2015. 10

한국물리학회 가을학술 논문발표회 초록집

the Korean Physical Society

2015. 10. 21(수)~23(금) 경주화백컨벤션센터

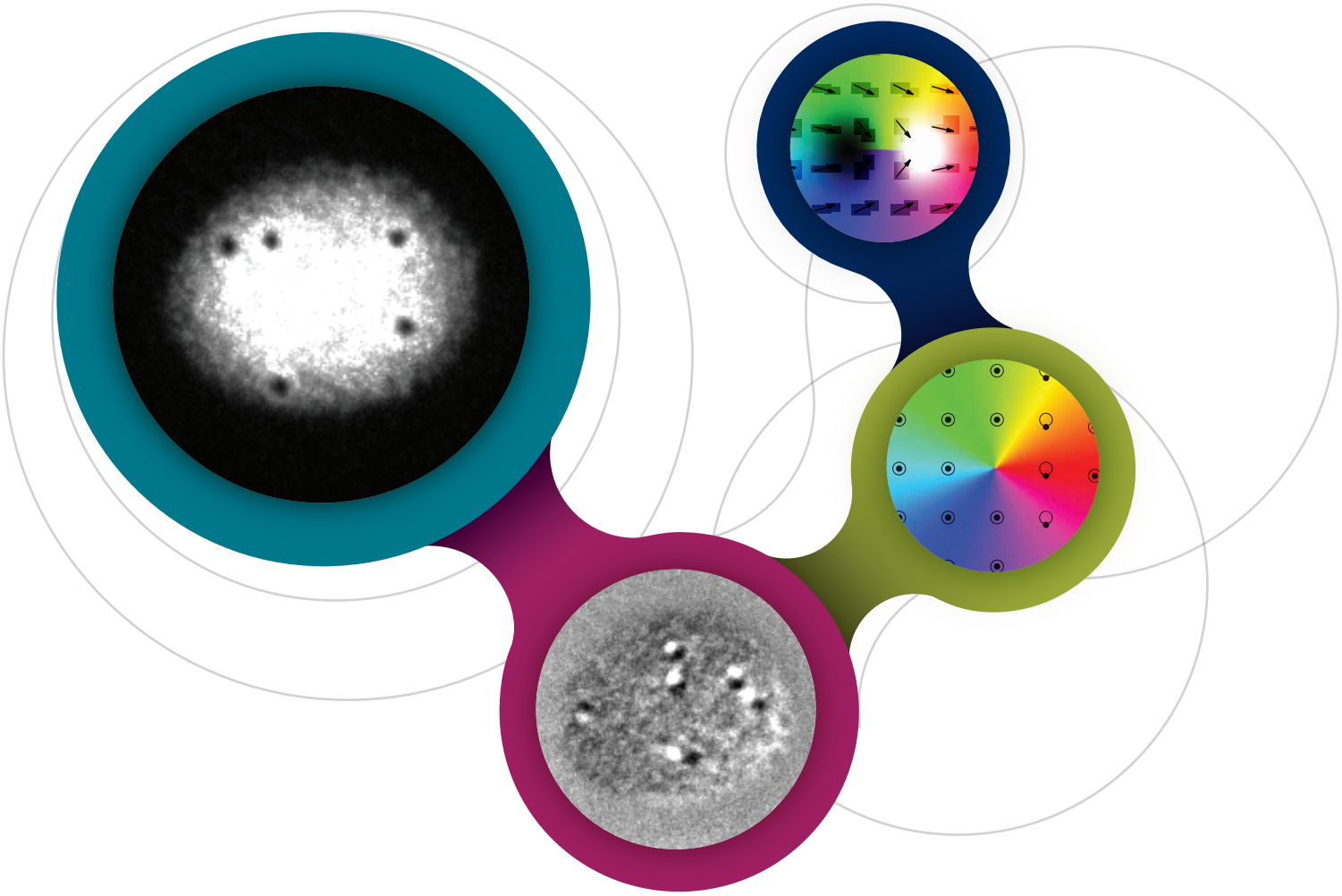

한국물리학회
The Korean Physical Society

구두발표논문

A1.01(초)

Terahertz Vibrational Spectroscopy of Condensed Matter

*Seiji Kojima
*Seiji. Kojima
University of Tsukuba.

Keyword : Terahertz spectroscopy, ferroelectrics, soft mode, polariton

The recent progress of broadband terahertz vibrational spectroscopy and its application to oxide dielectrics are reviewed. The new technique of the coherent terahertz generation using a femtosecond pulse laser enables the unique determination of a complex dielectric constant without using the Kramers-Kronig transformation, and terahertz time domain spectroscopy (THz-TDS) has attracted much attention [1]. However, the most of the THz-TDS works until now were below 2 THz. Very recently, the widely tunable monochromatic Cherenkov phase-matched THz wave generator has extended the high frequency limit up to 6.5 THz. THz-TDS enables the observation of Raman inactive soft mode of the incipient ferroelectrics [2]. The complex phonon-polariton dispersion relation including the damping of polariton was discussed on paraelectric and ferroelectric crystals as shown in Fig. 1 [3].

References

1. S. Kojima, N. Tsumura, M. W. Takeda, and S. Nishizawa, Phys. Rev. B 67, 035102 (2003).
2. M. A. Helal, T. Mori, and S. Kojima, Appl. Phys. Lett. 106, 182904 (2015).
3. S. Kojima and T. Mori, AIP Proc. 1627, 52; (2014).

A1.02(초)

Newly emerging phenomena in ultrathin ferroelectric films

*노태원
*Tae Won. Noh
서울대학교.

Keyword : Ferroelectric, ultrathin film, flexoelectric

Ferroelectricity, defined by the existence of a switchable spontaneous polarization, has attracted significant interest since its discovery in 1920. A lot of extensive researches has been done for deep understanding of ferroelectric phenomena. More recently, rapid advances in thin film fabrication techniques for oxide film has enabled us to study new fascinating emerging phenomena, particular to thin film ferroelectric materials. Especially, we are investigating a couple of intriguing effects, including ferroelectric critical thickness and flexoelectricity.

Studies on the ferroelectricity at the nanoscale enable us to understand the fundamental properties of this phenomenon. For instance, the minimum thickness for existence of ferroelectricity and its relation with the effect of the depolarizing field and interfaces, is the one of the long-standing issues in this field. This issue is particularly relevant in the context of the recent advent of memory devices based on ultrathin layers: so-called ferroelectric tunnel junction. Recently, we have successfully fabricated ferroelectric BaTiO3 films just a few unit cells in thickness, on SrRuO3-coated SrTiO3 substrates. Our studies on the heterostructure based on these ultrathin films show that the minimum thickness of 3.5 monolayers for ferroelectricity. We also found that the realizing the minimum thickness for ferroelectricity in the heterostructure only can done in specific interface termination sequences. This interface-termination-dependent critical thickness highlights the importance of the interfacial effect between the ferroelectric material and the electrode for stabilizing ferroelectricity.

The flexoelectric effect is the electro-mechanical coupling that generates an electric field by a strain gradient. Although this phenomenon exists in all dielectric materials, there have been few studies devoted to it due to the small size of the effects in bulk and difficulties in systematic control of strain gradient. Our recent studies, however, have shown that strain gradients in epitaxial thin films can be 6-7 orders of magnitude larger than in their bulk counterparts [1]. Here, I will review the recent progress regarding the flexoelectric effects in epitaxial ferroelectric thin films, suggesting that we can make use of flexoelectric effects by carefully controlling the strain gradient.

A1.03(초)

Combinatorial Substrate Epitaxy of Oxide Films

*Wilfrid Prellier
*Wilfrid. Prellier
ENSICAEN.

Keyword : Functional Oxides; thin Films, pulsed laser deposition, substrates

Interest in thin film transition metal oxides is driven in part by the potential technological application of devices exploiting intriguing phenomena, i.e. oxide electronics, and in part by the novel structures and properties observed in epitaxial oxide films, using phase, strain, and interfacial engineering. However, in spite of the large number of observations and promise of epitaxial oxide thin films, most of the investigations have been focused on films on low-index commercially-available single-crystal substrates, which have limited the scope of the study.
Here, we develop a high-throughput synthesis process (called combinatorial substrate epitaxy) where an oxide film is grown epitaxially on a polycrystalline substrate. Based on few examples like $BiFeO_3$ or Ca_2MnO_4, I will show how functional properties could be investigated across the entirety of epitaxial orientation space, and provide a library of physical property observations. Ultimately, this approach will expand our understanding of engineering function into transition metal oxides.
ANR, IDS FunMAT supports are acknowledged.

A1.04(초)

Electrical control of large magnetization reversal in a helimagnet

*김기훈
*Kee Hoon. Kim
서울대학교.

Keyword : multiferroic, magnetization reversal, giant magnetoelectric effect

Despite its technical and fundamental importance, reversal of macroscopic magnetization by an electric field (E) has rarely been achieved and remains a considerable challenge. Here, we report the strong modulation and large reversal of magnetization (M) by E in a multiferroic $Ba_{0.5}Sr_{1.5}Zn_2(Fe_{0.92}Al_{0.08})_{12}O_{22}$ crystal at zero magnetic field, in which a transverse conical spin state exhibits a remanent M and electric polarization below ~150 K. Upon sweeping E through the range of ±2 MV m^{-1}, M varied quasi-linearly in the range of ±2 μ_B per f.u., resulting in the reversal of M. Moreover, the remanent M exhibited non-volatile changes of ±0.15 μ_B per f.u., depending on the history of the applied electric fields. The strong modulation and non-volatile two-states of M at zero magnetic field were observable up to ~150 K. Nuclear magnetic resonance measurements provided microscopic evidence that the electric field and the magnetic field play equivalent roles in modulating the volume of magnetic domains. Our results suggest that soft ferrimagnetism with small magnetic anisotropy and the related transverse conical state are key ingredients to achieve the giant converse magnetoelectric effect, indicating a novel pathway toward achieving large magnetization reversal by electric fields at fairly high temperatures [1].
[1] Y. S. Chai et al., Nature comm. 5, 4208 (2014); Sae Hwan Chun et al., Phys. Rev. Lett. 108, 177201 (2012); ibid, 104, 037204 (2010);

In close collaboration with Prof. Soonchil Lee, Dr. Kwon, Sangil, Dr. Yisheng Chai, and Dr. Saehwan Chun

A2.01(초)

Engineering the band structure of black phosphorus

*김근수
*Keun Su. Kim
POSTECH.

Keyword : Black phosphorus, Phosphorene, Angle-resolved photoemission spectroscopy, tunable band gap, Dirac semimetal

Two-dimensional atomic crystals have emerged as a class of materials that may impact our future electronics technology. A key issue is controlling their electronic state to overcome the limit of natural properties. In this regard, there are growing interests in black phosphorus, a layered material that consists of phosphorene. The low-energy band structure of black phosphorus has been predicted to be tunable by various external perturbations, such as strain and electric field. In this talk, I will introduce our recent angle-resolved photoemission spectroscopy studies on the tunable band structure of black phosphorus. The in-situ deposition of alkali-metal atoms on the surface of black phosphorus induces a vertical electric field nearby, and tunes the band gap from a narrow-gap semiconductor to a band-overlapped semimetal. At the critical field, surface-doped black phosphorus becomes a Dirac semimetal whose band dispersion is highly anisotropic, linear in armchair and quadratic in zigzag directions.

A2.02(초)

Conductance quantization, universal terahertz absorption, and strong surface-phonon interaction in topological insulators

*김재훈
*Jae Hoon. KIM
연세대학교.

Keyword : "terahertz, Bi2Se3, topological insulator, topological surface state"

We report on our recent terahertz study on the novel aspects of the topological insulator Bi2Se3. Conductance quantization was observed and attributed to the presence of topological surface states and quantum-well states. In the 2D limit, a single conductance quantum was detected per surface, along with a universal terahertz absorption of 2.9% (four times the fine structure constant). The strong interaction between the surface state and the bulk phonon was analyzed in terms of Fano coupling.

A2.03(초)

$AMnBi_2$: Novel Anisotropic Dirac Materials

*김준성
*Jun Sung. Kim
포항공과대학교.

Keyword : Dirac materials

Dirac electronic structure, strong spin-orbit coupling, and magnetism are key elements for realizing various unconventional electronic states. Having these ingredients together in a single compound is extremely rare, and so far it has only been realized in a proximity-coupled interface of dissimilar layers having each property. In this talk, we report that a new layered compound $AMnBi_2$ provide a natural heterostructure of a Bi layer hosting a two dimensional Dirac fermions with large spin-orbit coupling. Due to the underlying sublattice symmetry in the double-sized Bi square net, the Dirac Fermi surface has the strong momentum dependence of the in-plane Fermi velocity. By applying high magnetic field, we show that the strong anisotropy of the interlayer coupling induces a valley-selective conduction. Also, by introducing a magnetic layer, we show that the transport properties of Dirac fermions are strongly coupled to the underlying spin structure. These results clearly demonstrates that the Bi square net, a common building block of various layered pnictide compounds, is a new platform for a highly anisotropic Dirac fermions coupled to external or internal magnetic fields.

A3.01(초)

Magnetic Van der Waals materials: opportunities and challenges

*박제근
*Je-Geun. PARK
서울대학교. IBS-CCES.

Keyword : Van der Waals

Van der Waals (VdW) materials entered the materials science well before the age of graphene. However, with the enormous success of graphene science one gets a certain, rightly or wrongly, impression that graphene brought us an entirely new waves of sciences and industrial applications as never seen before. True, we have now come to know various class of materials thanks to the extensive studies on several VdW materials. Strangely enough, however there is the conspicuous missing of one particular, otherwise popular, class of systems, which are magnetic VdW materials. With the intrinsic quantum number of spin, studies of this magnetic VdW systems would only enrich the science of VdW that has been so far successful in its own right. With this simple question in mind, I want to explore several possible magnetic VdW materials that are known in this talk. In particular, I will present some of our latest data on this topic.

A3.02

Two-dimensional massless Dirac fermions, chiral pseudo-spins, and Berry's phase in potassium doped few-layer black phosphorus

*백승수, 최형준
*Seung Su. Baik, Hyoung Joon. Choi
연세대학교.

Keyword : black phosphorus, potassium doping, massless Dirac fermions, chiral pseudo-spins, Berry's phase

Black phosphorus (BP) and its two-dimensional (2D) derivative phosphorene are rapidly emerging nanoelectronic materials with potential applicability to field effect transistors and optoelectronic devices. Unlike the gapless semiconductor graphene, multilayer BP has a substantial band gap of ~0.2 eV, and this band-gap size is predicted being sensitive to the external perturbations such as pressure and electric field. Very recently, a semiconductor-semimetal transition in BP was realized by the surface potassium (K) doping, producing a Dirac semimetal state with a linear dispersion in the armchair direction and a quadratic one in the zigzag direction [1,2]. Here, based on first-principles density functional calculations, we present that beyond the critical K density, 2D massless Dirac fermions emerge in K-doped few-layer BP, and the electronic states around Dirac points have chiral pseudo-spins and Berry's phase. These features are robust with respect to the spin-orbit interaction. The switchable massless Dirac fermions discussed here may open a new way for the development of high performance devices in 2D materials beyond graphene. This work was supported by NRF of Korea (Grant No. 2011-0018306) and KISTI supercomputing center (Project No. KSC-2014-C3-070).

[1] J. Kim, S. S. Baik, S. H. Ryu, Y. Sohn, S. Park, B. Park, J. Denlinger, Y. Yi, H. J. Choi, and K. S. Kim, Observation of tunable band gap and anisotropic Dirac semimetal state in black phosphorus, Science 349, 723-725, (2015).
[2] S. S. Baik, K. S. Kim, Y. Yi and H. J. Choi, Emergence of two-dimensional massless Dirac fermions, chiral pseudo-spins, and Berry's phase in potassium doped few-layer black phosphorus, arXiv:1508.04932.

A3.03

Tight-binding model study of few-layer black phosphorus

*도현진, 최형준
*Hyeonjin. Doh, Hyoung Joon. Choi
연세대학교.

Keyword : black phosphorus, Dirac semi-metal

We carry out a systematic study on the tight-binding model of few-layer black phosphorus. The black phosphorus can be a Dirac semi-metal with proper doping and electric field. We investigate the band structure changes depending on the hopping parameters and on-site potentials. For simplicity, we consider only dominating hopping parameters and find proper conditions of parameters for Dirac semi-metal in mono- and bi-layer black phosphorus. We also show that the tight-binding Hamiltonian can be reduced to the Dirac equation by expanding the momentum near the Dirac point. Our study suggests proper directions of experiments of the black phosphorus for controlling the gap at the Dirac point.

*This work is supported by the NRF of Korea (Grant No.2011-0018306). Computational resources have been provided by KISTI Supercomputing Center (Project No. KSC-2014-C3-070).

A3.04

Geometry, Electronic Structures and Optical Properties of Phosphorus Nanotubes

*타오후, Hashmi Arqum, 홍지상
*Tao. Hu, Hashmi. Arqum, Jisang. Hong
부경대학교.

Keyword : PNT, First principles

Using the first principles approach, we investigated the geometry, electronic structures, and optical properties of phosphorus nanotubes (PNTs). Two possible 1D configurations the so-called α-PNTs and β-PNTs are proposed, which are structurally related to blue and black phosphorus monolayer, respectively. Hereby, we predict that both armchair and zigzag geometries can be synthesized in α-PNTs, but the zigzag form of β-PNT is highly unfavorable because of large strain and conformation energies. The band gap of α-PNTs is expected to be ~2.67 eV, and this is insensitive to the chirality when the tube's inner diameter is larger than 1.3 nm, while the armchair β-PNTs have a much smaller band gap. Interestingly, we find nearly flat band structures in the zigzag α-PNT system. This may indicate that an excited particle-hole pair has a huge effective mass. We also find asymmetric optical properties with respect to the polarization direction. This work introduces a unique allotrope of phosphorus with interesting properties. This research was supported by Basic Science Research Program through the National Research Foundation of Korea (NRF) funded by the Ministry of Education, Science and Technology (No. 2013R1A1A2006071) and by the Supercomputing Center/Korea Institute of Science and Technology Information with supercomputing resources including technical support (KSC-2015-C3-021).

A3.05

Electronic band structures of bulk and few-layer black phosphorus with GW approximation

Kim Han-gyu, Seung Su Baik[1], Hyoung Joon CHOI
Han-gyu. Kim, Seung Su. Baik[1], Hyoung Joon. CHOI
Department of Physics and IPAP. Yonsei University. [1]Department of Physics. Yonsei University.

Keyword : black phosphorus, GW

We calculate the electronic band structures of bulk and few-layer black phosphorus (BP) by using the GW approximation. Compared with the generalized gradient approximation (GGA), GW method is shown to enhance the band-gap size in bulk and multilayer BP, while retaining the overall band shape in GGA results. This improvement of band-gap size tends to increase as the number of BP layers decreases from bulk to monolayer. Additionally, we calculate the band structures of potassium (K) doped four-layer BP and compare them with the experimental result of K-doped bulk BP. This work was supported by NRF of Korea (Grant No. 2011-0018306) and KISTI supercomputing center (Project No. KSC-2014-C3-070).

A3.06

Strain effect of monolayer and bilayer SnS2 for 1T and 1H structures

Abeera RAHMAN, 신영한
Abeera. RAHMAN, Young-Han. Shin
울산대학교.

Keyword : Strain effect, 2D material, Band-gap energy

Recently,many efforts have been paid to two-dimensional layered metal dichalcogenides (LMDs). Among them MoS2 has become a prototype LMD,and recent studies show surprising and rich new physics emerging in other van der Waals materials such as layered SnS2 [1-4]. SnS2 is a semiconducting earth-abundant material and Sn is a group IV element replacing the transition metal in MoS2. SnS2 shows new possibilities in various potential applications. However,the knowledge on basic properties of layered SnS2 is still not well understood. In this study,we consider two types of structures; 1T with P − 3m1 (164) space group and 1H with P63/mmc (194) space group. Our first principles calculations show that the 1T structure for SnS2 is more stable than the 1H structure whereas latter is more stable for MoS2. Moreover,in contrast to MoS2,SnS2 shows an indirect band gap both for 1T and 1H structures while 1T MoS2 is metal- lic and 1H has a direct band gap. We also study strain effect in the range of 0-10% on the band structure for monolayer and bilayer SnS2 (both for 1T and 1H structures).We find significant change in their band gaps. We also investigate the bilayer SnS2 with and without out-of-plane stress. As the possibility of tuning the band gap has an essential role to enrich device appli- cations, our results potentially offer a mechanism for controlling the electronic properties of monolayer and bilayer SnS2.

A4.01(초)

Enhancement of the superconductivity in optimally doped $Ba(Fe_{1-□x}Co_x)_2As_2$ through surface electron doping

*김용관, 경원식 [1], 고윤영 [2], 허순상 [1], 최기영 [3], 모성관 [4], 김창영 [1], Jonathan Denlinger[5]
*Yeoung kwan. Kim, Won shik. Kyung[1], Yoon Young. Koh[2], Soon Sang. Huh[1], KI YOUNG. CHOI[3], Sung-kwan. Mo[4], Changyoung. Kim[1], Jonathan. Denlinger[5]
Institute for Basic Science. [1] 연세대학교. [2] 포항가속기연구소. [3] 서울대학교. [4]Lawrence Berkeley national laboratory. USA. [5]Lawrence Berkeley national laboratory.

Keyword : Superconductivit, Iron-based superconductor, Angle resolved photoemission spectroscopy

Discovery of superconductivity with a striking transition temperature (T_C) as high as 100 K in heavily electron doped monolayer FeSe thin film on $SrTiO_3$ highlight a new insight on the mechanism of superconductivity in iron based superconductors. Together with relatively higer T_C found in bulk iron chalcogenide compounds with heavily electron doped nature, it suggests that higher T_C may be achieved through heavy electron doping, which results in Fermi surface only with electron pockets. It is far contrasting to what have found in iron pnictide, other family of IBS, so far that presence of both hole and electron pockets are regarded to be important to the superconductivity.

In this presentation, we report the observation of the T_C enhancement through surface doping in iron pnictide superconductor, up to 44.3 K from the original value of 23.1 K in optimally doped $Ba(Fe_{1□-x}Co_x)_2As_2$, concomitant with the overall FS topology change close to that of chalcogenides by a rigid band shift down to 14 meV. Our observation strongly implies FS nesting instability is not a crucial factor for the superconductivity for both iron chalcogenides and pnictides and call for a new understanding on the role of the hole bands in the superconductivity mechanism.

A4.02

Fermi arc Analyzed from Fitting of the Diverging Effective Mass Extracted from Quantum Oscillation in $YaBa_2Cu_3O_{6+x}$

*김현탁
*Hyun-Tak. KIM
한국전자통신연구원(ETRI).

Keyword : "YBCO", "d-wave MIT", "Brinkman-Rice picture", "high-Tc superconductivity", "Pairing symmetry"

For cuprate superconductors, the mechanism of high-T_c superconductivity is still an unclear and unsolved problem, because they are inhomogeneous. Here, we show analysis of superconductivity from the fitting result of the diverging-effective mass (DEM) extracted from the quantum-oscillation data in $YaBa_2Cu_3O_{6+x}$ [1]. The fitting was performed by extended Brinkman-Rice picture [2]. The fitting result presents the Fermi arc observed by angle-resolved-photoemission-spectroscopy data. In particular, the growing Fermi arc from the nodal Fermi point to the isotropic Fermi surface with increasing x and the nodal constant Fermi energy are revealed. Further, pairing symmetry of cuprate superconductors is analyzed as s-wave. The quantum critical point is regarded as the nodal Fermi point. The intrinsic superconducting gap is formed at node. The mass divergence is an average effect and the true effective mass is constant. [1] S. E. Sebastian et al., 2010 Proc. Natl. Acad. Sci. 107 (2010) 6179. [2] Physica C 341-348(2000)259; e-print arXiv:cond-mat/0110112

A4.03

The interplay of magnetism and superconductivity in $ErNi_2B_2C$ studied via a home-built magnetic force microscope

*Dirk Wulferding, 양일규 [1], 양진호 [2], 이민경 [1], Sergey L. Bud'ko[3], Paul C. Canfield[3], 최희철 [1], 염한웅, 김지훈 [1]
*Dirk. Wulferding, Il Kyu. Yang[1], Jin-Ho. YANG[2], MinKyung. Lee[1], Sergey. Bud'ko[3], Paul. Canfield[3], Hee Cheul. Choi[1], Han Woong. Yeom, Jeehoon. Kim[1]
포항공과대학교/기초과학연구원. [1] 포항공과대학교. [2]POSTECH. [3]Iowa State University.

Keyword : superconductivity, magnetism, scanning probe microscopy

We have designed and constructed a novel low temperature, ^{3}He magnetic force microscope operating within a vector magnet with field ranges of 2-2-9 T in x-y-z direction. We employ the system to investigate the ferromagnetic superconductor $ErNi_2B_2C$, which develops a long-range ferromagnetic order within the superconducting phase. Our data obtained at T=500 mK evidence the emergence of a structured magnetic background that has a profound influence on the London penetration depth λ. We present local measurements of absolute λ values with a sub-micrometer spatial resolution, as well as an estimation of the absolute pinning force for single Abrikosov vortices. Our data also support the scenario of spontaneous vortex formation due to the interplay of magnetism and superconductivity.

A4.04

The observation of coexistence of itinerant electronic states and local moments in parents compound superconductor $Sr_4V_2O_6Fe_2As_2$

*장원준, 최석환 [1], 옥종목 [2], 최현우 [1], 이현정 [1], 정진오 [1], 손동현 [1], 서환수 [3], 김준성 [2], 야니스 세메르치디스, 이진환 [1]
*Won-Jun. Jang, Seokhwan. Choi[1], JongMok. Ok[2], Hyun Woo. Choi[1], Hyun Jung. Lee[1], Jin Oh. Jung[1], Dong Hyun. Son[1], Hwansoo. Suh[3], Jun Sung. Kim[2], Yannis k.. Semertzidis, Jhinhwan. Lee[1]
Institute for Basic Science. [1]Korea Advanced Institute of Science and Technology. [2] 포항공과대학교. [3] 삼성전자 종합기술원.

Keyword : superconductivity, Fe based superconductivity, Kondo lattice, STM, QPI

The discovery of Fe based high-temperature superconductor (Fe-HTSC) has recently received significant attention, because of its possibilities of superconducting film growth with critical temperature over liquid nitrogen temperature. Unlike usual Fe-HTSC families, the parents compound superconductor, $Sr_4V_2O_6Fe_2As_2$ consists of two magnetic atomic layers of V and Fe.
Here, we studied about the electronic structures of $Sr_4V_2O_6Fe_2As_2$ using variable temperature scanning tunneling spectroscopy (STS) and quasi-particle interference (QPI) analysis. Temperature dependent STS measurements showed Fano resonances, resulting from the hybridization between the local moments of V atoms and the itinerant electrons of Fe atoms, near 100 K and revealed the superconducting coherence peaks near 30 K. Near 50 K, we found the signature of Fano lattices, which means the collective behaviors between local moments of V atoms. Also, spatially resolved STS measurements and QPI analysis showed the correlation between superconducting gap and V-Fe hybridization strength. Our results show the coexistence of itinerant electronic states and local moments, and the possibility of local moments contributing to superconductivity.

A4.05*

Pressure-induced superconductivity in the transition metal dichalcogenide 1T'-$MoTe_2$

*이상연, 박두선, 정순길, 김성일, 김지현, 김성웅
*Sangyun. Lee, Tuson. park, Soon-Gil. Jung, Sung il. Kim, JI HYUN. KIM, SungWng. Kim
성균관대학교.

Keyword : 1T-$MoTe_2$, superconductivity, transition-metal dichalcogenide, multi-band superconductivity, upper critical field

We report pressure-induced superconductivity in a single crystal of the transition-metal dichalcogenide 1T'-$MoTe_2$. At atmospheric pressure, this material goes through a structural phase transition near 210 K but pressure induces superconductivity at 0.47 K and 0.4 GPa. With increasing pressure, the monoclinic-to-orthorhombic transition temperature (T^*) decreases and electrical resistivity measurements do not show any anomaly associated with it above 1.2 GPa, where T^* and T_c become equal. In contrast, T_c increases with pressure and increases less rapidly for pressures higher than 1.2 GPa, suggesting a dome-like superconducting state. At 2.5 GPa, Tc is 4 K and the upper critical field H_{c2} is 2.8 kOe, which is ten times smaller than the Pauli limiting field, indicating that the orbital pair breaking effects are important. The linear-in-T dependence of H_{c2} and a positive curvature near T_c in $H_{c2}(T)$ indicate multi-band superconductivity in 1T'-$MoTe_2$

A4.06*

Thickness dependent structural and transport properties of $La_{1.85}Sr_{0.15}CuO_4$ epitaxial thin films.

*장한별
*HanByul. Jang
카이스트.

Keyword : Superconductivity, Thin film, Thickness, Pulsed laser deposition

For many years, copper-oxides-based superconductors have been extensively studied to obtain high critical superconducting temperature. $La_{2-x}Sr_xCuO_4$ is a well-known cuprate superconducting system which has a layered perovskite structure and various electronic properties as a function of Sr content. Especially, epitaxial thin layers of the compound show enormous increase of superconducting critical temperature (T_c) by compressive strain. It has been reported that the superconducting critical temperature can be controlled by misfit strain[1], thickness[2], and oxygen annealing[3]. In this study, we report structural and transport properties depend on thickness of the $La_{1.85}Sr_{0.15}CuO_4$ high quality epitaxial thin films synthesized by using pulsed laser deposition. Atomic force microscope image of the films presents step-terrace structure and roughness within atomic step level. According to x-ray theta-2theta scans and reciprocal space maps, c-axis lattice parameter increases as thickness of the films get thicker by relaxation of tensile strain. Electrical transport measurements of the films shows clear insulator-to-superconductor (I-S) transition, accompanying variation of T_c. We expect that film in boundary thickness of I-S transition is expected to have dramatic phase transition and T_c control by applying gate voltage control with ionic liquid or ferroelectric layer.

A4.07*

Construction of Tunnel Diode Oscillator setup and its application to the London penetration depth.

*신동우, O. E. Ayala-Valenzuela, 염한웅, 김지훈
*Dongwoo. Shin, Oscar. E. Ayala-Valenzuela, Han Woong. YEOM, Jeehoon. Kim
포항공과대학교/기초과학연구원.

Keyword : "TDO", "London penetration depth", "pairing symmetry", "superfluid density"

London penetration depth λ is one of the most important intrinsic parameters in superconductivity. Its temperature dependence is related to a superfluid density and superconducting pairing symmetry.
So far, a variety of experimental techniques have been employed to measure the absolute value of λ and its temperature dependence. The tunnel diode oscillator (TDO) technique is the most sensitive one among them to obtain the temperature dependence of λ. Here, we present home-built TDO and its preliminary results obtained from the Niobium and Ca10(Pt4As8)[(Fe1−xPtx)2As2]5 (10-4-8). Our TDO operates in the temperature range of 4 K ~ 300 K and the magnetic field of up to 9 tesla inside a cryogen free magnet system. The temperature dependent λ values measured from Niobium and 10-4-8 show s-wave pairing symmetry and multiband superconductivity, respectively.

A4.08

Real-space imaging of the temperature dependent magnetic structure and charge density waves in Sr_2VO_3FeAs

*최석환, 장원준, 옥종목 [1], 최현우, 이현정, 정진오, 손동현, 서환수 [2], 김준성 [1], Yannis K. Semertzidis, 이진환
*Seokhwan. Choi, Won Jun. Jang, JongMok. Ok[1], Hyun woo. Choi, Hyun-jung. Lee, JinOh. Jung, DongHyun. Son, Hwansoo. Suh[2], Jun Sung. Kim[1], Yannis. Semertzidis, Jhinhwan. Lee
KAIST. [1] 포항공과대학교. [2] 삼성전자 종합기술원.

Keyword : superconductivity, STM, magnetic order, spin fluctuation, charge density wave

Sr_2VO_3FeAs, which consists of superconducting FeAs layer and Mott insulating Sr_2VO_3 layer, exhibits superconductivity with Tc ~30 K despite being a parent compound material. Unlike typical Fe-based superconductors, the presence of two magnetic atomic layers of V and Fe added complexity to previous studies on its magnetic structure.
Here, we studied on the orbital and magnetic phase changes of Sr_2VO_3FeAs using temperature dependent (4 K ~ 180 K) scanning tunneling microscopy and spectroscopy with non-magnetic W tip and antiferromagnetic Cr tip. STM topography, obtained by non-magnetic tip, showed the changes of charge density waves of V atomic layer at 100 K and 150 K.
Spin-polarized STM topography showed the spin density waves of V atoms with the periodicity of (π/a, 0) and (0, π/a) below 50 K, resulting from spin ordering of underlying Fe atomic layer. Controlling the sample bias voltage, the hysteresis characteristics of magnetic domain is observed. Our result shows key clues that are able to solve controversy about the magnetic structure of Sr_2VO_3FeAs.

A5.01

Dark matter fusion research cluster based on computational science

*조기현
*Kihyeon. Cho
한국과학기술정보연구원.

Keyword : Beyond Standard Model, Dark Matter, Computational Science, Accelerator-based physic, Particle Physics

The Standard Model helps understanding visible matters that make up 4% of the universe. However, the universe seems to be made of 26% dark matter and remaining 70% dark energy which is beyond the Standard Model. Let me introduce dark matter fusion research cluster which is supported by National Research Council of Science and Technology. The goal is a fusion research to search for dark matter from accelerator-based physics to astrophysics using infrastructures at KISTI (Korea Institute of Science Technology Information) and KASI (Korea Astronomy and Space Science Institute). For this, computational science is used. The current status and plan will be discussed.

A5.02

Search for Hidden Particles - The SHiP experiment

*윤천실
*Chun Sil. YOON
경상대학교.

Keyword : SHiP experiment, Hidden particles, Heavy Neutral Lepton, CERN SPS, Tau neutrino

A new general purpose fixed target experiment, SHiP (Search for Hidden Particles), is proposed at the CERN SPS accelerator which is intended to hunt for new physics in the largely unexplored domain of hidden particles with masses below the Fermi scale, inaccessible to the LHC experiments, and to study tau neutrino physics. The hidden particles are predicted by a large number of recently elaborated models of hidden sectors which are capable of accommodating dark matter, neutrino oscillations, and the origin of the full baryon asymmetry in the Universe. The high intensity of the SPS and in particular the large production of charm mesons with the 400 GeV beam allow accessing a wide variety of light long-lived exotic particles with masses below O(10) GeV/c^2 of such models and of SUSY. Specifically, the experiment is aimed at searching for very weakly interacting long lived particles including Heavy Neutral Leptons (right-handed partners of the active neutrinos), light supersymmetric particles, dark photons etc. Moreover, the facility is ideally suited to study the interactions of tau neutrinos. In this talk, we will present the brief description of the conceptual design and the current status of the proposed experiment.

A5.03

SHiP experiment and dark matter

*최기영*Ki Young. Choi
한국천문연구원.

Keyword : dark matter, hidden particle

SHiP (Searching for Hidden Particles) experiment is the beam dump experiment proposed at the CERN using the proton beam at SPS. I will talk about the possibility to probe the new light particles beyond the standard model and the relation to the dark matter search.

A5.04

Theoretical Review of SHiP Experiment

*이강영
*Kang Young. Lee
경상대학교.

Keyword : SHiP, new physics, hidden particle, neutrino

CERN 의 SPS 가속기를 이용하는 고정 타깃 실험인 SHiP (Search for Hidden Particle)에서 검증하고자 하는 이론적인 모델 전반을 소개한다. SHiP 에서는 수 GeV 의 질량을 가지고 표준모형의 입자와 매우 약하게 상호작용은 하면서도 수십 m 정도를 날아갈 정도의 수명을 가지는 입자를 검출하게 된다. 따라서 이와 같은 입자를 포함하는 이론을 SHiP 에서 일어나는 매우 많은 수의 충돌 사건을 통해 검증한다.

A5.05

Status of the AMoRE-pilot experiment, a search for 0νββ of 100Mo with 1.5 kg of CaMoO4 crystals

*강찬석, AMoRE collaborators
*Chan Seok. KANG, AMoRE. collaborators
기초과학연구원.

Keyword : AMoRE,CaMoO4,0νββ

The Advanced Mo-based Rare process Experiment (AMoRE) is a search for neutrinoless double beta decay (0νββ) of Mo-100 with CaMoO4 crystals using cryogenic techniques. A pilot experiment with 1.5 kg of CaMoO4 crystals, named the AMoRE-pilot, was prepared and installed at the YangYang underground laboratory (Y2L) and now has been under operation for a few weeks. The status of the experiment will be presented and system improvements such as noise reduction will be discussed.

A5.06*

SIMP dark matter with discrete gauge symmetries

*최수민, 이현민
*Soo Min. Choi, Hyun Min. Lee
중앙대학교.

Keyword : Dark Matter, SIMP, Hidden sector

The SIMP miracle can provide a new possibility for thermal dark matter in the presence of strong interactions in the hidden sector. We consider Higgs-portal type interactions of SIMP dark matter to keep it in kinetic equilibrium with thermal bath until freeze-out in the early universe. As a consequence, we find bounds on the Higgs-portal couplings from the requirement that the 3-to-2 scattering is dominant mechanism for determining the thermal dark matter relic density as well as from the Higgs invisible decay.

A5.07*

Analysis of WIMP direct detection data beyond standard methods

*윤국현, 스코펠 [1]
*Kook hyun. Yoon, Scopel. Stefano[1]
서강대학교. [1]Sogang University.

Keyword : Dark matter, WIMP, Generalized WIMP-nucleus cross section, Halo-independent approach

We discuss compatibility of the DAMA modulation signal with other experimental constraints(xenon, fluorine, germanium, etc) and the correspoding allowed parameter space using a generalized WIMP-nucleus cross section beyond the standard spin-independent and spin-dependent cases. We also adopt a halo independent approach and consider in-elastic scattering. In this way, tension between DAMA and other experiments can be relaxed or eliminated.

A5.08*

Search for non-thermal dark matter and new scalar boson at the LHC

정남균, 김동희, *오영도
Nam Gyun. Jeong, DongHee. Kim, *Young Do. OH
경북대학교.

Keyword : Dark matter, non-thermal , pp-collisions , Delphe

Recent results from LHC experiment and Fermi-LAT experiment require new Dark matter self annihilation rate. Non thermal dark matter scenario as simple extended Standard Model is proposed to solve this problem as well as baryon-antibaryon asymmetry. This model introduces two scalar bosons with mass of O(TeV) which are isosinglet, colortriplet and one singlet fermion with mass of O(GeV) which can be a dark matter candidate. We perform simulation study of the non thermal dark matter model in pp collisions at sqrt(s)= 14 TeV using Delphe 3 program and determine the search limits of new scalar bosons as well as light dark matter.

A6.01*

Direct investigation of metal diffusion into organic layer after thermal annealing

*이시우, 조정형, 김효정, 이현휘 [1], 김남동 [1], 신현준 [1]
*Si Woo. Lee, Jeong Hyeung. Jo, Hyo Jung. KIM, Hyun Hwi. Lee[1], Namdong. KIM[1], Hyun Joon. SHIN[1]
부산대학교. [1] *포항가속기연구소.*

Keyword : STXM, metal diffusion, interface, solvent, thermal annealing

We directly observed the metal diffusion phenomena into the organic semiconductor layer at an Al metal-organic interface after thermal annealing by scanning transmission x-ray microscopy (STXM), optical microscopy, and x-ray reflectivity measurements. The spatial resolution of STXM was ~50 nm. The diffusion of Al metal was dependent on the annealing temperature as well as type of casting solvent used for the fabricating the organic layer. The organic layer was poly (3-hexylthiophene) (P3HT): phenyl-C61-butyric acid methyl ester (PCBM) which is an archetype active layer for organic photovoltaics (OPVs). In case of chlorobenzene (CB) solvent, Al atoms considerably diffused into the organic layer and aggregated to form pillar shaped grains of 500-700 nm diameter and therefore, Al layer was significantly deformed by the diffusion. On the other hand, the Al atom diffusion was adequately in case of dichlorobenzene (DCB) solvent. The presence of PCBM was also affected to the diffusion phenomena. We mixed the solvents with CB and DCB at various ratio of them, and confirmed the role of solvents by AFM and SEM measurements.

A6.02*

Laser irradiation-induced modification of the amorphous phase in GeTe films: The role of intermediate Ge-Te bonding in the crystallization mechanism

박승종, 박한진 [1], 장문형, *안민, 양원준, 한정화, 정홍식, 김철운 [1], 권영균 [1], 조만호
Seung Jong. Park, Hanjin. Park[1], Moon Hyung. Jang, *Min. Ahn, Won Jun. Yang, Jeong Hwa. Han, Hong-Sik. Jeong, Cheol-Woon. Kim[1], Young-Kyun. Kwon[1], Mann-Ho. Cho
연세대학교. [1] *경희대학교.*

Keyword : Phase-change, intermediate state, amorphization, first-principles density functional theory, molecular dynamics

Modified amorphous GeTe, formed by the pulsed laser irradiation of as-grown GeTe, was analyzed in terms of variations in the local bonding structure using Raman spectroscopy and x-ray absorption fine structure in tandem with first-principles density functional theory. Amorphized GeTe (acquired from the crystalline phase) was compared with the modified amorphous GeTe to investigate the similarities and discrepancies between these two amorphous phases. Raman spectroscopy showed that these materials have a similar distribution of Ge-centered local structure in both phases, which is mainly composed of an octahedral-like structure. However, extended X-ray absorption fine structure results show the presence of a unique second type of Ge-Te bonding in the amorphized GeTe, which can effectively reduce the energy required for recrystallization. A computational study based on molecular dynamics simulations verified our experimental observations, including the existence of a second type of Ge-Te bonding in the amorphized phase. Moreover we distinguished the structural characteristics underlying the different amorphous phases, such as local atomic configurations and structural symmetries.

A6.03*

Grain size and thickness effects on thermal transport of post-annealed antimony telluride (Sb_2Te_3) thin films via four-point probe 3-omega method

*박노원, 이원용, 윤순길 [1], 박태현, 조상혁, 이상권
*No-Won. Park, Won Yong. Lee, Soon-Gil. Yoon[1], Tae hyun. Park, sanghyeok. Cho, Sang-Kwon. Lee
중앙대학교. [1] *충남대학교.*

Keyword : Thermal conductivity, Antimony telluride (Sb_2Te_3), 3-omega technique, Grain size, Thermal transport

We report on the effects of the thickness and grain size on the thermal transport properties of antimony telluride (Sb_2Te_3) thin films in the temperature range of 20–300 K using a four-point-probe 3-omega method. For this study, 100-, 400-, and 500-nm-thick Sb_2Te_3 films were prepared by radio frequency magnetron sputtering. The average thermal conductivities of the films were determined to be between 0.8 and 3.9 W/m·K in the temperature range of 20–300 K, revealing a strong thickness and temperature dependences of the thermal transport properties of the films. We suggest that this reduction in the thermal conductivity of the films, compared to the bulk, may be attributed to the enhanced phonon scattering from the grain boundary that occurs when decreasing the thickness to 100 nm. To further investigate the effects of the thickness and grain size, the experimental results of the films were theoretically analyzed using the Sondheimer model, which showed a good agreement with the measured values, indicating that the thermal conductivity decreases appreciably from the bulk values.

A6.04*

The effects of Si impurities on the Schottky barrier height and effective work function at TiN/t-HfO_2 interface

*김근명, 오영준, 장기주
*Geun-Myeong. Kim, Young Jun. Oh, Kee Joo. Chang
한국과학기술원.

Keyword : Metal/high-k interface, Schottky barrier height, effective work function, impurity

High-k/metal gate stack has attracted much attention due to the replacement of SiO_2/poly-Si gate in metal-oxide-semiconductor field-effect transistor (MOSFET). Monoclinic HfO_2 (m-HfO_2) is one of widely used high-k dielectric materials. However, the dielectric constant of m-HfO_2 is not sufficiently high as the size of MOSFET device is continuously reduced. On the other hand, tetragonal HfO_2 (t-HfO_2) has a higher dielectric constant, so that the leakage current can be effectively reduced. It was reported that Si doping reduces the crystallization temperature of tetragonal HfO_2. However, there is a lack of studies for the effect of Si impurities on the work function at TiN/t-HfO2 interface.

In this work, we perform first-principles density functional calculations to investigate the effect of Si impurities on the p-type Schottky barrier height (p-SBH) at TiN/t-HfO_2 interface. We generate two interface interface structures, which consist of either Ti-O or N-Hf bonds at the interface. The effective work function is obtained by including the quasiparticle GW_o corrections to the band gap and the valence band edge state of HfO_2. When the Si atoms substitute for the interface N atoms, p-SBH tends to decrease, leading to the p-type shift of work function. Such a shift is attributed to the change of interface bonding by Si. On the other hand, when the Si atoms replace the Ti atoms inside the bulk region, p-SBH does not significantly change. Thus, the Si impurities mostly affect the effective work function at the N-terminated interface.

A6.05*

Gold Membrane as a Material for Two-Tone Nanolithography

*오창목, 장재원
*Changmok. Oh, Jae-Won. Jang
부경대학교.

Keyword : Membrane, Lithgraphy, PDMS

Recently, membrane based applications have been reported such as Li-ion battery, fuel cell, and transparent electrode. For this reason, membrane based lithography methods have been researched; two typed membrane based lithographies have been developed, which are the underneath lithography (UNL) and chemical imprint lithography (CIL). By means of the CIL, metal oxide structures with negative-tone (based on PDMS stamp) are fabricated. And UNL method creates channel-like structures. In addition, metamaterial structure of Al2O3/Au hole array was obtained by CIL. This structure has been designed as a metamaterial to work in infrared region. In this study, it is demonstrate that the membrane based lithography method can be conveniently used as various applications including optical and channel devices.

A6.06

Thickness-dependent strain effect on the optical and electrical properties of V_2O_5 thin films

*강만일, 김석원, 류지욱 [1]
*Manil. Kang, Sok Won. KIM, Ji-Wook. Ryu[1]
울산대학교. [1] *공주대학교.*

Keyword : "V_2O_5," "metal-insulator transition," "strain," "ellipsometry"

Thin-film vanadium pentoxide (V_2O_5) has attracted much attention owing to its unique electronic, chemical, and optical properties. These interesting properties have been attributed to the ease of oxygen removal from the lattice of V_2O_5. Much research has focused on the changes in electronic structure by the formation of oxygen vacancies. A reversible surface metal-insulator transition has been reported on a V_2O_5 (001) single crystal at 350–400 K by inducing oxygen vacancies in an ultrahigh vacuum. However, there is still no full understanding of the oxygen vacancy-induced lattice relaxations.
In the present study, we investigate thickness-dependent strain effect on the optical and electrical properties in V_2O_5 thin films prepared using an rf sputtering system. The optical and electrical properties with temperature in the films are characterized by measurements of the ellipsometry and resistance at temperatures ranging from room temperature to 400 °C. Also, the behaviors of the optical and electrical properties near the transition temperature are discussed.

A6.07

Interaction between x-ray and resistance switching materials

*장서형, 홍승범 [1], 김정호 [1]
*Seo Hyoung. Chang, Seungbum. Hong[1], Jungho. Kim[1]
부경대학교. [1]Argonne National Laboratory.

Keyword : Resistance switching, X-ray, irradiation, TiO2, RIXS

Resistance switching phenomenon has attracted great attention due to its scientific interests as well as potential applications. To unveil mechanisms of nanoscale-switching phenomena, synchrotron-based x-ray or electron-beam has been used as a powerful diagnostic tool. Despite recent efforts on developing advanced measurement tools based on x-ray, there is still a lack of fundamental understanding on how to interact between x-ray and resistance switching materials. Here, we investigate the x-ray-induced resistance change in Pt/TiO_2/Pt structures. We found that the two distinct resistance level changes induced by x-ray [1]: reversible and irreversible resistance changes. We will discuss the physical explanation of the intriguing phenomena. In addition, we will discuss how to promote or eliminate the x-ray effects and introduce advanced x-ray techniques for nanoscale resistance switching phenomena, e.g., resonant x-ray inelastic scattering (RIXS) and extended x-ray absorption spectroscopy (EXAFS).

[1] S. H. Chang et al., ACS Nano 8, 1584 (2014).

A7.01

Efficient stress-relaxation in InGaN/GaN light-emitting diodes using carbon nanotube interlayer

*박아현, 서태훈 [1], S. Chandramohan, 이건희, 민경현, 이슬아 [1], 김명종 [1], 서은경
*Ah Hyun. PARK, Tae Hoon. SEO[1], Samygounder. Chandramohan, Gun Hee. LEE, Kyung Hyun. MIN, Seula. LEE[1], Myung Jong. KIM[1], Eunkyung. SUH
전북대학교. [1] 한국과학기술연구원.

Keyword : carbon nanotubes, epitaxial lateral overgrowth, stress relaxation, light-emitting diode

We demonstrate facile methods to facilitate epitaxial lateral overgrowth of III-nitride materials and light emitting diode (LED) structures using single-walled carbon nanotubes (SWCNTs) in metalorganic chemical vapor deposition. High-quality GaN was achieved on sapphire by simply coating the SWCNTs as an intermediate layer for stress and defect mitigation. The SWCNTs allow epitaxial lateral overgrowth of GaN to occur, leading to the suppression of edge dislocations and stress relaxation by up to 0.32 GPa. High-resolution x-ray diffraction, micro-Raman, and photoluminescence studies revealed substantial improvements in the crystal and optical quality of the GaN layer. InGaN/GaN multi-quantum-well LEDs on this high-quality GaN template offered enhanced internal quantum efficiency and light output power with reduced efficiency droop.

A7.02

Investigation of direct transition energies in $Ge_{1-x}Sn_x$ thin films with various Sn contents by photoreflectance spectroscopy

Hyun-Jun Jo, Jong Su Kim, Mee-Yi RYU[1], Yung Kee Yeo[2], John Kouvetakis[3]
Hyun-Jun. Jo, Jong Su. KIM, Mee-Yi. RYU[1], Yung Kee. Yeo[2], John. Kouvetakisd[3]
Yeungnam University. [1]Kangwon National University. [2]Air Force Institute of Technology. [3]Arizona State University.

Keyword : GeSn, Photoreflectance, direct transition

Various $Ge_{1-x}Sn_x$ (x=0-7.5%) thin films were grown on i-Ge buffered i-Si substrate by ultra-high vacuum chemical vapor deposition method. Photoreflectance (PR) measurements at room temperature (RT) have been made to investigate the direct transition energies of $Ge_{1-x}Sn_x$ thin films. The PR spectra show the direct transitions from conduction Γ valley to valence and spin-orbit split-off bands of $Ge_{1-x}Sn_x$ thin films and Ge buffer layers. The PR signals of $Ge_{1-x}Sn_x$ thin films are red shifted with increasing Sn content as shown in Fig. 1. Temperature-dependent PR measurements are also performed as shown in Fig. 2. Behaviors of $Ge_{1-x}Sn_x$ and Ge buffer layer with Sn content and temperature are dicussed.

A7.03*

그래핀과 실리콘 사이의 전하 이동 특성 연구

*박홍기, 최재우
*Hong-Ki. Park, Jaewu. Choi
경희대학교.

Keyword : 그래핀 반도체 라만분광법

그래핀과 반도체 이종접합구조에서 존재하는 계면의 물리적 특성은 소자의 특성을 크게 조절한다. 따라서 라만분광법과 Impedance analyzer 를 통하여 계면 특성을 연구 조사하였다. 그래핀과 반도체이종접합구조가 형성되면서 전하의 이동이 있고, 또한 역전압을 인가하게 되면, 실리콘내에서 공핍영역(Depletion region)이 발생하게 되고, 이는 그래핀 내의 전하밀도의 변화로 나타난다. 그래핀의 낮은 상태밀도함수의 변화로 인하여 그래핀과 반도체 이종접합구조에서 쇼트키장벽(Shottky barrier)의 높이가 변화하게 되고, 그에 따라 전하의 이동량이 달라지게 된다. 따라서 라만분광법을 통해 나타나게 되는그래핀 특유의 G, 2D peak 의 위치변화를 통해 그래핀의 전하분포를 알 수 있게 되고, Impedance analyzer 를 통해 계면에 축척되는 전하량과 다이마믹 특성을 조사하였다.

A7.04*

Hierarchical nano/ microstructured polymer films combined with ZnO nanowires for piezo / triboelectric energy-harvesting device applications

*두뎀, 임정우, 유재수
*Bhaskar Dudem. , Jung Woo. Leem, Jae Su. Yu
경희대학교.

Keyword : Piezoelectric, triboelectric nanogenerator, hierarchical architecture PDMS.

Energy harvesting from nanogenerators is one of the foremost interest to efficiently convert vibrational, rotational, and mechanical energy into electricity based on the piezoelectric, triboelectric, electromagnetic, and pyroelectric effects. Especially, the flexible and transparent nanogenerators demand for most of the device applications such as sensors, displays, etc. In this work, we developed the prototype piezoelectric / triboelectric hybrid nanogenerators by employing the polydimethylsiloxane (PDMS) film with hierarchical architectures (HA) consisting of nanonipples on periodic microcone arrays and zinc oxide (ZnO) nanowires to produce the electricity by utilizing the mechanical pushing force. Moreover, it is possible to realize the transparent and flexible nanogenerators using PDMS and ZnO materials. Therefore, the transparent and flexible piezoelectric / triboelectric hybrid nanogenerator can be utilized as a pressure sensor. For the fabricated samples, the surface morphologies and profiles were observed by a scanning electron microscopy and optical properties were characterized by using a UV-VIS-NIR spectrophotometer. For an analysis of the output device performance, the multimeter and picoammeter were employed to measure the generated voltage and current of fabricated devices.

A7.05*

Hydrothermally synthesized hydroxyapatite nanopowders: study of structural and luminescent properties

*크리스나바랏, 유재수
*Krishna. bharat, Jae Su. Yu
경희대학교.

Keyword : Nanoparticles, Hydroxyapatite, Structural properties, optical properties

Nanoparticle which can bridge the bulk materials and atomic/molecular structures have great significance due to its wide range of applications in optical, electronics and biomedical fields. The nanoscale size particles have properties like high percentage of atoms on the surface of the material than the bulk materials. $Ca_{10}(PO_4)_6(OH)_2$ hydroxyapatie (HAp) belong to the apatite family with general formula $Ca_{10}(PO_4)_6X_2$. The synthetic HAp have the same chemical compositions as biological HAp. HAp is a good host material for doping different kinds of metal ions (dopants) and studying the optical properties. In the present work we synthesized the nanosize calcium hydroxyapatite structures through hydrothermal synthesis process. The as-prepared powders were characterized by X-ray diffraction, Fourier transform infrared spectroscopy, scanning electron microscopy and transmission electron microscopy. The doped HAp materials were used to study the optical properties.

A7.06*

Energy transfer mechanism and color-tunable luminescence in Dy^{3+}/Eu^{3+}-codoped $NaLa(MoO_4)_2$ phosphors

*두펭, 유재수
*Peng. Du, Jae Su. Yu
경희대학교.

Keyword : Phpsphors,Rare-earth,Luminescence,$NaLa(MoO_4)_2$

Nowadays, the trivalent rare-earth (RE) ions doped luminescent materials have drawn considerable as a result of their promising applications in solar cells, solid-state lasers, white light-emitting diodes and field emission displays. To meet the requirement of these applications, luminescent materials are expected to show high-efficiency photoluminescence (PL) emissions, color controllable emissions, high physical-chemical stability. Dysprosium (Dy^{3+}) ion, as a member of RE ions, has been intensively studied because of its unique luminescence properties. In general, Dy^{3+} ions exhibit two dominant emissions in blue and yellow regions, which are attributed to the $^4F_{9/2} \rightarrow {}^6H_{15/2}$ and $^4F_{9/2} \rightarrow {}^6H_{13/2}$ transitions, respectively. Furthermore, europium (Eu^{3+}) ions doped compounds are considered to be alternative candidates for red-emitting phosphors owing to their high efficiency characteristic red emission at about 615 nm corresponding to the $^5D_0 \rightarrow {}^7F_2$ transition. In addition, the energy can be efficiently transferred from Dy^{3+} to Eu^{3+} ions, thus, color controllable emissions are expected to be obtained in Dy^{3+}/Eu^{3+}-codoped phosphors. In this work, the Dy^{3+}/Eu^{3+}-codoped $NaLa(MoO_4)_2$ phosphors were prepared by a simple high temperature solid state reaction method. The X-ray diffraction (XRD) results indicated that all the samples had pure tetragonal phase. Meanwhile, the energy transfer mechanism between Dy^{3+} and Eu^{3+} ions was found to be electric dipole-dipole interaction. Ultimately, the color tunable emissions were observed in Dy^{3+}/Eu^{3+}-codoped $NaLa(MoO_4)_2$ phosphors by adjusting the ratio of Dy^{3+} and Eu^{3+} ion concentrations.

A8.01(초)

Big Bang Nucleosynthesis and the Origin and Evolution of Space-Time

*Grant Mathews
*Grant. Mathews
Univ. of Notre Dame.

Keyword : Big Bang, dark energy and dark matter, early universe

Primordial nucleosynthesis remains as one of the pillars of modern cosmology. It is the testing ground upon which all cosmological models must ultimately rest. It is our only probe of the universe during the first few minutes of cosmic expansion and in particular during the important radiation-dominated epoch. There have been significant recent advances in the understanding of the big bang including the recent detection of the inflation-generated gravity-wave background. This talk will review the current state of observational constraints on primordial abundances along with the key nuclear reactions, their uncertainties and how this knowledge places key constraints on cosmological models. In particular, we will summarize the connections between big bang nucleosynthesis and the birth of the universe, including cosmic gravity waves, inflation, the possible time variation of fundamental constants], the nature and origin of dark matter and dark energy, supersymmetry, and the primordial magnetic field.

A8.02(초)

Origin of r-Process Elements in Galactic Evolution

*Taka Kajino
*Taka. Kajino
The University of Tokyo.

Keyword : Supernovae, r-process

Both core-collapse supernovae (SNe) and binary neutron star mergers (NSMs) are viable candidates for the r-process elements. SN models such as magneto-hydro-dynamic jets can naturally explain the universality, but their explosion mechanism is till poorly known. On the other hand, binary NSMs could not have arrived very early in Galactic evolution because of their cosmologically long coalescence time scale 0.1Gy < t_c < 1000Gy, as estimated from the orbital motions of observed binary pulsars. We will first discuss the importance of nuclear data such as asymmetric fission mass-fragment distributions and beta-decay half-lives far from stability by taking account of recent experimental data from RIKEN-RIBF. We then apply these refined nuclear input data to the r-process nucleosynthesis calculations in both astrophysical models of SNe and binary NSMs. We would like to discuss how to solve the above twisted problem by carrying out numerical simulations of Galactic chemo-dynamical evolution of dwarf galaxies in a hierarchical structure formation scenario of the Milky Way. We then propose a best model for the origin of the r-process elements and their evolution from the early Galaxy to the epoch of solar-system formation.

A8.03

The low-energy effective theory for the nuclear interaction and its application to the dense nuclear matter by using $V_{low\ k}$

*팽원기, Thomas T. S. Kuo[1], 이현규 [2], Mannque Rho[3]
*Won-Gi. Paeng, Thomas. Kuo[1], Hyun Kyu. LEE[2], Mannque. Rho[3]
기초과학연구원. [1]Stony Brook University. [2] 한양대학교. [3]CEA Saclay.

Keyword : hidden local symmetry, dense nuclear matter, qcd, $V_{low\ k}$, neutron star

When the effective theory for the nuclear interaction is given for the low-energy strong interaction which accounts for the trace anomaly of QCD and is matched with QCD at the high energy scale, we apply the effective theory called “scale-invariant Hidden Local Symmetric(HLS) model” to dense baryonic matter relevant for heavy ion collision and massive compact stars. By performing a double-decimation procedure for the renormalization-group calculation employing the V_{low k} strategy, we compute the equation of the state for dense nuclear matter and discuss what the prediction of the ``scale-invariant HLS'' is for heavy ion collision like RAON or compact star observatory.

A8.04*

Effects of the Sterile Neutrino and Extra Dimension in Big Bang Nucleosynthesis

*장덕재, Motohiko Kusakabe[1], 천명기
*Dukjae. Jang, Motohiko. Kusakabe[1], Myung-Ki. Cheoun
숭실대학교. [1]University of Notre Dame.

Keyword : BBN, Sterile neutrino, expansion rate, extra dimension

Big bang nucleosynthesis (BBN) in the early Universe is an important topic on the origin of elements because it explains production of light nuclei.The BBN is described by many variables such as expansion rate that affect the abundances of light elements. These variables can be constrained by comparing theoretical and observed abundances. In this work, we study an extra dimension model which includes sterile neutrinos. The cosmic expansion rate in this model is affected by the extra dimension and sterile neutrinos. Then this model has a different cosmic expansion rate from the standard BBN. In this presentation, we will show the effects of the modified expansion rate on light element abundances.

A8.05

Nuclear Reactions during Supernova Explosion

*곽규진
*Kyujin. Kwak
울산과학기술대학교(UNIST).

Keyword : Nuclear Reaction, Supernova, Shock Wave, Particle Distribution

무거운 별의 진화의 마지막 단계에서 발생하는 초신성 폭발은 강력한 충격파를 동반한다. 최근 연구를 통해 충격파가 지나간 물질 (Shocked Matter or Matter in the Downstream) 내의 입자들이 열평형 상태에 근거한 맥스웰 분포를 벗어나 Power-law 를 따르는 것이 알려졌다. 본 연구에서는 충격파에 의해 형성된 power-law 를 따르는 입자들의 분포가 초신성 폭발과 관련한 핵자들의 핵반응에 미치는 영향을 조사하였다.

A8.06

Study of the ^{26}Al(d,p)^{27}Al reaction for the astrophysical ^{26g}Al(p,γ)^{27}Si reaction rate

*채경육, S.D. Pain[1], D.W. Bardayan[2], J.C. Blackmon[3], M.S. Smith[1], K.A. Chipps[4], J.A. Cizewski[4], R.L. Kozub[5], K.L. Jones[6], J.F. Liang[1], C. Matei[7], M. Matos[7], B.H. Moazen[6], C.D. Nesaraja[1], J. Okolowicz[8], P.D. O'Malley[4], W.A. Peters[7], M. Ploszajczak[9], K.T. Schmitt[6], J.F. Shriner Jr.[5]
*Kyung Yuk. Chae, S.D.. Pain[1], D.W.. Bardayan[2], J.C.. Blackmon[3], M.S.. Smith[1], K.A.. Chipps[4], J.A.. Cizewski[4], R.L.. Kozub[5], K.L.. Jones[6], J.F.. Liang[1], C.. Matei[7], M.. Matos[7], B.H.. Moazen[6], C.D.. Nesaraja[1], J.. Okolowicz[8], P.D.. O'Malley[4], W.A.. Peters[7], M.. Ploszajczak[9], K.T.. Schmitt[6], J.F.. Shriner. Jr.[5]
성균관대학교. [1]Oak Ridge National Laboratory. [2]University of Notre Dame. [3]Louisiana State University. [4]Rutgers University. [5]Tennessee Technological University. [6]University of Tennessee at Knoxville. [7]Oak Ridge Associated Universities. [8]Polish Academy of Sciences. [9]GANIL.

Keyword : nuclear astrophysics, ^{26}Al(d,p)^{27}Al, radioactive ion beam

The Galactic 1.809-MeV γ-ray signature from the β decay of ^{26g}Al is a dominant target of γ-ray astronomy, of which a significant component is understood to originate from massive stars. The ^{26g}Al(p,γ)^{27}Si reaction is a major destruction pathway for ^{26g}Al at stellar temperatures, but the reaction rate is poorly constrained due to uncertainties in the strengths of low-lying resonances in ^{27}Si. The ^{26g}Al(d,p)^{27}Al reaction has been employed in inverse kinematics to determine the spectroscopic factors at the Holofield Radioactive Ion Beam Facility of the Oak Ridge National Laboratory. The details of the experimental setup and results will be discussed.

A8.07

Pion emission in strong magnetic fields

*권영신, Tomoyuki Maruyama[1], 천명기, Toshitaka Kajino[2], Grant J. Mathews[3], 류충열
*Youngshin. Kwon, Tomoyuki. Maruyama[1], Myung-Ki. Cheoun, Toshitaka. Kajino[2], Grant. Mathews[3], Chung-Yeol. Ryu
숭실대학교. [1]Nihon University. [2]University of Tokyo. [3]University of Notre Dame.

Keyword : pion emission, magnetic field, high energy neutrinos

We study pion production from proton synchrotron radiation in the presence of strong magnetic fields by using the exact proton propagator in a strong magnetic field and explicitly including the anomalous magnetic moment. In this exact quantum field approach the magnitude of pion synchrotron emission turns out to be much smaller than that obtained in the semiclassical approach. However, we also find that the anomalous magnetic moment of the proton greatly enhances the production rate about by 2 orders of magnitude.

A9.01

교구 개발 활동이 예비 물리 교사의 전공 전자기 교육에 미치는 영향

*조광희
*JO Kwang-hee.
조선대학교.

Keyword : 교구, 예비 물리 교사, 전공 전자기학 교육

예비 물리 교사를 대상으로 교구 개발 활동을 진행하고 이러한 활동이 전공 전자기 교육에 미치는 영향을 알아보았다. 연구 참여자는 남부 지역 사범대학 물리교육과에 재학 중인 2 학년생 16 명이었다. 한명을 제외한 15 명은 전공 전자기학 강좌를 이수하는 중이었으며, 이와 별도로 개설된 과목을 통해 자발적으로 본 연구에 참여하였다. 연구 참여자들에게 전공 전자기학의 내용 및 물리적 상황을 나타낼 수 있는 교구를 개발하도록 요청하였다. 교구 개발은 2 인 1 조 형식으로 한 학기 동안 진행되었다. 5 차례의 진행 관련 보고서 작성, 5 차례 이상의 성찰 저널 작성, 설문 및 면담 등을 통해 인지 및 정의적 영역을 포괄하는 교육 관련 자료를 수집하여 교구 개발 활동의 효과를 알아보았다. 질적 자료를 중심으로 분석한 결과, 교구 개발 활동이 전반적으로 전공 전자기 내용에 대한 이해, 학습 동기 고취 등에 있어 다양하게 기여하는 것으로 나타났다. 예를 들어 교구 개발을 위해 해당 내용에 대한 개념 이해를 선행하는 과정을 거쳤고, 이를 쉽게 설명하기 위한 방법을 탐색하는 토론 시간을 가졌다. 아울러 내용에 대한 이해와 표현의 관계를 탐구하는 경험을 통해, 특히 교구 완성 단계에서 성취감과 교육에 대한 자신감 등을 가지게 되었다.

A9.02

과학자의 협업 유형에 관한 탐색적 연구

*이지원, 김중복
*Jiwon. Lee, Jung Bog. Kim
한국교원대학교.

Keyword : 과학적 협업, 협업 유형, 협업적 창의성

최근의 수많은 연구를 통해 사람들 사이의 협업이 강력한 통찰력을 이끌어낸다는 것이 밝혀지고 있다. 이 연구에서는 과학자들의 협업적 창의성이 발현되는 과정에서 나타난 협업 유형을 분류하기 위한 분류틀을 개발하고, 이 분류틀을 적용하여 과학자들의 사례를 분석하고자 한다. 개발된 분류틀에서 과학자들의 협업 방식은 개인, 과제, 집단의 세 축을 기반으로 나눌 수 있었다. 이 분류틀을 기반으로 CERN 의 LHC, 2013 년 노벨화학상을 수상한 CHARMM, Human Cunnectome Project 등의 과학적 협업사례를 분석하였다.

A9.03

사범대학 교과목과 부설학교 수업실습 간 연계성 탐색: 물리교사 지도수업을 중심으로

*이경호, 문홍주 [1], 신재성 [2], 유은지 [3], 안정곤, 이종선, 오지은
*Gyoungho. Lee, Hongju. [1], Jaesung. [2], Eunji. [3], Jeonggon. , Jongsun. , Jieun.
서울대학교. [1] 서울대학교사범대학부설고등학교. [2] 서울대학교사범대학부설여중학교. [3] 서울대학교사범대학부설중학교.

Keyword : 물리교과 수업실습, 연계성, 물리교사 지도수업

교육 실습은 예비교사들이 대학에서 배운 전문적인 지식과 이론을 교육현장에 적용해 보고
교사로서의 자질을 함양하도록 하는 데 그 목적이 있다. 이와 같은 교육실습의 목적이 성공적으로 달성되기 위해서는
사범대학과 부설학교 간에 다양한 차원의 연계성이 필요하다. 본 연구는 사범대학 물리교육과의 '물리교과수업실습 및
분석'과 부설학교 물리과 수업실습 간의 연계성을 강화하기 연구의 일환으로 진행되었다. 구체적으로, 본 발표에서는
사범대학 교수와 부설학교 교사들이 함께 지도교사의 시범수업을 분석하고 논의하면서 '좋은 과학수업'에 대한
서로간의 지평을 나누고 융합하는 과정에 대하여 소개할 예정이다.

A9.04

과학 고등학교 학생들에게 적용 가능한 융합형 STEAM 과제의 유형

*이승우, 김영민 [1]
*Seungwoo. Yi, Youngmin. Kim[1]
동서대학교. [1] *부산대학교.*

Keyword : "STEAM 융합과제","창의적문제해결력","과학고등학교"

본 연구에서는 과학고등학교 2 학년 3 명의 학생들이 과학 전람회 과제를 준비하면서 보인 창의성 변화의 과정을 탐구하였고 과학고 수준에 적합한 STEAM 융합과제의 한 예를 제시하였다.
과학고등학교 2 학년 학생들은 대학교 1 학년 수준의 교과목을 이수하고 있었으며 과학고등학교를 지원하는 과정에서 이미 수학과 과학에 대한 다양한 개인적인 역량을 가지고 있었다. 학생들은 전람회 준비를 위한 주제를 정하는 과정에서 잘 가이드 되어져야 했지만 주제가 결정되고 연구가 진행되어 가는 과정에서 개인적인 역량이 잘 드러났고 STEAM 융합과제로의 전환이 순조롭게 이루어 질 수 있었다. 연구결과 학생들의 주제선정의 어려움은 내신 대비를 위한 교과목 위주의 학습으로 인한 다양한 과학적인 정보와 관심의 부재에서 기인함을 발견하였다. 3 명의 과학고 학생들은 각자 수학과 과학에 대한 다양한 관심과 재능을 가지고 있었고 수학적 재능이 뛰어나 프로그래밍에 재능을 보인 학생과 물리, 화학의 원리에 깊은 이해를 하고 있는 학생, 그리고 실험을 계획하고 실천에 옮기는 추진력이 뛰어난 학생으로 구성되어 있었으며 이러한 구성은 의도되어지지 않은 조합이었다. 이러한 학생들의 조합에서 개인적인 역량이 잘 발휘되어질 수 있도록 가이드 되어 질 경우 과학고등학교 학생들의 특성을 잘 이끌어 낼 수 있는 STEAM 융합과제가 도출될 수 있음을 확인할 수 있었다.

A9.05*

통일 한국을 위한 아름다운 과학교육
- 물리영역을 중심으로 한 통합적 문항(SIP)의 개발-

*이수아, 나재원 [1], 권순재 [2]
*, [1], [2]
경북대학교. [1]West vancouver secondary school. [2] 덕화중학교.

Keyword : 통합적 문항, 과학과 예술, 창의적 사고, 통합적 사고, 독창성

오천년의 역사를 가진 우리나라는 분단 70 년이라는 암울함속에서도 눈부신 성장을 이루어왔다고 볼 수 있다. 이러한 시대적 상황 속에서 복잡한 문제들을 해결하기 위해서는 세밀한 분석과 창의적 사고(creative thinking)뿐만 아니라 폭넓은 지식에 의한 통합적 사고(integrated thinking)도 필요하다고 할 수 있다(Treffinger, 2004; Lehman, 1994; Hurd, 1991; Marzano, 1988). 특히, 독창성(originality)은 창의적 사고의 공통적 요소라고 할 수 있으며(Park, 2011) 특허 출원시 중요하게 다뤄진다고 볼 수 있다(2001, Kim). 따라서 국제적인 경쟁력을 갖추기 위해서는 한국의 상황과 문화가 깃든 독창적인 과학교육을 추구할 필요가 있다고 할 수 있다. 우리나라의 과학성취도는 교과서에서 배운 과학적 상황이 주로 제시되는 TIMSS 보다 다양한 상황을 제시하는 PISA 에서 낮게 나타나는 경향이 있다(M. Lee, 2007). 즉, 학생들은 비슷한 유형의 문항들을 반복 학습하는 경향이 있다고 할 수 있으며(S. Lee & Y. Park, 2008), 물리 과목의 경우 입시정책의 영향으로 CSAT(the College Scholastic Ability Test)에서 선택률이 낮다고 볼 수 있다. 과학과 예술의 통합 수업은 학생들의 창의적 사고를 일깨우고(Medina Jerez, 2012) 사고의 폭을 넓게 하며 과학에 대한 태도에 긍정적 영향을 끼친다고 볼 수 있다(Igal Galili, 2013). 최근, 문화적 정체성을 표현한 예술작품이 전시되기도 하였다(Yinka Shonibare, 2015). 그러나 예술적 상황은 첨단 기술적 상황을 적극적으로 도입한 2009 개정 교육과정에서 두드러지지 않았으며 CSAT 물리영역에서도 도입되지 않았다(Yang, 2003). 따라서 본 연구는 물리를 중심으로 한 통합적 문항(SIP:ScienArt for the Integrated Problem)을 제작하여 학생들의 문제해결 과정에 나타난 창의적, 통합적 사고에 대해 살펴보았다. 제작된 문항은 3 개의 질문(감상, 과학, 창의적 설계)으로 이루어져 있으며 연구 대상은 캐나다와 한국의 중학교 2 학년 각 1 명이며 상세한 분석을 위해 회상면접법을 이용하여 면담도 실시하였다. 이를 통해, 본 연구는 과학 수업과 문항개발, 평가에서 지향해야 할 바를 제시하고자 하였다.

A9.06

Bridging Moments of Inertia Between Solids and Shells

*홍석철, 홍석인 [1]
*Seok-Cheol. Hong, Seok-In. HONG[1]
고려대학교. [1] *경인교육대학교.*

Keyword : Moment of inertia, Rotational dynamics, Differentiation-based method.

We develop a differentiation-based method to relate the moments of inertia (MOIs) of symmetrical solid objects with only one characteristic length (rod, disk, sphere, equilateral triangle, square, and all five regular polyhedra) and those of the corresponding shells when the MOIs are measured about an axis of rotation passing through the center of mass.

A9.07

Why Coordination Class?

*김성용, 홍석인
*Seongyong. Kim, Seok-In. Hong
경인교육대학교.

Keyword : 개념변화, 전이

Coordination class supports the knowledge-in-piece perspective of conceptual change. We clarify its function, intrinsic difficulties (span, alignment), architecture (readout strategy, causal net), and implications to transfer of learning through a variety of episodes.

A9.08

전자 스페클 패턴 간섭계(ESPI)를 이용한 대류와 역전층의 관찰

*장도형, 허재혁, 전동렬
*Dohyeong. Jang, Jaehyuk. Hyh, JEON Dong-Ryul.
서울대학교.

Keyword : "대류", "역전층", "ESPI", "전자 스페클 패턴 간섭계"

대류는 열을 전달하는 중요한 현상 중의 하나지만 눈에 보이지 않기 때문에 학생들이 이 현상을 이해하는데 어려움을 겪는다. 역전층에서는 대류가 일어나기 힘들어 대기 오염의 원인이 되기도 하는데, 이 또한 눈에 보이지 않아 학생들에게 어려움을 준다. 우리는 이 어려움을 해소할 수 있도록 전자 스페클 간섭계를 이용하여 대류와 역전층을 눈으로 확인할 수 있는 무늬로 나타냈다. 스페클 간섭계 무늬를 분석하면 공기의 굴절율과 온도까지 잴 수 있으므로 이 간단한 학습 도구는 학생들이 기체의 순환을 이해하는데 많은 도움을 줄 수 있다.

A10.01

Detection of Cosmic ray and X-ray of GEM Detector by the Korea CMS

*류민상, 박인규, 정영군, 김현철, 최민규
*Min Sang. RYU, Inkyu. PARK, Young Gun. JENG, Hyunchul. KIM, Minkyoo. CHOI
서울시립대학교 (University of Seoul).

Keyword : Compact Muon Solenoid (CMS), gas electron multiplier (GEM), detector, pad readout

The Korea CMS (KCMS) has been studying and developing the gas electron multiplier (GEM) for the muon system upgrade project of CMS at CERN. The KCMS has built the quality control system for large GEM (50x120 cm^2) to measure the leakage current and to check whether the holes are good and surface damage on GEM. Also, the GEM detector (10x10 cm^2) designed by CERN RD51 has been made by the KCMS and tested with the cosmic ray muons and 5.9 keV X-ray (Fe-55). And we has been developing and making the prototype GEM detector (10x10 cm^2) with the pad readout system for 2D imaging. In this talk, we present the R & D status of GEM detector by the KCMS.

A10.02

Studies of the b-jet trigger using Level 1 Pixel tracks at CMS for the LHC Phase II upgrade

*유금봉, 양운기, 김준호, 오성빈, 박재균, 문창성 [1], SAVOY-NAVARRO Aurore[1]
*Geum Bong. Yu, Un-ki. Yang, JUN HO. Kim, Sung bin. Oh, Jae gyun. Park, Chang-seong. Moon[1], Aurore. Savoy-Navarro[1]
서울대학교. [1]University Paris-Diderot/CNRS.

Keyword : CMS, LHC PhaseII, L1 b-jet trigger

In the Phase II upgrade at the LHC, CMS experiment will install the track trigger in Level 1 (L1 track trigger) to make the most powerful tool in searching for new physics and precision measurements. The capability of the L1 track can be significantly improved by refitting the tracks with pixel hits (L1 pixel track). One big advantage is to have the b-jet trigger in Level 1. Here we present the physics motivation of the b-jet trigger and the feasibility study.

A10.03*

CMS Muon Trigger Performance in pp Collisions at sqrt(s) = 13 TeV

*남경욱, 이경필, 유휘동
*Kyungwook. Nam, Kyeongpil. Lee, Hwidong. Yoo
서울대학교.

Keyword : CMS, Muon, Trigger, 13TeV

A measurement of CMS muon trigger performance in pp collisions at sqrt(s) = 13 TeV is presented. The performance is tested in the data collected with the CMS detector during LHC 13 TeV operation in 2015. Single muon and double muon trigger rates are measured with respect to instantaneous luminosity. Also muon trigger efficiencies, including L3 intermediate steps, are measured through Tag & Probe method. In addition, tools to monitor trigger system using L2 & L3 muon variables are developed.

A10.04*

Performance of muon reconstruction and identification using Tag & Probe method with 13TeV data

*이경필, 남경욱, 유휘동
*KyeongPil. Lee, Kyungwook. Nam, Hwidong. Yoo
서울대학교.

Keyword : CMS, Muon, Tag & Probe

Performance of muon reconstruction and identification in pp collisions at 13 TeV is presented. Muon final states are analyzed in a data sample collected with the CMS detector. Efficiencies of muon reconstruction and identification are measured by Tag & Probe method. The measured values show fair agreement with next-to-leading-order Monte-Carlo prediction.

A10.05

Beam Profile Monitoring (BPM) system development for the low energy muon beam diagnostics in the J-PARC g-2/EDM experiment

*김봉호, 최선호, Yoshinori Fukao[1], Ryo Kitamura[2], Tsutomu Mibe[1], Masashi Otani[1], 원은일 [3], Kondo Yasuhiro[4]
*BongHo. Kim, SEONHO. CHOI, Yoshinori. Fukao[1], Ryo. Kitamura[2], Tsutomu. Mibe[1], Masashi. Otani[1], Eunil. Won[3], Kondo. Yasuhiro[4]
서울대학교. [1]KEK. [2]University of Tokyo. [3]Korea University.Center for Axion and Precision Physics Research. [4]JAEA.

Keyword : anomalous magnetic moment, delectric dipole moment, muon, Beam diagnostics, beam profile

A discrepancy between theory and experiment about 3 standard deviation of the muon anomalous magnetic moment was reported by the BNL E821 experiment. This deviation can be a hint of new physics beyond standard model. Additionally, measurement of muon EDM will be a doorway to new physics as CP violation in charged lepton sector has not been observed yet. The J-PARC g-2/EDM experiment aims to measure the anomalous magnetic moment (g-2) and electric dipole moment (EDM) of the positive muon with the sensitivity of 0.1 ppm for g-2 and 10e-21e·cm for EDM. This experiment uses novel technique by accelerating ultra-slow muon to 300 MeV/c with small transverse momentum spread that can be focused without electric-focusing field. It is complementary to the BNL E821 and the FNAL E989 that use 3.1 GeV/c muon beam as magic momentum to cancel the effects of electric-focusing field at muon storage. The ultra-cold muon generated from muonium ionization should be accelerated with high efficiency and this goal can be achieved by optimization of the beam line. The Beam Profile Monitor has been developed as a beam diagnostics to measure beam profile at low energy region. After conceptual design, the first proto-type is on the test stage. In this presentation, the R & D of the muon beam profile monitor will be discuss more in detail.

A10.06*

Studies of the electron trigger using pixel detector at Level 1 in CMS experiment for the Phase II upgrade.

*김준호, 유금봉, 오성빈, 박재균
*JUN HO. KIM, Geum-bong. YU, Sung bin. Oh, Jae gyun. Park
서울대학교.

Keyword : CMS

In Phase II upgrade, LHC plans to increase luminosity over 5x10^34 /cm^2/s to increase the capability for new physics and precision physics.The CMS experiment will replace the silicon tracker (pixel and strips detectors) to allow for efficient data taking at higher collision rates.This brings an opportunity to deploy the tracker into the trigger system at Level 1. We perform feasibility studiesof new Level-1 pixel electron trigger which provides higher trigger efficiency on electron and large rejection factor for fake electrons.

A10.07

The 3-dimensional level one track trigger for the Belle II experiment.

*김재박, 원은일, 김경태, 문현기, Yoshihito Iwasaki[1], Jing-Ge Shiu[2], Yun-Tsung Lai[2], Ming-Chuan Chang[3]
*Jae bak. Kim, Eunil. Won, KyungTae. Kim, HyunKi. Moon, Yoshihito. Iwasaki[1], Jing-Ge. Shiu[2], Yun-Tsung. Lai[2], Ming-Chuan. Chang[3]
고려대학교. [1]KEK. [2]National Taiwan University. [3]Fu Jen Catholic University.

Keyword : Belle II, level 1 trigger, CDC, FPGA, 3 dimensional tracker

The next generation e+ e- collision experiment called Belle II will start in the following few years. It will search for new physics using high precision measurements which were not possible before. The precision will be achieved by using a high luminosity beam. Due to the luminosity of the beam, there must be an fast and efficient trigger system in order to record the physics relavent data.
The Belle II level 1 trigger system is a combination of sub-trigger FPGA based systems. The main dectector triggers are the CDC (Central drift chamber) trigger and electromagnetic detector trigger. Between them the CDC trigger finds the momentum and vertex position of charged tracks. These precise information will then be used to determine whether the event has interesting physics or not. If the event is determined to be physics relavent, the DAQ system will record the detector data to disk.
The level 1 CDC trigger consistes of 7 types of boards. They are the Frontend boards, Merger boards, TSF boards, 2D finder board, Event time finder board, 3D tracker boards, and Neural Network boards. Each board has a specific function that makes tracking charged track possible with high precision.
Korea University is participating heavily in the development of the level 1 CDC trigger. We are developing the TSF firmware, Event time finder firmware, and 3D tracker firmware.
Details of the Belle II level 1 CDC trigger are presentated.

A10.08*

Data Acquisition for the Belle 2 experiment

*육영민, 권영준, 김한진
*Youngmin. Yook, Youngjoon. Kwon, Hanjin. Kim
연세대학교.

Keyword : Collider experiment, B physics, Data acquisition

The design of the new Data Acquisition system (DAQ) is under development for the upcoming Belle 2 experiment at the SuperKEKB asymmetric-energy e^+e^- collider. The DAQ system is consisted of timing distribution, data link, event building, and high level triggering, where it is expected to comply with the Belle 2 design luminosity of $8\times10^{35}cm^{-2}s^{-1}$, 40 times higher than the previous Belle experiment. We present the overall concept of the DAQ design and the contribution of Yonsei High Energy Group on the development.

A10.09

OPTIMASS : A Package for Kinematic Mass Function Minimization with Constraints

*조원상
*Won Sang. Cho
기초과학연구원 순수물리이론연구단.

Keyword : New physics search, Mass measurement, Top-quark, Supersymmetry, Optimization

Reconstructed mass variables, such as M_2, M_{2C}, M_T^*, and M_{T2}^W, play an essential role in searches for new physics at hadron colliders. The calculation of these variables generally involves constrained minimization in a large parameter space, which is numerically challenging. We provide a C++ code, OPTIMASS, which interfaces with the MINUIT library to perform this constrained minimization using the Augmented Lagrangian Method. The code can be applied to arbitrarily general event topologies and thus allows the user to significantly extend the existing set of kinematic variables. We describe this code and its motivation and demonstrate its use in the analysis of the fully leptonic decay of pair-produced top quarks using the M_2 variables.

A11.01(초)

Telescope Array 실험에 대한 현황 보고

*박일흥
*PARK IL Hung.
성균관대학교.

Keyword : 우주선, 극한에너지, TA

미국 유타사막에서 진행되고 있는 Telescope Array 극한에너지 우주선 실험에 대한 한국 기여에 대하여 보고하며, 또한 검출기 업그레이드 계획에 대하여 토의하고자 한다.

A11.02(초)

Galaxy Clustering Topology of Large-scale Structure in the Sloan Digital Sky Survey

*최윤영
*Yun-Young. Choi
경희대학교 국제캠퍼스.

Keyword : cosmology, large-scale structure, observation

Topology analysis was introduced by Gott et al. (1986) to test the Gaussianity of the primordial density fluctuations. At large scales where density fluctuations are still in the linear regime and maintain their initial topology, it is possible to check whether the primordial fluctuations were a Gaussian field or not. At smaller scales, the topology analysis is useful in constraining both cosmological parameters and galaxy formation mechanisms if the initial conditions were Gaussian distributed. In particular, differences in clustering topology for different types of galaxies reflect their different history of formation and evolution. In this talk, we present various three-dimensional genus topologies of large-scale structures traced by three different types of galaxies (Main galaxy, luminous red galaxy, and high redshift BOSS galaxy) from the Sloan Digital Sky Survey, and discuss their deviations of the observed topology from the theoretical expectation. To estimate the uncertainties in the measured genus and also to compare the result with the outputs of cosmological N-body simulations of a ΛCDM universe, we use mock surveys constructed along the past light cone from the Horizon Run 3, one of the largest N-body simulations to date, which evolved 72103 particles in a 10815 h^{-1} Mpc box.

A11.03(초)

Overview of 42 Years Research in Astrophysics

*양종만
*Jongmann. YANG
이화여자대학교.

Keyword : "big bang nucleosynthesis", "isotopes", "high energy astrophysics", "academic genealogy", "international collaboration"

Academic personal research experience in astrophysics will be described. Topics include academic genealogy, research topics, equipment, collaboration, travel, personal relations.

A12.01(초)

Thermodynamic second law in a feedback process with time delay

*엄재곤, 권철안 [1], 박형규
*Jaegon. Um, Chulan. KWON[1], Hyunggyu. PARK
고등과학원. [1] 명지대학교.

Keyword : information thermodynamics, nonequilibrium, thermodynamic second law, cold damping

We investigate a realistic feedback process repeated in multiple steps where a feedback protocol from measurement is applied with delay and maintains for a finite duration until next step. Unlike a feedback without delay, a composite system consists of the system and two memories where previous and present measurement outcomes are stored, leading to the 3-state Shannon entropy for the composite system. Then according to the thermodynamic second law, the change of the 3-state Shannon entropy provides the upper bound for heat flow from reservoir to system during the feedback and relaxation process. However, if the feedback protocol is depending on memory states sequentially, it turns out that the tighter bound for heat production can be obtained by integrating out the irrelevant memory state. We exemplify a cold damping case where a velocity of a particle is measured and a dissipative protocol is applied by feedback, and it is confirmed that the Shannon-entropy change of the reduced composite system gives the tighter bound for heat production.

A12.02

Reversibility-irreversibility transition in an elastoplastic model under cyclic shear

*이수도, 백승기
*Su Do. Yi, Seung Ki. Baek
부경대학교.

Keyword : Yield stress, plastic behavior, elastoplastic model, irreversibility

Some materials such as foams and granular matters show plastic behavior beyond a critical yield stress. Picard et al. have proposed an athermal elastoplastic model as a coarse-grained description of such materials. By considering the Eshelby inclusion problem to take into account consequences of a plastic event, this approach has successfully explained macroscopic properties of yield stress materials, including the formation of shear bands under a constant shear rate. By applying cyclic shear to the Picard model, we observe a discontinuous jump from finite to zero mean stress as the amplitude of the cyclic shear increases, which signals a transition between reversibility and irreversibility.

A12.03

Information and statistical mechanics

*김상락
*Sang Rak. KIM
경기대학교.

Keyword : statistical mechanics, information theory, ideal gas model, entropy

A new formulation of statistical mechanics based on the information theory is presented. Starting from a general ideal gas model, the exact entropy expressions for classical and quantum systems are systematically derived. The quantum effects and interaction between particles for real gases are regarded as mutual information. Coarse-graining of a system with a resolution l can be interpreted as a reduction of information by an amount log l.

A12.04

Spherical models of growing interface

DURANG XAVIER, HENKEL MALTE[1]
Xavier. Durang, Malte. HENKEL[1]
한국과학기술원. [1]Universite de Lorraine. France.

Keyword : Exactly solvable models
Non equilibrium phenomena
Ageing
Growth process

We study several surface growth models obtained by treating and replacing the non-linear term in the noisy Burgers equation or the KPZ equation by a mean spherical condition. We want to explore the consequences of such constraints on the Edwards-Wilkinson (EW) interface. In those exactly solvable models, one has to solve the spherical conditions and then we can derive the two-time quantities (the correlation function and the response function). Therefore, we have access to the non-equilibrium exponents and compare them to those of the EW model or the KPZ model.

A12.05

Phase transitions on multiplex lattices of percolations under cascade of activations and deactivations

*최지혜, 고광일, 민병준 [1]
*Jeehye. Choi, Kwang-Il. Goh, Byungjoon. Min[1]
고려대학교. [1]City College of New York.

Keyword : Multiplex networks

Multiplex networks which are constructed by various types of connections have been studied to understand complex systems, i.e. cooperation. We study the percolation transitions of two models, Cascade of Activations (CA) and Cascade of Deactivations (CD) which has multiple resource on boundaries on multiplex lattices. Two different cascading model have different order parameter scaling exponent. Activation process is similar to ordinary percolation transition, but the mean of viable cluster size diverges at the critical point. Deactivation process result is the same to the multiplex lattices result which shows slower phase transtiion than ordinary percolation. Preliminary results on the transitions and their critical phenomena will be presented.

A12.06*

Generalized Epidemic Process on Scale-Free Networks

*정기홍, 백용주 [1], 하미순 [2], 정하웅
*Kihong. Chung, Yongjoo. Baek[1], Meesoon. Ha[2], HAWOONG. JEONG
KAIST. [1]Technion. [2] 조선대학교.

Keyword : GEP, tricriticality, scale-free

We study the generalized epidemic process (GEP) on scale-free (SF) networks, which is a simple model of spreading process with synergetic effects. Previous studies on regular lattices [1] and Erdos–Renyi networks [2,3] found that the phase diagram of GEP exhibits both continuous and discontinuous transition lines, whose intersection exhibits tricritical behaviors that are distinct from ordinary bond percolation. Extending analytical approaches employed in these previous studies, we investigate how phase transitions and tricritical behaviors of GEP are affected by the power-law exponent of SF networks. Our theoretical predictions are compared with numerical results obtained from Monte Carlo simulations.

[1] H.–K. Janssen et al., Phys. Rev. E 70, 026114 (2004).
[2] K. Chung et al., Phys. Rev. E 89, 052811 (2014).
[3] K. Chung et al., to be submitted.

A12.07*

Two critical behaviors in percolation transitions in two dimensional interdependent networks

*최상민, 이덕재, 강병남
*Sangmin. CHOI, Deokjae. LEE, Byungnam. KAHNG
서울대학교.

Keyword : hybrid phase transition, mutually connected component, randomly interdependent network

Hybrid phase transition differs from conventional phase transition in that it exhibits the behaviors of both first- and second-order phase transitions. In a system with hybrid phase transition, not only does its order parameter display a discontinuity at the transition point, but the physical quantities also possess critical exponents. It is known that the cascading failure model on multilayered random networks exhibits hybrid phase transition, but the details of its critical properties were covered in veil due to the enormous amount of computational resources required for simulation. This problem has recently been resolved by an efficient algorithm that identifies the mutually connected components within O(N^1.2) computation time. Utilizing this algorithm, we investigate the critical behavior of the cascading failure model on randomly interdependent 2D lattices in the supercritical regime. Furthermore, we aim to identify the critical exponents of this system, as well as the scaling relations that they must satisfy.

A12.08*

Explosive percolation in growing networks

*오수민, 손승우 [1], 강병남
*Soo Min. Oh, Seung-Woo. Son[1], Byungnam. KAHNG
서울대학교. [1] *한양대학교 ERICA.*

Keyword : Explosive percolation, growing networks, Achlioptas process, phase transition

We study the percolation transition properties of growing and static networks under an Achlioptas-like process. In our growing networks model, a node is added in the network every time step and randomly m candidate nodes are chosen, which is not connected yet each other. After comparing the sizes of m clusters containing each candidate node, the two smallest clusters are selected. The two candidate nodes which belong to the selected clusters are connected with probability δ. And In our static networks model, the rule is same with growing case except for δ = 1 and nodes are not added. For m = 3, we found the rate equation of size distributions. And Using this rate equation and finite-size scaling, we extensively investigate the transition point δ_c and the critical exponent β,γ,τ,σ. We found that the percolation phase transitions are continuous with reference to whether there are growing networks or static networks for m = 3. And we expand this model for general m. For various m, we found that the percolation phase transitions are also continuous, but the scaling functions change. Using finite-size scaling and numerical analysis, we extensively investigate the transition point δ_c and the critical exponent β. Interestingly, 1-δ_c and β decay as power of m contrary to the exponential decay of static explosive percolation. And we investigate differences between infinite-order transitions and 2nd-order transitions analyzing the size distribution.

A15.01(초)

Overview of experimental systems in RISP

*권영관
*Young Kwan. Kwon
기초과학연구원.

Keyword : RISP, 희귀동위원소빔, 핵과학실험장치, 응용과학실험장치

현재 중이온가속기건설구축사업단 (RISP)에서는 안정동위원소빔과 희귀동위원소빔을 활용한 핵과학 및 응용과학 분야의 다양한 실험장치 개발을 진행 중이다. 본 발표에서는 해당 실험장치들에서 수행될 연구내용 및 개발 현황과 향후 계획 등을 소개할 예정이다.

A15.02(초)

중입자가속기(KHIMA) 가속기 시스템

*안동현, 임희중, 박차원, 한가람
*An Dong Hyun. , Yim Hee Joong. , Cha Won. Park, Hahn Garam.
한국원자력의학원.

Keyword : carbon, cancer, synchrotron, accelerator, KHIMA

한국원자력의학원(KIRAMS)은 암 치료를 위한 싱크로트론 기반 가속기 시스템을 개발 중에 있다. 본 발표에서는 암 치료를 위한 임상 요구조건을 기반으로 계산된 탄소 빔 사양과 탄소 6 가 이온을 최대 430 MeV/u 까지 가속시킬 수 있는 싱크로트론을 기반으로 한 의료용중입자가속기사업단(KHIMA)의 가속기 시스템을 소개하고자 한다.

A15.03(초)

Rare isotope beam production systems using high-power accelerators for RISP

*김종원
*Jong-Won. Kim
기초과학연구원.

Keyword : superconducting linac, heavy ion accelerator, in-flight method, ISOL, proton cyclotron

In the next generation rare isotope beam facilities, high-power accelerators will be used to produce isotope beams for nuclear science and for multidisciplinary applications. For the RISP a superconducting linac will accelerate primary heavy ion beams to produce RI beams using in-flight (IF) method at a maximum power of 400 kW. A large-acceptance fragment separator has been designed and main components prototyped. In addition, a proton cyclotron will be used to bombard a multi-kilowatt beam on a target system made of such as UCx to produce RI beam using the ISOL method. A superconducting linac will be then used to re-accelerate the beam above 10 MeV/u. Now we consider a scheme to accelerate both primary and RI beams from ISOL simultaneously. Electron Beam Ion Source (EBIS) is a key component to charge-breed an isotope beam of interest to a similar charge to mass ratio of the primary beam. The progress in the RI beam production systems will be presented.

A15.04(초)

PLS-II Operations and Improvements towards More Reliable User Facility

*신승환, 이태연, 박종도, 김경렬
*Seunghwan. Shin, Tae-Yeon. LEE, Chong Do. PARK, Kyung Ryul. KIM
포항가속기연구소.

Keyword : PLS-II, 탑업운전, 광자빔, 삽입장치, 시분해 실험

3 년 기간의 업그레이드를 통해 현재 PLS-II 는 성공적으로 운전중에 있다. PLS-II 의 주요 목표인 400 mA 탑업 운전을 성공적으로 수행하고 있으며 96 % 이상의 높은 빔제공율 달성하고 있다. 하지만, 좀 더 높은 이용자의 요구사항을 충족시키기 위해서는 계속된 성능 개선 연구가 진행되고 있는데 광자빔의 안정화, 삽입장치 운전의 최적화, 시분해 실험 (time resolved experiment)을 위한 운전모드 구축등이 주 연구 내용을 이룬다. 본 발표에서는 현재 PLS-II 운전의 상황을 기술하고 진행중인 개선 연구 내용을 소개할 예정이다.

B1.01(초)

Spontaneous instabilities in (anti)ferroelectrics of ABO3 perovskite structure: a case for $BaTiO_3$, $PbZrO_3$ and $PbHfO_3$

*Krystian Roleder
*Krystian. Roleder
University of Silesia ul.

Keyword : antiferroelectrics, lattice instabilities, phase transitions, local symmetry breaking, latent heat

It might be said that it would not be so intensive investigations of antiferroelectric materials if not reports on non-classical physical properties of the paraelectric phase in BaTiO3 and SrTiO3 [1-3]. It was connected with a discrepancy of the optical, dielectric, electrostrictive and piezoelectric properties, and Brillouin light scattering, from those expected for centrosymmetric paraelectric phase. Origin of this discrepancy was theoretically accounted for strong anharmonic interaction between the optical and acoustic phonons [4]. This interaction, which is caused mainly by high anisotropic polarity of oxygen ions, may break local symmetry and as a consequence leads to appearance of stable non-centrosymmetric nano-/microregions above Tc.

Similar behaviour has been found in antiferroelectrics PbZrO3 and PbHfO3 single crystals, although structural order of nano-/microregions regions with broken symmetry above Tc have not been revealed yet. I believe that based on recently performed precise observation of temperature changes at phase transitions, and also changes of permittivity and pyroelectric signals detected, its polar character - for the first time - has been proved. In the case of lead zirconate it will be shown that above Tc there is a temperature TBH = 292°C, from which fluctuations of local polarity start appearing approaching Tc from the high temperature side. A possibility of another transition at T*=265°C - i.e. inside temperature region (Tc - TBH) - to a phase of permanent polar regions existence, will be proposed and discussed.
It will also be mentioned that except very attractive, although quite complex physics of antiferroelectric phase transition, one can think of their practical application. It has been revealed that boundary between antiferroelectric domains may have ferroelectric properties [5]. Such boundaries of width of a few nanometers could be considered as a candidate for another, even more dense than todays', electronic memories.

Finally it is worth mentioning that phenomenon of local breaking symmetry above Tc have been proved to exist in the micro and nano-scale through the neutron diffuse scattering [6]. Thus, in my opinion, this breaking symmetry effect is a result of spontaneous lattice instabilities due to anharmonic interaction between optical and acoustic phonons above Tc, and not induced by defects.

References

[1] A. Ziębińska, D. Rytz, K. Szot, M. Górny, K. Roleder, J. Phys.: Condensed Matter, 20 (2008) 142202
[2] J.-H. Ko, S. Kojima, T.-Y. Koo, J.H. Jung, C.J. Won, N.J. Hur, Appl. Phys. Lett. 93 (2008) 102905
[3] K. Roleder, A. Bussmann-Holder, M. Górny, K. Szot, A.M. Glazer, Phase Transition 85 (2014) 939–948
[4] A. Bussmann-Holder, J-H. Ko, A. Majchrowski, M. Górny, K. Roleder, J. Phys.: Condens. Matter 25 (2013) 212202
[5] X.-K. Wei, A. K. Tagantsev, A. Kvasov, K. Roleder, Ch.-L. Jia, N. Setter, Nature Communications, 5 (2014) 3031 DOI: 10.1038/ncomms4031
[6] N. Zhang, M. Paściak, A. M. Glazer, J. Hlinka, M. Gutmann, H. Sparkes, T. R. Welberry, A. Majchrowski, K. Roleder, Y. Xie and Z-G. Ye. Submitted to J. Appl. Cryst. (2015)

B1.02(초)

New aspects unearthed from the temperature-dependent dielectric relaxations of relaxor PLZT

*Wook Jo
*Wook. Jo
울산과학기술대학교(유니스트).

Keyword : dielectric permittivity, relaxor ferroelectrics, PLZT

Frequency-dispersive dielectric responses of relaxor ferroelectrics have been of a great interest to the community largely due to the obscurity of the origin of such relaxational behavior. One of the most well-accepted is the random-field model that explains why and how relaxor properties arise satisfactorily though qualitatively. This means that no known model has successfully explained the relaxor properties quantitatively yet. As an attempt to develop such model, we investigated the Frequency-dependent dielectric spectra of a relaxor $Pb_{0.92}La_{0.08}(Zr_{0.65}Ti_{0.35})_{0.98}O_3$ (PLZT 8/65/35) at various temperatures ranging from 0 ^oC to 100 ^oC and analyzed them by a multiple relaxation process model. We identified that the overall permittivity spectra are a consequence of a convolution of three distinct relaxation processes, featuring different relaxation time and distribution as well as the symmetry in the distribution function. By extracting the contribution of each process to the permittivity at different temperatures and comparing the results with ε(T) plot, the overall permittivity of ε(T) can be deconvoluted into three non-relaxor components. The characteristics of the relaxor behavior such as frequency dispersion of the dielectric maxima, the disparity in peak positions of real and imaginary parts, and the unique feature during aging are explained by this model.

B1.03(초)

Large electric field induced strain of lead-free $Bi_{0.5}(Na,K)_{0.5}TiO_3$–based Actuators

*김일원, 안창원, 최시영 [1], 최강호, 이대수 [2], 정순종 [2], 장기봉 [3], 이재신
*ILL WON. Kim, Changwon. Ahn, Si Young. Choi[1], Gang ho. Choi, Dae Su. Lee[2], Soon Jong. Jeong[2], Ki Bong. Jang[3], Jae-Shin. Lee
울산대학교. [1] 한국기계연구원부설 재료연구소. [2] 한국전기연구원. [3](주) 삼전.

Keyword : Lead-free, Texture, Strain, Actuator, $Bi_{0.5}Na_{0.5}TiO$

Lead-free piezoelectric ceramics exhibited superior electromechanical responses near the morphotropic phase boundary (MPB). Among the lead-free piezoelectric ceramics so far developed, the binary $(1-x)Bi_{0.5}Na_{0.5}TiO_3$ - $xBi_{0.5}K_{0.5}TiO_3$ class of materials has received considerable attention due to its excellent ferroelectric and piezoelectric properties near the rhombohedral-tetragonal morphotropic phase boundary. Recently, a large electric field induced strain has been reported in $BiAlO_3$-modified $Bi_{0.5}(Na_{0.78}K_{0.22})_{0.5}TiO_3$ lead-free piezoceramics. However, the applied electric field (60kV/cm) for the observed large strain is also high, limiting its applications in actuator devices. On the other hand, it is widely known that textured ceramics showed enhanced piezoelectric properties.

In this work, textured $(1-x)(Bi_{0.5}(Na_{0.78}K_{0.22})_{0.5}TiO_3)$-$xBiAlO_3$ (BNKT-BA-x ; x = 0, 0.015) ceramics were fabricated by templated grain growth (TGG) method using plate-like $Na_{0.5}Bi_{4.5}Ti_4O_{15}$ (NBiT) templates with the viewpoint of improving the strain response and reducing the driving electric field. X-ray diffraction analysis shows pure perovskite phase with tetragonal symmetry. Moreover, it was found that, the textured ceramics show high orientation factor (lotgering's factor) > 90%. The textured BNKT-BA-0.015 ceramics exhibited large strain (S = 0.55%) at applied electric field of 40 kV/cm, which corresponds to a normalized strain (S_{max}/E_{max}) of ~1370 pm/V. Furthermore, the strain value is fairly temperature stable up to 110 ^oC, which is highly promising for actuator applications. In addition, we studied why occur the large strain for the stack actuators made by textured $Bi_{0.5}(Na,K)_{0.5}TiO_3$–based ceramics.

B1.04(초)

High-Performance Lead-Free Piezoceramics with High Curie Temperatures

*송태권, 이명환, 박진수, 김다정, 김명호
*Tae Kwon. SONG, Myanghwan. Lee, Jinsu. Park, DA JEONG. KIM, Myong Ho. Kim
창원대학교.

Keyword : Piezoelectric, Lead-free, Ceramic, Curie Temperature, Quenching

Lead-free piezoelectric materials have been studied to replace the commonly used lead zirconate titanate (PZT) because of environmental and health issues. Piezoelectric properties are usually inversely proportional to the phase transition Curie temperature (T_C), but PZT is an exception that has good piezoelectric properties with a high T_C. Here we show that a bismuth ferrite (BF) and barium titanate (BT) solid solution system can achieve good piezoelectric properties with a high T_C when fabricated with low-temperature sintering followed by a water-quenching process, with no complicated grain alignment processes performed. By adding the super-tetragonal compound of bismuth gallium oxide, the piezoelectric properties were equal to that of PZT ceramics and exhibited good long-term reliabilities.

B2.01

Abnormal electrical property of graphene on hBN-ferroelectric substrate

*강해용, 박나희, 박정민, 이유락, 윤유주, 이정호 [1], 이상구 [1], 이영희, 서동석
*Hae yong. Kang, Na Hee. Park, Jeongmin. Park, You Rack. Lee, Yang Hee. Yun, Jeong-Ho. Lee[1], Sang-Goo. Lee[1], Young Hee. LEE, Dongseok. Suh
성균관대학교. [1] 아이블포토닉스.

Keyword : graphene, ferroelectric, antihysteresis, charge trap, field effect transistor

To examine the effect of a ferroelectric polarization field on the charge transport in a two-dimensional (2D) material, a graphene monolayer on a hexagonal boron nitride (hBN) field-effect transistor (FET) was fabricated using a ferroelectric single-crystal substrate, (1-x)[$Pb(Mg_{1/3}Nb_{2/3})O_3$]-x[$PbTiO_3$] (PMN-PT). In this configuration, graphene conductance showed several abnormal behaviors with the help of hBN-protection. As gate-voltage swept a wider range, the overall I_D-V_G curves changed from normal to antihysteresis, which is opposite to what would be expected in normal ferroelectric switching. In addition, a hump-like increase of channel conductance occurred at the gate voltage corresponding to the ferroelectric switching and wide conductance saturation was shown in the positive gate voltage region. We developed a model to interpret the complex behaviors in relation with the ferroelectric switching and the polarization-assisted charge trapping, which can be generalized to explain the combination of 2D structured materials with ferroelectrics.

B2.02*

Causality of the Aharonov-Bohm effect and the gauge dependence

*김갑현, 강기천
*Gabhyun. Kim, Kicheon. KANG
전남대학교.

Keyword : Aharonov-Bohm effect, Causality, Lorentz gauge, gauge dependence

We investigate the causality in the Aharonov-Bohm (AB) effect. For this purpose, we consider a switching of the localized magnetic flux and its influence on the interference of a test charge (see the figure). The AB phase shift is analyzed for various spacetime separation between the flux and the charge. Naturally, we find that there is no violation of the causality, but that the interpretation of the result depends on the choice of gauge. In the Coulomb gauge, there appears space-like separated nonlocal interaction between the charge and the flux, but this interaction has no physical effect. In the Lorentz gauge, in contrast, there is no space-like separated interaction. Our discussion is closely related to the question on the locality/nonlocality of the Aharonov-Bohm-Casher effect [1].

Reference :
[1] K. Kang, "Aharonov-Bohm effect, local field interaction, and Lorentz invariance." arXiv:1308.2093 (2013); K. Kang, "Locality of the Aharonov-Bohm-Casher effect." Phys. Rev. A 91 052116 (2015).

B2.05*

Valley-symmetry-conserved quasi-one-dimensional ballistic transport in high-mobility graphene

*김민수, Kenji Watanabe[1], Takashi Taniguchi[1], 이후종
*Minsoo. Kim, Kenji. Watanabe[1], Takashi. Taniguchi[1], Hu-Jong. Lee
포항공과대학교. [1]NIMS.

Keyword : graphene, valleytronics, ballistic quasi-1D transport

One-dimensional (1D) graphene system, so-called graphene nanoribbons, with zigzag edges is predicted to exhibit interesting electronic properties stemming from its Dirac band structure. However, to date, investigation of the properties is highly limited because of the defects and the roughness at the edges, which mix valleys of graphene. Recent progress in preparing a high-quality graphene layer enables one to investigate the intrinsic carrier transport nature in the material. Here, we report the signature of conservation of the Berry's phase with preserved valley symmetry in two types of quasi-1D ballistic transport devices; one is a quantum point contact (QPC) and the other is an Aharonov-Bohm (AB) interferometer. Devices were fabricated on monolayer graphene with high carrier mobility, where the graphene was encapsulated between two thin hexagonal boron nitride (h-BN) layers. In measurements, charge carriers were confined in a potential well formed by the dual operation of the bottom and top gates and the four-terminal magneto-conductance (MC) was measured with varying charge carrier density, dc bias, and temperature. Graphene in the device was truly in the ballistic regime, exhibiting the conductance quantization in regular steps of $\Delta G = 4e^2/h$ starting from G = (2, 6), 10 × e^2/h in a constricted conducting channel of QPC-type devices. In AB interferometry, we observed h/e periodic modulation of MC and the zero-field conductance minimum with a negative MC background. All these results strongly suggest that carriers flowing qausi-1D channels built in our devices preserve the intrinsic Dirac transport nature, which would be conveniently utilized for valleytronics in graphene.

B2.06

Very Strong Josephson Coupling in PbS Nanowire Superconducting Junctions

*김범규, 김홍석, Yiming Yang[1], Xingyue Peng[1], Dong Yu[1], 도용주
*Bum kyu. Kim, Hong Seok. Kim, Yiming. Yang[1], Xingyue. Peng[1], Dong. Yu[1], Yong-Joo. Doh
고려대학교(세종). [1]University of California. Davis. CA 95616. USA.

Keyword : "PbS nanowire, Josephson junction, switching current distribution"

We report on the fabrication and electrical transport of the nano-hybrid Josephson junctions of PbS nanowires contacted with superconducting PbIn electrodes. The PbS nanowire-based Josephson junctions are fabricated by using conventional e-beam lithography and e-beam evaporation processes. At low temperatures below 7 K, the PbIn electrode becomes superconducting, which induces the superconducting proximity effect in the nanowire. We have observed the Josephson supercurrent up to a ten micro-Ampere at T_{base} = 300 mK, corresponding to the I_cR_n ~ 0.8 meV. From the subgap conductance structure, superconductor gap Δ_{PbIn} is estimated to be 0.8 meV. Switching current distribution is measured with varying temperature and magnetic field. As increasing temperature, the switching process shows transition behavior from thermal activation to phase diffusion regions. Also we are observation of monotonous decreased supercurrent with applied magnetic field, which is explained by magnetic pair-breaking effect in the narrow Josephson junction. Under the irradiation of an external microwave frequency (f_{mw}), the current vs. voltage characteristic curves display quantized voltage steps (so-called Shapiro steps) occurring at $V_n = nhf_{mw}/2e$. It is expected that the nano-hybrid Josephson junctions of PbS nanowires, exhibiting very strong Josephson coupling strength even at high temperature near liquid helium temperature, can be a promising building block to develop nanowire-based superconducting information devices.

B2.07*

Gate-tunable Superconducting Quantum Interference Devices of PbS Semiconductor Nanowires

*김홍석, 김범규, Yiming Yang[1], Xingyue Peng[1], Dong Yu[1], 도용주
*Hong-Seok. Kim, Bum kyu. Kim, Yiming. Yang[1], Xingyue. Peng[1], Dong. Yu[1], Yong-Joo. Doh
고려대학교(세종). [1]University of California. Davis.

Keyword : "superconducting quantum interference device (SQUID)", "PbS nanowire", "Josephson junction"

A superconducting quantum interference device (SQUID) is based on a superconducting loop including two Josephson junctions. We report on the fabrication and electrical transport properties of nano-hybrid dc SQUID devices, made of PbS nanowire contacted with three PbIn superconducting electrodes forming a supercurrent loop. The PbS nanowires with 100-nm diameter were synthesized via a chemical-vapor-deposition method. The devices have been fabricated by using the conventional e-beam lithography and subsequent e-beam evaporation of PbIn. The proximity effect is established through the PbS NW below the transition temperature of PbIn electrodes (T_c~7 K). At T = 2.8 K, the current versus voltage curve shows the Josephson supercurrent. When the magnetic field is applied perpendicular to the plane of the nanowire SQUID, clear Φ_0 periodic voltage and critical current oscillations are observed for devices with different flux area, where $\Phi_0 = h/2e$ is the magnetic flux quantum. We also observed the gate-tunable magnetic field modulation of the critical current at T = 0.3 K.

B3.01(초)

Creating lateral electronic interfaces in 2D materials with strong interactions; $IrTe_2$ and 1T-TaS_2

*염한웅
*Han Woong. Yeom
기초과학연구원.

Keyword : 2D materials, superconductivity, charge order, $IrTe_2$, 1T-TaS_2

$IrTe_2$ and 1T-TaS_2 exhibit intriguing charge ordered states together with strong spin-orbit interaction and electron Coulomb interaction, respectively. When doped, these materials fall into superconducting states with the charge orders suppressed. The nature of the superconducting states and their competition with charge orders are poorly understood. In our own project, we aim to clarify (i) the charge ordering nature of these quasi 2D systems and (ii) the competition of their charge orders with the superconductivity through high resolution and low temperature scanning tunneling microscopy/spectroscopy (STM/STS). In particular, we aim to observe or create laterally inhomogeneous domain structures of different charge orders with superconductivity to directly probe their competition with STM. Firstly, we characterize the various stripe charge order states of $IrTe_2$ in terms of the real-space structural and LDOS modulations [1, 2] and identify for the first time the coexisting hexagonal charge order state [3]. This newly found charge order state falls very intriguingly into a superconducting state below 3 K, creating lateral interfaces of the stripe charge order and the superconductivity [3]. These results both cast important open questions and provide an important physics platform. Secondly, we discuss the commensurate charge density wave (CDW) state of 1T-TaS_2, which has the Mott-Hubbard band gap [4]. For a superconducting state, this Mott-CDW state has to be broken into a metallic nearly-commensurate (NC) CDW state. We characterize this NC-CDW with unprecedented spatial and spectroscopic resolution and clarify the origin of the metallization as the Mott criticality [5]. In addition, we succeed in creating the lateral interfaces of the Mott-CDW state and the metallic phase. This result bears important implication for the superconducting state of this system, on which our own experiment is on going. Finally, borrowing this occasion, we would like to introduce the up-scaled ultra low temperature STM under construction, which can reach below 10 mK with vector magnetic field of 9-2-2 Tesla. When the construction is finished in early 2016, this instrument would become one of the most powerful STM on earth to serve for the Korea condensed matter physics community widely.

[1] Hyo Sung Kim et al., Phys. Rev. B 90, 201103(R) (2014).
[2] K.-T. Ko et al., Nature Communication 6, 7342 (2015).
[2] Hyo Sung Kim et al. to be submitted.
[3] Do-Hee Cho et al., Phys. Rev. B 92, 085132 (2015).
[4] Do-Hee Cho et al., Nature Communication, under review.

B3.02*

Topological edge states of MoS_2 : A first-principles study

*성하준, 최덕현, 장기주
*Ha Jun. Sung, Duk-Hyun. Choe, Kee Joo. Chang
KAIST.

Keyword : "Transition metal dichalcogenides". "Topological edge states", "Topological Insulators",

Layered transition metal dichalcogenides MX_2 (M = W, Mo and X = S, Se, Te) have attracted much attention owing to their diverse electronic properties depending on their polytypic structures such as 2H, 1T, and 1T'. The 2H phase is a semiconducting phase, while 1T phase is metallic. Interestingly, 1T'-MX_2 has been recently proposed to be two-dimensional (2D) topological insulators (TIs), non-trivial phase of quantum matter that exhibits unusual edge states. Spontaneous symmetry breaking of metallic 1T phase induces a distorted 1T' phase, while spin-orbit coupling (SOC) opens a non-trivial energy gap in 1T'-MX_2. Although the structural and electronic properties of 1T'-MX_2 in 2D form are well studied, the topological edge states of quasi-one-dimensional (Q1D) structures are poorly understood.

Based on first-principles density functional calculations, we investigate the electronic properties of Q1D 1T'-MoS_2 nanoribbons. In order to study the topological edge states of 1T'-MoS_2, we passivate the edge dangling bonds by hydrogen. We find that the topological edge states are formed around the center of Brillouin zone, exhibiting a single Dirac point. We discuss interactions between the bulk and edge states in 1T'-MoS_2 nanoribbons.

B3.03*

Manipulation of magnetic state in armchair black phosphorene nanoribbon by charge doping

*파루크우마, 칸임란, Hashmi arqum, 홍지상
*Farooq. Umar, Imran. Khan, Hashmi. Arqum, Jisang. Hong
부경대학교.

Keyword : phosphorene

Using the first principles studies, we investigated the width dependent magnetic properties of armchair black phosphorene nanoribbons (APNRs) by controlling the electron charge doping. In the unrelaxed APNRs the antiferromagnetic coupling between two phosphorus atoms in the same edge was found. However, the edge magnetic moment vanished after structure relaxation, and all the APNRs showed a semiconducting feature. Interestingly, the charge doping substantially altered the band structures of the APNRs because the metallic states reappeared in the charge doped APNRs. Besides, the magnetic moment was found in the charge doped systems. We found that the Stoner condition could nicely explain the magnetic moment at the edge atoms. Moreover, we propose that that the edge-to-edge magnetic coupling can be manipulated by charge doping because the transition from antiferromagnetic to ferromagnetic state was achieved. Our findings may bring interesting issues for spintronics applications. This research was supported by Basic Science Research Program through the National Research Foundation of Korea (NRF) funded by the Ministry of Education, Science and Technology (No. 2013R1A1A2006071) and by the Supercomputing Center/Korea Institute of Science and Technology Information with supercomputing resources including technical support (KSC-2015-C3-021).

B3.04

Reversible metal-insulator transition in the charge-ordered Mott insulator 1T-TaS_2

*조두희, 천상모, 김기석 [1], 이성훈, 조용흠 [1], 정상욱 [2], 염한웅
*Doohee. Cho, Sangmo. Cheon, Ki Seok. Kim[1], Sung Hoon. LEE, Yong-Heum. Cho[1], Sang-Wook. Cheong[2], Han Woong. Yeom
IBS (POSTECH). [1]POSTECH. [2]Rutgers University.

Keyword : 1T-TaS2, Mott insulator, Phase manipulation, Scanning tunneling microscopy

The phase manipulations has been a perennial issue in low dimensional correlated electron systems. Recently, it has been realized through various external tuning parameters, such as pressure, chemical doping, and optical pumping. Here, we demonstrate the controllability of a reversible metal-insulator transition in the charge-ordered Mott insulator 1T-TaS_2 using a scanning tunneling microscope. The metallic textured charge order state is locally generated by applying voltage pulses and coexists with the insulating domain. Our spatially resolved scanning tunneling spectroscopy results reveal the mechanism of the metallization as bandwidth controlling driven by melting the charge order. This work provides a promising pathway for realizing electronic devices based on correlated electrons.

B5.01(초)

Spin Dynamics of Chiral Spin Structures due to Spin Orbit Torques

*Mathias Kläui
*Mathias. Kläui
Johannes Gutenberg-Universität Mainz.

Keyword : he Dzyaloshinskii-Moriya interaction (DMI), Skyrmion, Spin-orbit torque

Topological spin structures that emerge due to the Dzyaloshinskii-Moriya interaction (DMI), such as chiral domain walls and skyrmions possess a high stability and are of key importance for magnetic memories and logic devices.
We have investigated in detail the dynamics of domain walls [1] and we find that in addition to conventional spin transfer torque, also spin orbit torques play a key role [2]. By comparing the wall motion with current-induced magnetization switching in our systems, we can deduce the spin-orbit torques independently of the DMI [2] and we find that the motion observed Ta(5nm)/Co20Fe60B20(1nm)/MgO(2nm) can be attributed to a DMI that is opposite to such stacks with a magnetic CoFe layer pointing to the B at the interface that governs the sign of the DMI [2].
For skyrmions we demonstrate for the first time that we can move a train of skyrmions in a “racetrack”-type device due to spin-orbit torques reliably [3] and we find skyrmion lattices at room temperature in confined geometries [3].
[1] O. Boulle et al., Mater.Sci Eng R 72, 159 (2011).
[2] R. Lo Conte et al.; Appl.Phys.Lett. 105, 122404 (2014); R. Lo Conte et al.; Phys.Rev B 91, 014433 (2015)
[3] S. Woo et al., arxiv:1502.07376 (2015)

B5.02(초)

Current-induced dynamics of antiferromagnetic domain wall in antiferromagnet/heavy metal bilayers

Takayuki Shiino, 오세혁 [1], 박병국, *이경진 [1]
Takayuki. Shiino, Se-Hyoek. Oh[1], Byong-Guk. Park, *Kyung-Jin. Lee[1]
KAIST. [1]Korea University.

Keyword : domain wall, antiferromagnet, spin-orbit torque

Antiferromagnetic spintronics is attracting considerable interest nowadays as the antiferromagnet is immune to external magnetic fields [1] and compatible with metal or semiconductor electronic structure [2]. To be used as functional devices, one has to find an efficient driving force to manipulate antiferromagnet spins. The effect of spin transfer torque (STT) on antiferromagnetic spins has been identified [3]. Recently, Hals et al. [4] reported a theory of STT-induced dynamics of antiferromagnetic domain wall (AF-DW) and found that the DW velocity is proportional to the ratio between the dissipative torque and the damping, as for ferromagnet (FM) DWs.
In this talk, we report theoretical and numerical results of current-induced AF-DW motion in antiferromagnet/heavy metal bilayers where the injection of in-plane current generates spin-orbit torque (SOT) as well as conventional STT (i.e. adiabatic and nonadiabatic STTs). Based on the nonlinear sigma model for the Néel vector [5], we derive analytical solution of steady-state domain wall velocity. We also perform numerical computation based on atomistic spin model [6]. We find that the DW velocity v_{DW} increases rapidly for a sign of the spin Hall angle q_{SH} (or current direction equivalently). This rapid increase of v_{DW} assisted by SOT is similar to the case of FM-DW [7] but an important difference is also observed; a current range for very high v_{DW} is quite narrow for FM-DW due to the Walker breakdown [7], whereas such a very high v_{DW} is obtained for the current above a certain threshold for AF-DW because the Walker breakdown of AF-DW occurs at a much higher current density (> 10^9 A/cm^2). We also observe a large deviation between analytic solution and modeling results at high current regime, caused by the breakdown of continuum approximation used for the nonlinear sigma model.

[1] X. Martí, I. Fina, and T. Jungwirth, IEEE Trans. Magn. 51, 1 (2015).
[2] T. Jungwirth et al., Phys. Rev. B 81, 212409 (2008); P. Wadley et al., Nat. Commun. 10, 347 (2011).
[3] A. S. Núñez, R. A. Duine, P. Haney, and A. H. MacDonald, Phys. Rev. B 73, 214426 (2006); Z. Wei et al., Phys. Rev. Lett. 98, 116603 (2007); S. Urazhdin and N. Anthony, Phys. Rev. Lett. 99, 046602 (2007); P. M. Haney and A. H. MacDonald, Phys. Rev. Lett. 100, 196801 (2008).
[4] K. M. D. Hals, Y. Tserkovnyak, and A. Brataas, Phys. Rev. Lett. 106, 107206 (2011).
[5] A. C. Swaving and R. A. Duine, Phys. Rev. B 83, 054428 (2011).
[6] R. F. L. Evans et al., J. Phys.: Condens. Matter 26, 103202 (2014).
[7] S.-M. Seo, K.-W. Kim, J. Ryu, H.-W. Lee, and K.-J. Lee, Appl. Phys. Lett. 101, 022405 (2012).

B5.03(초)

Relativistic spin-orbit torques in ferromagnets and anti-ferromagnets

*J. Sinova
*J.. Sinova
Johannes Gutenberg-Universität Mainz.

Keyword : Relativistic spin-orbit coupling, spin-current

Understanding the origin and properties of the different phases of materials and how to control them is at the heart of condensed matter physics and physics in general. One of the grand challenges of the field is to control spin-dependent properties without using magnetic fields. To do so, one must resort to the relativistic nature of electrons, which arises directly from its particle-antiparticle description that gives its spin. In the relatively slow world of solids this leads to the spin-orbit coupling (SOC) that connects the spin and charge of the electron. We have learned how to exploit the relativistic SOC to create new paradigms of spin control in complex materials and discover new unexpected connections between seemingly disparate ideas as topology, materials science, high energy physics, ferromagnetism, thermoelectricity, and current-induced magnetization manipulation. I will broadly describe joint theoretical and experimental efforts on how we now generate and manipulate spin-currents that are being used in devices relevant for future MRAM technology. I will also show in some detail how insights on the spin Hall effect have yielded novel ways to manipulate magnetization using relativistic torques, and how to extend these ideas to a new a phase of spintronics by exploiting anti-ferromagnetic materials in an active way.

B5.04(초)

Magnetic skyrmions and their current-driven dynamics at room temperature

*우성훈
*Seonghoon. Woo
한국과학기술연구원.

Keyword : Magnetic Skyrmion, Chiral Magnetism, Dzyalloshinski-Moriya Interaction

Magnetic skyrmions are topologically-protected spin textures that exhibit fascinating physical behaviors[1–2] and large potential in highly energy efficient spintronic device applications[3,4]. The main obstacles so far are that skyrmions have been observed in only a few exotic materials and at low temperatures[1–4], and fast current-driven motion of individual skyrmions has not yet been achieved. Here, we report the observation of stable magnetic skyrmions at room temperature in ultrathin transition metal ferromagnets with magnetic transmission soft x-ray microscopy. We demonstrate the ability to generate stable skyrmion lattices and drive trains of individual skyrmions by short current pulses along a magnetic racetrack at speeds approaching 50 m/s as required for applications. Our findings provide experimental evidence of recent predictions[5-6] and open the door to room-temperature skyrmion spintronics in robust thin-film heterostructures.

1. Rößler, U. K. et al., Nature 442, 797–801 (2006).
2. Mühlbauer, S. et al., Science 323, 915–919 (2009).
3. Jonietz, F. et al., Science 330, 1648–1651 (2010).
4. Schulz, T. et al., Nat. Phys. 8, 301–304 (2012).
5. Iwasaki, J. et al.,. Nat. Commun. 4, 1463 (2013).
6. Fert, A. et al., Nat. Nanotechnol. 8, 152–156 (2013).

B7.01*

근자외선에 민감한 그래핀/다공성 실리콘 광검출기의 제작 및 특성

김정길, 김주환, 이대훈, 김성, *최석호
Jungkil. Kim, Ju Hwan. Kim, Dae Hun. Lee, Sung. Kim, *CHOI Suk-Ho.
경희대학교.

Keyword : 그래핀, 다공성 실리콘, 광검출기, 다공성도, 근자외선

본 연구에서는 그래핀과 다공성 실리콘을 각각 전하운반자 수집층 및 발생층으로 이용하여 그래핀/다공성 실리콘 광검출기를 제작하고 그 특성을 분석하여 다공성 실리콘의 넓은 띠간격 에너지를 장점으로 하여 근자외선에서 민감한 광검출기를 구현하였다. 또한 그래핀의 높은 전하운반자 이동도에 의하여 그래핀/다공성 실리콘 광검출기가 기존의 그래핀/실리콘 광검출기보다 상대적으로 빠른 마이크로초의 반응속도를 보였다. 광검출기의 성능은 다공성 실리콘의 다공성도를 조절하여 체계적으로 분석함으로써 최적화하였다. 다공성도는 광검출기의 암전류 및 광전류의 가장 중요한 인자로서 광반응도, 광반응도 스펙트럼의 최고점에너지, 양자효율, 및 시분해 광전류에 큰 영향을 미쳤다. 그래핀/다공성 실리콘 광검출기는 기존의 그래핀/실리콘 광검출기에 비해 근자외선에서 향상된 광반응도를 보였다. 본 발표에서는 이러한 그래핀/다공성 실리콘 광검출기의 구동 메커니즘에 기반하여 그 특성을 자세히 분석한다.

B7.02*

First-Principle Study on Valley Convergence in MoS_2 and Its Thermoelectric Properties

*홍지숙, 이창훈, 박진성 [1], 심지훈
*Jisook. Hong, Changhoon. Lee, Jin-Seong. Park[1], Ji Hoon. Shim
포항공과대학교. [1] 한양대학교.

Keyword : Density functional theory, Thermoelectric, Molydisulfide

Various physical properties depending on the thickness of MoS_2 have been in spotlight in the field of nanoelectronics, spintronics, and newly arising valleytronics. MoS_2 also has been studied as a candidate for good thermoelectric material because of its high Seebeck coefficient. Because it is essential to enhance the electrical conductivity of MoS_2 for thermoelectric application, the band gap engineering has been suggested by using the control of layer thickness, pressure, and layer mixing. [1-5]
In this study, we have investigated the control of valley degeneracy in MoS_2 and its effect on thermoelectric properties by using ab-initio calculation. By modulating the layer thickness and external electric field, the valence band maximum (VBM) at Γ and K points and the conduction band minimum (CBM) at K and Σ_{min} points are differently shifted. The valley degeneracy of VBM is observed in MoS_2 monolayer, while that of CBM in MoS_2 monolayer under the external electric field. By tuning the valley degeneracy, the Seebeck coefficient and electrical conductivity can be separately controlled, and the maximum power factor can be obtained in n-type (p-type) MoS_2 monolayer with (without) the external electric field. We suggest that the transition metal dichalcogenides are good example to investigate the role of valley degeneracy in the thermoelectric properties with the control of interlayer interaction and external electric field strength.

[1] H. Guo, T. Yang, P. Tao, Y. Wang, and Z. Zhang, J. Appl. Phys. 113, 013709 (2013).
[2] C. Lee, J. Hong, M.-H. Whangbo, and J. H. Shim, Chem. Mater. 25, 3745 (2013).
[3] C. Lee, J. Hong, W. R. Lee, D. Y. Kim, and J. H. Shim, J. Solid State Chem. 211, 113 (2014).
[4] D. Wickramaratne, F. Zahid, and R. K. Lake, J. Chem. Phys. 140, 124710 (2014).
[5] W. Huang, X. Luo, C. K. Gan, S. Y. Quek, and G. Liang, Phys. Chem. Chem. Phys. 16, 10866 (2014).

B7.03*

Localised state and optical Aharonov-Bohm oscillations of a quatum ring on top of droplet quantum dot

*박성호, 김광석, Takayuki[1], Akihiro Murayama[1], Kyhm Jihoon[2], Song Jindong[2], Robert Taylor[3], Marek Potemski[4]
*Seong ho. Park, kwangseuk. kyhm, Takayuki. Kiba[1], Akihiro. Murayama[1], Jihoon. Kyhm[2], Jindong. Song[2], Robert. Taylor[3], Marek. Potemski[4]
부산대학교. [1]Hokkaido University. [2]KIST. [3]University of Oxford. [4]CNRS-UJF-UPS-INSA.

Keyword : Localization, Droplet Epitaxy, Quantum Dot, Optical Aharonov-Bohm oscillations, oscillator strength

Currently, droplet quantum dots (QDs) are great interest as its giant oscillator strength may significantly enhance the light-matter coupling in single-photon technology provided that the wavefunction is extended over the large size (~ 100 nm). However, this proposal seems overlook practical huddles. In particular, localization issue can be claimed, which likely arises from disorder effects such as impurity, defect, and structural non-uniformity. So far, no conclusive evidence has been reported to clarify the localized wavefunction despite of various optimistic proposals. In this work, we have performed time-resolved and magnetic dependence of micro-photoluminescence to confirm the presence of localized states in a single droplet quantum dot. The quantum dot-like local structure in a droplet quantum dot (~100 nm) were found to be significantly small (6 ~ 15 nm) in diameter, which were estimated from the size-dependence bi-exciton binding energy and the diamagnetic coefficient of excitons. We also observed optical Aharonov-Bohm oscillations from a local structure, where the diameter (~36 nm) and diamagnetic coefficient (~29 eV/T2) were found to be significantly large compared to quantum dot-like local structures. Those results suggest a quantum ring-like local structure is present on top of a droplet quantum dot.

B7.04

Irradiation effects of AlGaN/GaN HEMT devices

*장영준, 이인학, 김혁진, 오창원, 이철, 윤예슬, 장승엽 [1]
*Young Jun. Chang, In hak. Lee, Hyuck Jin. Kim, Changwon. Oh, Chul. Lee, Yeseul. Yun, Seung Yuo. Jang[1]
서울시립대학교. [1]*LG 전자 연구소.*

Keyword : GaN, HEMT, 2DEG, Proton, Exicmer laser annealing

The AlGaN/GaN HEMTs device grown on Si(111) substrate has been intensively studies for next-generation power transistor, which has better efficiency and higher operation voltage. However, it has natural defects such as dislocation because of the lattice mismatch with Si(111) substrate and reduces the electrical performance of the AlGaN/GaN HEMTs device. To improve performance of the HEMTs device, irradiations, such as excimer laser or high energy proton beam, can be considered for modifying the electrical property of AlGaN/GaN HEMTs device. In this report, we exposed excimer laser pulses or proton (5.2 MeV) beam to figure out the irradiation effects on AlGaN/GaN HEMTs device. Upon irradiation, we found out significant reduction of carrier concentration and mobility, except a case of carrier density enhancement for the medium proton dose. To understand the irradiation effects, we utilized several methods, such as XPS, Raman, and PL.

B7.05*

InAs/InGaAsP 양자점 레이저다이오드의 특성을 Rate-equation 으로 수치해석적으로 분석하여 얻어낸 양자점 에너지 상태 정보

*이종민, 백종서, 장유동, 이동한, 편수현 [1], 정원국 [1], 김정호 [2]
*JongMin. Lee, Jongseo. Baek, Yudong. Jang, Donghan. Lee, Suhyun. Pyun[1], Won-Guk. Jeong[1], Jungho. Kim[2]
충남대학교. [1] 성균관대학교. [2] 경희대학교.

Keyword : 양자점, 레이저다이오드, 반도체광학, 광특성

반도체 양자점은 0 차원적인 구조이기 때문에 에너지 상태가 불연속적이다. 그러나 1.5 um 대역에서 동작하는 InAs/InGaAsP 양자점 레이저다이오드의 경우 주입 전류밀도를 증가시키면 이득 peak 가 단파장쪽으로 연속적으로 이동하는 것을 볼 수 있다. 이는 InAs/InGaAsP 양자점의 바닥상태와 여기상태의 간격이 좁아서 나타나는 것으로 생각할 수 있다. 하지만 1550 nm 대역에서 동작하는 InAs/InGaAsP 양자점의 바닥상태와 여기상태의 간격에 대해 자세히 알려진 것은 없다. 본 연구에서는 InAs/InGaAsP 양자점 레이저다이오드를 제작하고 특성을 살펴보는 것으로 InAs/InGaAsP 양자점의 바닥상태와 여기상태의 에너지 간격에 대해 살펴보았다. 양자점이 여러 주기로 성장되어 있으면 해석에 어려움이 줄 것으로 예상하여 한 주기 양자점 층이 성장된 기판을 사용하여 레이저다이오드를 제작하여 특성을 측정하였다. 하지만 양자점의 바닥상태와 여기상태의 간격이 좁고 inhomogeneous broadening 이 넓기 때문에 측정 결과를 해석하는 것이 쉽지 않다. 그래서 양자점의 inhomogeneous broadening 을 고려하여 rate equation 을 작성하고 이를 통해 측정 결과를 해석하였다. 결과적으로 rate equation 을 사용하여 실험 결과를 잘 설명할 수 있었다. 그림.

그림. 1 주기 InAs/InGaAsP 레이저다이오드의 이득 곡선, (위) 계산 결과 (아래) 측정 결과

B7.06

Effect of Defects and Impurities on the Optical, Electrical, and Valley Properties of Monolayer MoS_2

*김동학, 임대영
*Dong Hak. Kim, Daeyoung. Lim
경희대학교.

Keyword : MoS_2, Vally polarization, chemical doping, vacuum annealing

We studied the effects of chemical doping and vacuum annealing on the optical, electrical and valley properties of monolayer MoS_2. Both the vacuum annealing and $AuCl_3$ chemical doping dramatically increase the photoluminescence (PL) intensity and reduce the valley polarization significantly. The huge PL enhancement after p-type chemical doping can be explained by the suppression of the fast non-radiative trionic decay path in the n-type as-exfoliated MoS_2. However, the PL increase in the vacuum-annealed MoS_2 cannot be attributed to the same trionic mechanism as suggested previously, where it is proposed that vacuum-annealing-induced S-vacancies play the role of p-type dopant. The shift of the threshold voltage of the vacuum-annealed MoS2 FET towards the negative voltage clearly shows that MoS2 becomes more n-type contrary to the previous explanations. The PL enhancement in the vacuum-annealed MoS2 seems to be rather due to the defect-related enhancement of radiative recombination.
A comparison between the PL intensity and the circular polarization reveals that the increased exciton lifetime after chemical doping or vacuum annealing, alone, cannot explain the observed large reduction in the valley polarization. The valley polarization change is also found to be more significant at high temperatures, which excludes the increased intervalley scattering due to the defects or impurities as its origin. A relaxation of valley-contrasting optical selection rule due to the increased disorder - defects or impurities - seems to better explain the reduced valley polarization.

B8.01

Topological susceptibility of QCD at fnite temperature and Axion

*남승일
*Seung-il. NAM
부경대학교.

Keyword : Topological susceptibility, instanton, caloron, thermodynamic potential

In this talk, I study an effective thermodynamic potential for the axion, which is the strong CP-violation agent in SM and one of the plausible candidates for the dark matter in BSM, in the presence of the fermionic degree of freedom, i.e. quarks. The variation of the topological charge and susceptibility are computed within the liquid-instanton model at finite temperature, being modified with the caloron solution. We compare our results with the lattice QCD and effective models.

B8.02*

Radiative decay of pion from the instanton vacuum

*심상인, 김현철
*Sang-In. Shim, Hyun-Chul. Kim
인하대학교.

Keyword : pion, instanton, form factor

We investigate the form factors for radiative decay of pion, based on the gauged low-energy chiral effective action from the instanton vacuum in the large N_c limit. The gauged effective action satisfies U(1) and chiral gauge transformations. We consider vector, axial and tensor form factors for the radiative pion decay. We separate those form factors into local and non-local parts. We first compute the local contribution to the form factors and discuss the results.

B8.03*

Asymmetric Hits from a Large Pb-Scintillator Barrel Calorimeter of the KOTO Experiment

*김준이, 이종원, 안정근, 임계엽 [1], 이건호 [2], 김은주 [2], 고재우 [3], 우종관 [3]
*JunLee. Kim, JongWon. Lee, Jung Keun. AHN, Gei Yub. LIM[1], GUNHO. LEE[2], Eun Joo. Kim[2], jae woo. Ko[3], Jong-Kwan. Woo[3]
고려대학교. [1]KEK. Japan. [2] 전북대학교. [3] 제주대학교.

Keyword : E14, J-PARC, Main Barrel, CBAR, KOTO

The KOTO main barrel (MB) detector is a large cylindrical array of lead-plastic scintillator sandwich calorimeters for vetoing high p_T particles from the K_L decays and the beam-associated interactions. The MB has a symmetric configuration about the beam axis. However, we observed an asymmetric azimuthal angular distribution of the beam-associated hits on the MB. Hit information from a two-layer structure of the MB enables us to reconstruct particle tracks, thereby pointing to a source of particles passing through the MB. We will present preliminary results of the MB data analysis with Geant4 simulation results

B8.04

Observation of a deeply bound state of Ξ^--^{14}N system

*윤천실, 김지현, K. Nakazawa[1], J. Yoshida[1]
*Chun Sil. YOON, Ji HYun. KIM, K.. Nakazawa[1], J.. Yoshida[1]
경상대학교. [1]Gifu University.

Keyword : Nuclear emulsion, E373 experiment, twin single-hypernuclei, ΞN interaction

We have observed a deeply bound state of Ξ^--^{14}N system, which decayed into twin single-hypernuclei in nuclear emulsion exposed in the E373 experiment at KEK-PS. The process was uniquely identified as $\Xi^- + {}^{14}N \; {}_{\Lambda}^{10}Be + {}_{\Lambda}^{5}He$. If both single-hypernuclei were emitted in the ground state from at rest capture of a Ξ^- hyperon, the binding energy of the Ξ^--^{14}N system, B_{Ξ^-}, was measured to be 4.38 ± 0.28 MeV, which is far from the Ξ^--^{14}N 3D atomic state (0.17 MeV). If the ${}_{\Lambda}^{10}Be$ nucleus is produced in an excited state, the B_{Ξ^-} value decreases by its excitation energy. Although there is no experimental data for its excited states, model calculations predicted two excited states in the bound region with consistent values of excitation energy based on known values for ^{9}Be excited states. Using Cluster and Shell model calculations, we obtained the B_{Ξ^-} values to be 2.03 ± 0.28 MeV, 1.25 ± 0.30 MeV and B_{Ξ^-} = 1.90 ± 0.28 MeV, 1.22 ± 0.28 MeV for the 1st and 2nd excited states, respectively. Even in the case of ${}_{\Lambda}^{10}Be$ production in the 2nd excited state, the B_{Ξ^-} values are far from 3D atomic level of the Ξ^--^{14}N system by more than 3.6 standard deviations. Therefore, the event provided the first clear evidence of a deeply bound state Ξ^--^{14}N system formed by attractive ΞN interaction.

B8.05

Diquark Sum Rules for Λ(1405)

*노성식, 김경일 [1], 이수형
*Sungsik. Noh, Kyung il. Kim[1], Su Houng. LEE
연세대학교. [1]RISP/IBS.

Keyword : "QCD Sum Rules","Hadron","Exotic"

We calculate the mass of Λ(1405) through the diquark sum rule with the interpolating field suggested by the diquark cluster picture for the penta-quark components in baryons. By introducing the masses of diquarks and condensates, we find that the sum rule for Λ(1405) works well. We also discuss the introduction to QCD Sum Rules with explicit diquarks.

B8.06*

Instanton effect in Quarkonium

*보부르, Hyun-Chul Kim
*Bobur. Turimov, Hyun-Chul. Kim
인하대학교.

Keyword : Instanton, Quarkonia

We investigate the instanton effects on the quarkonium system. We first derive the effective heavy quark potential from the instanton vacuum. Combining the confinement and colored Coulomb potential with that from the instanton vacuum. We calculate the mass spectrum of the quarqonia as well as radiative decays of them based on the Gaussian expansion method. We discuss the results in the context of the instanton effect.

B8.07*

Towards the construction of the extended chiral quark soliton model

*손현동, 김현철
*Hyeon-Dong. Son, Hyun-Chul. Kim
인하대학교.

Keyword : chiral quark-soliton model, excited baryons

Starting from the chiral quark soliton model, we show how to extend the model by incorporating the scalar, psuedoscalar, vector, axial-vector, and tensor fields, so that we are able to describe excited baryons.
Since the physics of the quark confinement plays an essential role in explaning the properties and structure of the excited baryons, we regard the scalar field as a confining background field.
We will present the single quark spectra, based on self-consistent profile functions and discuss the physical implications.

B8.08

Unveiling the Nature of Sigma(1670) Hyperons from Photoproduction and (K-,pi+) Reaction

*유선영, 안정근 [1]
*Sun Young. Ryu, Jung Keun. AHN[1]
핵물리연구센타오사카대학. [1] *고려대학교.*

Keyword : "J-Parc"

While formation experiments observe only one Sigma resonance in the 1670 MeV mass region with J^p=3/2- and decaying primarily
to NKbar, Lambda pi, and Sigma pi, production experiments have found evidence suggestive of two Sigma resonances in this mass region, based on a difference in the production angular distributions of Sigma(1670) decaying into Sigma pi and Sigma pi pi. To unveil this puzzle in the Sigma(1670) we have measured p(gamma, K+pi)X reactions in the energy range from 1.5 to 2.9 GeV at SPring-8. We would like to report some preliminary results on Sigma(1670) photoproduction from LEPS at SPring-8 and also discuss a proposed experiment at J-PARC.

B9.01

센서 활용 굴절률 측정 장치 개발 및 적용

*전종호
*Jongho. Jeon
대구일과학고등학교.

Keyword : 센서, 굴절률, 가변저항

물질의 굴절률을 측정하기 위해서는 스넬의 법칙(Snell's law of refraction)을 이용한다. 실험 시간에 굴절률을 측정할 때 스넬의 법칙을 이용하여 굴절률을 계산하지만 빛의 경로를 종이 위에 직접 작도해야 하는 불편함 때문에 측정 과정에서 발생하는 오차가 커 실제 이론값과 다소 차이가 발생한다는 것을 알게 되었다. 좀 더 간편하고 정밀한 측정 장치를 고민하여 가변저항 센서에 의해 각도 측정이 가능하고, 굴절률을 구하는 수식을 새롭게 정의하여 간단한 실험으로 물질의 굴절률을 쉽게 측정할 수 있도록 한 장치를 개발하여 수업에 적용해 보았다. (제 35 회 전국학생과학발명품경진대회 학습용품 부문 은상 수상)

B9.02

돌림힘에 관한 개념 이해를 돕기 위한 실험 장치의 제안

*조헌국, 신애경 [1], 현동걸 [1]
*Hunkoog. Jho, Ae Kyung. Shin[1], Hyun. Donggeul. [1]
단국대학교. [1] *제주대학교.*

Keyword : 돌림힘, 실험장치, 시범, 개념이해

본 연구는 돌림힘과 관련된 개념 이해의 어려움에 관한 선행 연구를 분석하고, 학생들의 개념 이해에 도움을 줄 수 있는 구체적인 실험 장치를 제안하고자 한다. 특히, 돌림힘에 관한 선행 연구들을 살펴보면 학생들은 돌림힘과 힘, 각운동량, 회전 관성 등을 올바로 구분하지 못하며 돌림힘을 매우 추상적인 개념으로 어려워하고 있다. 그럼에도 불구하고 이를 직접 실험적으로 확인할 수 있는 장치에 대한 제안은 매우 부족하다. 이에 본 연구는 돌림힘의 정의에 따른 다양한 특성들을 이해하고 다른 개념들과 구분지을 수 있는 실험 장치를 개발하고, 이를 실험을 통해 검증하였다. 본 연구의 실험 장치는 회전 원판과 이동형 고정쇠, 길이를 측정할 수 있는 자와 각도기 등으로 구성되어 있다. 회전 원판에 자를 부착하고 이동형 고정쇠에 각도기를 부착함으로써 손쉽게 회전축으로부터 떨어진 거리와 힘의 크기와 방향을 측정할 수 있도록 하였다. 실제 이를 수행할 수 있는 실험 장치를 만들고 실험해 본 결과 예측치와 매우 유사한 값을 얻을 수 있었다. 또한 힘의 크기와 각도, 거리 등을 한 번에 쉽게 측정함으로써 짧은 시간 안에 다양한 종류의 실험을 수행할 수 있는 장점이 있었다. 본 연구에서는 고등학교 물리수업에서 본 실험 장치를 활용한 여러 가지 교육방법과 시사점에 대해 제시하였다.

B9.03(초)

2015 교육과정 고등학교 물리학 Ⅰ,Ⅱ 교과서 집필에 필요한 신념

*안종제
*
덕수고.

Keyword : 2015 교육과정, 물리 교과서, 물리학 Ⅰ, 물리학 Ⅱ, 교과서 집필

2009 교육과정의 교과서를 집필하면서 교육과정이 의미하는 바가 정확히 무엇인지 몰라서 어려웠던 성취기준이 많았고, 수업 시수에 비해 지나치게 많은 양의 지식을 가르치게 되어 학생들의 과학적 사고력 훈련이 거의 이루어지지 않는 과목으로 취급될까 염려했다. 교육과정의 낯선 부분은 관련 전문 학술 서적들을 검토하여 고등학생이 이해하기 쉽도록 재구성하여 집필했다. 이러한 과정에서 교사의 사회적 역할 중 하나는 학생이 읽기 어려운 자료들을 대신 읽어서 학생이 쉽게 이해하도록 도와주는 것이란 신념이 좋은 지침이 되었다. 교과서와 관련된 또 다른 중요한 신념은 학교 수업이 학생들의 삶에 도움이 된다는 느낌이 강할수록 그 수업이 더 많이 선택되고 더 자발적인 학습이 일어나게 된다는 신념이라고 본다. 자발적인 학습이 많이 발생할수록 더 효과적인 수업이 될 것이다. 따라서 2015 교육과정의 물리 교과서는 학생들의 졸업 후 삶에 도움을 많이 줄 수 있는 내용과 형식을 담아내야 할 것이다.

B9.04

물리교과서 개발과 효용성에 대한 논의

*김영민
*Youngmin. KIM
부산대학교.

Keyword :
물리 I 교과서, 물리 II 교과서, 수학능력시험, 물리 참고서, 물리교과서 효용성

물리교과서는 당시의 물리교육과정 목표와 내용에 근거하여 개발된다. 현행 물리교과서는 2009 개정 교육과정에 근거하여 [물리 I] 교과서와 [물리 II] 교과서로 나누어져 있으며 이 과목을 선택한 학생들이 학습하게 된다. 실제로는 [물리 I]을 선택하는 학생들은 일부 있으나 [물리 II]를 선택하는 학생들은 거의 없다. 2015 학년도 대학수학능력시험에서의 [물리 Ⅰ] 선택자 수는 55,415 명으로 이는 [화학 I] 및 [생물 I]의 약 1/3 수준이며, [물리Ⅱ] 선택자 수는 4,631 명으로 아주 적은 수이다. 그나마 물리 교과서를 충실히 활용하여 공부한다기보다는 교육방송에서 개발된 참고서 중심으로 공부하고 있다고 한다. 물론 참고서는 교과서를 근간으로 개발된다고 볼 때 교과서의 중요성이 높다고 할 수 있지만 실제로 학생들이 참고서보다 더 중요하게 여길 수 있는 방안이 필요하다.

B9.05

물리교육 비전공자의 교과서 집필기

*박병윤
*PARK Byung-Yoon.
충남대학교.

Keyword : 교육과정, 교과서

우연한 기회에 2009 년 교육과정의 물리 교과서 집필에 참여하게 되었습니다. 과학교육을 전공하지 않은 사람이 열정과 이상만으로 덤비다 보니 아무래도 교육 현장에 대한 이해가 부족하여 여러 어려움이 있었고 의견 충돌도 많았습니다. 하지만 과학교육 현장과 과학연구 현장의 교류와 소통은 좋은 교육을 위해 반드시 필요하다고 생각합니다. 이에 대해 논의하고자 합니다.

B9.06

과학 교과서 개선을 위한 쟁점 분석과 제안

*박윤배, 윤은정
*Yunebae. Park, Eunjeong. Yun
경북대학교.

Keyword : 과학 교과서, 과학 용어, 목표 진술

설문조사에 의하면 우리나라 과학 교사 및 학생들은 현재 과학 교과서의 문제점으로 '읽고 이해하기 어렵다'와 '설명이 부족하다', '핵심이 잘 드러나 있지 않다', '실생활과의 연계가 부족하다', '지나치게 지식 개념 위주의 진술이다' 등을 꼽고 있다(윤은정, 박윤배, 2014). 이러한 사용자들의 의견들을 자칫 과학이라는 과목 특성에서 비롯되는 어쩔 수 없는 현상들로 여겨, 구태의연 또는 식상한 불만 정도로 받아들이고 지나칠 수 있다. 그러나 여러 선행 연구 결과 실제로 우리나라 과학교과서에는 위와 같은 불만을 야기할 만한 구체적 문제점들이 발견되고 있다. 발표에서는 선행 연구들을 통해 드러난 우리나라 과학교과서의 문제점을 목표 진술 측면, 문장 기술 측면, 과학용어 사용 측면, 교실 수업 개선 측면 등 다각도에서 사례를 통해 조명하고, 개선을 위한 제안을 한다. 이들이 차기 교과서 집필자들에게 참고 자료로 활용되기를, 그리고 전문가들에게는 과학교과서가 나아가야 할 방향에 대해 고민하는 계기가 되기를 기대한다.

B10.01

First measurement of the differential cross section for ttbar production in the dilepton final state at 13 TeV in CMS

전다정, 이상훈, 김동현 [1], 최영일 [1], 고정환 [1], 유인태 [1], 최수용 [2], *노연정 [2]
Da Jeong. Jeon, Jason. Lee, Dong Hyun. Kim[1], Young-Il. Choi[1], Junghwan. Goh[1], Intae. YU[1], Suyong. CHOI[2], *Youn Jung. Roh[2]
서울시립대학교. [1] *성균관대학교.* [2] *고려대학교.*

Keyword : top quark, differential cross section, CMS, LHC

First measurement of differential cross sections for top-quark pair production in the dilepton final state is performed with proton-proton collisions at a center-of-mass energy of 13 TeV. The measurement is performed with a early RunII data using CMS detector at the Large Hadron Collider. In this analysis, we measure the normalized differential cross sections with respect to kinematic variables of leptons, bjets, and top-quarks.

B10.02

Measurement of the transverse momentum spectra of vector bosons produced in charge and neutral Drell-Yan processes in proton-proton collisions at sqrt(s) = 8 TeV

*이상은
*Sang Eun. Lee
경북대학교.

Keyword : CMS, cross section, transverse momentum, W, Z

The transverse momentum spectra of vector bosons produced in charged and neutral current Drell-Yan processes are measured in the CMS experiment at the LHC. The measurement uses a sample of proton-proton collisions collected during a special low luminosity operation of the LHC at sqrt(s) = 8 TeV and corresponding to an integrated luminosity of 18.4+0.5/pb. The ratios of W- to W+, and Z to W cross sections are also measured. The measured differential cross sections and the thoretical predictions are in agreement within the uncertainties.

B10.03

Constraints on the Higgs boson width from off-shell production and decay to W boson pairs and from combination with decay to Z boson pairs

*이상은
*Sang Eun. Lee
경북대학교.

Keyword : CMS, Higgs, Width

We present constraints on the Higgs boson width based on its relative on-shell and off- shell production rates in gluon fusion and vector boson processes and decay rates to a W+W− pairs, both W decaying leptonically. The analysis is based on data collected by the CMS experiment at the LHC in 2011 and 2012, corresponding to integrated luminosities of 4.9 fb−1 at a centre-of-mass energy 7 TeV and 19.4 fb−1 at 8 TeV. The combination of this result with the Higgs boson decay to a pair of Z bosons is also performed, which further reduces the limit on the observed (expected) Higgs boson width.

B10.04

Study of ttbar+bbbar process at 13 TeV LHC

*조영권, 최수용, 노연정, 김태정 [1]
*Young-Kwon. Jo, Suyong. CHOI, Youn Jung. Roh, TAEJEONG. KIM[1]
고려대학교. [1] *한양대학교.*

Keyword : "CMS", "ttbb", "LHC"

We will present result of ttbar+bbbar analysis by using the CMS data.
We will show the result in the 2l final state.

B10.05

MET phi corrections at sqrt(s) = 13 TeV with the CMS detector

*견두연, 최수용
*Dooyeon. Gyun, Suyong. CHOI
고려대학교.

Keyword : "MET","METphi","phi modulation","phi corrections","PFtype1MET"

MET φ corrections are applied to 13 TeV collisions in the CMS experiment.
Removing the MET phi modulation by correcting the average x,y shifts induced by different particle species (charged, neutral, photons, forward hadrons, forward egamma) in bins of eta. Useful for some analysis which depend on Δφ(MET, X). It can be used together with type-1 corrections.

B10.06*

Search Results on Heavy Neutrinos in same-sign dielectron events at the CMS

*이한얼, 오성빈, 박재균, 유금봉, 서선희, John Almond, 양운기
*Haneol. Lee, Sung bin. Oh, Jae gyun. Park, Geum-bong. YU, Seon Hee. Seo, John. Almond, Un-ki. Yang
서울대학교.

Keyword : heavy neutrino, Majorana neutrino, CMS, LHC

The discovery of neutrino oscilations has opened a new window for heavy neutrinos at the LHC energy scale. The CMS experiment has performed searches for heavy neutrinos at the CMS. We present the search results of heavy Majorana neutrinos in the same-sign electron pairs plus two jets channel using proton-proton collision data at sqrt(s) = 8 TeV.

B10.07*

Search for light charged Higgs in top quark decays at pp collisions with 8 TeV in CMS experiment

*좌연재, 유금봉, 김도현, John Almond, 양운기
*Yeon-jae. Jwa, Geum-bong. YU, Do-hyun. Kim, John. Almond, Un-ki. Yang
서울대학교.

Keyword : Charged Higgs, CMS, 2HDM, tt-bar

We present the result of charged Higgs search using the CMS data from pp collisions at 8 TeV. If the charged Higgs bosons are lighter than top quark mass, they appear in top decay as t->H+b. In particular, the branching ratio of charged Higgs decay into cb-bar can be enhanced in type-Y two Higgs doublet model. In the lepton+jets channel of the Standard Model tt-bar event, the final state has one lepton, four jets (two b-jets and two light jets), and missing transverse energy. If the charged Higgs decaying to cb-bar is produced in the place of hadronic decaying W, one more b-jet is expected in the final state. A search for the light charged Higgs to cb-bar using at least two b-jets is performed using 19.7/fb of the data.

B10.08*

Search for Heavy Neutrinos in Tri-lepton Channel at the CMS

*김재성, 박재균, 서선희, 오성빈, 유금봉, 이한얼, John Almond, 전시현, 양운기
*Jae Sung. Kim, Jae gyun. Park, Seon Hee. Seo, Sung bin. Oh, Geum-bong. YU, Haneol. Lee, John. Almond, Si Hyun. Jeon, Un-ki. Yang
서울대학교.

Keyword : LHC, CMS, Heavy Majorana Neutrino,

Searches for heavy Majorana neutrinos at the CMS have been done in two same-sign leptons and two jets channels. We extend the searches into tri-leptons channel, and check a sensitivity on the limit and discovery potential. For the heavy Majorana neutrino with mass less than W boson, the production cross section will be enhanced due to on-shell W production which has a huge cross section. For events with tri-leptons and missing transverse energy, the invariant mass of the heavy neutrino can be fully constructed with a good mass resolution. We present a study of this channel and the discovery sensitivity.

B10.09*

Search Results on Heavy Neutrino in e-mu dilepton channel at the CMS

*오성빈, John Almond, 서선희, 유금봉, 이한얼, 박재균, 양운기
*SungBin. Oh, John. Almond, Seonhee. Seo, Geumbong. Yu, Haneol. Lee, Jaegyun. Park, Un-ki. Yang
서울대학교.

Keyword : CMS, LHC, Neutrino, Majorana, Seasaw Model

The discovery of non-zero neutrino masses has opened a big question about smallness of neutrino mass. The heavy Majorana neutrino has been considered as a strong candidate to solve this problem. The CMS experiment has performed searches for heavy neutrinos in same-sign di-lepton events with two jets. We present the first direct search results of same-sign electron-muon channel on the heavy Majorana neutrinos using 19.7 /fb of proton-proton collision data of LHC at sqrt(s) = 8 TeV.

B11.01(초)

Physics of Neutron Stars : From Dense Matter to Gravitational Waves

*이창환
*Chang-Hwan. Lee
부산대학교.

Keyword : 중성자별, 중력파, 초신성폭발, 고밀도 강입자 물질

중성자별은 내부 밀도가 매우 높아 고밀도 강입자 상태를 연구할 수 있는 천체이다. 또한 중성자별은, 관련 천체현상에 초신성폭발, 감마선폭발 및 중력파방출 등이 포함되어 있어, 상대론적 고에너지 천체물리 연구에 매우 중요한 천체이다. 본 발표에서는 고밀도 강입자 물질 연구에서 출발하여 중력파에 이르기까지, 중성자별과 관련된 다양한 물리 및 천체물리학 현상에 대해 논의한다.

B11.02(초)

Nuclear EOS and compact stars

*김영만
*Youngman. Kim
기초과학연구원.

Keyword : nuclear symmetry energy, neutron stars

The compact stars that we are interested in are neutron stars in which strong interaction dominates. The EOS of asymmetric nuclear matter is essential for the understanding of neutron stars. In this presentation we will discuss the relations between nuclear EOS (especially, nuclear symmetry energy) and neutron star properties such as the mass-radius relations.

B11.03(초)

상대론적 천체현상 감마선 폭발

*이현규
*Hyun Kyu. Lee
한양대학교.

Keyword : 감마선 폭발, 상대론, 천체물리학

감마선 폭발의(Gamma Ray Bursts) '표준모형', 중심엔진 모형, 그리고 중력파 발생등을 중심으로 상대론적 천체현상인 감마선 폭발 연구의 현재와 미래 연구방향을 토의한다.

B12.01(초)

Rotating pinwheel wave within a biological master clock, the Suprachiasmatic nucleus

*이경진, 정병하 [1]
*Kyoung Jin. LEE, Byeongha. Jeong[1]
고려대학교. [1] *고려대학교/세포동력학연구센터.*

Keyword : biological circadian clock, nonequilibrium patterns and waves, nonlinear phase response curve, phase resetting

Within every clock cell that comprises the biological master clock the suprachiasmatic nucleus (SCN), several biochemical markers oscillate in a circadian fashion and the oscillations propagate as a circadian phase wave over the whole clock cell population within the nucleus. However, little is known about their iophysical properties. Here, based on a realistic mathematical model as well as experiments with SCN slice cultures, we demonstrate that the wave can take any one of various modes including phase-coherent oscillation, planar or oval-shaped wave, complex wave states with fragmented domains, and most notably, a rotating pinwheel wave which conceptually resembles a wall clock with a rotating hand. All of these are stable and the transitions among them can be induced by an extrinsic, spatially-homogeneous perturbation. Thus, no spatially-fixed circadian phase ordering seems to exist at least within an ex vivo SCN.

B12.02(초)

Roles of noise in auditory transduction and speech perception

*안강헌, 홍성화 [1], 문일준 [1], 이은영 [2], 우지환 [3], 이경면 [4], 이우석, 유재연, 박설아
*Kang Hun. Ahn, Sung Hwa. Hong[1], Il Joon. Moon[1], Eunyoung. Yi[2], Jihwan. Wu[3], Kyung Myun. Lee[4], Woo Seok. Lee, Jaeyun. Yoo, Sul-Ah. Park
충남대학교. [1]Samsung Medical Center. [2] 목포대학교. [3] 울산대학교. [4] 서울대학교.

Keyword : hearing, noise, hair cell, speech perception, ribbon synapse

Hearing research is one of the most active interdisciplinary topics in the developed countries. It is important not only as due to its medical aspects but also fundamental issues. The ear can actively amplify weak signals to achieve great sensitivity and a wide dynamic range of hearing. Hair cells of the inner ear are the mechano-transducers which have been proposed to amplify weak signals with a great dynamic range. Through the complex dynamics of the cochlear and signal processing of the brain, humans understand speech in noise. The exact mechanisms for these are not yet clearly known. I will introduce our recent efforts and recent advances in the hearing research, in particular, on the positive and negative roles of noises in speech perception.

B12.03(초)

What is the dimension of molecular recognition?

*Tsvi Tlusty
*Tsvi. Tlusty
Ulsan National Institute of Science and Technology (UNIST).

Keyword : .

When an enzyme binds to a substrate, many of its atoms move around to accommodate the bound substrate. Such large-scale, many-body motion makes molecular recognition appear as an inherently multidimensional problem. This raises several basic questions: What is the effective dimension of the molecular phenotype space? What is the role of conformational changes? And practically, what is the structural resolution required to understand the function of biomolecules?
We will discuss these questions in the context of molecular information processing systems. Our prime example will be the ribosome, which has to select the right tRNA among numerous competitors during translation. Simple analysis of the ribosome function suggests a generic mechanism of enhancing molecular recognition. It also suggests a possible answer to the questions raised above regarding the dimensionality of living systems.

B12.04(초)

Mechano-Sensitive Adhesion and Dynamic Stabilization of Multicellular Assembly in Living Tissues

S. de Beco, J.-B. Perney, S. Coscoy, François Amblard[1]
. , . , . , . [1]
Institut Curie. [1]UNIST.

Keyword : cell biophysics, adhesion, dynamical systems, multi-agent systems

초록(500 단어 이내): Because biological systems are intrinsically out of equilibrium, they represent an extremely rich playground to explore how the individual dynamics of active and noisy interacting objects control the morphogenesis and the stability of multi-agent structures. In living tissues, the proper control of time-scales and synchronization among cells is probably a key issue for multicellular assemblies to achieve homeostasis or complex morphogenetic processes. In epithelia, cells are known to individually generate actomyosin contractile stress and transmit it in a regulated fashion through adhesive interfaces. Each individual interface is thus subjected to the opposed stresses independently generated by its two partner cells, and it should thus move unless the partners mechanically match. The geometric homeostasis of mature epithelia observed at short enough time-scale thus raises the problem to understand how cells, if considered as noisy individual actuators, do adapt across individual intercellular contacts to locally balance their time-average contractile stress. We found that adhesive structures are based on short-lived molecular bonds between cells (homotypic E-cadherin bonds), with mechano-sensitive life-times that probably reflects a self-limiting transmission of stress across bonds. We propose the concept of active adhesion, in which mutual adaptation and stability are dynamically achieved by a flux of transient mechano-sensitive bonds.

B13.01

초소형 Chip-Scale 원자시계 개발

*권택용, 박상언, 홍현규, 이상범, 허명선, 김희연 [1], 김태현 [1], 박종철 [1], 양충모 [1], 윤상준 [2], 이승일 [2], 전태현 [2]
*Taeg Yong. Kwon, Park Sang Eon. , Hong. Hyun-Gue. , . , . , . , . [1], . [1], . [1], . [1], . [2], . [2], . [2]
한국표준과학연구원. [1] 나노종합기술원. [2] 넵코어스(주).

Keyword : chip-scale 원자시계, CPT, 주파수발생기, 세슘원자

초소형 chip-scale 원자시계는 원자의 결맞은 밀도 포획(CPT) 현상을 이용하는, 즉, 광학 전이(optical transition)를 통해 마이크로파 시계전이 공진을 발생시키는 방식의 원자시계이다. 마이크로파 공진기를 사용하지 않기 때문에 기존의 원자시계에 비해 훨씬 더 작은 크기로 제작이 가능하고, 광원으로 VCSEL 을 사용하기 때문에 저전력 원자시계 개발이 가능하다. 한국표준과학연구원, 나노종합기술원, 그리고 넵코어스(주) 의 3 개 기관이 공동으로 크기가 25 cm^3 이하이고, 소모전력이 125 mW 이하인 초소형 원자시계를 개발하는 연구를 수행하고 있다. 초소형 원자시계 개발을 위해 VCSEL 변조(변조주파수 ~4.6 GHz) 및 CPT 분광, 마이크로 분광셀 제작, 저전력 마이크로파 합성기 개발 등의 연구가 진행하고 있다. 본 발표에서는 현재 진행 중인 초소형 chip-scale 원자시계 개발 현황에 대해 소개하고, 1 년 동안 연구수행으로 얻은 연구 결과를 발표하고자 한다.
* 이 연구는 민군겸용기술개발사업의 지원으로 수행되었습니다.

B13.02

기본물리상수와 새 국제단위계

*이호성
*Ho Seong. Lee
한국표준과학연구원.

Keyword : 기본물리상수, 국제단위계, 기본단위, 재정의, CODATA

기본물리상수란 물리학 법칙에 나오는 불변의 숫자라는 의미를 가진다. 가장 보편적인 기본상수로는 빛의 속력, 중력상수, 플랑크 상수 등이 있다. 2018 년도에 기본물리상수를 이용하여 국제단위계를 새롭게 정의한다. 7 개의 기본단위 (길이, 질량, 시간, 온도, 전류, 광도, 물질의 양)는 각각 해당되는 기본물리상수 (빛의 속력, 플랑크 상수, 세슘원자 초미세 준위간의 전이 주파수, 볼츠만 상수, 기본전하량, 시감효능, 아보가드로 상수)를 바탕으로 다시 정의된다. 이 때 해당 기본물리상수들의 값은 불확도가 0 인, 정의된 값을 가진다. 이를 위해 현재 세계적으로 진행되고 있는 연구현황과 CODATA 에서 4 년마다 발표하는 기본물리상수의 주요 이슈를 소개한다.

B13.03

Coupled-coherent-states for the one-dimensional model atom driven by strong laser pulses

*최낙렬, 변장우, 이민호, 김대성 [1]
*Nark Nyul. CHOI, Chang Woo. BYUN, Min-Ho. LEE, Dae-Soung. KIM[1]
금오공과대학교. [1] *경기과학기술대학.*

Keyword : driven ionization, coupled-coherent-states, tunneling, strong laser pulses

강하고 짧은 레이저 펄스에 노출된 일차원 원자 모형의 문턱 넘어 이온화 (ATI) 와 고차조화파 생성 (HHG) 현상을 양자역학적 관점에서 수치적으로 다루고자 한다. 시간에 따라 진행하는 Coherent States (CS) 를 basis set 으로 취하고 각 CS 사이의 coupling 을 도입하여 고전역학에서는 나타나지 않는 터널링과 같은 현상이 자연스럽게 다루어지도록 한다. Coupled-coherent-states 방법에서는 CS basis set 을 어떻게 정하느냐에 따라 계산량과 물리현상의 기술 여부가 크게 좌우된다. 우리는 특히 이 부분을 자세히 살펴 봄으로써 Coupled-coherent-states 방법을 자유도가 큰 시스템에 대해 적용할 수 있는 기틀을 마련하고자 한다.

B13.04

Measurement of gate fidelity of superconducting 3D transmon qubit

노태완, 박정환, 박관열, 이순걸 [1], 송운, *정연욱
Taewan. Noh, Jung Hwan. Park, Gwan Yeol. Park, Soon Gul. Lee[1], Woon. Song, *Yonuk. Chong
한국표준과학연구원. [1] *고려대학교.*

Keyword : superconducting qubit, gate fidelity, benchmarking, tomography

We present measurements of single-qubit gate fidelity in a superconducting transmon qubit strongly coupled to a 3D aluminum cavity. In order to measure the average gate fidelity from the accumulated error over a long sequence of gates, we applied randomized benchmarking (RB) protocol [1, 2]. Each sequence consists of an alternation of randomly generated Pauli randomization gate Pi ∈ P = {X±π, Y±π, Z±π, ±I} and computation Cllifford gate Ci ∈ C = {X±π/2, Y±π/2}. By taking the average of the results from 32 random sequences with 15 difference truncations, we obtained a minimum average gate fidelity of 98.3% in our setup in KRISS. Interleaved randomized benchmarking protocol [3] revealed an average fidelity ~ 99.5% for single-qubit gates X±π, Y±π. We also present results from quantum process tomography, which would serve as an essential tool to investigate the entanglement in a multi-qubit system.

B13.05

Quantum electrodynamic Aharonov-Bohm effect: nonlocal interaction of a charge qubit and an electromagnetic cavity

*김영완, 강기천
*Youngwan. Kim, Kicheon. KANG
전남대학교.

Keyword : Aharonov-Bohm effect, nonlocal exchange, circuit quantum electrodynamics, superconducting charge qubit, quantum electrodynamic potential

The Aharonov-Bohm effect is an intriguing quantum phenomenon which occurs due to the interaction between a "static" potential and a charge located even in a electromagnetic-field-free region. Here, we predict a new type of the Aharonov-Bohm effect under the influence of a quantum electrodynamic potential. The specific system considered here is a superconducting charge qubit nonlocally interacting with a cavity electromagnetic field. We find that the indirect interaction gives rise to the nonlocal exchange of the two quanta, charge and photon, and leads to remarkable quantum electrodynamic phenomena such as vacuum Rabi splitting and oscillation, and Lamb shift, under the condition that the qubit is located in an electromagnetic-field-free region. Our result can be verified in a realistic experimental setup, and provides a novel approach of investigating the Aharonov-Bohm effect combined with the cavity/circuit quantum electrodynamics.

B13.06

Periodic shedding of vortex dipoles in a highly oblate Bose Einstein condensate

*권우진, 서상원, 강세지, 김준현, 신용일
*Woo Jin. Kwon, Sang Won. Seo, Seji. Kang, Joon Hyun. Kim, Yong-il. Shin
서울대학교.

Keyword : Bose Einstein condensate, vortex, shedding, superfluid

We investigate vortex shedding from a moving penetrable obstacle in a highly oblate Bose-Einstein condensate. The penetrable obstacle is formed by a repulsive Gaussian laser beam that has the potential barrier height lower than the chemical potential of the condensate. The moving obstacle periodically generates vortex dipoles and the vortex shedding frequency f_v linearly increases with the obstacle velocity v as $f_v = a(v-\square v_c)$, where v_c is a critical velocity. Based on periodic shedding behavior, we demonstrate deterministic generation of a single vortex dipole by applying a short linear sweep of a laser beam. This method will allow further controlled vortex experiments such as dipole-dipole collisions.

B13.07*

Collisions of Half-Quantum Vortices and Quantum Turbulence in a Spinor Atomic Superfluid

*서상원, 권우진, 강세지, 김준현, 신용일
*Sang Won. Seo, Woo Jin. Kwon, Seji. Kang, Joon Hyun. Kim, Yong-il. Shin
서울대학교.

Keyword : Spinor Bose-Einstein condensate, half quantum vortex, topological defect

Half quantum vortices (HQVs) are a new type of vortices in spinor Bose-Einstein condensates which have fractional vorticity. These exotic vortices are one of the central topics in spinor superfuids such as 3He, triplet superconductors, exciton-polariton condensates, and atomic spinor gases. Here, we present experimental observation of HQVs dynamics caused by collisions of the HQVs in the easy-plane polar phase of an antiferromagnetic gaseous spinor BEC. We identify the HQVs as magnetized point defects using magnetization-sensitive imaging. We conducted a collision experiment of two HQV pairs and investigated the scattering patterns which gives us qualitative information on the interaction among the HQVs. Finally, we created spin turbulence by injecting many HQVs and investigated its temporal evolution.

B13.08*

Probing molecular states of ^{174}ytterbium atoms via intercombination line photoassociation spectroscopy of a Bose-Einstein condensate.

*김민석, 이정원 [1], 이재훈 [2], 신용일, 문종철 [1]
*Min-Seok. Kim, Jeongwon. Lee[1], Jae Hoon. Lee[2], Yong-il. Shin, Jongchul. Mun[1]
서울대학교. [1] 한국표준과학연구원. [2] 표준과학연구원.

Keyword : Bose-Einstein Condensate, photoassociation, optical Feshbach resonance, ytterbium dimer, qunatum control

We report the experimental results of the photoassociation spectroscopy (PAS) measurements of a 174 ytterbium Bose-Einstein condensate (BEC) using the intercombination transition ($^1S_0$-$^3P_1$) at 555.8nm. Photoassociation is a key tool for the optical Feshbach resonance [1] and could potentially be used for more complex quantum control of atom-atom collisions. Previous studies of ytterbium molecular transitions, i.e., dimers (Yb_2), have been done with a thermal distribution of laser cooled atoms [2]. In this presentation, we probe Yb_2 molecules using a quantum degenerate gas significantly reducing the thermal broadening of the sub-MHz linewidth molecular transitions. The high resolution molecular spectra obtained in these experiments can pave the way for further study of atomic interaction dynamics within a BEC and for precision measurements of collisional frequency shifts in optical lattice clocks [3].

References

1. K. Enomoto, K. Kasa, M. Kitagawa, and Y. Takahashi, Phys. Rev. Lett. 101, 203201 (2008).
2. S. Tojo, M. Kitagawa, K. Enomoto, Y. Kato, Y. Takasu, M. Kumakura, and Y. Takahashi, Phys. Rev. Lett. 96, 153201 (2006)
3. K. M. Jones, E. Tiesinga, P. D. Lett, and Paul S. Julienne, Rev. Mod. Phys. 78, 483 (2006).

B13.09*

Observation of quantum degenerate gas of Fermionic ytterbium atoms

*이무송, 한정호, 김민석, 강진현, 신용일
*Moosong. Lee, Jeong Ho. Han, Min-Seok. Kim, Jin Hyoun. Kang, Yong-il. Shin
서울대학교.

Keyword : degenerate Fermi gas. Ytterbium. Quantum degeneracy. Optical trap.

Quantum gases of alkaline-earth like atoms opened fascinating ways to study various many-body physics in optical lattice such as SU(N) quantum magnetism and heavy Fermion physics. Here, we present recent realization of degenerate Fermi gas of Yb^{173} atoms. Unlike the bosonic case, we used dark spot Zeeman slower beam to avoid strong pushing effect to the magneto optically trapped atoms. After 15 seconds loading and following compression step, we loaded 10^7 atoms in optical dipole trap. As a result of scattering property of Yb^{173} and tight optical dipole trap, only 4.3 seconds of evaporation is sufficient to observe Fermi degeneracy. We succeeded to produce degenerate Fermi gas of $T/T_F \sim 0.2$ and $\sim 10^5$ atoms. In future experiments, we're planning to transfer atoms to science chamber and load adiabatically into optical lattice.

B15.01(초)

KHIMA 치료시스템의 현황 소개

*조성호, 조일성
*Sungho. cho, Ilsung. Cho
한국원자력의학원.

Keyword : 중입자치료, 치료시스템

최근 입자치료 (양성자와 중이온)는 타켓 볼륨이내에 많은 빔 에너지를 전달하면서 브래그 피크 위치 이전의 조직에 대해서는 전체 선량에 비해서 낮은 에너지를 전달할 수 있는 장점으로 인해 우수한 기술로 평가되어 그 관심이 증가하고 있다. 이에 KIRAMS 에서도 2010 년도부터 입자치료를 위한 센터를 구축하고 있다. 이러한 치료시스템은 조사장치, 환자위치시스템 및 검증장치, 치료계획시스템, 선량검증시스템 및 네트워크 시스템 등으로 구성되고 있다. 본 논문에서는 이러한 치료시스템 구축을 위한 KIRAMS 의 현황을 보고하고, 이에 관한 세부적인 사항(치료방법, 해외치료센터현황 등)에 대해서 보고하고자 한다.

B15.02(초)

Commissioning Plan of Accelerators at PAL-XFEL

*한장희, 강흥식, 김광우, 고인수
*Jang-Hui. Han, Heung-Sik. Kang, Kwang-Woo. Kim, In Soo. Ko
PAL.

Keyword : free electron laser, x-ray, coherent, femtosecond, commissioning

The Pohang Accelerator Laboratory X-ray Free Electron Laser (PAL-XFEL) project aims at the generation of X-ray FEL radiation in the range of 0.06 to 10 nm for photon users with a bunch repetition rate of 60 Hz. The linear accelerator (linac) is based on the normal conducting S-band technology and the undulator system is a variable gap, out-vacuum type. The accelerator components are being installed for the 10 GeV linac and the undulator beamlines. Beam commissioning is planned to be started in early winter 2015. 0.25 nm FEL radiation with a 6 GeV electron beam by early summer 2016 is the first milestone. Finally, 0.1 nm FEL with 10 GeV is foreseen by end 2016. We present the beam commissioning plan for stepwise achievement of the commissioning milestones.

B15.03(초)

양성자가속기 이용 현황과 빔라인 확충 계획

*김계령, 권혁중, 김귀영, 조용섭
*Kye-Ryung. Kim, KWON Hyeok-Jung. , Kim Kui Young. , CHO Yong-Sub.
한국원자력연구원.

Keyword : 양성자가속기, 양성자빔, 이용, 빔라인, 표적실

한국원자력연구원 양성자가속기연구센터(KOMAC)에서는 2012 년말 100MeV 양성자가속기를 완공하고 2 개의 빔라인을 이용하여 2013 년 7 월부터 빔 서비스를 시작하였으며, 2015 년 6 월말까지 약 3,400 공정의, 4,000 여개의 시료에 대한 빔조사실험을 수행하였다. 연구과제수는 약 200 개이고 참여연구원의 수는 약 460 명에 달한다. 양성자빔의 활용분야를 살펴보면, 나노/재료/반도체, 생명/의료/의공학, 에너지/환경, 원자력/방사선/중성자, 우주항공/기초과학 등 매우 다양하였다. 양성자가속기연구센터는 10 개의 빔라인의 구축계획을 가지고 있으며, 각 빔라인과 표적실은 중성자원, 동위원소, 우주방사선, 반도체, 생명공학/의학 등 특정한 분야에서 활용될 수 있도록 설계되었다. 2015 년도에는 동위원소 생산을 위한 빔라인의 구축을 완료하고 향후 년차별로 이용자들의 요구를 반영한 우선 순위에 따라 빔라인을 확충해 나갈 예정이다.

B15.04(초)

차세대 우주용 박막 태양전지 개발을 위한 양성자 빔 조사 연구

*곽지혜, 김기환, 안승규, 송희은, 김계령 [1], 윤재호
*Jihye. Gwak, Kihwan. Kim, Seung Kyu. Ahn, Hee-eun. Song, KIM Kye-Ryung. [1], Jae Ho. Yun
한국에너지기술연구원. [1] 한국원자력연구원.

Keyword : 우주용, 화합물 박막 태양전지, 저가 경량, CIGS 계 광흡수층, 양성자 조사 특성

1958 년 처음으로 뱅가드(Vanguard) 위성에 태양전지가 사용된 이래, 지금까지 결정질 Si 및 GaAs 태양전지 기술이 우주에서 필수적인 역할을 해오는 동안 무게당 전력비(power to mass ratio, W/kg; specific power) 및 내방사선 특성은 개선이 필요한 두가지 중요사항으로 파악되어왔다. 그러나, 결정질 Si 재료의 경우 단일접합 효율 이상의 고효율 구현이 불가능하고, GaAs 를 비롯한 유사 III-V 족 우주용 태양전지의 경우 고효율의 장점을 가지나 공정이 복잡하고 고가인 단점을 가진다. 현재까지 국내 인공위성을 비롯한 우주비행체의 경우 위와 같은 고가의 III-V 족 태양전지를 전량 수입하여 사용하고 있으며, 고방사선, 극고온 및 극저온 등의 열악한 우주환경에 적합한 태양전지 성능 확보가 필요한 반면 국내에는 관련 제조 기술뿐만 아니라 평가 및 예측기술도 전무한 실정이다.
Cu, In, Ga, Se 의 4 원소로 구성된 화합물을 태양전지의 광흡수층으로 사용하는 $CuIn_{1-x}Ga_xSe_2$(CIGS) 박막 태양전지는 태양광의 광흡수계수가 높아 박막 태양전지 중 가장 높은 효율(독일 ZSW 21.7%)이 보고되었으며, 내방사선 특성이 우수할 뿐만 아니라 경량기판 상에 제조가 가능하고 상대적으로 높은 무게당 전력비를 가지므로, 위에서 언급한 우주용 태양전지에 대한 요구사항을 충족할 수 있다. 더불어, 기존의 우주용 태양전지 대비 제조단가가 낮을 뿐 아니라 결정질 Si 태양전지와 달리 탠덤화를 통해 효율 향상을 기대할 수 있다.
한국에너지기술연구원(KIER)에서는 1990 년대 초부터 CIGS 박막 태양전지 연구를 수행해 왔으며, AM1.5 조건에서 20%의 CIGS 박막 태양전지 효율을 달성한 바 있다. 이러한 지상용 CIGS 박막 태양전지에 대한 축적된 기술과 노하우를 기반으로 경량기판 상에 CIGS 박막 태양전지를 제조하여 우주용으로 개발하고자 하는 연구가 진행 중이며, 본 발표에서는 KIER 에서 제조된 CIGS 박막 태양전지에 대해 KOMAC 의 양성자가속기를 활용하여 수행된 내방사선 특성 연구의 초기 결과와 함께 관련 연구 동향을 소개하고자 한다.

C1.01*

Topological Phase Transition of Phosphorene Oxide induced by Tensile Strain

*강승훈, 박제준, 우성종 [1], 권영균
*Seoung-Hun. Kang, JEJUNE. PARK, Sungjong. Woo[1], Young-Kyun. Kwon
경희대학교. [1] *고등과학원.*

Keyword : phosphorene oxides, DFT, topological phase transition

Phosphorene, a new two-dimensional material produced by the exfoliation of black phosphorus, may be extremely reactive with oxygen because of the existence of a lone pair of electrons on each phosphorous atom, and thus the oxidation would be unavoidable during synthesis and/or fabrication processes. Here we investigate the structural stability and electronic properties of phosphorene oxides (PO_x) with different oxygen compositions x using density functional theory. We explore the strain effect on the electronic structure of the fully (x=1) oxidized phosphorene. At a particular strain without spin-orbit coupling (SOC) is observed a band gap closure originating from an interesting band inversion near the Γ point in the k space. The strain in tandem with SOC induces a very small band gap (~5 meV) reopened, and thus gives rise to a topological quantum phase transition from a normal insulator to a topological insulator. Such a topological phase transition is verified by evaluating z_2 invariant.

C1.02*

Curvature-induced stability in graphitic carbon nitride structures: ab initio study

*송호신, 김민관 [1], 강승훈, 권영균
*Hosin. Song, Min-Gwan. Kim[1], Seoung-Hun. Kang, Young-Kyun. Kwon
경희대학교. [1] *광주과학기술원.*

Keyword : "g-C_3N_4", "2D material", "nanotube", "curvature"

Using ab initio density functional theory, we investigate the structural and electronic properties of triazine-based graphitic carbon nitride (g-C_3N_4) structures in planar and tubular forms. The planar g-C_3N_4 is a layered material of vacancy-rich honeycomb lattice composed of C_3N_4 sub units cross-linked by a triply-coordinated nitrogen atom. Intriguingly, the g-C_3N_4 exhibits a band gap ranging from 2.1 to 2.7 eV and light electronic effective mass, and thus it is expected to be utilized future electronic devices. We find that a buckled structure is preferred to a flat one for a monolayer of g-C_3N_4 planar sheet, because of repulsion between lone pairs of electrons on the nitrogen atoms in a triazine ring. In case of g-C_3N_4 nanotubes (NTs), it is found that the (7,0) zigzag NT is more stable than not only any other NTs, but also surprisingly even the equilibrium planar sheet. This implies that such g-C_3N_4 NTs may be synthesized more easily than the sheet. To further explore the curvature effect on the structural stability, we investigate various g-C_3N_4 nanoribbons with difference cuvatures with armchair or zigzag edges.

C1.03*

Ab initio study of polaron dynamics in metal oxides

*신동빈, 박노정
*Dongbin. Shin, Noejung. Park
울산과학기술대학교.

Keyword : condensed matter, polaron, rt-TDDFT, DFT

Among the family of quasiparticles in condensed matters, polaron, that is bound state of electron and phonons, is involved in various physics in metal oxide, such as the life time of excited state, carrier conductivity, and electron-electron pairing in the strong coupling regime. Whereas polaron-related phenomena have been mostly studied with model Hamiltonian, here we use real-time evolution of time-dependent density functional theory plus Hubbard U to calculate them within the gear of ab initio. As a case study, we calculated the excitation of STO, and we found that some particular charge-ordered excitation can result in a resonant mode of oscillation. We also calculated the polaron transport in STO/LAO interface, and found that the interchange between polaronic state and the conduction band state can lead to a long range fast teleportation of Holstein-type polaron.

C1.04*

프레스노이트 단결정 $A_2TiSi_2O_8$ (A=Ba, Sr)의 구조적 상전이와 비선형 광학 상수에 관한 제일원리계산

*송나영, 김복기
*Nayoung. Song, KIM Bog-Gi.
부산대학교.

Keyword : 프레스노이트, 강유전체, 상전이, 자발분극, 제일원리계산

최근 들어 non-centrosymmetry phase 에 관한 다양한 계산 혹은 실험 결과들이 소개되고 있다. 우리는 본 발표 논문에서 프레스노이트 단결정 $Ba_2TiSi_2O_8$ (BTS) 와 새롭게 제시되는 $Sr_2TiSi_2O_8$ (STS) 를 비교 분석하였다.
우리는 밀도 범함수를 사용하는 VASP 을 이용하여, 구조적인 상변화와 자발 분극의 크기에 관한 계산을 수행하였다. 프레스노이트 단결정 BTS 와 STS 는 non-centrosymmetry P4bm 공간군을 가지며, centrosymmetry P4/mbm 공간군으로부터 허구의 상전이를 통해 나타난다. 본 발표에서 중점적으로 논의할 주제는 산소 결합 길이의 변화이다. 상전이가 일어날 때, 다면체의 한 꼭짓점에서 산소 원자가 비대칭적으로 떨어져 나간다. 우리는 이 변화가 본 물질에 어떠한 물리적 물성을 좌우하는 지 논의하고자 한다. 뿐만 아니라, 전자 구조 (band structure 와 desnity of state)와 mode 분석, 자발 분극의 크기에 관한 논의를 담고 있으며 비선형 광학 상수 계산 논의를 위해 ABINIT 프로그램 패키지를 활용하였으며 이 논문 발표를 통해 비선형 광학 상수에 관한 계산 결과도 논의하고자 한다.

C1.05*

Density functional study of ferroelectric domain dynamics responding to oxygen vacancy around domain wall

*송회철, 신영한
*Hoe-Cheol. Song, Young-Han. Shin
울산대학교.

Keyword : ferroelectrics, fatigue, domain wall, oxygen vacancy, DFT

Because of their promising properties for non-volatile random access memories and several other applications, ferroelectric materials have been extensively studied in recent years. Experimentally fabiricated materials include many defects such as vacancy, interstitial, and antisite, which affect significantly the properties of materials. For example, Bujakiewicz-Koronska and Natanzon showed that point defects alter the elastic constants of $Na_{1/2}Bi_{1/2}TiO_3$ significantly [1]. Also, it was known that oxygen vacancies moved to ferroelectric domain walls and pinned them [2,3]. In this work, we examine the domain dynamics around the 180° ferroelectric domain walls of tetragonal $PbTiO_3$ with and without the oxygen vacancy by using the first-principles calculations. In order to investigate the effect of oxygen vacancies on the ferroelectric domain dynamics of $PbTiO_3$, we consider three possible cases for migration of oxygen vacancies and domain walls. First, an oxygen vacancy that is initially located on the PbO-centered domain wall stays on the same PbO-centered plane while the domain wall migrates. In this case the energy barrier is obtained as 0.18 eV for the 8 x √2 x √2 unit cells. Second, the PbO-centered domain wall is fixed when an oxygen vacancy migrates. In this second case, two possible migration pathways of an oxygen vacancy exist. One is through the oxygen position on top of the Ti atom, and another is through the oxygen position at the same plane of the Ti atom. For these cases, the energy barriers are calculated as 0.45 eV and 0.55 eV, respectively. Third, the PbO-centered domain wall and oxygen vacancy migrates at the same time with two different energy barriers of 0.22 eV and 0.30 eV. Because of low energy barrier difference between domain wall and oxygen vacancy, migration of oxygen vancancy toward to grain boundary may occur during the switching process in ferroelectric applications. Due to this phenomenon, in ferroelectric materials, fixed grain appears in the material and it will cause the fatigue problems.

1. R. Bujakiewicz-Koronska and Y. Nantanzon, Intergr. Ferroelectr. 108, 21 (2009).
2. S. Pöykkö and D. J. Chadi, J. Phys. Chem. 61, 291 (2000).
3. A. Angoshtari and A. Yavari, Comp. Mater. Sci. 48 258 (2010).

C1.06

Off-centered "Walk on Spheres" (WOS) Algorithm

*황치옥
*Chi-Ok. Hwang
광주과학기술원.

Keyword : Materials science, Monte Carlo, Walk on Spheres, Off-Centered

Diffusion Monte Carlo methods has been computationally used for materials science, especially the bulk properties of porous and composite media such as the electrical or thermal conductivity or shear modulus of structural composites; the permeability of porous media; the electrostatic contribution to the free energy of a bio-molecule in solution; and the mutual capacitance matrix describing interaction of micro-components in a transistor matrix on a microchip. In the Diffusion Monte Carlo methods, "Walk on Spheres" (WOS) algorithm has played the central role to simulate the diffusion process. In this talk, based on the isomorphism between the electrostatic Poisson problem and the corresponding diffusion motion expectation of the first-passage, we develop an off-centered WOS algorithm to replace the WOS one. We find that the new off-centered WOS algorithm is much more efficient than the old WOS one.

C1.07

Non-thermal phase transition mechanism in Ge-Sb-Te alloys: Role of excited carrier dynamics

*방준혁, Y. Y. Sun[1], X.-Q. Liu[1], S. B. Zhang[1]
*Junhyeok. Bang, Y. Y.. Sun[1], X.-Q.. Liu[1], S. B.. Zhang[1]
한국기초과학지원연구원 (KBSI). [1]Rensselaer Polytechnic Institute.

Keyword : Non-thermal phase transition, Excited carrier dynamcis, Time-dependent density functional theory

Non-thermally driven phase transition has been observed by femtosecond laser experiments in numerous materials. For decades, the phenomenon has been explained by the plasma model: excitation of a large fraction of valence electrons to conduction bands weakens lattices and leads to the structural phase transition in low temperature. In contrast to ground state electrons, however, excited carriers undergo several dynamic processes such as scattering, relaxation, and recombination and the plasma model completely ignores such an effect of the carrier dynamics. In this presentation, we will discuss recent real-time ab initio time-dependent density functional studies on the non-thermal phase transition in Ge-Sb-Te alloys. We find a strong carrier energy dependence in the carrier relaxation process: for low energy carriers electron-phonon scattering becomes a dominant relaxation process, and for high energy carriers electron-electron scattering remains a dominant relaxation process. As a result, we observe significant ionic temperature increase from the initial stage of excitation for low energy excitation, which aids phase transition by ionic thermal activation, and non-thermal phase transition for high energy excitation significantly below the melting temperature. The results show that the excited carrier energy is a key factor in determining the phase transition mechanism in contrast to the plasma model, in which the excited carrier density is crucial in the phase transition processes. This provides a new conceptual framework in understanding fundamental physical phenomenon of the phase transition.

C1.08

Strain-Engineered Optoelectronic Properties of Two-Dimensional Transition Metal Dichalcogenide Lateral Heterostructures

*이재광
*Jaekwang. Lee
Department of Physics. Pusan National University.

Keyword : "two-dimensional materials", "strain engineering", " transition metal dichalcogenide", lateral (in-plane) heterostructures","power conversion efficiency"

Compared with their bulk counterparts, two-dimensional materials can sustain much higher elastic strains (up to ~10%), at which optical quantities such as bandgaps and absorption spectra governing optoelectronic device performance can be modified with relative ease. Using first-principles density functional theory, we demonstrate how uniaxial tensile strain can be utilized to optimize the electronic and optical properties of transition metal dichalcogenide lateral (in-plane) heterostructures such as MoX_2/WX_2 (X = S, Se, Te). In addition, we show that a lateral $MoS_2/MoTe_2$ heterostructure uniquely develops a continuously varying direct bandgap across the heterojunction, which is a particularly useful characteristic for broadband absorption across the solar spectrum. Consequently, we expect the lateral heterostructures to be promising for optimizing optoelectronic device performance by selectively tuning the energetic and spatial distributions of the bandgap.

C2.01(초)

Spin-dependent electrical transport in oxide hetero-structure

뉴엔타치, 장정원 [1], 이규준 [2], 한승주 [1], 이준성 [1], 김영헌 [3], 정명화 [2], 도용주 [1], 최만수 [1], 송종현 [4], *김진희 [3]
Thach D. N.. Ngo, Jung-Won. Chang[1], Kyujoon. Lee[2], Seungju. Han[1], Joon Sung. Lee[1], Young Heon. Kim[3], Myung-Hwa. Jung[2], Yong-Joo. Doh[1], Mahn-Soo. Choi[1], Jonghyun. Song[4], *Jinhee. KIM[3]
과학기술연합대학원 대학교.
표준과학연구원. [1] 고려대학교. [2] 서강대학교. [3] 한국표준과학연구원. [4] 충남대학교.

Keyword : perovskite oxide, oxide heterostructure, LAO/STO, TMR

Perovskite oxide heterostructures exhibit many interesting physical phenomena, including superconductivity, ferromagnetism, and ferroelectricity. Some system even shows multiples of these phenomena at the same time. Here we present electrical transport properties of heterostructured oxide interface of LAO/STO. Tunneling magnetic resistance device, utilizing LAO/STO interface, is realized and spin-dependent electrical transport properties at low temperatures are investigated. Hysteretic magnetoresistance was clearly seen and it shows strong anglular dependence with the crystallographic axis of STO.

C2.03(초)

Relativistic and Topological Dynamics of Topological Materials

*최만수, 한승주
*Mahn-Soo. Choi, Seungju. Han
고려대학교.

Keyword : topological insulator, Weyl semimetal, relativistic effects, topological dynamics

The topological materials such as topological insulators and Weyl semimetals are inherently characterized by the non-vanishing topological quantum numbers and the bulk-surface correspondence, hence topological. Another unmistakable common feature is that at low energies they are described by Lorentz-invariant relativistic Hamiltonians. A distinctive consequence was recently demonstrated by the length contraction effects on the excitation spectrum in a Lorentz boosted Majorana fermion. In this talk, I will focus on the (special and general) relativistic effects in topological materials, and seek their connections to the topological dynamics.

C3.01(초)

Topological origin of the nematicity in iron-based superconductor FeSe

*Dung-Hai Lee
*Dung-Hai. Lee
UC Berkeley.

Keyword : .

Magnetic systems which do not break spin rotation symmetry down to zero temperature, namely quantum paramagnet, has attracted strong interest in modern condensed matter physics. Finding materials in which these kind of novel magnetic states are realized is a focal point of research. In this talk I introduce a new type of quantum paramagnet and argue that it is realized in bulk FeSe.

C3.02(초)

Topological semimetal phases in spin-orbit-coupled systems

*Shuichi Murakami
*Shuichi. Murakami
Tokyo Institute of Technology.

Keyword : .

We analyze a novel type of phase transition that appears in the spin-rotationally invariant form of the underscreened Anderson Lattice Model and we obtain, with decreasing temperature, a continuous transition with opening of a gap. The novel transition is driven by the Hund's rule exchange and is promoted by interband nesting. The resulting ground state can be viewed as a combined spin and orbital density wave, in which the order parameter cannot be observed by probes that are purely sensitive to either charge or magnetism. The transition produces an anisotropy in the response to a magnetic field. The model also supports an antiferromagnetic phase which is promoted by interband nesting. We suggest that this model might describe the "Hidden Order" transition in URu2Si2. We compare the predictions of the model with experimental results.

C3.03(초)

Emergent supersymmetry and non-Fermi liquid phenomena in topological Weyl semimetals

*Hong Yao
*Hong. Yao
Tsinghua.

Keyword : .

We analyze a novel type of phase transition that appears in the spin-rotationally invariant form of the underscreened Anderson Lattice Model and we obtain, with decreasing temperature, a continuous transition with opening of a gap. The novel transition is driven by the Hund's rule exchange and is promoted by interband nesting. The resulting ground state can be viewed as a combined spin and orbital density wave, in which the order parameter cannot be observed by probes that are purely sensitive to either charge or magnetism. The transition produces an anisotropy in the response to a magnetic field. The model also supports an antiferromagnetic phase which is promoted by interband nesting. We suggest that this model might describe the "Hidden Order" transition in URu2Si2. We compare the predictions of the model with experimental results.

C4.01(초)

Enhancement of Critical Current Density in Iron-based Superconductors by Particle Irradiations

*T. Tamegai, F. Ohtake, A. Park, M. Morimoto, Y. Sun, T. Taen, S. Pyon, S. Okayasu[1], T. Kambara[2], H. Kitamura[3]
*T.. Tamegai, F.. Ohtake, A. Park. , M.. Morimoto, Y.. Sun, T.. Taen, S.. Pyon, S.. Okayasu[1], T.. Kambara[2], H.. Kitamura[3]
The University of Tokyo. [1]NIRS. [2]RIKEN. [3]JAEA.

Keyword : iron-based superconductors, critical current density, particle irradiation

Artificial defects created by irradiations of energetic particles into a superconductor can pin vortices, leading to an enhancement of critical current density (Jc). In cuprate superconductors, significant increase in Jc has been reported by proton [1] and heavy-ion irradiations [2]. We have demonstrated that 200 MeV Au irradiation into Ba(Fe,Co)2As2 is effective in creating columnar defects and enhance Jc by a factor of 5 even at the lowest temperature [3]. Similar effects have been demonstrated by 800 MeV Xe [4] and 1.4 GeV Pb irradiations [5]. The effect is even more dramatic in (Ba,K)Fe2As2. Jc as high as 6 MA/cm at 5 K has been reported in the case of 1.4 GeV Pb (BF=210 kG) [8]. We have also succeeded in enhancing Jc up to 10 MA/cm2 at 5 K by 320 MeV Au irradiation (BF=80 kG) in (Ba,K)Fe2As2 [7]. Furthermore, magnetic field dependence of Jc becomes very weak and pinning force density at 5 K and 40 kOe reaches 280 GN/m3, which is even larger than 2G-YBCO coated conductors and demonstrate a strong potential of iron-based superconductors for high-field applications. Attempts to further enhance Jc by increasing the dose [8], combining point and columnar defects, or splaying the direction of columnar defects will be also reported.

[1] L. Civale et al. Phys. Rev. Lett. 65, 1164 (1990).
[2] L. Civale et al., Phys. Rev. Lett. 67, 648 (1991).
[3] Y. Nakajima et al., Phys. Rev. B 80, 012510 (2009).
[4] T. Tamegai et al., Supercond. Sci. Technol. 25, 084008 (2012).
[5] R. Prozorov et al., Phys. Rev. B 81, 094509 (2010).
[6] L. Fang et al., Appl. Phys. Lett. 101, 012601 (2012).
[7] S. Pyon et al., Appl. Phys. Express 6, 123101 (2013).
[8] F. Ohtake et al., Physica C to be published.

C4.02(초)

Enhanced Flux-pinning Properties of $GdBa_2Cu_3O_{7-d}$ Superconducting Films by addition of $BaSnO_3$

*강병원, D.H. Tran, W.B.K. Putri, 이남훈 [1], 강원남 [2]
*Byeongwon. KANG, D.H.. Tran, W.B.K.. Putri, Nam Hun. LEE[1], Won Nam. KANG[2]
충북대학교. [1] 성균관 대학교. [2] 성균관대학교.

Keyword : GdBCO films, BSO, Critical current density, Flux pinning

We report a systematic study of field dependence of the critical current density of $GdBa_2Cu_3O_{7-d}$ (GdBCO) superconducting films with the addition of $BaSnO_3$ (BSO). Magnetization J_c's at different temperatures were obtained in both pure and 2 wt. % BSO-added GdBCO films with film thicknesses varying from 0.2 micro-m to 1.5 micro-m by using a pulsed laser deposition (PLD) technique. For pure GdBCO, the a values of the power-law relationship in the intermediate-field region were estimated to be a ~ 0.48-0.52 for both the thin- and the thick-film regions, which is in good agreement with the collective pinning theory of uncorrelated defects. A smaller value of a ~ 0.35 obtained for the 0.6 micron-thick film suggests a sudden increase in the pinning centers due to the evolution of a-axis oriented grains on the surface of the film. On the other hand, the a values of the BSO-added GdBCO films were estimated to be a ~ 0.31-0.33 for an entire film thickness range indicating that more effective pinning is induced by the BSO addition. Based on the thickness scaling of pinning force density and ion milling analyses, the enhanced pinning may be attributed to the formation of meandering grain boundaries through the film thickness of the BSO-added GdBCO films.

C4.03(초)

Pressure Evolution of the Critical Current Density for FeSe Single Crystals

*정순길, 강지훈, 박은성, 이상연, Jiunn-Yuan Lin[1], Dmitriy A. Chareev[2], Alexander N. Vasiliev[3], 박두선
*Soon-Gil. Jung, Ji Hoon. Kang, Eunsung. Park, SANG YUN. LEE, Jiunn-Yuan. Lin[1], Dmitriy A.. Chareev[2], Alexander N.. Vasiliev[3], Tuson. Park
성균관대학교. [1]National Chiao Tung University. [2]Russian Academy of Science. [3]Moscow State University.

Keyword : FeSe, critical current density, pressure, pinning mechanism

The binary Fe-based superconductor FeSe has attracted a great interest in part due to the significantly controllable superconducting transition temperature (T_c). The bulk T_c of 10 K increases up to 37 K by external pressure, while a tremendously high T_c above 100 K has been reported in FeSe monolayer, presenting its possibility for technological applications [1,2]. Critical current density (J_c) in superconductors is one of the most important factors for practical applications, and therefore investigation into the evolution of J_c with an increase in T_c is important. Here, we present the evolution of J_c for FeSe single crystals under pressure up to 2.4 GPa. The J_f determined as the onset of the free-flux flow regime monotonically increases with increasing T_c, whereas the J_c obtained from the criterion of 1 μV, corresponding to depinning current density, is not consistent with enhanced T_c. Interestingly, J_c showed a sudden enhancement at 1.22 GPa at which antiferromagnetic ordering emerges, whereas J_c at 2.4 GPa showed a decreasing feature despite an increase of T_c, considered due to disappearance of structure transition ~ 2.1 GPa. In addition, below 1.22 GPa the spatial variations of superconducting transition temperature (δT_c-pinning) play a main role for the J_c, while at higher pressures the spatial variations of charge carrier mean free path (l) fluctuations (δl-pinning) become important. These observations underline that the origin of the anomalous enhancement in J_c is closely tied to the pressure-induced antiferromagnetism.

[1] S. Medvedev et al. Electronic and magnetic phase diagram of β-$Fe_{1.01}Se$ with superconductivity at 36.7 K under pressure. Nature Mater. 8, 630-633, (2009).
[2] J.-F. Ge et al. Superconductivity above 100 K in single-layer FeSe films on doped $SrTiO_3$. Nature Mater. Doi:10.1038/NMAT4153 (2014).

C4.04(초)

Vortex dynamics in superconducting single crystals $NaFe_{1-x}Co_xAs$

*권용성, 다우드 아메드, 최우재, 서유일, 김영철 [1]
*Yong Seung. Kwon, Dawood. Ahmad, Woo Jae. Choi, Yu Il. Seo, Y. C.. Kim[1]
DGIST. [1] *부산대학교.*

Keyword : $NaFe_{1-x}Co_xAs$, Superconductivity, thermal fluctuation, vortex dynamics

We have studied on the fluctuation effect and the vortex dynamics in superconducting single crystals $NaFe_{1-x}Co_xAs$ (x = 0.01, 0.03, and 0.07). The superconducting fluctuations were analyzed through in-out-plane paraconductivity and magnetoconductivity in $NaFe_{1-x}Co_xAs$ single crystals. The Ginzburg-Landau and Lawrence-Doniach approaches were applied on the magnetoconductivity data of $NaFe_{1-x}Co_xAs$ single crystals well above their T_c. The results showed that the coherence lengths depend on the Co doping level. In particular, the transverse coherence length decreases on entering in the overdoped (x >0.07) region which justifies a 3D-2D transition in the overdoped sample. Furthermore, for the optimal doped sample (x = 0.03), x_c was estimated to be 2nm which is larger than the value for overdoped sample (0.2nm) thus indicated the 3D anisotropic superconductor. The field dependence magnetic hysteresis of the series samples showed that the secondary peak (SP) gets prominent from under doped to optimal doped region however less pronounced in the over doped region. We found large critical current density J_c in the optimal doped sample. Furthermore, from the time dependence magnetization, the analysis of the vortex dynamics supports a crossover from plastic creeping to collective pinning in the optimal doped region which justifies the prominent secondary peak (SP) in the sample.

C5.01(초)

Spin Hall magnetoresistance and its correlation to the spin-orbit torque in W/CoFeB/MgO structures

*박병국, 백승헌, 조영훈 [1], 조순하
*Byong Guk. Park, Seung-heon Chris. Baek, Younghun. Jo[1], Soonha. Cho
KAIST. [1]KBSI.

Keyword : Spin-orbit coupling, Spin Hall magnetoresistance, spin-orbit torque

We report a systematic study of the magnetoresistance (MR) of the W/CoFeB/MgO structures and its correlation to the current-induced torque to the magnetization. We observe that the MR is independent of the angle between magnetization and current direction, but is determined by the relative magnetization orientation with respect to the spin direction accumulated by spin Hall effect, which is the same symmetry of so-called spin Hall magnetoresistance. The MR of ~1% in W/CoFeB/MgO samples is considerably larger than those in other structures of Ta/CoFeB/MgO or Pt/Co/AlOx, which indicates a larger spin Hall angle of W. Moreover, the similar W thickness dependence of the MR and the current-induced magnetization switching efficiency demonstrates that they share the same underlying physics, which allows one to utilize the MR in non-magnet/ferromagnet structure in order to understand closely related other spin-orbit coupling effects such as inverse spin Hall effect, spin-orbit spin transfer torques, etc.

C5.02(초)

Domain Wall Manipulation using Spin Currents and Fields

*R. M. Reeve, J.-S. Kim, M.-A. Mawass, A. Bisig, T. Schulz, F. Büttner, A. Kronenberg, B. Krüger, M. Jourdan, M. Kläui
*R. M.. Reeve, J.-S.. Kim, M.-A.. Mawass, A.. Bisig, T.. Schulz, F.. Büttner, A.. Kronenberg, B.. Krüger, M.. Jourdan, M.. Kläui
Johannes Gutenberg-Universität Mainz.

Keyword : Domain wall, Scanning transmission X-ray microscopy

For improved functionalities and efficiencies of spintronic devices based on domain walls (DWs), novel approaches for manipulating magnetization states need to be understood. In particular ways to displace multiple DWs synchronously are required, which is not possible with conventional field induced motion. Here we present a radical new scheme which achieves this for a fixed chirality of transverse DWs, through the application of out-of-plane field pulses. Asymmetric pulses combined with tailored pinning potentials suppress back-ward motion of the DWs and provide net displacement. An experimental demonstration is provided through direct scanning transmission X-ray microscopy imaging [Nat. Commun. 5, 3429]. Spin currents (SCs) can also manipulate DWs efficiently, for instance using a non-local spin valve. To generate larger SCs and improve efficiencies highly spin polarized electrodes are attractive. We study electrically and thermally generated SCs in Co2MnSi/Cu structures. Measurements of the signal vs. temperature reveal a different behaviour in each case, demonstrating that it is not only the spin transport in the non-magnetic channel which plays a role but that additionally the spin injection mechanism contributes significantly [Appl. Phys. Lett. In Press; arXiv:1507.04868].

C5.03(초)

Huge negative spin-transfer torque in atomically thin Co layers and demonstration of magnetic Bubblecade memory

*최석봉, Soong-Geun Je, Kyoung-Woong Moon[1], Sang-Cheol Yoo, Duck-Ho Kim, Joo-Sung Kim, Joon Moon, Byoung-Chul Min[2], Chanyong Hwang[1]
*Sug-Bong. Choe, Soong-Geun. Je, Kyoung-Woong. Moon[1], Sang-Cheol. Yoo, Duck-Ho. Kim, Joo-Sung. Kim, Joon. Moon, Byoung-Chul. Min[2], Chanyong. Hwang[1]
Seoul National University. [1]Korea Research Institute of Standards and Science. [2]Korea Institute of Science and Technology.

Keyword : Spin Transfer Torque, Spin Orbit Torque, Bybblecade Memory

In the last decade, there have been remarkable advances in the study of current-induced domain wall (DW) motion as the key operation principle of emerging memory and logic devices. As the major driving mechanism of the DW motion, spin-orbit torque (SOT) with chiral DWs draws great attention nowadays, which explains the direction of DW motions in heavy metal/transition metal/oxide films. However, here we demonstrate that the spin-transfer torque (STT) is significantly enhanced in ultra-thin Co films sandwiched by Pt layers and consequently, plays a major role in determining the direction of DW motions. Such significant enhancement is attributed to the ultra-narrow DW width down to about 1 nm, which considerably boosts up the nonadiabaticity of the conduction electrons. Moreover, the sign of the enhanced STT is found to be negative, possibly caused by either a negative nonadiabaticity or a negative spin polarization, which results in the DW motion along the current direction. The detailed experimental procedures and results will be discussed.
In the second part of the talk, we demonstrate a new scheme for unidirectional motion of magnetic DWs without any current injection or structural modulation. This scheme utilizes the recently discovered chiral DWs induced by the Dzyaloshinskii-Moriya interaction (DMI), which exhibit asymmetry in their speed with respect to magnetic fields. Because of this asymmetry, an alternating magnetic field results in the coherent motion of the domain walls in one direction. Such coherent unidirectional motion is achieved even for an array of magnetic bubble domains, enabling the design of a new device prototype—magnetic bubblecade memory—with two-dimensional data-storage capability.

C5.04(초)

Static and Dynamic Properties of Skyrmions in Nanostructured Multilayers

*B. Krüger
*B.. Krüger
Johannes Gutenberg-Universität Mainz.

Keyword : Skyrmion, Pump-probe X-ray holography, The Dzyaloshinskii-Moriya interaction

In nano patterned magnetic thin-film elements highly stable topological defect spin structures such as Skyrmions emerge. They exhibit the dynamics of a composite quasi-particle which is of key importance for applications.
We study the properties of Skyrmions in thin multi layers. For the GHz gyrotropic motion it is found that the Skyrmion shows inertia [1] with a small dependence on the size of the film element and the pining strength [2]. Experimentally we track the motion of a Skyrmion with 3 nm accuracy using pump-probe X-ray holography and report the first experimental observation of the GHz gyrotropic motion of a Skyrmion. From a fit with the analytical model [1], we are able to deduce the inertial mass of the magnetic Skyrmion that is much larger than in any other magnetic system [2]. This high effective mass is also important for the displacement in a wire. We calculate the trajectories of Skyrmions with different masses. For Skyrmions with Dzyaloshinskii-Moriya interaction, the dynamics due to spin orbit torques was simulated and compared with first experimental results of a Skyrmion racetrack device [3].

References:
[1] I. Makhfudz et al., Phys. Rev. Lett. 109, 217201 (2012).
[2] F. Büttner et al., Nature Phys. 11, 225 (2015).
[3] S. Woo et al., arXiv:1502.07376 (2015).

C6.01(초)

InGaN Nano-Solar Cells with High Short-Circuit Current

*서혜원, Mehmet F. Cansizoglu[1]
*Hye-Won. Seo, Mehmet. Cansizoglu[1]
제주대학교. [1]University of Arkansas at Little Rock.

Keyword : InGaN, Solar cell, Nanorod, Nanowire

We have successfully grown nanostructured InGaN solar cells of Eg=~2.2 eV using plasma-assisted molecular beam epitaxy methods. By optimizing the nitrogen plasma power, III-V ratio, and substrate temperature, the high-qaulity P-i-N nitride nanorod was achieved. The glancing angle deposition and small angle deposition process were adapted to grow a continuous transparent oxide layers as metal contact. A short circuit current density of 4.6 mA/cm^2, an open circuit voltage of 0.22 V and a fill factor of 34% with a power conversion efficiency of 0.5% under 1 sun illumination was observed. The excellent photo-induced current density in the InGaN nanorod solar cells is attributed to the strain-free nature as well as the enhanced light concentration effects in the nanorod configuration.

C6.02*

Photocurrent of monolayer MoS_2 as a function of back gate bias

*이진희, Hamza Zad Gul, 김정호 [1], 김현 [2], 최호민, 이영희 [1], 임성주
*Jin-hee. Lee, Hamza Zad. Gul, Jung Ho. Kim[1], Hyun. Kim[2], Ho min. Choi, Young Hee. LEE[1], Seong-Chu. LIM
성균관대학교 나노구조물리연구단. [1] 성균관대학교. [2]IBS 나노구조물리연구단 성균관대학교.

Keyword : "Molybdenum disulfide (MoS_2)", "Photocurrent", "Metal-to-insultor(MIT) transition"

Molybdenum disulfide (MoS_2) is a 2-dimensional semiconductor and has exhibited metal-to-insulator transition depending on carrier concentration that can be modulated by a gate bias. Therefore, the optical property is also subject to change as a function of back gate bias. In this work, the photocurrent of MoS_2 is studied in two different regimes; semiconductor and metal. The optical behaviors of both semiconducting and metallic MoS_2 will be discussed in this presentation.

C6.03*

Polarization dependence of Raman spectra of WTe_2

*한송희, 김민정, 이재웅, 정현식
*Songhee. Han, Minjung. Kim, Jae-Ung. Lee, Hyeonsik. Cheong
서강대학교.

Keyword : Tungsten ditelluride (WTe_2), Raman spectroscopy, Low frequency, Polarization, Transition metal dichalcogenide (TMD)

Tungsten ditelluride (WTe_2) is a layered material with the Td structure which has a distorted orthorhombic phase. It has attracted interest owing to large, non-saturating magnetoresistance which can be applied for the information storage area. [1, 2] The large magnetoresistance is related with its Td structure. Therefore understanding the lattice dynamics is an important key to the study of WTe_2. [3]

Raman scattering measurements on WTe_2 have been reported, but the incident polarization dependence and low frequency measurements of Raman spectra have not been studied yet. We measured the Raman spectra of WTe_2 in the low frequency region. WTe_2 with the Td structure shows strong dependence on the incident laser polarization. We discovered new peaks which have not been observed. We also identified the Raman mode of each peak by comparing both the incident and the analyzer polarization dependence of the Raman spectrum.

[1] Mazhar N. Ali, Jun Xiong, Steven Flynn, Jing Tao, Quinn D. Gibson, Leslie M. Schoop, Tian Liang, Neel Haldolaarachchige, Max Hirschberger,N. P.Ong and R. J.Cava1, Nature 514, 13763 (2014).
[2] W.-D. Kong, S.-F. Wu, P. Richard, C.-S. Lian, J.-T. Wang, C.-L. Yang, Y.-G. Shi, and H. Ding, Applied Physics Letters 106, 081906 (2015).

C6.04*

Raman scattering studies of CIGSS/Mo interface under various annealing temperature in sulfurization process

*트랑, 문한결, 김지영, 조윌렴, 양정엽 [1], Junggyu Nam[1], 이동호 [1], 김동섭 [1], 권민수 [2], 전찬욱 [2], 윤석현
*Thi Thu Trang. Nguyen, Han kyoul. Moon, Geeyeong. Kim, William. JO, JungYup. Yang[1], Junggyu. Nam[1], Dong Ho. Lee[1], Dong seop. Kim[1], Min su. Kwon[2], Chan Wook. Jeon[2], Seokhyun. Yoon
이화여자대학교. [1]Samsung SDI. [2] 영남대학교.

Keyword : CIGSSe, Raman Spectroscopy, Sulfurization/Selenization

$CuInGa(S,Se)_2$ has many advantages in quaternary semiconductor-based absorber solar cell fabrication such as low cost and potential high efficiency. For example, Yang et al have achieved good results in fabricating CIGSSe solar cells modules with high efficiency by with a frameless glass to glass (G2G) of 15% or sulfurization/selenizattion with Cd-free buffer of 18% [1,2]. Recently, Raman scattering spectroscopy has been actively applied to study optical properties of CIGSSe thin film solar cells. In this study, we present Raman scattering results of $CuInGa(S,Se)_2$ (CIGSSe) thin films prepared by a two-step sputter and selenization/sulfurization method. The sulfurization processes were conducted in various annealing temperatures of 570 °C, 580 °C, and 590 °C as prepared by Yang group [3]. We observed phonons of CIGSSe (A_1 mode at 188 cm^{-1}) and CIGS (A_1 mode at 287 cm^{-1}) at the surface of thin films and also observed, with increased annealing temperature, the shift of the CIGSSe peak that is related to the Ga contents. We also studied the spatial variation of the samples by measuring Raman spectra near the front surface and near CIGSSe/Mo interface regions that were cut by a dimpling method. We observed the red shift of the CIGSSe A_1 mode at near surface for all films, which indicates decreasing of Ga contents near the absorber region. However, near interface, there was no frequency shift of the CIGSSe peak observed and A_1 mode of the CIGS peak disappeared. We also found that with the higher annealing temperature, the energy of the CIGSSe peak was higher and showed the Ga-rich CIGSSe phase. On the other hand, from the Raman spectra, the secondary phase of $Cu_{2-x}Se$ was least observed in the sample with the annealing temperature of 580 °C, which indicates the best material with intrinsic properties of the CIGSSe phase would be this sample. These results are also completely consistent with local electrical measurements that show the best annealing temperature for the sulfurization that provides the highest efficiency of 15% among three samples with different annealing temperatures is 580 °C [3].

[1] J. Y. Yang, D. Lee, D. H. Baek, D. Kim, J. Nam, G. Y. Kim, and P. H. Huh, RSC Advances 5, 51258 (2015).
[2] J. Nam, Y. Kang, D. Lee, J. Y. Yang, Y. S. Kim, C. B. Mo, S. Park, and D. Kim, Progress in Photovoltaics: Research and Application (2015) (online version, DOI: 10.1002/pip.2653).
[3] J. Y. Yang, D. Lee, K. S. Huh, S. J. Jung, J. W. Lee, H. C. Lee, D. H. Baek, B. J. Kim, D. Kim, J. Nam, G. Y. Kim, and W. Jo, RSC Advances 5, 40719 (2015).

C6.05*

Two-dimensional photonic crystal band-edge laser using colloidal quantum dots as gain material

*장호준, 이명재, 강민수, 민경택, 전헌수 [1]
*Hojun. Chang, Myungjae. Lee, Minsu. Kang, Kyungtaek. Min, Heon Su. JEON[1]
서울대학교 물리천문학부. [1] *서울대학교 생물물리 및 화학생물학과.*

Keyword : quantum dot, photonic crystal, band-edge laser, square lattice, M-point

core-shell 형태의 콜로이드 양자점은 넓은 파장 영역에 걸쳐 밴드갭을 튜닝할 수 있는 효율적인 발광 물질로 에피택시 증착법을 이용하여 성장한 반도체 물질을 대체할 수 있을 뿐만 아니라, 새로운 개념의 광소자 디자인과 제작에 응용할 수 있다. 본 연구에서는 고밀도의 양자점막을 광 이득 물질로 이용하여 이차원 광자결정 띠가장자리 레이저를 제작하였다. 광자결정 구조는 SiN (n ~ 2.01) 과 SiO_2 (n ~ 1.475) 로 이루어진 비대칭 슬랩 구조로 제작하되 FDTD 방법을 통하여, 간단한 square lattice 구조로 M-point 에서 air-band 에 해당하는 띠가장자리 모드를 가지도록 디자인 되었다. e-beam lithography 와 reactive ion etching 방법으로 다양한 지름의 2 차원으로 배열된 air-hole 광자결정을 제작하였다. 주기 255 nm, air-hole diameter 60 ~ 150 nm, SiN slab 두께 140 nm 의 광자결정 구조 위에 콜로이드 양자점을 스핀 코팅으로 도포하여 발광체로 작용하도록 하였다. 완성된 SiN-양자점 2 차원 광자결정 구조를 532 nm 펄스 레이저 (frequency-doubled Nd:YAG; repetition rate = 1 kHz, pulse duration ~ 400 psec.) 로 펌핑하여 630 nm 부근에서 단일 모드 레이저로 동작함을 확인하였다.

C6.06*

Improvement of polypyrrole nanowire device by plasmonic space charge generation: high photocurrent and wide spectral response by Ag nanoparticle decoration

*이승훈, 장재원
*Seung-Hoon. Lee, Jae-Won. Jang
부경대학교.

Keyword : "localized surface plasmon resonance", "space charge","polypyrrole", "nanowire", "photoccurent"

Improvement of opto-electronic properties of non-single crystallized nanowire devices with space charges generated by localized surface plasmon resonance (LSPR) is demonstrated. Photocurrent and spectral response of single polypyrrole (PPy) nanowire (NW) devices are improved by electrostatically attached Ag nanoparticles (Ag NPs). The improved photocurrent efficiency and spectral response are resulted from space charges generated by LSPR of Ag NPs. In addition, increasing exponent (m) of photocurrent ($J_{PC} \sim V^m$) and finite-differential time domain (FDTD) simulation are investigated for enlarged space charge region at the interface of PPy NW. These results prove that performance of non-single crystallized polymer nanowire devices can be improved by plasmonic enhancement.

C6.07*

은 나노 홀 어레이의 특이 광 투과 현상과 플라즈몬 에너지 밴드 구조 연구

*송보경, 한승훈, 조창희
*Bokyung. Song, Seunghoon. Han, Chang-Hee. Cho
DGIST.

Keyword : "표면 플라즈몬 폴라리톤", "특이 광 투과", "은 나노 홀 어레이", "에너지 밴드"

특이 광 투과 현상은 빛의 파장보다 작은 크기를 갖는 금속 홀 어레이를 통해 특정 파장대에서 큰 광투과도를 보이는 현상이다. 이 현상은 바이오 센서 [1], 컬러 필터 [2], 투명 전극 [3] 등 응용 가능한 분야가 넓기 때문에 기본적인 투과 메커니즘에 대해 이해하는 것은 매우 중요하다. 하지만 특이 광 투과 현상을 이해하기 위한 많은 연구들이 이루어지고 있음에도 불구하고 [4-6], 아직까지 그 메커니즘이 명확하게 밝혀지지 않고 있다. 따라서 본 연구에서는 특이 광 투과 현상이 표면 플라즈몬 폴라리톤과 밀접한 관련이 있다는 사실을 기반으로 표면 플라즈몬 폴라리톤의 에너지 밴드 구조를 통해 특이 광 투과 현상의 투과 특성을 분석하였다. 다양한 주기에 따른 은 나노 홀 어레이를 실험적으로 구현하여 광 투과 특성을 측정하였으며, 이는 이론적 모델을 통해 계산된 투과 특성과 일치함을 확인하였다. 또한 플라즈몬 폴라리톤의 에너지 밴드 구조를 계산함으로써 투과 스펙트럼과의 상관 관계에 대해 비교 분석을 하였다. [1] A. J. Haes et al., A localized surface plasmon resonance biosensor: First steps toward an assay for Alzheimer's disease, Nano Letters 4, 1029 (2004).

[2] D. Inoue et al., Polarization independent visible color filter comprising an aluminum film with surface-plasmon enhanced transmission through a subwavelength array of holes, Applied Physics Letters 98, 093113 (2011).

[3] J. Van de Groep et al., Transparent conducting silver nanowire networks, Nano Letters 12, 3138 (2012).

[4] E. Popov et al., Theory of light transmission through subwavelength periodic hole arrays, Physical Review B 62, 16100 (2000).

[5] L. Martin-Moreno et al., Theory of extraordinary optical transmission through subwavelength hole arrays, Physical Review Letters 86, 1114 (2001).

[6] S. H. Chang et al., Surface plasmon generation and light transmission by isolated nanoholes and arrays of nanoholes in thin metal films, Optics Express 13, 3150 (2005).

C6.08*

Structural, electrical and optical properties of proton-bombarded ZnO Nanorods

*박창인, 김정란, 황인희, 손재관, 한상욱
*Chang In. Park, ZHEN LAN. JIN, Inhee. Hwang, jaekuan. son, Sang Wook. Han
Jeonbuk National University.

Keyword : "ZnO nanords","proton bombardment","XAFS","I-V measurements","photoluminescence"

We investigated the structural and the electrical properties of proton-beam-bombarded ZnO nanorods. Vertically-aligned ZnO nanorods were synthesized on Al_2O_3 substrates by using a catalyst-free metal organic chemical vapor deposition (MOCVD). ZnO nanorods were bombarded by proton beam at energies of 10 ~ 40 MeV and fluxes of 1×10^{11} - 1×10^{12} particles/cm^2. Field-emission scanning electron microscopy (FE-SEM) measurements showed no visible distortion on the ZnO nanorods after proton-beam bombardment. High-resolution X-ray diffraction measurements (HR-XRD) demonstrated a small but substantial amount of lattice constant distortion in ZnO nanorods, compared with untouched ZnO nanorods. Polarization-dependent extended X-ray absorption fine structure (EXAFS) revealed that the bond length of Zn-O pairs along the c-axis of ZnO nanorods were more distorted than other atomic pairs. Photoluminescence revealed that optical properties of ZnO nanorods are changed as proton bombarded flux. From I-V measurements, we found that the electrical properties of proton-bombarded ZnO nanorods were enhanced by at least 5 time than that of untouched ZnO nanorods. Also, we will discuss annealing effect of the electrical property change of proton-bombarded ZnO nanorods.

C7.01(초)

나노 스케일 메타물질을 이용한 초고감도 테라헤르츠 분자 센서

*서민아
*Minah. Seo
한국과학기술연구원.

Keyword : 테라헤르츠 분광법, 메타물질, 나노 플라즈모닉스, 분자인식

테라헤르츠파 (Terahertz wave)는 가시광이나 적외선보다 파장이 길어 침투깊이가 길고 에너지는 낮아 비이온화 특성을 지니며 비파괴 검사에 이용될 수 있다. 특히 펄스 형태의 테라헤르츠파는 넓은 스펙트럼 영역에 존재하는 유기물이나 생화학 분자 고유의 진동 주파수를 구별하는 분광에 널리 이용되어 왔다. 그러나 기존의 전형적인 테라헤르츠파 분광법으로는 검출 대상의 농도가 매우 높을 경우에만 검출이 가능해 그 민감도를 높이는 연구가 매우 절실한 상황이다. 최근 들어 활발한 연구가 진행되고 있는 메타물질 (metamaterial)은 기존의 분광법의 성능을 향상시켜 관련 연구에 더욱 박차를 가할 것으로 큰 기대를 모으고 있다. 나노 스케일 플라즈모닉 구조 기반 메타물질을 이용하여 선택적으로 특정 주파수에서의 민감도를 극대화시키고 테라헤르츠 분광법 고유의 분자인식 특성을 활용하는 고감도 고선택성 테라헤르츠 분광법 응용에 대하여 자세하게 소개하고자 한다. 이러한 테라헤르츠 고감도 고선택성 센싱 기술을 이용하여 분자 구조가 비슷하여 저농도에서 구별이 어려운 것으로 알려진 당류를 수 밀리몰 (mM) 농도에서 선택적으로 검출 (그림) 할 수 있음을 보였다.

C7.02(초)

Scattering characteristics of metal and dielectric optical nanoantennas

*서민교, 이호석, 이은광, 김진형, 송정환
*Min Kyo. Seo, Ho Seok. Ee, Eun-Kwang. Lee, Jinhyung. Kim, Jung Hwan. Song
KAIST.

Keyword : plasmonics,optical antenna,scattering,far-field,near-field

Optical resonances of metallic or dielectric nanoantennas enable to effectively convert free-propagating electromagnetic waves to localized electromagnetic fields and vice versa. Plasmonic resonances of metal nanoantennas extremely modify the local density of optical states beyond the optical diffraction limit and thus facilitate highly-efficient light-emitting, nonlinear signal conversion, photovoltaics, and optical trapping. The leaky-mode resonances, or termed Mie resonances, allow dielectric nanoantennas to have a compact size even less than the wavelength scale. The dielectric nanoantennas exhibiting low optical losses and supporting both electric and magnetic resonances provide an alternative to their metallic counterparts. To extend the utility of metal and dielectric nanoantennas in further applications, e.g. metasurfaces and metamaterials, it is required to understand and engineer their scattering characteristics. At first, we characterize resonant plasmonic antenna radiations of a single-crystalline Ag nanowire over a wide spectral range from visible to near infrared regions. Dark-field optical microscope and direct far-field scanning measurements successfully identify the FP resonances and mode matching conditions of the antenna radiation, and reveal the mutual relation between the SPP dispersion and the far-field antenna radiation. Secondly, we perform a systematical study on resonant scattering properties of high-refractive-index dielectric nanoantennas. In this research, we examined Si nanoblock and electron-beam induced deposition (EBID) carbonaceous nanorod structures. Scattering spectra of the transverse-electric (TE) and transverse-magnetic (TM) leaky-mode resonances are measured by dark-field microscope spectroscopy. The leaky-mode resonances result a large scattering cross section approaching the theoretical single-channel scattering limit, and their wide tuning ranges enable vivid structural color generation over the full visible spectrum range from blue to green, yellow, and red. In particular, the lowest-order TM01 mode overcomes the diffraction limit. The finite-difference time-domain method and modal dispersion model successfully reproduce the experimental results.

C7.03(초)

Invisible Hyperbolic Metamaterial Nanotube

*박홍규, 김경호, 노유신
*Hong-Gyu. Park, Kyoung-Ho. Kim, You-Shin. No
고려대학교.

Keyword : metamaterial, nanowire

The suppression of the visibility of an object is one of the most exciting optical phenomena and attracts wide attention for developing camouflages or invisible sensors. In this talk, I will propose a low scattering metal/dielectric layered nanotube in the visible wavelength regime. To elucidate the low scattering, the layered nanotube is described as a radial anisotropic hyperbolic metamaterial nanotube, and the light scattering is analyzed. From the light scattering analysis, the near zero effective permittivity in angular direction of the hyperbolic nanotube dominates the low scattering characteristics. Such findings will be useful for invisible nanotube applications.

C7.04(초)

Plasmon-manipulated optical emission and transmission in nanostructured systems

*조창희
*Chang Hee. Cho
대구경북과학기술원.

Keyword : "Plasmonics", "Nanocavity"

Plasmonic materials are stimulating the intense activity in the area of photonics due to their unique ability of tailoring the optoelectronic properties. In particular, controlling the optical emission and transmission properties of materials with engineered structures has been of great importance for understanding the underlying physics and designing new optoelectronic devices. At first, we will discuss the non-thermalized hot luminescence in single semiconductor nanowires coupled with plasmon nanocavities, which is absent for simple photonic semiconductor nanowires. By tuning the plasmonic cavity size to match the cavity mode resonances, an almost complete transition from thermalized luminescence to hot luminescence was achieved, which reflects exceptionally high radiative rate enhancement. Time-resolved measurements for the plasmonic semiconductors showed the excited-state lifetime shortening by a factor of 1000, resulting in sub-picosecond lifetimes. Finally, we will discuss the extraordinary optical transmission in Ag nano-hole array with variable periods, which allow us to study the evolution of the optical transmission through the Ag nano-hole array as a function of the period. The spectral features in the optical transmission were measured to be sensitively changed with the period, and the measured spectra were correctly reproduced by the simulated optical transmission using finite-difference time-domain (FDTD) method. To obtain further insights into the extraordinary optical transmission in the Ag nano-hole array, we calculated the dispersion of surface plasmon polaritons, confirming the evolution of energy band structure with varying the period of nano-hole array. The comparative study between the transmission spectra and the plasmon dispersions clearly showed that the extraordinary optical transmission phenomena are directly correlated with the band structure of surface plasmon polaritons.

C7.05(초)

Control of multiple-scattered surface plasmon polaritons in disordered nanostructures

*최원식
*Wonshik. Choi
고려대학교.

Keyword : surface plasmon polaritons, wave front shaping, disordered media

Multiple light scattering occurring in a scattering medium poses problems in photonics applications as it obstructs imaging targets embedded in the medium and attenuates wave energy delivered to the targets. If properly controlled, however, they can be used to improve the functionalities of conventional optical elements. In this talk, I will introduce experimental methods that make use of the multiple-scattered suface plasmon polaritons in nano-plasmonic devices. Specifically, we performed wave front shaping of the far-field incident waves to a disordered array of nanoholes in the metal surface and demonstrated that we can control the shape of plasmonc waves and maximize their total intensity. Our study may provide an additional control to the optoelectronics to bridge the gap between the photonics and electronics.

C8.02

Projectile fragmentation cross sections at 140 MeV/n simulated by a transport model

*김경일, 김영만, 이강석 [1]
*Kyungil. Kim, Youngman. Kim, Kang Seog. Lee[1]
RISP. IBS. [1] *전남대학교.*

Keyword : QMD, Transport model, Projectile fragmentaion

We calculate projectile fragmentation cross sections at 140 MeV/n using a new QMD-type transport code. We write the new transport code and test it. At first, to examine the stability of an initialized nucleus, we check variation of its radius and binding energy during time evolution. To realize the fermionic nature of the nucleons in a nucleus, we try to implement a simplified Pauli blocking method. Then, we simulate nucleus-nucleus collisions at 140 MeV/n with well-initialized nuclei. The obtained cross sections are compared with experimental data and are analyzed according to impact parameter. We discuss the relevance of the code as an event generator and the future plan to improve the fermionic nature of nucleons in the code.

C8.03

Photonuclear reaction of molybdenum isotopes

Dong Yoon Han, B.S. Ishkhanov, A.A. Kuznetsov
Dong Yoon. Han, Boris. Ishkhanov, Alexander. Kuznetsov
Lomonosov Moscow State University.

Keyword : molybdenum isotopes, photonuclear reaction, excited states of nuclei

In order to investigate molybdenum's photodisintegration, experiments were conducted by gamma activation methods[1], using RTM-70 accelerator. Natural mixture of molybdenum isotopes was irradiated by bremsstrahlung photons under maximum energy of electrons 19.5, 29.1 and 67.7 MeV. As a result of these photonuclear reactions, accompanying ejection of maximum 4 neutrons, Mo, Nb isotopes were created. Their relative yields, that were normalized by yield of reaction $^{100}Mo(\gamma,n)^{99}Mo$, were calculated and compared with the theoretical calculation. This theoretical calculation is based on "Combined model of photonuclear reaction"[2], which was developed in Skobeltsyn Institute of Nuclear Physics, Lomonosov Moscow State University. The comparison shows that the theoretical model well describes the experimental results of photonuclear reactions for all molybdenum isotopes. As the mass number of molybdenum isotopes decreases, proton ejection threshold steeply decreases, accordingly the yield of photoproton reaction hardly increases and that of photoneutron reaction hardly decreases. This can be interpreted on the basis of shell structure of molybdenum.

1. Belyshev S. S., Ermakov A. N., Ishkhanov B. S. et al. // Nucl.Instrum. and Meth. in Phys. Res. Sect. A 745,133-137(2014)
2. Ishkhanov B.S., Orlin V.N. // Phys. Atom. Nucl. 74, 19 (2011)

C8.04*

소형가속기를 이용한 중성자 발생장치 전산모사 연구

*김정호, 문명국 [1], 허민구 [1], 이승욱
*Jeong Ho. Kim, MOON Myung Kook. [1], Min Goo. Hur[1], Seung Wook. Lee
부산대학교. [1] 한국원자력연구원.

Keyword : Cyclotron, Geant4, Compact Neutron Source, Neutron Radiography

중성자 영상(neutron radiography)을 위한 선원으로서 양성자 가속기의 이용가치는 매우 높다. 본 논문에서는 13 MeV 급 소형 사이클로트론을 이용하여 영상획득용 중성자 선원으로서의 타당성을 검증하고, 중성자 발생 표적에 대한 최적화 연구를 수행하였다. 양질의 중성자 영상을 얻기 위해서는 충분한 중성자속(neutron flux)과 적합한 에너지 분포(neutron energy spectrum)의 분석이 필수적이다. 본 연구에서는 Geant4 코드를 활용한 몬테 카를로 기법(Monte Carlo method)을 이용하여 발생된 중성자 빔의 표적 설계에 대한 의존성을 확인하였다. 베릴륨 층(Beryllium Layer), 금속층(metal layer), 아퍼쳐(Aperture) 그리고 냉각장치(cooling system)로 구성된 표적에 대하여, 서로 다른 두께와 아퍼쳐 직경의 조합에 대한 전산모사를 수행하였다. 표적으로부터 3m 거리에서 1.0E+03 이상의 중성자속을 얻을 수 있었으며, 이는 긴 노출시간 하에서 제한적으로 중성자 영상에 사용가능한 양이다.

C8.05

Neutrino-Nucleus quasielastic scatterings with Relativistic Fermi Gas model in the context of recent MiniBooNe and NOMAD experiments

*양길석, 천명기, 김경식 [1]
*Ghil-Seok. Yang, Myung-ki. CHEOUN, Kyungsik. KIM[1]
숭실대학교. [1] *한국항공대학교.*

Keyword : neutrions, relativistic fermi gas model, quasielastic scatterings, MiniBooNE, NOMAD

We investigated the neutrino and antineutrino quasielastic scatterings on the nucleon of the recent MiniBooNE and NOMAD experiments for Neutral Current (NC) and Charged Current (CC) processes. The CC differential and total cross sections are used to extract the value of the axial mass depending on the incident neutrino energy and the NC observables are taken into account in determining the values of the strangeness couplings as like g_A^s and μ_s. The properties of relevant observables and the applicable studies will be discussed.

C8.06

Long-range dynamic polarization potentials for ^{11}Li + ^{208}Pb and ^{6}He + ^{208}Pb systems

*최기석, 소운영 [1], 김경식 [2], 천명기
*Ki-Seok. Choi, WOON YOUNG. SO[1], Kyungsik. KIM[2], Myung-ki. CHEOUN
숭실대학교. [1] 강원대학교. [2] 한국항공대학교.

Keyword : dynamic polarization potential, Halo nuclei, elastic scattering

We investigate the effects of long-range dynamic polarization on elastic cross sections for heavy-ion collisions which comprise the Coulomb dipole excitation (CDE) potential and the long-range nuclear (LRN) potential. To study these effects, we perform a χ^2 analysis for the elastic cross sections of ^{11}Li + ^{208}Pb and ^{6}He + ^{208}Pb systems using the long-range dynamic polarization potentials. For the CDE we formulate some empirical models to reproduce the experimental Coulomb dipole strength B(E1) distribution and apply to the collision of ^{11}Li and ^{6}He. But the CDE potential turns out to be not enough to explain the experimental data relevant to the nuclei. It leads us to additionally take the LRN potential peculiar to these halo nuclei into account. Our model, which was constructed by adding the CDE and LRN potentials to the conventional short-range nuclear potential corrected by the Coulomb interaction, provides a good description of the experimental data. In particular, the surface type is shown to be more reasonable rather than the volume type in the LRN potential.

C8.07

Calculation of fission product yields for n+^{235}U using a semi-empirical method

*이종화, 길충섭 [1], 이영욱 [1], 박태선, 홍승우
*Jounghwa. Lee, Choong-sup. Gil[1], Young-Ouk. Lee[1], Tae-Sun. Park, Seong-Woo. Hong
성균관대학교. [1] 한국원자력연구원.

Keyword : Nuclear fission, Fission product yields, Fission barrier, Liquid drop model, Shell effect

Calculations of fission product yields are very important because they are related to nuclear safety by predicting decay heat from nuclear fuels. A huge amount of experimental data have been accumulated in the conditions related to the nuclear reactor, but there are no data for those rare, unusual cases where accidents can occur or experimental data are hard to obtain. For such cases, the models that have a theoretical ground and a prediction power need to be developed because we have to rely on the calculation results based on some theoretical models.
Our model is based on the model for the fission product yields proposed by Bohr and Brosa. The investigation of the fission barrier was done by using the semi-empirical method. The shape of the fission barrier at a scission point is determined by the macro potential and is corrected by the shell effect. In this study, shell correction terms are considered as a Gaussian function. The model can predict the mass distribution of fission products.

C9.01*

Prototype of the position-sensitive ionization chamber using multi-wire electrodes

*곽민식, 채경육, 차수미, 김아람, 이은지, 이재하
*Minsik. Kwag, Kyungyuk. Chae, Soomi. Cha, Aram. Kim, Eunji. Lee, Jaeha. Lee
성균관대학교.

Keyword : Ionization chamber, Position-sensitive, Multi-wire electrodes, Particle identification, Beam mornitoring

Many different types of particle detectors have been widely used for beam intensity monitoring and particle identification in various experiments in nuclear physics. An ionization chamber is well suited for this purpose because of its sturdiness against radiation damage. When the beams and beam-like heavy recoils are high atomic mass isotopes, however, standard energy loss technique is not enough for particle identification since Z-number is dominant to beam stopping power. In order to figure out this limitation, a position-sensitive ionization chamber is designed and constructed at the Sungkyunkwan University. Commissioning of the chamber was performed by using alpha source. Details of the experimental setup and results will be presented.

C9.02

Production of a neutrino source through proton induced reaction

*신재원, 천명기
*Jae Won. Shin, Myung-Ki. Cheoun
숭실대학교.

Keyword : Neutrino, Proton-induced reaction, GEANT4, ENDF/B-VII.1, ENSDF

Production of a neutrino source through proton induced reaction is studied by using particle transport code, GEANT4. Unstable isotopes such as ^{27}Si can be produced when the Al target is bombarded by energetic proton beams. Through the beta decay process of unstable isotopes, a neutrino source is obtained. Proton induced reactions are simulated with ENDF/B-VII.1 data. For radioactive decay processes, we use "G4RadioactiveDecay" model based on the Evaluated Nuclear Structure Data File (ENSDF).
We suggest beam current, target systems required for future's neutrino experiments.

C9.03*

Beam Test Results from Prototypes of Aerogel Cherenkov Detector for the E42 at J-PARC

*김민호, 안정근, 홍병식, 이종원, T. Ohta[1]
*Minho. Kim, Jungkeun. Ahn, Byungsik. Hong, Jongwon. Lee, Takeshi. Ohta[1]
Korea University. [1]RCNP. Osaka University.

Keyword : H-dibaryon, E42, Cherenkov detector, SPring-8, LEPS

We report the recent test results for performance of the forward aerogel Cherenkov detector (FAC) at SPring-8. FAC is a threshold Cherenkov detector that will be used for online pion veto detector against kaon signals in the E42, H-dibaryon search experiment. It is composed of a thin aluminum light box, a large volume (440x220x60 mm^3) aerogel radiator with refractive index of 1.04 and a both-sides parabolic reflector surface with specular reflection. The FAC system also employs the fine-mesh PMTs that are safe in magnetic field, because it should be operated in strong magnetic field up to 0.5 T by superconducting Helmholtz magnet. Three kinds of FAC prototypes were constructed and estimated their efficiencies for the pion rejection using pion and proton beam at SPring-8 LEPS spectrometer with which the charged particles can be clearly identified. In this presentation, tha analysis results on the pion efficiencies of the three different prototypes and the pulse-height distribution study of the fine-mesh PMT to estimate number of photoelectrons of FAC will be presented.

C9.04

Measurements of ^{89}Y(n,2n)^{88}Y, ^{93}Nb(n,2n)^{92m}Nb and ^{209}Bi(n,4n)^{206}Bi cross sections for fast neutrons by using KIRAMS MC-50 cyclotron.

*김도윤, 박상인, 함철민, 민경주, 인은진, 신재원, 박태선, V. N. BHORASKAR[1], 홍승우
*Do Yoon. KIM, Sang in. BAK, Chul Min. HAM, Kyung Joo. MIN, Eun Jin. IN, Jae Won. SHIN, Tae-Sun. PARK, V. N.. BHORASKAR[1], Seung-Woo. HONG
Sungkyunkwan University. [1]S. P. Pune University.

Keyword : (n,xn) cross section, ^{89}Y, ^{93}Nb, ^{209}Bi, Neutron activation, Neutron flux, KIRAMS MC-50, Gamma-ray activities

고속 중성자 원자로 개발을 위해서는 20 MeV 이상의 고속 중성자에 의해 유도된 핵반응단면적이 필요하다. 우리는 한국원자력의학원(KIRAMS)의 MC-50 양성자 사이클로트론에서 발생되는 넓은 에너지 영역의 중성자 스펙트럼을 이용해 (n,xn) 핵반응단면적을 얻는 시도를 했다. 원자로 구조재료 및 합금에 첨가되는 ^{27}Al, ^{56}Fe, ^{89}Y, ^{93}Nb 와 고속로 중 하나인 납비스무스 냉각 원자로의 냉각재로 이용되는 ^{209}Bi 를 고려했다. ^{89}Y(n,2n)^{88}Y, ^{93}Nb(n,2n)^{92m}Nb, ^{209}Bi(n,4n)^{206}Bi 의 (n,xn) 반응단면적을 얻기 위해 MC-50 사이클로트론의 연속 스펙트럼 중성자로 Y, Nb, Bi 샘플을 조사시켰고, HPGe 검출기를 이용하여 감마선을 측정했다. Geant4 시뮬레이션 결과로부터 얻어진 중성자 선속은 핵반응단면적이 비교적 잘 알려진 ^{56}Fe(n,p)^{56}Mn 와 ^{27}Al(n,α)^{24}Na 핵반응을 통해 간접적으로 검증했고 그렇게 확인된 중성자 선속과 알려진 핵자료 및 Talys 코드를 이용해 ^{89}Y(n,2n)^{88}Y, ^{93}Nb(n,2n)^{92m}Nb, ^{209}Bi(n,4n)^{206}Bi 핵반응단면적에 대한 예비분석 결과를 얻었다. 근사적인 방법을 이용하지만, 연속 스펙트럼을 갖는 중성자를 이용해서 (n,xn) 반응단면적을 얻을 수 있음을 보였다.

C9.05*

Lifetime measurement of the 81 keV excited state of ^{133}Cs formed by the decay of ^{133}Ba

*이노센트, 존, 이종원, 홍병식, 안정근
*Innocent Jimmy. Lugendo, John. Kumwenda Mwingereza, Jongwon. Lee, Byungsik. Hong, Jung Keun. Ahn
고려대학교.

Keyword : Lifetime of a state, Resonance Environment, Isomeric nucleus, Uncertainty

Observing the lifetime of the 81 keV state of ^{133m}Cs nucleus is particularly interesting when subjected to a resonance environment created by the presence of stable ^{133}Cs nuclei. In this environment, the lifetime is expected to be changed due to gamma radiation from isomeric nuclei ^{133m1}Cs which is newly produced upon the resonance capture of gamma rays from ^{133m}Cs by stable ^{133}Cs. As a preparatory experiment, we set up a table top system of two NaI(TI) detectors to measure the lifetime of the 81 keV state of ^{133m}Cs when there is no resonance effect. ^{133}Ba source which decay to ^{133m}Cs through electron capture was used in this experiment. The experimental results on the lifetime of 81 keV state fairly agrees with the measurements reported elsewhere. The uncertainty level for the present experiment was estimated to be about 1.6%.

C9.06*

Test and simulation results of prototype Si-CsI for the possible low-energy LAMPS at RAON

*박재범, 이경세 [1], 안정근 [1], 홍병식 [1], 김영진 [2], 문동호 [3], 이한슬 [3], 김은주 [4]
*Jae Beom. Park, Kyong-Sei. Lee[1], Jung Keun. Ahn[1], Byungsik. Hong[1], Young Jin. Kim[2], Dong Ho. Moon[3], Hanseul. Lee[3], Eun-Joo. Kim[4]
고려대학교. [1]Korea Univ. [2]IBS. [3]ChonNam National Univ. [4]ChonBuk National Univ.

Keyword : LAMPS,Symmetry Energy,RAON,Si-CsI,low-energy

Low-energy radioactive ion beams provided by RAON will play an important role in the study of the nuclear symmetry energy at sub-saturation densities. Conceptual design of the low-energy Large Acceptance Multi-Purpose Spectrometer (LAMPS) consists of the Si-CsI system and neutron detector array. The CsI detector in the Si-CsI system will be used for depositing the full energy of charged particles and measuring gammas from nucleus-nucleus collisions. In order to investigate the performance of the CsI detector, we performed the GEANT4 simulation and tested the prototype detector with various radioactive sources. In this presentation, we summarize the results of the simulation and tests. We also show the performance of the full simulation for the low-energy LAMPS.

C9.07

A gas ionization alpha particle detector at the Yangyang underground laboratory.

*하창현
*Chang Hyon. Ha
기초과학연구원.

Keyword : Alpha particle, ionization chamber

An ionization chamber for detecting alpha particles has been installed in the Yangyang underground laboratory (Y2L). The main purpose of the alpha detector is to assay detector materials that will be used for rare event search experiments such as KIMS and AMoRE. The instrument characterizes signals from ionization electrons that are produced by alpha particles in an Ar-filled gas chamber, exploiting the distinct rise time signature to identify alpha particles that originate from the specimen tray and vetoes those from other sources. Because of its location in the deep underground Y2L facility, the chamber can reach a sensitivity as low as 0.001 count/cm^2/hr. In this presentation, we review the principle of the detector and show results from preliminary measurements.

C10.01(초)

New Physics at the Terascale

*Tim Tait
*Tim. Tait
Univ. of California at Irvine.

Keyword : .

Abstract: LHC experiments have started to explore the physics at the TeV scale in 2015. This provides golden opportunities in searching for new phenomena. I present a broad review of new physics models at the Terascale and their LHC signatures. I will also discuss why the searches at the Terascale are so exciting program.

C10.02(초)

Precision Physics at the LHC

*Christopher Hays
*Christopher. Hays
Oxford University.

Keyword : .

Abstract: High-statistics LHC data enabled several precision tests on the electroweak observables and QCD tests. This provides not only precise knowledge of the Standard Model but also a window for new physics signature. I will present several precision measurements done by both ATLAS and CMS experiments and discuss the results and future prospects.

C10.03(초)

Searches for New Physics at the LHC

*Christopher Hill
*Christopher. Hill
Ohio State University.

Keyword : .

A new era at the Terascale physics was started with the Run II of the LHC in 2015, which will expand our understanding of the Standard Model, and will provide direct and indirect searches for beyond the Standard Model. I will discuss various search strategy and present search results and future prospects.

C10.04(초)

Flavor physics in the LHC era

*권영준
*Youngjoon. Kwon
연세대학교.

Keyword : flavor physics, Belle, intensity frontier

In the era of LHC physics by which energy frontier is explored, complementary knowledge can be obtained by exploring the luminosity frontier, in particular, in the subject of flavor physics. Currently, LHCb and the two e+ e- B-factory experiments, Belle and BaBar, have provided numerous new results on the flavor sector of particle physics. In this talk, we present a few highlights, e.g. B -> D(*) tau nu, dark sector searches, of flavor physics from the current experiments such as Belle, BaBar and LHCb, and near-future prospects focusing on the Belle II, the next-generation e+e- B-factory experiment using the SuperKEKB collider.

C11.01

Probing Dark Enegy with ISW and WL

*이석천
*SEOK CHEON. LEE
고등과학원.

Keyword : "Dark Energy", "CMB", "WL"

We show that the cross correlation between Integrated Sachs-Wolfe effect and Weak Lensing can be used to probe different dark enery models. If one uses the non-linear evolution of the matter density, then there exists the transition from the anti-correlation to the correlation on this cross correlation. This transition scale depends on dark energy models and thus be used to probe dark energy properties.

C11.02

Inverse transfer of magnetic energy in the free decaying MHD system: its application to the origin of magnetic field with a new dynamo model

*박기완
*Kiwan. Park
UNIST.

Keyword : Magnetohydrodynamics (MHD), decaying turbulence, dynamo, simulation, theory

Magnetic field is a ubiquitous phenomenon, and its interaction with conducting fluid (plasma) plays a crucial role in the evolution of celestial objects like pulsars, jets, galaxy, planetary nebulae, or GRBs etc. So better understanding their interactions, i.e., magnetohydrodynamic (MHD) phenomena will more clearly explain the past, present, and future universe. However, the origin and role of magnetic field in space and plasma are not yet completely understood. Since the interaction between magnetic field and plasma is essentially nonlinear, it is hard to intuitively understand the consequent phenomena in the MHD system. Instead we need a more simplified model and solve the coupled equations that describe the MHD phenomena. As of now the exact solution of the core MHD equations is not known yet. Only a few stochastic approaches (Kazantsev 1968, Kraichnan & Nagarajan 1967, Pouquet et al., 1976) and simplified mean field theory (Krause and Radler 1980, Brandenburg 2001, Park & Blackman 2012, Park 2013) are available in a limited way, which means our comprehension is also restricted as much.
We briefly introduce couple of models on the origin of magnetic field in the early universe (Turner and Widrow 1988, Grasso and Rubinstein 2001). Then we talk about the simulation results showing the amplification of magnetic field in a decaying MHD system, which looks unusual and contradictory. However, strictly speaking the decaying turbulence does not mean the interaction between magnetic field and fluid is forbidden. Due to the asymmetric properties in the conducting fluid and magnetic field, some intrinsic features of MHD turbulence show up. So far only a few dimensional analyses and numerical results on the inverse transfer in a decaying MHD system already have been reported. Oelsen 1997, Brandenburg et al. 2015 showed the possibility of inverse transfer of magnetic energy rescaling the MHD equations. But it is not enough to understand the unusual phenomenon by the typical dynamo model. Here we suggest a new dynamo model that explains the local or nonlocal magnetic energy transfer. This intuitive model is not limited to in decaying turbulence. Rather it covers the general mechanism of magnetic energy transfer and is complementary to the statistical Quasi Normal approach (Park 2015 submitted). Besides, we briefly introduce the inverse cascade of magnetic energy when there is a helicity in the MHD system (Park 2014). These introductions will be helpful to our more complete understanding the evolution of magnetic field in the plasma, which gives us some clues to the origin of currently observed magnetic field in a quiescent astrophysical system and fundamental relation between magnetic field and plasma.

C11.04

General Relativistic Effects on Curvature Radiation from Pulsars

*김동훈
*Dong Hoon. Kim
이화여자대학교.

Keyword : "pulsar" "electromagnetic field" "curvature radiation" "general relativisty" "linear polarization"

In this work we consider a magnetic dipole model of a pulsar and investigate general relativistic (GR) effects on electromagnetic (EM) radiation from the pulsar: in particular, curvature radiation. In the strongly curved spacetime of the pulsar, we identify the magnetic field lines with the trajectories of a charged particle, and compute the EM fields from curvature radiation; emitted by the charge moving along the field lines. Notable GR effects are shown, including modification of the magnetic field lines, which leads to modification of the curvature radii of the trajectories and hence to modulation of the frequency of curvature radiation. Then the Stokes parameters are calculated to exhibit a strong linear polarization in the plane of curvature, where GR effects are also investigated.

C11.05

Gravity on Relativistic Equation of State

*김형찬
*Hyeong-Chan. KIM
한국교통대학교.

Keyword : Equation of state, Unruh temperature,

In this work, we study how a strong graivty a ects on the equation of state (EoS) of matters.
To do this we employ a canonical ensemble of classical monatomic ideal gas inside a cylindrical box located in a Rindler spacetime. The total energy is shown to decrease monotonically with the increase of the external gravity representing its attractiveness. However, it is bounded below, which is crucially di erent from the results of the Newtonian gravity. As for the entropy, it decreases with the external gravity in the Newtonian regime. However, in the presence of strong gravity or ultra-relativistic high temperature, the entropy increases with the gravity. This result can be a resolution of the negative entropy problem of the ideal gas in the Newtonian gravity. In the Newtonian regime, the EoS gains relativistic correction of O(kT/c^2). In the presence of strong gravity, the bottom of the box is very close to the event horizon of the Rindler spacetime mimiking a blackhole. The system behaves as if it is on an e ective two dimensional surface. Investigating the EoS in the strong gravity regime, the temperature of the system is found to be not a free parameter but to approach to a xed value proportional to the external gravity, which is reminiscent of the Unruh temperature.

C11.06

Effects of neutron star spin in gravitational-wave parameter estimation

*김정리, 마크 파바타 [1], 김정초 [2], 이형원 [2]
*Chunglee. KIM, Mark. Favata[1], Jeongcho. KIM[2], Hyung Won. Lee[2]
연세대학교. [1]Montclair state university. USA. [2] 인제대학교.

Keyword : gravitational waves, neutron stars, binaries, parameter estimation

Neutron stars are remnants of supernova explosions of massive stars. Based on observed pulsars in our Galaxy, the spin of neutron stars has been considered to be small (a ~ 0.1 or less) compared to that of black holes. However,
the maximum spins of neutron stars containing normal matter can be as high as ~0.7. With the next generation gravitational-wave (GW) detectors such as advanced LIGO, it will be possible to detect GWs, identify the sources, and measure their physical parameters within a decade. In this talk, we present our effort in parameter estimation with simulated gravitational-wave signals from neutron star-neutron star (NS-NS) binary inspirals. Assuming aligned spins for both neutron stars, we perform Markov Chain Monte Carlo parameter estimation to compute systematic errors due to ignoring neutron star spin. We find that advanced LIGO will be able to distinguish some of spinning binary neutron stars from non-spinning ones.

C11.07

Thermodynamics of AdS Black Holes

*곽보근
*Bogeun. Gwak
CQUeST/서강대학교.

Keyword : black hole, thermodynamics, probe, stability, anti-de Sitter

The stability and thermodynamics of rotating anti-de Sitter black hole are investigated by a particle probe. When the particle comes into the black hole, the mass and momentum of the black hole changes by the conserved charges of the particle. The irreducible mass of the black hole always increases under the process. It leads to the 2nd law of thermodynamics. Under this condition, the horizon is stable even if the extremal black hole, because the mass of the black hole increases larger than the angular momentum.

C12.01*

Regulatory Roles of Dynamic Disorder in Transcription Initiation Control

*김철민, 장준일
*Cheol-Min. Ghim, Juneil. Jang
UNIST.

Keyword : dynamic disorder, gene expression, stochastic fluctuation, transcription factor

A norm in subcellular biochemistry is the changes in macromolecular conformations over the time scales longer than reaction cycle. The so-called dynamic disorder bears physiological consequences by way of not only enzymatic reactions but also gene expression machinery. In this work, we studied the effects of dynamic disorder in transcription factors on the noise level of various gene expression systems. In addition to the known mechanisms such as dimerization, we find that dynamic disorder in individual molecule has additional regulatory roles, which may provide a novel buffering mechanism to reduce the gene expression noise.

C12.02*

Intravital Quantitative Phase Imaging of Microvasculature in Live Mouse Mesentery

*김규현, 최기백, 김필한, 박용근 [1]
*Kyoohyun. Kim, Kibaek. Choe, Pilhan. Kim, YongKeun. Park[1]
카이스트. [1]KAIST.

Keyword : Optical diffraction tomography, Quantitative Phase Imaging, In vivo imaging, Intravital microscopy, Red blood cell

Intravital microscopy (IVM) has been an invaluable tool for studying various mechanisms taken place in biological cells and tissues under natural physiological conditions including temperature, molecules gradient, oxygen, CO_2 and pH concentration. IVM can be implemented by various imaging modalities including confocal scanning microscopy and multi-photon microscopy which measure excited light signals of fluorescent probes attached by target proteins. Since fluorescence imaging techniques measure light intensity, however, they have been lacking of quantitative information about biochemical and morphological properties of individual cells. In addition, since three-dimensional (3-D) images are obtained by axial stacking 2-D images, the limited acquisition speed hinders the video-rate 3-D imaging of cellular behaviors in live animals.
Here, we present a method to measure 2-D and 3-D quantitative phase imaging (QPI) of individual red blood cells (RBCs) flowing in the microvasculature of live mouse mesentery. QPI has been an emerging imaging technique which can measure optical phase delay of microscopic samples such as biological cells and tissues in label free. So far, various QPI techniques have been developed to study individual cells and tissues cultured in vitro, while in vivo QPI has remained unexplored due to multiple light scattering in tissues. We developed a post image-processing technique that remove the light scattering in tissues, and experimentally demonstrated that 2-D intravital QPI enables the investigation of the fluid dynamics of RBCs in capillaries of mouse mesentery and 3-D intravital optical diffraction tomography (ODT) measures chemical and morphological parameters of RBCs in capillaries. We expect the presented technique can be used for the in vivo investigation of various pathophysiological changes of RBCs inside micro-capillaries.

C12.03*

Optical Measurement of Membrane Fluctuations of Sickle Cell Trait Red Blood Cells

*정재황, Lucas Matemba[1], 김동진 [2], 박용근
*JaeHwang. Jung, Lucas. Matemba[1], Dong-Jin. Kim[2], YongKeun. Park
KAIST. [1]National Institute for Medical Research (NIMR). [2]The Nelson Mandela African Institute of Science and Technology.

Keyword : "sickle cell disease","sickle cell trait","quantitative phase imaging","QPIU","flucutation"

Sickle cell disease (SCD) is an inherited blood disorder caused by a point mutation in the β-globin gene, Val-His-Leu-Thr-Pro-Glu-Glu-Lys to Val-His-Leu-Thr-Pro-Val-Glu-Lys. This change leads production of Hemoglobin S (HbS) which shows self-assembling in a deoxygenated condition and intensively damages a membrane of red blood cells (RBCs), instead of Hemoglobin A (HbA) which is normal. While individuals having two copies of mutated genes suffers from fatal symptoms including vaso-occlusion and aplastic crisis, individuals having a single copy of HbS and HbA, called sickle cell traits (SCT), do not display the severe symptoms of SCD. Although SCT is typically considered as a benign condition, there are rare cases that present complications. Especially in extreme conditions such as heavy exercise and military training, there are reports of sudden deaths of people with SCT. There are still controversial debates whether individual with SCT have clinical differences compared to normal individuals. Most countries in Sub-Saharan Africa have unusually high populations of people who have sickle genes but most of them are under lack of management. Although worldwide attention is claimed as well as domestic effort, SCD is still major genetic problems and priority of public health in those countries. Due to the limited access of biomedical instruments in Sub-Saharan Africa, simple and cost-effective imaging tools are necessary for in situ study of SCD and SCT. In this work, we quantitatively measured the fluctuation of membranes of red blood cells (RBCs) obtained from individuals with SCD and SCD in Tanzania using quantitative phase imaging unit. Membrane fluctuations over 600 RBCs from 22 individual has been measured. We categorized the whole RBC samples to 4 groups: (1) RBCs from normal individuals, (2) RBCs from SCT individuals, (3) irreversibly sickled RBCs from SCD individuals, and (4) reversibly sickled RBCs from SCD individuals. As widely known, irreversibly sickled RBCs from SCD individuals present weakest fluctuations. We also noticed that SCT RBCs fluctuate similar to that of reversibly sickled RBCs while all HbS-containing RBCs fluctuate less than normal RBCs. This results implies that although the SCT RBCs do not show sickle shape in physiological oxygen level as normal RBCs do, mechanical properties of SCT RBCs is somehow different from normal RBCs and similar to non-sickle RBCs from SCD individuals.

C12.04(초)

Experimental Evidence for growing amorphous order and non-monotonic dynamic correlations in a colloidal glass forming liquid

*Manasa Kandula, 박혁규 [1]
*Hima Nagamanasa. Kandula, Hyuk Kyu. PAK[1]
기초과학연구원 (IBS). [1] 울산과학기술대학교.

Keyword : Colloids, Glass transition, pinning

Glass transition, transformation of a flowing liquid into a rigid solid on cooling without a perceptible change in structure, is one of the long standing puzzles of condensed matter physics. Numerous theories have been developed to understand the nature of this transition. Despite decades of research it is as yet unclear whether glass transition is dynamic or thermodynamic in nature [1, 2]. By pinning particles along a wall using holographic optical tweezers, we have provided experimental evidence in favor of Random First Order Transition (RFOT) theory, a thermodynamic theory of glass transition. Our experiments reveal growing amorphous order in the form of point-to-set correlation length with increasing supercooling. Interestingly, we find a non-monotonic density dependence of dynamic correlations. Further, we demonstrate that the non-monotonicity is accompanied by a change in morphology and internal structure of cooperatively rearranging regions – localized zones which govern relaxations in glass forming liquids. Together, our observations are consistent with a thermodynamic theory of the glass transition [3].

References:
[1] Berthier, L. & Biroli, G. Theoretical perspective on the glass transition and amorphous materials. Rev. Mod. Phys. 83, 587_645 (2011).
[2] Biroli, G & Garrahan J. P. Perspective: The Glass Transition. J. Chem. Phys. , 12A301 (2013).
[3] Nagamanasa, K. H., Gokhale, S., Sood, A. K., & G Ganapathy, R. Direct measurements of growing amorphous order and non-monotonic dynamic correlations in a colloidal glass-former. Nature. Phys. (2015)

C12.05(초)

Structural and dynamics studies of non-canonical DNAs

*홍석철
*Seok-Cheol. Hong
고려대학교.

Keyword : Single-molecule biophysics, non-canonical DNA, Z-DNA, i-motif, smFRET

Single-molecule biophysical techniques revolutionize the way we view the behavior of DNA molecules. The techniques are so powerful that they can allow us to uncover transitory intermediate states, keeping track of conformational states of individual molecules and reveal molecular heterogeneity, defying ensemble averaging, which is inevitable in many conventional methods. With single-molecule techniques, we directly observe that DNA, one of the most fundamental and essential biomolecules, can adopt various non-canonical conformations, which are often rare and masked by major molecular species. Non-canonical conformations often exhibit intriguing conformational dynamics, the kinetics of which permits us to gain new insight into the behavior and function of biomolecules. In this talk, I will mainly present our recent studies on left-handed Z-DNA and cytosine quadruplex called i-motif.

C12.06*

Queue Formations and Defect-Driven Phase Transitions in TASEP

*소형준, 백용주 [1], 하미순 [2], 정하웅
*Hyungjoon. Soh, Yongjoo. Baek[1], Meesoon. Ha[2], HAWOONG. JEONG
KAIST. [1]Technion. [2] 조선대학교.

Keyword : TASEP, KPZ Equation, Dynamical phase transition

The Kardar-Parisi-Zhang (KPZ) universality class covers lots of nonequillibrium growing interfaces, so it has been intensely studied for several decades. As a result, it is found that the analytic solution of one-dimensional (1D) KPZ fluctuating properties for such growth processes obey Tracy-Widom distributions, where its strong universality implies that the fluctuations strongly depends on initial and boundary conditions, but not on the details of the models. Although the model with translational symmetry has some rigorous form, the simplest broken symmetry of the system does not have analytic solutions. Among the many unresolved mysteries of such systems, one controversial issue is whether a localized defect at the middle of the system is always relevant. This is equivalent to the existence of a phase such that the site far from the defect cannot experience the effect. To resolve the issue, we numerically investigate the upper limit for the critical strength of the single-site defect that induces global queuing in 1D Totally Asymmetric Simple Exclusion Process (TASEP), as one instance of KPZ universality class. With two different temporal (transient and stationary) and initial conditions (wedge and flat), we measure the statistics for number of consecutive particles/holes as an indicator of global jamming. While the earlier studies focused on the values defined on a single site, we measure the quantities that spans multiple-site characteristics. In particular, we investigate the probability distribution of cluster sizes of the whole system and the cluster adjacent to the point defect, respectively, where we find that the abrupt growth of the effective cluster size in the strong-defect regime. Finally, we discuss the upper limit for the defect strength for the system being globally queued as well as the ensemble equivalence.

C12.07

Molecular Dynamics study for the friction coefficient on the overdamped case

*유동환, 정영균 [1], 권철안
*Dong Hwan. Yoo, Youngkyun. JUNG[1], Chulan. KWON
명지대학교. [1] 한국과학기술정보연구원.

Keyword : friction coefficient, molecular dynamics simulation

We estimate the friction coefficient of a colloidal particles for various size in fluid by investigating the position correlation functions in time. We use the molecular dynamics simulation that is alternative to the simulation based on the Langevin equation and is expected to mimic an experiment more realistically. We choose a heat bath composed of thousands of particles interacting to each other through the Lennard-Jones potential and impose the Langevin thermostat to maintain it in equilibrium. We prepare a colloidal particle to interact with the particles of the heat bath also by the Lenard-Jones potential while any dissipative force and noise are not employed explicitly. We estimate the friction coefficient of the colloidal particles for various size. We confirm the friction coefficients to follow Stokes' law.

C13.01(초)

Quantum computing with cold atoms and Rydberg blockade

*Mark Saffman
*Mark. Saffman
University of Wisconsin-Madison.

Keyword : Rydberg atom, Quantum computing

Optically trapped neutral atoms are one of several leading approaches to scalable quantum information processing. Atomic Rydberg states provide strong and controllable interactions that can be applied in a variety of for quantum information tasks. Examples include entanglement of single atom qubits, multi-atom ensemble qubits, and hybrid entanglement between different types of atoms, between atoms and photons, or between atoms and solid state qubits. I will present progress towards using strong Rydberg interactions for implementation of small scale quantum computing devices. In experiments with N~10 atom ensembles we demonstrate preparation of entangled W states, and strong blockade between spatially separated ensembles. In an array of single atom qubits we demonstrate high fidelity single qubit gates, and improved fidelity of Rydberg blockade mediated entanglement, surpassing all previous experiments. Prospects for very high fidelity Rydberg gates using new gate protocols will be presented.

C13.02(초)

Microwave spectroscopy of Rydberg atoms

*Hyungwook Park
*Hyungwook. Park
Ohio State University.

Keyword : .

A gas of Rydberg atom is a fascinating system for study of a broad range of quantum phenomena. Due to large transition dipole moments in Rydberg states ~n2, interactions between Rydberg atoms lead to intriguing consequences, including resonant energy transfer and formation of large Rydberg molecule. One of the most interesting aspects of cold Rydberg atoms is their potential application for quantum information researches. For the first step towards quantum logic operations in a quantum computer, intensive efforts have gone into making a quantum phase gate. As a candidate for the quantum gate, a notion of dipole blockade has been proposed and actively studied theoretical and experimental perspectives. Accordingly understanding dipole-dipole interaction is prerequisite for further applications and crucial to overcoming any realistic problems. On the other hand, studying Rydberg states requires a high-resolution probe to resolve narrow energy spacing ~n-3. Microwave field makes it possible to detect transitions between Rydberg states with extremely high accuracy and stability in frequency and power. In this work we present observations of coupling between nearby Rydberg atoms and precise measurement of small electric field by combination of Rydberg atom and high-resolution microwave spectroscopy.

C13.03(초)

Long-range interacting quantum magnets of Rydberg dressed atoms

*최재윤
*Jae-yoon. Choi
Max-Planck Institute of Quantum Optics.

Keyword : "Rydberg dressing", "Long-range interaction","Ramsey interrogation scheme"

Realizing long-range interacting and long-lived quantum state will open a new avenue for exploring novel quantum magnetism as well as supersolid phase. Rydberg atoms offer the possibility to study long range interacting systems of ultracold atoms due to their strong van der Waals interactions. Admixture of a Rydberg state to a ground state, known as Rydberg dressing, allows for a great experimental tunability of these interactions and therefore promises to substantially enlarge the variety of Hamiltonians that can be studied. Here we report on our progress towards the realization of Rydberg dressing in a many-body spin system. Starting from a two-dimensional spin-polarized Mott insulator state, we couple one spin component to a Rydberg p-state on a single photon ultra-violet transition at 297 nm. Employing microwave Ramsey interferometry in the ground state manifold, we measure the spin-spin correlations emerging due to the admixture of long range interactions to the ground state.

C15.01

The beam test of C-band beam position monitor with a position resolution of nano meter

*장시원, 김은산
*Siwon. Jang, Eun San. Kim
고려대학교.

Keyword : BPM, ATF, KEK, ILC, resolution

We developed and tested an C-band beam position monitor with position resolution of nano meter in ATF2. The C-band BPM was developed for the fast beam feedback system at the interaction point of ATF in KEK, which C-band beam position monitor called to IPBPM (Interaction Point Beam Position Monitor). The developed IPBPM was acheived 8nm position resolution with nominal ATF beam condition. In this talk, we will described about the development of IPBPM and the beam test results with 8nm beam positioin resolution.

C15.02

Simulation Study on Ridge Bar Shape for Biological Uniform Response in Ion Beam Therapy

*조일성, 유승훈, 조성호, 김은호, 송용근, 신재익, 정원균
*Ilsung. Cho, SeungHoon. Yoo, Sungho. Cho, Eun Ho. Kim, Yongkeun. Song, Jae-ik. Shin, Won-Gyun. Jung
한국원자력의학원.

Keyword : Therapy,carbon,SOBP,RBE,Simulation

Spread-out Bragg peak (SOBP) is commonly used to deliver a prescription dose to tumor region in charged particle therapy. In this study a simulation method for ridge bar shape is presented for a synchrotron based carbon accelerator facility. GEANT4 monte carlo simulation tool kit is employed to simulate 290 MeV/u C12 ion beam transport into water phantom. The microdosimetric kinetic model is applied to estimate the Relative Biological Effectiveness (RBE) for 10% survival of HSG cells along the beam incident direction. SOBP is designed using biologically photon equivalent Bagg peaks. Finally, ridge bar shape is designed in order to achieve a uniform biological response for KHIMA beam delivery line within 2% of dose uniformity around SOBP region

C15.03

X-ray energy measurement of a prototype 6 MeV C-band Electron LINAC

*이만우, 임희진, 이무진, 정동혁, 이준규 [1]
*Manwoo. LEE, Heuijin. Lim, Mu Jin. Lee, Dong Hyeok. Jeong, Jungyu. Yi[1]
동남권원자력의학원. [1] 동남권원자력의학원. 부산대학교.

Keyword : FADC DAQ, BGO detector, X-ray spectrum, C-band, Linac for medical application

X-ray energy spectrum of a prototype 6MeV C-band Electron LINAC which has been developing for radiation therapy at DIRAMS (Dongnam Institute of Radiological & Medical Sciences) was measured. 6 MeV electrons were bombarded to a tungsten target to produce X-rays by the process of Bremsstrahlung. BGO detector shows a good energy resolution in high energy X-ray due to high density and a low saturation of scintillation lights. BGO detector was shielded with lead blocks to reduce environmental background and overlapped X-rays during a electron pulse width. A 500MHz FADC measurement device which can save the whole shape of signals during the pulse width was used to analyze an individual signal. We will present the overview of the test set-up and the result of X-ray energy spectrum. (This research was supported by the DIRAMS (No. 50496-2015))

C15.04

6 MeV 소형전자가속기 개발과 전자빔 진단

*이준규, 이만우, 임희진, 이무진, 신상웅, 김성우, 이상진, 정동혁, 양광모, 고창오 [1], 고창빈 [1], 신성균 [2], 양해룡 [2], 조무현 [2], 남궁원 [2]
*Jungyu. Yi, Manwoo. Lee, Heuijin. Lim, Mu Jin. Lee, . , Sung-woo Kim. , Sangjin. Lee, Dong Hyeok. JEONG, . , Changoh. Koh[1], Chang Bin. Koh[1], Sung Gyun. Shin[2], Hae Ryong. Yang[2], Moo-Hyun. CHO[2], Won. NAMKUNG[2]
동남권원자력의학원. [1](주) 태성정밀. [2] 포항공과대학교.

Keyword : electron beam, C-band, Linac for medical application, high power RF test

X-선 및 전자선을 이용하는 방사선 치료기 개발을 목표로 소형 전자 선형가속기 시작품을 개발하였다. C-band 정상파형 가속관에 2.5 MW 출력의 마그네트론을 고주파원으로 사용하여 6 MeV 전자빔을 생성하였다. 제작된 가속기의 시운전과 빔진단을 위해 수행했던 고전압 펄스 고주파 테스트 내용과 이를 이용하여 생성한 전자빔의 단면 측정 및 에너지 측정 결과를 발표하고자 한다.

*본 연구는 정부(미래창조과학부)의 재원으로 동남권원자력의학원의 지원을 받아 수행되었음 (과제번호: 50496-2015)

C15.05

The status report of KBSI accelerator facility and application plans of 28 GHz ECR ion source

*이병섭, 옥정우, 최세용, 박진용, 김성준, 방정배 [1], 홍종기, 신창석, 윤장희, 김현규, 원미숙
*Byoung Seob. Lee, Jung-Woo. Ok, Seyong. Choi, Jin Yong. Park, Sung-Jun. KIM, Jungbae. Bahng[1], Jonggi. Hong, Chang Seouk. Shin, Jang-Hee. Yoon, Hyun Gyu. Kim, Mi-Sook. Won
한국기초과학지원연구원. [1] 경북대학교.

Keyword : KBSI accelerator facility, 28 GHz ECR ion source, ion beam application

The Korea Basic Science Institute (KBSI) is developing a compact linear accelerator that is composed with 28GHz ECR ion source, radio frequency quadrupole accelerator (RFQ), drift tube linear accelerator (DTL), and neutron radiography system. After the development of 28 GHz ECR ion source, we performed feasibility studies about the ion beam extraction of multi-charged ions from various species of gases that are O, Ar, N, Xe. In this report, we briefly present experimental results and discuss the application of ion beams. Also, we are performing development of RFQ system and design of accelerator building. The current status of KBSI accelerator project was reported in this presentation.

C15.06

의료용 가속기 제어용 실시간 방사선 출력 모니터링 시스템 개발

*이무진, 임희진, 이만우, 이준규, 강상구, 정동혁
*Mujin. Lee, Lim Heuijin. , Man-Woo. Lee, Jungyu. Yi, Sang-Koo. Kang, Dong-Hyeok. Jeong
동남권원자력의학원.

Keyword : 의료용 선형가속기, 모니터링 시스템, 제어 시스템

의료용 가속기에서는 가속기의 안정한 작동과 일정한 방사선의 발생을 위하여 방사선 출력을 실시간으로 측정하고 제어한다. 방사선 출력 모니터링 시스템은 발생되는 방사선의 출력을 측정하고 제어하는 장치로서 모니터 전리함, 신호획득 및 처리장치, 그리고 가속기 연결 인터페이스로 구성된다. 본 연구에서는 방사선 출력 모니터링 시스템을 제작하여 연구용 6 MeV 가속기 시스템에 장착하고 방사선 출력의 측정과 제어를 시험하였다. 방사선발생부에서 생성된 엑스선 또는 산란된 전자선에 대하여 측정한 모니터 전리함의 신호를 기준 거리의 실제 방사선량에 대하여 교정하였으며, 가속기 시스템과 연동시켜 가속기의 정상적 작동과 중단을 실험적으로 확인하였다. 본 시스템은 의료용 가속기 개발시 빔과 방사선의 정밀 제어 시스템의 일부로 활용될 것이다. (본 연구는 정부-미래창조과학부의 재원으로 동남권원자력의학원의 지원을 받아 수행되었음/과제번호: 50495-2015)

C15.07

Design Comparison of RISP and FRIB

*전동오
*Dong-O. Jeon
기초과학연구원(IBS).

Keyword : "heavy ion accelerator","superconducting linac"

Two large scale, high power heavy ion accelerator facilities are under construction : the RISP in Korea and the FRIB in US. The driver linac of the RISP is designed to accelerate uranium to proton beam up to 200 MeV/u (600 MeV), delivering 400 kW of beam power. The driver linac of the FRIB is designed to accelerate heavy ion beams with A/q > 3 up to 200 MeV/u. In this presentation, the design differences and their cons and pros are presented.

C15.08*

플라즈마 홀 추력기의 자기장에 따른 이온빔 특성과 성능 특성과의 관계 연구

*김호락, 임유봉, 이승훈 [1], 선종호 [2], 최원호
*Holak. Kim, Lim youbong. , Seunghun. Lee[1], Jongho SEON. [2], CHOE Wonho.
한국과학기술원. [1] 한국기계연구원 부설 재료연구소. [2] 경희대학교.

Keyword : Plasma Physics, Plasma Hall thrsuter, Cylindrical Hall thruster, Multiply charged ion

플라즈마 홀 추력기는 인공위성의 자세제어, 궤도수정, 궤도천이 등 다양한 우주 탐사활동 및 임무수행을 위한 우주선의 엔진으로 사용되며, 코팅 및 에칭 등 산업적인 목적과 용도로도 사용되고 있다. 홀 추력기는 외부에 위치한 음극을 통해 채널 내부로 전자를 공급하며, 전자와 중성 Xe 원자와 충돌을 통해 Xe 이온들을 발생시켜 양극과 음극 사이의 전기장에 의해 가속되어 추력을 발생시킨다. 이때, 자기장에 의해 감금된 전자들의 효과로 인하여 이온에너지 분포함수, 이온전류 분포, 다중전하 이온 분포 등 이온빔의 특성 및 추력, 비추력 등의 성능 특성이 달라진다. 본 연구에서는, 플라즈마 홀 추력기 내부의 자기장 특성이 두 전자석의 전류 방향이 같을 때(Co-current)와 반대일 때(Counter-current) 나타나는 두 자기장 구조에서 이온 빔 및 성능 특성을 측정하였다. Co-current 구조에서는 강한 축 방향 자기장으로 인하여 약 40%의 다중이온이 발생하였으며, 이를 통해 발생된 추력의 세기도 약 10%이상 높게 나타났다. 두 자기장 구조에 대한 빔 특성 및 성능 특성 대한 연구결과가 발표될 예정이다.

C15.09

Strike point splitting by non-axisymmetric magnetic fields in tokamaks

*김기민, J.-W. Ahn[1], F. Scotti[2], J.-K. Park[3], J. E. Menard[3]
*Kimin. Kim, J.-W.. Ahn[1], F.. Scotti[2], J.-K.. Park[3], J. E.. Menard[3]
KAIST (한국과학기술원). [1]Oak Ridge National Laboratory. [2]Lawrence Livermore National Laboratory. [3]Princeton Plasma Physics Laboratory.

Keyword : tokamak, non-axisymmetric fields, resonant magnetic perturbation, field line tracing, strike point splitting

Ideal plasma shielding and amplification of resonant magnetic perturbations in non-axisymmetric tokamak is presented by field line tracing simulation with full ideal plasma response, compared to vacuum field model and measurements of divertor lobe structures. Field line tracing simulations in NSTX with toroidal non-axisymmetry indicate the ideal plasma response can significantly shield/amplify and phase shift the vacuum resonant magnetic perturbations. Ideal plasma shielding is found to prevent magnetic islands from opening and modify the degree of stochasticity. The overall helical lobe structures of the vacuum field are not changed by the ideal plasma response for high toroidal mode n=3. On the other hand, strong amplification of vacuum fields by the ideal plasma response is predicted for low toroidal mode n=1, better reproducing measurements of strong striation of the field lines on the divertor plate.

D1.01

Calculation of the Hofstadter Butterfly arising in patterned superlattices in graphene

Nicolas Leconte, *정재일
Nicolas. Lecont, *Jeil. Jung
서울시립대.

Keyword : Hofstadter butterly, moire patterns, quantum transport, superlattices, zero-line modes

We present a novel approach to study the Hofstadter butterfly in the density of states due to superlattices and moire patterns that can be tailored through lithographic gating techniques on graphene or through controlled vertical heterojunctions with other 2D crystals. A real space implementation of the Kubo-Greenwood formalism together with the Lanczos recursion technique allows us to simulate millions of atoms size mesoscale systems without relying on exact diagonalization. The high computational efficiency of our method makes it possible to carry out a quantum mechanical calculation of the conductivity in the presence of magnetic field sizes and realistic disorder that would be prohibitive in conventional ab initio simulations. We use this technique to investigate the effects of patterned superlattices in graphene on the quantum transport and the Hofstadter butterfly in the density of states paying particular attention to the role of the zero-line valley Hall channels that can appear due to changing signs in the local band gap in real space.

D1.02

Modeling Atomic Layer Rearrangement in Interfacial Phase-Change Materials

*송영선, 지승훈
*Young-Sun. Song, Seung-Hoon. Jhi
Department of Physics. POSTECH.

Keyword : density functional theory (DFT), interfacial phase-change memory (iPCM), atomic layer rearrangement, nudged elastic band (NEB) method, interatomic potential model

GeTe-Sb2Te3 superlattices, known as interfacial phase change materials (iPCMs), have been claimed to outperform Ge-Sb-Te-based phase-change materials, candidate materials for the non-volatile memory devices, in terms of energy efficiency, switching rate, and durability. Despite its great potential as next-generation data storage medium, we still lack detailed knowledge of the mechanism of the phase change. Recently, the phase change between the "RESET" and the "SET" phases of iPCMs was attributed to the rearrangement of Ge and Te layers in the superlattices, but neither clear evidences supporting this nor detailed phase change processes have been revealed yet. In this work, we investigated the detailed characteristics of atomic layer rearrangements in iPCMs by calculating the energy barriers for several rearrangement paths. We used the climbing image nudged elastic band (CI-NEB) method and ab-initio calculations. In order to analyze the rearrangement paths and the energy barriers, we chose an interatomic potential model and tested it for the intermediate steps of the phase change processes. We found that rearrangement processes can be separated into intrinsically different two sub-processes, namely vertical and horizontal movements. We calculated the energy barriers by modeling the rearrangement of atoms as concurrent movement or successive chain movement.

D1.03

First-principles study of thickness dependent thermoelectric properties of Bi_2Te_3, Bi_2Se_3 and Sb_2Te_3 thin-film structures

*임명수, 지승훈
*Myung-Soo. Lim, Seung Hoon. Jhi
포항공과대학교.

Keyword : First-principles calculation, Thermoelectric property

Three-dimensional topological insulator Bi_2Te_3, Bi_2Se_3 and Sb_2Te_3 are good thermoelectric materials. In this study, we use first-principles calculations and semi-classical Boltzmann transport method to investigate the thermoelectric property of these compounds in a-few-layer structures. In particular, we study the effect of topological surface states and quantum-well states on the thermoelectric property. Our calculations show that the Seebeck coefficients of n-type and p-type doped films exhibit contrasting behavior upon variation in film thickness. We show that the thickness dependence of the Seebeck coefficient is associated with the interplay of the quantum well states and the surface states near the Fermi level in 2D structures.

D1.04

Strain effect on electronic structure and thermoelectric properties of orthorhombic SnSe: a first principles study

*도득궁, 임성현, 이주형 [1], 홍순철
*Duc Cuong. Do, Sonny. Rhim, Joo-Hyoung. Lee[1], Soon Cheol. HONG
울산대학교. [1] 광주 과학 기술원.

Keyword : "SnSe" , "first-principles" , "strain effect"

Strain effect on thermoelectricity of the orthorhombic SnSe is studied using density function theory. The Seebeck coefficients are obtained by solving Boltzmann Transport equation (BTE), where band energies are interpolated. As expected in crystal structure, calculated Seebeck coefficients are highly anisotropic and agree very well with experiment. Changes in the Seebeck coefficients when strain is applied along b and c direction with strength from -3% to +3% is presented, where influence by band gaps and band dispersions are significant. Moreover, for compressive strains, from the sign change of Seebeck coefficients at particular direction, suggests that the bipolar transport is possible for SnSe.

D1.05

Ab-initio thermal conductivity calculation of layered BiCuOQ (Q: S, Se, Te) compounds

*지효석, 심지훈
*Hyoseok. Ji, Ji Hoon. Shim
포항공과대학교.

Keyword : Thermoelectric, thermal conductivity, Boltzmann Equation, first-principle, Mixed layer

The p-type BiCuOSe is a new candidate for thermoelectric material which shows high ZT of 1.1 at 923 K. The origin of high ZT is the low thermal conductivity and high power factor. Electronic properties such as electrical conductivity and Seebeck coefficient, are well studied using ab initio calculations. The lattice properties, however, are not well studied. In this study, we investigated its thermal conductivity and lattice properties using combination of density functional theory and Boltzmann transport equation.
Calculated lattice properties of BiCuOQ show clear trend for elastic moduli and phonon dispersions. As the atomic mass increases(S to Te), phonon dispersion is suppressed which results low thermal conductivity of BiCuOTe compound rather than S and Se compounds. Also calculated thermal conductivity is well reasonable compared with experimental result. The detailed mechanism of low thermal conductivity of these compounds will be discussed.
We suggested that the mixing of two different layer can enhance the themoelectric properties as a consequence of reducing the band gap. This concept will also be aplied to lowering thermal conductivity caused by two mass-different layers.

D1.06*

Atomic and electronic structure of non-stoichiometric amorphous In-Ga-Zn-O semiconductors

*한우현, 오영준 [1], 장기주 [1]
*WOOHYUN. HAN, Young Jun. Oh[1], Kee Joo. CHANG[1]
카이스트. [1] 한국과학기술원.

Keyword : a-IGZO, First-principle calculation, semiconductor

Amorphous indium-gallium-zinc oxide (a-IGZO) semiconductors have attracted much attention because they are used as an active channel material in transparent thin film transistors (TFTs). Despite superior device properties, such as high field-effect mobility, as compared to amorphous Si TFTs, the instability of threshold voltage under negative bias illumination stress (NBIS) as well as positive bias stress (PBS) is the main obstacle for device applications. Our recent theoretical studies suggested that O-vacancy defects are responsible for the NBIS instability, and this defect model has been supported by numerous experiments. We have also proposed that excess O interstitials, which act as double acceptors, cause the PBS instability. In these previous studies, O-related defects were generated by eliminating the host O atoms or introducing excess O atoms in stoichiometric a-IGZO.
In this work, we investigate the atomic and electronic properties of O-related defects in non-stoichiometric a-IGZO through first-principles density functional calculations. We consider IGZO crystals with the composition ratio of In:Ga:Zn:O = 1:1:1:4 and introduce excess O atoms or O deficiencies which may lead to the generation of O-related defects. Then we generate non-stoichiometric amorphous samples through melt-and-quench ab initio molecular dynamics simulations. We discuss the role of O-related defects in device instability and compare our results with the previous theoretical models.

D1.07*

$Li_2Ge_4O_9$, $LiNaGe_4O_9$ 물질에서의 강유전상에 관한 제일원리계산

*박장희, 김복기
*Janghee. Park, KIM Bog-Gi.
부산대학교.

Keyword : 강유전체, 자발분극, $Li_2Ge_4O_9$, $LiNaGe_4O_9$, 상전이

최근에 stoichiometric glass 로부터 crystalize 된 $Li_2Ge_4O_9$ 의 orthorhombic $Pca2_1$ 구조에서 나타나는 강유전상에 대한 실험적인 보고가 있었다. $Li_2Ge_4O_9$(LGO), $LiNaGe_4O_9$(LNGO) 물질은 GeO_4 산소사면체와 GeO_6 산소팔면체가 3 차원적으로 연결되어 있는 입체구조를 가진다. 우리는 제일원리계산을 통해 $Li_2Ge_4O_9$(LGO), $LiNaGe_4O_9$(LNGO) 물질의 $Pca2_1$ 구조에서의 안정성을 확인하였고 군 이론을 이용한 모드 분석을 통해 Pcca 구조에서 $Pca2_1$ 구조로 가는 상전이 과정에서 나타나게 되는 원자들의 displacement 를 분석하였다. Born effective charge 방법을 통하여 LGO 와 LNGO 물질의 자발분극에 대한 Alkali 이온의 기여를 확인하였고, 우리는 이로부터 본 논문발표를 통해 강유전상의 주된 요인이 무엇인지 설명하고자 한다. 또한, LGO 와 LNGO 물질 내에서의 발생하는 강유전상을 Alkali 이온간의 자발분극의 배열 분석을 통하여 논의하고자 한다. 그리고 밴드구조와 상태밀도 분석을 통하여 Li 과 Na 가 각각 어떻게 강유전상의 발현에 차이를 주는지 분석해 보았다.

D1.08*

Origin of Negative Thermal Expansion in sp−sp^2 Hybridized Carbon Systems

*김철운, 강승훈, 권영균
*Cheol-Woon. Kim, Seoung-Hun. Kang, Young-Kyun. Kwon
경희대학교.

Keyword : "graphyne", "negative thermal expansion", "rigid unit mode"

Based on density functional theory combined with quasi-harmonic approximation, we investigate the thermal expansion behaviors of three different types (α, β, and γ) of graphyne which is a two-dimensional carbon allotrope composed of sp and sp^2 bonds. For each type of graphyne, we obtain the temperature dependent area variation by minimizing its free energy calculated by considering all the phonon modes in the whole Brillouin zone. We find that all three types of graphyne exhibit negative in-plane thermal expansion up to $T \lesssim 1000$ K. To reveal the origin of negative thermal expansion, we look into the phonon modes observed in graphyne and evaluate their corresponding mode Gruneisen parameters indicating the contribution to thermal expansion behaivor. Similarly in graphene, we find that the ripple effect contributes to the observed in-plane thermal contraction. We also observe that other modes with negative mode Gruneisen parameters, which are particular phonon modes with frequencies of around a few hundreds of cm^{-1} existing exclusively in graphyne, may fill empty spaces resulting in area reduction. These modes are identified as “rigid unit modes (RUMs)” corresponding to the libration of each rigid unit composed of sp^2 bonds.

D1.09*

First-Principles Study on Thermoelectric Properties of Phosphorene and Phosphoene Oxide

*이승준, 박제준, 강승훈, 권영균
*Seungjun. Lee, JEJUNE. PARK, Seoung-Hun. Kang, Young-Kyun. Kwon
경희대학교.

Keyword : phosphorene, phosphorene oxide, thermoelectric, boltzmann transport equation, deformation potential theory

Phosphorene, a single layer of black phosphorus, is expected to be one of notable 2D materials for future semiconductor devices. Phosphorene may have interesting thermoelectric properties such as its intrinsic thermoelectric anisotropy depending on the crystal anisotropy. To study the thermoelectric properties of phosphorene, we calculate electronic and thermal transport properties contributed from both electrons and phonons by solving the Boltzmann transport equation (BTE) based on first-principles calculations. For accurate calculations of electronic transport properties using BTE, the relaxation time (electron–phonon scattering time) is a signification and essential quantity. We estimate the relaxation time using the deformation potential theory for electron–phonon coupling. We observe that its electrical conductivity is higher along the armchair direction than along the zigzag direction, while thermal conductivity shows an opposite behavior. Because of this orthogonal relation between the electrical and thermal conductivities, phosphorene exhibits quite a large ZT value along the armchair direction. We also investigate the thermoelectric property of phosphorene oxide since phosphorene would be quite susceptible to the oxidation due to a lone pair of electrons in each P atom. Similarly, the BTE is also solved for phsophorene oxide to calculate various transport coefficients. It is found that phosphorene oxide also reveals strong anisotropic characteristics in its electrical and thermal conductivities. It turns out that its ZT value is comparable to that of phosphorene along the armchair direction, whereas its figure of merit along the zigzag direction is much larger than that of phosphorene implying that both direction can be utilized as thermoelectric system.

D2.01

Selective elemental vacancy control on physical properties in $SrTiO_3$ homoepitaxial thin films

*이상아, 정회동, 우성민, 황재열 [1], 최시영 [2], 최민석 [2], 노슬기, 유호성, 황정식, 김성웅, 최우석
*Sang A. Lee, Hoidong. Jeong, Sungmin. Woo, Jae-Yeol. Hwang[1], Si-Young. Choi[2], Minseok. Choi[2], Seulki. Roh, Hosung. Yu, Jungseek. Hwang, Sung Wng. Kim, Woo Seok. Choi
성균관대학교. [1] 기초과학연구원 (IBS). [2] 재료연구소.

Keyword : $SrTiO_3$, homoepitaxy, PLD, elemental vacancy

Perovskite strontium titanate ($SrTiO_3$, STO) is an exciting material which shows various physical property changes including superconductivity-metal-insulator and ferroelectric-paraelectric transition. It is therefore one of the most popular substances and substrates for epitaxial growth of perovskite transition metal oxide thin films and heterostructures. It is also well-known that elemental defects such as oxygen vacancies induce changes in the crystal and electronic structure of STO. However, it has not been clearly understood, how the elemental vacancies are related to specific physical properties and phase transitions in STO. In this study, we have systematically investigated the formation and the role of elemental vacancies in STO homoepitaxial thin films using pulsed laser epitaxy (PLE). We could selectively control Sr and oxygen vacancies in the thin film by carefully controlling various growth conditions, such as partial pressure, laser energy, and oxygen flow rate. Based on this selective elemental vacancy engineering, we identified that Sr and oxygen vacancies individually affect the crystal structure and electronic structure, respectively. X-ray diffraction analyses and theoretical calculation result showed that the cubic-to-tetragonal structural transition observed in the homoepitaxial thin films was due to the Sr-containing vacancies, indicating that oxygen vacancies alone cannot modify the crystal lattice of STO. On the other hand, the electronic structure of STO was closely coupled to the oxygen vacancies, where the insulator-to-metal transition was induced by introducing oxygen vacancies. Our results imply that selective elemental vacancy engineering is possible even in complex oxides and paves a way for exploiting defects for designing physical property and functionality tailored transition metal oxides thin films and heterostructures.

D2.02*

Radial quadrant domains in $BiFeO_3$ nanopillars

*김광은, 장병권, 이진홍, 김용진, 정스리, 김기엽 [1], 김성대 [1], 주강현, 최시영 [1], 양찬호
*Kwang-Eun. Kim, Byung-Kweon. Jang, Jin Hong. Lee, Yong Jin. Kim, Seuri. Jeong, Gi-Yeop. Kim[1], Sung-Dae. Kim[1], Kanghyun. Chu, Si-Young. Choi[1], Chan-Ho. Yang
한국과학기술원. [1]KIMS.

Keyword : "Ferroelectric","PFM","c-AFM","Nanostructure"

Understanding ferroelectric nanostructure has recently become as issue because of their broad applications in multifunctional electric devices. Ferroelectric nanostructures are expected to be sensitive to the system's size, geometry, and strain. In this study, we report that a new type charged domain structure which attracts the same polarities of polarizations at local area in the BFO nanopillar. Normally, these structures encountering same bound charge have been rarely observed because of their unstable electrostatic energy, but we realized the charged domain structure under large strain relaxation environment. The domain structures of BFO nanopillars were examined using angle-resolved piezoresponse force microscopy (AR-PFM). Average strain and strain gradient values were estimated by x-ray diffraction measurements. Moreover, electronic conductivity of nanopillars were investigated using conductive atomic force microscopy (c-AFM) by applying dc bias between the conductive tip and bottom electrode.

D2.03*

$BiFeO_3$-$BaTiO_3$ lead-free piezoceramics by using tape casting process

*김다정, 이명환, 박진수, 김명호, 송태권, 도달현 [1], 김상수, 장기완, 이호용 [2]
*Dajeong. KIM, Myanghwan. LEE, Jinsu. PARK, Myongho. KIM, Tae Kwon. SONG, Dalhyun. Do[1], Sang Su. KIM, Kiwan. JANG, Ho Yong. Lee[2]
창원대학교. [1] 계명대학교. [2] 선문대학교& (주)세라콤.

Keyword : BiFeO3, BaTiO3, Lead-free, Piezoceramics, Tape casting

$BiFeO_3$–$BaTiO_3$ (BF–BTx) solid solution bulk ceramic is presented as potential lead-free piezoelectric ceramic. The phase diagram of BF-BTx material show morphotropic phase boundary (MPB) at x = 33 mol% region, which is coexistence of both rhombohedral ($BiFeO_3$) and tetragonal ($BaTiO_3$) phase, the result of excellent piezoelectric properties in BF-BT33 system can be expected. For the piezoelectric application, it is needed for the Multi-layer actuators (MLAs) made by using tape casting or screen printing process. Fujii and co-workers reported Mn-modified BF-BT-Bi(Mg,Ti)O_3 ternary ceramics, however, unmodified BF-BT based ceramics have not been achieved yet. We have investigated 0.67BF-0.33BT (BF-BT33) ceramic prepared using tape casting method showed high Tc, of ~ 470 ^oC, and piezoelectric constants d_{33} , of 180 pC/N in ceramics quenched at temperature of 960 ^oC.

D2.04*

Atomistic aspect of carrier concentration variation in post-annealed ITO films

*김지웅, 김혜경, 이민영, 이두용, 이지성, 장윤형 [1], 배종성 [2], 이정수 [3], 박성균
*Ji Woong. KIM, Hyegyeong. Kim, Min-Young. Lee, Dooyong. Lee, Jisung. Lee, Yun Hyeong. Jang[1], Jong Seong. BAE[2], Jeong Soo. LEE[3], Sungkyun. PARK
부산대학교. [1] 넥스트론. [2] 한국기초과학지원연구원. [3] 한국원자력연구원.

Keyword : ITO, Oxygen vacancy, Sn^{4+}, Post-annealing, Electrical properties

Sn-doped indium oxide (ITO) has high transparency in the visible region with superior electrical conductivity, so it is widely used transparent electrodes for the optoelectronic applications. Despite its usefulness, there have been continues effort to improve and control the electrical and optical properties of the system. Among them, post-annealing process is one of the routes to achieve the desired properties for transparent electrodes. In this presentation, we explain the origin of the physical property variation in post-annealed ITO films in terms of spectroscopic view [1].
ITO films, deposited on glass substrate, were annealed at 400 ^{o}C for 10 min under various environments such as O_2, in-Air and N_2. After annealing, the amorphous films became poly-crystalline films regardless of annealing environments with improved optical transmittance. Furthermore, all annealed-films showed n-type characteristics. Interestingly, the electrical properties improved (higher carrier concentration, lower conductivity) with increasing oxygen content in annealing environment. The physical origin of electrical property variation with different annealing environments was examined by core-level X-ray photoelectron spectroscopy. As results, we found that the electrical properties of ITO films are affected by Sn^{4+} ion and oxygen vacancy. The amount of Sn^{4+} ion and oxygen vacancy in ITO films increased with oxygen content in annealing environment. Therefore, the reducing oxygen content by post-annealing is a key component for improving electrical properties for the transparent conducting oxide application.

[1] J.W. Kim et al, J. Phys. D: Appl. Phys. (2015).

This study was supported in part by NRF Korea (2011-0031933 and 2012H1B8A2026225) and Korea Basic Science Institute Research Grant (E35800).

D2.05*

Comprehensive understanding of physical property variations in annealed ZnO films

*김혜경, 이두용, 김지웅, 이지성, 이원재 [1], 배종성 [2], 이재광, 박성균
*Hyegyeong. Kim, Dooyong. Lee, Ji Woong. Kim, Jisung. Lee, Won-Jae. Lee[1], Jong-Seong. Bae[2], Jaekwang. Lee, Sungkyun. PARK
부산대학교. [1] 동의대학교. [2] 한국기초과학지원연구원.

Keyword : ZnO films, Annealing, Environmental stability, Oxygen vacancies

To achieve the stable and controllable properties of ZnO thin film, various growth environments such as annealing, oxygen contents have been used. However, comprehensive understanding of physical properties of annealed ZnO thin film was not sufficiently complete. Here, we implemented spectroscopic approach in conjunction with structural and electrical analysis to examine the environmental stability of ZnO thin film.
ZnO thin films were fabricated by RF-sputtering method and annealed under various environments (O_2, in-Air, N_2 and vacuum). The structural, electrical and chemical properties were investigated by X-ray diffraction (XRD), Hall effect and X-ray photoelectron spectroscopy (XPS) measurement. XRD measurements showed all the annealed films showed better crystallinity than as-grown film. Especially, the film annealed under the N_2 environment showed the highest peak intensity and the smallest -rocking curve suggesting better crystallinity than films annealed other environments. In electrical measurement, the film annealed under N_2 exhibited the highest conductivity, carrier concentration and mobility. XPS measurement revealed the particular correlation between physical (structural, electrical) and chemical properties in ZnO films: The crystallinity of ZnO films is closely related to the Zn-O bonding, while carrier concentration is associated with the Zn-V_O (oxygen vacancy) bonding.

This study was supported in part by NRF Korea (2011-0031933 and 2012H1B8A2026225) and Korea Basic Science Institute Research Grant (E35800).

D2.06

Synthesis and electrical properties of thermally-driven-MIT in VO_2 films

*김정란, 황인희, 박창인, 한상욱
*ZHEN LAN. JIN, Inhee. Hwang, Chang In. Park, Sang Wook. Han
전북대학교.

Keyword : VO_2 film, growth, local structure, XAFS, metal-insulator transition

B-oriented VO_2 films were synthesized on Al_2O_3 (0001) substrates using DC magnetron sputtering deposition. Vanadium has diverse oxides, such as V_2O_3, V_2O_5, and V_4O_7 and VO_2 exhibits a relatively weak anti-oxidization ability. Thus, the synthesis of b-oriented VO_2 films are quite difficult, particularly, during an annealing process at a high temperature in an oxygen-rich atmosphere. A monoclinic phase and b-orientation (0l0) of the VO_2 films were determined by using X-ray diffraction. The structural and the electrical transitions were observed from thermally driven VO_2 films. The temperature dependent local structures were investigated by using in-situ X-ray absorption fine structure (XAFS) measurements at the V K edge. XAFS revealed that the structural phase transition was occurred nearly 70°C for heating process and reproducible. Hysteretic MIT is also observed and critical transition temperature was near 75°C which was higher than 68°C reported from a VO_2 bulk. We will discuss the MIT of VO_2 films, comparing with the local structural properties determined by XAFS measurements.

D2.07*

Temperature-dependent local structural properties of metal-insulator-transition Ti_2O_3

*황인희, 강병식 [1], 김정란, 박창인, 한상욱
*Inhee. Hwang, Bingzhi. Jiang[1], Zhenlan. Jin, Chang-In. Park, Sang Wook. Han
전북대학교. [1]Yanbian University.

Keyword : XAFS, Ti_2O_3, MIT

We examined the local structural properties of metal-to-insulator-transition (MIT) Ti_2O_3 using in-situ X-ray absorption fine structure (XAFS) measurements at the Ti K edge in the temperature range of 300 – 750 K. Ti_2O_3 powder was synthesized by using a chemical reaction method. X-ray diffraction measurements with a Rietveld refinement demonstrated that Ti_2O_3 has a single-phased R -3 c symmetry. Extended-XAFS (EXAFS) demonstrated a zigzag patterned Ti position and an anomalous structural disorder of Ti-Ti pairs, accompanying with the bond length expansion of the Ti-Ti pairs along the c-axis for T > 450 K. The local structural distortion of the Ti ions would induce a band gap collapse between the Ti 3d a_{1g} and e_g^{π} bands with the bond length expansion for T > 450 K.

D2.08*

The origin of the thermally stimulated depolarization currents and the dielectric relaxations in non-multiferroic $YFe_{0.8}Mn_{0.2}O_3$ single crystals

Kwanghee Cho, Soonyong Park
Kwanghee. Cho, Soonyong. Park
중앙대학교.

Keyword : dielectric, relaxation, TSDC, defect, multiferroic

Dielectric relaxation and polarization properties were investigated in the solid solutions of orthorhombic $(YFeO_3)_{1-x}(YMnO_3)_x$ single crystals with x=0.2. The thermally stimulated depolarization currents (TSDC) were observed along all three orthorhombic axes at ~ 110 K, which was much lower than the observed spin reorientation temperature T_{SR} ~ 230 K. The electric field sweep bulk polarization measurements, however, showed neither hysteresis nor remnant polarization. Based on the result of the temperature and frequency dependent dielectric measurements, the defect-dipoles with the Mn^{4+}-Fe^{2+} centers are suggested as the origin of the observed TSDC and dielectric relaxation at ~ 110 K in the Mn-substituted yittrium orthoferrites.

D2.09*

Tunable Photoluminescence of $Sr(Zr,Hf)O_3$:Cu with respect to Photo-excitation energy

*이동재, 이윤상, 노한진 [1]
*Dong Jae. Lee, Yun Sang. LEE, Han-Jin. Noh[1]
숭실대학교. [1] *전남대학교.*

Keyword : "$SrZrO_3$", "$SrHfO_3$", "visible emission", "Cu doping"

We investigated the visible emission of Cu-ion-doped $Sr(Zr,Hf)O_3$ with the photo-excitation energy dependence. Polycrystalline $Sr(Zr,Hf)O_3$:Cu were prepared in the solid state reaction method, and the doping concentration of Cu ions were varied up to 10 %. In the Cu-ion-doped $SrZrO_3$ (SZO:Cu), the peak position of the visible emission changed from 400 nm (violet) to 600 nm (yellow) as the photo-excitation wavelength was tuned from 220 nm to 375 nm. This tunable multicolor behavior depended on the concentration of the Cu-ion doping. The Cu-ion-doped $SrHfO_3$ (SHO:Cu) showed optical properties similar to those of SZO:Cu. This unusual emission behavior is likely to be associated with the mixed valence states of the doped Cu ions, which were revealed by X-ray photoelectron spectroscopy. Our results suggest that the tunable multicolor emission in SZO:Cu and SHO:Cu could be utilized for ultraviolet sensors.

D3.01(초)

A Magnetic Nematic Hidden Ordered Phase in the Underscreened Anderson Model

*Peter S. Riseborough
*Peter S.. Riseborough
Temple University.

Keyword : .

We analyze a novel type of phase transition that appears in the spin-rotationally invariant form of the underscreened Anderson Lattice Model and we obtain, with decreasing temperature, a continuous transition with opening of a gap. The novel transition is driven by the Hund's rule exchange and is promoted by interband nesting. The resulting ground state can be viewed as a combined spin and orbital density wave, in which the order parameter cannot be observed by probes that are purely sensitive to either charge or magnetism. The transition produces an anisotropy in the response to a magnetic field. The model also supports an antiferromagnetic phase which is promoted by interband nesting. We suggest that this model might describe the "Hidden Order" transition in URu2Si2. We compare the predictions of the model with experimental results.

D3.02(초)

Effects of the spin-orbit interaction in correlated electron systems

*민병일
*BYUNG IL. MIN
포항공과대학교.

Keyword : spin-orbit coupling, correlated system, Po, mixed-valence, topological Kondo insulator

Materials of recent interest manifest the complex interplay of the spin and other lattice degrees of freedom. Among those, the spin-orbit interaction plays an essential role in determining electronic, magnetic, and structural properties of solids. We have investigated effects of the spin-orbit interaction in both weakly and strongly correlated electron systems, including metallic element Po with s,p valence electrons and rare-earth mixed-valent Kondo insulators with f valence electrons. The following properties are addressed: the origin of the stabilized simple-cubic structure for Po, and the topological properties of electronic structures in SmB6, YbB6, and SmS

D3.03(초)

Novel Quantum Criticality in Two Dimensional Topological Phase transitions

*조길영, 문은국
*Gil Young. Cho, Eun-Gook. Moon
KAIST (한국과학기술원).

Keyword : Topological quantum phase transitions, quantum criticality, Dirac Hamiltonian, Coulomb interaction

Topological quantum phase transitions intrinsically intertwine self-similarity and topology of many-electron wave-functions, and divining them is one of the most significant ways to advance understanding in condensed matter physics. Our focus is to investigate an unconventional class of the transitions between insulators and Dirac semimetals whose description is beyond conventional pseudo relativistic Dirac Hamiltonian. At the transition without the long-range Coulomb interaction, the electronic energy dispersion along one direction behaves like a relativistic particle, linear in momentum, but along the other direction it behaves like a non-relativistic particle, quadratic in momentum. Various physical systems ranging from TiO2-VO2 heterostructure to organic material α-(BEDT-TTF)2 I3 under pressure have been proposed to have such anisotropic dispersion relation. Here, we discover a novel quantum criticality at the phase transition by incorporating the 1/r long-range Coulomb interaction. Unique interplay between the Coulomb interaction and electronic critical modes enforces not only the anisotropic renormalization of the Coulomb interaction but also marginally modified electronic excitation. In connection with experiments, we investigate several striking effects in physical observables of our novel criticality.

D3.04(초)

Classification of three dimensional Dirac semimetals

*Bohm-Jung Yang
*Bohm-Jung. Yang
Seoul National University.

Keyword : .

A three-dimensional (3D) Dirac semimetal (SM) is the 3D analogue of graphene having linear energy dispersion around Fermi points. Owing to the nontrivial topology of electronic wave functions, the 3D Dirac SM shows nontrivial physical properties and hosts various exotic quantum states such as Weyl SMs and topological insulators under proper external conditions. There are several kinds of Dirac SMs proposed theoretically and partly confirmed experimentally, but its unified picture is still missing. In this talk, we propose a general framework to classify stable 3D Dirac SMs in systems having the time-reversal, inversion and uniaxial rotational symmetries. We show that there are two distinct classes of 3D Dirac SMs. In one class, the Dirac SM possesses a single Dirac point at a time-reversal invariant momentum on the rotation axis. Whereas the other class of Dirac SMs has a pair of Dirac points created by band inversion, and carries a quantized topological invariant. Moreover, we show that a quantized topological charge can be assigned to each Dirac point which ensures the stability of 3D Dirac semimetals.

D4.01(초)

Various pinning centers in Fe based superconductor thin films

*이상한
*Sanghan. Lee
광주과학기술원.

Keyword : Fe based superconductor, multilayer, BaZrO3, pinning effect, pulsed laser deposition

Since the discovery of Fe based superconductors (FeSCs), epitaxial thin films have been successfully grown by many groups and they have significantly advanced potential device applications and the understanding of the fundamental physical properties of these new superconductors. In particular, we recently have grown artificially engineered undoped $BaFe_2As_2$ /Co doped $BaFe_2As_2$ compositionally modulated superlattice structures grown on $SrTiO_3$/(La,Sr)(Al,Ta)O_3 substrate produces ab-aligned nanoparticle arrays and self-assembled c-axis aligned defects that combine to produce very large critical current density (J_c) and irreversibility field (H_{irr}) enhancements. We also fabricated BaO incorporated Co doped $BaFe_2As_2$/Co doped $BaFe_2As_2$ multilayer thin films on oxygen free CaF_2 substrate and it shows very high pinning force density reaching a maximum of 84 GN/m^3 at 22.5 T and 4.2 K. Not only multilayering but also 2nd phase incorporation approach which is relatively simple process is available to generate pinning centers in FeSCs. Recently, it has been reported that $BaZrO_3$ could exist as the nanoparticle second phase in $BaFe_2As_2$ matrix since it is chemically stable without suppressing the superconductivity. We incorporated various mol % $BaZrO_3$ in Co doped $BaFe_2As_2$ ceramic targets and have grown $BaZrO_3$ incorporated Co doped $BaFe_2As_2$ epitaxial thin films to maximize the pinning effect in $BaFe_2As_2$ system. Measured J_c was over $1MA/cm^2$ even at 13T which is the highest among reported FeSCs. We will discuss the structural properties of $BaZrO_3$ incorporated Co doped $BaFe_2As_2$ multilayer thin films examined by X-ray diffraction and T_c and J_c.

D4.02(초)

Study of vortex dynamics by magnetic force microscopy

*김지훈
*Jeehoon. Kim
IBS. POSTECH.

Keyword : vortex dynamics, magnetic penetration depth, MFM, high-T_c superconductors

The application of high-T_c superconductors has been a focus since its discovery. In general, superconductors lose superconductivity at the three critical parameters such as critical temperature (T_c), field (H_c), and current (J_c). The J_c is the most important for applications since it enhance directly power transportation and high field. However, the impediment of its increase takes place due mainly to the motion of vortices, resulting in a fast entrance of the vortex liquid state where J_c =0. For example, the maximum field at T=77 K is about 1 tesla that the coated YBCO conductor can generate. In this talk, we present a basic principle to increase J_c with the combination of extrinsic and intrinsic parameters obtained from global and local measurements. We measure the absolute magnetic penetration depth using magnetic force microscopy and investigate how it affects extrinsic parameters such as creep, fluctuations, and J_c in disordered high-T_c superconductors.

D4.03(초)

Deciphering Electron Matter in Unconventional Superconductors

*Laura H. Greene
*Laura H.. Greene
Florida State University.

Keyword : .

Point contact spectroscopy (PCS) is a bulk spectroscopic tool used to detect bozonic excitations through classical quasiparticle scattering and superconducting gap structure through Andreev scattering. We have found this technique to be sensitive to the non-Fermi liquid density of states arising from electronic nematic phases in the Fe pnictides and chalcogenides [1] and developed a quantum mechanical theory to account for this.[2] we have also used PCS to measure the bulk hybridization gap in the heavy-fermion URu_2Si_2, which opens at temperatures well above that of the hidden order transition.[3] Recently, we have studied the non-superconducting, non-magnetic, intermediate valence compound $YbAl_3$ and show that this heavy fermion exhibits a “slow crossover” to the coherent state, [3,4] We also show how PCS may provide a rigorous identification of the onset of hybridization. Collaborators: H.Z. Arham, E. D. Bauer, R.E. Baumbach, S.L. Bud’ko, P.C. Canfield, D.Y. Chung, S.D. Das, M. Dwyer, J. Gillett, G. Gu, C.R. Hunt, M.G. Kanatzidis W.-C. Lee, Q. Li, Z. W. Lin J. Misuraca, S. Narasiwodeyar, W.K. Park, P. Phillips, S. Ran F. Ronning, J.L. Sarrao, S.E. Sebastian, A. Thaler, J.D. Thompson, P.H. Tobash, J.S. Wen, and Z.J. Xu. H. Z. Arham, et al., Phys. Rev. B 85, 214515 (2012); Wei-Cheng Lee et al., Rev. B 86 245113 (2012);
Wei-Cheng Lee et al., Int’l J. Mod. Phys. B 27 1330014 (2013). Wei-Cheng Lee, et al., (PNAS) 112, 651 (2015). W. K. Park et al., Phys. Rev. Lett. 108, 246403 (2012); W. K. Park et al., Phil. Mag. 94, 3737 (2014). W. K. Park et al., arXiv:1411.7073; S. Burdin and V. Zlatić, Phys. Rev. B 79, 115139 (2009).

D5.01(초)

Spectroscopic Investigation of Magnetic Material Systems

*박재훈
*Jae-Hoon. Park
포항공과대학교.

Keyword : Magnetism, Spectroscopy, Interface, Thin film, Multilayer

Magnetic thin films and multilayers have intensively been studied in last a few decades due to potential magnetic device applications such as magnetic tunneling junctions and spin-torque magnetic random access memory devices. The magnetic device has rather complicated structure consisting of magnetic and non-magnetic metal films and oxide layers, and the functionality is determined not only by the property of magnetic thin films but also the interface states of metal-metal, metal-oxide, and even oxide-oxide films. The interface creates unusual effects, for examples lattice strain, unexpected oxidation of metal films, interface magnetism, etc, on the devices. Here we presents microscopic information and characterization on magnetic materials systems with metal-metal, metal-oxide, or oxide-oxide interfaces using various synchrotron-based spectroscopic techniques, which provide detailed chemical and structural information as well as physical properties. We will also discuss how such interfaces affect the magnetic properties and functionality of the system.

D5.02(초)

Anisotropic exchange interaction between a molecular spin and Fe3O4(100)

*E. Rentschler, J. Klanke[1], K. Medjanik, D. Kutnyakhov, G. Schönhense, S.K. Arora[2], I.V. Shvets[2], S. Schuppler[3], P. Nagel[3], H.J. Elmers
*E.. Rentschler, J.. Klanke[1], K.. Medjanik, D.. Kutnyakhov, G.. Schönhense, S. K.. Arora[2], I.V.. Shvets[2], S.. Schuppler[3], P.. Nagel[3], H. J.. Elmers
Instituet fuer Physik. [1]Johannes Gutenberg-Universität Mainz. [2]Centre for Research on Adaptive Nanostructures and Nanodevices (CRANN). [3]Institut für Festkörperphysik.

Keyword : Anisotropic exchange interaction, molecular magnets

Molecular magnetism is a fascinating interdisciplinary research field comprising aspects of materials science, chemistry and physics. Single molecule magnets have been proposed for the use as memory storage on the molecular level, quantum calculators and as building blocks of spintronic devices. They have also been shown to represent ideal model systems for studying exchange interactions between a finite number of localized magnetic moments. Usually the exchange coupling is described by a spin Hamiltonian considering an isotropic exchange constant. The exchange constant may depend on the distance and on the bond direction of the coupled spins but not on the spin direction itself. Only very recently a study of the exchange interaction in molecular magnets with unquenched orbital angular momenta describes the exchange interaction by an orbitally dependent exchange Hamiltonian, which is equivalent to an anisotropic Heisenberg exchange constant. We report an anisotropic coupling of a single magnetic moment comprising a large orbital moment coupled to a ferromagnetic substrate.

D5.03(초)

The effect of interface roughness on exchange bias coupling in $BiFeO_3/La_{0.7}Sr_{0.3}MnO_3$ heterostructures

*M. Vafaee, S. Finizio, R. Abrudan[1], H. Deniz[2], D. Hesse[2], H. Zabel, G. Jakob, M. Klaeui
*M.. Vafaee, S.. Finizio, R.. Abrudan[1], . [2], D.. Hesse[2], H.. Zabel, G.. Jakob, M.. Klaeui
Johannes-Gutenberg-Universitaet Mainz. [1]Albert-Einstein-Strasse. [2]Max-Planck Institute of Microstructure Physics.

Keyword : Multiferroic, X-ray resonant magnetic reflectometry measurements, Exchange bias effect

The electric field control of magnetization is a cost and energy efficient approach for future spintronics devices that can be realized using magnetoelectric effects. For instance, in artificial multiferroic $BiFeO_3/La_{0.7}Sr_{0.3}MnO_3$ (BFO/LSMO) heterostructures, the magnetization of the ferromagnetic LSMO can be altered by applying electric fields across ferroelectric/antiferromagnetic BFO in which the two ferroelectric and antiferromagnetic orders are coupled. The mechanism of the coupling at the interface is believed to be due to the exchange bias effect. We characterized the interface of the heterostructures with different stack sequences of LSMO/BFO and BFO/LSMO using TEM. The measurements show sharp and rough interfaces, respectively. The magnetometry and X-ray resonant magnetic reflectometry measurements (XRMR) show neither exchange coupling nor traces of ferromagnetic Fe atoms at the sharp interface between LSMO and BFO, respectively, in agreement with previous report [Bertinshaw et al., Phys. Rev. B 90, 041113(R) (2014)]. Instead, the heterostructures with rough and chemically intermixed interfaces exhibit coupling, and for these structures also ferromagnetic Fe atoms were detected at the interface via XRMR measurements.

D5.04(초)

Thermal spin generation

*최경민, 문철현, 민병철, 이경진 [1], David G. Cahill[2]
*Gyung-Min. Choi, Chul-Hyun. Moon, Byoung-Chul. Min, Kyung-Jin. Lee[1], David. Cahill[2]
한국과학기술연구원. [1] 고려대학교. [2]University of Illinois at Urbana-Champaign.

Keyword : spincaloritronics, spin transfer torque, thermal spin

The coupling of spin and heat gives rise to new physical phenomena in nanoscale spin devices. In particular, spin transfer torque (STT) driven by passing heat currents through magnetic layers provides a new way to manipulate local magnetization. Hatami et al. theoretically predicted thermally-driven STT in metallic spin valves [1]; Slonczewski suggested the initiation of thermally-driven STT in ferrite/metal structures and predicted a greatly enhanced quantum efficiency compared to charge-current-driven STT [2]. These new phenomena, namely, “thermal STT” rely on the transport of thermal energy, in contrast to the transport of electrical charge, and provide a new way to manipulate magnetization [1, 2]. To fully realize the envisioned advantages of thermal STT, it is important to observe thermal STT directly and quantify its sign and magnitude. Although thermal spin injections in ferromagnetic metal (FM)/normal metal (NM) [3], ferrite/NM [4], and FM/semiconductor [5] have been achieved, direct and conclusive evidence of thermal STT has remained elusive.
Here I provide direct evidence of thermal STT in metallic spin valves with the structure Pt/FM1/Cu/FM2. Heating by the ultra-fast pump optical pulse generates spin currents in the structure by two distinct mechanisms: i) volume spin generation in the FM1 layer by ultrafast heating and associated ultrafast demagnetization of FM1 [6]; ii) interfacial spin generation at the Pt/FM1 and FM1/Cu interfaces by heat current passing through the FM1 layer [7]. The spin-dependent Seebeck effect (SDSE) of FM1 converts the heat current into spin current. Both demagnetization-driven and SDSE-driven spin generation on FM1 can diffuse to FM2 and exert STT on FM2 magnetization.
The demagnetization-driven spin generation is due to thermal transport between electrons and magnons of FM1 and angular momentum conservation of electron-magnon coupling of FM1 [6]. The demagnetization-driven spin generation is significant for only the first ~3 ps after the pump optical pulse; 3 ps is approximately the time required for electrons, magnons, and phonons of FM1 to equilibrate.
The SDSE-driven spin generation is due to thermal transport between FM and NM at FM/NM interface. In contrast to ultrafast demagnetization, the heat current passing through FM1 persists for a much longer time, ~100 ps, the time required for the various layers in the structure (Pt, FM1, Cu, and FM2) to equilibrate. The amount of SDSE can be controlled by the composition of FM1, which is a spin source layer, and thickness of Cu, which is a heat sink layer.

References M. Hatami et al. Phys. Rev. Lett. 99, 066603 (2007).
J. C. Slonczewski, Phys. Rev. B 82, 054403 (2010).
A. Slachter et al. Nature Phys. 6, 879 (2010).
K. Uchida et al. Nature Mater. 9, 894 (2010).
J.-C. Le Breton et al. Nature 475, 82 (2011).
G.-M. Choi et al. Nature Commun. 5, 4334 (2014).
G.-M. Choi et al. Nature Phys. 11, 576 (2015).

D6.01

Status of the PAL-XFEL construction

*강흥식
*Heung Sik. Kang
포항공과대학교.

Keyword : hard X-ray FEL, S-band linac, undulator, lasing

The PAL-XFEL, a 0.1-nm hard X-ray FEL facility consisting of a 10-GeV S-band linac, is being constructed in Pohang, South Korea. Its building construction was completed at the end of 2014. The installation of the 10-GeV linac started in January 2015 will be completed by the end of 2015 together with undulators and beam lines. The commissioning will get started in January 2016 aiming for the first lasing of hard X-ray FEL. We will report the current status, construction progress, and commissioning plans for the PAL XFEL project, including major subsystem preparations.

D6.02(초)

Advanced X-rays in Japan

*Tetsuya Ishikawa
*Tetsuya. Ishikawa
RIKEN SPring-8 Center.

Keyword : .

SACLA, the X-ray Free Electron Laser (XFEL) in Japan, has been operated as a user facility since 2013[1]. High peak power (40GW: ~400 uJ/pulse & 10 fs pulse duration) with near complete spatial coherence characterizes the SACLA X-rays, which finds ideal applications in quantum X-ray optics, ultrafast dynamics, radiation damage-free structure investigations, etc. In this talk, I will introduce this SACLA XFEL facility and its performance during the last three years. Further the upgrade plan of SPring-8 will be introduced with the perspective for new X-ray science with those.

1 Ishikawa, T. et al. A compact X-ray free-electron laser emitting in the sub-angstrom region. Nat. Photon. 6, 540-544 (2012).

D6.03(초)

Progress of PAL-XFEL Beamlines

*김봉수, 고인수 [1], 김동언, 강흥식 [1], 김광우
*Bongsoo. KIM, In Soo. KO[1], Dong Eon. KIM, Hung Sik. KANG[1], Kwang Woo. KIM
포항가속기연구소. [1] 포항공과대학교.

Keyword : XFEL, Synchrotron, Beamline

Pohang Accelerator Laboratory(PAL) is developing a SASE X-ray Free Electron Laser based on 10 GeV linear accelerator (Pal-XFEL).
PAL-XFEL has two undulator halls, one for hard X-ray, the other for soft X-ray, which will provide XFEL light in a photon energy range from 2 keV to 20 keV, and from 300 eV to 2 keV respectively. The typical photon numbers at 10 keV is ~ 5x1011 in a pulse. The construction of the phase 1of PAL-XFEL started at yr 2009 and plan to begin the commissioning in 2016.
Tapering of undulator, and self-seeding are being developed and scheduled in next to phase 1 construction.
One hard X-ray FEL undulator and one soft X-ray undulator are in construction with 2 hard X-ray hutches and 1 soft X-ray hutch respectively.

D8.01*

Measuring correlation between flow harmonics with moments in ALICE experiment in LHC.

*송명근, 강주환, 김동조 [1]
*Myunggeun. Song, JuHwan. Kang, DongJo. Kim[1]
연세대학교. [1]University of Javaskila.

Keyword : ALICE, LHC, Flow, Correlation, AMPT

One of the important results in Heavy Ion collisions is anisotropic azimuthal distribution of particle production. This collective phenomena is know as Flow effect, and successfully explained by Fourier's harmonic decomposition. Especially large elliptic flow v_2(second order harmonics) in non-central collision has been described by initial geometric response of almond shaped collision regions, and asymmetric pressure gradient. Higher harmonics are understood as the hydrodynamic response to spatial deformation of initial density profile which fluctuate as event to event. And the correlation between different flow harmonics may provide a new window into both the early stage dynamics and transport properties of QGP.
Several flow observables have been studied by measuring moments[1,2], by using two symmetric sub-events group separated by a single rapidity gap. Advantage of using this method is that we can suppressing non-flow effect such as jet and resonance in addition to suppressing self-correlation. With this method, we measured the correlation between different harmonics flows (both magnitude and event plane angle direction) and and studied how the correlation between higher-order flow and lower-order flow is correlated and estimated the coefficient of nonlinear part of the hydrodynamic response.

In this presentation, the details of the method will be described and the final results will be compared to the AMPT simulation and various hydrodynamic calculations.

D8.02

Review of bottomonia measurements in pp and PbPb at CMS

*문동호
*Dong Ho. Moon
전남대학교.

Keyword : CMS, Quarkonia, Upsilon, QGP, heavy-ion

Quarkonia are very important probes to investigate Quark-Gluon-Plasma state of hot and densed medium created in high energy heavy-ion collisions. The results of upsilon productions in pp and PbPb at CMS are updated recently. So, in this talk, we would like to summarize the results presented so far and updated results.

D8.03

Review of the CMS results of charmonia from Run I

*김용선
*Yongsun. Kim
고려대학교.

Keyword : charmonia, CMS, heavy ion, quarkonia, Yongsun Kim

A multi-dimensional analysis of charmonia in pp, pA, and AA collisions with the CMS detector will be presented. The prompt J/psi results are obtained using the $L_{int}=5.4 pb^{-1}$ pp, the $L_{int}= 35 nb^{-1}$ pPb, and the $L_{int}=150\mu b^{-1}$ PbPb data recorded between 2011 and 2013. The prompt J/psi nuclear modification factors (R_{AA}) and azimuthal anisotropy (v_2) in PbPb will be presented, and their impact on the understanding of the charmonium production will be discussed. In addition, the suppression pattern of prompt psi(2S) and J/psi in pp and PbPb collisions will be compared, addressing the phenomenology of the charmonium excited state versus ground state in a medium. The pPb differential cross-sections of prompt J/psi will be shown in a wide kinematic region, for transverse momentum spanning from 2 to 30 GeV /c and a rapidity interval between -2.87 to 1.93 in the center of mass of the collision. The ratio of yields in forward (p-going beam) and backward (Pb-going beam) directions, R_{FB}, is measured, to quantify the asymmetry of cross-sections as a function of p_{T}, rapidity, and event activity. A significant asymmetry is observed for $2 < p_T < 10$ GeV/c region, with no rapidity dependence, and with the effect monotonically increasing for higher event activity.

D8.04*

Activity of INHA university for the ALICE ITS upgrade

*박종한, 권민정
*Jonghan. PARK, Minjung. KWEON
인하대학교.

Keyword : 박종한

ALICE 실험의 목표는 QGP 를 연구하는 것이고, 이론적으로 QGP 는 중이온 충돌을 통해 생성된다고 예측된다. 중이온 충돌 실험을 통해 생성된 입자들을 ALICE 검출기로부터 측정할 수 있는데 ALICE 검출기 중 실리 콘으로 만들어진 ITS 는 위치 분해능이 뛰어나기 때문에 충돌로부터 나오는 입자의 궤적과 충돌지점을 추적하는데 사용된다. 현재 ALICE 에서는 ITS 업그레이드가 진행되고 있고, 업그레이드 함으로써 더 좋은 위치분해능과 트랙킹 효율을 얻을 수 있다. 본 연구에서는 업그레이드 된 ITS 에서 사용될 chip prototype 중에서 pALPIDEfs 칩테스트에서 DAQ board 에 인가되는 supply voltage 변화에 따른 threshold 값의 변화와 방사선 소스에 대한 chip response 변화를 확인하였다.

D8.05*

Study on bulk damage of sensor volume of Explorer-1 with neutron irradiation

*김지영, 최경언, 유인권
*Jiyoung. Kim, KyungEon. Choi, In-Kwon. Yoo
부산대학교.

Keyword : ALICE, ITS, CMOS, MAPS, silicon tracking detector

for the ALICE collaboration

During the Long Shutdown 2 (LS2) of the LHC in 2018/2019, the ALICE (A Large Ion Collider Experiment) plans an upgrade of its Inner Tracking System (ITS). A new seven layer detector system using Monolithic Active Pixel Sensor (MAPS) will be installed with replacing the current ITS detector system. The MAPS detectors are being developed by the ALICE-ITS team and manufactured by the TowerJazz 0.18um CMOS Imaging Sensor Process. The main goal of the ALICE-ITS upgrade project is to improve tracking resolution and accordingly vertexing capabilities at low p_T, and readout rate of the system while coping with the expected increase in luminosity at LHC during LS2. Radiation hardness of the upgraded ITS is one of crucial elements in the overall performance of the system. The expected radiation level for the upgraded ITS are a maximum Total Ionizing Dose (TID) of 700krad and a Non-Ionizing Energy Loss (NIEL) of $1x10^{13}$ 1MeV n_{eq} /cm^2. We studied radiation-induced effect on CMOS pixel sensor, concentrating on the effect of NIEL which causes bulk damage in the silicon lattice through non-elastic displacement of Si-atoms. Using Explorer-1, one of the ALICE Pixel Detector (ALPIDE) prototypes for ITS upgrade, we measured the characteristics of different irradiated sensor in diverse sensor volume. Some results of bulk damage of sensor volume induced by neutron irradiation will be presented.

D8.06*

Jet energy loss through photon bremsstrahlung

*조소연, 박가영, 윤진희
*Soyeon. Cho, Kayoung. Park, Jin Hee. YOON
인하대학교.

Keyword : Jet energy loss mechanism, QGP, quark-gluon plasma, Bremsstrahlung

Jet loses its energy with emitted photon while traveling in quark-gluon plasma(QGP). We calculate the cross section for this energy loss mechanism and check the correlation of final medium or photon with final jet.

D8.07*

Double helicity asymmetries in charged pion production in longitudinally polarized proton proton collisions at sqrt(s) = 510 GeV at RHIC-PHENIX in 2013

*문태봉
*Taebong. Moon
RIKEN/PHENIX/연세대학교.

Keyword : PHENIX, Spin, Proton, Gluon, RHIC

The Relativistic Heavy Ion Collider (RHIC) is a unique facility to study the role of gluons in the intrinsic proton properties. In perturbative Quantum Chromodynamics, charged pion production at high transverse momentum is sensitive to the gluon distributions in the proton. Gluon helicity distribution can be constrained by measuring the double helicity asymmetry A_{LL} for charged pion production in longitudinally polarized proton proton collisions. PHENIX has accumulated large amount of data since it started taking data. Especially, in 2013 at sqrt(s) = 510 GeV, PHENIX recorded the total integrated luminosity of 150 pb^{-1} which is almost ten times higher than in 2009 at sqrt(s) = 200 GeV. Due to a significant increase of the total integrated luminosity, we can improve statistics, In this talk, the physics motivation, the analysis procedure, and the the current status of the analysis will be reported.

D8.08*

Inclusive cross section and longitudinally double helicity asymmetry for π^0 production in p+p collsions at GeV at PHENIX Mid-rapidity

*윤인석
*INSEOK. YOON
서울대학교.

Keyword : A_{LL}, inclusive π^0,GeV,gluon polarization

PHENIX results on cross section and longitudinally double helicity asymmetry (A_{LL}) in inclusive π^0 production in p+p collisions at GeV at mid-rapidity from 2012/2013 RHIC runs will be presented. The result of cross section measurement will show the maturity of our understanding of perturbative QCD (pQCD) processes and parton-to-hadron fragmentation function. The π^0 A_{LL} result will help improve the constraints on the gluon's contribution to the proton's spin (ΔG). The latest global next-to-leading order pQCD analysis of the world data set including the data from fixed target deep inelastic scattering (DIS) experiments, the inclusive pion and jet A_{LL} data from RHIC data at GeV, suggest a positive ΔG in the region of gluon momentum fraction x_g>0.05. The new data at GeV will extend the experimental measurement to lower x~0.01 and help reduce the uncertainty.

D9.01

Measurement of electrons from beauty-hadron decays in p-Pb collision at with ALICE at the LHC

윤진희, 권민정
Jin Hee. YOON, Min Jung. KWEON
인하대학교.

Keyword : ultra-relativistic heavy-ion collisions, heavy-quark, cold nuclear matter effects, Beauty-decays electron, ALICE

Heavy-flavour hadrons, the hadrons containing charm or beauty quarks, are valuable probes providing constraints on partonic energy-loss mechanisms in the medium formed in heavy-ion collisions since they are produced at an early stage in the initial hard scattering processes. In particular, the medium-induced parton energy loss is expected to depend on the parton mass and colour charge. The theoretical prediction about mass dependency of the parton energy loss in medium can be tested by the flavour-separated measurement of charm and beauty. Measurements of medium modifications of heavy- flavour transverse momentum distributions in p-Pb collisions allow us to quantify cold nuclear matter effects in the initial state and to deduce the role of final-state effects in Pb-Pb collisions. With the ALICE central barrel detectors, electrons can be identified with high purity down to low transverse momentum. The production of electrons from beauty-hadron decays can be measured using their displacement from the primary vertex thanks to the long lifetime of the beauty hadrons. Using the impact parameter distributions of the electrons to separate statistically the electrons from beauty hadron decays from the background electrons in p-Pb collisions. The status on the nuclear modification factor of electrons from beauty decays in p-Pb collisions at $\sqrt{s_\rm{NN}}= 5.02\rm{TeV}$ will be presented.

D9.02

Reduction of the K^* meson abundance in heavy ion collisions

*조성태, 이수형 [1]
*Sungtae. Cho, Su Houng. Lee[1]
강원대학교. [1] *연세대학교.*

Keyword : K^*, K^* meson abundance, hadronic effects

We study the K^* meson reduction in heavy ion collisions by focusing on the hadronic effects on the K^* meson abundance. We show how the interplay between the interaction of the K^* meson with light mesons in the hadronic medium and that of the kaon determines the final yield difference of the statistical hadronization model to the experimental measurements. For the central Au+Au collision at $\sqrt{s_{NN}}=200$ GeV, we find that the K^*/K yield ratio at chemical freeze-out decreases by 36% during the expansion of the hadronic matter, resulting in the final ratio comparable to STAR measurements of 0.23 ±0.05.

D9.03

Calculation of k*/k+ ratio assuming the partial chemical equilibration

*이강석, 최숙 [1]
*Kang Seog. Lee, Suk. Choi[1]
전남대학교. [1]IBS.

Keyword : relativistic heavy-ion collision, K*/pion ratio

Production of K* in the relativistic heavy-ion collisions at LHC draws strong interest since the ratio involving K* mesons such as K*/pi or K*/K+ doesn't fit to the statistical model calculations while most of other ratios fit nicely. The reason is possibly that the K* doesn't chemically freeze-out at the same temperature T_{ch} as other particles do. Rather K* maintains partial chemical equilibrium through the process $K* \rightarrow K+ + \pi$ until the thermal freeze-out temperature, T_{th}. In this presentation, after fitting the momentum spectra of measured hadrons and ratios involving them measured by the ALICE collaborations with a blast-wave model which assumes the chemical freeze-out at higher T_{ch} and the thermal freeze-out at lower T_{th}, the ratio $K*/\pi$ is calculated from the parameters thus obtained assuming the partial chemical equilibration of K*, K and pi until T_{th}, and the result is compared with the data.

D9.04

Hypernuclei in Halo/Cluster Effective Field Theory

*안도슝이치
*Shung-Ichi. Ando
선문대학교.

Keyword : Light double Lambda hypernuclei, three-body system, limit cycle, Efimov state, effective field theory

The light double Λ hypernuclei, ${}_{\Lambda\Lambda}^{\ \ 4}$H and ${}_{\Lambda\Lambda}^{\ \ 6}$He, are studied as three-body $\Lambda\Lambda d$ and $\Lambda\Lambda\alpha$ cluster systems in halo/cluster effective field theory at leading order. We find that the $\Lambda\Lambda d$ system in spin-0 channel does not exhibit the limit cycle whereas the $\Lambda\Lambda d$ system in spin-1 channel and the $\Lambda\Lambda\alpha$ system in spin-0 channel do. The limit cycle is associated with the formation of bound states, known as Efimov states, in unitary limit. For the $\Lambda\Lambda d$ system in the spin-0 channel we estimate the scattering length a_0 for S-wave Λ hyperon-hypertriton scattering as $a_0=16.0\pm 3.0$~fm. We also discuss that studying the cutoff dependences in the $\Lambda\Lambda d$ and $\Lambda\Lambda\alpha$ systems, the bound state of ${}_{\Lambda\Lambda}^{\ \ 4}$H is not the Efimov state but formed due to the mechanism in the high energy whereas that of ${}_{\Lambda\Lambda}^{\ \ 6}$He would be the Efimov state.

D9.05

Relic antineutrino Capture by Electron Capture Decaying Nuclei

*이정연, 김영덕
*Jeong-Yeon. LEE, Yeongduk. Kim
Institute for Basic Science.

Keyword : Relic antineutrino, electon capture, decay.

The low energy nuclear beta or electron capture decays are excellent tools for testing non-zero neutrino masses. Among all beta unstable nuclides, ^{3}H, ^{187}Re, and ^{163}Ho are attractive for non-zero neutrino mass experiment due to their low Q-values. The EC decay of the isotope ^{163}Ho has been proposed since a long time as a candidate for measuring the electron neutrino mass and the interest in ^{163}Ho has been renewed because of a possible relic antineutrino capture experiment. But if there is no overdensity in the antineutrino distribution, the detection using ^{163}Ho is not possible. In this talk we will describe new possible candidates for experiments of relic antineutrino capture by electron capture decaying nuclei.

D9.06

Symmetry energy effects in nuclear α decay

신은경, 임연환 [1], 현창호 [2], *오용석
Eun-Kyeong. Shin, Yeunhwan. Lim[1], Chang Ho. Hyun[2], *Yongseok. Oh
경북대학교. [1] 기초과학연구원. [2] 대구대학교.

Keyword : nuclear α decay; effective potential; empirical formula; symmetry energy

The effects of nuclear symmetry energy on the alpha decay lifetimes of heavy nuclei are investigated within various phenomenological models of nuclear potential for the α cluster. In addition to the widely used simple square-well potential and Woods-Saxon potential, we suggest a model for the potential of the α cluster motivated by a microscopic approach of the Skyrme force model. We then investigate the effects of the nuclear symmetry energy by including the isospin asymmetry term in the potentials. We also modify the empirical α decay lifetime formula of Viola and Seaborg by including an isospin-dependent term. The calculated α-decay half-lives are in good agreement with the experimental data and we find that including the nuclear symmetry energy improves the results. The predictions on the α decay lifetimes of superheavy elements are also presented.

D9.07

Optimization of SRG-evolved N3LO interaction

*신익재, 김영만, A. Shirokov[1], M. Sosonkina[2], P. Maris[3], J. Vary[3]
*Ik Jae. Shin, Youngman. Kim, Andrey. Shirokov[1], Masha. Sosonkina[2], Pieter. Maris[3], James. Vary[3]
기초과학연구원. [1]Skobeltsyn Institute of Nuclear Physics. [2]Old Dominion University. [3]Iowa State University.

Keyword : NN interaction, PET, light nuclei

Nucleon-nucleon (NN) interaction is one of the substantial topics in nuclear physics, and especially plays a critical role in ab initio calculations. A current tendency is to adopt NN interactions based on chiral effective field theory. We start from SRG-evolved N3LO interaction which is derived by similarity renormalization group (SRG) to improve relatively poor convergences of original interaction, and apply phase-equivalent-transformation (PET). PET parameters are fitted to produce the ground and some excited states energy of selected s-shell and p-shell nuclei. This interaction, so called Daejeon16, can describe the properties of other light nuclei well.

D10.01(초)

High Energy Physics After the Higgs Discovery

*Tao Han
*Tao. Han
U. Pittsburg, USA.

Keyword : Beyond Standard Model (BSM), LHC, Future Colliders

With the milestone discovery of the Higgs boson at the CERN LHC, high energy physics has entered a new era. The completion of the "Standard Model" (SM) implies, for the first time ever, that we have a relativistic, quantum-mechanical, self-consistent theoretical framework, valid up to exponentially high energies, perhaps to the Planck scale. Yet, there are compelling reasons to believe that new physics beyond the SM is not far from our reach. I discuss the need for the new physics, and motivate the future colliders beyond the LHC. I present the potential reach for the new physics at the future colliders.

D10.02(초)

Physics opportunities at the International Linear Collider

*Tomohiko Tanabe
*Tomohiko. Tanabe
Univ. of Tokyo.

Keyword : Linear Collider, Higgs boson, top quark, new particles

The International Linear Collider is a proposed electron-positron collider with a center-of-mass energy range of 250-500 GeV, upgradable to 1 TeV. The talk will review the prospects for the precise measurements of the Higgs boson, the top quark, and selected topics on new particle searches.

D10.03(초)

Overview of Future Circular Colliders

*Hongbo Zhu
*Hongbo. Zhu
IHEP, China.

Keyword : CEPC-SppC, FCC

The discovery of the Higgs boson at the LHC marked a major breakthrough in particle physics and deepened our understanding of the fundamental structure of matter. It becomes natural to measure its properties as precise as possible at future colliders. The lightness of the Higgs boson of ~125 GeV makes circular electron-positron collider technologically feasible as a Higgs Factory and the same tunnel could accommodate proton-proton collider in future to enable searches for new physics at the next energy frontier of ~100 TeV. In this presentation, I will review briefly the two major proposals on future circular colliders, i.e. CEPC-SppC and FCC, including their status and future development.

D11.01

Thermal Instability of Charged AdS Black Hole

*노대호, 이범훈, 곽보근
*Daeho. Ro, Bum-Hoon. Lee, Bogeun. Gwak
서강대학교.

Keyword : Instabiliity, Fragmentation, Black Hole

We study about the instability of charged anti-de Sitter black hole in higher-dimension under fragmentation. The fragmentation breaks the black hole when the electric repulsion with the cosmological constant is too strong. The detailes are numerically investigated in terms of the mass and charge with arbitrary fragmented ratios.

D11.02

The GroudnBIRD Experiment for The Studies of B-mode Polarziation From Cosmic Microwave Background Radiation Detection.

*최지훈, 원은일, Osamu Tajima[1], Shugo Oguri[1], Hikaru Ishitsuka[2], Nozomu Tomita[3], Mitsuhiro Yoshida[1], Masashi Hazumi[1], Masanori Kawai[1]
*Jihoon. Choi, Eunil. Won, Osamu. Tajima[1], Shugo. Oguri[1], Hikaru. Ishitsuka[2], Nozomu. Tomita[3], Mitsuhiro. Yoshida[1], Masashi. Hazumi[1], Masanori. Kawai[1]
고려대학교. [1]High Energy Accelerator Research Organization. [2]SOKENDAI. [3]The University of Tokyo.

Keyword : "Cosmology","CMB","GroundBIRD","MKID","B-mode"

일반적으로 인플레이션 우주의 연구는 원시 중력파(Primordial Gravitational Waves)의 존재를 통해서 이루어질 수 있으며 Degree-Scale 에서의 B-mode Polarization Pattern 의 측정은 원시 중력파의 존재의 명백한 증거가 될 수 있다.
GroundBIRD 는 이러한 우주 배경 복사 (CMB)로부터의 B-mode Polarization Pattern 의 측정을 위한 지상 기반의 실험이며 두 Band 의 주파수 영역, 145 GHz 와 220 GHz, 그리고 6~300 의 Multipole(l)의 범위를 측정하게 될 것이다.

GroundBIRD 는 보통 일반적인 망원경이 사용중인 Azimuth-Elevation Scan 대신에 20rpm 으로 일정하게 회전하는 회전테이블(Turn Table)을 도입했다.
이러한 회전테이블은 GroundBIRD 의 관측영역을 매우 빠르게 변화시킬 수 있으며 결과적으로 대기의 요동에 의해 생성되는 관측범위의 제한을 크게 확장시켜서 지상 기반의 실험임에도 불구하고 위성실험 수준의 관측 영역을 제공할 수 있다.
Focal Plane 에는 최근 주목받고 있는 MKID(Microwave Kinetic Inductane Detector)를 사용 예정에 있으며 하나의 Cell 에서 수직, 수평의 두 Polarizaton 성분을 측정하게 된다.
광학계는 Mizuguchi-Dragone Dual-Reflector Mirror 로서 이것은 낮은 Cross-Polarization 및 넓은 Focal Plane 영역을 제공해주어서 CMB Polarization 실험에 매우 이상적인 광학계이다.

현재 GroundBIRD 는 대부분의 구조가 완성되어서 장시간의 냉각 테스트가 이루어지고 있으며 Focal Plane Design 의 최종 설계 및 제작이 진행중에 있다. 2016 년에 일본 내에서 시험관측이 예정되어있으며 2017 년부터는 Canary Islands 에서 본격적인 과학적 관측이 시작될 예정이다.

D11.03*

Conductivity in Anisotropic-Einstein-Maxwell-Dilaton-Axion Black Hole

*순리킴푼, 이범훈, 박찬용
*Sunly. Khimphun, Bum-Hoon. LEE, Chan Yong. PARK
서강대학교.

Keyword : gauge/gravity duality, conductivity, anisotropic black brane, Einstein-Maxwell-Dilaton-Axion

We study The AC and DC conductivity in the Einstein-Maxwell-Dilaton-Axion model using two axions to turn on the anisotropic properties of the black brane in both x and y direction. We perturb metric, Axion and gauge field by using gauge/gravity duality to study the conductivity numerically.

D11.04*

UFFO-pathfinder integration test result

*김민빈, 박일흥, 이직
*Minbin. Kim, IL Hung. PARK, Jik. LEE
성균관대학교.

Keyword : UFFO-pathfinder,감마선폭발,

Ultra Fast Flash Observatory (UFFO)- pathfinder 는 감마선 폭발(Gamma Ray Burst;GRB) 관측을 통한 물리적 결과 도출을 위해 제안된 위성 탑재체로, Coded mask 기반의 광시야각 망원경인 X-선 트리거 망원경과 자외선, 가시광 초기 후광 관측을 측정하기위한 자외선/가시광 추적 망원경과 구성되어 있다. 우주에서 감마선 폭발이 발생하면 X-선 트리거 망원경을 통해 감마선 폭발의 위치를 계산해 그 위치정보를 자외선/가시광 추적 망원경에 전달하게 된다. 이 때, 위성체 전체가 아닌 거울을 움직여 자외선/가시광 추적 망원경이 감마선 폭발의 초기광을 수초내에 관측가능하도록 한다. UFFO-pathfinder 는 Lomonosov 위성에 탑재되어 2015 년 말 발사 예정에 있으며, 전체를 조립하여 integration 테스트를 진행하고, 그 결과에 대해 발표하고자 한다.

D11.05*

Effect of eccentricity in gravitational waves emitted from compact binary inspirals

*김정초, 김정리 [1], 이형원
*Jeong Cho. Kim, Chunglee. KIM[1], Hyung Won. Lee
인제대학교. [1] *연세대학교 천문우주학과.*

Keyword : "Gravitational Wave","eccentricity","data analysis","waveform","inspirals"

Advanced LIGO (USA) will operate from this september, searching for astrophysical objects via gravitational waves (GWs). Advanced Virgo (Europe) and KAGRA (Japan) will be functional in a few years. Compact binary inspirals, such as neutron star - neutron star binaries or more heavier black hole - black hole binaries, are promising candidates for advanced LIGO and other future GW detectors. Based on a simple two-body calculation, Peter (1964) showed that inspiral orbits of compact binaries are circularized by GW emission. Therefore, most GW data analysis piplines have not involved eccentricity. In this work, we present how eccentricities in binary orbits affect GW waveforms and discuss their implications in GW data analysis.

D11.06*

Primordial gravitational waves from the space-condensate ination model

*간수, 고석태 [1], 이범훈
*Gansukh. Tumurtushaa, Seoktae. KOH[1], Bum-Hoon. LEE
서강대학교. [1] *제주대학교.*

Keyword : primordial gravitational waves, space-condensate ination model

We consider space-condensate ination model to study primordial gravitational waves. The energy density spectrum of primordial gravitational wave for this model is calculated when the phase transition between two regimes is abrupt. We also investigate constraints on our model parameter in light of observational bounds from several gravitational wave data including pulsar timing, ground-based and satellite observations.

D11.07*

Dark energy with a space-condensate (stopper) field

*이가원, 고석태 [1], 이범훈 [2]
*Kawon. Lee, Seoktae. KOH[1], Bum-Hoon. LEE[2]
서강대학교 물리학과. [1] 제주대학교. [2] 서강대학교.

Keyword : Cosmology, Late-time Acceleration, Dark energy

Recent couple of decades, several observational results reported independently that the present Universe is on the epoch of acceleration expansion.The source for the acceleration is distinguished by the name of "Dark energy" because of it is totally away from the sources that are already known. The many types of candidates for dark energy are suggested. One of them is the Quintessence field model which can explain the 'late' and 'acceleration' behavior of the dynamic of present Universe with proper potential.The non-linear sigma model can be regarded as parametric extension of the Q-field model and we find that the non-linear sigma model gives more proper fits for the observational data than the Q-field. To show this, we compare our results to the PLANCK 2015 data using the equation of state parameter and to the Supernova Type Ia data using the distance modulus.

D11.08*

Status of the Top and Bottom Counting Detectors for ISS-CREAM Experiment

*박정민, 김홍주, 박환배, 전혜빈, 황용석 [1], 현효정 [2], 이무현 [3], 윤영수 [3]
*Jeongmin. Park, Hong Joo. KIM, Hwanbae. Park, Hyebin. Jeon, Young Seok. Hwang[1], Hyojung. Hyun[2], MOO HYUN. LEE[3], Young Soo. Yoon[3]
경북대학교. [1] 원자력연구원. [2] 포항가속기연구소. [3] 기초과학연구원.

Keyword : "ISS-CREAM", "TCD/BCD", "e/p Separation"

The Cosmic Ray Energetics And Mass (CREAM) experiment will be launched in 2016 to the International Space Station (ISS) for understanding of the origin, acceleration and propagation mechanism of high-energy cosmic rays. The Top and Bottom Counting Detectors (T/BCD) are designed for studying the electron/gamma-ray physics. The T/BCD separate electrons form protons by using the difference in shower shapes between electromagnetic and hadronic interactions. Each of TCD and BCD consists of a plastic scintillator attached with 20 by 20 photodiodes. The T/BCD were integrated into the payload at the NASA Wallops Flight Facility. After the Integration, the ISS-CREAM instrument has been under vibration and thermal vacuum tests to confirm the safety of the instrument under a space environment. We present the result of the environment test of the T/BCD.

D11.09(초)

Recent results from the Telescope Array experiment

*H. Sagawa
*H.. Sagawa
Univ. of Tokyo.

Keyword : Telescope Array Experiment, Ultra-high energy cosmic rays

The Telescope Array (TA) experiment is the largest cosmic ray observatory in the Northern Hemisphere to explore astrophysical phenomena at the highest ends (~10^20.3 eV) of the cosmic ray energies. We have expanded its reach down to lower energy (10^15.6 eV) in the energy spectrum thus allowing it to probe over an unprecedented 4.7 decades in energy, and have observed spectral features. We present evidence for anisotropy in the arrival direction of the highest-energy cosmic rays as well as updated measurements of the spectrum and primary composition.Finally we present the plan of the Telescope Array extension.

D12.01(초)

Onset of glassy dynamics of polymers in spherical confinement and its link to chromosome organization

*현창봉
*Changbong. Hyeon
Korea Institute for Advanced Study.

Keyword : Confinement, Glassy dynamics, Chromosome, Genome, Polymer

Recent experiments showing scaling of the intrachromosomal contact probability, P (s) $\sim s^{-1}$ with the genomic distance s, are interpreted to mean a self-similar fractal-like chromosome organization. However, scaling of P(s) varies across organisms, requiring an explanation. We illustrate that dynamical arrest in a highly confined space as a discriminating marker for genome organization, by modeling chromosome inside a nucleus as a self-avoiding homopolymer confined to a sphere of varying sizes. Brownian dynamics simulations show that the chain dynamics slows down as the polymer volume fraction (φ) inside the confinement approaches a critical value φc. Using finite size scaling analysis, we determine $\varphi_c^{\infty} \approx 0.44$ for a sufficiently long polymer ($N \gg 1$). Our study shows that the onset of glassy dynamics is the reason for the formation of segregated organization in human chromosomes ($N \approx 3\times10^9$, $\varphi > \varphi_c^{\infty}$), whereas chromosomes of budding yeast ($N \approx 1.2\times107$, $\varphi < \varphi_c^{\infty}$) are equilibrated with no clear signature of such organization.

D12.02(초)

Transformation of taxol-stabilized microtubules into inverted tubulin tubules triggered by a tubulin conformation switch

*송채연, Miguel A. Ojeda-Lopez[1], Daniel J. Needleman[2], Youli Li, Herbert P. Miller, Leslie Wilson, Myung Chul Choi[3], Cyrus R. Safinya
*Chaeyeon. Song, Miguel A.. Ojeda-Lopez[1], Daniel J.. Needleman[2], Youli. Li, Herbert P.. Miller, Leslie. Wilson, Myung Chul. Choi[3], Cyrus R.. Safinya
산타바바라대학교. [1]Universidad Autonoma de San Luis Potosi. [2]Harvard University. [3]KAIST.

Keyword : microtubule, small angle x-ray scattering

Bundles of taxol-stabilized microtubules (MTs) - hollow protein nanotubes comprised of assembled αβ-tubulin heterodimers - spontaneously assemble above a critical concentration of tetravalent spermine and are stable over long times at room temperature. Here we report that at concentrations of spermine several-fold higher the MT bundles (B_{MT}) quickly become unstable and undergo a shape transformation to bundles of inverted tubulin tubules (B_{ITT}), the outside surface of which corresponds to the inner surface of the B_{MT} tubules. Using transmission electron microscopy and synchrotron small-angle X-ray scattering, we quantitatively determined both the nature of the B_{MT}-to-B_{ITT} transformation pathway and the structure of the B_{ITT} phase. Inverted tubulin tubules provide a platform for studies requiring exposure and availability of the inside, luminal surface of MTs to MT-targeted drugs and MT-associated proteins. (ref. Nature Materials 2014, 13, 195-203)

D12.03(초)

Surface roughness and density profile of water-alcohol mixture surfaces

*김도석, 전윤남 [1], 성재호 [1], Wei Bu[2], David Vaknin[2]
*Doseok. KIM, Yoonnam. Jeon[1], Jaeho. Sung[1], Wei. Bu[2], David. Vaknin[2]
서강대학교. [1]Sogang University. [2]Ames National Lab.

Keyword : surface capillary wave, X-ray reflectivity, surface roughness,

The density profiles of liquid/vapor interfaces of water–alcohol (methanol, ethanol, and propanol) mixtures were studied by X-ray reflectivity and the data was analyzed in the framework of capillary wave theory to address the characteristic length scales of the intrinsic roughness and the shortest capillary wavelength (alternatively, the upper wavevector cutoff in capillary wave theory). Our results established that the intrinsic roughness is dominated by average interatomic distances. The extracted effective upper wavevector cutoff indicates capillary wave theory breaks down at distances of the order of bulk correlation lengths. Careful analysis of the X-ray reflectivity data using various density profiles shows an error-function like profile is the most adequate within experimental error. Our finding, together with recent observations from simulation studies on liquid surfaces, strongly suggests that the capillary-wave dynamics shapes the interfacial density profile in terms of the error function.

D12.04(초)

Watching Molecular Motions in Confocal Microscope

*Sung Chul Bae
*Sung Chul. Bae
Department of.

Keyword : .

Confocal fluorescence microscope has been a powerful tool in various fields, especially biological science. 3D sectional imaging capability provided enhanced image contract by excluding signals from the out-of-focus region with a tiny confocal pinhole. However, most of applications were limited to imaging application till now. In this presentation, I would like to introduce experimental techniques for molecular dynamics, which can be used in confocal microscope. First of all, fluorescence correlation spectroscopy(FCS) is a great tool to observe any molecular motions which are responsible for fluorescence signal fluctuation in a small excitation volume of sample. Among these molecular motions are diffusion, rotation, molecular binding, conformation dynamics and so on. Combined with stimulated emission depletion(STED) microscope, FCS opens up another opportunity in live cell system and we will discuss pros and cons of STED-FCS. Another interesting technique is a time-resolved fluorescence anisotropy, which can provide local information of molecular rotation dynamics. Together with confocal geometry and time-correlated single photon counting system, it can measure rotational relaxation time of probe dye molecules, which is related with micro environment of molecules. Some of application examples and future perspective will be presented

D13.01(초)

Microwave ionization of Rydberg atoms

*H. Maeda
*H.. Maeda
Aoyama Gakuin Univ.

Keyword : .

When exposed to intense microwave fields, Rydberg atoms are ionized. It is well known that microwave ionization of Rydberg atoms are described either by a photon point of view or treating the microwave as classical oscillating fields [1]. In extremely intense microwave fields, tunneling ionization or over-the-barrier ionization takes place, in which Rydberg atoms "feel" electric fields of the microwave fields.
In low frequency regime, i.e., $\Omega < 1$ where $\Omega = \omega n^3$ is a scaled frequency, ω is microwave (angular) frequency, and n is principal quantum number of the initial Rydberg state, alkali atoms such as Na or Li are ionized at the electric field amplitudes blow $1/n^4$, i.e., classical field ionization limit, to as low as $1/n^5$ [2]. We use atomic units unless otherwise specified. It is pointed out that the $1/n^5$ field correlates with Ingliss-Teller limit, at which n and n+1 Stark manifolds intersect [1]. At this field the atom can evolve from the initial n state to n+1 state via single Landau-Zener (LZ) transition. Once the atom undergoes the n→n+1 LZ transition, the atom is sooner or later driven into very high-lying states or even into continuum after many cycles of the microwave field, because the n→n+1 LZ transition is the rate limiting step. H.B. van Linden van den Heuvell et al. show that the ionization process of alkali Rydberg atoms via the LZ transition can be well understood based on the photon point of view [3].
Recently we have experimentally studied microwave ionization of Li Rydberg atoms in low-frequency regime. In our experiments we have measured final-state distribution of Li Rydberg atoms exposed to linearly polarized 17.5-GHz microwave pulses by varying microwave-field amplitudes in the energy region of $23 \le n \le 72$, which is equivalent to $0.03 \le \Omega \le 1$. Our measurements show that microwave field amplitudes at which 50-% ionization of initial Rydberg atoms occurs tend to deviate from $1/n^5$ scaling law and increase as n increases, whereas the microwave amplitudes at which transitions of the Rydberg atoms into neighboring state occur nearly match the Ingliss-Teller limit, $1/3n^5$. Our results indicate that the n→n+1 LZ transition does not necessarily play a role of the rate limiting step in the ionization process.
References
[1] see, for example, T.F. Gallagher, "Rydberg Atoms", (Cambridge Univ. Press, New York, 1994).
[2] P. Pillet et al, Phys. Rev. A 30, 280 (1984).
[3] H.B. van Linden van den Heuvell et al., Phys. Rev. Lett. 53, 1901 (1984).

D13.02(초)

Towards THz clock-speed quantum computing

*안재욱
*Jaewook. AHN
한국과학기술원.

Keyword : Quantum computing

Quantum computation has been evolved during the past two decades from a visionary idea to one of the most active research areas in modern physics. Various quantum gates and elementary quantum circuits have been tested with model systems including trapped ions, superconductor junction arrays, and entangled photons, to list a few, and, lately, scientists around the world are tackling unseen technical issues in scaling the systems to a large-scale quantum computer. In that regards, recent progress in Rydberg atom-based C-NOT gating suggests a promising possibility of neutral-atom-based large-scale quantum computers. In this presentation, we introduce our experimental efforts towards an N-neutral atom quantum computer, where shaped femtosecond laser pulses drive atoms at a THz clock-speed and the atoms are to be coupled through Rydberg dipole blockade. Most recently, we have demonstrated a scheme for deterministic single atom loading by a reconfigurable two-dimensional optical tweezer array, generating N filled sites out of 2N initial sites in 95% success probability.

D15.01

Structural changes of small amplitude kinetic Alfvén solitary waves due to second order corrections

*최정림
*Cheong Rim. Choi
한국과학기술원.

Keyword : kinetic Alfven solitary wave, KdV soliton, second order correction

The structural changes of the KdV solution of kinetic Alfvén solitary waves (KASWs) due to higher order terms are investigated. The reductive perturbation method (RPM) is used to obtain the second order and third order partial differential equations, while the first order differential equation provides the dispersion relation for the kinetic Alfvén waves and the second order differential equation provides the KdV solution. Using the techniques introduced by Kodama and Tanuiti [J. Phys. Soc. Japan 45, 298(1978)], the secularities in the third order differential equations are removed and a linear second order inhomogeneous differential equation is obtained.

D15.02

Viscous dissipation in magnetic reconnection of collisionless magnetized plasma

*윤건수, 지정영 [1]
*GUNSU. YUN, Jeong-young. Ji[1]
POSTECH. [1]Utah State University. Logan.

Keyword : viscosity, magnetic reconnection, fluid closure, collisionless plasma

The dissipation rate of the magnetic field energy of wave-like fluctuations in collisionless magnetized plasma due to finite electron viscosity is obtained analytically. The viscous resistivity can be several orders larger than the collisional (Spitzer) resistivity in high-temperature fusion plasma. Thus, for magnetic reconnection events where the magnetic field energy transforms into kinetic energy, the viscous dissipation will play a key role for enhancing the rate of magnetic reconnection. The viscous dissipation is more effective for shorter wavelength fluctuation. A preliminary interpretation is discussed on the broadband emission and chirping-down phenomena observed in the ion cyclotron harmonic frequency range at the crash onset of magnetohydrodynamic instability modes of the KSTAR tokamak plasma. *Work supported by the National Research Foundation of Korea (grant No. NRF-2014M1A7A1A03029881 and BK21+ program) and Asia-Pacific Center for Theoretical Physics.

D15.03*

Research on parallelization mechanism of inductively coupled plasma for large area plasma source

*이장재, 김시준, 김광기, 이바다, 박인용, 염희중, 김대웅 [1], 유신재
*Jang Jae. Lee, Si Jun. Kim, Kwang Ki. Kim, Ba Da. Lee, In Yong. Park, Hee Jung. Yeom, Dae Woong. Kim[1], Sin Jae. YU
충남대학교. [1] 한국과학기술원.

Keyword : "inductively coupled plasma","parallelization mechanism","large area plasma","transformer model"

Inductively coupled plasma having the high-density is often used in plasma processing. In large area processing, the plasma can be generated by using the coil connected in parallel. However, in case of this, the power cannot transfer to plasma uniformly. To address the problem, we studied the mechanism of inductively coupled plasma connected in parallel by using transformer model.

D15.04*

New Circuit Model of Cutoff Probe for precise measurement of high density plasma

*김시준, 이장재, 이바다, 김광기, 박인용, 염희중, 김대웅 [1], 김정형 [2], 유신재
*SiJun. Kim, Jang Jae. Lee, Ba Da. Lee, Kwang Ki. Kim, In Yong. Park, Hee Jung. Yeom, Dae Woong. Kim[1], Jeong Hyung. Kim[2], Shin Jae. You
충남대학교. [1] 한국과학기술원. [2] 한국표준과학연구원.

Keyword : "cutoff probe" , "plasma modeling" , "high density plasma" , "plasma diagnostics" , "circuit model"

Cutoff probe have been noticed due to interest of plasma density which related to the results in the plasma processing. Although the cutoff probe has a long history, physics of it is not sufficient, especially in high density plasma because circuit model of cutoff probe is limited in low density plasma. In this research, we suggest the new circuit model of cutoff probe for precise measurement of high density plasma. It is well agree with Finite-Difference Time-Domain(FDTD) simulation at high density plasma and also previous circuit model at low density.

D15.05*

Research on transmission line design for efficient RF power delivery to plasma

*박인용, 이장재, 김시준, 김광기, 염희중, 이바다, 유신재
*In-Yong. Park, Jang Jae. Lee, Si Jun. Kim, Kwang Ki. Kim, Hee Jung. Yeom, Ba Da. Lee, Shin Jae. You
충남대학교.

Keyword : "Transmission line", "Plasma", "Impedance", "Matching", "Smithchart"

Recently, RF plasma has been used in the many processing. When used RF generator, generated plasma has source impedance that it can be changed by pressure, frequency and so on during processing. However, if the range of source impedance excesses matching range of the matching box, this matching box can`t match all value of input impedance. So, we researched to address the problem by using transmission line. As a result, transmission line is able to reduce range of source impedance and to deliver efficient RF power to plasma.

D15.06*

Development of ICP modeling for Research E-H mode transition mechanism

*김광기, 김시준, 이장재, 염희중 [1], 박인용, 김대웅 [2], 이바다, 유신재
*Kwang_Ki. Kim, SiJun. Kim, Jang Jae. Lee, hee jung. yeom[1], In-Yong. Park, Dae Woong. Kim[2], Ba-Da. Lee, Sin Jae. Yu
충남대학교. [1] 충남대학교 물리학과. [2] 한국과학기술원.

Keyword : " Plasma " , " ICP modeling" , " hysteresis " , " E to H mode transition mechanism "

Abstract
The various researches on E-H mode transition have been studied on account of the reason that the E-H mode transition is quite interesting phenomenon in ICP source. However, the previous researches have studied on the low density region or the high density region due to the non-existence of analytic power absorption relation versus plasma density with respect to the whole plasma density region. As a result of the development of ICP modeling, we induced the analytic power absorption relation versus plasma density or skin layer. The analytic power absorption equation considerably fit the previous researches that have been studied at the low density region and high density region well. We expect the analytic power absorption equation can help the subsequent research on the E-H mode transition mechanism.

D15.07

Hafnium Carbide Coatings on Carbon/Carbon Composites Using a Vacuum Plasma Spray coating method

*문세연, 유희일, 김호석, 홍봉근
*Se Youn. Moon, Hee-Il. Yoo, Ho-Seok. Kim, Bong-Guen. Hong
전북대학교.

Keyword : "vacuum plasma spray,Hafnium carbide, Ultra-high-temperature ceramic"

The pure hafnium-carbide (HfC) coating layer was deposited on the carbon-carbon (C/C) composites using a vacuum plasma spray (VPS) system. Using the SiC buffer layer, we successfully integrated C/C composites with a protective coating layer of 100 mm HfC. Comparing to the conventional chemical vapor deposition process (CVD), the HfC coating process by VPS showed more competitive growth rate, thickness and hardness. The growth behavior and morphological study about HfC coatings were investigated FE-SEM, EDS and XRD. From the pre-heat surface treatment, it was shown that the addition of SiC intermediate layer provided optimal surface condition during VPS procedure to enhance the adhesion between C/C and HfC without delamination. From the result, we expect that this ultra-high temperature ceramic (UHTC) coating method and micro structure will be widely applied to thermal shock and oxidation resistance filed under the ultra-high temperature environment

D15.08

Disinfection of rice seeds by ozone, ultrasonic wave or arc discharged plasma

*강민호, Anchalee Pengkit, 최기홍, 전성실, 최효원 [1], 신동범 [2], 최은하, 엄환섭, 박경순
*Min Ho. Kang, Anchalee. Pengkit, Ki hong. Choi, seong sil. Jeon, Hyo-Won. Choi[1], Dong-Bum. Shin[2], Eun Ha. CHOI, Han S.. Uhm, Gyungsoon. Park
광운대학교. [1]National Academy of Agricultural Science. [2]National Institute of Crop Science.

Keyword : "bakanae diseases", "rice seeds", "arc discharge plasma", "ozone", "ultrasonic wave"

Seed borne fungal diseases have been controlled mostly by seed treatment using various tools such as fungicide, heat, electrons, natural antifungal products, and biological control agents. There is a great need for efficient and eco-friendly technologies controlling fungal diseases. Previously, we found that arc discharge plasma was effective in sterilizing rice seeds infected with Fusarium fujikuroi, causing rice bakanae disease. In this study we have examined the effects of combined treatment of ozone and ultrasonic wave or arc plasma. The ozone treatment with ultrasonification has disinfected rice seeds more effectively than separate treatment with ozone or arc discharge plasma. Combined treatment that has a condition of 40kHz frequency ultrasonic wave and a concentration of 10% ozone gas seems to have greater fungicidal effect than separate treatment. After treatment of arc discharged plasma and combined treatment of ozone and ultrasonic wave, germination of normal seeds was not much changed compared to control. And also mechanisms of fungal inactivation by ozone, arc discharge plasma, and ultrasonification are being investigated.

This work was supported by the National Research Foundation of Korea (NRF) grant funded by the Korea government (MSIP), (No. 2010-0027963), Rural Development Administration (RDA) grant, No. PJ009891, and National Fusion Research Institute (NFRI).

D15.09*

Hybrid resonance probe for determination of plasma density and its application

*김대웅, 유신재**[1], 유광호 [2], 김정형 [2], 김시준 [1], 오왕열 [3], 장홍영 [3]
*Dae Woong. Kim, ShinJae. You[1], KwangHo. You[2], JungHyung. Kim[2], SiJun. Kim[1], WangRhul. Oh[3], HongYoung. CHANG[3]
한국과학기술원/한국표준과학연구원. [1] 충남대학교. [2] 한국표준과학연구원. [3] 한국과학기술원.

Keyword : plasma diagnostics, plasma density measurement, microwave probe, resonance

The electrostatic and electromagnetic resonances are typical phenomena for measurement of the plasma density by observing them. The first device was developed for detecting the resonances on microwave transmission or reflection spectra several decades ago. Recently, Piejeck[1] and Kim[2] revised the techniques of hairpin and cutoff probes incorporating electromagnetic and electrostatic resonances, respectively. Abundant researches have been conducted to reveal the physics and improve the precision of the each probes. However, correspondence of the measured plasma density between them is still questionable.
In this presentation, we propose the hybrid resonance probe (HRP) for measurement of plasma density with electrostatic and electromagnetic resonances. The HRP makes both resonances on the same microwave transmission spectrum. It was possible by merged structure of antenna tip and holder of cutoff and hairpin probe. The plasma densities were measured from two resonance peaks on the same spectrum. They showed a qualitatively good agreement but, measured plasma density from electrostatic resonance was little higher than that from electromagnetic. When the effect of sheath on the measured densities was corrected, the quantitatively discrepancy was decreased. This research elucidates the discrepancy of measured density from electrostatic and electromagnetic resonances and allows complementary uses of them by the proposed HRP.

[1] R. B. Piejak et al., Jour. Appl. Phys. 95 (2004)
[2] J. H. Kim et al., Appl. Phys. Lett. 83 (2003)
**.corresponding author:sjyou@cnu.ac.kr

E1.01*

Antiferromagnetic order competing with topological state in $Ce_xBi_{2-x}Te_3$

*이현성, 정명화, 김진수, 이규준, Andreja Jelen[1], Stanislav Vrtnik[1], Zvonko Jagličić[1], Janez Dolinšek[1]
*Hyun Seong. Lee, Myung Hwa. JUNG, Jinsu. Kim, Kyu Joon. Lee, Andreja. Jelen[1], Stanislav. Vrtnik[1], Zvonko. Jagličić[1], Janez. Dolinšek[1]
서강대학교. [1]J. Stefan Institute and University of Ljubljana.

Keyword : "topological insulator", "magnetic doping"

The topological surface states in three-dimensional topological insulators are easily tuned by chemical doping, especially by magnetic impurities. We prepared single crystals of $Ce_xBi_{2-x}Te_3$ with various x (= 0.04, 0.06, 0.08, 0.10, and 0.12). The obtained crystals were characterized by X-ray diffraction and scanning electron microscopy. The magnetic susceptibility data revealed that the Ce atoms are well substituted for Bi into Bi_2Te_3. From the Curie-Weiss fits, we obtained that the effective magnetic moments μ_{eff} are close to 2.54 μ_B for free Ce ion and the paramagnetic Curie-Weiss temperatures θ_p are negatively increased from 2.87 K to -59.3 K with increasing x. The magnetization data clearly showed antiferromagnetic orders around T_N = 4.1 K for $x \geq 0.08$, where θ_p suddenly increases, and the electrical resistivity is simply metallic and the magnetoresistance is parabolic. Only for x = 0.06, exotic physical properties arising from topological states were observed such as non-metallic behavior in the electrical resistivity and linear dependence of the magnetoresistance. Moreover, the carrier concentration of x = 0.06 is one order lower than that of $x \geq 0.08$. These observations propose that the antiferromagnetic order is strongly competing with the topological state in $Ce_xBi_{2-x}Te_3$.

E1.02*

비대칭 자구 확장 패턴 분석을 통한 자구벽 형태 결정

*김대연, 김덕호, 문준, 최석봉
*Dae-Yun. Kim, Kim Duck ho. , Moon Joon. , Sug-Bong Choe.
서울대학교.

Keyword : 자구벽 (magnetic domain-wall)

자구벽이 전류에 의해 이동하는 현상은 학술적인 측면 뿐만 아니라 racetrack memory 와 같은 소자로서의 응용으로도 많은 관심을 받아오고 있다. 소자로서의 응용적인 측면에서 볼 때, 전류에 대한 자구벽의 이동 효율은 매우 중요하며, 최근 자구벽의 형태 (Néel or Bloch) 에 효율이 크게 의존한다는 것이 보고되었다. 따라서 물질의 자구벽 형태를 결정하는 것은 굉장히 중요하며, 이번 연구에서는 자구가 확장하는 패턴을 관측함으로써 그 자구벽의 형태를 결정할 수 있는 방법을 찾아내었다. 서로 다른 자구벽 형태 (right-handed Néel, left-handed Néel, Bloch) 를 갖는 세 가지 자성 박막에서 자구의 확장 형태를 관측한 결과, 각각이 서로 다른 방향을 지향하며 비대칭적으로 확장하는 것을 볼 수 있었다. 인가한 수평 자기장 방향에 대하여 right-handed Néel 타입의 자구는 평행한 방향으로, left-handed Néel 타입의 자구는 반평행한 방향으로, Bloch 타입 자구는 수직한 방향으로 길게 확장하였다. 따라서 수평 자기장 인가 하에서 자구 확장 패턴의 elongation 방향 측정을 통해, 자구벽의 형태를 결정할 수 있다. 이러한 방법은 자구가 확장된 단일 image 만을 필요로 하기 때문에, 다양한 자성 박막의 자구벽 형태를 빠르게 결정해 내는데 큰 도움을 줄 것으로 예상된다.

E1.03*

Strain-induced uniaxial magnetic anisotropy variation in epitaxial $CoFe_2O_4$ thin films

*이두용, 김지웅, 배종성 [1], 윤형중 [1], 원종한 [1], 이주한 [1], 박성균
*Dooyong. LEE, Ji Woong. KIM, Jong-Seongq. BAE[1], Hyung-Joong. YUN[1], Jonghan. WON[1], Jouhahn. LEE[1], Sungkyun. PARK
부산대학교. [1] 한국기초과학지원연구원.

Keyword : "$CoFe_2O_4$", "Spinel structure", "Strain", "Magnetic anisotropy",

Achieving the materials with high magnetic anisotropy is important subject for the technological applications, such as magnetic and magneto-optic recording media. Among many high magnetic anisotropic materials, $CoFe_2O_4$ (CFO) has attracted much interests because of its unique magnetic properties such as larger magnetic elastic constant (K_1 ~ 2.0 x 10^6 erg/cm^3 in), large magnetic anisotropy constant (λsp ~ -110 x 10^{-6}), excellent chemical stability and high Curie temperature. Furthermore, it has been suggested that these properties can be tuned by the degree of epitaxial strain in the thin film form [1]. In this presentation, we examined the effect of epitaxial strain-dependent magnetic anisotropy of CFO thin films grown on different substrates.
The epitaxial CFO thin films were grown on different temperature. X-ray diffraction measurement showed all films have a (004) orientation for thin films grown above 450 ^oC regardless of substrates. However, the films grown on $SrTiO_3$(001) substrate exhibited in-plane compressive strain while in-plane tensile strain was showed for the films grown on MgO(001) substrate. The core-level X-ray photoelectron spectroscopy measurement revealed the different cation distribution depending on the strain state. The room temperature magnetization measurement also showed a decreased in-plane (out-of-plane) magnetic anisotropy for the films grown on $SrTiO_3$ (MgO) substrate when the epitaxial strain was decreased. The calculated uniaxial magnetic anisotropy energy showed a direct correlation between the uniaxial magnetic anisotropy and degree of epitaxial strain of the films.

E1.04*

Creep 과 Flow 영역에서 Dzyloshinskii-Moriya 상호작용에 의한 Chiral 자구벽 운동의 보편성

*김덕호, 유상철, 김대연, 민병철 [1], 최석봉
*Duck-Ho. Kim, Yoo Sang Cheol. , Dae-Yun Kim. , MIN Byoung Chul. [1], Sug-Bong Choe.
서울대학교. [1] 한국과학기술연구원.

Keyword : 비대칭적 자구벽 운동, Dzyloshinskii-Moriya 상호작용, 보편성, Flow 영역, Creep 영역

최근 Dzyloshinskii-Moriya (DM) 상호작용으로 나타난 Chiral 자구벽(domain wall)과 관련된 많은 물리적인 흥미로운 현상과 이것을 이용한 기술적인 응용 가능성으로 많은 연구가 진행되어 왔다[1,2]. 자구벽에 수평 자기장 H_x를 걸어주면, 이에 따라 자구벽 구조가 변하여, 유한한 DM 상호작용이 있는 계에서는 비대칭적인 자구벽 운동을 한다[3]. 최근 Creep 영역에서 이런 비대칭적인 운동에 대한 많은 연구들이 수행되었는데, DM 상호작용에 의한 유효자기장 H_{DMI}에 관련된 대칭적 효과(자구벽 에너지 밀도 변화[3-5])와 비대칭적인 효과(Chiral damping 또는 기타 변화[6])를 이용해 비대칭적인 운동을 설명하였다. 본 연구에서는 비대칭적인 자구벽 운동에 대한 이해를 확장하기 위하여, Creep 영역과 Flow 영역에서 비대칭 자구벽 운동을 관찰해보았다. 이를 위해 Pt(2.0 nm)/Co(0.3 nm)/Pt(2.0 nm) 구조의 수직 자기 이방성 박막을 제작하였고, 광자기 Kerr 현미경(magneto-optical Kerr effect microscope)을 이용하여 수직자기장 H_z를 고정하고, 수평자기장 H_x에 따른 자구벽 속력 v를 측정하였다. 기존의 Creep 영역의 비대칭적 자구벽 운동은 H_{DMI} 축을 기준으로 구분 된 대칭과 비대칭 효과를 이용하여 설명 할 수 있다. 그림 1(a)는 Creep 영역에서(H_z = 1.7 mT 로 고정) H_x에 대한 v 결과이다. 이 결과를 최근 Appl. Phys. Lett.에 보고된 방법[5]을 이용하여 H_{DMI}을 구하면, H_{DMI}가 60±5 mT 로 얻을 수 있었다. 흥미롭게도, Flow 영역에서도 거의 비슷한 현상이 관찰되었다. 그림 1(b)는 Flow 영역에서(H_z = 51 mT 로 고정) H_x에 대한 v 결과이다. 이 결과에서 Flow 영역에서는 비대칭 효과가 없어지고, 대칭 효과만 나타나는데, 놀랍게도 Creep 에서 구한 H_{DMI}와 정확이 같은 값을 대칭축을 가지고 있었다. 이 결과로부터 H_{DMI}는 Creep 과 Flow 모든 동역학 구간들에서 보편적인 값임을 확인 하였다. 이는 자구벽 이동을 통한 H_{DMI} 측정법에 대한 이해에 많은 도움이 될 것으로 생각된다. 세부적인 내용은 추후 발표에서 논의할 예정이다.

참고문헌

[1] K.-S. Ryu, L. Thomas, S.-H. Yang, and S. Parkin, Nat. Nanotech. 8, 527 (2013).
[2] K.-W. Moon et al. Sci. Rep. 5, 9166; DOI:10.1038/srep09166 (2015).
[3] S.-G. Je et al. Phys. Rev. B 88, 214401 (2013).
[4] R. Lavrijsen et al. Phys. Rev. B 91, 104414 (2015).
[5] D.-Y. Kim, D.-H. Kim, J. Moon, and S.-B. Choe, Appl. Phys. Lett. 106, 262403 (2015).
[6] E. Jué et al. ArXiv 1504.04411 (2015).

E1.05*

The effect of the MgO(001) layer on molecular structure and spin transport in organic spintronic devices

*배유정, 이년종, Jessica Wade[1], Ji-Seon Kim[1], Eisuke Ito[2], 김태희
*Yu Jeong. Bae, Nyun Jong. Lee, Jessica. Wade[1], Ji-Seon. Kim[1], Eisuke. Ito[2], Tae Hee. Kim
이화여자대학교. [1]Imperial College London. [2]RIKEN Advanced Science Institute.

Keyword : Organic Spintronics, Cu-Phthalocyanine, Molecular Ordering, Organic/Inorganic Hybrid Barrier, Spin Transport

In this work, we investigated the improvement of molecular structure and spin transport in magnetic tunnel junctions (MTJs) of the Fe(001)/MgO(001)/Cu-phthalocyanine (CuPc)/Co structure. Using an ultra-high vacuum (UHV) dual inorganic/organic molecular beam epitaxy (MBE) system, the multi-stacks were prepared in all in situ process with a variation of the organic semiconductor (OSC) CuPc thickness in 1.2-5.0 nm. MTJs of the Fe(001)/CuPc/Co structure without MgO(001) showed no magneto-resistance (MR) behavior due to the spin scattering in the disordered CuPc films as well as the conductivity mismatch problems at the ferromagnetic metal (FM)/OSC interfaces. As a result of the MgO(001) insertion, we observed remarkable MR ratio (> 100%) at 77 K and an abrupt reduction of MR to ~10% at RT. The reflection high-energy electron diffraction (RHEED) and Raman studies showed CuPc molecular films have highly crystalline structures on the MgO(001) surface and CuPc molecules are re-ordered along a preferential direction at low temperature below 200 K. Such crystallinity and reordering were not observable for CuPc films on Fe(001) or amorphous SiO_2 substrates. The results imply that a new molecular ordering could result from balancing intermolecular and substrate-molecular interactions, which is mainly controlled by the under-layer effects. This low temperature phase transition observed for the CuPc films on MgO(001) can affect the transport phenomena through CuPc barriers. Temperature dependent junction resistance revealed also consistent with this, showing abrupt changes at around 220 K. Our work provides important clues to improve the organic spintronic device performance at RT. Recently, MR up to 30% has been achieved at RT in hybrid MTJs with a 5 nm thick CuPc barrier.

E1.06*

Antiferromagnetic order induced by gadolinium substitution in Bi_2Se_3 single crystals

김수환, *정명화, Stanislav Vrtnik[1], Janez Dolinšek[1]
Soo-Whan. Kim, *Myung Hwa. JUNG, Stanislav. Vrtnik[1], Janez. Dolinšek[1]
서강대학교. [1]Jožef Stefan Institute and University of Ljubljana. Jamova.

Keyword : "topological insulator", "magnetic doping"

Magnetic topological insulators can serve as a fundamental platform for various spin-based device applications. We report the antiferromagnetic order induced by the magnetic impurity dopants of Gd in $Gd_xBi_{2-x}Se_3$ and the systematic results with varying the Gd concentration x (= 0.14, 0.20, 0.30, and 0.40). The antiferromagnetic order is demonstrated by the magnetic susceptibility, electrical resistivity, and specific heat measurements. The anomaly observed at T_N = 6 K for $x \geqslant 0.30$ shifts towards lower temperature with increasing the magnetic field, indicative of antiferromagnetic ground state. The Gd substitution into Bi_2Se_3 enables not only tuning the magnetism from paramagnetic to antiferromagnetic for high x ($\geqslant 0.30$) but also giving a promising candidate for antiferromagnetic topological insulators.

E1.07*

Magnetic properties of an asymmetrically terminated FeRh(001) thin film

*제갈소영, 임성현, 홍순철
*Soyoung. Jekal, Sonny. Rhim, Soon Cheol. HONG
울산대학교.

Keyword : "first-principles calculation" , "electronic structure" , "thin film" , "magnetocrystalline anisotropy"

The surface-termination and film thickness dependence of FeRh (001) magnetism has been recently reported. While Fe-terminated film shows G-type antiferromagnetism (G-AFM) as in the bulk, Rh-terminated ones exhibit ferromagnetism (FM) when they are thinner than 17 monolayers (ML) [1]. In this work, we investigate magnetic properties of asymmetrically terminated FeRh(001) films: One surface is Fe-terminated and the other surface is Rh-terminated. Since the different element-terminations have the different magnetic ground states, it is plausible that AFM and FM states coexist in an asymmetrically terminated FeRh(001) film. From total energy calculations, we found the coexistence of FM and AFM states in thicker asymmetric films than 8-ML: It is most stable among all plausible magnetic configurations that three layers from the Rh-terminated surface are FM while other rest layers are G-AFM. However, the thinner films than 6-ML show FM states over the whole layers. For 10-ML film, the coexistent magnetic state has lower energy of 8.55 meV/Fe and 9.27 meV/Fe than G-AFM and FM states over the whole thin film, respectively. Diverse magnetism such as magnetocrystalline anisotropy energies of the asymmetric FeRh(001) films will also be discussed. We expect that the plentiful magnetism of the asymmetrically terminated FeRh(001) may be utilized in spintronic devises including an exchange bias of AFM/FM composed of a single alloy.

[1] S. Jekal, S. H. Rhim, S. C. Hong, W. J. Son, and A. B. Shick, Phys. Rev. B, 92, 064410 (2015).

Acknowledgement
This work was supported by the Priority Research Centers Program through NRF funded by the Ministry of Education of Korea (2009-0093818) and the Basic Science Research Program through NRF funded by the Ministry of Science, ICT and Future Planning (2015R1A2A2A01003621)

E2.01(초)

Site-dependent evolution of conduction channels from tunneling to point contact in atomic-scale superconducting junctions

*김호원
*Howon. Kim
동경대학교 물성연구소.

Keyword : electron transport, Josephson junction, atomic contact, scanning tunneling microscopy, scanning tunneling spectroscopy

Electron transport in a quantum coherent conductor can be characterized by the set of transmission probability, $\{\tau_i\}$, which is relevant to conductance channels through the junctions. The accurate determination of the $\{\tau_i\}$ for the junctions is crucial to understand the conduction mechanism of electron in both normal-state and superconducting state. Although there has been many efforts with various methods to unveil the relation between channel distributions and their contributions to the electron transport through the superconductor-superconductor (S-S) junction at atomic-size junctions, direct observation of that relation is still challenge because of the lack of the geometric information at the atomically-formed junctions.

Here, we investigated atomic-scale S-S junctions by using scanning tunneling microscopy and spectroscopy with highly stable and precise control of a tip. In our local conductance measurements between superconducting Pb islands on Ge(111) and Pb layers on the end of PtIr tip apex, we observed evolution of not only the normal-state conductance [1] but also a zero-bias peak from tunnel to atomic contact, which corresponds to the Josephson current, with a decrease in the tip-substrate distance. Additionally, we found that the amounts of Josephson supercurrent and their evolutions from tunneling to contact were strongly depending on the contact between tip-apex atom and atomic sites on the surface crystalline lattice of the substrate. With a help of multiple Andreev reflection analysis through the S-S junctions, the observed spatial variation of Josephson current can be explained in terms of atomic-sites dependent distributions of conductance channels. Our new observations based on the precisely-controlled STM measurements together with theoretical supports at the S-S junctions can be expected to shed a new light to understand conduction mechanism in the small superconducting device and their applications.[2]

[1] H. Kim and Y. Hasegawa, Phys Rev Lett 114, 206801 (2015)
[2] H. Kim and Y. Hasegawa, arXiv:1506.05528 (2015)

E2.02(초)

Pushing Si-based storages toward atomic scales

*엄대진, 문창연, 구자용
*Daejin. Eom, Chang-Youn. Moon, Ja-Yong. Koo
한구표준과학연구원.

Keyword : silicon, boron, atomic scale storage, electron-lattice coupling, scanning tunneling microscopy

Information storage devices have been scaled down exponentially during the past decades. Yet they do not reach the ultimate limit of the solid-state devices i.e. atomic scale storages whose virtue was appreciated by R. P. Feynman as early as 1959. An essential ingredient to the ultimate scaling is to incarnate the bistate conversion on the atomic scale. Despite ongoing quest for this with various technologies exploiting diverse material systems, Si is still in a privileged position in the sense that it is the mainstream material for the current device fabrication and its processing technology is exceedingly advanced now. In this talk, I will present our efforts to make atomic scale storages on Si beyond the limits of previous studies. We show that the electron-lattice coupling is enhanced at the surface of boron delta-doped Si, making individual surface atoms have two stable but electrically switchable charge states. The structural and electronic properties of the two charge states as well as their energetics are uncovered by employing scanning tunneling microscopy (STM) measurements and density functional theory (DFT) calculations, which reveals that one of the two is a surface bipolaron. We also execute single-atom bit operations on individual surface atoms by using an STM to verify that R. P. Feynman has made a correct estimate on the conceivable bit dimension. Though still away from a real application, our findings underscore a message that the electron-lattice coupling in Si can provide new methodologies to implement atomic scale storages.

E2.03(초)

Graphene-metal Interactions Revealed by Scanning Tunneling Microscopy

*김효원
*Hyo Won. Kim
삼성종합기술원.

Keyword : Graphene, STM, Pt(111), Interaction

Graphene is a promising building block for future electronic devices but actualizing this enormous promise and realizing graphene-based devices requires a thorough understanding of how the contact between graphene and the underlying metal substrate affects the electronic properties of graphene. Metallic contacts to graphene are known to influence doping and can result in the opening of a band gap, which in turn significantly modifies the transport properties. The electronic properties of graphene on metal substrates also strongly depend on the nature of the graphene–metal interaction. Here, I present the graphene-metal interactions revealed by various scanning tunneling microscopic and spectroscopic studies such as the electron confinement in graphene nanoislands grown on a Pt(111) substrate [1], strong interaction between a graphene edge and the underlying metal [2], and the phonon excitations in graphene controlled by the interaction strength between the graphene and the underlying metal [3].

[1] H. W. Kim, et al. Electron Confinement in Graphene Nanoislands with Free-electron-like Energy Dispersion, submitted.
[2] H. W. Kim, et al. Strong Interaction between Graphene edge and metal revealed by scanning tunneling microscopy, Carbon, 78, 190 (2014).
[3] H. W. Kim, et al. Nanoscale Control of Phonon Excitations in Graphene, Nature Commun. 6, 7528 (2015)

E2.04

Local Potential Variation in Alloyed Topological Insulator $Bi_{1.5}Sb_{0.5}Te_{1.7}Se_{1.3}$ Probed by Landau Level Spectroscopy

*고원희, 박준범 [1], 전인수, 김효원, 권혁신, 오영택, 김준성 [1], 서환수, 황성우
*Wonhee. Ko, JoonBum. Park[1], in su. Jeon, Hyo Won. Kim, Hyeokshin. Kwon, Youngtek. Oh, Jun Sung. Kim[1], Hwansoo. Suh, Sungwoo. Hwang
삼성종합기술원. [1] 포항공과대학교.

Keyword : Topological insulator, Scanning tunneling microscopy, Landau level, local potential variation

We report the observation of local potential variation in the alloyed topological insulator $Bi_{1.5}Sb_{0.5}Te_{1.7}Se_{1.3}$ by Landau level spectroscopy combined with scanning tunneling microscopy. In high magnetic fields, topological surface states became quantized and formed Landau levels, whose energy showed spatial variation and directly illustrated the local potential fluctuation and resulting charge puddles. The origin of local doping was investigated through correlation between various physical quantities. The small correlation between the local potential and the surface topography indicated that the doping should be induced by the subsurface structure. Moreover, the large correlation between the local potential and the Dirac point conductance implied that such subsurface structures affect the electron properties of the topological surface states.

E2.05

Topological phase transition of ultrathin Sb films on Bi_2Te_2Se

*김성환, 진경환 [1], 박준범 [1], 김준성 [1], 지승훈 [1], 염한웅
*Sung Hwan. Kim, Kyung-hwan. Jin[1], JoonBum. Park[1], Jun Sung. Kim[1], Seung Hoon. Jhi[1], Han Woong. Yeom
포항공과대학교/기초과학연구원. [1] 포항공과대학교.

Keyword : Topological insulator, scanning tunneling microscopy/spectroscopy, ultrathin Sb film, quantum spin Hall phase, phase transition

We investigate local electronic structures of ultrathin Sb films and their edges as two-dimensional (2D) topological insulator through scanning tunneling microscopy/spectroscopy (STM/STS) and density functional theory (DFT) calculations. The ultrathin Sb films are theoretically predicted to emerge a topological phase transition depending on their thickness [1]. The STS measurements near the Sb 3~5 BLs edges clearly show that their edge states are different depends on the thickness of the Sb films. Our DFT calculations for Sb nanoribbon and films structures also indicate the topological phase transition between 3 and 4 BLs. According to our calculations, we distinguish that the experimentally resolved edge states on 4 and 5 BLs corresponded to a quantum spin Hall (QSH) phase whereas the 3 BLs edge states are trivial. Our experimental and theoretical results clearly show the topological phase transition of the ultrathin Sb films from trivial to QSH phase.

[1] P. Zhang, Z. Liu, W. Duan, F. Liu, and J. Wu, Phys. Rev. B 85, 201410(R) (2012).

E3.01

Resistance switching in layered oxide of strontium cobaltite

*정창욱
*Chang Uk. Jung
Hankuk University of Foreign Studies.

Keyword : strontium cobaltite, brownmillerite, resistance switching

The strontium cobaltite ($SrCoO_x$) has been reported to show topotactic phase transformations between an insulating brownmillerite ($SrCoO_{2.5}$) phase and a conducting perovskite ($SrCoO_{3-d}$) phase. by various methods. In this talk, I will introduce our very recent observations of novel resistance switching phenomena in a thin film of $SrCoO_x$ having layered structure. Electric voltage scan changed the state of SCO films from insulator to metal transition reversibly. Together with the temperature dependent resistivity at each state, we proposed novel switching mechanism in this material and suggest new type of resistance switching device.

E3.02

Doping a J_{eff}=1/2 Mott insulator: An Infrared Spectroscopic Study

*문순재, G. H. Ahn, S. J. Song, T. Hogan[1], S. D. Wilson[1]
*Soonjae. Moon, G. H.. Ahn, S. J.. Song, T. Hogan[1], S. D.. Wilson[1]
한양대학교. [1]University of California. Santa Barbara.

Keyword : electronic correlatins, spin-orbit coupling, metal-insulator transition, infrared spectroscopy

Iridium oxides (iridates) with layered perovksite structure have been attracting much attention as they were suggested to be 5d counterparts of high-T_c cuprates. Indeed extensive experimental studies of layered iridates revealed a number of commonalties of the electronic and magnetic properties of the iridates and cuprates. In this presentation, we will present our infrared spectroscopic data of electron-doped $Sr_3Ir_2O_7$, $(Sr_{1-x}La_x)_3Ir_2O_7$. We observed a filling-controlled insulator-metal transition with La doping. In the parent compound, a two-peak structure associated with the optical transitions between the effective total angular momentum J_{eff}=1/2 and 3/2 states were clearly resolved in optical conductivity spectra. Upon electron doping, the two peaks were suppressed and a Drude-like response accompanying a peculiar pseudogap structure appeared. The change in the electronic structure involves a transfer of the spectral weight over a wide energy region. Our observations parallel with the doping-induced evolution of optical response of strongly correlated electron materials including high-T_c cuprates and thus indicate a critical role of electronic correlations in $(Sr_{1-x}La_x)_3Ir_2O_7$.

E3.03

극초단 펄스로 유도된 LaMnO3 박막의 광학적 비등방성

*김명훈
*KIM Myung Whun.
전북대학교.

Keyword : LaMnO3, 극초단 펄스레이저

광학적 비등방성은 유용한 성질인데 그것을 조절하기는 어려운 경우가 대부분이다. 만약 극초단 레이저 펄스 빛을 이용해서 비등방성의 정도를 수 피코초 수준에서 조절할 수 있는 물질이 있다면, 이러한 물질은 초고속 소자를 개발하는데 사용될 수 있다. LaMnO3 라는 물질은 통상적인 투과율 실험에서는 비등방성이 관찰되지 않는다. 그러나 레이저 펄스를 쪼이면 상황이 달라질 수 있다. 우리는 LaMnO3 라는 물질에서 극초단 펄스에 의해 유도된 광학적 비등방성이 상온에서도 2 mJ/cm2 이하의 펄스 빛세기에 의해서 생길 수 있음을 발견했다. 이러한 비등방성의 원인을 이해하기 위해서 허버드 해밀토니안에 기반해서 물질계를 시늉낼 수 있는 간단한 모델을 수립하고 수치적으로 반사율과 투과율의 변화를 계산한 결과와 실험결과를 비교해 보겠다. 실험의 유효성 검증을 위해 Nd0.5Sr0.5MnO3 라는 물질과 기판으로 사용된 SrTiO3 의 실험결과도 함께 제시할 것이다.

E3.04

Nanoscale arrays of Kondo-cross-coupled one dimensional Heisenberg spin chains and metallic nanowires in $Nb_{12}O_{29}$

*이관우, W. E. Pickett[1]
*Kwan-Woo. Lee, Warren. Pickett[1]
고려대학교 세종캠퍼스. [1]Univ. of California. Davis.

Keyword : $Nb_{12}O_{29}$, Heisenberg-Kondo lattice, first principles calculations

In 1991, $Nb_{12}O_{29}$ was revealed in two papers to have very unexpected behavior: magnetic Nb ions (Nb is practically never magnetic) in the midst of conducting electrons (Nb_2O_5 is a well studied, common insulator). Using first principles theoretical methods, we have established that this materials has a distinctive, in fact unique, electronic and magnetic structure: a single Nb-based electronic state is very large in size (as in metallo-organics) yet localized ("flat band"). These local moments form spin chains in one direction, while there are conducting Nb-based "nanowires" in a perpendicular. This is a 2D system, essentially uncoupled to the next layer in the third direction. We describe this situation clearly, and show that its underlying properties should be contained within a new type of electronic model. Its array of 1D spin chains interlaced with a perpendicular array of conducting nanowires suggests novel electronic behavior, but that direction remains to be studied.

This new information on a 2D magnetic transition metal oxide (TMO) comes during a period (spanning roughly the past decade) where magnetic 2D TMOs are being designed (and synthesized layer by layer) for the numerous unusual phases that are found to result. $Nb_{12}O_{29}$ is naturally strongly layered, we show, and it displays the interplay between charge [Nb^{5+} and Nb^{4+} ions], spin [fluctuating spin-half magnetic moments], and orbital [specific 4d orbital occupation is crucial] that is so important in artificially synthesized materials. We suspect this compound forming the new 2D Heisenberg-Kondo lattice may also house superconducting pairing correlations.

E3.05

Characterization of the Weyl semimetal via the "Fermi arc" of Wannier-Stark ladder

*김건우, 이우람, 김용백 [1], 박권
*Kun Woo. Kim, Woo-Ram. Lee, Yong-Baek. Kim[1], Kwon. Park
고등과학원. [1]University of Toronto.

Keyword : Weyl semimetal, Fermi arc, Wannier-Stark ladder, DC E field, topological surface states

Weyl semimetals have been characterized unequivocally by the Fermi-arc spectrum of the surface states in photoemission experiments. While successful, such a method reveals the topological nature of the Weyl phase in the bulk indirectly via the surface spectrum. In this talk, we propose an alternative method to characterize the Weyl phase via the bulk spectrum of the Wannier-Stark ladder (WSL) emerging under an electric field. Specifically, we show that, for weak-to-moderate strengths of electric field, the WSL exhibits its own "Fermi arc" precisely corresponding to the surface spectrum counterpart, which can be used to characterize the Weyl phase directly in the bulk spectrum.

E3.06

Competing states for the fractional quantum Hall effect in the 1/3-filled second Landau level

*정재승, Hantao Lu[1], Kenji Hashimoto[2], 박권 [3]
*Jae-Seung. Jeong, Hantao. Lu[1], Kenji. Hashimoto[2], Kwon. Park[3]
IBS 강상관계물질연구단 / 서울대학교. [1]Lanzhou University. [2]Max Planck Institute for Mathematics. [3]Korea Institute for Advanced Study.

Keyword : fractional quantum Hall, second Landau level, 1/3

The fractional quantum Hall (FQH) states occurring in the second Landau level (SLL) exhibit qualitatively different behaviors in comparison with those occurring in the lowest Landau level, which provides a possibility of different FQH phases other than the composite fermion (CF) states. One of the most celebrated examples is the FQH state in the half-filled SLL, where there is a delicate competition between various states including the Moore-Read Pfaffian state and the antisymmetrized product state (APS) of CF seas (CFS) at quarter filling. While widely believed to be in the same universality class as the Laughlin state, the true nature of the FQH state in the 1/3- filled SLL has remained elusive. In this work, we perform exact diagonalization (ED) study of the wave function overlap between the exact ground state in the 1/3-filled SLL and various competing states including the Laughlin state, the Haffnian state, the particle-hole conjugate of the Z4 parafermion state, and the APS of CFS at 1/6 filling.

E3.07

Kondo screening in mixed valence and heavy fermion compounds and the signatures of Nozieres' exhaustion

*이현정, 강한힘 [1], 심지훈 [1]
*Hyun-jung. LEE, Hanhim. Kang[1], Ji Hoon. Shim[1]
Korea Advanced Institute of Science and Technology. [1]Pohang University of Science and Technology.

Keyword : Kondo lattice, heavy fermion, mixed valence, DMFT, NRG

How can few electrons screen many magnetic impurities, the so called "exhaustion problem" is an interesting issue in Kondo alloys, which is supposed to control the physics of heavy fermions in the mixed-valence regime. It also enters indirectly in the issue of Mott metal insulator transitions, where few charge carriers in a resonant narrow band are acting to screen a large number of localized spins in a broad Hubbard band, making isomorphic correspondence between heavy fermions superconductors and high-Tc cuprates.
In order to understand the exhaustion problem in Kondo alloys, we examine the dynamical properties of the periodic Anderson model such as the local spectral density and the spin excitation spectrum within the dynamical mean-field theory using the numerical renormalization-group technique. Pursuing the high impurity-concentration and the strong coupling limit simultaneously, we find a transition between coherent and incoherent Kondo regime, characterized by closing of the hybridization gap (pseudo-gap) and the extinct zero-energy bound state (Majorana mode). In the incoherent Kondo regime, where the heavy fermion quasiparticles lose the lattice coherence, spin and charge degrees of freedom of the correlated electron are decoupled, yielding separate two-peak structure in the spectral density.

E3.08

Observation of many-body localization transition in two-dimensional Hubbard model

*최재윤
*Jae-yoon. Choi
Max-Planck Institute of Quantum Optics.

Keyword : "Eigenstate thermalization hypothesis","Many-body localization","Dynamical phase transition"

Under which conditions isolated quantum systems do thermalize is one of the fundamental questions in modern statistical physics. Many-body localization (MBL) marks a general example that does not thermalize and has been a central theme in this field. Experimental demonstration of one-dimensional MBL is reported only recently by studying relaxation dynamics of charge density wave. However, microscopic detection of diverging length scale near critical disorder remains experimental challenges, and demonstration of the MBL in a higher dimension is highly demanding. Here, we report divergence of decaying length near many-body localization transition with two-dimensional Bose gases in an optical lattice. Employing single-site-addressing system, we engineer a density step at the center and observe dynamics of the initial state after lattice ramp. The density profile evolves into exponential decaying curve after long time evolution. We observe divergence of decaying exponent at a finite disorder and enhancement of decaying length because of interaction. Our results mark a first step to understand many-body localization near critical point, stimulating theoretical works to understand MBL in higher dimension and develop a novel scheme that probes local conserved quantities.

E3.09*

Reversible phase transition in $BaBiO_3$ thin films via oxygen stoichiometry control

*김기덕, 김지현, 김민우, 노태원
*Gideok. Kim, Jeehyun. KIM, Minu. Kim, Tae Won. Noh
서울대학교.

Keyword : charge density wave, oxide thin film, real-time ellipsometry, oxygen vacancy

Reversible phase transition in $BaBiO_3$ thin films via oxygen stoichiometry control

Jeehyun Kim[1,2], Gideok Kim[1,2], Minu Kim[1,2], Tae Won Noh[1,2]
[1]Center for Correlated Electron Systems, Institute for Basic Science (IBS), Seoul 151-747, South Korea
[2]Department of Physics and Astronomy, Seoul National University, Seoul 151-747, South Korea

Controlling oxygen vacancy in perovskite oxides has been a key quest for studying novel physical phenomena [1, 2]. Also, the formation of oxygen vacancy, closely related to oxygen diffusion process in solids, is crucial for the development of oxygen ion conductor [3, 4]. A perovskite bismuthate, $BaBiO_3$ (BBO), may be an intriguing candidate to study the effect of oxygen vacancy on its electronic properties: BBO is an insulator that exhibits a dominant optical absorption peak at 2 eV, which originated from a charge density wave (CDW) order [5]. The CDW order in BBO is understood by unfavored Bi^{4+} valence ($6s^1$), which disproportionates into Bi^{3+} ($6s^2$) and Bi^{5+} ($6s^0$), and thus is expected to be susceptible to additional charge carriers doped by oxygen vacancy.
Here, we investigate the effect of oxygen vacancy on the electronic properties of epitaxial BBO films grown by pulsed laser deposition. By using real-time spectroscopic ellipsometry, we found that the CDW absorption peak of BBO films is strongly suppressed by annealing below 10^{-8} Torr, meaning that the formation of oxygen vacancy can suppress CDW order. Interestingly, the CDW peak revives when annealed at high oxygen partial pressure (P_{O2} = 200 Torr), indicating that the CDW order can be reversibly controlled with oxygen vacancy concentration. We revealed that oxygen ions migration starts to occur at around 250 °C, substantially low compared to existing ion conductors, suggesting that BBO films might be promising for an oxygen ion conductor [4, 6]. In this presentation, the transition from oxygen deficient to oxygen stoichiometric phases depending on oxygen partial pressure and annealing temperature will be discussed in detail.

[1] Woo Seok Choi et al., Phys. Rev. Lett 111, 097401 (2013)
[2] D. A. Muller et al., Nature 430, 657 (2004).
[3] M. Cherry, M. S. Islam, C. R. A. Catlow, J. Solid State Chem 118, 125 (1995).
[4] S. Sanna et al., Nature Mater. 14, 500 (2015).
[5] S. Uchida, K. Kitazawa, S. Tanaka, Phase Transitions 8, 95 (1987).
[6] E. D. Wachsman, K. T. Lee, Science 334, 935 (2011).

E4.01(초)

Features of spin fluctuation mediated superconductivity for cuprates

*최한용, 복진모 [1], 배종주
*Han-Yong. CHOI, Jin Mo. Bok[1], Jong Ju. Bae
성균관대학교. [1]Chinese Academy of Sciences. Beijing. China.

Keyword : Pairing self-energy, Eliashberg theory, spin fluctuation, ARPES

We perform a consistency check of the spin-fuctuation-mediated d-wave pairing against the angle resolved photoemission spectroscopy (ARPES) results for the cuprate superconductors. Using the inelastic neutron scattering (INS) spin susceptibility spectrum reported by Vignolle et al in the Eliashberg equation, we calculate the quasi-particle self-energy for the optimally doped La2-xSrxCuO4. The self-energy can also be determined by analyzing the ARPES intensity. The angle and frequency dependence of the calculated normal and pairing self-energies from the spin fluctuations does not seem to be consistent with that deduced from ARPES.

E4.02(초)

Superconductivity and antiferromagnetism in iron pnictides and copper oxides

Hyoung Joon Choi
Hyoung Joon. Choi
Yonsei University.

Keyword : superconductivity, iron pnictide, copper oxide

Iron pnictides and copper oxides have a common feature that superconductivity appears near antiferromagnetism. A scenario for the microscopic mechanism of superconductivity in these materials is spin-fluctuation-mediated superconductivity. We develop a theory of spin-fluctuation-mediated superconductivity based on first-principles calculations of electronic structures and magnetic properties of iron pnictides. We calculate magnetic exchange couplings of Fe magnetic moments and construct Heisenberg spin Hamiltonians to obtain magnetic excitation spectra. We present superconducting properties of iron pnictides obtained using our theory of spin-fluctuation-mediated superconductivity and discuss its application to copper oxides. This work is supported by the NRF of Korea (Grant No. 2011-0018306). Computational resources have been provided by KISTI Supercomputing Center (Project No. KSC-2014-C3-070).

E4.03(초)

Quasiparticle self-consistent GW study of cuprates: electronic structure, model parameters, and the two-band theory for Tc

*MyungJoon Han
*MyungJoon. Han
KAIST.

Keyword : .

An important open question for high-Tc cuprates is about the material dependence of the superconducting properties. Using the quasiparticle self-consistent GW (QSGW) method, we re-examine the electronic structure of the parent compounds of copper oxide high-Tc materials. We show that QSGW captures several important features, distinctive from the conventional LDA results. The energy level splitting between dx2-y2 and d3z2-r2 is significantly enlarged and the van Hove singularity point is lowered. The calculated results compare better than LDA with recent experimental results from resonant inelastic xray scattering and angle resolved photoemission experiments. This agreement with the experiments supports the previously suggested two-band theory for the material dependence of the superconducting transition temperature, Tc.

E5.02*

경락의 연결망 규명을 위한 토끼에 지질다당류와 알시안블루-자성비드가 흡착된 프리모관의 자기적 특성 연구

이해리, 김지영, 하예은, 홍예지, 김근호, 노민석, 강석윤 [1], *이상석
Hye-Rie. LEE, Ji-Young. KIM, Yae-Eun. HA, Ye-Ji. HONG, Keun-Ho. KIM, Min-Suk. RHO, Suk-Yun. KANG[1], *Sang Suk. LEE
상지대학교. [1] *한국한의학연구원.*

Keyword : 염증유발, LPS, 자성비드, 프리모관, 림프관

염증유발 지질다당류 리포폴리사카라이드를 토끼의 림프관 면역체계가 활성화 되도록 림프노드에 주입하였다. 림프관에 떠있는 프리모관을 찾기 위해 알시안블루(Alcian blue) 염색액에 1 ml 당 50 mg 의 양으로 있는 1 μm 의 초상자성체 자성비드(Co-Si-OH)를 고르게 혼합시켰다. 자성비드와 혼합된 염색액을 림프노드에 주입한 후 림프관내에 진한 녹색으로 염색된 프리모관이 남게 된 것을 관찰하였다. 림프관 내의 떠있는 상태로 프리모관의 존재를 확인한 후, 50 G ~ 80 G 정도 자기장이 인가된 프리모관은 영구자석의 주기적인 움직임에 따라 같이 운동하는 프리모관의 자기적 특성을 관찰하였다.

E5.03*

Enhanced Electrochemical Supramolecular Recognition by β-Cyclodextrin−Graphite Oxide−Carbon Nanotube Composite

*정혜경, 래히옌
*Hae Kyung. Jeong, Le Thi Ngoc. Hien
대구대학교.

Keyword : Supramolecular recognition, graphite oxide, cyclodextrin, carbon nanotube

The synthesis of βCD−GO−CNT and βCD−CNT composite is presented by the simple chemical method. The electrochemical characterization of βCD−GO−CNT composite displayed not only the typical EDLC behavior with the highest current intensity but also excellent supramolecular recognition capability with three kinds of biomolecules (dopamine, thioridazine, L-tyrosine) than individual CNT and βCD−CNT composites, illustrating the role of GO in the βCD−GO−CNT composite could immobilize βCD molecules effectively. It's represented the new material, βCD−GO−CNT, supplied a synergistic effect of high electric conductivity from CNT and high supramolecular recognition capability from βCD effectively immobilized in GO for future biosensor applications.
* Corresponding author: outron@gmail.com, Tel: 82-53-850-6438, Fax: 82-53-850-6439

E5.04

Serial segmentation of bone specimen: computed microtomography using synchrotron radiation

*박정웅, 서승준 [1], 임재홍 [2], 김용건 [3]
*Chung Wung. Bark, Seung-jun. Seo[1], Jae-Hong. Lim[2], Yong Gun. Kim[3]
가천대학교. [1] 대구가톨릭대학교. [2] 포항방사광 가속기. [3] 경북대학교.

Keyword : maxillary sinus floor elevation, synchrotron radiation X-ray microtomography, serial segmentation, new bone formation

Maxillary sinus floor augmentation has been shown to be the most predictable surgical techniques to enhance bone volume in posterior area of maxilla. The purpose of this study was to analysis serial slice image segmentation of newly formed bone and bone substitutes after sinus floor elevation using synchrotron radiation X-ray microtomography (SRuCT).

After 6 months of sinus floor augmentation, bone biopsy specimens were collected. From six-bone biopsy specimens, the cross-sectional images at every 8 um along apical direction from inferior border using the serial segmentation from 3D reconstructed x-ray images were analyzed. The amount of new bone and bone substitues were measured at each slicing images (300~430 images per specimen).

The bone dynamics between new bone and bone substitutes along inferior-superior direction in human after MSFE can be analyzed with whole sample region. Even though our observation suggests that the specimens are structurally not homogenous, we confirmed that sinus floor elevation is a reliable surgical procedure which aims to increase the amount of bone.

We demonstrated that using of SR-μCT is highly effective to obtain high resolution images. The analysis of biological specimen using SR-μCT is very reliable and this technique would be important tool in the wide field of tissue engineering.

E5.05*

Role of G bases in Long Human Telomere investigated by Fluorescence Correlation Spectroscopy

정석현, 김수용, *김석원 [1]
Seokhyun. Jung, Soo Yong. Kim, *Sok Won. KIM[1]
Korea advanced institute of science and technology. [1]*University of ulsan.*

Keyword : Human telomere, Fluorescence correlation spectroscopy, $(TTAGGG)_{12}$

The human telomeric sequence $(TTAGGG)_{12}$ is widely adopted and studied due to its 3D structure forming property in the monovalent cation environment. However, the interpretation of the human telomeric sequence in terms of wormlike chain model seems to be limited by its 3D structure even though its significance role in a cell. In this paper, we investigated the property of human telomeric sequence $(TTAGGG)_{12}$ in a wormlike chain model. To compare its property, the same base number but different base composition T72 is adopted due to it have played a role as a model system in various researches. Moreover, for comparison, we adopted another sequence called CT72 which has the same base number but less number of guanine.

E6.01(초)

Damage-free protein crystallography with the XFEL

*Hideo Ago
*Hideo. Ago
RIKEN SPring-8 Center.

Keyword : .

Biological molecules like proteins contain hundreds of thousands of atoms, and identifying exact atomic structures of these complex macromolecules is essential to understand their functions. The importance of knowing atomic structures in biological studies and drug discovery puts an emphasis on the intense X-rays, which however inevitably cause significant radiation damage to the specimens themselves. We have developed a new measurement technique using SACLA, which enables to study large, complex biomolecules without radiation damage[1]. Scanning of large protein crystals across micron focused femtosecond X-ray pulses allowed us to successfully acquire radiation damage-free structures of metalloproteins and membrane proteins[2]. In this talk, I will share the perspective of damage-free crystallography using femtosecond X-ray pulses from XFELs.

1 Hirata, K. et al. Determination of damage-free crystal structure of an X-ray-sensitive protein using an XFEL. Nat Meth 11, 734-736 (2014).
2 Suga, M. et al. Native structure of photosystem II at 1.95 A resolution viewed by femtosecond X-ray pulses. Nature 517, 99-103 (2015).

E6.02(초)

X-Ray Free Electron Laser Studies of Nano Scale Dynamics in Materials : Applications and Perspective on Coherent properties

*김현정
*Hyunjung. KIM
서강대학교.

Keyword : XFEL, dynamics, nanoscale, structure

The recent advent of hard x-ray free electron lasers (XFELs) opens new areas of science due to their exceptional brightness, coherence, and time structure. In principle, such sources enable studies of dynamics of condensed matter systems over times ranging from femtoseconds to seconds. However, the studies of the dynamics in, for example, polymeric materials still remain in question due to the characteristics of the XFEL beam and concerns about sample damage. Recently we demonstrate the feasibility of measuring the relaxation dynamics of gold nanoparticles suspended in polymer melts using X-ray photon correlation spectroscopy (XPCS), while also monitoring eventual X-ray induced damage. In spite of inherently large pulse-to-pulse intensity and position variations of the XFEL beam, measurements can be realized at slow time scales. The X-ray induced damage and heating are less than initially expected for soft matter materials.
In this talk, I present the recent results obtained in LCLS and the perspectives on coherent properties of XFEL in addition to the unique time structures for the future experiments in XFELs.
This research was supported by NRF-2014R1A2A1A10052454 and NRF-2015R1A5A1009962.

E6.03(초)

Time resolved photoemission spectroscopy

*Masaki Oura
*Masaki. Oura
RIKEN SPring-8 Center.

Keyword : .

We have established the time-resolved hard x-ray photoelectron spectroscopy (trHAXPES) using SACLA. The technique by extending to the hard X-ray as a core-level spectroscopy combines element and atomic-site specificity to probe bulk (sub-surface) electron dynamics at femtosecond scale. The viability of trHAXPES at XFELs is demonstrated by studying vacuum space-charge effects induced by a pump laser as well as probe. Evolution of the spectral shifts and broadenings is compared with the numerical simulations and mean-field models with good agreements[1]. The trHAXPES expects to open a new avenue in the study of ultrafast electron dynamics in bulk materials and also at buried interfaces.

1 Oloff, L. P. et al. Time-resolved HAXPES at SACLA: probe and pump pulse-induced space-charge effects. New Journal of Physics 16, 123045 (2014).

E6.04(초)

High Energy Density Science on XFELs

*조병익
*Byoung Ick. Cho
광주과학기술원.

Keyword : x-ray free electron laser, high energy density science, x-ray photonics, plasmas

The ultrafast and ultraintense x-ray pulses generated by x-ray free electron laser (XFEL) have opened the new era for various fields of research. High energy density science (HEDS), investigating materials properties under extremely high temperature - pressures and their interactions with photons and particles, is one of those benefited enormously from the new light source. In this talk, I'll briefly introduce several key experiments for HEDS in the XFEL facilities and their physical interpretations, such as isochoric heating of matter, ionization potential depression, saturable and reverse saturable absorptions. The open questions and new research opportunities will be also discussed.

E7.01(초)

for Organic Electronics

*나석인
*Seok-In. Na
전북대학교.

Keyword : "Organic Electronics", "Organic Solar Cells", "Transparent Electrode", "Conducting Polyemr", "Carbon nanosheet",

For emerging flexible electronics, polymer-based solution-processable transparent electrodes with low-cost and large-area should be preferentially developed. As is well known, indium tin oxide (ITO) are typically used due to its high transparency and conductivity. However, ITO is not an ideal conductive material due to inherent problems, as follows: release of oxygen and indium into the organic layer; poor transparency in the blue region; and, complete crystallization of ITO films requires high temperature processing. In particular, the ever-increasing cost of indium, limited mechanical flexibility, and readily crack upon substrate bending prevent realization of flexible and large-area electronics; thus, it is clear that novel electrode materials should be intensively developed for realization of flexible and low-cost electronics. Herein, we are dedicated to develop conducting polymer and carbon nanosheet based transparent electrodes and to apply into electronics in order to realize low-cost and flexible electronics. These overall approaches could be very beneficial for low-cost, high efficiency, and all-solution-processed next-generation organic/inorganic electronics.

E7.02(초)

투명 전도성 고분자 PEDOT:PSS 필름의 전도도 개선 및 투명 태양전지 적용 연구

*윤선진, 연창봉 [1], 김주미
*Sun Jin. Yun, Changbong. Yeon[1], Jumi.
한국전자통신연구원. [1] 과학기술연합대학원대학교.

Keyword : 투명전극, PEDOT:PSS, 전도성고분자, 전도도, 태양전지

최근 투명전극은 디스플레이, 센서, 터치패널, 전자소자 등에 광범위하게 사용되면서 많은 기술 개발이 이루어지고 있다. 특히 유연성 디스플레이와 전자소자, 유연태양전지를 비롯한 flexibility, stretchability 를 가지는 소자들에 대한 필요성이 대두되면서 투명전도성 고분자가 더욱 큰 관심을 끌고 있다. 그 중에서 가장 대표적으로 많이 연구되고 있는 전도성고분자인 poly(3,4-ethylenedioxythiophene):poly(4-styrenesulfonate) (PEDOT:PSS)는 태양전지와 디스플레이소자의 투명전극으로 활용하기에는 전도도가 낮아서 전도도 개선을 위한 다양한 방법들이 연구, 시도되고 있다. 본 논문에서는 간단하고 비용이 저렴한 방법을 사용하여 PEDOT:PSS 의 전도도를 크게 개선한 결과를 보고하고자 한다.
본 연구에서 PEDOT:PSS 의 전도도를 4100 S cm^{-1} 까지 증가시킬 수 있는 방법을 개발하였다. 이 전도도는 산행연구들과 비교하여 실온 공정으로 얻은 전도도 중에서 가장 높은 값으로서 저렴하고 간단한 고농도 질산처리로부터 얻었다는 데에 큰 의미가 있다. 또한 질산처리에 의해 전도도가 개선되는 메커니즘을 제안하고, 이를 설명하기위해 다양한 분석을 수행하였다. 고농도의 질선처리는 전도도에 부정적인 영향을 미치는 PSS 의 선택적인 제거를 통해 (100), (200) 결정 방향의 결정화와 상분리를 촉진함으로써 전도도를 개선하는 것으로 보인다. 본 연구에서 개발한 질산처리 공정으로 전도도가 크게 향상된 PEDOT:PSS 박막을 염료감응 태양전지의 투명전극으로 활용하여 우수한 결과를 얻었는데, 이 전극으로 Pt/FTO 전극을 대체했을 때 8.6%의 높은 광변환 효율을 얻을 수 있었다.

E7.03(초)

Nano-sized Ag inserted into ITO films prepared by roll-to-roll sputtering for high-performance, transparent, flexible film heaters

*Han-Ki Kim
*Han-Ki. Kim
Kyung Hee University.

Keyword : .

We demonstrate high-performance, flexible, transparent film heaters fabricated on a conductive Ag layer inserted ITO films prepared by pilot-scale roll-to-roll (RTR) sputtering. The RTR sputtered ITO/Ag/ITO multilayer on a 700 mm wide PET substrate at room temperature exhibits a high optical transmittance of 88.2 % and a very low sheet resistance of 3.0 Ohm/square, which are ideal for a low-voltage transparent film heater. The time-temperature profiles and heat distribution analysis demonstrate that the performance of the transparent film heater with the ITO/Ag/ITO multilayer is superior to that of a film heater with graphene, carbon nanotubes, amorphous ITO, Ag nanowires, and a Ag network, due to its very low sheet resistance (3-17 Ohm/square). In particular, the thickness of the Ag interlayer in the ITO/Ag/ITO multilayer critically impedes the voltage for attaining 100 ºC in the transparent film heater because the Ag interlayer provides a main conduction path in the ITO/Ag/ITO multilayer. In addition, the bending and cycling fatigue tests demonstrate comparable flexibility of the ITO/Ag/ITO multilayer to other transparent electrodes, indicating the potential of the ITO/Ag/ITO multilayer as an electrode for a highly flexible film heater. Therefore, the RTR sputtered ITO/Ag/ITO multilayer is the best substitute for conventional metallic or ITO film heaters in order to realize a large-area, transparent, flexible film heater that is applicable to flexible defogging/deicing and heating systems.

E7.04(초)

Nanoscale metal network-based electrodes for wearable devices

*Jung-Yong Lee
*Jung-Yong. Lee
KAIST.

Keyword : .

Wearable devices draw much attention in various electronic applications such as displays and touch screen panels. Although indium tin oxide (ITO) has been most widely and commonly used as transparent electrodes for the applications, ITO shows disadvantages such as relatively unstable, expensive production cost and poor mechanical robustness on flexible and stretchable substrates. Here, we present a novel method for fabricating high-performance transparent and conductive nanonetworks on various types of substrates. The nanonetworks are monolithically etched using nanoscale shadow masks and exhibit figure of merit (FoM) values greater than 3000. They also exhibit excellent optoelectrical characteristics, primarily because they intrinsically have zero contact resistance. Further, the nanonetworks also show high thermal and mechanical robustness. We also demonstrate that such etched nanonetworks can be formed readily on various types of substrates, regardless of the surface properties of the substrates.

E8.01(초)

Saturation and scaling properties in high energy scattering : from deep inelastic scattering to heavyioncollisions.

*Michal Praszalowicz
*Michal. Praszalowicz
Instytut Fizyki UJ.

Keyword : satuation, scaling, DIS, sacttering

By scaling we understand a property of certain physical observables that in principle should depend on two kinematical variables but in reality depend only on a particular combination of them. A prominent example is so called Bjorken scaling that paved the road to the present understanding of the proton structure. After a short reminder of the Bjorken scaling we shall introduce geometrical scaling(GS). GS follows from the fact that there exists an intermediate momentum scale, called saturation scale. We shall give physical interpretation of GS. By inspecting different pieces of data we shall demonstrate the existence of GS invarious high energy reactions.

E8.02(초)

Structure of few-body light Lambda hypernuclei

*E. Hiyama
*E.. Hiyama
RIKEN.

Keyword : Lambda hypernuclei, CSB, neutron halo structure

In 2013, a neutron rich $Lambda$ hypernucleus,
$^7_{\Lambda}$He was observed via the $(e,e' K^+$) reaction and
an observed Λ separation energy of $B_{\Lambda}=5.68 \pm 0.03 \pm 0.25$ MeV was reported. This observation is important for the study of CSB and neutron halo structure. To explore these phenomena, we study this hypernucleus within the framework of \alpha+\Lambda+n+n four-body problem and I will report recent result.

E8.03(초)

Brueckner G-matrix approach for neutron-proton pairing correlations in the deformed BCS approach

*하은자, 천명기
*Eun ja. Ha, Myung-Ki. Cheoun
숭실대학교.

Keyword : np-pairing correlation, BCS

Ground states of even-even Ge isotopes with mass number A=64-76 have been studied in the deformed Bardeen Cooper Schrieffer (BCS) theory by taking neutronproton (np) pairing correlations as well as neutron-neutron (nn) and proton-proton (pp) pairing correlations. The np pairing has two different modes J = 0; T = 1 (iso-triplet) and J = 1; T = 0 (iso-singlet). In this work, Brueckner G-matrix, based on the CD Bonn potential, has been exploited to reduce the ambiguity on nucleon-nucleon interactions inside nuclei and compared to the results by a simple schematic phenomenological force. We found that the G-matrix plays important roles to obtain reasonable descriptions of even-even nuclei rather than the schematic force. The np pairing strength has been shown to have a clear correlation with quadrupole deformation parameter 2 for the isotopes and affect the smearing of the Fermi surfaces of not only N = Z nuclei but also N≠ Z nuclei. In particular, the coexistence of the like-particle (nn and pp) and the np pairing mode was found to become more salient by the G-matrix approach rather than the schematic force approach.

E8.04(초)

Systematic study of double hypernuclei by a hybrid-emulsion method at J-PARC

*황상훈
*Sanghoon. Hwang
Japan Atomic Energy Agency.

Keyword : Double strangeness, J-PARC, E07, KURAMA spectrometer

Double strangeness (S=-2) systems have gained considerable attention over the past decades, because of their important role to understand baryon-baryon (B-B) interaction in SU(3) flavor. Only one double Lambda-hypernucleus event, called NAGARA event, was clearly identified as the decay of ${}_{6\Lambda\Lambda}$He hyper nuclei in the hybrid emulsion experiment at the old KEK experiment. An upgrade experiment will be performed at a high intensity Kaon beam line (K1.8) at the J-PARC hadron hall facility. For the new experiment, we are constructing new detector systems, which are the KURAMA spectrometer, a SSD and a Germanium array detector (Hyperball-X). The KURAMA spectrometer identifies the Ξ^- production in the (K^-,K^+) reactions off a diamond target. The SSDs are located in the upstream and downstream of the emulsion plates to tag the Ξ^- stopped events in the emulsion plate. In addition, the Hyperball-X measures Ξ^- atomic X-ray for the first time. In this talk, we will discuss physics motivation and current status of the E07 experiment.

E9.01(초)

Nature Physics Editor 와의 만남

*박제근
*Je-Geun. PARK
서울대학교. IBS-CCES.

Keyword : Nature Physics Editor

Nature-branded journals continue to strive to publish the most significant advances in science, whose importance can be appreciated not only by specialists, but can be communicated to broad audiences. This talk will give insight into the journals, policies and procedures of the Nature Publishing Group.

E12.01(초)

Conserved mechanism of Rad51/RecA family in homology search and strand exchange during homologous recombination

*이자일
*Ja Yil. Lee
Columbia University.

Keyword : Homologous recombination, Rad51/RecA family, Homology search, Strand exchange, DNA curtain

Homologous recombination is one of the most important DNA metabolisms because it repairs DNA double-strand break and induces genetic diversity. The homologous recombination is mediated by recombinases of RecA/Rad51 family. The recombinases form nucleoprotein filament on single-stranded DNA, which is resected from double-strand break. Then the recombinases search for homologous sequence and then exchange strand, which is followed by DNA synthesis and branch migration. Even though the homology search and strand exchange processes have been intensively and/or extensively studied, the physical basis of the reactions is not clearly established yet. Using the single-stranded DNA curtain technique, we investigate the homology search and strand exchange for the recombinases. Firstly we find that 8 nucleotides are minimal requirement to search for homologous sequence. In addition, this search process is accelerated by facilitated exchange. Then we show that strand exchange intermediates are stabilized in precise 3-nucleotide steps. Furthermore a mismatched base in triplets can be stepped over during strand exchange. Our study for bacterial RecA and eukaryotic Rad51 and Dmc1 demonstrates that all the mechanisms of homology search and strand exchange are conserved from bacteria to human.

E12.02(초)

Non-Gaussian dynamics in RBC membrane fluctuation

*박용근
*YongKeun. Park
KAIST.

Keyword : Nonequillibrium, Nongaussian, biophysics, red blood cells, membrane

There is a strong correlation between the membrane fluctuations and the mechanical properties of living cells. The dynamic membrane fluctuation consisting of submicron displacements can be altered by changing the cells' pathophysiological conditions. Here, we present that the presence of adenosine 5'-triphosphate (ATP) facilitates non-Gaussian dynamic fluctuations in the RBC membrane, which are highly correlated with the biconcave shape of RBCs. Spatial analysis reveals that these non-Gaussian dynamics are enhanced at the scale of spectrin structures.
These results have significant relevance to the understanding of RBC biophysics and pathology, as follows. RBCs must withstand large mechanical deformations during repeated passages through the microvasculature and the fenestrated walls of the splenic sinusoids. This essential ability is diminished with senescence, resulting in physiological destruction of the aging RBCs. Pathological destruction of the red cells, however, occurs in cells affected by a host of diseases such as spherocytosis, malaria, and Sickle cell disease, as RBCs depart from their normal discoid shape and lose their deformability. Therefore, quantifying the effects of ATP on the RBC deformability insight into a variety of problems regarding the interplay of cell structure, dynamics, and function. Furthermore, the ability to monitor mechanical properties of RBCs is of vital interest in monitoring disease progression or response to treatment as molecular and pharmaceutical approaches for treatment of chronic diseases.
In addition to its clinical relevance, understanding the coincident morphological and mechanical control via ATP hydrolysis is fundamental to membrane biology, RBC circulation, and basic studies of cellular mechanics. The RBC is a uniquely suitable model system for studying viscoelastic membrane dynamics with broad technological implications for encapsulation and drug delivery applications.

[1] Y. Park, C. Best, K. Badizadegan et al., "Measurement of red blood cell mechanics during morphological changes," Proc Natl Acad Sci U S A, 107(15), 6731 (2010).
[2] Y. Park, C. Best, K. Badizadegan et al., "Metabolic remodeling of the human red blood cell membrane," Proc Natl Acad Sci U S A, 107(4) 1289-1294 (2010).
[3] S. Cho et al., in preparation
[4] H. Park et al., in preparation.

E12.03(초)

Single-molecule FRET studies on human Argonaute 2

*홍성철
*Sungchul. Hohng
서울대학교.

Keyword : RISC, single-molecule FRET, Argonaute

Argonaute is a key enzyme of various RNA silencing pathways. We use single-molecule fluorescence measurements to characterize the reaction mechanisms of the core-RISC (RNA Induced Silencing Complex) composed of human Argonaute 2 and a small RNA, and reveal the followings. Target binding of core-RISC starts at the seed region, resulting in four distinct reaction pathways: target cleavage, transient binding, stable binding, and Argonaute unloading. The target cleavage requires extensive sequence complementarity and dramatically accelerates core-RISC recycling. The stable binding of core-RISC is efficiently established with the seed-match only, providing a potential explanation for the seed-match rule of miRNA (microRNA) target selection. Target cleavage on perfect match targets sensitively depend on RNA sequences, providing an insight into designing more efficient siRNAs (small interfering RNAs).

E12.04(초)

Dynamic Regulation of DNA Mismatch Removal

*이종봉
*Jong-Bong. LEE
포항공과대학교.

Keyword : DNA mismatch; Single-molecule; DNA repair; Diffusion Mechanics

DNA mismatch repair (MMR) is a catalytic reaction of a strand-specific degradation and resynthesis dependent on the mismatch by coordination of sequential signaling pathways. MutS homolog (MSH) binding to mismatched nucleotides transmits the mismatch-finding signal ultimately to a distant strand scission site. To remove the mismatch, the excision reaction proceeds from the strand break to the mismatch either in the 5' or 3' direction. These two distinct mechanisms of the strand excision have commonly raised a mechanical question of how the excision reaction is terminated since no component in the excision machinery recognizes the mismatch after the excision begins. I will present the mechanics of strand excision in the 5' to 3' direction. The model we propose elegantly explains the mechanical processes of the elimination of the mismatch during DNA mismatch repair, combined with its upstream event, the transmission of the mismatch-finding signal.

E13.01(초)

Femto-second, high brightness radiation from hard X-ray FEL

*강흥식
*Heung Sik. Kang
포항공과대학교.

Keyword : X-ray Free electron laser, electron Linac, light source, brightness

A hard X-ray Free electron laser facility using 10-GeV electron Linac is under construction at PAL, will be commissioned in 2016, and be used for the scientific experiments in 2017. The X-ray FEL radiation, which is typically a few tens of femto-seconds long and even shorter a few femto-seconds, is 10 billions times brighter than the 3-rd generation light source. The characteristics of this FEL radiation will presented in comparison with other radiation sources.

E13.02(초)

초고속 전자회절 기술

*정영욱
*JEONG Young Uk.
한국원자력연구원.

Keyword : 초고속 전자 회절, 펨토초 전자빔, 광전자총, 상대론적 전자빔, 펨토초 시간동기화, 테라헤르츠 펌프

원자나 분자와 같은 미시세계는 전통적으로 높은 에너지의 전자기파 (엑스선)나 고속의 입자 (전자)로 측정하여 왔다. 대표적인 기술들이 엑스선 회절이나 전자현미경이다. 한편, 원자나 분자의 빠른 움직임을 보고자 하는 노력들 역시 끊임없이 이어져 왔다. 최근 4 세대 방사광 (엑스선 자유전자레이저) 시설과 초고속 전자회절 장치는 각기 엑스선과 전자를 이용하여 약 100 펨토초 시간 분해능으로 미시세계를 직접 관측하게 되었다. 본 포커스 세션은 초고속 세계를 들여다보는 새로운 도구들과 이를 이용하는 연구들을 물리학회 회원 일반에게 소개한다. 그리고, 본 발표는 전자빔을 이용하여 상대적으로 용이하게 초고속의 세계를 탐구할 수 있는 기술에 대해서 개관한다.

E13.03(초)

Ultrafast spin and lattice dynamics of BaFe2As2 seen by infrared and X-ray pulses

*김경완
*Kyungwan. KIM
충북대학교.

Keyword : ultrafast dynamics, spin density waves, time domain spectroscopy, coherent lattice vibrations

We investigate ultrafast dynamics of $BaFe_2As_2$ by utilizing broadband terahertz-infrared time domain spectroscopy and ultrafast X-ray diffraction techniques. The pump pulses destroy the magnetic order in the low temperature spin density wave state. We observe that strong pump pulses launch coherent lattice vibrations of As ions at 5.5 THz, which modulate the infrared response. Interestingly, the normal state spectral response of the modulation resembles the gap opening behavior upon cooling below the magnetic transition temperature. Direct measurement of the ultrafast lattice motion by the X-ray diffraction method reveals that the As ions move away from the Fe plane and the Fe-As-Fe bond angle can become smaller by more than 0.5°. Density functional theory finds that such a lattice motion modifies the Fermi surface and an orbital dependent nesting instability can be enhanced, giving rise to the magnetic order.

E15.01(초)

Numerical Relativity: Status and Korean Activities

*강궁원
*Gungwon. Kang
한국과학기술정보연구원.

Keyword : Numerical relativity, Gravitational radiation capture

Numerical Relativity (NR) is to investigate gravitational phenomena by computationally solving Einstein equations which are so complicated and highly non-linear that analytic approaches are limited for most cases. Especially, NR becomes very powerful for the cases of strong gravitational interactions such as black hole formations, compact star coalescences and early universe where approximate methods such as Post-Newtonian theory and perturbation theory break down. In this talk, the status of NR simulations is briefly summarized, focusing on eccentric binary black hole merger simulations. Some of Korean activities are also introduced, which include gravitational radiation captures of two black holes with equal/non-equal masses and with/without spins, general relativistic hydrodynamics and black hole universe. Finally, recent activity of using NR in holographic theory of string theory is mentioned.

E15.02(초)

Current status of gravitational wave research

*이형목
*Hyung Mok. LEE
Seoul National University.

Keyword : General relativity, Gravitational waves, neutron star, black hole, pulsar

Gravitational waves have been predicted by the general theory of relativity, but they never have been directly detected yet. The ground based detectors based on laser interferometry are now thought to be able to detect the gravitational waves coming from merger of binaries composed of neutron stars or black holes. Frequent detection of gravitational waves will become enable us to study highly relativistic objects such as black holes and neutron stars as they will provide information that is not accessible through the observation of electromagnetic waves. Accurate measurements of pulsar arrival times also can provide the evidence for the low-frequency gravitational waves that can originate from supermassive black holes. The pulsar timing studies already began imposing strong constraints on the scenarios of the growth of the supermassive black holes. Thus we are now witnessing a birth of gravitaitional wave astronomy. This talk is intended to provide a comprehensive summary of the recent development of gravitational wave research and its perspectives.

E15.03(초)

Status of KAGRA

*Toshikazu Suzuki
*Toshikazu Suzuki.
KEK. Japan.

Keyword : Gravitational waves, KAGRA

KAGRA is a gravitational wave detector under construction in the Ikenoyama mountain of Kamioka-mine. The excavation of the tunnel was finished by the end of 2014fy. Installation of instruments is in progress by each subsystem. An initial operation of KAGRA at room temperature, which is called as iKAGRA will be planed in the end of 2015. The iKAGRA operation will include a comprehensive test of detector system however the operation will be terminated in a relatively short period. A cryogenic operation of KAGRA will be planed in 2017.

My talk will contain status of construction and installation from engineering / scientific point of view. Less theoretical matter will be included.

F1.01

Magnetic phase transitions in hexagonal manganites studied through magnon scattering

*민혠, 진상백 [1], 한기옥, Ji-Yeon Nam, 응원티후옌, Sang-Wook Cheong[2], 노태원 [3], 조병기 [4], 양인상
*Nguyen Thi Minh. HIEN, Xiang Bai. Chen[1], Ki-Ok. Han, Ji-Yeon. Nam, NGUYEN THI. HUYEN, Sang-Wook. Cheong[2], Tae Won. NOH[3], Beongki. Cho[4], In-Sang. YANG
이화여자대학교. [1] 건국대학교. [2]Rutgers University. USA. [3] 서울대학교. [4] 광주과학기술원.

Keyword : Hexagonal RMnO3, Raman spectroscopy, temperature dependence, spin ordering transition, spin-reorientation transition

Phase transition is a subject of great interest in physics. Magnon scattering, when clearly observed by Raman spectroscopy, can be a simple and powerful tool for studying magnetic phase transitions. We found that, by choosing the excitation energy close to the peak of “on-site Coulomb energy” (~1.7 eV) and the appropriate polarization configuration to reduce strong phonon scattering signal, the hexagonal RMnO3 can gain strongest resonance effect of magnon scattering. And the temperature dependence of magnon scattering can be powerful quantity for investigating not only the spin-ordering but also spin-reorientation transitions. Especially, the Raman method would be very helpful for investigating the weak spin-reorientation transitions by selectively probing the magnons in the Mn3+ sublattice, while leaving out the strong effects of paramagnetic moments of the rare earth.

F1.02

Electrical Manipulation of Reversible Magnetization at the Ferromagnet/Ferroelectric Interface

*엇후돌즈
*Dorj. Odkhuu
인천대학교.

Keyword : Multiferroic interface, Magnetic anisotropy, First-principles calculation

Electrically addressable magnetic memory applications seek magnetization reversal induced by an electric field alone. Based on first principles calculations, we demonstrate that the magnetic anisotropy of Fe films on $PbTiO_3$ is reversible and undergoes a transition from in-plane to perpendicular magnetization as ferroelectric polarization reverses. This magnetization switching is mainly driven by the mutual interfacial effects of the interstitial free electron like gas and Fe d-O p hybridization, as reversible polarization of Ti displacement alters the Fe-O atomic separation at the interface. We will also discuss results on the alternative routes for magnetization reversal of other ferromagnet/ferroelectric interfaces. These results indicate significance of highly-polarized ferroelectrics for achieving the full control of the electric-field induced switching of magnetization, and would motivate an experimental investigation in the area of spintronics.

F1.03

Plasma arc synthesis and magnetocaloric properties of HoN nanoparticles

K. P. Shinde, 장세훈, 김종우, 김동수, M. Ranot, *정국채
Kiran. Shinde, S. H.. Jang, J. W.. Kim, D. S.. Kim, Mahipal. Ranot, *K. C.. Chung
Korea Institute of Materials Science.

Keyword : Magneto-caloric effect, HoN, Plasma Arc Discharge, Nano-particles

The study of magnetocaloric properties of materials is a fascinating area of research from the standpoint of both application and basic understanding. Due to its high cooling efficiency, environmental friendliness, and compactness, magnetic refrigeration based on the magnetocaloric effect (MCE) is considered as a promising alternative to conventional gas compression refrigeration techniques. The rare earth mononitrides have been studied for their interesting magnetic properties as potential magnetic refrigerants for the applications in liquefaction of hydrogen.
HoN nanoparticles were prepared by the plasma arc discharge, where the particle size was tailored by using different composition of nitrogen and hydrogen gas inside the discharge chamber. The HoN prepared by using the 40% N_2 and 60% H_2 (S1), 60% N_2 and 40% H_2 (S2), 80% N_2 and 20% H_2 (S3) and 100% N_2 have an average particle size of 45, 67, 74 and 38 nm, respectively. It is also observed that for samples S1, S2 and S3 particle size distribution is wide while in case of sample S4 it is narrow. The x-ray diffraction analysis confirms the cubic crystal structure without any impurity phases. The prepared particles are commonly shaped like cubes. The paramagnetic–ferromagnetic transition temperature T_C is observed to be 13.9, 14.2, 14.5 and 14.2 K for all samples respectively. All the samples shows second order paramagnetic to ferromagnetic phase transition at T_C. The magnetic entropy change is found to be extended over a wide range of temperature around T_C, and its maximum value at an applied magnetic field of 5 T is obtained to be 27.7, 29.8, 30.2 and 34.2 J/kgK for samples S1, S2, S3 and S4 respectively.

F1.04

Quantum Magnetism of Isolated tetrahedron in pyrochlore antiferromagnet $Ba_3Yb_2Zn_5O_{11}$

*박상연, 지성대 [1]
*Sang-Youn. Park, Sungdae. Ji[1]
막스플랑크 한국/포스텍 연구소. [1] 막스플랑크 한국포스텍 연구소.

Keyword : Inelastic Neutron Scattering, Pyrochlore, DM interaction

Spin-1/2 quantum pyrochlore Heisenberg antiferromagnets are known to be promising candidates for three-dimensional quantum spin liquids. Despite numerous experimental and theoretical efforts, their ground state properties have not yet been established because of the lack of a model material and the unavailability of exact solutions. A popular theoretical approach to this problem is to first decouple the full pyrochlore lattice into a set of independent tetrahedra and then reconnect them perturbatively. Kimura et al. have reported the new material $Ba_3Yb_2Zn_5O_{11}$ to be a model system of a bond alternating pyrochlore lattice antiferromagnet; their pyrochlore lattice consists of an alternating array of small and large tetrahedron [4]. This material crystallizes with the cubic space group F-43m, and intra- and inter-Yb-tetrahedron distances are ~3.29 Å and ~6.25 Å. Analysis of inelastic neutron scattering, magnetization and heat capacity data show the formation of quantum spin-singlet state of total spin S = 2. An exact diagonalization calculation taking account of Dzyaloshinsky-Moriya interactions reproduces the experimental results very well.

F1.05

Asymmetric H_2 dissociation by Pt nano-particle loaded NaY zeolite investigated by in situ neutron diffraction and spectroscopies

*이희주, KIM Hyunjung, 최용남 [1], 임대운 [1], 김용일 [2], 조인화 [1], 전철호 [3], 강현욱 [1], 윤경병
*Heeju. Lee, Hyunjung. KIM, Yong Nam. CHOI[1], Dae-Woon. Lim[1], Yong-Il. Kim[2], In Hwa. Cho[1], Cheolho. Jeon[3], Hyun Wook. Kang[1], Kyung Byung. Yoon
서강대학교. [1] 한국원자력연구원. [2] 한국표준과학연구원. [3] 한국기초과학지원연구원.

Keyword : Neutron diffraction, Zeolite, FT-IR, NMR, XPS

Pt nanoparticle-loaded sodium zeolite Y (Pt_x/NaY) has been widely used as an important cracking catalyst for upgrading less-valuable heavy gasoil into more-valuable lighter hydrocarbons in the petrochemical industry, and has been studied for hydrogen spillover mechanism. However, the role of Pt_x, the Na^+ ion, and the negatively charged zeolite framework, the whereabouts of the incorporated hydrogen and the final forms of the chemisorbed hydrogen in Pt_x/NaY have not been well understood.
NaY zeolite loaded with Pt nano-particles in physical method (sputtering and vacuum annealing) was used for the study of hydrogen storage mechanism near ambient temperature. In situ neutron powder diffraction result reveals the occurrence of hydrogen chemisorption. From the Rietveld analysis and maximum entropy method analysis, hydride ions are found to locate near NaII site. 1H and 23Na MAS-NMR data, O 1s and Na 1s XPS, in situ FT-IR data are consistently evidenced the formation of -OH and -NaH after the hydrogen treatment at 400K under 10 bar. We found for the first time that H_2 undergoes heterolysis in Pt_x/NaY into sodium hydride (-NaH) and the framework oxygen-bound proton (-OH). This implies that a pair of Lewis base and acid, FLP (frustrated Lewis pair), was formed inside the nanopore of zeolite as a result of asymmetric H_2 dissociation by Pt_x/NaY. The existence and the catalytic function of –NaH in zeolite was verified by a set of Tishchenko reactions, the coupling of two aldehyde molecules to the corresponding ester, using three comparative materials (Pt_x/NaY, H_2-Pt_x/NaY and authentic NaH powders) and acetaldehyde.

F1.06

Picosecond Time-resolved x-ray scattering at PLS-II

*조원혁, 이수형 [1]
*Won Hyuk. Jo, Sooheyong. Lee[1]
숭실대학교. [1] *한국표준과학연구원.*

Keyword : X-ray, Time Resolved experiment, InSb, PLS-II

Essentially all fundamental processes in nature, such as chemical reaction and phase transitions involve rapid structural changes in a matter via rearrangements of the constituent atoms and molecules. Such atomic-scale dynamics usually occur on the time-scales that are comparable to natural oscillation periods of atoms and molecules (fs~ps). Owing to significant developments of ultrafast laser technologies, various types of time-resolved experiments have been performed, in which optical laser pulses are used for both exciting and then probing the sample. While such methods excel in time-resolution, the interpretation of the result becomes quite non-trivial, often requiring extensive numerical simulation to confirm the validity of the experimental data. Arrivals of pulsed hard x-ray sources such as synchrotrons and XFELs during recent decades have enabled direct studies of the structural evolution of the excited medium. However, implementation of such instrument is rare because it requires both a designated x-ray beamline at synchrotrons and a precise timing-synchronization between laser and x-ray pulses. In our work, we demonstrate the very first time-resolved x-rays scattering (TRXS) experiment in Korea, which was performed at Photon Test Facility at PLS-II. In particular, we successfully measured structural evolution of an InSb semiconductor after irradiation of femtosecond near-infrared pulses. Sub-atomic scale high-spatial and picosecond time resolution allow us to clearly differentiate each contribution from free-carrier population and thermal diffusion on the crystal lattice.

F2.01(초)

Recent Development of Ambient Pressure XPS

*문봉진
*Bongjin Simon. Mun
광주과학기술원.

Keyword : Ambient Pressure XPS, Surface Physics, Gas/Solid Interface

X-ray photoelectron spectroscopy (XPS) is one of the major tools in the fields of surface chemistry due to its excellent capabilities in studying surface chemical and electronic properties. However, due to the short inelastic attenuation lengths of photoelectrons, as well as the requirement of high vacuum in the electron spectrometer, only the model studies or ex-situ systems have been carried out, and thus creating so-called "pressure-gap". In an effort to bridge this pressure-gap, the ambient pressure x-ray photoelectron spectroscopy (AP-XPS) has been continuously developed and now puts a new road map in the world of surface science with use of synchrotron radiation facility. [1]

In this presentation, the basic principles and the latest instrumental developments of AP-XPS will be presented. Also, the applications of AP-XPS to several practical systems will be given, including electrochemical system. Now, with the use of high-energy photon source, it becomes possible to run in-situ analysis of liquid/solid interface under operating condition.

Reference

[1] Bongjin Simon Mun, Hiroshi Kondoh, Zhi Liu, Phil N. Ross Jr., Zahid Hussain, Current Trends of Surface Science and Catalysis, Springer, 2014, edited by Jeong Young Park

F2.02(초)

Ambient Pressure XPS at PAL : Goal and Present status

*김기정, 백재윤, 김남동, 임규욱
*Ki-jeong. Kim, Jaeyoon. Baik, Namdong. Kim, Kyuwook. Ihm
포항가속기연구소.

Keyword : "APXPS", "Soft x-ray", "PAL", "KBSI"

Recent advanced technologies have resulted in the development of specialized instruments at synchrotron facilities which allow performing the so-called ambient pressure photoelectron spectroscopy (APXPS) measurements. APXPS experienced its breakthrough through the third-generation synchrotron radiation sources and has been recognized again as an important in-situ tool to study water, environmental science, catalysis and many other important fields. Therefore, PAL and KBSI agreed a MOU for APXPS experimental system to study these fast emerging fields. Here, we present current status on the way of constructing beamline and optical design dedicated to AP-XPS endstation. Newly designed optics will replace of that of 8A (U6.8) which has been under operational for 20 years. Total budget is 3.0 billion won including moving cost of 8A2 HRPES II beamline to 10A2 port. Through this project two beamlines at 8A, AP-XPS and SPEM, leads top edge science by exploring brands new scientific world without pressure gap based on the powerful photon source covering medium energy range.

F2.03(초)

The latest near ambient pressure X-ray photoelectron spectroscopy at korea basic science institute and its performance

*윤형중, 이두용 [1], 정창길 [2], 문봉진 [2], 이주한
*Hyung Joong. Yun, Doo Yong. Lee[1], chang kil. jeong[2], Bongjin Simon. Mun[2], Jouhahn. Lee
한국기초과학지원연구원 (KBSI). [1] 부산대학교. [2] 광주과학기술원.

Keyword : XPS, ambient pressure, surface

X-ray photoelectron spectroscopy (XPS) is a spectroscopic method that determines elemental composition of surfaces. XPS has conventionally been conducted under ultra-high vacuum (UHV) conditions, however most of the important surface processes in the environment take place under non-UHV conditions. Therefore, an XPS unit capable of working under environmental condition has now been developed. In 2014, Korea Basic Science Institute (KBSI) successfully completes the commissioning of NAP-XPS. The chamber is equipped with PHOIBOS NAP-150 analyzer and 2-dimensional-delay line detector, which provides improved detection efficiency with a) 2-dimensional angle resolved mode, b) 1-dimensional chemical imaging mode c) time resolved XPS at picosecond scale. The in-situ gas-pressure cell is designed to operate at pressure up to 25mbar with differential pumping system. As a photon source, Al Kα X-ray source can be focused with special monochromator with beam spot size 300μm. the main chamber is attached to preparation chamber, which houses a low energy electron diffraction (LEED), a high pressure cell (HPC), an ion sputter gun, a multi-cell E-beam evaporators, and a four-axis manipulator with heating and cooling functions. The usual characterization capabilities of NAP-XPS @ KBSI are extended to the study of gas-solid and gas-liquid interphases, with applications to in-situ characterization of heterogeneous catalysts, corrosion processes, wetting, fuel cells, photovoltaics, etc.

F3.01(초)

Present status and bright future of spin-resolved photoelectron spectroscopy with potential of full spin and momentum analyses

*Shigemasa Suga
*Shigemasa Suga.
Max-Planck-Institute.

Keyword : SP-2D-ARPES, VLEED, PEEM

Spin-resolved two-dimensional angle-resolved photoelectron spectroscopy (SP-2D-ARPES) with high resolutions in energy and momentum in a wide (kx,ky) region has been desired since few decades.
Spin detectors were upgraded from Au Mott detector, W(001) SP-LEED detector with the single channel figure of merit f0 of 10^-4 to Fe-O VLEED detector and Au/Ir(001) detector with f0 of 10^-2 in recent years [1,2].
Still higher spin detection efficiency is required to study reactive surfaces of various materials.
In addition, SP-ARPES is expected to provide fruitful information on electron correlation, hybridization, stability of charge, spin, as well as various transitions in bulk and buried interface electronic structures when performed in the soft and hard X-ray regions.
Owing to the development of the momentum microscope in Max-Planck Institute of Microstructure Physics, composed of a PEEM (photoelectron emission microscope) optics, S-type tandem arranged 2 hemispherical deflection analyzers (HDAs for aberration correction), decelerating lens and a 2D detector, almost two orders of magnitude higher efficiency ARPES than conventional ARPES by a single HDA with a 2D detector became feasible.
With using a 2D imaging spin filter made of Au/Ir(001), the spin detection with 2D figure of merit of 100 is now feasible in MPI-Halle.
Thus the SP-ARPES detection efficiency is now 106 times higher than Mott detector.
As far as a very flat clean surface is realized, very efficient SP-2D-ARPES is now feasible.
Even SP-2D-ARPES is possible for micro- and nano-regions owing to the PEEM optics.
If the instrument is installed on synchrotron radiation beam line, 9D-Px,Py,Pz(EB(kx,ky,kz)) SP-ARPES can provide rich information and enable the check of the validity of any theoretical approaches.

[1] S.Suga and A.Sekiyama, Photoelectron Spectroscopy, Bulk and Surface Electronic Structures, Springer Series in Optical Sciences 176 (Springer, Heiderberg, 2014).
[2] S.Suga and C.Tusche, J.Electron Spectrosc. Rel. Phenom.200 (2015), in press.

F3.02(초)

Resonant inelastic x-ray scattering spectroscopy for strongly correlated systems

*Jung Ho Kim
*Jung Ho. Kim
Advanced Photon Source. Argonne National Laboratory.

Keyword : RIXS, strongly correlated systems, spin-orbit coupling

Resonant Inelastic X-ray Scattering (RIXS) has made remarkable progress as a spectroscopic technique over the past decade, at third-generation synchrotron sources such as the Advanced Photon Source (APS).[1] The technique's unique capability to provide the excitation spectrum in strongly correlated systems by measuring their momentum- and energy- dependences has brought RIXS to the forefront of experimental spectroscopic studies. In this talk, I will briefly review on the technical and scientific developments over the past decade and present the current status and the on-going development of the hard x-ray RIXS facilities at the APS. Traditionally, 3d transition metal oxide systems such as cuprates and manganites has been studied at the K-edge absorption. Dynamics of Mott gap excitations, orbital excitations, and spin excitations have been studied, revealing those strongly correlated nature, which is otherwise difficult or impossible to obtain.[1] Recently, its technical capability has been extended to the L-edge of 5d transition metal[2] and rare-earth[3] systems. In particular, elementary excitations such as magnon and orbiton have been successfully measured in the case of the Iridium oxide system, revealing essential aspects of exchange interactions of the spin-orbit coupled composite states. This success opens up new possibilities for the study of all other 5d transition metal systems. Other than the bulk systems, quantum phenomena controlled by heterostructure thin films[4] and high pressure[5] have been successfully studied. Advances in RIXS have come in lockstep with improvements in energy resolution. The recent R & D for the order-of magnitude improvement in the energy resolution will be presented.

[1] Luuk J. P. Ament, et al. Rev. Mod. Phys. 83, 705–767 (2011).
[2] Jungho Kim, et al. Phys. Rev. Lett. 109, 157402 (2012).
[3] I. Jarrige, et al. Phys. Rev. Lett. 114, 126401 (2015)
[4] A. Lupascu, et al. Phys. Rev. Lett. 112, 147201 (2014)
[5] Jungho Kim, et al., EPL, 108, 37001 (2014)

F3.03(초)

Inelastic Neutron Scattering: Facilities and Scientific Opportunities

*박승일
*J. M. Sungil. Park
한국원자력연구원.

Keyword : inelastic neutron scattering

Inelastic neutron scattering, since its inception in 1950's, has become an indispensable tool for studying the lattice and spin dynamics of strongly correlated electron systems. East Asia and the surrounding region host a variety of inelastic neutron scattering instruments at a few prominent neutron sources, with several new instruments under construction or commissioning thanks to the vibrant condensed matter communities in the region. Korea's only large scale neutron source, the 30 MW research reactor HANARO, will have three working inelastic neutron scattering instruments in late 2016 when the reactor resumes operation after a long hiatus. A brief introduction will be given on their inner workings and the characteristics as well as the scientific opportunities they present to the strongly correlated electron community.

F4.01

Tyrannosaurs as long-lived species

*원병묵
*Byung Mook. Weon
성균관대학교.

Keyword : tyrannosaurs, population ecology, aging, stretched exponential

Biodemographic analysis would be essential to understand population ecology and aging of tyrannosaurs. Here, we address a methodology that quantifies tyrannosaur survival and mortality curves by utilizing modified stretched exponential survival functions. Our analysis clearly shows that mortality patterns and aging dynamics for tyrannosaurs resemble those for humans. This result implies that tyrannosaurs would live so long to undergo aging after reproduction, which would be plausible as benefit from predation relief by rapid growth.

F4.02

Air bubble motion by symmetric breaking in homogeneous nematic cell

*김성조, 김종현, Bohdan Lev
*Sung-Jo. Kim, Jong-Hyun. Kim, Bohdan. Lev
충남대학교.

Keyword : liquid crystal

5CB nematic liquid crystal molecules align vertically on air-nematic interface. Hyperbolic hedgehog point defect or Saturn-ring disclination line defect are accompanied around air bubble for conserving topological charge in homogeneous nematic cell. The symmetry of distribution of liquid crystal molecules is determined by combination with air bubble and defect and it leads to anisotropic evaporation of air molecules. We investigate the air bubble motion by such a symmetric breaking.

F4.03

DMSO disorders water structure and enhances water diffusion near phospholipid bilayer surfaces

*이윤호, 현창봉
*Yuno. Lee, Changbong. Hyeon
고등과학원.

Keyword : DMSO, lipid bilayer, MD simulation

Dimethyl sulfoxide (DMSO) prevents ice formation by disrupting the hydrogen bond network among water molecules. Despite its broad use as a cryoprotectant and long-lasting efforts to probe water dynamics in the presence of DMSO, the microscopic underpinnings by which DMSO prevents ice formation on cell surfaces are not fully understood.
Here, using all atom molecular dynamics simulations of POPC/water systems at varying DMSO concentrations, we probe the structural and dynamical properties of water and DMSO in the vicinity of phospholipid bilayers. Our study is consistent with the recent studies pointing to DMSO-induced dehyration, but critically reveals the presence of fine structures in hydration layer near bilayer surfaces.

F4.04

X-ray-induced volume change of a colloidal sphere

*조건, 황인규, 김예슬, 임준 [1], 원병묵
*Kun. Cho, In Gyu. Hwang, Yeseul. Kim, Jun. Lim[1], Byung Mook. Weon
성균관대학교. [1] 포항가속기연구소.

Keyword : X-ray microscopy, colloids, radiation effects, volume change

X-ray microscopy would be powerful for biomedical imaging and soft matter studies. Controlling radiation effects of X-ray photons is important for appropriate applications of X-ray imaging. We find an efficient and practical protocol to quantify X-ray radiation effects by using a colloidal particle in atmospheric and room-temperature conditions. We present quantitative evidence for X-ray-induced chain scission of polystyrene (PS) colloidal particles. A cluster of PS colloids was capsulated with a nonvolatile liquid to prevent evaporation and then irradiated with hard X-rays. We show that the initial volume of a PS sphere constantly decreases with X-ray irradiation time, demonstrating a possibility of X-ray-induced chain scission of PS. These data can be used to estimate X-ray radiation effects.

F4.05*

X-ray nanotomography of colloid random packing

*김예슬, 임준 [1], 원병묵
*Yeseul. Kim, Jun. Lim[1], Byung Mook. Weon
성균관대학교. [1] 포항가속기연구소.

Keyword : X-ray nanotomography, colloids, packing, complex fluids

Colloidal suspensions are complex fluids that include colloidal nanoparticles or microparticles uniformly suspended in a liquid medium. In-situ characterizations of colloidal suspensions are required in many topics: for instance, wetting properties for colloidal particles on a fluid-fluid interface are essential but hard to be directly taken with conventional imaging techniques. Here we show that hard X-ray nanotomography clearly visualizes individual colloidal particles inside fluids in three dimensions (3D). In particular, we demonstrate 3D images for monodispersed colloidal particles with various sizes from 500 nm to 2,000 nm. We believe that hard X-ray nanotomography would be a powerful tool to identify the packing nature of colloidal particles inside or on fluids.

F4.06*

Coffee-ring effects in a dense limit

*김진영, 류슬아, 김형대 [1], 김준헌 [2], 박정수 [2], 박용석, 오정수, 원병묵
*Jin Young. Kim, Seul-a. Ryu, Hyungdae. Kim[1], Joon Heon. Kim[2], Jung Su. Park[2], Yong Seok. Park, Jeong Su. Oh, Byung Mook. Weon
성균관대학교. [1] 경희대학교. [2] 광주과학기술원.

Keyword : "coffee-ring effect", "evaporation", "drying", "droplet", "complex fluid"

The coffee-ring effect, which is a natural generation of outward capillary flows inside drying coffee drops, is valid when solute is dilute. This effect is significant in modern technologies such as self-assembly of nanoparticles, ink-jet printing, painting, particle deposition applications, and DNA chip manufacturing. As the solute becomes dense, the ring width cannot be negligible: the ring deposit is forced to have a non-zero width. In general, a higher initial concentration leads to a wider ring. Here we study the coffee-ring effect in a dense limit by demonstrating differences with various initial coffee concentrations from 0.1% to 60%. The coffee drops with high initial concentrations of real coffee particles show specific evaporation dynamics: dense coffee drops tend to evaporate slowly. This result is different from the classic coffee-ring effect in the dilute limit. We suppose that the slow evaporation of dense coffee drops is associated with the ring growth dynamics. The complexity in evaporation dynamics of colloidal fluids can be understood by expanding the coffee-ring effect in the dilute as well as the dense limits.

F4.07*

Plasticity in cancer survival curves

*임수진, 이세라 [1], 강태홍 [1], 임선희 [1], 원병묵
*Su Jin. Lim, Se-Ra. Lee[1], Tae-Hong. Kang[1], Sun-Hee. Leem[1], Byung Mook. Weon
성균관대학교. [1] 동아대학교.

Keyword : survival curve, cancer, plasticity

Precise analysis of survival statistics for cancer patients is important for optimal patient care and prognosis. Survival curves can be made from reliable data for survival years from diagnosis to death. We develop a useful method to precisely analyze survival curves for cancer patients with a modified stretched exponential function. Here we show an availability of our method by using a public database of the Surveillance, Epidemiology, and End Results (SEER) program for the United States that is annually under update by the National Cancer Institute. Our analysis shows how cancer survival curves have changed over time, demonstrating plasticity of cancer survival curves, particularly during recent three decades. As a result, survival trends of patients can be classified as four different types. This result would be important for tracking recent improvements in diagnosis and treatment of cancer as well as suggesting effective ways to fight cancer in the near future.

F5.01(초)

Versatile Surface Plasmon Resonance of Silver Nanoparticles in Polymer Solar Cells

*김진영
*Jin Young. Kim
울산과학기술대학교.

Keyword : Surface plasmon resonance, polymer solar cells, silver nanoparticles

The coupling of surface plasmons and excitons in organic materials can improve the performance of organic optoelectronic devices. The surface plasmon resonance effect of carbon dot-supported silver nanoparticles (Ag NPs) allows additional light absorption, leading to remarkably enhanced a power conversion efficiency (PCE) of 8.31% and an internal quantum efficiency of 99% in polymer solar cells (PSCs) compared with control devices. Furthermore, we have demonstrated high-performance PSCs using the plasmonic effect of multi-positional silica-coated silver nanoparticles. The location of the nanoparticles is critical for increasing light absorption and scattering via enhanced electric field distribution. The device incorporating silica-coated silver nanoparticles between the hole transport layer and the active layer achieves a PCE of 8.92% with an external quantum efficiency of 81.5%. These results demonstrate that Ag NPs constitute a versatile and effective route for achieving high-performance polymer optoelectronic devices.

F5.02(초)

Zwitterionic Electrode Modifiers for Inverted Organic Electronics

*이현복
*Hyunbok. Lee
강원대학교.

Keyword : "zwitterion","UPS","low work function","electron injection","OPV"

Organic electronics, such as organic photovoltaics (OPVs), organic light-emitting diodes (OLEDs), and organic field-effect transistors (OFETs), have attracted significant interest due to the unique advantages such as simple fabrication method, light weight, and flexibility. In organic electronics, reducing the charge injection barrier between an electrode and an organic semiconductor plays a critical role in device performance. To improve charge injection efficiency, the insertion of an ultrathin interlayer modifying the work function of an electrode is often employed. For inverted organic electronics, low work function electrodes having air stability are necessary which show the low electron injection barrier with an adjacent n-type organic semiconductor. In this respect, solution-processable and dipole-rich zwitterions are regarded as efficient electrode modifiers for inverted organic electronics which lower the work function of an electrode significantly. Here we investigated the electronic structures and structural properties of poly(sulfobetein methacrylate) (PSBMA).[1] The work functions of various electrodes with a PSBAM interlayer were reduced by more than 1 eV. The origin of the work function reduction was the interface dipole formation due to the strong intramolecular dipole moment of a sulfobetain zwitterion. As a result, the electron injection barrier between ITO and C_{70} was significantly reduced from the 0.76 to 0.09 eV. The power conversion efficiency (PCE) of inverted OPVs with a PSBMA interlayer dramatically improved from 0.71 to 3.35%. Especially, the S-shaped kink in J-V characteristics due to charge accumulation at the interface between C_{70} and ITO was removed. The zwitterions can be widely applicable to electronic devices requiring a low work function electrode.

F5.03*

Morphology Modifier for a Graphene Electrode: CuPc/HAT-CN/Graphene

*정준경, 박수형, 강성준 [1], 이현복 [2], 이연진
*Junkyeong. Jeong, SOO HYUNG. PARK, Seong Jun. Kang[1], Hyungbok. Lee[2], Yeonjin. Yi
연세대학교. [1] 경희대학교. [2] 강원대학교.

Keyword : graphene, HAT-CN, CuPc, energy level alignment, molecular orientation

As a transparent electrode for future optoelectronic devices, graphene is one of promising materials for replacing an indium-tin oxide (ITO). However, the work function of graphene, ca. 4.5 eV, is not quite high or low to be used as either an anode or a cathode in organic photovoltaics (OPVs). Although PEDOT:PSS is commonly used to increase the work function of an anode, it is not suitable to a graphene electrode due to its hydrophobic characteristic.[1] Accordingly, hexaazatriphenylene hexacarbonitrile (HAT-CN) which has a high work function would be an alternative to a hole injection layer with a graphene substrate. In addition, since the lowest unoccupied molecular orbital (LUMO) level of HAT-CN is very close to the Fermi level, it is regarded as a charge-generation layer. Therefore, it dramatically improved the performance of devices.[2]

While the electronic properties and applications of HAT-CN have been studied, the morphological effects have not been investigated in detail. Graphene has a flat π-surface which leads organic molecule to orient face-on geometry. On the other hands, the HAT-CN layer does not provide a flat surface as compared to graphene. Fundamental study on morphological difference which would change the electronic structure for each system is still lacking.

In this study, the morphological effect of graphene and HAT-CN on the electronic structures of a copper phthalocyanine (CuPc) overlayer was demonstrated. To investigate the molecular orientation of CuPc in each sample, Raman spectroscopy and grazing incident wide angle x-ray scattering (GIWAXS) measurements were conducted. In addition, in situ ultraviolet photoelectron spectroscopy (UPS) and x-ray photoelectron spectroscopy (XPS) measurements were carried out for the interface of CuPc/HAT-CN/graphene and CuPc/graphene. These measurements showed the significant reduction of a hole injection barrier of CuPc overlayer with the insertion of HAT-CN.

[1] Park, H.; Kong, J. Adv. Energy Mater. 4, 1301280 (2014)
[2] Lee, H.; et. al Carbon 71, 268–275 (2014)

F5.04*

Electrical characteristics of vertically stacked microscale organic nonvolatile memory

*유대경, 송영걸, 장진곤, 김영록, 정석헌 [1], 이진균 [1], 이탁희
*Daekyoung. Yoo, Young gul. Song, Jingon. Jang, Youngrok. Kim, Seok-Heon. Jung[1], Jin-Kyun. Lee[1], Tak Hee. LEE
서울대학교. [1] *인하대학교.*

Keyword : "Organic electronics", "Non-volatile memory", "Microscale"

Recently organic electronics is widely studied due to its material variety, easy and low cost fabrication, spin coating process, and flexibility. In particular, organic nonvolatile memory has been spotlighted for data-storage device [1]. However in spite of these merits, most organic non-volatile memory (ONVM) devices so far have been fabricated with very large cell size of ~100 μm. To overcome this large cell size problem, fabricating microscale three-dimensionally (3D) integrated ONVM can be a solution for the high density ONVM [2]. Such works may propose the possibility of high density 3D stacked ONVM devices with uniform electric parameters.

In this presentation, I will report micro-scale 3D integrated ONVM devices with a 7 μm × 7 μm memory cell size in a 32 × 32 crossbar structure on a silicon substrate by orthogonal photolithography using highly fluorinated photoresist and development solvent. Because highly fluorinated photoresist material has orthogonal property to the most organic materials, there is no damage for organic memory layer or Al electrodes during orthogonal photolithography [3]. Our 3D integrated micro-scale ONVM devices showed reproducibility with good endurance cycle and stability with long retention time over 10^4 s for the vertically stacked layers [4]. And, the operative memory cells in each layer have uniform and stable electric parameters. Our study suggests that the realization of 3D integrated micro-scale ONVM may enable the production of functioning organic electronic devices in practical configurations such as micro-scale 3D integrated flexible organic devices.

[1]. B. Cho, S. Song, Y. Ji, T.-W. Kim & T. Lee, Adv. Funct. Mater. 21, 2806 (2011).
[2]. S. Song, B. Cho, T.-W. Kim, Y. Ji & T. Lee Adv. Mater. 22, 5048 (2010).
[3]. Y. Song, J. Jang, D. Yoo, S.-H. Jung, S. Hong, J.-K. Lee, T. Lee, Org. Electron. 17, 192 (2015).
[4]. D. Yoo, Y. Song, J. Jang, W.-T. Hwang, S.-H. Jung, S. Hong, J.-K. Lee, and T. Lee, Org. Electron. 21, 198 (2015).

F5.05*

Interfacial electronic structure of C_{60}/ZnPc/AZO on photoemission spectroscopy for organic photovoltaic applications

정윤우, 이나래, 김종훈, 임영지, 천수영, 조수행, *조상완, 박수형, 이연진
Yunwoo. Jung, Nalae. Lee, Jonghoon. Kim, Yeong Ji. Im, Suyoung. Cheon, Soohaeng. Cho, *Sang Wan. Cho, SOO HYUNG. PARK, Yeonjin. Yi
연세대학교.

Keyword : organic semiconductors, ultraviolet photoemission spectroscopy, ZnPc, AZO

The interfacial electronic structure of a bilayer of fullerene (C_{60}) and zinc phthalocyanine (ZnPc) grown on aluminum-doped zinc oxide (AZO) substrates has been evaluated by X-ray and ultraviolet photoemission spectroscopy. The energy difference between the highest occupied molecular orbital (HOMO) level of the ZnPc layer and the lowest unoccupied molecular orbital (LUMO) level of the C_{60} layer ($E^{D}_{HOMO} - E^{A}_{LUMO}$) was determined and compared to that grown on an indium tin oxide (ITO) substrate. The $E^{D}_{HOMO} - E^{A}_{LUMO}$ value of the heterojunction on AZO was 1.4 eV, while that on ITO was 1.1 eV. This result is discussed in terms of the differences of the work function and resistivity of each transparent conductive oxide. We also obtained complete energy level diagrams of C_{60}/ZnPc/AZO and C_{60}/ZnPc/ITO.

F5.06*

고전류 구동 구현을 위한 수직형 유기전계트랜지스터의 제작과 이해

*권혁윤, 김민철, 조현수, 유승협
*Hyukyun. Kwon, KIM Mincheol. , Cho Hyun su. , Seuunghyup Yoo.
한국과학기술원 (KAIST).

Keyword : 유기 수직 전계 트랜지스터, 소자 시뮬레이션, C60, 하부 반도체 층, 유기 발광 다이오드 구동

유기 박막 트랜지스터 (OTFTs) 는 유기 반도체 고유의 특성으로 인해 플렉서블하고 투명하며 저가의 공정이 가능해 다양하고 새로운 분야에 쓰일 잠재력이 있는 소자이다. 그러나 유기 반도체 고유의 낮은 이동도는 소자의 성능에 제한이 된다. 제한된 유기 반도체의 이동도에서 출력 전류량을 늘리고자 소자의 구조적인 연구가 다양하게 진행되어 왔는데 이중 하나가 수직 방향의 채널을 갖는 유기 수직 전계 트랜지스터 (VFETs) 이다. 유기 수직 전계 트랜지스터는 전하가 수직으로 흐르므로 반도체 층의 두께가 채널의 길이가 되어서 효과적으로 채널의 길이를 줄일 수 있다. 하지만 대부분의 경우 구조적인 특성과 동작 원리로 인해 소스 전극의 복잡한 패터닝 공정이 요구되어 왔으며 패터닝에 따라 소자의 성능이 달라지는 문제가 발생되었다.
이에 본 연구에서는 증착 공정만을 이용해 소스 전극을 반도체층 사이에 삽입하여 복잡한 전극 패터닝이 요구되지 않는 구조의 유기 수직 전계 트랜지스터를 제작하고 분석하였다 [1]. 소자의 동작 원리를 파악하고 성능에 영향을 주는 파라미터를 결정하기 위해 실험과 소자 시뮬레이션을 동시에 진행하였다. 그 결과, 소스-드레인 전극의 폭, 소스 전극 아래에 존재하는 하부 반도체 층의 두께를 소자의 성능을 결정짓는 요소로 정하였다. 위의 과정들을 거쳐 최적화된 구조는 기존의 수평 방향 채널을 가지는 유기 박막 트랜지스터에 비해 약 20 배 이상의 전류 값을 가졌으며 OLED 구동을 통해 전류 구동 소자로의 실제 적용 가능성을 확인해 보았다.

[1] H. Kleemann, A. A. Günther, K. Leo, and B. Lüssem, Small, 21(9), pp. 3670-3677 (2013).

F5.07*

Efficient inverted organic solar cells using graphene as a cathode

*김호범, 이태우
*Hobeom. Kim, Tae-Woo. Lee
포항공과대학교.

Keyword : graphene electrodes, organic solar cells, ZnO, Zonyl, graphene doping

In this report, we developed efficient OSCs of inverted structure (iOSCs) with graphene bottom cathodes grown by chemical vapor deposition method. Because graphene is hydrophobic, coating a hydrophilic ZnO solution and forming a uniform layer of ZnO on graphene surface have been constantly pointed out as a big problem to fabricate iOSCs with graphene electrodes. By adding fluorosurfactant, Zonyl, to a precursor solution of ZnO (ZZO), we successfully made a uniform ZZO layer on graphene surface and fabricated iOSCs with graphene cathodes. The iOSC with a graphene cathode achieved a PCE = 7.5% which was identical to that of an otherwise-identical device with an ITO cathode. To the best of our knowledge, the PCE of iOSCs with the graphene cathode we developed is the highest value among single junction OSCs with graphene electrodes ever reported up to date and this is the first result to show that the PCE of OSCs with graphene electrodes can reach an equivalent level of PCE of OSCs with ITO electrodes. Furthermore, we conducted systematic analysis of light harvesting and recombination kinetics of devices to understand the device result. Lastly, we also observed n-doping effect of the ZZO layer on graphene by Raman spectroscopy and the Dirac point shift in graphene field effect transistors.

F6.01*

Grain Boundary – Free Growth of Monolayer Hexagonal Boron Nitride on Liquid Metal

*이주송, 박지훈 [1], 이승희 [2], 이영희 [1], 김기강 [3], 김수민
*Joo Song. Lee, Ji Hoon. Park[1], SEUNG HEE. LEE[2], Young Hee. LEE[1], Ki Kang. Kim[3], soo Min. Kim
한국과학기술연구원. [1] 성균관대학교. [2] 전북대학교. [3] 동국대학교.

Keyword : hexagonal boron nitride, single crystal, self-alignment, synthesis, liquid metal

We report the synthesis of grain boundary-free monolayer hexagonal boron nitride (h-BN) on liquid metal. Hexagon-shaped monolayer h-BN grains were initially grown on liquid metal and merged to form the single crystal monolayer h-BN via self-alignment of hexagon h-BN grains over a prolonged growth time. Both the liquid surface of metal and hexagon-shaped h-BN grains are essential in order to obtain the single crystal h-BN. The optimum ratio of hydrogen and argon is the key for the formation of the hexagon h-BN island. As-grown h-BN film was transferred to a target substrate by using the conventional bubble transfer method and metal foil was reused for the repeated growth of h-BN film. The large-area single crystal monolayer h-BN film was characterized by selective area diffraction pattern in transmission electron microscopy and polarizing optical microscopy assisted by the nematic liquid crystal, confirming that a single grain size of monolayer h-BN is larger than 8 mm^2, which is highest reported value from previous reports of CVD-grown monolayer h-BN film.

F6.02*

New approach of Synthesis of Molybdenum Disulfide using Liquid-phase Precursor

*최수호, 보안도스테펜, 이주송 [1], 김수민 [1], 양우철, 김기강
*Soo Ho. Choi, Stephen. Boandoh, Joo Song. Lee[1], soo Min. Kim[1], woo chul. yang, Ki Kang. Kim
동국대학교. [1] *한국과학기술연구원 전북분원.*

Keyword : "molybdenum disulfide", "synthesis", "dimethyl disulfide", "molybdenum hexacarbonyl", "liquid precursor"

Finding of alternative molybdenum and sulfur precursors remains of importance for the synthesis of molybdenum disulfide (MoS_2). Here, we report the development of liquid-phase precursor to synthesize monolayer MoS_2 in chemical vapor deposition. The liquid precursor is prepared by dissolving of molybdenum hexacarbonyl in dimethyl disulfide. It contains the complex of Mo ion, S compound, and Mo-S compound confirmed by mass spectrometry. The liquid precursor is supplied with a conventional bubbling system. Monolayer MoS_2 flakes as large as an order of few micrometer sizes on SiO_2/Si substrate are grown. The kinetics for the growth is also studied with the controlling of hydrogen, precursor flow rate, and the growth temperature. Our liquid-phase precursor not only provides inexpensive and facile ways to grow MoS_2 compared with other precursors, but also hastens the commercialization of MoS_2 in near future.

F6.03*

Universal transfer of 2D materials with ethyl cellulose onto arbitrary substrates

*보안도스테펜, 최수호, 이주송 [1], 양우철, 김수민 [1], 김기강
*Stephen. Boandoh, SooHo. Choi, Joo Song. Lee[1], woo chul. yang, soo Min. Kim[1], Ki Kang. Kim
동국대학교. [1] *한국과학기술연구원 전북분원.*

Keyword : "2D materials", "transfer", "Support layer", "Ethyl cellulose"

Chemical vapor deposition (CVD) among the several methods is the most promising way to produce large-area and high-quality 2D materials. To study their fundamental properties and practical application, 2D materials after growth on a substrate in CVD need to be transferred onto a target substrate. The desire is to transfer the materials onto a target substrate without any negative impact on their properties. The most widely used among several methods is the wet transfer with Poly(methyl methacrylate) (PMMA) as the support layer. However, the effective removal of the PMMA has been an issue, hence alternatives to PMMA are being sort after. In this study, we report new supporting layer of ethyl cellulose for the transfer of 2D materials onto target substrates. The diverse solubility of ethyl cellulose in a wide range of organic solvents makes it a clean and cheap alternative. This support layer can be removed with appropriate solvents at room temperature without further annealing which is suitable for transfer onto flexible substrates.

F6.04*

Graphene and nickel oxide composite with glucose for supercapacitor application

*정혜경, 전하이
*Hae Kyung. Jeong, Minh-Hai. Tran
대구대학교.

Keyword : graphene oxide, nickel oxide, glucose, supercapacitor

Nickel oxide composites with graphene have been a promising electrode material for supercapacitor based on synergistic of both electric double-layer capacitance and pseudo-capacitance. However, the re-agglomeration phenomenon of reduced graphene oxide still a drawback for increasing its capacitance. Therefore, we considered and investigated a simple and green synthesis method for improving capacitance of reduced graphene oxide/nickel oxide based supercapacitor electrode by compositing with glucose, considered as a cheap and eco-friendly chemical nowadays. The specific capacitance of the ternary composite can be improved up to about five times higher than that of the reduced GO and two times higher than that of nickel oxide-graphene composite without glucose in an aqueous electrolyte based on not only synergistic effect of graphene and metal oxide but also ameliorative surface modification when compositing with glucose.
* Corresponding author: outron@daegu.ac.kr

F6.05*

Photoconductive characteristics of copper phthalocyanine-stacked MoS_2 field effect transistors

*박진수, Jingon Jang[1], Kyungjune Cho[1], Tae-Young Kim[1], Jae-Keun Kim[1], Younggul Song[1], Woong-Ki Hong[2], Misook Min[1], Hyoyoung Lee[3], 이탁희
*Jin Su. Pak, Jingon. Jang[1], Kyungjune. Cho[1], Tae-Young. Kim[1], Jae-Keun. Kim[1], Younggul. Song[1], Woong-Ki. Hong[2], Misook. Min[1], Hyoyoung. Lee[3], Tak Hee. LEE
서울대학교. [1]Seoul National University. [2]Jeonju Center. Korea Basic Science Institute. [3]Sungkyunkwan University.

Keyword : "Molybdenum disulfide", "Photodetector", "Field effect transistor","Copper phthalocyanine", "Heterostructure"

Recently, transition metal dichalcogenide (TMD) two-dimensional (2D) materials have gained a considerable interest as a candidate for next generation nanoelectronics devices. Among the various TMD materials, molybdenum disulfide (MoS_2) has been widely researched as 2D field-effect transistors (FETs) and exhibited the outstanding electrical properties about high carrier mobility, low subthreshold swing value, and high on/off ratio [1]. In contrast to graphene which lacks an energy band gap, MoS_2 has a direct band gap of 1.8 eV as a single layer and an indirect band gap of 1.2 eV as a multilayer MoS_2. Becuase of these band gap properties of MoS_2, the photodetectors made with MoS_2 have exhibited excellent photoreponse properties. Beyound the structure of MoS_2 FET alone, it has been demonstrated the MoS_2-based heterostructure through stacking other materials results in higher photoreponsivity [2].
In this study, we have investigated the electrical and photoresponsive properties of MoS_2 FET-based photodetectors by stacking copper phthalocyanine (CuPc) layers on the MoS_2 surface [3]. We characterized and compared the shift of threshold voltage and the photodetection characteristics of MoS_2 devices prior to and after the devices were stacked with p-type organic semiconductor (CuPc) layers on the MoS_2 surface. In addition, we found the optimized CuPc thickness (~2 nm) on MoS_2 surface for the best performance as a photodetector. Consequentially, we could enhance the photoresponsivity of devices throughout the wavelength ranges and under different intensity. And our results suggest that the height of p-type organic material for vertical heterostructure is also an important factor to exhibit the best performance as a photodetector.

References
[1] B. Radisavljevic, A. Radenovic, J. Brivio, V. Giacometti and A. Kis, Nature Nanotechnology, 6, 147 (2011).
[2] D. Kufer, I. Nikitskiy, T. Lasanta, G. Navickaite, F.H.L. koppens, and G. Konstantaos, Adv. Mater. 27, 176 (2015).
[3] Jinsu Pak, Jingon Jang, Kyungjune Cho, Tae-Young Kim, Jae-Keun Kim, Younggul Song, Woong-Ki Hong, Misook Min, Hyoyoung Lee, and Takhee Lee, submitted (2015).

F6.06*

Phase Patterning for Ohmic Homojunction Contact in $MoTe_2$

*김세라, 조수연, 김정호, 석진봉, 금동훈, 이영희, 김성웅, 양희준
*Se Ra. Kim, Suyeon. Cho, Jung Ho. Kim, jinbong. seok, dong hoon. Keum, Young Hee. LEE, SungWng. Kim, HeeJun. Yang
성균관대학교.

Keyword : "phase trasition", "$MoTe_2$", "2D device", "ohmic contact"

반도체 특성을 보이는 2H-$MoTe_2$ 에 532nm 파장의 레이저를 조사함으로써 레이저를 조사한 부분만 도체의 특성을 보이는 1T' phase 로의 상전이를 일으켰다. 이 국소적인 상전이를 소자에 응용하여 Ohmic Homojunction Contact 을 만들어 10^6 의 높은 on/off ratio 를 유지하면서도 mobility 를 약 50 배 향상시켰다. Tellurium vacancy 가 기존 800 도 이상의 상전이 온도를 약 400 도 까지 내려주었으나 이 때문에 1T'에서 2H phase 로 돌아올 순 없었음을 STEM 분석을 통해 확인하였다.

F6.07

High-performance Graphene Field Effect Transistors using h-BN as a Dielectric Layer

Huynh Van NGOC, *강대준
Huynh Van. NGOC, *Dae Joon. KANG
성균관대학교.

Keyword : Graphene transistor, h-BN, Chemical vapor deposition, PMMA assisted transfer

Hexagonal boron nitride (h-BN) has emerged as an exceptional dielectric for graphene based field effect transistor (GFET). GFETs based on mechanically exfoliated h-BN dielectric were found to exhibit an order of magnitude improvement in device mobility, reduced carrier in-homogeneity, lower extrinsic doping, reduced chemical reactivity, and improved high-bias performance when compared to FET devices fabricated with conventional oxide dielectrics. However, the chemical vapor deposition (CVD) growth of h-BN dielectric has not been fully explored yet for high-performance GFETs. This is mainly due to residues originated from incomplete etching of polymethylmethacrylate (PMMA) during a typical PMMA-assisted transfer on to the surface of transferred h-BN. This creates additional trapping sites, thus degrading the performance of GFETs. In this report, we demonstrate that GFETs based on CVD grown h-BN dielectric layer can show excellent electrical properties by adding a water soluble layer in-between PMMA and 2D materials, graphene and h-BN. This transfer method allows not only an effective transfer of 2D materials to various target substrates with a high degree of freedom but also an metal etching-free process of PMMA-assisted-transfer, minimizing the effects of undesirable contaminations on the surface. This facile transfer technique presents a great potential for future research and application suitable for high performance large area mechanical, optical and electronic devices based on graphene/h-BN heterostructures.

F6.08*

Raman investigation of molybdenum disulfide with different stacking orders

*이재웅, 김강원, 한송희, 류경희 [1], 이종훈 [1], 정현식
*Jae-Ung. Lee, Kangwon. Kim, Songhee. Han, Gyeong Hee. Ryu[1], Zonghoon. Lee[1], Hyeonsik. Cheong
서강대학교. [1] 울산과기대.

Keyword : Molybdenum disulfide, Raman spectroscopy, Stacking orders, 3R phase

The effects of stacking order in the Raman spectra of molybdenum disulfide (MoS_2) are investigated. 2H-MoS_2 is representative of semiconducting transition metal dichalcogenides (TMDCs). Although 2H-MoS_2 is most common in nature, the 3R phase can exist due to a small difference in the formation energy. However, most studies so far have focused on the 2H phase, and only few studies are reported for 3R phase. We found the 2H, 3R and mixed phase of exfoliated MoS_2 from natural molybdenite crystals. The crystal structures are confirmed by the HR-TEM measurements. By using 3 different excitation energies, we compared the Raman spectra of samples with different stacking orders in detail. We show that the Raman spectroscopy can be used to identify not only the number of layers but also stacking orders of MoS_2.

F6.09*

Optical Properties of Single Layer MoS_2 Nanoflakes

심유민, 김진배, *성맹제
Yumin. SIM, Jinbae. KIM, *Maeng-Je. SEONG
중앙대학교.

Keyword : MoS2, nanoflake, Raman, photoluminescence, quantum confinement

We have synthesized nanoflakes of molybdenum disulfide (MoS_2) layers using simple chemical vapor deposition method with sulfur (S) and molybdenum trioxide (MoO_3) as the reactant and precursor, respectively. The synthesized MoS_2 nanoflakes, from mono- to few-layer, were characterized using Raman spectroscopy and photoluminescence (PL) spectroscopy. Raman spectra exhibited typical Raman features of two vibrational modes E_{2g} and A_{1g} at ~387cm^{-1} and ~407cm^{-1}, respectively. The room-temperature PL peak position of our MoS_2 nanoflakes was blue-shifted up to 30 meV with respect to that previously reported in the literature, which can be attributed to quantum confinement effect. Temperature dependence of the PL spectrum was also studied from 10K to 300K.

F7.01(초)

Suppress technology of nodule formation on the magnetron sputtering ITO target.

Pung-keun Song
Pung-keun. Song
Pusan National University.

Keyword : .

Magnetron sputtering is a very important technology for preparation of the high performance transparent conductive oxide (TCO) films because it has advantage of obtaining homogeneous large-area coatings with high reproducibility. Nodule are formed on the surface of sputter ITO target near the race track region, redeposit area, and sometimes race track region during the sputtering. There are some kinds of nodule shape type, hillock (grain), cone, and pyramid, etc. Usually formed nodule tend to grow during the sputtering and deposition, which induce various effects such as arcing generation, change in sputtering yield, angle distribution of sputtered atoms, and instability of discharge, etc. As a result, a sputtering system has to be shut down for cleaning of sputtering target or substitution of new target because they lead to degradation of the film quality. This is one of the reasons for rising production cost of the ITO films. However, we cannot understand still now in detail as to mechanism of nodule formation, growth, arcing generation, etc.
Therefore, in this study, we will discuss key factors dominating nodule formation and arcing generation on the point of view sputtering TCO target preparation and sputtering parameters such as target density, micro-pore size, secondary phase distribution, impurity doping, sputtering power density, cooling efficiency, etc.

F7.02(초)

Stretchable, Transparent Electrodes and Their Applications in Wearable Electronics

*Jang-Ung Park
*Jang-Ung. Park
Ulsan National Institute of Science and Technology (UNIST).

Keyword : .

Transparent conductive electrodes (TCEs), which have transparency and conductivity, are of increasing significance and demand for diverse application areas such as information (displays, touch screen), energy (solar cell, architectural), and environment (sensors). Nowadays, indium tin oxide (ITO) deposited by sputtering process is used as the main TCE material. Although the ITO presents low sheet resistance (~ 30 Ohm/sq) and high transparency (~ 90 %), its fragility limits many potential applications in flexible and stretchable electronics. For these reason, many types of alternative materials such as conducting polymers, carbon nanotubes, graphene, and metal nanowires, have been studied as candidates of the flexible and stretchable TCEs. Although many of these candidates exhibit good mechanical flexibility and stretchability, none shows significantly higher conductivity and transparency together, compared to ITO. Here, we present a simple fabrication process of high-performance, stretchable TCEs based on the metal nanofibers which have long and continuous web geometries, hybrid with 2D material graphene. These TCEs show superb electric conductivity (~ 1 Ohm/sq) with high transparency (~ 91 %) as well as substantial flexibility and stretchability. Hybrid transparent electrode shows very stable electrical property under 500 μm radius bending and 50% stretching (sheet resistance changed less than 20%). Also hybrid film shows great uniformity, sheet resistance standard deviation reduced one-tenth compare to only metal nanofiber. Based on high mechanical property and electrical property, we demonstrated transparent and flexible TFT backplane. Single TFT consisted of AgNW-graphene hybrid film, ZAO, IO, and metal nanofiber-graphene hybrid film. TFT show high electrical performance up to 100 $cm^2/V•s$, also represents ~90 % transparency (without substrate). TFT backplane can transfer to various substrates such as leaf, glass cup, glasses and human skin. We believe these TCEs based on the nanostructures present a promising strategy toward flexible and wearable electronics, and indicate the promise of future electronics beyond the limits of conventional ITO.

F7.03(초)

Recent Progress of Synthesis of Transition Metal Dichalcogenides and Hexagonal Boron Nitride Films in Chemical Vapor Deposition

*김기강
*Ki Kang. Kim
동국대학교.

Keyword : synthesis, transition metal dichalcogenides, hexagonal boron nitride

Recently, two dimensional (2D) materials including transition metal dichalcogenides (TMdCs) and hexagonal boron nitride (hBN) have been highlighted due to their unique physical, chemical, and optical properties. However, it is challenge to obtain large-area and high-quality 2D materials with controlling number of layers. Here, we present recent progress of the synthesis of large-area and high-quality 2D materials. First, we introduce the catalytic metal substrate and new precursors for the growth of TMdCs with full coverage. Second, we discuss how to control their thickness with maintaining high quality. Lastly, we propose new approaches for the synthesis of single crystal monolayer hBN with millimeter scale and extremely high-quality thick hBN film with large area. Our strategies will not only pave the way to synthesize large-area and high-quality 2D, but also promote their real applications.

F7.04(초)

Controlled synthesis of pristine and doped graphene using chemical vapor deposition method based on organic precursors

*김근수
*Keun Soo. KIM
세종대학교.

Keyword : graphene, CVD, organic precursors, controlled synthesis

We have investigated the synthesis conditions of pristine and doped graphene using chemical vapor deposition (CVD) method with various organic precursors, such as methane(CH_4), ethanol(C_2H_6O), methanol(CH_4O), pyridine(C_5H_5N), and so on.
For the synthesis of high-quality graphene, the growth condition has optimized by controlling the CVD parameters. As a result, we have successfully grown the graphene and doped graphene under very short growth time. It has shown 10 times faster than typical growth condition using CVD with methane (CH_4), previously.
In Raman spectra, 2D/G ratio and D/G ratio of samples have shown significantly different results according to supplying sources. Especially, in the case of N-doped graphene grown by pyridine source, D-peak intensity is increase, G-peak is blue shift and 2D-peak intensity is suppressed.
In x-ray photoelectron spectra, our pristine graphene has shown clear C1s-peak, and N-doped graphene has shown asymmetric broad C1s-peak from C-N bond and N1s-peak from graphitic-N bond, dominantly.
In addition, according to electrical characterizations, positions of Dirac point have shown neutral (methane), p-type (alcohol) and n-type (pyridine) behavior depend on the organic precursors. More details will be provided in the presentation.

F7.05(초)

대면적 2 차원 금속칼코겐 합성

*이창구, 이진환, 김영찬
*Changgu. Lee, Jinhwan. Lee, Youngchan. Kim
성균관대학교.

Keyword : 2 차원 금속칼코겐, 대면적 합성, 증기화학증착법

2 차원 금속 칼코겐물질은 금속, 반도체, 부도체성의 다양한 전기적물성을 지닌다. 그중에서 반도체성 금속칼코겐박막은 높은 전하이동도와 기계적 유연성, 그리고 투명도로 인해 차세대 유연전자소자의 재료로써 가장 적합한 물질에 포함된다. 본 발표에서는 MoS2 를 비롯한 원자수준두께의 2 차원 금속칼코겐을 증기화학증착법 등의 방법을 이용하여 대면적/균일한 두께의 필름을 합성한 결과를 소개하도록 한다. 특별히 이황화몰리브덴 필름합성을 위해서 H2S 가스와 고체의 Mo 전구체를 사용하여 전기적 물성이 우수하고 균일하고 투명한 필름을 합성하였다.

F8.01(초)

Selected results on nuclei and hadrons with strangeness from J-PARC

*Kiyoshi Tanida
*Kiyoshi. Tanida
Japan Atomic Energy Agency.

Keyword : hadron, strangeness, J-PARC

I will overview the experimental results on hadrons and nuclei with strangeness from the Hadron Hall facility of J-PARC. Especially interesting results are obtained on kaonic nuclei from E15 and E27, and on charge symmetry breaking effect in mirror hypernuclei (E13).
I also will show the status and future of nuclear and hadron physics at J-PARC.

F8.02(초)

Hyperons in neutron stars and their effects on neutron star cooling

*임연환
*Yeunhwan. Lim
기초과학연구원.

Keyword : Hyperons, Neutron Stars, Neutron Star Cooling

The existence of hyperons is expected in the core of neutron stars. As the baryon number density increases, the ground state of nuclear matter is supposed to have nucleons, hyperons, or some exotic particles to make lower energy states.
The so called 'Hyperon Puzzle' appears since the presence of hyperons make the equation of state (EOS) softer than the pure nuclear matter EOS, thus the maximum mass of neutron stars is unlikely to be greater than 2.0 Solar mass.
In this work, we present the EOS which satisfies the observational constraints for the mass of neutron stars and radius of them analyzed by the low mass X-ray bursts.
Both non-relativistic and relativistic mean field models are employed to construct EOS for neutron stars.
Using the EOS constructed by both both models, we investigate neutron star cooling curves in the presence of hyperons with and without hyperon superfluidity.

F8.03(초)

Photon induced multi-kaon production

*류휘영, 김현철 [1], 오용석, 아츄시 호사카 [2]
*Hui-Young. RYU, Hyun-Chul. Kim[1], Youngseok. Oh, Atushi. Hosaka[2]
경북대학교. [1] 인하대학교. [2]Osaka university.

Keyword : photoproduction, effective Lagrangian, Omega baryon

In the present work, we investigated in photoproduction of multi kaon with in an effective Lagrangian method. Firstly omega baryon porduction, , is considered. Not only known hyperons are included to estimate the cross section of the omega baryon productions but also unknown resonances are considered for other possible contribution separately. Secondly we study scattering process with possible intemediate states. We are interested in not only the cross section but the interference among each channels.
Both process are considered in the gague invariant formalism. To keep the gague invariance, we define the interaction current which remedy the broken gauge invariance by the other current.

F8.04(초)

Recent results and prospects from the LEPS and LEPS2 experiments at SPring-8

*Tomoaki Hotta
*Tomoaki. Hotta
Osaka University.

Keyword : LEPS/LEPS2, photon beams, BGOegg

We have been studying meson/baryon photoproduction reactions with linearly polarized photon beams in the energy range of 1.5-3.0 GeV. The photon beams are produced by the backward Compton scattering of ultraviolet laser photons off the 8-GeV electrons in the SPring-8 synchrotron radiation facility. At LEPS, one of two such beamlines operated by us, we are focusing on measuring charged particles in the forward direction with a dipole magnetic spectrometer. At the newly constructed LEPS2 beamline, the BGOegg experiment is being conducted, where a large-acceptance electromagnetic calorimeter (BGOegg) is used in combination with a high-resolution time-of-flight detector in the forward direction. In this talk, the recent results from the LEPS and LEPS2 experiments are reported. We are also constructing a large-acceptance detector system with a solenoidal magnetic spectrometer at the LEPS2 beamline. Th

F9.01(초)

범물리학과장협의회의 정책방향

*정윤철
*
부산대.

Keyword : 물리교육, 연구비감소, 지방물리학과 활성화 대책

현재 국내 물리학의 발전은 교육, 연구 모든 부분에서 과거와 비교해 비교적 정체되어 있는 것으로 보인다. 이러한 어려움을 극복하고자 전국 범물리학과장 협의회가 발족 되었다. 현재 물리학계가 겪고 있는 어려움을 분석하고 이를 통해 현실적으로 대처할 수 있는 방향을 모색하고자 한다. 특히 개인과제 연구비 감소, 물리학 교육의 문제, 지방 물리학과의 역할 감소 등에 대한 대응책을 적극 마련하고자 한다.

F9.02(초)

지역대 물리학과가 직면한 현실 및 극복 방안

*노태익

동아대.

학령인구 감소에 따른 대학 정원 감축과 관련된 지역대학의 구조조정과 물리학과가 처한 상황을 알아 보고 대처방안을 숙고해 본다. 대학평가와 학과 평가에서 물리학과가 받고 있는 불이익 요인과 평가지표로 인정 받지 못하고 있는 사항들을 분석해 본다. 물리학과의 순기능 특성 요인들은 새지표에 포함 되어야하고, 낮은 지표는 가중치를 높혀야 하며, 제도적 미흡으로 인한 불이익과 중복손해 지표들은 신속 과감하게 시정되어야 한다. 물리학을 둘러싸고 있는 현재의 중요한 사회적 환경은 기초과학으로서 물리학이 1/n 의 취급을 당하고, 교육과정에서 수업시수가 줄어들고 있으며, 학입학제도에 의해 고교생이 기피하는 과목으로 전락되었다. 중등 및 대학의 물리교육 과정의 개혁과 사회적 물리활동 봉사를 통해 새로운 전기를 만들어야한다.

F9.03(초)

대학물리교육 개선을 위한 활동 방안: 협력과 공유

*김진승

전북대.

우리나라의 인구 변화 추세, 산업구조 및 경제상황, 교육환경의 변화는 대학물리교육의 변화를 요구하고 있다. 이러한 변화에 대한 대응은 전국 대학의 공통 문제이므로, 각 대학이 따로 노력하는 것보다는 물리학회를 중심으로 집단적으로 노력하고 추진하는 것이 더 좋다. 이 강연에서는 여러 대학의 협력과 공유를 통해 대학물리교육 개선을 효율적으로 추진할 수 있는 방안을 제시한다.

F9.04(초)

효과적 연구비 재원마련 방안에 대하여

*이긍원

고려대.

최근 들어 여러 상황에 의해 기초연구비 재원의 마련이 어려운 국면을 맡고 있다. 이는 우리 나라의 역량 있는 연구인력의 수는 늘었으나 기초연구에 대한 지원이 갈수록 초대형 프로젝트에 매몰되고 이로써 잘못된 선택과 집중을 실행하고 있는 실정에 의한 것이라 판단된다. 이는 기초과학의 다양성을 가로막을 수 있으며 그동안 줄기차게 여러 회원들에 의해 제기되었던 풀뿌리 정신에도 매우 어긋난다 할 수 있다. 이번 강연에서는 물리학과 회원들의 효과적인 연구비 재원마련 방안에 대하여 토론하고 이로써 현실 개선 방안을 찾고자 한다.

F12.01(초)

Abundance of strategies in the iterated prisoner's dilemma in well-mixed populations

*백승기, 정형채 [1], 크리스티안 힐베 [2], 마틴 노박 [2]
*Seung Ki. Baek, Hyeong Chai. JEONG[1], Christian. Hilbe[2], Martin. Nowak[2]
부경대학교. [1] 세종대학교. [2] 하버드 대학교.

Keyword : Iterated prisoner's dilemma, Moran process, Win-Stay-Lose-Shift

The condition for emergence of cooperation in the prisoner's dilemma is an important question in evolutionary game theory. If the dilemma is formulated as a donation game, its payoff structure can be parametrized by a cost-benefit ratio of cooperation. This work investigates the iterated prisoner's dilemma in a well-mixed finite population with a general cost-benefit ratio. We consider the Moran process among strategies with memory one in the presence of implementation error. If we suitably separate relevant time scales of this dynamics, the abundance calculation of deterministic strategies reduces to an eigenvector problem. In addition, we calculate the most abundant strategy in the uncountable set of stochastic strategies with memory one in the weak-selection limit. Our calculation shows that Win-Stay-Lose-Shift is the most abundant when the cost of cooperation is low, whereas defectors are favored when the cost is high.

F12.02(초)

Large Variance and Fat Tail of Damage by Natural Disaster

*조항현, 고유리 [1]
*Hang-Hyun. Jo, Yu-li. Ko[1]
POSTECH. [1]Rensselaer Polytechnic Institute.

Keyword : natural disaster, damage, fat-tailed distribution, power-law distribution

In order to account for large variance and fat tail of damage by natural disaster, we study a simple model by combining distributions of disaster and population/property with their spatial correlation. We assume fat-tailed or power-law distributions for disaster and population/property exposed to the disaster, and a constant vulnerability for exposed population/property. Our model suggests that the fat tail property of damage can be determined either by that of disaster or by those of population/property depending on which tail is fatter. It is also found that the spatial correlations of population/property can enhance or reduce the variance of damage depending on how fat the tails of population/property are. In case of tornadoes in the United States, we show that the damage does have fat tail property. Our results support that the standard cost-benefit analysis would not be reliable for social investment in vulnerability reduction and disaster prevention.

F12.03

Mobile prisoners' dilemma game with reputation

*김영진, 정선영, 정현우, 손승우 [1]
*Young Jin. Kim, Seon Young. Jeong, Hyunwoo. Jung, Seung-Woo. Son[1]
한양대학교. [1] 한양대학교 ERICA.

Keyword : prisoners' dilemma game, reputation, mobile agents

The origin of altruism is an important issue of psychology and behavioral ecology (economy). Recently Cuesta et al. [Sci. Rep., 5, 7843 (2015)] show that reputation plays a significant role to drive the cooperative state from the experiment among humans. In this study, we investigate the spatial prisoners' dilemma (PD) game with mobile agents having a sort of reputation as global information. Each agent plays the PD game with only the agents in the interaction radius $R_{a,}$ and then updates agents' reputation according to the ratio of the cooperative behavior. While doing the PD game, agents determine whether cooperate or defeat on the basis of the opponent's reputation. From the agent-based model simulation, we found that the cooperative state is promoted at an optimal interaction range determined from the density and mobility of agents.

F12.04

Building Blocks of Synchronization Stability Transition on Power Grid

*김희태, 이상훈 [1], 페터홀메
*Heetae. Kim, Sang Hoon. Lee[1], Petter. Holme
성균관대학교. [1] 고등과학원.

Keyword : sunchronization, basin stability, power grid, complex network

Stable supply of electricity is crucial for secure energy systems in our society. Researchers have utilized various methods in nonlinear dynamics and network science to investigate the stability of electric power systems. For instance, Menck et al. [1] introduced basin stability measuring the stability of the synchronization of a power-grid node. Basin stability is the probability of convergence of a node after a phase perturbation. As the basin stability does not necessarily monotonically increase as the transmission strength varies, the investigation on the entire shape or pattern of basin stability transition is required for comprehensive understanding of the power-grid stability as presented in our previous work [2]. In this study, we systemically analyze such a basin transition pattern, including particularly interesting peak and valley structures. Instead of large networks, where such a level of systematic approach is prohibited due to the sheer size of the system, we focus on small networks that enable us to investigate the transition pattern by exhaustively enumerating every possible configuration. Furthermore, the results from such small networks are meaningful as they are effectively motifs or building blocks of larger networks. We find that the transition shape of basin stability changes sensitively to the network topology and parameter values.

F12.05

About generating general frequency in hamiltonian cube

*이호중
*Ho Joong. LEE
카톨릭대학교.

Keyword : N body, entropy, generating frequency, plasma frequency, hamiltonian cube

I implement mathematical formulation using differential equations for N body in hamiltonian cube creating characteristical general frequencies representing the resolution of the interactions of the N body. Since Poincaré's conclusion that the three body problem represents of chaos in nature, statistical approach develop in to numerous research center and in school. asymptotic solutions, characteristic exponents and the non existence of new single valued integrals. carateristic plasma frequency. Eigenvalues are classified as the form of trajectories. In this context, I discuss a connection between general frequency, entropy and three body problem. The analogy between three body problem and a large number of particles in a single thermodynamics.

F13.01(초)

Nanoscale Ultrafast Dynamics in Materials by X-ray Free Electron Laser

*김현정
*Hyunjung. KIM
서강대학교.

Keyword : XFEL, Ultrafast, dynamics

The recent advent of hard x-ray free electron lasers (XFELs) opens new areas of science due to their exceptional brightness, coherence, and time structure. In principle, such sources enable studies of dynamics of condensed matter systems over times ranging from femtoseconds to seconds. The dynamics can be studied by a technique based on pump-probe method and single shot analysis. In this talk, I review the studies of dynamics with XFELs and present the recent results obtained in LCLS and the perspectives on coherent properties of XFEL in addition to the unique time structures for the future experiments in XFELs.
This research was supported by NRF-2014R1A2A1A10052454 and NRF-2015R1A5A1009962.

F13.02(초)

초고속 현상 관찰을 가능하게 하는 광기반 타이밍 측정제어 기술

*김정원
*
한국과학기술원.

Keyword : 펨토초, 아토초, 자유전자레이저, 초고속전자회절, 타이밍

최근 X-선 자유전자레이저(XFEL)와 초고속전자회절(UED) 장치를 이용하여 펨토초 시간 분해능과 원자 크기 공간 분해능으로 초고속 현상을 관찰하고자 하는 연구가 활발히 진행되고 있다. 이를 위해서는 전자 펄스를 생성하고 펌프 펄스를 제공하는 초고속 레이저들과 전자빔을 제어하는 RF 기반 시스템들 간 타이밍의 정밀한 측정과 제어가 요구된다. 본 발표는 우리 연구팀이 최근 초고속 레이저와 광섬유 광학을 이용하여 개발한 펨토초 정밀도 타이밍 측정제어 기술들과 이들의 국내외 가속기에서의 실제 적용 사례들을 소개하고자 한다.

F13.03(초)

Table-top Ultrafast Microscopy using Compact X-ray Sources

*이경환, 윤혁 [1], 성재희 [2], 이성구 [2], 이황운, 김형택 [2], 남창희 [2]
*Kyoung Hwan. Lee, Hyeok. Yun[1], Jae Hee. Sung[2], Seong Ku. LEE[2], Hwang Woon. Lee, Hyung Taek. KIM[2], Chang Hee. NAM[2]
기초과학연구원. [1]Institute for Basic Science. [2] 광주과학기술원.

Keyword : "Ultrafast microscopy", "X-ray microscopy", "High harmonics", "X-ray laser"

Ultrafast microscopes with nanometer spatial resolution have been developed to visualize ultrafast phenomena occurring in complex nano-structures. To this end, single-shot soft x-ray microscopy, utilizing ultrashort light sources, can be a promising technology, since the single-shot microscopy can offer comparable spatio-temporal resolution set by the wavelength and pulse duration of an x-ray source. While previous works on single-shot x-ray imaging were carried out mostly using large x-ray facilities, such as synchrotron and x-ray free electron laser, the development of compact x-ray sources enabled the single-shot soft x-ray microscopy in a small laboratory. Several imaging approaches, including transmission microscopy using Fresnel zone plates, Fourier transform holography, and coherent diffraction imaging (CDI), have been successfully applied to single-shot imaging using table-top x-ray sources, such as high harmonics and x-ray laser. Although the demonstrations provided microscope images with femto/picosecond temporal resolution, the spatial resolutions remained around 100 nm. Through a detailed analysis of the factors affecting the resolution of single-shot imaging, we could substantially improve the achievable resolution. We present our works on resolution enhanced single-shot soft x-ray imaging performed using a high-harmonic source and a Ni-like Ag x-ray laser.

F15.01(초)

The Remarkable Power of General Relativity

*Gary Horowitz
*Gary Horowitz.
UC Santa Barbara. USA.

Keyword : General relativity, Gauge/gravity duality

This year marks the 100th anniversary of Einstein's discovery of general relativity. This theory has been very successful in reproducing a wide range of gravitational phenomena. I will briefly review this success, and then explain how general relativity can describe other areas of physics as well, including aspects of particle physics and condensed matter physics. This is a result of the gauge/gravity duality that emerged from string theory. I will explain this remarkable development and show how general relativity reproduces properties of QCD and superconductivity.

F15.02(초)

Memorable Event of Gauge, Gravity and String

*이수종
*Soo-Jong. Rey
서울대학교.

Keyword : Christoudou, gauge, gravity, string, memory

How would I know gauge, gravitational or string wave has just passed in front of my nose? In this talk, I first recall the Christodoulou effect for detecting gravitational wave and propose how it can be generalized to electromagnetic and string waves. I then explain that these memory effects are simple consequence of the asymptotic spacetime and internal symmetries in any theories that encompass the diffeomorphism invariance. Extending this line of reasoning, I put forward a proposal for experimentally testing the string theory at low energies and at low budget.

F15.03(초)

Calibrated Geometry and Schroedinger Atoms

*이필진
*Piljin. Yi
고등과학원.

Keyword : Calibrated Geometry, Calabi-Yau Manifold, Wall-Crossing, Supersymmetry, Quantum Bound States

Superstring Theory is naturally formulated in ten spacetime dimensions, rather than four. The invisible six dimensions are expected curled up into small manifold, simplest class of which would be Ricci flat manifolds called Calabi-Yau-3's. The spacetime is still governed by Einstein's general relativity, or its ten-dimensional cousin, in a manner that physics of the visible four dimenisons and geometry of the invisible six dimensions are tighly correlated. This correlation has enormous implications not only for construction of a string theoretical model of our universe, but also for some intrinsical mathematical questions. In this review, we woul like to outline one such example, widely known as the Wall-Crossing problem, where a purely geometrical task of classifying calibrated cycles in Calabi-Yau-3 manifolds translates to finding and counting supersymmetric quantum bound states of certain charge particles living in the four extended dimensions. This can be considered an example of string theory dualities, and again suggests that the string theory framework goes well beyond the earlier goal of providing a unified model of our universe.

G1.01*

Angle-resolved photoemission study on surface-doped black phosphorus

*김지민, 류세희, 손영섭, 김근수
*Jimin. Kim, Sae Hee. Ryu, Yeong Seop. Son, Keun Su. Kim
포항공과대학교. 기초과학연구원 (IBS).

Keyword : APRES, band structure, surface physics, 2D materials, black phosphorus

Black phosphorus is attracting growing interests owing to its promising device characteristics and tunable electronic properties. Black phosphorus consists of phosphorene layers, and interlayer coupling between them results in a thickness-dependent band gap in the range of 0.3 ~ 2.0 eV. Moreover, individual phosphorene layers have characteristic puckered honeycomb structure that is naturally susceptible to external perturbations, such as electric field and strain. In this work, we studied the electronic band structure of black phosphorus, and how it changes upon the deposition of potassium atoms on the surface to induce a vertical electric field. Using angle-resolved photoemission spectroscopy, we could directly observe a widely tunable band gap as a function of electric field controlled by the density of potassium atoms. At the critical dopant density, black phosphorus shows anisotropic dispersion, linear in armchair and quadratic in zigzag directions.

G1.02

Enhanced Rashba-Dresselhaus spin-orbit interaction near the band saddle point in 5d transition metal oxide heterostructures

김민성, *정석범
Minsung Kim. , *Suk Bum Chung.
서울대학교.

Keyword : Rashba-Dresselhaus spin-orbit interaction, perovskite oxide, quantum well band, heterostructure, 5d transition metal

While crystalline systems allow for the Rashba-Dresselhaus spin-orbit interaction not only around the k=0 point but also around other time-reversal invariant momenta in the 1st Brillouin zone, the current studies in the perovskite oxide surface and interface focus exclusively on the band minimum at k=0. In this paper, we calculate the surface band structure of the 5d transition metal oxide heterostructure, e.g. tantalate/hafnate, using the first-principles density functional theory and find an enhanced Rashba-Dresselhaus type spin-orbit interaction around the band saddle points at X = (π,0) and (0,π). These points are readily accessible due to the anisotropy of the t_{2g} orbital dispersion. However, we find that the magnitude of the interaction owes to the contributions from the e_g orbitals.

G1.03*

Chiral orbital angular momentum and subband structures in the (001) surface states of $SrTiO_3$

*솔타니쇼레쉬, 조수현, 유한영 [1], 한가람 [2], 김범영 [3], Timur Kim[4], Moritz Hoesch[4], Cheng-Maw Cheng[5], 김창영 [2]
*SHORESH. SOLTANI, Soohyun. Cho, Hanyoung. Ryo[1], Garam. Han[2], Beomyoung. Kim[3], Timur. Kim[4], Moritz. Hoesch[4], Cheng-Maw. Cheng[5], Changyoung. Kim[2]
연세대학교. IBS-CCES. Seoul National University. [1]IBS-CCES. Seoul National University. Seoul. Korea. [2]IBS-CCES. Seoul National University. [3] 연세대학교. [4]Diamond Light Source. Harwell Campus. [5]National Synchrotron Radiation Research Center.

Keyword : Orbital angular momentum, Chiral, Surface, ARPES, Subband

Angle resolved photoemission spectroscopy performed We (ARPES) measurements on the surface states of $SrTiO_3$ to investigate the existence of orbital angular momentum (OAM) chiral structure. Our results not only show circular dichroism (CD) signal which is an indirect proof for OAM but also reveal new subband structures for out-of-plane orbitals which are not seen in previous studies. Existence of OAM through CD signal could help to explain the origin of surface band splitting and existence of cubic term in the splitting.

G1.04

Giant spin-orbit-induced spin splitting in Bi zigzag chains on GaAs(110)

*김현중, 조준형 [1]
*Hyun-Jung. Kim, Jun Hyung. Cho[1]
고등과학원. [1] 한양대학교.

Keyword : Rashba effect, spin-orbit coupling, Bi zigzag chain, GaAs(110), DFT

The search for one-dimensional electron systems with a giant Rashba-type spin splitting is of importance for the application of spin transport. Here we report [1], based on a first-principles density-functional-theory calculation, that Bi zigzag chains formed on a heterogeneous GaAs(110) surface have a giant spin splitting of surface states. This giant spin splitting is revealed to originate from spin-orbit coupling (SOC) and electric dipole interaction that are significantly enhanced by (i) the asymmetric surface charge distribution due to the strong SOC-induced hybridization of the Bi px , py , and pz orbitals and (ii) the large out-of-plane and in-plane potential gradients generated by two geometrically and electronically inequivalent Bi atoms bonding to Ga and As atoms. The results demonstrate an important implication of the in-plane and out-of-plane asymmetry of the Bi/GaAs(110) interface system in producing the giant spin splitting with the in-plane and out-of-plane spin components.

Ref.
[1] Hyun-Jung Kim and Jun-Hyung Cho, Phys. Rev. B 92, 085303 (2015).

G1.05*

Partial Dislocations and Si Dopants in Graphene: Cooperative Study of Aberration Corrected Transmission Electron Microscopy and Simulation

Sungwoo Lee, Alex W. Robertson[1], Jamie H. Warner[1], Euijoon Yoon, Gun-Do Lee
Sungwoo. Lee, Alex. Robertson[1], Jamie. Warner[1], Euijoon. Yoon, Gun-Do. Lee
Seoul National University. [1]University of Oxford.

Keyword : Graphene, Dislocations, Dopants, Ab initio calculations, Tight-binding molecular dynamics simulations

Recently, we demonstrated the formation of partial dislocations in graphene at elevated temperatures of ≥ 500 °C with single atom resolution aberration corrected transmission electron microscopy (AC-TEM) [1]. The partial dislocations spatially redistribute strain in the lattice, providing an energetically more favorable configuration to the perfect dislocation. Ab initio calculations were performed for various levels of lattice contraction to show that stability of the partial dislocations at high temperature. Low energy migration paths mediated by partial dislocation formation have been observed and ab initio calculations and tight-binding molecular dynamics (TBMD) simulations revealed that its mechanism is a kink migration via a repeating sequence of Stone-Wales (SW) bond rotations. Similar partial dislocation type mechanisms are expected to occur in other two-dimensional materials as well, and so it will be of particular interest to investigate if the migration mechanisms identified here are applicable to other 2D and 3D materials.

We also studied the atomic structure and dynamics of silicon nanoclusters covalently bonded to graphene [2]. Anisotropic crystals are formed due to higher stability of the Si-C bond under electron beam irradiation compared to the Si-Si bond. Dynamics of the anisotropic crystalline Si nanoclusters revealed that they could rotate perpendicular to the graphene plane, with oscillations between the two geometric configurations and ab initio calculations showed that stability and energy barrier of the rotating Si pair. These results are important for understanding structures and dynamics of defects and dopants in graphene and related other 2D and 3D materials.

References

[1] Alex W. Robertson, Gun-Do Lee, Kuang He, Ye Fan, Christopher S. Allen, Sungwoo Lee, Heeyeon Kim, Euijoon Yoon, Haimei Zheng, Angus I. Kirkland, and Jamie H. Warner. Nano Letters DOI: 10.1021/acs.nanolett.5b02080 (2015)
[2] Qu Chen, Ai Leen Koh, Alex W. Robertson, Kuang He, Sungwoo Lee, Euijoon Yoon, Gun-Do Lee, Robert Sinclair, and Jamie H. Warner. ACS Nano DOI: 10.1021/acsnano.5b03476 (2015)

G1.06

Atomic structure of the silicene double layer on Ag(111)-√3x√3: density-functional theory

*권세갑, 강명호
*Se Gab. Kwon, Myung Ho. Kang
포스텍.

Keyword : "Silicene" "Ag(111)" "Atomic structure" "Density functional theroy"

We have performed density functional calculations to theoretically examine a structural model for the Si-deposited Ag(111)-√3x√3 surface proposed by recent experimental studies [1,2]. The model consists of Ag and Si mixed double layer (Figure (a)), contrary to the prevailing idea that the overlayer on Ag(111) is a double-layer silicene (Figure (b)) [3]. The Ag and Si mixed double-layer model is energetically favored over the double-layer silicene model and well reproduces the previously reported STM images showing the hexagonal and honeycomb configurations [4]. Moreover, this √3x√3 mixed double-layer model is energetically unfavored over the well-known single-layer 3x3 model, compatible with an experimental report that the √3x√3 phase appears after completely covered with 3x3 phase, as increasing the Si coverage [5].

[참고문헌]
[1] T Shirai, T. Shirasawa, T. Hirahara, N. Fukui, T. Takahashi, and S. Hasegawa, Phys. Rev. B 89, 241403 (2014).
[2] A. J. Mannix, B. Kiraly, B. L. Fisher, M. C. Hersam, and N. P. Guisinger, ACS Nano 8, 7538 (2014).
[3] Z. X. Guo and A. Oshiyama, Rhys. Rev. B 89, 155418 (2014).
[4] Chen, H. Li, B. Feng, Z. Ding, J. Qiu, P. Cheng, K. Wu, and S. Meng, Phys. Rev. Lett. 110, 085504 (2013).
[5] P. Vogt, P. Capiod, M. Berthe, A. Resta, P. De Padova, T. Bruhn, G. Le Lay, and B. Grandidier, Appl. Phys. Lett. 104, 0216002 (2014).

G1.07*

Study on the high spectral intensity at the Dirac energy of epitaxially grown single-layer graphene on an SiC(0001) substrate.

*황진웅, 황춘규
*Jinwoong. Hwang, Choongyu. Hwang
부산대학교.

Keyword : graphene, Dirac energy

The origin of the high spectral intensity at the Dirac energy of single-layer graphene epitaxially grown on an SiC (0001) substrate has been controversial between in-gap states induced by the buffer layer and electron-plasmon interactions, so-called plasmaron. By using angle-resolved photoemission spectroscopy, we have investigated the origin of the high spectral intensity from the two perspectives of in-gap states and plasmaron. Our work reports that the in-gap states picture well explains the high spectral intensity based on the comparison of the electron band structure of single-layer graphene to that of buffer layer and double-layer graphene. Our work will provide better insight on the mysterious spectral weight at the Dirac energy of the epitaxial single-layer graphene, and stimulate further theoretical and experimental investigations to understand the spectral features in the presence of many-body interactions in graphene.

G2.01

Fermi level control of a Sb_2Te_3 topological insulator by strain

*박상한, 채지민 [1], 정광식 [1], 김태현 [1], 최혜진 [1], 조만호 [1], 배명호 [2], 강철 [3], 권순남
*Sang Han. Park, Jimin. Chae[1], Kwang Sik. Jeong[1], Tae hyeon. Kim[1], Hyejin. Choi[1], Mann-Ho. Cho[1], Myung Ho. Bae[2], Chul. KANG[3], Soonnam. Kwon
포항 가속기 연구소. [1] 연세대학교. [2] 표준과학연구원. [3] 고등광기술연구소.

Keyword : topological insulator, strain, Fermi level, Sb_2Te_3

Many studies of topological insulators have demonstrated their potential for use in a wide variety of devices. However, in order to apply topological insulators to specialized devices, it is necessary to electrochemically modify them. Specifically, chemical doping is one of most common approaches for modifying the properties of topological insulators. Although chemical doping can be a very effective method, modifications of the Fermi level (E_f) using chemical doping are static and irreversible. For electronic devices, the dynamic control of the E_f could be more useful than static doping. Sb_2Te_3, a 3D topological insulator, has a layered structure in which E_f is sensitive to in-plane strain. Because of this it is possible to reversibly control E_f using strain. We showed the modulation of E_f for a Sb_2Te_3 topological insulator. Mechanical substrate bending was used to induce tensile strain in a Sb_2Te_3 film. Sheet resistance was then increased by increasing the strain and vice versa. Based on the temperature dependent resistance and magneto resistance measurements, in-plane strain was found to decrease bulk carrier density while accentuating transport of topological surface state. The changes of Sb_2Te_3 film were optically confirmed in a large area using THz-time domain spectroscopy. The induced strain was confirmed by transmittance X-ray scattering measurements. In addition, density functional theory calculations were conducted to support the E_f shift mechanism from a theoretical point of view. The results show that reversible device control is possible using structural deformation and enabled a clear study of controlling the topological surface state of a material by reducing excessive bulk carriers.

G2.02*

라만 분광법을 이용한 그래핀 소자 산처리 효과의 실시간 분석

김세진, 박세준, 박지용, *안영환
Se-Jin. Kim, Sae June. Park, Ji-Yong. Park, *Yeong Hwan. Ahn
아주대학교.

Keyword : 라만분광학, 그래핀, 도핑

라만 분광법은 탄소 나노 구조체의 특성을 평가하는 주된 측정 법으로 사용되고 있다. 그래핀의 경우, 뚜렷한 D, G, 2D 라만 공명을 확인 할 수 있는데, 특히 단일층 그래핀의 경우 G 공명 대비 상대적으로 강한 2D 공명을 확인 할 수 있다. 이러한 공명들은 격자구조 변화에 강하게 반응하여 도핑 혹은 산화와 같은 그래핀의 물리적, 화학적 변화를 규명하는데 응용된다. 본 연구에서는 실시간 라만 분광법을 이용하여 그래핀의 질산 처리 효과로 인한 D, G, 2D 공명의 변화 과정을 분석하였다. 다양한 농도의 질산을 가했을 경우 나타나는 G, 2D 공명 주파수의 청색 편이과정을 실시간으로 관측하였다. 반면, 그래핀 내의 결함형성과 관련이 깊은 D 공명의 경우 상대적으로 완만한 진폭의 증가 및 적색 편이를 보였다. 이러한 라만 스펙트럼의 변화를 통해 산처리 효과가 야기하는 도핑효과를 정량화 했으며, 그래핀 나노소자의 동작특성과의 상관관계를 연구할 수 있었다. 본 연구는 향후 그래핀을 비롯한 다양한 나노물질 기반 소자를 최적화하는데 중요한 단초를 제공할 것이다.

G2.03*

Large current transport through vertical multi-heterojunction 2D layered materials and active gate-tunable photocurrent generation

Muhammad Farooq Khan, Ghazanfar Nazir, *엄종화
Muhammad Farooq. Khan, Ghazanfar. Nazir, *Jonghwa. Eom
세종대학교 물리학과.

Keyword : 그래핀, MoS_2, 전이금속 칼코겐 화합물, 트랜지스터, electrical transport, photocurrent

The fast vertical field effect transistors of two-dimensional (2D) materials are fascinating devices in electronics field. We report a fast switching and large current modulation through graphene/MoS_2/Mo vertical field effect transistors (VFETs). We fabricated VFETs on h-BN dielectrics, which is almost residue free devices by deep ultraviolet (DUV) light treatment and annealing treatment at 200 ^{o}C in high vacuum (~10^{-6} torr) to clean the graphene-MoS_2 interface. We obtained high (~10^6) ON-OFF current ratios with large current density (~10^5 A/cm^2) through Schottky barrier at graphene-MoS_2 interface. The rapid and significant performance of our vertical devices is attributed to clean interface and compatible top metal contact. Moreover, we investigated the efficient back-gate tuning of photocurrent generation in graphene-based MoS_2 vertical transistors. The approach to simultaneously achieve a high on-off ratio and large current density in vertically stacked 2D multi-heterostructures transistors can boost up the electronics industry.

G2.04*

Comparison of field-effect and Hall mobilities for atomically thin layered materials

Ghazanfar Nazir, Muhammad Farooq Khan, Volodymyr M. Iermolenko, *엄종화
Ghazanfar. Nazir, Muhammad Farooq. Khan, Volodymyr M.. Iermolenko, *Jonghwa. Eom
세종대학교 물리학과.

Keyword : 전이금속 칼코겐 화합물, 이차원 물질, 전하이동도, electrical transport, ohmic contact

Here we report the characteristic of field-effect transistors consists of multilayer (WS_2 or MoS_2) flake using well-known mechanically exfoliation method onto SiO_2/Si substrate. We performed two- and four-probe field-effect and Hall mobility measurements, as well as Raman spectroscopy and atomic force microscopy. Both WS_2 and MoS_2 field-effect transistors appeared to be electron-doped, showing on/off ratios more than 10^6 and 10^4 respectively. Both field-effect and Hall mobilities are in good agreement with previously reported data for multilayer WS_2 and MoS_2 on Si substrates at room temperature without utilizing any kind of dielectric engineering. Raman spectroscopy indicates sharp modes consistent with previous reports which confirm multilayer nature for both WS_2 and MoS_2. We discuss the comparison among two- and four-probe field-effect mobility and Hall mobility for both WS_2 and MoS_2 flakes. The quality of ohmic contacts in WS_2 and MoS_2 field-effect transistors plays an important role to measure mobility in WS_2 and MoS_2 field-effect transistors.

G2.05*

1-D conducting channel induced between inverted band regions in bilayer graphene

*이장희, Kenji Watanabe[1], Takashi Taniguchi[1], 이후종
*Janghee. Lee, Kenji. Watanabe[1], Takashi. Taniguchi[1], Hu-Jong. Lee
포항공과대학교. [1]Advanced Materials Laboratory. NIMS.

Keyword : Graphene, Valleytronics, Mesoscopic system, Topological state, Zero energy state.

Bilayer graphene (BLG), consisting of two layers of graphene with Bernal stacking, has no energy gap between the particle and hole bands. However, the on-site energy difference (U) can be induced between two layers of BLG by applying an external electric field perpendicular to the BLG plane. The U produces a bulk energy gap between the particle and hole bands of low energy states in BLG. Motivated by the tunability of this bulk energy gap, zero energy modes have been predicted in BLG [1]. If directions of the electric fields in two adjacent regions in BLG are opposite, zero energy modes emerge at the interface with chiral nature [2]. To realize these one-dimensional (1-D) chiral modes in BLG, two pairs of aligned split gates with a narrow spacing should be attached to the top and bottom surfaces of a BLG flake while the four gate voltages (two pairs of split gates) can be controlled independently. In this presentation, we introduce a method for fabricating the four split gates attached to a BLG flake, which is sandwiched between two atomically clean hexagonal boron nitride (h-BN) single crystals and thus allows ballistic transport of carriers at least within the device size. Current-voltage characteristics of the BLG flake show large transport gap, which is comparable to the results obtained previously from optical measurements and numerical calculations. Opening the band gap in two adjacent regions of the BLG flake by oppositely gated electric fields, we observed metallic behavior (a few kW) in transport characteristics along the boundary between the two regions although the resistance of two gapped regions are a few hundreds of kW. These results indicate that a 1-D conducting channel formed between the two regions where the induced band gaps were inverted to each other. The formation of this 1-D conducting channel mimics the topological edge conducting channels emerging at the boundary of a two-dimensional topological insulator and may be utilized for applying BLG to valleytronic devices.

[1] I. Martin, Y. M. Blanter, and A. F. Morpurgo, Phys. Rev. Lett. 100, 036804 (2008).
[2] Z. Qiao, J. Jung, Q. Niu, and A. H. MacDonald, Nano Lett. 11, 3453 (2011).

G3.01(초)

Nanoscale graphene oxidized and hydrogenated using AFM lithography

*박배호
*Bae Ho. PARK
건국대학교.

Keyword : 산화 그래핀, 수소화 그래핀, AFM 리쏘그라피, 소자특성, 강자성

단일 원자층 그래핀은 독특한 전도 특성으로 인해 차세대 전자 소자용 신소재로 많은 관심을 받고 있다. 그래핀 기반 소자의 실현을 위해서는 그래핀에 적절한 크기의 band gap 을 유도할 수 있는 방법과 나노크기의 리쏘그라피 방법이 확보되어야 한다. 나노크기의 수소화 및 산소화는 그래핀의 표면 구조를 변화시켜 band gap 을 유도할 수 있는 방법인 동시에 그래핀 나노리본과 같은 나노구조를 제작할 수 있는 방법이다. 지금까지 그래핀 수소화는 대면적 화학적 변형, 나노구조 패터닝, 에칭으로 구성된 복잡한 공정을 거쳐야 했기 때문에, 수소화 그래핀 및 산화 그래핀으로 구성된 나노크기의 소자를 형성하는 것이 쉽지 않았다.
이번 발표에서는 AFM 리쏘그라피 방법을 통해서 인가하는 외부 전압을 조절함으로써 에칭, 습식 공정, 가스 처리 등의 추가 공정 없이 상온, 상압에서 그래핀의 나노크기 영역을 수소화 혹은 산화시키는 방법을 소개하고자 한다. AFM 리쏘그라피 방법을 사용해서 인가 전압 제어만으로 그래핀의 나노크기 기능화 및 선택적 작용기 흡착을 조절할 수 있으며 이렇게 흡착된 작용기들은 적절한 열처리를 통해 대부분 제거가 가능하다. 우리는 또한 AFM 리쏘그라피 방법으로 형성한 나노크기 산화 그래핀을 기반으로 한 소자구조도 제작하고 특성을 확인했다. 자기력 현미경 측정을 통해 나노크기의 수소화 및 산화된 그래핀이 상온에서 강자성을 가질 수 있음도 확인하였다.

G3.02*

Temperature evolution of the optical conductivity in heavy fermion compound Ce2IrIn8: a first-principles dynamical mean field theory approach

*김재녕, 최홍철 [1], Kristjan Haule[2], Gabriel Kotliar[2], 심지훈
*Jae Nyeong. Kim, Hong-chul. Choi[1], Kristjan. Haule[2], Gabriel. Kotliar[2], Ji Hoon. Shim
POSTECH. [1]Los Alamos National Laboratory. [2]Rutgers University.

Keyword : Heavy Fermion, Density Functional Theory, Dynamical Mean Feld Theory, Optical conductivity

We have investigated the temperature evolution of the spectral function, optical conductivity and resistivity of heavy fermion compound Ce2IrIn8 by using the density functional theory and dynamical mean field theory (DFT+DMFT). In the formation of heavy fermion, there are three important factors: carrier concentration, effective mass, and scattering rate. In the previous work (H. C. Choi, et al. PRL 108, 016402 (2012)) on dHvA analysis, we revealed that the change of carrier concentration, which corresponds to the FS area, show a crossover around local Kondo temperature (T_K). Although the f electrons are still incoherent around T_K, they contribute to the conduction bands near the Fermi level, so the number of carrier increases below T_K. We also showed that the effective mass and the scattering rate of conduction carriers are shown to be clearly changed around coherence temperature (T*), where the f electrons become coherent. In this work, we have performed similar analysis for heavy fermionic Drude peak structure below T*. For better description of low temperature peak structure in optical conductivity, we have employed crystalline electric field (CEF) basis. Resulting peak positions of the optical conductivity shows good agreement with the size of CEF splitting. The optical conductivity have been more analyzed from the temperature dependent band structures. We suggest that measurement of the optical conductivity and its analysis on the effective mass and scattering rate will be a reasonable way to estimate T*.

G3.03*

Effects of Spin-Orbit Coupling in Dirac Mott-Insulating 2D Ising Ferromagnetic $BaFe_2(PO_4)_2$

송영준, W. E. Pickett[1], *이관우 [2]
Young-Joon. Song, Warren. Pickett[1], *Kwan-Woo. Lee[2]
고려대학교 세종캠퍼스. [1]Univ. of California. Davis. [2]CA.

Keyword : $BaFe_2(PO_4)_2$, Ising ferromagnet, Spin-orbit coupling, J_{eff}=3 Dirac Mott insulator, first principles calculations

Recently, Montre and coworkers have synthesized a quasi-2 dimensional Fe honeycomb lattice $BaFe_2(PO_4)_2$, which is suggested as the first 2-dimensional Ising ferromagnetic(FM) oxide with T_C~65 K.[1,2] The observed Curie-Weiss and saturated moments are 6.16 and 5 (in units of μ_B/Fe), respectively, indicating a large orbital contribution. Additionally, this system shows a very rare re-entrant structure transition, R-3 at room T→ P-1 at T=135K → R-3 at T = 75K.
Throughout density functional theory based calculations, including both correlation (U) and SOC effects, we investigate the electronic and magnetic structures of the ground FM state. A large exchange splitting of 3 eV leads to an effective minority d^1 configuration for this high spin ($t_{2g}^{3\uparrow,1\downarrow}$, $e_g^{2\uparrow}$) S = 2 Fe^{2+} system. Interestingly, when neglecting SOC, a Dirac point appears at the Fermi level in the spin-down channel, leading to a Dirac half-semimetallic state. Inclusion of pure correlation effects fails to obtain the observed insulating state. Although the strength of SOC is tiny in this 3d system, SOC lowers the degeneracy of the Dirac point and inclusion of both SOC and correlation results in a Mott insulating state with a large orbital moment of 0.7 μ_B (corresponding to essentially L=1) . We obtained a large magnetocrystalline anisotropy, consistent with the Ising character. In this presentation, we will address on the mechanism of the semimetal to insulator transition and the large orbital moment. Besides, we will discuss the unique re-entrant structure transition.

Acknowledgements: This research was supported by NRF-2013R1A1A2A10008946.

[1] H. Kabbour, R. David, A. Pautrat, H.-J. Koo, M.-H. Whangbo, G. Andre, and O. Mentre, Angew. Chem. Int. Ed. 51, 11745(2012)
[2] R. David, A. Pautrat, D. filimonov, H. Kabbour, H. Verin, M.-H. whangbo, and O. Mentre, J. Am. Chem. SOC. 135, 13023(2013)
[3] Y.-J. Song, K.-W. Lee, and W. E. Pickett, Phys. Rev. B (in press).

G3.04*

Nature of the Insulating Ground State of the 5d Postperovskite $CaIrO_3$

*김선우, 김현중 [1], 이준호 [1], 조준형
*Sun-Woo. Kim, Hyun-Jung. Kim[1], Jun-Ho. Lee[1], Jun-Hyung. Cho
한양대학교. [1] 고등과학원.

Keyword : $CaIrO_3$, Mott insulator, Slater insulator, Spin-Orbit Coupling, DFT+DMFT

The insulating ground state of the 5d transition metal oxide $CaIrO_3$ has been classified as a Mott-type insulator. Based on a systematic density functional theory (DFT) study with local, semilocal, and hybrid exchange-correlation functionals, we reveal that the Ir t_{2g} states exhibit large splittings and one-dimensional electronic states along the c axis due to a tetragonal crystal field. Our hybrid DFT calculation adequately describes the antiferromagnetic (AFM) order along the c direction via a superexchange interaction between Ir^{4+} spins. Furthermore, the spin-orbit coupling (SOC) hybridizes the t_{2g} states to open an insulating gap. These results indicate that $CaIrO_3$ can be represented as a spin-orbit Slater insulator, diven by the interplay between a long-range AFM order and the SOC. Such a Slater mechanism for the gap fomation is also demonstrated by the DFT + dynamical mean field theory calculation, where the metal-insulator transition and the paramagnetic to AFM phase transition are concomitant with each other.

G3.05*

Electrical rotation of antiferromagnetic easy axis around strain-driven morphotropic phase boundary of lanthanum doped bismuth ferrite thin films

*이진홍, 김광은, 장병권, Ahmet A. Unal[1], Sergio Valencia[1], Florian Kronast[1], 고경태 [2], Stefan Kowarik[3], Jan Seidel[4], 양찬호
*Jin Hong. Lee, Kwang-Eun. Kim, Byung-Kweon. Jang, Ahmet. Ünal[1], Sergio. Valencia[1], Florian. Kronast[1], Kyung-Tae. Ko[2], Stefan. Kowarik[3], Jan. Seidel[4], Chan-Ho. Yang
KAIST. [1]Helmholtz Zentrum Berlin. [2]Max Planck Institute for Chemical Physics of Solids. [3]Humboldt-Universität zu Berlin. [4]University of New South Wales.

Keyword : Multiferroic, La doped $BiFeO_3$, Strain-driven morphotropic phase boundary, Antiferromagnetism, Photoemission electron microscope

Bismuth ferrite (a_{pc} ~ 3.965 Å), $BiFeO_3$ (BFO), is one of few multiferroic materials which exhibit both ferroelectricity and magnetism at room temperature. The stream of BFO research has entered a new era after a discovery of the metastable tetragonal-like BFO (T-BFO) which can be stabilized in compressive-strained BFO thin films. Especially, the strain-driven morphotropic phase boundary (MPB) between two distinctive phases of BFO, i.e., T-BFO and rhombohedral-like monoclinic BFO (R-BFO), has been observed in strain-relaxed BFO thin films on $LaAlO_3$ (a_{pc} ~ 3.789 Å) substrates. The MPB has brought a variety of interesting phenomena such as colossal electromechanical response, enhanced magnetic moment, and electronic conductivity. The controllability of MPB patterns also has been demonstrated via electrical and mechanical switching. Recently, it has been reported that the curved MPB patterns of pure BFO thin films can be straightened by La 5% doping, and the straight MPB patterns of La 5% doped BFO can become tens of microns long and its alignment direction can be rotated through the atomic force microscope tip-based electrical formation [1]. The long-and-straight MPB patterns in La 5% doped BFO thin films provide a better test-bed for studying the electronic and spin structure of MPB as compared with the curved MPB patterns of pure BFO which display more complex strains around MPBs.

In this presentation, we report on the experimental results of photoemission electron microscope measurements around the electrically aligned MPB patterns in a La 5% doped BFO thin film. By analyzing the azimuthal-angle-dependent x-ray absorption spectra near Fe L-edge and O K-edge energy, we argue about the correlation between the spin structure, e.g., antiferromagnetic easy axis, and the alignment direction of spatially uniform MPB patterns. The configuration interaction model calculations including the full atomic multiplets and crystal field splitting are provided to investigate the antiferromagnetic easy axis of the straight MPB pattern.

[1] K.-E. Kim et al., NPG Asia Mater. 6, e81 (2014).

G4.01(초)

Nonequilibrium Fluctuations for a Single-Particle Analog of Gas in a Soft Wall

*박혁규, 이동윤 [1], 권철안 [2]
*Hyuk Kyu. Pak, Dong Yun. Lee[1], Chulan. Kwon[2]
울산과학기술대학교. [1]IBS Center for Soft and Living Matter. [2] 명지대학교.

Keyword : nonequilibrium, fluctuations, optical tweezers, harmonic potential

We investigate the motion of a colloidal particle driven out of equilibrium by a time-varying stiffness of the optical trap that produces persistent nonequilibrium work. Measurements of work production for repeated cycles composed of the compression and expansion processes for the optical potential show huge fluctuations due to thermal motion. Using a precise technique to modulate the stiffness in time, we accurately estimate the probability distributions of work produced for the compression and expansion processes.We confirm the fluctuation theorem from the ratio of the two distributions.We also show that the average values of work for the two processes comply with the Jarzynski equality. This system has an analogy with a gas in a breathing soft wall. We discuss about its applicability to a heat engine and an information engine operated by feedback control.

G4.02

Decoding dynamic heterogeneity in single molecule data

*황원석, 이일범 [1], 홍석철 [1], 현창봉
*Wonseok. Hwang, Il Buem. Lee[1], Seok Cheol. Hong[1], Changbong. Hyeon
고등과학원. [1] 고려대학교.

Keyword : dynamic disorder, heterogeneity, H-DNA, single molecule, smFRET

Single molecule time trajectories of biomolecules provide glimpses into complex folding landscapes which are dicult to visualize using conventional ensemble experiments. Recent single molecule data and theoretical analysis have highlighted static or dynamic heterogeneity, a hallmark
of rugged energy landscapes, in certain classes of biomolecules. Although data suggestive of molecular heterogeneities from single molecule measurements have recently increased, a systematic method for analyzing such data is currently missing. Here we report a new method to analyze single molecule time trajectories with dynamic heterogeneity such that kinetics of conformational transitions varies along the time due to a slowly changing hidden internal state of the molecule. Our method can detect, if any, the presence of dynamic heterogeneity in each trajectory, identify how many internal states are mixed in the individual trajectories, and enable us to estimate interconversion rates between internal states as well as the kinetic rates of conformational dynamics of each internal state. Finally, we applied our method to analyze single molecule data of H-DNA whose duplex-triplex transitions exhibit dynamic heterogeneity.

G4.03

Dynamic release of bending energy in short double-stranded DNA by two types of deformation

*김철희, 이오철, 김재열 [1], 성우경, 이남기
*Cheolhee. Kim, O chul. Lee, Jae-Yeol. Kim[1], Wokyung. SUNG, Nam Ki. Lee
포항공과대학교. [1]National Institutes of Health.

Keyword : DNA bending, single-molecule, FRET, fork, kink

Bending with high curvature is one of the major mechanical properties of double-stranded DNA (dsDNA) which is critical to its biological functions. The emergence of a kink due to local melting in the middle of dsDNA has been suggested as a mechanism of releasing the energy cost of bending. Here, we report that strong bending induces two types of short dsDNA deformations, induced by two types of local melting, i.e., a kink in the middle and forks at the ends, which we demonstrate using D-shaped DNA nanostructures. The two types of deformed dsDNA structures dynamically interconvert with each other on a millisecond scale. The transition from a fork to a kink is dominated by entropic contribution (anti-Arrhenius behavior), while the transition from a kink to a fork is dominated by enthalpy contribution. The presence of mismatches in dsDNA accelerates kink formation, and the transition from a kink to a fork is removed when the mismatch size is three base pairs

G4.04

Mapping the energy landscape for second stage folding of a single membrane protein

민두영, Robert E. Jefferson[1], *김현우 [2], James U. Bowie[1], 윤태영
Duyoung. Min, Robert E.. Jefferson[1], *HyunWoo. Kim[2], James. Bowie[1], Tae-Young. Yoon
KAIST. [1]University of California. Los Angeles. [2] 한국과학기술원 (KAIST).

Keyword : Membrane protein, GlpG, Magnetic tweezers, energy landscape

Membrane proteins are designed to fold and function in a lipid membrane, yet folding experiments within a native membrane environment are challenging to design. Here we show that single molecule forced unfolding experiments can be adapted to study helical membrane protein folding under native-like bicelle conditions. Applying force using magnetic tweezers, we find that the unfolding of a transmembrane helix protein, the rhomboid protease GlpG, is highly cooperative, largely unraveling as one physical unit in response to mechanical tension above 25 pN. Considerable hysteresis is observed, with refolding occurring only at forces below 5 pN. Characterizing the energy landscape reveals only modest thermodynamic stability (DG = 6.5 k_BT) but a large unfolding barrier (21.3 k_BT) that can maintain the protein in a folded state for long periods of time ($t_{1/2}$ ~3.5 hrs). The observed energy landscape may have evolved to limit the existence of troublesome partially unfolded states and impart rigidity to the structure.

G4.05*

smFRET analysis of Nucleosome remodeling by CHD1

*곽재원, 홍성철
*Jaewon. Kirk, Sungchul. Hohng
서울대학교.

Keyword : Nucleosome, Chromatin, CHD1, Chromatin remodeling

Nucleosome is unit of DNA package in eukaryotes, contains 147bp of DNA and histone octamer. These nucleosomes allow DNA to form chromatin by making successive higher-order structure, and nucleosome itself or these higher-order structures provide regulatory function of gene expression. This gene expression control, or transcription regulation is achived by chromatin remodeling which is done by a set of enzymes, chromatin remodellers. These enzymes form/deform, or translocate nucleosomes to hide/reveal certain DNA region, and related to regulation of chromatin structure.

helicase-DNA-binding protein 1 (CHD1) is one of chromatin remodeller, and well conserved in eukaryotes including human. CHD1 regulates nucleosome dynamics and it is especially important in transcription regulation, since CHD1 is known to be a component of transcription elongation complex.

single molecule Fluorescent Resonance Enegy Transfer (smFRET) assay allows direct, real-time observation of molecular dynamics. Using this technique, we observed interaction of single nucleosome and CHD1 in vitro. From this assay, we revealed characteristic behavior of nucleosome remodeling induced by ATP binding/hydrolysis of CHD1.

G5.01(초)

High-resolution magnetic soft x-ray microscopy of nanoscale spin phenomena

*M.-Y. Im, K.-S. Lee[1], P. Fischer, J.-I. Hong[2], Weilun Chao
*M.-Y.. Im, K.-S.. Lee[1], P.. Fischer, J.-I.. Hong[2], Weilun. Chao
Lawrence Berkeley National Laboratory. [1]Ulsan National Institute of Science and Technology. [2]Daegu Gyeongbuk Institute of Science and Technology.

Keyword : High-resolution magnetic soft x-ray microscopy, vortex core, stochastic

Understanding of spin phenomena at the nanometer length scale is not only scientifically intriguing but also technologically of highest relevant. Magnetic transmission soft X-ray microscopy (MTXM) with a high lateral resolution down to 20 nm provided by Fresnel zone plate optics [1] allows to study on spin phenomena in magnetic nanostructures.
We tackled some critical issues in spin phenomena such as asymmetry and stochasticity by direct imaging of in-plane (circularity) and out-of-plane (polarity) magnetic structures in vortex system utilizing soft x-ray microscopy (BL6.1.2 at ALS)[2]. We observed a symmetry breaking and a stochastic behavior in the formation process of vortex structures in circular and asymmetric shaped permalloy ($Ni_{80}Fe_{20}$) disks, respectively. It was interpreted that the symmetry breaking in circular disks is possibly triggered by “intrinsic” Dzyaloshinskii-Moriya interaction (DMI) and “extrinsic” factors such as roughness and defects [3]. In the study of stochastic behavior, we found that the dynamics at the initial stages of vortex formation, which has a character of chaos such as the Butterfly effect, plays a dominating role for the stochastic nature observed at steady state in asymmetric disks [4]. From extended stocasticity study we provided the possibility for the reliable and complete control of vortex structure, both circularity and polarity, in asymmetrically shaped magnetic disk [5].
Furthermore, we firstly observed field (pulse)-driven motions of nontrivially deformed vortex core formed in 100 nm thick Py disks with a flat edge [6]. Depending whether the vortex core includes Bloch-point or not, the static and dynamical behaviors of the core were significantly changed.
This work is supported by BES MSD DOE Contract No. DE-AC02-05-CH11231. This research was also supported by Leading Foreign Research Institute Recruitment Program through the National Research Foundation (NRF) of Korea funded by the Ministry of Education, Science and Technology (MEST) (2012K1A4A3053565).
[1] W. Chao, B. H. Harteneck, J. A. Liddle, E. H. Anderson, D. T. Attwood, Nature 435, 1210 (2005).
[2] P. Fischer et al., Materials Today 9, 26 (2006).
[3] M.-Y. Im et al., Nature Communications 3, 1978 (2012).
[4] M.-Y. Im et al., Nature Communications 5, 5620 (2014).
[5] M.-Y. Im et al., will be submitted (2015).
[6] M.-Y. Im et al., will be submitted (2015).

G5.02(초)

Materials with large MCA and design principles of large MCA

*임성현, 홍순철
*Sonny. Rhim, Soon-Cheol. Hong
울산대학교.

Keyword : density functional theory, MCA, magnetism, spin-orbit interaction, Dzyaloshinskii-Moriya

With advances and interests in spintronics, materials with large magnetocrystalline anisotropy (MCA) have become highly attractive. We review here recent studies on MCA, on Fe/MgO and Fe layer with transition metal capping using first-principles calculations.. While d-d hybridization between Fe and transition metals enlarges spin-orbit matrix, the large MCA found in Fe/MgO can be attributed to perfect epitaxy of the interface rather than widely accepted hybridization between Fe and O. Furthermore, design principles of MCA will be presented relying on the irreducible representation of crystal symmetry. Some other spin-orbit related phenomena, Dzyaloshinskii-Moriya interaction, are discussed within scheme of density functional theory.

G5.03(초)

Direct terahertz probes of Mott conductivity in metals and fundamental observation of GMR.

*D. Turchinovich, Z. Jin[1], A. Tkach, F. Casper, V. Spetter[2], H. Grimm[2], A. Thomas, T. Kampfrath[3], M. Bonn[1], M. Kläui
*D.. Turchinovich, Z.. Jin[1], A.. Tkach, F.. Casper, V.. Spetter[2], H.. Grimm[2], A.. Thomas, T.. Kampfrath[3], M.. Bonn[1], M.. Kläui
Johannes-Gutenberg-Universitaet Mainz. [1]Max Planck Institute for Polymer Research. [2]Sensitec GmbH. [3]6Fritz Haber Institute of the Max Planck Society.

Keyword : Giant magnetoresistance (GMR), Terahertz electromagnetic probes, Mott model

The spin-dependent conduction in metals, explained by Sir Nevill Mott as early as in 1936, underlies all modern magnetic memory technologies such as giant magnetoresistance (GMR). In Mott's picture, the current in ferromagnetic transition metals is carried by non-mixing populations of majority- and minority-spin sp-band Fermi-level electrons, experiencing the spin-dependent momentum scattering with localized electrons originating from the spin-split d-band. Yet the direct observation of magneto-transport under such fundamental conditions has remained a challenge, as it requires a non-perturbative magneto-transport measurement performed on an elementary, sub-100 femtosecond timescale defined by electron momentum scattering dynamics in metals. Here, using terahertz electromagnetic probes, we directly observe the magneto-transport in a metallic system under the fundamental conditions of Mott model, and unambigously determine its parameters: the spin-dependent densities and momentum scattering times of conducting electrons. In particular, we find that traditional measurements in fact significantly underestimate the spin-asymmetry in electron scattering, a key parameter responsible for effects such as GMR. We furthermore demonstrate the possibility of magnetic modulation of terahertz waves, and heat- and contact-free GMR readout with ultrafast terahertz signals.

G5.04(초)

Determination of the interfacial Dzyaloshinskii-Moriya interaction energy density in the inversion symmetry broken systems

Chun-Yeol You, Jaehun Cho, Nam-Hui Kim, June-Seo Kim[1], Reinoud Lavrijsen[1], Aurelie Solignac[1], Yuxiang Yin[1], Dong-Soo Han[1], Niels J. J. van Hoof[1], Henk J. M. Swagten[1], Bert Koopmans[1]
Chun-Yeol. You, Jaehun. Cho, Nam-Hui. Kim, June-Seo. Kim[1], Reinoud. Lavrijsen[1], Aurelie. Solignac[1], Yuxiang. Yin[1], Dong-Soo. Han[1], Niels. van Hoof[1], Henk. Swagten[1], Bert. Koopmans[1]
Inha University. [1]Eindhoven University of Technology.

Keyword : "The interfacial Dzyaloshinskii-Moriya interaction, Brillouin light scattering"

We determined the interfacial Dzyaloshinskii-Moriya (iDM) energy density by using Brillouin Light Scattering (BLS). Since BLS measurement provides Stokes and anti-Stokes spin waves, corresponding to propagation spin wave vectors, simultaneously, the frequency difference, , can be obtained, where finite is a finger point of the iDM [2]. We performed three different measurements (1) as a function of the external field, (2) as a function of the angle between spin wave propagation direction, and (3) spin wave dispersion relations as shown in Fig. 1 (a)~(c). Based those three independent measurements, we can successfully rule out other possible sources of in our experiments, and determine iDM energy density precisely. By virtue of local probing nature of BLS, we investigated the thickness dependent iDM in Pt/Co(t_{Co})/AlO_x and Pt/CoFeB(t_{CoFeB})/AlO_x wedge samples. In order to extract iDM energy density from the , the only additional necessary physical quantity is the saturation magnetization , and it can be determined in the BLS measurement, which is one of the strong advantages of the BLS measurement compared to other methods. The maximum iDM energy densities are 1.2 mJ/m^2 for 1-nm thick Co and 0.7 mJ/m^2 for 1.6-nm thick CoFeB samples. Furthermore, we found the inverse proportionality of iDM energy density to the t_{Co} and t_{CoFeB}, it implies the measured iDM in our system is true interfacial term.

[1] Jaehun Cho et al. http://arxiv.org/abs/1505.05965 (accepted in Nat. Comm.)
[2] J. H. Moon et al. Phys. Rev. B 88, 184404 (2013).

G6.01*

High thermoelectric figure-of-merit in Sb_2Te_3/Ag_2Te bulk composites as Pb-free p-type thermoelectric materials

*이민호, 김가령, 이종수
*MIn Ho. Lee, KaRyeong. Kim, Jong-Soo. Rhyee
경희대학교.

Keyword : Thermoelectric, Topological insulator, Thermal conductivity, Lattice thermal conductivity, composites

We investigated thermoelectric properties of the Sb_2Te_3/Ag_2Te (ST/AT) composites with molar ratios of ST/AT = 1/1, 2/1, 4/1, 8/1, 16/1, and 32/1. The extrinsic composites, synthesized by wet ball milling of two separate powders of Sb_2Te_3 and Ag_2Te, are differentiated with intrinsic composites by high temperature phase separation in that it is low temperature synthesis process. The thermoelectric properties of the composites show systematic behaviour of decreased electrical and thermal conductivities with increasing Ag_2Te dispersion concentration. The ST/AT = 1/1 composite exhibits extremely low lattice thermal conductivity with high power factor over a wide temperature range, resulting in high ZT value 1.5 at 700 K, which is the significantly enhanced value of ZT compared with other Pb-free p-type chalcogenide thermoelectric materials.

G6.02

음이온 치환 도핑을 통한 이차원 층상구조 소재의 금속전도 전이현상

*이기문
*Kimoon. Lee
군산대학교.

Keyword : "이차원 물질 (2D materials)", "금속 전도 (metallic conduction)", "치환형 도핑 (interstitial doping)"

Graphene 의 발견 이후, 이차원 물성을 발현할 수 있는 이차원 층상구조 물질계에 대한 연구가 활발히 이뤄지고 있다. 실질적인 전자 소재로의 응용을 위해서는, 기존의 Si 소재에서 그러했듯이, 화학적인 도핑을 통한 전도도 제어 기술의 확보가 절실하나, 현재까지의 이차원 전자 소재군의 경우 화학적인 치환형 도핑을 통해 반도체에서 금속성까지 전도성을 제어한 연구가 부재한 실정이다. 본 연구에서는 이차원 층상구조 화합물인 $SnSe_2$ 소재의 음이온 치환 도핑을 통한 반도체에서 금속 전도로의 전이 현상을 보고한다. Cl 원소의 Se-site 의 안정적인 치환형 도핑을 통해 $SnSe_2$ 반도체 소재의 전하농도를 10^{20} cm^{-3} 까지 향상시킬 수 있었으며, ~10^{19} cm^{-3} 을 기점으로 반도체 전도에서 금속 전도로의 전이가 일어남을 확인하였다. 기존의 전이금속 화합물과 달리 금속 전도가 쉽게 일어나는 원리를 제일원리 계산을 통해 고찰하였다.

G6.03

Thermoelectric, thermodynamic, and structural properties in $Cu_{1.94}A_{0.02}Se$ (A =Al, Ga, and In) polycrystalline compounds

*김진희, 오수경, 김민재, 이종수, 안도천 [1], 박수동 [2]
*Jin hee. Kim, Sue kyung. Oh, Min jae. Kim, Jong-Soo. Rhyee, Do cheon. Ahn[1], Su-Dong. Park[2]
경희대학교. [1] *포항공대 가속기연구소.* [2] *한국전기연구원.*

Keyword : thermoelectric, Cu2Se, thermal stability, structure phase transition

We investigated thermoelectric and thermal stability properties of the cation doped polycrystalline compounds of $Cu_{1.94}A_{0.02}Se$ (A = Al, Ga, and In). The thermoelectric properties of the doped compounds are inferior to the reported Al-doped compound $Cu_{1.94}Al_{0.02}Se$. The maximum ZT value of In-doped sample (0.8 at 973 K) is also still lower than the previous Al-doped one (1.0 along the layer plane and 1.5 along the inter-layer plane at 973 K). The thermo-gravimetric analysis (TGA) showed that the dissociation temperature of the doped compounds significantly enhanced comparing with parent compound $Cu_{2-x}Se$, indicating the enhancement of thermal stability by cation doping. The enhancement of thermodynamic stability might be related with hybridization of cation element with Se. However, the thermal hysteresis behavior upon heating to 90 ℃ and cooling to room temperature with 0.28 % reduction of lattice volume indicates that the Se evaporation during thermal cycling cannot be resolved completely in spite of the enhancement of thermal stability by cation doping.

G6.04*

나노초 열반사율 시스템을 이용한 온도에 따른 V_2O_5 박막의 열확산도 측정

김태성, 박현우, 강만일, *김석원, 이상현 [1]
Taesueng Kim. , Hyungwoo Park. , Manil Kang. , *KIM Sok Won. , Sang Hyun Lee. [1]
울산대학교. [1] *한국표준과학연구원.*

Keyword : V_2O_5, 열확산도, 나노초 열반사율

오산화바나듐(V_2O_5)은 우수한 열적, 화학적, 전기적 특성에 의해 화학 센서, 측온 및 열 감지 영상 센서 등에 활용되고 있다. 이러한 V_2O_5 는 다양한 바나듐산화물 중 가장 안정하며, 스퍼터링법을 이용해서 박막으로 성장시 ~500℃의 기판온도에서 사방정계 구조(orthorhombic structure)로 결정화된다. 결정화된 V_2O_5 박막은 260℃ 근처의 온도에서 금속-절연체 전이(MIT; metal-insulator transition)를 보인다.
본 연구에서는 전이온도 근처에서의 V_2O_5 박막의 열확산도를 측정하기 위해 Nd:YAG 레이저 기반의 후면가열-전면측정 방법의 나노초 열반사율 장치를 구성하였고, 이를 이용하여 300-680K 의 온도범위에서 V2O5 박막의 열확산도를 측정하였다. 나노초 열반사율법은 나노초 펄스에 의해 발생한 박막에서의 열에 의한 반사율 변화를 매우 빠르게 측정하기 때문에 박막의 열물성 측정에 아주 유용한 방법이다. V_2O_5 박막의 열확산도는 Cape-Lehman 의 열확산 방정식을 이용한 열반사율 신호의 분석을 통해 얻었으며, 얻어진 결과를 통해 상전이 구간에서의 V_2O_5 박막의 열물성의 온도의존성에 대해 논하였다.

00507 – No-show

[No-show]Electronic structures and optical properties of α-$BiFeO_3$: an ab-initio study

*Ishrat Naz, AHMAD FAYYAZ, 장재경, 이주열 [1]
*Ishrat. Naz, FAYYAZ. AHMAD, Jae Kyung. JANG, Joo Yull. RHEE[1]
물리학과/성균관대학교. [1] *성균관대학교.*

Keyword : "α-$BiFeO_3$", "mBJ", "Ab initio", "optical"

By means of density-functional-theory the electronic structure and optical properties of multiferroic bismuth ferrite α-$BiFeO_3$ are investigated by using the so-called GGA+U and modified Becke-Johnson (mBJ) methods for the exchange-correlation functional. The modified Becke-Johnson potential (mBJ) shows that α-$BiFeO_3$ has a direct band gap of 2.43 eV is in good agreement with experiment (2.5 eV), while the GGA+U method bears 2.37 eV. The density of states predicted that the valence band was mainly composed with Fe 3d, O 2p states. We find a close accordance between experiment and calculated results with mBJ including dielectric function, absorption spectra, refractive index, extinction coefficient, energy-loss spectrum and reflectivity.

G6.05*

자기장 각도와 세기 조절을 통한 자기 Bubblecade 속력 최적화

*김덕호, 문경웅 [1], 유상철, 김대연, 민병철 [2], 황찬용 [1], 최석봉
*Duck-Ho. Kim, Moon. Kyoung-Woong. [1], Yoo Sang Cheol. , Dae-Yun Kim. , MIN Byoung Chul. [2], HWANG Chanyong. [1], Sug-Bong Choe.
서울대학교. [1] 한국표준과학연구원. [2] 한국과학기술연구원.

Keyword : 자기 Bubblecade 메모리, 속력 최적화, 교류 자기장, Creep, 광자기 Kerr 현미경

자구벽(domain wall)을 한쪽 방향으로 동시에 이동시키는 방법은 차세대 메모리와 논리 소자 적용에 중요한 요소이다. 이를 위해, 나노선에 전류 주입[1]과 복잡한 구조를 이용한 DW 의 포텐셜에너지 조절[2]과 교류자기장[3] 등 여러 가지 방법들이 제안되었고, 이를 바탕으로 많은 연구가 활발히 수행되어 왔다. 이 중 교류 자기장을 이용하여, 2 차원 면적에서 bubble domain 을 같은 모양을 한쪽 방향으로 움직이는 "자기 Bubblecade 메모리"가 최근에 제안되고, 실험적으로 입증이 되었다[3]. 메모리 소자는 빠른 속력으로 구동하는 것이 중요한데, Bubblecade 메모리에서는 자기장 세기 H 와 자기장의 기울인 각도 θ 에 의해 속력 v 이 결정된다. 본 연구에서는 H 와 θ 가 v 에 미치는 영향에 대하여 살펴보았다. 본 연구를 위해 Pt(2.5 nm)/Co(0.3 nm)/Pt(1.0 nm) 수직 자기 이방성 박막을 준비하였고, 광자기 Kerr 현미경(magneto-optical Kerr microscope)을 이용해 자구벽 속력을 측정하였다. 그림 1 는 다양한 H 에서 θ 에 따른 v 변화를 보여주고 있다. 여기에서 v 는 특정 임계각도 θ_c 에서 최대값을 보여주고 있다. 특히, 이 임계각도 θ_c 는 H 에 따라 달라진다. 이 현상을 이해하기 위해서 Creep 이론을 이용하여 분석하였더니, θ_c 는 H 에 대한 관계식을 얻어, 본 현상에 대한 이해를 할 수 있었다. 본 연구는 특정 자기장에서 각도 최적화를 통해 자기 Bubblecade 메모리 소자 구동 속력을 최적화하여, 차세대 메모리 소자 연구에 도움이 될 것으로 생각된다.

참고문헌

[1] S. S. P. Parkin, M. Hayashi, and L. Thomas, Science 320, 190 (2008).
[2] D. A. Allwood et al., Science 309, 1688 (2005).
[3] K.-W. Moon, et al., Sci. Rep. 5, 9166; DOI:10.1038/srep09166 (2015).

G6.06*

The physical properties change of sputtered film via working pressure manipulation

*김동석, 김지민, 김범진, 장영재, 주성중 [1], 이병찬 [2], 이긍원
*Dong Seok. Kim, Ji Min. Kim, Bumjin. Kim, Young-jae. Jang, Sung-Jung. Joo[1], Byung-Chan. LEE[2], Kungwon. Rhie
고려대학교. [1] 한국표준과학연구원. [2] 인하대학교.

Keyword : structural phase, surface tension, FeZr, CoFeB, voids

Perpendicular-Magnetic tunnel junction (p-MTJs) structure is a good candidate for nonvolatile magnetoresistive random access memory (MRAM) devices [1, 2]. Both high quality of multi-layers and large anisotropic constant K are the essential requirements. The flat surface and high densitiy of sputtered film is very important to make a good quality of PMA layer, because the perpendicular magnetic anisotropy is affected by the interface between ferromagnetic layer and the other layer. The effect of sputtering energy for better perpendicular magnetic anisotropy (PMA) of CoFeB [3] is studied.
SiO_2/X(50 or 150) (in nm.) samples are grown by conventional magnetron sputtering techniques, where X is FeZr, Co, CoFeB, and Ta. The sputtering energy was controlled by changing sputtering pressure and distance between samples and sputtering gun. The sputtering particles may lose energy they arrive substrate, because they experience multiple scattering by Ar particles along the path to the substrate. Therefore, sputtering particle energy at substrate is small when both working pressure and distance is high. In a low sputtering energy case, sputtered particles cannot make a uniform surface and voids may be formed inside a film, which results lower film density. We observed that the film growth pattern changes from 2 dimensional to 3 dimensional growth by crossing a critical sputtering condition. The best pressure and distance to make the best film quality is less than 5mTorr and below 10.5 cm, respectively.
Figure 1(a) shows the resistivity vs. working pressure with a 50 nm thickness of FeZr layer on top of SiO_2 substrate. We measured the resistivity with 4-point-probe method. The gap between whole tips are 1 mm. The resistivity of FeZr film increase with a working pressure. Because of the voids in film, increasing of the resistivity is appeared. In Fig. 1(b), the RMS and average roughness of FeZr layer is plotted as a function of working pressure. As the working pressure increases above 7 mTorr, the roughness of film become 10 times larger than low working pressure case. The 7 mTorr is the boundary of 2-dimensional growth and 3-dimensional growth of the film.
Low resistivity and high density of film could be achieved by controlling the sputtering energy.

[1] S. Ikeda, K. Miura, H. Yamamoto, K. Mizunuma, H. D. Gan, M. Endo, S. Kanai, J. Hayakawa, F. Matsukura, and H. Ohno, Nat. Mater. 9, 721 (2010).
[2] W. X. Wang, Y. Yang, H. Naganuma, Y. Ando, R. C. Yu, and X. F. Han, Applied Physics Letters 99, 012502 (2011).
[3] D. S. Kim, K. Y. Jung, S. J. Joo, Y. J. Jang, J. K. Hong, B. C. Lee, C. Y. You, J. H. Cho, M. Y. Kim, and K. Rhie, J. Magn. Magn. Mater. 374, 350 (2015).

G7.01(초)

Direct Measurement of Energy Level Alignment in Single Molecular Junctions

*김태경
*Taekyeong. Kim
한국외국어대학교.

Keyword : single molecule, scanning tunneling microscope-based break-junction, energy level alignment, density functional theory, graphite

There is an increased interest in understanding electron transfer across single molecule junctions and metal/organic interfaces as this has implications in the field of organic electronics and photovoltaics. In this presentation, I will show how to measure directly the electronic energy level alignment in single molecular junctions by using a scanning tunneling microscope-based break-junction technique. We find that these values are in excellent agreement with density functional theory calculations. Furthermore, I will introduce a hybrid device structure with a single molecule between the gold and the graphite electrodes, which shows the highest rectification ratios reported for a single molecular junction. This work opens a new path to the layered two-dimensional material based molecular electronic devices.

G7.02(초)

Electronic Transport in Molecular Tunneling Transistors

*송현욱
*Hyunwook. Song
경희대학교.

Keyword : Molecular transistors, Molecular electronics, Tunneling, Inelastic electron tunneling spectroscopy

We report the observation of direct gate modulation of the orbital energy in molecular transistors where transport current is controlled by an external gate. We show this using a multiprobe approach combining a variety of transport techniques that elucidates the transport mechanisms and electronic structure of molecular transistors. To make the transistors, individual molecules are connected to tiny gaps between source and drain electrodes with a bottom-gate control electrode using an electromigration-induced break junction technique. We have examined two prototype molecules: (a) the control, octanedithiol with an alkyl σ-backbone as a saturated aliphatic molecule, and (b) the active device, benzenedithiol with a delocalized π-electron aromatic ring as a conjugated molecule. We also demonstrate that a change of the molecule attachment endgroups (specifically, from thiol, -SH to cyanide, -CN) can dramatically change the orbital alignment with respect to the contact Fermi level, transforming the behavior from HOMO-dominated (i.e., p-type) to LUMO-dominated transport (i.e., n-type). These results show that a complementary set of molecular transistors can be created with appropriate chemical design of the metal-molecule contact. Resonant-enhanced coupling to the frontier molecular orbitals is revealed by electron tunneling spectroscopy to verify the identity of the molecule in the transistors and to determine the amount of orbital coupling, demonstrating direct molecular orbital gating in an electronic device. In particular, we contrast molecular structures that have near-resonant coupling to ones that have far-from-resonant coupling. Our findings provide direct, clear evidence of an orbital-modulated molecular transistor and so validate the concept of such an electronic device.

G7.03(초)

Charge transport and optoelectronic process in an atomically thin p-n junction

*이철호
*Chul-Ho. Lee
고려대학교.

Keyword : 2D materials, transition metal dichalcogenides, van der Waals heterostructure, optoelectronics

Van der Waals (vdW) heterostructures built from two-dimensional layered materials provide an unprecedented opportunity in designing new material systems because the lack of dangling bonds on the vdW surfaces enables the creation of high-quality heterointerfaces without the constraint of atomically precise commensurability. In particular, the ability to build artificial heterostructures, combined with the recent advent of transition metal dichalcogenides, allows the fabrication of unique semiconductor heterostructures in an ultimate thickness limit for fundamental studies as well as novel device applications. In this talk, we will present the characterization of the electronic and optoelectronic properties of atomically thin p-n junctions consisting of vertically stacked WSe_2 and MoS_2 monolayers. We observed gate-tunable diode-like current rectification and a photovoltaic response across the p-n interface. Unlike conventional bulk p-n junctions, the tunneling-assisted interlayer recombination of the majority carriers is responsible for the tenability of the charge transport and the photovoltaic response. Furthermore, we will discuss the enhanced optoelectronic characteristics in graphene-sandwiched vdW p-n junctions.

G7.04(초)

Electrical and photoresponse properties in Al/n-typeMoS$_2$/p- type Si heterojunction structures

Fu Huang, Seung Bae Son, Jong-Bae Park, Tae-Sung Bae, Jung Hee Park[1], *Woong Ki Hong
Fu. Huang, Seung Bae. Son, Jong-Bae. Park, Tae-Sung. Bae, Jung Hee. Park[1], *Woong Ki. Hong
Korea Basic Science Institute. [1]Chonbuk National University.

Keyword : Two-Dimensional materials, Molybdenum Disulfide, Heterojunction, PN diode

Recently, atomically thin two-dimensional materials, such as transition metal dichalcogenides (TMDs), especially molybdenum disulfide (MoS_2), have attracted considerable interest for future electronic and optoelectronic applications, such as transistors, logic circuits, solar cells, photodetectors, and sensors. Intrinsic MoS_2 is a n-type semiconducting material with an indirect bandgap of ~1.3 eV in bulk and a direct bandgap of ~1.9 eV for a monolayer. In particular, MoS_2 has a great potential for the applications in photodetection due to the excellent sensitivity of light, the formation of large area film, extreme flexibility, and high transparency. For the applications in photodetection, the use of heterojunction devices can be an effective way of manipulating the electronic and optoelectronic properties of semiconductor devices based two-dimensional nanomaterials. In this work, we demonstrate electrical and photoresponse properties in heterojunction devices based on an Al/n-type MoS_2/p-type Si structure. We investigated three different types of heterojunction devices: (1) metal/Si junction devices without a MoS_2 layer, (2) metal/as-grown MoS_2/Si junction devices in which a MoS_2 layer was directly grown on a Si substrate, (3) metal/transferred MoS_2/Si junction devices in which a MoS_2 layer was transferred onto a Si substrate.

G8.01(초)

Perspectives of nuclear structure studies on exotic nuclei

*Takaharu Otsuka
*Takaharu. Otsuka
Univ. of Tokyo.

Keyword : exotic nuclei, shell evolution, dual quantum liquid picture

I would like to present recent outcome on conceptual and computational studies on the structure of exotic nuclei. This includes shell evolution, dual quantum liquid picture, and Monte Carlo Shell Model calculations. I will select some topics depending on the duration of the talk and the audience.

G8.02(초)

Activities of nuclear physics theory at RISP

*김영만
*Youngman. Kim
기초과학연구원.

Keyword : nuclear reactions, nuclear structures, nuclear transport, nuclear astrophysics

In this presentation we will discuss nuclear theories at RISP for rare isotope science.

G8.03(초)

Nuclear forces and applications to nuclear structure calculations

*Furong Xu
*Furong. Xu
Peking Univ.

Keyword : N3LO force, HF, MBPT, BHF

Starting from the nuclear N3LO force, we perform the Hartree-Fock approximation first. Taking the HF solution as the reference and using many-body perturbation theory (MBPT), we make corrections to the HF calculation, up to the third-order correction in nuclear energy and up to the second order in nuclear radius. As preliminary calculations, we have investigated the closed-shell nuclei, He-4 and O-16, obtaining quite good results in both binding energies and radii. As another ab-initio method, we have made Bruckner-Hatree-Fock calculations of nuclear structures.

G9.01

Supersymmetric Localization for BPS Black Hole Entropy: 1-loop Partition Function from Vector Multiplets

*전임탁, Rajesh Kumar Gupta[1], Yuto Ito
*Imtak. Jeon, Rajesh. Gupta[1], Yuto. Ito
고등과학원. [1]ICTP.

Keyword : black holes in string theory, BPS black hole entropy, supersymmetric localization, AdS/CFT

We use the techniques of supersymmetric localization to compute the BPS black hole entropy in N=2 supergravity. We focus on the n_v+1 vector multiplets on the black hole near horizon background which is $AdS_2 \times S^2$ space. We find the localizing saddle point of the vector multiplets by solving the localization equations, and compute the exact one loop partition function on the saddle point. Furthermore, we propose the appropriate functional integration measure. Through this measure, the one loop determinant is written in terms of the radius of the physical metric, which depends on the localizing saddle point value of the vector multiplets. The result for the one loop determinant is consistent with the logarithmic corrections to the BPS black hole entropy from vector multiplets.

G9.02

Non-existence of Zitterbewegung

*최태승
*Taeseung. Choi
서울여자대학교.

Keyword : DIrac particle, Zitterbewegung, relativitisc spin operator, relativistic position operator, Poincare group

We derived the new spin operator that gives the representation of the Poincare group at the last meeting. This new spin operator naturally define the new position operator, which is local in the sense [x_i, x_j]=0, through the total angular momentum. We have shown that the time derivative of this position operator -velocity- has no Zitterbewegung solution other than the ordinary Dirac position operator. This requires the reinterpretation of recent experiment of Zitterbewegung in 1+1 dimension.

G9.03

Ward Identity and holography

*김경규, 김근영 [1], 박미옥 [2]
*Kyung Kiu. Kim, Keun-Young. Kim[1], Miok. Park[2]
광주과학기술원 물리·광과학과. [1] 광주과기원 물리광과학과. [2] 고등과학원.

Keyword : gauge/gravity correspondence, Ward identity, superfluid density

We derive a Ward identity for a field theory with sources and we construct a dual holographic system. This system can reproduce the Ward identity through numerical calculations. In addition, we will provide the physical meaning of the superfluid density in a holographic superconductor model by using the Ward identity.

G9.04

Chiral Fermion and Boundary State Formulation: Resonant Point-Contact Tunneling

*이태진
*Taejin. Lee
강원대학교.

Keyword : chiral fermion, boundary state, Luttinger liquid, point-contact tunneling

We study a model of resonant point-contact tunneling of a single Luttinger-liquid lead, using the boundary state formulation. The model is described by a single chiral fermion in one dimensional space with one point contact interaction at the origin. It is the simplest model of this type.
By folding the infinite line we map the model onto a non-chiral model on the half-line and transcribe the point-contact tunneling intraction into a boundary interaction. The tunneling interaction yields a non-local effective action at the boundary. We explicitly construc the boundary state and evaluate the current correlation functions.

G9.05

Instantons as Bulk Local Operators in pp-wave holography

*김낙우
*NAKWOO. KIM
경희대학교.

Keyword : Holography, pp-wave, bulk locality, instanton

The surface/state correspondence relates an arbitrary surface in spacetime with gravity to a density matrix of the holographic dual field theory. It should be particularly useful for backgrounds without obvious boundary, such as Minkowski or pp-waves. We consider the BMN sector/pp-wave relation and argue that D-instantons provide bulk local operators. We present simple calculations and illustrate how to extract the spacetime metric from D-instanton states.

G9.06

Magnetic Impurities from Holography

*서윤석, 신상진, 김근영 [1], 김경규 [2]
*Yunseok. SEO, Sang-Jin. SIN, Keun-Young. Kim[1], Kyung Kiu. Kim[2]
한양대학교. [1] 광주과기원. [2] 광주과학기술원 물리·광과학과.

Keyword : AdS/CMT correspondence, strongly correlated system, ferromagnetism, anomalous Hall effect

We study the magnetic properties of the system with impurities by using holography.We start from Einstein-Maxwell-dilaton system. We introduce scalar field in the bulk to break momentum conservation and turn on the Chern-Simons like interaction between gague field and scalar. We find analytic background solution and calculate magnetization of the system. The system has finite magnetization in the absence of the external magnetic field and hence it can be understood as ferromagnetic system. We also calculate DC transport coefficiens from the black hole horizon data and investgate temperatue and external field dependence of the DC conductivities.

G9.07

3d superconformal index and Seiberg-like dualities with an adjoint matter

*황치웅, 박재모 [1]
*Chiung. Hwang, Jaemo. Park[1]
고등과학원. [1] 포항공과대학교.

Keyword : superconformal index, factorization, supersymmetric gauge theory, Seiberg-like duality

We work out the factorization of the 3d superconformal index for N = 2 $U(N_c)$ gauge theory with one adjoint chiral multiplet as well as N_f fundamental, N_a anti-fundamental chiral multiplets. Using the factorization, one can prove the Seiberg-like duality for N = 4 $U(N_c)$ theory with N_f hypermultiplets at the index level. We explicitly show that monopole operators violating unitarity bound in a bad theory are mapped to free hypermultiplets in the dual side. For N = 2 $U(N_c)$ theory with one adjoint matter X, N_f fundamental, N_a anti-fundamental chiral multiplets with superpotential W = tr X^n+1, we work out Seiberg-like duality for this theory. The index computation provides combinatorial identities for a dual pair, which we carry out intensive numerical checks.

G9.08

6d SCFTs, 5d dualities and Tao diagrams

*김성수
*Sung-Soo. Kim
고등과학원.

Keyword : 6d superconformal theories, 5d superconformal theories, Brane dynamics.

We discuss a circle compactification of 6d superconformal theories (SCFTs). From the perspective of the (p,q) 5-brane web diagram, circle compactified SCFTs are 5d SCFTs with the critical number of flavors which have 6d UV completion. Such 5d theories are depicted as a new web diagram of spiral shape called Tao diagram. We report new 5d dualities among 5d SCFTs through the Tao diagrams.

G9.09*

Supersymmetric gauged Double Field Theory: Systematic derivation by virtue of Twist

*조원영, 박정혁, 전임탁 [1]
*Wonyoung. Cho, Jeong-Hyuck. Park, Imtak. Jeon[1]
서강대학교. [1] *고등과학원.*

Keyword : "Double Field Theory", "twist", "reduction", "gauged", "supersymmetric"

In a completely systematic and geometric way, we derive maximal and half-maximal supersymmetric gauged double field theories in lower than ten dimensions. To this end, we apply a simple twisting ansatz to the D=10 ungauged maximal and half-maximal supersymmetric double field theories constructed previously within the so-called semi-covariant formalism. The twisting ansatz may not satisfy the section condition. Nonetheless, all the features of the semi-covariant formalism, including its complete covariantizability, are still valid after the twist under alternative consistency conditions. The twist allows gaugings as supersymmetry preserving deformations of the D=10 untwisted theories after Scherk-Schwarz-type dimensional reductions. The maximal supersymmetric twist requires an extra condition to ensure both the Ramond-Ramond gauge symmetry and the 32 supersymmetries unbroken.

G10.01

Discovery of ν_τ appearance in the CNGS neutrino beam with the OPERA experiment

*윤천실, 박인곤, 김성현 [1], 박병도 [2], 김지현
*Chun Sil. YOON, In Gon. PARK, Sung Hyun. KIM[1], Byung Do. PARK[2], Ji Hyun. KIM
경상대학교. [1]IBS. [2] 성균관대학교 삼성창원병원.

Keyword : Tau neutrino, OPERA experiment, Neutrino oscillation

The 5th Tau neutrino candidate event was found in the OPERA experiment. The experiment is designed to search for oscillations in appearance mode, i.e. by detecting the tau leptons produced in charged current interactions. And data were taken from 2008 to 2012 in the CERN Neutrinos to Gran Sasso beam. The observation of appearance, obtained with four candidate events in a sub-sample of the data, was previously reported. In this talk, a fifth candidate event, found in an enlarged data sample, is presented. Together with a further reduction of the expected background, the five candidate events detected so far allow assessing the discovery of oscillations in appearance mode with a significance larger than 5.

G10.02

Highlights and Future Plan of Telescope Array Experiment

*천병구
*Hiro.. Sagawa
동경대학교.

Keyword : Telescope Array Experiment, Ultra-high energy cosmic rays, TAx4 Extension

The Telescope Array (TA), located in Utah, USA, observes highest energy cosmic rays using Surface Detectors (SDs) and Fluorescence Detectors (FDs). The SD array consists of 507 scintillation detectors on a 1.2-km square grid covering 700 km^2. The FD sets located at three sites look over the surface array. Using the first 6-year data collected by the surface detectors, we found a cluster of cosmic rays with energies above 57 EeV that we call the hotspot. With enhanced statistics, we expect to observe the structure of that hotspot, other excess spots, point sources and the correlation with extreme phenomena in the nearby universe. Therefore, we plan to quadruple the SD array, which covers 3,000 km^2, by adding 500 surface detectors with 2.1-km spacing. Two FD stations will be constructed at the new SD array. This TA extension that we call TAx4 would speed up in the detection rate to elucidate the above objectives, the measurement of energy spectrum and composition study in the highest energy region. Here we present TA physics highlights and the plan of TAx4 as well.

G10.03

A Method of Pulse-separation in Pulse Shape Discrimination Searching for the non-Baryonic Heavy Particle.

*우종관, 고재우, 유동
*Jong-Kwan. Woo, JeWou. Ko, Dong. Liu
제주대학교.

Keyword : PSD, MIP, HIP

We will introduce a way to discriminate the neutral particles, such as a gamma ray from a neutron, using a pulse shape discrimination (PSD) method. An elastic scattering between an incident particle and a target nucleus provides a scintillation photon through an excitation process and an ionization process simultaneously. The ratios of amount of signal induced by excitation to the amount of signal induced by ionization are different by the incident particles, Minimum Ionization Particles (MIP), such as a neutron, to the Heavy Ionization particles (HIP), such as a gamma ray. We will introduce a way to separate a signal into two sub signals induced by ionization and excitation. Our PSD method will provide a good solution to identify a heavy non-Baryonic particles.

G10.04

Status of the KIMS-NaI experiment

*하창현
*Chang Hyon. Ha
기초과학연구원.

Keyword : NaI(Tl) crystal, WIMP, scintillation, KIMS

The Korea Invisible Mass Search (KIMS) is a sequence of dark matter searches that use arrays of scintillating crystals that serve both as a WIMP-interaction target and detector in the low-background environment of the Yangyang underground laboratory. After ten years of operation with CsI(Tl) crystals, KIMS is currently making a transition to new program that uses recently developed low-background, high light yield NaI(Tl) crystals for a WIMP dark matter search. The goal of the KIMS-NaI experiment is to make an unambiguous test of the controversial DAMA/LIBRA annual modulation signature. Studies with six prototype NaI(Tl) crystals have shown considerable progress in the reduction of internal contaminations of radioisotopes. We expect to achieve a background level of less than 1~counts/day/keV/kg for recoil energies around 2~keV in an operational array of NaI(Tl) crystals with a total mass of 200~kg. The current status of the KIMS-NaI experiment is reported.

G10.05*

Performance of liquid scintillator veto systemin KIMS experiment.

*푸시파
*Pushparaj. Adhikari
세종대학교.

Keyword : dark matter, WIMP, KIMS-NAI, NaI, Liquid Scintillator

Rejection of external and internal background is one of the most crucial part for the wimp search using NaI crystal. For this purpose, we designed and constructed liquid scintillator veto system by dipping one NaI crystal into the liquid scintillator. LS veto system consist of acrylic box, which contained LS, and attached 10 PMTs to acrylic vessel wall and it surrounded by copper box. We analyzed the recorded signal from all PMTs and estimate rejection efficiency, dru level, energy threshold, etc. The result from the data analysis and comparison of dru level with and without veto system will be discussed.

G10.06*

Resolving nonlinear behavior of photomultiplier tubes in the KIMS-NaI experiment

*고빈다
*GOVINDA. ADHIKARI
세종대학교.

Keyword : dark matter, WIMP, KIMS-NaI, PMT

The Korea Invisible Mass Search experiment uses the 3-inch diameter R12669SEL made by Hamamatsu Photonics to detect a faint scintillation light from dark matter interactions in NaI(Tl) crystals. While the photomultiplier tube (PMT) is a low-radioactivity light sensor, widely used for direct dark matter searches, the anode readout from these PMTs in high energy region above 2 MeV shows anomalous behavior of early saturation and shape distortion. In this talk, the study to resolve this nonlinearity issue by reading out both anode and dynode signals simultaneously is presented.

G10.07*

A Study of Initial State Gluon Radiation on the Drell-Yan process from Proton

양운기, *박재균, 김준호, John Leslie Almond, 유금봉
Un-ki. Yang, *Jae gyun. Park, JUN HO. KIM, John Leslie. Almond, Geum-bong. YU
서울대학교.

Keyword : "ISR", "LHC", "CMS", "DGLAP", "QCD"

We present the updated results of initial state gluon radiation (ISR) study with the Drell-Yan process from proton-proton collisions at = 8 TeV. The effect of the ISR in the Drell-Yan events is studied using the transverse momentum p_T of dilepton in electron and muon channels. We found that the average p_T of the dilepton has a logarithmic dependence on the invariant mass squared of the dilepton and measured the logarithmic slope using 19.7 fb^{-1} of the data. In addition to this, we continued studying systematic uncertainties, and updated the result. This measurement provides not only a useful QCD information, but also a way to estimate the ISR effect on other similar physics processes.

G10.08*

The Current Status of the AMoRE-Pilot Experiment Analysis

*김인욱
*Inwook. Kim
기초과학연구원.

Keyword : neutrino, low temperature physics, mmc, molybdenum

The Advanced Mo-based Rare process Experiment (AMoRE) is a search for neutrinoless double beta decay (0νββ) of 100Mo using CaMoO4 crystals as the source and the detector. A pilot experiment, AMoRE-Pilot, was installed at Yangyang underground laboratory and the experimental conditions are being studied in preparation for a year-long data-taking period. Here we present the basic idea behind the AMoRE-Pilot technique, i.e., the simultaneous detection of both phonons and photons, and event discrimination power that it provides. The energy calibration of the AMoRE-Pilot and measured internal backgrounds of the crystals are also described.

G10.09

HPGe detector array 구축을 위한 샘플들의 감마선 측정 및 시뮬레이션

*김고운, 한인식, 김영덕 [1], 강운구 [2], Elena Sala[2], Douglas Lenard[2], 이무현 [3], 박수연
*Go Woon. Kim, Insik. HAHN, Yeong Duk. KIM[1], Woon Gu. Kang[2], Elena. Sala[2], Douglas. Lenard[2], MOO HYUN. LEE[3], Su-yeon. Park
이화여자대학교. [1] 기초과학연구원/세종대학교. [2] 기초과학연구원(IBS). [3] 기초과학연구원.

Keyword : HPGe detector, GEANT4

{180m}^Ta 과 같이 핵, 입자, 천체물리적으로 중요한 핵들의 반감기 측정과 다양한 연구 목적으로 지하실험연구단(CUP)에서는 14 개의 HPGe detector 를 사용한 Array 를 구축하고자 준비 중이다. 이 때에 사용될 개별 HPGe detector 를 구성하고 있는 Copper, Lead, Aluminum 등 각 material 의 샘플들과 주변 부속물로 사용될 O-ring 샘플의 Background 를 양양실험실에 이미 구축되어 있는 HPGe 를 사용하여 측정 및 분석하였다. 이 측정 결과와 더불어 GEANT4 시뮬레이션을 통하여 HPGe Array 의 Background 결과를 예측하고 그 level 을 줄일 수 있는 방안에 대한 연구결과를 발표하고자 한다. 이 연구를 바탕으로 최적화된 HPGe Array System 과 차폐체를 구축하고자 한다.

G12.01(초)

Cellular Organization and Controllable Synchronization of Pancreatic Islets

Danh-Tai Hoang, *조정효
Danh-Tai. Hoang, *Junghyo. Jo
아시아태평양이론물리센터.

Keyword : Synchronization, Desynchronization, Cellular Network, Pancreatic Islet, Diabetes

Understanding structure-function relationships is one of the most fundamental problems in biology. Pancreatic islets, critical micro-organ for glucose homeostasis, are composed mainly of alpha, beta, and delta cells. The alpha and beta cells are complementary to increase and decrease glucose levels by producing glucagon and insulin pulses, while the role of delta cells is unclear. Although the spatial organization and paracrine interactions between the endocrine cells have been well studied, we still lack their functional implications. In this study, we made a mathematical model that combines the islet architecture and the pulsatile hormone secretions with the paracrine interactions, and examined the synchronization of hormone pulses within islets. We found that the islet architecture and the paracrine interactions were special for controlling synchronization: islet cells were highly synchronized to concentrate hormone pulses at emergency such as low and high glucose conditions, while they were desynchronized to hide unnecessary hormone actions at normal glucose conditions. The controllable synchronization may provide a new viewpoint on the malfunction of diabetic islets.

G12.02(초)

Quantitative Measurement of Charged Lipid Vesicle Interaction by Optical Confinement

*김보필, 박성민 [1], 김만원 [2], 최명철 [2]
*Bopil. Gim, Seongmin. Park[1], Mahn Won. Kim[2], Myung Chul. Choi[2]
한국과학기술원 (KAIST). [1]LG Chem Research Park. [2] 한국과학기술원.

Keyword : lipid vesicle, optical trapping, second virial coefficient, charge interaction, drug delivery

Lipid vesicles are are the most useful as encapsulated carriers which can transport inside living organisms. Due to this property, research of lipid vesicles mainly focuses on understanding their transports and inter-vesicle interactions for applications of drug delivery systems. Although many interests in modern science, the basic studies, particularly in terms of thermodynamics and phase transitions, had not been actively investigated because of limit of experimental technology to measure such a small size of vesicles (much less than micron size) in lab.

In this talk, we will show the recent results of measuring charged lipid vesicle interaction via decent optical trapping method, called “optical bottle”, using capturing multi-vesicles inside of laser confinement. Throughout number density change of vesicles by switching on/off laser beam, we define isothermal pressure difference (or the isothermal compressibility) and eventually work out second virial coefficient, B2, in the virial theory. Indeed, from experimental data, we set theoretical model to determine vesicle-vesicle interactions in various conditions of lipid composite and volume fraction of vesicles. As a result, we have quantitatively good agreement with both experimental results and theoretical results.

G12.03

Functional connectomes of the clock cells within Suprachiasmatic nucleus based on optogenetic light stimulation and whole-cell patch recording

*민철홍, 김현, 정병하, 이경진
*Cheol Hong. Min, Hyun. Kim, Byeongha. Jeong, Kyoung Jin. LEE
세포동력학연구센터/고려대학교.

Keyword : Suprachiasmatic nucleus (SCN), whole-cell patch recording, optogenetic light stimulation, channelrhodopsin-2, cell-to-cell connectivity

The biological master clock, Suprachiasmatic nucleus (SCN), governs the autonomous circadian rhythm in all mammals. It is composed of thousands of clock cells that work in concert to produce slowly propagating coherent phase waves. However, some recent studies including ours [Hong et. al 2012, EJN] suggest that SCN clock cells form very extensive, interdigital, sub-networks that may span almost the entire SCN. The cell-to-cell interactions mediated by action potentials can confer phase coherence to the clock cells that are coupled together within a sub-network. On the other hand, the co-existence of many sub-networks, each supporting a different circadian phase, can render a situation in which two neighboring clock cells in a close proximity to exhibit two rather different circadian phases. So far, we have no quantitative understanding of the extent over which clock cells are coupled together by action potentials and of their network morphologies. In this work we report our experimental findings regarding functional connectomes among clock cells. They are based on a time-correlated optogenetic light stimulation and response test protocol, in which 5 successive light stimuli are delivered to a small square area (either 25x25 or 50x50 micron^2) of a ChR2 (blue-light triggerable cation channel) expressing SCN tissue at a time interval of 100 ms and the time correlated response of a chosen clock cell is monitored by a whole-cell recording while the square box is scanned systematically throughout the whole tissue. Then, the test protocol is repeated at least for 5 times to ensure the stimulation-induced response. With different voltage-clamping and current-clamping recording modes in conjunction with different pharmacological interventions, including CNQX, bicuculline, we confirm that most clock cells in “core” region have a extensive excitatory receptive field, typically covering an area larger than 50% of the entire SCN, while there are only a small sub-population of clock cells (less than 10%) showing an inhibitory receptive field. The observed inhibitory receptive field is generally very small compared to the typical size of excitatory receptive field. We also find that the excitatory receptive field of the clock cells in “shell” area tend to be much smaller than those of clock cells in “core” area. In conclusion, we have established an optogenetic light-stimulation system for mapping out SCN clock cell connectomes and estimated the range of cell-to-cell connectivity, both excitatory and inhibitory. The biological or biophysical implication of these structure are elusive at the moment and warrants further investigation.

G12.04

Mechanical Properties of Branched Actin Filaments

*판베네타토스, M. Razbin[1], M. Falcke[2], A. Zippelius[1]
*Panayotis. Benetatos, Mohammadhosein. Razbin[1], Martin. Falcke[2], Annette. Zippelius[1]
Kyungpook National Univ. [1]University of Goettingen. [2]Max Delbruck Center.

Keyword : elasticity, semiflexible, actin, Arp2/3, lamellipodia

Cells moving on two-dimensional substrates generate motion through the polymerization of branched actin networks inside flat membrane protrusions (lamellipodia). We investigate the force-extension relation of branched filaments, grafted on an elastic structure at one end and pushing with the free ends against the leading edge cell membrane. We model the filaments as worm-like chains whose thermal fluctuations are restricted by the leading edge cell membrane giving rise to an effective force. We show that branching increases the effective stiffness considerably.

G12.05

Inter-islet synchronization

*박동호, Jin Xu[1], 조정효
*Dong-Ho. Park, Jin. Xu[1], Junghyo. Jo
아시아태평양이론물리센터. [1]Pohang University of Science and Technology.

Keyword : synchronization

Pancreatic islets secrete hormones such as glucagon, insulin and somatostatin for glucose homeostasis. On a certain condition, it is observed that they are released into blood in a pulsatile way. It suggests that there exist a synchronization mechanism in the islet system. Based on the Stuart-Landau type coupled oscillator model with a pinning term, islets can be synchronized or desynchronized depending on the glucose level. We suggest that the known cell-cell interactions in the islet is the unique natural choice among other possibilities.

G12.06

Optogenetic Regulation of Cellular Activities through a Scattering Skull using Wavefront Shaping

*윤종희, 박용근
*Jonghee. Yoon, YongKeun. Park
KAIST.

Keyword : wavefront shaping, optogenetics, adaptive optics, cellular signaling, scattering

Recent advances in optogenetics, which optically regulate biological processes by using genetically engineered proteins, have shown its importance and potential. Optogenetics has shown many applications in various research fields ranging from neuroscience and cardiology to genetics. While optogenetics has advantages in in vivo functional studies, multiple light scattering caused by biological tissues such as brain or skull layers significantly prevents non-invasive in vivo applications. To overcome aforementioned issue resulted from multiple light scattering, invasive approaches including implementation of endoscopes or optical fibers and cranial windows have been used. While invasive methods provide deep light penetration, it inevitably causes deleterious effects on tissues. Recently, genetically modified proteins which response to near-infrared (NIR) light have been developed, but penetration depths of NIR light is still limited to a few millimeter.
Toward the development of non-invasive in vivo optogenetic applications, we exploited a wavefront shaping method. We demonstrated that an illumination with shaped waves make a focus through a scattering skull, and it enables spatiotemporal control of intracellular Ca^{2+} concentrations by activating photoactivatable proteins.

G13.01(초)

Interaction of clusters with intense, few-cycle, long wavelength fields

*Hyunwook Park, Zhou Wang, P. Agostini, L. F. DiMauro
*Hyunwook. Park, Zhou. Wang, P.. Agostini, L. F.. DiMauro
Ohio State University.

Keyword : femtosecond (fs) laser, ultrafast interaction, cluster, high-order harmonic generation (HHG)

Interaction of matter with intense laser has attracted a lot of attention for both fundamental importance and potential applications. Understanding atoms, also molecules to a great extent, in a strong field has been quite successful in both classical and quantum mechanical perspectives, yet understanding more complex systems like solid material is still in its infancy stage due to difficulties of properly coupling such a high field energy to the high density target as well as theoretical challenges. Alternatively, van der Waals clusters are proposed as a way of bottom-to-top approach to understand the intense laser-matter interaction, bridging atom and solid phase. Cluster sources generally have advantageous properties such as large inter-cluster distances (gas-like) but high local density (solid-like) so that the incident light can be efficiently and homogeneously deposited into the small solid targets. As a result, clusters confine a great amount of photon energy with a high level of tolerance and finally the highly condensed photon energy can be released as forms of photon up-conversion like high-order harmonic generation (HHG) or energetic particles. Here we report a systematic study of cluster heating by intense femtosecond (fs) lasers in the infrared (IR) to near-infrared (NIR) range for the first time. We observed that clusters display a wavelength-dependence in their heating process. After heating, the nanoplasma emits high-energy electrons and ions during relaxation. The wavelength dependent behaviors are attributed to two heating mechanisms- inverse Bremsstrahlung (IB) volume and Brunel-like, field-driven surface heating. The detected ion energy first decreases rapidly and subsides gradually with increasing wavelength, which indicates a strong signature of IB collisional heating. The surface heating appears to be relatively too weak to be resolved in the ion energy measurement due to the small surface-to-volume ratio and short effective active duration. Alternatively, we carried out more detailed measurements of the anisotropy of the ion emission and sensitivity of heating to the circularly polarized light (CPL). Progressive growth of the anisotropy and higher sensitivity to CPL with longer wavelengths testifies to the existence of the field-driven surface heating.

G13.02*

Propagation of surge-current-induced THz pulse into the medium investigated in a near-field zone

*한정우, 이종석 [1], 최영관 [2]
*Jeong Woo. Han, Jongseok. LEE[1], Younggwan. Choi[2]
GIST. [1] 광주과학기술원. [2] 광주과학기술원(GIST).

Keyword : Terahertz, refractive index, near field zone

Characteristics of propagated terahertz (THz) radiation into a medium emitted from photo-excited carriers have been diagnosed in the near field zone by conducting a knife-edge experiment. In order to characterize an initial amplitude profile of THz wave, we have modelled the motion of photo-excited carriers in terms of position- and time-dependent electric dipoles, and confirmed that THz pulse has a Gaussian distribution of its amplitude. By comparing the experimental results with the calculation results, we have demonstrated that THz pulses propagate in the medium following the prediction based on paraxial wave equation. In addition, we discuss a minimum spatial resolution in performing THz time-domain spectroscopy exploiting a recently introduced technique based on the multiple reflections in a THz emitter-sample hybrid structure (J. W. Han et al., Opt. Lett. 39, 19 (2014)).

G13.03

Current Status of HES-I Construction Project in PAL-XFEL

*김수남, 박재구, 김봉수
*Sunam. Kim, Jaeku. Park, Bongsoo. Kim
포항가속기 연구소.

Keyword : Pohang Accelerator Laboratory, X-ray Free Electron Laser, Ultrafast Dynamics

The HES-I (Hard X-ray Pump and Probe end-station) in PAL-XFEL (Pohang Accelerator Laboratory X-ray Free Electron Laser) will be a new tool to observe dynamics of physical and chemical systems within femto-second time resolution. Current status of construction project will be reported: science opportunity, XFEL photons, experimental apparatus, construction concept and plan, and additions. Since the HXPP is user facility, we believe that reflection of user opinion in beamline construction. All staffs is constructing the new facility with passion, and has a plan for user support since 2017 after one year commissioning in 2016. We wish to have time for communication with future HXPP users in various research fields.

G13.04

Vis-NIR emission analysis of Pr^{3+} doped borosilicate glasses for broad band signal amplification

*Varnakavi Naresh, 함병승
*Varnakavi. Naresh, Byoung Seung. HAM
광주과학기술원.

Keyword : Energy transfer, Multi-phonon, Cross-relaxations, Pr^{3+} Vis-NIR emission

Here, we discuss on results pertaining to non-radiative relaxations of visible-near infrared emissions originating from $^3P_0$ and $^1D_2$ levels of Pr^{3+}: LABS glasses. The effect of OH content and phonon energy on luminescence features of Pr^{3+} is analysed from Fourier transform infrared and Raman spectral profiles. Luminescence from Pr^{3+} glasses in visible region exhibited two bands at 493 nm ($^3P_0 \dashrightarrow {}^3H_4$) and 605 nm ($^1D_2 \dashrightarrow {}^3H_4$) when excited by 448 nm. In a NIR region a narrow and ultra-broad emission bands are observed at 1.06 µm ($^1D_2 \dashrightarrow {}^3F_3$) and 1.49 µm ($^1D_2 \dashrightarrow {}^1G_4$) for 488 nm excitation. For these emission transitions, emission decay curves exhibited shortening in their lifetime due to multiphonon interactions and cross-relaxation routes. The ion-ion interactions in $^3P_0$ and $^1D_2$ states of Pr^{3+} causing quenching in emission intensities and lifetimes is governed by electric dipole-dipole mechanism. The large absorption and stimulated emission cross-sections of Pr^{3+} ions around 1.49 µm suggests suitability of a host material operating for broadband signal amplifications at low-loss optical telecommunication windows. Besides, emission parameters like stimulated emission cross-section (σ_{emi}), effective band width ($\Delta\lambda_{eff}$) and figure of merit are calculated for 1.49 µm ($^1D_2 \dashrightarrow {}^1G_4$) of Pr^{3+} doped silicate based glasses.

G13.05*

Single strand DNA 와 G-quadruplex 의 병진 및 회전확산 분석

이재란, 이동근 [1], 김수용 [1], *김석원
Jaeran Lee. , Dongkeun Lee. [1], Soo Yong Kim. [1], *KIM Sok Won.
울산대학교. [1] *한국과학기술원.*

Keyword : Fluorescence correlation spectroscopy, G-quadruplex, rotational diffusion

DNA(deoxyribonucleic acid)는 세포의 핵 안에서 아데닌(A), 구아닌(G), 시토신(C), 티민(T)의 4 개의 염기 서열 조합에 의해 생물의 유전 정보를 저장하는 물질로 잘 알려져 있다. 일반적으로는 1 nm 의 반지름으로 오른쪽으로 꼬여있는 이중 나선 구조의 B-DNA 가 잘 알려져 있지만, 왼쪽으로 꼬인 Z-DNA, 십자가 형태나 슬리피드 루프 형태, 트리플 헬릭스인 H-DNA, G-rich strand 인 G-quadruplex 와 같이 다양한 형태들의 DNA 가 존재한다. 그 중에서 G-quadruplex 는 single-strand DNA 형태에서 음이온의 농도에 의해 구형으로 변형된 구조를 띠고 있어 형태에 따른 입자의 확산 운동을 분석하기가 용이하다. 본 연구에서는 편광-형광상관분광법을 이용하여 d(GGGT)4 single-strand DNA 에서 G-quadruplex 로 변형될 때의 회전 확산과 병진확산의 특성 변화를 분석하였다. 이온의 농도를 변화시키기 위해 KCl 을 1 M 에서 10 nM 까지 1/10 씩 변화시키고 10 mM Tris-HCl 버퍼로 희석하여, 각각의 농도에서 온도에 따른 G-quadruplex 의 안정도를 분석하였다. 시료의 온도는 25 ~ 45 ℃까지 5 ℃ 간격으로 증가시켰고, 각 시료들의 회전 확산과 병진 확산 시간을 통해 입자의 크기 변화를 확인하였다. 본 연구는 온도와 이온의 농도가 DNA 의 말단에 존재하는 G-rich DNA 에 미치는 영향을 분석하기 위해 활용될 것이다.

G13.06*

Organic dopant modified PEDOT:PSS as an efficient anode buffer layer in polymer solar cells

*쉬빈루에이, 강신원 [1], 사이아난드 고파란, 이광돈, 이재성, 김세완, 이상원
*Binrui. Xu, Shin Won. Kang[1], Sai-anand. Gopalan, Kwang-Don. Lee, Jae-Sung. Lee, Sae-Wan. Kim, Sang-Won. Lee
경북대학교. [1] 경북대학교 IT 대학.

Keyword : Organic dopant, Polymer Solar Cells (PSCs), Poly(ethylenedioxythiophene):polystyrene sulfonate (PEDOT: PSS), Anode buffer layer,

Poly(ethylenedioxythiophene):polystyrene sulfonate (PEDOT: PSS) is widely used as a standard anode buffer layer in polymer solar cells (PSCs), because of its excellent transport properties, high transparency and textured surface [1]. However, the major demerits of using PEDOT: PSS film as buffer layer in PSCs are the highly acidic and hygroscopic nature, poor device air/thermal stability, low electrical conductivity etc [2, 3]. In this work, we utilize a new organic dopant (DOH) modified PEDOT:PSS to influence the optoelectronic/photovoltaic (PV) characteristics. The organic dopant modified PEDOT:PSS based device exhibited superior PV characteristics than the pristine PEDOT:PSS. The device performance of the PSCs fabricated with modified PEDOT:PSS buffer layer found to depend on the doping concentration of DOH. Fig.1 presents the photocurrent density-voltage (J-V) curves for the pristine device and dopant modified device. The device fabricated with modified PEDOT:PSS (P3HT:PCBM photoactive system) by utilizing optimized concentration of the dopant, exhibited a significant power conversion efficiency (PCE) of 3.44 % with open-ciruit voltage of 0.60 V, short circuit current density of 9.127 mA/cm^2 and fill factor of 0.63. On the contrary, device fabricated with pristine PEDOT buffer layer showed a PCE of 2.94%. The superior device characteristics for the modified PEDOT:PSS buffer layer are attributed to the stronger light absorption capability, improved conductivity and hole mobility, enhanced charge extraction/collection and decreased interfacial contact resistance. In addition, we believe that the dopant modified PEDOT:PSS device will remain air stable for longer period than the pristine device, due to its relatively low pH.

Acknowledgment
This work was supported by the national research foundation of Korea (NRF) Grant funded by the Korean Government (MSIP) (No. NRF2014R1A2A1A11050377).
References
[1] Wang. X., et al. (2015). “Inducting effects of ionic liquid crystal modified-PEDOT:PSS on the performance of bulk heterojunction polymer solar cells”, RSC Advances, 5: 52874-52881.
[2] Sai-Anand, G., et al. (2015). “A futuristic strategy to influnece the solar cell performance using fixed and mobile dopants incorporated sulfonated polyaniline based buffer layer”, Solar Energy Materials and Solar Cells 141: 275-290.
[3] Li, Z., et al. (2015). “A nonionic surfactant simultaneously enhancing wetting property and electrical conductivity of PEDOT:PSS for vacuum-free organic solar cells”, Solar Energy Materials and Solar Cells 137: 311-318.

G13.07*

Electric field enhancement measurements of metallic nanogaps in near infrared wavelengths

*강태희, 이지예, 박주현 [1], 박영미, 안재성, 양효심, 이재우, 김다솜, 전형탁 [1], 김대식
*Taehee. Kang, Jiyeah. Rhie, Joohyun. Park[1], Young mi. Bahk, Jae sung. Ahn, Hyosim. Yang, Jaiu. Lee, Dasom. Kim, Hyeongtag. JEON[1], Dai Sik. Ghim
서울대학교. [1] 한양대학교.

Keyword : "Electric field enhancement", "Kirchhoff integral"

We quantify the electric field enhancement factor of metallic nanogaps experimentally and theoretically. First we fabricated the metallic nanogap aligned vertically in the silver film. By the far field transmission measurement on the nanogaps and applying Kirchhoff integral formalism on the transmission data, we demonstrate the field enhancement factors of 1.5, 3, 8 nm gaps in near infrared frequency range. From the resonant features arising from the Fabry-Perot effect, field enhancement factor spectrum shows characteristic peaks and the enhancement factor reaches up to ~40 for 1.5 nm gap at wavelength of 2.2 um.

H1.01*

First-principles calculations on the interaction between impurities and the charge density wave in indium atomic wires on Si(111)

*현정민, 심형준 [1], 이근섭 [1], 김한철
*Jung-Min. Hyun, Hyungjoon. Shim[1], Geun Seop. LEE[1], Hanchul. KIM
숙명여자대학교. [1] 인하대학교.

Keyword : charge density wave, phase transition, impurity

Metal adsorbed semiconductors have attracted much interest in surface science because they provide useful platforms to study low-dimensional phenomena including phase transition. In nanowires self-assembled on the Si(111) surface undergo phase transition from room-temperature (RT) Si(111)In-4×1 to low-temperature Si(111)In-8×2 at ~120K. O adatoms are known to increase the critical temperature (T_c) while a number of adsorbates such as Al, Ga, Ag, or In adatoms are decrease T_c. However, its mechanism remained veiled. In this presentation, we have investigated the interaction between oxygen impurities and the charge density wave (CDW).
This work was supported by the EDISON program (No. 2012M3C1A6035684) through the National Research Foundation of Korea(NRF) and partly by the Supercomputing Center/Korea Institute of Science and Technology Information (No. KSC-2013-C3-061).

H1.02*

Interface states of Bi_2Se_3 thin films revealed by second harmonic generation and terahertz emission

*함선영, 박순희, 정상균 [1], 전재호 [1], 천승현 [1], 전정흠 [2], 강세종 [2], 유광남 [3], 최은집 [3], 김성 [4], 최석호 [4], Namrata Bansal[5], 오성식 [5], 고병우 [6], 박준범 [6], 김준성 [6], 이종석
*Sun Young. Hamh, Soon-Hee. Park, Sahng kyoon. Jeong[1], jaeho. jeon[1], Seung Hyun. CHUN[1], Heum Jeon. Jeong[2], Se-Jong. KAHNG[2], Kwangnam. Yu[3], E. J.. Choi[3], Sung. KIM[4], Suk-Ho. CHOI[4], Namrata. Bansal[5], Seongshik. OH[5], Byung Woo. Kho[6], JoonBum. Park[6], Jun Sung. Kim[6], Jongseok. LEE
광주과학기술원. [1] 세종대학교. [2] 고려대학교. [3] 서울시립대학교. [4] 경희대학교. [5]Rutgers. The state University of New Jersey. [6] 포항공과대학교.

Keyword : topological insualtor, Bi_2Se_3, interface, second harmonic generation, terahertz emission

We investigate the surface and the interface states of Bi_2Se_3 thin films by exploiting two surface-sensitive optical methods, i.e., second harmonic generation and terahertz emission experiment. The film surface and interface generate azimuth-independent second harmonic wave which is distinct from the response of the bulk crystal, and is ascribed to the twin domain formation on the both interfaces. By looking more details of nonlinear susceptibility deduced from the second harmonic intensities, we demonstrate that the surface band bending caused in a space charge region appears relatively strong at the interface facing the Al_2O_3 substrate or capping layer compared to the surface facing the air. We demonstrate that terahertz electric fields emitted from the samples can supply further information about the surface electronic state of Bi_2Se_3. Finally, we discuss the charge-current-induced spin transport behavior originating from the exotic surface state of Bi_2Se_3 thin films.

H1.03

Two-dimensional free-electron nature of the indium thin films

*박재환, 강명호
*Jae whan. Park, Myung Ho. KANG
포항공과대학교.

Keyword : indium, thin film, two-dimensional free-electron, density functional calculation

Indium overlayers on Si(111)-√7x√3 have been assumed to be one atom thick and widely used to explore the two-dimensional (2D) limits of metal overlayer properties. Recently, however, the representative rectangular and hexagonal In/Si(111)-√7x√3 surfaces were found to represent indium double-layer structures [1, 2]. It is thus a compelling question to find a true indium single overlayer representing the ultimated 2D metallic limit. Here, we use density-functional theory calculations to investigate the 2D electronic properties of freestanding indium thin films. Our calculations demonstrate that the free-electron character of bulk indium is well preserved in indium thin films, even in a single-layer limit. By comparing with the In/Si(111)-√7x√3 surfaces, we understand the Si-substrate effects on the overlayer properties and provide insight into the 2D free-electron nature of the observed indium overlayers.

[참고문헌]
[1] J. W. Park and M. H. Kang, Phys. Rev. Lett. 109, 166102 (2012).
[2] J. W. Park and M. H. Kang, Phys. Rev. B 92, 045306 (2015).

H1.04

Physical properties of zinc-tin-oxide thin films deposited on sapphire and quartz

*박주영, 김재용
*Jooyoung. Park, Jaeyong. Kim
한양대학교.

Keyword : Sputtering, ZTO, ZnO,

최근 투명전도산화물 물질로 잘 알려진 ITO 의 비싼 가격과 대기에서의 독성, 그리고 희소성 문제로 인한 대체 물질이 활발히 연구되고 있다. ZnO 기반의 투명전화산화물 물질들은 넓은 밴드갭 에너지와 높은 광투과율, 그리고 전도성으로 각광받고 있고, 이 중 SnO_2 가 첨가된 zinc-tin-oxide(ZTO) 박막의 대한 연구가 활발하게 이루어 지고 있다. 특히 Zn_2SnO_4 구조의 ZTO 박막은 높은 홀 모빌리티와 우수한 전도성, 그리고 열적 안정성을 가지고 있기 때문에 차세대 투명전도산화물의 대표적인 후보이다. 본 연구에서는 ZnO, SnO_2 가 각각 50:50 wt.%로 섞여있는 타켓을 이용하여 스퍼터링 방법으로 쿼츠 기판과 사파이어 기판에 각각 증착 하였다. X-ray 회절법을 이용하여 기판과 열처리에 따른 구조를 분석하였고 이를 통해, 박막시료가 비정질에서 F.C.C 결정 구조를 갖는 ZTO 박막으로 변화하는 것을 확인하다. 또한, 사파이어 기판에 증착된 ZTO 박막은 (222) 방향으로 우선 성장하는 것을 확인하였고, 그에 따른 박막의 표면 분석, 전기적, 그리고 광학적 특성을 AFM, Hall measurement system, UV-VIS Spectrometer 를 이용해 분석하였다.

H1.05*

Change of the HOMO-LUMO states by the N dopant in the nano-crystalline Si embedded in the a-SiO_2 matrix

*김규형, 정석민
*Gyu Hyeong. Kim, Suk Min. Jeong
전북대학교.

Keyword : Quantum dot, Nano crystalline Silicon, N impurity, Interface state, DFT calculation

Nano-scale structures have attracted great attention to scientists and engineers for their unveiled physical concepts and industrial applications. The nano-crystalline (NC) Si is one of the hottest nano-materials for its preferable optical properties. It is well known that the NC-Si has a direct band gap, which is in contrast to the indirect band gap of bulk Si, and the gap size between HOMO-LUMO states varies with the NC-Si size and the type of the functional group passivating the NC-Si surface. Recently, Zacharias group [1] reported that the N atoms incorporated at the NC-Si and a-SiO_2 interface change the position of the photoluminescence (PL) main peak toward the blue region and enhance the PL intensity. They explained the blue shift mainly originates from the larger Si-N bond polarity compared to the Si-O bond polarity. However, the microscopic origin of the effect is still vague due to the experimental difficulties. We have studied the effect of the N doping in the NC-Si and a-SiO_2 system by using the first-principles calculation. We find that the N atoms form a N pair (N_p) structure at the NC-Si and a-SiO_2 interface, and is more stable than other structures by amount of ~2 eV/N (Fig. 1). The N_p dopants change the eigen-energies of the HOMO-LUMO states with the interface state character, and as a result they increase the gap of the system by the amount of 7~17 meV/N_p.

[1] M. Zacharias et al., J. Appl. Phys. 116, 223501 (2014)

H1.06*

Electrical Resistivity and Improvement of Quasi-crystallinity of TiZrNi Quasicrystals by Addition of Ag

*이상화, 이근우 [1], 김재용
*Sang-hwa. Lee, Geun Woo. Lee[1], Jae-yong. Kim.
한양대학교. [1] 한국표준과학연구원.

Keyword : "TiZrNi alloy", "Quasicrystal", "electrical resistivity", "Ag"

TiZrNi 준결정체는 시료에 인가된 전압을 증가시킴에 따라 전류가 선형으로 증가하는데 이는 금속이 갖는 전형적인 전기적 특성이다. TiZrNi 준결정체의 비저항값은 일반적으로 상온에서 10^{-6} Ω·cm 의 order 를 갖는데, 이러한 비저항은 20 K 에서 가장 낮은 값을 갖으며, 이후 온도에 비례하여 증가한다.[1] 본 연구에서는 TiZrNi 준결정체의 특이한 비저항 현상을 규명하고 전기전도도를 최대화하기 위해, Ag 를 첨가하여 이에 따른 구조 변화와 전기저항의 변화를 조사하였다.

시료의 제작을 위해, $(Ti_{35.2}Zr_{43.8}Ni_{21})_{100-x}Ag_x$ (x=0, 2, 3 and 4) 혼합물을 준비하였고, 이는 각각 quenching 과 suction casting 방법으로 Ar 분위기에서 만들었다. 수소흡수는 P-c-T 곡선 측정을 통해 진행하였으며, 각각의 전기저항 평가는 I-V 곡선 측정으로 분석하였다.

Ag 를 첨가한 $(Ti_{35.2}Zr_{43.8}Ni_{21})_{100-x}Ag_x$ 준결정 시료에 대해서는 Ag 의 양을 0 에서 4 at. %로 증가시킴에 따라, 가간섭성 길이가 100 에서 153 Å 으로 증가하였고, 이는 시료의 결정성이 증가하였음을 의미한다. 비저항은 2.94 x 10^{-6} 에서 2.76 x 10^{-6} Ω·cm 으로 감소하였다. 이러한 이유는 두 가지로 설명할 수 있는데 첫번째는 시료의 가간섭성 길이가 증가한다는 것은 입자크기 (grain size)가 커지는 것을 의미하는데 이에 따라 결정립계 (garin boundary)가 줄어드므로, 자유전자의 이동이 용이해질 수 있다.[2] 두 번째로는 시료에 수소나 Ag 를 도핑함으로써 시료의 홀이동도 (Hall mobility), 혹은 캐리어농도 (Carrier concentration)가 증가하기 때문이라고 판단된다.[3]

참고문헌

1. V. Azhazha, V. Khadzhay, G. Malikhin, Phys. Lett. A 319, 539 (2003).
2. A. S. Wochnik, M. Handloser, D. Durach, A. Hartschuh and C. Scheu, Appl. Mater. Inter. 5, 5696 (2013).
3. N. Abbas, M. Abbas, W. A. Syed and W. Magmood, Iranica. J. Energy. Environment, 5, 87 (2014).

H2.01(초)

Quantum measurements of qubit states in semiconductor quantum dots

*김도헌
*Dohun. Kim
연세대학교.

Keyword : semiconductor quantum dot, quantum point contact, RF-reflectometry, quantum tomography

The charge and spin degrees of freedom of an electron constitute natural bases for constructing quantum two level systems, or qubits, in semiconductor quantum dots. The quantum dot charge qubit offers a simple architecture and high-speed operation, but generally suffers from fast dephasing due to strong coupling of the environment to the electron's charge. On the other hand, quantum dot spin qubits have demonstrated long coherence times, but their manipulation is often slower than desired for important future applications. This talk will present a broad introduction to experimental progress of a few different types of qubits focusing on qubit manipulation and quantum state measurement by a quantum point contact acting as a charge sensor. Basic operation sequence for rotating qubit states and how to measure intrinsic relaxation and coherence times of semiconductor quantum dot qubits will be discussed. Moreover, method of state and process tomography in semiconductor quantum dot qubits will be introduced in depth.

H2.02(초)

Quantum measurements of macroscopic mechanical oscillators

*서준호
*Junho. Suh
한국표준과학연구원.

Keyword : quantum measurement, mechanical oscillator, optomechanics

Started from theoretical studies of quantum limits in force measurements, quantum measurements of macroscopic mechanical oscillators recently reached the point of observing phenomena dominated by quantum effects of electromagnetic and acoustic fields. In this light, I discuss three recent experiments conducted with radio-frequency mechanical oscillators cooled down to near-ground state, which are tightly coupled to and probed by microwave photons - quantum back-action evading measurement of mechanical quadratures, motional sideband asymmetry, and quantum squeezing of motion. Here, the interplay between the mechanical oscillator and microwave photons manifests Heisenberg's uncertainty relations in various ways, and their strong mutual interaction allows manipulation and utilization of the fundamental quantum fluctuations.

H2.03(초)

Superconducting qubit and its applications

*조성운
*Sung Un. Cho
서울대학교 물리천문학부.

Keyword : quantum optics, optomechanics, superconducting qubit, electromagnetically induced transparency, Autler-Townes doublet

As an artificial atom, superconducting qubit (quantum bit) is efficient system to study quantum optics and to implement quantum information processing on a chip, because of its high sensitivity to external parameter and adjustability of discrete energy levels. In this talk, we introduce our recent two experimental results using superconducting qubit system.

First, we focus on a multi-level qubit system, so-called qudit, in a dressed state by microwave photons. The higher-levels above the two lowest levels of a qubit can serve an important role of reducing the number of elemental quantum gate operation and of quantum information storage. Especially, in a dressed state, the study of electromagnetically induced transparency (EIT) phenomenon is received much attention, because of its potential application as a quantum information storage. But EIT phenomenon accompany ac-Stark splitting, Autler-Townes (AT) doublet, thereby experimental discrimination between these two is still an important task. We investigated the occupation behavior of the levels for the applied photon strength in spectroscopy. Because, on the other hand, splitting of the AT doublet depends on the strength of photon which are resonant with the level transition, it is considered that the AT doublet is tunable effective multi-level system controlled by photon strength. We observed the Rabi oscillation through the AT doublet and this implies that the phase coherences of the AT doublet is useful as multivalued quantum logic elements.

Finally, we introduce another possible application of a superconducting qubit. Cavity or circuit optomechanical system is one of the studies for the light-matter interaction in the quantum regime. With sideband cooling technique, less than unity of mechanical phonon number can be observed, but the coupling strength between cavity photon mode and mechanical modes is still weak in current systems. We developed superconducting qubit integrated circuit optomechanical system to effectively increase the coupling strength. The radiation pressure interaction between two modes is mediated by charge-based qubit inserted between microwave cavity and charged mechanical resonator.

H3.01

First-principles studies of $Sr_2Ru_xIr_{1-x}O_4$ near metal-insulator transition

*고은정, 최형준
*Eunjung. Ko, Hyoung Joon. CHOI
연세대학교.

Keyword : metal-insulator transition, doped iridates, doped ruthanates

We study changes in electronic and magnetic structures from Sr_2IrO_4 to Sr_2RuO_4 by Ru doping from first-principles. The 5d transition-metal Ir compound Sr_2IrO_4 is a canted antiferromagnetic insulator with the novel J_{eff}=1/2 states while the 4d transition-metal Ru compound Sr_2RuO_4 is a nonmagnetic superconducting metal. Thus Ru-doped Sr_2IrO_4, $Sr_2Ru_xIr_{1-x}O_4$, shows a metal-insulator (MI) transition as x increases. Current interesting issues are where the MI transition occurs, how the J_{eff}=1/2 insulating bands of Sr_2IrO_4 evolve to metallic bands of Sr_2RuO_4 as x increases, and what magnetic properties of $Sr_2Ru_xIr_{1-x}O_4$ are near the MI transition. We will show electronic and magnetic properties of $Sr_2Ru_xIr_{1-x}O_4$ at x=0.4, 0.5, and 0.6 obtained by performing LSDA+U+SOI calculations. This work is supported by the NRF of Korea (Grant No. 2011-0018306). Computational resources have been provided by KISTI Supercomputing Center (Project No. KSC-2014-C3-070).

H3.02

Electronic Structure and Band Topology of Divalent YbB_6

Chang-Jong Kang, J. D. Denlinger[1], J. W. Allen[2], Chul-Hee Min[3], F. Reinert[3], B. Y. Kang[4], B. K. Cho[4], J.-S. Kang[5], J. H. Shim[6], B. I. Min
Chang-Jong. Kang, Jonathan. Denlinger[1], James. Allen[2], Chul-Hee. Min[3], Friedrich. Reinert[3], B. Y.. Kang[4], B. K.. Cho[4], J.-S.. Kang[5], J. H.. Shim[6], B. I.. Min
Dept. of Physics. POSTECH. [1]Advanced Light Source. Lawrence Berkeley Laboratory. [2]Randall Laboratory. University of Michigan. [3]Universitat Wurzburg. Experimentelle Physik. [4]School of Materials Science and Engineering. GIST. [5]Dept. of Physics. The Catholic University of Korea. [6]Dept. of Chemistry. POSTECH.

Keyword : Electronic structure, Band topology, Topological Kondo insulator

To resolve the controversial issue of the topological nature of the electronic structure of YbB_6, we have made a combined study using density functional theory (DFT) and angle resolved photoemission spectroscopy (ARPES). Accurate determination of the low energy band topology in DFT requires the use of modified Becke-Johnson exchange potential incorporating the spin-orbit coupling and the on-site Coulomb interaction U of Yb 4f electrons as large as 7 eV. We have double-checked the DFT result with the more precise GW band calculation. ARPES is done with the non-polar (110) surface termination to avoid band bending and quantum well confinement that have confused ARPES spectra taken on the polar (001) surface termination. Thereby we show definitively that YbB_6 has a topologically trivial B 2p-Yb 5d semiconductor band gap, and hence is a non-Kondo non-topological insulator (TI). In agreement with theory, ARPES shows pure divalency for Yb and a p-d band gap of 0.3 eV, which clearly rules out both of the previous scenarios of f-d band inversion Kondo TI and p-d band inversion non-Kondo TI. We have also examined the pressure-dependent electronic structure of YbB_6, and found that the high pressure phase is not a Kondo TI but a p-d overlap semimetal.

H3.03*

Field-induced quantum criticality in α-$RuCl_3$

*최광용, 도승환
*Kwang Yong. Choi, S. –H.. Do
중앙대학교.

Keyword : Kitaev honeycomb lattice, quantum criticality, spin liquid, structural phase transition

Kitaev spins on a honeycomb lattice offer a benchmark to explore topological and quantum spin liquids whose emergent excitations are dispersive Majorana fermions and static Z_2 gauge fluxes. We have successfully grown high-quality single crystals of α-$RuCl_3$ using a vacuum sublimation method, which is regarded as a prime candidate for the Kitaev honeycomb magnet. Our crystals are nearly free from stacking faults, judging from the large suppression of the magnetic anomalies around 14 K. In this talk, we present magnetic and structural properties of α-$RuCl_3$ as a function of temperature and external magnetic field. We observe a first-order structural phase transition from a monoclinic (C2/m) to rhombohedral (R-3) structure with huge hysteresis loop. The major finding is that when an external field is applied along the honeycomb plane, a long-range magnetic order is melted to a quantum disordered phase, providing evidence for a quantum critical point at about 8 T. This result suggests that α-$RuCl_3$ provides us with a platform for studying two-dimensional quantum criticality in a Heisenberg-Kitaev system.

H3.04*

Strain engineering of $BaBiO_3$ thin films via using buffer layers

*김기덕, 이한결 [1], 김민우, 노태원
*Gideok. Kim, Hangyeol. Lee[1], Minu. Kim, Tae Won. Noh
서울대학교. [1] *서울대학교 물리천문학부.*

Keyword : charge density wave, strain control, heterostructure engineering, oxide thin film

Strain engineering of $BaBiO_3$ thin films via using buffer layers

Han Gyeol Lee[1,2], Gideok Kim[1,2], Minu Kim[1,2], Tae Won Noh[1,2]
[1]Center for Correlated Electron Systems, Institute for Basic Science (IBS), Seoul 151-742, South Korea
[2]Department of Physics and Astronomy, Seoul National University, Seoul 151-742, South Korea

Recently, perovskite oxide heterostructure has attracted wide interest as a playground of novel electronic phases [1]. Strain engineering is a crucial method in the realization of such phases, which allows us to modify oxygen octahedral structure that dominates physical properties of perovskite oxides [2, 3]. $BaBiO_3$, known as a charge density wave insulator and a parent compound of high-T_c superconductors [4], can be a prime candidate to apply such a method: The significant interplay of breathing distortion and octahedral tilting distortion is predicted to alter the electronic properties of this compound [5]. However, lack of commercial substrates commensurate with $BaBiO_3$ ($a_{pseudo\text{-}cubic}$ = 4.34 Å) has hindered further experimental studies.
Here, we utilize a buffer layer for the control of strain in $BaBiO_3$ films. $BaZrO_3$ and $BaCeO_3$ are used as a buffer layer, because of their small mismatch with $BaBiO_3$ (3 % and -1 %, respectively). First, we grow high-quality thick $BaZrO_3$ and $BaCeO_3$ thin films on a $SrTiO_3$ substrate by pulsed laser deposition, and make them relaxed. Subsequently, $BaBiO_3$ films are grown on top of the $BaXO_3$ (X = Zr, Ce) films. X-ray diffraction reciprocal space mapping is conducted to confirm that our films are strained. These results show not only the first experimental realization of strained $BaBiO_3$ films, but also a model system to synthesize other perovskite oxides with large lattice constant (> 4 Å). In this talk, we will discuss about structural and electronic properties of strained $BaBiO_3$ films in detail.

[1] A. Ohtomo and H. Y. Hwang, Nature 427, 423 (2004).
[2] J. M. Rondinelli et al., MRS Bulletin 37 (2012)
[3] W. Lu et al., Sci. Rep. 5, 10245 (2015).
[4] A. W. Sleight, Physica C 514, 152 (2015).
[5] K. Foyevtsova et al., Phys. Rev. B 91, 121114 (2015).

H3.05*

Anomalous optical properties of $SrMnSb_2$ due to thermal effect in multiband system

*박현주, 루크, 유정상 [1], 지효석 [1], 손창희, 한정우 [2], 문순재 [3], 김경완 [4], 심지훈 [1], 김준성 [1], 노태원
*H. J.. Park, Luke. Sandilands, J. S.. YOU[1], Hyo Seok. Ji[1], C. H.. Sohn, J. W.. Han[2], S. J.. Moon[3], K. W.. Kim[4], J. H.. Shim[1], Jun Sung. Kim[1], T. W.. NOH
서울대학교. [1] 포항공과대학교. [2] 광주과학기술원. [3] 한양대학교. [4] 충북대학교.

Keyword : "SrMnSb2","optical spectroscopy","multiband system","thermal effect"

We report an optical spectroscopic study of $SnMnSb_2$, a low carrier density metal. As temperature is decreased, our measurements reveal a large increase in the free carrier plasma frequency, which is highly unusual for a metal. This seemingly anomalous behavior can be accounted for using a 'three band' model of the multiband electronic structure of $SrMnSb_2$ that includes two conduction bands and one valence band close to the Fermi level. The temperature dependence of the low-lying interband optical transitions and the Hall number can also be understood using our model. The phenomenology of such a 'three band' scenario has not been widely considered and our results provide a possible explanation for the puzzling optical properties that have been reported in a number of topical low carrier density metals and semimetals.

H3.06*

Spin-orbit coupling induced band structure topology and orbital character of epitaxial IrO_2 film

*김우진, 김소연 [1], 김충현 [2], 손창희 [3], O. B. Korneta[3], 채승철 [4], 노태원 [5]
*Woo Jin. Kim, Soyeun. Kim[1], Choong Hyun. Kim[2], Chang hee. Sohn[3], O. B.. Korneta[3], Seung Chul. Chae[4], Tae Won. Noh[5]
서울대학교. [1]Center for Correlated Electron Systems. Institute for Basic Scie. [2]Center for Correlated Electron Systems. Institute for Basic Science (IBS). [3]Center for Correlated Electron Systems. IBS. [4]Department of Physics Education. Seoul National University. [5]Seoul 151-747.

Keyword : Spin-orbit coupling, IrO_2, J_{eff} = 1/2 state

We investigated the electronic structure of IrO_2 to address the controversy regarding spin-orbit coupling (SOC) effects in metallic 5d transition metal oxides. The effects of SOC on the physical properties of IrO_2 have been studied extensively, but have recently received much attention. Two issues have come to the forefront: (1) SOC effects on the behavior and electronic structure of IrO_2 and (2) the possible formation of a novel ground state in this material, called as the J_{eff} = 1/2 state. To better understand the SOC mechanism, we grew epitaxial IrO_2 films, whose dc resistivity values were comparable with those of a single crystal. We measured obtained polarization-dependent optical and X-ray absorption spectra and compared these results with those acquired using the generalized gradient approximation plus Hubbard U (GGA+U) and GGA+U+SOC calculations. From the optical spectra, peak structures were identified at 0.5 and 2.0 eV, which could only be explained using the GGA+U+SOC) calculation. This suggests that SOC plays an important role in the electronic structure of IrO_2. From the polarization-dependent O 1s XAS spectra, we observed that the empty state near the Fermi level is formed mainly composed by of Ir d_{yz} and d_{xz} orbitals, hybridized with O $2p_z$ orbitals. The lack of involvement of the Ir d_{xy} orbital suggests that, despite the importance of SOC in IrO_2, it is not strong enough to result in the J_{eff} = 1/2 state does not form in metallic IrO_2.

H3.07*

Temperature evolution of Fermi surface of the Anderson lattice model in the Kondo lattice regime studied by DMFT with CTQMC impurity solver

*강한힘, 최홍철, 김재녕, 심지훈
*Hanhim. Kang, Hong Chul. Choi, Jae Nyeong. Kim, Ji Hoon. Shim
포항공과대학교.

Keyword : DMFT, Anderson Lattice Model, Heavy Fermion, Temperature evolution

We have investigated the temperature evolution of the Fermi surface of the Anderson lattice model with two-dimensional square lattice in the Kondo lattice regime by the dynamical mean-field theory (DMFT) with continuous-time Monte Carlo (CTQMC) impurity solver. As temperature increases, the Fermi surface evolves continuously from the large Fermi surface of heavy Fermi liquid to the small Fermi surface with local spin moment. In addition to the area of the Fermi surface, the coherency of the Fermi surface dramatically changes during the large-to-small phase transition. We also report the temperature evolution of the quasi-particle interference (QPI) pattern and transports such as the resistivity (ρ) and Hall angle (θ_H).

H4.01(초)

천연 단백질 실크를 활용한 광학소자 연구

*김성환
*Sunghwan. Kim
아주대학교.

Keyword : 실크 단백질, 나노광학, 광소자, 생체적합성, 의공학

누에에서 추출한 천연 단백질 중 하나인 실크 피브로인은 생체적합성과 더불어 독특한 기계적, 화학적 물성을 지녀 의공학 분야에 활발하게 적용되어 온 물질이다. 최근 마이크로/나노 공정기술의 적용과 광학적 특성을 활용한 다양한 전기/광학 소자가 연구되고 있으며, 생체적합성을 기반에 둔 첨단기술기반 의공학 소자로의 적용이 활발하게 이루어지고 있다. 본 발표에서는 실크 단백질을 활용한 다양한 광학소자 연구를 본 연구실 연구 성과를 바탕으로 논의하고자 한다.

H4.02

Understanding PI3K in Cancer at the Single-Molecule Level

*손민주, 윤태영
*Min Ju. Shon, Tae-Young. Yoon
KAIST.

Keyword : Single-molecule imaging, Fluorescence, PI3K, Cancer

PI3K-Akt signaling pathway controls cell growth, proliferation, and motility, and is frequently deregulated in many types of cancer. PI3K is a lipid kinase that converts PIP2 into PIP3 on membrane, which then recruits downstream signaling proteins such as Akt. Traditionally, the activity of PI3K has been probed indirectly by the phosphorylation of Akt. Here, we developed a technique that directly measures the activity of PI3K by single-molecule fluorescence. In this method, surface-tethered PI3K phosphorylates PIP2 on nearby vesicles, fluorescently-tagged Akt is introduced, and its binding to vesicles is imaged to quantify PI3K activity. After validating the method with fluorescent protein-tagged PI3K, we extend this assay to endogenous PI3K from breast cancer cells to understand the response of cancer cells to PI3K inhibitors. We hope this assay could be useful in screening for PI3K inhibitors or guide selection of cancer patients for PI3K-targeted therapy.

H4.03*

Probing transcriptional dynamics by fluorescent imaging in living cells

*양소라, 김승현, 김동균, 김철희, 안형전, 이남기
*Sora. Yang, Seunghyeon. Kim, Dong-Kyun. Kim, Cheolhee. Kim, Hyeong Jeon. An, Nam Ki. Lee
포항공과대학교.

Keyword : Fluorescence imaging, Transcription

Unlike eukaryotes, transcription and translation in bacteria happen on the same space simultaneously. It has been reported that the transcription elongation rate is tightly controlled by translation rate of ribosome. However, fluorescence imaging have revealed that ribosomes are separated from the DNA and RNA polymerase (RNAP). Thus it is still unknown how the problem of spatial separation between transcription and translation is solved in living cell. Using in vivo single-molecule detection techniques, we found that the gene transcribed by RNAP is moved toward the outside of nucleoid by the translating ribosome. As a result, the transcription initiation rate is increased in living E.coli. Collectively, this cellular spatial organization by cooperation between transcription and translation play a crucial role in gene expression in E.coli.

H4.04*

Simultaneous kinetic analysis of multiple states of EGFR in a living cell using single-particle tracking

*김동균, 안형전, 이남기
*Dong-Kyun. Kim, Hyeong Jeon. An, Nam Ki. Lee
포항공과대학교.

Keyword : Single-particle tracking, Live cell imaging, Reaction progress kinetic analysis,

Cellular processes occur through the regulation of multiple molecular reactions. Reaction progress kinetic analysis (RPKA) of these molecular reactions can provide mechanistic information to understand the cellular processes generated by multi-step reactions. However, current tools are limited to simultaneously measure the variations of the multiple states in a living cell. Here, we combine single-particle tracking (spt) and RPKA methods to simultaneously analyze the kinetics of the multiple states of membrane protein in a living cell. Based on different intrinsic diffusivities of states, we extracted relative concentration of each state from the diffusion-coefficient distribution acquired by single particle tracking using stochastic super-resolution microscopy. Using this approach, we investigated the simultaneous kinetics of the four distinct complex states of EGFR induced by Cetuximab. And we also performed simulation at various situations for interpretation and comparison.

H5.01(초)

드론기술개발 최근 동향과 전망

*이충희
*RHEE Chunghi.
한국과학기술정보연구원 ReSEAT 프로그램.

Keyword : "드론, 무인항공기, 자율조종, 원격조종, 항법"

드론(무인항공기)은 조종사가 탑승하지 않고 자율비행과 원격조종이 가능한 비행체를 말하며, 신성장동력이 될 수 있는 이머징기술로서 군사적 목적 외에 민간용과 상업용으로 확대될 것으로 전망된다. 본 논문에서는 드론의 핵심기술해설과 국내외 연구개발 현황, 기술정보 현황 등을 분석하여 미국, 유럽, 일본, 한국, 이스라엘 등 주요국의 드론기술의 수준을 평가하고, 관련기술의 당면과제와 발전방향을 제시하였다. 드론기술은 1) 드론의 설계와 제작, 2) 센싱과 제어, 3) 감지·회피기술, 4) 인지무선기술 등으로 분류하여 기술하였다. 미국, 유럽, 일본, 한국, 이스라엘 등 주요국의 드론기술 수준을 비교분석한 결과 미국이 압도적으로 우세하여 1 위이며, 다음은 이스라엘, 유럽, 한국, 일본 순이다. 한국은 핵심기술 분야에서 선진국 대비 기술력이 상대적으로 취약하며, 기술개발을 위한 전문인력 및 장비 등 인프라가 부족하다. 본 연구는 한국과학기술정보연구원이 수행하고 있는 미래창조과학부의 과학기술진흥기금 출연사업인 ReSEAT 프로그램에 의해 수행되었다.

H5.02*

Multi-Level Memory Effect of CVD Graphene Transferred on SiO_2 by Gate-Voltage Controlled Hydron Adsorption

Sungchul Jung, Junhyoung Kim, Hoon Hahn Yoon, Han Byul Jin, Gahyun Choi, Jung-Yong Lee, Daejin Eom[1], *박기복
Sungchul. Jung, Junhyoung. Kim, Hoon Hahn. Yoon, Han Byul. Jin, Gahyun. Choi, Jung-Yong. Lee, Daejin. Eom[1], *Kibog. Park
Ulsan National Institute of Science and Technology. [1]*Korea Research Institute of Standards and Science.*

Keyword : Graphene, Multi-Level Memory, Hydron Adsorption, Charge Neutrality Point, Conductivity Modulation

Memory effect of graphene has been studied in various ways based on the Fermi-level shift driven by external electric field. From the current hysteresis loop obtained by changing the gate voltage of Graphene/SiO_2/Si field effect transistor, the existence of two different channel conductivity states has been observed which can be used for a two-level memory device. [1] This phenomenon has been explained by the motion of hydroxides and hydrons ionized from the water molecules trapped between the graphene channel and the SiO_2 gate insulator. [2] In this study, we fabricated a CVD-grown graphene field effect transistor on SiO_2/Si substrate and found four different channel conductivity states tunable by varying the applied gate voltage pulse. It is shown that the stabilization of the reset state (off-state), which is one of the challenging issues in fabricating memory devices with this phenomenon, can be achieved by positioning the Fermi-level in the off-state as close to the charge neutrality point as possible during read-out. A constant gate voltage which is chosen to ensure the proper positioning of the off-state Fermi-level is always applied in read-out steps. This study demonstrates the possibility of fabricating graphene-based multi-bit memory devices.

[1] E. U. Stützel, M. Burghard, K. Kern, F. Traversi, F. Nichele, R. Sordan, Small 6, 2822-2825 (2010).
[2] X. Hong, J. Hoffman, A. Posadas, K. Zou, C. H. Ahn, J. Zhu, Appl. Phys. Lett. 97, 033114 (2010).

H5.03

Computational Study of the Recovery of Dirac Point Energy by Self-Assembled HTC Layers on Graphene

*최지일, 심윤수, 유영준 [1], 안석훈 [2], 김용훈
*JI IL. CHOI, Yoon su. Shim, Young-Jun. Yu[1], Seok Hoon. Ahn[2], Yong-Hoon. Kim
KAIST. [1]ETRI. [2]KIST.

Keyword : Graphene, HTC, silica

We present a computational study of graphene surface about the relaxation of surface geometry on amorphous silica. Corrugated surface geometry of the graphene has reported and implied to take detrimental effects on electronic mobility. Recent studies show that the mobility could be improved using the self-assembly of ordered molecular lattices. To investigate the improvement of electronic properties, we have developed computational models and studied the intriguing phenomena due to the self-assembly of hexatriacontane (HTC) using density functional theory and classical forcefield based molecular dynamics. It is found that the electronic mobility of the graphene is deteriorated by the close adhesion to the irregular silica surface. To recover the flatten geometry, the graphene sheet should be detached from pitfalls, more than 4 Å. Simulations demonstrates that the surface morphology of graphene comes after the shape of silica surface, and also it could be recovered by employing the self-assembling HTC layers. The interactions between graphene and HTC are calculated to overcome the competitive binding strength between graphene and silica surface, and contribute to the recovery of the structural properties, and thereby electronic properties of the graphene. The recovery of the electronic properties are discussed in terms the position of the Dirac point, and recovery from the p-type nature of graphene on the amorphous silica.

H5.04*

구조적 비대칭을 갖는 H 모양의 나노 메타물질에서 상쇄간섭 현상에 대한 양자적 분석

*이동현, 함병승
*Donghyun. Lee, ByoungSeung. Ham
광주과학기술원.

Keyword : "나노 메타물질","플라즈몬 유도투과현상","플라즈몬 스위칭","간섭 효과"

구조적 비대칭을 갖는 H-모양의 나노 메타물질에서 나타나는 상쇄간섭 효과인 플라즈몬 유도투과현상을 양자광학적 접근법으로 분석하였다. 양자광학의 전자기유도투과와 같이 전자기파에 의해 발생한 메타물질 경계면에서의 국소적 표면플라즈몬은 대칭적 보강간섭과 상쇄간섭 효과에 의해 플라즈몬 스위칭 현상이 일어남을 규명하였고, 기존의 다양한 모델에서의 표면플라즈몬 유도투과 관측을 동일한 이론으로 설명하였다. 결과적으로 나노메타물질의 구조적 변화를 선제적으로 통제하여 표면 플라즈몬 회로구성에 대한 기초이해를 확립할 수 있는 계기가 되었다.

H5.05

Synthesis parameter adjustments for better performing reduced graphene oxide transparent electrodes and supercapacitor electrodes

*강영호, 김용재 [1], 이광희 [1]
*Yung Ho. Kahng, Yong Jae. Kim[1], Kwanghee. Lee[1]
전남대학교. [1]Gwangju Institute of Science and Technology (GIST).

Keyword : Graphene, Graphene oxides, Transparent electrode, Supercapacitor

Solution-processed graphene oxides are mass production compatible. They can be made to conducting graphene after a reduction. Graphene films have potentials for various applications such as transparent electrodes for organic optoelectronics and energy-storing porous electrodes for supercapacitors. The modified Hummers' method is a major synthesis method. For the applications, precise control of the synthesized properties of graphene oxide is needed. However, the effects of the synthesis parameters are still not well understood, hindering the advance of the applications for graphene oxides. Here, we present our study results on the effects of the various synthesis parameters on the properties of the graphene oxides. The properties of graphene electrodes were investigated using UV-visible spectroscopy, Hall measurements, atomic force microscopy, X-ray photoelectron spectroscopy, and cyclic voltammetry. Our focus was on the transparent electrode and the supercapacitor electrode applications. The results reveal that increasing the oxidization parameters improves morphological and optoelectrical properties of the graphene thin films. On the other hand, the synthesis parameter improvements had little role in the performance for the supercapacitor electrodes applications, instead, the thermal reduction using thermal shocking was found to show a bigger effect.
Fig. 1. Synthesis parameter adjustment for GO improved the morphology of the spin-coated thin films.

H5.06

ZnO-Graphene oxide- based Piezo-triboelectric Hybrid Nanogenerator

Viyada HARNCHANA, Hyunh Van NGOC, Simgeon OH, *강대준
Viyada. HARNCHANA, Hyunh Van. NGOC, Simgeon. OH, *Dae Joon. KANG
성균관대학교.

Keyword : ZnO-Graphene oxide, Piezo-triboelectric Hybrid Nanogenerator

A hybrid piezo-triboelectric nanogenerator based on ZnO and graphene oxide (GO) is developed. Piezoelectric ZnO nanoflakes (NFs) are firstly grown onto indium tin oxide (ITO) substrate via a solution based hydrothermal method. GO triboelectric layer is then directly coated onto the prepared ZnO NFs film by a simple dip-coating technique. The piezo-triboelectric nanogenerator device is assembled using polyethylene terephthalate (PET) as a moving electrode. Under periodic compressive stress, short-circuit current (I_{sc}) and open-circuit voltage (V_{oc}) of 8 μA and 60 V were achieved from the ZnO-GO based nanogenerator, which are higher than those of ZnO-based piezoelectric nanogenerators (I_{sc} = 5 μA and V_{oc} of 30 V). This may be attributed to oxygen-containing functional groups in GO that enhance charge generation and storage during electrification and electrostatic induction processes. This finding could be beneficial for the development of high efficiency and low cost energy harvesting devices.

H5.07*

Control-factors for colloidal nanoparticle assembly fabrication on a self-assembled monolayer-patterned substrate

*양미선, 문병기, 장재원
*Mi Sun. Yang, Byung Kee. MOON, Jae-Won. Jang
부경대학교.

Keyword : colloidal assembly, nanoparticle patterning, soft lithography

This study investigates which factors mainly influence fabrication of colloidal nanoparticle (NP) assembly on a self-assembled monolayer (SAM) patterned substrate with using zirconia (ZrO_2) NP assembly on a poly(dimethylsiloxane) (PDMS)-stamped Au substrate. The ZrO_2 NP assembly was carried out by changing size of the NPs, polarity of the substrate, and surface charge of both the NPs and the substrate. ZrO_2 particles with diameters of 300 nm, 600 nm, and 1300 nm were employed to examine the effect of NP size on the assembly. Besides bare ZrO_2, NPs with a negatively charged surface and ZrO_2 NPs with a positively charged surface through 3-aminopropyltriethoxysilane (APTES) encapsulation were prepared for the NP assembly. Moreover, the substrate polarity effect on the NP assembly was evaluated by comparing the assembly on substrates with the PDMS-patterned SAMs of thiols with polar and non-polar functional groups. In conclusion, it was found that the dispersion of NPs and contrast of polarity of SAMs work more effectively on the assembly of colloidal NPs on the SAM-patterned substrate than electrostatic interaction.

H6.01

Real-time Evolution of Poly (3-hexylthiophene) type-II Phase and its Super-lattice Structure in P3HT:PCBM Blend thin films

*이현휘, 이시우 [1], 금희성 [1], 김효정 [1], 이동렬 [2], 김제한
*Hyun Hwi. Lee, Si Woo. Lee[1], 희성. 금 [1], Hyo Jung. Kim[1], Dong Ryeol. LEE[2], Jehan. KIM
포항가속기연구소. [1] 부산대학교. [2] 숭실대학교.

Keyword : P3HT, type-II phase, temperature-dependence, cryogelation, super-lattice, crystal alignment

We observed the temperature-dependent evolution and behavior of P3HT type-II phase during a real time annealing process from a cryo-cooled low temperature in the absence and presence of an Al electrode. A poly (3-hexylthiophene) (P3HT) Type-II phase in the P3HT:PCBM films started to form near at -10℃, regardless of Al layer presence. In the absence of an Al layer, type-II phase was extinct at 30℃. However, the extinction temperature was extended to 50℃ in the presence of the Al layer. Simultaneously, combined with the type-II phase, a 1:3 ordered P3HT type-II (1/3,0,0) super-lattice peak evolved. These type-II domains tended to be formed near the Al electrode layer with higher aligned status than host P3HT crystals.

H6.02*

Photoluminescent Intermediate Layer for Organic Tandem Solar Cell

Ho Nhu Thuy, *김용수
Nhu Thuy. Ho, *Yong Soo. Kim
울산대학교 물리학과 및 EHRSC.

Keyword : Organic Tandem Solar Cell, Intermediate Layer, Graphene Quantum Dot

Graphene quantum dot (GQD) thin films with high transparent and good conductivity have been demonstrated to be efficient holes transport layer (HTL) for organic solar cells [1]. The performances of devices with GQDs as the HTLs are comparable to those of the cells using either conventional PEDOT:PSS or reduced GO-based material. Importantly, GQD exhibits strong photoluminescence effect in visible light region when their diameter is less than 10 nm. Therefore, GQD shows a big potential for further applications in organic solar cell. At present, the most common method to improve power conversion efficiencies of organic solar cell is stacking two sub-cells in serial tandem configuration. By using GQD and PEI as an intermediate connecting layer, our P3HT:PCBM tandem device show significant improvement in fill factor (10%) and efficiency (15%) in compare to devices using PEDOT:PSS polymer. The optimal tandem cells with GQD show the double open-circuit voltage of 1.16 V, short-circuit current density of of 5.67 mA/cm^2, fill factor of 0.55 and power conversion efficiency of 3.60 % under AM 1.5G solar irradiation.

[1] M Li, W Ni, B Kan, X Wan, L Zhang, Q Zhang, Q Long, Y Zuo and Y Chen, Phys. Chem. Chem. Phys. 15, 18973 (2013)

H6.03

High efficient inverted bulk-heterojunction solar cells with a gradiently-doped ZnO layer

노성호, *조신욱
SUNGHO. NHO, *Shinuk. Cho
울산대학교.

Keyword : Organic Solar Cells; ZnO; doping; metal carbonate

In this study, we demonstrate a highly efficient inverted bulk heterojunction (BHJ) polymer solar cell using a wet-chemically prepared doped ZnO with a self-organized ripple nanostructure as an electron extraction layer and a blend of poly[[4,8-bis[(2-ethylhexyl)oxy]benzo[1,2-b:4,5-b′]dithiophene-2,6-diyl][3-fluoro-2-[(2-ethylhexyl)-carbonyl]-thieno-[3,4-b]thiophenediyl]] (PTB7) and [6,6]-phenyl C71 butyric acid methyl ester ($PC_{71}BM$) as an active light absorbing layer. In order to enhance the electron extraction efficiency, the ZnO ripple surface was modified with various alkali metal carbonate materials including Li_2CO_3, K_2CO_3, Na_2CO_3, Cs_2CO_3, and $(NH_4)_2CO_3$. The inclusion of an additional metal carbonate layer led to gradient doping of the ZnO ripple layer and improved the electron extraction properties by modifying the energy level without destroying the ZnO ripple structures. The highest performing solar cells were fabricated with Li_2CO_3 and yielded a PCE of 10.08%; this value represents a ~14% increase in the efficiency compared to solar cells without a metal carbonate treatment.

H6.05

Optical spin Hall effect in out-of-plane refraction

*이연의, 우정원
*Yeon Ui. Lee, Jeong Weon. Wu
이화여자대학교.

Keyword : Optical spin Hall effect, metasurface

In this report, we study optical spin Hall effect (OSHE) at 2D-phase-discontinuity metasurface (PMS). Spin-dependent beam shift is not restricted to the direction perpendicular to incidence plane and can be controlled by manipulating additional momentum of metasurface. OSHE at PMS shows a new type of spin separation which has in-plane spin separation component, different from the Goos-Hanchen shift induced by total internal reflection and optical spin Hall effect at traditional medium interface.

H6.06*

레이저 간섭 리쏘그래피를 이용한 점진적 주기 변화 패턴 제작

*김한빛, 정현호, 전헌수
*Kim Hanbit. , Jung Hyun ho. , JEON Heon Su.
서울대학교.

Keyword : 레이저 간섭 리쏘그래피, 점진적 주기 변화 패턴, Laser interference lithography, Period-chirped grating

오늘날 LED, 태양광전지 산업을 비롯한 여러 분야에서 나노 혹은 마이크론 이하 (sub-micron) 크기의 패턴을 제작할 수 있는 리쏘그래피 기법은 점점 더 중요해지고 있다. 이러한 중요성 때문에 레이저 간섭 리쏘그래피(laser interference lithography)나 나노스피어 리쏘그래피(nanosphere lithography) 등과 같이 대면적에 마이크론 이하 크기의 패턴을 제작할 수 있는 리쏘그래피 기법에 대한 연구가 활발하게 이루어지고 있다. 그 중에서도 레이저 간섭 리쏘그래피는 대면적에 빠른 생산률(high-throughput)로 패턴을 제작할 수 있으면서도 비용이 적게 드는 리쏘그래피 기법이다. 그러나 레이저 간섭 리쏘그래피로는 주기가 일정한 패턴만 제작 가능하다는 한계가 있다. 본 연구에서는 이러한 레이저 간섭 리쏘그래피의 한계를 극복하여 대면적의 단일 샘플 내에서 점진적으로 주기가 변화하는 패턴을 제작할 수 있는 레이저 간섭 리쏘그래피 기법을 제안한다. 우리가 사용한 레이저 간섭 리쏘그래피 시스템은 샘플 면과 수직한 방향으로 반사 거울을 배치하는 Lloyd 거울 구성을 채용하고 있으며, 이 때 Lloyd 거울 구성에서 평면 반사 거울 대신에 원통형의 오목 반사 거울을 사용하면 샘플로 입사되는 두 빛 중 하나의 입사각을 점진적으로 변화시킬 수 있고, 점진적인 입사각의 변화는 곧 제작하는 패턴의 주기 상에 점진적인 변화로 이어진다. 원통형의 오목 반사 거울을 이용하여 2 X 2 cm^2 크기의 샘플에 중심 주기가 ~600 nm, 주기의 변화 범위가 80 nm 인 period-chirped grating 을 제작하였다. 본 연구에서 제안한 period-chirped grating 제작 방법은 가변 파장 레이저나 가변 색상 필터 등 다양한 광소자 분야에서 응용 가능성이 큰 리쏘그래피 기법으로 판단된다.

H6.07*

Light collection strategies from truncated conical single quantum dot structures

*바산단, 장유동, 이동한
*Vasanthan. Devaraj, Yudong. Jang, Donghan. Lee
충남대학교.

Keyword : Single quantum dot, Single photon source, Photon extraction efficiency, Photon collection efficiency, Simulations

In recent years development of single photon sources (SPS) became more important in field of telecommunications such as quantum cryptography, quantum teleportation, quantum computation etc. Single quantum dot (SQD) based structures have gained greater interest in realization of SPS which are highly efficient in quantum light generation. Introduction of semiconductors in field of SPS is not an easy task. While coming to bare semiconductor structures with n = 3.5, photons generated from QD suffer serious total internal reflection. So by fact, even though QD has a high internal quantum efficiency, probability of collecting them in experimental system remains very low (~ < 1 %). Therefore necessity of designing an effective SQD structure becomes so important in realization of a good SPS as well as investigation of SQD physics. With the help of 3D finite element method (FEM) and finite difference time domain (FDTD) simulations, we designed a truncated conical single quantum dot structure which exhibited good photon collection efficiency (PCE). A parabolic solid immersion lens structure on top of the truncated conical structure further helps in improving PCE which leads us to a very bright SPS.

Figure: Far-field profile of our optimized single quantum dot structure which shows very good PCE within 0.41 NA.

H6.08*

광 흡수 증가를 위한 실리콘 나노와이어 광학 안테나의 형상 제어 연구

*고민지, 백성호, 송보경, 김신애, 조창희
*Minjee. Ko, Seong-Ho. Baek, Bokyung. Song, Shin-Ae. Kim, Chang-Hee. Cho
DGIST.

Keyword : "나노와이어", "형상 제어", "광 흡수"

태양전지나 광 검출 소자의 표면에 광학 안테나 구조를 적용시킴으로써 광 흡수 효율을 증가시키는 연구가 많이 진행되고 있다. 특히, 반도체 나노와이어 구조의 경우, 리키 모드(leaky mode)에 의한 광 가둠 효과로 인하여 광 흡수 효율이 향상된다는 점이 알려져 있다. 넓은 파장 대역에 걸쳐 광 흡수 효율을 증가시킬 수 있는 광학 안테나 구조를 구현한다면 고효율 광 소자 개발에 응용할 수 있을 것으로 기대된다. 본 연구에서는 지름이 주기적으로 변화되는 물결 형상 실리콘 나노와이어 어레이의 광 흡수 현상을 연구하였다. 일반적인 실리콘 반도체 공정기술을 사용하여 나노와이어 표면에 물결 형상 구조를 형성하였다. 450 ~ 900 nm 파장 대역에서 물결 형상 실리콘 나노와이어의 광 흡수는 평면의 벌크 실리콘과 비교하여 약 41.6% 증가하였고, 단일 지름을 가지는 실린더 나노와이어와 비교하여 약 25% 증가함을 확인하였다. 또한, Finite-difference time-domain 방법을 이용한 계산을 통하여 물결 형상 나노와이어의 광 흡수 향상 효과를 이론적으로 검증하였다. 그 결과, 물결 형상 나노와이어의 주기적인 지름에 의해 단일 지름을 가지는 나노와이어 보다 넓은 파장 대에 걸쳐 다중의 증강된 공명 현상이 일어나며, 이를 통해 물결 형상 나노와이어가 향상된 광 흡수 특성을 갖는다는 것을 확인하였다.

H7.01(초)

물질연구를 위한 양자계산 튜토리얼

*한승우
*HAN Seungwu.
서울대학교.

Keyword : 양자계산, 고체물리, 재료물리, 전자구조

본 강의에서는 최근 물질연구 분야에서 많은 주목을 받고 있는 제일원리 기반 양자계산 방법에 대해서 초보자 수준의 튜토리얼을 하고자 한다. 배경 지식으로는 고체물리에 학부생 수준의 이해만 있으면 된다. 이를 바탕으로 제일원리 계산법의 기초이론과 간단한 물질에 적용하는 사례를 소개하고 결과를 물리적으로 어떻게 해석하는지 소개할 계획이다.

H7.02(초)

제 1 원리 계산 온라인소프트웨어 구축 및 교육/연구 활용

*김용훈, 김후성
*Yong-Hoon. Kim, Hu Sung. Kim
한국과학기술원.

Keyword : First-principles calculation, Atomistic multiscale simulation, Nanomaterials, Physics education

First-principles and force-fields simulation softwares have matured into powerful and accessible platforms for education as well as research in nanosicence and nanotechnology. Since 2008, our group has actively developing a Python-based software toolkit NanoCore that provides easy-to-use interfaces for modeling various nanostructrures and automating electronic structure and multiscale computations [1]. Several nanostructure modelers and interfaces to simulators SIESTA and LAMMPS have been uploaded on EDISON Nano-Physics webpage [2]. In this presentation, after describing our protocol of develping steering interfaces for legacy codes in Python, I will demonstrate examples of using these tools in solid-state physics class and research on low-dimensional nanomaterials.

[1] H. S. Kim and Y.-H. Kim, Phys. Rev. B 82, 075412 (2010).
[2] https://www.edison.re.kr/web/nano

H7.03(초)

나노 전자 소자 해석을 위한 계산 방법 및 SW 소개

*신민철
*
한국과학기술원.

Keyword : . 나노 전자 소자, 시뮬레이션, 양자 수송, Tight-binding, 비평형 그린함수 방법

고전적 방정식에 기반을 둔 기존의 소자 시뮬레이터는 반도체 트랜지스터 동작을 분석하고 성능을 예측하는데 있어 성공을 거두었고 무어의 법칙으로 대변되는 반도체 소자의 눈부신 발전에 일조를 하였다. 그러나 트랜지스터의 크기가 나노 스케일로 작아지면서 전자의 파동성에 의한 양자화, 터널링 등이 전하 수송에 있어 중요한 이슈가 되었고 소자 특성에 직접적인 영향을 미치게 되었다. 이러한 양자 효과는 기존 상용 소자 시뮬레이터에서 지원하는 기능 및 범위를 벗어나며, 적절한 양자 모듈이 상용 툴에 탑재되기까지는 아직 요원한 실정이다.
지난 십 여 년간 Computational Electronics 분야에서는 나노 스케일 트랜지스터에서 양자 역학적 전자 수송을 다루기 위한 새로운 소자 전산 모사 기법 및 툴 개발이 활발히 이루어졌다. 해밀토니안으로는 유효 질량 방법, k.p 방법, tight-binding (TB) 기법 등이 동원되었고 최근에는 제일원리 영역으로 확장되는 추세이며, 양자 전자 수송을 기술하기 위하여 양자 투과 경계 방법, 비평형 그린함수 방법 (NEGF), 위그너 함수 방법 등이 다루어졌다. 본 발표에서는 이러한 동향에 대하여 간략히 소개한 후, 주된 주제로서 TB 방법을 통한 원자 수준의 나노 트랜지스터에서의 전자 수송 문제를 NEGF 방법을 사용하여 접근하는 기법에 대하여 소개하고자 한다. State-of-the-Art 라고 할 수 있는 TB-NEGF 방법은, 나노 소자의 전기적 특성을 해석하는데 있어서 엄밀하다고 평가를 받으나 실제 구현에 있어서는 매우 큰 해밀토니안 행렬을 다루어야 하고 멀티 코어 클러스터에서도 수십 시간 계산을 해야 하는 등 제한적이다. 이를 극복하고자 최신 기법이 적용되어 자체 개발된 매우 효율적인 TB-NEGF 소자 시뮬레이션 SW 를 소개하고, 웹을 통한 활용 방법 및 응용 가능성 등에 대하여 발표하고자 한다

H7.04(초)

소프트웨어를 이용한 가상실험 및 온라인 커리큘럼을 통한 학습

*유재준
*Jaejun. Yu
서울대학교.

Keyword : 계산과학, 물리교육, 온라인 교육허브,

최근 비약적인 발전을 거듭하는 컴퓨터 하드웨어와 알고리즘의 발달은 이론과 실험으로 구분되어 진행된 과학의 패턴에서 벗어난 '계산과학'이라는 새로운 장을 열어 주었다. 계산과학의 패러다임은 연구분야에만 국한되지 않고 교육적으로도 중요한 도구로 부각되고 있다. 대학 물리교육에서도 기존의 해석학적 방법을 통한 교육 방법으로는 접근이 불가능한 복잡하고 어려운 그러나 개념 습득에 매우 중요한 현상이나 실험 등을 컴퓨터 시뮬레이션을 통해 접근할 수 있게 되었다. 최근 첨단사이언스교육허브개발사업(EDISON; EDucation-research Integration through Simulation On the Net)의 일환으로 진행된 교육연구용 시뮬레이션 프로젝트에서 물리교육, 특히 일반물리학 강의의 시뮬레이션 프로젝트 개발이 진행되었고, 그 연장선에서 여러 물리학 교육관련 주제의 시뮬레이션과 실험을 네트워크 상에서 진행할 수 있는 방법적 도구인 가상실험 소프트웨어 기반이 확보되고 있다. 본 발표에서는 대학의 일반물리학 및 전공과정에 관련된 온라인 커리큘럼과 시뮬레이션 과제, 그리고 실험교육 등에 활용할 수 있는 가상 공간의 소프트웨어 기반과 도구 등을 소개하고, 향후 창의적 교육 콘텐츠 개발과 운영을 통해 물리학 교육에 기여할 수 있는 방향을 논의하고자 한다.

H8.01(초)

RI beam facilities worldwide - present and future -

*Tohru Motobayashi
*Tohru. Motobayashi
RIKEN.

Keyword : short-lived nuclei, RI beams

Since the first experiments with energetic beams of short-lived nuclei in mid 80s, people have developed various new paradigms for nuclear physics and astrophysics along with worldwide constructions of dedicated facilities and equipment. An overview will be provided for world facilities for radioactive isotope (RI) beams.

H8.02(초)

Nuclear astrophysics in China and JUNA progress

*Weiping Liu
*Weiping. Liu
CIAE.

Keyword : nuclear astrophysics, network calculation, JUNA

Progress of nuclear astrophysics in China will be given, and some highlights will be presented. The progress is including nuclear reaction, decay, mass, theory and network calculation of astrophysics interest. Finally, the progress of Jinpin underground nuclear astrophysics laboratory (JUNA) will be presented. The relevant experimental programs and their progress will be reported.

H8.03(초)

Current and future programs at RIBF

*Hiroyoshi Sakurai
*Hiroyoshi. Sakurai
RIKEN.

Keyword : science program, RIBF, RIKEN

This presentation will give an overview of the science program of RIBF at RIKEN, Japan.

H9.01*

Dynamics of Perturbations in Double Field Theory and Non-Relativistic String Theory

*고성문, 박정혁
*Sung Moon. Ko, Jeong-Hyuck. Park
서강대학교.

Keyword : Differntial Geometry, String Theory, Double Field Theory, Non-relativistic String Theory, Non-Riemannian Geometry

Double Field Theory provides a geometric framework capable of describing string theory backgrounds that cannot be understood purely in terms of Riemannian geometry -- not only globally ('non-geometry'), but even locally ('non-Riemannian'). In this work, we show that the non-relativistic closed string theory of Gomis and Ooguri arises precisely as such a non-Riemannian string background, and that the Gomis-Ooguri sigma model is equivalent to the Double Field Theory sigma model of on this background. We further show that the target-space formulation of Double Field Theory on this non-Riemannian background correctly reproduces the appropriate sector of the Gomis-Ooguri string spectrum. To do this, we develop a general semi-covariant formalism describing perturbations in Double Field Theory. We derive compact expressions for the linearized equations of motion around a generic on-shell background, and construct the corresponding fluctuation Lagrangian in terms of novel completely covariant second order differential operators. We also present a new non-Riemannian solution featuring Schr\"odinger conformal symmetry.

H9.02*

Scaling symmetry and the Smarr relation for Lifshitz black holes

*박상아, 현승준, 정재훈 [1], 이상헌
*Sang-A. PARK, Seungjoon. HYUN, Jaehoon. JEONG[1], Sang-Heon. YI
연세대학교. [1]Aristotle University of Thessaloniki.

Keyword : Black Hole, Scaling symmetery, Smarr relation, Lifshitz geometry, Conserved charge

By utilizing the scaling symmetry of the reduced action for planar black holes, we obtain the corresponding conserved charge. We use the conserved charge to find the generalized Smarr relation of static hairy planar black holes in various dimensions. Our results not only reproduce the relation in the various known cases but also give the new relation in the Lifshitz planar black holes with the scalar hair.

H9.03(초)

Recent results from the Telescope Array experiment

*H. Sagawa
*H.. Sagawa
Univ. of Tokyo.

Keyword : Telescope Array Experiment, Ultra-high energy cosmic rays

The Telescope Array (TA) experiment is the largest cosmic ray observatory in the Northern Hemisphere to explore astrophysical phenomena at the highest ends (~10^20.3 eV) of the cosmic ray energies. We have expanded its reach down to lower energy (10^15.6 eV) in the energy spectrum thus allowing it to probe over an unprecedented 4.7 decades in energy, and have observed spectral features. We present evidence for anisotropy in the arrival direction of the highest-energy cosmic rays as well as updated measurements of the spectrum and primary composition.Finally we present the plan of the Telescope Array extension.

H9.04

Diboson Excesses from Effective Field Theory Approach

*이현민, 박성찬 [1]
*Hyun Min. Lee, Seong Chan. Park[1]
중앙대학교. [1] *연세대학교.*

Keyword : LHC, Resonances, Effective Field Theories.

We study the collider implication of a neutral resonance which decays to several diboson final states such as W+W−, ZZ, and Zγ via a minimal set of effective operators. We consider both CP-even and CP-odd bosonic states with spin 0, 1, or 2. The production cross sections for the bosonic resonance states are obtained with the effective operators involving gluons (and quarks), and the branching fractions are obtained with the operators responsible for the interactions with electroweak gauge bosons. We demonstrate that each scenario allows for a broad parameter space which could accommodate the recently-reported intriguing excesses in the ATLAS diboson final states, and discuss how the CP states and spin information of the resonance can be extracted at the LHC run II.

H9.05

Shifted Focus Point and Naturalness-guided Gluino Mass Bound

*계범석, 김도윤 [1]
*Bumseok. Kyae, Doyoun. Kim[1]
부산대학교. [1]APCTP.

Keyword : focus point scenario, minimal gravity mediation, minimal gauge mediation

In order to significantly reduce the fine-tuning associated with the electroweak symmetry breaking in the minimal supersymmetric standard model (MSSM), we consider not only the minimal gravity mediation effects but also the minimal gauge mediation ones for a common supersymmetry breaking source at a hidden sector. In this "Minimal Mixed Mediation model," the minimal forms for the Kahler potential and the gauge kinetic function are employed at tree level. The MSSM gaugino masses are radiatively generated through the gauge mediations. Since a "focus point" of the soft Higgs mass parameter, m_hu^2 appears around 3-4TeV energy scale in this case, m_hu^2 is quite insensitive to stop masses. Instead, the naturalness of the small m_hu^2 is more closely associated with the gluino mass rather than the stop mass unlike the conventional scenario. As a result, even a 3-4TeV stop mass, which is known to explain the 125-126 GeV Higgs mass at three loop level, can still be compatible with the naturalness of the electroweak scale. On the other hand, the requirements of various fine-tuning measures much smaller than 100 and |\mu| < 600 GeV constrain the gluino mass to be 1.6 TeV < M_3 < 2.2 TeV, which is well-inside the discovery potential range of LHC Run 2.

H9.06

Top-philic resonances at the LHC

*박성찬
*Seong Chan. Park
연세대학교.

Keyword : top quark, resonance, LHC

We investigate the collider phenomenology of a color-singlet vector resonance, which couples to the heaviest quarks, the top quarks, but very weakly to the rest of the fermions in the Standard Model. We find that the dominant production of such a resonance does not appear at the tree level -- it rather occurs at the one-loop level in association with an extra jet. Signatures like t anti-t plus jets readily emerge as a result of the subsequent decay of the resonance into a pair of top quarks. Without the additional jet, the resonance can still be produced off-shell, which gives a sizeable contribution at low masses. The lower top quark multiplicity of the loop induced resonance production facilitates its reconstruction as compared to the tree level production that gives rise to more exotic signatures involving three or even four top quarks in the final state. For all these cases, we discuss the constraints on the resonance production stemming from recent experimental measurements in the top quark sector. We find that the top-philic vector resonance remains largely unconstrained for the majority of the parameter space, although this will be scrutinized closely in the Run 2 phase of the LHC.

H9.07

Fragmenation contributions to J/ψ production at HERA

*김유래, 이정일, Geoffrey T. Bodwin[1], 정희석 [1]
*U-Rae. Kim, Jungil. LEE, Geoffrey T.. Bodwin[1], Hee Sok. Chung[1]
고려대학교. [1]Argonne national laboratory.

Keyword : QCD, photoproduction, DESY HERA, J/ψ, heavy quarkonium

We evaluate leading-power fragmentation corrections to J/ψ production at DESY HERA, based on the nonrelativistic QCD factorization. We consider parton production cross sections through order α_s^3, fragmentation functions though order α_s^2, and leading logarithms of the transverse momentum divided by the charm-quark mass to all orders in α_s. We find that the leading-power fragmentation corrections are small relative to the fixed-order contributions through next-to-leading order in α_s.

H9.08*

Measurement of energy dependent reactor neutrino disappearance

*최원국
*Wonqook. Choi
서울대학교.

Keyword : Neutrino, Oscillation, Reactor

The Reactor Experiment for Neutrino Oscillation(RENO) started data-taking from August, 2011 and has observed the disappearance of reactor electron antineutrinos to measure the neutrino mixing angle theta_13. The experiment has accumulated roughly 800 days of data and this increased events make possible to improve our measurement of the reactor neutrino flux and spectral shape. The Antineutrino spectra from six reactors at Hanbit Nuclear Power Plant in Korea are compared by two identical detectors each located near and far from the reactor array center. In this talk, we present new results on theta_13,and reactor neutrino spectra and flux based on the 800 day data sample.

H9.09

Holographic Entanglement Entropy in Time-Dependent Backgrounds

*김낙우, 이정훈
*NAKWOO. KIM, Jung Hun. Lee
경희대학교.

Keyword : Holography, Entanglement Entropy

We study the time-dependent entanglement entropy. We consider small deformation of anti-de Sitter space and compute
holographic entanglement entropy. Our main object of interest is the time-periodic solutions which were constructed in scalar fields coupled to Einstein gravity.

H10.01

Search for sterile neutrinos at RENO

*여인성, 김우영 [1], 박인곤 [2], 장지승 [3], 박명렬 [4], 장한일 [5], 김상용 [6], 유인태 [7], 김영덕 [8], 김현수 [9], 김바로 [10], 김시연 [11], 박성우 [1], 최준호 [4], 김수봉 [12], 박정식 [12], 서선희 [12], 서현관 [12], 이동하 [12], 최원국 [12], 양장희 [13], 최영일 [13], 전은주 [14], 김재률 [10], 박령균 [10], 신창동 [10], 임인택 [10], 주경광 [10], 고영주 [15]
*In Sung. Yeo, Wooyoung. KIM[1], In-Gon. PARK[2], Jee Seung. Jang[3], Myoung Youl. PAC[4], Han Il. JANG[5], Sang yong. Kim[6], Intae. YU[7], Yeong Duk. KIM[8], Hyunsoo. Kim[9], Ba Ro. Kim[10], Siyeon. Kim[11], Sung Woo. Park[1], JUNE HO. CHOI[4], Soo-Bong. KIM[12], Jungsic. Park[12], Seon Hee. Seo[12], Hyun Kwan. Seo[12], Dong ha. Lee[12], won qook. Choi[12], Janghee. Yang[13], Young-Il. Choi[13], Eun Ju. Jeon[14], Jae Yool. KIM[10], Ryeong Gyoon. Park[10], Changdong. Shin[10], In Taek. Lim[10], Kyung Kwang. Joo[10], Youngju. Ko[15]
전남대학교. [1] 경북대. [2] 경상대. [3] 광주과기원. [4] 동신대. [5] 서영대. [6] 서울대. [7] 성균관대. [8]IBS/세종대. [9] 세종대. [10] 전남대. [11] 중앙대. [12] 서울대학교. [13] 성균관대학교. [14]IBS/세종대학교. [15] 중앙대학교.

Keyword : RENO,

The RENO experiment was designed to measure an neutrino mixing angle, theta13, by detecting anti-electron neutrinos emitted from the Hanbit nuclear reactors (known as Yonggwang before) in Korea, and succeeded to measure theta_13 from the disappearance mode of reactor anti-electron neutrinos at a few km-order baselines in three-neutrino frame.
We investigate the possibility of sterile neutrinos existence at RENO experiment. We compare data with four-neutrino scenario. In this talk, we present some recent results, including the probability deficit curve .vs. distance and the excluded contour in sin^2(2theta14) – Delta(m41)^2 space using chi-square analysis

H10.02

New Result from RENO

*서현관, 김우영 [1], 박인곤 [2], 장지승 [3], 박명렬 [4], 장한일 [5], 김상용 [6], 서선희 [7], 이동하 [8], 최원국 [9], 양장희 [10], 김영덕 [11], 박성우 [12], 최준호 [13], 김수봉, 박정식, 유인태 [14], 최영일 [14], 전은주 [15]
*Hyunkwan. Seo, Wooyoung. KIM[1], In-Gon. PARK[2], Jee Seung. Jang[3], Myoung Youl. PAC[4], Han Il. JANG[5], Sang yong. Kim[6], Seon Hee. Seo[7], Dong ha. Lee[8], Won Kook. CHOI[9], Janghee. Yang[10], Yeong Duk. KIM[11], Sung Woo. Park[12], JUNE HO. CHOI[13], Soo-Bong. KIM, Jungsic. Park, Intae. YU[14], Young-Il. Choi[14], Eun Ju. Jeon[15]
서울대학교. [1] 경북대. [2] 경상대. [3] 광주과기원. [4] 동신대. [5] 서영대. [6] 서울대. [7] 성균관대. [8]IBS/세종대. [9] 세종대. [10] 전남대. [11] 중앙대. [12] 경북대학교. [13] 동신대학교. [14] 전남대학교. [15] 중앙대학교.

Keyword : neutrino, reactor, RENO, oscillation

The Reactor Experiment for Neutrino Oscillation (RENO) started data-taking from August, 2011 and has successfully measured the smallest neutrino mixing angle θ_13 by observing the disappearance of reactor antineutrinos. Antineutrinos from the six reactors at Hanbit Nuclear Power Plant in Korea are detected and compared by the two identical detectors located in the near and far distances from the reactor array center. We present new results on precisely measured sin^2(2θ_13) value and our first measurement of dm^2_ee based on spectral analysis using the 500 days of data sample, which are taken from August, 2011 to January, 2013. In addition, the recent result of theta_13 measurement with neutron capture on hydrogen and the search for sterile neutrinos will be reported.

H10.03

R＆D efforts for RENO-50

*서선희, 김수봉, 서현관, 최원국, 김상용, 이동하, 김재률 [1], 임인택 [1], 주경광 [1]
*Seon Hee. Seo, Soo Bong. Kim, Hyun Kwan. Seo, Won Qook. Choi, Sang Yong. Kim, Dong Ha. Lee, Jae Lyool. Kim[1], In Taek. Lim[1], kyung Kwang. Joo[1]
서울대학교. [1] 전남대학교.

Keyword : neutrino oscillation, mass ordering, reactor neutrinos

RENO-50 is a 18kt liquid scintillator detector to determine neutrino mass ordering, one of the most fundamental puzzles. It will also make unprecedentedly accurate measurements of neutrino oscillation parameters, essential for the next discoveries. In addiion, it will detect neutrinos from Supernova, the Earth, and the Sun as a large neutrino telescope to provide valuable information on neutrino cooling mechanisms in the early stage of neutron star formation, thermal energy generation inside the Earth, and metallicity of stars.

H10.04

Search for solar axions using CsI crystal detector

Yoon Young Soo
Young Soo. Yoon
기초과학연구원.

Keyword : CsI detector, solar axions, underground physics, particle experiment

The Korea Invisible Mass Search (KIMS) experiment has taken data for several years at the YangYang Underground Laboratory. While the experiment was designed to be search for dark-matter with CsI crystal detector, this detector can be used for solar axion search via axio-electric process. In this talk, we will present current status of the data analysis using part of full data sample.

H10.05

Status of the NEOS

*오유민, 이재승, 고영주 [1], 김시연 [1], 김현수 [2], 이주영 [3], 김영덕 [4], 박강순, 박향규, 이무현, 이정연 [5], 전은주, 김진유 [2], 김바로 [6], 여인성 [6], 주경광 [6], 서경민 [7], 박현서 [8], 선광민 [9], 한보영 [9]
*Yoomin. Oh, Jaison. Lee, Youngju. Ko[1], Siyeon. Kim[1], Hyunsoo. Kim[2], Joo Young. Lee[3], Yeong Duk. KIM[4], Kang Soon. Park, HyangKyu. Park, MOO HYUN. LEE, Jeong Yeon. LEE[5], Eun Ju. Jeon, Jin Yu. Kim[2], Ba Ro. Kim[6], In Sung. Yeo[6], Kyung Kwang. Joo[6], kyung min. seo[7], Hyeonseo. PARK[8], Kwang Min. SUN[9], Bo Young. Han[9]
기초과학연구원. [1] 중앙대학교. [2] 세종대학교. [3] 경북대학교. [4] 기초과학연구원/세종대학교. [5] 기초과학연구원 (IBS). [6] 전남대학교. [7] 전북대학교. [8] 한국표준과학연구원. [9] 한국원자력연구원.

Keyword : reactor neutrino, sterile neutrino, neutrino oscillation, short baseline experiment

The Neutrino Experiment for Oscillation at Short baseline (NEOS) has completed its installation at the Hanbit nuclear power plant and has started taking data from August 2015. We report the overall features and status of the experiment.

H10.06*

Pulse Shape Discrimination Analysis with NaI(Tl) Crystal

*김경원, KIMS Collaboration[1]
*Kyung Won. Kim, KIMS. Collaboration[1]
서울대학교. [1]IBS.

Keyword : WIMP,PSD,KIMS,dark matter

The KIMS-NaI experiment is aimed at the direct detection of Weakly Interacting Massive Particle (WIMP) via weak interactions with nuclei in low-background NaI(Tl) crystals. KIMS-NaI installed one 9.15 kg NaI(Tl) crystal in Yang Yang underground laboratory in 2014 and crystal R & D and some data-taking has been underway since that time. We use pulse shape discrimination (PSD) to distinguish between WIMP nuclear recoil signals and beta/gamma-induced backgrounds in the crystal. In order to quantify the effectiveness of the PSD, we measured the pulse shapes produced by neutrons, gamma rays and surface alpha sources in a test NaI(Tl) crystal that was exposed to a neutron source and a gamma-source. In this talk, the status of the PSD analysis study based on a 133 day underground exposure of the NaI(Tl) detector will be presented.

H10.07*

Measurement of theta13 with neutron capture on hydrogen

*신창동, 김바로, 김우영 [1], 박인곤 [2], 장지승 [3], 박명렬 [4], 장한일 [5], 김상용 [6], 양장희 [7], 김영덕 [8], 김현수 [8], 김시연 [9], 김재률, 박령균, 여인성, 임인택, 주경광, 박성우 [1], 최준호 [4], 김수봉 [6], 박정식 [6], 서선희 [6], 서현관 [6], 이동하 [6], 최원국 [6], 유인태 [7], 최영일 [7], 전은주 [10], 고영주 [9]
*Changdong. Shin, Ba Ro. Kim, Wooyoung. Kim[1], In-Gon. PARK[2], Jee Seung. Jang[3], Myoung Youl. PAC[4], Han Il. JANG[5], Sang yong. Kim[6], Janghee. Yang[7], Young Duck. Kim[8], Hyunsoo. Kim[8], Siyeon. Kim[9], Jae Yool. KIM, Ryeong Gyoon. Park, In Sung. Yeo, In Taek. Lim, Kyung Kwang. Joo, Sung Woo. Park[1], JUNE HO. CHOI[4], Soo-Bong. KIM[6], Jungsic. Park[6], Seon Hee. Seo[6], Hyun Kwan. Seo[6], Dong ha. Lee[6], won qook. Choi[6], Intae. YU[7], Young-Il. Choi[7], Eun Ju. Jeon[10], Youngju. Ko[9]
전남대학교. [1] 경북대학교. [2] 경상대학교. [3] 광주과학기술원. [4] 동신대학교. [5] 서영대학교. [6] 서울대학교. [7] 성균관대학교. [8] 세종대학교. [9] 중앙대학교. [10]IBS/세종대학교.

Keyword : RENO

RENO has been taking data since August, 2011 and successfully measured the smallest neutrino mixing angle, theta_13. This measurement was based on reactor neutrino events with neutron captures on gadolinium. Furthemore, RENO can also measure the theta_13 with reactor neutrino samples of neutron captures on hydrogen. The background subtraction in the case of hydrogen capture is more difficult than that of gadolinium capture case. However, this independent measurement provides a valuable cross-check on the systematic uncertainties of the earlier measured theta_13 results. In this talk, the recent results from the hydrogen capture analysis will be presented.

H10.08*

Low-temperature heat and light detection system to search for scintillating crystal candidates for rare process experiments

*김혜림, 김용함 [1], 조현석 [2], 강찬석 [1], 김건보 [1], 김홍주, 김인욱 [3], 김소라 [1], 이혜진 [1], 오승윤 [4], 소중호 [1], 윤원식 [1]
*Hye lim. Kim, Yong-Hamb. Kim[1], Hyon-Suk. Jo[2], Chan Seok. KANG[1], Geon-Bo. Kim[1], Hong Joo. KIM, Inwook. Kim[3], So Ra. kim[1], Hye Jin. Lee[1], Seung yoon. Oh[4], Jung Ho. So[1], Wonsik. Yoon[1]
경북대학교. [1] 기초과학연구원. [2] 기초과학 연구원. [3] 서울대학교. [4] 세종대학교.

Keyword : scintillating crystal, low-temperature detector, rare event search experiment

Low-temperature detectors with scintillating crystal absorbers are a promising tool for rare event search experiments due to their powerful particle discrimination capabilities. In general, heat and scintillation light are generated by energy deposition in a scintillating crystal. At room temperature, only scintillation light can be detected. However, at milli-Kelvin (mK) temperatures, the simultaneous measurements of heat and scintillation light can be performed, providing a powerful method to discriminate particles with different scintillation-light efficiencies, such as alpha, beta, and neutral particles. Studies on the properties of both heat and light signals of scintillation crystals at tens of mK temperatures are essential in the search for proper crystals for various research activities.
We developed a compact detection system to investigate various crystals. It is designed to measure heat and light signals from a 1 cm3 crystal with readout via metallic magnetic calorimeters (MMCs) and the crystal is easily replaceable for an effective search of crystal candidates. Recent results using a Nb-doped $CaMoO_4$ scintillation crystal will be reported.

H10.09

Data Analisys for NEOS Experiment

*김바로, 주경광, 김영덕 [1], 이재승 [1], 박강순 [1], 이무현 [1], 박향규 [1], 이정연 [2], 김현수 [3], 김진유 [3], 김시연 [4], 고영주 [4], 김홍주 [5], 이주영 [5], 전은주 [1], 여인성, 서경민 [6], 박현서 [7], 선광민 [8], 한보영 [8]
*Ba Ro. Kim, Kyung Kwang. Joo, Yeong Duk. KIM[1], Jaison. Lee[1], Kang Soon. Park[1], MOO HYUN. LEE[1], HyangKyu. Park[1], Jeong Yeon. LEE[2], Hyunsoo. Kim[3], Jin Yu. Kim[3], Siyeon. Kim[4], Youngju. Ko[4], Hong Joo. KIM[5], Joo Young. Lee[5], Eun Ju. Jeon[1], In Sung. Yeo, kyung min. seo[6], Hyeonseo. PARK[7], Kwang Min. SUN[8], Bo Young. Han[8]
전남대학교. [1] 기초과학연구원. [2] 기초과학연구원 (IBS). [3] 세종대학교. [4] 중앙대학교. [5] 경북대학교. [6] 전북대학교. [7] 한국표준과학연구원. [8] 한국원자력연구원.

Keyword : sterile neutrino, reactor neutrino experiment

Existing reactor short baseline neutrino data show the possible existence of sterile neutrino. Neutrino Experiment for Oscillation at Short baseline (NEOS) has started data taking since August 2015. We present the analysis status and the preliminary data of NEOS.

H12.01

Navigation on Temporal Networks

*이상훈, Petter Holme[1]
*Sang Hoon. Lee, Petter. Holme[1]
고등과학원. [1] 성균관대학교.

Keyword : complex network, temporal network, navigability, network centrality, diffusion

The temporal network framework represents dynamically changing interactions between nodes that describe more realistic situations. The static representation or simplification of those interacting nodes ignores possibly nontrivial temporal trends that we can harness for better understanding of complex systems. To demonstrate the effectiveness of such temporal information, in this work, we take the navigability or packet delivery problem on temporal networks as an example to show that using even a small portion of past information such as the distance to the destination from other nodes may significantly improve the navigability in real temporal networks. We quantify such efficiency of navigability in the real temporal networks and find that the navigability measures of our model are relatively uncorrelated with many aggregated network centralities and temporal correlation measures, compared to those of the random diffusion model and the model where the agent indefinitely waits for the direct contact with the destination. The result indicates that in contrast to the navigation strategies without using temporal information, our simple model effectively uses intrinsic temporal patterns for better navigability.

H12.02

Diffusion with memory on complex networks

*김강훈, 경재구, 이덕선
*Kanghun. Kim, jaegu. Kyoung, Deok-Sun. LEE
인하대학교.

Keyword : self-attracting walk, generalized random walk, human mobility, complex network, scale-free network

Understanding the human mobility is important to efficiently design and manage diverse infrastructures. While the relevance of memory in human mobility and the heterogeneous topology of many infrastructures are known recently, yet there is no work of considering memory and topology simultaneously in the human mobility. Here we study the self-attracting walk (SATW) on scale-free (SF) networks, in which a walker is more likely to move to visited nodes than to unvisited ones. We find that the number of distinct visited nodes S grows faster in SF networks with γ 3 but goes through crossovers in time. The memory makes the walker move recurrently around hubs and consequently the hubs help a fast exploration in first but hinder later. Our result indicate that hubs are essential for efficient transportations carried by humans.

H12.03*

Spread of Political Opinions Based On Human Migrations in Presidential Elections

*조우성, 김범준
*WooSeong. Jo, Beom Jun. Kim
성균관대학교.

Keyword : voter nodel, election

The voter model has been studied in various systems to understand how opinions spread. Recently, several studies showed that election results can be addressed by applying the voter model with commuter flow. However, political opinions of individuals can be strongly affected by their birthplaces as well as where they are. We apply the voter model to presidential election in South Korea from 1971 to 2012, considering the annual inter-province flow of migration. Keeping information of birthplace, agents change their political opinions with given probability which is assigned by birthplace. We optimize the probability of changing opinions, comparing the outcome from real elections with simulation results. From several presidential elections, traces of the probability show the evolution of political bias based on a province. In addition, results are robust on fluctuation of population growth. We expect that the long-term evolution of the probability may show the changes in province-wise political opinions.

H12.04*

Quantitative analysis of history of Joseon using half-millenium chronological historical data and its visualization

*이병휘, 김영호 [1], 조항현 [2], 정하웅
*Byung Hwee. Lee, Daniel. Kim[1], Hang-Hyun. JO[2], HAWOONG. JEONG
KAIST. [1] 한국과학기술원. [2]POSTECH.

Keyword : historical data, temporal data, event categories, geographic locations

The Annals of the Joseon Dynasty are the historical records of the Joseon Dynasty, one of the major kingdoms in the history of Korea, composed of 1893 books covering 472 years (1392- 1863) written in chronological order. The chronologically ordered historical document provide us a variety of opportunities of studying historical contents changing across time. We extracted temporal information on subject categories, geographic locations and mentioned people from the Annals. Here we reveal distinct trends of different types of historical events. We also investigate how geographical locations are correlated with event categories and different people. This work may overcome the limits of previous studies focusing on specific events within a narrow time period, and provide a new insight into systematic understanding on historical processes.

H12.05*

Editing dynamics of Wikipedia based on real time series.

*윤진혁, 이상훈 [1], 정하웅 [2]
*Jinhyuk. Yun, Sang Hoon. Lee[1], HAWOONG. JEONG[2]
한국과학기술원. [1] 고등과학원. [2]KAIST.

Keyword : Complex System, Data Science, Wikipedia

Wikipedia is a free Internet encyclopedia with enormous amount of contents. This encyclopedia is written by volunteers with various backgrounds in a collective fashion; anyone can access and edit most of the articles. This new paradigm of sharing knowledge is one of the most famous examples of "collective intelligence," yet occasionally regarded ambiguous and even inaccurate to utilize in scientific context due to the very nature of open-edit policy. However, many studies suggest that Wikipedia is even more accurate and self-consistent than traditional encyclopedias. Scholars have attempted to understand such extraordinary credibility, but usually used the edit number without consideration of real time. In this work, we find the existence of various growth patterns only appearing with real-time, and suggest an intuitive model of Wikipedia editing process employing both time-step and edit-step.The model adopts both the article editing dynamics, and editors-editor and editor-article interactions. We present the condition to reproduce various growth patterns of a Wikipedia's article, which can effectively classify articles.

H12.06*

Modeling of social uprising with inhomogeneous status distribution

*이은, 이상훈 [1], 페터홀메
*Eun. Lee, Sang Hoon. Lee[1], Petter. Holme
성균관대학교. [1] *고등과학원.*

Keyword : Social status, complex network, opinion spreading, convergence, inhomogeneous degree distribution

We model an uprising phenomenon of the opinion held by the agents belonging to socially lower classes, against a different opinion held by higher classes in an authoritarian system. The celebrated Pareto or power-law distribution represents the inequality in the social status assigned to each agent. For individual characteristics of agents besides such a social setting, we introduce additional parameters corresponding to acceptance of others' opinions and the will to change the society to the correct direction. First, we predict the phase separation between uprising and suppressing by a mean-field argument and verify it in the well-mixed system. We also test the effect of different types of social interactions than the mean-field case. The social uprising is qualitatively more difficult on the scale-free networks where the number of neighbors (degree) and the social status are strongly correlated, compared to other homogeneous networks without the correlation between the degree and social status. Therefore, our results indicate that the type of networks and their intricate relation to the social status play an important role in the opinion dynamics of uprising phenomena.

H12.07*

Crisis-spreading model on the multiplex global economic network

*이규민, 고광일
*Kyu-Min. Lee, Kwang-Il. Goh
고려대학교.

Keyword : Multiplex network, Crisis spreading model, Systemic risk, Global economic system

Many real-world complex systems such as the modern infrastructure, human society, cellular network, human brain network, and global economic system operate through various types of interactions. In this respect, the structural and dynamical properties of multiplex network systems draws much attention in the network science and have been intensively studied recently. Here we study the dynamic model of crisis spreading on the multiplex global economic network. With introducing the measure of individual countries impact as an epicenter and comparing the results of multiplex model with the simplex case, we found that the multiplex network produces more catastrophic avalanche dynamics than the simplex framework. Through the direct and indirect avalanche analysis, we found that most of facilitation of avalanche dynamics were collective behaviors between layers rather than just summation e
ect of layers. Our simple model would have some implications about real complex systems to investigate the better systemic design for security.

H12.08*

Strategy for optimal spreading in multilayer networks

*곽상환, 민병준 [1], 고광일
*Sang-Hwan. Gwak, Byungjoon. Min[1], Kwang-Il. Goh
고려대학교. [1]City College of New York.

Keyword : "Spreading dynamics", "Multilayer networks"

Epidemic spreading is one of the most important and emergent phenomena which arise from complex system. In particular, the complex problem of disease dynamics that have been infected by a variety of routes and optimal strategy for spreading dynamics.
In this study, we study the dynamics of spreading on the multilayer networks based on the SIR(susceptible-infected-recovered) framework for the spreading of information or diseases.
The model represents two effects for spreading dynamics in multilayer networks, the layer crossing effect and the different link densities between two layers.
Our formalism reflects the optimal strategy for spreading dynamics in multilayer networks and not the only spreading of disease or information through various channels on multilayer networks, but also the effect of the density of the network and ratio of spread on both networks.

H13.01

Optics at 0.1 nm scale: colossal terahertz nonlinearities of 1 cm-long van der Waals gaps

박영미, 강봉주 [1], 김용승 [2], *김준연, 김원태 [1], 김태윤, 이지예, 한상훈, 박철환, 이상민 [1], 김대식
Young mi. Bahk, Bong Joo. Kang[1], Yong Seung. Kim[2], *Joonyeon. Kim, Won Tae. Kim[1], Tae Yun. Kim, Jiyeah. Rhie, Sanghoon. Han, Cheol Hwan. Park, Rotermund. Fabian[1], Dai Sik. Ghim
서울대학교. [1] 아주대학교. [2] 세종대학교.

Keyword : Terahertz nonlinearity, Quantum plasmonics, Van der Waals gap, Graphene, Angstrom optics

We observed a ninety-seven percent decrease of terahertz transmittance in five-millimeter long, angstrom-sized optical gaps of copper-graphene-copper hybrid structure when irradiated with intense terahertz pulses. To understand the origin of the nonlinear response, we plotted the induced voltage across the gap by multiplying the incident electric field with the field enhancement factor. The maximum voltage across the gap is changed from 5 mV to 5 V when the incident electric field increases from 30 V/cm to 192 kV/cm. The induced voltage is sufficiently strong to deform the quantum mechanical potential barrier of the angstrom gap and facilitate electron tunneling. Based on a quantum corrected plasmonic model of the dielectric constant as a function of the funneling-induced voltage across an effective gap size of 3 Å with the barrier height of 3 eV, the calculated transmittance matches well with the experimental results. As a result, it is well explained that the giant nonlinearity originates from terahertz funneling-induced electron tunneling across the angstrom gap, which modifies the effective dielectric constant of the fictitious material inside the gap.

H13.02*

LCD Panel Complex Spatial Light Modulators for Wave Optical Applications

*최민호, 최재우
*MINHO. CHOI, Jaewu. Choi
경희대학교.

Keyword : Polarization independent phase modulator, Phase and amplitude independent SLM, Commercial LCD, Spatial Light Modulator

본 연구에서는 간단한 배열을 이용하여, 기존의 상업용 LCD 를 위상과 진폭 모두 조절할 수 있는 SLM(Spatial Light Modulator)으로 이용하는 방법을 개발하였다. 기존의 연구들과는 달리 위상과 진폭을 독립적으로 조절 할 수 있으며, 여러 화소를 하나의 큰 화소로 만들지 않고, 원래의 화소 크기를 유지한다. 2 층 혹은 3 층 구조로 이루어져 있으며, 3 층 구조의 경우 약간의 조건이 필요하지만, 거의 대부분의 LCD 로 사용이 가능하며, 3 층 구조의 위상 조절 부분만을 사용하면 편광에 무관한 위상 조절이 가능하다.

H13.03

Firsthand in situ observation of active fine laser tuning by combining a temperature gradient and a CLC wedge cell structure

*정미윤, 차지훈
*Mi-Yun. Jeong, Jihun. Cha
경상대학교.

Keyword : cholesteric liquid crystal (CLC) laser array, spatial temperature gradient, active fine laser tuning, active tunable laser array

In situ direct observation of the lasing process in a cholesteric liquid crystal (CLC) laser array using a CMOS camera was used to investigate discontinuous laser tuning in a parallel CLC cell. In accordance with the discontinuous pitch change by thermal energy transfer, at the same time the laser wavelength undergoes an immediate and discontinuous shift. And we found out the reason why the CLC phase has domain textures. And this work develops a simple active tunable laser array by forming a spatial temperature gradient along a wedge CLC cell. With this new strategy, only just about 7 nm laser tuning range at room temperature is extremely widened over the 105 nm wavelength range with about 0.2 nm tuning resolution. Furthermore, there is no aging effect because the employed CLC array has only one chiral molecular concentration. This strategy could be used in a practical CLC laser device application.

H13.04*

Dynamics of surface plasmon lasing in Ag/InGaAsP nano structure

*이향록, 김승현, 정태영, 안광준 [1], 이기주
*Hyang rok. Lee, Seung-hyun. Kim, TaeYoung. Jeong, Kwang Jun. Ahn[1], Ki Ju. YEE
충남대학교. [1] *아주대학교.*

Keyword : "surface plasmon", "lasing"

표면 플라즈몬(surface plasmon)은 유전상수가 음수인 금속과 양수인 유전체 사이 경계면을 전하가 진동하는 현상을 말한다. 본 실험에서는 up-conversion 실험을 통해 표면플라즈몬 레이징 동역학을 알아보았다. 이 때, 표면 플라즈몬 레이징을 보기 위하여 InP 기판 위에 InGaAsP 를 400nm 증착한 후 그 위에 Ag 가 증착된 시료를 사용하였다. Ag 는 일정한 주기를 가지는 금속격자로 제작하였다. up-conversion 실험 결과 표면플라즈몬 레이징 파장이 시간지연에 따라 장파장으로 변화하였다. 표면플라즈몬 분산관계(dispersion relation for surface plasmons)와 kramer-kronig relation 을 통해 표면플라즈몬 레이징 파장 변화와 여기전자의 밀도와의 관계를 알아보았다. 그 결과, 시간지연에 따라 여기 전자의 밀도가 점점 감소하는 것을 알 수 있었다.

H13.05*

Theoretical study of the propagation and the mode conversion of electromagnetic waves in stratified magnetoelectric media

김슬옹, *김기홍
Seulong. Kim, *Kihong. Kim
아주대학교.

Keyword : magnetoelectric media, Tellegen media, topological insulator, invariant imbedding method, mode conversion

We develop a generalized version of the invariant imbedding method for the study of wave propagation in stratified magnetoelectric media. In general magnetoelectric media, which include chiral media and Tellegen media as special examples, the electric displacement D and the magnetic flux B are related to both the electric field E and the magnetic field H. Topological insulators, which have been studied extensively in recent years, are a special case of Tellegen media. Using the invariant imbedding method, we investigate the surface waves and the mode conversion of transverse electromagnetic waves into longitudinal electromagnetic waves in magnetoelectric media. We compare our results on topological insulators and general magnetoelectric media with those of previous researches and clarify the reasons of some discrepancies. In the following figure, we plot the mode conversion coefficient A versus incident angle in a stratified magnetoelectric medium. Linearly-polarized electromagnetic waves of wave length λ are incident from a vacuum to an inhomogeneous medium of thickness 5λ. In the inhomogeneous medium, only the dielectric permittivity ε changes linearly from 1 to 0. The magnetic permeability μ has a constant value of 1. The Tellegen parameter χ is 0.5 and the chirality index is zero in the medium. We find that the mode conversion coefficient is strongly dependent on the wave polarization and discuss the underlying physics in detail.

H13.06

An Auxiliary Differential Equation Finite-Difference Time-Domain Method for the 3-level Maxwell-Bloch System

*전경원, 함병승
*Kyungwon. Chun, Byoung Seung. Ham
광주과학기술원.

Keyword : FDTD, finite-difference time-domain, Maxwell-Bloch equations, nonlinear, Lie algebra

An auxiliary differential equation finite-difference time-domain method is used to model the semiclassical interaction between electromagnetic waves and nonlinear media, represented by the 3-level Maxwell-Bloch equations. The Bloch equations are represented as an 8-dimensional pseudo vector, and combined to the Maxwell's curl equation as multiple macroscopic polarizations. The proposed algorithm can handle an ultra-short pulse response, because it does not rely on the rotating wave approximation. Moreover, the algorithm is affordable to the full vector simulation with multi-dimensional fields. Here we have studied the light atom interaction in n(n=2, 3)-level systems.

H13.07*

Effective medium Theory 를 이용한 자연산화막을 지닌 티타늄 박막의 특성 연구

*이창묵, 최재우
*Lee Chang Mook. , Choi Jaewu.
경희대학교.

Keyword : Effective medium Theory, 티타늄, 광학적모델링, Lorentz-Drude 모델

본 연구에서는 전기전도도 또는 유전율과 같은 물리적인 값의 근사를 설명하는 Effective medium Theory (EMT)를 도입하여 자연산화막을 지닌 티타늄 박막을 티타늄과 이산화티타늄이 서로 다른 물질 (inhomogeneous medium)로 보고 서로 섞여 있는 혼합체로 간주하여 EMT 중의 한 예로써, Newtonian, Maxwell-Garnett 모델과 Bruggeman 모델을 사용하여 자연산화막이 형성된 티타늄 박막의 빛의 투과도 정보로부터 광학적 특성을 분석하였다. 추가적으로, 자연산화막을 지닌 티타늄 박막을 한 물질 (homogeneous medium)로 보고 Loretz-Drude 모델을 이용한 광학적 모델 결과와 비교 분석 하였다. EMT 모델을 이용하여 광학적 모델링을 한 결과, 두께에 따른 티타늄과 이산화티타늄의 volume filling factor 및 광학적 두께를 예측 할 수 있었다.

H13.08

Ultrafast carrier dynamics study on semiconductors using terahertz-nano metamaterial

*최근창, 박영미, 서민아 [1], 손병희 [2], 안영환 [2], 김대식
*geunchang. choi, Young mi. Bahk, Minah. Seo[1], Byung Hee. Son[2], Yeong Hwan. Ahn[2], Dai-Sik. Kim
서울대학교. [1] 한국과학기술연구원. [2] 아주대학교.

Keyword : "Terahertz spectroscopy", "Nano metamaterial", "optical-pump terahertz-probe"

펨토초 레이저 기반 기술은 다양한 물질의 광학적 특성, 전기적 특성, 초고속 동역학 등을 연구하는데 이용되며, 그 중 광학-펌프 테라헤르츠-프로브 방법을 이용하면 광학적으로 여기된 캐리어들의 피코초 시간단위 동역학을 직접적으로 측정할 수 있다. 테라헤르츠파 영역에서 특정 주파수에 공명을 일으키는 나노 슬랏 안테나 구조를 이용하여 파장보다 훨씬 작은 공간 (나노 스케일)에 집속시키면 기존의 방법으로 관찰할 수 없는 나노 스케일에서의 물질 표면 관찰이 가능해진다. 본 연구에서는 나노 슬랏 안테나 어레이를 이용하여 GaAs 등 반도체 크리스탈 표면에 테라헤르츠파를 강하게 집속시킴으로써 광학적 여기에 의한 표면 캐리어들의 초고속 동역학을 효과적으로 관측하였다. 이를 통해 다양한 반도체 물질 표면에 일어나는 광학적 현상을 초고속 시간 해상도와 나노 스케일의 공간적 해상도로 측정할 수 있다. 특히 이 방법은 관찰하고자 하는 물질을 어려운 공정을 통해 얇은 필름형태 또는 막대 형태로 만드는 등의 복잡한 과정을 거치지 않고 벌크 상태의 물질을 그대로 이용할 수 있다는 점에서 그 파급효과가 매우 클 것이다.

J8.01(초)

Overview of Rare Isotope Science Project (RISP)

*정순찬, 김재홍
*Sunchan. Chung, Jaehong. Kim
기초과학연구원.

Keyword : .

Rare Isotope Science Project (RISP) of IBS has been initiated along with a construction of a heavy ion linear accelerator and experimental facilities at Sindong in Dajeon. This superconducting LINAC can accelerate beams from proton to uranium with 200 MeV/u, 400 kW (for uranium beam). The LINAC is in-progress with the development of rare isotope production facilities, where two different production methods of an In-flight Fragment (IF) and an Isotope Separation On-Line (ISOL) are employed. At present major components for LINAC, such as superconducting cavities and cryomodules are fabricated and tested at both domestic and abroad test facilities. These facilities provide high-intensity stable ion and rare isotope (RI) beams for domestic and international users. For applications of RI beams, low and intermediate energy nuclear science and applied science facilities are well underway. This presentation will overview the progress of the RISP facilities.

J8.02(초)

Rare isotope beam production systems for RISP

*김종원
*Jong-Won. Kim
기초과학연구원.

Keyword : in-flight separator, ISOL, rare isotope beam, UCx target

The Rare Isotope Science Project (RISP) aims to provide isotope beams with users in nuclear science and for multidisciplinary applications. A superconducting linear accelerator with a voltage of 600 MV will provide primary beams for the RI beam production using in-flight (IF) method. The energy of ^{238}U is 200 MeV/u at a maximum power of 400 kW. A large-acceptance fragment separator has been designed and prototyping of main components are underway. RISP also adopts an ISOL method to produce RI beams using a proton cyclotron and a target system made of such as UCx. Electron Beam Ion Source (EBIS) is a key component to charge-breed an isotope beam of interest for post-acceleration. An RI beam with a similar charge to mass ratio to that of primary beam can be accelerated by the same superconducting linac for stable beams in a time shared way. The progress in the RI beam production systems will be presented.

J8.03(초)

KOBRA for low energy nuclear physics study at RISP

*권영관
*Young Kwan. Kwon
기초과학연구원.

Keyword : RISP, RAON, KOBRA

The Korea Broad acceptance Recoil spectrometer and Apparatus (KOBRA) is a low energy nuclear facility planned at the RAON accelerator complex in Daejeon, South Korea. KOBRA will consist primarily of a series of magnetic dipoles, quadrupoles and Wien lters, separated into two distinct separation stages. The design will allow for the transport and separation of RI beams produced in Fight (IF) at the separator, or at an earlier stage via the ISOL method, or a combination of these methods. The production of such beams is necessary to probe the experimental limits of nuclear structure and astrophysics. The first stage of the facility will comprise of a production target, that will receive either stable or rare isotope (RI) beam from RAON, with the resulting IF beam directed onto a reaction target located downstream. Recoil products formed at the reaction target, the position of which along the beamline can vary depending on the mode of operation, can be separated from unreacted beam ions via a large acceptance spectrometer. This will allow for the observation of low cross section capture and transfer reactions relevant to both astrophysics and nuclear structure studies. An array of germanium detectors positioned at the reaction target will aid this endeavor, together with a silicon array encompassing the target, allowing for both gamma spectroscopy and inelastic/elastic scattering experiments to be performed. Alternatively, the initial separation stage can be used for primary beam transport, with dispersion matching employed with the second stage, allowing for high resolution momentum measurements of recoil products at the final focal plane. Fabrication and installation of the facilities components is planned to be completed by the end of 2019, with stable beam commissioning nished midway through 2020. The current status of KOBRA will be presented

K8.01(초)

LAMPS for nuclear symmetry energy study at RISP

*김영진
*Young Jin. Kim
기초과학연구원.

Keyword : RISP, RAON, Rare Isotope, Symmetry Energy, LAMPS

The Rare Isotope Science Project(RISP) was established in December 2011 for the establishment of the accelerator complex(RAON) for the rare isotope science in Korea. The rare isotope accelerator at RAON will provide rare isotope(RI) beams via both the Isotope Separation On-Line(ISOL) and the In-Flight Fragmentation(IF) methods. The energy range of RI beams will be from a few MeV/nucleon to a few hundreds of MeV/nucleon for researches in fields of basic and applied science. Large Acceptance Multi-Purpose Spectrometer(LAMPS) at RAON is a heavy-ion collision experimental facility for studying nuclear symmetry energy by using RI beams. At the end of the IF separator, LAMPS experimental setup will be located for completing an event reconstruction by detecting all the particles produced in heavy-ion collisions within a large acceptance angle to measure particle spectrum, yield, ratio and collective flow of pions, protons, neutrons, and intermediate fragments at the same time. LAMPS consists of a solenoid spectrometer and a neutron detector array. A Time Projection Chamber(TPC) and a time-of-flight(ToF) detector will be placed inside of cylindrical solenoid magnet of 0.5 T for charged particle tracking and particle identification. The neutron detector array will be made of 8 layers of plastic scintillators for neutron tracking. In this presentation, the detail physics and design of LAMPS will be discussed.

K8.02(초)

Present status and future plans of J-PARC hadron experimental facility

*Kazuhiro Tanaka
*Kazuhiro. Tanaka
KEK.

Keyword : Hadron Experimental Facility, J-PARC

The hadron experimental Facility (HEF) of J-PARC restarted its operation on April 24th in 2015. Approximately two years have passed after the radioactive-materials leak incident happened on May 23rd in 2013. Now HEF is running stably with 33kW primary proton beam, which is already 9kW higher than previous (before the incident) beam power. Now main research subjects in nuclear physics at HEF are gamma ray spectroscopy of single lambda hypernuclei and search for high density nuclear matter of ppK- bound state. Soon we will start the experimental study of S=-2 hyper nuclei, which contains two lambda or single Xi. In the coming ANPhA symposium, some details of the physics results from J-PARC HEF as well as its recovery program and future plans will be given.

K8.03(초)

Study nucleon partonic structure at high-momentum beamline at J-PARC

*Wen-Chen Chang
*Wen-Chen. Chang
Academia Sinica.

Keyword : DIS, PDFs, GPDs, DVCS, DVMP

Nucleon partonic structure can be accessed either by deep inelastic scattering (DIS) with lepton beams or by Drell-Yan (DY) processes with hadron beams. With great experimental efforts, the nucleon parton distributions as a function of longitudinal-momentum fraction x (PDFs) have been obtained. Nevertheless the structures of valance and sea quarks at large-x regions are still not well known. In addition the next-generation nucleon parton distribution with additional dependence on the transverse size has been formulated as “generalized parton distributions” (GPDs) such that the role of partonic orbital angular momentum in the overall nucleon spin could be. The determination of GPDs is mostly done by the exclusive hard processes with lepton beams such like deeply virtual Compton scattering (DVCS) and deeply virtual meson production (DVMP). After the completion of the high-momentum beamline project, 10-20 GeV/c high-intensity pion and kaon beams will be available in the Hadron Hall of J-PARC. In this talk we will introduce how the large-x partonic structures and the GPDs of nucleons could be measured by the inclusive and exclusive Drell-Yan processes with the hadron beams at J-PARC. The results of feasibility study within the future E50 setup will be shown.

T1.01

Introduction to Superconductivity and Recent Development.

*방윤규
*Yunkyu. BANG
전남대학교.

Keyword : Superconductivity, Fe-based superconductors, high-Tc curates, heavy fermion superconductors, topological superconductors

After a brief explanation of key principles of the superconductivity, I will discuss the Fe-based superconductors: their unusual superconducting properties and their theoretical understandings, and some remaining puzzles. I will then briefly discuss the connections to other unconventional superconductors such as high-Tc curates and heavy fermion superconductors. Finally, switching gears I will overview the theory of the topological superconductors and their future direction.

T2.01(초)

산화물 반도체 소재 및 소자의 이슈 및 최신 연구 동향

*Jin-Seong Park
*Jin-Seong. Park
Hanyang University.

Keyword : .

Recently, AMOLED TVs are rapidly emerging and settling down on next display markets. A decade ago, many researchers have looked for proper poly-silicon structures/processes as an active layer on AMOLED backplanes. Fortunately, a novel class such as an oxide semiconductor (amorphous InGaZnO) was reported its possibility, exhibiting a reasonable mobility and process for applying on large area. Since this report, the AMOLED TV's technology has been experienced to develop/improve materials, processes, and device performance marvelously. In this tutorial, I will introduce the brief history of oxide semiconductor thin film transistors (TFTs) and show their developments for 10 years. In particular, I will discuss the fundamental of oxide semiconductor materials, device structures, and process issues. Finally, the basic device stability of oxide TFTs will be discussed in terms of oxygen and hydrogen defects.

W1.01(초)

아인슈타인 세계에서의 시간여행

*박명구
*
경북대학교.

Keyword : .

아인슈타인은 1905 년 특수상대성이론과 1915 년 일반상대성이론을 발표하면서 시간과 공간을 시공간으로 통합하였다. 통합된 시공간에서는 사건을 어떻게 표시하는지 알아본다. 또 상대성이론에서 시공간은 관찰자에 따라 어떻게 달라지며 중력의 영향은 어떠한지 살펴본다. 마지막으로 상대성이론의 체계하에서 미래로의 시간여행과 과거로의 시간여행이 어떤 조건하에서 가능해질 수 있는지 이해하고 시간여행의 특징들도 알아본다.

W1.02(초)

일반상대론으로 가는 길

*강궁원
*
KISTI. 한국과학기술정보연구원.

Keyword : .

일반상대성 이론이 출현한 지 올해로 100 년이 되었다. 일반상대론은 태양계 행성의 운동뿐만 아니라 중성자별, 블랙홀 그리고 우주팽창 등을 이해하는데 필수불가결한 사고의 틀이 되었다. 또한, GPS 등으로 일상생활에서도 활용하지 않으면 안 될 중요한 원리가 되어 가고 있다. 한편 라이고(LIGO) 등 지상에서 중력파를 검출하고자 하는 실험이 활발히 수행되고 있어 조만간 "중력파 천문학" 시대의 도래를 예고하고 있다. 본 강연에서는 일반상대론이 성립하는 데 중요한 역할을 한 몇 가지 사고실험을 위주로 일반상대론의 핵심내용을 쉽고 간략하게 소개하고자 한다. 빛속도의 불변, 시공간 연속체, 중력 적색편이, 등가원리, 중력과 시공간, 아인슈타인 방정식 등이 그것이다. 마지막으로 일반상대론의 향후 전망을 살펴보고자 한다.

Y1.01

Cosmology and Cosmic Microwave Background measurements

*François R. Bouchet
Institut d'Astrophysique de Paris CNRS & Sorbonne Universités-UPMC

Cosmology enjoyed a remarkable development over the last century, which revealed that galaxies like our own are not distributed at random into space, but rather delineate a complex structure reminiscent of the skeletal framework of a sponge. We now have developed a compelling model of how these large scale structures developed over time, and trace their origin to the earliest moment of the Big Bang. Most effective into this lightning progress has been the study of the background light called the Cosmic microwave background. This residual light, from early times when the universe was hot, dense, and very homogeneous, bear witness to the infancy of these structures. Its study allows us to determine the content of the Universe and to study the process which initiated their growth. It brings amazing confirmation of ideas put forward in the 80's and opens a window on physics in a range of scales, time and energies which was hitherto inaccessible. The most powerful tool we used so far in this endeavour is the Planck satellite mission which we entirely devoted to the study of this residual light, and which released its latest results just a few month ago. I will overview the Planck space experiment and survey some of our key results, in particular concerning precision tests of key hypotheses of the standard model of cosmology, like the flat spatial geometry or Gaussianity, adiabaticity and deviation from scale invariance of the primordial fluctuations.

Y2.01

FAIR chances for nuclear astrophysics

*Karlheinz Lang
GSI Helmholtz Centre for Heavy Ion Research

Keyword : Cosmology, Late-time Acceleration, Dark energy

The Facility for Antiprotons and Ion Research (FAIR) is currently under construction at the campus of the GSI Helmholtzzentrum in Darmstadt, Germany. FAIR will boost a new set of accelerators, storage rings and detectors which allows unprecedented research in hadron, nuclear, atomic and plasma physics and in applied sciences. In particular, FAIR will open a new era in nuclear astrophysics. It allows international experimental collaborations to probe the nuclear equation of state at high densities (CBM), to study atomic properties in extreme electromagnetic fields (SPARC) and to explore meson interactions (PANDA). The NuSTAR collaboration will use FAIR as a next-generation facility for radioactive ion beams to produce many short-lived nuclei with extreme neutron excess for the first time and to determine their properties. These nuclei play crucial roles in the dynamics of supernovae and in the nucleosynthesis of the heavy elements in the Universe.

포스터발표논문

P1-Ap.001

In-plane propagation of incident electromagnetic waves in subwavelength antenna/hole array

*이창현, 이주열, 이영백 [1]
*Changhyun. Yi, Joo Yull. Rhee, Young Pak. LEE[1]
성균관대학교. [1] *한양대학교.*

Keyword : Metamaterial, subwavelength antenna array, FDTD

It is generally believed that there is no electromagnetic wave propagating along the plane in a planar metamaterial. In this presentation, results of investigations on subwavenglth antenna/hole array by using reliable computational-electrodynamics codes, especially finite-difference time-domain(FDTD) method are reported, while there are various methods like transfer-matrix method and finite integration techniques. Some of subwavelength antenna/hole arrays show considerable in-plane propagation. Due to this in-plane propagation we had to give up the use of periodic boundary condition. In this case, we have found that time gating and/or wavesource must be chosen carefully to get the accurate result. We have investigated several structures and analyzed their FDTD simulation results and discussed the methods of optimization of simulation conditions.

P1-Ap.002*

Highly crystalline monolayer $MoSe_2$ flakes and continuous film by selenization of pre-deposited Molybdenum trioxide (MoO_3) thin film by pulse laser deposition

Farman Ullah, V. Senthilkumar, C. T. Le, 김선호, *김용수
Farman. Ullah, V.. Senthilkumar, C. T.. Le, Sun-Ho. Kim, *Yong Soo. Kim
울산대학교 물리학과 및 EHRSC.

Keyword : Pulse laser deposition, Monolayer $MoSe_2$, chemical vapor deposition, Molybdenum Trioxide. Selenization

Layered transition metal di-chalcogenides has tremendous applications in diverse fields, such as lithium ion batteries, energy harvesting, non-linear optics, electronics and optoelectronics. Monolayer $MoSe_2$ of transition metal chalcogenides is one of the promising material in this regard. However, reports on good quality, large area and continuous synthesis of monolayer $MoSe_2$ is still rare. Here, in this study we demonstrates two step growth mechanism for high quality monolayer $MoSe_2$ flakes and continuous film. Initially, we deposit MoO_3 thin film by pulse laser deposition and in second step the as grown MoO_3 film was converted to $MoSe_2$ by selenization in hot-wall furnace at 900°C. Microscopic images reveals that the grown sample comprise of monolayer $MoSe_2$ triangular flakes and continues film of approximately ~ 1 mm^2 area. Atomic force microscopy and Raman spectra confirms that $MoSe_2$ flakes are single layer. Photoluminance intensity and peak position (~1.51 eV) indicates direct band gap for monolayer $MoSe_2$.

[1]. X. Wang, Y. Gong, G. Shi, W. L. Chow, K. Keyshar, G. Ye, R. Vajtai, J. Lou, Z. Liu, E. Ringe, B. K. Tay, and P. M. Ajayan, Nano Lett, 2014 ,8,5125.

P1-Ap.003

표면조도 향상을 위한 일인산암모늄이 첨가된 알루미늄 양극산화을 통해 형성된 Al_2O_3 막의 광 특성 연구

*유재인, 윤재곤, 유재용, 고훈 [1], 김기홍 [2], 배연주 [2], 고다영 [2]
*Jae-In. Yu, JAE GON. YUN, Jae Yong. Yu, K. H[1], Ki Hong. KIM[2], Y. J. Bae[2], D.Y. K[2]
영남대학교. [1](주)테크트랜스. [2] 대구가톨릭대학교.

Keyword : 알루미늄합금, 아노다이징, 알루미나, 일인산암모늄, 표면조도

The anodization method is attractive for the formation of ordered nanochannel or nanotubular films onto the surface of valve metals. In the last few decades this method has been successfully applied for fabrication of self-ordered porous templates of aluminum oxide for subsequent production arrays of various nanostructured materials. Al plate was anodized in an acid electrolyte with Pt counter electrodes. The anodization temperature was 5 C for sulfuric acid (1.5 M) and 15 ℃ for Monoammonium phosphate (0.3 M), respectively. The anodization voltage and time were 5 ~ 30 V and 1 h. In this study, we investigated the roughness and optical properties of films produced by anodizing of Al surface in $NH_4H_2PO_4$ –containing Etg solutions.

P1-Ap.004

전기도금 BiTe 박막의 조성 및 물성

*홍기민, 진영환, 김지현
*HONG Kimin. , Jin Young Hwan. , KIM Ji Hyun.
충남대학교.

Keyword : BiTe, electroplating, thermoelectric, thin film, composition, carrier concentration

열전소자로 많은 연구가 진행되고 있는 BiTe 박막을 전기도금 방법으로 제작하였다. 도금용 전해액 내 Bi 와 Te 의 농도는 10-100 mM 이다. 전해액의 조성과 도금 전압을 변화함으로써 BiTe 박막의 조성을 조절하였다. 상대적으로 Bi 농도가 높은 전해액을 이용했을 때 도금 박막의 조성조절이 보다 용이했다. 즉, 전해액 내 Bi 농도와 전기도금 인가전압에 따라서 BiTe 박막의 조성과 carrier concentration 을 일관성 있게 조절할 수 있었다. 최적화된 도금 조건에서 Bi2Te3 박막을 제작하고 공정 조건의 변화에 따른 물성의 변화를 분석하였다.

P1-Ap.005

Temperature-dependent structures and chemical bonding states of the rare-earth-ions-doped calcium chlorapatite powders

*홍경수, 하명규, 이민정 [1], 양호순 [1]
*Kyong-Soo. HONG, Myoung Gyu. HA, Min-Jeong. LEE[1], Ho-Soon. YANG[1]
한국기초과학지원연구원. [1] 부산대학교.

Keyword : calcium chlorapatite, structures, chemical bonding states

Rare-earth ions-doped phosphors attract lots of interests because of their promising luminescent features. Among these phosphor materials, apatite compounds are widely examined because of the various application areas such as biocompatible ceramics, catalysts, ionic exchangers, oxide ion conductors, and fluorescent lightings. Apatites are inorganic components of calcified tissues such as teeth and bones of vertebrates, a basis for many pathologic solid formations, and the main raw materials in the production of phosphorus fertilizers and phosphor-organic compounds.

In this study, temperature-dependent structures and chemical bonding states in calcium chlorapatite phosphors are reported. Rare-earth-ions-doped calcium chlorapatite phosphors are synthesized by using the solid-state reaction method sintering at 1,100 ^{o}C and 1,300 ^{o}C, respectively. The characterized physical properties show that the apatite phosphors exhibit two phases with the sintering temperatures: the ones sintered below 1,100 ^{o}C form in hexagonal structure, while the others sintered at 1,300 ^{o}C form in monoclinic structure. In other words, the apatite compounds sintered at higher temperature show the structure with lower space symmetry. The chemical bonding states of the synthesized powders remain unchanged regardless of the amount of doped rare earths and the sintering temperatures.

P1-Ap.006

Preparation and optical characterization of the tristrontium silicate phosphors

*홍경수, 하명규, 이민정 [1], 양호순 [1]
*Kyong-Soo. HONG, Myoung-Gyu. HA, Min-Jeong. LEE[1], Ho-Soon. YANG[1]
한국기초과학지원연구원. [1] 부산대학교.

Keyword : tristrontium silicate, phosphors

The silicate ceramics is a useful luminescent host material with a stable crystal structure. Thus, lots of studies on silicate materials have been conducted. Among the silicate ceramics, Eu^{2+}-doped tristrontium silicate (Sr_3SiO_5:Eu^{2+}) is known as a yellow emitting phosphor and attracted due to the white light-emitting diodes (LEDs) applications because White LEDs are made from blue LEDs and a yellow emitting phosphor. Up to now, Sr_3SiO_5:Eu^{2+} phosphors are studied on focusing the effect of Eu^{2+} concentration and various fluxing agents, etc. However, there are not many reports about the other rare-earth-doped Sr_3SiO_5 phosphors.

In this study, preparation process and optical properties of the Sm^{3+}-doped Sr_3SiO_5 phosphors are reported. The Sr_3SiO_5 phosphors are synthesized by using the solid-state reaction method sintering at 1,300 ^oC for 6 h. The basic physical properties are characterized by using XRD, SEM, and XPS, with the variation of the doped Sm^{3+} amount. Optical properties are studied by measuring the absorption, excitation, and emission spectra. The Sm^{3+}-doped Sr_3SiO_5 phosphors are red-emitting phosphors under the excitation of near ultra-violet region.

P1-Ap.007*

Electrochemical properties of graphite modified by plasma treatment

*정혜경, 김호준
*Hae Kyung. Jeong, Hojun. Kim
대구대학교.

Keyword : Graphite, plasma, supercapacitor

Usually, supercapacitor is used carbon allotrope for electrode such as activated carbon, carbon nanotube, graphene. Graphene is a high specific surface area, lightweight and high electrical conductivity. In this paper, the Highly Ordered Pyrolysis Graphite (HOPG) was investigated by plasma treatment. HOPG with water layer and HOPG without water layer showed different result after treatment with plasma. The result is investigated by using Cyclic Voltammetry(CV) for capacitance characterization and impedance measurement is using Electrochemical Impedance Spectroscope(EIS). Also, Scanning Electron Microscope(SEM) used for their surface morphology and Energy Dispersive X-ray Spectroscope(EDX) to investigate the quantity of element in each HOPG. The experiment result is showed that the surface of HOPG change at different interval of time. It is caused the change of electrochemical properties such as capacitance and impedance by plasma treatment which physical bonding oxygen on HOPG surface area.

P1-Ap.008

Innovative three-dimensional(3D) eco-TiO_2 photocatalysts for practical environmental and bio-medical applications

박소영, 이현욱, 서순주, 김혜란, *윤형중, 이순창 [1], 이주한
So young. Park, Hyun Uk. Lee, Soonjoo. Seo, Hyeran. Kim, *Hyung Joong. Yun, Soon Chang. Lee[1], Jouhahn. Lee
한국기초과학지원연구원 (KBSI). [1] 충남대학교.

Keyword : TiO2, photocatalyst, Bio, AAO, environment

It is known that water purified by conventional TiO_2 photocatalysts may not be safe enough for drinking, due to the toxicity by tiny existence of TiO_2 nanoparticles after water treatment. We herein demonstrate a facile design of a three-dimensional (3D) TiO_2 photocatalyst structure with which both the efficiency of purification and the safety level of the final purified water can be improved and ensured, respectively. The structure, consisting of 3D sulfur-doped TiO_2 microtubes in nanotubes (eco-TiO_2), is suitable for both environmental and bio-medical applications. Investigation of its formation mechanism reveals that anodic aluminum oxide (AAO), owing to a spatial constraint, causes a simple, nanoparticles-to-nanotubes structural rearrangement as a template for nanotube growth. It is found that eco-TiO_2 can be activated under visible-light irradiation by non-metal (sulfur; S) doping, after which it shows visible-light photocatalytic activities over a range of solar energy. Importantly, an in vitro cytotoxicity test of well-purified water by eco-TiO_2 confirms that eco-TiO_2 satisfies the key human safety conditions.

P1-Ap.009*

타원평광분석법을 이용한 $SrTiO_3$ 유전율 함수의 온도 의존성 연구

*김화섭, 박한결, 김태중, Mangesh S. Diware, Van Long Le, 유창현, 김영동
*Hwa Seob. Kim, Han Gyeol. Park, Tae Jung. Kim, Mangesh. Diware, Van Long. Le, Chang Hyun. Yoo, Young Dong. Kim
경희대학교.

Keyword : Perovskite 기반 산화물, $SrTiO_3$, 타원편광분석법, 유전율 함수, 전이점

일반적으로 강유전성을 가진 perovskite 기반 산화물은 압전소자 센서, 소형 콘덴서의 유전체로 널리 활용되어, 반도체 이론 및 실험 분야에서 연구되고 있다. 그 중에서도 $SrTiO_3$ (STO)는 높은 절연성을 가졌으며 자발 분극 고온 초전도체와 게이트 유전체와 같은 특수 목적의 얇은 산화막에 이상적인 기판으로 사용된다. STO 를 더욱 정밀하고 심도 있게 응용하기 위해서는 유전율 함수 정보가 필요하지만, 온도 변화에 대한 연구는 수행되지 않았다. 타원편광분석법은 빛의 편광을 이용한 비파괴검사로써 물질의 광특성을 측정하는데 정확하고 민감한 기술이다. 본 연구에서는 top-seed 용액 성장된 STO 단결정의 유전율 함수를 26 – 674 K 온도 범위와 0.74 – 6.42 eV 에너지 범위에서 타원편광분석법으로 얻었다. 전이점의 에너지 값은 이차미분 표준해석법 (standard analytic critical point expression) 으로 결정하였고, 그 결과 전자-포논 상호작용이 적은 26K 에서 두 개의 전이점을 추가로 확인할 수 있었다. 본 연구결과는 STO 특성의 물리적 이해 및 이를 기반으로 하는 소자 응용에 유용하게 이용될 수 있을 것이다.

P1-Ap.010*

Reduction of Graphene Oxide by using atmospheric pressure plasma treatment

*정혜경, Niyitanga Theophile
*Hae Kyung. Jeong, Niyitanga. Theophile
대구대학교.

Keyword : Graphite oxide, Reduction, Plasma

we present a simple, fast, eco-friendly and low cost method to reduce graphene oxide by using atmospheric pressure plasma treatment. The morphology of graphene oxide (GO) before and after plasma treatment (PGO) and were analyzed by scanning electroscope, and energy dispersive x-ray was used to analyze weight and atomic % of C/O ratio where PGO shows C/O ratio of 2.8. Cyclic voltammetry , galvanostatic charging and discharging profile and electron impedance spectroscopy were used to investigate electrochemical properties and the result shows that PGO has good electrochemical properties comparing to that of GO ,where specific capacitance of PGO was almost twice to that of GO. we also used X-ray diffraction to investigate atomic structure and interlayer spacing, and PGO has shown the presence of interlayer of few-layer of graphene sheets., which demonstrates its potential for energy storage applications.

P1-Ap.012*

Strategy of a thermal conductivity measurement of topological insulators using a time-domain thermoreflectance technique

*최영관, 이종석 [1]
*Younggwan. Choi, Jongseok. LEE[1]
광주과학기술원(GIST). [1] *광주과학기술원.*

Keyword : Time-domain thermoreflectance, topological insulator

There has been a significant interest in the study of thermoelectric (TE) materials for several decades, and topological insulator (TI) is considered as one of the most challenging TE candidate materials; as they are prepared to have nanostructures, grain boundaries between two different TIs can contribute to enhance an electrical conduction and thermal insulation simultaneously, and hence increase the figure of merit of the thermoelectric application. To investigate thermal properties of TI materials, we have been preparing time-domain thermoreflectance (TDTR) technique which is one of the most powerful tools to measure the thermal conductivity of film and bulk materials. In this presentation, we present simulation results of the TDTR responses of TI materials and discuss the strategy for the efficient characterization of thermal properties of nanostructure TI materials.

P1-Ap.013

Mesoporous ZrO_2 spheres with hollow interior by a solvothermal reaction

문주영, *양현경, 문병기, 정중현
Ju Young. Mun, *Hyun Kyoung. Yang, Kee Moon. Byung, Jung-Hyun. Jeong
부경대학교.

Keyword : "Mesoporous" , "ZrO_2 spheres" , "solvothermal"

Mesoporous material has pores as a porosity of between 1 ~ 100 nm of less than micro and macro size. That is known by the size of the pores to selectively shortcomings of zeolites in microporous material in technology to secure there. Recently, Mesoporous materials have attracted extensive attention owing to their promising applications in the optical science, catalysis, energy materials, CO_2 adsorption separation, electrochemical, battery materials, filter and drug delivery carrier and so on.
ZrO_2 is one of the most important oxide materials with wide band-gap energy (≈ 5.0 - 5.85 eV). ZrO_2 has gained much considerable attention owing to its potential applications in many fields, such as catalytic activity, photo catalysis, photo-electrochemical conversion and so on.
We report the synthesis of ZrO_2 spheres with hollow interiors, using a solvothermal reaction method. ZrO_2 spheres were found to form through the aggregation of small ZrO_2 particles with diameter of tens of nanometers, which could be observed by controlling the reaction temperature. Furthermore, the structural and morphological properties such as diffraction patterns, surface and interior morphology, and thermal changes of the mesoporous materials spheres have been studied.

P1-Ap.014*

PLD 방법을 이용한 Pyrochlore 구조의 $Tl_2Ru_2O_7$ 박막 제작 및 금속-비금속 전이 특성 관찰

*김용환, 허남정
*yonghwan. kim, Namjung Hur.
인하대학교.

Keyword : Pulsed Laser Deposition, Metal-Insulator transition, Pyrochlore, $Tl_2Ru_2O_7$

기존의 $Tl_2Ru_2O_7$ 다결정 및 단결정 제작은 3GPa 의 높은 산소 분압에서 이루어졌다. 그러나 PLD 에서 제작하는 박막의 경우 기존의 실험결과와는 달리, 낮은 산소 분압 과 낮은 온도에서 제작하여도 금속-비금속 전이가 나타나는 것을 확인하였다. 박막 증착을 위해 기판은 YSZ(111) 기판을 사용하였으며, 기판 온도 300℃, 산소 분압 300mTorr 에서 증착하였다. 저항 측정은 4 침법을 이용하여 측정하였고 온도에 따른 박막의 저항을 측정하여 금속-비금속 전이가 나타남을 확인하였다. 제작 분위기에 따른 금속-비금속 전이 특성의 차이를 알아 보기 위해, 제작 시, 산소분압을 50~400mTorr 으로 바꿔가면서 저항 특성을 관찰해 보았다. 그 결과 산소 분압이 낮을수록 금속-비금속 전이가 억제되는 것을 확인하였다.

P1-Ap.015*

Electrical properties of electrospun carbon-PVA nanofiber

김혁준, *여창수, 신민균, 한준범 [1], 송윤규, 주상현 [1], 박상윤
Hyuk-joon. KIM, *Chang Su. Yeo, Min Kyoon. Shin, June Beam. Han[1], Yoon-Kyu. Song, Sang Hyun. Ju[1], SangYoon. Park
서울대학교 차세대융합기술연구원. [1] 경기대학교.

Keyword : "카본나노튜브" , "그래핀", "전기방사", "나노섬유"

전기방사법은 고분자 또는 고분자-나노복합체를 수십나노에서 수백나노의 크기로 섬유형태로 간단히 제조할 수 있어 생명공학과 전자소자에 응용가능성이 매우 높아 많은 연구가 진행되어 왔다. 특히 전도성 나노섬유는 높은 유연성과 기계적 내구성으로 인해 투명전극으로써의 활용가능성이 높다. 본 연구에서는 전기방사법으로 탄소나노입자(graphene, CNT)-PVA 나노섬유를 core-shell 구조, composite 구조, core-shell composite 구조로 제조하고 전기적 특성과 기계적 특성을 비교하여, 최적화된 전기전도도와 탄성특성을 가진 제조기법을 제시하고자 한다. 또한, tunneling, percolation charge transport 모델을 통해 carbon-PVA 나노섬유의 전도특성을 제시하고자 한다.

P1-Ap.016

Growth mechanism and controlled synthesis of single-crystal monolayer graphene on germanium

김유석, 김지선 [1], 심지니 [1], 송우석 [2], 전철호, 이주한, 박종윤[1]
*Yooseok. Kim, Ji Sun. Kim[1], Jeeny. Shim[1], Wooseok. Song[2], Cheolho. Jeon, Jouhahn. Lee, Chong-Yun. Park[1]
한국기초과학지원연구원 (KBSI). [1] 성균관대학교. [2] 한국화학연구원.

Keyword : Graphene, Chemical vapor deposition, germanium

Mechanically exfoliated graphene demonstrates extraordinary electrical and physical properties that could be harnessed to enable exceptional advances in technology. However, the initially reported micromechanical exfoliation of highly oriented pyrolytic graphite can only yield a minute amount of small single-crystal graphene, limiting the practicality of this method. Recently developed chemical vapor deposition (CVD) methods could produce large-size and uniform polycrystalline graphene, but the electronic properties of CVD graphene are degraded by domain boundaries. Thus, the fabrication of large-size single-crystal graphene using CVD has attracted much interest among materials scientists. In addition, single-crystal monolayer graphene with a predefined orientation will allow various applications of graphene's orientation-dependent properties.
In this research, we present the growth of single-crystal monolayer graphene on hydrogen-terminated germanium (Ge) surface. A single-crystal Ge substrate is a promising candidate for the growth of single-crystal graphene, because of its catalytic activity for the catalytic decomposition of the formation of graphitic carbon on the surface; the extremely low solubility of carbon in Ge even at its melting temperature, enabling growth of complete monolayer graphene; the availability of a large area single-crystal surface via epitaxial Ge growth on Si wafers. The structural features such as surface morphology crystallinity were investigated by scanning electron microscopy (SEM) and atomic force microscopy (AFM), transmission electron microscopy (TEM) and resonant Raman spectroscopy. We believe that our approach for the synthesis of single-crystal monolayer graphene may be potentially useful for the development of many electronic devices.

P1-Ap.017*

Nb 가 치환된 $CaBi_4Ti_4O_{15}$ 세라믹스의 구조 및 전기적 특성 변화

*조삼연, 김진우, 최기쁨, 부상돈
*Cho Sam Yeon. , Kim Jin woo. , Choi Gi ppeum. , Bu Sang Don.
전북대학교.

Keyword : 비스무스 층상구조, 고온/고방사선 환경, CBTO, 압전체

최근 우주 항공 산업과 원자력 등의 에너지 산업이 발전 함에 따라서 고온/고방사선 환경에서 구동하기 위한 액추에이터 (actuator), 센서 (sensor), 메모리 소자 (memory device)에 대한 요구가 지속적으로 증가하고 있다. 비스무스 층상구조 형 강유전체 (bismuth layer-structured ferroelectrics, BLSFs)는 일반적으로 $(Bi_2O_2)^{2+}(A_{m-1}B_mO_{3m+1})^{2-}$ 의 식으로 표현되며, $(Bi_2O_2)^{2+}$ 의 비스무스 층 사이에 $(A_{m-1}B_mO_{3m+1})^{2-}$ 의 페로브스카이트 (perovskite) 층이 삽입된 구조를 갖는다. BLSFs 는 높은 큐리 온도 (the Curie temperature, T_c)를 갖는 것으로 알려져 있으며 특히, $CaBi_4Ti_4O_{15}$ (CBTO)는 BLSFs 에서도 가장 높은 T_c (790 ºC)를 보이며, 높은 전기 저항성 (500 ºC 에서 4.2 X 10^6 Ω cm)을 보이기 때문에 고온 환경 적용에 있어 유망한 물질 중 하나이다. 그러나 낮은 압전특성은 (d_{33} = ~8 pC/N) 응용 분야에 한계를 갖게 한다. 따라서, 본 연구에서는 CBTO 의 고온 T_c 특성은 유지하면서 압전 특성을 향상시키기 위한 방법의 하나로 페로브스카이트 구조의 B-site 위치에 Nb 를 치환하였다. Nb 치환은 $CaBi_4Ti_{4-x}Nb_xO_{15}$ (x=0.0 ~ 0.20) 범위에서 이루어 졌으며, Nb 와 Ti 이온의 반경 차이에 의해 페로브스카이트 구조내의 산소 팔면체 (BO_6)의 뒤틀림 (distortion)을 유도하여 압전 특성을 향상 시킬 것으로 예상하였다. 그 결과 x-선 회절에서는 Nb 치환에 따른 주목할 만한 변화는 나타나지 않았지만, 압전상수 측정결과에서는 순수한 CBTO (~8 pC/N)에 비해 2 배 정도 향상된 ~15 pC/N 값을 보였다. Thermal depoling 온도 (T_d) 측정 결과에서는 모든시료에서 800 ºC 까지 탈분극 (depolarization)현상이 나타나지 않았다. 이러한 결과들에서 Nb 가 치환된 CBTO 세라믹스의 고온 압전 소자로써의 가능성을 확인 하였다. 이와 함께 감마선 조사 실험을 통해 내방사선 특성도 함께 조사하였다.

P1-Ap.018*

High conductive wet-spun carbon-PVA fiber and wearable device applications

*여창수, 김혁준, 신민균, 이주열 [1], 박상윤
*Chang Su. Yeo, Hyuk-Joon. Kim, Min Kyoon. Shin, Joo yull. Rhee[1], Sang Yoon. Park
서울대학교 차세대융합기술연구원. [1] 성균관대학교.

Keyword : "탄소섬유", "카본나노튜브", "그래핀", "습식방사"

탄소섬유는 우수한 기계적, 전기적 특성으로 인해 다양한 분야에 핵심소재로써 사용되고 있다. 특히 최근 carbon nanotube (CNT), graphene 과 같은 나노크기의 탄소입자는 기존 탄소섬유에 비해 이론적으로 더 우수한 특성이 예상되므로 섬유로 제조하기 위한 방법이 제시되었다. 본 연구에서는 습식방사로 CNT, graphene 섬유를 제조하고 나노입자의 nematic liquid crystal 특성이 기계적 강도, 전기전도도에 미치는 효과를 보여주고자 한다. 또한, 실제로 실형태로 섬유를 제조하고, 일반적인 sewing machine 을 이용하여 wearable device 의 전도성 섬유로 실용화 할 수 있음을 보여주고자 한다.

P1-Ap.019

Luminescence properties of near-infrared excited blue emission in $La_{(0.87-x)}NbO_4$:$Yb_{0.13}^{3+}$, Tm_x^{3+} phosphors

*이성수, 남기원, 최성우, 김종원
*Soung Soo. Yi, Ki Won. Nam, Sung Woo. Choi, Jong Won. Kim
신라대학교.

Keyword : Upconversion, luminescence, $La_{(0.87-x)}NbO_4$:$Yb_{0.13}^{3+}$, Tm_x^{3+}, phosphors, crystallinity

Different concentrations of Tm3+ ions-doped La(0.87-x)NbO4 : Yb0.133+, Tmx3+(x=0.003, 0.006, 0.009, 0.012) polycrystalline powder phosphors were prepared by the conventional solid state reaction method. The crystalline structure, morphology and chemical analysis of the as-prepared phosphors were characterized by X-ray diffraction(XRD), scanning electron microscopy (SEM), and energy-dispersive spectroscopy(EDS) techniques, respectively. The photoluminescence properties of the as-prepared powder samples were studied. The spectrum consisted of 1G4-3H6, weak 1G4-3F4, and intense 3H4-3H6 transition bands with in the f12 configuration of Tm3+, together with the 2F5/2-2F7/2 transition of Yb3+. The up-converted emission of La(0.87-x)NbO4 : Yb0.133+, Tmx3+ powders was observed under laser diode excitation of 980 nm. Obvious differences in up-converted emission spectra among the as-obtained products were observed, and possible reasons were discussed. The corresponding up-conversion mechanism was also proposed. The energy transfer and upconversion luminescence properties of the La(0.87-x)NbO4 : Yb0.133+, Tmx3+ phosphors have been discussed.

P1-Ap.020

Up-conversion luminescence properties of $La_{(0.94-x)}NbO_4$:Yb_x^{3+} ,$Tm_{0.06}^{3+}$ phosphors

*이성수, 정지훈, 신상수
*Soung Soo. YI, Ji Hoon. Jeong, Sang Su. Shin
신라대학교.

Keyword : Up-conversion, luminescence, LaNbO4 :Yb3+ ,Tm3+, phosphors

La(0.94-x)NbO4 : Ybx3+ ,Tm0.063+(x=0.05, 0.01, 0.125, 0.15) phosphors were synthesized by solid state reaction. Phosphor powder were measured by using the X-ray diffraction (XRD : Rigaku, Ultima IV) radiated by Cu-Kα1 (λ=0.1540596 nm). Particle sizes of crystal and surface shapes were investigated by a FE-SEM(field emission-scanning electron microscopy, Hi-tachi S4200). In the presence of Yb3+ ions, the emission is also achieved by near infrared excitation through a typical up-conversion process under 980 nm. The photoluminescence properties of the as-prepared powder samples were studied. The spectrum consisted of 1G4-3H6, weak 1G4-3F4, and intense 3H4-3H6 transition bands with in the f12 configuration of Tm3+, together with the 2F5/2-2F7/2 transition of Yb3+. The suitability of material in increasing the efficiency of silicon solar cell has been realized. This phosphor show that for co-doped(Tm3+, Yb3+) samples one emission from the each activator which is obtained the blue and red(Tm3+) emissions.

P1-Ap.022

생분해성 열전도 절연 복합소재를 활용한 고방사율 LED 히트싱크 개발연구

유삼주, 이주현, 주정식, *양현경
YOO SAM-JOO. , LEE JOO HYUN. , JOO JUNG SIK. , *Yang Hyun Kyoung.
부경대학교.

Keyword : "PLA" , "LED heatsink" , "heatsink"

기존에 사용되는 LED heatsink 는 알루미늄 다이케스팅 및 판재를 활용한 LED Chip 에 열을 외부로 방출하는 제품이 대다수였지만, 누설전류로 인해 발생되는 LED Chips 에 손상과 안전문제 대두로 인해 알루미늄 heatsink 에 절연 코팅을 하는 번거로움이 있었다.
친환경 소재인 BIO 소재를 활용한 LED heatsink 제조를 하기 위해 비표면적이 많은 활성탄 나노 기공에 나노 은을 침투 후 표면 및 기공에 접착력이 탁월한 에폭시 수지를 반응시켜 열전도에 issue 가 될 수 있는 공기층을 최소화하고 방사율이 우수한 복사열전도 기능을 증가 시킬 수 있다. 특히 복사 열전도성이 좋은 Graphite, CNT, Carbon fiber 는 전기가 통하여 절연기능이 없고, 금속파우더는 열전도율은 우수하나 상기와 같이 절연기능을 부여하기 위해 표면 절연 코팅을 하는 번거로움이 있다.
친환경 절연 열전도성 복합 플라스틱 제조에 있어 heatsink 와 대기중 자연자류에 효율을 상승시키고 기존 전도성 filler 충전제에 비해 복사열전도 기능이 탁월한 효과를 얻을 수 있다.
본 연구는 분해성 복합플라스틱 제조를 위해 PLA(Poly Lactic Acid)소재에 물성이 약하고 브리틀한 특성을 보강하기 위해 생분해성 소재인 PBS, PBAT, PBSA, PCL, PVA 소재중 비교적 내열성이 우수한 PBAT 소재와 혼합 사용하여, 활성탄 기공에 나노은침투 및 건조 단계, 에폭시수지 침투 및 표면코팅단계, 열경화 단계를 거쳐 제작한다. 제작된 시료는 열전도율, 열방사율을 측정하여 열특성을 분석한다.

P1-Ap.023

High-quality and color-tunable InP/ZnS quantum dots using amine-derived synthetic approach

*정도영, 정진주, 원하연, 김도형
*Do Yeong. Jeong, Jinjoo. Jung, Ha Yeon. Won, Do Hyung. Kim
경북대학교.

Keyword : "non-cadmium", "InP/ZnS QDs", "tris(dimethylamino)phosphine(P(N(CH_3)$_2$)", "the shelling time "

Non-Cadmium and High-quality InP quantum dots(QDs) have been synthesized by using tris(trimethylsilyl)phosphine(P(TMS)$_3$) as a phosphorus precursor source. However, P(TMS)$_3$ is expensive and dangerous to treat because of its chemical instability. So we synthesized using tris(dimethylamino)phosphine(P(N(CH_3)$_2$)$_3$) as an alternative P source, which is far safer during hot-injection process and much cheaper. In this study, we researched physical and optical properties of InP/ZnS QDs. And we confirmed the effect of the dependence on the shelling time of ZnS. The diameters and FWHM(full width at half maximum) of the QDs were 5-8nm, 50nm respectively. As the shelling time of ZnS is increased, photoluminescence intensity was enhanced by approximately 5 times.

P1-Ap.024*

Investigation of the electrical properties of benzenethiol self-assembled monolayers in graphene-electrode molecular electronic devices

*장연식, 정현학, 김동구, 황왕택, 민미숙, 이탁희
*Yeonsik. Jang, Hyunhak. Jeong, dong ku. Kim, Wang taek. Hwang, Misook. Min, Tak Hee. LEE
서울대학교.

Keyword : Molecular Devices. Multilayer Graphene (MLG), Benzenethiols

Molecular electronics deals with a single molecule or molecular monolayer as an active device component. In particular, vertical-type solid state device based on molecular self-assembled monolayer junction has gained a large attention as a testbed to study charge transport characteristics of molecular-scale junction. However, such fabrication technique usually incorporates evaporating top metal directly onto the molecular layer, which may often cause filamentary path formation resulting in electrical short circuit in the junctions. As a new approach to solve this problem and fabricate reliable molecular junctions, multilayer graphene film has been applied as an interlayer between the molecular layer and top electrode, and this method exhibited an excellent electrical stability and high device yield [1].

In this presentation, we report a fabrication of two types of benzenethiol (4-methylbenzenethiol and benzene-1,4-dithiol) based molecular self-assembled monolayers with multilayer graphene electrode in vertical-type molecular junction. We compared electrical characteristics of these two molecules which have the same backbone structure but different end-group. We observed that no significant difference of electrical properties were occurred between two types of molecular devices. This investigation supports insensitive charge transport nature in spite of end-group substitution in molecular electronic system where weak van der Waals force exerts on the physisorbed interface system.

References

[1] Wang et al., Adv. Mater. 23, 755 (2011).

P1-Ap.025

몬테카를로 방법을 이용한 나노구조 회절격자 엑스선 영상장치 차폐계산

*김인수, 이현우, 표성환, 김은광, 김숭구, 한범수, 강창무 [1], 우혜영 [2], 안치원 [2], 이세호 [3], 김영주 [3], 이승욱 [3]
*KIM INSOO. , . , . , . , . , . , . , Chang M. Kang. [1], . [2], . [2], . [3], . [3], Seung Wook LEE. [3]
이비테크(주). [1] 한국과학기술정보연구원. [2] 나노종합기술원. [3] 부산대학교.

Keyword : phase contrast grating, X-ray phase contrast image, MCNP code

나노구조 회절격자를 이용한 엑스선 영상장치는 종래의 엑스선 투과 영상(흡수영상)과 더불어 엑스선 회절격자를 이용한 위상차(phase contrast) 영상 및 가시도(darkfield) 영상 획득을 통하여 피조사체의 구조결함 및 부패정도를 영상으로 구현가능하다.
본 연구에서는 나노구조 회절격자를 이용한 엑스선 영상장치 시제품을 제작하기 위하여 엑스선에 의한 외부 누설선량을 MCNP(Monte Carlo N-Patricle transport) 코드를 사용하여, 시제품의 3 차원 기하학적 구조 모델링을 하였으며 32 multi-thread 를 갖는 시뮬레이션 컴퓨터를 사용하여 계산하였다.
MCNP 모델링은 내부필터가 존재하는 엑스선발생장치에서 120kV 4mA 로 엑스선을 방출할 때 에너지별 스펙트럼을 갖는 선원의 모델과 동 상황에서 단일 유효에너지일 경우 선원의 모델을 비교평가 하였다. 선원으로부터 1m 떨어진 곳에서의 방사선량 측정데이터를 표준으로, MCNP 모델링된 선원으로부터 거리에 따른 선량 분포와 일정한 거리에 반가층(HVL)에 해당되는 알루미늄을 삽입하여 선량을 확인하였다. 또한 MCNP 모델링에 추가 외부필터를 적용하여 나노구조회절격자 제작 시 설정한 유효에너지와 반가층 추가에 따른 선량분포를 비교평가 하였다. 최종적으로 엑스선 회절영상 영상장치에 대한 차폐평가를 몬테카를로 방법을 사용하여 검증하였다.

P1-Ap.026*

Dissociative hydrogen adsorption on bilayer graphene/hexagonal boron nitride

*홍성주, 강호진, 박민, 이민우, 다비드, 정대홍, 박영우, 김병훈 [1]
*Sung Ju. Hong, Hojin. Kang, Min. Park, Minwoo. Lee, David Soler. Delgado, Dae Hong. Jeong, Yung Woo. PARK, Byung Hoon. KIM[1]
서울대학교. [1] *인천대학교.*

Keyword : Bilayer graphene, Hydrogen, Electron doping, Raman spectroscopy, Hexagonal boron nitride

We have investigated dissociative hydrogen (H_2) adsorption on bilayer graphene (BLG)/hexagonal boron nitride (h-BN). The BLG/h-BN heterostructure provides an advantage to study intrinsic chemical interaction between BLG and H_2. Temporal evolution of electrical conductivity vs gate voltage (σ vs V_g) showed that the H_2 adsorption follows first order Langmuir type and results in electron doping. In addition to the charge transfer phenomena, we observed that the H atom behaves like short-range scatterer, which is analyzed by impurity density dependent mobility. Raman spectroscopy supports the supplemental results such as electron doping, short-range scattering, and compressive lattice strain.

P1-Ap.027*

N-type doping in CVD-grown bilayer graphene by hydrogen exposure

*다비드, 홍성주, 박민, 강호진, 이민우, 정대홍, 박영우, 김병훈 [1]
*David. Soler Delgado, Sung Ju. Hong, Min. Park, Hojin. Kang, Minwoo. Lee, Dae Hong. Jeong, Yung Woo. PARK, Byung Hoon. KIM[1]
서울대학교. [1] *인천대학교.*

Keyword : Chemical vapor deposition, bilayer graphene, Thermoelectric power, Hydrogen

We report progressive n-type doping of chemical vapor deposition (CVD) grown bilayer graphene (BLG) due to hydrogen exposure. Charge neutrality point (CNP) in transfer characteristic (I vs Vg) moved to negative gate voltage region, which means BLG become n-doped. In addition, thermoelectric power (TEP) measurements are used to verify this trend. The n-type doping was observed on BLGs regardless of the twist angles. Our results can be used as an aid for exploring further functionalities of hydrogenated BLG devices.

P1-Ap.028*

Temperature and polarization dependence of Raman spectra of 1T- and 2H-TaS_2

*김민정, 김학성 [1], 이재웅, 이상욱 [1], 정현식
*Minjung. Kim, Hakseong. Kim[1], Jae-Ung. Lee, Sang Wook. Lee[1], Hyeonsik. Cheong
서강대학교. [1] *건국대학교.*

Keyword : Tantalum disulfide (TaS_2),Charge density wave (CDW), Raman spectroscopy, phase transition

Tantalum disulfide (TaS_2) which has 1T and 2H polytypes is intriguing due to the formation of the charge density waves (CDW) and the related phase transition by varying temperature. The dynamics of the CDW in 1T-TaS_2 have been investigated by Raman scattering measurements [1-3]. In this work, we measured the temperature dependence of the Raman spectra and the resistance of 1T- and 2H-TaS_2. Because the transition temperature of 1T-TaS_2 depends on the thickness of the material and has hysteresis [4], the Raman spectrum and the resistance were measured at each temperature as the temperature is varied in order to pinpoint the transition temperature. We also measured the polarization dependence of the Raman spectra when TaS_2 is in the CDW state.

[1] J.R. Duffey et al., Solid State Communications 20, 617 (1976).
[2] S. Sugai et al., Physica B 105, 405 (1981).
[3] T. Hirata et al., Solid State Communications 117, 361 (2001).
[4] Y. Yu et al., Nature Nanotechnology 10, 270 (2015)

P1-Ap.029*

Evaluation of gas barrier property of graphene formed by two-step growth process and electro-chemical polishing

*이슬아, 서태훈, 조현진, 김준희, 민경현, 박아현 [1], 서은경 [1], 이재관 [2], 김명종
*Seula. Lee, Tae Hoon. Seo, Hyunjin. Cho, Jun Hee. Kim, Kyung Hyun. Min, Ah Hyun. Park[1], Eun-kyung. Suh[1], Jae Kwan. Lee[2], Myung Jong. Kim
한국과학기술연구원. [1] 전북대학교. [2] 조선대학교.

Keyword : graphene, gas barrier, two-step growth, electro-chemical polishing, water vapor transmission rate

We introduce a two-step growth process of graphene on electrochemically polished Cu foil to achieve large graphene domains and improved graphene quality by low pressure chemical vapor deposition (LPCVD). The performance of resulting graphene as a gas barrier was systematically evaluated and compared to graphene obtained by one-step growth on polished and unpolished Cu foils. Scanning electron microscopy (SEM), atomic force microscopy (AFM), and micro-Raman studies revealed large graphene domains and low defect density in graphene grown by two-step growth process. This is attributed to the suppression of early graphene nucleation and reduction of surface roughness as well as defects and impurities that exist on Cu foils. When transferred on to poly ethylene terephthalate (PET) film, the water vapor transmission rate (WVTR) and permeability of graphene/PET significantly decreased, compared to other two graphene and pure PET films. The results indicate that the use of electro-chemical polishing and two-step growth methods for the growth of high quality graphene could open up the possibility for exploring graphene-based gas barrier.

This work was supported by grants from the Korea Institute of Science and Technology (KIST) Institutional Program, the Converging Research Center Program funded by the Ministry of Science, ICT & Future Planning Technology (2014M3C1A8054009), and the Graphene Materials/Components Development Project (10044366) through the Ministry of Trade, Industry, and Energy (MOTIE), Republic of Korea.

P1-Ap.030*

Raman spectra of 2D metal monochalcogenide semiconductor GaSe

*임수연, 이재웅, 정현식
*Soo Yeon. Lim, Jae-Ung. Lee, Hyeonsik. Cheong
서강대학교.

Keyword : Raman spectroscopy, GaSe, monochalcogenide

We measured the Raman spectra of few-layer GaSe. Although most studies have focused on 2D transition metal dichalcogenides (TMDCs), 2D layered metal monochalcogenides, such as GaS, GaSe, and InSe, have recently attracted increasing interest. 2D metal monochacogenides show significantly different electronic and optoelectronic properties from those of TMDCs.[1] For examples, GaSe-nanosheet-based photodetectors show better performance compared to existing photodetectors such as graphene-based photodetectors.[2] Few-layer GaSe samples were mechanically exfoliated on silicon substrates with oxidized layer of 90 nm thickness. We performed Raman measurements in vacuum to avoid damaging the sample.

References
[1] Xufan Li et al, Scientific reports 4, 5497 (2014)
[2] PingAn Hu et al, ACS nano 6, 5988 (2012)

P1-Ap.031*

Polarized Raman Spectra in Few-layer Black Phosphorus

*김중철, 이재웅, 정현식
*Jungcheol. Kim, Jae-Ung. Lee, Hyeonsik. Cheong
서강대학교.

Keyword : Black phosphorus, Raman spectroscopy

Few-layer black phosphorus is attracting interest recently as a promising candidate for field effect transistor devices with a high carrier mobility (~300 V cm^2/s) and a high on/off ratio (~10^5) which are important for logic circuits [1]. It has been known that the mobility depends on the crystallographic orientation of the sample due to anisotropy.

We performed Raman measurements on few-layer black phosphorus in vacuum. We prepared the samples on SiO_2/Si substrates by mechanical exfoliation. The thickness was confirmed by low frequency interlayer breathing Raman modes [2]. In backscattering geometry, there are three Raman vibration modes: the out-of-plane (A_g^1) mode at around 360cm^{-1} and the in-plane (B_{2g}, A_g^2) modes at around 440cm^{-1} and 467 cm^{-1} [3]. We investigated the excitation wavelength and polarization dependence of each Raman mode. The spectra with different excitation wavelengths were compared at the same polarization direction.

[1] S. P. Koenig et al, Appl. Phys. Lett. 104, 103106 (2014)
[2] L. Xi et al, Nano Lett. 1, 4080 (2015)
[3] A. Castellanos-Gomez et al, 2D Mat. 1, 025001 (2014)

P1-Ap.032*

High Performance Solid Electrolytes based on Lithium Salt Soluble in Plasticizer Mixed with Polyvinyl Alcohol

오심건, *강대준
Simgeon. OH, *Dae Joon. Kang
성균관대학교.

Keyword : solid electrolytes, dimethyl phthalate, LiClO4, PVA

Much attention has been paid recently to improve the ionic conductivity of solid electrolytes for the development of next generation batteries. In this work, we report on our efforts to seek out novel additive polymeric materials that can be used both as a liquid electrolyte and as a plasticizer. We have successfully synthesized a high ionic conductive polymer based solid electrolyte (PSE) in which polyvinyl alcohol (PVA) and dimethyl phthalate (DMP), $LiClO_4$ were employed as polymer electrolyte, plasticizer and lithium salt, respectively. Here, we chose DMP as a plasticizer, which can also dissolve $LiClO_4$, thus enabling DMP to be utilized not only as a plasticizer but also as an organic electrolyte. This results in improving the content of $LiClO_4$ in the solid electrolytes, facilitating the transport of Li ion through the electrolyte. High contents of DMP and $LiClO_4$ in solid electrolytes are desirable and can be achieved via a volatile liquid surfactant avoiding surfactant pollution. The PSE film was prepared by a solvent casting method, which shows good dispersion stability in PVA matrix. The ionic conductivity of the as-produced PSEs was determined by AC impedance measurement. It was found that the PSE has a good ionic conductivity of 1.308 mS/cm at room temperature. Furthermore, they also exhibited good mechanical property and optical transparency even without subsequent treatments. We expect that our approach to develop novel PSEs may present a facile route for the fabrication of next-generation transparent and flexible batteries.

P1-Ap.033*

Electric Field Induced Metal-Insulator Transition of Vanadium Dioxide Thin Films on Sapphire Substrates Deposited by RF Sputtering System

배가람, 양형우, 황재석, *강대준
Garam. BAE, Hyoungwoo. YANG, Jaeseok. HWANG, *Dae Joon. KANG
성균관대학교.

Keyword : Electric field induced metal insulator transition, VO2, on-state slope resistivity, on-state current density

Single phase monoclinic vanadium dioxide (VO_2) films were successfully grown on sapphire (001) substrates by RF sputtering. In x-ray diffraction patterns, we observed reflections originating from monoclinic VO_2 with a peak at $2\theta = 39.77°$ corresponding to VO_2 (020) for films on sapphire (001) substrates. The VO_2 films exhibited metal-insulator transition (MIT) at temperature around 337 K with three orders of change in resistivity. A simple two-terminal device based on VO_2 films on sapphire (001) substrates using gold/titanium electrodes with different channel lengths and widths showed current jump dependency of channel length by an applied voltage at 332 K. The break-over voltage increases linearly with increasing a channel length. The two-terminal VO_2 devices showed high electrical performance with the on-state slope resistivity of 7.02×10^{-4} Ωcm and on-state current density of 2.1×10^5 A/cm^2 which is suitable for high electric-power switching devices.

P1-Ap.034*

Understanding Growth Mechanism of Epitaxially Grown Ultra-long VO_2 Nanowires on X-cut and Y-cut Quartz Substrates

곽래협, 황재석, 양형우, *강대준
Rae Hyob. KWAK, Jaeseok. HWANG, Hyoungwoo. YANG, *Dae Joon. KANG
성균관대학교.

Keyword : VO2, metal insulator transition, ultra-long nanowires growth

In this work, vanadium dioxide (VO_2) nanowires have been successfully grown on both x-cut and y-cut quartz substrates by vapor transport deposition process, in which VO_2 powder was employed as a source material without the use of catalyst. The growth mechanism of VO_2 nanowires on both substrates were studied by high resolution transmission electron microscopy (TEM) and X-ray diffraction technique. The study revealed that the VO_2 nanowires grown on x-cut and y-cut quartz substrates had different growth behaviors implying the growth mechanism were different. Furthermore, we attempted to grow ultra-long (over 500 μm) VO_2 nanowires from both substrates and investigated its electrical transport properties to understand its subtle difference in metal-insulator transition behaviors. We discussed potential applications of such ultra-long high quality VO_2 nanowires in novel electronic and optical devices.

P1-Ap.035*

Creating Sub-micrometer Featured Functional Structures Using Magnetohydrodynamic Lithography

천명현, 문충만, *강대준
Myung Hyun. CHEON, Choong Man. MOON, *Dae Joon. KANG
성균관대학교.

Keyword : Magnetogydrodynamic lithography, Magnetic fluid, Pattern transfer

Magnetohydrodynamic behaviors of a magnetic fluid, a colloidal suspension of nanoparticles dispersed with the aid of surfactants in a continuous carrier phase, has been studied over decades using magnetic field and Hele-shaw cell. In these studies, it was found that the pattern size obtained ranged from tens to several hundred micrometers and the pattern shape was limited in a form of random dots or labyrinths. However, applying this interesting and unique physical phenomenon for regular and sub-micron scale pattern formations has not been fully explored yet. Here in this study, we report that the magnetic fluid can be structured into a particular pattern we design. We found that the replication of a particular pattern engraved in the cell and reduction of the pattern critical dimension to sub-micrometer scale is possible by a careful optimization of the replication process conditions. The effects of different cell thickness and magnetic field strength have critical influence on the magnetic fluid pattern formation behaviors. We also performed a computer simulation to better understand a pattern formation of magnetic fluid upon varying replication process conditions. We exploited our simulation results to realize the desirable pattern formation by carefully controlling the magnetic field distribution in the magnetic fluid. Thus, we believe our efforts in developing sub-micrometer nanostructures based on magnetohydrodyamic lithography will improve the potential uses of magnetic fluids for the development of a next generation large-area pattern transfer technique.

P1-Ap.036

Voltage Oscillations in 2-Terminal Devices based on VO_2 Thin Films with Negative Differential Resistance

양형우, *강대준
Hyoungwoo. YANG, *Dae Joon. KANG
성균관대학교.

Keyword : VO2, Voltage Oscillation, Negative differential resistance, phase transition

Many strongly correlated electron systems exhibit complex nonlinear behaviors with electric fields. The origin of the electrical instabilities is closely related to a negative differential resistance (NDR). Here, we report electrical characteristics of two-terminal devices based on vanadium dioxide (VO_2) thin films fabricated on c-cut sapphire substrates, exhibiting NDR behavior in their I-V characteristics that may work as a voltage oscillator of high efficiency. We show that the NDR behavior can be better understood in the context of metal-insulator phase transition. Furthermore, we found that the source voltage and frequency affect greatly the NDR behaviors, which is indicated by an evident shift of oscillation voltage from 10 V to 1 V. Based on the experimental results, with the source voltage and the frequency systematically varied, the mechanism of the oscillation was found to be the ascribed to an alternate occurrence of an electric-field-induced resistance switching in the MIT of VO_2. We discuss herein, the origin and potential applications of NDR based devices in detail and investigated the voltage oscillation behaviors of VO_2 to elucidate the underlying physics of its metal insulator transition behavior.

P1-Ap.037*

Large Scale Synthesis of Sea-urchin Like Carbon/ZnO Heterostructures with Enhanced Photocatalytic Efficiency

Wen He, Viyada HARNCHANA, Huynh Van NGOC, *강대준
Wen. He, Viyada. HARNCHANA, Huynh Van. NGOC, *Dae Joon. KANG
성균관대학교.

Keyword : Photocatalyst, ZnO/carbon composites

A large scale synthesis of sea-urchin like Carbon/ZnO heterostructures has been successfully demonstrated by using a novel low temperature hydrothermal method, in which glucose and zinc acetate were employed as carbon and ZnO source, respectively. ZnO nanowires with average diameter of 40-50 nm were grown on the surface of carbon microspheres forming carbon/ZnO nanocomposites. Owing to large surface area, superior conductivity, and strong light absorption in ultraviolet region, the hybrid structures show excellent photocatalytic efficiency for the degradation of Methylene Orange under ultra-violet (UV) light photo-irradiation. We believe that as-synthesized sea-urchin like carbon/ZnO hybrid composites could be a potential UV sensitive photocatalyst suitable for the efficient degradation of organic pollutants.

P1-Ap.038*

A Multilevel Resistive Switching in Vanadium Dioxide Based FET Devices by using Gate Bias Voltage

Kaleem ABBAS, *강대준
Kaleem. ABBAS, *Dae Joon. KANG
성균관대학교.

Keyword : VO2, Multilevel Resistive Switching, FET

The field effect transition in vanadium dioxide (VO_2) is employed to study the phase transitions, and electrical properties. This work demonstrates a multilevel, fast resistive switching in VO_2 by using a gate bias configuration. The resistance levels in VO_2 film was controlled by using the back gate. The vanadium dioxide film was prepared by a sol gel method on the SiO_2/Si^+ substrate. FET devices were fabricated on VO_2 films and gold electrodes used as source and drain. The quality of the VO_2 film was characterized by using X-ray diffraction, Raman spectroscopy, field emission scanning electron microscopy and high resolution transmission electron microscopy. The current-voltage characteristics of the FET devices were measured by changing the gate voltage. The effects of gate polarity on its resistance change, hysteresis behavior and the emergence of metallic phase are discussed in detail.

P1-Ap.039*

Hydrothermal Synthesis of $Zn_xCo_y(OH)F$ Nanoflakes for Supercapacitor Electrodes

Yaping YAN, Wen HE, *강대준
Yaping. YAN, Wen. HE, *Dae Joon. KANG
성균관대학교.

Keyword : Zinc Cobalt fluoride hydroxides, supercapacitors

Zinc Cobalt fluoride hydroxides, $Zn_xCo_y(OH)F$ have been successfully synthesized via a facile one-pot hydrothermal method. The morphology and the crystal structure of the as-prepared $Zn_xCo_y(OH)F$ nanoflakes were characterized by field emission scanning electron microscopy (FE-SEM), X-ray diffraction and transmission electron microscopy. The electrochemical performance of the as-prepared $Zn_xCo_y(OH)F$ electrode was investigated using C-V and GCD measurements. Our results present a great potential to be further developed as a high performance supercapacitor.

P1-Ap.041*

Hydrothermally Synthesized $NiCo_2S_4$ Nanoparticles for High-Performance Supercapcitor Electrodes

Yongteng QIAN, *강대준
Yongteng. Qian, *Dae Joon. KANG
성균관대학교.

Keyword : Hydrothermal Synthesis, $NiCo_2S_4$ Nanoparticles, Supercapcitor Electrodes

$NiCo_2S_4$ nanoparticles are successfully synthesized by using a facile one-pot hydrothermal method using manganese acetate and cobalt acetate as manganese and cobalt sources, respectively. The crystalline structure, morphologies and surface area of as-synthesized samples are characterized by X-ray diffraction (XRD), field-emission scanning electron microscope (FE-SEM) and Brunauer-Emmet-Teller (BET) techniques. Owing to mesoporous nature and small crystalline size, the as-prepared $NiCo_2S_4$ electrode shows a high specific capacitance of 465 F g^{-1} at 1 A g^{-1} and excellent cycling stability with the retention capacity of 93.75 % after 1000 cycles in the KOH aqueous solution electrolyte (3 mol/L). This study presents the potential in using $NiCo_2S_4$ nanoparticles for high performance energy storage applications.

P1-Ap.042*

Thermochromic Smart Windows based on VO_2 Nano-gratings Using Electrohydrodynamic Lithography

Aniruddha CHATTERJEE, 문충만, 양형우, *강대준
Aniruddha. CHATTERJEE, Choongman. MOON, Hyoungwoo. YANG, *Dae Joon. Kang
성균관대학교.

Keyword : Thermochromic Smart Windows, VO_2 Nano-gratings, Electrohydrodynamic Lithography

Electrohydrodynamic lithography (EHL) as an alternative patterning method has attracted a great deal of attention over the past decade. Here, EHL allows easy and accurate transfer of nano-grating pattern with a desirable aspect ratio onto Vanadium dioxide (VO_2) thin film for easy and large-area fabrication of thermochromic smart windows used in housetops, wall periphery, etc. VO_2 is a widely used thermochromic material which is optically transparent in the semiconductor (insulating) phase and highly reflective in the metallic phase, making it an attractive material for smart windows. Here, VO_2 nano-grating pattern fabricated using EHL is serving as the working electrode, which is sandwiched between ITO electrodes. It is known that in thin film VO_2, the opaque wavelength is near the infrared region and hence it is optically transparent throughout the visible range. However, our results show that configuring nano-grating on VO_2 films allow shifting the opaque wavelength to be within the visible range. This paper describes the EHL patterning technique and spectral performance of the next-generation large area thermochromic ‘smart window’.

P1-Ap.043

Morphology control of indium tin oxide nanorods fabricated using thermal chemical vapor deposition

*이성엽, 김홍탁, 김찬, 이형락
*Sung-Youp. LEE, Hong-tak. KIM, Chan. KIM, Hyeong-rag. LEE
경북대학교.

Keyword : indium tin oxide, nanorod,

ITO (indium tin oxide) is a promising degenerate wide band gap n-type semiconductor, and has become the best-known transparent conductive oxide material in optoelectronics due to its relatively low resistivity, high optical transmittance in the visible and near-infrared regions and high reflectance in the infrared region. In this work, we synthesized ITO nanorods by carbothermal reduction of a mixture of ITO and graphite powders. This method is very well known for fabrication of metal oxide nanostructures. The various ITO nanorods were grown on silicon substrate coated gold and cobalt. The cone-like nanorods and pin-like nanorods were fabricated at 1000 ℃ and 700 ℃ for 1 hour with argon as the carrier gas. Comparing the measured values with the JCPDS cards on ITO, The XRD pattern of the ITO nanorods indexed to the body centered cubic structure with lattice constants of a=10.118Å. This result clearly shows that the ITO nanorods are structurally uniform single crystal. The tip morphologies of ITO nanorods were readily controlled by changing the stoichiometric ratio of tin and oxygen, which was determined by flow rate and temperature.

P1-Ap.044

Lattice-matched lateral p-n diode of monolayer WSe_2 and MoS_2

*이종윤, 허호석 [1], 이장희, 조문호 [1], 이후종
*Jongyoon. Yi, Hoseok. Heo[1], Janghee. Lee, Moon Ho. Jo[1], Hu-Jong. Lee
포항공과대학교. [1]Institute for Basic Science. Korea.

Keyword : MoS_2, WSe_2, heterojunction, FET, diode

After the discovery of graphene, studies on graphene have increased enormously. Graphene has various special characteristics; good electrical and thermal conductivity, Dirac electronic structure, exceptionally strong mechanical properties, along with providing a truly two-dimensional system due to its extreme thinness. Following the 'graphene rush', realization of MoS_2–based monolayer field effect transistor (FET) was reported [1]. Starting with MoS_2, various transition metal dichalcogenides (TMDs) receive high attention as 2D materials. TMDs are expected to be applied to pn junctions, photoelectronic devices, and other devices. Recently, using these 2D materials, novel transport properties have been reported in various heterostructures. But most of heterostructures consist of random crystal orientation of each material, although precise identifying the momentum space structure is important for electronic transport. Because of the randomness of the crystal orientations, systematic study on the orientation dependence of heterostructure has not been reported. Recent studies on the effect of lattice orientation of heterostructure on electron tunnelling reveal the importance of lattice matched heterostructures [2]. To examine the effect, we prepared lattice matched lateral heterojunctions of monolayer WSe_2 and MoS_2 by serial CVD growth technique. To make electronic devices, good metallic electrode contacts are essential by suppressing the formation of the Schottky interfacial barrier, the formation of which depends on work functions of metal and semiconductor. We examined the contact characteristics between semiconductor and metal, by fabricating FETs, with Au and Ti employed for the contact metals with WSe_2 and MoS_2, respectively. Measuring electrical properties of these FETs, we confirmed that monolayer WSe_2 is a p-type semiconductor and monolayer MoS_2 is a n-type semiconductor. We will discuss on fabrication processes and characteristics of pn diodes with lattice-matched lateral heterojunctions of monolayer WSe_2 and MoS_2.

P1-Ap.045*

Annealing 온도 조절을 통한 다중벽 탄소나노튜브 위에 성장시킨 $Pb(Zr_{0.52}Ti_{0.48})O_3$ 의 구조 분석 연구

*강신욱, 한진규 [1], 김은영, 부상돈
*Sin Wook. Kang, Han Jin Kyu. [1], Eunyoung. Kim, Sang Don. Bu
전북대학교. [1] 한국화학연구원.

Keyword : PZT, CNT, Composite

탄소나노튜브(CNTs)는 높은 화학적 열적 안정성과 넓은 표면적을 가지기 때문에 금속 산화물의 안정성을 도와주는 물질로서 알려져 있다. 최근, CNT 와 강유전체 금속산화물의 혼합 nanocomposite 은 전자파 흡수재와 강유전 전계효과 트랜지스터와 같은 곳에 사용될 잠재성 때문에 큰 관심을 받고 있다. Nanocomposites 의 전기적 특성은 CNT 위에 nanocrystal 을 어떻게 성장시키느냐에 따라서 변화할 수 있다. 하지만 CNT 와 nanocrystal 사이의 원자단위의 결합의 분석에 대한 연구는 많이 진행되지 않았다. 본 연구에서, 우리는 CNT 표면위에 성장한 $Pb(Zr_{0.52}Ti_{0.48})O_3$ (PZT) nanocrystal 의 구조적·형태적 특성을 분석하였다. 이러한 CNT 표면 위에 성장한 PZT nanocrystal 은 PTFE 주사기 필터를 이용해서 주사기 필터링을 진행해서 파우더를 제작하였고, 이렇게 제작된 파우더를 annealing 온도 조건 600, 650, 700 ℃에서 진행하였다. annealing 온도가 증가함에 따라서 CNT 위의 PZT 의 페로브스카이트 구조가 잘 형성되는 것을 확인 할 수 있었다.

P1-Ap.046*

Excitation energy dependent Raman spectrum of bulk $MoSe_2$

*남다현, 이재웅, 정현식
*Dahyun. Nam, Jae-Ung. Lee, Hyeonsik. Cheong
서강대학교.

Keyword : $MoSe_2$, Resonance Raman

Raman investigation of bulk $MoSe_2$ was carried out with eight different excitation energies. Seven peaks, including E_{1g}, A_{1g}, E_{2g}^1, and A_{2u}^2 peaks are observed in the range of 100 – 400 cm^{-1}. The phonon modes are assigned by comparing the peak positions with theoretical calculations. The intensities of the peaks are enhanced at different excitation energies through resonance with different optical transitions. The A_{1g} mode is enhanced at 1.58 and 3.82 eV, which are near the A exciton energy and the band-to-band transition between higher energy bands, respectively. The E_{2g}^1 mode is strongly enhanced with respect to the A_{1g} mode for the 2.71- and 2.81-eV excitations, which are close to the C exciton energy. The different enhancements of the A_{1g} and E_{2g}^1 modes are explained in terms of the symmetries of the exciton states and the exciton-phonon coupling. Other smaller peaks including E_{1g} and A_{2u}^2 are forbidden but appear due to the resonance effect near optical transition energies.

P1-Ap.047

Synergy effect of mixed molybdenum-tungsten oxide with controllable phase and morphology for supercapacitor

*정진주, 원하연, 정도영, 김도형
*Jinjoo. Jung, Ha Yeon. Won, Do Yeong. Jeong, Do Hyung. Kim
경북대학교.

Keyword : nanostructure, molybdenum tungsten oxide, supercapacitor, solvothermal method

Substoiciometric molybdenum–tungsten mixed oxide nanostructures (MTMON) were prepared by solvothermal method to examine the dependence of their phase and morphological properties on the relative percentage of the constituent compounds for supercapacitor application. The phase and morphology of MTMONs were changed simultaneously by mixing different molar ratio of tungsten to molybdenum sources. The MTMONs synthesized with 50:50 is related to the well-defined peaks derived from H^+ intercalation/deintercalation and redox process in the MTMONs. The result of cyclic voltammogram confirm that both materials synergistically contribute to the charge-storage process. The molybdenum tungsten oxide synthesized by solvothermal method is attractive material due to controllable morphology and phase to obtain high volume to surface ratio and electrochemically activity.

P1-Ap.048

Size, emission wavelength, and shape controlled LaF_3:Ce/CdSeS-polymer nanocomposite as X-ray scintillator

*원하연, 정진주, 정도영, 김도형
*Hayeon. Won, Jinjoo. Jung, Do Yeong. Jeong, Do Hyung. Kim
경북대학교.

Keyword : LaF_3:Ce/CdSeS-polymer nanocomposite, scintillator, X-ray detection

LaF_3:Ce/CdSeS nanocomposites were investigated for their potential application as X-ray scintillator. LaF_3:Ce/CdSeS nanocomposites were synthesized by wet chemical method and fabricated the cylindrical form with polymer matrix. The LaF_3:Ce/CdSeS-polymer nanocomposites could overcome the shortcomings of LaF_3:Ce nanoparticle scintillator because the ultra-violet emission of LaF_3:Ce nanoparticle can absorbed in polymer matrix. The X-ray excited luminescence of LaF_3:Ce/CdSeS-polymer nanocomposites showed the emission peak at 603 nm, while the LaF_3:Ce nanoparticles have the emission peak at 300 nm. The emission peak of LaF_3:Ce/CdSeS-polymer nanocomposites can be controlled by the size control of CdSeS quantum dots (QDs), which cannot be obtained in LaF_3:Ce nanoparticles. The emission peak form LaF_3:Ce/CdSeS-polymer nanocomposites is mainly originated by CdSeS QDs, which can be attributed to the resonance energy transfer (RET) from LaF_3:Ce to CdSeS. The LaF_3:Ce/CdSeS-polymer nanocomposite scintillators based on the RET could be a candidate as an effective radiation detection material with the controllability of size, emission wavelength, and shape.

P1-Ap.049

Fixed Target Single-shot Imaging of Nanostructures using Thin Solid Membranes at SACLA

*남대웅, 김찬 [1], 김윤희 [1], Tomio Ebisu[2], Marcus Gallagher-Jones[3], 박재현 [4], 김수남 [4], 김상수 [4], Kensuke Tono[5], 노도영 [1], Makina Yabashi[2], Tetsuya Ishikawa[2], 송창용
*Daewoong. Nam, Chan. Kim[1], Yoonhee. Kim[1], Tomio. Ebisu[2], Marcus. Gallagher-Jones[3], Jae-hyun. PARK[4], Sunam. Kim[4], Sang Soo. Kim[4], Kensuke. Tono[5], Do Young. NOH[1], Makina. Yabashi[2], Tetsuya. Ishikawa[2], Changyong. Song
포항공과대학교. [1] 광주과학기술원. [2]RIKEN SPring-8 Center. [3]University of California. Los Angele **Size, emission wavelength, and shape controlled LaF3:Ce/CdSeS-.** *[4] 포항가속기연구소. [5]Japan Synchrotron Radiation Research Institute.*

Keyword : XFEL, single-shot imaging, fixed target, coherent diffraction imaging

X-ray free electron lasers (XFELs) have enabled to obtain intact structures with nanoscale details without the radiation damages. As the specimens are destroyed eventually by intense X-ray pulses, it becomes essential to provide fresh and intact specimens to each X-ray pulses reliably. The flying-type injectors, liquid jet injectors and aerosol injectors, are widely accepted for single-shot diffraction experiments at XFELs. In contrast to common approaches to inject specimens continuously, we introduce an alterative method, fixed-target using thin membrane. It allows an issue such as high sample consumption to be considered. This study reveals the structures of Au nanoparticles and biological macromolecular complexes at nanoscale resolution by using thin solid membranes. It was found that we can reduce the sample consumption as low as ~ 350 times comparing with flying-type injectors with the maximum data acquisition rate, 30 Hz, at SACLA.

P1-Ap.050*

Coherent diffraction imaging of gold patterns at 9C, PLS-Ⅱ

*전병현, 성대호, 남대웅, 김찬 [1], 김윤희 [1], 김준형 [1], 이수용 [2], 김용삼 [2], 안도천 [2], 유청종 [2], 노도영 [1], 송창용
*Byeonghyun. Jeon, Daeho. Sung, Daewoong. Nam, Chan. Kim[1], Yoonhee. Kim[1], JUNHYEONG. Kim[1], Su Yong. Lee[2], yongsam. kim[2], Do cheon. Ahn[2], Chungjong. Yu[2], Do Young. NOH[1], Changyong. Song
포항공과대학교(POSTECH). [1] 광주과학기술원. [2] 포항가속기연구소.

Keyword : Coherent diffracion imaging, PLS, phase retrieval, GHIO

결맞은 X 선 회절 현미경은 렌즈 없이 결맞은 X 선을 시료에 직접 입사하여 얻어지는 회절 무늬를 통하여 시료의 구조를 규명하는 방법이다. 이는 다른 광학계가 없어 실험 설계가 간단하고 광학계로 인한 측정의 한계 또한 없기에 극미세 구조 규명에 매우 효과적이다.
우리는 PLS-Ⅱ의 9C 빔라인에서 결맞은 X 선 회절 현미경을 이용하여 금으로 만들어진 패턴을 이미징 하였다. 실험에서 얻은 회절 무늬 정보를 GHIO 알고리듬에 입력하여 나노스케일 해상도를 지닌 이미지를 복원해내었다. 이 과정에서 GHIO 알고리듬을 파이썬과 매트랩으로 구현하여 위상복원 과정의 효율성 및 신속성을 비교하였다. 본 발표를 통하여 우리는 9C 빔라인을 이용해 얻은 이미지 해상도의 질적 요소를 평가하고, 이를 분석하는데 사용된 두 코드의 데이터 처리 방법 및 계산 시간 등을 비교 분석하였다.향후 우리는 9C 빔라인을 이용한 3 차원 이미징 뿐 아니라 위상복원 알고리듬을 병렬화를 할 예정이다.

P1-Ap.051*

결맞는 회절영상 기법을 이용한 생체시료 이미지 구현

*성대호, 남대웅, 김찬 [1], 김윤희 [1], 김준형 [1], 전병현, 노도영 [1], Yoshiki Kohmura[2], Tetsuya Ishikawa[2], 송창용
*Daeho. Sung, Daewoong. Nam, Kim Chan. [1], Yoonhee Kim. [1], JUNHYEONG. Kim[1], Byeonghyun. Jeon, NOH Do Young. [1], Yoshiki. Kohmura[2], Tetsuya. Ishikawa[2], Changyong. Song
포항공과대학교(POSTECH). [1] 광주과학기술원. [2]RIKEN SPring-8 Center.

Keyword : 결맞은 회절 영상기법, GHIO, 위상 복원, bio imaging

결맞는 엑스선을 이용한 이미징 기법은 시료에 결맞는 엑스선을 조사하여 회절패턴을 얻고, 이를 이용해 시료의 외부 및 내부 구조를 규명하는데 쓰인다. 이 기법을 통해 결정화가 어렵거나 불가능한 물질의 회절패턴을 얻을 수 있다. 또한 사용되는 엑스선은 짧은 파장을 갖기 때문에 이론적으로는 엑스선의 파장에 근접하는 분해능을 가질 수 있다. 실험에 쓰이는 엑스선의 장시간 노출에 의하여 시료에 방사선 손상을 야기시키는데, 이는 이미지 해상도의 한계를 가지게 한다. 이런 한계를 극복 하기 위하여 우리는 시료를 극저온 하에 유지함으로써 방사선 피해를 완화 할 수 있었다. 본 발표를 통하여 급속 동결된 시료의 회절 이미징 실험이 가능한 장치를 소개하고, 이를 이용해 염색체 구조를 분석하는 과정을 보일 것이다. 향후, 우리는 염색체의 3 차원 구조 연구를 수행할 예정이며, 이는 나노스케일에서 염색체 내부 구조를 이해하는데 도움이 되리라 기대된다.

P1-Ap.052

Ta thickness dependence of inverse-spin Hall effect voltage for Ta/CoFeB structure

*김상일, 김동준 [1], 서민수 [2], 박병국 [1], 박승영 [2]
*Sang-Il. Kim, Dong Jun. Kim[1], Min-Su. Seo[2], Byong Guk. Park[1], Seung young. Park[2]
고려대학교. [1] 한국과학기술원. [2] 한국기초과학지원연구원.

Keyword : spin pumping, ferromagnetic resonance, inverse spin Hall effect, spin current, spin Hall angle

Generation and detection of a pure spin current are the important technique in the field of spintronic devices [1,2]. The spin-pumping method enables the generation of spin current from the ferromagnetic resonance (FMR) at a ferromagnet (FM)/normal-metal (NM) interface. This spin current is converted into a charge current via the inverse-spin Hall effect (ISHE). In case of the resonant cavity systems, the unwanted spin-rectified effect (SRE) interfered with measuring the ISHE voltages (V_{ISHE}) [1,3]. In this study, at the TE_{011} cavity (for X-band), the V induced by the ISHE and SRE is investigated for the Ta (t_{Ta} nm)/CoFeB (10 nm) samples with changing t_{Ta}. Figure 1 shows the magnetic field H dependence of V under the FMR condition. The V shows a decrease with increasing t_{Ta} when t_{Ta} is greater than the spin-diffusion length of Ta (λ_{Ta})[4]. Figure 2 shows the t_{Ta} dependence of V_{ISHE} and SRE voltages (V_{SRE}) from the fitting curves of V-spectra. V_{SRE} shows monotonic decrease with increasing t_{Ta}. From this result, SRE contribution to the V in the resonant cavity system is practically negligible at the $t_{Ta} >> \lambda_{Ta}$. [1] E. Saitoh et al., Appl. Phys. Lett., 88, 182509 (2006). [2] K. Ando et al., Phys. Rev. B, 78, 014413 (2008). [3] K. Harii et al., J. Appl. Phys., 103, 07F311 (2008). [4] H. Nakayama et al., Phys. Rev. B, 85, 144408 (2012).

P1-Ap.053*

Enhancement of the Diffusion Barrier Property of the Capping Layer by Controlling its Grain Size for High Performance p-MTJ

*최진영, 홍송화 [1], 이승은 [1], 이두영 [1], 심태헌 [1], 박재근 [1]
*JinYoung. Choi, Hong Songhwa. [1], Lee Seung-Eun. [1], Lee Du yeong. [1], Shim Tae-Hun. [1], PARK Jeagun. [1]
한양대학교 대학원. [1] 한양대학교.

Keyword : MRAM, grain, diffusion, annealing

With the physical scaling limitation of Dynamic Random Access Memory (DRAM) cells, researchers turned their eyes on Magnetic Random Access Memory (MRAM) cells because of its high-density, non-volatile, high thermal stability, and low switching current to replace DRAM cells. It should be noted that the diffusion of the Pt atoms from the synthetic anti-ferromagnetic layer (SyAF) disrupts the crystallinity of the tunnel barrier and lowers the tunneling magnetoresistance (TMR) ratio. As a result, the MRAM cells breakdown at the annealing temperature of 400℃ during the back-end of Line (BEOL) process due to Pt diffusion. Therefore, the goal of this experiment is to enhance the diffusion barrier property of the capping layer so MRAM cells endure its magnetic properties during BEOL process.

For the experiment, we split the in-situ annealing condition of the capping layer in the perpendicular magnetic anisotropy (PMA) structure [substrate/Ta/CoFeB/MgO/CoFeB/capping layer] to increase the grain size of the capping layer. It is expected that the larger grain size of the capping layer leads to the decrease of the diffusion in Pt atoms. The grain size of the capping layer was determined by atomic force microscopy (AFM). Conventional spin valve structure of Ta/CoFeB/MgO/CoFeB/capping layer/SyAF layer was sputtered and analyzed by SIMS to actually see the difference in the penetration of the Pt atoms into the magnetic layer with different grain sizes of the capping layer. H_{ex} was calculated to see how much of the spin coupling is retained from the vibrating sample magnetometer (VSM). H_{ex} is an externally magnetic field that the exchange coupling strength can withstand to keep an exchange coupling state. We report the enhancement of the diffusion barrier property of the capping layer by controlling its grain size for high performance perpendicular magnetic tunneling junction (p-MTJ)

This work was supported by Basic Science Research program through the National Research Foundation of Korea (NRF) grant funded by the Korea government (MSIP) (No.2014R1A2A1A01006474) and Brain Korea 21 PLUS Program in 2014.

P1-Ap.054

Investigation of Cu2+ion-SHP in BaO-B2O3-CuO Glasses

*김영훈, 노태호, 최덕, 송승기
*Young Hoon. KIM, Tea Ho. NOH, Dock. CHOI, Seung-Kee. SONG
명지대학교.

Keyword : Electron paramagnetic resonance (EPR) , spin Hamiltonian parameters (SHP)

Glasses with composition xBaO-B2O3-yCuO(x=BaOmol% / B2O3mol% and y=CuOmol% / B2O3mol%) in the range x=0.1~0.7 with y=0.01 and 0.03 have been prepared using melt-quenching technique. Electron paramagnetic resonance (EPR) spectra of Cu2+ions for the samples have been observed at room temperature, showing resonance peaks characteristic of Cu2+ions. From the observed EPR spectra the spin Hamiltonian parameters (SHP) have been estimated. The values of SHP indicate that the site symmetry around Cu2+ions is tetragonally distorted octahedral.
Values of the density, molar volume and optical basicity have also been reported.

P1-Ap.055*

Structural and Magnetic properties of FeMn2O4 epitaxial film grown on MgO(100) substrate by molercular beam epitaxy

*둥반티엣, 조성래, 당득둥, 드엉안투안, 웬반쾅
*Duong Van. Thiet, Sunglae. CHO, Duc Dung. Dang, Duong Anh. Tuan, Nguyen Van. Quang
울산대학교.

Keyword : Spinel, Ferrimangetism, Spin, Ferromagnetism, Spintronics

FeM2X4 spinel structures, where M is a transition metal and X is oxygen or sulfur, are candidate materials for spin filters, one of the key devices in spintronics. Both the Fe and M ions can occupy tetrahedral and octahedral sites; therefore, these types of compounds can display various physical and chemical properties [1]. On the other hand, the electronic and magnetic properties of these spinel structures could be modified via the control of cation distribution [2-3]. Among the spinel oxides, iron manganese oxide is one of promising materials for applications. FeMn2O4 shows inverse spinel structure above 390 K and ferrimagnetic properties below the temperature [4]. In this work, we report on the structural and magnetic properties of epitaxial FeMn2O4 thin film on MgO(100) substrate. The reflection high energy electron diffraction (RHEED) and X-ray diffraction (XRD) results indicated that films were epitaxially grown on MgO(100) without the impurity phases. The valance states of Fe and Mn in the FeMn2O4 film were carried out using x-ray photoelectron spectrometer (XPS). The magnetic properties were measured by vibrating sample magnetometer (VSM), indicating that the samples are ferromagnetic at room temperature. The structural detail and origin of magnetic ordering in FeMn2O4 will be discussed.

References

[1] D. Santos-Carballal et al., Phys. Rev. B 91, 195106 (2015).
[2] C. Tenailleau et al., Am. Mineral. 91, 1442 (2006).
[3] P. Waldner et al., J. Chem. Thermodyn. 41, 171 (2009).
[4] J. Van Landuyt et al., Mater. Res. Bull. 7, 327 (1972).

P1-Ap.056*

Current induced switching in Transition-metal/Ferromagnetic multilayers

*김지민, 김범진, 김동석, 장영재, 주성중 [1], 이병찬 [2], 이긍원
*Ji Min. Kim, Bumjin. Kim, Dong Seok. Kim, Young-jae. Jang, Sung-Jung. Joo[1], Byung-Chan. LEE[2], Kungwon. Rhie
고려대학교. [1] 한국표준과학연구원. [2] 인하대학교.

Keyword : "spin orbit torque","CoFeB","Ta","FeZr","Magnetization switching"

The spin orbit torque (SOT) may lead to a better conceptual basis for developing 3-terminal magnetic memory cells [1]. After the Miron's work [2], many results shown that SOT is a good mechanism to change a magnetization direction of ferromagnetic layers which include a transition-metal (TM)/ferromagnetic (FM) multilayers structure. [3, 4]
In this study, we use Pt/Co, FeZr(amorphous paramagnetic)/CoFeB, and Ta/CoFeB multilayers to understand an effect of SOT in each structure. In Pt (t_1)/Co/Pt (t_2) case, the thickness of both upper (t_2) and lower (t_1) Pt layers are varied separately. The sign of SOT is changed when t_2 is thicker than t_1, which means injected spin currents from upper and lower Pt layers have different spin directions. Since the amount of injected spin current is proportional to thickness of TM, one is able to observe the competitions of spins injected from upper and lower paramagnetic layers. The critical current to switch magnetization decreases with the increase of in plane magnetic field strength. And the sign of Hall voltage is changed when the direction of applied filed is switched. We observed magnetic field dependence of switching current and thickness dependence of spin Hall sign

[1] L. Liu, C. F. Pai, Y. Li, H. W. Tseng, D. C. Ralph, and R. A. Buhrman, Science 336, 555 (2012).
[2] I. M. miron, k. Garello, G. Gaudin, P. J. Zermatten, M. V. Costache, S. Auffret, S. Bandiera, B. Rodmacq, A. Schuhl and P. Gambardella, Nature (Lond on) 476, 189 (2011).
[3] K. Ando, S. Takahashi, k Harii, K. Sasage, J. Idea, S. Maekawa and E. Saitoh, Phys. Rev. Lett. 101, 036601 (2008).
[4] L. Q. Liu, T. Moriyama, D. C. Ralph and R. A. Buhrman, Phys. Rev. Lett. 106, 036601 (2011).

P1-Ap.057*

The study for sign of the interfacial Dzyaloshinskii-Moriya interaction in an inversion broken symmetry structures by employing Brillouin light scattering.

*정진용, 김남희, 조재훈, 강승구, 유천열
*Jinyong. Jung, Nam-Hui. Kim, Jaehun. Cho, Seung Ku. Kang, Chun-Yeol. You
인하대학교.

Keyword : interfacial Dzyaloshinskii-Moriya interaction, Brillouin light scattering

The interfacial Dzyaloshinskii-Moriya interaction (iDMI) has been attracted attention from many researchers because it could open new paths to control spin orientations.[1] It has been already predicted by Fert[2,3] in 1980, only recently experimental evidences of iDMI were reported.[4,5] In this work, the iDMI energy density and its sign investigated by employing Brillouin light scattering (BLS) on the Pt/CoFeB/Ta and Ta/CoFeB/Pt structures. Series of 2-nm-thick CoFeB films are sandwiched with different HMs such as Ta or Pt are fabricated on Si/SiO_2 substrate by employing DC magnetron sputtering. The films were grown at a 3×10^{-8} Torr of base pressure. We find that zero or ignorable iDMI on the symmetric Pt/CoFeB/Pt and Ta/CoFeB/Ta structures, and finite iDMI on the Pt/CoFeB/Ta and Ta/CoFeB/Pt structures. We also find that signs of iDMI are opposite for Pt/CoFeB/Ta and Ta/CoFeB/Pt structures. Fig. 1 clearly shows iDMI as a function of the angle θ_α between the spin wave propagation directions and the direction of the magnetizations. D. Cortés-Ortuño[6] claimed the relation of $\Delta f(\theta_\alpha)=\Delta f_0 \sin\theta_\alpha$, for inversion broken symmetry structure. In our results, opposite signs of iDMI energy density is arisen by different position of Pt/CoFeB interface. It means that Pt/CoFeB interface is leading the observed iDMI. Furthermore, it is revealed that the iDM energy densities are -0.64 ± 0.05 mJ/m^2 and 0.50 ± 0.1 mJ/m^2 for Pt/CoFeB/Ta and Ta/CoFeB/Pt samples, respectively. The difference are within experimental errors, and it implies that Pt/CoFeB and CoFeB/Pt interfaces are almost identical in our samples, despite of the stacking order is reversed. We believed that it is due to the amorphous nature of CoFeB layer.

1 J. Sampaio, et al., Nat. Nanotech. 8, 839-844 (2013).
2 A. Fert, and M. Levy, Phys. Rev. Lett. 44, 1538 (1980).
3 A. Fert, Mater. Sci. Forum 59-60, 439-480 (1990).
4 K. Di, et al., Phys. Rev. Lett. 114, 047201 (2015).
5 J. Cho, et al., Nat. Commun. 6, 7635 (2015).
6 D. Cortés-Ortuño, et al., J. Phys. Cond. Matter 25, 156001 (2013).

P1-Ap.058*

The interfacial Dzyaloshinskii-Moriya interaction in Pt/Co/AlO_x with Tantalum buffer layer

Nam-Hui Kim, Dong-Soo Han[1], Jinyong Jung, Jaehun Cho, June-Seo Kim[1], Henk J. M. Swagten[1], Chun-Yeol You
Nam-Hui. Kim, Dong-Soo. Han[1], Jinyong. Jung, Jaehun. Cho, June-Seo. Kim[1], Henk. Swagten[1], Chun-Yeol. You
Inha University. [1]Eindhoven University of Technology.

Keyword : "The interfacial Dzaloshinskii-Moriya interaction, Brillouin light scattering, Tantalum buffer layer"

The interfacial Dzyaloshinskii-Moriya interaction (iDMI),[1-4] an asymmetric exchange interaction, based on a spin-orbit coupling in an inversion symmetry broken system such as heavy metal/ferromagnet/insulator is experimentally investigated by performing Brillouin light scattering (BLS).[5-7] In order to extract the interfacial DM energy density by using BLS, the first step is the observation of the frequency differences (Df) between Stokes and anti-Stokes peaks in BLS spectra. The second step is to convert the iDM energy density from the measured Df over the saturation magnetization.
From our systematic BLS measurements of Co layer thickness, we achieve that the interfacial DM energy densities are averagely 88% improved via a tantalum buffer layer. Since the interfacial DM energy density is a function of the saturation magnetization and the Df, we clearly explain this significant enhancement of the iDM energy densities. Compare with our previous results (without buffer layer),[5] the Df increases 24% and the saturation magnetization is also enhanced as close as the bulk value of Cobalt. There are two possible scenarios. First, the improved interface quality between the heavy metal and Cobalt layers makes the better defined Cobalt with less intermixing. The second scenario is the proximity effect of the heavy metal (Pt).[8] Moreover, the interfacial perpendicular magnetic anisotropy (PMA) is improved as well.
Additionally, we show the inverse proportionality of the interfacial DM energy densities as a function of the Cobalt thickness, which is direct evidence that the DM interaction is purely originated from the interface. The improvement and inverse proportionality are clearly shown in Fig. 1

References
[1]A. Fert and P. M. Levy, Phys. Rev. Lett. 44, 1538-1541 (1980).
[2]A. Fert, Mater. Sci. Forum 59, 439-480 (1990).
[3]A. Thiaville et al., EPL 100, 57002 (2012).
[4]R. Yanes et al., Phys. Rev. Lett. 111, 217202 (2013).
[5]J. Cho et al., Nat. Comm. 6, 7635 (2015).
[6]M. Belmeguenai et al., Phys. Rev. B 91, 180405(R) (2015).
[7]K. Di, et al., Phys. Rev. Lett. 114, 047201 (2015).
[8]K.-S. Ryu et al., Nat. Comm. 5, 3910 (2014).

P1-Ap.059*

Mn 이 도핑된 Mg_2Si 의 열전 성질과 자성 성질에 대한 연구

*김충만, 김수현 [1], 정명화, 오민욱 [2]
*Chung Man. Kim, Soo Hyun. Kim[1], JUNG Myung Hwa. , Min-Wook. Oh[2]
서강대학교. [1] 한국과학기술연구원(KIST). [2] 한밭대학교.

Keyword : magnetic properties, thermoelectric properties

수직 Bridgman 법을 이용하여 망간을 도핑한 $Mg_{2-x}Mn_xSi$ (x=0, 0.1, 0.2, 0.3, 0.4) 단결정을 제작하여 Mn 에 의한 자기적 성질이 열전 성능에 어떤 영향을 끼치는지 연구하였다. 단결정 $Mg_{2-x}Mn_xSi$ 은 x = 0.2 에서 가장 높은 ZT 값을 가진다. 온도 변화에 따른 열전 성질과 자기적 성질을 측정한 결과, Mn 이 도핑된 모든 시료에서 85 K 근방에서 제벡 계수의 경향이 갑자기 변화하고 전기 전도도는 피크를 형성한다. 이 온도 영역에서 자기 모멘트도 역시 넓은 피크를 형성하는 것을 관측하였다. 특히, x = 0.1 시료에서는 저온에서 운반자 형이 변화하는 구간이 나타나고, 이 구간에서 전기 전도도와 제백 계수가 급격히 변화하는 것을 관측하였다. 이러한 실험 결과는 Mn 의 3d 전도전자가 Mg_2Si 에 도핑되면서 자기적 성질을 부여하고 그 열전 성질에 영향을 준 것으로 해석된다.

P1-Ap.060*

Enhanced tunneling magnetoresistance and perpendicular magnetic anisotropy by using Mo seed layer

Julie Lee, Jong-Ung Baek, Yasutaka Takemura, Tae-Hun Shim, Jea-Gun Park
Julie. Lee, Jong-Ung. Baek, Yasutaka. Takemura, Tae-Hun. Shim, Jea-Gun. Park
Hanyang University.

Keyword : Mo,TMR,perpendicular

Recently, many researchers have studied perpendicular spin-transfer-torque magnetoresistance RAM (p-STT-MRAM) as an alternative terra-bit-integration non-volatile memory to overcome the physical scaling limit (i.e: less than 20 nm) imposed on current silicon-based dynamic-random-access-memory (DRAM). In particular, p-STT-MRAM has demonstrated a fast write time of about 10 ns, non-volatile memory operation, and extremely low power consumption. A p-STT-MRAM cell is fabricated with a metal-insulator-semiconductor (MOS) transistor and a p-MTJ spin-value. However, to satisfy a commercial specification as a terra-bit-integration non-volatile memory, p-STT-MRAM essentially needs to satisfy critical device performances for p-MTJ spin-values, namely, a high TMR ratio, a high J_{ex}, a good thermal stability, and a low critical switching current density (J_c). In order to get high TMR ratio, structural, magnetic, and transported studies have been performed on perpendicular magnetic tunnel junctions (p-MTJ) with Ta as a capping and seed layer. The experiments show us the TMR ratio of the samples composed of the Ta seed was so low at 400 ^{o}C. Therefore, in our study, we applied the Mo seed instead of the Ta seed to improve the TMR ratio.

p-MTJ spin-valves were fabricated with a vertically stacked structure consisting of a silicon substrate, a SiO_2 layer, a tantalum (Ta) layer (5 nm thick), a molybdenum (Mo) seed layer (t nm thick), a CoFeB layer(1.05 nm thick), a MgO tunneling barrier(1.15 nm thick) and a tantalum (Ta) layer(2 nm thick). The mechanism of the samples was reviewed in detail by the out-of-plane magnetic moment versus applied magnetic field (M-H) curves and crystallinity observation between the CFB free layer/ MgO tunneling barrier by using the vibrating sampling magnetometer (VSM) at room temperature and high resolution TEM. In addition, the dependency of the TMR ratio on the sample of the p-MTJ spin-valves was estimated by using current-in-plane tunneling (CIPT). In the presentation, we report enhanced tunneling magnetoresistance and perpendicular magnetic anisotropy by using Mo seed layer.

This work was supported by Basic Science Research Program through the National Research Foundation of Korea (NRF) grant funded by the Korea government (MSIP) (No. 2014R1A2A1A01006474) and Brain Korea 21 PLUS Program in 2014.

P1-Ap.061*

Co 를 도핑한 Mn_3Ga 박막의 전기적 및 자기적 특성

*유우석, 방현우, 유천열 [1], 홍정일 [2], 정명화
*Woosuk. Yoo, Hyun-Woo. Bang, Chun-Yeol. You[1], HONG JUNG IL. [2], JUNG Myung Hwa.
서강대학교. [1] 인하대학교. [2] 대구경북과학기술원.

Keyword : "perpendicular magnetic anisotropy", "exchange bias"

최근 차세대 메모리 소자로서 수직 자기 이방성을 가진 물질에 대한 관심이 증대되었고, 특히 Mn 계열의 정방성 Heusler 합금에 관해서 주목할 만한 연구들이 발표되고 있다. Mn 계열의 정방성 Heusler 합금 중 주목 받고 있는 Mn_3Ga 은 준강자성(ferrimagnetic) 성질을 가지며 수직자기이방성(perpendicular magnetic anisotropy)을 가지는 동시에 상대적으로 높은 Curie 온도(700 K 이상)와 높은 스핀 분극률을 가진다는 점에서 차세대 메모리 소자로서의 응용가능성이 높은 물질이다. 본 연구는 Mn_3Ga 에 Co 를 도핑한 박막을 스퍼터링 방법으로 최초로 증착하여 Mn_3Ga 의 전기적 및 자기적 특성의 변화를 관찰하였다. Co 도핑량이 증가함에 따라 보자력(coercivity)이 급격히 변화하면서 경자성체(hard magnet)에서 연자성체(soft magnet)으로 변화함과 동시에 정방체 구조에서 입방체 구조로의 전이가 관찰되었다. 또한, Co 의 강자성 성질과 Mn_3Ga 자체의 준강자성 성질에 의한 복합상(mixed phase)으로 인하여 교환 바이어스(exchange bias) 효과가 나타났다.

P1-Ap.062*

Structural, electrical, and magnetic properties of cubic Mn_3Ga films deposited on MgO(100)

*방현우, 유우석, 정명화
*Hyun-Woo. Bang, Woosuk. Yoo, Myung Hwa. JUNG
서강대학교.

Keyword : perpendicular magnetic anisotropy, structural phase transition

Mn_3Ga has received renewed attention in recent years because of the variation of magnetic properties depending on the crystal structure. One is a triangular antiferromagnetism for the hexagonal ($D0_{19}$) phase, which is easily obtained by arc melting. The other is a ferrimagnetism for the tetragonal ($D0_{22}$) phase, which is achieved by annealing the hexagonal material at high temperatures. Another is an antiferromagnetism for the cubic Heusler ($D0_3$) phase, which is synthesized using a nonequilibrium technique, but is not stable in experiments. In this study, we first succeeded to fabricate the cubic phase by using a RF/DC magnetron sputtering as varying the power of sputtering gun. X-ray diffraction data revealed that the tetragonal Mn_3Ga is changed into the cubic structure with decreasing RF gun power. The surface morphology was investigated by scanning electron microscope images. The electrical transport and magnetic data showed that the cubic Mn_3Ga is semiconducting and antiferromagnetic, while the tetragonal Mn_3Ga is metallic and ferromagnetic. Antiferromagnetic thin films of cubic Mn_3Ga can be used to pin the magnetization of reference layer through the interfacial exchange interaction in magnetic-tunnel-junction.

P1-Ap.063

Optimizing the effect of seed materials on PMA characteristics in p-MTJ

윤동한, 주문환, 최진영 [1], LIJUNLI, 홍송화, 이승은, 이두영, 박재근
*DONGHAN. YOON, MOONHWAN. JU, JinYoung. Choi[1], JUNLI. LEE, Songhwa. Hong, Seung-Eun. Lee, Du yeong. Lee, Jeagun. PARK
한양대학교. [1] 한양대학교 대학원.

Keyword : MTJ, CoFeB, MgO, seed layer

A Spin-transfer torque magnetic random access memory (STT-MRAM) is one of the promising memories to replace a DRAM (dynamic random access memory) as it has a great potential for realizing advanced high-density and non-volatile memory. Magnetic Tunnel Junction (MTJ) is the most important component in STT-MRAM in which MgO tunnel barrier is stacked between two ferromagnetic layers: free layer and pinned layer. The arrangement of the spin direction between two ferromagnetic layers decides the resistance of MTJ. It is low when the spin direction of two ferromagnetic layers is parallel, while it is high when the spin direction is antiparallel. The difference of the resistance between two different magnetic states is defined as tunnelling magnetoresistance(TMR) ratio and this should be large to make it clear to distinguish binary states. Another parameter which defines the cell productivity is thermal stability. It is related with the energy barrier, given as $E_b = M_s H_K V/2$. Therefore, high thermal stability is needed to prevent the shifting of the two different spin direction, where M_s is the saturation magnetization and H_K is the anisotropy field. We can calculate the value of the total anisotropy energy per unit area $K_u t$ if we measure both M_s and H_K, where the effective anisotropy energy density is defined as $K_u = H_K M_S/2$ and t is an actual magnetic layer thickness, which is the thickness of the magnetic layer with the exception of the dead layer.

After a few decades of research and experiments obtained by researchers, we use the perpendicular MTJ consisting of CoFeB/MgO/CoFeB as it shows a high TMR ratio and high thermal stability in nanoscale cells. Furthermore, it is known that MgO induces high perpendicular magnetic anisotropy at the CoFeB-MgO interfaces. However CoFeB is sensitively affected by the type and the thickness of the seed layer materials stacked under the CoFeB layer. Additionally, because it is important for semiconductor used in STT-MRAM to endure high temperature upper 400℃ in heat treatment process, we differentiate the annealing temperature to observe the degradation of the cell.

Samples were prepared by sputtering into a SiO_2 / seed layer / CoFeB 1 / MgO 2 / Ta 2 (numbers indicate layer thickness in nanometers), and they were annealed with various temperatures. We measured the magnetization versus external magnetic field (M-H curves) of the samples using Vibrating Sample Magnetometer (VSM) which is used to measure and analyze the magnetic properties of a sample. We compared the M-H curves of the various thickness of Ta, Ru and Hf seed layer, and gained H_k and M_s of each sample. Also, we obtained actual magnetic layer thickness (t) from experiment with various CoFeB thicknesses. In this presentation, we showed optimum perpendicular magnetic anisotropy energy ($K_u t$) with various types and thicknesses of seed.

This work was supported by Basic Science Research program through the National Research Foundation of Korea (NRF) grant funded by the Korea government (MSIP) (No.2014R1A2A1A01006474) and Brain Korea 21 PLUS Program in 2014.

P1-As.001

Unification of gravitational and electromagnetic field equation through the gauge conditions

*윤영환, 장기호 [1]
*younghwan. yun, kiho. jang[1]
SK 하이닉스. [1]ETPL 연구소.

Keyword : electromagnetic filed, gravitational field, gauge, kaluza-klein, symmetry

In this paper, we show that the rank 1 field equation representing electromagnetic field equation can be derived from the gravitational field equation by using the gauge term to reduce the rank of field equation. Although the well-known Kaluza-Klein theory (KK theory below) of unification using 5th dimension as the electromagnetic term can explain only the gauge symmetry of electromagnetic field, our approach can explain almost of all features of electromagnetic field without any additional dimension. Our methodology is obtaining the specialized picture of field equation from the most general field equation.

P1-As.002*

Camera system for the IceCube Neutrino Telescope

*카르스텐로트, 김명철, 드반잔 보스, 전민진, 강우식, 김종현, 두이모위즈 흐르보예
*Carsten. Rott, Myoungchul. Kim, Debanjan. Bose, Minjin. Jeong, Woosik. Kang, JongHyun. Kim, Dujmovic. Hrvoje
물리학과/성균관대학교.

Keyword : "Astroparticle Physics", "IceCube", "CMOS Camera"

The IceCube Neutrino Observatory, located deep within the geographic South Pole ice, is the world's largest neutrino detector designed to observe astrophysical neutrinos. More than 5000 optical sensors for observing Cherenkov light from neutrinos make IceCube a powerful tool to reveal the physical processes associated with the origin of the highest energy particles. Building on the successful observation of high energy astrophysical neutrinos, the collaboration is planning an extension to the detector. The properties of the ice surrounding the sensors represent a major source of uncertainty for event reconstruction in IceCube. A camera system integrated with optical sensor modules could be beneficial to better understand ice properties. We describe several candidates for camera systems and compare their performance characteristics, including low temperature measurements. we perform a simulation to determine the requirements of a camera system in ice.

P1-As.003

Event Trigger Generator for Gravitational-Wave Data based on Hilbert-Huang Transform

*손재주, 추형석, 김영민 [1], 김환선, 오정근, 오상훈, Lindy Blackburn[2], Kazuhiro Hayama[3], Florent Robinet[4]
*Edwin J.. Son, Hyoungseok. Chu, Young min. Kim[1], Hwansun. Kim, John J.. OH, Sang Hoon. Oh, Lindy. Blackburn[2], Kazuhiro. Hayama[3], Florent. Robinet[4]
국가수리과학연구소. [1] 부산대학교. [2]Harvard-Smithsonian Center for Astrophysics. [3]Osaka City University. [4]Laboratoire de l'Accélérateur Linéaire.

Keyword : Gravitational Wave, Event Trigger Generator, Hilbert-Huang Transform

The Hilbert-Huang Transform (HHT) is composed of the Empirical Mode Decomposition (EMD) and the Hilbert Spectral Analysis (HSA). The EMD decomposes any time series data into a small number of components called the Intrinsic Mode Functions (IMFs), compared to the Discrete Fourier Transform which decomposes a data into a large number of harmonic functions. Each IMF has varying amplitude and frequency with respect to time, which can be obtained by HSA. The time resolution of the modes in HHT is the same as that of the given time series, while in the Wavelet Transform, Constant Q Transform and Short-Time Fourier Transform, there is a tradeoff between the resolutions in frequency and time. Based on the time-dependent amplitudes of IMFs, we develop an Event Trigger Generator and demonstrate its efficiency by applying it to gravitational-wave data.

P1-As.004

GAGMon: Correlation-based Glitch Monitor for Gravitational Wave Detection

*오정근, 김영민 [1], 손재주, 오상훈, 김환선, 추형석, 플로랑 로비넷 [2], 카즈히로 하야마 [3]
*John J.. OH, Young-Min. Kim[1], Edwin J.. Son, Sang Hoon. Oh, Hwansun. Kim, Hyoungseok. Chu, Florent. Robinet[2], Kazuhiro. Hayama[3]
국가수리과학연구소. [1] 부산대학교. [2]Universite Paris-Sud 11. [3]Osaka City University.

Keyword : Gravitational Waves, LIGO, KAGRA, Detecter Characterization

We study the possibility of new approach for identifying instrumental noise artifacts and sources of gravitational wave (GW) data such as LIGO and CLIO using various correlation analyses.To improve the quality of data for the GW signal search, the instrumental noises should be reduced in an appropriate way. Furthermore, it is important to understand the correlation between auxiliary channels of the GW detector. In this study, we investigate the possible way of identifying glitch triggers by generating time- frequency-correlation (TFC) maps between the related channels and compare the result to the current conventional schemes.

P1-At.001

Cross Sections for Electron Collisions with Acetylene

*송미영, 윤정식, 조혁 [1], G. P. Karwasz[2], V. Kokoouline[3], Y. Nakamura[4], J. Tennyson[5]
*Mi-Young. SONG, Jung-Sik. YOON, Hyuck. CHO[1], G. P.. Karwasz[2], V.. Kokoouline[3], Y.. Nakamura[4], J.. Tennyson[5]
국가핵융합연구소. [1] 충남대학교. [2]University Nicolaus Copernicus. Poland. [3]University of Central Florida. USA. [4]Tokyo Denki Univ.. Japan. [5]University College London. UK.

Keyword : total scattering, elastic scattering, momentum transfer, ionization, dissociative attachment

Acetylene (C_2H_2) is a hydrocarbon and the simplest alkyne. It is linear, symmetric and isoelectronic with N_2 and CO. It has triggered many theoretical and experimental studies. Electron collisions with C_2H_2 are important in the plasma processing, and acetylene has been detected in natural environments where free electrons may occur, including the interstellar medium and the atmospheres of Jupiter and other planets. Electron collision cross sections with acetylene for various processes have been reported and reviewed in the literature. In this presentation, cross section data have been compiled from the literature for electron collisions with acetylene molecules. Cross sections are collected and reviewed for total scattering, elastic scattering, momentum transfer, ionization, excitations of rotational, vibrational and electronic states, and dissociative attachment. The data extracted from swarm experiments are also considered. For each of these processes, the recommended values and associated uncertainties for the cross sections are derived if possible. The literature has been surveyed through early 2015. As group we are actively collaborating on the evaluation and recommendation of electron collision cross sections with key molecules, especially those of interest for plasma studies. A comprehensive review of electron-methane data was our first project; this was followed by the present study on acetylene. Further reviews will follow in due course.

P1-At.002

Photoionization cross section of Be atom using a B-spline R-matrix method

*이민호, 김 대성 [1], 변창우, 최낙렬
*Min-Ho. Lee, Daesoung. Kim[1], ChangWoo. Byun, NarkNyul. Choi
금오공과대학교. [1] 경기과학기술대학교.

Keyword : Be, photoionization cross section, Bspline, R-matrix

The photoionization of Be atom has been investigated using a B-spline R-matrix method. For the calculation of this photoionization process, non-orthogonal orbitals are used for describing both the target states and the R-matrix basis functions. In particular, a B-spline basis is used for the description of continuum states in the inner region and the target states may be obtained from independent calculations. This leads to a generalized eigenvalue problem but has the advantage of requiring much smaller bases for accurate representation of target wave functions and to achieve convergence in the close-coupling expansion. The present approach is applicable to a general atom, and their efficiency is demonstrated by this calculation. A detailed analysis of the resonance structure is given. The present results for the photoionization cross sections are in very good agreement with previous calculations and experimental data.

P1-At.003

Solving Schroedinger equations in an overcomplete basis set

*최낙렬, 변창우, 이민호, 김대성 [1]
*Nark Nyul. CHOI, Chang Woo. BYUN, Min-Ho. LEE, Dae-Soung. KIM[1]
금오공과대학교. [1] *경기과학기술대학.*

Keyword : coherent states, overcomplete basis set, time-dependent Schroedinger equations

최근들어, 시간 의존 슈뢰딩거 방정식을 풀기 위해 CS (Coherent States) 를 basis set 으로 사용하는 방법이 주목을 받고 있다. 그런데 CS basis set 은 대표적인 overcomplete set 으로서, 이러한 overcomplete basis set 을 사용하여 고유에너지 문제와 시간 의존슈뢰딩거 방정식을 푸는데 있어서 기존에 complete basis set 을 사용할 때 적용하던 방법을 그대로 적용할 수는 없다. 우리는 이에 대한 해결 방안을 소개하고 예를 들어 설명한다.

P1-At.004

Photo-association and wave-packet dynamics in the interaction of cold rubidium atoms with shaped femtosecond laser pulses

*이한결, 조한래, Hoang-Van Do[1], 고광훈 [2], 안재욱
*Han-gyeol. LEE, Han Lae. JO, Hoang-Van. DO[1], Kwang Hoon. KO[2], Jaewook. AHN
한국과학기술원. [1]Ecole Normale Supérieure (ENS). [2] 한국원자력연구원.

Keyword : photo-association, cold molecule, femtosecond pulse shaping

We report photo-association of cold rubidium atoms to the 0^-_g molecular state by shaped femtosecond laser pulses. When ground-state rubidium atoms colliding in a magneto-optical trap were excited to the superposition of near-dissociation vibrational levels of the given electronic state, vibrational motions of about 5-ps period were probed by time-resolved photo-ionization. It is estimated that this unseen molecular wave-packet occurs under the experimental condition of low atom density (5×10^9 /cm^3) and high laser intensity (1.3×10^{11} W/m^2).

P1-At.005*

Arbitrary transformation of single atom arrangement in holographic dipole traps

*이우준, 김효섭, 안재욱 [1]
*Woojun. Lee, Hyosub. Kim, Jaewook. Ahn[1]
KAIST. [1] *한국과학기술원.*

Keyword : Atomic and molecular physics, Single atom trap, Quantum computation

We experimentally demonstrated arbitrary transformation of single atom array in two-dimensional holographic dipole trap. An ultracold atom cloud was prepared by a magneto-optical trap and single atoms were dipole-trapped by a holographic micro-trap generated by a phase-modulating spatial light modulator (SLM). Employing the capability of SLM to generate arbitrary shape of the holographic trap, it was possible to place single atoms at arbitrary locations and even continuously reconfigure the array by conveying each atom. For this purpose, we loaded a series of computer-generated phase masks in the full frame rate of 60Hz of SLM, so the animation of phase mask transformed the holographic trap in real time, driving each atom along the assigned trajectory. Possible applications of this scheme of transformation of atom array include preparation of deterministic single atom array for quantum computation and novel atom collision experiments.

P1-At.006*

Simulation of the small number of qubits in 1D array using MPS method

*이동근, 손원민
*Dong Geun. Lee, Wonmin. Son
서강대학교.

Keyword : Matrix Product State(MPS)

Description of many-body quantum system has been known as a intractable problem in physics. Within the framework of Quantum Information, we have been researched the physical properties of the many-body system by using the analytical methods and embark on the numerical methods. Matrix Product State (MPS) method for one-dimensional system is one of the most popular and powerful numerical methods in tensor network theory. By using this method, the exponential order of the quantum system O(exp N) can be reduced to the linear order O(N), which results in the efficient simulation of the many-body quantum system. There is a brief explanation for the decomposition of the high-rank tensor into some matrices of the pure state and the Hamiltonian, and the algorithms for searching the many-body ground state. Then, we test the s=1/2 Heisenberg model and analyze its error.

P1-At.007*

Toeplitz matrix for generalized entanglement witness

Bae Kwang Il, Son Wonmin
Kwang Il. Bae, Wonmin. Son
Sogang University.

Keyword : Multipartite high-dimensional Bell's inequality, SLK inequality, Toeplitz matrices, Entanglement witness

We present a formalism which gives maximal quantum bound of generalized correlation. SLK correlation is one of generalized Bell correlation constructed for arbitrary N-partite d-dimensional system. By employing dimensional weight factor on SLK, we derived slightly generalized version of it. Quantum operator for the generalized SLK is derived in the form of real symmetric Toeplitz maxtrix and the bound can be obtained from diagonalizing corresponding matrix. We also shows that this approach is valid for various known Bell correlations, CHSH, Svetlichny, CGLMP, etc.. On this viewpoint, changing dimensional weight factor of the generalized SLK, we analyze the influence of high dimensional correlation in quantum violation of generalized correlation.

P1-At.008*

Measurement-device-independent Quantum Key Distribution with 3-dimensional Quantum States

*조용기, 손원민
*Yonggi. Jo, Wonmin. Son
서강대학교.

Keyword : quantum information, quantum key distribution, quantum cryptography, measurement-device-independent

Quantum Key Distribution(QKD) is one of the application of quantum physics which is sharing secure symmetric key between two parties. Theoretically, QKD has absolute security against eavesdropping, but it can be hacked because of imperfection of implements. The solution for is measurement-device-independent QKD(MDI QKD) protocol, which is immune to most of attacks against detectors by separating detectors from parties. And there is the postprocessing method including imperfection of qubit source in security analysis of MDI QKD by incorporating the mismatched-basis statistics data. Here, we analyze the security of MDI QKD with 3 dimensional quantum states and compare the key rate to qubit case. And we also consider the case that the bases of source are not mutually unbiased.

P1-At.009*

Analytical solutions of optical Bloch equations for a two-level atom revisited

*최경원, 노흥렬
*Gyeong Won. Choi, Heung Ryoul. Noh
전남대학교.

Keyword : "Optical Bloch Equations", "Two-Level Atom", "Analytical Solution"

An analytical study of the optical Bloch equations for a two-level atom with a cycling transition is presented. We obtained a map in phase space of the Rabi frequency and the laser frequency detuning, discriminating the characteristics of solutions to the optical Bloch equations: outside the boundary, oscillatory behavior is shown, while simple decaying behavior is shown inside the boundary. We find that the behavior of the solutions depends on the relative magnitude of the decay rates of the optical coherence and the excited state population.

P1-At.011*

Polarization dependence of electromagnetically induced transparency in a V-type system of rubidium

*강현종, 노흥렬
*HyunJong. Kang, Heung Ryoul. Noh
전남대학교.

Keyword : "V-type" "Electromagnetic Induced Transparency" "Polarization Dependence"

3 준위 원자계인 V 형 구도에서 루비듐 원자의 전자기 유도 투과 신호를 연구하였다. 결합광의 편광을 바꿔가면서 전자기 유도 투과의 편광 의존성을 실험적으로 분석하였다. 조사광의 주파수는 D1 전이선과 공명할 수 있도록 주파수를 고정하여 사용하였고, 결합광의 주파수는 D2 전이선 근처에서 변화를 주며 전자기 유도 투과 신호를 관찰하였다. 또한 실험 결과는 계산 결과와 비교 분석하였다.

P1-At.012*

Observation of polarization rotation for the D2 line of 87Rb

*양승철, 노흥렬
*Seung Chul. Yang, Heung Ryoul. Noh
전남대학교.

Keyword : "Polarization-rotation","Rubidium Atoms"

We present an experimental study on the polarization-rotation resonances for the Fg=2->Fe= 3 transition of 87Rb-D2 line by using two independent laser sources. The probe beam was locked to the resonant Fg=2->Fe= 3 transition, while the control beam was scanned around the same transition line. We observed the phenomenon of polarization-rotation resonances for various control laser intensities. The experimentally observed rotation spectra were compared with the calculated results obtained by solving density matrix equations.

P1-At.013*

Quench dynamics of quasi-2D antiferromagnetic spinor condensates

*강세지, 서상원, 신용일
*Seji. Kang, Sang Won. Seo, Yong-il. Shin
서울대학교.

Keyword : spinor condensate, quench dynamics, Kibble-Zurek mechanism

Depending on the sign of the quadratic Zeeman energy q, the antiferromagnetic spinor condensate of spin-1sodium atoms have two distinctive ground states: the easy-axis polar phase for q>0 and the easy-plane antiferromagnetic phase for q

P1-At.014

Effect of three-photon coherence on electromagnetically induced absorption in ladder system

*노흥렬, 문한섭 [1]
*Heung Ryoul. Noh, Han Seb. Moon[1]
전남대학교. [1] *부산대학교.*

Keyword : three-photon coherence, electromagnetically induced absorption

We study the effect of three-photon coherence on electromagnetically induced absorption for a ladder-type three-level atomic system. A probe beam was tuned to the lower line and two counterpropagating coupling beams were tuned to the upper line. The system can be modeled with a three-level scheme when the polarization directions of the coupling beams are parallel. By calculating the absorption coefficients analytically, we found that the three-photon coherence was the main cause of three-photon electromagnetically induced absorption.

P1-At.015*

Three-photon resonance in Rydberg Rb atom

*곽효민, 이윤석, 문한섭
*Hyo Min. Kwak, younseok. lee, Han Seb. Moon
부산대학교.

Keyword : "Rydberg atom", "three-photon absorption"

We studied three-photon absorption due to three-photon resonance for the $5S_{1/2}$-$5P_{3/2}$-$50D_{5/2}$-$51P_{3/2}$ transition of Rydberg ^{85}Rb atoms.

P1-At.016*

Optical Pumping Effect in the Imaging of Spinor Bose-Einstein Condensates of Spin-1 Atoms

*김수신, 서상원, 노흥렬 [1], 신용일
*Sooshin. Kim, Sang Won. Seo, Heung-Ryoul. Noh[1], Yong-il. Shin
서울대학교. [1] *전남대학교.*

Keyword : Absorption imaging, Phase-contrast imaging, Bose-Einstein condensate, Beam intensity, Pulse duration

Atomic Bose-Einstein Condensates (BECs) provide useful systems to research on quantum vortices and topological objects with internal spin degrees of freedom. However, it is sometimes difficult to quantitatively understand and analyze images of the spinor BECs because the D_2 transition of the atom has relatively large linewidth comparing to the energy differences among the excited hyperfine states. In this study, we investigate atom-light interactions in F=1 sodium spinor BECs to give advanced interpretation of imaging. Absorption spectra at the F=1 initial state are derived from calculations including the temporal evolution of the populations in the all magnetic sublevels, m_F=-1, 0, and 1, predicting that the spectral strength and linewidth are affected by the imaging beam intensity and its pulse duration. The theoretical results are verified by experiments, showing that the optical pumping effect should be taken into account for quantitative interpretation of the image. We apply the outcome to precisely predict the phase-contrast imaging signals for given magnetizations and atom numbers of the spinor BECs, which is found to be compatible with experimental data.

P1-At.017

VCSEL 과 칩스케일 증기셀을 이용한 세슘 D1 전이선 분광

*홍현규, 박상언, 이상범, 허명선, 김희연 [1], 김태현 [1], 박종철 [1], 양충모 [1], 윤상준 [2], 이승일 [2], 전태현 [2], 권택용
*Hyun-Gue. Hong, Sang Eon. Park, Sang Bum. Lee, Myoung-Sun. Heo, Hee Yeoun. Kim[1], Tae Hyun. Kim[1], Jongchul. Park[1], Chungmo. Yang[1], Sangjun. Yun[2], Seung Il. Lee[2], Tae Hyun. Jun[2], Taeg Yong. Kwon
한국표준과학연구원. [1] 나노종합기술원. [2] 넵코어스(주).

Keyword : VCSEL, CPT, MEMS

VCSEL 은 저전력으로 동작하고 고주파 전류 변조가 가능하며 적층형 패키지에 유리하여 칩스케일 원자 센서의 광원으로 널리 쓰이고 있다. 본 논문에서는 세슘 D1 전이선을 이용하여 VCSEL 의 직접 전류 변조를 통해 얻어진 결맞은 밀도 포획 현상을 보고한다. 또한 VCSEL 을 이용하여 MEMS 기반 소형 증기셀에서 얻어진 흡수 분광 신호를 분석한다.

P1-At.018

Progress in Development of an Atomic Interferometer in ADD

*이상경, 김태현, 임신혁, 노희숙, 심규민
*Sangkyung. Lee, Tae Hyun. Kim, Sin Hyuk. Yim, Hee Sook. ROH, 규민. 심
국방과학연구소.

Keyword : Atom interferometer, stimulated Raman transition, cold atom

We report current progress in development of an atomic interferometer in ADD. Rubidium 87 atoms are trapped and cooled by a 3D magneto-optical trap and optical molasses technique. The optical pumping technique is applied to prepare the free-falling atoms in the magnetic insensitive state ($F = 2$, $m_F = 2$). After the cooling and preparaton stage, they are illuminated by the two phase-locked Raman lasers wich induce the two photon Raman transition between the $F = 2$, $m_F = 0$ and $F = 1$, $m_F = 0$ states. By applying a $\pi/2$-π-$\pi/2$ Raman pulse sequence with counter-propagating Raman lasers configuration, an atomic Mach-Zehnder interferometer is implemented. We obtain the interference fringes as a function of frequency sweeping rates of the Raman laser.

P1-At.019*

Development of interference filter stabilized external cavity diode laser

*이동진, 박지웅, 권혁민, 강석태, 김중복 [1]
*DONGJIN. LEE, JIWOONG. PARK, HYEOKMIN. KWON, SUGTAE. KANG, Jung Bog. KIM[1]
Korea National University of Education. [1] 한국교원대학교.

Keyword : atomic physics, external cavity diode laser, interference filter, rubidium, saturated absorption spectroscopy

We have developed interference filter stabilized ECDL(external cavity diode laser). For stability, this ECDL design employs interference filter instead of generally used diffraction grating for wavelength selection and out-coupler for optical feedback. We used cateye configuration for feedback efficiency and compensation which is caused by optical misalignment in cavity. We observed ^{85}Rb(F=3->F') , ^{87}Rb(F=2->F') signals by saturated absorption spectroscopy.

P1-At.020

^{87}Rb Bose Einstein condensation on atom chip with T-wire

*강석태, 김승진, 전윤성, 민동훈, 이동진, 김중복
*SUGTAE. KANG, SEUNGJIN. KIM, YOONSUNG. JEON, DONGHOON. MIN, DONGJIN. LEE, Jung Bog. KIM
Korea National University of Education.

Keyword : Atom chip, Bose Einstein condensation, Magneto optical trap, Polarization gradient cooling, Evaporative cooling

We are trying to produce the ^{87}Rb Bose Einstein condensation (BEC) on an external atom chip with T-wire. Initially we produce atomic flux from $2D^+$ Magneto Optical Trap (MOT) in the $2D^+$ MOT chamber. The flux is trapped by 3D MOT in the 3D MOT chamber and further cooled by performing compressed MOT and polarization gradient cooling. After optical pumping stage, We transfer the cold atoms toward the atom chip surface by performing external Z coil trap. The external Z coil trap is completely switched to atom chip trap by using T wire on the atom chip with external bias fields. The T trap make tight confinement of cold atoms in axial direction. After compressing the atom chip trap to increase trap frequencies, we perform the RF evaporative cooling in the RF frequency range.

P1-At.021

Demonstration of Yb+ ion trapping/shuttling on a chip and measurement of secular frequency and Rabi oscillation

Kwon Yeong Dae, Seokjun Hong, Minjae Lee, Hongjin Cheon, Dongil, Jun Sik Ahn[1], Taehyun Kim[1]
Yeong Dae. Kwon, Seokjun. Hong, Minjae. Lee, Hongjin. Cheon, Cho. , Jun Sik. Ahn[1], Taehyun. Kim[1]
서울대학교. [1]SK Telecom.

Keyword : ion trap, quantum repeater, Rabi oscillation, quantum computation

Ion trap technology is a promising ground for realizaing various quantum information processors. For example, QKD systems have limitations on transmission distance (roughly 100 km) because of the attenuation inside the fiber, and this problem can be overcome using two entangled trapped ions as a quantum repeater. We designed ion trap chips based on MEMS (micro-electro-mechanical system) process and implemented laser control systems, UHV (ultra-high vacuum) chambers, and high NA (numerical aperture) imaging and detection systems. We have successfully trapped up to six 174Yb+ ions and three 171Yb+ ions that can be used as quantum bits (qubits) for quantum repeater. We demonstrated that trapped ions can be shuttled along the trap axis, and confirmed that we can prepare intended quantum states through Rabi oscillation. Measurements of trap frequencies are also presented.

P1-At.022

Optical Properties of Metal Ion-Doped DNA-Based Nanostructures

*정택선, 하태우, Sreekantha Reddy Dugasani[1], Bramaramba Gnapareddy[1], 최규진, 김병훈 [1], 박성하 [1], 김재훈
*TaekSun. Jung, Taewoo. Ha, Sreekantha Reddy. Dugasani[1], Bramaramba. Gnapareddy[1], Kyujin. Choi, Byeonghoon. Kim[1], Sung Ha. Park[1], Jae Hoon. KIM
연세대학교. [1] 성균관대학교.

Keyword : "DNA", "band gap", "optical transition"

We investigated the energy band gap and optical transitions of divalent metal ion (Cu^{2+}, Ni^{2+}, Zn^{2+} and Co^{2+}) modified DNA (M-DNA) double crossover (DX) crystals fabricated on fused silica by the substrate assisted growth (SAG) method. The energy band gap between the lowest unoccupied molecular orbital (LUMO) and the highest occupied molecular orbital (HOMO) varies with the doping concentration while the onset of the second absorption band also shifts. Our study shows that metal ion doping is an effective method to tune the band gap energy of DNA-based nanostructures.

P1-At.023

Optical Properties of Doxorubicin Hydrochloride Drug-Doped Salmon DNA Thin films

*하태우, Bramaramba Gnapareddy[1], Sreekantha Reddy Dugasani[1], Bjorn Paulson, 황태현 [1], 김태성 [1], 오경환, 박성하 [1], 김재훈
*Taewoo. Ha, Bramaramba. Gnapareddy[1], Sreekantha Reddy. Dugasani[1], Bjorn. Paulson, Taehyun. Hwang[1], Taesung. Kim[1], Kyunghwan. Oh, Sung Ha. Park[1], Jae Hoon. KIM
연세대학교. [1] 성균관대학교.

Keyword : Salmon DNA, DOX, optical band gap, second band onset, spectrophotometry

Double-stranded salmon DNA (SDNA) was doped with doxorubicin hydrochloride drug molecules (DOX) to determine the binding between DOX and SDNA, and DOX optimum doping concentration in SDNA. SDNA thin films were prepared with various concentrations of DOX by drop-casting on oxygen plasma treated glass and quartz substrates. Fourier transform infrared (FTIR) spectroscopy was employed to investigate the binding sites for DOX in SDNA, and electrical and photoluminescence (PL) analyses were used to determine the optimum doping concentration of DOX. The FTIR spectra showed that up to a concentration of 30 μM of DOX, there was a tendency for binding with a periodic orientation via intercalation between nucleosides. The current and PL intensity increased as the DOX concentration increased up to 30 μM, and then as the concentration of DOX further increased, we observed a decrease in current as well as PL quenching. Finally, the optical band gap and second band onset of the transmittance spectra were analyzed to further verify the DOX binding and optimum doping concentration into SDNA thin films as a function of the DOX concentration.

P1-At.024

Physical Properties of Lanthanide-Ion Modified DNA Crystal

*김장원, 하태우, 김시준, Sreekantha Reddy Dugasani[1], Bramaramba Gnapareddy[1], 유상현 [1], 이근우 [1], 정태수, 김현재, 박성하 [1], 김재훈
*Jangwon. Kim, Taewoo. Ha, Si Joon. Kim, Sreekantha Reddy. Dugasani[1], Bramaramba. Gnapareddy[1], Sanghyun. Yoo[1], Keun Woo. Lee[1], Tae Soo. Jung, Hyun Jae. Kim, Sung Ha. Park[1], Jae Hoon. KIM
연세대학교. [1] 성균관대학교.

Keyword : "lanthanide-ion", "optical band gap", "Hall transport", " DNA crystal"

We have studied the optical band gap and Hall transport in lanthanide-ion-modified DNA crystals fabricated on quartz and silica substrates via surface-assisted growth. The optical band gap of these crystals exhibits a dependence on ion species and the second band onset showed an inverted V shape upon increasing the lanthanide ion concentration. At a critical concentration, each lanthanide-ion-doped DNA crystals exhibits low resistivity, low Hall mobility, and high free-carrier concentration. Our study suggests a way to control the optical band gap and Hall parameters of DNA crystals by adjusting the concentration of the lanthanide ions.

P1-At.025

Terahertz spectroscopic analysis of traditional Chinese pigments

*이호원, 김종현, 조영찬, 심경익, 김장원, 하태우, 김재훈
*howon. Lee, Jong Hyeon. Kim, young chan. Jo, Kyung Ik. Sim, Jangwon. Kim, Taewoo. Ha, Jae Hoon. KIM
연세대학교.

Keyword : Terahertz, traditional pigments, time domain spectroscopy, cultural heritage

We studied the optical properties of traditional Chinese pigments with terahertz time-domain spectroscopy (THz-TDS) over the spectral range of 0.1 - 3 THz and determined their refractive index n, extinction coefficient k, and absorption coefficient α. Chinese pigments which were pressed into pellets exhibited terahertz absorption peaks the corresponding refractive index decreased as the grain size increased. Our study on traditional Chinese pigments will provide valuable tools for terahertz imaging of cultural heritage materials and their conservation and restoration.

P1-Co.101*

flexoelectric switching in $BiFeO_3$ thin film

*박성민, 노태원
*Sungmin. Park, Tae Won. NOH
서울대학교.

Keyword : "Mechanical switching", "Flexoelectric effect", "$BiFeO_3$"

In 2012, mechanical switching of polarization in barrium titanum oxide thin film was demonstrated. The most plausible explanation of the mechanically induced polarization switching is the flexoelectric coupling, which is a coupling between a strain gradient and polarization. Also, recent study computationally simulated the spatial distribution of the tip-induced flexoelectricity and compared with experiments. However, since they used the ultra thin film of barrium titanum oxide , only polarization of out-of-plane component was considered. In this work, We examine the phenomenon of flexoelectric switching of polarization induced by a tip of an atomic force microscope with thin film of bismuth iron oxide, which posses polarization components along both out-of-plane and in-plane directction.

P1-Co.102*

Strain distribution near mixed phase nano-domains in epitaxial T-like phase $BiFeO_3$ thin films probed by X-ray microdiffraction

위상원, 박정현, *정진석
Sangwon. Wi, Jung Hyun. Park, *Jin-Seok. CHUNG
숭실대학교.

Keyword : BiFeO3, T-phase, multiferroic, X-ray microdiffraction

$BiFeO_3$(BFO) under compressive strain from the substrate like $LaAlO_3$:~4.5% or $YAlO_3$:~7.3%, can have the tetragonal-like(T-like) structure with a large tetragonality or c/a ratio ~1.24. This T-like phase attracted a lot of attention from researchers due to their potential large remnant polarization from the highly elongated unit cell, predicted by first principle calculations. It is reported that BFO films under compressive strain usually have mixtures of the rhombohedral like(R-like) phase and T-like phase when they are thicker than a few tens of nm's. The X-ray Reciprocal Space Mapping(RSM) and TEM studies suggested BFO film of ~100 nm had drastic local variations of structures, the T-like phase and the mixed phase nano-domains(MPN), which consisted of alternating strip like grains of the tilted R-like phase and the tilted T-like phase.
But most structural studies have been either in a macroscopic scale like X-ray RSM or in a microscopic scale as TEM studies. In this study, X-ray microdiffraction set up at Pohang Light Source(PLS) was used to investigate the local structural variations in the intermediate scale, which enabled to get the statistics of local structures. X-ray white beam from the synchrotron radiation source was focused down to 1x1 $micron^2$ by a pair of K-B mirrors, and scanned over the area of several tens of microns. From Laue patterns of the PLD grown BFO films on $LaAlO_3$ substrate, peaks from the T-phase grain and the MPN were separated and their strain states were compared. At each point, the c/a ratio, distortion angle, the abundance ratio of non-tilted/tilted T phase were calculated and their correlations were investigated. The statistics suggested that strain and the distortion of the T-phase decreased near the area where peaks from the MPN were strong. This implied that the formation of the MPN was one way of relaxation of the strong strain from the substrate.
*The experiments were done at the 4B beamline at PLS.

Figure 1 (a) Diagram of MPN with tilted grains of alternating structures arrayed on the substrate. It is reported that Tt-phase has 1.3˚ tilt with surface normal and Rt-phase has 2.5˚. (b) The (001) satellite peaks from the Rt-phase and the Tt-phase near the substrate peak in Laue image (c) Distortion of the T-phase(untilted) vs. the intensity of tilted phases.

P1-Co.103*

Migration of oxygen vacancies in Ca doped $BiFeO_3$ film

*임지수, 양찬호
*Ji Soo. Lim, Chan-Ho. Yang
카이스트.

Keyword : oxygen vacancy,$BiFeO_3$,resistive switching memory,ferroelectric

Control of oxygen vacancies is important in resistive switching memory. Concentration of oxygen vacancies controlled by electric field determines whether resistance of its system is high or low. Dynamics of oxygen vacancies is still needed to study to understand resistive switching process. In this study, divalent ion doping (Ca^{2+}) on $BiFeO_3$ film is grown to investigate a migration of oxygen vacancies. As-grown Ca-doped $BiFeO_3$ produces oxygen vacancies due to a stable oxidation number of Fe^{3+} ions. These oxygen vacancies, positively charged defects, can be controllable by an application of external electric field. Time resolved current value at constant electric field during a migration of oxygen vacancies gives an intuition of dynamic of oxygen vacancies. For various doping ratios, which are related to amount of oxygen vacancies, measurement of current value is beneficial to study a movement of oxygen vacancies. Especially, at x = 0.3 doping ratio, current value is monitored at various temperature and electric field.

P1-Co.104

다강체 $BiFeO_3$ 비정질의 상전이 구조 변화 및 동역학 연구

*최현우, 임영훈 [1], 양용석
*현우., RIM Young-Hoon. [1], Yang Y. S..
부산대학교. [1] 세명대학교.

Keyword : 다강체, $BiFeO_3$, 상전이, 동역학

전기 절연체 중 전기장에 의해 분극이 형성되는 물질은 유전체라고 하며, 이들 중 외부전기장 없이 온도가 변함에 따라 자발적 전기분극이 가능한 물질을 강유전체라고 한다. 이같은 강유전성을 가지며 강자성, 강탄성과 같은 성질을 2 가지 이상 동시에 가지는 물질을 다강체라고 한다. 다강체 물질 중 상온에서의 다강성을 지닌 물질이 $BiFeO_3$ (BFO)이다. 다강체 BFO 는 강자성, 강유전성이 동시에 있으며, 페로브스카이트 구조로, 퀴리온도(T_c=830 ℃)와 반강자성 전이온도 (T_N=370 ℃)를 가지는 물질이다.
본 연구에서는 다강체 BFO 를 비정질로 제조하고, 비정질 BFO 의 결정화에 따른 물성의 변화를 관찰하였다. 비정질 BFO 의 열처리 온도에 따른 결정구조 변화를 관찰하였으며, 열처리 온도가 증가함에 따라 $Bi_{36}Fe_2O_{57}$ 과 $Bi_2Fe_4O_9$ 결정상이 BFO 결정상과 혼합하여 나타나고 있음을 알 수 있었다. 상전이와 관련된 발열봉우리는 3 개의 봉우리가 나타났고 이는 각각 $Bi_2Fe_4O_9$ 상과 $Bi_{36}Fe_2O_{57}$ 상, $BiFeO_3$ 상으로 대응됨을 XRD 를 통하여 알 수 있었다. 또한 780 ℃와 825 ℃에서 각각 흡열 봉우리가 나타났으며, 780 ℃에서의 흡열 봉우리는 $Bi_{36}Fe_2O_{57}$ 결정상에 의한 흡열봉우리임을 알 수 있었다. DSC 와 DTA 장비를 이용하여 열분석을 하였고, 비정질 시료의 유리전이 온도(T_g)는 380 ℃, 결정화 온도(T_c)는 400 ℃, 녹는점(T_m)은 936 ℃에서 나타남을 확인하였다. 열출입 곡선을 이용하여 상전이에 따른 동역학적 분석을 하였으며, 감소 또는 증가하는 핵생성율을 가진 확산 제어 메카니즘임을 확인하였다.

P1-Co.105

Structural and electrical properties of $BiFeO_3$ thin film deposited on a Ge-doped ZnO electrode

*김상수, 최지야, 송태권
*Sang Su. Kim, Ji Ya. Choi, Tae Kwon. SONG
창원대학교.

Keyword : $BiFeO_3$ thin film, Pulsed laser deposion, Structure, Electrical Property, Ferroelectric property

In this study, Ge-doped ZnO (GZO) was used as the electrode material for the top and bottom electrodes of a capacitor, to explore the electrical and ferroelectric properties of the perovskite $BiFeO_3$ (BFO) thin film. Thin films of BFO were deposited on GZO/Si(100) and Pt(111)/Ti/SiO_2/Si(100) substrates by using a pulsed laser deposition technique. An improved crystal growth property was observed for the BFO thin film grown on the GZO/Si(100) substrate. The BFO thin film, which is deposited on a (00l) textured GZO/Si(100) substrate, exhibited preferred (l00) orientated grains, while randomly orientated grains were observed for the thin film grown on the Pt(111)/Ti/SiO_2/Si(100) substrate. When compared with the Pt/BFO/Pt capacitor, the GZO/BFO/GZO capacitor exhibited improved electrical properties, namely low leakage current density and high stability against electrical breakdown. Furthermore, a large ferroelectric polarization and enhanced resistance against polarization fatigue were observed for the GZO/BFO/GZO capacitor. The observed results suggest that GZO would be a reliable electrode material for use in ferroelectric capacitors.

P1-Co.106

Enhanced ferroelectric properties of sulpher doped $Pb[Zr_{0.52}Ti_{0.48}]O_3$ PZT thin film

*Sheeraz Muhammad, 안창원, 김일원
*Sheeraz. Muhammad, Changwon. AHN, ILL WON. KIM
울산대학교.

Keyword : "sulpher doped $Pb[Zr_{0.52}Ti_{0.48}]O_3$, thin film, ferroelectric property"

Among ferroelectric materials $Pb(Zr,Ti)O_3$ (PZT) with high electric polarization, low coercive field and high curie temperature has drawn researchers attentions due to their wide range of applications, such as, energy harvesting, non-volatile memory devices, electro-optic materials for data storage applications and micro electro mechanical systems (MEMS).
The aim of this experiment is to enhance the ferroelectric response by replacing the oxygen in PZT through sulpher doping. As sulpher has high ionic radius compared to oxygen, it has been expected that sulpher will replace the oxygen and modify the electronic structure PZT and as a result ferroelectric effect can be improved.
In this work, $Pb(Zr_{0.52}Ti_{0.48})O_3$ thin film was prepared by conventional sol-gel method. An additional top sulpher layer was spin coated on $Pb(Zr_{0.52}Ti_{0.48})O_3$ film using thiourea solution. P-E loop measurement clearly reveals that the ferroelectric properties had been greatly improved by the additional sulpher layer which will be discussed.

P1-Co.107*

Flexible piezoelectric/pyroelectric nanogenerator base on Pb(Zr,Ti)O3 thin film

JongHoon Jung, Young Joon Ko, Dong Yeong Kim
JongHoon. Jung, Young Joon. Ko, Dong Yeong. Kim
Inha University.

Keyword : Pb(Zr,Ti)O3, Hybrid nanogenerator, mechanical vibration, thermal fluctuation

A great deal of attention has been paid to the harvesting of energy from ambient or wasted energy sources, such as mechanical vibrations, heat, and light, due to the limitations of global energy resources. Although the energy that could be harvested from such sources is rather small, a great reduction in power consumption may provide an opportunity to operate modern devices without batteries. For mechanical-vibration and heat sources, piezoelectric and ferroelectric materials have been considered to be the most appropriate candidates to convert mechanical and thermal energy into electrical energy due to their high piezoelectricity and pyroelectricity.
We report the hybrid piezoelectric and pyroelectric energy harvesting using flexible Pb(Zr,Ti)O3 film. The PZT film scavenges biomechanical and cold/hot wind based mechanical vibration and thermal fluctuation. In addition, the PZT film based nanogenerator works well even in elevated temperature, high humidity, and high base conditions. These results imply that the PZT film based nanogenerator is useful in harsh environments.

P1-Co.108

Influence of Annealing Conditions on the Structural and Ferroelectric Properties of $PbZr_{0.52}Ti_{0.48}O_3$.

*부상돈, Trent Johnson
*Sang Don. Bu, Trent. Johnson
전북대학교.

Keyword : "PZT" "PFM"

We investigated the effects of annealing temperature and duration on the microstructural and ferroelectric properties of $PbZr_{0.52}Ti_{0.48}O_3$ (PZT) thin films prepared by sol-gel technique. The films were deposited on Pt(111)/Ti/SiO_2/Si(100) substrates and annealed under oxygen at ambient pressure at temperatures between 500 °C to 900 °C for a range of time durations. The specific annealing conditions influenced the formation and distribution of vacancies within the films, in turn modifying their structural and electrical properties. The microstructural surface morphology of the samples was studied by atomic force microscopy (AFM), while the native ferroelectric structure and switching characteristics were observed via piezoresponse force microscopy (PFM).

P1-Co.109*

Strain and vacancy engineering of opto-electronic properties in hetero-epitaxial $LiNbO_3$ thin films

*유태섭, 이상아 [1], 강경태 [1], 최우석 [1]
*Tae Sup. Yoo, Sang A. Lee[1], Kyeong Tae. Kang[1], Woo Seok. Choi[1]
물리학과/성균관대학교. [1] 성균관대학교.

Keyword : $LiNbO_3$, ferroelectric, bandgap tuning, optoelectronic, PLD

Bandgap tuning in ferroelectric materials is useful for fabricating efficient opto-electronic devices, such as ferroelectric photovoltaic devices. However, since ferroelectric materials have usually large bandgap and it is rather difficult to reduce it without sacrificing the functionalities, e.g. ferroelectricity, bandgap tuning in ferroelectric materials has been a formidable task. In this sense, $LiNbO_3$ (LNO) is an interesting system to search for the possibilities of bandgap tuning, since it is one of the most widely studied ferroelectric materials due to its advantageous optical properties for various photonic device applications. In this study, we investigated strain and elemental vacancy induced optical and ferroelectric properties of hetero-epitaxial LNO thin films grown on (111) $SrTiO_3$ and c-Al_2O_3 substrates using pulsed laser epitaxy. Atomic arrangements of oxygen in LNO (006) plane contain distorted hexagonal-like structure, and the extended atomic distance mismatch for LNO layer on $SrTiO_3$(111) and on c-Al_2O_3 substrate is –7.13% (tensile) and +7.50% (compressive), respectively. We could also systematically control the electronic structure and optical properties, and therefore, the bandgap, by changing the elemental vacancy concentration of LNO thin films. The custom-tailored physical properties in LNO thin films due to elemental vacancy concentration and epitaxial strain could lead to discovery of novel opto-electronic devices as well as better clarification of the origin of the ferroelectricity in LNO.

P1-Co.110*

Ferroelectric properties of (1−x)$BiFeO_3$–x$BaTiO_3$ films by pulsed laser deposition

*박진수, 이명환, 김다정, 한성진, 김명호, 김원정, 김상수, 도달현 [1], 송태권
*Jinsu. Park, Myanghwan. Lee, DA JEONG. KIM, Sung Jin. Han, Myong Ho. Kim, Won-jeong. KIM, Sang Su. KIM, Dalhyun. Do[1], Tae Kwon. SONG
창원대학교. [1] *계명대학교.*

Keyword : $BiFeO_3$, $BaTiO_3$, Thin film, ferroelectric

Thin films of lead-free ferroelectric material (1−x)$BiFeO_3$–x$BaTiO_3$ [(BF-BT), x=0.1, 0.2, 0.3, 0.33, 0.4 mol] were deposited on a Pt(111)/Ti/SiO_2/Si(100) substrates at 560°C~580°C by pulsed laser deposition at various oxygen partial pressure, such as 30, 50, and 100 mTorr, respectively. The crystal structures were investigated by using X-ray diffraction. Deposited at various oxygen partial pressure, BF-BT films were exhibited single-phase perovskite structure. The crystal structure were change from rhombohedral phase to tetragonal phase at x~0.33 composition. Interestingly, the P-E loops were exhibited change from hard to soft type as increasing of BT in BF film.

P1-Co.111*

Ferroelectric properties of lead-free sulfur doped $(K_{0.5}Na_{0.5})(Mn_{0.005}Nb_{0.995})O_3$ thin films

*석해진, 안창원, 간수지아마르사나, 김일원
*Hae Jin. Seog, Chang Won. Ahn, Gantsooj. Amarsanaa, ILL WON. Kim
울산대학교.

Keyword : ferroelectric, lead-free, $(K,Na)NbO_3$, thin film, sol-gel

Lead-free piezoelectric materials have been receiving special attention due to the recent environmental issues. $K_{0.5}Na_{0.5}NbO_3$ (KNN) is a promising candidate, as it has a good ferroelectric as well as biocompatibility. Sulfur (S), which has proven viable in recent $SrTiO_3$ perovskite alloy experiments and is isoelectronic to oxygen (O), is a good candidate. Amarsanaa et al. [1] studied that the effect of S doped $KNbO_3$ using first principles calculated and reported excellent ferroelectric properties due to the large out-of-plane opposing displacements of the ions. However, almost systematic experiment work did not report the ferroelectric properties of sulfur doped ferroelectric thin films. In this study, we have deposited S doped $(K_{0.5}Na_{0.5})(Mn_{0.005}Nb_{0.995})O_3$ (KNMN) thin films on $Pt(111)/TiO_2/SiO_2/Si(100)$ substrates with submicron meter thickness using chemical solution deposition method and investigated the effect of S doping by measuring on the surface morphology, crystal structure, electrical and ferroelectric properties.

P1-Co.112

Effects of Nb-doping on structural, electrical and ferroelectric properties of $Na_{0.5}Bi_{4.5}Ti_4O_{15}$ thin films

*김상수, 최지야, 송태권
*Sang Su. Kim, Ji Ya. Choi, Tae Kwon. SONG
창원대학교.

Keyword : Nb-doped $Na_{0.5}Bi_{4.5}Ti_4O_{15}$ thin film, Chemical solution deposition, Structure, Electrical property, Ferroelectric property

Ferroelectric $Na_{0.5}Bi_{4.5}Ti_4O_{15}$ (NaBTi) and donor Nb-doped $Na_{0.5}Bi_{4.5}Ti_{3.94}Nb_{0.06}O_{15}$ (NaBTiNb) thin films were prepared on Pt(111)/Ti/SiO_2/Si(100) substrates by using a chemical solution deposition method. The doping with Nb^{5+}-ions leads to tremendous improvements in the ferroelectric properties of the NaBTiNb thin film. Room-temperature ferroelectricity with a large remnant polarization ($2P_r$) of 64.1 μC/cm^2 and a low coercive field ($2E_c$) of 165 kV/cm at an applied electric field of 475 kV/cm was observed for the NaBTiNb thin film. The polarization fatigue study revealed that the NaBTiNb thin film exhibited good fatigue endurance compared with the NaBTi thin film. Furthermore, the NaBTiNb thin film showed a low leakage current density, which was $1.48´10^{-6}$ A/cm^2 at an applied electric field of 100 kV/cm.

P1-Co.113

High energy storage density of $Bi_{0.5}(Na_{0.82}K_{0.18})TiO_3$–based relaxor ferroelectric thin film

*채송아, 안창원, 김일원
*Song A. Chae, Changwon. AHN, ILL WON. Kim
울산대학교.

Keyword : "lead-free, BNKT, thin film, energy storage density"

Commercial electrical energy storage and energy supply devices include fuel cells, batteries, electrochemical supercapacitors and dielectric capacitors. Especially, dielectric capacitor is a promising technology for energy storage devices. Based on the physical principle, the materials with high saturated polarization, smaller remnant polarization, and higher electrical breakdown field are the most promising candidates. In general, antiferroelectrics, dielectrics, relaxor ferroelectric and polymer based ferroelectrics, are believed to be the most promising candidates for high energy-storage application. Among of that, relaxor ferroelectrics with slim type P-E hysteresis loops are the promising candidates due to their diffused phase transition.
We have grown a lead-free $Bi_{0.5}(Na_{0.82}K_{0.18})_{0.5}TiO_3$ (BNKT)-based ferroelectric thin films on $Pt/TiO_2/SiO_2/Si$ substrate by using chemical solution deposition. The physical properties of BNKT thin films were investigated by measuring SEM, XRD, P-E hysteresis loop, fatigue. Also, the high energy storage density and efficiency of thin films were investigated as a function of applied electric field and increase operation temperature. The energy storage density and efficiency BNKT-based thin films Showed high energy storage density with good temperature stability which is promising candidate material for high power electric applications.

P1-Co.114

Piezoresponse in epitaxial WO_3 thin films

*윤신희, 우창수, 이진홍, 최시영 [1], 김기엽 [1], 양찬호
*Shinhee. Yun, Chang-Su. Woo, Jin Hong. Lee, Si Young. Choi[1], Gi Yeop. Kim[1], Chan Ho. Yang
KAIST. [1]KIMS.

Keyword : WO_3, epitaxial, piezoresponse

In the early 20th century, WO_3 single crystal had been considered as a ferroelectric material because of the stripe domain structure [1,2]. However, the studies on crystalline structure revealed that the unit cell of bulk WO_3 at room temperature is centrosymmetric monoclinic phase (space group: $P2_1/n$), which is non-ferroelectric. By using misfit strain, we have grown heteroepitaxial WO_3 films showing piezoresponses of well-aligned ferroelastic twin domains. In addition, the crystal-structural analyses on the as-grown films were performed.

[1] B. T. Matthias, Phys. Rev., 76, 430 (1949)
[2] R. Ueda et al., Phys. Rev., 80, 1106 (1950)

P1-Co.115

Optical properties of doped Zinc Oxides

윤가화, 전기완, 이철의, *최동민, 이규원, 정승교, 이연호
Ka Hwa. Yoon, Gi Wan. Jeon, Cheol Eui. LEE, *Dong Min. Choi, Kyu Won. Lee, Seung Gyo. Jeong, Yeon Ho. Lee
고려대학교.

Keyword : Zinc Oxide, Photoluminescence

Currently, Zinc Oxide is widely studied for use as semiconductors and magnetic materials and even in the cosmetic fields. Here, optical properties of ZnO with various metal doping including aluminium, cobalt, manganese, and magnesium were investigated and compared with those of polymerized ZnO (added PVP). The study was focused on use for screening ultraviolet rays by reflecting 355 nm laser beams with shifted wavelength to visible light range, as radicals emerging from UV rays may break down the stable structure of ZnO, causing malicious effect on skin and even on life leading to skin cancer, aging due to destroyed cells and nucleotides.

P1-Co.116

유전체 박막의 열전도도 측정과 온도 의존성

강준구, 이두용, 이준혁, 김지웅, 박성균, 진형진, 양호순, *홍경수 [1]
Joon Ku. KANG, Doo Yong. LEE, Joon Hyuck. LEE, Ji Woong. KIM, Sung Kyun. PARK, Hyung Jeen. JEEN, Ho-Soon. YANG, *Kyong-Soo. Hong[1]
부산대학교. [1] *한국기초과학지원연구원.*

Keyword : 열전도도, $Gd_2Zr_2O_7$, 3-오메가 방법,

차세대 산업이 고집적화기술을 토대로 생산성 향상을 꾀하고 있고 이로 인해 전자 및 첨단 부품이 나노미터 단위로 미세화 되고 있다. 그러나 부품 크기의 축소에 따른 열부하의 증가는 성능이 저하되고 기기 수명을 단축시키는 요인이 되기 때문에 집적화의 기술적 한계로 작용하게 된다. 따라서 나노미터 단위에서 열의 흐름을 제어하고 관리하는 일과 물리적 성질을 이해하고 응용하는 일은 더욱 중요해졌다.

열의 흐름을 특정 짓는 대표적인 값인 열전도도는 어떤 물질이 가지는 고유한 물리적 성질 중 하나이지만 시스템의 온도가 변함에 따라 그 값이 변하고 변화의 양상은 물질에 따라 상이하다. $Gd_2Zr_2O_7$ 의 경우는 1000 K 이상의 고온에서 작동하는 터빈의 날개를 보호하는 열차단막으로 응용되는 반면 35 K 이하에서 초전도성을 띄는 $YBa_2Cu_3O_{7-\delta}$ 초전도체의 완충층으로도 응용되고 있어 두 경우에 동일한 물성을 적용하기 힘들다. 또한 산화물연료전지의 음극물질로 상용되고 있는 $La_{1-x}Sr_xMnO_3$ 의 경우는 함량에 따라 150 - 350 K 사이에서 상전이가 일어난다. 이런 상전이는 열전도도의 변화에도 영향을 미칠 것이므로 온도에 따른 정확한 변화 양상은 상전이의 새로운 지표를 제시할 수 있다.

본 연구에서는 RF 마그네트론 스퍼터링법을 이용하여 Al_2O_3 기판 위에 $Gd_2Zr_2O_7$ 박막을, 그리고 Si 기판 위에는 $CoFe_2O_4$ 박막을 증착하였다. 또한 펄스레이저증착 (PLD)법을 이용하여 $SrTiO_3$ 기판 위에는 $La_{1-x}Sr_xMnO_3$ 박막을 증착하였다. 3-오메가 측정 방법을 이용하여 다양한 온도 범위에서 박막의 열전도도를 측정하였다.

P1-Co.117*

Piezoelectric P(VDF-TrFE) thin film-based power generators using paper substrates for wearable device applications

*원성식, 안창원, Angus I. Kingon[1], 김일원, 김승현 [1]
*sung sik. won, Changwon. AHN, Angus. Kingon[1], ILL WON. KIM, Seung-Hyun. Kim[1]
울산대학교. [1] *브라운대학교.*

Keyword : P(VDF-TrFE) thin film, Piezoelectric, Power Generator, Wearable Device

The objective of this research is to develop a new class of flexible energy harvesting devices for self-powered wearable electronic systems. A critical issue of all piezoelectric wearable devices is the need to reduce the size and the weight so that devices with increased functionality can be incorporated into a wider range of physiological locations and applications. Use of polymeric piezoelectric thin films on paper substrates, however, is potentially beneficial for the fabrication of large-area and complicated-shaped devices with low cost, light weight and size scaling.
In this study, Solution-derived P(VDF-TrFE) piezoelectric thin films on cellulose paper substrates were successfully prepared as flexible power generators for wearable device applications. Optimization of appropriate annealing and cooling sequences of the co-polymer films resulted in the formation of dense and uniform microstructures exhibiting a well-developed β-phase. A maximum open-circuit voltage of 1.5 V was generated from the periodic bending and releasing the paper power generator at approximately 1 Hz. To demonstrate the wearable applications, P(VDF-TrFE) piezoelectric film-based paper power generators were directly attached on the back of a human hand and generated a maximum output open-circuit voltage of 0.4 V at low bending frequencies of 0.25 Hz. Good open-circuit voltage performance at low frequencies makes P(VDF-TrFE) piezoelectric thin films on paper substrates a strong candidate for future self-powered wearable devices.

P1-Co.118

Switchable photocurrents and electrical transports in organic-inorganic hybrid halide single crystals

*원충재, 허남정, 김용환
*Choongjae. Won, Namjung. Hur, yonghwan. kim
인하대학교.

Keyword : Inorganic-organic perovskites, Photocurent, asymmetrical eletric transport

Organic-inorganic halide perovskite is the one of powerful pioneering solar cell material although there has been a controversy in the existence of the ferroelectricity in the fundamental aspect. Here we report on the switchable photocurrents in organic-inorganic halide perovskites CH3NH3PbI3 single crystal, and light-induced diode-like electrical transport. The directions of photocurrent and electrical transports are dependent on the poling direction. At the low temperatures below the structure transition temperature, diode-like electrical transports appeared when the crystal was illuminated. We suggest that asymmetrical potential induced by the ion migration is responsible for the intriguing electrical transport and photocurrent.

P1-Co.119*

Enhanced triboelectric energy harvesting performance in surface-treated polydimethylsiloxane

JongHoon Jung, Byung Kil Yun, Jae Woong Kim, Hyun Soo Kim
JongHoon. Jung, Byung Kil. Yun, Jae Woong. Kim, Hyun Soo. Kim
Inha University.

Keyword : triboelectricity, PDMS, surface treatment

We report a facile method to increase the triboelectric performance of polydimethylsiloxane (PDMS) after a surface treatment using ultra-violet (UV)-ozone and base. In case of fresh PDMS-based devices, the open-circuit voltage and closed-circuit current were 3.8 V and 65 nA during contact/separation from an indium tin oxide (ITO) electrode, respectively. After the treatment of the PDMS surface using 1 M NaOH, in contrast, the resulting device generated voltage of 10.4 V and current of 179 nA. On the other hand, the UV-ozone and base treated PDMS resulted in a voltage and current of 49.3 V and 1.16 μA, respectively, which are almost 15 times larger than those of fresh PDMS. Attenuated total internal reflection and X-ray photoemission spectroscopic measurements indicated significant changes in Si–OH vibrations, the atomic ratio of O/Si, and the oxidation state of Si. These changes can be explained by a modification of Si–CH3 bonds to Si–O bonds after UVO and NaOH treatments.

P1-Co.120*

Piezoelectric and ferroelectric properties of $Bi(Ni_{0.5}Ti_{0.5})O_3$ substituted $0.67BiFeO_3$-$0.33BaTiO_3$ lead-free ceramics

*황인지, 도달현, 이명환 [1], 김다정 [1], 박진수 [1], 송태권 [1], 김명호 [1], 김원정 [1]
*In ji. Hwang, Dalhyun. Do, Myanghwan. Lee[1], DA JEONG. KIM[1], jin su. Park[1], Tae Kwon. SONG[1], Myong Ho. Kim[1], Won-jeong. KIM[1]
계명대학교. [1] 창원대학교.

Keyword : lead-free piezoelectric ceramics,(1-x)$BiFeO_3$-x$BaTiO_3$

Piezoelectric ceramics are widely used for electromechanical system such as sensors and actuators. Most piezoelectric ceramics which is commercially available are based on lead-based materials such as $Pb(Zr,Ti)O_3$ system. The use of lead-based ceramics has caused serious environmental problems and is harmful to human body. Therefore, the development of lead-free piezoelectric ceramics is an urgent issue. Recently lead-free (1-x)$BiFeO_3$-x$BaTiO_3$ system has been introduced. (1-x)$BiFeO_3$-x$BaTiO_3$ system has been reported to be a promising candidate with a high Curie temperature and good piezoelectric properties. This system has a morphotropic phase boundary with the coexistence of both rombohedral and psudocubic phases at x=0.33. However, the study on (1-x)$BiFeO_3$-x$BaTiO_3$ is rare due to high leakage current.
In this study, piezoelectric and ferroelectric properties of $Bi(Ni_{0.5}Ti_{0.5})O_3$ substituted $0.67BiFeO_3$-$0.33BaTiO_3$ ceramics were studied. The ceramics were sintered in a range of 980℃ - 1040℃, followed by water quenching. The best piezoelectric and ferroelectric properties were observed in the sample sintered at 980℃. The piezoelectric coefficient (d_{33}) of $0.97(0.67BiFeO_3$-$0.33BaTiO_3)$-$0.03Bi(Ni_{0.5}Ti_{0.5})O_3$ sintered at 980℃ was 201 pC/N. The remnant polarization($2P_r$) and the coercive electric field ($2E_c$) of $0.97(0.67BiFeO_3$-$0.33BaTiO_3)$-$0.03Bi(Ni_{0.5}Ti_{0.5})O_3$ sintered at 980℃ were 68 $\mu C/cm^2$ and 40 kV/cm at an applied electric field of 50 kV/cm, respectively. This result indicates that (1-x)$BiFeO_3$-x$BaTiO_3$ ceramic can be one of the promising candidates for lead-free piezoelectric ceramics.

P1-Co.121

Structure, electrical properties of Co doped $BiFeO_3$-$BaTiO_3$ lead free ceramics.

*한성진, 이명환, 김다정, 박진수, 최해인, 김명호, 송태권, 김원정, 김상수
*Sung Jin. Han, Myanghwan. Lee, DA JEONG. KIM, Jinsu. Park, Hai In. Choi, Myong Ho. Kim, Tae Kwon. SONG, Won-jeong. KIM, Sang Su. KIM
창원대학교.

Keyword : " $BiFeO_3$-$BaTiO_3$ ", "$BiCoO_3$", "piezoelectric property"

Recently, $BiFeO_3$-$BaTiO_3$ ceramic system is kind of replacement lead based piezoelectric ceramic, because $BiFeO_3$-$BaTiO_3$ system has a high Curie temperature without toxic materials. However, $BiFeO_3$-$BaTiO_3$ ceramics have not enough piezoelectric properties for replacement lead- based piezoelectric ceramic. The $BiCoO_3$ is a perovskite with a tetragonal symmetry and a large lattice c/a ratio 1.27, which indicates a high ferroelectric polarization.
In this study, the structure and the piezoelectric properties of $BiCoO_3$ modified $BiFeO_3$–$BaTiO_3$ ceramics were investigated. Detail of information will be present.

P1-Co.122

Giant electric-field-induced strain and crystallographic orientation of textured $Bi_{0.5}(Na,K)_{0.5}TiO_3$ templates

*abdul khaliq, 안창원, 김일원
*abdul. khaliq, Changwon. AHN, ILL WON. KIM
울산대학교.

Keyword : "Textured templates, giant strain, crystallographic orientation"

It has been an active research area for a considerable time span to prove improvements in the crystallographic orientation of textured ceramics. They are, on the other hand, the most suitable options for properties like electromechanical response. We are following reactive templated grain growth (RTGG) technique to fabricate $Bi_{0.5}Na_{0.5}TiO_3$ textured templates having large strain at low driving electric field values. Because of this high strain, these templates are likely to hold the place of other commercial materials which show electromechanical response at high electric fields. Here $Na_{0.5}Bi_{4.5}Ti_4O_{15}$ templates are used as precursor material. The composite textured ceramics are manufactured from $Bi_{0.5}(Na,K)_{0.5}TiO_3$ a ferroelectric and $Bi_{0.5}(Na,K)_{0.5}TiO_3$-$BiAlO_3$ a relaxor material. This gives us $Bi_{0.5}Na_{0.5}TiO_3$ as final textured plate like particles with enhanced crystallographic orientation. It is expected that these fabricated textured templates will come out as piezoelectric material with large dielectric and electromechanical properties. In comparison with other materials of the same nature like single crystals, this will be a good replacement being less expensive and delivering fine results.

P1-Co.123*

Fabrication and electrical properties of Intergrowth $Na_{0.5}Bi_{2.5}Nb_2O_6$-$Bi_4Ti_3O_{12}$ piezoelectric ceramics.

*최기쁨, 조삼연, 부상돈
*Gi Ppeum. Choi, Sam Yeon. Cho, Sang Don. Bu
전북대학교.

Keyword : Intergrowth, superlattice, piezoelectric, ferroelectric, ceramics

Intergrowth Bismuth layer-structured ferroelectric ceramics (BLSFs) $Na_{0.5}Bi_{2.5}Nb_2O_6$-$Bi_4Ti_3O_{12}$ (NBN-BIT) 세라믹스는 고상반응법으로 제작하였다. X-ray diffraction (XRD) 분석을 통해서 단일상의 NBN-BIT 세라믹스가 만들어짐을 확인하였다. 온도에 따른 유전상수를 측정한 결과 유전상수에서 두 개의 최대값이 나타났고, 큐리 온도 (T_c)가 780 ºC 인 것을 확인하였다. 유전 손실은 400 ºC 까지 우수한 열 안정성을 보였다. 압전 상수 (d_{33})가 순수한 NBN, BIT 보다 향상되었고, 온도 증가에 따라서 일정한 압전 상수가 나타남을 확인하였다. Scanning electron microscopic (SEM)을 사용하여 NBN-BIT 의 단면을 비교한 결과 grain size 가 감소되었다.
NBN-BIT 세라믹스의 P-E hysteresis loop 을 통해서 P_r 값과 E_c 값이 각각 10.5μC/cm^2, 18.5 kV/cm 이였고, 이 것은 BIT 의 강유전 특성보다 향상된 것을 알 수 있었다. 결과 적으로 NBN-BIT 세라믹스는 BIT 세라믹스에 비해서 T_c, 강유전 특성 그리고 압전 특성이 향상된 것을 알 수 있으며, 이것은 극한 환경에서도 사용될 수 있음을 시사한다.

P1-Co.124*

비납계 KNbO3 나노 막대를 이용한 압전 에너지 수확 및 비선형 광학성 응용

JongHoon Jung, Pil Gu Kang, Tae Kwon Lee
JongHoon. Jung, Pil Gu. Kang, Tae Kwon. Lee
Inha University.

Keyword : KNbO3, 나노 로드, 압전 에너지 수확, 비선형 광학

강유전체 나노제네레이터(NG)는 그 다양한 응용법 덕분에 최근 많은 주목을 받고 있는 소자이다. 이번 연구에서 비납계열 소자인 KNbO3(KNO)를 Nb:SrTiO3 기판 위에 150 도의 상대적인 저온에서 수열합성하여 성장시켰다. 이렇게 만든 나노제네레이터는 세로 방향으로 정렬된 평균길이 2 μm 의 1 차원 나노로드들임을 확인하였다. 이 소자를 이용하여 압전소자로서의 성질과 Second Harmonic Generator(SHG) 측정을 통해 광학소자로서의 성질을 확인하였다. 이렇게 성장한 KNO 나노제네레이터는 약 140 pm/V 의 높은 압전계수를 가지고 있고, 이 나노제네레이터의 외부에서 10N 의 압력을 가하여 최대 0.5 V, 10 nA 의 개방회로 전압과 단락회로 전류를 확인 할 수 있었다. 또한 이 나노제네레이터를 특정 파장대의 적외선 광선에 노출시켰더니 각각 그 파장대의 절반대역인 가시광선을 관측 할 수 있었다. 이러한 결과를 통해 이렇게 만들어진 나노제네레이터가 비단 압력센서로서의 사용법만 아닌, 광필터로서의 가능성을 확인 할 수 있었다.

P1-Co.125

Field-induced Effects on Phase Transition Behaviors of Lead-Free $(Na_{1/2}Bi_{1/2})TiO_3$-$BaTiO_3$ Single Crystals Studied by Brillouin Scattering

Byoung Wan Lee, *고재현, Xiaobing Li[1], Haosu Luo[1]
Byoung Wan. Lee, *Jae-Hyeon. Ko, Xiaobing. Li[1], Haosu. Luo[1]
Hallym University. [1]*Chinese Academy of Sciences.*

Keyword : lead-free, NBT-BT, Brillouin scattering, piezoelectric, phase transition

Lead-free piezoelectric materials have recently been studied intensively due to their potential in the field environmentally-friendly technology. The present piezoelectric performances of lead-free materials are in general inferior to those of lead-based materials, $Pb(Zr_{1-x}Ti_x)O_3$ being the most representative example. In this study, we used Brillouin scattering experiment to investigate phase transition behaviors of $0.95(Na_{1/2}Bi_{1/2})TiO_3$-$0.05BaTiO_3$ (NBT-5%BT) single crystals in a wide temperature range along different crystallographic axes and under different poling conditions. The crystals were grown by carefully controlled top-seeded solution growth method[1], and the Brillouin spectrum was measured by using conventional tandem 6-pass Fabry-Perot interferometer and a compact cryostat cell [2]. This method was successfully applied to derive elastic constants of NBT-5%BT at room temperature [3]. The temperature dependences of the Brillouin frequency shifts of the longitudinal acoustic (LA) and the transverse acoustic (TA) modes, as well as their half widths, of NBT-5%BT were determined under unpoled and poled conditions. While the unpoled crystals showed typical relaxor behaviors such as softening over a large temperature range and substantial hypersonic damping, the poled crystals displayed a sharp discontinuous change at ~110°C. The broad acoustic anomalies of unpoled crystals suggest the existence of noncentrosymmetric polar clusters in the paraelectric phase which do not evolve in long-range ferroelectric order. On the other hand, the sharp change in both the Brillouin frequency shift and the formation of a Landau-Khalatnikov-type damping peak at ~110°C indicates the transition from ergodic relaxor phase into long-range ferroelectric phase. The critical electric field is located at ~1.4 kV/mm.

P1-Co.126*

First-principle study of 180° head-to-head and tail-to-tail domain wall in $BaTiO_3$

*윤성우, 신영한
*Sung-woo. Yun, Young-Han. Shin
울산대학교.

Keyword : First principles calculation, DFT, $BaTiO_3$, Domain wall

Ferroelectric materials have a spontaneous electric polarization that can be switched by an external electric field, and the different polarization directions of ferroelectric domains form diverse domain walls [1]. The head-to-head (HH) and tail-to-tail (TT) domain walls have antiparallel polarization directions that lead to charge accommodation or depletion at the interface. $BaTiO_3$ and $PbTiO_3$ were studied to keep ferroelectricity for the HH and TT domain walls by substituting titanium and oxygen atoms at the boundary [2, 3]. It was shown that HH and TT ferroelectric domain walls disappeared to nullify the depolarization field without such substitution. But, another research was reported to form the inclined HH & TT domain walls without substitution by using Landau-Ginzburg-Devonshire theory (LGD) [4]. In order to estimate the intrinsic properties of HH and TT domain walls of $BaTiO_3$, we fixed the internal atomic coordinates to the bulk values and relaxed the other coordinates using first-principles calculations based on density functional theory (DFT). From this calculation, we found the ferroelectric domain wall was more diffuse than the non charged domain wall. We expect that we can extend our study to understand the ferroelectric domain dynamics by including the HH and TT domain wall energies and strain in the phenomenological Hamiltonian. Additionally, in order to compare LGD results and our DFT calculations, we form the domain wall in step formation and calculate the domain wall energies and polarization, electrostatic potential.

References:
1. M.E. Lines and A.M, Glass, Principles and applications of ferroelectrics and related materials (Clarendon Press, Oxford, 1977).
2. X. Wu and D. Vanderbilt, Phys. Rev. B 73, 020103(R) (2006).
3. K. Rahmanizadeh, D. Wortmann, G. Bihlmayer, S. Blugel, Phys Rev. B 90, 114104 (2014). 4. E. A. Eliseev, A. N. Morozovska, G. S. Svechnikov, Venkatraman Gopalan and V. Ya. Shur, Phys Rev. B 83, 235313 (2011).
4. E. A. Eliseev, A. N. Morozovska, G. S. Svechnikov, Venkatraman Gopalan and V. Ya. Shur, Phys Rev. B 83, 235313 (2011).

P1-Co.127

Sulfate disorder in potassium alum. X-ray single crystal study.

*오인환, 박가람, 김호성 [1], 박현민 [2]
*In-Hwan. Oh, Garam. Park, Ho-Sung. Kim[1], Hyun Min. Park[2]
한국원자력연구원. [1] 전남대학교. [2] 표준연구원.

Keyword : diorder, sulfate group. hydrogen bond, X-ray single crystal

$KAl(SO_4)_2 \cdot 12H2O$ belongs to the alum family whose general formula is $AB(SO_4)_2 \cdot 12H_2O$, where A=monovalent cation, B=trivalent cation, respectively. Among these, potassium alum is a representative of the naturally occuring sulfate compound and used for industrial applications. The atoms in the crystal move around. Diffraction method can give an just averaged crystal structure over the time. Therefore, the only hint for the atomic motions in the crystal structure is the atomic displacement factor. Based on our result, the two oxygen atoms related with sulfate group in alum show unusually large thermal factor and this indicates the disordered character in the crystal structure. It seems that the sulfate grops are disordered one of the two possible sites in a 70:30 proportion at room temperature. Generally, heavy atoms in the inorganic solid state material have the atomic displacement factor between 0.005 and 0.02. Organic molecular has the typical values between 0.02-0.06. In the case of weak bounded terminal atoms, this value may lie between 0.1-0.2. If the one of the principla axes of the thermal factor is greater than 0.2 or 0.3, then this is evidence for the disorder in the crystal structure. In this work, we will show a single crystal structure from X-ray diffraction and data treatment method in the case of disordered crystal structure.

P1-Co.128

Comparisons of Dielectric Relaxations and Modulus Relaxations in the Ferroelectric Barium Europium Titanate Ceramics

*전병억, 이종림, 김민기, 오승민
*Byeong-Eog. Jun, Jong-Rim. Lee, Minki. Kim, Seung-min. Oh
카이스트 부설 한국과학영재학교.

Keyword : Diffused ferroelectric phase transion, Dielectric relaxation, Modulus relaxation, Cole-Cole formula

We have studied the dielectric properties of the ferroelectric phase transitions barium europium titanate $Ba_{1-x}Eu_xTiO_3$ (BET, x = 0 ~ 0.3) ceramics. It is considered that the c-axis lattice constant and the ferroelectric phase transition temperature decrease with proportional to the increasing x in the BET solid solution. We are studying the ferroelectric phase transition of the BET solid solution by using the dielectric spectroscopy and the ferroelectric hysteresis behaviors in the temperature range below 600 °C. The dielectric relaxation times were characterized as the thermally activated behaviors in the temperature range below 500 °C. Both in the complex dielectric constant formalism and in the complex modulus formalism, the Cole-Cole type dielectric relaxations were characterized in the frequency range from 10^{-2} Hz to 10^5 Hz during the ferroelectric phase transition. The relaxation time and the exponent of the Cole-Cole type formula, , where is the imaginary unit, is the angular frequency. It is considered that there was a similarity of the Cole-Cole type relaxations in the two formalism.

P1-Co.129*

Physical properties of hybrid perovskites $CH_3NH_3PbI_3$ and $CH_3NH_3PbBr_3$ single crystals

*우원석, 안창원, 김일원
*Won Seok. Woo, Chang won. Ahn, Ill Won. Kim
울산대학교.

Keyword : Perovskite solar cell, single crystal, $CH_3NH_3PbX_3$

Photovoltaic devices based on the hybrid perovskites $MAPbX_3$ (MA= CH_3NH_3, X= I, Br and Cl) have recently emerged as a new generation of solution process with low-cost and high power conversion efficiency of around 20% in just a few years. Though progress in device efficiencies has been remarkable, the lead-halide perovskite fabricated by chemical solution deposition have as main drawback for the instability of the material to atmospheric moisture. For this reason, the fundamental physical properties and performance limits of organolead trihalide $MAPbX_3$ remain obscured by extensive disorder in the polycrystalline $MAPbX_3$ films. In this study, we have grown $MAPbI_3$ and $MAPbBr_3$ single crystals using inverse temperature crystallization technique. The black and orange color single crystals of $MAPbI_3$ and $MAPbBr_3$ with the size of 7 mm x 7 mm x 2 mm were successfully grown in the bottom of the crystallizing dishes after several days. The physical properties and crystal structure of $MAPbI_3$ and $MAPbBr_3$ single crystals were investigated by measuring XRD, SEM, dielectric, P-E hysteresis loop and I-V characteristic for the different crystal axis.

P1-Co.130

양성자 조사를 통한 비정질 $Li_2B_4O_7$(LBO)의 유전특성 변화

*김수재, 정명환, 김계령, 김맥 [1]
*Su Jae. KIM, Myung hwan. Jung, Kye-Ryung. KIM, Mac. Kim[1]
한국원자력연구원. [1] *부산대학교.*

Keyword : $Li_2B_4O_7$, Proton irradiation, Proton accelerator, Amorphous, Dielectric

회로가 소형화되면서 배선간격이 작아지고 이에 따라 고유전율을 가진 물질에 대한 요구도 커지고 있다. 다양한 불순물 도핑등을 통하여 유전율을 향상시키기 위한 시도가 수행되고 있다. 양성자빔 조사를 통한 LBO 비정질의 유전율 변화를 시도하였다. LBO 파우더를 1000℃에서 30 분 녹인 후 공기 중에서 냉각하여 비정질을 제조하였다. 제조된 비정질의 유전율을 변화시키기 위하여 양성자 빔을 LBO 에 조사하고 더불어 양성자가 불순물로 작용하도록 시료 내부에 존재 하게 조절하였다. 양성자를 조사한 LBO 의 유전율이 증가하는 것을 확인하였다. LBO 내부로 조사된 양성자는 에너지를 전달한 후 느슨한 상호작용을 가지고 LBO 내부에 존재 할 것으로 예상되며 LBO 를 구성하는 다른 원소에 비해 쉽게 전기장에 반응할 수 있을 것으로 생각된다. 또한 양성자 조사에 의하여 생겨난 defect 또한 유전율의 변화에 기여할 것으로 기대된다.

미래창조과학부로부터 지원을 받은 양성자가속기연구센터 운영기금의 지원을 받은 연구임.

P1-Co.131

Elastic moduli of Zerodur® glass ceramic studied by micro-Brillouin scattering

*김태현, 임신혁, 이상경, 노희숙, 심규민
*Tae Hyun. Kim, Sin Hyuk. Yim, Sangkyung. Lee, Hee Sook. Roh, Kyu Min. Shim
국방과학연구소.

Keyword : "elastic constant", "light scattering", "glass ceramics"

We investigated the temperature dependence of elastic properties of Zerodur®, which is a glass-ceramic material exhibiting a very low coefficient of thermal expansion. The material is therefore used as a mirror substrate for astronomical telescopes or as a mechanical component when geometrical dimensions and shapes are required to be extremely stable against temperature changes. The Brillouin frequency shift allowed the calculation of longitudinal sound velocity and longitudinal modulus from liquid N_2 to 1300 ^oC . The values of elastic moduli (including Young's modulus, bulk modulus, and shear modulus) derived from experimental data by non-contact measurement. No signs of any structureal phase transition at temperatures between -190 ^oC and the melting point of Zerodur®, i.e.~1250 ^oC, were obserced.

P1-Co.132

Nonlinear magnetodielectric effect in double-perovskite Gd_2NiMnO_6

*오상협, 최환영, 문재영, 김미경, 조영훈 [1], 이나라, 최영재
*SANGHYUP. OH, Hwan Young. Choi, Jae Young. Moon, M. K.. Kim, Younghun. Jo[1], Nara. Lee, Y.J.. Choi
연세대학교. [1] 한국기초과학지원연구원.

Keyword : Magnetodielectric

Magnetic and dielectric properties of the double perovskite Gd_2NiMnO_6 were investigated. Ferromagnetic order of alternating Ni^{2+} and Mn^{4+} spins arises below T_C=134 K and additional order of Gd^{3+} spins occurs at T_{Gd}=33 K. The formation of short-range ferromagnetic clusters accompanied by Griffiths phase-like feature below T_G=230 K is also suggested. Under the low enough dielectric loss at low temperature regime excluding the influence of extrinsic effect, highly non-linear variation of dielectric constant was achieved in application of magnetic fields. Our finding offers an efficient approach to accomplish intrinsically coupled functionality utilizing both magnetic and dielectric quantities

P1-Co.133

Phonon and piezoelectric propertiex of C_2HF and SnX_2(X=S, Se)

*이건희, 신영한
*Geon Hui. Lee, Young-Han. Shin
울산대학교.

Keyword : "two-dimensional materials" "graphene" "SnS_2" "piezoelectric" "phonon"

Recently two-dimensional materials have drawn a great attention, mainly because of their promising applications for nanoelectromechanical devices. By breaking centro-symmetry of graphene, H and F co-decoration engineers piezoelectricity into non-piezoelectric graphene. Based on first principles calculations, we investigate the phonon properties of H and F co-decorated graphene (C_2HF). Our calculations suggest that free standing C_2HF monolayer is vibrationally stable without imaginary frequencies in the phonon band structure. We also study other two-dimensional monolayers: SnS_2 and $SnSe_2$. Unlike stable 1H-MoS_2, SnS_2 and $SnSe_2$ monolayers have a hexagonal CdI_2-type structure with Sn atoms sandwiched between two layers of S atoms, where two S planes are off-set from each other with inversion symmetry. We extend the study of SnS_2 and $SnSe_2$ in bulk and bilayer forms as well as the S-vacancy or S/Se substitution. Our results suggest that those stable free standing two-dimensional piezoelectric materials could lead to tunable piezoelectric materials and devices for extremely small force generation and sensing.

P1-Co.134

Ferroelastic phase transition in $(C_6H_5CH_2CH_2NH_3)_2CuCl_4$ (Cu-PEA)

박가람, *오인환 [1], 박승일 [1], 박성훈 [2]
Garam. Park, *In-Hwan. Oh[1], J.M. Sungil. Park[1], Seong-Hun. Park[2]
원자력연구원. [1] *한국원자력연구원.* [2] *경기과학고등학교.*

Keyword : structural phase transition, ferroelastic, X-ray powder diffraction, group-subgroup relation

Pervoskite type inorganic-organic hybrid compounds draw many attentions due to the possible various applications in the field of solar cell, multiferroics, low-dimensional magnetism and thermoelectrics. In the previous investigation (Polyakov et al., (2012)), the layered inorganic-organic hybrid material $(C_6H_5CH_2CH_2NH_3)_2CuCl_4$ (Cu-PEA) is reported as multiferroics (ferromagnetic and ferroelectrics). Two structural phase transitions are observed at T_{c1} = 408K and T_{c2} = 372K. Cu-PEA crystallized in the space group Pbma at room temperature and the polarization is incompatible with the inversion center in the crystal structure. To study this contradiction, we carried out temperature dependent X-ray powder diffraction measurements. Our results together with the previous optical observations strongly suggest that Cu-PEA should be not ferroelectric at room temperature but ferroelastic. The color change at the phase transition is attributed to an alteration of the optical birefringence resulted from a cell doubling from primitive cell at room temperature to a-centered cell at high temperature. In this work, we will present group-maximal subgroup relations to explain the domain building and the phase transitions.

Reference

[1] Polyakov et al., Chem. Mater. Vol. 24, 133 (2012)

P1-Co.135

Raman scattering studies of Topological insulator SmB_6

*응원티후옌, 민헨, Kang Boyoun[1], 조병기 [1], 양인상
*Nguyen Thi. HUYEN, Nguyen Thi Minh. HIEN, Boyoun. Kang[1], Beongki. Cho[1], In-Sang. YANG
이화여자대학교. [1] 광주과학기술원.

Keyword : Raman scattering, Samarium hexaboride, Topological insulator, temperature dependent

We present the results of temperature-dependent Raman spectroscopy of SmB_6 single crystals grown from boron with a purity of 99.9% (3N) or 99.9999% (6N) from 12 K to 300 K. The Raman active phonon modes T_{2g}, E_g, A_{1g} of SmB_6 (6N) are sharp peaks. However, the Raman modes of SmB_6 (3N) appear at higher wavenumbers compared with SmB_6 (6N). In SmB_6 (6N), A_{1g} peak has Fano line shape (asymmetric) and the temperature dependence of spectral weight shows anomalous change near 150 K, while in 3N sample, the A_{1g} shape is more symmetric. In addition, anomalous temperature dependences near 50 K of the E_g and A_{1g} phonon modes were observed in SmB_6 (3N). It may related to a gap opening due to the hybridization between f-electron and the electron in conduction band. These differences of the Raman behavior of the SmB_6 (6N) and SmB_6 (3N) samples may be due to subtle structural distortions in SmB_6 (3N), which may be triggered by the existence of small amount of impurities in SmB_6 (3N).

P1-Co.136

Color-Tunable Ca_2SiO_4 : Eu^{2+} phosphors prepared with differently aged PGMS

Hyun-Joo Woo, Sakthivel Gandhi, Bong-Joon Kwon, kyungmi CHO[1], Dong-Soo Shin[2], Kiwan JANG[1]
Hyun-Joo. Woo, Gandhi. Sakthivel, Bong joon. Kwon, kyungmi. CHO[1], Dong-Soo. Shin[2], Kiwan. JANG[1]
Research Institute of Basic Sciences/ Changwon Nat'l Univ. [1]Department of Physics/Changwon Nat'l Univ. [2]Department of Chemistry/Changwon Nat'l Univ.

Keyword : Ca_2SiO_4 : Eu^{2+} , PGMS, phosphor, w-LEDs

White light emitting diodes (w-LEDs) are the most important solid-state light source due to many advantages over traditional light sources such as long lifetime, high luminance efficiency, high brightness, low power consumption and environmental friendliness. White light is generally created by the combination of blue LED chips and a yellow phosphor, which has low color rendering index and high color correlated temperature. Therefore, development of phosphor along with enough red spectral components is required, to improve the performance of w-LEDs.

The Ca_2SiO_4 based Eu^{2+} doped phosphor was prepared using differently aged PGMS as silica source. The powder XRD patterns of all the samples prepared with different aged PGMS as silica source. The peaks obtained for all the $Ca_{2-x}SiO_4$:2xEu^{2+} (2x = 0.05) phosphors are in good agreement with ICSD standard card (390060) which proves that the different aged PGMS as silica source did not influence on the host crystal structure. The emission spectra of the Eu^{2+}:Ca_2SiO_4 phosphors showed a band near the visible region which might have occurred from the $4f^65d^1 \rightarrow 4f^7$ ($^8S_{7/2}$) transition of Eu^{2+} ions. A pcLED that has been fabricated using a single crystal host materials possess the ability to give red, green and blue colors along with a high color rendering index.

P1-Co.137

Photoluminescent Properties and Electronic Structures of $NaY(MoO_4)_2:Eu^{3+}$ Phosphors

*박성욱, 김도림, 정중현, 김중환 [1]
*Sung Wook. Park, Dorim. Kim, Jung Hyun. Jeong, Jung Hwan. KIM[1]
부경대학교. [1] *동의대학교.*

Keyword : Photoluminescent,$NaY(MoO_4)_2:Eu^{3+}$,Phosphor

The $NaR(MoO_4)_2:Eu^{3+}$, with R = Y, Gd, La, phosphors have been fabricated by using high energy ball milling process. Calculations of the band structures, partial densities of states of perfect $NaY(MoO_4)_2$ and $NaLa(MoO_4)_2$ crystals were performed. In the phosphor series, $NaY(MoO_4)_2:Eu^{3+}$ was chosen owing to the most suitable characteristics, which was sintered from 800 to 1100°C to optimize microstructure and performance. The optimal synthesistemperature for the $NaY(MoO_4)_2:Eu^{3+}$ phosphor powder was defined at 1100°C. The XRD and FE-SEM microscopy indicate that the crystallinity is improved and the particles grow up with increasing sintering temperature up to 1100°C. The absorption edge gradually shifts to lower energy side with increasing the sintering temperature. The increase in the particle size is considered to respond to the trend. Highly pure and single-phased $NaY(MoO_4)_2:Eu^{3+}$ phosphor exhibits intense red emission with good color chromaticity attributed to efficient energy transfer from MoO_4^{2-} to Eu^{3+}.

P1-Co.138

SILICATE BASED FLEXIBLE REMOTE PHOSPHOR FOR WARM WHITE LED APPLICATIONS – AN IMPORTANT ROLE PLAYED BY SILICA NANOPARTICLES

Sakthivel Gandhi, Bong-Joon Kwon, Hyun-Joo Woo, Dong-Soo Shin[1], JANG Kiwan[2]
Gandhi. Sakthivel, Bong- joon. Kwon, Hyun- Joo. Woo, Dong-Soo. Shin[1], Kiwan. JANG[2]
Research Institute for Basic Sciences/ Changwon Nat'l Univ. [1]Department of Chemistry/Changwon Nat'l Univ. [2]Department of Physics/Changwon Nat'l Univ.

Keyword : Calcium strontium silicate, Eu^{2+},warm white LED

Once the problem in accessing blue LED was solved by Prof. Nakammura, there were enormous technologies developed for creating white light. It is correct to say, the phosphor is a prime source for creating white light from the solid state illuminating chips. There are several researches talk about the different kinds of organic & inorganic hosts which are self activated or activated by a particular element. The commercially available YAG:Ce fails in making warm white light due to the insufficient red spectral components in it. To overcome the challenges, a novel material has been used here to develop a silicate phosphor.

Calcium strontium silicate, activated by Eu^{2+} has been prepared via wet-solid phase reaction technique using silica nanoparticles for the first time. The prepared phosphor can be efficiently excited by a broad range of spectrum from 200 to 500 nm and emit in the red region at 605 nm, covering the entire spectrum from blue to red. This reddish yellow emitting phosphor was fabricated as a thin film using silicon resin and used as remote phosphor to produce warm white light. The prototype LED was fabricated using a commercial 450 nm blue emitting LED with the developed phosphor. The result shows a production of warm white light along with CCT 90. The temperature dependant luminescence profile shows the instability of luminescence against increasing temperature. So, the silica nanoparticles assisted $CaSrEuSiO_4$ remote type phosphor can be well utilized for warm white light production under various commercial LEDs.

P1-Co.139

Mechanism of tri-color upconversion luminescence on adjusting Yb^{3+} concentrations

*오주현, 정중현, 김중환 [1]
*Ju Hyun. Oh, Jung Hyun. Jeong, Jung Hwan. KIM[1]
부경대학교. [1] *동의대학교.*

Keyword : Upconversion,Phosphor,Energy transfer

Upconversion (UC) luminescent nanomaterials have attracted much research interest due to their applications in various optical devices such as solid state lasers, three-dimensional flat-panel displays. Among a lot of host materials, the β-$NaYF_4$ is known as one of the most efficient NIR to visible UC materials. Mechanism for the green and red emission on Yb^{3+} and Er^{3+} co-doped UC phosphors was much reported. However, the currently accepted mechanism for production of green, red, and blue emission is not appropriate to explain the Yb^{3+}, Er^{3+} co-doped $NaYF_4$ phosphors.
We propose mechanism to explain tri-color UC luminescence on adjusting Yb^{3+} concentrations in $NaYF_4$:Er^{3+} UC phosphors. We measured lifetime and pump power dependence of UC photoluminescence on various Yb^{3+} concentrations to examine mechanism of the blue, green, red emission.

P1-Co.140

Multi wavelength excited white-emitting Dy^{3+}doped $Sr_3Y(PO_4)_3$ phosphor

*서연우, 오주현, 정중현, 김중환 [1]
*Yeon Woo. Seo, Ju Hyun. Oh, Jung Hyun. Jeong, Jung Hwan. Kim[1]
부경대학교. [1] *동의대학교.*

Keyword : White light-emitting diodes,Phosphor,Photoluminescence

White light-emitting diodes (WLEDs)are the promising new emitting light source for common illumination due to their extensive application in the lighting industry base on the advantages of energy saving capability, long operation lifetime and environment friendly characteristics.In recent years, trivalent dysprosium ions (Dy^{3+}) doped phosphors have been extensively studied due to its two dominant emission bands in the blue region owing to the $^4F_{9/2}\rightarrow{}^6H_{13/2}$ transition and in the yellow region owing to the $^4F_{9/2}\rightarrow{}^6H_{15/2}$ transition. It is possible to achieve near white light emission by adjusting the yellow to blue intensity ratio value.
In this study, white emitting phosphor Dy^{3+} doped $Sr_3Y(PO_4)_3$ powder samples by high-energy ball milling method. The structural and luminescence properties of the phosphors were investigated by X-ray diffraction (XRD), field-emission scanning electron microscopy (FE-SEM), and photoluminescence (PL) excitation and emission spectra.These phosphors showed double emissions at wave lengths of 483 nm and 576 nm under the excitation of near-ultraviolet light.

P1-Co.141

Li^+ 또는 La^{3+}를 첨가한 $CaSrSiO_4:Eu^{3+}$, $CaSrSiO_4:Eu^{2+}$ 형광체의 합성과 광학적 특성 연구

조경미, 우현주, 간디삭티벨, 권봉준, 신동수, *장기완
KYUNG MI. CHO, Hyun - Joo. Woo, Gandhi. Sakthivel, Bong joon. Kwon, Dong-Soo. Shin, *Kiwan. Jang
창원대학교.

Keyword : Li^+, La^{3+}, 형광체, 고상반응법

차세대 조명광원으로 각광받고 있는 백색 LED 는 적색, 녹색 및 청색 LED 를 결합하여 구현하거나 청색 LED 또는 자외선 LED 와 청색, 녹색, 황색, 적색 형광체를 조합하는 방법이 사용되고 있다. 형광체와 함께 사용되는 백색 LED 의 경우에 색지수 및 색온도 등의 향상을 위해 형광체의 기능은 매우 중요하다.
본 연구에서는, 고상 반응법을 이용하여 Li^+와 La^{3+}가 소량 첨가된 $Ca_{0.9975}Sr_{0.9975}SiO_4:Eu^{3+}{}_{0.005}$ 형광체 분말을 소결하여 제조하였다. Li^+와 La^{3+}가 발광효율에 미치는 영향을 조사하였다. Li^+이온의 농도는 Li_2CO_3 의 첨가량 조절을 통하여 조절하였으며, La^{3+}이온의 농도는 La_2CO_3 를 첨가하여 La^+이온의 농도를 변화시켰다. Li^+와 La^{3+}가 발광효율에 미치는 영향을 조사하기 위하여 Eu 의 양은 0.5 mol%로 고정하였다. $CaSrSiO_4$ 첨가된 Eu^{3+}의 발광에 미치는 Li^+ 또는 La^{3+} 이온의 영향을 조사보기 위하여 Li_2CO_3 의 농도를 0.1~3 mol% 변화시키고, La_2CO_3 의 농도를 0.1~2 mol% 변화시키면서 시료들을 합성하였다. 또한 Li^+ 또는 La^{3+} 이온들이 $CaSrSiO_4$ 첨가된 Eu^{2+}의 발광에 미치는 영향을 조사하기 위하여 환원분위기에서 2 차 열처리한 후 농도에 따른 발광세기를 측정하였다. 본 연구를 통하여 Li^+ 또는 La^{3+} 이온들의 농도를 증가시키면 Eu^{3+}에서 Li^+1.25mol%, Eu^{2+}에서 La^{3+}2mol%까지는 발광세기가 증가하다가 특정농도이상이 되면 발광세기가 감소한다. 이러한 현상은 다른 연구자들의 실험결과와 같지만, 다시 농도를 Eu^{3+}에서 Li^+1.25mol% 이상으로 증가시키면 다시 발광세기가 증가하다가 이들의 농도가 더욱 증가하면 다시 감소하는 경향이 나타났다. 이러한 현상은 $CaSrSiO_4$ 모체에 첨가된 경우에만 발견되는 특이현상이다.

P1-Co.142

Luminescence properties and energy transfer of Sm^{3+} doped $Sr_2CaMo_{1-x}W_xO_6$ as a potential phosphor for white LEDs

*왕리리, 노현미, 최병춘, 정중현
*Lili. Wang, Hyeon Mi. Noh, Byung Chun. Choi, Jung Hyun. Jeong
부경대학교.

Keyword : White LED,Energy transfer,Luminescence

A series of Sm^{3+} doped $Sr_2CaMo_{1-x}W_xO_6$ phosphors were synthesized through solid state reaction process and their luminescence properties have been investigated. The phosphors presented effective excitation bands in UV, near UV and blue regions, which originating from the charge transfer band of $Mo(W)O_6$ and Sm^{3+} f-f transitions. There exists energy transfer blockage from MoO_6 to Sm^{3+} ions because the configuration of Mo^{6+}, O^{2-} and Sm^{3+} (Sr^{2+}) is not collinear and concentration quenching usually happens among MoO_6 groups in Mo-rich samples. Efficient energy transfer from WO_6 to Sm^{3+} was discovered by directly observing significant overlap of the excitation of Sm^{3+} and the emission of WO_6. Appropriate amount of W was used to replace Mo in $Sr_2CaMo_{1-x}W_xO_6$ phosphors. MoO_6 groups can enhance the absorption capability of the host lattice in the near UV region and WO_6 groups can act as energy obstacles to block the energy migration among MoO_6 groups, resulting in more energy being transferred to Sm^{3+} ions to give red luminescence. To understand cation substitution and charge transfer transitions in the phosphors, Raman spectra were collected and first-principle calculations on the band structure and density of states were conducted. Optical band gap were also calculated based on the diffuse reflectance spectra.

P1-Co.143

Luminescent properties of host-sensitized Dy^{3+} doped double-perovskite $SrLaMgTaO_6$ for white LEDs

*곽월, 노현미, 문병기, 정중현
*Yue. Guo, Hyeon Mi. Noh, Byung Kee. Moon, Jung Hyun. Jeong
부경대학교.

Keyword : White LED,Luminescence,Double-perovskite

Luminescent properties of host-sensitized Dy^{3+} doped double-perovskite $SrLaMgTaO_6$ for white LEDs

P1-Co.144

Luminescence properties of double perovskite $SrLa_{(1-x)}MgTaO_6:xEu^{3+}$ phosphor for white light-emitting diodes

*김도림, 박성욱, 정중현, 김중환 [1]
*Dorim. Kim, Sung Wook. Park, Jung Hyun. Jeong, Jung Hwan. Kim[1]
부경대학교. [1] 동의대학교.

Keyword : Double perovskite,White light-emitting diode,$SrLaMgTaO_6$

$SrLa_{(1-x)}MgTaO_6$ phosphors with a high quantum efficiency have recently been reported by our group, which were synthesized by conventional solid reaction method. To enhance the luminescence efficiency, we fabricated $SrLa_{(1-x)}MgTaO_6:xEu^{3+}$ phosphors using high mechanical energy milling technique. Nano crystalline $SrLaMgTaO_6$:Eu powder was produced by the high energy ball mill machine. The Eu doping concentration was varied from 0.30 to 0.60 mol and sintering was carried out at temperature of 1400°C in air. Under the excitation of the near ultraviolet (UV) and blue light, this perovskite type phosphor emitted a red light. The luminescence process is attributed to the energy transfer from the excited states of $SrLaMgTaO_6$ host to Eu^{3+} ion and then relaxed to ground states of Eu^{3+}. The characteristic Eu^{3+} emission of 617 nm due to the $^5D_0$-$^7F_2$ transition was observed. The effects of the doped Eu^{3+} concentration in $SrLaMgTaO_6$ were also investigated in detail. The results showed that increasing Eu^{3+} concentration increases until a maximum intensity is reached, and then it decreases because of the concentration quenching effect, which are explained satisfactorily with the luminescent theory. At the optimum Eu^{3+} concentration of 50 mol%, quantum efficiency is not only 1.5times higher than the $SrLaMgTaO_6$:Eu sample which was synthesized by conventional solid state reaction method but also 2.4 times higher than the sulfides that are used now as red phosphors in white LEDs. Accordingly, it is a promising material for warm-white light-emitting diodes.

P1-Co.201*

Negative longitudinal magnetoresistance of Weyl semi-metal candidate $ZrTe_5$

Byung Woo Kho, Joonbum Park[1], ErikKampert[2], Jun Sung Kim
Byung Woo. Kho, Joonbum. Park[1], Erik. Kampert[2], Jun Sung. Kim
Pohang University of Science and Technology. [1]Max Planck institutes. [2]Helmholtz-Zentrum Dresden-Rossendorf.

Keyword : "Weyl semimetal" "Negative magnetoresistance" "Chiral anomaly"

We report the negative longitudinal magnetoresistance of $ZrTe_5$ single crystals and their systemic changes temperature field orientation. $ZrTe_5$ is one of the candidates of Dirac semimetals that can host Weyl points as the external magnetic field split the Dirac nodes. In this case, the magnetic field aligned to the electric field can produce additional chiral charge flow between two Weyl nodes, leading to negative magnetoresistance. For $ZrTe_5$, the longitudinal negative magnetoresistance is completely suppressed when the magnetic fields and currents are mis-oriented by only ~2 deg. Such an extremely sensitivity is one of the defining signature of the chiral anomaly, thus supporting that ZrTe5 is indeed Weyl semimetal under magnetic fields.

P1-Co.202*

Field effect operation of 2-Dimensional Electron Gas at SrTiO3/LaAlO3 heterointerface from normal metal to superconductor region

*곽용수, 김진희 [1], 송종현
*yong su. kwak, Jinhee. KIM[1], Jong Hyun. SONG
충남대학교. [1] 한국표준과학연구원.

Keyword : "superconductor","heterostructure","2-Dimensional Electron Gas","pulsed laser deposion","field effect transistor"

We have investigated field effect operation of 2-Dimensional Electron Gas (2DEG) formed on LaAlO3/SrTiO3 heterostructure from normal metal to superconductor region. The heterostructure was grown by pulsed laser deposition and hall-bar geometry was fabricated by photo lithography. Hardly exposed poly methyl methacrylate (PMMA) by Scanning Electron Microscope(SEM) was used as a gate insulator and Au electrode was sputtered as gate electrode. Conductivity of 2DEG channel was modulated as a field effect transistor device. We also observed that the superconducting tunnel junction is formed at superconducting channel in LaAlO3/SrTiO3 heterostructure by applying gate voltage. Our result could contribute to fundamental investigation in oxide electronics by using oxide heterointerface.

P1-Co.203*

Excitation Energy Dependent Raman Scattering of Few-layer $MoSe_2$

*김강원, 이재웅, 남다현, 정현식
*Kangwon. Kim, Jae-Ung. Lee, Da Hyun. Nam, Hyeonsik. Cheong
서강대학교.

Keyword : Resonant Raman, Raman scattering, $MoSe_2$

We investigated the effects of excitation energies on the Raman spectra from 5 to 600 cm^{-1} of few-layered $MoSe_2$ thin films up to 7-layers. In Raman measurements, if the excitation energy matches an exciton state, resonance effects are observed. Due to these effects, there are several anomalous behaviors as in the case of MoS_2[1]. In addition, we measured and compared the Raman spectra in the low-frequency region ($^{-1}$). As the thickness of $MoSe_2$ is increased, the number of inter-layer vibration modes (breathing and shear modes) and positions of those are changed. By combining these results, we can establish fingerprints for determining the number of layers.

References
[1] J.-U. Lee et al., Nanoscale 7, 3229 (2015)

P1-Co.204*

The modulation of types of charge carrier in WSe_2 field effect transistor with source/drain electrodes of different work function

*김상민, 김태광, 두혜원, 신소명, 김다혜, 구형준, 김선영, 송민호, 김승준, 서순애
*SANGMIN. KIM, Tae Kwang. Kim, hyewon. Du, So Myeong. Shin, Da hye. Kim, Hyung Jun. Koo, SeonYeong. Kim, Min ho. Song, Seungjun. Kim, sunae. seo
세종대학교.

Keyword : TMD, WSe_2, ambipolar, 2D semiconductor, work function

The ambipolar behavior of WSe_2 lies in the accessibility of the electrons and holes for charge transport. In metal/WSe_2 junction, the relative position of metal Fermi level and semiconductor conduction band or valance band determines preference of carrier type with no Fermi-level pinning. Thus, low (high) work function metals can be utilized to improve injection efficiency of electron (hole) by lowering the height of respective Schottky barrier (SB). However, due to dominance of SB in WSe_2, device parameters such as off-current, threshold voltage, subthreshold swing and field effect mobility as well as on-current are highly affected by combined effect of source/drain voltage and gate voltage because both voltages can modulate depletion width and change the injection mechanism. Here, we fabricated WSe_2 field effect transistor (FET) with different source/drain electrode of Sc, Al, Ti, graphene, Ni and Pd. Multi-layer WSe_2 is exfoliated onto a 300nm thick SiO_2 with back-gated Si substrate. Source/drain contacts were defined by electron-beam lithography. We measured transfer curves and output curves of WSe_2 FET with different source/drain, and analyzed device parameters using SB modulation in each device.

P1-Co.205*

Al_2O_3 high-k passivation effect depending on MoS2 thickness

*김승준, 김태광, 신소명, 두혜원, 김다혜, 구형준, 김선영, 송민호, 김상민, 서순애
*Seungjun. Kim, Tae Kwang. Kim, So Myeong. Shin, hyewon. Du, Da hye. Kim, Hyung Jun. Koo, SeonYeong. Kim, Min ho. Song, SANGMIN. KIM, sunae. seo
세종대학교.

Keyword : TMD, MoS_2 , 2-D semiconductor, passivation,

Two-dimensional transition metal dichalcogenides (TMDs), in particular, molybdenum disulfide (MoS_2), have attracted considerable attention due to unique structure and remarkable properties. MoS2 combined with high mobility and semiconducting band gap of 1.3~1.8 eV range, offers an attractive possibility of using field-effect transistor (FET). However, electronic mobility of mechanically exfoliated MoS_2 on SiO_2 did not reach the expectation, in particular for mono- or bi-layer MoS_2. The lower than expected mobility is partially due to the charge disorder caused by chemical bonding or roughness at the interfaces as well as optical phonon scattering. Also, electron transport in n-type MoS_2 transistor is strongly affected by extrinsic effects, such as absorption of H_2O and O_2 from the environment. In this work, we investigated the passivation effect of high-k oxide layer in order to prevent the adsorption of H_2O and O_2 and obtain improve carrier mobility. However, due to the active channel around 5 layers, transport property showed thickness dependent passivation effect, less considerable with thickness. Along with passivation effect, additional oxide layer enhances contact resistance and modulate device parameters in subthreshold regime by influencing Schottky barrier existed between source/drain electrode and MoS_2.

P1-Co.206

Terahertz study of topological insulator Bi_2Te_3 nanowires

*김종현, 박병철 [1], 한날애, 김하영 [2], 김성진 [2], 유경화, 김재훈
*Jong Hyeon. Kim, Byung Cheol. Park[1], Nal ae. Han, Ha-Yeong. Kim[2], Sung-Jin. Kim[2], Kyung-Hwa. YOO, Jae Hoon. KIM
연세대학교. [1]Max Planck Institute for Polymer Research. [2] 이화여자대학교.

Keyword : Topological insulator, Bi2Te3, nanowire, terahertz time-domain spectroscopy, topological surface state

We studied the aging effect of topological insulator Bi_2Te_3 nonowires via terahertz time-domain transmission spectroscopy. We measured the optical conductance G of Bi_2Te_3 nanowires after milling and then after aging. The DC conductance G_0 decreased from around 50 to 1 after aging and increased from 1 to around 20 after milling in units of the fundamental conductance quantum. We verified that the topological surface state of Bi_2Te_3 nanowires vanished as a result of aging but reappears after milling.

P1-Co.207*

Tunable n-Doping of Multilayer WS_2 field effect transistor by Lithium Fluoride

Hafiz M W Khalil, M Farooq Khan, 엄종화, *노화용
Hafiz M W. Khalil, M Farooq. Khan, Jonghwa. Eom, *Hwayong. Noh
Sejong University.

Keyword : WS_2, doping, FET, contact resistance

Tungsten disulfide (WS_2) has recently emerged as a promising two-dimensional semiconducting material for nanoelectronics and optoelectronics devices. Here we investigate the effect of chemical doping on contact resistance and electrical properties. After doping with Lithium fluoride (LiF), WS_2 FET shows an enhanced carrier mobility and photocurrent response. The threshold voltage of ML-WS_2 FETs shifted towards more negative voltage and the positions of E^1_{2g} and A_{1g} peaks in Raman spectra also shifted to lower wavenumbers, indicating the n-type doping effect. The transfer length method (TLM) has been used to extract the contact resistance (R_c). After doping, the R_c of multilayer (ML) WS_2 has been reduced to 0.9 kΩ·μm. The significant reduction of the R_c is mainly due to the high electron doping density, thus a reduction in schottky barrier height, which limits the device performance. The potential of using LiF doping in contact engineering of TMDCs open new ways to enhance the performance of WS_2 FET.

P1-Co.208

Ab initio Study of Atom-passivated Au(111)-MoS_2 Interfaces

Kyung-Ah Min, Kyeongjae Cho[1], Suklyun Hong
Kyung-Ah. Min, Kyeongjae. Cho[1], Suklyun. Hong
Sejong University. [1]The University of Texas at Dallas.

Keyword : MoS_2, Fermi level pinning, First-principles calculation

Monolayer molybdenum disulfide (MoS_2) is a semiconducting material with direct band gap of ~1.8 eV [1]. Such a monolayer MoS_2 has drawn much attention for application in electronic devices such as field effect transistors (FETs). In this connection, the Fermi level (FL) pinning, which occurs at metal-semiconductor interface, was very recently investigated at metal-MoS_2 interface [2]. However, for application of MoS_2 in FETs, it is very important to reduce the FL pinning.
In this study, we investigate the atomic and electronic structure of atom-passivated Au(111)-MoS_2 interfaces using first-principles calculations. For reduction of the FL pinning at Au(111)-MoS_2 interface, we consider H, N, O, F and S atoms that can passivate the surface of Au(111). Our calculations show that FL pinning is reduced by passivating atoms on Au(111) with modification of metal work function. Details are analyzed by work function, partial density of states (PDOS) and charge density difference.

[1] Kin Fai Mak, Changgu Lee, James Hone, Jie Shan, and Tony F. Heinz, Phys. Rev. Lett. 105, 136805 (2010).
[2] Cheng Gong, Luigi Colombo, Robert M. Wallace, and Kyeongjae Cho, Nano Lett. 14, 1714 (2014).

Corresponding author: hong@sejong.ac.kr

P1-Co.209*

Search for Andreev Reflection of Graphene in Quantum-Hall Regime

*박건형, 이길호 [1], 김민수, 신윤석 [2], Takashi Taniguchi[3], Kenji Watanabe[3], 이후종
*Geon-Hyoung. Park, Gil-Ho. Lee[1], Minsoo. Kim, Yun Sok. Shin[2], Takashi. Taniguchi[3], Kenji. Watanabe[3], Hu-Jong. LEE
포항공과대학교. [1]Harvard University. [2]Korea University Sejong Campus. [3]National Insititue for Materials Science.

Keyword : graphene, Andreev reflection, quantum Hall effect

Andreev reflection (AR), the retro-reflection of an incident electron as a hole at the superconductor (S)-normal metal (N) junction, gives rise to the formation of Andreev edge state, which consists of a coherent pair of an electron and a hole in strong magnetic field [1]. Up to now the experimental proofs of co-existence of AR and quantum-Hall effect in two-dimensional electron systems has been studied in several ways. Since the recent progresses on the fabrication methods allow graphene (G) to be noble candidate for hybrid devices, we contacted niobium (Nb) electrodes at the edges of hexagonal boron nitride (BN)-G-BN stack [2] and their electrical transport properties were examined. We found that the normalized differential conductance (1.5 K/4.4 K) exhibited ~6 % of maximal enhancement close to the quantum-Hall plateaus. Inclusion of the contact resistance in the two-terminal measurement may have reduced the effect of proximity-induced conductance enhancement. To examine the Andreev edge state in the quantum-Hall regime in more conclusive manner, a study is under way employing BN-encapsulated bilayer graphene Hall-bar devices with local dual gates, which enables opening the band gap at the Dirac point in the region of graphene where the superconducting proximity effect is introduced to the graphene sheet. In this manner, we expect that the superconducting proximity effect can be clearly separated from the quantum-Hall conductance as the proximity effect is modulated by the progressive opening of the band gap without any change in temperature or magnetic field to suppress the superconducting proximity effect.

[1] H. Hoppe et al., PRL, 84, 1804 (2000).
[2] L. Wang et al., Science, 342, 614 (2013).

P1-Co.210

Temperature-dependent Structure of Thiophene Multilayers on Si(100)

Jinwoo Park, Han-Koo Lee[1], Aloysius Soon[2], B. D. Yu[3], Suklyun Hong
Jinwoo. Park, Han-Koo. Lee[1], Aloysius. Soon[2], Byung Deok. Yu[3], Suklyun. Hong
Sejong University. [1]Pohang Accelerator Laboratory. [2]Yonsei University. [3]University of Seoul.

Keyword : Thiophene, NEXAFS, DFT

We have studied multilayer structures of thiophene molecules on the Si(100)-2x1 surface at 170 K and its evolution upon annealing by using near-edge X-ray absorption fine structure (NEXAFS) measurement and ab initio calculations. NEXAFS spectra show that thiophene molecules are predominantly physisorbed on Si(100)-2x1 for multilayer films with an upright molecular orientation at 170 K, while the molecules are chemisorbed on Si(100)-2x1 for monolayer in a flat lying position at 240 K. Especially, thiophene molecules are chemically adsorbed on Si(100)-2x1 through the formation of 2,5-dihydrothiophene structure. For analysis of adsorption behaviors of thiophene multilayer structures depending on temperature, we investigate their structural evolution and energetics using ab initio calculations. It is found that the intermediate flat lying phase is favorable for monolayer coverage, while film formation of molecules perpendicular to Si(100) is favored for multilayer coverage.

Corresponding author: hong@sejong.ac.kr

P1-Co.211

D peak evolution of graphene by ion beam irradiation.

*여순목, 이동수 [1], 배수강 [1], 한지윤 [1], 오예린 [1], 한지윤 [1]
*Sunmog. YEO, Dong Su. Lee[1], Sukang. Bae[1], Jiyoon. Han[1], Yelin. Oh[1], Jiyoon. Han[1]
한국원자력연구원. [1]KIST.

Keyword : Graphene, Ion Beam irradiation, Raman spectroscopy

We investigate D peak evolution via Raman spectroscopy by means of various ion beam irradiation such as H, N. Ar. The D peak intensity is systematically increased by increasing ion beam dose. The ion size and irradiation energy are important factors to evolve the intensity of D peak. It is natural that the smaller ion size makes the smaller evolution of D peak. In addition, the higher irradiation energy affects the smaller evolution of D peak. We discuss the physical meaning of D peak evolution in Raman spectroscopy.

P1-Co.212*

Anomalous current-phase relation of Josephson coupling via surface channels of a 3D topological insulator

*이재형, 이길호 [1], 고병우, 김준성, 이후종
*Jae Hyeong. Lee, Gil-Ho. Lee[1], Byung Woo. Kho, Jun Sung. Kim, Hu-Jong. Lee
포항공과대학교. [1]Harvard University.

Keyword : "Current-phase relation of Josephson junctions", "TI Josephson junction", "topological insulator (TI)"

In this talk, we report the preliminary measurement results of the current-phase relation (CPR) in a Josephson junction prepared on the surface of a $Bi_{1.5}Sb_{0.5}Te_{1.7}Se_{1.3}$ (BSTS) topological insulator (TI) flake [1], known as three-dimensional topological insulator (3D TI). We form a SQUID by putting the TI Josephson junction and an Al tunnel junction in an s-wave Al superconducting ring. 3D TIs are characterized by the presence of an inverted band gap in their bulk state and a gapless Dirac band structure for their surface state, which induce a topologically robust surface conducting channels. Recently, many experimental schemes have been proposed in search of Majorana fermionic excitations [2] at an interface between an s-wave superconductor (S) and a TI, where the spinless p_x+ip_y superconductivity is predicted to emerge. In general, a conventional tunneling Josephson junction has a 2π sinusoidal CPR. But a S-TI-S Josephson junction is predicted to have a 4π-periodic CPR or skewed oscillation resulting from Josephson coupling via the Majorana bound states [3]. In our measurements we obtained a 2π-periodic and skewed CPR. We will discuss the possible scenario for the observed results.

[1] J. Lee, "Local and nonlocal Fraunhofer-like pattern from an edge-stepped topological surface Josephson current distribution", Nano Lett. 14, 5029 (2014).
[2] L. Fu and C. L. Kane, "Superconducting proximity effect and Majorana fermions at the surface of a topological insulator", Phys. Rev. Lett. 100, 096407 (2008).
[3] C. T. Olund and E. Zhao, "Current-phase relation for Josephson effect through helical metal", Phys. Rev. B 86, 214515 (2012).

P1-Co.213*

Raman mapping of graphene domains

*이태건, F. A. Mas'ud[1], 조현진 [1], 김명종 [1], 노희석
*Taegeon. Lee, Felisita Annisanti. Mas'ud[1], Hyun Jin. Cho[1], Myung Jong. Kim[1], Heesuk. Rho
전북대학교. [1] *한국과학기술연구원.*

Keyword : "Raman scattering", "Graphene", "Domain", "Defect"

높은 공간 분해능의 라만 산란 연구를 통해서 단층 그래핀의 도메인 크기와 결정 방향 및 결함의 관계에 대한 연구를 진행하였다. 화학증기증착 방법을 이용하여 구리 기판 위에 그래핀을 성장 시켜 단층의 다결정 그래핀을 얻었다. 그래핀의 단일 도메인 크기는 기판의 표면 처리 방식에 따라서 변하게 된다. 그래핀에 대한 라만 산란을 통해 G, 2D, D 피크들을 관측하였고 이를 통해 단일 도메인의 크기에 따른 결정 방향 및 결함 분포 변화에 대해서 연구할 수 있었다. G band 의 라만 산란 세기는 결정 방향에 대한 변화가 미미한 반면에 2D band 의 이에 대한 변화는 상대적으로 크게 나타난다. 따라서 2D/G 라만 산란 세기 비율의 변화를 통해서 단일 도메인의 크기에 대한 정보를 관측할 수 있었다. D band 는 그래핀 내 결함에 대한 정보를 제공한다. 특이한 결과로써 D/G 라만 산란 세기 비율을 통해서 단일 도메인의 크기가 클수록 평균적인 결함의 분포가 상대적으로 증가함을 확인할 수 있었다. 이번 연구를 통해서 구리 기판의 표면 처리 변화에 따라서 도메인의 크기가 변화되며 이에 따라 그래핀 내의 결함 분포가 변화함을 확인할 수 있었다. 이 논문은 2014 년도 정부(교육부)의 재원으로 한국연구재단(과제번호: 2014R1A1A2057173), 미래창조과학부(과제번호: 2014M3C1A8054009), 산업통상자원부(과제번호: 10044366), KIST 기관고유 사업의 지원을 받아 수행되었음.

P1-Co.214*

PMMA 기판 위의 탄소나노튜브에 대한 이온 조사 효과

*임웅빈, 박지용, 이순일, 안영환, 정희성, 박세준
*Yim Woong bin. , Ji-Yong. Park, LEE Soonil. , Yeong Hwan Ahn. , Huiseong Jeong. , Park Sae june.
아주대학교.

Keyword : CNT, PMMA, nanostructure

이온 조사는 일반적으로 물질의 표면특성을 바꾸기 위해 사용된다. 우리는 PMMA(Poly(methyl methacrylate))기판 위의 단일벽 탄소나노튜브(SWCNT)에 대한 이온 조사 효과를 연구하였다. 이를 위해 SiO2/Si 기판에 열화학기상증착법(Thermal chemical vapor deposition)으로 성장시킨 SWCNT 를 PMMA 를 필름 및 전사매개체로 이용하여 SiO2 층을 BOE(Buffered oxide etch)로 에칭하여 PMMA/SWCNT 를 기판에서 떼어냈다. 떼어낸 PMMA/SWCNT 를 뒤집은 후 Ar 이온을 조사하면 PMMA 와 SWCNT 간에 이온스퍼터링율의 차이로 인해 SWCNT 가 에칭 마스크로 작용하여 SWCNT 의 너비와 비슷한 PMMA 나노벽을 형성할 수 있다. 나노벽의 종횡비는 이온 조사의 파워와 시간에 따라 조절 가능하다. 이러한 형성과정을 원자힘현미경, 전자현미경, 전압-전류 측정 및 라만 분광법으로 관찰하였으며, 나노선 및 나노갭에서의 응용가능성을 확인했다.

P1-Co.215

Optical study of CVD graphene

*조영찬, 이종영, 이관형, 김재훈
*young chan. Jo, Jong-Young. Lee, Gwan-Hyoung. Lee, Jae Hoon. KIM
연세대학교.

Keyword : "graphene, spectroscopy, terahertz, optical conductance"

We studied large area monolayer graphene thin films grown by chemical vapor deposition (CVD) on silicon substrates via terahertz time-domain spectroscopy (THz-TDS) and visible-ultraviolet (VUV) spectroscopy. To analyze of the optical conductance of monolayer graphene, we calculated the real part conductance from the measured THz complex transmittance. The universal absorbance () of monolayer graphene (about 0.018) was confirmed from the VUV transmission. We observed that the DC optical conductance of monolayer graphene films are about 25-40G0 ($G_0=e^2/h$) in the spectral range of 0.1-3 THz.

P1-Co.216

Electrical properties of Bi_2Se_3 nanoparticles synthesized by hydrothermal treatment

*최동민, 이철의 [1], 이규원 [1], 김도완 [1]
*Dong Min. Choi, Cheol Eui. LEE[1], Kyu Won. Lee[1], Do wan. Kim[1]
고려대학교 이과대학 물리학과. [1] 고려대학교.

Keyword : topological insulator, Bi_2Se_3

Recently, Bi_2Se_3 has been receiving great attention due to a topologically-protected metallic surface state, where polarized spin current can flow without backscattering. However, at room-temperature, typical transport properties of the bulk overwhelms that of the surface, preventing detection of the metallic surface states. One of the ways to resolve the problem is to increase the surface-to-volume ratio. In this work, we show that the size of the Bi_2Se_3 nanoparticles can be controlled by hydrothermal treatment, and report the transport properties of the nanopaticles studied by the impedance spectroscopic measurements.

P1-Co.217

CdSe 양자점의 표면 상태에 따른 광학적 특성 연구

이민정, 양호순, *홍경수 [1]
Min Jeong. LEE, Ho-Soon. YANG, *Kyong-Soo. Hong[1]
부산대학교. [1] *한국기초과학지원연구원.*

Keyword : CdSe, quantum dot, TCSPC

점차 전자 기기가 초소형화 되어 가고 있는 현재 나노 구조에 대한 연구는 매우 중요해지고 있다. 특히 소자의 소형화에 큰 기여를 할 수 있으며 입자의 크기가 나노 크기가 될수록 벌크상태일 때와는 다른 독특한 특성을 띄게 되어 흥미롭다. 그 중 양자점은 크기에 따라 다른 band gap 을 가져 다른 발광파장을 가지는 특성을 보인다. 크기가 나노미터에 가까워지면 quantum confinement effect 가 일어나 크기가 작아질수록 넓은 band gap 을 가지는 quantum size effect 를 확인할 수 있다. 여기서 quantum confinement effect 는 물체의 크기가 보어 반지름만큼 작아지게 되면 bulk 상태일 때보다 band gap 이 넓어지는 현상을 말한다. 최근 양자점의 이러한 특성을 이용해 양자점 TV 가 나오는 등 실제 산업과도 밀접한 관련을 맺고 있는 만큼 앞으로가 더욱 기대된다.

본 연구는 양자점의 합성조건에 따른 광학적 특성에 중점을 두고 있다. 화학적 콜로이드 방법으로 CdSe 양자점을 얻을 수 있는데 이 때 합성조건에 따라 다른 크기와 표면 상태를 가지는 양자점이 만들어진다. 크기 변화에 주요한 조작변인은 합성온도와 반응시간 등이 있다.

실제 Cd solution 과 Se solution 만으로 합성을 진행하게 되면 매우 순식간에 합성이 진행돼 원하는 크기의 양자점을 얻기 힘들다. 따라서 최대한 Cd solution 과 Se solution 의 반응속도를 늦춰 고른 크기의 양자점을 얻기 위해 두 가지 유기물을 사용하고 있다. 하나는 TOPO (trioctlyphosphine oxide)이며 다른 하나는 HDA(1-hexadecylamine)이다. 이 두 가지 유기물에 따라 양자점의 다른 표면 상태를 가지게 되어 광학적 특성이 다르게 나타나는 것이 확인되었다.

PL (photoluminescence), OD (optical density)를 통해 발광 파장과 흡수파장의 스펙트럼을 측정하였으며 그 메커니즘을 이해하기 위해 TCSPC (time-correlated single-photon counting)를 측정해보았다. 또한 저온이 되면 광학적 특성이 어떻게 달라지는지 측정해 보았다.

P1-Co.218

Influence of metal-oxide supports on dispersion of Pt nanoparticles

*황인희, 정은석, 박창인, 김정란, 김미영 [1], 최재순 [2], 한상욱
*Inhee. Hwang, Eun-Seok. Jeong, Chang-In. Park, Zhelan. Jin, Mi-yeong. Kim[1], jae Soon. Choi[2], Sang Wook. Han
전북대학교. [1]Heesung Catalysts Corp. [2]Oak Ridge National Laboratory.

Keyword : XAFS, Pt, TiO_2

We examined the local structural properties around Pt and Ti atoms in Pt-nanoparticles/TiO_2 incorporated with silica-based supports with and without a H_2O_2 treatment using X-ray absorption fine structure (XAFS) measurements at the Pt L_3 and the Ti K edges. Pt nanoparticles with the size of ~1-4 nm were synthesized on SiO_2 and TiO_2-SiO_2 supports using a solution method with H_2O_2 treatments at each steps to understand H_2O_2 effects. XAFS measurements at Pt L_3 edge demonstrated that Pt nanoparticles on TiO_2-fumed silica were highly dispersed by H_2O_2 treatment and reduction, whereas they on TiO_2-silica gel were slightly aggregated. XAFS at the Ti K edge revealed that H_2O_2 considerably affected local structural properties around Ti atoms on both fumed silica and silica gel. XAFS results suggested that the dispersion of Pt nanoparticles on TiO_2-silica supports was greatly affected by crystal-quality of TiO_2 in the supports.

P1-Co.301

Effect of nitrogen annealing on the crystal structure and magnetic properties of $(Ru_{0.75}Cu_{0.25})(Sr_{1.67}Nd_{0.33})(Nd_{0.6}Tb_{0.6}Ce_{0.8})Cu_2O_{10-\delta}$ compound

*이호근, 엄주원
*Ho Keun. LEE, Ju Won. Um
강원대학교.

Keyword : (Ru,Cu)-1222, structure, neutron diffraction, oxygen vacancy

To search the influence of oxygen content on the structural and magnetic properties of Ru-1222 ruthenates, Two $(Ru_{0.75}Cu_{0.25})(Sr_{1.67}Nd_{0.33})(Nd_{0.6}Tb_{0.6}Ce_{0.8})Cu_2O_{10-\delta}$ samples with different oxygen contents were prepared and studied by using neutron diffraction and magnetization measurements. For the as-prepared sample in O_2 atmosphere, the dc magnetization data measured in an applied field of 20 Oe showed a branching of the zero-field-cooled(ZFC) and field-cooled (FC) curves around 90 K. Annealing the as-prepared sample in N_2 atmosphere at 400 °C increased the magnetic transition temperature. The Rietveld refinements of the neutron diffraction data showed that both samples exhibited the 1222 structure with space group I4/mmm and oxygen vacancies were located on both the O(1) site of the RuO_2 basal plane and the O(4) site of the fluorite-type $(Nd,Ce)O_{2-\delta}$ block. Magnetization data were discussed in connection with the refined structural properties of the sample.

P1-Co.302

Nitrogen flow-rate dependence of Transition Temperatures and Upper Critical Fields for NbN Thin Films

*김동호, 황태종
*Dong Ho. KIM, Tae Jong. Hwang
영남대학교.

Keyword : Niobium nitride thin film, reactive magnetron sputtering, granular superconductivity, nitrogen flow rate

NbN thin films were deposited on thermally oxidized Si substrate at room temperature by using reactive magnetron sputtering in an Ar-N_2 gas mixture. Total sputtering gas pressure was fixed while varying N_2 flow rate from 1.4 sccm to 2.9 sccm. X-ray diffraction pattern analysis revealed dominant NbN(200) orientation in the low N_2 flow rate but emerging of (111) orientation with diminishing (200) orientation at higher flow rate. The nitrogen flow-rate dependence of transition temperature and upper critical field were investigated. Our results are discussed with the polycrystalline nature of NbN thin films

P1-Co.304

Doping effect of NiO magnetic nanoparticles on flux pinning behavior of MgB_2 bulk superconductor

M. Ranot, 장세훈, K. P. Shinde, 강성훈, *정국채
Mahipal. Ranot, S. H.. Jang, Kiran. Shinde, S. H.. Kang, *Kookchae. Chung
Korea Institute of Materials Science.

Keyword : MgB_2, magnetic nano-particles, flux pinning

Pinning of magnetic flux lines is an essential requirement for any superconductor to carry high critical currents at high temperatures and in high magnetic fields for various practical applications. Pinning of flux lines can be achieved by introducing pinning centers of different nature, concentration, distribution and geometry. In this work, magnetic nanoparticles of NiO (mean particle size < 50 nm) were used as a dopant for MgB_2 to introduce magnetic impurities. Magnetic impurities usually have a stronger interaction with magnetic flux line than nonmagnetic impurities and may exert a stronger force to trap the flux lines if they can be properly introduced into the superconducting matrix. NiO-doped MgB_2 bulk samples were synthesized by the solid-state reaction route. The NiO with 0, 1, 3, 5, and 10 % of MgB_2 was mixed with an appropriate amount of boron and magnesium powders. The mixed samples were palletized under 10 ton pressure using mechanical hydraulic press. The pellets were sintered at 700 ^{o}C for 30 min under flowing Ar atmosphere. The effect of NiO-doping was investigated for all prepared samples. A systematic decrease in the T_c of the samples was found with the increase of doping level. At 5 K and low fields, enhancement in the critical current density (J_c) was observed for NiO-doped MgB_2 samples, whereas a cross-over in J_c with undoped-MgB_2 sample was noticed at high fields. The effect of NiO-doping on crystal structure, surface morphologies and superconducting properties [T_c, J_c(H), flux-pinning (F_p)] of MgB_2 will be discussed in detail.

P1-Co.305

Vortex states in Extended - s-wave superconductor by Simulated Annealing Method.

*정현희, 김남미, 김희상
*Hyun Hee. CHUNG, Nammee. Kim, Heesang. Kim
숭실대학교.

Keyword : supersonductor, vortex, Ginzburg-Landau equation, simulating annealing

Simulated annealing 이용하여 Ginzburg-Landau energy 최소화하는 방법으로 extended s-wave 초전도체에서의 vortex 구조를 연구한다. extended s-wave 의 구체적인 예로 nonmagnetic borocarbide 초전도체의 order parameter 로 관심을 가졌던 s+g wave 에 weighting factor 를 도입하여 s-wave g-wave 로 변해가는 과정에서 vortex 의 구조가 어떻게 변하는지 연구한다.

P1-Co.306*

Synthesis and Thermal Annealing Effects on Superconductivity of $Ca_{0.8}La_{0.2}Fe_2As_2$

*신수현, 정순길, 박두선
*Soohyeon. Shin, Soon-Gil. Jung, Tuson. Park
성균관대학교.

Keyword : "La doped $CaFe_2As_2$", "Thermal annealing effects", "Superconductivity"

Single crystals of $CaFe_2As_2$ (Ca122) form in a $ThCr_2Si_2$-type (I4/mmm) tetragonal structure and undergo an orthorhombic structural as well as a spin density wave (SDW) phase transition at 170K. Chemical substation of La for Ca suppresses both structure transition and magnetic ordering, but increases superconducting phase transition up to 43K with 20% La-doping concentration. The origin of this unusual high T_c superconducting phase is still unresolved. One of the candidate explanations is the effect of chemical interfaces[1] that form a boundary between two different inhomogeneous phases. In order to clarify the role of chemical interfaces in producing the high-T_c superconducting phase in 20% La doped Ca122, we synthesized $Ca_{0.8}La_{0.2}Fe_2As_2$ by using FeAs self-flux method. X-ray diffraction and energy dispersive X-ray spectroscopy confirmed the single phase and doping concentration of the $Ca_{0.8}La_{0.2}Fe_2As_2$ within their experimental resolution. Thermal annealing was performed in the excess arsenic environments at 500, 600, 700, 800°C for 4hours, respectively. In this presentation, we report the effects of thermal annealing on superconducting properties, which were probed by electrical resistivity, AC and DC magnetization measurements.

P1-Co.307*

Study on thermal annealing effects via electrical resistivity of $Ba(Fe_{1-x}Co_x)_2As_2$ single crystals under pressure

*신동원, 서순범, 최기영 [1], 김기훈 [1], 박두선
*Dongwon. Shin, Soonbeom. Seo, KI YOUNG. CHOI[1], Kee Hoon. Kim[1], Tuson. Park
성균관대학교. [1] *서울대학교.*

Keyword : Superconductivity, Annealing, Co doped BaFe2As2, Non-Fermi liquid (NFL) behavior

Superconducting transition temperature (T_c) of the Co doped $BaFe_2As_2$ (Co-Ba122) can be controlled either by applied external pressure or chemical doping. Recently it was reported that thermal annealing can significantly enhance not only T_c but also other physical properties in the underdoped Co-Ba122. However, the underlying origin of the thermal annealing effect has yet to be clarified whose understanding may play a crucial role to elucidate the SC pairing mechanism. To our knowledge the combined effects of annealing and pressure have not been reported. We have performed the temperature and pressure dependence of the electrical resistivity of the as-grown and annealed Co-doped Ba122 single crystals, respectively. In this presentation, we comparatively report the comprehensive temperature-pressure phase diagram and non-Fermi liquid behavior (NFL) in normal state for the as-grown and annealed single crystals.

P1-Co.308*

Synthesis of the Ni-doped ternary compound $Ba(Fe_{1-x}Ni_x)_2Se_3$

*박현범, 신수현 [1], 박두선 [1]
*Hyeon Beom. Park, Soo Hyeon. Shin[1], Tuson. Park[1]
성균관대 양자물질 초전도 연구소. [1] 성균관대학교.

Keyword : Fe-based material, Nickel doped $BaFe_2Se_3$, superconductivity

Fe-based superconductors have attracted great interest partly because it has high superconducting transition temperature. The recently discovered $BaFe_2Se_3$ is not superconducting, but shows an insulating behavior. A possibility of superconductivity was raised for Cobalt-doped $BaFe_2Se_3$, where the band gap decreases with increasing Co concentration[1]. In this presentation, we report synthesis of the nickel doped $BaFe_2Se_3$ by using flux method. X-ray diffraction (XRD) data of $Ba(Fe_xNi_{1-x})_2Se_3$ shows a gradual shift in the diffraction peaks due to the decrease in the unit cell volume from x = 0 to x = 0.1. Temperature dependence of magnetic susceptibility as well as the electrical resistivity for different Ni concentrations will be discussed.

[1] Fei Du et al, " Doping- and pressure-induced change of electrical and magnetic properties in the Fe-based spin-ladder compound BaFe2Se3", PRB 90, 085143 (2014)

P1-Co.309*

Heat capacity study on the pressure-induced superconductor CrAs

*김성일, 박두선
*Sung il. Kim, Tuson. Park
성균관대학교.

Keyword : "Quantum critical point", "transition metal", "unconventional superconductivity"

Heavy fermion compounds, high-Tc cuprate and iron-pnictide superconductors, which show unconventional superconductivity, commonly exhibit a superconductivity dome in the vicinity of a long-range ordered state. CrAs belongs to the family of transition metal pnictides, where Cr moments are anti-aligned below 265 K. Superconductivity appears at a critical pressure when the first order antiferromagnetic (AFM) transition temperature TN is suppressed to zero Kelvin, indicating a close relationship between the AFM quantum critical point (QCP) and superconducting state. Here we report heat capacity and electrical resistivity of CrAs under pressure. Temperature dependence of the specific heat and electrical resistivity under magnetic field and pressure will be presented to understand the superconducting phase as well as the normal state behavior.

[1] Wei Wu, “Superconductivity in the vicinity of antiferromagnetic order in CrAs”(2014)
[2] H. Boller, A. Kallel, “First doere crystallographic and magnetic phase transition in CrAs”(1971)

P1-Co.310*

Construction of Tunnel Diode Oscillator setup and its application to the London penetration depth.

*신동우, O. E. Ayala-Valenzuela, 염한웅, 김지훈
*Dongwoo. Shin, Oscar Ayala. Valenzuela, Han Woong. YEOM, Jeehoon. Kim
포항공과대학교/기초과학연구원.

Keyword : "TDO", "London penetration depth", "pairing symmetry", "superfluid density"

London penetration depth λ is one of the most important intrinsic parameters in superconductivity. Its temperature dependence is related to a superfluid density and superconducting pairing symmetry.
So far, a variety of experimental techniques have been employed to measure the absolute value of λ and its temperature dependence. The tunnel diode oscillator (TDO) technique is the most sensitive one among them to obtain the temperature dependence of λ. Here, we present home-built TDO and its preliminary results obtained from the Niobium and Ca10(Pt4As8)[(Fe1−xPtx)2As2]5 (10-4-8). Our TDO operates in the temperature range of 4 K ~ 300 K and the magnetic field of up to 9 tesla inside a cryogen free magnet system. The temperature dependent λ values measured from Niobium and 10-4-8 show s-wave pairing symmetry and multiband superconductivity, respectively.

P1-Co.311*

저역통과 금속분말 필터의 제작 및 감쇄특성 연구

*이성훈, 이순걸
*Lee Sung Hoon. , LEE Soon-Gul.
고려대학교 세종캠퍼스.

Keyword : 저역통과필터, Stainless steel 304L powder, 벡터회로망분석기

필터의 길이와 모양, 제작 방법에 따른 저역통과 금속분말 필터의 감쇄 특성을 스펙트럼분석기와 벡터회로망분석기를 사용하여 20GHz 까지 측정하였다. 금속분말은 상대적으로 비저항이 큰 SUS 304L 분말를 사용하였고, 저온에서의 열전도성을 향상시키기 위하여 저온에폭시 (stycast 2850FT+23LV) 를 혼합하여 제작하였다. 필터는 지름 0.1 mm 절연 구리선을 원기둥과 타원형 솔레노이드 그리고 토로이드 모양으로 코일을 감아 제작하였다. 절연 구리선이 필터의 단위길이당 감긴수와 SUS 304L 분말·에폭시 혼합물에 닿는 표면적에 따른 특성을 조사하였다. 제작된 필터들의 감쇄특성은 일정한 경향성을 나타내었으며, 토로이드 코일 필터에서 공진에 의한 노이즈가 두르러지게 관측되었다. SUS 304L 분말·에폭시 혼합물의 비율이 1:1(무게비)이고 구리선의 길이가 1,533 mm 인 필터는 4 GHz 에서 -93 dB 이하의 값을 보였고, 와이어의 길이에 비례하여 필터 감쇄특성이 증가하였다. 또한, 절연 구리선이 SUS 304L 분말·에폭시 혼합물에 닿는 표면적이 2 배 증가함에 따라 1GHz 에서 -10dB 이상 향상된 감쇄특성을 보였다. SUS 분말 100%로 제작한 필터는 0.3 GHz 에서 -40 dB 이하가 되었으며, 1.4GHz 에서 noise floor 에 도달하는 확연히 향상된 감쇄특성이 관측 되었다.

P1-Co.312*

Study on Hall coefficient in the electron doped heavy fermion superconductor $CeCoIn_{5-x}Sn_x$ (x = 0 ~ 0.18)

*김지현, 정순길, 이상연, 박두선
*Jihyun. Kim, Soon-Gil. Jung, SANG YUN. LEE, Tuson. Park
성균관대학교.

Keyword : Heavy fermion, unconventional Superconductivity, CeCoIn5, Hall effect

Heavy fermion (HF) compounds belong to the class of unconventional superconducting (SC) materials. CeCoIn5 is a prototypical HF superconductor, which has the highest superconducting transition temperature (Tc = 2.3 K) among the HF SCs. Measurements of the Hall coefficient in the non-doped CeCoIn5 revealed that non-Fermi liquid properties appear below the Kondo coherence temperature, where the electrical resistivity shows a maximum [1]. At low enough temperatures, however, a Fermi liquid state was restored and ascribed to the vanishing of the anisotropic spin fluctuations. Sn doping to CeCoIn5 is expected to increase the hybridization between Ce 4f and itinerant electrons, therefore providing a knob to tune the spin fluctuations in CeCoIn5. In order to probe the evolution of the spin fluctuations under Sn doping and their relationship with unconventional superconductivity, we synthesized CeCoIn5-xSnx with x=0 to 0.18. In this presentation, we will discuss the synthesis as well as Hall measurements on the Sn-doped CeCoIn5.

[1] Y. Nakajima et al., J. Phys. Soc. Jpn. 75, 023705 (2006).

P1-Co.313

Superconductivity in Y_2C_3 : role of C-C dumbbell

정명철, *이관우 [1]
Myung-Chul. Jung, *Kwan Woo. Lee[1]
대학원 응용물리학과/고려대학교 세종캠퍼스. [1] *고려대학교 세종캠퍼스.*

Keyword : Y_2C_3, superconductivity, C-C dumbbell, ab initio calculations, phonon dispersion

In 1960's, rare-earth sesquicarbide superconductors R_2C_3, containing the C-C dumbbells, were discovered. In 2000's, Amano and Coworkers were synthesized Y_2C_3 with T_c~18 K.[1] This system has a body-centered cubic structure with the 12 C-C dumbbells (3-Dimensional bonding direction). Recently, Kuroiwa et al. suggested a double gap superconducting property in this compound, using muon-spin measurement.[2] Besides, its 2-dimensional version AC_2 (A=Y and La) compounds show superconductivity around 4K and 2K, respectively. In spite of many researches, the mechanism of these C-C dumbbell superconductivity is still unclear..
Since no full phonon data are available in the system, we carried out full phonon calculations to understand the superconductivity Y_2C_3 and compared with the 2-dimensional sister compounds AC_2. We will discuss on the role of C-C vibrating mode in these superconductors.

Acknowledgements: This research was supported by NRF-2013R1A1A2A10008946.

[1] G. Amano et al., J. Phys. Soc. Jpn. 73, 530 (2004).
[2] S. Kuroiwa et al., Phys. Rev. Lett. 100, 097002 (2008).

P1-Co.314

Pressure-induced phase diagram in $FeSe_{1-x}$

*김지혜, 조연정, 서동필, 오명준, 옥종목 [1], 김준성 [1], 강원 [2]
*Ji Hye. Kim, Youn Jung. Jo, dongpil. Seo, Myeongjun. Oh, JongMok. Ok[1], Jun Sung. Kim[1], Woun. KANG[2]
경북대학교. [1] *포항공과대학교.* [2] *이화여자대학교.*

Keyword : Fe-based superconductor, Activation energy

Iron selenide is the simplest crystal among Fe-based superconductors and has the interesting feature that its critical temperature(T_c) increases up to 36.7 K under the pressure. Superconductivity of $FeSe_{1-x}$ has close relation to its crystal structure parameter such as lattice constant and Se height from Fe plane. Therefore, clarifying the interplay between them is regarded as a key factor to describe superconducting mechanism of $FeSe_{1-x}$. We established the pressure induced phase diagram of a high quality $FeSe_{1-x}$ from the ambient pressure to 3 GPa. In this pressure range, a local maximum and minimum of T_c are found where the competition between superconducting state and magnetism exists. Remarkably, an anomaly of temperature(T_x) is shown up just above the local maximum temperature. Compared with previous muon spin resonance(μSR) and nuclear magnetic resonance(NMR) experiments, an antiferromagnetic transition takes place below T_x.

P1-Co.315

The various local magnetic superconducting properties of stirated GdBCO coated conductors by using Low Temperature Scanning Hall Probe Microscopy

*김찬, 김무용, 박희연, 이형철
*Chan. Kim, Mu Yong. Kim, Hee yeon. Park, H.-C.. RI
경북대학교.

Keyword : Coated superconductor , Local magnetization , Local hysteresis loss , Local magnetic relaxation

Various local superconducting magnetic properties of GdBCO coated conductors were measured by using Low Temperature Scanning Hall Probe Microscopy. We obtained local current densities in the superconductor from the measured local magnetization by the inversion calculation. We investigated the distribution of local hysteresis losses and local relaxation rates. According to the critical state model, these two local magnetic properties are strongly correlated to local remanent magnetic fields. In this study, we analyzed our experiment results in terms of modified Bean's model

P1-Co.316

Terahertz Metamaterial of Superconducting NbN Thin Films

*심경익, 장호욱, 조영찬, 김종현, 하태우, Hirotake Yamamori[1], 안종현, 김재훈
*Kyung Ik. Sim, Houk. Jang, young chan. Jo, Jong Hyeon. Kim, Taewoo. Ha, Yamamori. Hirotake[1], Jong-Hyun. Ahn, Jae Hoon. KIM
연세대학교. [1]AIST.

Keyword : "Terahertz","Metamaterial","Superconductor","NbN"

We performed intaglio lithography on NbN thin film (20 nm) grown on Si, and conducted THz time-domain spectroscopy. We studied the low-temperature electrodynamics of DSRR (Double Split Ring Resonator) structure with angle dependence, which exhibited open and closed resonance modes emerging from the low frequency region. The modes yield a quality factor of maximum 30 at 3.8 K. Our results demonstrate that traditional BCS superconductors provide useful frameworks for terahertz metamaterials.

P1-Co.317

Synthesis superconducting BSCCO thin films by Pulsed Laser Deposition

*김두리, 송종현
*DuRi. Kim, Jong Hyun. Song
충남대학교.

Keyword : BSCCO, Superconducting, PLD

We successfully grew superconducting Bi_2 Sr_2 $CaCu_2$ O8 (BSCCO) thin films by using Pulsed Laser Deposition (PLD) technique with post-growth ex situ treatment. To perform experiments, we controlled a number of variables to find the optimum condition to fabricate targets. Targets were made by using a soild state reaction method. Temperature dependence of resistance at the target showed superconducting at 77K. BSCCO thin film grow with the non-superconducting target showed non-superconducting behavior. However these observation indicate that target quality is important to grow superconducting BSCCO thin film. Films were grown on the single crystal MgO (100) substrate. It was maintained at 880˚C in 15min and annealed at 850˚C in 5h in ambient air. X-Ray Diffraction (XRD) patterns were well matching with JCPDS data.

P1-Nu.001*

Prototype Test Results of the COSMUS Detector Array

*김영준, 안정근 [1]
*Young Jun. Kim, Jung Keun. AHN[1]
고려대학교 물리학과 핵 및 고에너지 연구실. [1] *고려대학교.*

Keyword : "low-energy muon"

"Prototype Test Results of the COSMUS Detector Array"

김영준, 정우승, 박재범, 이종원, 안정근

We have been developing the COsmic-ray MUlti-layer Scintillation (COSMUS) detector array for measuring low-energy cosmic-ray muons at Earth surface. The COSMUS is composed of 24 long plastic scintillators, 30 CsI(pure) scintillating crystals, a 0.5 T permanent magnet, and additional trigger counters. Momenta of cosmic muons are reconstructed from time-of-flight and position measurement results. In addition, stopping pions and protons could be identified from energy deposited in CsI scintillators. We will report prototype test results of the COSMUS with special emphasis on timing and position resolutions.

P1-Nu.002

Reanalysis of the $f_0(980)$ structure as $K\bar{K}$ bound state within QCD sum rule

*이희정
*Hee Jung. Lee
충북대학교.

Keyword : "scalar meson" "QCD sum rule" "instanton"

We discuss again if the scalar meson $f_0(980)$ can be understood as a bound state of K and $\bar{K}$ mesons by using the QCD sum rule. From analysis of the QCD sum rule consisting of the contributions from the operator product expansion up to dimension 10 operators and the contributions from the instanton, it looks hard to understand $f_0(980)$ as a bound state of K and $\bar{K}$ mesons.

P1-Nu.003*

Simulation of energy spectrum of a fast ionization chamber using GEANT4

*이재하, 채경육, 김아람, 곽민식, 차수미, 이은지
*Jaeha. Lee, Kyung Yuk. Chae, Aram. KIM, Min sik. Gwak, Soo Mi. Cha, Eun Ji. Lee
성균관대학교.

Keyword : "ionization chamber", "GEANT4", "alpha-energy spectra"

The fast gas-filled ionization chamber developed by Chae et al. in 2012 was tested with an 241Am alpha-emitting radioactive source at the Sungkyunkwan University. The energy spectra obtained from the anode showed, however, somewhat broad peaks than expected especially when no optical component such as a collimator was used. In order to understand this phenomena more precisely, a Monte Carlo simulation was conducted by adopting the GEANT4 framework. The details of the methods employed in the simulation and the results will be presented. The plan for the further considerations by introducing the ion pair mechanism in the simulation will also be discussed.

P1-Nu.004*

X-선 검출기용 광 센서의 성능 확인 실험

*김보배, 강국현, 김태훈, 김홍주, 박환배, 이승철, 전혜빈
*Bobae. Kim, Kang Kook Hyun. , kim tae hun. , KIM Hong Joo. , Park. Hwanbae. , Lee Seung Chul. , Jeon Hyebin.
경북대학교.

Keyword : 실리콘 광 센서, 광 다이오드 센서, CsI(Tl) 섬광체, 방사선 검출, 센서 성능 확인

$CdWO_4$ (CWO) 결정 섬광체와 실리콘 광 센서를 결합한 형태인 X-선 검출기를 현재 개발하고 있다. 본 연구실에서 X-선 검출을 목적으로 실리콘 광 센서를 디자인 및 제작하고, 광 센서의 성능을 측정하였다. 제작된 광 센서로 Am-241 선원의 24.8 keV 와 26.3 keV 의 저에너지 감마, 5.48 MeV 의 알파입자를 검출하여 에너지 분해능을 측정하고, Sr-90 베타선원으로 신호대잡음비를 측정하였다. 또한 CsI(Tl) 섬광체를 광 센서와 결합하여, Am-241 선원의 알파입자, Cs-137 과 Na-22 선원의 감마를 측정하여 에너지 분해능을 측정하였다. 에너지 분해능과 신호대잡음비 측정 결과를 소개하고, 이를 바탕으로 제작한 센서의 성능을 확인한다.

P1-Nu.005*

실리콘 핀 다이오드를 사용한 저에너지 감마선의 에너지에 따른 신호 변환 효율 및 분해능 비교

*이승철, 박환배, 강국현, 김보배, 김태훈, 전혜빈
*Seung Chul. Lee, Park. Hwanbae. , Kang Kook Hyun. , Kim Bobae. , kim tae hun. , Jeon Hyebin.
경북대학교.

Keyword : 저에너지 감마선, 실리콘 핀 다이오드, 에너지 변환 효율, 에너지 분해능

저에너지 감마선의 에너지에 따른 신호 변환 효율 및 분해능을 비교한다. 저에너지 감마선 검출은 핵의학에서 진단, 단층 촬영 등에 주로 사용되며 중력파 연구에도 중요한 역할을 한다. Am241, Ba133, Co57 선원을 사용하여 14.4 keV ~ 136.5 keV 의 다양한 저에너지 감마선을 실리콘 핀 다이오드로 검출하였다. 실리콘 핀 다이오드는 빠른 응답 속도, 높은 신호 생성, 작은 부피 등의 장점을 가지고 있다. 또한, 저에너지 감마선은 고에너지 감마선과 달리 신틸레이터를 사용하지 않아도 검출이 가능하여 좋은 분해능을 보인다. 본 포스터에서는 저에너지 감마선의 에너지에 따른 신호 변환 효율 및 분해능을 발표할 것이다.

P1-Nu.006*

Back-thinning fabrication procedure of the silicon sensor and the detector's properties

*전혜빈, 박환배, 강국현, 김보배, 이승철, 김태훈
*Hyebin. Jeon, Hwanbae. Park, Kookhyun. Kang, Bobae. Kim, Seungcheol. Lee, Taehun. Kim
경북대학교.

Keyword : Thin silicon detector, back-thinning, Si-CsI detector

A thin silicon sensor as a part of Si-CsI detector in RAON accelerator is considered to identify isotopes with low energy. The typical thickness of 6-in silicon wafer is about 600 um, therefore reliable fabrication processes are needed to make a thin silicon sensor. We have developed the photodiode with 180 um thickness by mechanical grinding and a laser annealing methods starting with 650 um-thick silicon wafer. In the procedure, a laser annealing is performed to protect metal patterns on the front side of the photodiode. We present the back-thinning procedures and measurements of electrical characteristics and signal-to-noise ratio before and after the thinning, and the production yield of the thin photodiode.

P1-Nu.007

Optimized NMR Set-up at 217 G for ^{129}Xe Polarizer

*조슈아알뎀단, 선용근, 김우영, 블라디미르카탄욱, 사뮤엘스테판얀, 안도유, 알렉세이글라드코브, 박성우, 소지은
*Joshua Artem. TAN, Yonggeun. SEON, Wooyoung. KIM, Vladimir. KAVTANYUK, Samuel. STEPANYAN, ANDO. Yu, Aleksey. GLADKOV, Seongwoo. PARK, Ji-eun. SO
경북대학교.

Keyword : Polarized ^{129}Xe, Proton-in-water NMR

We present an optimized nuclear magnetic resonance (NMR) set-up for polarization measurement of ^{129}Xe polarized via spin-exchange optical pumping. NMR is observed when the motion of the net magnetic moment of the spins immersed in the static holding field and driven by the oscillating field of resonance frequency generated by the drive coil induces current to the surrounding pick-up coil. We construct the upgraded NMR set-up in response to the poor performance of the previous NMR set-up whose effective holding field's inhomogeneity, >7%, is a stumbling-block in acquiring NMR signal. The new NMR set-up uses a permanent magnet whose 217.3 G effective field is just 0.6% inhomogeneous. New drive and pick-up coils were constructed for higher frequency operations and other new electrical components with better performance were installed to the set-up. The settings of the NMR measurement software essential in acquiring signal of good quality were also optimized. The new set-up was tested through NMR measurements using free induction decay (FID) mode with water sample. Water FID NMR signal was acquired, reproduced, and verified. FID NMR signals acquired with 100 measurement scans from water, in general, had peak magnitude of 134.5×10^3 arbitrary units in the frequency domain.

P1-Nu.008

Growth and characterization of Li_2MoO_4 crystal

*손주경, 김홍주, 천종규 [1]
*Ju-Kyung. Son, Hong Joo. KIM, Jong kyu. Cheon[1]
경북대학교. [1] *서라벌대학.*

Keyword : "AMoRE" , "Crystal" , "Czochralski" , "Li_2MoO_4"

The AMoRE (Advanced Mo-based Rare process Experiment) is searching for neutrinoless double beta decay by using Mo based crystals in the cryogenic system. So, we continually develop the Mo based crystals for AMoRE experiment. In this study, the Li_2MoO_4 crystal is grown successfully by Czochralski method and then check about emission spectrum of laser source from room temperature to 10 K. We also try to grow Li and Mo based new crystal and results will be presented.

P1-Nu.009

Characterization of a $CaMoO_4$ Crystal grown by Low Temperature Gradient Czochralski technique

*이주영, 김홍주, 이무현 [1], 김영덕 [2], V.N. Shlegel[3]
*Jooyoung. Lee, Hong Joo. Kim, Moo Hyun. Lee[1], Yeong Duk. KIM[2], V.N.. Shlegel[3]
경북대학교. [1] 기초과학연구원. [2] 기초과학연구원/세종대학교. [3]Nikolaev Institute of Inorganic Chemistry.

Keyword : Low temperature gradient, Czochralski, CaMoO4, neutrinoless double beta decay, AMoRE

Low temperature gradient Czochralski technique is a new method to complement traditional scintillation crystal growing technique. It has several advantages in growing crystals. It rarely makes thermoelastic stress which could destroy crystal and the diffusion wall in this machine suppressed evaporation and decomposition well. Therefore, we expect a better quality crystal grown by this method than the traditional one. We have studied the luminescence and scintillation properties of $CaMoO_4$ crystal grown by the low temperature gradient Czochralski technique at Nikolaev Institute of Inorganic Chemistry and compare it with crystals grown by the traditional Czochralski method for the AMoRE (Advanced Molybdenum based Rare process Experiment) experiment which is searching for neutrinoless double beta decays of ^{100}Mo in $CaMoO_4$ crystals.

P1-Nu.010

Synthesis of $CaMoO_4$ powder from the purified $(NH_4)_2MoO_4$ solution and Ca $(NO_3)_2$ solution.

*카르키수지타, 김홍주
*SUJITA. KARKI, Hong Joo. Kim
경북대학교.

Keyword : "AMoRE" , "Synthesis" , "Purification" , "Crystal"

The AMoRE (Advanced Mo Based Rare Proces Experiment) collaboration is going to use calcium molybdate CaMoO4 crystals to search for neutrinoless double beta decay of ^{100}Mo. Hence, the CaMoO4 powder is synthesized directly by purifying the low background impurities present in MoO_3 powder in the form of $(NH_4)_2MoO_4$ solution and the $CaCO_3$ powder are purified in the form of $Ca(NO_3)_2$ solution. These, purified solution is mixed together to synthesize the $CaMoO_4$ powder. The synthesized $CaMoO_4$ powder is further used for growing CMO crystal.

P1-Nu.011*

Growth and Scintillation Properties of $Li_2Mg_2(MoO_4)_3$ Crystal

*인드라라즈, 김홍주, 천종규 [1]
*Indra Raj. Pandey, Hong Joo. Kim, Jong kyu. Cheon[1]
경북대학교. [1] *서라벌대학.*

Keyword : "AMoRE" , "Crystal" , "Scintillation " , "$Li_2Mg_2(MoO_4)_3$"

The AMoRE (Advanced Mo Based Rare Process Experiment) collaboration is going to use Mo based crystals to search for neutrino less double beta decay of ^{100}Mo. $Li_2Mg_2(MoO_4)_3$ might be the promising candidate of Molybdenum contained crystal for searching 0ν2β decay due to the absence of intrinsic radioactive isotopes. Synthesis of $Li_2Mg_2(MoO_4)_3$ single crystal was grown successfully by Czochralski technique using flux method. We present the detail procedure and difficulties of the grown process. Luminescence properties of cut and polished crystal were studied under LASER of 260nm source at room and low temperature. Crystal exhibited a broad band emission spectrum between 280nm and 900nm at 50 K.

P1-Nu.012

Measured x-ray spectra at ECR ion source

*박진용, 원미숙 [1], 이병섭 [1], 김성준 [1], 옥정우 [1], 윤장희 [1], 최세용 [1]
*Jin Yong. Park, Mi-Sook. Won[1], Byoung Seob. Lee[1], Sung-Jun. KIM[1], Jung-Woo. Ok[1], Jang-Hee. Yoon[1], Seyong. Choi[1]
한국기초과학지원연구원 (KBSI). [1] 한국기초과학지원연구원.

Keyword : ECR, ECRIS, X-ray,electron cyclotron resonance, superconducting ECR

A large amount of x-rays can be produced from an electron cyclotron resonance (ECR) ion source. It is well known that X-rays that are emitted from the inside of a plasma chamber affect the cryogenic system due to the extra heat load that is produced. Therefore, a knowledge of x-ray spectra provides the information concerning the electron heating process and electron confinement. The measurements of x-ray spectra were carried out using a Cd-Zn-Te detector combined with a collimator in this study. The x-ray emission during 28 GHz superconducting ECR ion source operation at the Korea Basic Science Institute was quantitatively analyzed. The effect of microwave power, injected gas pressure on the x-ray energy was investigated. The findings confirmed that the effectiveness of an x-ray shield is function of the thickness of the lead sheet used.

P1-Nu.013*

HPGe 를 이용한 환경 및 생활방사선 측정을 위한 효율적인 차폐체 연구

*박수연, 김고운, 김아람, 이은경, 허장용, 한인식
*Su-yeon. Park, Gowoon. , Aram. , Eunkyung. , Jangyong. , HAHN Insik.
이화여자대학교.

Keyword : 차폐체, 배경방사선, 생활방사선

일본 후쿠시마에서 발생한 원전 사고로 인위적으로 만들어진 방사능 물질이 유출되었다. 이에 환경 및 생활방사선에 대한 대중들의 불안과 관심이 조성되었고 정확한 환경 및 생활방사선의 측정이 요구되고 있다. 대중의 요구에 맞추어 심층 지하에서 자연에서 쉽게 구할 수 있는 각종 시료에서 방출되는 방사선을 측정하고 오염도를 분석하고자 한다. 현재 청평양수발전소 내에 심층 지하 방사선 연구 센터를 구축 중에 있으며, 방사선 측정에는 주로 HPGe 를 사용할 예정이다. 보다 정확한 방사선량을 측정하기 위해선 우주선과 배경방사선을 차단시킬 필요가 있어 납, 구리, 알루미늄, 주석 등을 이용하여 차폐체를 설치하고자 한다. 본 포스터에서는 GEANT4 를 활용, 다양한 물질, 두께로 시뮬레이션하여 찾은 효율적인 차폐체에 대해 논의하고자 한다.

P1-Nu.014*

External & internal background simulation for AMoRE-pilot experiment

*하대훈, 김홍주, 전은주 [1], 윤영수 [1]
*Daehoon. Ha, Hong Joo. KIM, Eun Ju. Jeon[1], Young Soo. Yoon[1]
경북대학교. [1] 기초과학연구원.

Keyword : AMoRE-Pilot,CMO crystal, Geant4, Simulation

AMoRE(Advanced Mo based Rare process Experiment)-pilot is an experiment to search neutrinoless double beta decay of ^{100}Mo with five $CaMoO_4$ crystals, approximately 1.5 kg in total mass, and is planned to operate at the Yang-yang underground laboratory.
One of goals of this experiment is to achieve a better understanding of internal and external backgrounds and we studied the effect of backgrounds from ^{238}U, ^{232}Th, and ^{40}K at inside crystal, surrounding materials, and shielding materials by simulating with Geant4 toolkit. We also estimated the expected background rates based on measurements. In this poster, background studies by Geant4-based simulation will be presented.

P1-Nu.015

The study on the cascade summing correction for HPGe detector

*김효진, 김현, 노성진, 강영록, 정동혁, 양광모, 노태익 [1], 이만우
*Hyo Jin. Kim, Hyun. Kim, sungjin. NOH, Yeong Rok. Kang, Dong Hyeok. JEONG, kwangmo. Yang, Tae Ik. Ro[1], Manwoo. LEE
동남권원자력의학원. [1] 동아대학교.

Keyword : HPGe-detector, Coincidence summing ,efficiency

Coincidence summing takes place when two or more gamma rays which are emitted in a cascade from an excited nucleus are detected within the resolving time of the detector. This leads to a loss in count from the peaks corresponding to two gamma rays and addition of count at the sum of two energies. This results in inaccurate count rate and hence erroneous results.
In this study, the calibrated sources (^{133}Ba, ^{137}Cs, ^{22}Na, ^{57}Co and ^{60}Co) were used to calculate the efficiency of the HPGe-detector. In order to eliminate the coincidence loss, all sources were individually placed at 20 cm above the surface of the detector, and only ^{137}Cs was placed (emits single gamma peak) on the surface of the detector to obtain the normalizing factor. The normalizing factor was then calculated from the ratio of the efficiencies of ^{137}Cs on the surface of the detector to the 20cm above the surface of the detector.

P1-Nu.016

Fundamental resolution limit studies in high-resolution alpha spectroscopy

*김소라
*So Ra. kim
기초과학연구원.

Keyword : "metallic magnetic calorimeters, alpha spectroscopy , lattice damage"

We report on the development of high-resolution alpha spectrometers and their energy resolution limit. Alpha spectrometers based on metallic magnetic calorimeters (MMCs) achieved a detector resolution better than 1 keV FWHM for 5.5 MeV alpha particles, that is one order of magnitude better than the theoretical limit of semiconductor-based detectors. These MMC-based alpha spectrometers seem to have a resolution limit of 0.9 keV FWHM. On the other hand, the energy resolution measured for baseline and gamma-ray signals seems to follow the signal-to-noise ratio, and do not show a saturation behavior in the measurement conditions. We discuss how this resolution limit was determined with lattice damage effect as a possible origin for the limit in comparison with Monte-Carlo simulations.

P1-Nu.017

핵전자기펄스 전산모사 연구

*가동하
*Dong Ha. Kah
국방과학연구소.

Keyword : 핵전자기펄스, Nuclear EMP

핵폭발은 폭풍충격파, 열복사, 방사능으로 인한 대규모 피해를 유발 할 수 있는 강력한 폭탄이지만, 고고도에서 폭발 시 핵폭발로 인해 발생되는 감마선 등으로 인해 대기가 이온화되며 이 때 생성되는 컴프턴 전자들이 지상으로 운동하면서 지구자기장의 영향으로 강력한 전자기파를 지구에 전파하게 된다. 이 때 전자기파는 펄스형태로 아주 넓은지역에 도달하게 되며, 지상에 강한 전압(전류)가 유도되어 전기전자기기에 심각한 영향을 줄 수 있다. 이로 인하여 국가기간망인 전력망, 통신망 등의 피해가 예측된다. 이러한 핵전자기펄스(핵 EMP)의 피해를 예측하기 핵 EMP 의 발생원리를 기반으로 과학적 모델의 시뮬레이션 프로그램을 개발하였고, 계산시간 단축을 위해서 수치 해석기법을 이용한 시뮬레이션 프로그램을 동시에 개발하였다. 핵 EMP 의 발생원리와 예전 고고도핵실험 결과를 바탕으로 이 두 가지 프로그램을 소개할 것이다.

P1-Nu.018

BHCV Calibration of KOTO experiment

*이건호
*GUNHO. LEE
전북대학교.

Keyword : "KOTO","BHCV","Calibration

- J-PARC E14(KOTO)실험은 K_L->^{0} Decay 관측을 목표로 한다. 우리는 이 Decay 모드를 관측하여 표준모형을 넘어서는 새로운 물리법칙의 존재를 발견할 수 있다. BHCV 는 Beam Hole Charged Veto 의 줄임말로 하전입자 검출을 위해 유기 섬광체로 제작하여 빔라인에 설치 하였다. 2015 년 6 월 빔 데이터를 가지고 뮤온 신호를 이용하여 Energy Calibration 과 Time Calibration 을 분석하고, LED 신호를 이용하여 Beamloading effect, PMT 의 Gain drop 문제를 분석하였다. 이번 발표에서는 Calibration 과 Beamloading effect 의 결과를 말하고 PMT Gain drop 의 문제에 대해서 논의할 것이다.

P1-Nu.019*

Bridgeman growth and characterization of Ce doped Tl_2LiYCl_6 crystals for PET

*장종훈, 김홍주, Gul Rooh[1], 김성환 [2], 기문광 [3], 김헌덕 [3], 우원희 [3]
*JongHun. Jang, Hong Joo. KIM, Gul. Rooh[1], Sunghwan. KIM[2], MoonKwang. KI[3], HeonDuk. KIM[3], WonHee. Woo[3]
경북대학교. [1]Abdul Wali Khan University. [2] 청주대학교. [3]TPS.

Keyword : "Bridgeman","PET","Tl_2LiYCl_6","Scintillation"," Positron Emission Tomography"

We develop Ce doped Tl_2LiYCl_6 single crystals different doping ratio grown by Bridgeman method. The one is pure and others Ce doped with 1%, 2%, 5% and 10% respectively. The crystals were grown at a temperature from 280 °C to 600 °C with the pulling down of 0.5 mm/h. The result of X-ray powder diffraction (XRD) shows that the grown crystals have the tetragonal structure. Crystals shaped cylinder were cut with the dimension of 10 x 5 mm3. The X-ray induced emission spectrum showed a emission band in the wavelength range from 370 to 500 nm. We measured the pulse height spectra and fluorescence decay time with a bi-alkali photomultiplier tube (PMT) using Cs-137 gamma ray source for Ce doped Tl_2LiYCl_6 single crystals.
This study showed that good quality crystals. The scintillation properties of the 1%Ce doped Tl_2LiYCl_6 crystal show that it could be used for Positron Emission Tomography (PET) instead of $Lu_{1.8}Y_{0.2}Si0_5$ (LYSO), Lu_2Si0_5 (LSO) and $Bi_4Ge_30_{12}$ (BGO).

P1-Nu.020

B4C 박막을 이용한 다층 환형 구조의 고효율 중성자 모니터

*임창휘, 문명국 [1], 이수현 [1], 김종열 [1], 박종원, 이정희
*Chang Hwy. Lim, Myung Kook. Moon[1], Suhyun. Lee[1], Jongyul. Kim[1], Jong Won. Park, Jeonghee. Lee
선박해양플랜트연구소. [1] 한국원자력연구원.

Keyword : 중성자 모니터, B-10, 비례계수기, MCNP

He-3 는 높은 반응효율과 안정적인 물질상태, 그리고 가격적 이점으로 인해 중성자 계측을 위한 물질로 가장 흔히 사용되어왔다. 하지만 최근 10 여년동안 다양한 원인으로 인해 He-3 의 공급이 줄어들고 수요가 늘어나게 되었다. 결과적으로 He-3 의 부족현상이 심각하게 발생하여 중성자 계측을 위한 방안으로 He-3 를 대체한 물질을 이용한 검출 방식이 각광을 받게 되었다. 이러한 물질들 중에서 가장 활발히 연구되고 있는 물질은 BF3, B-10, Li-6 이다. 이중 B-10 은 상대적으로 높은 중성자 반응확률과 수급의 원활함 등으로 인해 많은 연구그룹에서 중성자 계측을 위한 대체 물질로 연구가 수행되고 있다. 하지만 B-10 을 이용한 중성자 검출 방법은 중성자와 B-10 이 반응하여 생성되는 2 차 방사선의 짧은 이동거리 때문에 수 um 두께로 얇게 제작되어야 한다. 그러므로 중성자 반응확률을 높이기에는 한계가 있다. 이러한 문제점을 해결하기 위해 다층 구조의 B-10 박막을 이용한 중성자 계측이 수행될 수 있다. 본 연구에서는 기체충진형 비례계수기를 이용한 환형의 다층 구조의 중성자 모니터를 개발하였다. 전방향에서 입사되는 중성자 수집효율을 일정하게 유지할 수 있는 환형구조로 중성자 모니터를 개발함으로써 360 도 중성자 모니터링이 가능하게 하였다. 본 연구에서는 중성자 모니터의 개발과 더불어 개발 전 몬테칼로 전산모사 기법을 이용하는 MCNP 를 이용하여 환형 구조의 다층 중성자 모니터의 개발 가능성을 타진하였다.

ACKNOWLEDGMENT
This research was a part of the project titled “Research on Fundamental Core Technology for Ubiquitous Shipping and Logistics” funded by the Ministry of Oceans and Fisheries (MOF), Korea.

P1-Nu.021

Dirac coupled channel analyses of proton inelastic scattering from ^{40}Ar nucleus

*심숙이, 김문원
*Sugie. SHIM, Moon-Won. KIm
공주대학교.

Keyword : Dirac phynomenology, coupled channel analyses, optical potential model, proton inelastic scattering

0.8 GeV proton inelastic scatterings from ^{40}Ar nucleus are analyzed using an optical potential model in the Dirac coupled channel formalism. A rotational collective model is used to obtain the transition optical potentials for the low lying excited states of the rotational band. The optical potential parameters of a Woods-Saxon shape and the deformation parameters of the excited states are searched phenomenologically to reproduce the experimental differential cross-section data by using the sequential iteration method. The effect of a multistep process is investigated by including the channel coupling between two excited states in addition to the couplings between the ground state and the excited states. The calculated deformation parameters of the excited states are compared with those obtained by using the nonrelativistic calculations. The results of the Dirac coupled channel calculations are found to show pretty good agreements with the experimental data of the ground state and the low-lying excited states. The multistep excitation process via the channel coupling with the second 2^+ state is found to be important for the excitation of the 4^+ state at the inelastic scatterings from the deformed nucleus, ^{40}Ar.

P1-Nu.022

Dirac coupled channel analyses of the high-lying excited states at ^{22}Ne(p,p')

*심숙이, 김문원
*Sugie. SHIM, Moon-Won. KIM
공주대학교.

Keyword : Dirac coupled channel analysis; Optical potential model; Proton inelastic scattering; Collective model.

Dirac phenomenological coupled channel analyses are performed using an optical potential model for the high-lying excited vibrational states at 800 MeV unpolarized proton inelastic scatterings from ^{22}Ne nucleus. Lorentz-covariant scalar and time-like vector potentials are used as direct optical potentials and the first-order vibrational collective model is used for the transition optical potentials to describe the high-lying excited vibrational collective states. The complicated Dirac coupled channel equations are solved phenomenologically using a sequential iteration method by varying the optical potential and the deformation parameters. Relativistic Dirac coupled channel calculations are able to describe the high-lying excited states of the vibrational bands in ^{22}Ne clearly better than the nonrelativistic coupled channel calculations. The channel-coupling effects of the multistep process for the excited states of the vibrational bands are investigated. The deformation parameters obtained from the Dirac phenomenological calculations for the high-lying vibrational excited states in ^{22}Ne are found to agree well with those obtained from the nonrelativistic calculations using the same Woods-Saxon potential shape.

P1-Nu.023

Measurement of Relative Cross-Sections and Gamma Ray Energy Spectrum from ^{Nat}Pb(p,x)Bi Proton Induced Reactions by Using 100 MeV Proton Linear Accelerator at KOMAC

Ji eun Lee, Jungran Yoon, Taeik Ro, Samyol Lee[1]
Ji eun. Lee, Jungran. Yoon, Tae Ik. Ro, Samyol. Lee[1]
Dong-A University. [1]Dongseo University.

Keyword : proton nuclear reaction, 100 MeV proton accelerator, Natural Pb, Relative cross-section

Proton induced nuclear cross-section data in the high energy region are increasing importance for a wide variety of applications : radiation and shielding effects in space, technology development of an accelerator-driven system for transmutation of nuclear waste of energy production. We measured the production relative cross-sections of Bi radioisotopes for proton-induced reactions on natural lead(Pb) by using a stacked-foil activation technique in the energy of 100 MeV at the proton accelerator of the KOMAC. Reactions induced on the relative cross-section by measuring branching ratio reaction of ^{Nat}Pb(p,x)Bi. The gamma ray energy spectrum were measured from the foil sample by using HPGe detector. The new experimental data were compared with the few earlier experimental results and with the analysis of the ENDF/B-VII and EXFOR.

Acknowledgement:
• Regarding this experiment, it was honor to have an opportunity to be offered all of relative stuff, especially the people who let us conduct our successful research in KOMAC.
• This work was supported by Dongseo University, “Dongseo Frontier Project” Research Fund of 2014

P1-Nu.024

Thermal neutron capture cross-section of ^{108}Pd(n,g)^{109}Pd reaction and using MCNPX code at Pohang Neutron Facility for experimental set-up

*김광수, 누엔 티 히엔, 김귀년, 무함마드 샤히드, 무함마드 자만, 무함마드 나딤
*KwangSoo. Kim, Nguyen Thi. Hien, Gui Nyun. KIM, Shahid. Muhammad, Zaman. Muhammad, Nadeem. Muhammad
경북대학교.

Keyword : Neutron, MCNPX code, Pohang Neutron Facility

The measurement of neutron cross-sections directly involves fundamental information for the study of neutron interactions with nuclei. They also give great importance for the safety design of nuclear reactors and for the evaluation of the neutron flux density and energy spectrum around a reactor.
This work focuses on simulation of experimental set-up using MCNPX code for neutron capture reaction at Pohang Neutron Facility. The Pohang Neutron Facility (PNF) based on an electron linac was operated for total neutron cross-section measurements by using the pulsed neutrons produced at a water-cooled Ta-target with a water moderator. By using Monte-Carlo simulation code, the Ta-target system was optimized to achieve the maximum thermal neutron flux.
This work also reports results about thermal neutron capture cross-section of the ^{108}Pd(n,g)^{109}Pd reaction using pulsed neutrons. Thermal neutron capture cross-section of the ^{108}Pd(n,g)^{109}Pd reaction has been measured relative to that of the ^{197}Au(n,g)^{198}Au reaction by activation method. The induced activities in the activated foils were measured by a g-ray spectrometer based on a calibrated high purity germanium (HPGe) detector. The measured results are compared with literature values and Talys code.

P1-Nu.025

Measurements of high energy neutron induced activation cross sections of ^{nat}Ag

*김광수, 무함마드 나딤, 김귀년, 누엔 티 히엔, 무함마드 샤히드, 무함마드 자만
*KwangSoo. Kim, Nadeem. Muhammad, Gui Nyun. KIM, Nguyen Thi. Hien, Shahid. Muhammad, Zaman. Muhammad
경북대학교.

Keyword : ^{nat}Ag, KIRAMS, MCNPX code, Neutron

The neutron induced cross-sections for the ^{nat}Ag(n, x)^{106g,m,105,104g,m}Ag reactions were determined at the Korean Institute of Radiological and Medical Sciences (KIRAMS) in the neutron energy range of 22.50 to 29.10 MeV by an activation and off-line γ-spectrometric technique. The quasi-mono energetic neutron beam was produce from the 9Be(p,xn) reaction with the proton energy of 35 MeV. For a given experimental geometry neutron flux was simulated by MCNPX code. The natAg(n, x)^{106g,m,105,104g,m}Ag reaction cross-sections were also calculated from TALYS 1.6 code and are found to be in good agreement, which shows the validity of the code. It was also found that for the same neutron spectrum, the ^{nat}Ag(n, x)^{106g,m}Ag reaction is higher than the ^{nat}Ag(n, x)^{105}Ag, which in turn higher than the ^{nat}Ag(n, x)^{104g,m}Ag. This is due the increases number of neutron emission from the former to the latter.
It was also studied that cross-sections for isotopes with higher spin have higher cross-section values.

P1-Nu.026

Unbound excited states in ^{17}C

*김선지
*SUNJI. KIM
서울대학교.

Keyword : neutron-rich nucleus, unbound state, ^{17}C, knockout reaction, SAMURAI

Neutron-rich carbon isotopes have attracted attention in recent years due to their anomalous level structures. In particular, the first 2^+ excitation energy of $^{20}C_{14}$, $E_x(2_1^+)$ = 1588(20) keV, was found to be not much different from that of neighboring even-even $^{18}C_{12}$ of 1585(10) keV [1]. This migration of the 2_1^+ energy is distinct from that of oxygen isotopes, where $E_x(2_1^+)$ exhibits a sudden jump at $^{22}O_{14}$, signifying the emergence of the shell gap at the neutron number N = 14 [2]. The breakdown of the N = 14 gap in carbon isotopes has been ascribed to the near degeneracy of the $s_{1/2}$ and $d_{5/2}$ orbits and to the reduced neutron-neutron interaction when going from oxygen to carbon nuclei [1]. Detailed mechanisms and interplay of these effects, however, remain to be answered.

In order to furnish information on energy levels and understand the behavior of p-sd orbits, we performed a spectroscopic study on a neutron-rich odd carbon isotope, ^{17}C, above the neutron threshold. The experiment was performed during the first physics runs of SAMURAI spectrometer [3] at RIKEN-RIBF. Neutron unbound states in ^{17}C were populated via one-neutron knockout reaction from ^{18}C, and the excitation energies of them were reconstructed by the momentum vectors of the ^{16}C fragments and neutrons. Here, we also conducted γ-ray measurements in coincidence with the fragments and neutrons to determine the final states in ^{16}C. In the present work, three unbound states in ^{17}C at the excitation energies of 2.66(2), 3.16(5), and 3.97(3) MeV were observed. The presentation will describe the analysis and results together with spin-parity assignments and possible interpretations.

[1] M. Stanoiu et al., Phys. Rev. C 78, 034315 (2008)
[2] M. Stanoiu et al., Eur. Phys. J. A 20, 95 (2004)
[3] T. Kobayashi et al., Nucl. Instrum. Methods Phys. Res., Sect. B 317, 294 (2013)

P1-Nu.027

Spectroscopy of ^{19}C by one-neutron knockout reaction

*황종원
*Jongwon. Hwang
서울대학교.

Keyword : neutron-rich nuclei, knockout reaction, invariant mass method, shell model

The spectroscopic structure of ^{19}C has been investigated by one-neutron knockout reaction with a ^{20}C beam of 280 MeV/nucleon and carbon target. Three neutron-unbound states were observed in the relative energy spectrum by means of the invariant mass method. Spin and parities of those states were determined by comparing the parallel momentum distributions to the thoretical ones calculated with using the Glauber-model code. The shell-model calculations with different interactions were tested with the experimentally observed low-lying levels of ^{19}C.

P1-Nu.028*

$^{144-154}$Nd 핵에서 외각 핵자수에 따른 핵구조 변화 연구

*이수연, 이영준, 이종환
*LEE Su-youn. , Lee Young-jun. , LEE Jong-hwan.
동의대학교.

Keyword : IBM, Phase transition, Bohr Hamiltonian, Nuclear structure, $^{144-154}$Nd

본 연구는 $^{144-154}$Nd 핵을 구성하는 핵심(core) 외각핵자 쌍인 보오존 수에 따라 핵구조가 어떤 변화를 보이는지를 조사하였다. 질량수 146 인 네오디뮴(neodymium)은 대표적인 회전핵에 속하며 이는 대수적 핵모형인 IBM(interacting boson model)의 SU(3) 대칭을 이용하여 설명할 수 있다. 또한 질량수 148 과 150 인 네오디뮴은 대칭전이경로에 놓여 있는 핵으로 IBM 의 X(5) 대칭을 통해 핵구조의 설명이 가능하다. 이들을 제외한 나머지 네오디뮴 핵은 완전한 대칭핵이 아니므로 대칭깨짐을 나타내는 섭동항을 추가하여 기술할 수 있다.
네오디뮴 핵종 중 질량수가 144 에서 154 사이인 핵의 구조 변화에 관한 경향을 파악하기 위해 다음 세 가지 방법을 통해 계산하였다. 첫 번째로 IBM 의 SU(3) 극한의 기저상태와 전자기전이 연산자를 이용하여 ^{146}Nd 핵의 구조를 나타내었다. 두 번째로 IBM 의 SU(3) 해밀토니안에 U(5)군의 1 차 캐시미르연산자(casimir operator)를 섭동항으로 추가하였고, 이로부터 섭동파동함수를 구성하여 측정가능한 물리량인 에너지 준위와 전자기(M1, E2)전이율을 계산하였다. 이 결과를 ^{144,148,152,154}Nd 핵의 실험데이터와 비교하였다. 마지막으로 ^{148,150}Nd 핵은 보어 해밀토니언의 퍼텐셜을 조화진동자로 표현한 후 근사 변수분리법을 통해 핵의 구조를 닫힌표현으로 기술하여 실험결과와 비교하였다. 최종적으로 본 연구에서 이론적으로 예측한 결과를 바탕으로 네오디뮴의 핵심을 제외한 외각핵자 쌍(보오존)의 수에 따른 핵구조 변화에 관하여 분석하였다.

P1-Nu.029

Measuring low-x gluons in gold nucleus using MPC-EX in PHENIX experiment

*도재현
*Jae hyeon. Do
연세대학교.

Keyword : RHIC, PHENIX, Correlation, MPC, MPC-EX

Proton-Gold collide ran first in 2015 on PHENIX(RHIC) experiment with 200GeV colliding energy.
Heavy nucleus gluon structrure is not simple superposition of each proton or neutrons, its partonic structure distorted by interaction between each nucleon.
RHIC experiments have previously measured suppression of forward rapidity particle production relative to p+p scaled by the number of binary Au-Au collisions.
MPC-EX is located on high rapidity region (3.1<|y|
We will probe saturation effect of heavy nucleus using 2 particle correlation with large rapidity gap which is sensitive to low-x gluon structure and provides insight of saturation effect by comparing same quantity from p-p collision

P1-Nu.031*

Bethe-Heitler formula 를 이용한 전자 쌍 생성 산란단면적 및 전자의 분포 Simulation

*방혜선
*Bang Hye sun.
인하대학교.

Keyword : "쌍 생성, 산란단면적"

특정 물질에 광자가 입사하여 매질을 통과하는 경우 매질과의 상호작용을 통해 에너지를 잃으면서 전자-양전자 쌍(Pair production)을 생성한다. 전자-양전자 쌍 생성 산란단면적(Pair production Differential Cross Section)은 양자역학을 기반으로 얻을 수 있으며 Bethe-Heitler 공식에 의해 기술된다. 본 연구에서는 Bethe-Heitler formula 를 C++을 기반으로 한 프로그램을 이용하여 주어진 광자의 에너지로부터 생성되는 전자의 산란단면적을 구하려고 한다. 그리고 Tsai 공식을 이용하여 전자의 각 분포를 구해 전자의 운동학적 변수(kinematic variable)인 전자의 산란각도, 횡방향 운동량을 알아내려고 한다. 이를 통하여 전자와 상호작용을 일으키는 충돌 지점간의 최단거리를 구할 수 있고 이론으로 구한 값과 GEANT4 의 Simulation 결과 값을 비교해봄으로써 타당한 실험인지를 알 수 있다.

P1-Pa.001*

Time-periodic solutions of pure AdS5 and cancellation of secular terms

*김낙우, 김세진
*Nakwoo. Kim, Sejin. Kim
경희대학교.

Keyword : AdS, secular terms, instability

We construct time-dependent solutions perturbatively in AdS5 pure gravity system, and also illustrate cancellation of certain secular terms up to quartic order in perturbative expansion.

P1-Pa.002*

Scaling symmetry and scalar hairy rotating AdS_3 black holes

*안병준, 현승준, 이상헌, 박상아
*Byoungjoon. Ahn, Seungjoon. Hyun, Sang Heon. Yi, Sang-A. Park
연세대학교.

Keyword : scaling symmetry, hairy black holes, Smarr relation, thermodynamic stability

By using the scaling symmetry in the reduced action formalism, we derive the novel Smarr relation which holds even for the hairy rotating AdS_3 black holes. And then, by using the Smarr relation we argue that the hairy rotating AdS_3 black holes are stable thermodynamically, compared to the non-hairy ones.

P1-Pa.003*

Wire bonding study and quality assurance for the "Origami" modules of the Belle II Silicon Vertex Detector.

*강국현, 전혜빈, 김보배, 김홍주, 김태훈, 이승철, 박환배
*Kook Hyun. Kang, Hyebin. Jeon, Bobae. Kim, Hong Joo. KIM, tae hun. kim, Seung Chul. Lee, Hwanbae. Park
경북대학교.

Keyword : Belle II, Silicon Detector, Vertex Detector, Tracker, Wire Bonding

The silicon vertex detector (SVD) for the Belle-II experiment has been developed to improve the precision of vertexing and tracking under high luminosity environment of Super-KEKB in Japan. One of the key concepts of SVD is chip-on-sensor, called "Origami", to minimize material budget and capacitive noise (important for a good signal-to-noise ratio). This poster describes the wire-bonding procedures for four different bonding points on the "Origami" module toelectrically connect between the sensor and the read-out chip. The wire bonding performance depends on the gluing quality of "Origami" module and on the bonding parameters. It is represented by the pull force, the bonding efficiency and the break types occurring measurement of pull force. The bonding parameters are optimized to satisfy requirements of quality assurance on the above four bonding points where at least 30 wires each are bonded to guarantee enough statistics.

P1-Pa.004*

Canted-Pole 교번자장기를 이용한 테라헤르츠 자유전자레이저 개발

*배상윤, 문정호, 김현우 [1], 박선정 [2], 장규하 [3], 이기태 [3], 박성희 [3], 전민용 [4], Nicolay A. Vinokurov[3], 정영욱 [3]
*Sangyoon. Bae, Jung Ho. Mun, Hyun Woo. Kim[1], Sun jeong. Pakr[2], Kyu Ha. Jang[3], Ki Tae. LEE[3], Seong Hee. PARK[3], JEON Min Yong. [4], Nicolay. Vinokurov[3], Young Uk. JEONG[3]
한국원자력연구원/충남대학교. [1] 한국원자력연구원/과학기술연합대학원대학교. [2] 한국원자력연구원/경북대학교. [3] 한국원자력연구원. [4] 충남대학교.

Keyword : "THz", "교번자장기", "FEL"

자 유전자레이저에서 발생되는 빛의 파장은 전자빔의 에너지, 교번자장기의 자기장의 세기, 교번자장기의 주기에 따라 결정된다. 본 연구에서는 전자빔의 진행 방향에 수직인 면에서 자기장의 세기가 달라지게끔 교번자장기의 자석을 기울인 “Canted-Pole” 교번자장기를 설계하였다. 교번자장기를 횡축방향으로 이동시켜 전자빔이 받는 자기장의 세기를 0.5 – 0.7 T 로 변화시킬 수 있으며, 이때 발생된 빛의 파장은 400 - 600 μm 로 조절할 수 있다. 이 장치에 사용될 전자빔은 마이크로트론을 사용하여 가속되며, 전자빔의 에너지는 5 MeV, 최대 전류는 ~1 A, 에너지분산은 0.4 - 0.5%이다. 이 장치는 간단하면서 낮은 제작비용의 장점이 있다.

P1-Pa.005

Measurement of the inclusive and differential ttbar production cross section in lepton+jets channel at 13 TeV with the CMS detector

*이아리, 김태정, 하비어, 최수용 [1]
*Ari. Lee, TAEJEONG. KIM, Javier. Brochero, Suyong. CHOI[1]
전북대학교. [1] *고려대학교.*

Keyword : "Top quark","CMS","cross section"

We present the total inclusive and differential top pair production cross section in e/mu+jets decay modes in proton-proton collisions using the data collected by the CMS detector at 13TeV. The measurement is performed using an integrated luminosity of 42 pb-1 collected during the first months of detector operations in 2015. The differential cross section is measured as a function of kinematic top variables like pT and eta. Finally, we compare the results with the latest NNLO-NNLL predictions.

P1-Pa.006*

가속기기반 초고속 펌프-프로브 장치의 전자빔 변수 측정

*김현우, 박선정 [1], 백인형 [1], 장규하, 이기태, 박성희, Sadiq Setiniyaz[1], Boris Gudkov[1], Sergey Miginsky, Nikolay Vinokurov, 정영욱
*Hyun Woo. Kim, Pakr Sun jeong. [1], In Hyung. Baek[1], Kyu Ha. Jang, Ki Tae. LEE, Seong Hee. PARK, Sadiq. Setiniyaz[1], Boris. Gudkov[1], Sergey. Miginsky, Nikolay Vinokurov. Vinokurov, Young Uk. JEONG
과학기술연합대학원대학교. [1] 한국원자력연구원.

Keyword : 광전자총, 초고속 전자회절, 에미턴스

한국원자력연구원에서는 펨토초 정밀도의 초고속 전자회절 (Ultrafast Electron Diffraction) 및 펌프-프로브 실험을 위한 극초단 가속기 시설을 개발하고 있다. 광전자총에서 1 pC 의 전하량으로 발생된 전자빔은 3 MeV 까지 가속된다. 극초단 전자빔을 얻기 위해서 가속된 전자빔을 2 개의 45 도 이극 자석과 6 개의 사극자석을 통과시켜 시료위치에서 펄스 길이를 50 펨토초 이하로 줄인다. 전자회절에서 선명한 전자회절 무늬를 얻기 위해서는 낮은 에미턴스가 요구되므로 이를 정확히 측정하는 것이 중요하다. 공간 전하 효과가 크게 작용하는 저에너지 전자빔의 에미턴스는 'quad scan' 방법을 통해 측정하였다. 이 발표에서는 에미턴스 측정 방법 그리고 시뮬레이션과 측정 데이터를 비교한 결과를 발표할 계획이다.

P1-Pa.007

극초단 전자빔 펄스폭 측정을 위한 고주파 휨 공동 개발 및 전자빔 동역학 연구

*박선정, 정영욱 [1], 박성희 [1], 이기태 [1], 장규하 [1], 문정호 [2], 배상윤 [3], 김현우 [4], 김은산, 김홍주, Nicolay A. Vinokurov[1]
*Sunjeong. Park, Young Uk. JEONG[1], Seong Hee. PARK[1], Ki Tae. LEE[1], Kyu Ha. Jang[1], Jung Ho. Mun[2], Sangyoon. Bae[3], Hyun Woo. Kim[4], Eun San. Kim, Hong Joo. KIM, Nicolay. Vinokurov[1]
경북대학교. [1] 한국원자력연구원. [2] 충남대학교. [3]KAERI. [4] 과학기술연합대학원대학교.

Keyword : 초고속 전자회절, UED, 고주파 휨 공동, 극초단 전자빔 펄스폭 측정

한국원자력연구원에서는 원자나 분자의 구조 분석을 위하여 초고속 전자회절 (Ultrafast Electron Diffraction) 장치를 개발 중에 있다. 현재 개발 중인 UED 장치에 사용되는 전자빔의 에너지는 약 3 MeV 이고, 50 fs 이하의 펄스 폭과 약 1 pC 의 전하량을 갖고 있다.
이러한 조건의 펄스폭 측정을 위해 TM120 모드로 구동하는 S-band 고주파 휨 공동을 제작하였다. 실제 장치를 모사하기 위하여 삼차원 입자동역학계산 (Particle-In-Cell, PIC) 코드를 사용해 펄스폭 측정에 필요한 고주파 출력 및 고주파 위상에 따른 전자빔 동역학 계산을 수행하였다.

P1-Pa.008

Search for the rare decays $B^0 \rightarrow e^+ e^- e^+ e^-$, $B^0 \rightarrow \mu^+ \mu^- \mu^+ \mu^-$ and $B^0 \rightarrow e^+ e^- \mu^+ \mu^-$ at the Belle experiment.

*박석희, 권영준
*Seokhee. PARK, Youngjoon. Kwon
연세대학교 물리및응용물리.

Keyword : Belle

We present a status report of a search for the rare B^0 decays to 4 leptons using the full \Upsilon (4S) data sample of 772M B\bar{B} pairs collected with the Belle detector at the KEKB asymmetric-energy e^+ e^- collider. We reconstruct a B meson in a B\bar{B} pair requiring it to be composed of 4 leptons and further enhance the sensitivity to the signal using kinematical variables in a Monte Carlo study. We expect this study to be extended to a New Physics particle search by assuming the final state leptons to be produced in pairs via undetected intermediate state particles such as dark photons.

P1-Pa.009

Study of $B^+ \rightarrow \pi^+\pi^0\pi^0$ at Belle

*김경호, 권영준
*Kyungho. Kim, Youngjoon. Kwon
연세대학교.

Keyword : Belle

We report signal and background study of hadronic B decays $B^+ \rightarrow \pi^+\pi^0\pi^0$ decay mode by using MC samples based on a data sample of 711 fb^{-1} collected at the Y(4S) resonance energy, recorded by KEKB collider.

P1-Pa.010

기울어진 파두를 이용한 전자빔의 정밀 측정기술

*백인형, 한병헌, 김영찬, 박선정, 장규하, 이기태, 박성희, 정영욱, Nikolay Vinokurov
*In Hyung. Baek, Byung Heon. Han, Young-chan. Kim, Sun Jeong. Park, Kyu Ha. Jang, Kitae. Lee, Seong Hee. Park, Young Uk. Jeong, Nikolay. Vinokurov
한국원자력연구원.

Keyword : "전자가속기", "전자빔 측정기술", "전광효과"

입자빔의 특성을 측정하는 기술은 입자가속기 기반의 물리학을 연구하는 데 있어 가장 기본적인 연구테마이다. 전자빔의 경우, 전자 뭉치(Electron Bunch) 형태로 진행하기 때문에 전자 뭉치의 길이(Bunch Length)뿐만 아니라 에너지 퍼짐도(Energy Spread)와 에미턴스(Emittance) 등이 전자빔을 이용한 실험의 정밀도를 좌우하게 된다. 본 연구에서는 한국원자력연구원 양자빔기반방사선연구센터의 레이저-펌프/전자빔-프로브 기반 초고속 전자회절(Ultrafast Electron Diffraction) 측정 시스템에서 전자총으로부터 발생된 전자빔의 펄스폭과 펌프빔으로 사용되는 레이저빔과의 상대적인 시간차(Timing Jitter)를 전광결정(Electro-Optic Crystal)을 이용하여 측정하는 방법을 발표한다. 전자빔의 진행 경로에 대해 수직 방향으로 입사되는 레이저빔을 ZnTe 전광결정에서 서로 교차시켜 전자빔으로부터 발생되는 전기장에 의해 변하는 전광결정의 굴절률 차이를 검출용 레이저빔과 두 개의 편광자를 이용하여 검출하게 된다. 전자빔 특성 측정 시스템의 시간해상도를 높이기 위한 방법으로 레이저빔의 파두(pulse-front)를 45 도만큼 기울여 진행시킴으로써, 평면 파두로 입사될 때 전광결정 내에서의 전자빔과 레이저빔간의 상호작용 한계를 극복할 수 있으리라 기대한다.

P1-Pa.011*

Inclusive study on using hadronic tagging method at Belle

*김한진, 권영준
*Hanjin. Kim, Youngjoon. KWON
연세대학교.

Keyword : Belle, fullrecon, Xs, gamma

We present an inclusive study on the measurement of the branching fraction of the radiative meson decay, using the full data sample collected with the Belle detector at the KEKB asymmetric-energy collider, corresponding to pairs. One of the mesons in the decay is fully reconstructed in hadronic modes, and the radiative photon is sought in the decay of the other B meson. We plan to obtain the CP asymmetry and the isospin asymmetry according to the measured photon energy spectrum.

P1-Pa.012*

Higgs to dimuon at upgrade CMS detector.

*김병준, 박인규, 류민상, 이상훈, 김지현, 김현철, 최민규, 류건모, 김현용, 전다정
*Byoung jun. Kim, Inkyu. PARK, Min Sang. Ryu, Jason. Lee, Ji Hyun. Kim, Hyunchul. Kim, Minkyoo. Choi, Geonmo. Ryu, Hyunyong. Kim, Da Jeong. Jeon
서울시립대학교.

Keyword : higgs, muon, dimuon,

The proposed upgrade of the CMS detector to the muon system is the addition of GEM detectors. This will improve our potential to see the Higgs decaying to dimuons. The reconstruction performance of the upgrade detector scenarios is shown for the higgs to dimuon decay.

P1-Pa.013*

GEM mass production in KOREA

*최민규, 박인규, 류민상, 정영군, 김지현, 이상훈, 류건모, 김현용, 전다정, 김병준
*Minkyoo. Choi, Inkyu. PARK, Min Sang. Ryu, Young Gun. JEONG, Ji Hyun. Kim, Jason. Lee, geon mo. Ryu, Hyunyong. Kim, Da Jeong. Jeon, Byoung jun. Kim
서울시립대학교.

Keyword : GEM foil , CERN , CMS , Detector , Muon

CERN Longterm Shutdown 2 기간중에 GE1/1 파트에 한국 CMS 실험 사업팀의
GEM 을 이용한 전방뮤온검출기 업그레이드 활동을 보고한다. 이에 맞추어 한국에서 그간 생산된 GEM foil production 과 그것을 바탕으로 만들어진 소형 GEM 검출기의 성능을 알아보았다. 한국에서 Single Method 와 Double Method 방법으로 Mass Production 에 기반을 갖추었으며 또한 각 Method 별 특성을 리포트하고자 한다.

P1-Pa.014*

Study of top quark mass measurement using J/psi inside jets at LHC

*류건모, 박인규, 류민상, 이상훈, 김지현, 최민규, 김현용, 전다정, 김병준, 김현철
*Geonmo. Ryu, Inkyu. PARK, Min Sang. Ryu, Jason. Lee, Ji Hyun. Kim, Min kyoo. Choi, Hyunyong. Kim, Da Jeong. Jeon, Byoung jun. Kim, Hyunchul. Kim
서울시립대학교.

Keyword : jpsi, bjet, top quark, LHC, CMS

The measurement of the top quark mass is very important topic at LHC because top quark mass is one of fundamental parameters to research “Standard Model”. The large dependence of one loop corrections to the higgs boson mass on top quark mass makes its precise determination of extreme importance for constraining the model itself. In this poster, we researched ttbar events include jpsi-in-jet to measure top quark mass. These events were extracted from 8TeV LHC data in 2012. In order to measure top quark mass precisely, a classical method have limitations to reduce systematic errors because this method has uncertainties of jet energy scale and jet resolution. However, a method which use jpsi-in-jet can reduce systematic errors attributable to jet because it does not use jets to determine top quark mass. This method only use an isolated lepton from W boson and 2 muons from jpsi in b jet. LHC accelerator provides a highest energy and luminosity for particle collision in the world. Although jpsi-in-jet events have very small statistics, we are expecting to find considerable jpsi-in-jet events from LHC data.

P1-Pa.015

Analysis of J/Ψ as charged particle multiplicity at 8TeV in ALICE muon spectrometer

*공병윤, 오선근, 백용욱
*Byung yun. Kong, Sun Kun. OH, Yongwook. Baek
건국대학교.

Keyword : ALICE,muon,multiplicity,8TeV

Production of J/Ψ as charged particle multiplicity at 8TeV in ALICE muon spectrometer

P1-Pa.016*

Measurement of the differential cross section for ttbar production in the dilepton final state at 13 TeV in CMS

*전다정, 최수용 [1], 노연정 [1], 이상훈, 최영일 [2], 고정환 [2], 김동현 [2], 유인태 [2]
*Dajeong. JEON, Suyong. CHOI[1], Youn Jung. Roh[1], Jason. Lee, Young-Il. Choi[2], Junghwan. Goh[2], Dong Hyun. Kim[2], Intae. YU[2]
서울시립대학교. [1] 고려대학교. [2] 성균관대학교.

Keyword : top quark, differential cross section, CMS, LHC

Differential cross sections of top-quark pair production are measured in dilepton decay channel with proton-proton collisions at a center-of-mass energy of 13 TeV. The measurement is performed with a RunII data using CMS detector at the Large Hadron Collider. In this analysis, we measure the differential cross sections with respect to kinematic variables of leptons, bjets, and top-quarks.

P1-Pa.017

Analysis of Neutral Kaon Decay, $K_L \rightarrow \pi^0 \pi^0 \gamma$

*고재우, 우종관, 임계엽 [1], 안정근 [2], 김은주 [3], 김준이 [2], 이건호 [3], 이종원 [2], 김용주, 유동
*jae woo. Ko, Jong-Kwan. Woo, Gei Yub. LIM[1], Jung Keun. AHN[2], Eun Joo. Kim[3], JunLee. Kim[2], GUNHO. LEE[3], Jongwon. Lee[2], Yong Joo. Kim, DONG. LIU
제주대학교. [1]KEK. Japan. [2] 고려대학교. [3] 전북대학교.

Keyword : Chiral Perturbation Theory, Kaon

E14(KOTO)실험을 통해 중성 K 중간자 붕괴인 K0L -> pi0 pi0 gamma 붕괴에서 최종상태인 pi0 가 5 개의 광자로 붕괴하는 것을 CsI 검출기로 측정하였다. K0L -> pi0 pi0 gamma 붕괴모드는 KTeV 실험에서 제시한 붕괴비인 2.43×10^{-7} (90% CL)의 upper limit 에 대한 결과를 확인할 수 있는 좋은 붕괴 모드이다. 이 붕괴를 통해 카이랄 섭동 이론을 측정하고자 하는 것이 목표이다. K0L-> pi0 pi0 pi0 붕괴는 K0L->pi0 pi0 gamma 붕괴의 주요 배경사상이 된다. 그 이유는 K0L-> pi0 pi0 pi0 붕괴의 최종상태는 6 개의 감마가 생성이 되는데 이중 하나의 감마가 검출이 안되었거나 아니면 2 개의 감마가 하나의 클러스터를 생성하여 CsI 검출기로 입사된 경우이다. 본 발표에서는 전산모사를 통한 K0L-> pi0 pi0 pi0 붕괴에 대한 결과를 발표할 예정이다.

P1-Pa.018

Low-temperature photon detector for KIMS-LT and its MMC fabrication

*오승윤
*Seung-Yoon. Oh
세종대학교.

Keyword : dark matter, WIMP, KIMS, cryogenic detector

Korean Invisible Mass Search (KIMS) is an experiment searching for Weakly Interacting Massive Particles (WIMPs) which are among the major particle candidates for dark matter. It searches for possible rare WIMP-nucleon recoil events with a scintillating crystal. The KIMS-LT project proposes to use a high-sensitivity low-temperature (near 10 mK) calorimeter which has been developed for a neutrinoless double-beta decay search experiment (AMoRE), using scintillation crystals (CaMoO4) and metallic magnetic calorimeters (MMCs), for dark matter search. Particle absorption in a CaMoO4 scintillating crystal generates both photons and phonons. Simultaneous measurements of photon and phonon signals will allow us to isolate nuclear-recoil induced signals that would be produced by WIMPs. The phonons generate a heat signal that can be read out with an MMC temperature-sensor in thermal contact with a thin phonon-collecting film coated onto the crystal. The phonon sensor developed for the AMoRE project shows good performances (similar to that of CRESST) in terms of energy resolution and energy threshold. Photon sensor also measures excess phonons made by the photons in the light-absorbing wafer with an MMC temperature-sensor in a thermal contact with a phonon collection film. It can be improved by integrating the phonon collection film and the Au:Er layer of the MMC. In this poster, a fabrication process for those MMC and plan for the integrated photon detector for KIMS-LT will be presented.

P1-Pa.019*

Background understanding of NaI(Tl) crystals for KIMS-NaI experiment

*푸시파
*Pushparaj. Adhikari
세종대학교.

Keyword : dark matter, WIMP, KIMS-NaI, NaI

The DAMA experiment has reported a low-energy, annual-modulation signal in an array of low-background NaI(Tl) detectors, which may be caused by WIMP interaction, but no direct confirmation with the same material has yet been done. The aim of the KIMS-NaI experiment is to try to reproduce the DAMA result with same type NaI(Tl) crystals. Tis requires the development of ultra-low background NaI(Tl) crystals. We tested seven crystals made from different powders to understand internal backgrounds and develop methods to reduce them. The results of these NaI(Tl) crystal measurements as well as future prospects will be presented.

P1-Pa.020

Development of scintillation light detectors for cryogenic rare event search experiments

*이혜진, 조현석, 강찬석, 김건보, 김혜림 [1], 김인욱 [2], 김소라, 김용함, 이민규 [3], 오승윤 [4], 소중호
*Hyejin. Lee, Hyon-Suk. Jo, Chan Seok. KANG, Geon-Bo. Kim, Hye lim. Kim[1], Inwook. Kim[2], So Ra. kim, Yong-Hamb. Kim, Min Kyu. LEE[3], Seung yoon. Oh[4], Jung Ho. So
기초과학연구원. [1] 경북대학교. [2] 서울대학교. [3] 한국표준과학연구원. [4] 세종대학교.

Keyword : scintillation, light detector

We report on the development of light detectors based on metallic magnetic calorimeters (MMCs). These light detectors are to be used for simultaneous measurements of heat and light signals from scintillation crystals in rare event search experiments. A 2-inch Ge wafer was used as the light absorber. Gold films evaporated on the Ge wafer and annealed gold wires make the thermal connection between the wafer and the MMC sensor. Thermal and athermal heat flows between the thermal components of the detector were investigated to improve the energy and timing resolutions of the signals. We present recent results on the signal size and rise time depending on thermal connections expected by the heat flow model.

P1-Pa.021

Receiver electronics for axion experiment at CAPP/IBS

*장승표, 김영임 [1], 이명재 [1], 야니스 [2]
*SeungPyo. Chang, Young Im. Kim[1], Myeong Jae. Lee[1], Yannis K.. Semertzidis[2]
기초과학연구원 (IBS)/한국과학기술원 (KAIST). [1] 기초과학연구원 (IBS). [2] 기초과학연구원 (IBS)/한국과학기술원(KAIST).

Keyword : Axion, radio frequency (RF), Heterodyne system

The Center for Axion and Precision Physics (CAPP), one of the centers of Institute for Basic Science (IBS), is on the progress of constructing the axion cavity experiment. The axion is supposed to decay into two photons in the very low-temperature cavity (~ 100 mK) which is in high magnetic field (> 8 T). In theory, the signal is thought to be radio frequency (RF, 2 ~ 8 GHz), and extremely weak (10^{-24} W). The frequency of the signal depends on the mass of the axion. The signal comes out of the cryogenic cavity and goes into the room temperature part. To detect this signal, we need to downconvert the signal and reduce the additional noise. In that purpose, the RF signal processing system at room temperature is designed. The individual component of this system and the whole system are tested.

P1-Pa.022

Development of oil-based liquid scintillators using various surfactants

*신창동, 최규정, 주경광
*Changdong. Shin, 규정. 최, Kyung Kwang. Joo
전남대학교.

Keyword : Liquid scintillators, 액체섬광검출용액

액체섬광검출용액은 입자물리실험에 있어서 유용히 사용된다. 기본적으로 액체섬광검출요액은 낮은에너지 영역을 정밀측정하는데 유용하며, 입자의 방향성에 대해서는 측정이 어렵다. 하지만 물을 포함하여 체렌코프효과를 이용하면 입자의 방향성을 측정할수 있다. 그래서 현재 액체섬광검출용액에 물을 일정량 포함시키기 위한 시도를 하고 있으며, 그에 따라 기름과 물을 섞기 위하여 다양한 계면활성제를 사용가능 여부 및 조합비율을 확인하였다.

P1-Pa.023

Development of measurement device for liquid scintillator attenuation-length

*신창동, 김바로, 김우영 [1], 박인곤 [2], 장지승 [3], 박명렬 [4], 장한일 [5], 김상용 [6], 양장희 [7], 김영덕 [8], 김현수 [9], 김시연 [10], 김재률, 박령균, 여인성, 임인택, 주경광, 박성우 [1], 최준호 [4], 김수봉 [6], 박정식 [6], 서선희 [6], 서현관 [6], 이동하 [6], 최원국 [6], 유인태 [7], 최영일 [7], 전은주 [8], 고영주 [10]
*Changdong. Shin, Ba Ro. Kim, Wooyoung. Kim[1], In-Gon. PARK[2], Jee Seung. Jang[3], Myoung Youl. PAC[4], Han Il. JANG[5], Sang yong. Kim[6], Janghee. Yang[7], Yeong Duk. Kim[8], Hyunsoo. Kim[9], Siyeon. Kim[10], Jae Yool. Kim, Ryeong Gyoon. Park, In Sung. Yeo, In Taek. Lim, Kyung Kwang. Joo, Sung Woo. Park[1], JUNE HO. CHOI[4], Soo-Bong. Kim[6], Jungsic. Park[6], Seon Hee. Seo[6], Hyun Kwan. Seo[6], Dong ha. Lee[6], won qook. Choi[6], Intae. Yu[7], Young-Il. Choi[7], Eun Ju. Jeon[8], Youngju. Ko[10]
전남대학교. [1] 경북대학교. [2] 경상대학교. [3] 광주과학기술원. [4] 동신대학교. [5] 서영대학교. [6] 서울대학교. [7] 성균관대학교. [8]IBD/세종대학교. [9] 세종대학교. [10] 중앙대학교.

Keyword : RENO, LS, Attenuation length

RENO 실험에서 검출기 내부에는 중성미자를 검출하기 위하여 내부에 액체섬광검출용액을 사용한다. 액체섬광검출용액은 입자를 검출할때 나오는 빛의 양과 감쇄거리가 아주 중요하게 작용한다. 특히 감쇄거리는 검출장비로 사용하는 PMT 까지 도달하기 위해서 큰값을 가질 필요가 있다. 이는 검출기의 크기가 클 수록 중요한 요인으로 작용된다. 이에 따라 감쇄거리를 정확하게 측정하기 위하여 액체섬광검출용액의 감쇄거리 측정장비를 설계하여 측정을 시도한 결과에 대하여 정리하였다.

P1-Pa.024

Detector and Trigger Simulation for NEOS Experiment

*고영주, 김시연, 김홍주 [1], 이주영 [1], 김영덕 [2], 박강순 [3], 박향규 [3], 이무현 [3], 이재승 [3], 이정연 [3], 전은주 [3], 김진유 [4], 김현수 [4], 김바로 [5], 여인성 [5], 주경광 [5], 서경민 [6], 박현서 [7], 선광민 [8], 한보영 [8]
*Youngju. Ko, Siyeon. Kim, Hong Joo. KIM[1], Joo Young. Lee[1], Yeong Duk. KIM[2], Kang Soon. Park[3], HyangKyu. Park[3], MOO HYUN. LEE[3], Jaison. Lee[3], Jeong Yeon. LEE[3], Eun Ju. Jeon[3], Jin Yu. Kim[4], Hyunsoo. Kim[4], Ba Ro. Kim[5], In Sung. Yeo[5], Kyung Kwang. Joo[5], kyung min. seo[6], Hyeonseo. PARK[7], Kwang Min. SUN[8], Bo Young. Han[8]
중앙대학교. [1] 경북대학교. [2] 기초과학연구원/세종대학교. [3] 기초과학연구원. [4] 세종대학교. [5] 전남대학교. [6] 전북대학교. [7] 한국표준과학연구원. [8] 한국원자력연구원.

Keyword : sterrile neutrino, reactor neutrino experiment, simulation

By combining results of previous experiments performed in short baseline (th neutrino, possibly a sterile neutrino. The Neutrino Experiment for Oscillation at Short baseline (NEOS) is a short-baseline experiment near reactors in Korea to find out the existence of the sterile neutrino. We have developed detector and trigger simulation tools of the NEOS experiment. A comparison between the simulation data and the real data is presented.

P1-Pa.025*

Background understanding of the KIMS-NaI crystal cleaning and PMT attachment process.

*고빈다
*GOVINDA. ADHIKARI
세종대학교.

Keyword : dark matter, WIMP, KIMS-NaI, NaI

The KIMS (Korean Invisible Mass Search) experiment aim is to reproduce the DAMA observation of a WIMP-induced dark matter signal using the same target/detector material. As part of this effort, we have to develop ultra-low-background NaI(Tl) crystal detectors. We are studying backgrounds in test NaI(Tl) crystal detectors produced by different vendors (Alpha Spectra and Beijing Hamamatsu) and identifying the levels of natural and cosmogenic radioactive backgrounds. Based on these results, we will prepare a 200 kg array of pure NaI(Tl) crystal and operate them in the Yang Yang underground laboratory in Korea. To reduce backgrounds from surface contaminations, we have applied various cleaning techniques with the goal of reaching a background count level in KIMS-NaI that is below 1 count/kg/keV/day. In this poster, the status of our understanding of low- and high-energy background levels in NaI(Tl) crystal after different methods of cleaning the NaI crystal assemblies and their readout PMTs, as well as the characteristics of high energy alpha emitters will be presented.

P1-Pl.001

Design of a drift-tube of C-band klystron by simulation

*황지현, 박성주 [1], 남궁원 [1], 조무현
*Jihyun. Hwang, Sung-Ju. Park[1], Won. Namkung[1], Moo-Hyun. CHO
포항공과대학교. [1] 포항가속기연구소.

Keyword : Klystron, FCI, klystron simulation, efficiency, tube design

A klystron is a linear-beam vacuum tube which amplifies RF signals by converting the kinetic energy in DC electron beams into radio frequency power. It consists of an electron gun to produce electron beams, a drift tube which is connected to series of reentrant cavities and a collector to dump the spent electron beams at the end. In the drift tube region, the electron beams are bunched in consequence of a velocity modulation by interacting with cavities. The amplified signals are extracted when the bunched beam enter the output cavity. Therefore, the drift tube design plays a vital role to decide the tube performance parameters like gain, bandwidth and overall efficiency; the cavity parameters like resonant frequencies and R/Q of each cavity can be calculated by SUPERFISH code or white noise method. Through the simulation and experiment, we tried to find out the proper design of the drift-tube of C-band klystron to get the goal efficiency and gain. Also, it needs to be considered the system stability to avoid the self-oscillation producing by the multi-gap output cavity.

P1-Pl.002

4 결정 채널컷 분광기의 조정장치 개발

*길계환, 최효진, 임재홍
*Kyehwan. Gil, Hyo-Jin. Choi, Jae-Hong. Lim
포항가속기연구소.

Keyword : X-선 마이크로빔, 미세실험, 4 결정 채널컷 분광기, 분광기 조정기구, 에너지 주사

포항방사광가속기-II 의 4B 빔라인은 X-선 마이크로빔을 이용한 미세회절 실험과 미세형광 실험에 이용되고 있다. K-B(Kirkpatrick-Baez) 거울시스템에 의해서 집속된 마이크로빔은 분광된 빔으로서도 이용될 수 있으며, 이를 위하여 4 결정 채널컷 분광기가 운용되고 있다. 하지만, 분광기 몸체가 K-B 거울시스템과 함께 단일 광학 테이블상에 설치되어 광학 테이블만으로 조정되므로 그 조정성에 있어서 극히 제한적이었다.
본 연구에서는 분광기를 독립적으로 조정하기 위한 분광기 조정기구가 개발되었다. 광학 테이블 상부의 하판에 부착된 세 개의 스크루잭으로 중판의 높이, 롤(roll)각 및 피치(pitch)각을 조정하고, 중판에 부착된 두 개의 평행 볼스크루로 상판의 좌우 방향 이동과 요(yaw)각을 조정한다. 따라서 상판 상부에 설치된 분광기는 5 자유도 구동성을 갖추게 된다.
분광기의 5 자유도 구동은 LabVIEW 프로그램에 의해서 수행된다. 특히 4 결정 분광기의 단점인 낮은 출력을 보완하기 위하여, 분광기의 에너지 주사 중에 첫 번째 결정블록에 대한 두 번째 결정블록의 상대적인 피치각을 최고 반사율의 각도로 조정하는 알고리듬이 에너지 주사 프로그램에 구축되었다.
본 발표에서는 분광기 조정기구의 설계와 구동 프로그램을 상세히 기술하고, 시운전 결과를 보고한다.

P1-Pl.003

자기차폐 방식의 고리형 홀 추력기 특성 연구

*이승훈, 김호락 [1], 임유봉 [1], 최원호 [1]
*Seunghun. Lee, Kim Ho lak. [1], Lim youbong. [1], CHOE Wonho. [1]
한국기계연구원 부설 재료연구소. [1] *한국과학기술원.*

Keyword : 추력기, 자기차폐, 자기장, 플라즈마

고리형 홀 추력기는 인공위성의 자세제어 및 행성탐사 등의 우주 임무수행을 위한 전기추력기로 널리 활용된다. 최근 고리형 홀 추력기의 장시간 운전성 확보 및 방전효율 향상을 위해 플라즈마와 방전영역 내 유전체 벽 간의 충돌을 줄임으로써 전극 식각 및 전자온도 손실을 감소시키기 위한 연구가 활발히 진행되고 있다. 특히 ExB 운동을 유지하기 위한 전자석 코일 이외에 추가적인 전자석 코일을 활용해 방전 채널과 평행한 자기장을 형성하여 플라즈마와 유전체 벽 간의 충돌을 감소시키는 연구들이 소개되고 있으며, 이러한 방법을 자기차폐(magnetic shielding)라 한다.
본 발표에서는 추가적인 전자석 코일없이 자기차폐가 가능한 고리형 홀 추력기에 대해 소개하고자 한다. 자기차폐 구조형성을 위해 자성체 구조물을 활용한 내부 자기장 회로를 사용하였으며, 추가적인 전력 소모 없이 기존에 보고된 자기차폐 방법의 자기장 구조와 유사한 형태를 가진다. 한국과학기술원 전기추력기 연구팀에서는 본 자기차폐 방식이 적용된 300 W 급 추력기를 제작하였으며, 방전실험을 통해 자기차폐에 의한 플라즈마 구속 거동 및 추력 특성들을 보고하고자 한다.

P1-Pl.004*

마이크로 위성용 저전력 홀 추력기의 개발 및 특성 연구

*김호락, 임유봉, 이승훈 [1], 선종호 [2], 최원호
*Kim Ho lak. , Lim youbong. , Seunghun. Lee[1], Jongho SEON. [2], CHOE Wonho.
한국과학기술원. [1] 한국기계연구원 부설 재료연구소. [2] 경희대학교.

Keyword : Plasma Physics, Hall Thruster, Ion Beam Source, Micro-thruster

홀 추력기는 전기추력기 중 하나로, 화학식 추력기에 비해 비추력이 높아 인공위성의 자세제어, 궤도수정, 궤도천이를 포함한 행성간 탐사활동 및 우주 임무수행을 위한 우주선의 엔진 등으로 다양하게 활용된다. 특히, 저전력 홀 추력기는 큐브셋(cubesat) 및 마이크로 위성(microsatellite)의 증가하는 수요에 따라 필요성이 증가하고 있으며, 활용도가 높아 다양하게 연구 및 개발되고 있다. 홀 추력기는 자기장과 전기장을 서로 수직되게 인가하여, 자화된 전자는 플라즈마 방전을 유지시키고 자화되지 않은 이온은 전기장 방향으로 가속되어 이온빔을 발생시킨다. 하지만, 저전력 소형 추력기는 작은 소모전력과 방전채널로 인한 성능 저하 및 자기장 구조 설계 등 많은 어려움들을 가지고 있다. 본 연구에서는, 약 50 W 의 소모전력을 바탕으로 영구자석을 이용한 저전력 플라즈마 추력기를 개발하였다. 방전 채널은 지름 15 mm, 길이 16 mm, 무게는 약 0.6 kg 으로 원통형 구조의 채널로 제작되었다. 저전력 홀 추력기의 제작 과정과 성능 및 빔 특성에 대한 연구결과가 발표될 예정이다.

P1-Pl.005*

Transmission calculation for Reverse Saturable Absorption of X-ray Free Electron Laser Pulse in Aluminum

*조민상, 조병익 [1]
*Min Sang. Cho, Byoung Ick. Cho[1]
광주과학기술원 물리·광과학과. [1] *광주과학기술원.*

Keyword : "SCFLY" "Reverse saturable absorption" "Aluminum transmission" "Collisional Radiative Simulation"

The development of XFEL, capable of producing high energy and intensity coherent beam even in X-ray regime, makes a lot of interesting optical phenomena with related to light-matter interaction. One of these phenomena reported is Reverse Saturable Absorption. When the energy of XFEL beam is large enough to interact with each electron of atoms in inner shells, non-linear absorption effect whose excited state absorption is larger than the ground state absorption is observed. Therefore, a phenomenon of the increase in light absorption at higher intensity happens and is referred to as reverse saturable absorption.

A collisional radiative simulation code, SCFLY, is used to study detailed RSA mechanism. SCFLY is a simulation code to solve rate equations for level population by considering collisional and radiative atomic processes. It also provides a spectrum of light-matter interaction and even ionization and population distribution of plasma. Recently, SCFLY has become important tool to study the hot dense matter, warm dense matter, and highly transient states of matter, etc. and successfully applied to various research fields.

Using SCFLY, RSA mechanism was analyzed and we have tried to match simulation results and experimental data of RSA on aluminum in this poster. The experiment was performed on an instrument of LCLS using XFEL. The x-ray beam was set in the range of 1480 ~ 1510 eV below the K-edge of aluminum (1560 eV) and pulse duration was approximately 100fs bound by the electron pulse length. Also, the focal spot diameter was 3 μm and the corresponding peak intensity of 1017 W/cm2 on the target. Therefore, conditions of SCFLY simulation were set to match up with these conditions. Consequential simulation results comparable with experimental data will be discussed.

This work was supported by Institute of Basic Science (IBS-R012-D1) and National Research Foundation of Korea (No. 2013R1A1A1007084).

P1-Pl.007

분석용 이온빔 가속기 빔라인 빔광학 기초 연구

*권혁중, 김한성, 박성균, 조용섭
*KWON Hyeok-Jung. , Kim Han Sung. , park sung kyun. , CHO Yong-Sub.
한국원자력연구원.

Keyword : Tandem accelerator, PIXE, RBS

양성자가속기연구센터에서는 이온빔 서비스의 품질보증을 위하여 표면 분석용 이온빔 가속기를 설치하고 있다. 이온빔 가속기는 탄뎀 형태이며 최대 전압 1.7 MV 이다. 가속기에는 4 개의 빔라인을 설치할 예정이며, PIXE 빔라인, RBS 빔라인, 이온주입 빔라인, 표준 중성자 생산용 빔라인이 그것이다. 본 연구에서는 새로 설치되는 4 개 빔라인에 대한 빔 수송 특성에 대해서 논한다.

* 본 연구는 미래창조과학부의 연구비 지원을 받았음.

P1-Pl.008

헬륨빔 조사를 위한 200 MHz RFQ 설계 변수 최적화 및 공학 설계

*김한성, 권혁중, 조용섭, 박성균, 설경태
*Han Sung. Kim, Hyeok-Jung. Kwon, Yong-Sub. Cho, Sung Kyun. Park, Kyung tae. Seol
한국원자력연구원.

Keyword : RFQ, helium beam, Radio-frequency, linac

양성자가속기연구센터에서는 전력 반도체 특성 개선을 위한 헬륨빔 조사용 RFQ (Radio-Frequency Quadrupole)를 개발하고 있다. 사용 가능한 고주파 시스템 및 제작의 용이성 등을 고려하여 RFQ 의 공진주파수는 200 MHz, 구조는 4 vane 타입으로 설계하였다. 헬륨빔 기준으로 RFQ 의 입력 에너지는 100 keV, 출력 에너지는 4 MeV 이다. 설계시 빔전력을 포함한 고주파 전력은 200 kW 이하가 되도록 하였으며, 공진기의 총 길이는 3.2 m 이하가 되도록 하여 세 개의 섹션으로 제작이 가능하도록 하였다. RFQ 의 재질은 무산소동이며 진공 브레이징을 통해 제작된다. 본 발표에서는 헬륨빔 조사용 RFQ 의 설계 변수 최적화 및 공학 설계에 대해 보고한다.

본 연구는 미래창조과학부의 연구비 지원을 받았음.

P1-Pl.009

PAL-XFEL Girder 위치변화 측정용 WPS 측정원리 소개

*최효진, 서광원, 이상봉, 길계환, 이홍기, 강흥식
*최. , 서. , 이. , 길. , 이. , 강.
포항가속기연구소.

Keyword : PAL-XFEL, WPS, 측량센서

이집트 피라미드 건설 과정에서 돌의 높이를 일정하게 쌓거나, 돌을 직선으로 놓기 위해 줄(Wire)을 이용했다고 한다. 광학 및 Laser 측량기기가 개발되기 전에는 토목 및 건축에서 줄을 이용하여 정렬(Alignment)작업을 하였다. 광학 및 Laser 측량기가 발달된 오늘날, PAL-XFEL 에 줄을 이용한 정렬장치를 설치하는 이유는 (1) Radiation 지역의 장치들을 장기간 지속적으로 관측기록하며 (2) 저렴한 비용으로 설치 및 유지관리가 되어야 하고 (3) 200 미터 측정구간에 대한 측정 분해능(High resolution)이 1~2 micrometer 로서, 모든 요구조건을 만족시키는 것이 Wire Position Sensor (WPS)이기 때문이다. 과거에는 사람의 눈으로 확인해야 했지만, 전자기기의 발전으로 인해 다양한 방식의 전자센서가 판매되고 있다. PAL-XFEL 은 Capacitive 형태로서, 선형성(Linearity)과 안정성(Stability)을 높이기 위해 Dual 형태이다. 본 논문에서는 WPS 의 측정원리에 대해 자세히 소개한다.

P1-Pl.010

Front-end beam simulations in post accelerator of the RAON accelerator

*진현창, 장지호, 홍인석, 김형진
*Hyunchang. Jin, Ji-Ho. Jang, In-Seok. Hong, Hyung Jin. Kim
기초과학연구원.

Keyword : "RAON accelerator","RISP"

RAON accelerator proposed by the Rare Isotope Science Project (RISP) has been built to create and accelerate a variety of stable heavy ion beams and rare isotope beams. In the RAON accelerator, the rare isotope beams are generated by the Isotope Separation On-Line (ISOL) system and will be transported through the post accelerator, which includes the post Low Energy Beam Transport (LEBT) system, the post Radio Frequency Quadrupole (RFQ), and the superconducting linac (SCL3) section, to the low energy experimental hall or to the superconducting linac (SCL2) section. To identify the stability of the post accelerator, we will describe and discuss the results of the beam dynamics simulations at the front-end beamline of the post accelerator in the RAON accelerator.

P1-Pl.011

RAON Beam Optics in the Charge Stripper Section

*장지호, 진현창, 송정석, 전동오, 김형진
*Ji-Ho. JANG, Hyun Chang. Jin, Jeong Seog. Song, Dong-O. Jeon, Hyung Jin. Kim
중이온가속기건설구축사업단 / 기초과학연구원.

Keyword : RISP, linac, charge stripper

RISP (Rare Isotope Science Project) is developing a superconducting linear accelerator called RAON. It is separated by a charge stripper which increases the charge states of the heavy ions in order to effectively accelerate heavy ions in the higher energy part of the linac. Because the charge stripper degrades beam qualities, we need to evaluate the charger stripper effects on beam optics. This work summarized the beam optics in the charge stripper section.

P1-Pl.012

Beam tracking on the High Energy Beam Transport line in KHIMA medical machine

*박차원, 안동현, 임희중
*Cha Won. Park, Dong Hyun. An, Hee Joong. Yim
한국원자력의학원.

Keyword : KHIMA, KIRAMS, HEBT, TRACK, Opera3D

The Korea Heavy Ion Medical Accelerator (KHIMA) has launched the synchrotron based hadron beam therapy facility for combined medical cancer treatment and cancer research. The Korea Institute of Radiological & Medical Sciences (KIRAMS) synchrotron has been designed to accelerate the particle beams having the kinetic energy interval of 60-230 MeV proton and 110-430 MeV/u carbon ions respectively. An accelerated beam from the synchrotron is transported to the patient position through the High Energy Beam Transport (HEBT) lines. In the HEBT lines, the lattice are designed with beam optics codes. In order to check and conform the beam loss at the HEBT lines, the tracking code, TRACK, has been used with encoded field map and also with simulated field map by Opera3D code. The performances are described and compared for manufacturing the components in the HEBT lines.

P1-Pl.013

PAL-XFEL 전자석 설계와 자기장 측정 결과

*서형석, 이상봉, 오봉기, 정영규, 정성훈, 이홍기, 박기현 [1], 박기현, 강흥식, 고인수
*Hyung Seok. Suh, Sang-Bong. Lee, Bonggi. Oh, Young-Gyu. Jung, Seong Hun. Jeong, Hong-Gi. Lee, Park ki Hyeon. [1], Ki-Hyeon. Park, Heung-Sik. Kang, In Soo. Ko
포항공과대학교. [1] 포항가속기연구소.

Keyword : 전자석설계, 2 극전자석, 4 극전자석, 전자기해석, 열해석

PAL-XFEL 은 10 GeV 에너지로 0.1 nm X-ray 를 발생시키는 선형가속기이다. 첫 건설 단계에서는 Hard X-ray 한 빔라인과 Soft X-ray 한 빔라인을 목표로 하고, 2015 년말까지 이에 필요한 모든 장치를 설치할 예정이다. 첫 단계에 필요한 모든 전자석을 자체 설계했고, 현재 제작 및 자기장 측정 중이다. 2 극전자석 6 종류, 4 극전자석 11 종류, 보정전자석 3 종류 등 총 전자석 수는 308 대이다. 지금까지 자장측정 결과는 전자석 요구조건을 만족시키며 무난하게 진행되고 있다. 이 발표에서는 전자석 설계와 자기장 측정 결과를 설명한다.

P1-Pl.014

The design of low noise magnet power supply

*박기현, 정성훈 [1], 정영규, 김동언, 서형석 [1], 이홍기, 강흥식 [1]
*Ki-Hyeon. Park, Seong Hun. Jeong[1], YoungGyu. Jung, Dong Eon. KIM, Hyung Seok. SUH[1], Hong Gi. Lee, Hung Sik. KANG[1]
포항가속기연구소. [1] 포항공과대학교.

Keyword : "Magnet power supply","low noise"

The accelerator facility needs a high stable magnet power supply (MPS). The stability requirements of the some MPSs in accelerator facility were in the range of the ~10 ppm. There are many noise sources which affect the stability of the MPS. Thus the design of the MPS requests much attention on the noise reduction scheme from the beginning stage. The noise on the MPS divided into some sources such as the ripple voltage coming from rectifier on the DC link, switching noise from the high voltage switch, and so on. This paper dealt with ripple components analysis, simulation on the overall system control of the MPS.

P1-Pl.015

Installation of Pal-xfel magnet power supplies

*정성훈, 박기현 [1], 서형석, 이상봉, 오봉기, 정영규 [1], 이홍기 [1], 김동언 [1], 강흥식, 고인수
*Seong Hun. Jeong, ki Hyeon. Park[1], Hyung Seok. SUH, Sang-Bong. Lee, Bongi. Oh, YoungGyu. Jung[1], Hong Gi. Lee[1], Dong Eon. KIM[1], Hung Sik. KANG, In Soo. KO
포항공과대학교. [1] 포항가속기연구소.

Keyword : MPS

The PAL-XFEL has in the order of six hundreds of magnet power supply (MPS) installed, ranging from 4A/9V bipolar PS to 310A/250V unipolar PS. The eight different prototypes of MPS are developing to confirm the performance, functions, size, heat load and so on. This paper describes the acceptance test results of the prototype MPS in major specifications from the manufacturers. All MPSs have to be installed until the end of October in 2015. .

P1-Pl.016

Metal seal 을 이용한 KOMAC 빔창의 설계, 제작 및 테스트

*김초롱, 정보현, 김한성, 권혁중, 조용섭
*Chorong. Kim, Chung Bo hyun. , Kim Han Sung. , KWON Hyeok-Jung. , CHO Yong-Sub.
한국원자력연구원.

Keyword : 빔창, 유한요소, 열 해석, 구조 해석

KOMAC 은 20 MeV 와 100 MeV 에 이용자를 위한 빔라인을 운영 중이다. 100 MeV 양성자 빔을 대기 중으로 인출하기 위해 양성자 빔의 투과가 좋으며, 이로 인한 방사화가 적은 재질이 요구된다. 이를 위하여 강도가 좋은 Beryllium 과 방사화가 적은 Aluminium 을 고려하였고 이의 합금인 AlBeMet 162(Al≒38% Be≒62%)를 선택하였다. 진공 기밀을 위한 seal 은 기계적, 열적 특성이 좋은 Helicoflex seal 을 고려하였다. 빔창의 설계를 위하여 열 및 압력의 구조적 안정성파악을 위하여 유한요소코드를 사용하였고 이 결과를 바탕으로 빔창을 제작하여 실험하고 도출된 결과를 유한요소해석의 결과와 비교하였다. 빔창은 300 mm(∅)와 100 mm(∅) 두가지 경우를 고려하였다. 본 발표에서는 빔창의 설계 및 테스트에 대하여 논한다.

P1-Pl.018*

Investigation and interpretation for transparency of laser-driven ion bunch by using one-dimentional PIC simulation

*강태연, 김영국, 허민섭
*Teyoun. Kang, Young kuk. Kim, Min Sup. Hur
울산과학기술대학교.

Keyword : PIC, ion, acceleration, laser

임의의 plasma 의 trancparency 를 fluid equation 을 통해 이론적으로 예측하고, 이를 1D PIC simulation 결과와 비교했다. 이를 laser 에 의해 가속된 ion bunch 에도 적용할 수 있는지 검토했다.

P1-Pl.019

Ion acceleration on electrostatic shock through relativistic transparency in an intense laser-plasma interaction.

*김영국, 강태연, 허민섭 [1]
*Young kuk. Kim, Teyoun. Kang, Min Sup. Hur[1]
UNIST. [1] 울산과학기술대학교.

Keyword : ion acceleration, laser, plasma, shock

레이저의 상대론적 투과현상을 이용하여 electrostatic shock 을 만들어 이온을 가속시키고자 한다. 매우 짧은 펄스들의 경우 플라즈마를 높은 온도로 충분히 가열시키지 못하는데 상대론적 투과현상을 통해 추가적인 플라즈마 가열 과정을 거친다. 그리고 더 낮은 플라즈마 밀도를 사용할 수 있기 때문에 높은 shock velocity 를 얻을 수 있다. 따라서 상대적으로 적은 레이저 에너지로 높은 속도의 shock ion acceleration 을 구현할 수 있을것으로 전망한다.

P1-Pl.020*

Measurement of Onset Time of Plasma Breakdown under various Low Pressurized Gaseous States Using a High Power Gyrotron

*김동성, 김성국, 최은미
*Dongsung. Kim, Sunggug. Kim, Eunmi. CHOI
울산과학기술대학교.

Keyword : plasma, breakdown, gyrotron

In this paper, we present experimental study on plasma breakdown in a pressurized chamber filled with Argon gas to measure an avalanche onset time of plasma breakdown by using a high power gyrotron. Breakdown threshold electric fields at different pressure are in a good agreement with theoretically calculated values from the well-known Paschen curve. As the gas pressure increases from the value at which the threshold electric field is a minimum, the required characteristic time occurring plasma breakdown is delayed. We also determine a velocity of propagating the plasma wave along the opposite direction of RF beam using the discharge image. From the study, we find a relationship between the breakdown delay time and the gas pressure with careful analysis of probability of breakdown events using the RF signal and photo diode.

P1-Pl.021

Sr-82, Cu-67 생산용 KOMAC 빔라인 구축 및 진공테스트

*정보현, 윤상필, 설경태, 김한성, 권혁중, 조용섭
*Bo hyun. Chung, Sang pil. Yun, Kyung tae. Seol, Han Sung. Kim, Hyeok-Jung. KWON, Yong-Sub. CHO
한국원자력연구원.

Keyword : KOMAC, RI product beamline, Construction, Vacuum leak test

KOMAC (Korea Multi-Purpose Accelerator Complex)은 20 MeV 와 100 MeV 에 각각 5 개의 빔라인이 고려중이다. 이중 각각 1 개씩의 빔라인(TR23, TR103)이 구축되어 이용자에게 양성자 빔을 공급하고 있으며 올해 말을 목표로 동위원소 생산 빔라인(TR101)이 구축중이다. 이의 추가구축은 고부가가치 의료용 동위원소 전용 생산 빔라인으로 양성자가속기의 활용성을 극대화 할수 있으며 우리나라 동위원소 공급과 외화 유출방지에도 영향을 미칠 것이라 기대한다. 이 빔라인은 Sr-82 와 Cu-67 을 목표로 구축중이며 빔수송을 위하여 2 극자석과 4 극자석으로 구성하였다. 양성자 빔진단을 위하여 BPM 과 CT 등을 설치하였고, 고진공을 위하여 Scroll, TMP, Ion pump 로 구성하였다. 본 발표에서는 현재 구축된 동위원소 빔라인 구축과 이의 진공누설테스트에 대하여 논한다.

P1-Pl.022*

High energy electron beam generation by using a tapered gas-cell in laser-plasma accelerator

*김민석, 남인혁, 이승우, 김진주, 석희용
*Minseok. Kim, Inhyuk. NAM, Seungwoo. Lee, Jinju. Kim, Hyyong. Suk
광주과학기술원.

Keyword : Laser wakefield acceleration, Tapered gas-cell, Dephasing length, High power laser

The electron energy obtained by a laser wakefield accelerator (LWFA) is determined by an acceleration length. Compared to the capillary plasma with uniform density the acceleration length of electron from the tapered density plasma is able to be extended and higher energies can be achieved. For this reason, we developed a density-tapering gas-cell and conducted an electron acceleration experiment with the gas-cell. In addition, we performed the PIC (particle-in-cell) simulation and we confirmed that the experimental results are well matched with simulation results. In this presentation, we present the detailed results about laser wakefield electron acceleration with density-tapering plasma source.

P1-Pl.023*

Transmission Line Resonator 를 이용한 Microwave 대기압 플라즈마의 발생 장치 제작 및 플라즈마 특성연구

*엄인섭, 정태훈, 최준 [1]
*in sub. Eom, CHUNG Tae Hun. , jun. choi[1]
동아대학교. [1]KITECH.

Keyword : 마이크로웨이브(Microwave, MW)

마이크로웨이브(Microwave, MW)를 구동하기에 적합한 대기압 플라즈마 발생 장치 제작을 위해, 직경 6.5 mm 인 스테인리스 와이어 2 개를 이용하여 Two Parallel Wires Resonator (TPWR)를 구성하여 설계제작 하였다. Transmission line 이론을 기반으로 제작한 MW 발생 장치는 저주파에 비해 전자로 인한 파장의 왜곡 현상이 적으며 높은 진동수를 이용하기 때문에 전자의 운동에너지를 높일 수 있으므로 저전력으로 플라즈마의 생성이 가능하다는 장점을 가지고 있다. 따라서, HFSS(High Frequency Structural Simulator) 프로그램으로 반사계수, Feeding Point 그리고 전기장 구조를 확인하면서 안정적인 마이크로웨이브 플라즈마 발생이 가능한 조건을 찾고, 플라즈마 발생에 적합한 실험 변수를 Network Analyzer 를 이용하여 분석하였다.

P1-Pl.024*

대기압 플라즈마 젯의 방전 특성 및 플라즈마 처리된 액체내의 OH 의 변화 측정

*백은정, 조혜민, 김선자, 정태훈
*Baek Eun Jeong. , . , . , .
동아대학교.

Keyword : "플라즈마" "대기압플라즈마"

대기압 플라즈마 젯은 재료공정, 생의학적 응용 등에 널리 활용되는 저온 플라즈마를 발생시킨다. 전극 재료로는 직경이 1mm 인 구리를 이용하였고, 방전관은 내부에 구동전극을 석영관으로 감싸고 외부에 펜슬모형의 석영관으로 한번 더 감싸주는 대기압 플라즈마 젯을 설계 제작하였다. 플라즈마 젯에 헬륨기체를 주입하여 대기압에서 플라즈마를 발생시켜보았다. 이 때 플라즈마에 인가해주는 전압, 진동수, 기체유량, pulse width 의 변화에 따라서 전압 프로브와 전류 모니터를 이용하여 발생된 플라즈마의 I-V 특성 곡선을 얻었고, 플라즈마 방전 시 발생되는 입자 종들의 성분을 알아보기 위하여 OES (Optical Emission Spectroscopy)를 이용한 광 방출 특성을 조사하였다. 또한 다양한 조건에서 플라즈마의 기체 온도, plume 의 변화를 알아보았고, UV 흡수분광법을 이용하여 플라즈마-액체 계면에서의 OH 입자밀도를 측정하여 OES 방법으로 측정한 OH 밀도와 비교하였다. 그리고 TA solution 을 이용하여 다양한 조건에서 액체 내의 OH 양을 측정해보았다.

P1-Pl.025*

Experimental Apparatus of Ultrafast EUV Absorption Spectroscopy for Non-equilibrium Warm and Dense State of Matters

*이종원, Xiaotao Geng[1], 김동언 [1], 조병익
*Jong-Won. Lee, Xiaotao. Geng[1], Dong-Eon. Kim[1], Byoung-ick. Cho
GIST. [1]Max Planck POSTECH/KOREA Res. Init.

Keyword : Warm Dense Matter, High Harmonic Generation, Absorption Spectroscopy

The absorption spectroscopy is a versatile technique to study electronic structures and/or the local geometries of matter. The extreme ultraviolet (EUV) generated by high harmonic generation (HHG) has a few tens femtoseconds to a few hundreds attoseconds pulse duration, and has enormous potential for ultrafast pump-probe study. Combining the ultrafast nature of HHG with absorption spectroscopy technique, EUV absorption spectroscopy could be used to investigate ultrafast dynamics of matter in femtoand atto-second time scales. Ti:Sapphire pulse laser (800 nm of central wavelength, ~50 mJ of pulse energy, ~50 fs of pulse duration) mainly performs creating EUV and even heating solid target. Fs laser increase temperature of target near ~ 1eV, matter falls in warm dense matter condition.
This work is supported by the NRF of Korea (No. 2013R1A1A1007084) and MPK Research Initiative Program (No. 2011-0031558).

P1-Pl.026*

Semi-analytic shape function of high-harmonic electron cyclotron emission in tenuous plasma

*조자원, 윤건수
*Jawon. Jo, GUNSU. YUN
POSTECH.

Keyword : electron cyclotron emission, emissivity, shape function, plasma diagnostics

The power spectrum of the electron cyclotron emission (ECE) from magnetized tenuous plasma contains very useful information on the electron velocity distribution. The first and second harmonic ECEs are commonly used for the electron temperature measurement in the case of large optical depths whereas the higher harmonic ECEs can provide information on the electron temperature and density as well as the energetic electron population deviating from the Maxwellian distribution. The ECE emissivity is represented by the "shape function", which is a function of frequency and harmonic number for given plasma temperature, density, and magnetic field intensity. The calculation of the shape function involves complicated numerical integration over the electron velocity distribution, which makes difficult the analysis of high harmonic ECEs. This work presents a general method for obtaining semi-analytic form of shape functions for high harmonic ECEs by fitting the integrand to an analytic function that can be readily integrated. Examples of high-harmonic (4th to 10th) ECE shape functions are provided for perpendicular view angle (perpendicular to magnetic field).

P1-Pl.028*

External magnetic Field Effect For Enhanced Raman Amplification in TeraHertz Regime with Plasma by using PIC code.

*라욱주, 허민섭 [1]
*Ook Joo. Ra, Min Sup. Hur[1]
울산과학기술대학교 (유니스트). [1] 울산과학기술대학교.

Keyword : Raman Amplification, Plasma , Simulation , PIC , TeraHertz

Three waves model 로 설명되는 Plasma 에서의 Raman Amplification 을 확인하고 외부 자기장의 효과로 인한 Wave Breaking Regime 에서의 변화를 분석, 설명하는 모델을 Terahertz 영역에 대하여 Simulation 하였다.

P1-Pl.029*

Ultraintense, Directional, Frequency Selective THz Radiation from Collision of Two Laser Pulses in a Tapered Plasma

*권규빈, 허민섭 [1]
*KyuBeen. Kwon, Min Sup. Hur[1]
울산과학기술대학교 (유니스트). [1] 울산과학기술대학교.

Keyword : Plamsa, Simulation, PIC, THz

We present a novel idea of generating terahertz (THz) pulses with ultraintense amplitude up to GV/m, high directionality, and well defined career frequency, from interaction of two counter-propagating laser pulses and a plasma. The colliding laser pulses induce a strong nonlinear current of electron plasma in the propagation direction of the laser pulses. By tapering down the plasma density near the collision point, a storng THz pulse is emitted with a high directionality. As the plasma oscillation is a fundamental source of radiating current, selection of radiation frequency up to several tens of THz is readily available just by changing the plasma density. Furthermore no low pass filter is required to seperate the laser pulses from the THz pulse which emits in perpendicular direction. Such a THz pulse has potentially wide applications in science research, such as selective pumping of phonon modes in solid target, or THz particle accelerators.

P1-Pl.031*

Control of Electron Energy in a Capacitively Coupled Discharge Combined with Inductive Source

*김진석, 허민영, 이해준
*Jin Seok. Kim, Min Young. Hur, Hae June. LEE
부산대학교.

Keyword : "Partice-in-Cell", "CCP", "ICP"

반도체, 디스플레이등의 많은 산업분야에서 플라즈마를 이용한 건식 식각 및 증착 공정은 매우 중요한 역할을 하고 있다. 용량결합형 (Capacitively coupled) 와 유도결합형 (Inductive coupled) 플라즈마 장비는 이러한 공정에서 필수적으로 쓰인다[1].

일반적으로 저압에서 용량결합형 플라즈마는 bi-maxwellian 전자분포를 가진다. 이러한 전자분포에서는 5 eV 이상의 에너지를 가지는 전자밀도는 급격하게 줄어든다. 하지만 CF_4, O_2, F_2 등의 플라즈마에서는 5 eV 이상의 에너지 범위에서 excitation, ionization, dissociative attachment 등이 활발하게 일어나므로 이 범위의 전자밀도를 조절하게 되면 식각공정에서 식각률이나 증착공정에서 증착률, 박막의 조성등을 조정할 수 있다[2].

이 연구에서 우리는 입자-셀 시뮬레이션 (Particle-in-cell simulation)을 이용하여 아르곤 가스에서 용량결합형 및 유도결합형 플라즈마가 결합된 시뮬레이션을 수행하고 경계에서 전압 및 $E_{y,wall}$ field 를 가해주면서 전자 에너지 확률 분포함수의 변화를 보았다. 그 결과 경계에서의 $E_{y,wall}$ field 가 증가할 수록 5 eV 이하의 전자밀도는 줄어들고 5 eV 이상의 전자밀도는 증가하는 모습을 관찰 하였다.

References

[1] D. B. Graves, IEEE Trans. Plasma Sci., 22, 31 (1994)
[2] H. C. Lee and C. W. Chung, Plasma Source Sci. and Tech., 24, 024001 (2015)

P1-Se.001

Investigation of Schottky barrier inhomogeneity in Cu/n-type Ge Schottky diodes

정찬영, 김세현, *김호경
Chan Yeong. Jung, Se Hyun. Kim, *Hogyoung. Kim
서울과학기술대학교.

Keyword : Germanium, Oxygen plasma, Barrier inhomogeneity

Germanium (Ge) has gained considerable interest as an alternative channel material for high-speed complementary metal-oxide-semiconductor (CMOS) devices due to its higher electron and hole mobilities compared to Si. However, strong Fermi-level pinning at the chare neutrality level, close to the valence band edge of Ge, creates a high Schottky barrier height at the metal/n-Ge interface, leading to a high contact resistance between metal/n-Ge contacts. Various surface treatments such as sulfur treatment, Se treatment, and plasma treatment have been employed to improve the device performance of the metal/Ge contacts. Oxygen plasma is known to be an effective, economical, environmentally safe method of cleaning surfaces during device fabrication. Temperature-dependent electrical characteristics provide insight into the conduction mechanism in thermionic emission theory; however, studies of n-Ge Schottky contacts have been limited to electrical characterization at room temperature. In this work, we fabricated Cu Schottky contacts to oxygen plasma-treated n-type Ge and investigated their temperature-dependent electrical properties over the temperature range of 100–300 K, with considering barrier inhomogeneity. Based on these results, further investigation will be discussed later.

P1-Se.002*

The CVD Grown Multilayer $MoSe_2$ Field-effect-transistor As a Highly Responsible Sensing Device for Detecting NO_2 gas

*백종열, 김선국 [1], Inturu Omkaram[1], 김승민 [2], 임혜린 [1], 홍영기 [1], 허재현 [3], 윤영기 [4]
*Jong-Yeol. Baek, Sunkook. Kim[1], Inturu. Omkaram[1], Seung Min. Kim[2], Hae Lin. Im[1], Young Ki. Hong[1], Jaehyun. Hur[3], Youngki. Yoon[4]
경희대학교 국제캠퍼스. [1] 경희대학교. [2] 한국과학기술연구원(KIST). [3] 가천대학교. [4]University of Waterloo.

Keyword : "$MoSe_2$", "NO_2 gas", "sensor", "CVD", "transistor"

Graphene-like 2-dimensional transition metal dichalcogenide (TMDC) materials has been largely enhanced for field-effect-transistors (FETs). They have many advantages, low cost, high sensitivity, high reliability and fast responsibility. 2-D multilayer semiconducting materials are prospective candidates for sensor applications because the TMDCs show highly sensitive electrical characteristics. These days, there are plenty of sensors for detecting lots of harmful gases using resistor type. But the resistor type sensors performance have a limitations, and have a comparably slow response time. On the contrary, transistor type, we can modulate the current by the gate electrode, so we can amplify the sensor response. Here, we present the possibility of the alternative gas sensor using $MoSe_2$ FET. We detected the NO_2 gas is one of the harmful toxic chemical gas. It can be easily faced with our lives. If we exposed at 3ppm of NO_2 environments about 8 hours, our lung functions decreased, so respitory circulation is getting worse. NO_2 gas is easily generated from the smoke of automobiles and power plants meet with acid rain. Our CVD grown $MoSe_2$ FET shows 5 $cm^2V^{-1}s^{-1}$ of field-effect mobility (μ), 10^5 of the on-off current ratio (I_{on}/I_{off}). So, our device seems proper candidates. When the device exposed at the different NO_2 environment, the channel materials absorbed the NO_2 molecules and the off current has increased. NO_2 molecules and $MoSe_2$ surface make physical bindings and it lead electrons accumulation. We performed 60 to 300ppm of NO_2 gas. The highest sensor response is calculated by almost 1900%. The physical bindings of NO_2 molecules and $MoSe_2$ surface induced electron generations in conduction band at the off region. So, the off current level is increased. And it can be easily break up the physical bindings by biasing high negative voltage at the gate.

P1-Se.003

Ferromagnetic properties of Si-doped GaN rods grown on Si(111) by plasma asisted molecular beam epitaxy

*레데파 마다카, 박병권, 이상태, 김문덕, 오재응 [1]
*Maddaka. Reddeppa, Byung-Guon. Park, Sang-Tae. Lee, Moon-Deock. Kim, Jae-Eung. Oh[1]
충남대학교. [1] *한양대학교.*

Keyword : Si-doped GaN rods, Ferromagnetism, Hydrogenation

In this paper, we have been investigated room temperature ferromagnetism on before and after hydrogenation of Si-doped GaN rods grown on Si (111) by plasma assisted molecular beam epitaxy. Hydrogenation was performed using a RIE system (13.56 MHz frequency), and processing parameters namely H_2 plasma power, pressure, gas flow were maintained as 150 W, 100 mtorr and 100 sccm respectively. Samples were characterized by X-ray diffraction, photoluminescence (PL) measurements, vibrating sample magnetometer (VSM). VSM measurements revealed that saturation of magnetization (M_s) and coercivity (H_c) at 300 k were about 1.67×10^{-4} emu and 230 Oe respectively with silicon concentration of 6×10^{18} cm^{-3} after subtracting effect of substrate diamagnetism. Hydrogenation of Si-doped GaN rods strongly suppresses the ferromagnetic behavior due to compensation of defects, impurities by the hydrogen. Thermal annealing of hydrogenated GaN rods at 400 ^{o}C revealed that recovery of ferromagnetic properties. Optical properties correlate with magnetic properties in order to find origin of ferromagnetism in Si-doped GaN rods. These results suggest ferromagnetism arises from defects like vacancies, impurities created by incorporation of Si into GaN nanorods.

P1-Se.004*

Achieving Thermodynamic Limit of Subthreshold Slope by Inserting Pillar Structure in Nanoscale Schottky Barrier Field Effect Transistor

Jung-Yong Lee, Sungchul Jung, *박기복
Jung-Yong. Lee, Sungchul. Jung, *Kibog. Park
Ulsan National Institute of Science and Technology.

Keyword : Schottky Barrier Field Effect Transistor, Subthreshold Slope, Thermodynamic Limit, TCAD, Pillar Structure

As the device size shrinks continuously by scaling in the current Si CMOS technology, subthreshold slope which is related to device operation and leakage current goes from “bad” to “worse”. Especially, the subthreshold slope modulation that is one of the most interesting topics in metal/oxide/semiconductor field effect transistor (MOSFET) technology is quite difficult to achieve. We propose a new device structure, edge-over Schottky barrier field effect transistor (SBFET) which turns out to show subthreshold slope around the thermodynamic limit of Si MOSFET, 60 mV/dec. The edge-over SBFET has a unique pillar structure where the transistor channel is elongated by going over the edge of pillar. Hence, the edge-over SBFET has a much longer channel compared with the conventional planar MOSFET with the same transistor pitch. The interfaces between thin poly-silicon channel and Al electrodes (source and drain) form Schottky junctions with small Schottky barriers < 0.2 eV. We performed 2-dimensional TCAD modeling on an edge-over SBFET with horizontal channel length of 5.5 nm and ultra-thin channel thickness of 2.0 nm. The TCAD modeling predicts subthreshold slope of ~67.2 mV/dec and OFF-state current of ~13.5 nA . It is also noticed that subthreshold slope gets closer to the thermodynamic limit as the pillar height increases.

P1-Se.005*

$(In_{0.53}Ga_{0.47}As)_n/(In_{0.52}Al_{0.48}As)_n$ SPS 구조의 두께(n=1-5 ML)에 따른 발광 특성

*조일욱, 류미이, 송진동 [1]
*Il-Wook. Cho, Mee-Yi. RYU, JIN DONG. SONG[1]
강원대학교. [1] *한국과학기술연구원.*

Keyword : 디지털합금, SPS, InGaAlAs, PL, TRPL

InP 기판 위에 성장한 디지털 합금 $(In_{0.53}Ga_{0.47}As)_n/(In_{0.52}Al_{0.48}As)_n$ SPS(short-period superlattice) 구조의 광학적 특성을 PL(photoluminescence)과 TRPL(time-resolved PL) 측정을 이용하여 분석하였다. $(In_{0.53}Ga_{0.47}As)_n/(In_{0.52}Al_{0.48}As)_n$ SPS 구조는 $In_{0.53}Ga_{0.47}As$ 와 $In_{0.52}Al_{0.48}As$ 의 단분자층(ML; monolayer)의 두께(n)를 1, 2, 4, 그리고 5 ML 로 조절하여 성장하였다. 10 K 에서 측정한 PL 피크 에너지는 1 ML 에서 5 ML 로 증가함에 따라 1.12 eV 에서 1.07 eV 로 적색편이 하였다. 이것은 n 이 증가함에 따라 양자우물의 폭이 증가하는 것으로 설명할 수 있다. 또한 5 ML 로 성장한 시료가 10 K 에서 가장 좁은 반치폭을 보였는데, 이것은 시료가 더 균일하게 성장되었음을 의미한다. 여기 광의 세기를 0.001 I_0 에서 I_0 까지 증가함에 따라 각 시료의 PL 피크 에너지는 각각 7.3, 6.9, 5.5, 그리고 3.3 meV 만큼 청색편이 하였다. 이 청색편이는 potential fluctuation state 와 관련된 band filling 효과에 의한 것으로 설명할 수 있다. 온도를 10 K 에서 300 K 까지 증가하였을 때, 약 40 K 까지는 PL 피크가 청색편이 하다가 그 이상의 온도에서는 적색편이 하였다. 또한 $(In_{0.53}Ga_{0.47}As)_n/(In_{0.52}Al_{0.48}As)_n$ SPS 구조의 운반자 동력학을 발광 에너지와 온도에 따른 TRPL 측정을 이용하여 분석하였다. PL 피크에서 측정한 PL 소멸시간은 n 이 2 ML 와 5 ML 인 시료에서 각각 0.78 ns 와 0.44 ns 로 측정되었다. n 이 증가함에 따라 양자우물의 폭이 증가하기 때문에 구속에너지가 감소하여 PL 소멸시간이 짧아진다. 또한 모든 시료가 발광 에너지가 증가함에 따라 PL 소멸시간이 감소하였는데, 이것은 높은 에너지 영역의 캐리어들이 낮은 에너지 영역으로 이완하는 것으로 설명할 수 있다. 온도를 증가함에 따라 각 시료의 PL 피크에서 측정한 소멸 시간은 점점 증가하였다. 이러한 결과로부터 $(In_{0.53}Ga_{0.47}As)_n/(In_{0.52}Al_{0.48}As)_n$ SPS 구조의 두께 n 을 적절히 조절함으로써 1.3-1.55 μm 영역대의 광통신 소자에 응용할 수 있는 최적의 조건을 찾을 수 있음을 확인하였다.

P1-Se.006

UHV RF magnetron sputtering 법으로 제작된 ZTO 박막의 특성 연구

홍승환, 오규진, *김은규
Seunghwan. Hong, Gyujin. Oh, *KIM Eun Kyu.
한양대학교.

Keyword : zinc tin oxide, ZTO, 산화물 반도체, UHV RF magnetron sputtering

Indium gallium zinc oxide (IGZO)로 대표되는 산화물 반도체(oxide semiconductor)는 높은 전기전도도와 가시광 영역에서의 우수한 투과성을 바탕으로 LCD(Liquid crystal display), PDP(Plasma display panel), OLED(Organic light-emitting diode)등의 다양한 표시 소자 및 TFT(Thin film transistor)등에 널리 사용되고 있다. 하지만 산화물 반도체에 가장 많이 사용되는 인듐(In)의 경우 가격이 비싸므로 비용절감을 위해 인듐(In)을 대체하는 산화물 반도체의 개발을 필요로 하며 또한, 초고화질, 고속 구동 및 대형화의 방향으로 발전하는 최신 디스플레이 기술에 산화물 반도체를 적용하기 위해서는 고이동도를 가지는 산화물 반도체의 개발이 필요하다. 이에 본 연구에서는 UHV RF magnetron sputter 를 이용하여 인듐(In)을 포함하지 않는 산화물 반도체 zinc tin oxide(ZTO) 박막을 성장시키고 ZTO 박막의 전기적 특성을 알아보는 연구를 진행하였다. UHV RF magnetron sputtering 방법으로 성장시킨 zinc tin oxide(ZTO) 박막은 X-ray diffraction(XRD)를 이용하여 박막의 결정구조를 확인하고, Hall measurement 를 이용하여 박막의 전기적 특성을 측정하였다.

P1-Se.007

The change of deposition time on the secondary direction and abnormal shape of grains growth of SnO_2 thin films

*정진
*Jin. Jeong
조선대학교.

Keyword : SnO_2
Thin Films
Abnormal Grain Growth
Hall Effect

Observations made under a high-resolution transmission electron microscope reveal the lattice shape characteristic of thin films, with an overlapped or wrinkled flower form, and indicate that thin films growth takes place in different directions during the secondary growth. Measurements of the Hall effect show that the carriers mobility in the thin films increases linearly with the deposition time, whereas the carrier density decreases. The Hall Rh value increased linearly until 20 min deposition time, whereas for thin film grown for 30 min it decreased rapidly, showing a relatively similar behaviour to the carrier density. This is because as the deposition time becomes longer, the second growth and atypical shape occurs, leading to an increase of the thin films Rh value.

P1-Se.008

Cu_2ZnSnS_4 나노입자가 포함된 PMMA 층의 두께 변화에 따른 비휘발성 메모리 소자의 전기적 특성과 동작 메커니즘

*이현재, 김유나, 김태환
*Lee. Hyun Jae, Kim. Yu Na, Kim. Tae Whan
한양대학교.

Keyword : CZTS, PMMA

이현재 [1,*], 김유나 [2], 김태환 [1,2,3]
[1] 한양대학교 융합전자공학부
[2] 한양대학교 나노반도체공학과
[3] 한양대학교 전자통신컴퓨터공학과
*E-mail: poporia527@hanyang.ac.kr

나노입자가 포함된 폴리머층으로 이루어진 나노복합체를 사용하여 제작한 비휘발성 메모리 소자에 대한 연구가 많이 진행되고 있다. 나노입자중에서 Cu_2ZnSnS_4 (CZTS)는 지각에 풍부하게 존재하는 원소로 구성되어 있어 저비용 제작이 가능하고, 밴드갭 조절과 비독성 성질을 가진다는 점에서 메모리 분야에 연구가 시도되고 있다. 이 실험에서는 용액공정과 스핀코팅 방법을 사용하여 polymethyl methacrylate (PMMA) 층에 삽입된 CZTS 나노입자를 전하 트랩 영역으로 활용하여 제작한 비휘발성 메모리의 동작 메커니즘에 대하여 연구하였다. 톨루엔에 PMMA 와 CZTS 나노입자를 녹여 혼합용액을 제작하였고, 스핀코팅 장비를 사용하여 CZTS 나노입자가 포함된 PMMA 층의 두께를 다양하게 조절하여 메모리 소자를 제작하였다. 제작한 소자의 전류-전압 측정 결과가 메모리 특성을 나타내는 것을 확인하였다. 에너지 밴드 대역도와 전류-전압 측정결과를 사용하여 제작한 메모리 소자의 동작 메커니즘을 규명하고 CZTS 나노입자가 전하 저장 영역으로서의 역할을 수행함을 확인하였다.

Acknowledgements
This research was supported by Basic Science Research Program through the National Research Foundation of Korea (NRF) funded by the Ministry of Education, Science and Technology (2013R1A2A1A01016467).

P1-Se.009

Study of Photon Trigger Efficiency of Silicon PhotoMutiplier

*이직, 이혜영, 전진아, 김민빈, 박일흥
*Jik. LEE, Hye Young. Lee, JinA. Jeon, Minbin. Kim, Il Hung. Park
성균관대학교.

Keyword : Silicon PhotoMutiplier, Trigger Efficiency

It is important to trigger photons with optimal singal to noise ratio for most photon-counting photo-sensors. We carried on a study of the photon trigger efficiency of two Silicon PhotoMutiplier devices a function of various operation parameters. We present the optimized result of the photon trigger efficiency for the devices.

P1-Se.010

co-sputtering 방법으로 증착한 Al 을 첨가한 ZnO 박막의 특성 분석

*오병성, 김재석
*Byungsung. O, Jaesuk. Kim
충남대학교.

Keyword : ZnO, Aluminuim, Transparent Conductive Oxide, co-sputtering

유리 기판 (Corning 2948 glass) 위에 ZnO(99.99%) target 과 Al(99.99%) target 을 사용하여 co-sputtering 방법으로 ZnO:Al 박막을 증착하였다. ZnO 증착 RF power 는 60 W 로 고정하고 Al 증착 DC power 를 조절하여 Al 의 함량을 조절하였고 증착 온도를 400℃로 고정하였다.

증착한 ZnO:Al 박막을 XRD 결과 모든 박막이 wurtzite 구조의 c-축 배향성을 가진 (002)면으로 성장하였고, Al DC power 를 증가시켜줌에 따라 피크가 증가하다 15 W 이상에서 감소하는 것을 관찰하였다. SEM 으로 측정한 두께는 모두 200 nm 내외이었고 Al DC power 가 증가할수록 결정입자의 크기가 커지다 다시 감소하였다. 사탐침법으로 측정한 면저항은 Al DC power 가 증가할수록 급격히 감소하다가 15 W 에서 최소값을 나타내고 그 이상에서는 증가함을 확인하였다. spectrophotometer 로 측정한 가시광 투과율은 유리기판 대비 80%이상으로 측정되었다.

P1-Se.011*

Effect of wet thermal oxidation on the intermixing in InGaAs/GaAs quantum well

*장영준, 윤예슬 [1], 김상현 [2], 박민수 [2], 최원준 [2]
*Young Jun. Chang, Ye Seul. Yun[1], SangHyeon. Kim[2], Min-Su. Park[2], Won Jun. Choi[2]
서울시립대학교. [1] 한국과학기술연구원. 서울시립대학교. [2] 한국과학기술연구원.

Keyword : InGaAs quantum well, QWI, wet thermal oxidation, photoluminescence

Quantum well intermixing (QWI) is a technique which tunes the band gap through the inter-diffusion between quantum well and barrier. In recent years, QWI has attracted for many applications such as non-absorbing mirrors for high power laser diodes and optoelectronic integrated circuits. Among various methods used to achieve the QWI, impurity-free vacancy disordering (IFVD) has shown to be effective since it can maintain good crystal quality. In this study, we report the effect of wet thermal oxidation-induced QWI with oxidation condition variation in InGaAs/GaAs QW. We performed the wet thermal oxidation at 400-550°C for 1 h using wet O_2, with followed with annealing at 850°C for 10 min. Also we investigated the effect of oxidation time by changing oxidation time from 30 min to 3 h at 450°C. As the oxidation temperature and time increases, the blue-shifts increase. Maximum blue-shift was about 60 meV for oxidized at 450°C for 3 h. [NRF-2014R1A1A1002868]

P1-Se.012*

디지털 합금 $(In_{0.53}Ga_{0.47}As)_{1-z}/(In_{0.52}Al_{0.48}As)_z$ 구조의 광학적 특성

*조일욱, 류미이, 송진동 [1]
*Cho Il-Wook. , RYU Mee-Yi. , SONG JIN DONG. [1]
강원대학교. [1] *한국과학기술연구원.*

Keyword : 디지털합금, InGaAlAs, PL, TRPL

MBE 로 성장한 디지털 합금(digital-alloy) $(In_{0.53}Ga_{0.47}As)_{1-z}/(In_{0.52}Al_{0.48}As)_z$ 구조의 광학적 특성을 PL (photoluminescence)과 TRPL (time-resolved PL) 측정을 이용하여 분석하였다. 디지털 합금 $(In_{0.53}Ga_{0.47}As)_{1-z}/(In_{0.52}Al_{0.48}As)_z$ 는 InP 기판 위에 성장하였으며, $In_{0.53}Ga_{0.47}As$ (우물)와 $In_{0.52}Al_{0.48}As$ (장벽)의 두께를 2 monolayer 로 고정하고 $In_{0.52}Al_{0.48}As$ 의 두께(z)를 0.2, 0.4, 그리고 0.6 으로 조절시키며 성장하였다. 10 K 에서 측정한 PL 세기는 z=0.6 으로 성장한 시료가 가장 강하게 나타났고, PL 피크 에너지는 z 가 0.2 에서 0.6 으로 증가함에 따라 0.96 eV 에서 1.24 eV 로 청색편이 하였다. z 가 0.6 인 시료의 PL 세기가 가장 큰 것은 $In_{0.52}Al_{0.48}As$ 의 두께가 증가함에 따라 양자우물의 폭이 좁아지기 때문에 양자 구속 효과(quantum confinement effect)가 증가하는 것으로 설명할 수 있다. 여기 광의 세기가 증가함에 따라 PL 피크는 높은 에너지 쪽으로 이동하였다. 이것은 여기 광의 세기가 증가함에 따라 potential fluctuation state 와 관련된 band filling 효과에 의한 것으로 설명할 수 있다. 온도를 증가함에 따른 PL 피크 에너지는 ~50 K 까지는 높은 에너지로 이동하다가 그 이상의 온도에서는 적색편이를 보였다. PL 피크에서의 PL 소멸시간은 z 가 0.2 와 0.6 인 시료에서 각각 1.36 ns 와 1.52 ns 로 측정되었다. 이것은 $In_{0.52}Al_{0.48}As$ 의 두께가 증가함에 따라 양자 구속 효과가 증가하여 더 긴 소멸시간을 갖는 것으로 설명할 수 있다. 또한 z 가 0.2 인 시료는 에너지에 따라 일정한 PL 소멸시간을 보인 반면, z 가 0.6 인 시료의 PL 소멸시간은 에너지가 증가함에 따라 감소하는 것을 보였다. 본 논문에서는 $In_{0.52}Al_{0.48}As$ 의 두께의 변화에 따른 광학적 특성을 PL 과 TRPL 을 이용하여 분석하였고, 이러한 결과로부터 1.3-1.55 μm 영역대의 광통신 소자에 응용할 수 있음을 확인하였다.

P1-Se.013*

In-plane Fowler-Nordheim tunneling and resistive switching memory devices enabled by thin oxide barriers designed on mono-layer graphene using atomic force microscope lithography

*김철겸, 이덕현, 이미정, 기은희, 오다예, 김종호, 원은아, 신민정, 박배호
*Cheol Kyeom. Kim, Duk hyun. Lee, Mi Jung. Lee, Eun Hee. Ki, DaYea. Oh, Jong Ho. Kim, EunA. Won, minjung. shin, Bae Ho. PARK
건국대학교.

Keyword : Graphene, Graphene oxide, Transistor, Memory, AFM lithography

Recently, various electronic components including transistor, barristor, memory, and transparent electrode were implemented using graphene. While integrated circuits (IC) were demonstrated by combining graphene transistors and passive components, system on chip (SoC) platform, state-of-the-art CMOS technology, by combining transistors and memories on the same chip, has not yet been demonstrated. The main obstacle of the realization of SoC is the complexity of fabrication processes originated from the process differences between the transistors and the memories. In this study, using simple and clean atomic force microscope (AFM) lithography, we fabricated both the switching devices and the memories by forming very thin graphene oxide (GO) barriers in mono-layer graphene at the controlled oxidation voltages. Formed with 7V (9V), the lateral graphene/GO/graphene junction exhibits switching of Fowler-Nordheim tunneling (FNT) current (resistive memory behaviors). The combination of high Ion/Ioff (~ 1000) of the switching device and nonvolatility of the memory device fabricated by the same process demonstrates the possibility of graphene SoC platform.

P1-Se.014*

고감도 센서로의 적용을 위한 아민 기능화된 단일벽탄소나노튜브 연구

*김재성, 정영철 [1], 이제행, 최선우, 변영태
*Jaeseong. KIM, Youngchul. CHUNG[1], Je Haeng. LEE, Sun-Woo. CHOI, Young Tae. BYUN
한국과학기술연구원. [1] 광운대학교.

Keyword : SWCNT, Amine, 고감도센서, 표면처리, 선택성

1993 년 Sumio Iijima 에 의해 단일벽탄소나노튜브 (SWCNTs : Single Walled Carbon Nanotubes)가 발견된 이래로, SWCNT 의 뛰어난 전기적, 화학적, 기계적 성질이 알려지면서 다양한 분야로의 연구 및 개발이 확장되고 있다. 그 중 SWCNT 의 외벽에 특정 가스 분자가 흡착될 때 전기 전도성이 크게 변화한다는 연구결과가 보고되면서, SWCNT 는 고감도 센서의 촉망 받는 소재중 하나로 큰 주목을 받고 있다. 고감도 센서로 SWCNT 를 적용하기 위해서는 미량의 가스에도 반응할 수 있는 민감도와 다종의 가스에서 특정 가스를 선별하여 검지할 수 있는 선택성이 보장되어야 한다. 본 연구에서는 SWCNT 기반의 센서가 특정 가스에 대한 높은 반응도와 선택성을 갖게 하기 위해 아민 기능화 기법이 사용되었다. 아민 그룹 중 아미노 실란을 포함하는 APTES 와 en-APTAS 가 SWCNT 에 표면처리된 후 센서가 제작되었다. 그 후, 포토리소그래피로 인해 생기는 오염을 방지함으로서 센서 특성의 안정성과 신뢰성 확보를 위해 섀도우 마스크 (shadow mask)를 이용하여 전극이 제작되었다. 특정 가스에 대한 감응도를 평가하기 위해 제작된 센서가 NO 분위기에서 시간에 따른 저항의 변화가 측정되었다.

P1-Se.015

산화물-단일벽 탄소 나노튜브 헤테로 구조를 이용한 나노센서의 가스 감응특성
(Gas sensing performances of nanosensors using oxides-single walled carbon nanotube heterostructures)

*최선우, 김재성, 이제행, 김신근, 김선호, 변영태
*Sun-Woo. Choi, Kim jaeseong. , Lee Je Haeng. , Shin Gun. Kim, Sunho. Kim, BYUN Young Tae.
한국과학기술연구원.

Keyword : 산화물, 단일벽 탄소 나노튜브, 헤테로 구조, 나노센서

단일벽 탄소나노튜브 (single-walled carbon nanotube : SWCNT)를 포함한 탄소기반 나노물질은 그들이 가진 탁월한 물성 (뛰어난 체적 대비 표면적비, 우수한 전기전도도 등)으로 인해 극미량의 화학물질 검출을 위한 화학센서 분야에서의 연구가 활발히 진행 중에 있다. 그러나 나노화학 센서로서 실용화되기 위해서는 특정 화학물질에 대한 선택성과 감응특성의 증진이 더욱 요구되고 있다. 특히, 표면 기능화 또는 표면 개질을 이용한 탄소기반 나노센서에 관련된 연구가 활발히 보고되고 있다. 탄소기반 나노센서의 표면 기능화를 위한 연구들 중에서는 작용기 (functional group), 결함 (defect), 그리고 촉매 물질 (catalyst) 등을 활용한 연구들이 진행되고 있는데, 본 연구에서는 스프레이 기법을 이용하여 네트워킹된 SWCNTs 기반 센서 플랫폼이 제작되고, 기상증착법을 이용하여 SWCNT 표면이 산화물로 기능화된 후, 이에 따른 가스 감응 특성이 평가되었다. 특히, 산화물 기능화 처리가 NO2 가스에 대한 감도와 감응 특성 (반응 시간, 회복 시간 등)에 미치는 영향이 조사되었다.

P1-Se.016

Study of Metal-insulator Transitions of VO_2 thin films grown on various sapphire substrates using RF magnetron sputtering deposition

*정대호, 이호선, 소현섭, 고건희, 박준우
*Daeho. JUNG, Hosun. LEE, Hyeon Seob. So, KunHee. Ko, Jun Woo. Park
경희대학교.

Keyword : VO_2, RF magnetron sputtering, c- r- a- and m-plane sapphire, XRD, SEM

Vanadium dioxide (VO_2) has been studied most intensively owing to its near-room-temperature phase transition as well as its high phase stability. VO_2 thin films with ~120 nm in thickness were grown on c-, r-, a-, and m-plane sapphire substrates under identical conditions by RF magnetron sputtering deposition using a VO_2 target. The sputtering pressure was set at 6 mTorr with 10 sccm flow of O_2 gas. All samples were grown at 500℃. After sputtering deposition, all samples were annealed with 1 sccm of O_2 flow for 20min. The structural and morphological properties of all samples were studied by X-ray diffraction (XRD), scanning electron microscopy (SEM), and Raman spectroscopy. We measured the sheet resistivities as a function of temperature. We discussed the stress dependence of the thermal hysteresis of the sheet resistivity of the VO2 thin films which wer4e grown on various planes of sapphire substrates.

P1-Se.017*

Variation of Raman scattering of stacked molybdenum disulfide bilayer depending on twisted angle

*박세기, 이용준, 김현, 김용범, 김정용
*Seki. Park, Yongjun. Lee, Hyun. Kim, Youngbum. Kim, Jeongyong. Kim
나노구조물리연구단. 기초과학연구원. 성균관대학교.

Keyword : molybdenum disulfide, interlayer coupling, raman scattering, vertically herterostructure

Stacking of triangular MoS_2 grown by chemical vapor deposition is an intriguing method to investigate the physical properties affected by subtle interlayer interaction. The difference of relative crystal orientation in vertically prepared heterostructure affects the interlayer interaction that have different effect of the electrical and optical properties. Here, we show that Raman spectroscopy studies of mechanically stacked bilayer MoS_2 changes in Raman frequencies and intensities depending on twisted angle. In addition, the variation in the Raman properties for twisted MoS_2 through near-resonance excitation will be discussed. Our observation can be extended to the investigation of the influence of interlayer interaction by twist angle other transition metal dichalcogenide heterostructures.

P1-Se.018

Characterization of Heterostructured ZnO-SnO_2 Superlattice Thin Films and Their Field Effect Electronics Properties

*이수재, 황치선 [1], 조경익 [1], 조성행 [1]
*Su Jae. Lee, Chi-Sun. Hwang[1], Kyoung-Ik. Cho[1], Sung Haeng. Cho[1]
한국전자통신연구원(ETRI). [1]ETRI.

Keyword : Oxide semiconductor, ZnO, SnO2, superlattice, TFT

Heterostructured ZnO-SnO_2 superlattice thin films consisting of ZnO and SnO_2 layers were produced by alternating the pulsed laser ablation of ZnO and SnO_2 targets, and their structural and field effect electronic transport properties were investigated as a function of the thickness of the ZnO and SnO_2 layers. The performance parameters of heterostructured ZnO-SnO_2 superlattice thin film transistors (TFTs) are highly dependent on the thickness of the ZnO and SnO_2 layers. The highest electron mobility of 43 $cm^2/V{\cdot}s$, a low subthreshold swing of a 0.22 V/dec. threshold voltage of 1 V, and a high drain current on-to-off ratio of 10^{10} were obtained for the heterostructured ZnO(1.5 nm)-SnO_2(1.5 nm) superlattice TFTs, which are enough to operate next-generation microelectronic devices. These results are presumed to be due to the unique electronic structure of an heterostructured ZnO-SnO_2 superlattice thin films consisting of ZnO, SnO_2 and ZnO-SnO_2 interface layers. Figure shows (a) high-resolution cross-sectional STEM images and (inset) SAED patterns for heterostructured ZnO-SnO_2 superlattice thin film, and (b) performance parameters including the saturation mobility (m_{sat}), subthreshold swing (ss) and threshold voltage (V_{th}) of amorphous ZnO-SnO_2 superlattice TFTs as a function of ZnO and SnO_2 layer thicknesses.

P1-Se.019*

Extraction of interfacial and border traps from conductance method in MOS structures

*황수빈, 정광식, 조만호
*Soobin. Hwang, Kwang Sik. Jeong, Mann-Ho. Cho
연세대학교.

Keyword : defect, interface trap, border trap, III-V compound semiconductors, conductance method

With rapid growth of device density, silicon is reaching its physical limitation, which is classical substrate for MOS devices. III-V compound semiconductors such as GaAs, GaN, InGaAs, and InP are expected to replace Si. They have faster electronic carrier mobility than that of Si, so they have better electrical performance than Si. Simultaneously, high-k materials are replacing SiO_2 to reduce leakage current. However, since high-k materials have more defects than SiO_2 and hard to be controlled, many researchers have been concerned about defect of oxides. Conductance method is one of the well-known measurement to find defect density. Measured defect density with conductance method often contains both interface trap density and border trap density.
In this study, 3D contours of conductance could be acquired in TiN-HfO_2-InP MOS capacitor by multiple measurement of conductance method for a range of frequencies. By fitting contours, two defect states could be extracted, which are regarded as interface trap and border trap. Spatial profile of border trap was also acquired with calculating border trap density for the defect depth. Moreover, step-by-step rising electrical stresses were given to generate the defects in oxide. Sets of electrical measurements, which consist of C-V measurement, conductance method, and I-V measurement, were performed after each step of stress, by which we could trace defect generation in both spatial and energy profile. This study showed that both spatial distribution and energy distribution can be observed and classified by single measurement, the conductance method.

P1-Se.020

Bi-stable resistance switching property and Ferroelectric behavior in Potassium-doped ZnO thin films

*이주원, 손윤, 가나파티, 강태원, 박창수 [1], 김은규 [1]
*Ju Won. Lee, Yoon. Shon, N.G.. Subramaniam, Tae Won. KANG, Chang Soo. PARK[1], Eun Kyu. KIM[1]
동국대학교. [1] *한양대학교.*

Keyword : ZnO, Ferroelectric property, Electrodeposition

Potassium(K)-doped ZnO thin films electrodeposited on Indium Tin Oxide (ITO) coated glass substrates exhibited ferroelectric behavior with a remnant polarization of 0.2μC/cm^2. Especially, wave forms showing the applied input voltage V_i and output voltage V_o were obtained for Al/ZnO:K/ITO structure. It exhibits a superposition of V_i(input) and V_o (output) signal from Al/ZnO:K/ITO structure with a clear phase shift between the two wave forms which again confirms that the observed ferroelectric hysteresis curve is not related to leaky dielectric materials. The Current-Voltage characteristics of Al/ZnO:K/ITO structures measured for several cycles revealed bi-stable switching characteristics. The reproducible bi-stable switching characteristics for the mentioned structures had good retention in one particular resistance state. Around one order of switching was realized between low and high resistance states. The switching property thought to be polarization induced originating out from the ferroelectric properties of the potassium doped ZnO thin film. The switching between ZnO:K/ITO interface is assumed to be critical for stability in switching for several cycles. Possible application of this structure in non-volatile memories is explored.

P1-Se.021*

Fast Photodetector based on CVD-grown Multilayer $MoSe_2$ Thin Film Transistor

*문현성, 정철승, 김선국 [1]
*Hyunsung. MOON, Chulseung. Jung, Sunkook. Kim[1]
경희대학교 국제캠퍼스. [1] *경희대학교.*

Keyword : "$MoSe_2$", "TMDCs" , "CVD" , "photodetector"

Two-dimensional materials have large potential for photo-device. In order to large area synthesis of Transition metal dichalcogenides (TMDCs), many people think Chemical vapor deposition (CVD) is best way. So we grow hexagonal multilayer Molybdenum diselenide ($MoSe_2$) by CVD. Commonly, TMDCs grown by CVD is mono or few layer. However, if we use high pressure condition (>760 Torr), we can grow multilayer $MoSe_2$ which has 12nm thickness. We use MoO_3 and Se powder as a source. Ar gas is a carrier gas and H2 gas acts as a catalyst. Left side of furnace temperature was ramped up to 800℃ for the source and right side of furnace temperature 750℃ for the substrate. Commonly, $MoSe_2$ is n-type semiconductor. But, Our CVD grown multilayer $MoSe_2$ thin film transistor (TFT) show p-type dominant ambiploar behaviors We assume that large density of trap sites created by high temperature during the CVD growth influence the band structure of hexagonal $MoSe_2$ multilayers. In order to derive the sub gap states, we measure transfer curve of CVD grown hexagonal $MoSe_2$ TFT at different temperatures between T = 300 and 400K. We can calculate Density of state (DOS) using temperature dependent characteristics. DOS show CVD grown Hexagonal $MoSe_2$ has many trap sites. So Our $MoSe_2$ TFT show an ambipolar behavior with a p-tddddddddype characteristic. Our $MoSe_2$ has the highest field effect mobility 10 $cm^2/V{\cdot}s$ and an ON/OFF current ratio of ~10^3 , and the electron mobility was extracted as 2.14 $cm^2/V{\cdot}s$, at the positive region. The output characteristics (I_{ds}–V_{ds}) show depict clear p-type behaviors in the negative V_{ds} range.
In order to measure the optoelectronic properties of $MoSe_2$ multilayers, we examine the photoresponse of the TFTs. We measure the transfer characteristics under illumination with a 638nm laser as a function of V_{gs} at various incident power densities (from 20 to 2560 mW/cm^2). Our CVD grown $MoSe_2$ TFT show a high photoresponsivity (93.7 A/W) and a fast photoresponse time (τ_{rise} ~0.4 s). This is the highest value reported up to date concerning CVD-grown $MoSe_2$ TFTs, and the photoresponsivity is also comparable to that of mechanically exfoliated $MoSe_2$ TFT. So CVD grown multilayer MoSe2 TFT has possibility for photodetector application.

P1-Se.022

Growth and Characterization of Intermediate Band Solar Cell Structures with ZnO/CdS/ZnTe:Cr/GaAs

이경수, 오규진, *김은규
Kyoung Su. Lee, Gyujin. Oh, *Eun Kyu. Kim
한양대학교.

Keyword : Pulsed laser deposition, CdS, ZnTe:Cr

Low-cost, high efficiency solar cells are tremendous interests for the realization of a renewable and clean energy source. ZnTe based solar cells have a possibility of high efficiency with formation of an intermediated energy band structure by impurity doping. In this work, the ZnO/CdS/ZnTe:Cr/GaAs structure was fabricated by pulsed laser deposition (PLD) technique. A pulsed (10 Hz) Nd:YAG laser operating at a wavelength of 266 nm was used to produce a plasma plume from an ablated a ZnTe target, whose density of laser energy was 4.5J/cm^2. The base pressure of the chamber was kept at a pressure of approximately 4x10^{-7} Torr. ZnTe:Cr thin film with thickness of 400 nm was grown on to p$^+$-GaAs, and then CdS and ZnO thin film were grown on ZnTe:Cr thin film. Thickness of CdS and ZnTe:Cr were 100 nm and 500 nm, respectively. The Cr content in the ZnTe:Cr thin film was about 4.0 at%. For fabricating ZnO/CdS/ZnTe:Cr solar cells, Al metal was deposited on the ZnO thin film by thermal evaporation method. For ZnO/CdS/ZnTe:Cr solar cell structures, the electrical property was characterized by using HP 4156-a semiconductor parameter analyzer. Their solar cell performance was also measured using an Air Mass 1.5 Global (AM 1.5 G) solar simulator with an irradiation intensity of 100 mW cm^{-2}.

P1-Se.023

수소 처리된 $Zn_{0.8}Co_{0.2}O$ 의 gate 전압에 따른 자기수송 현상

*천미연, 조용찬 [1], 박철홍, 이근우 [1], 정세영
*CHEON Miyeon. , CHO Yong Chan. [1], PARK Chul-Hong. , LEE Geun Woo. [1], JEONG Se-Young.
부산대학교. [1] 한국표준과학연구원.

Keyword : ZnO, Hydrogen, magnetotransport

수소 처리된 $Zn_{0.8}Co_{0.2}O$ 를 field effect transitor 구조로 만든 후 7 K 의 자기적 수송 현상을 연구하였다. 자기장을 가하지 않았을 때의 저항은 양의 gate 전압이 가해진 경우에는 조금 감소한 반면 음의 게이트(gate) 전압이 가해진 경우에는 증가하였다. 이것은 본 시료가 전기 수송현상이 전자에 의해 일어나는 n-type 채널을 가졌다는 것을 의미한다. 또한 gate 전압이 0 인 경우 자기장 μ_0H= 3 T 에서 거의 31 %에 이르는 큰 양(positive)의 자기저항을 보였고 이 자기저항은 gate 전압이 음의 값으로 절대값이 점점 커지면 커질수록 증가하였다. 자기장에 따라 변하는 자기저항의 거동으로부터 전하의 밀도와 이동도(mobility)가 게이트 전압에 따라 어떻게 변하는지를 계산하였다.

P1-Se.024

Diamagnetic Shift of a InGaP-AlInGaP Semiconductor Single Quantum Well under Pulsed-magnetic Fields

*김용민, 신용호, 송진동 [1]
*Yongmin. KIM, Y. H.. Shin, J. D.. Song[1]
단국대학교. [1]KIST.

Keyword : high magnetic fields, semiconductor quantum well, photoluminescence, exciton

Application of magnetic fields is important to characterize the carrier dynamics in semiconductor quantum structures. We performed photoluminescence (PL) measurements from an InGaP-AlInGaP single quantum well under pulsed magnetic fields to 50 T. The zero field interband PL transition energy matches well with the self-consistent Poisson-Schrödinger equation. We attempted to analyze the dimensionality of the quantum well by using the diamagnetic shift of the magnetoexciton. The real quantum well has finite thickness that causes the quasi-two-dimensional behavior of the exciton diamagnetic shift. The PL intensity diminishes with increasing magnetic field because of the exciton motion in the presence of magnetic field.

P1-Se.025

Ammonia 와 Na_2EDTA 가 CBD-ZnS 박막에 미치는 영향

이동찬, 안희진, *엄영호
Dong Chan. Lee, Hee Jin. Ahn, *UM Young Ho.
울산대학교.

Keyword : Chemical Bath Deposition, Zinc Sulfide, CIGS

CIS 계 박막태양전지에서 버퍼층으로 사용되고 있는 CdS 는 Cd 의 독성으로 인해 Cd-free 인 대체 버퍼층이 요구되고 있다. ZnS 계 물질은 3.4~3.9 eV 정도의 광학적 띠 간격 에너지를 가지는데, ZnS 계 버퍼층을 증착하는 공정으로는 chemical bath deposition (CBD), molecular beam epitaxy (MBE), thermal evaporation, spray pyrolysis, sputtering, electro-deposition 등의 다양한 공정이 사용되는데, 이 중에서 CBD 공정은 여러 공정 중 제조 단가가 낮고 성장 시간이 짧으며 효율이 비교적 높아 많이 사용된다. 본 연구는 CBD 공정으로 성장시키는 ZnS 박막의 특성을 결정하는데 있어서 중요한 요소인 용액의 pH 를 조절할 수 있는 암모니아 및 Na_2EDTA 의 양을 조절해서 박막의 표면을 pin-hole 을 최대한 억제시켜 박막의 효율을 극대화시키려 했다. Zn 의 원료로는 zinc sulfate heptahydrate($ZnSO_4 \cdot 7H_2O$), S 의 원료로는 thiourea($(NH_2)_2CS$) 를 그리고 용매로는 증류수(distilled water)를 사용하였다. 그리고 ZnS 박막의 특성을 변화시킬 요소인 complexing agent 로 염기용액에서 ammonium hydroxide(NH_4OH)를, 산성용액에서 Na_2EDTA 를 사용하였다. ammonium hydroxide 와 Na_2EDTA 를 complexing agent 로 썼을 경우 모두 투과율은 가시광선 영역에서 대략 60%이상으로 비슷한 경향을 보였다. 하지만 ammonium hydroxide 의 첨가량이 증가함에 따라 띠 간격 에너지는 3.6 ~ 3.4 eV 로 줄어들었고 Na_2EDTA 첨가량이 증가함에 따라 띠 간격 에너지는 3.3 ~ 3.6 eV 로 늘어나는 경향을 보였다.

P1-Se.026

FTO glass 기판에 성장된 ZnSe 나노선의 성장과 결정구조 및 광학적 특성 분석

*송만석, 김용
*Man Suk. Song, Yong. Kim
동아대학교.

Keyword : 나노선, nanowire, FTO, ZnSe, VLS, polytypism

금(gold) 나노입자는 기상-액상-고상 (vapor-liquid-solid) 기구에 의한 나노선 성장에서 널리 사용되는 촉매이다. 그러나 금은 나노선에 깊은 준위를 형성하므로 이를 대체할 새로운 촉매가 널리 탐색되고 있다. 하나의 가능성으로 저온의 융점을 가진 Sn 은 촉매로 성장된 나노선 연구를 수행된 바 있다. 이를 응용하여 감광형 태양전지에서 널리 사용되는 FTO (Fluorine-doped tin oxide) glass 기판에서의 촉매를 이용한다. FTO 기판을 저온부에 놓고 고온부에 ZnSe 가 담긴 보트를 두어 물리기상수송법에 의하여 ZnSe 나노구조물을 성장하였다. 전계방출주사전자현미경(FESEM), 투과전자현미경(TEM), X 선 회절(XRD)을 이용해 결정학적 구조와 성장원리를 분석하였고, micro-PL 을 이용하여 광학적 특성을 알아보았다. II-VI 화합물 반도체 물질의 나노선 성장에서 자주 나타나는 Zinc blende 와 Wurtzite 의 polytypism 현상에 대해 분석한다. This research was supported by the Basic Science Research Program through the National Research Foundation of Korea (NRF) funded by the Ministry of Education, Science and Technology (2015R1D1A3A01015615).

P1-Se.027

Structural and optical properties of GaN epitaxial layer grown on nano-patterned Si(111) substrate by MOCVD

*임기영, 김종옥, 이훈기
*Kee Young. Lim, Jong Ock. Kim, Hoon Ki. Lee
전북대학교.

Keyword : GaN, Si(111), Nano-pattern, MOCVD

In this work, we investigate the structural and optical properties of the GaN epitaxial layer grown on nano-patterned Si(111) substrate by metal organic chemical vapor deposition(MOCVD). Thin Platinum(Pt) layer was deposited on Si(111) substrate using ion-sputtering, followed by thermal annealing to form Pt nano-droplets which act as masking layer during dry-etched with inductively coupled plasma-reactive ion etching to generate nano-patterned Si (111) substrate. The pattern-free and micro-patterned Si(111) substrates were prepared to compare with nano-patterned Si(111) substrate. GaN epitaxial layers were grown on pattern-free, micro- and nano-patterned Si (111) substrate under identical growth conditions for comparison. The structural and optical properties of the GaN epilayers were investigated by using optical microscopy (OM), scanning electron microscopy (SEM), atomic force microscopy (AFM), x-ray diffraction (XRD), transmission electron microscopy (TEM) and photoluminescence(PL) measurement.

P1-Se.028*

Current-Voltage characteristics-based extraction of interface states in $In_{0.7}Ga_{0.3}As$ MOSFETs

*김성광, 금대명, 박민수, 김상현, 최원준
*Seong Kwang. Kim, Dae-Myeong. Geum, Min-Su. Park, SangHyeon. Kim, Won Jun. Choi
한국과학기술연구원.

Keyword : III-V MOSFETs, Interface trap density

We propose a technique for extraction of interface trap density D_{it} in III-V metal-oxide-semiconductor field-effect transistors (MOSFETs). This technique is simultaneous extraction of surface potential and D_{it}. It is based on the only experimental I-V characteristics under subthreshold region and advantageous to apply to III-V MOSFETs with nonlinearity in the subthreshold swing caused by a none-uniform distribution of interface trap over the bandgap. We applied the technique to $In_{0.7}Ga_{0.3}As$-on insulator (-OI) III-V nMOSFETs with W/L = 20/100, 20/50, 20/25 mm/mm on the same wafer. Extracted interface trap density ranges $D_{it} = 10^{11}$~10^{12} $eV^{-1}cm^{-2}$.

P1-Se.029

Composition dependence of optical and electrical properties of $Zn_{1-x}Sn_xO$ thin films grown using RF sputtering deposition

*고건희, 이호선, 소현섭, 정대호, 박준우
*KunHee. Ko, Hosun. LEE, Hyeon Seob. So, Dae ho. Jung, Jun Woo. Park
경희대학교.

Keyword : zinc tin oxide,transparent thin film transistors,rf sputtering,ellipsometry,optical gap

Transparent amorphous semiconductor oxides have wide range of application areas in flat panel displays, photovoltaics, transparent thin film transistors (TTFT), and transparent memory devices. $InGaZnO_4$ are the most popular thin-film material for TTFT applications, because it has a high electron mobility, even in an amorphous material. However, the complicated composition of IGZO makes precise control of the composition and oxygen stoichiometry rather difficult, and In and Ga are scarce. This has caused the investigation of zinc tin oxide (ZTO, $Zn_{1-x}Sn_xO$) for use in the channel layer of TTFTs. Here, we investigated the optical and electrical properties of amorphous and crystalline zinc tin oxide thin films grown by using co-sputtering deposition method at room temperature. Co-sputtered targets were SnO_2 and ZnO targets. Varying the relative power ratio of the two targets, we controlled the Sn and Zn composition of ZTO. Through annealing, the as-grown amorphous oxides were transformed to crystalline oxides. The dielectric functions were obtained from the measured ellipsometry angles, ψ and Δ. We determined the absorption coefficients and optical gap energies of ZTO thin films from the dielectric functions with varying compositions. Using Hall effect measurements, we measured the carrier concentrations and electron mobilities with varying compositions.

P1-Se.030*

Synthesis of Mg Doped ZnO Thin Film by Pulse Laser Deposition and Its Optical, Electrical Properties

김선호, Farman Ullah, *김용수
Sun-Ho. Kim, Farman. Ullah, *Yong Soo. Kim
울산대학교 물리학과 및 EHRSC.

Keyword : Oxide, Mg doped ZnO, Hall mobility, transparent

Transparent thin films have drawn researcher's attentions across the globe due to its great importance in practical applications, such as, display systems. Indium Gallium doped Zinc Oxide (InGaZnO) is the most studied material in this regard. α-InGaZnO is a rare earth material having good optical and electrical properties. α-InGaZnO is approximately 80% transparent with good mobility (~10 $cm^2/V\cdot s$) [1]. On the other hand, MgZnO is naturally abundant material offering the approximately the same optical and electrical properties. Here in this study, we evaluate the optical and electrical properties $Mg_xZn_{1-x}O$ (x=0.1) thin film deposited by pulse laser deposition technique (PLD). The films were characterized by UV-vis spectrum, scanning electron microscopy and Hall measurement system. The 180 nm thick thin film was found to be approximately 78% transparent at visible range. From transmission spectra the optical band gap was calculated and was found to be 3.62 eV. Finally, the Hall measurement was done to evaluate the electrical properties. The $Mg_xZn_{1-x}O$ (x=0.1) thin film show n-type semiconducting behavior with carrier concentration 6.29 x 10^{17} #/cm^3 Moreover, the resistivity and hall mobility were found to be 2.398 Ω·cm, 4.14 $cm^2/V\cdot s$ respectively.
[1] J. B. Kim, et al., Appl. Phys. Lett. 93, 242111 (2008).

P1-Se.031*

H_2O_2 표면처리에 의한 unintentionally doped GaN Schottky 다이오드의 전기적 특성변화 연구

*오의영, 레데파 마다카, 박병권, 이상태, 김문덕, 김송강 [1]
*Eui-Young. Oh, Maddaka. Reddeppa, Byung-Guon. Park, Sang-Tae. Lee, Moon-Deock. Kim, Song-Gang. Kim[1]
충남대학교. [1] 중부대학교.

Keyword : defect,DLTS,GaN,leakage current,Shottky diode

본 연구는 GaN Schottky 다이오드 제작 시, H_2O_2 표면처리에 따른 전기적 특성 변화를 current-voltage(I-V) 측정과 deep level transient spectroscopy (DLTS) 법을 이용하여 조사하였다. 실험에 사용된 GaN 박막은 Si(111) 기판 위에 plasma-assisted molecular beam epitaxy 법으로 성장되었으며, 표면처리하지 않은 GaN 박막과 상온에서 H_2O_2 수용액에 표면처리 한 GaN 박막 위에 Schottky 및 저항성 접촉의 금속으로 Ni(20 nm)/Au(100 nm)와 Cr(20 nm)/Au(100 nm)를 각각 사용하였다. I-V 측정 결과, 표면처리하지 않은 GaN Schottky 다이오드 및 상온에서 표면처리한 GaN Schottky 다이오드의 경우 -5 V 에서 각각 -3.41×10^{-4} A 와 -5.62×10^{-5} A 로 H_2O_2 표면처리 이 후 누설전류가 감소하는 것을 확인하였다. 표면 처리하지 않은 GaN Schottky 다이오드의 DLTS 측정을 통하여 E_1=0.46 eV 와 E_2=0.70 eV 에 해당하는 결함 신호를 각각 관측한 반면에 상온에서 표면 처리한 GaN Schottky 다이오드의 경우 E_1=0.46 eV 의 신호만 관측되었다. I-V 측정과 DLTS 신호를 통하여 GaN Schottky 다이오드 제작 시 형성되는 결함의 종류를 확인하였으며 H_2O_2 표면처리 및 측정 조건 변화에 따른 결함의 거동과 누설 전류의 원인에 대하여 분석 설명하였다.

P1-Se.032*

단일 실리콘 나노선/그래핀 나노리본 이종접합 다이오드의 소자 특성 연구

김주환, 김정길, 김정현, 이대훈, *최석호
Ju Hwan. Kim, Jungkil. Kim, Jung Hyun. Kim, Dae Hun. Lee, *CHOI Suk-Ho.
경희대학교.

Keyword : 실리콘 나노선, 그래핀 나노리본, 이종접합, 다이오드, 화학적 식각기술

Si 은 거의 모든 전자소자의 재료로 사용되고 있으나 웨어러블 디바이스 측면에서는 유연성, 투과도 등의 특성이 뛰어난 물질로의 가공이 필요하다. 실리콘 나노선은 배터리, 태양전지, 바이오 센서, 및 트랜지스터 등, 많은 소자에 응용되고 있으며 그래핀은 뛰어난 물리화학적 특성들 때문에 최근에 투명하고 휘어지는 전극의 소재로서 주목을 받고 있다. 본 연구에서는 간단한 방법으로 실리콘 나노선과 그래핀 나노리본을 이용하여 이종접합 다이오드 소자를 제작하였다. Si 으로부터 금속촉매를 사용한 화학적 식각기술 (Metal-assisted chemical etching)을 이용하여 균일한 직경과 부드러운 표면을 가지는 실리콘 나노선을 제작하고 Si 기판에서 뜯어내어 에탄올에 분산시켰다. 이렇게 혼합된 용액을 화학기상 증착법으로 성장한 단층 그래핀 위에 스핀코팅한 후, O_2 플라즈마 처리를 하였다. 그 결과, 노출된 그래핀은 O_2 플라즈마에 의해 식각되고, 실리콘 나노선 밑의 그래핀은 선택적으로 남아 그래핀 나노리본을 형성하였다. 즉, 단일 실리콘 나노선/단일 그래핀 나노리본 이종접합 구조를 제작하였으며 그 광학적 및 구조적 특성을 라만 분광법, 주사 전자 현미경, 및 원자 힘 현미경으로 분석하였다. 이 이종접합 소자에 대해 전류 힘 현미경으로 측정한 전류-전압 곡선으로부터 비대칭의 정류작용을 확인하였다. 이러한 결과와 다른 분석결과를 바탕으로 단일 실리콘 나노선/단일 그래핀 나노리본 이종접합 다이오드 소자의 새로운 특성들을 물리학 메커니즘을 바탕으로 규명한다.

P1-Se.033*

전기영동법을 이용한 그래핀에 부착되는 Au 나노입자의 위치제어 및 전기적 특성 연구

*박진우, 원재식, 이인열 [1], Servin Rathi, 임동석 [2], 이윤태, Lijun Li, Muhammad Atif Khan, 강문식, 김길호 [3]
*JinWoo. Park, Jae Sik. Won, Lee In yeal. [1], Servin. , Dong Suk. Lim[2], Yoon Tae. Lee, Lijun. Li, Atif. Khan, Moon Sik. Kang, Gil Ho. Kim[3]
성균관대학교 전자전기공학부. [1] *성균관대학교 나노과학기술원.* [2] *성균관대학교 신소재공학과.* [3] *성균관대학교 전자전기공학부 및 성균나노과학기술원.*

Keyword : 전기영동법, 그래핀, 금 나노입자

최근 다양한 이차원 물질을 이용한 전자, 광학 및 센서 소자가 연구되고 있다. 이차원 물질을 기반으로 한 전자 소자의 특성을 향상시키기 위한 다양한 방법으로 가열, 도핑 및 이종접합구조와 같은 연구들이 진행되고 있다. 본 연구에서는 그래핀 및 전이금속 디칼코겐 화합물의 전기적 및 광학적 특성을 조절하기 위하여 금속 나노 입자를 표면 및 가장자리에 부착하는 실험을 진행 하였다. 상대적으로 미세한 나노입자를 그래핀의 특정 위치에 부착하기 위하여, 나노 입자를 전기장안에서 하전 시켜 부착하는 전기영동법을 이용하였다. 전기영동법이 진행되는 동안 두 전극 사이의 전압이 조절되었으며, 이로 인해 나노 입자는 선택적으로 표면 및 가장자리에 성공적으로 부착되었다. 선택적으로 부착된 나노입자는 온도 변화에 따른 가열로 인한 그래핀의 전기적 특성 변화를 관찰 하였다.

P1-Se.034

유기물박막에 삽입된 graphene oxide 기반 비휘발성 메모리 소자의 전기적 특성과 동작 메카니즘

*윤지영, 김유나, 김태환
*Jiyoung. Yoon, Kim Yu na. , KIM Tae Whan.
한양대학교.

Keyword : Graphene,GO,polymer,나노복합체

Organic/inorganic 나노복합체 기반 메모리 소자의 연구가 flexible 전자 및 광소자의 응용 가능성때문에 활발하게 이루어지고 있다. Graphene oxide (GO)가 trap 층 역할을 하는 비휘발성 메모리 소자의 전기적 특성에 대한 연구를 하였다. GO 는 절연성 특성을 가지고 있지만 외부에서 전압전 인가되었을 때 반도체의 성질을 가지게 된다. GO 의 물리적 변화 특성을 활용하여 차세대 비휘발성 메모리 소자 제작에 다양하게 응용하고 있다. 단순하고 저렴한 방법인 spin-coating 방법을 사용하여 polymer/GO/polymer 의 구조에서 각각의 층의 두께를 변화하여 메모리 소자를 제작 하였다. 주사전자현미경 관측을 통해 제작한 소자의 단면을 관측하였다. 제작한 소자의 전기적 특성은 I-V 실험으로 관측하였다. 관측한 I-V 특성을 통해 이 소자가 메모리 특성을 보여주었다. 메모리 소자의 동작 메커니즘을 I-V 결과와 energy band diagram 을 사용하여 설명하였다. polymer/GO/polymer 기반으로 한 메모리 소자의 응용성을 논의한다.

Acknowledgements
This research was supported by Basic Science Research Program through the National Research Foundation of Korea (NRF) funded by the Ministry of Education, Science and Technology (2013R1A2A1A01016467).

P1-Se.035*

Controllable Grain Size Distribution and Readily Transferable Growth of MoS_2 Monolayer Flakes Using a Seed Layer of PTAS by CVD Process

조흥열, V. Senthilkumar, C. T. Le, *김용수
H. -Y.. Cho, V.. Senthilkumar, C. T.. Le, *Yong Soo. Kim
울산대학교 물리학과 및 EHRSC.

Keyword : transition metal dichalcogenides, chemical vapor deposition, PTAS, seed, non-linear optics

Recently two-dimensional (2D) transition metal dichalcogenides (TMDCs) has gained much attention with respect to its interesting physical and optoelectronic properties. Graphene is a well-known 2D material, however it is too hard to be used in electronic devices as it possess zero band gap. Unlike graphene, 2D TMDCs, including MX_2 (M=Mo, W; X=S, Se), has a wide range of band gap from 1.2 – 2.0 eV. Bulk MoS_2 has indirect band gap, while mono-layer (ML) MoS_2 has direct band gap and show excellent electrical mobility ~200 $cm^2/V{\cdot}s$, for mechanical exfoliated flake. There are many reports available for the growth of large size and high quality MoS_2 by chemical vapor deposition (CVD) method. Nevertheless, one of the foremost issue of CVD process is the lack of uniform grain size distribution. In this study, we reports the scalable growth of uniform grain size MoS_2 flakes on sapphire and SiO_2 substrate using perylene-tetracarboxylic acid tetrapotassium salt (PTAS) as a seed by the CVD method. Further, as prepared fresh MoS_2 flakes were readily transferred to de-ionized water without PMMA for non-linear optical studies applications.

P1-Se.036

실리카 나노입자/그래핀 양자점 복합구조의 에너지 전달 특성 및 이를 이용한 광검출기 특성 향상 연구

김성, 김정길, 장찬욱, 김종민, 이대훈, 김정현, *최석호, 황성원 [1]
Sung. Kim, Jungkil. Kim, Chan. Jang, Jong Min. Kim, Dae Hun. Lee, Jung Hyun. Kim, *Suk-Ho. CHOI, Sung Won. Hwang[1]
경희대학교. [1] *건국대학교.*

Keyword : 그래핀 양자점, 실리카 나노입자, 에너지 전달, 광검출기,

최근에 그래핀 양자점(graphene quantum dots)은 새로운 전기적 및 광학적 특성 때문에 크게 주목 받고 있다. 특히 2 차원 물질인 그래핀 양자점을 주게(donor)나 받게(acceptor)로 이용하여 에너지 전달이 가능한 구조를 구현하게 된다면 이는 흥미로운 물리적인 현상으로서 그래핀 양자점 단독으로 발현할 수 없는 광효율의 증대가 기대된다. 그래핀 양자점과 서로 에너지 전환이 가능한 물질들 중에서 실리카 나노입자(Silica nanoparticles)는 그래핀 양자점의 발광 스펙트럼 영역에서 높은 광흡수를 가지기 때문에 상호간의 에너지 전달작용이 가능하다. 본 연구에서는 실리카 나노입자와 그래핀 양자점를 각각 주게와 받게로서 활용하여 에너지 전달이 가능한 시스템을 구현하고 그 특성들을 규명하였다. 특히 Förster resonant energy transfer (FRET) 원리를 바탕으로 에너지 전달과정을 분석하였으며, 여기 에너지에 따른 광루미네센스(photoluminescence, PL)와 PL 감쇄곡선의 측정을 통하여 실리카 나노입자와 그래핀 양자점 간의 FRET 에 의한 에너지 전환효율이 ~78%임을 도출하였다. 또한 실리카 나노입자/그래핀 양자점 FRET 시스템을 이용하여 광검출기를 제작하여 그 특성을 평가하였다. 그래핀 양자점만 있는 광검출기에 비해 FERT 시스템 광검출기의 광반응도는 순방향 및 역방향 바이어스에 대하여 각각 10^2 배와 10^3 배 이상씩 증가하였다. 이러한 광반응도의 증가는 실리카 나노입자로부터 그래핀 양자점으로 전하운반자 (또는 에너지)가 전달되어 그래핀 양자점의 광전류를 증가시키기 때문이다.

P1-Se.037*

Back-Gate Tunable Schottky Barriers in Multi-layered Graphene/MoS_2 Field-Effect-Transistor

추동일, *김은규
DONGRI. QIU, *Eun Kyu. KIM
한양대학교.

Keyword : transition metal dichalcogenides, MoS_2, graphene, Schottky barriers, ohmic contact

Transition metal dichalcogenides (TMDs) have been received much attention due to novel physical and chemical phenomena. Among them, molybdenum disulfide (MoS_2) has novel physical phenomena such as absence of dangling bonds, lack of inversion symmetry, valley degrees of freedom. Unlike graphene, the semiconducting MoS_2 exhibit controllable indirect or direct band gap (depending on its layer numbers). Two interfaces such as dielectric/MoS_2 and metal/MoS_2 have showed significant effect on device performance due to trapped charge and a scalable Schottky barrier height in their interface. In this study, we report a new device structure by using multi-layered graphene (MGr) as the bottom interconnections, in order to offer Schottky barrier free contact to bi-layer MoS_2. The multi-layered graphene was mechanically exfoliated from single crystal graphite by using standard Scotch tape-based cleavage method. The semiconducting MoS_2 flake was deposited onto a SiO_2 (280 nm-thick)/Si (n^{++}-type) substrate in which graphene electrodes were pre-deposited. The evaluated field-effect mobility for our bi -layer MGr/MoS_2 device appears to be about 17.9 cm^2/Vs in the bi-layer MoS_2 channel. Experimental reveal that Schottky barrier height dramatically decreases from 300 to 0 meV and further becomes negative to saturate near -45.5 meV. This result will be discussed with the role of graphene layer for ohmic contact formation.

P1-Se.038

Optical imaging of grain boundary in CVD-grown monolayer WS_2 using near-field photoluminescence imaging.

*이용준, 윤석준 [1], 박세기, 김정용 [1]
*Yongjun. Lee, Seok Jun. Yoon[1], Seki. Park, Jeongyong. Kim[1]
나노구조물리연구단. 기초과학연구원. [1] 성균관대학교.

Keyword : monolayer tungsten disulfide, near-field imaging, photoluminescence, grain boundary, spatial resolution

Structural defects can critically influence the electrical and optical properties of monolayer tungsten disulfide (1L-WS_2) grown by chemical vapor deposition; thus, convenient optical methods that can visualize grain boundaries (GBs) and other structural defects are in great demand. Although photoluminescence (PL) imaging can identify the presence of relatively large defects, the limited spatial resolution of PL imaging prevents the identification of nano-size structural defects in 1L-WS_2. Here, nanoscale PL images of 1L-WS_2 was obtained using near-field scanning optical microscope (NSOM) that provide high resolution below the diffraction limit in two-dimensional systems. By far-field microscope, the PL enhancement was observed in the vicinity of grain boundary (GB) of 1L-WS_2, whereas PL reduction was observed right on the GB location of 1L-WS_2 with near-field PL imaging. We believe that decreased PL along the expected GBs is due to the local physical damage of 1L- WS_2.

P1-Se.039

Cl-oxide 이온이 흡착된 그래핀의 반도체 특성

*박창수, 손윤 [1], 김은규
*Chang Soo. Park, Yoon. Shon[1], KIM Eun Kyu.
한양대학교. [1] 동국대학교.

Keyword : 그래핀, 흡착, 라만, XPS, FET

그래핀은 전기적, 물리적 특성이 우수하여 여러 응용분야의 연구에 유망한 원자단위의 물질이다. 그러나 밴드갭이 없는 준금속이어서 실제 소자에 적용하기에는 제한이 된다. 이러한 이유로 그래핀 내에 밴드갭을 생성시키려는 시도가 많이 이루어졌다. 그럼에도 불구하고 그래핀의 밴드갭을 생성 및 조절하는 것은 여전히 주목 받고 있다. 특히 그래핀은 표면에 댕글링 본드를 통해 표면 제어를 할 수 있어 도핑을 유도할 수 있다. 본 연구에서는 전기화학법을 이용하여 그래핀의 표면에 염소산화물을 흡착시켜 반도체 특성을 구현하였다. 사용된 그래핀은 라만측정 결과 단일층 그래핀으로 확인되었다. 염소산화물 이온의 조성과 전자구조의 변화를 조사하기 위하여 XPS 를 측정하였고 탄소 원자의 결합에너지에서 낮은 에너지대로의 이동이 있음을 확인하였고 염소원자의 존재를 확인하였다. 도핑을 통한 전기적 특성변화를 온도변화에 따른 비저항을 측정하여 알아보았다. 일반적인 그래핀이 금속성의 특성을 보여 온도가 상승함에 따라 저항이 증가하는 것과 달리 본 시료에서는 감소하는 거동을 보였고 계산한 결과 94 meV 의 밴드갭이 나타났다. 또한 FET 소자를 제작하여 I-V_g 특성을 조사한 결과 p-type 반도체 특성을 보였다.

P1-Se.040

A study of ultra-thin resistive switching oxide layers self-assembled by field-induced oxygen migration (FIOM) technique

*이상익, 이지혜, 윤찬수, 남윤승, 오태준, 김연수, 오광택, 전지훈, 김진수, 이민주, 박배호
*sang ik. Lee, Ji Hye. Lee, Chansoo. Yoon, Yoon Seung. Nam, Taejun. Oh, Yeon Soo. Kim, Gwangtaek. Oh, JiHoon. Jeon, Jin soo. Kim, Minju. Lee, Bae Ho. PARK
건국대학교.

Keyword : "ReRAM", "Ultra thin film", "Oxygen migration"

Ultra-thin oxide layers with excellent performances are required for various next-generation electronic and optical devices. Especially, ultra-thin resistive switching (RS) oxide layers are expected to be good building blocks of three-dimensional high-density non-volatile memory devices. Up to now, special deposition techniques have been introduced for realization of high quality ultra-thin oxide layers. Here, we report that ultra-thin oxide layers with reliable RS behaviors can be self-assembled by field-induced oxygen migration (FIOM) at the interfaces of oxide-conductor/oxide-insulator or oxide-conductor/metal. The formation of a ultra-thin oxide layer with 2~5 nm thickness and 2.5% excess oxygen content by FIOM is demonstrated using cross-sectional transmission electron microscopy and secondary ion mass spectroscopy depth profile. Observed RS behaviors, such as polarity dependent forming process, can be well explained by the formation of an ultra-thin oxide layer using FIOM. Because oxygen ions are mobile in many oxide-conductors, FIOM can be generally used for the formation of ultra-thin oxide layers with desired properties at the interfaces or surfaces of oxide-conductors in high-performance oxide-based devices.

P1-Se.041*

Effect of Germanium Composition and Doping Type of Pillar Components on Current-Voltage Characteristics in Cylindrical Tunneling Field-Effect Transistor

Min-Won Kim, Hyo-Jun Kwon, Seung-Hyun Song, Jong-Sun Lee, Tae-Hun Shim, Jea-Gun Park
Min-Won. Kim, Hyo-Jun. Kwon, Seung-Hyun. Song, Jong-Sun. Lee, Tae-Hun. Shim, Jea-Gun. Park
Hanyang University.

Keyword : "Tunneling FET", "Silicon Germanium", "ATLAS", "Band Structure"

The tunneling field-effect transistor (TFET) has been interested due to its steeper subthreshold slope, smaller OFF Sfcurrent and higher power efficiency compared to conventional complementary metal-oxide-semiconductor (CMOS) devices. However, the low ON current of TFETs resulting from tunneling-based conducting mechanism is one of the main issues. The TFETs using $Si_{1-x}Ge_x$ instead of silicon channel can be a good solution of the problem since $Si_{1-x}Ge_x$ (0.66-1.12 eV) has smaller energy bandgap compared to silicon (1.12 eV). In addition, replacing current material of pillar components (source, drain and channel) with germanium and changing doping types of pillar components can bring a better ON/OFF characteristic. Nevertheless, the studies on such effects of germanium composition and doping type of pillar components have not been performed sufficiently so far. In our study, therefore, we investigated how germanium composition and doping type of pillar components affect current-voltage characteristics in cylindrical TFETs by performing simulations using ATLAS device simulator. The results showed that $Si_{1-x}Ge_x$ with x=0.8 has the highest ON current among x values and that the pillar with p^+ doped germanium source, n^- doped silicon channel and n^+ doped silicon drain has the highest ON/OFF ratio among various doping conditions. Finally, we report the simulation results on the effect of germanium composition and doping type of pillar components on current-voltage characteristics, energy band structures, and so on.

Acknowledgment
* This research was supported by Brain Korea 21 PLUS Program in 2015.

P1-Se.042

투명 플렉서블 MoS_2 전계 효과 트랜지스터

*원동연, 김상윤 [1], 유우종 [1]
*DONGYEUN. WON, SangYun. Kim[1], Yu Woo jong. [1]
성균관대학교전자전기공학부. [1] *성균관대학교.*

Keyword : Graphene, h-BN, MoS2, Flexible, Transparent

2 차원 물질은 투명성과 유연성을 갖춘 전자 제품의 응용에 유망한 후보로 연구되어왔다. 본 실험에서는 2 차원 물질인 그래핀(Graphene), 질화붕소(h-BN), 황화몰리브덴(MoS2)을 쌓는 방식을 이용하여 FET 소자를 제작하였다. 전극으로 그래핀, 절연층으로 질화붕소, 채널에는 황화몰리브덴을 이용하였다. 이 소자는 2 차원 물질만으로 제작되어 뛰어난 유연성과 투명성을 보여주었고, 높은 수준의 on/off ratio 를 보여주었다. 2 차원 물질만으로 구성된 이 소자를 통해 고성능의 투명하고 유연한 소자제작의 가능성을 확인할 수 있었다.

P1-Se.043*

2 차원 물질 이용한 투명하고 유연한 전계효과트랜지스터

*정동섭, 유우종
*Dong Seob. Chung, Yu Woo jong.
성균관대학교.

Keyword : "그래핀","TMD","실리콘 반도체","전계효과트랜지스터"

그래핀과 WSe2, MoS2 등의 TMD(transition metal dichalcogenide)물질은 뛰어난 전기적, 기계적 특성으로 현재 반도체 재료로 쓰이고 있는 실리콘을 대체할 새로운 전자 재료로 각광 받고 있다. 이러한 물질들은 2 차원 나노물질로 기존 3 차원 물질인 실리콘으로는 실현하기 힘든 유연한 전자 소자의 실현을 가능하게 할 물질의 후보들이다. 그래핀은 뛰어난 전자 이동도를 갖는 반금속(semi-metal)물질이고 WSe2, MoS2 등의 TMD 물질은 높은 전자 이동도와 그래핀과는 다르게 밴드갭이 존재하는 반도체 물질이다. 이 논문에서 나는 유연한 기판 위에 이러한 2 차원 나노 물질들을 이용하여 전계 효과 트랜지스터(field effect transistor)를 제작하여 투명하고 구부러지는 나노 전자 소자를 만들고자 한다.

P1-Se.044

다중파장 측정이 가능한 실리콘 반도체기반의 실리콘 광증배 소자 연구

*전진아, 이혜영 [1], 박일흥 [1], 이직 [1]
*Jeon Jin-A. , Lee Hye Young. [1], PARK IL Hung. [1], LEE Jik. [1]
성균관대학교 기초과학연구소. [1] 성균관대학교.

Keyword : SiPM, PMT, APD

기존 광증배 소자를 실리콘 반도체기반의 실리콘 광증배 소자로의 개발 연구의 진행과 함께, 기존 광증배 소자가 특히 가시광 영역에서만 일정 효율을 달성하는 것이 극복해야할 과제이다. 이에 기존 실리콘 광증배 소자로서 가이거 모드에서 동작하면서도 자외선 영역에서 근적외선 영역까지의 (350 ~800nm) 다중파장 측정이 가능한 광증배 소자에 대한 연구를 진행하였다. 이를 제작하기 위해서 본 연구에서는 기존의 평면적 소자 구조를 수직적 구조로 설계하여 다중파장의 측정이 가능하도록 새로운 단위 소자를 설계하였고, 이번 발표에서 연구 중인 소자의 설계 및 동작 시뮬레이션 결과와 제작 공정 설계에 대해 논의 하겠다.

P1-Se.045

가이거 모드 실리콘 광센서(SiPM)의 대화소 설계에 있어 감도 향상을 위한 연구

*이혜영, 전진아 [1], 박일흥, 이직
*Lee Hye Young. , Jeon Jin-A. [1], PARK IL Hung. , LEE Jik.
성균관대학교. [1] 성균관대학교 기초과학연구소.

Keyword : Multi-SiPM, APD, PMTs

실리콘 광증배소자(Silicon Photomultiplier, SiPM)는 기존의 광전자증배관(Photomultiplier tube)과 같이 단일광자까지 측정할 수 있는 광센서이면서 실리콘 반도체 기반의 장점인 초고속 반응속도, 저전력, 저중량 등의 특성을 가지고 있어 다양한 응용분야에 적용이 가능하다. 특히 이미지 센서로의 활용을 위해 다채널 대화소의 구현이 무엇보다 중요하였다. 이는 소자를 어레이로 배열함으로써 달성 할 수 있고, 이때 단일 소자에 비해 광 비활성화 영역의 증가로 감도가 낮아지는 문제가 생길 수 있다. 이에 본 연구에서는 소자의 어레이 배열 기술 및 센서 자체의 기하학적 효율을 높여 광 비활성화 영역을 최소화하는 설계 및 제작을 진행 하였다. 이와 같은 다채널 실리콘 광증배 소자 연구 내용 및 결과를 본 발표에서 논하고자 한다.

P1-Se.046

다채널 실리콘 광증배소자용 신호 처리 장치 개발

*이직, 이혜영, 전진아, 김민빈, 박일흥
*LEE Jik. , Hye Young. Lee, JinA. Jeon, Minbin. Kim, PARK IL Hung.
성균관대학교.

Keyword : 실리콘 광증배관, SiPM

다채널 실리콘 광증배관 SiPM 소자용 신호처리 장치를 개발하였다. 신호처리 장치는 Analog part, Digital part, Data Aquisition part 로 구성된다. 본 발표에서는 64 채널을 기반으로하여 다채널로 확장 가능한 신호처리 장치의 설계 및 제작 결과를 제시한다. 또한 전하입력 및 SiPM 광입력 신호에 대한 신호 처리 장치의 성능을 제시한다.

P1-Se.047

10-nm tri-gate 소자의 전기적 특성 향상을 위한 연구

*유주태, 정현수, 김태환
*Jutae Ryu. , Jung Hyun Soo. , KIM Tae Whan.
한양대학교.

Keyword : "10-nm" "tri-gate" "MOSFET"

휴대폰, 태블릿과 같은 모바일 기기 시장의 성장으로 인해 저전력 반도체 소자에 대한 수요가 급격히 증가하고 있다. 이를 위해 비례 축소를 통한 더욱 작은 크기의 소자에 대한 연구가 활발히 진행 되고 있다. 작은 크기의 소자는 높은 집적도와 적은 소비전력, 빠른 속도의 장점을 가지지만 게이트 누설 전류, 셀간 간섭, 단 채널 효과 같은 문제점을 가지고 있다. 이로 인해 20 nm 이하 소자 크기에서 기존의 평면 MOSFET 을 대체할 여러 가지 차세대 소자에 대한 연구가 활발히 진행 되고 있다. 그 중에서 tri-gate 소자는 비례 축소가 용이하고 단 채널 효과와 누설전류 문제에 대한 장점으로 인해 많은 연구가 이루어져 왔다. 기존의 연구는 소자에 사용되는 물질 특성 대한 연구가 주로 진행되었으나 게이트 구조의 의한 특성 변화 연구는 많이 진행 되지 않았다.

이에 본 연구에서는 10-nm tri-gate 소자의 전기적 특성 향상을 위한 게이트 구조 최적화 연구를 진행하였다. Tri-gate 소자의 게이트 두께, 모양, 위치에 따라 여러 가지 전기적 특성들을 계산하여 관찰하였다. Tri-gate 소자의 게이트의 접촉면의 형태 변화에 따라 채널영역의 orientation 의 변화로 인한 효과를 계산하기 위해서 multi-orientation mobility model 을 포함한 three-dimensional technology computer aided design tool 을 사용하였다. Tri-gate 소자의 게이트 모서리의 곡률이 증가함에 따라 채널 영역의 부피 변화, 채널에서의 전자의 밀도와 전자 이동도의 변화를 관찰하였다.

Acknowledgements
This research was supported by Basic Science Research Program through the National Research Foundation of Korea (NRF) funded by the Ministry of Education, Science and Technology (2013-016467).

P1-Se.048

산화 알류미늄 게이트 산화막을 가진 플래시 메모리 소자의 전기적 특성에 관한 연구

*안준성, 정현수, 김태환
*Joonsung. Ahn, Hyun Soo. Jung, Tae Whan. Kim
한양대학교.

Keyword : SANOS, SONOS, electrical properties, flash memory

적층 구조의 플래시 메모리 소자를 제작하기 위해 높은 유전 상수를 가진 산화 알루미늄을 실리콘-실리콘 산화물-실리콘 질화물-실리콘 산화물-실리콘 (SONOS) 메모리 소자의 게이트 절연막으로 사용하는 폴리실리콘-산화 알루미늄-실리콘 질화물-실리콘 산화물-실리콘 (SANOS) 구조를 가진 메모리 소자가 있다 [1]. 하지만 SANOS 구조를 가진 기억 소자는 빠른 프로그램 속도에도 불구하고, 산화 알루미늄에서의 전하의 누설로 인해 SONOS 기억 소자의 저장 시간에 비하여 SANOS 메모리 소자의 저장 시간이 크게 감소하였다.
본 연구에서는 SANOS 기억 소자에서의 전자의 누설을 이론적으로 규명하기 위해 SANOS 메모리 소자의 저장 시간에 대한 변화 모델을 사용한 시뮬레이션으로 접근하였다. 실리콘 질화물의 포획된 전자 및 실리콘 질화물의 전도대의 자유 전자의 밀도를 시간에 따라 얻기 위해 Shockley-Reed-Hall 에 다양한 메커니즘을 가진 전자 누설에 대한 방정식들을 사용하여 계산하였다. 동일한 두께의 게이트 절연막을 가질 때, SONOS 기억 소자에 비해 SANOS 기억 소자의 저장 시간이 크게 줄어들었다. SONOS 메모리 소자에서 전자의 누설은 절연막의 터널링에 의한 것이었으며, SANOS 메모리 소자의 경우는 게이트 절연막의 터널링이 전자의 누설이 원인이며 누설 전자의 양이 훨씬 컸다. 시뮬레이션 결과를 통하여 SANOS 메모리 소자의 저장 시간의 단축은 게이트 절연막인 산화 알루미늄에서의 전자의 누설을 확인할 수 있었다.

Acknowledgment
This research was supported by Basic Science Research Program through the National Research Foundation of Korea (NRF) funded by the Ministry of Education, Science and Technology (2013-016467).
Reference
[1] M. F. Beug, T. Melde, M. Czernohorsky, R. Hoffmann, J. Paul, R. Knoefler, and A. T. Tilke, IEEE Trans. Electron Devices 57, 1590 (2010).

P1-Se.049

Thickness Effect of Tungsten Oxide Interfacial Layer for Silicon Solar Cells

오규진, *김은규
Gyujin. Oh, *Eun Kyu. KIM
Hanyang University.

Keyword : tungsten oxide, RF magnetron sputtering, interfacial layer, solar cell application

In the research field of organic solar cells, tungsten oxide (WO_3) is usually hole extraction layer. In this study, tungsten oxide interfacial layer was deposited with sputtering method. The band gap of sputtered tungsten oxide is ranging from 4.15 to 3.75 depending on its deposition conditions. Alignment mechanism of this n-type material as a hole extraction layer is now progressing research field. In the previous report, we found that the defect state of WO_3 is at 1.86 eV under the conduction band with ultraviolet photoelectron spectroscopy (UPS). With spectroscopic ellipsometry, the optical response near the energy of defect state was enhanced. In accordance with the defect states density, their contact resistance was also enhanced. In this study, the thickness of tungsten oxide was controlled by sputtering technique. The thickness control was performed by time measurement with previously found deposition condition. With the optimized thickness conditions, simple device was tested. The layer was deposited between the silicon substrate and indium tin oxide layer fabricated by sputtering method and their conducting mechanism was carefully discussed.

P1-Se.050

Structure and Optical properties of WS_2 nano-sheets

*박준우, 소현섭, 김성, 이호선
*Jun-Woo. Park, Hyeon Seob. So, Sung. Kim, Hosun. LEE
경희대학교.

Keyword : WS2 nano-sheet, optical property, dielectric function, photoluminescence, raman

We investigated the optical property of monolayer WS_2 and its nanosheets on c-Al_2O_3 substrate by using spectroscopic ellipsometry (SE), Raman, and photoluminescence (PL) spectroscopy. WS_2 nanosheets were prepared by chemical exfoliation and grown by spin coating method on the substrate. The dielectric function of WS_2 nanosheets was estimated via layer model analysis of the ellipsometric angles. Optical transition energies of WS_2 nanosheets were obtained by using the second derivative spectra of the dielectric functions and the standard critical point (SCP) model. We observed the exciton energy peaks in PL spectrum of WS_2 nanosheets. We discussed the change of the exciton energy between the monolayer and the nanosheets of WS_2.

P1-Se.051

Effect of Potassium Phosphate oxidizer on CMP performance for low corrosive Cobalt plug process in next generation application process (AP)

*조도연, 윤상수 [1], 박진형 [2], 박재근 [1]
*Do-Yeon. Cho, Sang-Su. Yun[1], Jin-Hyung. Park[2], Jae-Gun. Park[1]
한양대학교 대학원. [1] 한양대학교. [2]UB materials Inc.

Keyword : CMP,oxydizer,cobalt,slurry,passivation

Semiconductor industry has used the metal tungsten (W) as a contact plug material in the AP manufacturing process of 14nm design rule. In addition, the AP manufacturing process of the design rule less than 10 nm is expected to apply to cobalt (Co) as a material to replace the W for reducing the wiring resistance. However, the cobalt (standard reduction potential : $Co^{3+} + e^{-} \rightarrow Co^{2+}$) in the CMP process has generates more reactivity than the material such as Ru and Cu. In addition, it can generate the corrosion easily due to the difficult in forming a Co3O4 film. In order to solve this problem, we intended to inhibit the corrosion by forming a passivation film on the surface of the Co film, which is the alkali slurry (pH 8~10) including the Potassium Phosphate (K_2HPO_4) as an oxidizer to enhance polishing rate, as shown in Fig.1.
In particular, we investigated how Potassium Phosphate oxidizer affect CMP purformance in cobalt plug process to improve polishing selectivity ratio (Co vs. SiO_2 polishing rate). In addition, we designed the Co slurry based ZrO_2nano-crystal particle in the plug process of Co/SiO_2 structure and studied the electrochemical properties of Co and polishing principle. Furthermore, we proposed the post-cleaning solution of Co/SiO_2 structure.

P1-Se.052

HRXRD 를 이용한 경면 연마된 사파이어 웨이퍼의 잔류응력 분석

*정인영, 김창수 [1], 정양수 [2], 전현구 [2]
*Jung In young. , KIM Chang Soo. [1], CHUNG Yang-Soo. [2], Jeon Hyeon gu. [2]
충남대학교. 한국표준과학연구원. [1] 한국표준과학연구원. [2] 충남대학교.

Keyword : XRD, 잔류응력, 격자상수정밀측정

반도체의 기판 또는 윈도우로 사용되는 사파이어 웨이퍼(wafer)는, 사용 용도에 따라 단면 또는 양면으로 경면 연마를 진행한다. 경면 연마 공정은 타 공정과 같이 양면이 모두 경면화되는 과정도 있지만, 웨이퍼의 한쪽면만 가공되는 단면 공정도 있다. 이와 같은 가공 종류는 진행되는 공정에 따라 웨이퍼의 응력 특성에 차이를 주게 된다. 그래서 경면 연마가 양·단면 가공이 이루어진 시료를 HRXRD(High-resolution X-ray Diffractometry)를 이용한 정밀 격자상수 측정을 통해 잔류응력을 분석한다.
본 연구에서는 육방정계 구조를 가지고 있는 사파이어 웨이퍼의 a-축의 격자상수를 통해 잔류응력을 분석한다. 사파이어 웨이퍼의 a-축 잔류응력 분석을 위해 4 반사 Ge(220) monochromator 와 3 반사 분석결정(crystal analyzer) 장착한 HRXRD 를 이용하였다. 4 반사 monochromator 는 X-ray 의 단색화를 위해 사용하였고, 3 반사 분석결정은 면간거리에 해당하는 회절빔만 검출하기 위해 이용하였다. 그리고 a-축 격자상수 계산을 위해 (10·8)면과 (006)면의 브래그 회절 각도를 정밀 측정하였다. 각 면의 회절각도를 정밀 측정 하여 브래그 법칙을 통해 면간거리를 계산하여 격자상수를 산출하였고, 이를 이용하여 임의로 선택된 앞면을 기준으로 a-축의 앞·뒷면 차이를 통해 잔류응력 분석을 진행 하였다. 시료는 6 인치 양·단면 웨이퍼를 이용하였으며, 측정 위치는 중심을 포함하여 5 점을 측정 하였다. 단면 경면화된 경우 잔류응력이 58 MPa 로 나타나며, 양면 경면화된 웨이퍼는 -12 MPa 로 나타난다. 웨이퍼의 양면이 서로 다른 가공과정을 거친 경우에 잔류응력이 더 크게 나타나며, 같은 가공과정을 거친 경우 잔류응력이 줄어드는 것을 확인 할 수 있었다.

P1-Se.053*

석영 기판 위의 주기적 Ag 금속 홀에 의한 장적외선 표면 플라즈몬 투과특성

*이병우, 곽희민 [1], 김하술
*Byungwoo. Lee, Heo min. Kwak[1], Ha sul. Kim
전남대학교. [1] 광주과학기술원.

Keyword : surface plasmon, long wavelength infrared, transmittance

주기적 금속 홀 격자/SiO2 기판으로 구성된 장적외선 투과용 플라즈모닉스 소자가 포토리쏘그래피와 열전자 증착법에 의하여 제작되었다. 금속 박막 홀의 주기에 최대 투과도의 파장 대역을 임의적으로 조절 가능하도록 제작되었다. 장적외선이 플라즈모닉스 소자 표면에 수직 입사할 때, 주기 5.0 μm 와 홀 3 μm 의 크기로 구성된 디바이스는 파장 15.4 μm 에서 최대 투과도가 측정되었다. 또한 홀의 크기가 주기의 반 이상이 될 때, 최대 투과도가 두 개의 값으로 분리되는 것을 관측할 수 있었다. 입사광의 각도가 0° 일 때는 6 개의 축퇴된 모드가 하나의 (1,0) Ag/SiO2 표면 플라즈몬 모드로서 투과도의 최댓값이 동일한 파장에서 관측되었다. 입사광의 각도가 45° 일 때는 5 개의 표면 플라즈몬 모드로 분리되면서 장파장 및 단파장으로 파장 편이가 동시에 측정되었다.

P1-Se.054*

Comparison of I-V Characteristics of Fin Field-Effect Transistor with Different Gate Structures

Ui-Hyeon Jung, Min-Won Kim, Hyo-Jun Kwon, Seung-Hyun Song, Jong-Sun Lee, Tae-Hun Shim, Jea-Gun Park
Ui-Hyeon. Jung, Min-Won. Kim, Hyo-Jun. Kwon, Seung-Hyun. Song, Jong-Sun. Lee, Tae-Hun. Shim, Jea-Gun. Park
Hanyang University.

Keyword : "FinFET", "Gate Structure", "ATLAS"

Recently, the fin field-effect transistor (FinFET) has been used in advanced transistor technology since it can compensate the drain current which is decreased as a result of scaling down. The three-dimensional structure of FinFET makes the area of channel larger than conventional two-dimensional metal-oxide-semiconductor field-effect transistors (MOSFET), which leads to high drain current. There are many kinds of FinFETs with different gate structures such as double-gate FinFET, triple-gate FinFET, surrounding gate FinFET, and so on. However, the studies on relation between drain current and gate structure in FinFET have not been performed sufficiently so far. Therefore, we performed simulations using ATLAS device simulator by Silvaco International. The simulation results showed that the drain current increased as the area of channel increases. We report the simulation results on the difference of Current-Voltage characteristics caused by various gate structures (double, triple and surrounding gate). Multiple independent gate field-effect transistor (MIGFET) is used as double-gate FinFET, Trigate FET as triple-gate FinFET, and quadruple gate FET as surrounding gate.

P1-Se.055

알루미늄이 첨가된 산화카드뮴의 성장 변화

*정진, 이봉주
*Jeong Jin. , LEE Bong Ju.
조선대학교.

Keyword : ALCDO, THIN FILMS, AFM

알루니늄이 첨가된 산화카드뮴의 성장을 증착조건을 변화시켜서 박막의 표면과 성장방향, 게면등을 관찰하였다. 증착시간, 증착온도, 유입되는 산소의 양에 따라서 박막의 거칠기는 일정하게 변화되었다. 원자적으로 관찰한 결과 박막의 거칠기 정도는 온도가 올라갈수록 유입되는 산소의 양이 증가할수록 쳄버내의 진공의 변화가 클수록 증가하였다. 박박의 거칠기 정도는 전기적인 성질에 영향을 줌을 보였다

P1-Se.057

절연층 구조의 변화에 대한 채널의 이동도 감소 매커니즘 연구

*정현수, 김태환
*Hyun Soo. Jung, Tea Whan. Kim
한양대학교.

Keyword : "플래시메모리" "분극 효과" "이동도" "TCAD" "RPS"

반도체 소자의 집적도가 높아짐에 따라 소자의 크기의 비례 축소에 대한 연구가 많이 진행 되고 있다. 특히 높은 유전율을 가지는 물질을 절연층으로 사용하여 제작한 소자가 기존의 소자와 비교하여 게이트 커패시턴스 양을 유지하면서 적은 누설전류를 가지는 장점으로 인해 많은 연구가 이루어지고 있다. 높은 유전율을 가지는 물질을 이용하여 제작한 소자의 전기적 특성에 대한 연구가 많이 이루어졌지만, 절연층에서 발생하는 분극 효과로 인한 이동도 감소 메커니즘은 아직 연구가 많이 진행되지 않았다. 본 연구에서는 높은 유전율을 가지는 절연층을 가지는 채널에서 절연층 유전체의 분극현상으로 인한 전하 이동도에 대하여 관찰하였다. 높은 유전율을 가지는 절연층을 가지는 소자의 채널에서의 전하 이동도, 채널에서의 전기장의 분포와 채널에서의 전하 밀도를 remote phonon scattering (RPS) 모델을 포함한 3 차원 TCAD 시뮬레이션 툴을 이용하여 계산하였다. 절연층의 분극현상을 적용한 RPS 모델을 사용하여 계산하였을 때 소자의 on-current 값은 분극현상을 적용하지 않았을 때 보다 10% 정도 감소하였다. 또한 채널에서의 전자의 이동도도 분극현상을 적용한 모델을 사용하여 계산하였을때 적용하지 않았을 때보다 현격히 감소 하였다. 이 결과들은 높은 유전율을 사용한 메모리 소자의 전기적 특성을 관찰하는데 큰 도움을 줄 것이다.

Acknowledgements
This research was supported by Basic Science Research Program through the National Research Foundation of Korea (NRF) funded by the Ministry of Education, Science and Technology (2013-016467).

P1-Se.058*

Design of New NAND Flash Memory Structure using Second Channel Created by Buried Floating Gate (BFG) Charge

Hyo-jun Kwon, Jae-Hoon Choi, Seung-Hyun Song, Min-Won Kim, Jong-Sun Lee, Jea-Gun Park
Hyo-jun. Kwon, Jae-Hoon. Choi, Seung-Hyun. Song, Min-Won. Kim, Jong-Sun. Lee, Jea-Gun. Park
Hanyang University.

Keyword : "memory device","next generation memory","NAND flash memory","hot hole injection","buried floating gate"

Recently, in accordance with the limits of integration and scaling, the next generation memory devices such as phase change random access memory (PCRAM) and resistive random access memory (ReRAM) have been actively studied to replace the existing NAND flash memory. Furthermore, the semiconductor maker's announcement of the 3D X-point memory indicates the importance and potential of the next generation memory devices. Thus, in this study, we came up with a new memory device structure operated by current difference and investigated its electrical characteristics by Technology computer aided design (TCAD) simulation. The memory device structure was fabricated by adding poly-silicon in buried oxide (BOX) layer of conventional silicon-on-insulator metal-oxide-semiconductor field effect transistor (SOI-MOSFET) with 10-angstrom-thick tunnel oxide below top silicon layer. This poly-silicon can store charges like a floating gate of flash memory and generate second channel which makes current difference, which is named as a buried floating gate (BFG). This device is operated by hot hole injection mechanism in a program process and Fowler-Nordheim (FN) tunneling mechanism in an erase process, respectively. It was confirmed that the memory device needs lower power consumption than flash memories in a program process. We present a device structure, operating mechanisms, current-voltage characteristics, integrated charges in BFG, output pulse characteristics and read current characteristics. Our simulation results show the possibility for the other next generation NAND Flash memory.

Acknowledgment
* This research was supported by Brain Korea 21 PLUS Program in 2015.

P1-Te.001

상 관찰을 위한 투명 스크린의 개발과 특성에 대한 연구

*현동걸, 신애경, 조헌국 [1]
*Donggeul. Hyun, Aekyung. Shin, Hunkoog. Jho[1]
제주대학교. [1] *단국대학교.*

Keyword : "상 관찰", "투명 스크린", "빛다발"

물리교육에서 다루는 내용 중에서 교사와 학생들이 어려워하는 분야 중의 하나가 기하광학 분야이다 (권경필 등, 2006; 이양락 등, 2006; Galili et al., 1993; Clough & Driver, 1986; 이봉우, 2012). 특히 기하광학 관련 학습에서 대부분의 학생들은 상이 생기는 원리를 이해하지 못하여 이들 현상에 대한 설명이나 그 원인을 설명하는 것이 어려워 한다. 이들 연구에서 제시한 교수-학습 전략으로는 광선추적법을 활용하여 거울에 반사되거나 렌즈를 통과하는 빛들의 경로를 추적함에 의하여 상이 생기는 원리를 학생들이 이해하게 한다는 것이 공통적이다.
물체로부터 나온 빛이 직진이나 반사, 굴절 등을 통해 눈에 들어오면, 물체의 상을 인식하고 빛의 경로를 추론하려면 상에 대한 정확한 개념도 명확히 할 필요가 있으며 (김영심과 백성혜, 2008), 광선추적에 의하지 않고 실험적으로 상의 종류를 판별할 수 있는 실질적인 기준이 필요하다. 또한 광선추적의 어려움을 극복하기 위하여 소수의 특별한 광선보다는 보이는 전 영역을 표현하는 빛다발(beam)에 근거를 두어야 하며, 눈의 역할과 기능에 결부하여 한다 (Ronen and Eylon, 1993; Grayson, 1995; Galili and Hazan, 2000; 이재봉, 2004).
이 연구는 상을 관찰하고, 이로부터 빛의 경로를 추론하여 광학 현상을 효율적으로 이해하기 위해서는 물체에서 나온 빛이 광학기구를 통과하거나 반사하는 상태를 빛다발의 형태로 인식할 수 있으며, 상의 형태를 관찰할 수 있을 뿐만 아니라 눈으로 들어가는 빛다발의 상태를 인식할 수 있는 투명 스크린을 개발하고 그 특징을 설명하는 것을 목적으로 한다.

P1-Te.002

투명 스크린을 활용한 상의 관찰 및 광선 추적 실험 장치의 개발에 대한 연구

*현동걸, 신애경, 조헌국 [1]
*Hyun. Donggeul. , Shin. Aekyung. , Jho. Hunkoog. [1]
제주대학교. [1] *단국대학교.*

Keyword : "투명 스크린", '상 관찰", "광선추적법", "빛다발"

광선추적법을 배운 학생들이 광선추적을 근거로 상이 생기는 원리와 상의 위치를 묻는 질문에는 바른 대답을 할 수는 있지만, 실제 물리계와 관련시키지 못하며, 많은 학생들이 렌즈나 거울, 스크린, 눈의 기능을 이해하지 못한다는 것이다 (McDermott 등, 1987; Ronen and Eylon, 1993; 황민정, 2011). McDermott 등(1987)은 이러한 이유를 광선에 대한 개념과 그래픽의 역할에 대한 이해가 부족하기 때문인 것으로 설명하며, 전통적인 교육방법으로는 개선되지 않는다고 하였다. 빛의 경로를 효율적으로 추론하기 위해서는 상과 광학 개념 사이 관계를 연결지울 수 있는 실험적인 근거를 제공할 수 있는 교수 전략이 필요하다는 것이다 (김영심과 백성혜, 2008).
이 연구는 상을 관찰하고, 이로부터 빛의 경로를 추론하여 광학 현상을 효율적으로 이해하기 위해서는 물체에서 나온 빛이 광학기구를 통과하거나 반사하는 상태를 빛다발의 형태로 인식할 수 있으며, 상의 형태를 관찰할 수 있을 뿐만 아니라 눈으로 들어가는 빛다발의 상태를 인식할 수 있도록 개발된 투명 스크린(현동걸과 신애경, 2015)을 활용하여 상의 관찰 및 광선 추적의 의미를 실험적으로 학습할 수 있는 실험 장치를 개발하고 그 유용성을 보이는 것이다. 아울러 이 연구에서 개발된 새로운 광원/물체를 소개할 것이다.

P1-Te.003

Practical Experiments of Mirror and Shadow in Primary School Science

*김태규
*Taekyu. KIM
전주교육대학교.

Keyword : Primary School Science, Shadow

The title of Mirror and Shadow include the 10th unit of "To change a size of shadow" in primary school science developed for 2009 national curriculum. The contents and activity of unit contain to find out the shadow size depended on the distance between object and screen, relied on the distance between light source and object, and to look into the method to change the shadow size. It had been analyzed the inquiry activity of changing the size of shadows to measure the size of shadow changed by the distance between object and screen under fixing light source and screen (1) and by the distance between light source and object under fixing object and screen (2). And the experimental equipments had been manufactured for conducting experiments. Inquiry activity (1) has one parameter of distance between light source and screen based on the reference position of light source and inquiry activity (2) have two parameters of distances between light source and object and between light source and screen. Accordingly the light source approach to the object in the inquiry activity (2), the shadow size is increased with the distance between light source and object (A) but is decreased with the distance between light source and screen (B). Two parameters in inquiry activity (2) are contrary to each other but the shadow size is more dominant parameter (A) than (B). It is not sufficient to understand for teacher the results of inquiry activity (2) stated in teacher guidebook without detail explanation. Experimental equipment composed of light source, object, screen and track had been manufactured for shadow experiments and shadow size depended on parameters analyzed.

P1-Te.004

Practical Experiments of Weighting in Primary School Science

*김태규
*Taekyu. KIM
전주교육대학교.

Keyword : Primary School Science, Weighting

The title of Weighting include the 7th unit of "To find out the principle of keeping horizontality" in primary school science developed for 2009 national curriculum. Study objects are to keep the same or different objects of weight horizontality and to understand the horizontality. The plate used in keeping horizontality should be horizontal in inquiry activity in this unit. Figure in the textbook shows only the case of pivot above center of mass. Reference material in teacher guidebook explains the principle of keeping horizontality using springs, which can occur a little error due to mass of spring and the limited range of linearity. It is very important to keep horizontal the plate because the pivot is located above the position of center of mass. To reduce the error an experimental tools should be designed and experimental methods explained in detail
Objects are in stable, unstable, and critical state according to the position of center of mass.
Why should the plate be horizontal? How can the plate be horizontal in cases of pivot under center of mass or same? In this study, the principle of keeping horizontality had been analyzed in numerical methods. Based on the physical parameter of plate, the positions of rotating axis, load, and effort, the initial angles of load and effort, and the distances between rotating axis and load, effort, and center of mass are calculated. From force versus angles calculated for various parameters, the load and the physical shape of plate should be categorized.

P1-Te.005

특수 상대성 이론의 두 가지 가설에 관한 물리교사들의 이해 정도와 오개념 조사

*박동규, 윤성현 [1]
*Park. Dongkyu, YOON Sung Hyun. [1]
한국교원대학교 대학원. [1] *한국교원대학교.*

Keyword : 2009 개정 교육과정, 상대성 이론, 상대성 원리, 광속 불변 원리

2009 개정 교육과정 물리 I ‘시공간과 우주’ 단원 중 상대성 이론은 교사가 수업을 구성하거나 학생을 이해시키는 데 많은 어려움이 있는 것으로 알려져 있다. 이 연구는 상대성 이론에 나오는 여러 가지 개념들 중 특히 두 가지 가설에 대한 교사들의 이해 정도를 분석하여 교수·학습에 필요한 교육적 시사점을 얻고자 하는데 그 목적이 있다.
이 연구를 위해 전국의 물리교사 50 명을 대상으로 상대성 원리와 관련된 6 문항과 광속 불변 원리와 관련된 6 문항의 총 12 문항으로 구성된 검사 도구로 상대성 이론의 두 가설에 관한 이해 정도를 조사했다.
본 연구에서는 문항에 대한 교사들의 응답을 분석하여 상대성 이론의 두 가설에 대한 이해 정도와 오개념에 관한 반응을 유형별로 분류하고, 교사들이 가지고 있는 개념의 실태와 개선 방안에 대해 논의하고자 한다.

P1-Te.006*

토론 문제가 예고된 거꾸로 물리 학습의 학업 성취도와 수업 선호도 조사

*양영도, 윤성현 [1]
*YOUNG DO. YANG, YOON Sung Hyun. [1]
한국교원대학교 대학원. [1] *한국교원대학교.*

Keyword : 거꾸로 학습(flipped learning), 토론 학습, 학습 양식

본 연구는 토론을 기반으로 하는 거꾸로 물리 학습에 대한 수업의 선호도와 학업 성취도를 조사하여 교육적 시사점을 얻는데 목적이 있다.
서울에 소재하는 인문계 고등학교에서 물리 II 를 이수 중인 22 명의 3 학년 학생들을 대상으로, 힘과 운동 단원의 관성력과 단진동 부분을 학생들이 유튜브를 통해 제공된 동영상을 과제로 학습하고 미리 주어진 토론 문제를 생각해 본 후 본 수업 시간에 그 문제를 토론과 질의 응답을 통해 학습하는 거꾸로 학습(flipped learning)으로 진행할 때 나타나는 학생들의 학업 성취도와 수업 선호도 조사를 실시하고 이 결과에 대하여 논의하고자 한다.

P1-Te.007

TRIZ 의 발명원리를 이용하여 모순을 해결하는 온라인 글쓰기와 초등 과학 영재학급 학생들의 발명에 대한 태도

*양미선, 윤성현
*Miseon. Yang, Sung Hyun. YOON
한국교원대학교.

Keyword : "TRIZ" "초등 과학 영재" "모순 해결 글쓰기"

TRIZ 는 특허 분석을 통해 해결되기 어려운 문제에는 모순이 있다는데 착안하여 러시아의 G. Altshuller 가 고안한 창의적 문제 해결 기법이다. TRIZ 의 발명원리는 교육 현장에 적용이 가능하고 효과적이다. TRIZ 를 구성하는 요소의 하나인 발명원리 중 생활 속 적용 사례 수와 적용이 쉬운 정도를 감안하고 확산적 사고가 가능한 원리 8 가지를 추출하고, 이를 적용하여 모순을 해결하는 글쓰기 프로그램을 실시하고 이를 통해 나타난 초등학교 과학영재학급 학생들의 발명에 대한 태도 등을 논의하고자 한다.

P1-Te.008

기술수용모형(TAM)을 이용한 예비과학교사의 컴퓨터기반실험(MBL) 수용에 관한 연구

*임성민, 이상원
*_, .
대구대학교.

Keyword : 기술수용모형, 지각된 용이성, 지각된 유용성, 컴퓨터기반실험, 품질 요인

본 연구는 기술수용모형 (Technology Acceptance Model : TAM) 을 예비과학교사의 컴퓨터기반실험 (Microcomputer Based Laboratory : MBL) 수용에 확장 적용하여 기술수용모형에서 제시하는 지각된 용이성과 지각된 유용성에 영향을 미치는 외부변수를 도출하고자 하였다. 기술수용모형의 이러한 외부변수는 컴퓨터기반실험의 수용에 필요한 품질요인으로 시스템품질과 정보품질, 개인적 요인은 컴퓨터 자기효능감으로 구성하였다. 각 요인의 분석결과, 컴퓨터기반실험의 품질요인은 시스템품질과 정보품질로 나누어져 있고, 기술수용모형의 지각된 용이성, 지각된 유용성, 컴퓨터 자기효능감과 사용의도는 단일차원으로 구분되었다. 가설검증결과 시스템품질은 컴퓨터기반실험의 지각된 용이성과 지각된 유용성에 유의한 영향을 미치고, 정보 품질과 컴퓨터 자기효능감은 컴퓨터기반실험의 지각된 유용성에 유의한 영향을 미치는 것으로 나타났으며, 지각된 용이성과 지각된 유용성은 사용의도에 유의한 영향을 미치는 것으로 나타났다.

P1-Te.009*

예비 물리교사들의 '좋은 물리 1' 교과서에 관한 관점의 변화

*김형진, 이경호
*Kim Hyungjin. , LEE Gyoungho.
서울대학교.

Keyword : 교과서, 물리 1, 예비 교사, 2009 개정 교육과정

교과서는 교사에게는 수업 준비의 원천으로, 학생들에게는 물리학습을 위한 충실한 교재로 쓰이며 학교 현장에서 교사, 학생과 함께 필수적인 요소를 이루고 있다. 하지만 그 중요도에 비해 만들어진 교과서의 완성도는 기대에 미치지 못하는 경우가 많다. 현재 적용되고 있는 2009 개정 교육과정의 '공통과학'은 이제껏 시도되지 않았던 융합을 적극적으로 도입하며 인류의 근본 질문을 과목의 경계를 넘어 과학적으로 담으려는 큰 변화를 꽤하였으나 교과서에 담고 학교 현장에 적용하기엔 교사, 학생들의 거부감이 컸다. '물리 1' 역시 '공통과학'과 같은 연장선상에서 만들어져 혼란을 피할 수 없었다. 본 연구는 물리교육과 3,4 학년 예비교사들이 '물리교과교재 및 연구법'수업을 통해 2009 개정 교육과정의 '공통과학', '물리 1'교재를 분석하고 제작한 그들이 생각하는 이상적인 '물리 1'교재를 바탕으로 하였다. 목차를 통해 교육과정으로 담아야 할 내용을 구상하였고, 본문을 통해 이상적으로 생각하는 방식으로 내용을 담고 기술하며 몇 차례 수정을 거쳐 교과서를 만들었다. 본 연구의 목적은 예비물리교사들이 생각하는 이상적인 '물리 1' 교과서가 나오기까지 학생들의 생각의 변화를 수업의 내용과 비교하며 알아보는 것이다. 이를 위하여 정기적으로 반성적 실천지와 주간보고서를 통해 학생들의 생각을 듣고 표현하는 과정을 거치며 학생들이 개발한 물리 1 교과서를 분석하였다.

P1-Te.010*

입자해석에서 나타나는 빛의 세기 문제(광전효과 그래프 해석을 중심으로)

*김은선, 이경호, 김홍빈
*EUN SUN. KIM, LEE Gyoungho. , .
서울대학교.

Keyword : 광자의 개수, 광전효과

광자 1 개의 에너지는 진동수에 비례한다. 반면 광전류를 통해 측정되는 빛의 세기는 진동수에 비례하지 않는다. 빛의 세기를 nhf 로 나타냈을 때 빛의 세기가 일정할 때 단위시간 단위면적당 입사하는 광자의 수(flux)는 진동수에 반비례하게 된다. 그러나 광전효과 그래프에서 일정한 세기에서 최대로 측정되는 광전류의 값은 진동수에 관계없이 일정하다. 본 연구에서는 측정의 의미를 통하여 위의 모순을 설명하고자 노력하였다.

P2-Ap.001*

Simulation Study for the Radiation Damage to the Tumor Cell in Proton Boron Fusion Therapy

*유동, 우종관, 이세병 [1], 고재우
*DONG. LIU, Jong-Kwan. Woo, Se Byeong. LEE[1], jae woo. Ko
제주대학교. [1] 국립암센터.

Keyword : Proton Boron Fusion Therapy (PBFT), Radiation Damage, Monte Carlo Method

Proton boron fusion therapy (PBFT) is a radiation therapy method based on the proton boron fusion reaction, which has been investigated through the nuclear physics research since 1960. In proton boron fusion reaction, 3 alpha particles are emitted from the point of fusion reaction between a proton and boron, these alpha emitters are used to destroy the tumor cell in PBFT. In radionuclide therapy, the distribution of ionizing energy in the tumor cells is important to assess the therapy effects. In order to study the characteristics of distribution of ionizing energy in the tumor cells, in this study, we developed an innovation tumor cell model and summarized the various interaction models of the alpha articles and cells. Then we analyzed the distribution of ionizing energy deposition of the three alpha particles from a proton boron fusion reaction in the cellular level through simulate the interaction of alpha particles and cell using Monte Carlo simulation method. Through analyze the characteristics of distribution of ionizing energy of alpha particles in the cells, it can be concluded that the position of boron is significant to affect the ionizing energy distribution in the cells. This is significant to improve and perfect the elementary therapy of PBFT.

P2-Ap.002

Skull modeling for Dose calculation in Gamma Knife Radiosurgery for Intracanial Brain Lesions

SA HOE LIM, SHIN JUNG, IN YOUNG KIM, KYUNG SUB MOON, TAE YOUNG JUNG, WOO YOUL JANG
SA HOE. LIM, SHIN. JUNG, IN YOUNG. KIM, KYUNG SUB. MOON, TAE YOUNG. JUNG, WOO YOUL. JANG
Chonnam National University Hwasun Hospital.

Keyword :
Gamma Knife, Brain Tumor, Skull Modeling

Leksell Gamma Knife provides a non-invasive treatment option for patients with brain lesions. We reviewed 8 patients underwent Leksell Gamma Knife radiosurgery. Leksell GammaPlan(LGP) requires that distances from the center of Leksell stereotactic space to the outer surface of the patient's head are measured. From these skull measurements, patient's skull model which offers the basis of the treatment dose calculation is defined. The LGP skull model can result in discrepancy with the actual head shape due to the limited number of measurement point of the skull scaling instrument. In this study, the treatment time differences between LGP skull model and actual skull shape was investigated. TMR (Tissue Maximum Ratio) 10-dose algorithm was used to calculate treatment time. Effect of skull modeling methods in dose calculations for Gamma Knife Radiosurgery was discussed as well.

P2-Ap.003*

FCS 를 이용한 솔루션 상의 G-quadruplex 의 반응성 연구

이동근, 김수용, *김석원 [1]
Dongkeun. Lee, Soo Yong. Kim, *Sok Won. Kim[1]
한국과학기술원. [1] *울산대학교.*

Keyword : G-quadruplex, telomere, fluorescence correlation spectroscopy, potassium ion, tamra

G-quadruplex 는 세포 수명과의 연관성 (G-quadruplex telomere), 구조 특이성을 이용한 drug delivery 등에 응용되면서 중요한 연구토픽으로 급부상하고 있다. 이에 대한 기본적인 연구방향으로서 G-quadruplex 의 구조 및 성질 변화에 대해 다양한 연구가 이루어지고 있다. 본 연구에서는 FCS 를 적용하여 G-quadruplex 와 결합하는 다양한 물질에 대하여 솔루션 상에서의 성질 변화를 정량적으로 측정하였다. 이를 위해 d(TTAGGG)4 sequence 에 Tamra 를 부착하고 potassium 이온농도를 조절하여 G-quadruplex 를 생성시킨 뒤 G-quadruplex 와 결합하는 물질의 존재 여부에 따라 fluorescence signal 을 바탕으로 FCS 를 수행하였다. FCS curve 를 바탕으로 diffusion time, molecular weight 등을 측정하고 결합률 및 반응성을 분석하였다.

P2-Ap.004*

A novel aptamer-based capacitance sensor for real-time and specific detection of Escherichia coli and Salmonella

*이서원, 한날애, 이선미, 유경화
*Seo Won. Lee, Nal ae. Han, Sun Mi. Lee, Kyung-Hwa. YOO
연세대학교.

Keyword : "biosensor", "aptamer", "capacitance biosensor", "E. coli"

Various biosensors for the detection of pathogenic bacteria, including ELISA and PCR, have been developed because of their diverse applications from water-quality monitoring to testing of pharmaceutical products for bacterial contamination. Here, we report a novel aptamer-based capacitance biosensor for real-time and selective detection of pathogenic bacteria. Interdigited gold electrodes were fabricated on a SiO2/Si substrate and then anti-E. coli or anti-salmonella aptamers were immobilized using dithiodipropionic acid. Bacteria in solution was detected by measuring the capacitance change caused by bacteria bound to aptamers on the gold surface. This biosensor could detect as low as 10^2 CFU/ml of target bacteria within 1 hour with high selectivity.

P2-Ap.005*

Flexible Single-Walled Carbon Nanotubes Multi Electrodes Array for Image of Capacitance for Label-free Deference of Lipid Region in Atherosclerosis tissue ex vivo

*송준호, 이선미, 김형준, 한날애, 유경화
*Jun Ho. Song, Sun Mi. Lee, Hyung Joon. Kim, Nal ae. Han, Kyung-Hwa. YOO
연세대학교.

Keyword : "Capacitance sensor"
"Atherosclerosis"
"Flexible multi electrodes array(f-MEA)"
"polypyrrole-coated multi walled carbon nanotubes MEA"

Recently, there are a lot of diseases all around the world. Out of them, Atherosclerosis (AS) is the most common cause of stroke, cardiovascular mortality, and myocardial infarction. The macrophage-derived foam cell, which is formed by oxidized low-density lipoprotein (oxLDL), is the crucial marker for AS. In this study, we report a label-free capacitance imaging technique with multi-electrode array (MEA). The lipid-rich aorta arch lesions, which are derived from an apolipoprotein-E receptor-deficient (apoE$^{-/-}$) mouse, exhibit higher capacitance than the lipid-free aorta arch, allowing the capacitance imaging of lipid region in atherosclerosis. To improve the contacts between MEA and tissue, polypyrrole(PPy)-coated multi walled carbon nanotubes (MWNTs) multi electrode array (PPy-MWNTs-MEA) was fabricated. Compared to TiN-MEA, PPy-MWNTs-MEA yielded lower contact impedance and better capacitance images. In addition, we have also developed a Fflexible MEA using single walled carbon nanotubes on a PET substrate. The lipid region could be discriminated in the capacitance images of the lipid-rich aorta arch lesions measured using flexible MEA, demonstrating a feasibility of in vivo applications.

P2-Ap.006*

Enhanced capture sensitivity for circulating tumor cells in a breast cancer patient's bloods by silicon nanowire substrate

*임정택, 정진탁, 최문기, 이상권
*Jung-Taek. Lim, Jin tak. Jeong, mun ki. choi, Sang-Kwon. Lee
중앙대학교.

Keyword : Cell capture, circulating tumor cells (CTCs), silicon nanowires, Poly-l-lysine (PLL), breast cancer patient blood

The separation of circulating tumor cells (CTCs) from the blood of cancer patients with high sensitivity is an essential technique for selecting drug treatment at a patient-by-patient level. Recently, various research has been reported a nanostructure-based substrate for rare cell capture due to its high surface area and 3D nanotopographic features. However, evaluation of capture sensitivity based on chemical modification of the nanostructure surface has not yet been performed. In this work, we evaluated the capture sensitivity for CTCs from the blood of three breast cancer patients diagnosed with stage IV metastatic breast cancer by using the following three substrate: streptavidin-conjugated silicon nanowire (STR-SiNW), poly-l-lysine–coated silicon nanowire (PLL-SiNW), and poly-l-lysine–coated glass (PLL-glass). From our experiments, the number of evaluated CTCs/0.5 ml on STR-SiNW, PLL-SiNW, and PLL-glass were 16.2 ± 5.5 cells, 7.3 ± 2.9 cells, and 4.7 ± 1.5 cells, respectively, per 0.5 ml.

P2-Ap.007

반사광 측정 모드에서 표면 플라즈몬 공명 쌍금속 칩의 반응 특성

김형진, 이성엽 [1], 김홍탁 [1], *손영수
Hyung Jin. Kim, Sung-Youp. Lee[1], Hong Tak. Kim[1], *Young-Soo. Sohn
대구가톨릭대학교. [1] *경북대학교.*

Keyword : 표면 플라즈몬 공명, 쌍금속, 반사광 측정 모드

최근 생명 공학 연구에 표면 플라즈몬 공명(surface plasmon resonance) 센서의 연구가 활발히 이루어지고 있다. 일반적으로 표면 플라즈몬 공명을 일으키기 위해 금 박막을 이용한다. 유리 기판 위의 금 박막에 생분자 등의 흡착으로 굴절률이 변화하면 SPR 센서의 반사도 곡선(반사광-입사각 그래프)에 변화를 야기한다. 일반적으로 이러한 변화에서 공명각(반사광의 크기가 가장 작을 때의 입사각)의 변화를 측정한다. 본 연구는 은과 금이 결합된 쌍금속 칩을 이용하여 반사도 곡선의 반치폭(FWHM)을 좁히면 반사도 곡선에서 접선의 기울기가 가파르게 된다. 이 곡선에서 접선의 기울기가 가장 가파른 입사각에 광원을 고정하고 생분자 등의 흡착에 의한 반사광 변화를 측정하여 기존의 상용 금 칩과 비교하였다. 반사광의 변화를 측정하는 모드에서 은과 금만의 쌍금속 칩을 이용하는 것이 금만을 이용하는 것보다 동일한 굴절률 변화에 대해 더 많은 반사광 변화를 야기하는 것을 확인하였다. (This research was supported by Basic Science Research Program through the National Research Foundation of Korea (NRF) funded by the Ministry of Education (NRF-2013R1A1A2010028).)

P2-Ap.008*

Rapid and Checkable Annealing Method by Static Electrical Field for Organic Photovoltaic Devices

*박상헌, 서유성, 신원석 [1], 문상진 [1], 황정식
*Sangheon. Park, Yu seong. Seo, Wonsuk. Shin[1], Sangjin. Moon[1], Jungseek. Hwang
성균관대학교. [1] 한국화학연구원.

Keyword : Organic Photovoltaic, Electrical Annealing, P3HT/PCBM

To improve the performance of bulk-heterojunction (BHJ) organic photovoltaic (OPV) devices thermal annealing and chemical annealing (solvent vapor annealing: SVA) processes have been used widely. The annealing process has been known to improve the device performance by changing microscopic morphology and configuration of vertical phase separation in the active layer. In this work we introduce a new annealing process using an external electrical field. We have applied only external electrical field to a BHJ-OPV device for the annealing process. By monitoring applied voltage and current to the device we can tell when the annealing process is completed. Our electrical annealing process is also rapider and simpler than other annealing processes. We used the commercial photovoltaic materials, P3HT [Poly(3-hexylthiophene)] and $PC_{61}BM$ (Phenyl-C61-Butyric acid Methyl ester) as donor and acceptor, respectively. The performance of electrically annealed solar cell is comparable to that of the reference (thermally annealed) device. Our results indicate that our new rapid and checkable annealing process can be used to fabricate high performance BHJ-OPV devices.

P2-Ap.009

Fabrication and electrical properties of single wall carbon nanotube channel and graphene electrode based transistors; Toward all carbon electronics

*김학성, 서미리, 김용현, 나준홍 [1], 이병주 [2], 윤호열, 커스티 맥알리스터, 이임복 [3], 김근수 [3], 정구환 [2], 김규태 [1], 이상욱, 신동훈
*Hak Seong. Kim, Miri. Seo, Yong Hyun. Kim, Jun hong. Na[1], Byung Ju. Lee[2], Hoyeol. Yun, Mcallister. Kirstie, Im Bok. Lee[3], Keunsoo. Kim[3], Goo Hwan. Jeong[2], Gyu Tae. Kim[1], Sang-Wook. LEE, Dong Hoon. Shin
건국대학교. [1] 고려대학교. [2] 강원대학교. [3] 세종대학교.

Keyword : Graphene, CNT, Carbon, junction

We investigated the electrical properties of all carbon transistors, composed of a single-walled carbon nanotube (SWNT) channel and graphene electrodes. By using CVD grown large scale graphene and well-aligned SWNT, the highly integrated transistor arrays were prepared by transferring patterned graphene electrode patterns on top of the SWNT. Both single and multi-layer graphene were used to make the electrodes. In our graphene-SWNT junction transistor, typical p-type transistor and Schottky diode behaviors were observed in single and multi-layer graphene cases, respectively. Based on our fabrication method and device performances, several issues are suggested and discussed to improve the device reliability and finally to realize all carbon based future electronic systems.

P2-Ap.010*

Wide-band microwave metamaterial absorber based on resistive layers

김영주, 유영준, 황지섭, 손혜미, 이주열 [1], 김기원 [2], 박상윤 [3], *이영백
Young Ju. Kim, Young Joon. Yoo, Ji Sub. Hwang, Hye Mi. Son, Joo Yull. Rhee[1], Ki Won. Kim[2], Sang Yoon. Park[3], *YoungPak. Lee
한양대학교. [1] 성균관대학교. [2] 선문대학교. [3] 서울대학교.

Keyword : Absorption, Metamaterial, Broadband, Perfect absorption, Microwave applications

The electromagnetic (EM) properties of media such as propagation, focusing and scattering strongly depend on the electric permittivity and the magnetic permeability of media. Recently, artificially-created metamaterials (MMs) composed of periodically-arranged unit cells with adjustable electric permittivity and magnetic permeability have drawn wide interest due to their capability in tailoring the EM response. MM absorbers (MM-As) utilizing the conventional sandwich structures usually exhibit very high absorption at certain frequency, and the absorption properties of MMs can be tuned simply by changing the geometrical parameters of unit cell. In this work, we numerically and experimentally studied an incident-angle-independent broadband perfect absorber based on resistive layers. We analyze the absorption mechanism in terms of impedance matching with the free space and the distribution of surface currents at specific frequencies. From the simulation, the absorption was expected to be higher than 96% in 1.4 – 6.0 GHz. The corresponding experimental absorption was found to be higher than 96% in 1.4 – 4.0 GHz, and the absorption turned out to be slightly lower than 96% in 4.0 – 6.0 GHz owing to the rather irregular thickness of resistive layers.
This work was supported by the ICT R & D program of MSIP/IITP, Korea (13-911-01-101).

P2-Ap.011*

Reduced-size metamaterial absorbers at low frequency

부이쑤안쿠웬, 부이선퉁, 응웬반둥, 유영준, 김영주, 김기원 [1], 부딘람 [2], *이영백
Xuan Khuyen. Bui, Son Tung. Bui, Van Dung. Nguyen, Young Joon. Yoo, Young Ju. Kim, Ki Won. Kim[1], Dinh Lam. Vu[2], *YoungPak. Lee
한양대학교. [1] 선문대학교. [2]Vietnamese Academy of Science and Technology.

Keyword : Metamaterials, Perfect absorption, Low frequency, Enhanced bandwidth

In this work, we numerically and experimentally demonstrated a metamaterial perfect absorber (MPA) in the MHz regime based on a planar sandwiched metal-dielectric-metal structure. Firstly, single-peak perfect absorption was obtained at 400 MHz by exploiting the magnetic resonance. The ratios of the periodicity of unit cells and the thickness to the absorption wavelength are 1/12 and 1/94, respectively. The advantage of structural design and the mechanism for the low-frequency MPA are described in detail, based on the comparison among calculation, simulation and experiment. Influence of the incident angle of electromagnetic wave for both transverse-electric (TE) and transverse-magnetic (TM) polarization on absorption was also investigated, and the absorption was maintained to be above 95% at wide incident angles (up to 30°). Finally, we propose a self-asymmetric structure to enhance the bandwidth (full width at half maximum) of MPA. The results indicate that the bandwidth of absorption spectrum is enhanced to be nearly twice times wider than that in case of symmetric structure. The enhanced bandwidth is still well preserved even by varying the incident angle up to 30° for both TE and TM polarization. These results were confirmed by both simulation and experiment. Our work is promising for potential practical applications in the radio range, such as radio-frequency shielding devices, single/dual-frequency filters, mutual coupling reduction in antennas and switching devices.
This work was supported by the ICT R & D program of MSIP/IITP, Korea (13-911-01-101).

P2-Ap.012*

Tunable electromagnetically-induced transparency-like metamaterials using a snake-shape resonator array

황지섭, 유영준, 김영주, 김기원 [1], 이주열 [2], 박상윤 [3], *이영백
Ji Sub. Hwang, Young Joon. Yoo, Young ju. Kim, Ki Won. Kim[1], Joo Yull. Rhee[2], Sang Yoon. Park[3], *YoungPak. Lee
한양대학교. [1] *선문대학교.* [2] *성균관대학교.* [3] *서울대학교.*

Keyword : Metamaterials, Electromagnetically-induced transparency

Recently, the electromagnetically-induced transparency (EIT)-like effect in metamaterials (MMs) with resonant unit cells has been proposed. Generally, the EIT phenomenon in atomic system is activated by coherent interaction between atomic ensembles, which results in enhancing nonlinear interaction and reducing the group velocity of electromagnetic wave. Unlike the EIT in atomic system, the EIT-like effect in MMs are induced by a coupling of the plasmonic unit cells and simple tuning can be realized by varying their geometry. The MMs can dramatically reduce the difficulty in the experimental realization owing to the room-temperature operation and to no need for external activation through pumping lasers.

In this work, we experimentally and numerically studied a bilayer MM for controllable EIT-like feature at microwave frequencies. Two kind of snake-shape resonators (SSRs) were fabricated at the top (with one bar) and the bottom (with two bars) of FR4 substrate, respectively. The transmission spectra were measured in a frequency range of 4 – 8 GHz in an anechoic chamber at normal incidence. It was found that two SSRs in the MM were activated in bright modes, and the coupling between two bright modes led to the EIT-like effect, which resulted in the enhanced transmission at 5.61 GHz. Furthermore, it is confirmed that the EIT-like feature could be controlled by adjusting the geometric parameters of MM. The measured transmission spectra were in good agreement with the simulation in general shape and frequency. Our work provides a way to tunable EIT-like effect and a number of potential applications including filters, sensors, and other microwave devices.

This work was supported by the ICT R & D program of MSIP/IITP, Korea (13-911-01-101).

P2-Ap.013*

Towards High Resolution Mass Detectors Using Electromechanical Resonators

*커스티매칼리스터, 김학성, 이홍준, 이상욱
*Kirstie. McAllister, Hak Seong. Kim, Hong Jun. Lee, Sang-Wook. LEE
건국대학교.

Keyword : mass sensor, graphene, resonator, frequency

Here we present the development of two electromechanical resonators which function as highly sensitive mass detectors, using suspended graphene ribbons and silicon nitride beam-like structures. Each material holds specific properties which are desirable for enhancing mass resolution, for example, silicon nitride's high quality factor and graphene's low effective mass. Using an electromechanical actuation method and an optical interferometry detection setup, we could observe their fundamental resonance frequency behaviour. Detection of these frequencies pre- and post- loading Cr of 2Å thickness aided us in calculating their mass sensitivities. By monitoring each device's fluctuations in frequency, a more accurate determination of their mass sensitivities was established, with both being in the attogram (10^{-18}g) range at room temperature and in low vacuum conditions. One of the devices presented here shows great potential for improvement. In this poster we introduce the theoretical estimations and experimental results as well as suggesting various approaches for improvement of these devices for realisation of an ultra-sensitive mass detector.

P2-Ap.014*

RTP temperature dependence of CZTSSe absorber layer

*조소연, 남다현, 임수연, 고병수 [1], 황대규 [1], 김대환 [1], 강진규 [1], 정현식
*Soyeon. Cho, Dahyun. Nam, Soo Yeon. Lim, Byoung Soo. Ko[1], Dea-Kue. Hwang[1], Dae-Hwan. Kim[1], Jin-Kyu. Kang[1], Hyeonsik. Cheong
서강대학교. [1] 대구경북과학기술원.

Keyword : Raman spectroscopy, CZTSSe, solar cell

Raman measurements were carried out in order to study the absorber layer of Cu2ZnSn(S,Se)4 (CZTSSe) solar cells. The absorber layer was fabricated by co-evaporation and sulfurized by rapid thermal processing (RTP). Since the S/Se ratio change in the absorber layer is associated with the energy band gap, it is an important characteristics of the CZTSSe absorber layer. In order to study the effect of the RTP condition on the absorber layer, we changed the RTP temperatures: 550°C, 570°C, 590°C, 610°C, and 630°C. Macro-Raman measurements showed that the S/Se ratio increases as the RTP temperature increases. The scanning electron microscopy (SEM) images showed that the absorber layer is made up of two layers. The layers were further investigated by depth-resolved micro-Raman measurements. It was revealed that the S/Se ratio depends on the depth of the samples. Also, we found that the S/Se ratio change is different for each RTP temperature. Similar results were shown by the secondary ion mass spectroscopy (SIMS) as well. In order to investigate the effect of the band gap grading, we performed simulations using the SCAPS software.

P2-Ap.015

The Radio-Frequency Atmospheric Pressure Plasma Jet for Bio-Sciences

*곽형신, 엄환섭, 강민호, 전성실, 최은하, 홍영준
*HYOUNG SIN. KWAK, Han S.. Uhm, Min Ho. Kang, seong sil. Jeon, Eun Ha. CHOI, Young June. Hong
광운대학교.

Keyword : Non-thermal plasma, Plasma jet, Radio-frequency plasma, Optical emission spectrocopy, Plasma diagnosis

Various researches and tests have been performed according to the applications of plasma. Among them, non-thermal atmospheric-pressure plasma jets (APPJ) have many applications such as surface treatment, thin film deposition and biomedical treatment. In order to apply the plasma in bio-sciences, APPJ has to satisfy several requirements. First, it should be cold plasma. Second, it should be operated in atmospheric pressure. Third, it should be able to treat small area. In this study, we have developed the continuous radio-frequency (RF) APPJ to study its plasma gas temperature, plasma shape, chemically reactive species such as OH, NO and the possibility of applying bio-sciences. It has been investigated by means of optical emissions spectroscopy (OES). The RF-APPJ operated by 13.56 MHz RF power source was improved by a stepped-electrode, which enables the argon gas adding various gases such as oxygen, nitrogen to generate stable glow plasma at atmospheric pressure. In this reactor, the stepped-electrode used to make a strong electric field, which makes to pre-ionize electronegative gases. Due to the pre-ionization process, working gases are generated stable glow discharges.

P2-Ap.016*

Hydrogen treated graphene-based gas sensor

*박성진, 박민지, 이섬균, 유경화
*Sung Jin. Park, Min Ji. Park, Sum-gyun. Yi, Kyung-Hwa. Yoo
연세대학교.

Keyword : Hydrogen graphene, gas sensor

Graphene exhibits a number of unique properties that make it an intriguing candidate for use in sensor. Here, we report graphene-based gas sensor. Graphene was grown using CVD. Then, the sensor was made using standard lithography techniques. The sensor conductance increased upon exposure to NH3, whereas it decreased upon NO2, suggesting that NH3 and NO2 might be discriminated using the graphene-based sensor. To improve the sensitivity, graphene was treated with hydrogen plasma. After hydrogen treatment, the electrical properties of graphene changed from ambipolar to p-type semiconductors. In addition, the sensor performance was improved probably due to an opening of bandgap.

P2-Ap.017

Charge Transport in the Thick Reduced Graphene Oxide Films.

*김호종, 김대희 [1], 정수용 [1], 장수경, 하동한 [1]
*Ho Jong. Kim, dae hee. kim[1], Suyong. Jung[1], Soo-Kyung. CHANG, Dong Han. Ha[1]
연세대학교. [1] *한국표준과학연구원.*

Keyword : "reduced graphene oxide (RGO)", "variable range hopping (VRH)", "quantum tunneling", "thermal activation" , "charge transport",

We have investigated temperature-dependent charge transport behaviors in thick reduced graphene oxide (RGO) films. RGO films were prepared by attaching small RGO flakes on SiO_2/Si substrates in aqueous solutions using BSA as an adhesive layer. Disordered regions composing the percolating conducting networks are categorized as small, medium, and large ones. With temperature-dependent conductance measurements and numerical analyses, we showed that the charges transport in three dimensions and there are two types of parallel percolating conducting pathways in the RGO films. One contains large disordered regions as one of the constituents, so its conductance is determined dominantly by variable range hopping (VRH). The other is composed of small and medium disordered regions and crystalline sp^2 domains, so the conductance is given by a serial connection of quantum tunneling and thermal activation at low temperature. The more oxygen functional groups are removed from the GO films upon the progressive reduction, the more the potential barriers between crystalline sp^2 domains and disordered regions get lower. The contribution of thermal activation to the conductance does not appear evidently for the highly-reduced GO films having low potential barriers, while it causes the conductance of the moderately-reduced ones to change continuously even at low temperatures where the VRH is almost frozen out.

P2-Ap.018

Application of plasma generated nitric oxide(PGNO) to plant development

*전성실, 강민호, 신소민, 신재호, 최은하, 엄환섭, 박경순
*seong sil. Jeon, Min Ho. Kang, Somin. Shin, Jae Ho. Shin, Eun Ha. CHOI, Han S.. Uhm, Gyungsoon. Park
광운대학교.

Keyword : plasma, activate, nitric oxide(NO), seed germination

Beneficial effects of plasma on biological processes have been occasionally demonstrated. Free radicals (reactive oxygen and nitrogen species) generated from plasma can activate physiological processes such as wound healing and regeneration. However, tremendous experimental studies are still needed. In this study, we have analyzed the effects of plasma generated nitric oxide (PGNO) on plant development using spinach (Spinacia oleracea), Korean angelica (Angelica gigas), and deodeok (Codonopsis lanceolata). Seeds were exposed to the various level of PGNO produced by using nitrogen (10 lpm) and different flow rate of oxygen 100, 200, and 300 sccm. Our preliminary results showed that there was no significant changes in seed germination after plasma treatment, compared to control. As an alternative source of treatment, we have generated NO treated solution in order to treat plant seeds for testing the effects on germination and growth. Level of nitric oxide in water was dramatically increased after treatment but pH of water was concomitantly decreased. Treatment on phosphate buffer is under investigation in order to improve pH control of solution.
This work was supported by the National Research Foundation of Korea (NRF) grant funded by the Korea government (MSIP), (No. 2010-0027963) and National Fusion Research Institute (NFRI).

P2-Ap.019*

Design Variable Analysis of ALIP for the Circulation of Sodium in the IHTS of PGSFR

*곽재식, 김희령
*Jaesik. Kwak, Hee Reyoung. Kim
울산과학기술대학교.

Keyword : "Annular Linear Induction electromagnetic Pump (ALIP)", "P-Q characteristic curves", "Intermediate Heat Transport System (IHTS)" , "Prototype Generation-IV Sodium cooled Fast Reactor (PGSFR)"

The design variables of the Annular Linear Induction electromagnetic Pump (ALIP) were analyzed for the circulation of liquid sodium in the Intermediate Heat Transport System (IHTS) of the Prototype Generation-IV Sodium cooled Fast Reactor (PGSFR) of 150 MWe, which is being developed in the Korea Atomic Energy Research Institute (KAERI). Electromagnetic pumps have been employed for the transportation of the liquid metal with high electrical conductivity such as sodium, lithium and lead bismuth. An electromagnetic pump is developed by Lorentz' force generated from driving current and magnetic field perpendicular to it. It is operated without any contact with liquid metal because of no rotating part like the impellor and sealing while a mechanical pump transports liquid metal using impeller which contacts with the liquid metal. The change of physical property including the decrease of strength or corrosion can be caused by the contact between impeller and liquid metal. Therefore, in the sodium fast reactor (SFR), an electromagnetic pump can be effectively used in the environment of sodium with the high chemical reactivity avoiding direct contact with sodium due to the advantage of structural simplicity by no sealing over mechanical pumps. In this research, the design variables of the ALIP, which was composed of a stator core, exciting coils and duct wall, with the flowrate of 0.86 m3/s and developed pressure of 3.6 bar were analyzed magnetohydrodynamically according to the change of geometrical, hydrodynamic and electromagnetic ones. The maximum length and diameter of the ALIP were limited to 3 m and 2.2 m, respectively, because of geometrical restriction of the space. The condition for the minimum thickness of the outer duct and inner duct of the pump was set to 0.015 m and 0.025 m taking into thermal property of the stainless steel duct material, respectively. The developed pressure and efficiency of the pump were analyzed on the changes of pump geometrical and electromagnetic variables solving MHD equations, where the commercially used software of MATLAB was employed for the calculation. The magnetic field, linear current density and pressure loss were dependent on the flowrate of the pump. The dominant factors affecting on the pump performance were core length, flow gap, number of pole pairs, pole pitch. The P-Q characteristic curves were theoretically predicted on the change of the input current, voltage and power for the pump with the optimized design variables.

P2-Ap.020*

열파법에 의한 투명한 고체시료의 열확산도 측정

천보관, 황보현, 이재란, *김석원
Bokwan Cheon. , Hyeon Hwangbo. , Jaeran Lee. , *KIM Sok Won.
울산대학교.

Keyword : 열확산도, 투명광학유리, 열파법, 내열유리

열확산(thermal diffusion)은 시료내부에 온도분포가 균일하지 않기 때문에 물체에 온도차이가 생겨 열이 높은 온도에서 낮은 온도로 옮겨 가는 현상이다. 열파법(Thermal wave method)은 열확산도를 측정하는 한 방법으로서 간단한 장치구성으로 벌크 형태의 투명한 시료에 열확산도를 측정할 수 있다.
본 연구에서는 온도차에 의한 시료의 굴절률 구배현상을 열파법에 적용하여 광학유리인 BK7 그리고 내열유리로 쓰이는 Quartz 와 Pyrex 등 세가지 유리의 열확산도를 측정하였다. 투명한 시료 양면에 열판을 장치하여 각각의 열판에 전류를 흘려 열판의 온도를 조정하였다. 한쪽 열판에는 전원공급장치를 이용하여 6V 의 전압을 인가하여 시료온도가 30℃가 되도록 하였고, 다른 열판에는 1 분주기로 7V 의 전원을 on-off 하여 시료의 온도를 30℃에서 32℃까지 주기적으로 변화시켰다. 이 후 He-Ne 레이저 빔이 시료를 통과할 때 주기적인 굴절률 구배현상에 의해 주기적으로 편향이 되었다. 이 레이저빔의 편향정도를 광검출기(Photo detector)로 측정하여, 열판의 주기적 온도변화와 시료의 주기적 온도변화에 의한 두 사인파 곡선의 시간차로 위상차를 얻어서 열확산도를 구하였다.

P2-Ap.021

Sensing Low Magnetic Field by using Planar Hall Effect Sensor

*김성준, 송인철 [1], 김철기 [1]
*SungJoon. Kim, InCheol. Song[1], CheolGi. Kim[1]
DGIST(대구경북과학기술원). [1]DGIST.

Keyword : Planar Hall effect, Magnetoresistive sensor

The sensors can detect low magnetic field. The detection of picoTesla of magnetic field at room temperature has been used in many places where required the low magnetic field detection. However, it is hard to miniaturize systems now-a-day such as nano and pico-satelites or IC compass in mobile devices etc. Therefore, many magnetoresistive (MR) sensors have been developed to decrease the detective field. (for example as tunneling magnetoresistive (TMR), spin-valve, giant magnetoresistive (GMR), and anisotropy magnetoresistive (AMR) The detective field of these sensors has been stated around 100 pT at the frequency range from hundred Hz to few hundred kHz. However the AMR has more advantages in detection at lower frequency and it can detect 100 pT at around 10 Hz. Among MR sensors, the voltage noise of PHE-AMR sensor is lower several order of magnitude compared to others such as TMR sensor or GMR and AMR sensor, because of its off-diagonal geometry. However, the dectection of the magnetic field by MR sensor is difficult. In order to resolve this problem, we develop a highest sensitivity MR sensor based on the thin film with low magnetic noise. (i) We use the NiFe/Cu/IrMn trilayer structure; NiFe structure (the sensing layer) is amorphous state to minimize its structural noise. (ii) The sensor geometry is designed as a high sensitivity configuration–multi-ring, in which the current and voltage electrodes of the sensor is arranged in the way that the bridge has smallest off-set voltage to minimize the thermal noise. The limitation of the detective field is interpolating from drift voltage as a function of temperature from a set of the sensors where the length of one arm is changed.

P2-Ap.022

낮은 분산 특성의 메타 물질을 이용한 음향 GRIN 렌즈의 제작

*이상훈, 박춘만 [1], 김초희, 박희택
*Sang Hun. Lee, Park Choon mahn. [1], Cho Hee. Kim, Hee Tack. Park
서남대학교. [1](주)삼진.

Keyword : "메타물질", "음향학", "음향 메타물질", "그린렌즈", "광학"

오리피스를 포함한 단위 셀로 이루어진 음향 메타 물질 GRIN 렌즈를 제작하였다. FCOC (Face-centered-orifice-cubic) 단위 셀의 오리피스의 크기를 음파의 진행에 수직한 방향으로 다르게 줌으로써 음향 굴절률의 차이를 구현하였으며 이를 이용하여 음향 GRIN 렌즈를 설계하였다. 설계된 GRIN 렌즈를 메타물질의 균질 조건을 만족시키는 주파수에서 전산 시뮬하여 음파의 집중현상을 볼 수 있었으며 실험을 통해 확인하였다. 실험과 전산시뮬에서 얻은 결과를 GRIN 렌즈 분석 방법을 이용하여 분석한 결과 잘 맞음을 알 수 있었다. 이 결과로부터 제작에 사용된 비대칭 FCOC 단위 셀로 이루어진 음향 메타 물질이 비교적 넓은 주파수 대역에서 다양하게 응용될 수 있음을 확인하였다.

P2-Ap.023*

Active hydrogen evolution reaction over semi metallic phase MoTe2

*석진봉, 조수연 [1], 지병도 [2], 이준호 [3], 김효원 [4], 이영희 [5], 손영우 [6], 양희준 [5]
*Jinbong. Seok, Suyeon. Cho[1], Byeongdo. Ji[2], Junho. Lee[3], Hyowon. Kim[4], Young Hee. LEE[5], Young-Woo. Son[6], HeeJun. Yang[5]
성균관대학교 에너지과학과.
나노구조물리연구단. [1] 나노구조물리연구단. [2] 에너지과학과. [3]KIAS. [4] 삼성종합기술원. [5] 성균관대학교. [6] 고등과학원.

Keyword : TMD, MoTe2, Hydrogen evolution reaction,

Abstract: Engineering surface atoms of layered transition metal dichalcogenides (TMDs) is a promising way to design ideal electronic and chemical properties of catalysts for efficient electrochemical reactions including hydrogen evolution reaction (HER). While unprocessed single-crystalline TMDs have revealed poor HER performances, optimization of hybrid catalysts based on TMDs remains limited by incomplete understanding of catalytic active sites in the less-crystalline artificial hybrid structures. Here, we present an efficient HER by 1T' phase single-crystalline MoTe2. It has a lot of active site on wide basal plane and semi metallic properties which induce increasing of hydrogen evolution performance. Moreover, an exceptional HER performance, Tafel slope of 22 mV per decade and exchange current density of 1.0 mA/cm2, was realized by hybridizing the MoTe2 with platinum, which paves the way for the hydrogen economy.

P2-Ap.024*

액체내 기포를 이용한 광강도조절장치의 개발

*김나경, 한성범, 김현우, 함성길, 이재준, 이기원
*Kim Nagyeong. , Han. Seongbeom, Kom. Hyeonwoo, Ham-sounggil. , Lee Jaejoon. , LEE Ki-Won.
공주대학교.

Keyword : "기포", "광강도조절장치"

액체내 기포의 성장과정과 기포를 투과하는 빛의 강도와의 관련성에 대한 연구가 진행된바 있다. 이 연구에 의하면 기포의 부피가 일정하게 증가할 때 기포를 투과하는 빛의 강도는 시간에 따라 선형적으로 감소된다. 이 현상은 기포 성장과정에서 기포와 접촉한 접촉면의 변화에 의해 나타나는 것으로 밝혀졌다. 따라서 액체속 기포의 부피를 일정하게 유지하고 접촉면의 변화만을 이끌어내도 기포를 활용하여 빛의 강도를 조정하는 장치의 제작이 이론적으로 가능하다.
이에 따라 본 연구에서는 액체내에 형성된 기포를 이용하여 빛의 강도를 조정하는 광강도조절장치를 개발하였다. 이 장치는 폐쇄된 용액안에 일정한 부피를 갖는 기포를 형성하고, 기포와 접촉면의 변화를 고전압을 통해 조정함으로서 기포를 투과하는 빛의 강도를 조정한다. 그 결과 전압에 따라 빛의 강도가 변화됨을 실제로 관찰하였으며, 액체내 기포의 성장과정에 대한 선행 연구를 이용하여 관찰 결과를 해석하였다.

P2-Ap.025

방사능, 열, 빛의 자극에 의한 발광스펙트럼 측정장치의 개발

박창영, 고지영, *정기수, 장인수 [1], 이정일 [1], 김장렬 [1]
PARK Chang Young. , GO Ji Young. , *CHUNG Ki Soo. , JANG In Su. [1], LEE Jungil. [1], KIM Jang Lyul. [1]
경상대학교. [1] *한국원자력연구원.*

Keyword : RL, TL, OSL, Dosimetry

방사선 조사와 뒤이은 열과 빛의 자극에 의해 빛이 나오는 방사선발광(radioluminescence: RL), 열자극발광(thermally stimulated luminescence: TL)과 광자극발광(optically stimulated luminescence: OSL)을 통합해서 측정하는 장치를 개발하였다. 이들 발광은 모두 방사선과 관련된 것으로 노출선량측정, 연대측정, 물질의 에너지 준위 해석 등에 널리 쓰인다. 상용의 선량측정기(TL reader, OSL reader)는 모두 RL 과 TL, 혹은 OSL 을 발광총량(glow curve)으로 별개로 측정하도록 구성되어 있으나 본 연구에서 개발한 장치는 세 형태의 자극이 연속적으로나 동시에 가해지는 동일한 환경으로 측정한다. 또한 장치에는 분광계가 장착되어 있어 발광총량과 병행해서 발광스펙트럼을 측정한다. 이에 따라 선량평가 등 고유의 분석에 이용할 수 있을뿐더러 발광을 결정하는 물질의 물리적 파라미터들을 세부적으로 규명하는데 활용할 수 있게 된다. 특히 재결합트랩 준위의 정보는 스펙트럼을 결정하므로 기존의 장치가 가질 수 없는 분광발광특성도 추가로 해석할 수 있다. 장치의 방사선원으로는 X-선원(Moxtek 사, 50 kV, 0.2 mA, Pd 표적)을, 열자극을 위한 온도제어는 35 kHz 을 고주파를, 또한 광자극은 532 nm 의 녹색 레이저와 475 nm 의 LED 를 이용하였다. 이들 여러 형태의 자극량은 시퀀서 형태로 제어되며, 시료에 조사되는 X-선량은 PIN 다이오드(Vishay 사, BPW34)를 이용하였다. 발광은 자체 제작한 스캐너 형태의 분광계(Spex 사, 1681A)로 250 ~ 750nm 범위로 측정하였다. 컴퓨터와 범용 데이터취득장치를 조합하여 C#으로 프로그램으로 제어와 측정이 이루어지며, 아울러 측정 후 분석까지 수행된다. 선량계에서 널리 이용하는 Al_2O_3:C, LiF:Mg,Cu,P 등 물질의 RL+OSL, RL+TL 을 측정하여 개발한 장치의 성능을 평가하였다.

P2-Ap.026*

Near-field transmitted power loss behaviors of magnetic composite sheet on complex permittivity and permeability

이준식, 김진우, 남백일, *김기현
Joonsik. Lee, Jinu. Kim, Baekil. Nam, *Ki Hyeon. Kim
영남대학교.

Keyword : power absoption, magnetic composite sheet, microstrip line method, radio-frequency, complex permeability and permittivity

The transmission power absorption by the composite sheet was evaluated by microstrip line method (IEC 62333 standard) in the broadband radio-frequency range from 0.2 GHz to 10 GHz. The power absorptions simulated by using a 3D FEM method. The power loss of magnetic composite sheets were simulated by the variation of conditions such as complex permeability and permittivity values. As results with the increment of real part of permeability and permittivity, the power losses were decrease, which was caused by the reduction of loss tan (μ″/μ′). On the contrary, the power losses were increased with the increment of imaginary part of permeability and permittivity. The high real part of permittivity implies the enhancement of the dielectric and conductive effects. It should be resulted in improvement of power loss. To optimize the magnetic composite sheet for EM noise reduction, we will present the dielectric, magnetic and eddy current loss of the magnetic composite sheet as well as the complex permeability and permittivity variations, in magnetic composite sheets.

P2-Ap.027*

Electrical transport characteristics of PEDOT:PSS/n-Si Schottky junction diodes and electrical degradation in hybrid PEDOT:PSS/n-Si solar cells

*안재영, 박노원, 이상권
*Jay-Young. Ahn, No won. Park, Sang-Kwon. Lee
중앙대학교.

Keyword : : PEDOT:PSS, Schottky junction diode, Electrical degradation, Current voltage measurement, Power conversion efficiency.

We have recently reported on the electrical transport characteristics of PEDOT:PSS/n-Si Schottky junction diodes, which demonstrated excellent rectifying behavior. In this study, we investigate both the electrical transport of Schottky diodes and the electrical degradation in PEDOT:PSS-based solar cells. To examine the electrical properties, such as Schottky barrier heights and ideality factors of Au/PEDOT:PSS/n-Si Schottky diodes, both current–voltage and capacitance–voltage measurements were conducted at room temperature. In addition, we fabricated hybrid PEDOT:PSS/n-Si solar cells to compare the electrical degradation of the devices with and without polymethylmethacrylate (PMMA) layers, which were used as passivation layer. Our experimental results suggest that hybrid PEDOT:PSS/n-Si solar cells with PMMA layers exhibit superior surface passivation and PCEs compared to those of PEDOT:PSS/n-Si solar cells without PMMA layers when exposed to air for up to 0 days.

P2-Ap.028*

Al_2O_3 (0001) 기판에 성장된 V_2O_5 박막의 두께에 따른 구조적, 광학적 특성의 변화

김인혁, 김성호, 강만일, *김석원
Inhyuk Kim. , Suengho Kim. , Manil Kang. , *KIM Sok Won.
울산대학교.

Keyword : V_2O_5, 분광타원계, metal-insulator transition

오산화바나듐(V_2O_5)은 사방정계 결정구조(orthorhombic structure)를 갖는 n 형 반도체 물질로 ~2.2 eV 의 간접전이(indirect transition) 밴드갭을 가지고 있다. 또한, V_2O_5 는 박막으로 성장시 260℃ 근처에서 광학적, 전기적 특성의 큰 변화를 수반하는 금속-절연체 전이(MIT; metal-insulator transition)를 일으키는 것으로 알려져 있다.
본 연구에서는 V_2O_5 박막의 성장두께에 따른 구조적, 광학적 특성의 변화를 분석하기 위해 RF 스퍼터링법을 이용하여 박막을 제작하였다. 박막의 두께는 증착시간에 의해 조절되었으며, RF 파워, 기판온도, 산소분압 등과 같은 증착변수들은 모두 동일하게 하였다. 제작된 박막의 두께와 광학적 특성은 분광타원계(spectroscopic ellipsometer)와 UV-Vis 분광광도계를 이용하여 측정 및 분석하였으며, SEM 과 XRD 측정을 통해 박막의 두께에 따른 구조적 특성의 변화를 분석하였다. 또한, 얻어진 결과를 바탕으로 박막의 구조적 특성의 변화가 광학적 특성에 미치는 영향에 대해 논의 하였다.

P2-Ap.029

Analog-to-Digital Converter 의 성능 평가

*조혜리, 이형규, 김문석
*Hehree. CHO, Hyung-Kew. Lee, Mun-Seog. Kim
한국표준과학연구원.

Keyword : Analog-to-Digital Converter, 응답특성, 위상지연, 동적범위

Analog-to-Digital Converter (ADC)는 아날로그 신호를 이진 디지털 값으로 변환시켜주는 기기로 전기 측정분야 외에도 다양한 분야 (온도, 힘, 음향진동, 지진파 및 생체신호 측정 등)에서 활용되고 있다. ADC 를 이용하여 임의의 신호를 정확하게 측정하기 위해서는 ADC 의 응답특성 (response characteristic) 및 시각 오차 (timing error) 등이 사전에 엄밀하게 평가되어야 한다. ADC 의 응답특성은 이득오차 (gain error), 선형성 (linearity), 오프셋 (offset) 및 분해능 (resolution) 등으로 수치화될 수 있다. 본 연구에서는 이러한 특성을 평가하기 위한 샘플링 (sampling) 기반 ADC 평가시스템을 개발하였으며, 디지털 전압계, 디지타이저 및 지진기록계에 대한 평가를 수행하였다. 또한 ADC 자체의 클럭 (clock)을 사용하는 신호측정에서 발생하는 위상지연 (phase lag)을 기술하는 모델을 개발하여 위상지연이 측정결과에 미치는 영향을 평가하였다. 끝으로 ADC 의 동적범위 (dynamic range) 평가 및 검증을 위한 측정방법을 개발하였다.

P2-Ap.030*

대기 중 중성분자 흐름을 이용한 이온 속도 측정 연구

*성용규, 최명철 [1], 김명원 [2]
*Yong Gyu. Seong, CHOI Myoung Choul. [1], KIM Myoung Won. [2]
한국기초과학지원연구원/충북대학교. [1] *한국기초과학지원연구원.* [2] *충북대학교.*

Keyword : 이온운동, 대기압중 이온운동, 이온이동도

이번 연구는 대기 중 전기장 내 중성분자의 흐름을 이용하여 이온의 속도를 측정하는 연구이다. 이 연구는 대기 중 이온이 중성분자의 흐름과 수많은 충돌에 의해 통계적인 경향성을 갖을 것 이라는 가정하에 시작했다. 중성분자의 흐름을 전기장에 수직인 방향으로 만들어 주면 이온이 전기장으로부터의 영향과 함께 중성분자와의 충돌에 의한 영향을 받을 것이다. 이때 전기장을 조절하여 중성분자와의 충돌에 의한 이온은 영향을 측정하였다.

이번 연구에서 사용한 이온화원은 코로나 방전이고, 중성분자의 흐름은 팬에 의해서 제어하는 직사각형의 관을 제작하였다. 관 내부 4 면 중 한쪽 면에 이온화원을 부착하고, 반대쪽 면에 여러 개의 이온 전류센서를 부착하였다. 또한, 여러 개의 전류센서 중 각각의 센서마다 전류를 검출할 수 있도록 제작하여, 특정 전류센서에서 검출되는 전류 값을 측정하였다. 또한, 이온화원의 오른쪽에 팬을 부착하여 전기장의 수직인 방향으로 중성분자의 흐름을 만들어주고, 팬의 세기를 제어하면서 특정 전류센서에서 검출되는 전류를 측정하면서 팬의 세기에 따른 전류 변화를 관찰하였다.
실험 결과, 코로나 방전에 의해 이온화 된 이온들의 전류 분포를 알 수 있었고, 특정 전류센서에서 검출되는 전류 값이 팬의 세기가 커질수록 증가하다가 감소하는 현상을 확인할 수 있었다. 이 때, 최대 전류 값에서의 풍속을 이용하여 대기 중 이온의 운동속도를 구할 수 있었다.

P2-Ap.031

스마트로거를 이용한 실험실 온/습도 분포의 시간적 변화측정

*최명철, 김세진, 고재준 [1]
*CHOI Myoung Choul. , Sejin. Kim, KO Jae Jun. [1]
한국기초과학지원연구원. [1] *주식회사 에프티랩.*

Keyword : 로거, 온도 습도, 실험실 온도 습도, 스마트로거

최근 국내에서 개발된 초소형의 휴대용 전압 측정 및 저장장치를 이용하여 온/습도 센서와 결합하였다. 이러한 소형의 측정장치는 동시에 실험실 여러 곳에 설치하여 장시간동안 온/습도의 시간적, 공간적인 변화를 측정하여 온/습도조건이 중요한 실험실에서 발생할 수 있는 문제점을 파악할 수 있는 장치로 구현, 제작하였다.

이번 연구에서 온/습도의 영향을 민감하게 받는 다양한 실험실에 개발한 장치를 설치하여 12 시간 이상 변화의 시간적, 공간적 추이를 측정하였다. 일반적으로 이러한 민감한 실험실에서는 온/습도 측정 장치를 한곳에 고정하여 설치하고 이를 기준으로 조절을 한다. 따라서 국부적인 문제점 파악이 어렵고 장비에 치명적일 수 있는 영향을 미치게 된다. 국내 업체인 ㈜FTLAB 에서 개발된 “스마트로거”는 저렴하고 소형이고 장시간 독립작동이 가능하여 국부적인 변화를 장시간, 간단하게 측정하기 위해 개발된 장치이다. 이 장치를 이용하여 실험실에서 밤사이 혹은 며칠 동안 일어나는 변화를 동시에 여러 위치에서 측정, 저장이 가능한 간단한 방법이 제시된다.

P2-Ap.032

Loss tangent of r-cut Sapphire Measured by Using Microstrip Resonators

*김지웅, 정호상, 박유리, 정연욱 [1], 김선후 [1], 이상영
*Jee Woong. Kim, Ho samg. Jung, Yuri. Park, Yonuk. Chong[1], seonhoo. Kim[1], Sang Young. LEE
건국대학교. [1] 한국표준과학연구원.

Keyword : Microstrip resonator, Loss tangent

고온초전도체가 발견된 이후, 고온초전도체를 이용한 고주파 소자의 제작 및 응용성 연구는 활발하게 진행되어 qubit, particle detector 등이 발전되었다. 초전도 qubit 의 경우 소자의 기판으로 사용되는 유전체의 loss tangent 가 신호 손실률에 큰 영향을 끼치기 때문에 소자의 특성 및 사용방법에 따른 loss tangent 의 정확한 측정 방법이 요구되고 있다. 고온초전도체를 이용한 고주파 소자에서 사용되는 기판 소재의 loss tangent 를 정확하게 측정하기 위한 방법으로서 microstrip resonator 를 설계하고, 시뮬레이션 함으로서 loss tangent 를 측정하기 위한 사전작업을 시행하였다. 이미 선행 연구로서, r-cut sapphire 의 한쪽 면에 YBCO 를 성장시켜 제작한 ring resonator 로 측정한 RS 와 rutile-loaded cavity 에서의 측정값이 50 K 이하의 온도에서는 거의 같은 값을 지니는 것이 확인된 바 있다. 따라서 본 연구에서는 r-cut sapphire 의 양면에 성장시킨 YBCO 박막을 이용한 ring resonator 를 통해 선행연구의 확인 작업 및 r-cut sapphire 의 loss tangent 를 측정하였다.

P2-Ap.033

Effects of Neutron Irradiations on the Microwave Properties of Undoped n-type Si Crystals at Cryogenic Temperatures

*정호상, 김지웅, 박유리, 조만순 [1], 주기남 [1], 박병우 [2], 이상영
*Ho samg. Jung, Jee Woong. Kim, Yuri. Park, Man Soon. Cho[1], Kee Nam. Joo[1], Byung woo. PARK[2], Sang Young. LEE
건국대학교. [1] 한국원자력연구원. [2] 서울대학교.

Keyword : neutron irradiation, microwave loss, silicon crystal, freeze out

Si 는 가장 널리 사용되는 반도체로서 특히 최근 널리 연구되는 QUBIT 의 기판을 포함하여 초전도 microwave 소자의 기판으로 많이 응용되고 있다. Microwave 의 중요한 특성 중 하나인 loss tangent(tan δ)는 microwave 신호 손실의 척도로 tan δ 가 작을수록 고주파 소자용 기판으로 사용하기에 유리하다. 유전체 공진기법은 microwave 특성을 측정하는 방법 중 하나로 최근 건국대에서 제안한 바 유전체공진기를 이용한 초전도체의 표면저항 측정법은 2011 년에 IEC 에 의해 국제표준측정법으로 채택된 바 있다. 이번 연구에서는 YBCO 가 사용된 Si 공진기를 이용하여 Si 의 tan δ 를 측정하였으며, undoped n-type Si 과 n-type 및 p–type 으로 doping 된 Si 에 neutron 을 조사 한 후 그 특성 변화를 관측하였다. 고저항 undoped Si 의 경우 시편 내에 극히 일부의 donor (또는 acceptor)가 존재하더라도 극저온(50 K 이하)에서 존재하는 freeze-out 영역으로 인해 일정 온도 이하에서 resistivity 가 급격히 증가한다. Loss tangent 에 기여하는 요인들 중 유전적 손실을 무시할 수 있는 경우 resistivity 가 tan δ 를 결정하게 되는데, 본 연구에서는 tan δ 를 측정한 후 이 측정값으로부터 resistivity 를 구하였다. 그 결과 undoped pristine Si 은 25 K – 50 K 에서 freeze-out 이 관측되었으며 중성자 조사된 undoped Si 의 경우 freeze-out 영역이 사라졌으며 중성자 조사 전의 undoped Si 보다 25 K 이상 저온 영역에서 상당히 작은(50 K 에서 3 만배) tan δ 값을 보였다. 이는 thermal neutron 에 의한 Neutron Transmutation Doping(NTD) 효과로는 설명되지 않으며, fast neutron 의 영향으로 인해 이러한 결과를 보였다고 설명된다.

P2-Ap.034*

The electrical properties of molecular monolayer devices with a PEDOT:PSS interlayer

*정인호, 송현욱, 황왕택 [1], 장연식 [1], 정현학 [1], 이탁희 [1]
*Inho. Jeong, Hyunwook. Song, Wang-Taek. Hwang[1], Yeonsik. Jang[1], Hyunhak. Jeong[1], Tak Hee. LEE[1]
경희대학교. [1] *서울대학교.*

Keyword : Molecular electronics, Tunneling, PEDOT:PSS

We fabricate a large number of 4-methylbenzenethiol (MBT) and 1,4-benzenedithiol (BDT) monolayer devices with a dimethyl sulfoxide (DMSO)-modified PEDOT:PSS (3,4-ethylenedioxythiophene) interlayer and performed the electrical characterization of these devices. We, in this study, demonstrate the effect of the contact properties between the constituent molecules and the PEDOT:PSS interlayer on the charge transport in the molecular junctions. The electrical characteristics of the PEDOT:PSS interlayer is affected by the experimental conditions such as temperature and humidity. The conductance of MBT and BDT molecular devices with the PEDOT:PSS interlayer is dependent on temperature in the range of high temperature from 300K to 400K. The high temperature gives rise to the changes in the morphology and phase of PEDOT:PSS interlayer, then which are related to the junction conductance. Also, the electrical characteristics of PEDOT:PSS interlayer would be influenced by the humidity condition. Our observation is explained by the change of the interfacial properties of the PEDOT:PSS molecule contact.

P2-Ap.035*

Study of charge transport mechanism of organic semiconductor devices by electrical and optical second harmonic generation measurement

*복문정, 이주호, 다구찌 다이 [1], 이와모토 미쯔마사 [1], 임은주
*Moonjeong. Bok, Ju ho. Lee, Dai. Taguchi[1], Iwamoto. mitsumasa[1], Eun Ju. Lim
단국대학교. [1] 동경공업대학.

Keyword : TIPS-pentacene, CNT, Fullerene,

We studied the carrier behavior in TIPS-pentacene organic field effect transistors and organic double-layer diodes with doped carbon nanotube and fullerene, which are anticipated to be easily heat treated by microwave radiation. The experiments were carried out on focusing carrier injection and transport. By using time-resolved optical electric field induced second hargmonic generation (TR-EFISHG) and electrical measurements, i.e. I-V and C-V measurements, we studied the carrier transport mechanism in organic semiconductor devices. Theses experiments were analyzed in terms of carrier injection and tranport properties on the basis of the Maxwell-Wagner effect model. Under microwave radiation condition, carrier transport mechanism is observed and it is allowed to study the device performance in terms of carrerier behavior

P2-Ap.036*

Analysis of hysteresis behavior of ITO/PI/TIPS-Pentacene/Au diode using electrical and optical measurements

*조성집, 다구찌다이 [1], 이와모토미쯔마사 [1], 임은주
*seongjip. CHO, Dai. Taguchi[1], Mitsumasa. Iwamoto[1], Eun Ju. Lim
단국대학교. [1] 동경공대.

Keyword : TIPS-Pentacene, Hysteresis, Trapping, Maxwell-Wagner effect element, Charge Modulation Spectroscopy measurement.

The carrier mechanisms in actual organic devices are not so simple, owing to the dielectric nature of active organic semiconductor layers, the complexity of interfaces, trapping effect by stress biasing, and others. By coupling the conventional Current–Voltage and Capacitance–Voltage measurement we studied the hysteresis behavior and the temperature dependence to understand the effect of trapping caused by injected carriers. The electrical measurements were shown to be helpful to clarify carrier injection that followed carrier trapping, meanwhile Charge Modulation Spectroscopy measurement was found effective for studying the carrier behaviors in energy space. Finally, these carrier mechanisms in organic semiconductor device were discussed in greater detail by analyzing the device as Maxwell-Wagner effect element.

P2-Ap.037*

Study of polymer material characteristics and organic semiconductor device with proton irradiation

*김민지, 임은주
*Min Jee. KiM, Eun Ju. Lim
단국대학교.

Keyword : proton beam. organic diode. polymer.

By using high energy particle radiation on organic semiconductor device, we studied the effect that appears on the polymer and the device performance. Properties of material with and without high energy particle radiation were explored by using UV-Vis spectroscopy, FT-IR, Nanoindentation measurements and so on. In experiment with and without the radiation, we used the same polymer materials and devices. We studied the carrier behaviors on organic devices with and without high energy particle radiation by using electrical measurements. Using the Maxwell-Wagner model, we analyzed the results with taking into account the carrier trapping for development of high efficient injection type organic devices.

P2-Ap.038

Light management effects of Ag and Au nanoparticles at ITO/PEDOT:PSS interface

정재윤, 김학용, 이지수, 김현숙, *이강재, 이충훈
Jaeyoun. Jung, Hak Young. Kim, Jee Su. Lee, Hyun Suk. Kim, *Kang Jea. Lee, Choong Hun. LEE
원광대학교.

Keyword : Au nanoparticles, organic solar cells, localized surface plasmon

For the photovoltaic performance enhancement of the heterojunction organic solar cells, gold and silver nanoparticles were introduced into the interface between indium-tin-oxide anode layer and PEDOT:PSS hole transfer layer, and we improved the PCEs of organic solar cells by incorporating Au-NPs between ITO and the PEDOT:PSS layer. The PCEs enhancement effect occurs in the spectral region that coincident with the Au-NPs plasmon extinction band, whereas Ag-NPs do not. The degree of light absorption in the plasmonic-enhanced organic solar cells increased significantly as a result of Au-NPs LSPs resonance induced local field enhancement. The characterization results revealed that both optical and electrical properties of the fabricated organic solar cells were improved with Au-NPs.

P2-Ap.039*

실크 단백질 기반 금속-절연체-금속 공진기 구현 및 공진 모드 분석

권현수, 조성용, *김성환
Hyunsoo. Kwon, Sung-yong. Cho, *Sunghwan. Kim
아주대학교.

Keyword : 실크, 공진기, 변조, 금속-절연체-금속

금속-절연체-금속으로 이루어진 공진기 구조는 가장 기본적인 공진기 구조이다. 그리고 절연체로 주로 사용되는 물질은 산화규소와 같은 단단한 물질이 주로 사용되기에 공진기는 공진 모드를 크게 변조시키는 것에 한계가 존재한다. 그러나 외부 자극에 따라 절연체의 두께를 조절 할 수 있다면 큰 공진 모드 변조가 가능하며 다양한 응용이 가능하다. 본 연구에서는 생체친화 고분자 단백질인 실크를 절연체로 적용하여 큰 공진 모드의 변조를 유도했다. 결정화 된 실크는 물과 만났을 때 두께가 팽창하는 수화제의 특성을 가지며 두께가 팽창한다면 공진 모드 또한 크게 변할 것이다. 이러한 특성을 이용하여 물과 반응하기 전후의 투과율을 측정하여 공진 모드의 변조가 크게 나타나는 것을 확인했다. 뿐만 아니라 실크는 광학적으로 투명하며 인체에 무해한 생체친화 물질이므로 실크를 절연체로 사용한 공진기는 인체에 집적 할 수 있는 바이오 센서로서의 활용 가능성을 가진다.

P2-Ap.040*

비등방 나노 크기 구조에서 편광에 의존하는 Fano 공명 현상에 관한 연구

김민재, 김지수, *이연의, 우정원
Min Jae. Kim, Jisu. Kim, *Yeon Ui. Lee, Jeong Weon. Wu
이화여자대학교.

Keyword : Fano resonance

가로 250nm, 세로 500nm, 두께 100nm 인 직사각형 금 막대들 사이 가로간격을 50nm 에서 250nm 까지 50nm 간격으로 바꾸고, 세로간격을 100nm 에서 500nm 까지 50nm 간격으로 바꾼 메타 구조에서 일어나는 Fano 공명현상을 연구하였다. 금 막대들 사이의 간격을 가로, 세로 방향으로 조절하면서 각각 가로편광, 세로편광의 빛이 입사할 때 반사스펙트럼과 투과스펙트럼을 FDTD 로 계산하였다. 그 결과 세로편광의 빛이 입사할 때 가로간격의 변화에 따른 반사스펙트럼은 직사각형 금 막대의 플라즈몬공명의 변화가 없었고, 세로간격의 변화에 따른 반사스펙트럼은 Fano 공명을 보이는데 세로간격이 작아질수록 Fano 공명이 더 두드러진다. 한편 가로편광의 빛이 입사할 때는 플라즈몬공명의 적색편이 이외에 특이한 현상을 보이지 않았다. 이것은 세로편광의 빛에 의해 구동되는 직사각형 금 막대들 사이의 전기쌍극자 상호작용에 의한 간섭효과가 가로편광의 경우보다 훨씬 두드러지기 때문인 것으로 이해한다.

P2-Ap.041*

호이겐스 음각 사변체 메타표면에서 일어나는 비정상 굴절에 관한 연구

김지수, 김민재, *이연의, 우정원
Jisu. Kim, Min Jea. Kim, *Yeon Ui. Lee, Jeong Weon. Wu
이화여자대학교.

Keyword : 비정상 굴절, 메타표면

가로방향으로 일정하게 크기가 증가하는 사변체 메타표면에서 비정상 굴절을 관찰하였다. 두께 30nm 인 금 박막에 Focused Ion Beam 을 사용하여 가로변이 800nm 이고, 세로변이 각각 30nm 와 150nm 인 사변체모양을 가로 1000nm, 세로 200nm 주기로 총 크기 100 micro meter*100 micro meter 인 음각시료를 제작하였다. 가로방향의 위치에 따라 나노입자의 크기가 다르고, 이에 따라 고유진동수가 다르다. 외부에서 주어진 파장의 빛을 보내는 경우, 보낸 빛의 진동수와 사변체의 가로방향 위치에 놓여있는 나노입자의 고유진동수의 차이 때문에 산란된 빛이 갖는 위상은 느려진다. 사변체 메타 표면에서 산란된 빛의 전파 현상은 호이겐스 원리를 이용하여 이해할 수 있다. 본 논문에서는 파장에 따른 비정상 굴절을 실험으로 측정하고 또한 FDTD 를 이용하여 빛의 산란을 컴퓨터 시뮬레이션 하였고, 위상 차이를 이론적으로 계산하여 얻은 빛의 전파 결과와 비교 분석하였다.

P2-Ap.042*

The Effect of UV-Treated Iron Doped Bismuth Titanate-Doped TiO_2 Layer in Dye-Sensitized Solar Cells

*박정웅, 송명근
*Chung Wung. Bark, Myoung Geun. Song
가천대학교.

Keyword : Bismuth titanate, UV treatment, Hydrophilic, Hydrophobic

Dye-sensitized solar cells (DSSCs) have received considerable interest recently because they are cost-effective and eco friendly with efficiencies comparable to those of the traditional silicon-based cells. However, much of the effort aimed at achieving high conversion efficiencies has focused on dye and liquid electrolytes. In this work, we report the photovoltaic characteristics of DSSCs fabricated by mixing TiO_2 with Fe-doped bismuth titanate (Fe-BLT). Additionally, we were UV radiation-ozone (UV-O_3) treated to change the hydrophobic to hydrophilic of TiO_2. Because Fe-BLT mixed TiO_2 was easly seperated on the FTO glass. A remarkable surface wettability transition can be easily achieved by ultraviolet illumination. This result is attributed to prevent of metal oxide materials separated from the FTO glass.

P2-Ap.043*

Red Emission Enhancement of the YAG:Ce^{3+} by Co-doping Gd^{3+} ions

홍우태, 이주현, 주정식, *양현경
Woo Tae. Hong, Joo Hyun. Lee, Jung Sik. Joo, *Hyun Kyoung. Yang
부경대학교.

Keyword : "YAG:Ce^{3+}", "phosphor", "white LEDs" , "Gd^{3+}"

Most white LEDs (WLEDs) are based on InGaN blue LED chip with cerium doped yttrium aluminum garnet (YAG:Ce^{3+}) yellow phosphor. The YAG:Ce^{3+} phosphor has high stability in junction temperature of LED chip and high humidity environment, high quantum efficiency and blue absorption efficiency. However, there exist several problem in the application, including poor color-rendering index and high color temperature due to the lack of red emission.
To solve these problem, some sulfides and nitrides phosphors of $Y_2O_2S:Eu^{2+}$, $CaAlSiN_3:Eu^{2+}$, $(Ca,Sr)S:Eu^{2+}$ have been used commercially as red component for warm white LED. Unfortunately, these phosphor has poor chemical stability, low efficiency and short lifetime. Another solution is to use and UV LED chip, combined with red/green/blue (RGB) tri-color phosphors as the excitation light source. These method has a disadvantage with interaction between RGB phosphors which decrease the luminescence efficiency.
In recent years, researchers have developed garnet phosphors, which are emitting green or yellow light containing with more red emission intensity by and doping other ion in yttrium site or aluminum ion site. Also, the photoluminescence properties of the YAG:Ce^{3+} can be controlled by different synthesis methods. $Y_3Al_5O_{12}:Ce^{3+}$, Gd^{3+} (YAG:Ce^{3+}, Gd^{3+}) phosphors synthesized by using a high-energy ball milling method. The X-ray diffraction patterns, photoluminescence spectra, scanning electron microscope image and the International Commission on Illumination (CIE) chromaticity coordinates of YAG:Ce^{3+}, Gd^{3+} phosphors were characterized and analyzed for concentration of Gd^{3+} ion.

P2-Ap.044*

Properties of morphology and size changing Gd(III) by the various types and ratios of solvents

박성준, 문주영, 장형일, *양현경
Sung Jun. Park, Ju Young. Mun, Hyeong Il. Jang, *Hyun Kyoung. Yang
부경대학교.

Keyword : "morphology" , "Gd(III)" , "solvothermal"

In recent years, the synthesis of inorganic micro- and nanostructure materials with tunable size and morphology with different dimensions (zero, one, two, and three) have received great attention because of unique and useful electronic, optical, and magnetic properties.
The hydrothermal or solvothermal method is an important technology for the preparation of low dimension nanostructures. Solvents used in solvothermal have property from non-polar to polar and interact host materials. The morphology and size of materials is changed by the intensity of solvent polar.
The Gd-based nanoparticles are promising multifunctional properties. The Gd_2O_3 is also a useful host material because of its good chemical durability, thermal stability, and low phonon energy.
In this research, $Gd(NO_3)_3$ phosphors were synthesized by a hydro- and solvothermal method used in ethylene glycol, acetone, 2-propanol, toluene, and hexane as solvents, and each solvent added different ratio with mixed water (40/0, 30/10, 20/20, 10/30 and 0/40). A series of powders were characterized by X-ray diffraction (XRD) using a Philips X'pert/MPD diffraction system with Cu-Kα radiation (λ = 1.54056 Å). The surface morphology of the powders were investigated with the field emission scanning electron microscopy (FE-SEM). The PL and PLE spectra of the prepared samples were recorded on a PTI (Photon Technology International) fluorimeter using a Xe-arc lamp.

P2-Ap.045

Triplet–triplet annihilation-induced upconverted delayed luminescence in bicomponent organic systems by using a gap plasmon resonator

*박준규, 고형덕 [1], 권혁중
*Jun Kue. Park, Hyungduk. Ko[1], Hyeok-Jung. Kweon
Korea Atomic Energy Research Institute. [1]Korea Institute of Science and Technology.

Keyword : DPA, PtOEP, Triplet-triplet annihilation, gap plasmon resonator

The triplet–triplet annihilation (TTA) efficiency in bicomponent organic systems is investigated by employing a gap plasmon resonator. In our structure, strong absorption peaks arising from coupling between localized surface plasmons and surface plasmon polaritons closely overlap the Q band of porphyrin, leading to higher triplet concentrations within the film. We find that at ultralow excitation intensities on the order of watts per square centimeter (W cm^{-2}), TTA becomes predominant for the organic system on a gap plasmon resonator. A strong surface-enhanced Raman scattering intensity is observed in this substrate, verifying the nearfield enhancement.

* 본 연구는 미래창조과학부의 연구비 지원을 받았음.

P2-Ap.046*

그래핀과 WSe2 이종접합의 Metal Contact 변화에 따른 Photocurrent 효율 증대

*최원록, 김광진, 유우종
*wonrok. choe, kwangjin. kim, Yu Woo jong.
성균관대학교.

Keyword : Graphene, WSe_2, Metal contact, Photocurrent, Heterostructure

그래핀은 Planar 구조, 높은 전자 전도도, high mobility 등의 좋은 특성을 갖고있으며, 미래 지향적 물질로 탁월함을 보였다. 그러나 Bandgap 의 부재로 인하여 특정 파장의 광학 소자로서는의 사용에 어려운 점이 있다. 이를 보완하기 위하여 최근, Transition-metal dichalcogenides(TMDs) 물질과 결합하여 그 특성을 보완하는 연구가 진행되고 있다. TMDs 의 경우, 훌륭한 전기적, Optical 특성을 가지고 있으며, 그래핀과 동일하게 exfoliation 을 통하여 heterostructure 제작에 용이하다. 특히, mono-layer TMDs 물질의 경우, direct semiconductor 의 특성을 가져 특정 파장의 빛을 쉽게 흡수 또는 방출하여, 광학 소자로서의 연구에서 많이 활용된다. 여기서 우리는 Graphene 과 WSe2 의 이종접합을 통하여 광학적 특성을 보였으며, Metal Contact 의 변화에 따른 Schottky Barrier 의 변화를 연구하여 Graphene/WSe2 Heterostructure 의 Photocurrent 의 효율을 증대시켰다.

P2-Ap.047

3D 프린팅 기술을 이용한 선택적 박막 증착 방법

*박정웅, 김도현, 진종언 [1], 전성수 [1], 정종흠 [1]
*Chung Wung Bark. , KIM. DOHYUN, Jin. Jong Un[1], Chun. Sungsu[1], Jeong. Jongheum[1]
가천대학교. [1] 경기과학고등학교.

Keyword : 3D 프린팅,박막증착

실리콘 기반 소자를 포함한 나노 소자 대다수가 고직접화 회로설계로 복잡하기 때문에, 다양한 박막증착 기술을 구현 하는데 있어 문제점을 가지고 있다.
포토리소그래피(Photolithography)는 원하는 회로설계를 유리판 위에 금속패턴으로 만들어 놓은 마스크(mask)라는 원판 에 빛을 쬐어 생기는 그림자를 웨이퍼 상에 전사시켜 복사하는 기술이며, 반도체의 제조 공정에서 설계된 패턴을 웨이퍼 상에 형성하는 가장 중요한 공정이다. 그러나 고집적화 회로 설계에 있어서 각각 다른 패턴을 가지는 마스크를 제작하는 과정은 복잡할 뿐만 아니라, 고가의 공정기술을 필요로 한다. 이와 같은 문제점을 해결하고자, 3D 프린팅 기술을 이용하여 마스크 제작을 다양한 패턴으로 단시간에 구현해 낼 수 있으며, 무엇보다 저가의 공정기술로 제작할 수 있다는 큰 장점을 가진다. 따라서, 기존의 복잡하고 고가의 리소그래피 과정 없이 물성 조절이 가능한 나노소자 박막 시스템 구현이 가능하다.

P2-Ap.048*

Current control of GFET by Light

*유광남, 김지호, 최은집
*Kwangnam. Yu, Jiho. Kim, E. J.. Choi
서울시립대학교.

Keyword : GFET, Light, Low-doped Silicon

이 연구에서는 빛을 이용해 GFET 의 전류를 조절하는 방법에 대해 제시한다. GFET 는 게이트 역할을 하는 실리콘, 절연체인 실리콘옥사이드, 그리고 전자 수송 통로인 그래핀으로 이루어진다. 이 때 4~6 Ωcm 의 면저항을 가지는 실리콘을 사용하면 때 빛의 유무에 따라 GFET 의 전류를 약 2.5 배 까지 차이나게 만들 수 있다. GFET 의 빛에 의한 반응이 실리콘에 의해 나타남을 보이기 위해 단파장 빛을 이용해 실리콘 밴드갭인 1.1eV 보다 높은 빛에 의해서만 반응이 일어나는 확인했다. 또한 적외선 투과율을 통해서 빛의 유무에 상관없이 그래핀 내의 전자 산란 정도는 변화하지 않음을 보였다.

P2-Ap.049*

투명적극 ITO 와 Cu 다층 박막의
전기적, 광학적 특성에 관한 연구

박정일, 김경민, 이기문, *차덕준
Jeoungil. Park, Keongmin. Kim, Kimoon. Lee, *Deokjoon. Cha
군산대학교.

Keyword : "ITO, Cu, 다층박막"

투명전극으로 사용되는 ITO 는 높은 투과율과 낮은 전기저항을 가진다. 그러하여 ITO 는 OLED, PDP, LCD 등의 다양한 많은 분야에 활용되는 물질이다. 여러 분야에 널리 활용되는 만큼 보다 우수한 전기적 특성과 높은 투과율이 필요하다. 현재 ITO 의 성능을 높이기 위해 ITO 박막 내부에 얇은 금속층을 삽입하여 다층 박막으로 증착하는 연구가 활발히 진행되고 있다. 얇은 금속층으로 주로 Al, Cu, Ag 와 같은 금속이 주로 활용된다. 이중 Al 의 경우 산소에 민감하며, Ag 같은 경우 금속 자체의 가격이 비싸므로 여러 문제가 될 수 있다. 그러므로 가장 무난히 많이 사용 할 수 있는 Cu 를 선택하였다. 본 실험은 DC 마그네트론 스퍼터링으로 저온 공정에서 진행되었으며, 투명전극인 ITO 와 ITO 중간에 Cu 를 삽입한 ITO/Cu/ITO 인 3 층 박막 그리고 ITO/Cu/ITO/Cu/ITO 인 5 층 박막의 전기적, 광학적, 그리고 구조적 특징을 Four-point meter, UV-vis, FE-SEM 을 이용하여 분석하였다. 또한 광 투과율과 전기적 특성의 성능을 평가하기 위해 면 저항과 광 투과율 데이터를 통해 Haack's figure of merit 을 계산하여 분석하였다. 이 결과에서 다층투명전극의 제작에 긍정적인 영향을 미칠 것이라 생각한다.

P2-Ap.050

Thermal evaporation 방식을 적용한 Indium Zinc Oxide (IZO) 박막 제작 및 특성 분석

*김이도, 최명운 [1], 정광호, 최진철
*Yi do. Kim, Myung woon. Choi[1], Kwang ho. Jeong, Jin chul. Choi
연세대학교. [1](주) 야스.

Keyword : "Thermal evaporation", "Indium Zinc Oxide", "Low damage CIGS solar cell"

CIGS 태양전지는 다른 태양전지와 비교하여 고효율 및 열적, 전기적 안정성 등의 장점으로 활발한 연구가 진행되고 있다. CIGS 태양전지는 기판 위에 Back contact 을 올리고 그 위로 Absorber 층, Buffer 층, Window 층 그리고 Grid 순으로 구성이 되며 기판재료에 제약이 없어 Flexible 기판의 사용이 가능하여 Flexible 한 박막태양전지로써 높게 평가되고 있다. 이러한 CIGS 태양전지의 Window 층으로 사용되는 TCO 는 ITO, AZO, IZO 등이 사용되며, 일반적으로 Sputter 방식으로 Buffer 층(CdS, ZnS, InS 등) 위에 증착 된다. 이때 증착 과정에서 발생되는 고에너지 입자에 의해 Buffer 층이 손상되어 소자 효율이 저하되는 문제가 있다.

본 연구에서는 Window 층을 형성하면서 발생하는 Buffer 층 손상을 원천적으로 없앨 수 있는 Thermal Evaporation 방식을 이용하여 Window 층을 형성하는 방법에 대한 연구를 진행 하였다. 산소 분위기에서 Indium 과 Zinc 각 물질의 증발 속도 제어를 통한 조성비 변화 및 기판 온도에 변화를 주어 Indium Zinc Oxide (IZO) 박막을 Soda-lime glass 위에 증착 후 분석하였다. 기판 온도 200℃에서 특정 조성비의 IZO 박막은 XRD 분석 결과 amorphous 상태로 존재하였으며, UV-Vis-NIR Spectrophotometer 분석 결과 400nm 에서 800nm 까지는 85% 이상, 800nm 에서 1500nm 까지는 80% 이상의 광 투과도를 보이고, Hall Measurement 장치를 이용한 비저항 측정 값은 $5x10^{-4}$ Ω·cm 로 Sputter 방식으로 증착한 IZO 박막과 동등 수준의 전기적, 광학적 특성을 보임을 확인 하였다. 향후 Thermal evaporation 방식으로 제작된 Low Damage TCO 박막을 CIGS window 층에 적용하여 그 특성 분석을 진행하려 한다.

P2-Ap.051

Co-sputtering 법에 의한 Indium Molybdenum Oxide 박막의 증착온도 변화에 따른 광학적 및 전기적 특성 연구

*전지아, 오규진, 김은규
*Jeon Jia. , OH GYUJIN. , KIM Eun Kyu.
한양대학교.

Keyword : IMO, Indium oxide, Molybdenum, thin film

Transparent conducting oxides (TCOs)는 전기광학적 특성과 더불어 공정 편의성, 화학적 안정성, 그리고 경제성 등에 대해 수 십 년간 널리 연구되어 왔다. 특히, Indium oxide 계열의 TCO 박막은 3.6 eV 범위의 wide bandgap 으로 인한 높은 가시광 투과율과 함께 우수한 전기 전도도 특성 (

P2-Ap.052

Properties of ZnO:Yb_2O_3 nano-clustering films as a transparent down-conversion layer in poly-crystalline Si solar cells

*김홍탁, 이성엽 [1], 박종구 [1], 박진호
*Hong Tak. KIM, Sung-Yup. Lee[1], Jong Goo. Bhak[1], Chinho. Park
영남대학교. [1] *경북대학교.*

Keyword : Down-conversion, Nano-clustering, Solar cell, ZnO, Yb_2O_3

ZnO:Yb_2O_3 nano-clustering films (NCFs) were deposited on quartz substrates using spin-coating method. The formation mechanism of the NCFs could be summarized as out-diffusions of Yb elements dispersed inside ZnO hosts due to different ionic radii and oxidation state of Zn^{2+} and Yb^{3+} ions. This implied Yb elements did not incorporated into ZnO hosts, and the clustering structure between nano-sized Yb_2O_3 and ZnO hosts was formed by this mechanism. In addition, the energy transfer process from ZnO hosts to Yb_2O_3 was mainly followed by a quantum cutting process, and happened efficiently, although there is not substitution of Yb element in Zn sites. The improvement ratio of CE for the ZnO:Yb_2O_3 NCFs/pc-Si cell (9.3%) compared to the bare pc-Si cell (8.6%) was about 10% and this meant the NCFs was an effective down-conversion layer for Si-solar cells. However, the formation temperature of NCFs with high performance was relatively high (~750 ^{o}C), and the decrease of transmittance declined the improvement of CE, seriously.

P2-Ap.053*

AC 전기장 내에서 DC 전압이 인가된 다공성실리콘 박막의 진동 특성 해석

*함성길, 한성범, 이재준, 김나경, 이기원
*Ham sounggil. , Han. Seongbeom, Lee Jaejoon. , Kim Nagyeong. , LEE Ki-Won.
공주대학교.

Keyword : 다공성실리콘, 다공성실리콘 박막, 박막 진동, AC 전기장

실리콘웨이퍼를 HF 용액 속에서 전기화학적으로 에칭하면, 웨이퍼의 표면으로부터 깊이방향으로 수십 nm 의 무수한 기공을 갖는 다공성실리콘이 만들어진다. 다공성실리콘은 80% 이상의 다공도를 가질 수 있고 200m2/cm3 정도의 큰 표면적을 갖기 때문에 분자의 물리화학적 흡착 특성을 이용한 유기증기센서, 약물 전달체 등 다양한 연구가 이뤄지고 있다. 제작된 다공성실리콘은 2 차 에칭을 통해 실리콘 기판으로부터 완벽히 분리되어 박막으로도 제조될 수 있다.
본 연구에서는 DC 전압이 인가된 다공성실리콘 박막을 50Hz~20kHz 의 균일한 AC 전기장내에 평행하게 설치함으로서 다공성실리콘 박막을 진동시킬 수 있는 장치를 제작하였다. 그리고 박막의 진동으로 만들어지는 음파의 세기를 콘덴서 마이크로 측정하였다. 박막의 진동 특성을 상세히 조사하기 위해 DC 전압의 부호와 크기에 따른 음파 세기의 주파수응답특성, AC 전기장을 형성하는 참조신호와 측정된 음파신호 간의 위상차 등을 조사하였다. 그 결과 다양한 봉우리들이 주파수응답특성에서 관찰되었으며, 이 봉우리들의 세기와 위상은 박막에 인가한 DC 전압의 부호와 크기에 따라 변화되었다. 이 현상을 설명하기 위해 AC 전기장 주파수에 따른 다공성실리콘의 전하분포 변화에 대한 모델을 수립하고 해석하였다.

P2-Ap.054

Surface structure of ultra-thin Al films on a W(110) surface at high temperature

*최대선, 김지철, 박미미
*Dae Sun. Choi, JeeCheol. Kim, Mi Mi. Park
강원대학교.

Keyword : "Al", " W(110)", "growth mode"

The surface structures of ultra- thin Al films on a W(110) surface have been studied using LEED.
When the Al coverage is 0.5 ML, and annealed at 1100 K, the surface reveals a p(2x1) double domain structure.
When the Al coverage is 1.0 ML, the surface has mixted structure of various surface, i.e., a W(110) surface and a Al(111) surface rotated ±2.5° and a p(2x2)-R25.24° from [1,0,1] direction were revealed at the same time. Finally, we suggest that Al grow on a W(110) surface at high temperature with VW mode.

P2-Ap.055

Polarity Control of Semipolar GaN Domains

윤한섭, 주미연, 장동수, *김진교
Habsub. Yoon, Miyeon. Jue, Dongsoo. Jang, *Chinkyo. Kim
경희대학교.

Keyword : GaN, semipolar, polarity

Semipolar GaN draws much attention as a candidate to effectively suppress quantum confined Stark effect, which is commonly observed in GaN grown along the polar direction. For the effective suppression of quantum confined Stark effect, it is well known that the tilt angle between +c orientation and the surface normal should be about 45 degrees. In this work, we report that the polarity of semipolar GaN can be controlled in such a way that quantum confined Stark effect can be effectively suppressed.

P2-Ap.056

In-situ synchrotron radiation photoemission spectroscopy study of property variation of Ta_2O_5 film during the atomic layer deposition

*이승엽, 전철호, 이주한
*Seung Youb. Lee, Cheolho. Jeon, Jouhahn. Lee
한국기초과학지원연구원 (KBSI).

Keyword : “Atomic layer deposition”, “Tantalum pentoxide (Ta_2O_5)”, “In-situ SRPES”

Atomic layer deposition (ALD) can be regarded as a special variation of the chemical vapor deposition method for reducing film thickness. ALD is based on sequential self-limiting reactions from the gas phase to produce thin films and over-layers in the nanometer scale with perfect conformality and process controllability. These characteristics make ALD an important film deposition technique for nanoelectronics. Tantalum pentoxide (Ta_2O_5) has a number of applications in optics and electronics due to its superior properties, such as thermal and chemical stability, high refractive index (>2.0), low absorption in near-UV to IR regions, and high-k. In particular, the dielectric constant of amorphous Ta_2O_5 is typically close to 25. Accordingly, Ta_2O_5 has been extensively studied in various electronics such as metal oxide semiconductor field-effect transistors (FET), organic FET, dynamic random access memories (RAM), resistance RAM, etc. In this experiment, the variations of chemical and interfacial state during the growth of Ta_2O_5 films on the Si substrate by ALD was investigated using in-situ synchrotron radiation photoemission spectroscopy. A newly synthesized liquid precursor $Ta(N^tBu)(dmamp)_2Me$ was used as the metal precursor, with Ar as a purging gas and H_2O as the oxidant source. The core-level spectra of Si 2p, Ta 4f, and O 1s revealed that Ta suboxide and Si dioxide were formed at the initial stages of Ta_2O_5 growth. However, the Ta suboxide states almost disappeared as the ALD cycles progressed. Consequently, the Ta^{5+} state, which corresponds with the stoichiometric Ta_2O_5, only appeared after 4.0 cycles. Additionally, tantalum silicide was not detected at the interfacial states between Ta_2O_5 and Si. The measured valence band offset value between Ta_2O_5 and the Si substrate was 3.08 eV after 2.5 cycles.

P2-Ap.057*

Electrical Properties of Tantalum Nitride Film Prepared by Reactive Sputter Deposition

이수민, 유명재 [1], 선호정, *이용제
Sumin. Lee, Myungjae. Yoo[1], Hojung. Sun, *YongJei. Lee
군산대학교. [1] *전자부품연구원.*

Keyword : TaN, Thin flim resistor, Reactive RF sputtering

Tantalum Nitride (TaN) thin films were deposited onto Si(111) and plastic substrate at room temperature by reactive radio frequency (RF) magnetron sputtering with adjusted deposition parameters. the films were investigated by 4-point probe, High Resolution X-ray Diffraction (HR-XRD) and Field Emission Scanning Electron Microscope (FESEM, S-4800). The electrical resistivity was increased as the amount of N_2 was increased. The electrical resistivity of plastic substrates was higher than that of Si(111) substrates. Two TaN main peaks were identified as TaN(111) and TaN(200) orientations. From electrical and structural analysis, TaN(111) phase made the higher electrical resistivity. columnar structures were observed in the deposited films and increased with decreasing the N2 amount and increasing powers.

P2-Ap.058

The characteristics improvement of silicon nitride thin film using ArF excimer-laser annealing method

최도현, *김현숙, 이충훈
Do Hyun. Choi, *Hyun Suk. Kim, Choong Hun. LEE
Wonkwang University.

Keyword : Hydrogen-free silicon-nitride, Reactive sputtering, Stoichiometry, Excimer-laser annealing, X-ray photoelectron spectroscopy

Hydrogen-free silicon-nitride films have been deposited on 1200-Å-thick Si (100) wafers by using reactive sputtering at room temperature and annealed by ArF excimer-laser at room temperature. In-situ X-ray photoelectron spectroscopy (XPS) analyses showed that the 1200-Å-thick as-sputtered films were completely and uniformly annealed by ArF excimer-laser with the various energy densities leaving no unannealed portion in the depth direction. An as-sputtered film was also annealed in furnace at 1000 ℃ for comparison. The influence of the energy density was further investigated by comparing the etch rate of the SiN film with the N/Si ratio adjusted by separating the unreacted-Si and N components from the SiN film. For the excimer-laser-annealed SiN films, the results of quantitative XPS analysis were in good agreement with the etching characteristics.
The as-sputtered SiN film contained slightly higher Si than the stoichiometric ratio, with an adjusted-N/Si-ratio value 0.902, possibly due to sporadic presence unreacted-Si. At the laser energy densities ranging from 100 to 175 mJ/cm^2, the excimer-laser-annealed SiN films displayed a much better film quality than the SiN film annealed at 1000 ℃, due to a higher N/Si ratio.

P2-Ap.059*

Cu/Cr 금속 박막을 이용한 thin film thermocouple 의 특성 연구

김휘린, 박정일, 김경민, *차덕준
huirin. Kim, Jeoungil. Park, kyeongmin. Kim, *Deokjoon. Cha
군산대학교.

Keyword : Thin film thermocouples(TFTCs), Cu/Cr thin film, Thermoelectric

Cu, Cr 을 이용한 thin film thermocouple 를 제작했다. Cu 와 Cr 의 두께는 각각 100nm 의 두께로 DC 마그네트론 스퍼터링을 이용하여 유리기판위에 증착하여 제작했다. Hot junction 의 크기는 2mm x 2mm 로 하고 증착시간을 조절하여 두께를 조절했다. 두 금속의 접합면이 잘 스며들게 하기위한 공정을 하고, 단면의 이미지는 주사전자현미경(scanning electron microscopy)를 이용하여 정확히 확인하였다. 만들어진 thin film thermocouple 의 온도에 따른 열기전력을 측정하여 잘 완성된 실험인지 확인했다. thin film thermocouple 의 이점은 제조의 단순성과 작은 크기, 회로를 쉽게 구성할 수 있다.

P2-Ap.060

X-선 토포그래피에 의한 사파이어 웨이퍼의 표면 결함 분석

*전현구, 김창수 [1], 정인영
*Jeon Hyeon gu. , KIM Chang Soo. [1], Jung In young.
충남대학교. 한국표준과학연구원. [1] 한국표준과학연구원.

Keyword : XRT, X-선 토포그래피, X-ray topography, surface damage, 표면결함

사파이어 웨이퍼의 표면 결함은 에피 박막의 물성에 크게 영향을 미치며, 특히 에피 박막의 결정성 및 균질성에 영향을 미침으로서 광학 또는 반도체 소자의 특성에 영향을 주게 된다. 따라서 표면연마공정의 목적은 웨이퍼 제조공정 중에 생성된 표면 결함을 제거하여 우수한 결정성의 박막을 성장시키는데 있다. 그리고 이를 달성하기 위해 산업체에서는 광학현미경, AFM 등의 장비를 이용해 표면 결함의 검사하고 있다.
본 연구에서는 X-선 토포그래피의 결함 이미징 기술을 이용하여 사파이어 웨이퍼 연마 공정에 따른 표면 결함을 분석하였다. X-선 토포그래의 결함 이미징 메커니즘은 결함에 의해 생성된 결정학적 strain field 에 의해 회절 X-선의 산란강도가 증가하는 현상으로 설명할 수 있다. 따라서 표면 결함의 유무 또는 정도에 따라 X-선 산란강도가 달라지며, 이를 비교함으로서 표면 결함의 유무 또는 정도를 평가할 수 있다. 사파이어 웨이퍼를 표면 연마공정 조건을 달리하여 XRT 를 이용해 그 결과를 비교, 분석하였다. 분석 결과, 공정 조건에 따른 표면 결함의 유무, 분포 그리고 정도를 확인할 수 있었으며, 고분해능 XRD 를 이용해 표면 결함에 의한 diffuse scatter 를 분석함으로서 본 연구의 결과를 검증하였다.

P2-Ap.061

미려한 펄감을 표현하는 전자기기용 고기능 전착기술에 관한 연구

*장호경, 이일봉
*CHANG. Ho Gyeong, LEE. IL-BONG
대구한의대학교.

Keyword : "전착도장", "펄감", "Texture", "음이온전착도료"

미려한 펄감을 표현하는 전자기기용 고기능 전착기술에 대한 산업적 수요가 크게 요구되고 있으며, 전착도장으로 펄감을 가지는 도막을 형성하기 위해서는 일반적으로 전착도료에 펄 분말을 첨가하여 도장하지만, 펄 분말을 사용하지 않고 미려한 펄감을 표현할 수 있는 새로운 방식의 펄감을 표현하는 전착도장방법으로 전자기기용 고기능 전착 기술을 연구하였다. 연구결과 펄 분말을 첨가하여 도장하는 과정에서 미려한 펄감을 표현하는 전자기기용 고기능 전착의 수율과 품질향상을 위해 획기적으로 문제점을 해소할 수 있는 방법으로 전착도료에 펄 분말을 첨가하지 않고도 피도물의 표면에서 자연물에 의한 표현이라는 느낌을 주는 감성품질을 표현하는 새로운 방식의 펄감을 표현하는 전착도장 기술을 얻게 되었다.
본 연구에서는 센딩을 통한 Texture 형성하고, Dilution Recipe 를 구하기 위해 안료(Pigment)인 ED-600 과 ED-600S, ED-MX, ED-M 를 이용한 실험에서 안료들의 조성물 배합비를 찾기 위해 각 안료들의 여러 농도로 실험하여 ED-600 과 ED-MX (15% 고형분)의 적합한 농도에서 가장 정착이 우수함을 확인할 수 있었다.
이러한 정착 시료를 여러 온도(20~40℃) 조건에서 수세 후 검사 및 테스트하였으며, 건조 과정의 실험 결과 180±10℃와 30±5 min 건조 조건에서 가장 좋은 결과를 나타냄을 알 수 있었다.

P2-Ap.062

Post Annealing of the Gallium doped Zinc Magnesium Oxides ceramics

*전병억, 이성민, 권도윤, 이정현, 황수영
*Byeong-Eog. Jun, Seongmin. Lee, Doyoon. Kweon, Jeonghyun. Lee, Soo Young. Hwang
카이스트 부설 한국과학영재학교.

Keyword : RF magntron sputtering, Thin film coating, Surface morphology, Optical bandgap

Gallium doped $Zn_{1-x}Mg_xO$ (ZMO:Ga, x = 0.1, Ga 3 at.%) thin films were prepared by using the RF-magnetron sputtering methods. The ZMO:Ga target ceramic was prepared by using the conventional solid state reaction methods. ZMO:Ga thin films were coated on the Al_2O_3 (001) substrates at room temperature. The structural and surface morphology of ZMO:Ga thin films were analyzed by using the X-ray diffraction analysis and the scanning probe microscopy. The electrical properties of the post-annealed ZMO:Ga thin films were investigated by using the Hall Effect measurements and the 4-wire surface conductivities. Optical transmittance was measured by using the UV-Vis spectrometer. As the annealing temperature is increased in the temperature range from 200°C to 800°C, the X-ray scattering intensity of the (002) peak was increased but the surface conductivity was decreased. The optical band gap was increased as the annealing temperature was increased in the temperature range from 300°C to 500°C. It is considered that the nano sized particles were grown to sub micron sized grains. The band gap was increased with the lattice constant decreasing in the ZMO:Ga thin films.

P2-Ap.063*

Si(111) 위에서의 B20 나선형 FeGe(111) 박막 성장 조건과 원자 구조 연구

*노승균, 윤지수 [1], 김재성 [1], 황찬용 [2], 김원동 [2]
*Seung-Kyun. Noh, Ji-Soo. Yoon[1], KIM Jae Sung. [1], HWANG Chanyong. [2], KIM Wondong. [2]
과학기술연합대학원. [1] 숙명여자대학교. [2] 한국표준과학연구원.

Keyword : STM, LEED, FeGe, Magnetic Skyrmion, Bulk Chrome tip

자성 스커미온 상태는 그 위상학적 특성으로 향후 스핀트로닉스로의 응용 가능성이 매우 커 최근 많은 관심의 대상이 되고 있다. 특히 최근 B20 나선형 구조를 가지는 전이금속-4 족 화합물에서 자성 스커미온 격자 구조가 실험적으로 관찰되어 이러한 관심을 더욱 증폭시키는 계기가 되었다.[1] 이중 FeGe 는 다른 전이금속-4 족 화합물에 비해 더 낮은 자기장 및 더 높은 온도에서 자성 스커미온 격자 상태가 형성됨이 알려져 큰 주목을 받고 있다.[2] 이 연구에서는 이러한 FeGe 을 Si(111) 기판 위에 5 nm 이하 두께의 박막상태로 성장시켜 저에너지 전자회절(Low Energy Electron Diffraction, LEED)와 주사 터널링 전자 현미경(Scanning Tunneling Microscopy, STM)을 통하여 표면 상태와 원자 구조를 관찰하였다. 기존에 알려진 고온 성장 조건에서는 박막 표면이 매우 거칠게 됨을 확인한 반면, 상온 성장후 열처리하였을 때 매우 평평한 표면이 형성됨을 알아내었다. 또한 원자 분해능 STM 실험을 통하여 이러한 표면의 원자 구조가 FeGe 의 B20 나선형 구조와 일치함을 알아내어 실제로 FeGe(111) 단결정 박막이 형성되었음을 확인하였다. 성장 초기 과정에 대한 STM 및 LEED 관찰을 통해 Ge(111) 5x5 구조의 원자층이 Si 표면에 형성됨을 알아내었으며 이를 통해 Ge 원자층이 Si(111)과 FeGe(111)의 격자 어긋남을 완화시켜줄 수 있는 완충층이 됨을 유추할 수 있었다. 이러한 결과는 향후 고품질의 FeGe 박막 성장 및 이에 기반한 박막의 자성 스커미온 격자 상태 연구의 가능성을 높여준다고 할 수 있다.

[1] N. Nagaosa and Y. Tokura, Nature Nanotechnology 8, 899(2013).
[2] X. Z. Yu et al., Nature Materials 10, 106(2010).

P2-Co.101

Characterization of primary microRNA processing in single-molecule level

*조명현, 홍성철
*Myung Hyun. Jo, Sungchul. Hohng
서울대학교.

Keyword : MicroRNA, Drosha, DGCR8, single-molecule

MicroRNAs are short non-coding single-stranded RNA molecules of ~22 nt in length, which perform integral roles in post-transcriptional gene regulation in eukaryotes. In the early stage of biogenesis of miRNAs, RNase III DROSHA cleaves a long primary microRNA in an exact manner. The accurate process of DROSHA is critical for the production of functional microRNAs. How DROSHA recognize and cleave the various substrates precisely for successive processes remains enigmatic. In this study, we tried to clarify the mechanism of the Microprocessor in single-molecule level.

P2-Co.102

Unraveling the Unwinding Mechanism of E1 Hexameric Helicase from Papillomavirus using Ensemble and Single Molecule FRET Methods

*이승재, 홍성철 [1]
*Seung-Jae. Lee, Sungchul. Hohng[1]
서울대학교 기초과학연구원. [1] *서울대학교.*

Keyword : "ATPase" "helicase" "smFRET" "DNA replication"

A prerequisite for DNA replication is the unwinding of duplex DNA catalyzed by a replicative hexameric helicase. Despite a growing body of research, key elements of helicase mechanism remain under substantial debate. In particular, the number of DNA strands encircled by the helicase ring during unwinding and the ring orientation at the replication fork completely contrast in contemporary mechanistic models. Here we use single-molecule and ensemble assays to address these questions for the papillomavirus E1 helicase. We find that E1 unwinds DNA with a strand-exclusion mechanism, with the N-terminal side of the helicase ring facing the replication fork. We show that E1 generates strikingly heterogeneous unwinding patterns stemming from varying degrees of repetitive movements, which is modulated by the DNA-binding domain. Together, our studies reveal previously unrecognized dynamic facets of replicative helicase unwinding mechanisms

P2-Co.103

Nap1L1 regulates the enzymatic activity of CSB on the alteration of chromatin structure

*이주연, 홍성철, Robert J. Lake[1], Hua-Ying Fan[1]
*Ju Yeon. Lee, Sungchul. Hohng, Robert J.. Lake[1], Hua-Ying. Fan[1]
서울대학교. [1]University of Pennsylvania.

Keyword : Single molecule FRET, Cockayne syndrome complementation group B protein, Chromatin remodeling, Transcription-coupled nucleotide excision repair.

The Cockayne syndrome complementation group B (CSB) protein plays pivotal roles in transcription-coupled nucleotide excision repair (TC-NER). The mutations in CSB lead to defects in TC-NER, which is implicated in Cockayne syndrome characterized by photosensitivity, progressive neurological degeneration and premature-aging. CSB possesses a DNA-stimulated ATPase activity and can inefficiently repositions a nucleosome in an ATP-dependent manner. Recently, NAP1-like histone chaperone1 (Nap1L1) is discovered as a non-catalytic CSB-binding partner, which enhances nucleosome remodeling activity of CSB. However, how Nap1L1 impacts CSB's activity in the remodeling mechanism is not known. Here, we studied the underlying mechanism of the nucleosome remodeling by CSB in the absence or presence of Nap1L1, using a single molecule FRET technique. Interestingly, while ATP decreased the probability and the dwell time of transient DNA wrapping by CSB, Nap1L1 significantly prevented the nonspecific binding of CSB to free DNA, suppressing unnecessary ATP consumption for remodeling. In addition, the activation of the remodeling was 2-fold increased along with the higher translocation rate in the presence of Nap1L1. Our studies reveal a distinctive role of the histone chaperone Nap1L1 during the chromatin remodeling in preventing the formation of the nonfunctional CSB-chromatin interactions.

P2-Co.104

Metal-Ion Exchange Causes Catalytic Disorder that Interrupts Processive Enzyme Activity

유정민, *이광록
Jungmin. Yoo, *Gwangrog. Lee
광주과학기술원.

Keyword : "exonuclease", "metal ion", "cofactor", "single molecule", "FRET"

Metal ions as cofactors play a key role in enzymatic catalysis. Their coordination dynamics at the active-site greatly influences enzymatic activity. But little attention has been paid to dynamic aspects of how the exchange of metal ions influences the enzymatic activity. We employed lambda exonuclease and investigated how the enzyme activity is altered by competition of divalent ions via single-molecule fluorescence energy transfer (FRET). We found that the metal-ligand coordination is highly dynamic during each catalytic cycle, facilitating metal-ion exchange. We also tested competition among different metal-ions, and found that the enzyme exhibits fluctuation in the enzymatic rate in the presence of inhibitory cofactors. Our study provides new insight into how fluctuations in metal binding stability propagate into enzymatic activities.

P2-Co.105

Structural stability of aglycosylated IgG Fc variants affects the FcγRI binding affinity.

주만석, 정상택, *정철현 [1]
Man-Seok. JU, Sang Taek. JUNG, *Cherlhyun. JEONG[1]
국민대학교. [1] *한국과학기술연구원.*

Keyword : IgG Antibofy, FcγRI ,Single molecule FRET, alternating-laser excitation (ALEX)

In contrast to the glycosylated IgG antibodies secreted by human plasma cells, the aglycosylated IgG antibodies produced by bacteria are unable to bind FcγRs expressed on the surface of immune effector cells and cannot trigger immune effector functions. To avoid glycan heterogeneity problems, elicit novel effector functions, and produce therapeutic antibodies with effector function using a simple bacterial expression system, FcγRI-specific Fc-engineered aglycosylated antibodies, Fc11 (E382V) and Fc (E382V/M428I), containing mutations in the CH3 region, were isolated in a previous study. To elucidate the relationship between FcγRI binding affinity and the structural dynamics of the upper CH2 region of Fc induced by the CH3 mutations, the conformational variation of Fc variants was observed by single-molecule Förster resonance energy transfer (FRET) analysis using alternating-laser excitation (ALEX). In sharp contrast to wild-type Fc, which exhibits a highly dynamic upper CH2 region, the mutations in the CH3 region significantly stabilized the upper CH2 region. The results indicate that conformational plasticity, as well as the openness of the upper CH2 region, is critical for FcγR binding and therapeutic effector functions of IgG antibodies.

P2-Co.106

Predicting responses to targeted cancer therapy with single-molecule co-immunoprecipitation

*이홍원, 최병산, 손진영 [1], 민아름 [2], 강한나 [3], 차민권, 임석아 [4], 조병철 [1], 윤태영
*Hong-Won. Lee, Byung San. Choi, Jinyoung. Son[1], Ahrum. Min[2], Han Na. Kang[3], Min Kwon. Cha, Seock-Ah. Im[4], Byoung Chul. CHO[1], Tae-Young. Yoon
KAIST. [1]Yonsei University College of Medicine. [2]Seoul National University College of Medicine. [3]Yonsei University. College of Medicine. [4]Seoul National University. College of Medicine.

Keyword : protein-protein interaction, targeted cancer therapy, drug response prediction

Extensive profiling of cancer genome has comprehensively characterized the critical and recurrent genomic alterations from various cancer types. These genomic portraits of human cancer provided potential therapeutic targets in cancer therapy. However, whether the identified mutation is functionally important in maintaining individual cancer has still remained to be elucidated due to lack of functional analysis of altered genes. In this presentation, I will present about predicting the efficacy of targeted cancer therapy by profiling the signaling pathways at single-molecule level. Single-molecule co-immunoprecipitation enabled to measure protein-protein interaction (PPI) quantitatively between pulled down receptor tyrosine kinases (RTKs) and related downstream proteins, which gauged the RTK-signaling. We demonstrated that normalized sum of RTK-PPIs showed strong correlation to the EGFR- and HER2-targeted drug efficacy in lung adenocarcinoma and breast cancer cell lines, respectively. In addition, we predicted the responses of gefitinib at the preclinical model for which there is no current genetic biomarker based on the result of PPI profiling. Our approach provides functional context of individual signaling proteins in tumors and suggests a new concept to analyze cancer signaling in the post-genomic era.

P2-Co.107

Understanding PI3K in Cancer at the Single-Molecule Level

*손민주, 윤태영
*Min Ju. Shon, Tae-Young. Yoon
KAIST.

Keyword : Single-molecule imaging, Fluorescence, PI3K, Cancer

PI3K-Akt signaling pathway controls cell growth, proliferation, and motility, and is frequently deregulated in many types of cancer. PI3K is a lipid kinase that converts PIP2 into PIP3 on membrane, which then recruits downstream signaling proteins such as Akt. Traditionally, the activity of PI3K has been probed indirectly by the phosphorylation of Akt. Here, we developed a technique that directly measures the activity of PI3K by single-molecule fluorescence. In this method, surface-tethered PI3K phosphorylates PIP2 on nearby vesicles, fluorescently-tagged Akt is introduced, and its binding to vesicles is imaged to quantify PI3K activity. After validating the method with fluorescent protein-tagged PI3K, we extend this assay to endogenous PI3K from breast cancer cells to understand the response of cancer cells to PI3K inhibitors. We hope this assay could be useful in screening for PI3K inhibitors or guide selection of cancer patients for PI3K-targeted therapy.

P2-Co.108

Development of an in-vitro assay to study mechanosensitive NOMPC TRP channel

*김지철, 김해수, 윤태영
*Jichul. Kim, Haesoo. Kim, Tae-Young. Yoon
한국과학기술원 (KAIST).

Keyword : NOMPC, Mechanotransduction

The senses of touch, hearing and balance start with opening of mechanically sensitive ion channels in the subcellular level - the process known as mechanotransduction. Although cumulated physiological and functional data reveal important features regarding mechanotransduction activation, its biophysical mechanisms in the molecular scale are still largely unknown. To this end, we study Drosophila no mechanoreceptor potential C (NOMPC) that encodes transient receptor potential (TRP) channels – the mechanotransducer channel of touch, hearing and balance in Drosophila. As an initial step, we developed an assay for force spectroscopy study of a small unilamellar vesicle (SUV) using magnetic tweezer technique. Applying pN scale force to the SUVs, displacements of the vesicle show good agreement with the prediction of theoretical models. Secondary, we expressed green fluorescent protein (GFP) tagged NOMPC in Schneider 2 (S2) cells. Functional study of the cell using fluorescence imaging technique confirms its mechanosensitivity with respect to applied stress. Finally, the study will be continued to investigate SUV-NOMPC complex where we can directly characterize cooperative molecular interactions between the lipid membrane and the channel subunit for mechanotransduction activation.

P2-Co.109*

Reconstitution of RNA Transcription Machinery and Co-transcriptional Effect on RNA Folding

*엄희수, 강우영, 홍성철
*Heesoo. Uhm, Wooyoung. Kang, Sungchul. Hohng
서울대학교.

Keyword : FRET, Transcription, Riboswitch, Co-transcriptional effect, Ligand binding

A riboswitch is a non-coding region of an mRNA which recognizes a specific metabolite and regulates the expression of the mRNA itself. Recently, the fact that RNA folds sequentially as it is being transcribed is carefully considered for RNA structure prediction and dynamics study. It has been shown that this co-transcriptional effect strongly influences RNA folding pathway suggesting that the formation of transient conformations serves as a guideline for the following co-transcriptional folding.

We used fluorescence resonance energy transfer (FRET) to study conformational dynamics of the Escherichia coli thiM TPP (thiamine pyrophosphate) riboswitch. Previously, we found that the open form and the closed form of the riboswitch recognize the ligand with similar preference and the final conformational transition of it is induced by the ligand. Using RNA polymerase elongation complex system, we will show that these processes including ligand bindings are strongly related to the co-transcriptional RNA folding.

P2-Co.110*

A Single Molecule Study of Saccharomyces cerevisiae Modifier of Transcription 1

*정용제, 홍성철
*Yongje. Junge, Sungchul. Hohng
서울대학교.

Keyword : "Transcription", "Transcription regulation", "Modifier of Transcription", "TATA-bind protein", "single-molecule FRET"

Saccharomyces cerevisiae(brewer's yeast) is an eukaryotic unicellular organism, which has an elaborated transcription mechanism. Before transcription, transcriptional complex with RNA polymerase should find its initiation site with the assistance of TATA-binding protein(TBP), which is a part of a transcription factor II D(TFIID) protein. TBP has well-known capability of finding proper initiation site, generally has a series of bases as TATAAAA, which is the origin of the protein's name.
The affinity of TBP to various binding site is inhomogeneous. Some TATA-rich site can show high affinity, but the other initiating sites perform low affinity, which induces unwanted gradation of transcription. There are some groups of proteins redistribute this TBP to control transcription process. Modifier of Transcription 1(Mot1) is a member of these proteins, which regulate TBP in the vicinity of the protein. We imported single molecule FRET(smFRET) techniques to measure the dynamics of this TBP-Mot1-DNA complex at nanometer scale, which will help to understand the mechanism of transcription regulation, and beside the whole transcriptional process.

P2-Co.111*

Multi-Color Single Particle Tracking of Membrane Protein in Living Cell

*안형전, 김동균, 이남기
*Hyeong Jeon. An, Dong-Kyun. Kim, Nam Ki. Lee
포항공과대학교.

Keyword : "Single particle tracking", "Super resolution", "Fluorescent imaging", "DNA PAINT", "ErbB family"

Recently, super-resolution techniques using photoactivatable fluorescent particle enabled imaging individual molecules distributed closer than classical diffraction limit. Furthermore, tracking each localized particle provides information on dynamics of single molecule, acquiring heterogeneity of motions based on their complex environment in living cell. However, the method to track high density of single particle in living cell, named sptPALM, uses photo-activation which not only limit excitation and emission channel for fluorophore but also is unsuitable for controlling density of fluorescent particles when used for multi-color tracking. Here DNA-PAINT which uses binding and detaching of DNA oligonucleotides to control density of single particle trajectories is adapted to simultaneously track different targets. The DNA strands binds specifically to its complementary strand that enables regulation of each particle density by simply adjusting each concentration of imaging strands in the media. With ErbB family as a model system, the individual dynamics information of the family member is gained by single particle tracking DNA-PAINT and their interaction within the family is observed using spatial co-localization analysis.

P2-Co.112*

Single-molecule Study of Intercellular EGFR Transport on Cellular Nanotubes

*장민혁, 오정식, 이량근, 이종봉
*Minhyeok. Chang, JUNGSIC. OH, Ryanggeun. Lee, Jong-Bong. LEE
포항공과대학교.

Keyword : "Cellular nanotube","Single-molecule force-fluorescence spectroscopy","F-actin dynamics","EGFR transport"

Cellular nanotubes (CNT) are thin (50~200 nm), long-ranged (up to few hundreds micrometer) membrane tubes supported by actin filaments while transporting diverse cellular compounds and signals between cells and tissues. Though recent reports have revealed the biological significances of CNTs, their detailed morphology and functions are uncovered. We developed the single-molecule force-fluorescence spectroscopy combining optical tweezers and 3D line-scan confocal microscopy to observe CNTs and mechanics of intercellular transports through them simultaneously.
Examined CNTs between F-actin labeled living cells with different fluorophores show that diverse morphologies of F-actin bundles exist in CNTs, which decide the direction of transports. Also, resolved intercellular transports of activated EGFRs on CNTs suggest that dynamics of F-actin bundles in CNT induces the EGFR transport as it does in filopodium, the origin of CNT before linkage, while their behaviors are separated distinctly. We expect that the analysis based on the molecular clutch model will propose new physical model of actin filament dynamics and following transport in CNT.

P2-Co.113*

Observation of the fusion pore flickering using high affinity supramolecular interaction

*최봉규, 이남기
*Bong-Kyu. Choi, Nam Ki. Lee
포항공과대학교.

Keyword : FRET, host-guest interaction, fusion pore, single-vesicle content mixing assay

Fluorescence-based single-vesicle fusion assays provide a powerful method for studying mechanisms underlying complex biological processes of SNARE (soluble N-ethylmaleimide-sensitive factor attachment protein receptor)-mediated vesicle fusion and neurotrasmitter release. A crucial element of these assays is the ability of the fluorescent probe(s) to reliably detect key intermediate events of fusion pore opening and content release/mixing. Here, we report a new, reliable and efficient single-vesicle content-mixing assay using a high affinity, fluorophore tagged host-guest pair, cucurbit[7]uril-Cy3 and adamantane-Cy5 as a FRET pair. The power of these probes is demonstrated by the first successful in vitro observation of reversible flickering dynamics of the fusion pore during neuronal-SNARE mediated vesicle fusion. We further discover that Ca2+ accelerates fusion pore opening after docking and helps pore dilation during the first pore opening but has no effect on the re-opening of fusion pore during reversible fusion pore flickering.

P2-Co.114*

Liposome tethering single molecule FRET analysis measures real-time submillisecond observation of freely diffusing molecules.

*여상훈, 김재열 [1], 김철희, 이남기
*Sanghun. Yeou, Jae-Yeol. Kim[1], Cheolhee. Kim, Nam Ki. Lee
포항공과대학교. [1]National Institutes of Health.

Keyword : Single-molesule FRET, liposome tethering

Single-molecule fluorescence resonance energy transfer (smFRET) is powerful techniques for deciphering the dynamics of nanoscale biomolecules. However, smFRET is limited in its temporal resolution for the observing single molecule dynamics. Here, we report a nice method for observing real-time dynamics with sub-millisecond resolution by tethering FRET molecules to freely diffusing 100-nm-sized liposomes. The observation time for a single diffusing molecule was extended to 100 ms with a sub-millisecond temporal FRET resolution, which allowed for direct analysis of the transition states based on the FRET time trace using hidden Markov modeling. Using this method, we measured transition rates of up to 1,500 s-1 (~ 0.7-ms dwell time) between two conformers of a Holliday junction from the transition density plot. The rapid diffusional migration of dimeric single-stranded DNA-binding protein (SSB) from Deinococcus radiodurans on single-stranded DNA was directly observed in the FRET time traces at room temperature; this diffusion is faster than that of the tetrameric E.coli SSB by more than an order of magnitude. This result suggests that the diffusion of SSB on ssDNA is a general phenomenon. These results demonstrate that our approach is a powerful method for studying the conformational dynamics and movements of biomolecules at sub-millisecond time scales.

P2-Co.115*

Observing a Levy walk in mRNA transport in neurons

*송민호, 박혜윤, 전재형 [1], 문형석
*Minho. Song, Hyeyoon. Park, Jae-Hyung. Jeon[1], Hyungseok. Moon
서울대학교. [1] *고등과학원.*

Keyword : "Levy", "RNA", neuron", "transport"

In neurons, messenger RNAs are transported by motor proteins on microtubules. The movement phase of mRNAs continuously alters among anterograde, retrograde, and subdiffusive motions. To explain the mechanism of this movement, many biological models have been suggested, but the statistical details of the endogenous mRNA's movement remain unknown. In this work, we analyze in detail the transport of single mRNA molecules in living neurons via single-particle tracking. Using the obtained single trajectories we study its motion with a variety of quantities including the mean squared displacement and the probability distributions of run length and run time. Through this analysis with a supporting simulation material, we demonstrate that the mRNA motion in neurons follows a Levy walk. Our combined experimental and theoretical study is expected to give an insight into the regulatory mechanisms of mRNA transport in neuronal cells.

P2-Co.116*

FRET-based in vitro vesicle fusion assay for Investigating the synergistic effect in pathogenesis of neurodegenerative diseases on SNARE-dependent vesicle fusion

*유경지, 최봉규, 김재열 [1], 이남기
*Gyeongji. Yoo, Bong-Kyu. Choi, Jae-Yeol. Kim[1], Nam Ki. Lee
포항공과대학교. [1]National Institutes of Health (NIH).

Keyword : FRET, vesicle fusion, neurodegenerative disease

Alzheimer's disease (AD) and Parkinson's disease (PD) are caused by β-amyloid (Aβ) and α-synuclein (αS), respectively. Ample evidence suggests that these two pathogenic proteins have a synergistic effect on eliciting neurodegenerative disorders. However, the pathophysiological consequences of Aβ and αS coexistence are still elusive. Here, we show that large-sized αS oligomers are readily formed by Aβ42-seeding and that these oligomers efficiently block SNARE-mediated vesicle fusion in neuron. The direct binding of the Aβ-seeded αS oligomers to the N-terminal domain of synaptobrevin-2, a vesicular SNARE protein, is responsible for the inhibition of fusion. In contrast, large-sized Aβ42 oligomers (or aggregates) or the products of αS incubated without Aβ42 have no effect on vesicle fusion. These results are confirmed by examining PC12 cell exocytosis. Our results suggest that Aβ and αS cooperate to escalate the production of toxic oligomers, whose main toxicity is the inhibition of vesicle fusion and consequently prompts synaptic dysfunction.

P2-Co.117*

Bioinspired Nanogenerators Based on Vertically Aligned Phage Nanopillars

*신동명, 한혜지, 김원근, 김은종, 김춘태, 홍석원, 김형국, 오진우, 황윤회
*Dong myeong. Shin, Hye Ji. Han, Won-Geun. Kim, Eunjong. Kim, Chuntae. Kim, Suck Won. Hong, Hyung Kook. Kim, Jin-Woo. Oh, Yoon-Hwae. Hwang
부산대학교.

Keyword : Bioinspired Nanogenerator, M13 bacteriophage, Implantable device, Piezoelectric, Phage nanopillars

Considerable research attention has focused on the M13 bacteriophage as a potential piezoelectric material due to their remarkable advantages in mass production of genetically modified phages and environmentally friendly approach. Here, we report a simple strategy for fabricating the infiltrated M13 phage pillar in anodic aluminum oxide (AAO) by using an extrusion technique. The characterization of the M13 phage pillar by using scanning electron microscopy, and piezoresponse force microscopy reveals the key process of the formation of the M13 phage pillar. We then fabricate a phage-based pieozoelectric nanogenerator by utilizing the infiltrated M13 phage pillar with different lengths. The piezoelectric nanogenerator with the longest phage pillar produces up to ~9nA of current, 140 mV of voltage. The facile extrusion technique provides highly controllable M13 phage microstructure, which enables us to extend the promising applications for the electronic and optoelectronic devices.

P2-Co.118*

HER2 & HER3 activity as a new biomarker of Breast Cancer

*최병산, 윤태영
*Byung San. Choi, Tae Young. Yoon
KAIST.

Keyword : HER2, HER3, Breast Cancer, Protein Protein Interaction

HER2-positive(overexpression, gene amplification, or both) breast cancer has been found in about 20% of all breast cancer. HER3, one of the HER family member, plays important role in HER2-positive breast cancer, because HER3 forms the most proliferative dimer with HER2. Currently, HER2-positive breast cancer prognosis usually depends on immunohistochemistry(IHC) and fluorescence in situ hybridization(FISH). They reveals HER2 expression level, however, actual signaling strength depends on HER2 and HER3 activities. Using single-molecule co-immunoprecipitation, we measured PPI of native HER2 and HER3 extracted from some breast cancer cell lines. We observed three major signaling pathways(PI3K, MAPK, and PLC) for HER2, and one pathway(PI3K) for HER3. We also observed the effect of epidermal growth factor(EGF) and neuregulin beta 1 on various breast cancer cell lines.

P2-Co.119

Three-dimensional Super-resolution Imaging of Cell with DNA-PAINT

*박상준, 권영대, 강우영, 홍성철
*Sangjun. Park, Yeongdae. Kwon, Wooyoung. Kang, Sungchul. Hohng
서울대학교.

Keyword : super-resolution imaging, line-illumination confocal microscopy, DNA-PAINT, STORM

We study the three-dimensional super-resolution imaging of a whole cell using DNA-PAINT technique combined with line-illumination confocal microscopy (LICM). Optical sectioning (about 2 μm) with LICM decreased the background noise of DNA-PAINT to suppress the fluorescent signal from the coverglass–medium interface. DNA-PAINT method, in addition, provides clearer single molecule images than STORM method that allows LICM to be used reliably for single molecule localization microscopy. As DNA-PAINT imaging is not affected by photo-bleaching, we can get three-dimensional image as many focal planes as necessary to make the full-thickness (about 5 μm) three-dimensional reconstruction in super-resolution imaging.

P2-Co.120

Single molecule study on fork regression activity of yeast Rad5 protein

*신수철, 현광범 [1], 김재훈 [1], 홍성철
*Soochul. Shin, Kwang-Beom. Hyun[1], Jaehoon. Kim[1], Sungchul. Hohng
서울대학교. [1]KAIST.

Keyword : smFRET, Rad5, Fork regression

DNA lesions in the template strand block the replication process. If the damage is on the lagging strand template, the gap can be filled by synthesis from the adjacent Okajaki fragment. However, if the lesion is on the leading strand template, the gap cannot be repaired by fill-in synthesis using DNA polymerases. One method to bypass the leading strand lesions is to use the fork regression, a postreplicational pathway. In the yeast Saccharomyces cerevisiae, this postreplicational repair is dependent on Rad5 protein which has a helicase activity that is specialized for replication fork regression. In this study, we characterize the fork regression mechanism of Rad5 at the single molecule level, using single molecule fluorescence technique.

P2-Co.121

Single Molecule Study on TR2F terminatoer

*강우영, 홍성철
*Wooyoung. Kang, Sungchul. Hohng
서울대학교.

Keyword : TR2F terminator, sm FRET, RNA polymerase

The bacterial intrinsic terminator is composed of a stem-loop hairpin structure and a poly-uracil(U) chain. We know these structures can induce the termination event, but how it is happening remains unsolved. In this study, we would define which model can explain the mechanism of the termination through single-molecule FRET. Using wild type TR2F terminator and artificial terminator with Escherichia coli polymerase, we observed the FRET change and Protein Induced Fluorescence Enhancement(PIFE). There was the PIFE after RNA dissociation and the signal indicating RNA dissociation on wild type sample. We will study the movement of RNA polymerase during the termination by labeling other kinds of dye on DNA and RNA polymerase.

P2-Co.122

Single-Molecule studies on the Mechanism of mis-synthesized DNA strand removal in Human

*전용문, 김대형, Richard Fishel[1], 이종봉
*Yongmoon. Jeon, Daehyung. Kim, Richard. Fishel[1], Jong-Bong. LEE
포항공과대학교. [1]The Ohio State University Medical Center.

Keyword : Biophysics, single-molecule, mismatch repair, hExo1, flow-stretching

Single-molecule studies have improved our understanding of the mechanism of the mismatch recognition and the downstream signaling in DNA mismatch repair (MMR). However, the recognition mechanism of the mismatch by MMR proteins after the strand excision is less clear although the biochemical and structural studies have proposed models of the mismatched-strand removal by the hMsh2-hMsh6, hExoI, hsRPA, hMlh1-hPms2 proteins. hExoI is 5' à 3' exonuclease and only one exonuclease that is has been shown to be required for eukaryotic MMR. hMsh2-hMsh6 heterodimer is responsible for recognition of mismatch and downstream signaling. hsRPA is an eukaryotic single-strand DNA binding protein and protects a ssDNA during MMR, recombination, replication processes. We have developed a novel single-molecule technique for monitoring DNA strand excision by hExoI and hMSH2-hMSH6 in real time. We will present the dynamic feature of hExoI regulated by RPA and hMsh2-hMsh6. The results suggest that the removal of the mismatch is completely regulated by ATP-bound hMsh2-hMsh6 formed at a mismatch through the dynamic interaction with hExoI.

P2-Co.123

Interplay MutS, β clamp and MutL on Mismatched DNA

*오정식, 김대형, 조원기, Jiaquan Liu[1], Slobodan Jergic[2], Nicholas Dixon[2], Richard Fishel[1], 이종봉
*JUNGSIC. OH, Daehyung. Kim, Won ki. Cho, Jiaquan. Liu[1], Slobodan. Jergic[2], Nicholas. Dixon[2], Richard. Fishel[1], Jong-Bong. LEE
포항공과대학교. [1]The Ohio State University. [2]University of Wollongong.

Keyword : MutS, beta-clamp, MMR, single-molecule

The β clamp encircles duplex DNA, which results in the extremely stable conformation, and diffuses along the DNA. During DNA replication, β clamp act as processive factor of polymerase III. However, the long dwell time of the sliding β clamp on DNA results in its accumulation on the lagging strand, which may affect other associated proteins or downstream pathway. The DNA mismatch repair(MMR) is immediately occurred when mismatched DNA is synthesized during DNA replication. Thus, β clamp may interact with MutS, a mismatch repair initiation protein, which undergoes at least two distinct conformational changes during DNA MMR. Here, we show that β clamp make searching MutS, ADP-bound form, more stable on DNA before and at mismatch recognition, but weakly interact with ATP-bound MutS after mismatch recognition. Also, we directly observe β clamp and MutS complex diffuse on DNA. We suggest that β clamp help MutS recognize mismatch well, after that, dissociate from ATP-bond MutS to give chance to interact other downstream proteins such as MutL.

P2-Co.124

Single-molecule studies on maltose transport system

*이종진, 홍성철
*Jongjin. LEE, Sungchul. Hohng
서울대학교.

Keyword : single-molecule, maltose transporter, MalFGK2, maltose binding protein, MBP

Efficient carbon utilization is critical to the survival of microorganisms in competitive environments. To optimize energy usage, bacteria have developed an integrated control system to preferentially uptake carbohydrates that support rapid growth.

Maltose is one of the carbohydrates that is transported across the cytoplasmic membrane of Escherichia coli by a binding protein(MalE)-dependent transport system. The three membrane-associated components of the transport system are MalK, MalF, and MalG proteins.

This system has been studied extensively by crystallography and biochemical assays. Although crystal structures provide crucial snapshots of discrete states of the translocation cycle, but do not resolve the dynamics of the processes. Additionally, “bulk” biochemical experiments cannot provide insights into rare and/or transient events, crucial for the transport process, as these are lost in the ensemble averaging.
Thus we are studying this transport system by using single-molecule technique to overcome these limitations.

P2-Co.125

Probing the relationship between translation initiation efficiency from upstream RBS and transcriptional delay by quantitative mRNA analysis

*김승현, 양소라, 이남기
*Seunghyeon. Kim, Sora. Yang, Nam Ki. Lee
포항공과대학교.

Keyword : RNA polymerase, Ribosome, Transcription-translation coupling

Transcription-translation coupling is a unique phenomenon that occurs in bacteria only. Although it is known that RNA polymerase (RNAP) and ribosome are physically connected during the expression of a gene, less is known about how RNAP and ribosome affect the other's activity. We measured transcription elongation rate to describe the movement of RNAP on lacZ gene in E. coli. We found that transcription elongation rate from lacZ500 to lacZ3000 is almost same in both wildtype lacZ and Δrbs mutant, but time need to pass lacZ500 is different in two strains. Two models may explain our results : (1) temporal stop of RNAP near translation initiation region or (2) two phase in transcription elongation rate. Our results discriminate which effect is dominant on transcriptional delay.

P2-Co.126

Inositol Pyrophosphates Inhibit Synaptotagmin-Dependent Exocytosis

*이태선, 윤태영
*Tae Sun. Lee, Tae-Young. Yoon
KAIST.

Keyword : membrane fusion, inositol pyrophosphate, synaptotagmin, single vesicle docking assay,

The ability of 5-diphosphoinositol pentakisphosphate (5-IP7) to regulate specific target proteins is critical for fulfilling their signaling functions in controlling specific biological events like growth and metabolism. Inositol phosphates have been speculated as regulators for synaptic exocytosis, but exactly how they affect has been obscure. By analyzing synaptic vesicle fusion at the cell and single-molecule levels, here, we demonstrate that 5-IP7 markedly inhibits Ca2+-induced synaptic membrane fusion in the sub-micromolar range. We have further elucidated the molecular mechanism responsible for IP7 actions; it directly binds to synaptotagmin1 (Syt-1), a major Ca2+ sensor, suppressing the fusogenic activity of Ca2+-dependent Syt-1. Thus our data propose 5-IP7 as the key determinant for Syt1 actions on Ca2+-mediated synaptic vesicle fusion.

P2-Co.127

Full-length Ras-Raf kinetics revealed by single-molecule co-IP

*유장현, 최병산 [1], 차민권 [2], 배우리 [1], 윤태영 [1]
*Janghyun. Yoo, Byung San. Choi[1], Min Kwon. Cha[2], Wooli. Bae[1], Tae-Young. Yoon[1]
한국과학기술원. [1]KAIST. [2] 카이스트.

Keyword : Raf, Ras, single-molecule co-IP, melanoma, dimerization

The Ras-Raf-MEK-ERK signal transduction cascade regulates various cell processes including differentiation and proliferation, and their dysregulation often lead to cancer. Among the three Raf paralogs (ARaf, BRaf and CRaf) BRaf mutants are frequently found in cancer cell lines and tumors. Especially, BRafV600E which has a point mutation at kinase domain is a leading cause of melanomas. Normally, Raf activation is followed by activation of Ras which is a membrane anchored small GTPase. As a serine/threonine kinase, Raf needs to form a dimer to be fully functional and active Ras is required in the dimerization process. On the other hands, BRafV600E shows elaborated kinase activity even in a monomeric form independent of Ras activity. In August 2011, Vemurafenib was approved for the treatment of BRafV600E metastatic melanoma in the United States. Vemurafenib treatment has shown some degree of tumor regression, but most patient developed resistance within a year. Soon, it was revealed that ATP-competitive small-molecule inhibitors, including vemurafenib, accelerate CRaf activity through dimerization of BRafV600E (BRaf)/CRaf in Ras active environment and its resistance mechanism frequently involves Raf dimerization. Therefore, interplay between BRafV600E, CRaf and Ras is important to understand BRafV600E dependent tumors.
Currently, the importance of the Raf dimerization and its Ras dependency is well known. However, detailed Raf dimerization kinetics is rarely addressed. Moreover, Ras binding and its membrane recruitment effects on Raf: Raf conformation change, Ras dimerization, effect of Raf membrane recruitment or the membrane micro-environment itself make the mechanism of Ras-mediated Raf dimerization elusive. To overcome this complication and investigate interactions of Ras, BRafV600E and CRaf , we use single-molecule co-IP. In the previous study, we have quantitatively analyzed interactions of signaling proteins using unpurified cell extracts. Here, we studied Ras-Raf kinetics and Raf dimerization kinetics of HRas, BRafV600E and CRaf using single-molecule co-IP analysis. Using HRas as baits and BRafV600E or CRaf as preys, on/off kinetics of Ras-Raf interaction was addressed. And by differentiating heterogeneity in individual single-molecule binding events, BRafV600E and CRaf homo-dimerization kinetics was quantified. Lastly, the effect of Ras-Raf interaction on BRafV600E /CRaf hetero-dimerization was directly investigated.

P2-Co.201

DFT investigation on the stability of α-$BiFeO_3$ crystal structure

*AHMAD FAYYAZ, Ishrat Naz, 장재경, 이주열 [1]
*FAYYAZ. AHMAD, Ishrat. Naz, Jae Kyung. JANG, Joo Yull. RHEE[1]
물리학과/성균관대학교. [1] *성균관대학교.*

Keyword : "ab-initio", "α-$BiFeO_3$", "Electronic structure", "AIM"

It was experimentally suggested that there are several different crystal structures for α-$BiFeO_3$, which is a typically multiferroic material. The first-principles calculations on the electronic structures and valence-charge density of α-$BiFeO_3$ reveal that the triclinic phase (space group: P1) with semiconducting ground state is more stable than other possible configurations [1]. The valence-charge density was calculated by using the atoms-in-molecules method. The hybridization of Bi-O and Fe-O leads to spin magnetic moment to 3.60 μ_B. The band gap is predicted to be 0.63 eV. The calculated results show that the ionic bondings of Fe-O and Bi-O in triclinic phase is stronger than other models which leads to stability of α-$BiFeO_3$.

[1] H. Wang, C. Yang, J. Lu, M. Wu, J. Su, K. Li, J. Zhang, G. Li, T. Jin, T. Kamiyama, On the Structure of α-$BiFeO_3$, Inorganic chemistry, 52 (2013) 2388-2392.

P2-Co.203

Designing of narrow band gap alloys for optoelectronic and thermoelectric applications.

*Bakhtiar, Rashid Ahmed[1], 이주열 [2]
*Bakhtiar. Ul Haq, Rashid. Ahmed[1], Joo Yull. RHEE[2]
물리학과/성균관대학교. [1]Universiti Teknologi Malaysia. [2] 성균관대학교.

Keyword : "DFT", "FP-L(APW+lo)", "Electronic structure", "Seebeck coefficient", "Power factor"

The severe environmental pollution due to the globalization, industrialization and the population growth have trickled up the need for green and renewable energy resources. The solar-thermal-power generation devices based on highly efficient thermoelectric materials are among the most attractive ways to utilize the solar energy. Among the many developed thermoelectric materials, semiconductors with narrower band gap are considered as most effecient and have received particular interest of researchers. In this work, we are aiming to design narrow-band-gap thermoelectric materials through alloying of GaSb (E_g = 0.73eV) and GaBi (Semimetal). The resulting materials are expected to exhibit tunable energy gap in the energy span of 0.73 to 0 eV as a function of alloying composition. This study was carried out using density functional theory-based full-potential-linearized-augmented-plane-wave method implemented in WIEN2k code. The present investigations will address the engineering of the energy gap and its influence on the transport properties including free carrier concentration, thermal conductivity, Seebeck coefficient, power factor, and figure of merits. The designed alloys are expected to exhibit interesting electronic and thermoelectric properties desirable for solar thermal-power-generation devices and other optoelectronic applications.

P2-Co.204

Length Scaling of Metal-Graphene Contact Resistance: An ab inito study

*고관호, 김용훈
*Kwan Ho. Ko, Yong-Hoon. Kim
한국과학기술원.

Keyword : density functional theory, graphene, contact resistance

Despite many efforts to improve the performance of Si transistors, their performance has been pushed close to its physical limits. Thus, there is a high demand in searching for new materials suitable to replace Si by offering superior current transport properties and improved electrostatics. One of the most promising materials to replace Si is graphene due to its small size and superior electrical properties. In spite of the impressive intrinsic electronic properties, there are still many issues that have to be solved before carbon-based nanoelectronic devices can actually be manufactured. Contact resistance at the interface is a crucial property for nanoelectronic devices and understanding the profound effect of the graphene-metal contact on carrier transport is a major challenge. In this work, contact resistances for “end-contacted” metal-graphene is investigated. Particularly, the scaling of resistance with the length of channel materials and the effect of different metals on contact resistance have been studied.

P2-Co.205

Study of Dielectric Functions of Cubic Perovskite Structure $MAPbBr_3$

Janghwan Cha, Jun-Woo Park[1], Christoph Wolf[2], Tae-Woo Lee[2], Hosun Lee[1], Suklyun Hong
Janghwan. Cha, Jun-Woo. Park[1], Christoph. Wolf[2], Tae-Woo. Lee[2], Hosun. Lee[1], Suklyun. Hong
Sejong University. [1]Kyung Hee University. [2]POSTECH.

Keyword : Dielectric function, Optical properties, Metal halide perovskite, Density functional Theory, Ellepsometric angle

Recently, hybrid organic–inorganic perovskites have given rise to worldwide attention due to highly efficient solar cells based on methylammonium lead halides ($MAPbX_3$, MA = CH_3NH_3 and X = halogen atoms). We focus on $MAPbBr_3$ that is cubic perovskite structure phase at room temperature. To investigate optical properties of cubic perovskite structure $MAPbBr_3$, we have calculated dielectric functions of $MAPbBr_3$ using density functional theory calculations within generalized gradient approximation (GGA). On the other hand, we measure the ellipsometric angles (Ψ, Δ) using spectroscopic ellipsometry, and estimate the dielectric functions of $MAPbBr_3$ using layer model analysis. We discuss the difference between the measured and the calculated dielectric functions in terms of exciton effects and DFT band gap.

Corresponding author : hong@sejong.ac.kr

P2-Co.206*

First principle analysis of lattice dynamics and thermal conductivity of PbX(X=Te, Se, and S)

*김수지, 지효석, 심지훈
*Sujee. Kim, Hyoseok. Ji, Ji Hoon. Shim
포항공과대학교.

Keyword : lead chalcogenides, lattice thermal conductivity, first-principle, boltzman eqauation, thermoelectric

The lead chalcogenides have attracted much attention in recent years, in particular due to the high-temperature thermoelectric performance of PbTe. A number of recent investigations, experiment and theoretical, have aimed to gather insight into their unique lattice dynamics and electronic structure. The electronic structure, especially, has been well studied using first principle calculations. The lattice properties also have been studied using various theoretical methods such as molecular dynamics and lattice dynamics with Boltzmann equation. However, the detailed analysis of lattice dynamics should be needed for providing insights into the phonon properties and designing better thermoelectric materials.
In this study, we report thermal conductivity and lattice dynamics of the lead chalcogenides PbX(X=Te, Se, and S) using combination of density functional theory calculation and Boltzmann transport equation with a direct force-constant method. Calculated lattice properties such as elastic moduli and phonon dispersions are compared with reported experimental results. Based on lattice properties, the thermal conductivities of PbX compounds are investigated. By analyzing anharmonic phonon scattering, we have found phonon modes determining the lattice thermal conductivity. Our results suggest the effective way to reduce the lattice thermal conductivity of lead chalcogenide compounds by using phonon band engineering.

P2-Co.207*

Development of an ab initio method for the vertically-stacked 2D layered materials

*김한슬, 김용훈
*Han Seul. Kim, Yong-Hoon. Kim
한국과학기술원.

Keyword : Density functional theory, ΔSCF method, 2D layered materials, electronic devices

We report on the development of a first-principles method for the calculation of tunneling devices based on vertically-stacked 2D layered materials. Applying region-dependent Δ self-consistent field method, the new scheme efficiently simulates the device operation with different bias voltages. In particular, we will explicitly extract the ab initio energy level alignments and device characteristics in response to source-drain and gate bias which has been only schematically estimated otherwise. For the various types of realistic devices, we then discuss the working mechanisms in depth and provide the guidelines on designing new devices.

P2-Co.208*

First-principles study of ligand-dependent CdS/ZnS core/shell nanowire growth and band engineering

*김효석, 김용훈 [1]
*Hyo Seok. Kim, Yong-Hoon. Kim[1]
KAIST. [1] *한국과학기술원.*

Keyword : density functional theory calculations, CdS/ZnS nanowire

Using first-principles density functional theory (DFT) calculations, we studied the energetics and electronic structures of the core/shell and shell/ligand interfaces of the CdS/ZnS nanowires. We first calculated the binding energies of carboxylic acid and amine ligands to a range of CdS/ZnS surface facets, which were then compared with experimental data on the synthesis of CdS/ZnS nanowires. Next, we examined the relative effects of quantum confinement and strain on the electronic structure of CdS/ZnS nanowires which experience large lattice mismatches. Band level alignment of the CdS/ZnS nanowires are analyzed in terms of the core radii and shell thickness. Implication of our findings in the context of understanding of the growth of nanoscale haterostructures and band gap engineering will be discussed.

P2-Co.209*

Photoinduced ultrafast phenomena in rubrene molecular layer

*차웅탁, 이재동 [1]
*Woongtak. Cha, JaeDong. LEE[1]
DGIST. [1] 대구경북과학기술원.

Keyword : ultrafast phenomena, molecular crystal, rubrene

To investigate the photoinduced ultrafast phenomena in layered molecular-crystalline rubrene, we employ a model of electrons coupled to local vibrations incorporating the intermolecular electron hopping. Dynamics of molecular polarization, vibration propagation, charge transport, and electron population are described in the ultrafast time span by solving the time-dependent Schroedinger equation.

P2-Co.210*

Abnormal Thermal Expansion Behaviors in Cubic T-Carbon.

*최호식, 강승훈, 권영균
*Ho-Sik. Choi, Seoung-Hun. Kang, Young-Kyun. Kwon
경희대학교.

Keyword : "T-carbon","negative thermal expansion","rigid unit modes","thermal property"

Using first-principles density functional theory, we investigate the thermal property and the thermal expansion behavior of a “T-carbon” structure, a carbon allotrope, which can be constructed from the diamond by replacing every carbon atom with a tetrahedron composed of four carbon atoms. We search for its equilibrium structure by scanning its energy landscape while changing two inequivalent C-C bond lengths, the one within the tetrahedron and the other connecting any two neighboring tetrahedra. With the identified equilibrium structure, we apply the finite displacement method to calculate the phonon dispersion and its vibrational modes to explore its thermal property. The quasi-harmonic approximation allow us to explore unusual thermal expansion behavior of T-carbon exhibiting a negative thermal expansion in the cubic structure. Such an abnormal negative thermal expansion behavior is attributed to the existence of rigid unit modes originated from the tetrahedron structure. We analyze the rigid unit modes as well as the effects of the structural deformations. We also calculate their corresponding mode gruneisen parameters to verify their contribution to the negative thermal expansion behavior.

P2-Co.211*

양자 몬테카를로 방법을 이용한 1 차원 카바인 사슬들의 응집 에너지 계산

*홍의균, 신현덕, 권용경
*Iue Gyun. Hong, Shin Hyeondeok. , KWON Yong Kyung.
건국대학교.

Keyword : 양자 몬테카를로, 카바인, 응집에너지

일차원 탄소동소체이며 sp-결합으로 이루어진 카바인은 DFT(Density Functional Theory) 계산을 통해 가장 강한 강도와 인장력을 가질 것으로 예측되어온 물질이며, 일반적으로 두 개의 이중결합으로 이루어진 Cumulene 구조와 단일결합과 삼중결합이 교차하는 Polyyne 구조로 존재한다고 알려져 있다. 상기 구조들은 결합 방법이 다르므로 전기적 특성 차이를 보이는데, 기존 연구들에 의하면 Polyyne 구조가 Cumulene 구조 보다 에너지적으로 더 안정적인 것으로 평가되어 왔다. 그러나 최근의 QMC (Quantum Monte Carlo) 연구에서는 DFT 계산으로 구한 저차원 탄소 동소체의 응집 에너지가 일반적으로 높게 계산된다는 것으로 알려져 있으며, 이 과대 평가의 정도가 해당 구조에서 sp-결합의 비율이 증가 할 수록 커진다는 것이 밝혀졌다 [1]. 이에 따라 주로 DFT 로 예측되어 온 카바인 사슬의 전기적 특성들을 정확하게 제시하기 위해 본 연구에서는 제일원리 다체계 계산 방법인 QMC 를 사용하여 두 종류의 1 차원 카바인 사슬에 대한 응집 에너지를 계산하고 기존 DFT 계산을 통해 예측되어온 결과와 비교하였다. 최종적으로 두 구조들의 결합 길이에 따른 에너지 변화를 통해 구조의 안정성을 비교하였다. 또한 각각의 인장강도와 탄성계수를 계산하여 두 구조의 강도 차이를 비교 분석하였다.

1) Hyeondeok Shin et al J. Chem. Phys. 140, 114702 (2014)

P2-Co.212*

Development of a Python-based Platform for Atomistic Modeling and Simulations of Nanomaterials and Nanodevices

*김후성, 김용훈
*Hu Sung. Kim, Yong-Hoon. Kim
한국과학기술원.

Keyword : "first-principles calculation", "Nanomaterials", "Nanodevices", "Python", "Simulation Platform"

We will report on the progress of our effort to build a Python-based atomic-scale modeling and simulation platform. The project aims to provide an environment that contains the functionality of file input/output, manipulation/modeling, and interfaces for structure visualization and simulation codes. Currently, the simulation interfaces for first-principles codes such as SeqQuest [1], SIESTA [2], and VASP [3] and force-fields code LAMMPS [4] are available. Its advantages include the possibility of easily (1) adopting available Python libraries such as NumPy and matplotlib, (2) conducting all the modeling/visualization/simulation/analysis within the Python shell (in the style of MATLAB or Mathematica), (3) constructing utility scripts for various modeling/simulation/analysis tasks, (4) being able to access other Python-based modeling/simulation codes such as ASE [5] and Phonopy [6], etc. In addition, we integrated our in-house simulation tools for electron and phonon transmissions based on interatomic forces obtained via extended Phonopy from first-principles calculations and force-field parameters. Part of the package has been included on the EDISON project site [7], which aims to construct an integrated web-based research and learning environment.

References
[1] Peter A. Schultz et al., “SeqQuest Electronic Structure Code” (http://dft.sandia.gov/Quest/)
[2] Emilio Artacho et al., “SIESTA Electronic Structure Code” (http://icmab.cat/leem/siesta/)
[3] Jürgen Hafner et al., “The Vienna Ab initio Simulation Package” (http://www.vasp.at/)
[4] Steve Plimpton et al., “LAMMPS Molecular Dynamics Simulator” (http://lammps.sandia.gov/)
[5] K. W. Jacobsen et al., “Atomic Simulation Environment Project” (https://wiki.fysik.dtu.dk/ase/).
[6] A. Togo, “Phonopy project” (http://phonopy.sourceforge.net/)
[7] The EDISON project (https://nano.edison.re.kr/)

P2-Co.213*

Origin of an anomalous first semicircle in electrochemical impedance spectra for carbon-based counter electrodes with the I^-/I_3^- redox couple: an ab initio study

*노민종, 김한슬 [1], 김용훈 [1]
*Min Jong. Noh, Han Seul. Kim[1], Yong-Hoon. Kim[1]
KAIST. [1] 한국과학기술원.

Keyword : Density functional theory, Electrochemical impedance spectra, Dye sensitized solar cell, Counter elecctrodes, Non equilibrium Green's function formulism

Recently, various types of graphene-based materials have been utilized as counter electrodes (CEs) in dye sensitized solar cell. In terms of electrochemical impedance spectra (EIS), the porous carbon-based CEs with I^-/I_3^- redox couple commonly shows an additional first high-frequency semicircle (low-resistance operation) which has no relation to the electrocatalytic activities, different from conventional metal CEs. Due to its voltage-independency, such reduce in electrical resistance of carbon-based CEs can be thought of as a result of I_3^- (or I^-) adsorption. In this presentation, by using combined density functional theory and the non-equilibrium Green's function calculation, we investigate the effect of I_3^- (or I^-) adsorption on the current-voltage (I-V) characteristics of carbon-based CE, graphene. First of all, [e1] we obtain the binding energies and equilibrium distances of I^- and I_3^- adsorbed on graphene with several different configurations. Then, we systematically analyze the electron population, transmission and corresponding I-V characteristics of graphene with I^- and I_3^- adsorbent. Through these results, we discuss the relationship between graphene conductivity and I_3^- (or I^-) adsorption and elucidate the origin of first semicircle in EIS of carbon-based CEs.

P2-Co.214*

First Principle Study on Structural Properties and Phase Change Mechanism of GeTe, a Phase Change Material

*박한진, 김철운, 권영균
*Hanjin. Park, Cheol-Woon. Kim, Young-Kyun. Kwon
경희대학교.

Keyword : "PCM", "Phase Transition", GeTe"

Using ab initio density functional theory, we investigate the structural properties of the ordered crystalline and disordered amorphous phases of GeTe, which would be used for phase change random access memory and the phase transition between different phases. Different amorphous phases were modeled based on experimental data and a melt-quench process. We performed molecular dynamics (MD) simulations composed of various stages including several thermal equilibration at different temperatures, a high-temperature pre-melting process with a low gravimetric density, and a quenching process from high temperature to room temperature. To explore phase transition process, we evaluate the characteristics of local structures in several phases using their radial distribution functions (RDFs) and angle distribution functions (ADFs) in accordance with coordination number. Our calculated RDFs were analyzed and compared to EXAFS data available. We utilized ADFs to identify the local geometry of each phase. Furthermore, to investigate the thermal properties of various phases, we computed the phonon densities of states by Fourier-transforming the velocity autocorrelation functions (VAFs). The interfacial characteristics between crystalline and amorphous phases were studied by generating a amorphous phase enclosed by a crystalline structure.

P2-Co.215*

Widely tunable band gaps of graphdiyne

*배현후, 구자현, 박민우, 황승현 [1], 이승한, 이훈경
*Hyeonhu. Bae, Jahyun. Koo, Minwoo. Park, Seunghyun. Hwang[1], Seunghan. Lee, Hoonkyung Lee.
건국대학교. [1] 광주과학기술원.

Keyword : graphdiyne, functionalization, band gap tuning, DFT

Functionalization of graphdiyne, a two-dimensional atomic layer of sp-sp2 hybrid carbon networks, was investigated through first-principles calculations. Hydrogen or halogen atoms priorly adsorb on sp-bonded carbon atoms rather than on sp2-bonded carbon atoms, forming sp2- or sp3- hubridization. The energy band gap of graphdiyne is increased from ~0.5 eV to ~5.2 eV through the hydrogenation or halogenation Unlike graphene, segregation of adsorbed atoms is energetically unfavorable. Our results show that hydrogenation or halogenation can be utilized for modifying the electronic properties of graphdiyne for applications to nano-electronics and nano-photonics.

P2-Co.216*

Understanding Role of Crystal Violet and Its Polarity on MoS_2 Growth Scrutinized by Ab Initio Calculations

*수피안, 김용훈 [1]
*Muhammad Sufyan. Ramzan, Yong-Hoon. Kim[1]
KAIST (한국과학기술원). [1] 한국과학기술원.

Keyword : Crystal violet, MoS_2 growth mechanism, binding energy, ab initio calculation, transition metal disulfide

Thinnest semiconductor material molybdenum disulfide (MoS_2) exhibits promising facets in applications of optoelectronics and solar energy absorption. High quality monolayer of MoS_2 is highly desirable for fundamental studies and demanded applications. A number of techniques has been developed to grow MoS_2 layers but atomistic understanding of growth mechanism has been largely overlooked. In this work, using first-principles calculations, we try to understand the growth mechanism and effect of organic ligand (crystal violet) on MoS_2 growth. Here, we conduct the binding energy calculation at different adsorption sites and for different configurations of ligands. Based on our binding strength calculations, we will give insights into atomic geometry of transition metal disulfides and organic ligands as well as electronic charge transfer between surface and ligands.

P2-Co.217*

Development of a method to find the most stable spin configuration using first principle calculation

*이규현, 윤용, 한승우
*Kyuhyun. Lee, Yong. Youn, Seungwu. HAN
서울대학교.

Keyword : First principle calculation, Magnetism

Finding the most stable magnetic structure of antiferromagnetic material is one of physical issue since material properties are affected by spin configuration. Currently, empirical method such as combination of some well-known structure has been used to find the most stable magnetic structure. However, the methods depend on one's intuition and do not work well in complex materials. To suggest nonempirical method for this issue, we use Ising model to find the most stable spin configuration of antiferromagnetic materials. To generate Ising model, we categorize atom pairs according to the pair distance and symmetry condition and set a parameter for each pair. Each parameter is obtained by calculating energy contribution of each parameter. Energy is calculated the ab initio approach based on the density functional theory. With the complete Ising model, we use genetic algorithm to find the most stable spin configuration. Using this strategy, we check some well-known antiferromagnetic oxides such as NiO, Fe_2O_3 and $LaTiO_3$ and confirm the reliability of our model. Through this method, we find the most stable magnetic structure of unknown antiferromagnetic oxide in future.

P2-Co.218*

Electronic properties of atomic layered black phosphorus-metal contacts

*이수영, 윤원석, 이재동
*Su Yeong. Lee, Won Seok. Yun, JaeDong. Lee
대구경북과학기술원.

Keyword : black phosphorus, semiconductor-metal contact, first principles calculations, unfolding method

Layered black phosphorus (BP) attract great attention as promising candidates for the nanoelectronics and the field-effect transistor (FET) due to their excellent mechanical, optical, thermoelectric, and electronic properties. For a practical device realization, it is important to control electronic transport properties and contact resistance at the interfaces between semiconducting BP and metal electrode. In this work, based on the first-principles calculations, the electronic properties of the interface at semiconductor-metal contacts are investigated.

P2-Co.219*

Structural and Electronic Properties of Acetylsalicylic Acid adsorbed on Carbon and Carbon Nitride(C_3N_4) Nanotubes : Ab initio study

*이용주, 강승훈, 김건 [1], 권영균
*Yong ju. Lee, Seoung-Hun. Kang, Gunn. KIM[1], Young-Kyun. Kwon
경희대학교. [1] *세종대학교.*

Keyword : "CNT","Carbon nitride nanotube"

Using the first-principle study based on density functional theory, we investigate the structural and electronic properties of acetylsalicylic acid (ASA), a major component of aspirin, adsorbed on a carbon nanotube (CNT) and a triazine-based graphitic carbon nitride (g-C_3N_4) nanotube (CNNT). We use a plane-wave basis set and the projector augmented wave method with the generalized gradient approximation implemented with van der Waals interaction. It is found that the ASA molecule binds stronger on the CNNT with its adsorption energy of ~0.67 eV and the CNT with ~0.51 eV. The stronger adsorption energy on the CNNT is ascribed to the high reactivity of the N atoms containing electron lone pair. Binding enhancement in CNNT is ascribed to the buckling effect. The buckling structure by N atoms and C atoms can exhibit local electric dipole moments, which enhances ASA molecular adsorption through the dipole-dipole interaction between CNNT and ASA molecule. We further investigate the effect of an electric field externally applied parallel or perpendicular to the molecule, on the electronic structures of CNT and CNNT.

P2-Co.220*

Possible topological insulators in ASnX3-type halide perovskites

*이일영, 유재준
*Il Young. Lee, Jaejun. Yu
서울대학교.

Keyword : "Topological Insulator", "halide perovskite"

We investigate a possible topological insulator in a family of halide perovskite compounds consisting of ASnX3 with A = H, Li, Na, K, Rb, Cs and X = Cl, Br, I by carrying out first-principles electronic structure calculations. Topological insulators in a perovskite structure can be useful because of its various heterostructure interfaces with multifunctional properties. It is experimentally known that the halide perovskite CsSnI3 (CSI) has a cubic-α structure above 450K, and a tetragonal-β structure at a lower temperature, and then an orthorhombic-γ structure below 351K. CSI-α is found to have an “inverted” band structure with a non-degenerate s-like valence band maximum and triply degenerate p-like conduction band minimum, which is a signature of topological insulators. However, when hybrid functional is used to get a better description of band gap, the inverted band structure turns into a normal insulator band gap. The change of band gap in ASnX3-series shows an anomalous behavior with the change of lattice constant, that is, the band gap increases with increasing lattice constant. Such behavior is attributed to the decreasing valence band width due to the reduced interaction between Sn s and anion p states. HSnI3 exhibits a peculiar band structure with neutral H atom, while the compounds with Li and Na become unstable due to their small atomic size.

P2-Co.221*

High-throughput fist-principles study on doped-ZnO

*임강훈, 이주희, 한승우
*Kanghoon. Yim, Joo hee. Lee, Seungwu. HAN
서울대학교.

Keyword : Doped-ZnO, density functional theory, high-throughput calculation

Zinc oxide (ZnO) has been receiving lots of attentions due to its great potential in optical and optoelectronic applications as a transparent conducting oxide (TCO). ZnO has high mobility of carriers because of its dispersive band structure and it is transparent as it has wide direct band gap. On the other hand, intrinsic carrier concentrations of ZnO are not large enough for an electrode material. To utilize ZnO as an electrode, heavy donor or acceptor doping has to play an important role. For example, heavy doping of Al or Ga in ZnO has achieved n-typle conductivity of ~10^{-4} Ωcm which is comparable to In-Ga-Zn-Oxide. If reliable p-type doping on ZnO is achieved, applications with p-n junction could be activated but it has not discovered yet. In addition, doping can facilitates band gap engineering to absorb visible light, and application for spintronics is also possible when a transition metal is doped. However, though there are massive studies on several dopants for ZnO, defect types and behaviors of all the possible dopants are still unknown in both experiments and theoretical studies.
To find optimal dopants for various applications, we extensively study doped-ZnO with every element in periodic table as a single dopant by ab-initio calculations. In order to find the most stable doping configurations for each dopant, we closely search possible doping configurations including substitutions, interstitials according to bonding and anti-bonding framework, and split interstitials using density functional theory(DFT) calculation. We also considered various charge state of each doping types. To search those massive space, we develop an automatic code for high-throughput simulation of doped-ZnO. As a result, characterizations doped-ZnO such as formation energies and carrier concentrations are obtained for a wide range of dopants. We also figure out some interesting doping types that have not been reported to date, though most dopants are found to prefer general doping site that have been reported from former studies.

P2-Co.222*

Spin- and orbital-ordered magnetic structures in oxygen deficient $SrCoO_{2.5+x}$

*임진영, 유재준
*Jinyoung. Lim, Jaejun. Yu
서울대학교.

Keyword : $SrCoO_{2.5}$,magnetism,oxygen vacancy,orbital ordering

Layered $SrCoO_{2.5+x}$, a family of non-stoichiometric perovskites, has been reported to undergo topotactic ion exchange and intercalation reactions. Its property is expected to be useful for technology applications involving oxygen ion transport, such as solid oxide fuel cells and electrochemical sensors. We investigate the electronic structure and magnetic properties of the antiferromagnetically ordered $SrCoO_{2.5}$ with brownmillerite-type structure and the ferromagnetic $SrCoO_3$ with cubic-type perovskite structure by using first-principles electronic structure calculations. The relaxed structure of $SrCoO_{2.5}$ is compared with the experimental structure. The magnetic and orbital orderings related to the structural feature are observed in each layer. The magnetic exchange interaction parameters between nearest-neighbor Co ions are obtained through fitting the total energy results to model hamiltonians. The results are found to be consistent with the observed magnetic structures of $SrCoO_3$ and $SrCoO_{2.5}$. A magnetic and structural configuration for the $SrCoO_{2.75}$ oxygen deficient structure is suggested from the results of electronic structure calculations. This finding provides us a way to understand how the electronic and magnetic ground states of $SrCoO_{2.5+x}$ vary depending on the amount of oxygen vacancies.
*Supported by the National Research Foundation of Korea funded by the Ministry of Science, ICT & Future Planning (no. 2013R1A2A2A01067950).

P2-Co.223

Identification of Small Bipolaron Induced by Substitutional Hydrogen in TiO_2

*이동헌, 한승우, 남호현 [1]
*Dongheon. Lee, Seungwu. HAN, Ho Hyun. Nahm[1]
서울대학교. [1] *서울대학교 IBS 외부연구단.*

Keyword : TiO_2, Hydrogen impurity, bipolaron, photocatalyst

TiO2 is a promising candidate for photocatalyst for water splitting or hydrogen production [1]. To promote the efficient chemical reaction (H2 or O2) by light, both the large portion of the light absorption and the high mobility of the excited carriers into the reaction surface should be achieved. It is well-known that small polarons in TiO2, i.e., self-trapped polarons [2] and polarons induced by oxygen vacancies or dopants [3], are easily formed, implying that they act as a cause of poor carrier mobility. In spite of the fact that interstitial and substitutional hydrogen impurities, easily incorporated into oxides as shallow donors [4], can affect the electronic properties of materials, there are few researches. Thus, understanding the transport properties of H-related excited carriers for these electrochemical applications is essential. However, the polaronic behavior of hydrogen impurities has not been studied still. In this study, we investigated the microscopic structures of hydrogen impurities in TiO2 through the first-principles calculation. Surprisingly, we find that substitutional hydrogen (HO) in the (-)-charge state can be formed as a bipolaron state through the Ti-Ti bonding near HO in both anatase and rutile TiO2. The bipolaron state originates from antiferromagnetic interaction between two nearest Ti-d orbitals atoms. Conclusively, our results show that (i) substitutional hydrogen impurities do not simply plays a role as shallow donor, because the negatively-charged HO- make the thermal transition level of HO located below conduction band minimum, and (ii) the bipolaron state of HO can affect the transport of the carriers excited by light.

[1] Detlef W. Bahnemann et al., Chem. Rev. 114 (19), 9919 (2014).
[2] C. G. Van de Walle et al., Phys. Status Solidi RRL 7 (3), 199 (2013).
[3] G. W. Watson et al., Journal of Materials Chemistry 19, 5175 (2009).
[4] A. T. Brant et al., Journal of Applied Physics 110, 053714 (2011).

P2-Co.224

Electronic structures and optical properties of transition metal dichalcogenides heterobilayers

*이예리, 박철환, 임지순
*Yea-Lee. Lee, Cheol Hwan. Park, Jisoon. IHM
서울대학교.

Keyword : transition metal dichalcogenides, electronic structures, optical absorption, van der Waals interaction

We investigate the electronic structures and optical properties of transition metal dichalcogenides (TMD) heterobilayers without any arbitrary strain. The van der Waals (vdW) interactions, work function difference between the layers, and the constituting elements are intimately associated to determine the band structures of the heterobilayers. The weak interlayer interaction also gives rise to the substantial interlayer optical transition which will be corresponding to the interlayer exciton. The band structures and optical properties of the TMD heterobilayers are highly dependent on the weak vdW interlayer interactions, and our study will be helpful to design the new electronic and optoelectronic devices.

P2-Co.301*

Non-magnetic impurity effect on thermal properties of $YMnO_3$

*심하성, 최기영, 박제근
*HASUNG. SIM, KI YOUNG. CHOI, Je-Geun. PARK
서울대학교.

Keyword : hexagonal manganite, Non-magnetic impurity effect

Non-magnetic impurities on the hexagonal manganite can induce canted surrounding spins due to fractional impurity spin and a spin texture, which will affect several physical properties. To investigate the non-magnetic impurity effect on the hexagonal manganite, we prepared single crystals of Al doped $Y(Mn_{1-x}Al_x)O_3$ with x = 0, 0.02, 0.05 and 0.1 by using the floating zone furnace. Non-magnetic Al doping effects over the entire concentration of $Y(Mn_{1-x}Al_x)O_3$ were investigated by measuring bulk properties such as susceptibility, heat capacity, and thermal conductivity.

P2-Co.302*

방사광의 변광성을 이용한 $SrRu_{1-x}Ir_xO_3$ ($0 \le x \le 1$) 루티네이트 박막의 전자구조 연구

*김대현, 이은숙, 김현우, 강정수, 비스워스 [1], 정윤희 [1], 김재영 [2]
*Dae hyun. Kim, Lee Eun Sook. , Kim Hyun Woo. , KANG Jeongsoo. , Abhijit Biswas. [1], JEONG Yoon Hee. [1], Jae-Young Kim. [2]
가톨릭대학교. [1] 포항공과대학교. [2] 포항가속기연구소.

Keyword : PAL, XAS, XLD

Ir 4+ 이온과 Ru 4+ 이온은 매우 유사한 이온 반지름 (ionic radii)을 가지지만 페로브스카이트 산화물인 ABO_3 (A : Ca, Sr, Ba; B : Ir, Ru) 에서는 물성과 구조가 두드러지게 다르다. $SrRuO_3$ 은 금속성(metallic)을 갖는 강자성 (ferromagnetism)이며 상온에서 $CaTiO_3$-type 의 사방정계 (orthorhombic) 구조를 가지지만 $SrIrO_3$ 는 금속성을 갖는 상자성 (paramagnetism)이고 구조는 $BaTiO_3$-type 의 단사정계 형태로 찌그러진(monoclinic distortion) 6 방정계(hexagonal)이다. [1] 특히 SrIrO3 는 스핀-궤도 상호작용 (spin-orbit coupling) 이 큰 물질로 최근 많은 연구가 보고되고 있다.[2] $SrRu_{1-x}Ir_xO_3$ ($0 \le x \le 1$) 박막에서는 x=0($SrRuO_3$)에서 강자성을 띠며 Ir 의 양이 증가하면 x=0.2~0.3 부근에서 스핀 유리(spin glass)로 바뀌며 x=0.6 부근에서 상자성으로 바뀌는 현상이 관찰되었다[2]. 이 연구에서는 방사광의 편광성을 이용하여 Ir 의 치환 양에 따른 $SrRu_{1-x}Ir_xO_3$ 의 전자구조를 연구 하였다. 연 X 선 선편광 이색성 (soft X-ray linear dichroism : XLD)과 연 X 선 자기 원편광 이색성 (soft X-ray magnetic circular dichroism : XMCD)실험을 수행함으로써 Ru 과 Ir 이온들의 원자가와 Ru 4d, Ir 5d 전자들의 스핀 배열 상태 및 오비털 배열 상태를 결정하였다. O 1s XLD 의 결과로부터 Ir 이 첨가되면 Ir 의 양에 관계 없이 t_{2g}, e_g 의 오비털 배열이 매우 유사하고 $SrRuO_3$ 와는 배열이 다른 것을 확인하였다. 이번 발표에서는 x 별 O 1s XLD 결과와 오비털 배열들에 대한 발표를 진행 할 예정이다.

[1] Ilyas Qasim et al., J. Solid State Chem. 206, 242 (2013)
[2] S. J. Moon et al., Phys. Rev. Lett. 101, 226402 (2008)
[2] A. Biswas et al., arXiv:1312.2716 (2013)

P2-Co.303*

(La,Sr)MnO3 박막의 Electrolyte 와 Ionic liquid 게이트 효과에 대한 연구

*정종훈, 이태권, 송한성
*JongHoon. Jung, 태권. 이, 한성. 송
인하대학교.

Keyword : (La,Sr)MnO3 , Electrolyte, Ionic liquid, Electric Double layer

Electrolyte 와 Ionic liquid 는 기존 부도체 층에 비하여, 강한 전기장을 인가할 수 있어, 전이 금속 산화물의 ELECTROSTATIC DOPING 에 활용되고 있다. 본 연구에서는 대표적인 산화물 강자성체인 (La,Sr)MnO3 (LSMO) 박막의 Electrolyte 와 Ionic liquid 에 의한 gating 특성을 연구하였다. 강자성 전이 온도는 양의 전압 혹은 음의 전압에 따라 변화 폭이 다름을 확인하였고, 전기 저항 역시 전압의 극성에 따라 변화양상이 다름을 확인하였다. 홀 저항 측정을 통해, Gating 에 따른 carrier density 와 mobility 의 변화를 측정하였다. 이와 같은 변화는 Electric Double layer 에 의한 LSMO 박막 표면의 hole doping 에 의해 설명가능함을 보였다.

P2-Co.304*

Orthoferrite : Pristine And Rare Earth (Ho, Sm) Doped BaFeO3 Study For Bubble domain Applications

*김장건
*Jang Gun. Kim
서울대학교 물리천문학부.

Keyword : 거품자구, BaFeO3, 희토류, 박막, 자성

In principle, small cylindrical magnetic domains, which are usually called “magnetic bubbles”, can be formed in thin films of ferrites or garnets. Their field-controlled property makes magnetic bubbles to be potential candidates for data storage. The point is how at room temperature we can store a huge amount of data into smallest bubble memory chip as possible. $BaFeO_3$ was predicted to be a potential candidate. We have studied pristine and rare earth (Ho, Sm) doped BaFeO3 in both polycrystalline powder and thin film forms with hope to improve its magnetic properties such as transition temperature and magnetic moment. The results show that surprisingly, their magnetic behaviors are quite different between powder and film forms. By lowering the size of particles, BaFeO3 could be ferromagnetic even above room temperature and thin film of BaFeO3 showed a highly enhanced magnetization by Ho doping. Further studies concerning these dopants, $Ho_{1-x}Sm_xFeO3$ (x=0, 0.5, 1), were also carried out, resulting in somewhat interesting magnetic features, such as a magnetization reversal of HoFeO3 film. Some of these films showed magnetic anisotropies and their aging effects were also studied.

P2-Co.305*

Physical properties of the polycrystalline $CuRE_2Ge_2O_8$ (RE = Y, La, Pr, Nd, Eu, Tm)

*조환범, 피츠데런 [1], 최기영 [1], 박제근 [1]
*Hwanbeom. Cho, Darren. Peets[1], KI YOUNG. CHOI[1], Je-Geun. PARK[1]
서울대학교 자연과학대학. [1] 서울대학교.

Keyword : Heisenberg chain, one dimensional physics, copper, magnetism

$CuRE_2Ge_2O_8$ (RE = Y, La, Pr, Nd, Eu, Tm) has a monoclinic structure (space group C1m1) [1] with two oxygen sites which are departed from the centrosymmetric position and quasi one-dimensional Copper oxide chains between rare earth layers [2]. Emergent phenomena from the non-centrosymmetic and one-dimensional structure as well as the rare earth magnetism are expected in these compounds. We synthesize the polycrystalline $CuRE_2Ge_2O_8$ samples and observe the structural phase transition at high temperature region and the antiferromagnetic transition at low temperature region which are confirmed with X-ray and neutron diffraction, specific heat and magnetic measurements. We will discuss the direction of the copper oxide of the compounds which is different from the previous reports.

[1] U. Lambert and W. Eysel, Powder Diffr. 1, 256 (1986).
[2] J. A. Campa, E. Gutierrez-Puebla, M. A. Monge, C. Ruiz Valero, J. Mira, J. Rivas, C. Cascales and I. Rasines, J. Solid State Chem. 120, 254 (1995).

P2-Co.306*

Crystal grain distribution in a ferromagnetic $La_{0.7}Sr_{0.3}MnO_3$ single crystal revealed by magneto-optical imaging technique

*이지원, 함선영, 권준현, 김재명, 길계환 [1], 이종석
*Jiwon. Lee, Sun Young. Hamh, Jun-Hyun. Kwon, Jae Myung. Kim, Kyehwan. GIL[1], Jongseok. LEE
광주과학기술원. [1] 포항가속기연구소.

Keyword : magneto-optical imaging, $La_{0.7}Sr_{0.3}MnO_3$ (LSMO), Faraday rotation, magnetocrystalline anisotropy

We performed the magneto-optical (MO) imaging experiment using a magneto-optical indicator film (MOIF), $(LuBi)_3(FeGa)_5O_{12,}$ on a single crystalline $La_{0.7}Sr_{0.3}MnO_3$ (LSMO), and observed two distinguishable areas with a size of tens of micromters when the magnetic field is applied along the in-plane direction. From the detailed analysis about the X-ray micro diffraction results obtained on the same crystal, we found that the crystallographic orientation mapping results reproduce the MO imaging pattern quite well. Interestingly, each crystallographic grain has a tiny orientation difference, i.e., less than 1 degree along all three directions of [100], [010] and [001] of LSMO crystal. After all, the crystallographic distribution can give a similar pattern in the MO imaging due to the magnetocrystalline anisotropy, and therefore, MO imaging technique with a use of MOIF can provide reliable information about the crystallographic distribution for ferromagnetic material with a rapid data acquisition and high sensitivity.

P2-Co.307*

Orbital angular momentum based Hamiltonian in cycloidal magnets

*권준영, 정원식, 김창영
*Jun Young. Kwon, Won Sig. Jung, Changyoung. Kim
연세대학교.

Keyword : cycloidal, spiral, oribtla angular momentum

Cycloidal magnetic structure have been gathered interest as it can create electric polarization, hence multiferroicity. It is known that the electric polarization is created via the Dzyaloshinskii-Moriya (DM) interaction. The theory suggests that spin canting of two magnetic atoms from cycloidal structure can create displacement of atom between the two. However, we suggests that there can be possible orbital angular momentum contribution in the polarization. Mainly, canting of orbital angular momentums can create interference of wave function of electrons, hence there can be a charge anisotropy.

P2-Co.308*

Engineering shape of Ferromagnetic nanostructure in $BiFeO_3$-$CoFe_2O_4$ self-assembled thin films

*정스리, 김광은, 양찬호
*Seuri. Jeong, Kwang-Eun. Kim, Chan-Ho. Yang
한국과학기술원 (KAIST).

Keyword : " $BiFeO_3$-$CoFe_2O_4$ ", "magnetic anisotropy", "self assembly"

Magnetic Oxide have attracted considerable interest due to their potential applications in novel technological devices. $CoFe_2O_4$ (CFO) has been received a lot of attention due to large magnetocrystalline anisotropy and magnetostriction of $\lambda = -350 \times 10^{-6}$. Magnetic properties of CFO nanostructures depend on shape and size due to boundary condition. Recently, manipulation of magnetic easy axis by using various oriented substrates have been reported. In this study, we report growth of BFO-CFO nanocomposite thin films on (001)-, (110)-, (111)-oriented $SrTiO_3$ (STO) substrates. The films were synthesized by using pulse laser deposition at various growth temperature. We observed that size of CFO nanopillars depend on growth temperature. Our samples were characterized by using scanning probe microscopy. Our results show that CFO nanostructure forms rectangular, stripe, triangular-shape embedded in a BFO matrix on (001)-, (110)-, (111)-oriented STO substrates.

P2-Co.309*

Growth of MnBi nanorods on MgO (100) by molecular beam epitaxy

*민하이, 드엉안투안, 웬반쾅, 두엉반티엣, 웬안프엉, 웬티흐엉, 팜안투안, 웬티탄흐엉, 부티호아, 조성래
*Nguyen Thi Minh. Hai, Duong Anh. Tuan, Nguyen Van. Quang, Duong Van. Thiet, Nguyen Anh. Phuong, Nguyen Thi. Huong, Pham Anh. Tuan, Nguyen Thi Thanh. Huong, Vu Thi. Hoa, Sunglae. CHO
울산대학교.

Keyword : MnBi, nanorods, Molecular beam epitaxy

The intermetallic compound MnBi has long been a material of interest because of its unusual magnetic properties, attractive magneto-optical properties and complex diagram [1, 2]. Various techniques were used for fabricating MnBi. However there were a few reports for MnBi rods fabrication [3-6]. In the present study, we report on the growth of MnBi nanorods on MgO(100) substrate at 400 oC by molecular beam epitaxy (MBE). Scanning electron microscopy (SEM) indicated that MnBi nanorods were formed. XRD result showed that the polycrystalline film has a hexagonal NiAs crystal structure with impurity phases of Mn and Bi. Temperature dependence resistance curve suggested there was a phase transition at about 100 K. SQUID results will be discussed.

[1] Di G Q, Iwata S, Tsunashima S and Uchiyama S, J. Magn. Magn. Mater. 104, 1023 (1992).
[2] T. Chen and W. E. Stutius, IEEE Trans. Magn. 10, 581 (1974).
[3] K. Kang, L. H Lewis, A. R. Moodenbaugh, J. Appl. Phys. 97, 10K302 (2005).
[4] K. Kang, L. H. Lewis, A. R. Moodenbaugh, Appl. Phys. Lett. 87, 062505 (2005).
[5] K. Kang, L. H. Lewis, A. R. Moodenbaugh, Appl. Phys. Lett. 90, 153112 (2007).
[6] K. Kang, L. H. Lewis, Y. F. Hu, Quiang Li, A. R. Moodenbaugh, Y.-S. Choi, J. Appl. Phys. 99, 08N703 (2006).

P2-Co.310*

Temperature Dependent Anomalous Hall Effect and Anomalous Nernst-Ettingshausen Effect in perpendicularly magnetized [CoSiB/Pt] Multilayer film

Praveen Gautam, Hafiz M W Khalil, 김영광, 김태완, *노화용
Praveen. Gautam, Hafiz M W. Khalil, Young Gwang. Kim, Taewan. Kim, *Hwayong. Noh
Sejong University.

Keyword : perpendicular magnetic anisotropy, anomalous Nernst effect, multilayer

Materials with perpendicular magnetic anisotropy are the possible candidates for future perpendicular magnetic recording applications. Here we report experimental observation of temperature correlated behavior of anomalous Nernst effect induced by temperature gradient in [CoSiB/Pt] multilayer films, with an out of plane magnetization. The layered structure of sample was SiO_2/Ta(50Å)/Pt(30Å)/[CoSiB(6Å)/Pt(14Å)]$_n$. Furthermore, we also studied the variation of anomalous Hall signal with temperature ranging from 25K to 300K in the same device. There is a clear decrease in both signals with decrease in temperature. We discovered that keeping a heater current fixed at certain value during measurement maintains constant thermal gradient across the sample at that particular current, for all temperatures. Results clearly indicate that decrease in Nernst signal with temperature is larger than the Hall signal. Fractional drop in Nernst signal is approximately 10 fold larger than Hall signal.

P2-Co.311*

Gd 이 도입된 Bi_2Te_3 의 열처리에 따른 물리적 성질 변화

*김진수, 이현성, Manoj K. Sharma[1], 임규욱 [1], 황찬용 [2], Otgonbayar Dugerjav[2], 정명화
*Jinsu. Kim, Hyun Seong. Lee, Manoj. Sharma[1], Kyuwook. Ihm[1], HWANG Chanyong. [2], Otgonbayar. [2], JUNG Myung Hwa.
서강대학교. [1] 포항가속기연구소. [2] 한국표준과학연구원.

Keyword : topological insulator, magnetic doping, annealing effect

위상절연체인 Bi_2Te_3 에 희토류 자성체인 Gd 를 도입한 후, 열처리에 의한 물리적 성질 변화를 연구하였다. X-ray photoelectron spectroscopy 실험과 scanning tunneling microscopy 측정을 통해 열처리 전에 고르게 분포하던 Gd 이온이 열처리 후에 시료 표면으로 확산되어 나오는 것을 관측하였다. 열처리에 의해 확산된 Gd 이온들은 자기적 배열이 바뀌게 되고, 이로 인해 상자성(paramagnetic) 상태에서 반강자성(antiferromagnetic) 상태로 변화하게 된다. 특히 가해준 자기장 방향에 따라 확연히 다른 자기 이방성을 보였다. 이는 열처리 후에만 나타나는 현상으로, 시료가 가진 자기적 성질이 벌크가 아닌 표면에 존재하는 Gd 이온에 의한 것임을 의미한다. 열처리에 의한 자기적 성질뿐만 아니라 전기적 특성도 크게 변화하였다. 또한, 각분해 광전자 분광 실험을 통해서 자기적 배열에 따라 변화하는 위상절연체의 표면 전자구조를 관측하였다. 이러한 실험 결과들은 도핑된 Gd 이온의 자기적 배열에 따라 위상절연체인 Bi_2Te_3 의 물리적 특성에 어떠한 영향을 주는지 알 수 있게 한다.

P2-Co.312*

Unusual magnetic interactions in A-site deficient spinel Ir2O4

*박창휘, 강승진, 유재준 [1]
*Changhwi. Park, Seungjin. Kang, Jaejun. Yu[1]
서울대학교 물리천문학부. [1] *서울대학교.*

Keyword : spin, magnetism, Ir2O4, iridium, pyrochlore

We predict an unusual magnetic ground state of A-site deficient spinel Ir2O4 based on first-principles calculations with LDA+U+SOC method as implemented in the OpenMX code. The A-site deficient spinel Ir2O4 is a Mott-Hubbard insulator driven by the formation of the J=1/2 band due to strong spin-orbit coupling, where the effective on-site Coulomb interaction U of 2.4 eV Ir 5d orbitals is used to give a direct band gap of about 0.5 eV in agreement with experimental observation. The magnetic ground state of the spinel is shown to have a non-collinear spin structure with competing ground states of so-called XY pyrochlore configurations. Using the contraint calculations for non-collinear spin orientation together with various models for the effective spin interactions, we investigate the origin of unusual magnetic ordering in spinel Ir2O4. Both Heisenberg and Dzyloshinskii-Moriya interactions are found to be effective while a strong on-site anisotropy appears to be crucial for the J=1/2 spin configuration of Ir 5d orbitals.

P2-Co.313*

Synthesis of MPS_3 (M = Fe, Ni, Mn, and Co) by Chemical Vapor Transport Method

*이성민, 발라간, 김동직, 전세영, 박제근
*Sungmin. Lee, K.. BALAMURUGAN, Dong Jik. Kim, Seyyoung. Jeon, Je-Geun. Park
서울대학교.

Keyword : MPS3, Metal Phosphorus Trisulfides, Chemical Vapor Transport, Layered Structure, van der Waals Material

Honeycomb layered metal phosphorus trisulfides are the good candidate to investigate the magnetism in the low dimensional structure materials [1,2]. For this research, we have prepared single crystals of MPS_3 (M = Fe, Ni, Mn, Co) by chemical vapor transport method. The quality of single crystals were confirmed by single crystal XRD, SEM and EDX, and the typical size of the sample is about 2 ´ 2 mm^2. The physical properties of single crystals of MPS_3 (M = Fe, Ni, Mn, Co) will be presented.

References:
[1] Raymond Brec, Solid State Ionics 22, 3-30 (1986).
[2] P. A. Joy and S. Vasudevan, Phys. Rev. B 46, 5425 (1992).

P2-Co.314

Computational design of compensated half-metal in trigonally distorted perovskites

진효선, *이관우
Hyo-Sun. Jin, *Kwan-Woo. Lee
고려대학교 세종캠퍼스.

Keyword : Compensated half-metal, Half-metal Antiferromagnet, first principles calculations

Compensated half-metal (CHM) or called half-metallic antiferromagnet is a half-metal, which is metallic in one spin channel and insulating in the other channel, but has the zero net moment. CHM, a good candidate for spintronics applications, was theoretically suggested by de Groot and coworkers in 1995[1]. So far, the double perovskites, the Heusler structures, and tetragonally coordinated transition metallic system have been investigated for the last 20 years. We have investigated trigonally distorted perovskite-like systems. Lee and Pickett suggest that CHM in trigonally distorted perovskite-type $NiCrO_3$[2]. Motivate by this, we studies an isostructural and isovalent $PdCrO_3$[3]. Very recently, C. Felser's group has first synthesized CHM in a Pt-doped ferrimagnetic Heusler alloy[4].
We have performed first principles calculations to find new CHM compounds in the distorted perovskite structure. Our studies are expected to provide a new direction in CHM research.

Acknowledgements: This research was supported by NRF-2013R1A1A2A10008946.

[1] H. van Leuken and R. A. de Groot, Phys. Rev. Lett. 74, 1171 (1995)
[2] K.-W. Lee and W. E. Pickett, Phys. Rev. B 83, 180406(R) (2011)
[3] H.-S. Jin and K.-W. Lee, Phys. Rev. B 84, 172405 (2011)
[4] A. K. Nayak, et al., Nat. Mater. 14, 679-684 (2015)

P2-Co.315

Ba 대신 Bi 치환에 따른 $BaTi_{0.9}Fe_{0.1}O_3$ 의 다강성 산화물의 방사광 분광 연구

*김현우, 김대현, 이은숙, 김덕현 [1], 이보화 [1], 고윤영 [2], 김재영 [2], 강정수
*Hyun Woo. Kim, Dae hyun. Kim, Lee Eun Sook. , Kim Deok Hyeon. [1], LEE Bo Wha. [1], Koh Yoon Young. [2], Jae-Young Kim. [2], KANG Jeongsoo.
가톨릭대학교. [1] 한국외국어대학교. [2] 포항가속기연구소.

Keyword : Ba1-xBixTi0.9Fe0.1O3, XAS, XMCD,ferromagnetic,ferroelectric

최근 강유전성과 자성을 동시에 나타내는 다강체 (multiferroic) 물질이 발견됨에 따라 차세대 소자의 개발 가능성에 대한 응용 연구의 측면과 함께 이러한 물성의 원인규명에 대한 기초 연구의 관점에서 세계적으로 활발한 연구가 진행되고 있다. 다강체 물질의 한 예로 강유전 물질로 잘 알려진 $BaTiO_3$ 에 강자성 Fe 이온을 치환시켜 합성된 $BaTi_{1-x}Fe_xO_{3-d}$ 가 상온에서 강유전성과 강자성의 특성을 동시에 나타낸다는 사실이 많은 연구를 통해 보고 되었다. [1,2,3] 앞선 연구결과에 따르면 다결정 $BaTi_{1-x}Fe_xO_3$ 에서 Fe 치환양 x 가 7%인 $BaTi_{0.93}Fe_{0.07}O_{3-d}$ 에서 Fe 이온 치환에 의해 유도된 강자성 특성이 급격하게 변화되는 것이 발견된 바 있다. [2] 한편 $BaTi_{1-y}Fe_yO_3$ 에서 Ba 대신 Bi 이온을 치환시킨 $Ba_{1-x}Bi_xTi_{1-y}Fe_yO_3$ 는 Bi 이온의 치환양에 따라 Fe 이온의 원자가가 변할 것으로 예상되며 특정 치환양 x 에서 다강성 물성이 좋을 것으로 예상된다. [3] 이 연구에서는 방사광을 이용한 연 X-선 흡수 분광법 (soft X-ray absorption spectroscopy: XAS)과 연 X-선 자기원편광 이색성 (soft X-ray magnetic circular dichroism: XMCD) 분광법을 이용하여 $Ba_{1-x}Bi_xTi_{0.9}Fe_{0.1}O_3$ ($0 \le x \le 0.12$)의 전자 구조를 연구하였다. 이 연구에 의하면, 상온에서 Fe 는 Fe^{2+}와 Fe^{3+}가 섞여있는 혼합 원자가 상태로 관찰되었으며, Ba 는 Ba^{2+} 상태, Ti 는 거의 Ti^{4+} 상태로 관찰되었다. 또한 Fe 이온의 XMCD 신호의 크기가 거의 0 으로 측정되었다. 이 연구 발표에서는 $Ba_{1-x}Bi_xTi_{0.9}Fe_{0.1}O_3$ 산화물의 전자구조 및 전자구조가 이 물질의 다강성에 미치는 영향에 관하여 발표할 예정이다.

[1] S. Ray et al., Physical Review B 77, 104416 (2008).
[2] Qui. S. Y. et al., Transaction of Nonferrous Metal Society of China 20, 1911-1915 (2010).
[3] 김덕현 et al., 한국자기학회 자성 및 자성재료 국제학술대회 초록집 MO02, 49 (2013).

P2-Co.316

에피탁시 니켈 페라이트 박막의 수직 자기 이방성과 도메인 구조 연구

*김병건, 기상훈, 정웅현, 도중회
*Kim byeong geon. , Kisanghoon. , Woong-hyun Jung. , DHO Joong Hoe.
경북대학교.

Keyword : 니켈 페라이트, 자기적 도메인, 수직 자기 이방성

$NiFe_2O_4$(NFO)는 역스피넬 구조를 가지는 산화물로서 약 864 K 이하에서 준강자성을 가지는 물질로 알려져 있으며 NFO 박막은 마이크로파 및 스핀트로닉스 응용을 위한 물질로서 꾸준히 연구되어 왔다. 지금까지 스피넬 구조를 가진 페라이트 박막들의 자기 이방성이 열적 변형력, 결정화 방향, 변형 효과로 인하여 박막의 수직방향 또는 평면내 방향에서 증가된다는 결과가 보고되어 왔다. [1-2] 이번 실험에서는 NFO 박막을 $MgAl_2O_4$(MAO)(110) 기판 위에 다양한 온도(300-800℃)에서 펄스 레이저 증착법 (Pulsed laser deposition)으로 약 80 nm 두께로 성장시키고 그에 따른 수직 자기 이방성을 연구하였다. X 선 회절을 이용하여 박막들의 결정성을 확인하였으며 락킹 커브의 반치전폭 값들은 0.32-0.7° 범위이었다. 원자 힘 현미경을 통해 확인한 박막들의 표면의 거침도는 0.12-0.48 nm 범위이었다. X 선 회절의 박막 피크는 증착시 기판 온도가 증가함에 따라 이미 알려진 벌크 샘플의 피크 각도로 이동하였다. 박막의 수직 방향 자기 도메인을 자기힘 현미경으로 상온에서 확인하였다. 모든 박막들의 자기 이미지는 명암이 섞여있는 덩어리 형태의 자기 도메인 구조를 보였으며 박막 증착 시 기판 온도가 증가함에 따라 명암의 구분 정도가 보다 뚜렷해졌는데 이것은 압축변형 효과가 약해졌기 때문으로 보인다. [3] 추가적으로 고정된 기판 온도에서 박막의 두께 효과를 확인하였다. 이와 유사한 자기 도메인 구조는 MAO(100), $SrTiO_3$(100), $SrTiO_3$(110), MgO(100), MgO(110) 기판에 증착한 NFO 박막에서도 관찰됨을 확인했다.

P2-Co.317

Enhanced magnetic coercivity and maximum energy product in double-perovskite Y_2CoMnO_6 single crystals

*최환영, 오상협, 문재영, 김미경, 오동건, 이나라, 최영재
*Hwan Young. Choi, SANGHYUP. OH, Jae Young. Moon, Mi Kyung. Kim, DONG GUN. OH, Nara. Lee, Y.J.. Choi
연세대학교.

Keyword : Double perovskite, ferromagnet, single crystals, coericivity, maximum energy production

We have investigated the influence of different annealing conditions on the magnetic properties on the single crystals of double-perovskite Y_2CoMnO_6. The ferromagnetic moment along the c-axis with the large magnetic coercivity and high squareness ratio was observed. Particularly, in the quenched specimen, the magnetic functionality has been greatly improved compared to that of the as-grown crystal. The magnetic coercivity and maximum energy product have been increased by ~120 % and ~50 %, respectively, by comprising substantial disorders and defects. Our result renders an efficient route to improve the magnetic functionalilty in mixed-valent magnets.

P2-Co.318

덩치 및 박막 $CrPt_3$ 의 자성 제일원리 계산

*정태성, 제갈소영, 권오룡, 임성현, 홍순철
*Jeong Taesung. , Jekal Soyoung. , Kwon Oryong. , Sonny Rhim. , HONG Soon Cheol.
울산대학교.

Keyword : "자성" "박막"

본 논문에서는 제일원리 계산방법을 이용하여 계산한 $L1_2$ 구조 $CrPt_3$ 의 자성에 대해 보고한다. 계산방법으로는 Vienna Ab-initio Simulation Package (VASP)을 이용하였고 교환-상관 전위는 일반화 물매 근사 (GGA: generalized gradient approximation)로 표현하였다. 총에너지 계산결과에 의하면 강자성 상태가 가장 안정하였고 평형 상태에서의 격자상수는 3.925 Å 이였는데 이는 실험치 3.877 Å 보다 0.048 Å 컸다. 반강자성 상태는 A-type, C-type, G-type 에 대해 계산을 하였는데 강자성 상태에 비해 각각 0.517 eV, 0.591 eV, 0.184 eV 높았다. 강자성 상태일 때 Cr 과 Pt 의 자기모멘트는 각각 2.748 μ_B, -0.44 μ_B 으로 계산되었다. A-type, C-type, G-type 반강자성 상태일 때 Cr 자기모멘트는 각각 2.805 μ_B, 2.794 μ_B, 2.869 μ_B 이였고 Pt 는 각각 0.012μ_B, 0.010μ_B, 0.027μ_B 나왔다. Pt 혹은 CrPt 로 끝나는 $CrPt_3$ 박막의 자성에 대해서도 부가해서 논의할 예정이다.

P2-Co.319

하나로 수직형 냉중성자 반사율 장치 최적화 분석

*이준혁
*June Hyuk. Lee
한국원자력연구원.

Keyword : neutron, 중성자, 반사율측정, 박막

중성자를 이용한 박막의 반사율 측정은 나노단위에서 깊이에 따른 화학 조성 분포와 자화 크기와 방향 분포에 대한 정량적 해석이 가능한 매우 중요한 분석법이다. 국내 유일의 연구용 원자로 하나로에는 냉중성자 산란 시설이 있으며, 박막의 반사율 측정을 위한 수직형 반사율 측정 장치를 운영 중이다. 본 연구는 McStas 시뮬레이션 분석을 통해서 수직형 반사율 장치의 성능 향상을 위한 다양한 가능성을 찾고 최적의 장치 구성을 도출하였다. 최적화된 상황에서 2 배이상의 중성자속의 증가와 함께 중성자를 작은 영역으로 집속함으로써 기존에 측정이 어려웠던 소형 박막 시료에 대한 분석이 가능해질 전망이다.

P2-Co.320

디스크쵸퍼 비행시간 분광장치(DC-ToF)의 개발 및 응집물질연구에의 이용

*소지용
*SO Ji-Yong.
한국원자력연구원.

Keyword : 비행시간 분광장치, 중성자 산란, 비탄성 산란, 준탄성 산란,

국내 유일의 연구용 원자로인 하나로에 설치된 디스크쵸퍼 비행시간 분광장치(Disk Chopper Time-of-Flight Spectrometer)는 국내 최초로 개발된 비탄성 중성자 산란장치중의 하나이다. 2013 년도 첫 빔 입사시험에 성공하였으며 이후 장치 커미셔닝과 테스트 실험을 수행하였다. 이 장비는 50 μeV 에서 100 meV 에 이르는 넓은 영역의 준탄성 및 비탄성 산란을 통해 다양한 물질의 동역학을 측정할 수 있으며, 동종 장비가 널리 이용되는 외국의 경우 자성체, 초전도체, 고분자 및 생체분자, 소자등의 동역학 연구 및 다양한 화학 반응을 연구하는데 이용된다. 본 발표를 통해 DC-ToiF 의 현황 및 특성 및 이 장치를 통해 수행할 수 있는 다양한 연구 분야를 소개하고자 한다.

P2-Co.321

Internal Deformation Field Distribution of ZSM5 zeolites by Cu Ion Exchang

*이희주, 김현정, 강진백, 윤경병
*Heeju. Lee, Hyunjung. KIM, Jinback. Kang, Kyung Byung. Yoon
서강대학교.

Keyword : Zeolite, Catalyst, FT-IR, CXD

Cu-ZSM5 zeolites are well known catalysts for the selective reduction of NOx. They are obtained from H-ZSM5 zeolites by Cu ion exchange from the solution of $CuCl_2$, $Cu(NO_3)_2$, or $Cu(CH_3COO)_2$. Depending on the kinds of Cu donators, the exchange efficiency and the activity of catalysts are affected. In this study, we studied internal structural changes of ZSM5 after Cu ion exchange. We examined two kinds of Cu-ZSM5 zeolites exchanged by aqueous $CuCl_2$ and $Cu(CH_3COO)_2$ with same concentration. The sample exchanged by $Cu(CH_3COO)_2$ shows high Cu/Al ratio, but contains residual acetate organics. With employing coherent x-ray diffraction (CXD), a distorted diffraction pattern was observed in the one exchanged by $Cu(CH_3COO)_2$, in contrast with the other by $CuCl_2$. The deformation of the pattern was retained up to 200°C. After the phase retrieval process to the CXD patterns, we found that the deformation in the diffraction pattern is related to the internal strain of the crystal originated from the residual organics. This result contributes to the development of the applications of Cu-ZSM5 zeolites.

P2-Co.322*

X-ray Free-Electron Laser Study of Deformation Field Distribution of Zeolites during Catalytic Process

*강진백, 카르니스 제롬, 김동진, 정명우, 차원석 [1], Ross Harder[2], 송상훈 [3], Marcin Sikorski[3], Tung Chao Thanh Pham, 윤경병, 김현정
*Jinback. Kang, Jerome. Carnis, Dongjin. Kim, Myungwoo. Chung, Wonsuk. Cha[1], Ross. Harder[2], Sanghoon. Song[3], Marcin. Sikorski[3], Tung Chao Thanh. Pham, Kyung Byung. Yoon, Hyunjung. KIM
Sogang University. Korea. [1]Argonne National Laboratory. USA. [2]Advanced Photon Source. Argonne National Laboratory. USA. [3]SLAC National Accelerator Laboratory. USA.

Keyword : Coherent X-ray diffraction imaging, Zeolites, X-ray Free-electron Laser

Zeolites are well-known heterogeneous catalysts due to their aluminum sites of the nanometer-sized pore structure. It is important to understand the structural change of zeolites during catalytic process including adsorption and desorption of molecules. In this study, we measured time-resolved coherent X-ray scattering from ZSM-5 zeolites during the catalytic process. The highly coherent beam from the X-ray free-electron laser allows obtaining a map of internal deformation field distribution in zeolite microcrystals by applying phase retrieval methods, with unprecedented time resolution. The results show remarkable changes in the internal strain field along the catalytic process and give better insights of the new design of catalysts with high efficiency.
This research was supported by the National Research Foundation of Korea, ICT & Future Planning of Korea. (Nos. NRF-2015R1A5A1009962 and NRF-2014R1A2A1A10052454)

P2-Co.401

Surface electronic state of the $Bi_{1.5}Sb_{0.5}Te_{1.7}Se_{1.3}$ single crystal investigated by terahertz emission techniques

*박순희, 함선영, 박준범 [1], 김준성 [1], 이종석
*SoonHee. Park, Sun Young. Hamh, JoonBum. Park[1], Jun Sung. Kim[1], Jongseok. LEE
광주과학기술원. [1] 포항공과대학교.

Keyword : $Bi_{1.5}Sb_{0.5}Te_{1.7}Se_{1.3}$,terahertz emission spectroscopy,surface state

We investigate the surface state of $Bi_{1.5}Sb_{0.5}Te_{1.7}Se_{1.3}$ (BSTS) single crystal, which is one of the most bulk-insulating topological insulators, using terahertz emission spectroscopy. We monitor electric field profiles of emitted THz wave as a function of time after the sample cleavage, and find strong variations in the amplitude and phase, in particular, in an ambient environment with a relatively high humidity. By comparing the results obtained in different environments, such as inert gas or dry air, we discuss distributions of external ions at the sample surface and their contribution to the surface electronic states.

P2-Co.402

Investigation of Single Crystalline GeTe (111) by Using The Low Temperature Scanning Tunneling Microscopy and Spectroscopy

*김지호, 정인 [1], 여인환
*Ji ho. Kim, In. Chung[1], In-Whan. LYO
연세대학교. [1] 서울 대학교.

Keyword : GeTe (111), ferroelectricity, domain, scanning tunneling microscopy, scanning tunnelig spectroscopy

GeTe is the prototype material used in a wide range of data-storage applications. Despite much interest in GeTe itself and many derivatives, no atomic-scale resolution STM investigation of pristine GeTe has been performed to our knowledge, primarily due to the lack of high quality GeTe single crystals. Here we report on the study of GeTe(111) cleaved from single crystals at 120 K in UHV. Our low temperature scanning tunneling microscopy (STM) and spectroscopy (STS) show there exist at least two types of terraces; while both exhibit apparently similar structures with metallic characteristics, they show very distinctive I-V spectra. We attribute these different terraces to Ge-terminated, and Te-terminated surfaces respectively. At the same time, each domain exhibits a distinctive set of atomic-scale defects. We will present our analysis of these domains and defects, in comparison with other works.

P2-Co.403

STM 을 이용한 SnSe 표면구조와 defects 연구

*김상의, 드엉안투안, 임성현, 조성래, 김정대
*sang-ui. kim, Duong Anh Tuan. , Sonny Rhim. , CHO Sunglae. , KIM Jungdae.
울산대학교.

Keyword : "STM","SnSe"

SnSe 는 HOPG(Highly Ordered Pyrolytic Graphite)와 같은 2D layered material 로서 각 층들은 Van der waals force 로 결합되어 쉽게 분리할 수 있는 특성을 가진 반도체 물질이다. 최근 발표된 연구에선 bulk SnSe 에서 아주 뛰어난 열전특성(ZT = 2.6 at 932K)을 보이는 것으로 보고되어 관련 연구분야에서 큰 관심을 받고 있다(Zhao et al, Nature 508 373(2014)). 이번 발표에선 본 연구실에서 자체 제작한 저온주사터널링현미경(low temperature Scanning Tunneling Microscopy, STM)을 이용하여 원자수준의 SnSe 표면구조에 대해 연구한 결과를 소개하고자 한다. SnSe 표면에 대해 filled state 와 empty state 에서 각각 원자 이미지를 관찰하였으며, 세부적인 원자 구조는 DFT image simulation 을 통해 비교 분석하였다. 추가적으로 SnSe 에 존재하는 다양한 종류의 intrinsic defect 들에 대한 원자수준의 연구 결과도 언급할 것이다.

P2-Co.404

Non-metal catalytic behaviors of pristine and halogen-doped graphene

SUNG Dongchul, PARK Noejung[1], HONG Suklyun
Dongchul. SUNG, Noejung. Park[1], Suklyun. HONG
Sejong University. [1]UNIST.

Keyword : Density functional theory (DFT), Graphene, Solar cells, Halogen molecules

The importance of development of next generation clean energy has been increasing for several decades due to serious air pollution and depletion of fossil fuels. The solution of energy problem can be obtained from the sun because solar energy is clean and renewable source of energy. These days the interest for dye-sensitized solar cells (DSSCs) is increasing owing to its simple preparation process, low cost of fabrication, and high energy conversion efficiency. Graphene has been suggested useful for the transparent conductive electrodes (TCEs) and counter electrode (CE) for DSSCs. To examine the features of graphene used as electrode interfacing with halogen electrolytes, we performed density functional theory (DFT) calculations. We investigate the stability of halogen anionic species on the graphene surface and examine electro-catalytic activity of graphene in terms of the energy barrier for transformation between tri-iodide anion and atomic iodine (I) anions. Similarly, other halogens such as fluorine (F), chlorine (Cl), and bromine (Br) are also considered. We compare the formation energetics of linear trimer anions of halogens with that of monatomic anions on the surface of graphene. We show that the reduction process, in which the linear trimer anions transform into monatomic anions, experiences very high energy barrier on pure graphene. This suggests that, in order to use graphene as counter electrode, a source of catalyst is required to lower the reaction barrier from halogen trimer anions into atomic anions. We find that noble metal nanoparticles, such as Pt and Au, anchored onto graphene surfaces are very effective for this purpose. We suggest that a combination of noble metal nanoparticles and graphene can lead to an efficient stable catalytic behavior that is necessary for the transparent electrode.

*Corresponding author : hong@sejong.ac.kr

P2-Co.405

K^+ ion-induced electronic properties of bilayer graphene

*류민태, 이팽로 [1], 김진걸, 박희민, 정진욱
*Min Tae. Ryu, Paeng Ro. Lee[1], Jin gul. Kim, Hee min. Park, Jinwook. CHUNG
포항공과대학교. [1]POSTECH.

Keyword : Single-, Bi- layer graphene, potassium ion, band conversion

We have investigated electronic properties of Li-intercalated bilayer graphene (Li-BLG) formed on 6H-SiC(0001) substrate induced by the doping of low energy (5eV) K^+ ions. By using angle-resolved photoemission spectroscopy (ARPES) and high-resolution photoemission spectroscopy (HRPES) with synchrotron radiations, we find that K^+ ions intercalate into the interface between SiC-bilayer and second graphene layer formed by the intercalation of Li and induce a unique change in the p-band of graphene. The intercalation of K^+ ions under Li-BLG at room temperature (RT) converts the BLG into a single layer graphene (SLG). This SLG induced by K^+ ions is converted again back to BLG upon annealing. Such a back and forth conversion between SLG and BLG is interesting in its own right to understand the driving mechanism of the changes upon different surface treatments and may find its industrial applications in nano-sensing devices.

P2-Co.406

Opto-electric study of high-energy proton irradiated few layer WS_2

*오창원, 최은집
*ChangWon. O, E. J.. Choi
서울시립대학교.

Keyword : "WS_2" , "Proton irradiaiton", "Hole trap"

We investigated the effect of proton beam irradiation on CVD grown WS_2 thin film by FTIR spectroscopy, UV-VIS range absorbance, Raman spectroscopy and Resistance measurement. 5MeV proton beam (dose density : $10^{14} \sim 10^{16}$ particle/cm^2) irradiated onto the few layer WS_2(~10L) which are grown on various substrates. We have measured optical and electrical measurements before and after irradiation, to figure out the effect of high energy proton beam on WS_2 thin film. Despite of high energy proton penetrated the sample, the ratio of in-plane and out-of-plane phonon of WS_2 and its band gap enegy showed little change. On the other hand, the resistance of WS_2 were clearly raised after the proton irradiation. We guess this changes are induced from hole traps in SiO_2 dielectric layer by high energy proton irradiation which can modulate the electric properties of WS_2 chanel layer.

P2-Co.407

N_2^+ ion-induced modification of the Dirac band in graphene

*박희민, 이팽로 [1], 김진걸, 류민태, 최성수, 정진욱
*Heemin. Park, Paeng Ro. Lee[1], Jin gul. Kim, Min Tae. Ryu, Seong Soo. CHOI, Jinwook. CHUNG
포항공과대학교. [1]POSTECH.

Keyword : Graphene, N_2^+ ion, Dirac band, Doping

We have doped nitrogen ions on single layer graphene (SLG) with a variety of energies (50, 100, 300, 500eV) to induced modification on the π-band (or Dirac band) of graphene. We find that the Dirac-point (DP) of the p-band changes critically near 100 eV, i.e., it shifts away from the Fermi level (E_F) with increasing energy up to 100 eV where it begins to move up toward E_F with increasing energy up to 500 eV. From the behavior of the N 1s core level with increasing ion energy, we find the presence of two different forms of nitrogen ions embedded on graphene depending on binding sites and kinetic energy of the ions. Graphitic nitrogen appears only at the low energy while pyridinic nitrogen is seen at both low and high energy. The graphitic nitrogen ions cause the n-doping while pyridinic nitrogen the p-doping effect on carbon atoms of graphene. Band calculations based on density functional theory (DFT) reveal such a behavior of the DP with varying ion energy.

P2-Co.408

화학기상증착법을 이용한 이종접합 그래핀의 합성

*남정태, 배동재, 이동윤, 김지호 [1], 최은집 [1], 김근수
*Jungtae. Nam, Bae Dong Jae. , Dong Yun. Lee, Jiho Kim. [1], E. J. Choi. [1], KIM Keun Soo.
세종대학교. [1] 서울시립대학교.

Keyword : 그래핀, 화학기상증착법, 도핑

그래핀을 얻는 방법은 크게 흑연으로부터 떼어내는 방법과 인공적으로 합성하는 방법중의 대표적인 방법인 화학기상증착(CVD)법이 있다.
한편, 전자는 고품질로 거의 이론적으로 예측된 진성 특성을 갖는 장점이 있는 반면에 후자는 품질은 다소 떨어질 수 있으나, 인위적으로 물성을 조절할 수 있는 장점이 있다.
우리는 그래핀을 전자소자나 대면적 투명 전극으로 응용에 맞게 물성을 조절하기 위해 CVD 방법을 이용하여 순수그래핀과 도핑된 그래핀의 합성에 관한 연구를 수행하였다.
CVD 방법에 의해 메탄(CH_4) 가스를 소스로 하여 그래핀을 합성할 경우, 순수한 그래핀을 얻을 수 있다.
한편, 액상의 피리딘(pyridine, C_5H_5N)을 소스로 사용하게 되면, 질소(N)가 도핑 된 그래핀을 합성이 가능하며, 질소의 결합 사이트에 따라 그래핀의 물성이 조절 가능하다.
이를 기반으로, 촉매로 사용되는 구리포일에 메탄을 이용하여 부분적으로 순수 그래핀을 성장하고, 나머지 부분은 피리딘을 이용하여 도핑된 그래핀을 합성함으로써 이종접합 그래핀의 합성을 시도하였다.
두 단계의 CVD 공정을 이용하여 메탄과 피리딘을 소스로 합성 된 그래핀을 실리콘 기판 위에 전사하여 그래핀의 물성을 라만분광법을 이용하여 광물성을 평가하였고, FET 소자구조를 만들어 게이트 전압에 따른 전류-전압 응답특성을 통한 전기적물성을 평가하였다.

P2-Co.409

A bifractal nature of reticular patterns induced by oxygen plasma on polymer films

*배준완, 이인재
*Junwan. Bae, Injae. Lee
전북대학교.

Keyword : "Parylene", "Polymer films", "Plasma etching", "Surface", "Nano-structure"

Plasma etching was demonstrated to be a promising tool for generating self-organized nano-patterns on various commercial films. Unfortunately, dynamic scaling approach toward fundamental understanding of the formation and growth of the plasma-induced nano-structure has not always been straightforward. The temporal evolution of self-aligned nano-patterns may often evolve with an additional scale-invariance, which leads to breakdown of the well-established dynamic scaling law. The concept of a bifractal interface is successfully applied to reticular patterns induced by oxygen plasma on the surface of polymer films. The reticular pattern, composed of nano-size self-aligned protuberances and underlying structure, develops two types of anomalous dynamic scaling characterized by super-roughening and intrinsic anomalous scaling, respectively. The diffusion and aggregation of short-cleaved chains under the plasma environment are responsible for the regular distribution of the nano-size protuberances. Remarkably, it is uncovered that the dynamic roughening of the underlying structure is governed by a relaxation mechanism described by the Edwards-Wilkinson universality class with a conservative noise. The evidence for the basic phase, characterized by the negative roughness and growth exponents, has been elusive since its first theoretical consideration more than two decades ago.

P2-Co.410

Existence of nano-sized particles in azurite/malachite pigments studied by XRD and Raman Spectroscopy

*한기옥, 남지연, Jeong-Eun, 양인상, 강대일 [1], 이한형 [1], 송유나 [2]
*Kiok. Han, Ji Yeon. Nam, Jeong-Eun. jI, In-Sang. YANG, Daeill. Kang[1], Hanhyuong. Lee[1], Youna. Song[2]
이화여자대학교. [1] 한국전통문화대학교. [2] 공주대학교.

Keyword : pigment, nano-sized particle, Raman spectroscopy, XRD, line broadening

Crystalline ore pigments like azurite and malachite have been used by artists from ancient times both in the East and West. Being ground and levigated in water these pigments are separated into several grades of grain sizes which have different lightness.
Nanoparticles of the crystalline pigments are supposed to break off from the mass crystal in the grinding course. The ground material is levigated in water for the bigger particles in the range of micrometer-size settle down in order. But nano-sized particles float very long time in the water resulting in the lager population in the finer pigment grain size.
The difference of population of nanoparticles in six grades of grain sizes could be detected by X-ray diffraction measurement as well as Raman Spectroscopy. We observed the broadening of X-ray diffraction peaks by nanoparticles which is consistent with our previous measurements with Raman spectroscopy.
These results could be potentially useful in conservation and restoration of art heritage.

P2-Co.411

Embrittlement Characteristics of Austenitic Stainless Steels by Hydrogen at High and Low Temperature

*이현수, 박주영, 이석관, 김재용
*Hyun su. Lee, Jooyoung. Park, Seok Kwan. Lee, Jae-yong. Kim
한양대학교.

Keyword : "Hydrogen embrittlemnet(수소 취화)", "Hydrogen permeation(수소 투과)", "Hydrogen absorption(수소 흡수)", Austenitic stainless steel(오스테나이트계 스테인레스강)"

미래 신 에너지원으로 대두되고 있는 수소는 금속에 대해 강한 침투성을 가지고 있다. 이러한 침투 특성에 의한 금속 물질의 결함은, 변형, 강도저하, 갈라짐 등 많은 물성 변화를 일으킨다. 따라서 수소를 연료로 사용하는 에너지원의 안전성 확보를 위해서는 금속에 대한 수소 취화 특성을 연구함과 동시에 취성이 가장 적게 일어나는 물질의 선정이 필요하다. 스테인레스강은 액화수소 저장 물질 및 핵융합의 구조 재료로 거론되고 있는 물질이며, 이중 내식성이 뛰어나다고 알려진 오스테나이트계 스테인레스강은 기계적 성질이 우수할 뿐만 아니라 극저온에서부터 500 ℃ 까지 강도를 유지하는 고온 및 저온 특성을 가지고 있다. 또한 1073 K 에서 10^{-9} $mol \cdot s^{-1} \cdot m^{-1} \cdot pa^{-1/2}$ 이하의 수소 투과도를 가지고 있기 때문에 저온, 고온 및 고압의 수소 노출 환경하에서 활용되고 있다.
본 연구에서는 오스테나이트계 스테인레스강의 수소 취화 특성을 파악하고자 계의 대표적인 물질인 SS304 강과 SS316 강을 준비하였으며, 실험 전 시편을 표면 처리 함으로써 20 ~ 1073 K 의 온도범위에서 수소 장입된 시편의 특징을 분석하였다. X-ray Diffraction(XRD)를 통한 구조 분석에서 오스테나이트계 스테인레스강은 매우 낮은 수소 용해도를 가지고 있기 때문에 수소 첨가 반응 후의 구조적 변화를 관찰할 수 없었지만 광학현미경 및 전자현미경을 통한 관찰에서 수소가 노출된 표면의 갈라짐, 크롬 석출물과 같은 취화 현상을 발견할 수 있었다. 또한 수소 투과를 통한 스테인레스강의 취화 특성이 수소 장입 실험에 비해 뚜렷하게 나타나는 것을 확인함으로써 금속 시편에서의 수소 확산이 취성에 영향을 미치는 것을 확인하였고, 동시에 수소의 확산이 제한되는 20 K 의 극저온에서의 수소 취화 특성 또한 발견하였다.

P2-Co.412

TiO2 나노입자의 합성 및 초음파에너지에 따른 초음파 SILAR 법을 이용한 CdS 양자점 합성 연구

*서새롬, 김재호, 하혜진, 손상호
*Saerom. Seo, Kim Jaeho. , Ha Hyejin. , SOHN Sang Ho.
경북대학교.

Keyword : 양자점태양전지, 초음파화학반응(Sono-Chemical SILAR 법), CdS 양자점

FTO 기판 위에 TiO2 paste 를 스크린 프린터를 이용해 프린팅하여 TiO2 나노 입자를 합성하고 SILAR 방법을 이용하여 CdS 양자점을 합성하였다. 또 기존 SILAR 공법으로 양자점을 형성할 때 효율이 떨어지는 것을 보완하고자 초음파주입 공정을 사이에 넣어 양자점 형성 효율이 어떻게 변하는지 알아보았다. 초음파 SILAR 과정에서는 에너지를 바꿔가며 실험을 수행하였다. 초음파 주입 유무에 따른 CdS 양자점의 합성과 초음파의 에너지 변화에 따른 특성은 UV-Visible 스펙트럼, EDS, 그리고 TEM 으로 분석하였다. 초음파 SILAR 법은 다른 태양전지 제조공정에 비해 비교적 용이하여 실용화 단계에서도 수월할 것이다.

P2-Co.413

초음파 SILAR 를 이용한 양자점 태양전지용 CdS 양자점 합성 및 광학적 특성 연구

*김재호, 서새롬, 하혜진, 손상호
*Kim Jae ho. , saerom. seo, Ha Hyejin. , SOHN Sang Ho.
경북대학교.

Keyword : 양자점태양전지, 초음파화학법(Sono-chemical SILAR 법), CdS 양자점

양자점 태양전지는 염료감응형 태양전지의 염료 대신 양자점을 광흡수 및 전자 발생 물질로 사용함으로써 차세대 태양전지로 큰 이목을 끌고 있다. 양자점 태양전지의 대표적인 특성은 반도체 감응제로 사용되는 양자점의 양자 구속 효과를 들 수 있다. 양자점 입자의 크기를 조절함으로써 밴드갭 조절이 가능하여 전 파장 영역의 맞춤형 흡수가 가능하다. 또한 MEG(Multiple exciton generation)현상을 이용하여 hot electron 에 의한 열손실 에너지를 전류로 생산시킬 수 있다. 따라서, 양자점 태양전지는 이론상으로 Shockley-Queisser limit 를 극복할 수 있다.
본 연구에서는 CdS 양자점/TiO2 광전극을 기반으로 하는 CdS 양자점 태양전지의 효율을 높이기 위해, 전자 생성층으로 사용되는 CdS 양자점을 초음파 화학 방법으로 광 수송층인 TiO2 나노결정상에 형성하였다. Cd 전구체와 S 전구체에 TiO2 나노결정을 연속적으로 담그어 CdS 양자점/TiO2 광전극 구조로 합성시키는 기존의 Successive Ionic Layer Adsorption and Reaction (SILAR)방법에 초음파 에너지를 인가하여, 빠르고 균일하게 CdS 양자점을 TiO2 나노결정에 형성 및 흡착할 수 있다는 것은 본 연구진이 증명한 바 있다. 본 실험에서는 Cd 전구체와 S 전구체의 몰농도를 변화시킴으로써 초음파 에너지에 의해 TiO2 나노결정상에 형성될 CdS 양자점의 특성을 연구하였다. 이렇게 합성시킨 CdS 양자점/TiO2 광전극의 광학적 특성을 비교, 분석하였다.

P2-Co.414

Magnetic properties of $Ca_{0.97}La_{0.03}MnO_3$ single-crystal and polycrystalline perovskite manganites

GuoDong Gong, 김덕현, T. Andrey[1], T. L. Phan, *유춘리, B W Lee, 유성초 [2]
GuoDong. Gong, Deokhyeon. Kim, T.. Andrey[1], The Long. Phan, *Chunli. Liu, Bowha. Lee, sungcho. Yu[2]
한국외국어대학교. [1]Ural Branch of RAS. [2] 충북대학교.

Keyword : magnetic property, (Ca,La)MnO3, single crystal, polycrystalline

It is known that perovskite-type $CaMnO_3$ is an antiferromagnetic (AFM) insulator with the Neél temperature T_N = 120~125 K, where the AFM phase are from super-exchange interactions between Mn^{4+} ions (i.e., Mn^{4+}-Mn^{4+} pairs). Doping a rare-earth (RE) element (RE = La, Pr or Nd) into $CaMnO_3$ leads to the appearance of Mn^{3+} ions, causing exchange interactions of Mn^{3+}-Mn^{4+} and Mn^{3+}-Mn^{3+} pairs. The former is ferromagnetic (FM) while the latter is AFM. A coexistence of FM and AFM interactions enriches the magnetic and magneto-transport phase diagrams of doped $CaMnO_3$ perovskite manganites because of the interplay of spin, orbital and lattice degrees of freedom. Two typical phenomena are usually observed in this material system to be colossal magnetoresistance, and magnetocaloric (MC) effect taking place around magnetic phase transitions. Though many works performed on RE-doped $CaMnO_3$ materials, detailed investigations into the influence of low RE concentrations on the magnetic and MC properties have not been performed. Also, there is still the lack of a detailed comparison between single-crystal (SC) and polycrystalline (PC) samples. Dealing with this issue, we prepared orthorhombic $Ca_{0.97}La_{0.03}MnO_3$ single- and polycrystalline samples crystallized in the space group Pnma. Magnetization measurements versus temperature, see Fig. 1, reveal a remarkable difference in their magnetic behaviors, particularly around the FM-PM phase-transition temperatures of 90 and 109 K for SC and PC samples, respectively. This is related to a coexistence of FM and AFM interactions and grain boundaries, making the MC effect in the PC sample smaller than that in the SC one.

P2-Co.415*

The role of symmetry and grain boundary in epitaxial poly-crystalline $SrRuO_3$ thin films

*우성민, 이상아, Morgane Lacotte[1], Adrian David[1], 오영훈, 강원남, Wilfred Prellier[1], 최우석
*Sungmin. Woo, Sang A. Lee, Morgane. Lacotte[1], Adrian. David[1], Young-Hoon. Oh, Won Nam. Kang, Wilfred. Prellier[1], Woo Seok. Choi
성균관대학교. [1]Laboratorie CRISMAT CNRS. Caen.

Keyword : "Poly-crystalline", "Epitaxial thin film", "Grain boundary", "$SrRuO_3$", "Symmetry"

It is well known that various physical properties of transition metal oxide (TMO) films can be tuned by introducing elemental vacancies and/or epitaxial strain. In addition, long-range translational symmetry and grain boundaries can also determine electrical, magnetic, and thermal properties of the crystalline solids. In this presentation, we focus on the modifications of various physical properties due to the symmetry breaking and/or introduction of grain boundaries by fabricating single- and poly-crystalline $SrRuO_3$ films grown epitaxially using the template method. The epitaxial poly-crystalline thin films are composed of grains oriented to different directions, which induce broken translational symmetry and grain boundary effect compared to the single-crystalline thin films. Using atomically flat poly-crystalline substrates, we achieved high quality epitaxial poly-crystalline $SrRuO_3$ thin films, of which the crystallinity of each grain is comparable to that of the single crystalline thin films. We measured electronic, magnetic, and thermal properties of the poly-crystalline thin films and discuss the results in comparison with the single crystalline thin films which have distinctive orientations, i.e., (100), (110), and (111) oriented thin films. We propose a novel method to design the crystal nature of epitaxial thin films.

P2-Co.416*

Structural Study of Vanadium Oxide Microstructures Grown on Al_2O_3 (0001) by Thermal Transport Method

*페이야즈, 서옥균, Sun Min Kim[1], 강현철 [2], 노도영
*Faiyaz. Mohd, Okkyun. Seo, Sun Min. Kim[1], Hyon Chol. KANG[2], Do Young. NOH
광주과학기술원. [1]GIST. [2] 조선대학교.

Keyword : VO_2,Nanowires,Microstructures,XRD,SEM

In the diverse potential applications such as catalysts, photo electronic, sensor, battery, and thermoelectric devices based on the metal-insulator transition in vanadium oxides, controlling their microstructures is an important issue. We report growth of vanadium-oxide microstructures including nano wires, plates, and particles by the vapor transport method using vanadium-pentoxide (V_2O_5) powder source under hydrogen reduction inviroment. The morphology and crystalline structure were characterized by X-ray diffraction (XRD), scanning electron microscope (SEM), and transmission electron microscope (TEM) in terms of the growth temperature, vapor flux, and growth time.

P2-Co.417*

Topological modification of electronic properties by embedded Bi-bilayers in bulk Bi_2Se_3

*이팽로, 김진웅 [1], 김진걸, 류민태, 박희민, 지승훈, 김남동 [2], 김용삼 [2], 이남석 [3], 정진욱
*Paeng Ro. Lee, Jin Woong. Kim[1], Jin gul. Kim, Min Tae. Ryu, Hee min. Park, Seung Hoon. Jhi, Namdong. KIM[2], yongsam. kim[2], Nam-Suk. Lee[3], Jinwook. CHUNG
포항공과대학교. [1]California State University. Northridge. [2] 포항가속기. [3] 나노융합기술원.

Keyword : $(Bi_2)_m(Bi_2Se_3)_n$, topological insulator

We have studied electronic properties of an epitaxial thin film of a homologous series of $(Bi_2)_m(Bi_2Se_3)_n$, as a topological insulator (TI), by a combined study of angle-resolved photoemission spectroscopy (ARPES) measurements and density functional theory (DFT) band calculations. The high-quality thin film with m:n=1:3 (Bi8Se9) has been grown with Bi-bilayers embedded every other three quintuple layers (QLs) of Bi_2Se_3. Our in-situ x-ray diffraction, transmission electron microscopy, and Bi 5d core-level data reveal that Bi-bilayers are inserted regularly between three QLs in bulk Bi_2Se_3 with the QL-terminated outermost surface. The ARPES data obtained from clean Bi8Se9 shows the topological surface states (TSSs) quite similar to those of Bi_2Se_3 except that they are shifted down by 0.3 eV from the Fermi level. Our DFT calculations show that the TSSs stem from the inverted Bi and Se states and the topologically nontrivial structures are mainly based on the prototype of three-dimensional TI Bi_2Se_3. The presence of two-dimensional Bi-bilayers modifies the chemical potential without affecting the overall topological order.

P2-Co.418*

Passivation of Graphene Field Effect Transistors on Top and Bottom Surfaces

*장근수, 박지용, 안영환, 이순일
*Geun soo. Jang, Ji-Yong. Park, Yeong Hwan. Ahn, Soonil. LEE
아주대학교.

Keyword : 그래핀 , Passivation, polymer suface, 그래핀 전계형 트랜지스터

그래핀은 탄소의 단원자층으로 구성된 2 차원 나노 물질로 흥미로운 전기적 특징을 가지고 있는 물질이다. 저압화학기상증착법(LPCVD)을 통해 구리 호일에 단일층 그래핀을 성장시킨후 Poly(methyl methacrylate) (PMMA)를 이용하여 SiO_2 /Si 기판에 전사시켜 만들어진 그래핀 전계형 트랜지스터 [Graphene Field Effect Transistors (GFETs)] 는 전형적으로 p-type 의 성질을 보여주고 있다. 이것은 대기 중에 존재하는 hydroxyl (-OH) group 또는 고분자 잔여물에 공기중의 H_2O 또는 O_2 의 흡수에 기인하는 것으로 알려지고 있다. 또한 SiO_2 에 존재하는 charge puddle 또한 GFETs 의 전기적 특성에 영향을 준다. 본 연구에서는, GFETs 의 윗면과 아래면의 Passivation 에 따른 GFETs 의 전기적 특성 변화에 초점을 맞추어 실험을 진행하였다. SiO_2 /Si 기판 위에 만들어진 GFETs 의 전기적 특성을 먼저 확인한 후 다양한 고분자 기판에 전사하여 아래면을 Passivation 시킨 효과를 관찰하였고, 만들어진 GFETs 에 다른 고분자물질을 스핀코팅 하여 윗면을 Passivation 시킴으로써 윗면과 아랫면의 Passivation 을 통해 그래핀 소자의 전자이동도나 히스테리시스의 변화를 조사하였다.

P2-Co.419*

Real-time monitoring of rotating molecules on graphene

Jeong Heon Choe, Yangjin Lee, Kwanpyo Kim
Jeong Heon. Choe, Yangjin. Lee, Kwanpyo. Kim
Ulsan National Institute of Science and Technology (UNIST).

Keyword : dynamics behavior of molecules, transmission electron microscopy, graphene, elastic scattering, rotational motion

Low-voltage aberration-corrected transmission electron microscopy (TEM) is applied to monitor rotational motions of nanoscale hydrocarbon molecules on single-layer-graphene sheet. Electron beam of TEM enables us to induce and detect rotational motions of molecules anchored at the graphene membrane. We observe the preferential directions of molecular axis along graphene zigzag or armchair lattice directions. The calculated cross section from elastic scattering with experimental imaging conditions for a given energy transfer to carbon atoms can be utilized to understand the molecular rotational motions.

P2-Co.420*

Enhancement of Spin Hall effect in CVD graphene with adaotms and selective metal pad

Park Jungmin, Mi-Jin, Yun Hyungduk, Jo Junhyeon, Vijayakumar Modepalli, Kwon Soon Yong, Yoo Jung-Woo
jungmin. Park, Mi-Jin. Jin, Hyungduk. Yun, Junhyeon. Jo, Modepalli. Vijayakumar, Soon Yong. Kwon, Jung-Woo. Yoo
UNIST.

Keyword : graphene, spin hall effect, spin current, spin orbit interaction

Graphene has attracted enormous interest because the its electric band structure with linear dispersion at K and K' point of the first Brillouin zone has led to the observation of unique electronic transport properties. This 2-dimensional graphene is also considered as a promising spin channel material for spintonics application for spin field effect transistor and spin logic device because graphene is theoretically expected to have long spin diffusion length with large spin life time arising from weak intrinsic spin-orbit interaction (SOI) and the low atomic number of carbon atoms. Incorporation of SOI into graphene can lead to many interesting phenomena; such as spin and anomalous Hall effect, topological quantum spin Hall effect. Several methods for strong SOI can be used such as extrinsic effect of adatoms and substrate. In this study, we have fabricated graphene H bar devices, which have width 5 nm and length of 1.5,2,3 μm. Then, we introduced doping of Au atoms and selective Au pad in CVD graphene via thermal deposition in order to implement extrinsic SOI. Nonlocal I-V signal have increased in the following order; pristine, Au adatoms and pad CVD graphene.

P2-Co.421*

Diffusion of oxygen in graphene and bilayer graphene

*이세호, 김현중 [1], 조준형
*Seho. Yi, Hyun-Jung. Kim[1], Jun Hyung. Cho
한양대학교. [1] 고등과학원.

Keyword : atomic diffusion, surface diffusion

Using first-principles density functional theory calculations, we investigate the diffusions of oxygen and fluorine either adsorbed on the surface of single layer graphene or between the layers of AB stacked bilayer graphene. We found that the two atoms exhibit the drastically different diffusion behaviors. The diffusion barrier of fluorine from the top to neighboring top sites in bilayer graphene is found to be smaller than the corresponding one on a single-layer graphene by about 20%, leading to an easy mobility between two graphene layers. On the other hand, in the case of oxygen, the mobility on a single-layer graphene is significantly larger than that between two graphene layers. We find that the oxygen atom is trapped around the TT site (on top site of the lower layer and top site of the upper layer) in bilayer graphene because (i) the energy barrier from the bridge site in the lower (upper) graphene layer to the bridge site in the upper (lower) graphene layer is much smaller than that from the bridge to the bridge site in the same layer and (ii) the oxygen adsorbs on the bridge site.

P2-Co.422*

Charge transport through the contacts of metal-MoS_2 heterojunctions : an ab-initio study

*심윤수, 김성식 [1], 김효석 [1], 김용훈
*Yoon su. Shim, Seongsik. Kim[1], Hyo Seok. Kim[1], Yong-Hoon. Kim
한국과학기술원. [1]KAIST.

Keyword : Density functional theory, NEGF, Molybdenum didulfide, contact

Molybdenum disulfide has been emerging as an excellent candidate for the channel material of future electronic device due to the superb direct band gap of 1.9 eV in their monolayer region. Using the first-principles calculations, we study the structural, electronic, and charge transport properties of the monolayer 2H-, 1T-MoS_2 and their junction geometries with metal electrodes.We investigate the nature of metal-MoS_2 interface, especially in the cases of edge- and side-contact, and why the contact of two phases of MoS_2 enhances the contact resistance between channel and metal lead region.We find that the charge injection is dominant in side contact rather than edge contact.We also find that homojunction with 1T- and 2H- MoS_2 makes better charge injection than 2H- MoS_2 channel.

P2-Co.423*

Atomic scale analysis of few-layer black phosphorus and related nanostructures

Yangjin Lee, Jun-Yeong Yoon, Hu Young Jeong, Kwanpyo Kim
Yangjin. Lee, Jun-Yeong. Yoon, Hu Young. Jeong, Kwanpyo. Kim
Ulsan National Institute of Science and Technology (UNIST).

Keyword : Black phosphorus, atomic structure, Transmission electron microscopy, nanoribbon

Black phosphorus (BP) has recently emerged as an alternative 2D semiconductor material owing to its interesting properties such as tunable bandgap (2.0eV for monolayer phosphorene and 0.3eV for bulk BP), high charge carrier mobility, and highly anisotropic electrical and optical properties. To fully understand its structural and electronic properties, the investigation of atomic-scale defects of few-layer BP is necessary. We investigate atomic structures of few-layer BP using aberration corrected transmission electron microscopy (acTEM). The crystal lattice structures at the various crystal zone axes are observed and compared with simulation results. To identify the layer number of BP, we perform image and diffraction simulations, which are compared to observed data. Moreover, we demonstrate that the electron beam can be utilized to form BP nanoribbons with crystalline edge structures.

P2-Co.424*

액정 배향의 텍스쳐 분석을 통한 MoS_2 결정 구조 연구

*황제준, 김종현, 유정선, 김동현
*제준. 황, 종현. 김, 정선. 유, 동현. 김
충남대학교.

Keyword : "액정" "MoS2" "배향" "광학" "편광"

MoS_2 가 소자로써 사용되기 위해서는 대면적으로 좋은 특성을 가져야 한다. 그러므로 결정을 균일하게 성장시키고 그 방향을 확인하는 것이 중요하다. MoS_2 의 결정 방향을 확인하기 위해 STM, TEM 을 주로 이용하는데 측정 방법이 까다롭고 많은 측정 시간이 요구된다. 우리는 MoS_2 의 결정 방향을 대면적에서 빠르게 알기 위해 이 연구를 진행했다. MoS2 위에 액정을 올리고, 액정 배향 텍스쳐를 관찰하고 방향자의 분포를 분석했다. 이 결과를 분석하여 MoS_2 결정 방향을 확인했다.

P2-Co.425*

Raman scattering studies of tungsten disulfide (WS_2) and tungsten diselenide (WSe_2)

*문한결, 김자영, 윤석현
*Han kyoul. Moon, Ja yeong. Kim, Seokhyun. Yoon
이화여자대학교.

Keyword : "Raman scattering spectroscopy","TMDCs","2-D materials"

Since the advent of new fabrication techniques of producing the single- and the multi-layered graphene, large amount of research has also been conducted over other 2-dimensional materials including transition metal dichalcogenide monolayers (TMDCs) such as MoS_2, WS_2, $MoSe_2$, WSe_2, and $MoTe_2$. These materials exhibit not only interesting 2-dimensional physics but also, in principle, can be utilized for semiconductor devices such as transistors, emitters, and detectors because monolayers of these materials have a direct band gap (between ~1.7 eV and 3.0 eV). Moreover, these two-dimensional materials show low losses through the Joule effect due to very high mobility. For example, a field-effect transistor (FET) made of WSe_2 shows the mobility near 500 $cm^2V^{-1}S^{-1}$ for p-type conductivity and also exhibits the high on/off ratio of ~10^8, which make TMDCs even more attractive for applications. In this study, we made WS_2 and WSe_2 samples by exfoliation method. We deposited WS_2 and WSe_2 flakes on Si substrates with a 300 nm SiO_2 layer, and the typical size of thin layer of WS_2 and WSe_2 flakes were about few micrometers. For measuring basic characteristics such as lattice properties and information regarding the electronic band structures of the samples, we performed Raman scattering spectroscopy using four different excitation energies of 457 nm (2.71 eV), 488 nm (2.54 eV), 532 nm (2.33 eV), and 632.8 nm (1.96 eV). We report anomalous phonon behavior that depends on the number of layers and the resonant effect reflecting the underlying electronic band structure.

P2-Co.426*

Ca/Si(111)-2x1 표면에서 Si 원자의 흡착과 확산에 대한 연구

*여강모, 정석민
*Kang mo. Yeo, Suk Min. JEONG
전북대학교.

Keyword : Si(111)-2x1, defect, First principle, direct band gap, solar cell

Si 은 값싸고 넓은 시설기반을 갖추고 있어, 발전산업에서 태양광소자의 주 원료로 널리 사용된다. 하지만 Si 은 간접 띠틈을 가지고 있기 때문에 직접 띠틈을 가지는 반도체 물질에 비해 광 흡수 효율이 떨어진다. 최근에는 이러한 간접 띠틈을 가지는 Si 을 결함을 이용해 직접 띠틈으로 바꿔 광 효율을 높이려는 시도가 있다. 올해 초에 Si 단결정에 [111]방향으로 Seiwatz-chain 형태의 결함이 있다면 직접 띠틈이 생길 것 이라고 이론적으로 예상했고, 제작방법으로 Ca/Si(111)과 Si(111)표면을 접합 후 가열을 통해 Ca 을 빼내는 방법을 제시했다[1]. 본 연구에서는 이 제작방법 외에 Ca/Si(111)-2x1 표면에서[2] 에피성장으로 결함이 유지된 Si 단결정 형성가능성을 제일원리 계산을 통해 연구 했다. 제일원리 계산방법으로는 VASP(Vienna Ab-initio Simulation Package)를 이용하였다. Si 원자 한 개, 두 개, 세 개가 흡착될 경우 원자당 흡착에너지는 각각 3.73eV, 3.73eV, 3.91eV 였다. 따라서 Si 원자는 무리형태로 흡착될 것으로 예상되어 결함을 유지하며 단결정으로 성장하기는 어려울 것으로 보인다.

[1] Young Jun Oh et al., arXiv:1504.04134 (2015)
[2] Sukmin Jeong et al., Phys. Rev. B 72, 193309 (2005)

P2-Co.427*

In-situ coherent x-ray diffractive imaging (CXDI) study of oxidation process of Ni nano crystals

*김준형, 김윤희 [1], 김찬 [1], 노도영 [1]
*JUNHYEONG. Kim, Yoonhee. Kim[1], Chan. Kim[1], Do Young. NOH[1]
광주과기원. [1] 광주과학기술원.

Keyword : Coherent X-ray diffractive imaging, Oxidation, Nickel

We visualized oxide formation on a Ni nanocrystal using coherent x-ray diffraction imaging (CXDI) performed at the beamline 9C at Pohang Light Source (PLS)-II. Reconstructed images of an oxidized Ni particle exhibited oxide crust with much less density than Ni. The image reconstruction was conducted using the guided hybrid input and output algorithm (GHIO), which provided quantitative electron density in the Ni oxide with a resolution about 15 nm. We anticipate that our achievement could contribute to the understanding of oxidation process of nickel, which can be critical in the applications for storage devices, batteries, and catalysts.

P2-Co.428*

Internal deformation field distribution in Pt nanoparticles during catalytic process by coherent X-ray diffraction

Jerome Carnis, *김동진, 강진백, 정명우, 차원석 [1], Alexey Zozulya[2], 유병하 [3], 류도형 [3], Ross J. Harder[4], Michael Sprung[2], 김현정
Jerome. Carnis, *Dong jin. Kim, Jinback. Kang, Myungwoo. Chung, Wonsuk. Cha[1], Alexey. Zozulya[2], B.-H. You[3], Do Hyung. Ryu[3], Ross. Harder[4], Michael. Sprung[2], Hyunjung. KIM
서강대학교. [1]Argonne National Laboratory. USA. [2]PETRA III. Deutsches Elektronen-Synchrotron. Germany. [3] 서울과학기술대학교. [4]Advanced Photon Source. Argonne National Laboratory. USA.

Keyword : Catalysis , Platinum , Deformation , Nanoparticle , Coherent X-ray Diffraction

Catalysis plays a vital role in every aspect of modern life. Along with new ways of controlling the sizes and compositions of catalytic materials, understanding the mechanisms during catalysis in-situ and its kinetics are scientifically important. Platinum is widely used as catalytic converter in vehicle control devices where it contributes to the catalytic oxidation of unburned hydrocarbons. In this study we employ the coherent X-ray diffraction imaging to obtain the shape of the nanoparticles and the components of the crystal lattice displacement and strain perpendicular to crystal facets along the catalytic process. Our results show for the first time that the strain generated by the heterogeneous catalytic oxidation of methane on platinum single crystal propagates through the entire crystal lattice.

This research was supported by the National Research Foundation of Korea and ICT ＆ Future Planning of Korea (Nos. NRF-2015R1A5A1009962 , NRF-2014R1A2A1A10052454)

P2-Co.429*

방사광 분광법을 이용한 프러시안 블루유사계 $Rb_xBa_yMn_{[3-(x+2y)]/2}[Fe(CN)_6].zH_2O$ 의 전자 구조 연구

*이은숙, 김대현, 김현우, S.M. Yusuf[1], 김재영 [2], 강정수
*Eun Sook. Lee, Dae hyun. Kim, Kim Hyun Woo. , S.M.. Yusuf[1], Jae-Young Kim. [2], KANG Jeongsoo.
가톨릭대학교. [1]Bhabha Atomic Research Centre. [2] 포항가속기연구소.

Keyword : "Prussian blue", "nano particle", "XAS", "XMCD"

$A_nM_x\{M'(CN)_6\}_y\cdot zH_2O$ (M, M' : 전이금속 원소, A: 알칼리 금속 원소)형의 프러시안 블루(Prussian Blue analogues : PBAs)는 여러 가지 재미있는 물성을 나타내는 물질이다. 프러시안 블루 유사계 물질의 가장 대표적인 특징으로 빛에 유발된 스핀 전이 (photo-induced spin transition) 현상을 보인다는 것이다[1]. RbMn[Fe(CN)6]·zH2O 프러시안 블루는 225 K 와 300 K 에서 자기 상태 변화(magnetic phase transition)를 보이는데, 이 때 자기 상태 변화는 구조 변화를 동반한다. 높은 온도 (HT)의 원자가 및 스핀 상태는 Mn^{2+}(S=5/2)와 Fe^{3+}(S=1/2)이고, 낮은 온도 (LT)에서는 Mn^{3+}(S=2), Fe^{2+}(S=0)가 된다고 알려져 있다[2]. 또한 전이금속 원소인 M, M'에 다른 전이금속 원소를 치환해도 기본적인 결정 구조는 변화가 없다고 알려져 있으며, 시아나이드 리간드 (cyanide ligand)를 가지고 있어서 효과적인 자기 교환(magnetic exchange)이 가능하다고 알려져 있다[3]. 즉, 금속이온과 ligand 사이의 전자 이동이 용이하다. 이 연구에서는 연 x-선 흡수 분광법 (soft x-ray absorption spectroscopy: XAS)과 연 x-선 자기 원편광 이색성 (X-ray magnetic circular dichroism : XMCD)의 방사광 분광법을 이용하여 $Rb_xBa_yMn_{[3-(x+2y)]/2}[Fe(CN)_6]\cdot zH_2O$ (x, y)=(0.19, 0.3), (0.69, 0.19, 0.84, 0) 의 원자가 및 스핀 상태를 연구하였다. T=300 K 에서 측정했을 때, XAS 는 Fe 는 Fe^{2+}와 Fe^{3+}가 섞여 있지만 대체로 Fe^{3+}를 보이고, Mn 은 거의 Mn^{2+}로 관찰되었다. 또한 XMCD 는 Fe 는 거의 0 으로 XMCD 가 보이지 않았고, Mn 은 main peak 에서 negative 를 보였다. 마지막으로 빛에 시료를 노출시켜 노출 시간에 따른 전자 구조 변화를 연구하였는데, 노출시간에 따라 Fe 2p XAS 에 의하면 Fe 이온은 Fe3+에서 Fe2+로 점점 변하며, Mn 2p, O 1s, N 1s XAS 에서도 약하지만 변화가 일어나는 것을 관찰할 수 있었다.

[1] O. Sato, et al., Science 272, 704 (1996)
[2] Thakur et al., JAP 111, 063908 (2012)
[3] Thakur et al., Phys. Chem. Chem. Phys. 12, 12208 (2010)

P2-Co.430*

Photon energy dependent study of circular dichroism in angle-resolved photoemission spectroscopy on Au(111)

*유한영, 김범영 [1], 조수현 [1], Shoresh Soltani[1], Timur Kim[2], 김창영
*HAN YOUNG. YOO, BEOM YOUNG. KIM[1], SOOHYUN. CHO[1], Shoresh. Soltani[1], Timur. Kim[2], Changyoung. Kim
Seoul national university. [1]Yonsei university. [2]DIAMOND light source.

Keyword : ARPES, Circular dichroism, Au(111)

Circular dichroism in angle-resolved photoemission spectroscopy (CD-ARPES) is considered as useful tool for studying the electronic structure of material. However, there are controversies about interpretation of CD-ARPES. We performed CD-ARPES with varying incident photon energy ranging from 20eV to 100eV on surface state of Au(111), which is well known for showing Rashba-type spin splitting surface state. Our experimental data show variations of dichroism magnitude as varying incident photon energy. Analysis of dichroic signal from Au(111) surface state supports that CD-ARPES can observe orbital angular momentum(OAM) texture of initial state rather than spin texture.

P2-Co.501

First principles study on H_2S and $MoCl_5$ adsorption processes on (0001) SiO_2 surfaces

*김혜정, 신영한
*Hye Jung. Kim, Young-Han. Shin
울산대학교.

Keyword : Density functional theory, MoS_2 growth mechanism

Monolayer molybdenum disulfide (MoS_2), which has a finite direct band gap, high electron mobility and so on, is one of interesting two-dimensional (2D) layered materials, having potential applications in flexible electronic, optoelectronic, and photonic devices. Among the experimental growth methods of the 2D materials, the atomic layer deposition (ALD) has recently received much attention due to its ability to control the number of atomic layers during the growth process.

Using density functional calculations, we have studied MoS_2 growth process with ALD on two different O-terminated SiO_2 (0001) surfaces. Through the calculation of monolayer MoS_2 on the SiO_2 surfaces, we examine the most stable stacking pattern between a MoS_2 monolayer and a SiO_2 substate, and investigate the chemical adsorption pathway by comparing the energy barriers when $MoCl_5$ and H_2S approach to SiO_2 substrates alternatively.

P2-Co.502

Synthesis of epi-VO_2 films on AlN/Si (111) substrate

*테티아나, 조진철 [1], 김현탁
*Tetiana. Slusar, Jin-cheol. Cho[1], Hyun-tak. Kim
ETRI. [1]ETRI/UST.

Keyword : IMT, MIT, VO_2, Silicon

Vanadium dioxide (VO_2), a fascinating transition metal oxide with strongly correlated electrons, undergoes a first order insulator-to-metal transition (IMT) at a temperature of ~ 340 K with abrupt changes in its electrical and optical properties. These specifics make VO_2 a promising material for applications, in particular, in the electronic industry. However, important prerequisites for the widespread usage is its superior quality, reliability, compact size and integration with existing Si-based technology.

In this work we propose a new type of VO_2/AlN/Si heterostructures with the nanothick VO_2 films grown on purchased AlN/Si template, where ~ 200 nm thick epitaxial insulating AlN was used as a buffer layer between the film and Si (111) substrate. The samples were subjected to the appropriate investigations of their stoichiometry, structural and electrical properties. It is shown that regardless of a large film-substrate lattice mismatch, it is possible to fabricate the high-quality single-phase VO_2 thin films with epitaxial domains providing a significant, up to four orders, changes in the resistivity during IMT (see Fig.). This is an important result toward development and realization of VO_2-on-Si combined technology.

P2-Co.503

Room Temperature Multiferroism in Morphotropic Phase Mixture of $LuFeO_3$ film

*송승우, 한현, 장현명
*Seungwoo. Song, Hyun. Han, Hyun M.. Jang
포항공과대학교.

Keyword : LuFeO3, Multiferroics, Morphotropic phase mixture, Oxide heterostructure

Over the past decade, there has been a resurgence of interest about multiferroic materials driven for application of various electronic devices such as sensors, transducers, memories and spintronics. With tendency to manufacture electronic device smaller, multiferroic materials which have ferroelectricity and ferromagnetism (or antiferromagnetism) both could be remarkable solution for multifunctional device. Recently, Wenbin Wang et al., reported antiferromagnetic order in hexagonal-$LuFeO_3$ (h-LFO) film below T_N=440 K in addition to well-known room temperature ferroelectricity.[1] Moreover, Ujjal Chowdhury et al., reported a very small magnetization induced polarization in orhothormbic-$LuFeO_3$ (o-LFO) which is famous for weak ferromagnetic (WFM) materials.[2] However, unfortunately h-LFO film shows neither considerable magnetoelectric coupling nor net magnetization above room temperature and o-LFO shows too small remnant polarization to be used. Here to solve nonexistent net magnetization in h-LFO to manifest multiferroism above room temperature, we have synthesized orthorhombic-hexagonal morphotropic mixture of LFO film without any complex procedure changing only PLD depositional conditions at one time.

We successfully deposited orthorhombic-hexagonal morphotropic phase mixture of LFO film at higher temperature and higher oxygen partial pressure than those used for deposition of only h-LFO. XRD 2Θ- Θ scan, topographic analysis by AFM and STEM analysis confirmed microstructure of orthorhombic-hexagonal morphotropic phase mixture of LFO film. Finally, we can artificially obtained sufficient polarization (~5 $\mu C/cm^2$) from h-LFO and net magnetization from o-LFO showing enough multiferroism at room temperature. Magnetodielectric coupling coupling measurement shows a little positive magnetoelectric coupling in orthorhombic-hexagonal morphotropic phase mixture of LFO film.

Reference

[1] W. Wang, J. Zhao, W. Wang, Z. Gai, N. Balke, M. Chi, H. N. Lee, W. Tian, L. Zhu, X. Cheng, D. J. Keavney, J. Yi, T. Z. Ward, P. C. Snijders, H. M. Christen, W. Wu, J. Shen, X. Xu, Phys. Rev. Lett. 2013, 110, 237601.
[2] U. Chowdhury, S. Goswami, D. Bhattacharya, J. Ghosh, S. Basu, S. Neogi, Appl. Phys. Lett. 2014, 105, 052911.

P2-Co.504*

Structural and Orbital Conditions for Giant Spin-Splitting in Solids and Nanostructures

Sehoon Oh, Hyoung Joon Choi
Sehoon. Oh, Hyoung Joon. Choi
Department of Physics and IPAP. Yonsei University.

Keyword : spin-orbit coupling, orbital angular momentum, transition dichalcogenides, nanostructure

Giant spin-splitting of electronic bands, several orders of magnitude greater than Rashba splitting, has been observed in noble metal surfaces, transition-metal dichalcogenides (TMDC) materials thin films, and others. Here, we study structural and orbital conditions for the emergence of giant spin-splitting by using tight-binding and first-principles calculations. We find that broken mirror symmetry of local atomic structure around an atom can produce non-zero inter-atomic hopping matrix elements between different orbitals. These matrix elements produce non-zero orbital angular momentum (OAM) at the atom. The OAM results in the giant spin-splitting if the atom is a high-atomic number element. We demonstrate these structural and orbital conditions in the cases of simple atomic chains, WSe_2 monolayer, Au(111) surface, and bulk HgTe. Based on the mechanism of the spin-splitting, we suggest methods to control the magnitude and direction of spins, which can be used in applications such as spintronic devices. This work was supported by NRF of KOREA (Grant No. 2011-0018306) and KISTI supercomputing center (Project No. KSC-2014-C3-070).

P2-Co.505*

Raman characteristic of WSe_2 films with various thicknesses on sapphire

*장영준, 강건희, 최병기, 김지호, 양승준
*Young Jun. Chang, Kun hee. Kang, Byoung Ki. Choi, Ji Ho. Kim, Seung Jun. Yang
서울시립대학교.

Keyword : Raman spectroscopy, WSe_2

Raman spectroscopy is widely used to non-destructively check crystallinity and film thickness of transition metal dichalcogenides (TMDs) [1]. Using 514.5 nm laser, we studied Raman peak shift of WSe_2 thin films in wide range of thickness and growth conditions, which are not reported yet [2-3]. We prepared WSe_2 by selenization of WO_3 films with controlled thickness. We could map Raman peak intensities (E^1_{2g}, A_{1g}, and 2LA) and their ratio as a function of growth temperature and hydrogen gas ratio. For the case of WSe_2 made from 1 nm-thick WO_3 films, we note that WSe_2 shows the biggest at selected growth conditions (working pressure of 9 Torr, growth temperature of 875°C, and H_2 gas ratio of 15%). In addition, when we increase film thickness, the Raman peak shows both energy shift and peak intensity ratio change [4]. We further discuss additional measurements, such as x-ray diffraction and optical spectroscopy. [NRF-2014R1A1A1002868]

[1] C. Lee, H. Yan, L. E. Brus, T. F. Heinz, J. Hone, and S. Ryu, ACS nano, 4, 2695 (2010).
[2] E. del Corro, H. Terrones, A. Elias, C. Fantini, S. Feng, M. A. Nguyen, T. E. Mallouk, M. Terrones, and M. A. Pimenta, ACS Nano 8, 9629 (2014).
[3] H. Li, G. Lu, Y. Wang, Z. Yin, C. Cong, Q. He, L. Wang, F. Ding, T. Yu, and H. Zhang, Small 9, 1974 (2013).
[4] K.H. Kang, B.K. Choi, J.H. Kim, and Y.J. Chang, New Physics: Sae Mulli, 65, 633 (2015)

P2-Co.506*

Transport and thermoelectric properties of $SnSe_2$ grown by hot pressure method

*웬반쾅, 드엉안투안, 두엉반티엣, 송재용 [1], 박현민 [1], 조성래
*Nguyen Van. Quang, Duong Anh. Tuan, Duong Van. Thiet, JAE YONG. SONG[1], Huyn min. park[1], Sunglae. CHO
울산대학교. [1] 한국표준과학연구원.

Keyword : thermoelectric, 2D material, SnSe2, hot pressure

Recently, SnSe has been reported as ultralow thermal conductivity material which make it become a very high thermoelectric fingure of merit ZT material, up to 2.6 at 923 K. But, it is hard to use SnSe for applications in high temperature range because SnSe decomposes at 700 K. Therefore, searching for crystalline materials with high ZT value at lower temperature is still an attracted field of research. $SnSe_2$ is also 2D material which is expected to have low lattice thermal conductivity. However, less is known about thermoelectric property of $SnSe_2$. Eutectic $SnSe_2$-Bi_2Se_3 was repoted as a promsising low-temperature thermoelectric material with ZT=0.56 at 593 K. Here, we prepared the polycrystalline $SnSe_2$ by hot pressure method. At temperature range up to 573 K, it exhibit the anisotropic n-type charge carrier. The maximum ZT was 0.045 at 573 K, and increased with temperature. Interestingly, the non-magnetic materials $SnSe_2$ become magnetic at below 60 K without any insertion of magnetic impurities. A negative magnetoresistance (MR) was observed. The reasons of the observations will be discussed.

P2-Co.507*

Growth and thermoelectric properties of p-type layered GaTe single crystals

*부티호아, 조성래, 송재용 [1], 현 민 박 [1], 웬반쾅, 드엉안투안
*Vu Thi. Hoa, Sunglae. CHO, JAE YONG. SONG[1], Hyun-Min. Park[1], Nguyen Van. Quang, Duong Anh. Tuan
울산대학교. [1] 한국표준과학연구원.

Keyword : Gallium Telluride, thermoelectric properties, single crystal, Bridgman method, chalcogenide crystal

Gallium Telluride (GaTe) crystal is a member of chalcogenide crystal family as GaSe, GaS, InSe, InTe. Band gap energy of GaTe bulk crystal at room temperature which is suitable for room temperature x-ray and gamma–ray radiation detector applications and solar cells is about 1.7 eV [1]. GaTe was interesting because of its attractive electrical, optical and thermoelectric properties. However, due to the difficulty in growth of large-size high quality crystals, it is one of the less investigated materials. In this study, we reported on the crystal structure and thermoelectric properties of p-type GaTe single crystals. The sample was obtained by the modified vertical Bridgman method. The single crystal structure was determinded by XRD and FE-SEM measurement. Thermoelectric and transport properties both along and perpendicular to the layered planes were evaluated in the temperature range from 20 to 400K. Power factor of p-type GaTe increased with temperature and was 0.33 $mWcm^{-1}K^{-2}$ at 400K.We expect higher power factor at high temperature range.

Reference:

[1] O.A. Balitskii, B.Jaeckel, W. Jaegermann, Physics letters A 372 (2008) 3303-3306.

P2-Co.508*

Thermoelectric transport properties of bulk In_2Se_3 single crystal

조성래, 박 현민 [1], 송재용 [1], 웬반쾅, 두엉반티엣, 드엉안투안, *웬티흐엉
Sunglae. CHO, Hyun-Min. Park[1], JAE YONG. SONG[1], Nguyen Van. Quang, Duong Van. Thiet, Duong Anh. Tuan, *Nguyen Thi. Huong
울산대학교. [1] 한국표준과학연구원.

Keyword : 2D materials, In_2Se_3, single crystal, thermoelctric

Good thermoelectric materials should possess a combination of seemingly incompatible properties such as high electricalconductivity σ, high Seebeck coefficient S, and low lattice thermal conductivityk to achieve high thermoelectric figure of merit (ZT) value, which is calculated by $ZT=S^2\sigma T/k$. However, it is still a difficult mission because of strong coupling between these parameters each other. Recently, researchers focused on 2D materials which may be a good candidate due to its low lattice thermal conductivity. Members of III-VI layered structure compoundssuch as Ga_2Se_3 and Ga_2Te_3, In_2Se_3 could be interesting layered semiconductors for thermoelectric applications. In this study, we report on the transport and thermoelectric properties of In_2Se_3 single crystal. The layered crystal structure of In_2Se_3 was determined by XRD and FE-SEM measurements. Ellipsometry measurement illustratedthe indirect band gap of In_2Se_3, about 1.61 eV. Transport properties have been studied in the temperature range from 20 to 400 K along axis which is parallel to the layers direction. Interestingly, Seebeck coefficient was n-type and increased with temperature and the electrical conductivity increased with temperature. Therefore, power factor increased up to 2.69 $\mu Wcm^{-1}K^{-2}$ at 400 K. In this talk, we will discuss more on transport properties.

P2-Co.509*

Two-dimensional electron gas models in a honeycomb lattice with generalized low energy band chirality

*박영주, 한문섭, 정재일
*Youngju. Park, Moonsup. Han, Jeil. Jung
서울시립대학교.

Keyword : Graphene, bilayer graphene, chirality, topological phase, tight-binding

We present models of 2DEG with generalized band chirality that can be devised in a honeycomb lattice through a suitable choice of distant tight-binding hopping parameters that cancel the leading k-dependent power expansion terms in the low energy sector. This procedure allows to find an accurate representation of the Bernal stacked bilayer graphene near the Dirac points that possess a chirality index of two and a quadratic dispersion near the Fermi point when we eliminate the leading linear dispersion term. When we tailor a cubic band dispersion we can find a general chirality low energy band Hamiltonian whose chirality index and dispersion power near the K points are different. Our analysis provides a convenient platform for studying the physics of bilayer graphene in a single layer honeycomb lattice and can find applications in tailoring the band structure of cold atom optical lattices.

P2-Co.510*

Growth and thermoelectric properties of $SnSe_2$ single crystal grown by Bridgman method

*팜안투안, 웬반쾅, 드엉안투안, 두엉반티엣, 조성래
*Pham Anh Tuan. , Nguyen Van Quang. , Duong Anh Tuan. , Duong Van Thiet. , CHO Sunglae.
울산대학교.

Keyword : Tin diselenide, Bridgman method, Thermoelectric properties, Single crystal, 2D materials

The research for new efficient thermoelectric materials is very important in the development of alternative power generation technologies. The conversion efficiency of a thermoelectric material is related to the dimensionless figure of merit, $ZT= \alpha^2\sigma T/k$, where the $\alpha^2\sigma$ product is the thermoelectric power factor ($W/(mK^2)$) and T is the absolute temperature. The two-dimensional (2D) material, made up of layers of crystal, has unique properties that intensify electrical conductivity and decrease thermal conductivity. The tin diselenide ($SnSe_2$) is also one of promising 2D thermoelectric materials. $SnSe_2$ structure belongs to the hexagonal CdI_2-type lattice with band gap energy of about 1.01 eV. Single crystals $SnSe_2$ have been grown by vertical Bridgman technique. The confirmation of single crystallinity and composition determination of the grown crystals have been made by using EPMA Quantitative Analysis and X-ray diffraction techniques, respectively. The layered structure was observed via FE-SEM images. Seebeck coefficient, electrical conductivity and thermal conductivity were evaluated by transport properties measurement system (TPMS). At temperature range up to 520 K, it exhibit the anisotropic n-type charge carrier. The maximum ZT was 0.078 at 520 K. Specific results will be discussed.

P2-Co.511*

Growth and characterization of GaSe single crystal

*웬티탄흐엉, 웬반쾅, 드엉안투안, 조성래, 송재용 [1], 현 민 박 [1]
*Nguyen Thi Thanh Huong. , Nguyen Van Quang. , Duong Anh Tuan. , Sunglae. CHO, .JAE YONG. SONG[1], Hyun-Min. Park[1]
울산대학교. [1] *한국표준과학연구원.*

Keyword : Bridgman, GaSe, single crystal, EPMA, layer

Like other two dimensional semiconductor material in III - VI compounds group (GaTe, In_2Se_3), Gallium Selenide (GaSe) appears to be a promising candidate material for thermoelectric applications with high beta SE index. In this work, the GaSe single crystal was grown from the high purity Ga and Se by vertical Bridgman method. The grown crystal can be cleaved in layer by layer without difficulty, confirmed the layered structure of GaSe. Meanwhile, the X-ray diffraction (XRD) result indicates the crystalline perfection of the grown single crystal as a hexagonal structure. The compositional and optical properties of sample have also been investigated by Electron probe micro-analyzer and UV-visible spectroscopy techniques, respectively. The absorption spectra analysis revealed the energy band gap of 1.85 eV, which is comparable to the reference value of 2.03 eV.

P2-Co.512*

Far infrared properties of CVD graphene

*정일호, 황정식, 강대준
*Eilho. Jung, Jungseek. Hwang, Daejoon. Kang
Sungkyunkwan University.

Keyword : CVD Graphene, Far-IR, FTIR

We investigated multilayer graphene samples with different number of layers from 1 to 12 on Si-substrate or quartz-substrate using an optical spectroscopy technique. We measured transmittance spectra of our graphene samples in far- and mid-infrared range (50 ~ 7000 cm^{-1}). We obtained the optical conductivity spectra from the measured transmittance using the Tinkham's formula. We focused on charge carrier properties in the graphene samples in the far infrared range. By performing the Drude model fitting we also obtained the plasma frequency and the impurity scattering rate of the charge carriers and the dc conductivity. We will discuss layer number dependent transport properties of charge carriers.

P2-Co.513*

Electronic and Magnetic Phase Transitions in $SrRu_{1-x}Ir_xO_3$ Thin Films

*비스워스, 이용우, 정윤희 [1]
*Abhijit. Biswas, Yong Woo. Lee, Yoon Hee. Jeong[1]
POSTECH. [1] 포항공과대학교.

Keyword : Iridates, MIT, Non-Fermi liquid, Spin-glass, Localization

We have investigated the nature of transport and magnetic properties in $SrIr_{0.5}Ru_{0.5}O_3$, which falls in the intermediate region of correlated non-Fermi liquid state ($SrIrO_3$) and of an itinerant Fermi liquid state ($SrRuO_3$), by growing perovskite thin films on various substrates (e.g. $SrTiO_3$ (001), LSAT (001) and $LaAlO_3$ (001)). We observed systematic variation of underlying substrate dependent metal-to-insulator transition temperatures in resistivity. In the metallic side, resistivity shows $T^{3/2}$ power law dependence whereas insulating nature below T_{MIT} originates from localization effect. Magnetoresistance (MR) shows negative signature at low temperature and switches from negative to positive while increasing temperature, with negative MR μ and positive MR μ B^2; consistent with the localized to normal metal crossover dynamics. Furthermore, we observed spin-glass-like (T_{SG}) behavior of $SrIr_{0.5}Ru_{0.5}O_3$ on $SrTiO_3$ (001) at T_{SG}～ 25 K in the localized regime [1].
In the itinerant site, substituting Ir ($5d^{5+}$) for Ru ($4d^{4+}$) in $SrRuO_3$, films ($0.0 \leq x \leq 0.20$) showed fully-metallic behavior and ferromagnetic ordering, although resistivity (ρ) increased and the ferromagnetic T_C decreased. Films with x = 0.25 underwent the metal-to-insulator transition and spin-glass-like ordering (T_{SG}～45 K) with the elimination of ferromagnetic long-range ordering caused by the electron localization at the substitution sites. In ferromagnetic films ($0.0 \leq x \leq 0.20$), r increased near-linearly with T at $T > T_C$, but in paramagnetic film (x = 0.25) r increased as $T^{3/2}$ at $T > T_{MIT}$. Moreover, observed spin-glass-like (T_{SG}) ordering with the negative magnetoresistance at $T < T_{MIT}$ in film with x = 0.25; validates the hypothesis that (Anderson) localization favors glassy ordering at amply disorder limit. These observations provide a promising approach for future applications and of fundamental interest in 4d and 5d mixed perovskites thin films [2].

References:
[1] A. Biswas, Y. W. Lee, S. W. Kim, and Y. H. Jeong, J. Appl. Phys. 117, 115304 (2015).
[2] A. Biswas, Y. W. Lee, and Y. H. Jeong, accepted in J. Appl. Phys. 118, xxxxxx (2015).

P2-Co.514*

Highly anisotropic magnetism in Sr_2IrO_4 single crystals under the high magnetic field

*홍윤정, 최환영 [1], 이나라 [1], 최영재 [1], 강원 [2], 조연정
*Yun Jeong. Hong, Hwan Young. Choi[1], Nara. Lee[1], Y.J.. Choi[1], Woun. KANG[2], Youn Jung. Jo
경북대학교. [1] 연세대학교. [2] 이화여자대학교.

Keyword : "spin-orbit coupling", "magnetic anisotropy", "torque magnetometry"

Study on the Sr_2IrO_4 has emerged as their fascinating physical properties, such as semiconducting gap in electronic structure and canted antiferromagnetism in magnetic environment. Those exotic behaviors are attributed to the strong spin-orbit coupling. In order to detect magnetic anisotropy between the out-of-plane and the in-plane direction which appears below Neel temperature ($T_N \approx 240$ K), torque magnetometry experiment was performed. We fitted our high field torque data with a modelling equation composed of significant two terms; induced magnetic and canted antiferromagnetic term. The obtained parameters from the fitting indicate the origin of the magnetic anisotropy under the high magnetic field, furthermore, they are closely related to the lattice structure such as Ir-O-Ir bond angles.

P2-Co.515*

Oxygen-concentration dependent structural evolutino in $SrFeO_x$

*노슬기, 아밋 카리, 서유성, 이석배, 최우석, 황정식
*seulki. Roh, Amit. Khare, Yu seong. Seo, Seok Bae. Lee, Woo seok. Choi, Jungseek. Hwang
성균관대학교.

Keyword : Optical spectroscopy, Phonon, Oxide, TMO, MIT

We investigated 18 nm thick $SrFeO_x$ (SFO; x = 2.5 - 3) thin film on $SrTiO_3$ substrate with an optical spectroscopy in a spectral range (50 - 7000 cm^{-1}). The SFO shows two topotactic phases, the brownmillerite (BM) and the perovskite (P) with x = 2.5 and 3, respectively. Moreover, depending on the growth conditions, the direction of the oxygen vacancy channel in brownmillerite phase can be tuned from perpendicular (BM1) to parallel (BM2) to the sample surface. By tuning the direction of the oxygen vacancy channel we can observe phonons which appear in two different orientations. We also observed oxygen-concentration dependent phonon mode evolution. The BM and P samples show different electronic ground states: one is insulating and the other metallic. Our results may provide important information to understand better the role of oxygen in transition metal oxides.

P2-Co.516*

Electronic and phonon properties of $Lu(Pt_{1-x}Pd_x)_2In$

*김희정, 김규, 민병일
*Heejung. Kim, Kyoo. KIM, Byung IL. MIN
포항공과대학교.

Keyword : phonon, charge density wave, supperconductivity

It has been recently observed that $LuPt_2In$, having a simple cubic Heusler-type structure, experiences the anomalies in susceptibility, resistivity, and X-Ray Diffraction experiment below the structural transition temperature T_s=480 K. Further, the transition temperature is observed to be reduced by increasing substitution of Pd for Pt. Interestingly, the superconductivity occurs with increasing Pd composition, which is strongly enhanced at the structural quantum critical point for x~0.55 for $Lu(Pt_{1-x}Pd_x)_2In$.
To explore the underlying mechanism of the structural transition, we have investigated electronic band structure and phonon dispersion of $LuPt_2In$, LuPtPdIn, and $LuPd_2In$, using the ab initio density functional theory. We have found the Fermi surface nesting at the specific q vector in $LuPt_2In$. The Phonon softening instability occurs at the same q vector. This feature suggests that the structural instability of $LuPt_2In$ is driven by the charge density wave through electron-phonon coupling. We have also found that the phonon softening is suppressed by increasing the composition of Pd, as is consistent with experiment.

P2-Co.517*

Magnetic structure of a double perovskite Ba2YIrO6

*공호신, 민병일, 김범현
*Ho shin. Gong, Byung IL. MIN, Beom Hyun. Kim
포항공과대학교.

Keyword : "$5d^4$", "double perovskite", "antiferromagnetic", "Ba2YIrO6", "DFT"

Magnetic structures of double perovskite iridates with $5d^4$ electronic configuration have attracted recent attention.
A non-cubic system Sr2YIrO6 was reported to be antiferromagnetic below 1.3 K, which is expected to be derived from a non-cubic distortion. On the other hand, a cubic system Ba2YIrO6 was also reported to be antiferromagnetic below about 2 K. Because Ba2YIrO6 has the cubic symmetry, one could expect that the magnetic mechanism in Ba2YIrO6 would be different from that in Sr2YIrO6. To explore the magnetic mechanism in Ba2YIrO6, we have investigated electronic and magnetic properties using the DFT calculations. Our study suggests that the molecular bonding effect is as important as the spin-orbit coupling effect in the magnetic ordering.

P2-Co.518*

^{4}He adsorption on ^{3}He-plated graphite

*안정환, 권용경
*Jeong Hwan. Ahn, Yong Kyung. KWON
건국대학교.

Keyword : "helium", "commensurate", "supersolid", "graphite"

Noting that the first ^{3}He layer on graphite is completed at the areal density identical to the 7/12 commensurate density of 0.111 Å^{-2}, we have performed path-integral Monte Carlo calculations for a new configuration of the second layer of ^{4}He atoms on top of the first-layer ^{3}He atoms on graphite. The complete first ^{3}He layer on graphite is found to be a $C_{7/12}$ commensurate solid, which is a result of the simulations starting from initial configuration of ^{3}He atoms randomly distributed far enough from the graphite surface. Additional adsorption of ^{4}He atoms on top of the complete first ^{3}He layer does not disrupt the underlying ^{3}He commensurate structure and the second-layer 4/7 commensurate structure of ^{4}He atoms develops on the ^{3}He solid. Furthermore, this second-layer 4/7 commensurate structure is observed to be formed above a mixture of the first-layer ^{3}He and ^{4}He adatoms on graphite. We also find that the vacancies created in the second-layer ^{4}He 4/7 commensurate structure are mobile, regardless of whether the underlying first layer is made up of only ^{3}He atoms or a mixture of ^{3}He-^{4}He atoms, leading us to conjecture a possible realization of two-dimensional supersolidity.

P2-Co.519*

Infrared Spectroscopic Study of Filling-Controlled Metal-Insulator Transition in $(Sr,La)_3Ir_2O_7$

*안기현, 송승재, Tom Hogan[1], Stephen D. Wilson[1], 문순재
*Gihyeon. Ahn, Seung Jae. Song, Tom. Hogan[1], Stephen. D. Wilson[1], Soonjae. Moon
한양대학교. [1]University of California. Santa Barbara.

Keyword : Ruddlesden-Popper Series Iridates, Infrared Spectroscopy, Filling-Control, Metal-Insulator Transition, Correlated Metal

After the discovery of the J_{eff}=1/2 states in the Ruddlesden-Popper series of 5d iridium oxides $Sr_{n+1}Ir_nO_{3n+1}$, there have been wide interests in their physical properties. Recently, extensive studies have been carried out on the evolution of the J_{eff}=1/2 states of $Sr_3Ir_2O_7$ with electron doping. We investigated the charge dynamics of $(Sr_{1-x}La_x)_3Ir_2O_7$ by using infrared spectroscopy. Upon electron doping, we observed a collapse of the J_{eff}=1/2 Mott gap accompanying the transfer of the spectral weight from high energy region to in-gap region, which is a characteristic feature of correlated electron systems. At x=0.051, a clear Drude-like mode appeared. The extended Drude model analysis on $(Sr_{0.949}La_{0.051})_3Ir_2O_7$ revealed a large mass enhancement for the itinerant carriers, suggesting that it is a correlated metal. Our results indicate that the electronic correlations play important roles in the electrodynamics of electron-doped $Sr_3Ir_2O_7$.

P2-Co.520*

Experimental stabilization of electron-doped $BaBiO_3$ via controlling oxygen non-stoichiometry

*김기덕, 김지현, 김민우, 노태원
*Gideok. Kim, Jeehyn. KIM, Minu. Kim, Tae Won. Noh
서울대학교.

Keyword : charge density wave, real-time ellipsometry, electron-doping, thin film

Experimental stabilization of electron-doped $BaBiO_3$ via controlling oxygen non-stoichiometry

Gideok Kim[1,2], Jeehyun Kim[1,2], Minu Kim[1,2], Tae Won Noh[1,2]
[1]Center for Correlated Electron Systems, Institute for Basic Science, Seoul 151-747, Republic of Korea
[2]Department of Physics and Astronomy, Seoul National University, Seoul 151-747, Republic of Korea
gideokphysics@gmail.com

Perovskite oxide materials have received much attention because of their novel physical properties. One of the most representative phenomena is perhaps high-T_c superconductivity in cuprates, whose superconducting phase diagram has been explored with the insertion of holes or electrons [1]. Superconductivity is observed in both doping regimes, yet the phase diagram is not perfectly symmetric. For example, an antiferromagnetic insulating ground state of an undoped compound is more robust against electron doping. However, apart from cuprates not many high-T_c superconductors had been studied by electron doping [3].

Hole-doped barium bismuthates are known to be the first oxide high-T_c superconductors without copper ion, and also show remarkably high T_c exceeding 30 K [4]. The undoped compound, $BaBiO_3$, is a charge-disproportionation-type charge density wave (CDW) insulator, which is caused by Bi^{4+} valence skipping behavior [5]. Insulator-to-superconductor transition was revealed by chemical substitution that dopes holes . Recently, there are interesting theoretical predictions about a possible topological insulating state in an electron-doped $BaBiO_3$ [6, 7]. However, there has been little experimental report on electron doping in part owing to low feasibility of chemical substitution of electron donors. As an alternative approach, here we examine to utilize oxygen vacancy for electron doping in $BaBiO_3$. Oxygen vacancy is intentionally introduced in epitaxial $BaBiO_3$ thin films by annealing the films under vacuum, and optical spectra are measured simultaneously with real-time spectroscopic ellipsometry. We observed clear suppression of CDW with oxygen vacancy concentration increased. In this presentation, the lattice and electronic structures of oxygen-deficient $BaBiO_3$ observed by x-ray diffraction and photoemission spectroscopy will be discussed in detail.

Reference

[1] E. Dagotto, Rev. Mod. Phys. 66, 763-840 (1994).
[2] C. Weber et al., Nat. Phys. 6, 574-578 (2010).
[3] S. Segawa et al., Nat. Phys. 6, 579-583 (2010).
[4] A. W. Sleight et al., Physica C. 514, 152-165 (2015).
[5] D. E. Cox et al., Solid State Commun. 19, 969 (1976).
[6] H. Jin et al., Sci. Rep. 3, 1651 (2013).
[7] B. Yan et al., Nat. Phys. 9, 709-711 (2013).

P2-Co.521*

Epitaxial growth of MoO_2 thin films

*안은영, 서유성 [1], 황정식 [1], 진형진
*Eun Yung. Ahn, Yu seong. Seo[1], Jungseek. Hwang[1], Hyoungjeen. Jeen
부산대학교. [1] *성균관대학교.*

Keyword : Thin film, complex oxides, x-ray diffraction, energy materials

Molybdenum oxides have various crystal structures and physical properties due to their multiple valance states in the 4d transition metal element. Particularly MoO_2 with distorted rutile structure shows metallic behavior and robust chemical stability, which are promising properties for electrodes in electrochemical devices. Recently, MoO_2 has gotten a lot of attention as a new energy material due to high capacity of Li ions in mesoporous MoO_2 nanostructures. In this presentation, we will show optimal growth condition for epitaxial MoO_2 thin films by RF magnetron sputtering. We used Ar gas partial pressure and substrate temperature as control parameters. To confirm epitaxial growth of MoO_2 thin films and determine their crystallinity we used high resolution X-ray diffractometer (HR-XRD). After the optimization, electronic and optical properties of the optimized MoO_2 thin film were probed by spectroscopic ellipsometry and temperature dependent transport measurements.

P2-Co.522*

Solving the Hubbard Model Using DMFT with CTQMC

*고범준, 심지훈
*Beomjoon. Goh, Ji Hoon. Shim
포항공과대학교.

Keyword : QMC, impurity solver, DMFT, Hubbard

We developed the continuous-time quantum Monte Calro (CTQMC) impurity solver for the dynamical mean field theory(DMFT) and used it to reproduce the metal-insulator transition(MIT) of the 3-dimensional cubic 1-band Hubbard model successively. The impurity solver adopted the hybridisation expansion representation considering density-density interactions (segment representation). Currently the dimensional analysis is being carried out to monitor how the DMFT describes low dimensional strongly correlated systems by continuously reducing dimension 3 to 2. Further, the calculation method could be easily extended to handle multi-orbital systems, to the cluster type DMFT or to the non equilibrium DMFT. We are currently developing a new scheme beyond the conventional DMFT to include nonlocal effects of the Coulomb interaction.

P2-Co.523*

Strain engineering of heteroepitaxial lanthanum manganite thin films

*김용진, 이진홍, 송종현 [1], 구태영 [2], 양찬호
*Yong-Jin. Kim, Jin Hong. Lee, Jong Hyun. Song[1], Tae Yeong. Koo[2], Chan-Ho. Yang
KAIST. [1] 충남대학교. [2] 포항가속기연구소.

Keyword : $LaMnO_3$, Strain engineering, Resonant x-ray scattering, Resistivity

Strain engineering which controls the misfit strain of heteroepitaxial thin films leads to distinctive physical properties in contrast to the intrinsic properties of unstrained bulk materials [1]. Perovskite $LaMnO_3$ (LMO), the parent compound of colossal magnetoresistance materials, e.g., $La_{1-x}Sr_xMnO_4$, has attracted considerable attention due to strong coupling among the lattice, charge, spin and orbital degrees of freedom [2]. Stoichiometric LMO is known to be an A-type antiferromagnetic (Néel temperature ~ 140 K) Mott insulator, and its orbital ordering is established due to cooperative Jahn-Teller distortion below ~750 K [3]. However, the synthesis of stoichiometric LMO thin films has been difficult due to undesired defects (cation or oxygen vacancy) which easily appear during the film deposition [4], and non-stoichiometric LMO films would exhibit ferromagnetism and electronic conduction [5]. Our goal is to obtain epitaxial stoichiometric LMO thin films and investigate their strain-dependent physical properties. We have grown LMO thin films on four different substrates, i.e., $DyScO_3$(110), $GaScO_3$(110), $SrTiO_3$(001), and LSAT(001), using the pulsed laser deposition technique. The films have been characterized by atomic force microscopy and x-ray diffraction. Resistivity measurements have shown insulating behavior and negative magnetoresistance up to 30%. We have performed resonant x-ray scattering on each film and figured out that resonant behaviors can be modulated depending on misfit strain. Our observations will be a base for future studies of the strain dependence of LMO.

[1] K. J. Choi et al. Science 306, 1005–1009 (2004).
[2] Y. Tokura et al., Science 288, 462 (2000).
[3] Y. Murakami et al., Phys. Rev. Lett. 81, 582(1998).
[4] W. S. Choi et al., Korean Phys. Soc. 58, 569 (2011).
[5] P. Orgiani et al., Appl. Phys. Lett. 95, 013510 (2009).

P2-Co.524

Epitaxial MBE growth of $MoSe_2$ ultrathin films

최병기, 구민선, 김지호, 박수현 [1], 한문섭, 김민우 [1], *장영준
Byoung-Ki. Choi, Minsun. Goo, Jiho. Kim, Soo-hyun. Phark[1], Moonsup. Han, Minu. Kim[1], *Young Jun. Chang
서울시립대학교. [1] *서울대학교.*

Keyword : Molecular Beam Epitaxy, MoSe2, RHEED, XRD

Layered transition metal dichalcogenides (TMDCs) draw much attention, because of its unique optical properties and band structures depending on the layer thicknesses. We grew epitaxial $MoSe_2$ ultrathin films on both graphene/SiC and sapphire substrate by using molecular beam epitaxy (MBE) and confirm its thickness and crystalline properties using Raman spectra, x-ray diffraction (XRD), and in-situ reflective high energy electron diffraction (RHEED). We also characterize the surface morphology and stoichiometry by using atomic force microscopy (AFM) and x-ray photoemission spectroscopy (XPS). We discuss optimum growth condition by considering thermal stability of chalcogen under various ambient condition. [This research was supported by Nano·Material Technology Development Program through the National Research Foundation of Korea(NRF) funded by the Ministry of Science, ICT and Future Planning.(2009-0082580), NRF-2014R1A1A1002868]

P2-Co.525

Optical properties of g-C_4N_3/BN bilayer film: A first principles study

*손지철, Hashmi Arqum, 홍지상
*Jicheol. Son, Hashmi. Arqum, Jisang. Hong
부경대학교.

Keyword : First principles, g-C_4N_3/BN

Using the first principles method, the frequency dependent dielectric function, refractive index, reflectivity, optical conductivity, loss function, and absorption coefficient of g-C_4N_3/BN bilayer system were explored. Here, the optical properties of electric field polarization dependency were explored as well. Since the dielectric function was strongly dependent on the electric polarization, we obtained an anisotropic optical properties. For instance, the dielectric function was frequency independent regarding the perpendicular electric polarization while a frequency dependent dielectric function was observed. A high refractive index larger than 2 for parallel polarization in the infrared and visible frequency ranges was obtained, whereas a constant refractive index of approximately 1.5 was observed for perpendicular electric field polarization. We found that the electromagnetic wave propagating perpendicular to the film surface had a very small reflectivity in the ultraviolet frequency and this property can be utilized for anti-reflection ultraviolet coating application. In addition, the g-C_4N_3/BN bilayer may produce no meaningful joule heating for in-plan wave propagation because of extremely weak optical conductivity. We propose that the optical phonon can be generated by the incident of ultraviolet wave. Besides, the bilayer system can be transparent in the visible range. Overall, we have found that the metal free transparent half metallic g-C_4N_3 films can be utilized for spintronics and optical device applications. This research was supported by Basic Science Research Program through the National Research Foundation of Korea (NRF) funded by the Ministry of Education, Science and Technology (No. 2013R1A1A2006071) and by the Supercomputing Center/Korea Institute of Science and Technology Information with supercomputing resources including technical support (KSC-2015-C3-021).

P2-Co.526

Implementation of Dynamical Mean Field Theory with Spin-Orbit Coupling

HAN Mancheon, LEE Choong-Ki[1], CHOI Hyoung Joon
Mancheon. HAN, Choong-Ki. LEE[1], Hyoung Joon. CHOI
Department of Physics and IPAP. Yonsei University. [1]Department of Physics. Yonsei University.

Keyword : DMFT,CT-QMC,Monte-Carlo, Spin-Orbit,Iridate

Recently, iridium-based layered oxides such as Sr_2IrO_4 are intensively studied because of cuprate-like properties such as the Fermi arc and the d-wave gap. As these exotic properties come from the $J_{eff} = 1/2$ states induced by the strong spin-orbit coupling and the moderate Coulomb interaction, it is needed to deal with these two effects simultaneously. Practically, this can be done most appropriately by the dynamical mean field theory (DMFT). We have developed a continuous-time quantum monte carlo (CT-QMC) implementation of the dynamical mean field theory and included the spin-orbit coupling effect. We studied three-orbital systems with a semicircular density of states as an illustration. This work is supported by the NRF of Korea (Grant No.2011-0018306). Computational resources have been provided by KISTI Supercomputing Center (Project No. KSC-2014-C3-070).

P2-Co.527

Role of f-orbital occupation for ground states of heavy-fermion antiferromagnet $CeNMSb_2$ (NM = Cu and Au).

*장재경, 이주열 [1]
*Jae Kyung. JANG, Joo Yull. RHEE[1]
물리학과/성균관대학교. [1] *성균관대학교.*

Keyword : "electronic structures", "heavy-fermion", "spin-orbit coupling", "magnetic easy axis"

We investigated the electronic structures of antiferromagnetic $CeNMSb_2$ (NM = Cu and Au) by using the full-potential linearized-augmented-plane-wave method. Total-energy differences show that it is necessary to include both spin-orbit coupling (SOC) and the so-called LDA + U method, as well as the spin-polarized calculation, to predict correct magnetic easy axis for AFM $CeNMSb_2$ compounds. Spin-density plots, the density of states and SOC energy calculated by using matrix elements of f-orbitals indicate the effects of SOC of Ce atom, especially the Ce 4f electrons, play a crucial role to determine the magnetic easy axes of these systems. The on-site Coulomb interaction of Ce atom is also very important. Different occupations of f-orbitals in $CeCuSb_2$ and $CeAuSb_2$ lead to different ground states.

P2-Co.528

The electronic structure of $PdTe_2$ measured by angle-resolved photoemission spectroscopy

김은아, 정진원, 문현숙, *노한진
Euna. Kim, Jinwon. Jeong, Hyun Sook. Moon, *Han-Jin. Noh
전남대학교.

Keyword : PdTe2, ARPES, electronic structure, LMTO, topological insulator

We report the electronic structure of $PdTe_2$ measured by angle-resolved photoemission spectroscopy. The Fermi surface of the system has quite a complex shape of electron pockets and hole pockets, mosts of which are consistent with a band calculation performed by an LMTO method.[1] However, there are noticeable differences, also. In the presentaion, those differences will be discussed in terms of the topological properties of this system.

[1] J-P Jan and H L Skriver, J. Phys. F 7, 1719 (1977).

P2-Co.529

Cubic anvil press for investigations of matter under uniform, high pressure up to 10 GPa

*장동현, Keizo Murata, 김기훈
*Dong Hyun. Jang, Keizo. Murata, Kee Hoon. Kim
서울대학교.

Keyword : Cubic anvil press, Ideal high pressure,

Dong Hyun Jang, Keizo Murata, Kee Hoon Kim

CeNSCMR and Institute of Applied Physics, Department of physics and astronomy,
Seoul National University, Seoul 151-747, South Korea

Application of high pressure on various emergent correlated materials such as multiferroics, heavy-fermions and new superconductors, has played a vital role in extending physical dimension of exploration by controlling their lattice, electron density of states and electron-phonon coupling. In South Korea, however, transport and thermodynamic measurements under high pressure and high B/T conditions has been limited mostly below ~3 GPa. Here, we report our efforts to install a cubic anvil press which is specialized for exploration of materials under high pressure (< 10 GPa), high magnetic field (2 K). Cubic anvil press is superior to other pressure tools in a similar pressure range, particularly in the pressure quality. Other pressure apparatus such as a piston cylinder cell and a diamond anvil cell cannot avoid the inclusion of uniaxial pressure in addition to the isotropic one so that the effect of uncontrollable uniaxial strains should be considered in the analysis of physical properties. On the other hand, the cubic anvil press allows us to apply ideal hydrostatic, isotropic pressure because it pressurizes a specimen in a pressure medium Daphne 7373 in six directions encapsulated in a teflon cell embedded inside the gasket. Moreover, the apparatus provides an experiment condition of maintaining the constant pressure via automated feedback process during the temperature sweep. This enables us to obtain, e.g., intrinsic power law of transport properties at low temperature and under constant pressure conditions without being subject to the variation of pressure upon cooling as observed in other pressure tools. The information thus obtained could provide fruitful information on the materials of being investigated by providing the intrinsic power law near the classical and quantum critical point of a phase transition. Furthermore, the apparatus would allow investigating the intrinsic T-P phase diagram of emergent materials to look for their novel physical properties of specific problem and provide hints to develop new materials. This cubic anvil press is expected to provide unprecedented opportunities to search for novel physical properties of emergent materials.

P2-Co.530

Investigation of the magnetic properties in double perovskite R_2CoMnO_6 single crystals (R=rare earth: La to Lu)

*김미경, 문재영, 최환영, 오상협, 이나라, 최영재
*M. K.. Kim, Jae Young. Moon, Hwan Young. Choi, SANGHYUP. OH, Nara. Lee, Y.J.. Choi
연세대학교.

Keyword : R_2CoMnO_6, double-perovskite, single crystal, rare earth, ferromagnetic

We have successfully synthesized the series of the double-perovskite R_2CoMnO_6 (R=rare earth: La to Lu) single crystals and have investigated their magnetic properties. The ferromagnetic order of Co^{2+}/Mn^{4+} spins emerges mainly along the c axis. Upon decreasing the size of rare earth ion, the magnetic transition temperature decreases linearly from 204 K for La_2CoMnO_6 to 48 K for Lu_2CoMnO_6, along with the enhancement of monoclinic distortion. The temperature and magnetic-field dependences of magnetization reveal the various magnetic characteristics such as the metamagnetic transition in R=Eu, the isotropic nature of rare earth moment in R=Gd, and the reversal of magnetic anisotropy in R=Tb and Dy. Our results offer comprehensive information for understanding the roles of mixed-valent magnetic ions and rare earth magnetic moments on the magnetic properties.

P2-Co.531

Giant magnetocaloric effect in Gd_2NiMnO_6 compounds

*문재영, 김미경, 오동건, 오상협, 이나라, 최영재
*Jae Young. Moon, M. K.. Kim, DONG GUN. OH, SANG HYUP. OH, Nara. Lee, Y.J.. Choi
연세대학교.

Keyword : Magnetocaloric, Double perovskite

We have prepared polycrystalline Gd_2NiMnO_6(GNMO) sample by the standard solid-state reaction method and investigated magnetocaloric effect in them by magnetic measurements. Magnetic susceptibility of GNMO increases smoothly as temperature decrease and ferromagnetic order occurs below 134 K, and additional anomaly show at low temperature, indicative of the onset of Gd^{3+} spin arrangement. At the temperature, magnetic entropy change, $-\Delta S_M$, with the field changes of 0-7 T, calculated from isothermal M(H) data using Maxwell relation, exhibits sharp peak. This peak have 35.0 J/Kg K at 4 K which is gigantic and cryogenic, these make GNMO promising cryogenic magnetic refrigerant materials.

P2-Co.532

Separation of electronic and structural transition in VO_2/AlN/Si(111)

*조진철, 테티아나 슬루사 [1], 김현탁 [2]
*Jin-cheol. Cho, Tetiana. Slusar[1], Hyun-tak. Kim[2]
ETRI/UST. [1]ETRI. [2]MIT.

Keyword : MIT, IMT, Vanadium dioxide, VO_2

Vanadium dioxide (VO_2) is a promising compound because of its abrupt insulator-to-metal transition(IMT) at around 68°C. However there is physical issue that debate of transition phenomenon is to prove either Mott or Peierls transition.
In this work, the VO_2 thin films were deposited on AlN buffer layer/Si(111) substrate using pulsed laser deposition method. As the films quality confirmation method, temperature dependence of resistance was measured to see that electrical transition point. For samples crystallinity investigation the room temperature θ-2θ and Φ-scans were investigated as well. Temperature dependent x-ray diffraction (XRD) was performed along with measurement of the resistance of the VO_2 films in order to observe the dynamics of electronic and structural transition simultaneously. Based on the obtained data (see fig), the evidence of Mott transition was obtained from comparison between resistance and lattice constant change which obtained by using Gaussian model fitting and Bragg's law ($n\lambda = 2d\sin\Theta$).

P2-Co.533

Field induced Spin Reorientation Transition of $EuMnBi_2$ in Anisotropic Dirac Compound

*김성래, 김동환, 김준성, 박재훈
*Seong rae. Kim, dong hwan. Kim, Jun Sung. Kim, Jae Hoon. PARK
포항공과대학교.

Keyword : XAS, XMLD, spin reorientation transition(SRT),

We measured X-ray Absorption Spectroscopy (XAS) and Dichroism of EuMnBi2. EuMnBi2 single crystal has been recently synthesized by replacing Sr^{2+} ions with magnetic Eu^{2+} ions in order to modify and manipulate an anisotropic Dirac fermions of $SrMnBi_2$. $EuMnBi_2$ was reported that Eu^{2+} ions(J=7/2) of $EuMnBi_2$ form an antiferromagnetic ordering below 24K while Mn^{2+} ions give an AFM ordering at 310K and a spin reorientation transition(SRT) was observed under c-parallel magnetic fields(H_c~5.2T). To obtain an element specific information of the spin reorientation transition, we measured x-ray magnetic linear dichroism(XMLD) at Eu $M_{5,4}$-edge and Mn $L_{3,2}$-edge. Firstly we performed the measurements at 4.5K, 50K, and 335K. There are linear dichroisms in both Eu and Mn ion at 4.5K and Eu-MLD disappears at 50K and Mn-MLD disappears at 335K. Next, when field-dependent measurements was performed at 0T, 4.5T and 6T magnetic field, spin reorientation transition of Eu sublattice was clearly observed. But the spectra of Mn $L_{3,2}$-edge does not change under 6.5T magnetic field. We also measured magnetic circular dichroism spectra in order to examine the origin of large magnetic anisotropy of Mn sublattice. (All these data have been analyzing using cluster calculation and following investigation including magneto-transport measurement have been conduction.)

P2-Op.001*

Time-resolved x-ray absorption and fluorescence spectroscopy of Fe/Co using a femtosecond laser plasma x-ray source

*이자즈, 마자르 [1], 캐롤, 노도영
*Anwar. Mahar Muhammad Ijaz, Mazhar. Mazhar[1], Janulewicz. Janulewicz, Do Young. NOH
광주과학기술원. [1] 광주과학기술원 물리광과학과.

Keyword : X-ray absorption spectroscopy, Time resolved XANES, Fluorescence

Ultrafast time- resolved X-ray absorption and fluorescence spectroscopy experiment was performed on a Fe and Co foils of varying thickness by using a femtosecond laser plasma x-ray source [1] delivering Cu K_α (~ 8.05 keV) and Bremsstrahlung radiation. Temporal evolution of the absorption and fluorescence of Fe/Co after excited by a pump infra-red beam of 1 mJ/ cm^2, was observed using a jitter free pump-probe scheme with time resolution of 50 fs. The x-ray energy resolution achieved by a graphite crystal (HAPG) spectrometer was better than $E/\Delta E < 2000$ which was enough to resolve the x-ray absorption near edge spectrum (XANES) features. The absorption of x-rays started to increase for Fe and Co foils when pump and probe pulses overlap. The rise in absorption of x-rays occurred within a few hundred femtoseconds which is typically the time constant of non-thermal electronic distribution above the Fermi level. In fact, the rising time constant of the absorption was 116 ± 49 fs, which, we believe, was limited by the temporal resolution of our pump-probe set up. Interestingly, the time constant of the fluorescence signal was 315 ± 133 fs, which suggests that the recombination transition after x-ray absorption occurs within about 300 fs. Furthermore, we observed that the recovery of the absorption took a few picoseconds indicating that the electron-lattice relaxation is responsible for the recovery.
Using femto-second pump-probe x-ray absorption spectroscopy, we observed that there occurs ultrafast electronic rearrangement in Fe after excited by IR pumping signal, and determined relevant time constants. We believe that ultrafast electronic rearrangement can now be investigated using a laboratory scale table top x-ray source.

Reference M. Iqbal, Z. Urrehman, H. Im, J. G. Son, O. Seo, H. Stiel, P. V. Nickles, D. Y. Noh, K. A. Janulewicz, “Performance improvement of a Kα source by a high-resolution thin-layer-graphite spectrometer and a polycapillary lens”, Appl. Phys. B (2014) 116:305–311

P2-Op.002*

Surface-Enhanced Raman Scattering (SERS) of 5 nm-width Nanogaps

*윤형석, 최한규, 김나연, 김지환, 김대식
*Hyeong Seok. Yun, Han-Kyu. Choi, Na-Yeon. Kim, Zee Hwan. Kim, Dai-Sik. Kim
서울대학교.

Keyword : Raman, SERS, nanogap, enhancement

We studied surface-enhanced Raman scattering (SERS) of nanogaps. We fabricated 5 nm-width nanogaps filled with alumina (Al_2O_3), and etched alumina with KOH to fill Raman-active molecules inside the gap. To confirm the completeness of etching, we checked the terahertz transmission peak shift of nanogaps in the etching process and the etching rate was found to be 33 nm/min. After etching, we filled nanogaps with bezenethiol (C_6H_6S), which are Raman-active molecules as well as self-assembled monolayers (SAMs) attached to Au surface. Experimental results show strong electric field enhancement and high Raman peak intensity in the nanogaps compared to the smooth Au surface. Our results of nanogaps will be beneficial to measure SERS enhancement factor with more accurate volume ratio than that of nanodimers or bowtie nanoantennas, in which an arbitrary volume ratio is assumed to calculate SERS enhancement factor.

P2-Op.003*

나노 안테나 어레이 기반의 고감도 테라헤르츠 분광법을 이용한 잔류 농약 검출

*이동규, 김기영 [1], 손주혁 [2], 서민아
*Dong-Kyu. Lee, Giyoung. Kim[1], Joo-Hiuk. Son[2], Minah. Seo
한국과학기술연구원. [1] 농업진흥청. [2] 서울시립대학교.

Keyword : "테라헤르츠 전자기파", "테라헤르츠 시간축 분광학", "나노 안테나", "메타물질", "잔류농약"

테라헤르츠 전자기파를 이용한 물질 고유의 광학상수 추출과 이를 바탕으로 물질의 특성을 분석하는 방법은 다양한 분야에서 응용되고 있으며 농작물에 잔류하는 농약의 미량 검출에 적용해 볼 수 있다. 그러나 기존의 일반적 테라헤르츠 시간축 분광법은 미량의 분자 검출에는 한계점이 있으며 민감도 향상이 절실한 상황이다.
본 연구에서는 나노 안테나 어레이 기반 메타물질을 이용한 고감도 테라헤르츠 시간축 분광학 시스템을 구축하여 잔류농약을 실시간, 비침습, 비파괴적으로 검출하는 방법을 구현하였다. 농작물 보호를 위해 사용되는 다수의 농약들은 테라헤르츠 영역에서 서로 다른 주파수에서 흡수 밴드를 갖고 있다. 목표한 특정 농약의 흡수 밴드에 공명을 갖는 나노안테나 어레이를 제작하여 나노안테나 어레이에 농약을 도포하면 공명 주파수 위치에서 강한 테라헤르츠 전기장 증폭이 일어나고 흡수 단면도가 동시에 증가한다. 이러한 기본 원리를 바탕으로 제작된 나노 안테나는 특정 흡수 밴드의 민감도를 극적으로 향상 시킨다.
이러한 기본 원리를 바탕으로 구현된 나노안테나 어레이 기반의 고감도 테라헤르츠 시간축 분광학 시스템은 현재 수 ppm 농도 수준까지 잔류 농약의 검출이 가능하며, 농작물 표면에 도포된 잔류농약를 반사형태로 실시간, 비침습, 비파괴적 검출을 가능케 한다.

P2-Op.004*

THz resonance of split ring resonators with a few nanometer gap

*김나연, 이덕형, 이지예, 김대식
*Na-Yeon. Kim, Duckhyung. Lee, Jiyeah. Rhie, Dai-Sik. Kim
서울대학교.

Keyword : Split ring resonator, Metamaterials, Terahertz optics

We studied resonance behaviors of split ring resonators with a nanometer-sized gap. We fabricated split ring resonators which have gap size of 2 nm using atomic layer lithography. The individual structures have one side length of 120 um with 30 um line width and the lattice periodicity is 200 um. We measured the transmission spectra of nanogap split ring resonator arrays using THz time domain spectroscopy. There was a resonance peak near 0.4 THz which comes from the sides of split ring resonators. We also expect huge field enhancement in nanogap split ring resonators and giant nonlinear optical response of the system.

P2-Op.005*

단일 나노-브릿지 구조를 이용한 테라헤르츠파 다중 주파수 변조

*최근창, 김철기, 이동규, 최재빈, 김대식 [1], 서민아
*geunchang. choi, Chulki. Kim, dong-Kyu. Lee, Jaebin. choi, Dai-Sik. kim[1], Minah. Seo
한국과학기술연구원. [1] 서울대학교.

Keyword : "Fano interfew rence", "Terahertz spectroscopy", "Nano material sensing and detection"

테라헤르츠파는 넓은 주파수 영역에 존재하는 생화학 물질들의 분자 고유의 흡수 공명 특성 때문에 분자 인식 등의 분광법에 높은 응용 가능성을 가지고 있다. 그러나 상대적으로 파장이 길고 흡수단면적이 매우 작아 미량의 분자나 작은 크기의 물질과 상호작용을 관찰하기 어렵다. 본 연구에서는 메타물질 구조를 이용하여 작은 영역 (나노 스케일)에서도 테라헤르츠파의 상호작용을 증가시키고, 나노 크기의 물질을 이용한 테라헤르츠파 주파수 변조가 일어남을 보였다. 테라헤르츠파 주파수 영역에서 공명을 갖는 단일 슬랏-안테나를 제작하여 특정 주파수에서 강한 집속과 증폭이 일어나게 한다. 이 때 나노 크기의 단일 막대로 나노-브릿지를 형성하고, 나노-브릿지의 위치를 바꾸며 테라헤르츠파의 투과 주파수가 다양하게 변조되며, 이중 및 다중 공명 모드가 관찰됨을 보였다. 슬랏-안테나와 나노-브릿지 사이의 강한 결합은 Fano-간섭에 의해 설명되며, 브릿지가 놓인 위치와 사용된 물질의 종류(금속과 반도체, 반도체의 도핑 정도)에 따라 결합의 정도가 달라지는 것을 보였다. 이러한 결과는 동시에 테라헤르츠파를 이용한 나노 스케일에서의 물질의 탐지와 특성 연구를 가능하게 할 것으로 기대된다.

P2-Op.006*

Terahertz generation in two-color laser filamentation

*장도근, 강기곤, 석희용
*Do geun. Jang, Keekon. Kang, Hyyong. Suk
광주과학기술원.

Keyword : plasma, femtosecond laser, terahertz, two-color laser, filamentation

Terahertz (THz) generation in two-color laser filamentation has attracted much attention for broadband THz spectroscopy, THz imaging and nonlinear THz studies. In the two-color scheme, a femtosecond laser's fundamental and its second harmonic pulses are focused together in air or gaseous to produce a plasma via ionization.
In this presentation, we demonstrate the THz generation according to the laser pulse energy, gases, gaseous pressure, and focal length of the lens. For experiments, we employ a Ti:sapphire laser system which is capable of delivering a central wavelength of 800 nm, pulse duration of 40 fs, and 1 kHz repetition rate. The laser pulse is focused by a lens and then propagates through 0.1 mm thick BBO crystal (type-I) which generates a second harmonic pulse. The two-color (a fundamental and its second harmonic) pulses co-propagate and produce a plasma filament at the focus area, generating THz pulses. Then the laser pulses are blocked by a 0.3 mm thick silicon (Si) wafer, while the generated THz pulse is being collected and focused by two off-axis parabolic mirrors. In detection, the electric-optics (EO) sampling method with a 1 mm thick ZnTe crystal and a pryoelectric detector are used to detect the THz pulse waveform and its energy.
We can see that THz waveform and their spectrums in this presentation. The two-color laser scheme can provide a half-cycle THz pulse with a bandwidth of > 2 THz. In addition, we have developed a one-dimensional numerical simulation using the plasma current model to understand the THz generation process. Using this simulation, we have simulated the conditions for optimal THz generation.

P2-Op.007*

고출력 레이저용 안정화 주사광학계 설계

*김다애, 이소영, 이종웅
*KIM Da Ae. , soyoung. Lee, LEE Jong Ung.
청주대학교.

Keyword : achromat design, athermalization, laser scanning system

광학소재의 굴절률은 입사 파장과 주변 온도에 따라 변화한다. 이 연구에서는 2 종의 광학유리를 조합하여 특정한 파장과 온도에서 광학적 특성 변화가 없는 광학계를 설계하는 방법을 연구하고, 이를 기반으로 고출력 레이저에서 발진파장과 주변 온도가 변화하여도 주사 특성의 변화가 없는 레이저 주사광학계를 설계하였다.

P2-Op.008*

Broadband Epsilon-Near-Zero Perfect Absorption of Indium Tin Oxide Thin Films in the Near-Infrared

*윤준호, 바드샤, 김태영, 김원영, 전영철 [1], 황보창권
*Junho. Yoon, Md. Alamgir. Badsha, Tae Young. Kim, Wonyoung. Kim, Young Chul. Jun[1], Chang Kwon. Hwangbo
인하대학교. [1] *울산과학기술대학교.*

Keyword : Thin Film, Perfect Absorption, Plasmonics, Epsilon near zero, ITO.

Perfect absorption (PA) of incident light is important for both fundamental light-matter interaction studies and device applications. Recently transparent conductive oxides (TCOs) have been considered as alternative plasmonic materials in the near infrared (NIR) since they have an advantage of low optical losses and adjustable optical properties. Indium tin oxide (ITO), one of TCOs, shows the ENZ wavelength at NIR wavelengths.

At an ENZ wavelength, the normal electric field in an ENZ thin film becomes very strong, and this leads to large light absorption with a low optical loss.The maximum absorptance of a free-standing thin film is limited to A=0.5, but it is possible to increase it up to A=1. For example, if an ENZ film is coated on a metallic substrate or the attenuated total reflection (ATR) configuration is employed, the destructive interference condition of reflected light can be satisfied. This condition can be approximately written as [1],

(when $\mathrm{Re}[\varepsilon] \rightarrow 0$), (1)

From Eq. (1) it is noted that PA can be achieved in an ultra-thin, flat film even with a very low optical loss. However, Eq. (1) can be satisfied only at a single wavelength for a given film thickness and incidence angle, and thus it is limited in practical use.

We adjust the growth condition of an ITO film and control its ENZ wavelength. Then, using an ITO multilayer of different ENZ wavelengths, we demonstrate broadband PA that covers a wide range of NIR wavelengths [2]. We obtained the dielectric constant of the ITO multilayer film using ellipsometry. Figure 1(a) shows the real and imaginary parts of the effective dielectric constant of the ITO multilayer (red and blue curves, respectively). The real part of the effective dielectric constant is close to zero over the broad spectral region (i.e. broadband ENZ is achieved). Using this effective dielectric constant, we could retrieve the broadband absorption spectrum (blue curve). Broadband PA relaxes the single wavelength condition in previous PA studies, and thus it is suitable for many practical device applications, including sensors, photodetectors, and energy harvesting devices.

[1] M. A. Badsha, Y. C. Jun, C. K. Hwangbo, “Admittance matching analysis of perfect absorption in unpatterned thin films,” Opt. Commun. 332, 206-213 (2014).
[2] J. Yoon, M. Zhou, M. A. Badsha, T. Y. Kim, Y. C. Jun, C. K. Hwangbo, “Broadband Epsilon-Near-Zero Perfect Absorption in the Near-Infrared,” Sci. Rep. 5, 12788 (2015).

P2-Op.009*

Hilbert 변환을 이용한 3 차원 측정연구

*유영훈, 나실인
*Young Hun. YU, silin. Na
제주대학교.

Keyword : Deflectometry, Phase measuring deflectometry, Fringe, Hilbert transform

편향법 중에서 측정 정밀도가 상대적으로 높고, 주사 방법을 사용하지 않고 일정 면적을 한번에 측정 할 수 있고, 비교적 측정 시스템이 간단하며 외부환경에 덜 민감한 3 차원 측정법으로 위상 측정 편향법 (PMD: Phase measuring deflectonetry or fringe reflection method)이 제안되고 연구 되고 있다[10-13]. 위상 측정 편향법은 투과형과 반사형이 있는데 둘 다 기준 패턴 모양이 시료에 의해 변형된 모양을 분석하여 시료의 3 차원 형상을 측정하는 방식이다. 그리고 편향법은 일반적인 3 차원 측정법, 즉 간섭법 혹은 모아레법과는 달리 시료의 높이를 직접 측정하는 것이 아니고, 시료의 국소적 기울기를 구하고 이를 적분 혹은 least square 방법을 이용하여 시료의 형상을 측정하는 방식이다.
본 연구에서는 투과형 편향법을 이용하여 파면의 변화를 측정하였고, 파면 변화 정도를 계산하기 위해 hilbert 변환을 이용하여 위상을 추출하여 3 차원 형상을 측정 하였다. 편향법은 면적이 비교적 크고 거울과 같이 산란이 거의 없는 물체의 3 차원 측정을 하는데 유용하다. 편향법을 통해 얻은 왜곡 무늬로부터 위상 기울기를 구하기 위해 hilbert 변환을 이용하여 파면의 기울기를 측정하고, 구한 기울기로부터 3 차원 프로파일을 구하기 위해 최소자승법을 이용하였다.

P2-Op.010*

나선형 박막증착을 이용한 최외층 저굴절 무반사 코팅의 제작
Anti-reflection coatings using low-index helical material prepared by oblique angle deposition.

*김원영, 김태영, 설주환, 황보창권
*Wonyoung. Kim, Tae young. Kim, Juhwan. Seol, Chang Kwon. HWANGBO
인하대학교.

Keyword : oblique angle deposition. Thinfilm. Anti-reflection coating.

무반사 코팅은 카메라, 디스플레이 등 대부분의 광부품이나 광학산업에서 사용되고 있고 많은 연구가 이루어지고 있는 분야이다. 특히 카메라렌즈 부분에서는 고스트이미지등과 같은 문제를 해결하기 위해 더욱더 성능이 좋은 무반사 코팅이 요구 되고 있다. 더욱 낮은 반사율의 무반사 코팅을 만들기 위해서는 이론적으론 1.2 의 굴절률을 가지는 물질로 박막을 구성하거나, 박막을 구성하는 고굴절률 물질과 저굴절률 물질의 굴절률 차이가 커야 하거나, 박막의 층수가 많아져야 한다. 최근에는 graded index 를 이용한 무반사 코팅도 연구 되고 있다. 본 실험에서는 나선형 박막증착법을 이용하여 맨 마지막 층을 저굴절 물질로 코팅하여 무반사 코팅을 만드는 방법을 사용하여 평균반사율 0.11%(파장 440nm~740nm)의 6 층 무반사 코팅을 설계 제작 하였다.
나선형 박막은 OAD(Oblique Angle Deposition)을 이용하여 제작을 하였다. OAD 란 기판을 기울이거나 돌려서 기둥구조를 기울이거나 회전이 되게 하여 나노구조가 될 수 있도록 증착 시키는 방법이다. 이렇게 증착을 하게 되면 증착 시 기판의 각도와 회전수에 따라 기울어진 기둥구조나 나선형 구조를 만들 수 있게 된다. 또한 이러한 박막은 기울어진 각도에 의해 그림자효과로 빈 공간이 생기게 되고 이는 일반적인 기둥구조의 박막보다 박막의 다공성을 증가시켜 굴절률이 낮아지는 효과를 초래 한다. 이렇게 굴절률이 낮은 물질을 사용하게 되면 층수를 늘리지 않으면서 반사율을 더욱 낮은 박막을 얻을 수 있다. 본 실험에서는 증착물질로 저굴절 물질은 SiO_2, 고굴절 물질은 TiO_2 를 사용하였으며, 마지막 층의 SiO_2 는 기판을 85°로 기울이고 회전수는 0.3rpm 을 주어 나선형 나노사이즈 패턴을 형성하게 하여 낮은 굴절률의 SiO_2 박막을 증착 시켰다.
매우 낮은 반사율의 박막으로 작은 두께와 굴절률차이로도 최종결과물이 달라질 수 있으므로 각 층의 굴절률과 두께를 보다 정확히 알아야 할 필요성이 있다. 이를 위하여 엘립소미터와 분광광도계를 이용하여 다층박막의 굴절률과 두께를 분석하였다. 기존의 엘립소미터를 이용한 박막의 분석은 단층박막에 한정되어 있었다. 이를 보완하기 위해 분광광도계의 반사율 혹은 투과율 데이터를 함께 사용하여 보다 정확한 다층박막의 굴절률과 두께를 분석한 후, 이러한 분석결과들을 바탕으로 OAD 를 이용한 무반사 코팅의 설계 및 제작을 진행하였다. 그 결과 다층 박막의 분석에서 엘립소미터로 측정한 Δ 와 Ψ 값과도 일치하며(1)(2), 분광광도계의 반사율 결과와도 일치하는 각 층의 굴절률과 두께를 찾아내게 되었고, 이를 토대로 한 무반사 코팅 역시 시뮬레이션 결과와 측정결과가 매우 흡사하게 나옴을 확인 하여 엘립소미터를 이용한 다층박막의 분석이 효과적임을 알 수 있었다. 이러한 분석을 토대로 각층의 굴절률과 두께를 설계단계에서부터 반영하여 평균반사율 0.11% 대의 무반사 코팅을 설계 및 제작하였다. 이와 같은 결과들을 통하여 단층박막의 분석에만 쓰이던 엘립소미터를 분광광도계와 상호보완적으로 다층박막의 분석에도 이용하도록 확장하였으며, OAD 를 이용한 나노구조의 저굴절률 박막을 실제 무반사 코팅에도 적용시켜 적은층수로도 효과적인 무반사 코팅을 설계, 제작하였다. 이러한 결과는 향후 OAD 박막을 응용한 여러 가지 박막에도 도움이 될 것으로 보인다.

참고문헌
1. Bernhard von Blanckenhagen, Applied Optics, Vol. 41, Issue 16, pp. 3137-3141 (2002)
2. G.E. Jellison, Jr, Thin Solid Films, Volumes 313–314, Pages 33–39, (1998)

P2-Op.011*

Design of Bidirectional Epsilon-Near-Zero Coherent Perfect Absorption with Indium Tin Oxide Thin Films Using Admittance Matching Method

*김태영, 김원영, 윤준호, 함원규, 전영철 [1], 황보창권
*Kim. Tae Young, Wonyoung. Kim, Junho. Yoon, Ham. Wonguy, Young Chul. Jun[1], Chang Kwon. HWANGBO
인하대학교. [1] *울산과학기술대학교.*

Keyword : perfect absorption, epsilon-near-zero, ITO, thin film

Coherent perfect absorption (CPA) is an optical phenomenon in an absorbing medium by interaction of two counter-propagating coherent waves and turns it into some form of internal energy. It is the time-reversed counterpart of a laser and this is why a coherent perfect absorber is called as an anti-laser. It has many potential applications in the fields of detectors, transducers, optical switches and radiology. Many researches are focused on CPA with nanostructured metamaterials (MMs). In this study we employ unpatterned indium tin oxide (ITO) thin films for CPA at epsilon-near-zero (ENZ) wavelength in the near infrared (NIR) regime. Recently transparent conductive oxides (TCOs) have been studied as alternative MMs in NIR since they have an advantage of low optical loss and adjustable optical properties. At an epsilon-near-zero (ENZ) wavelength the normal component (E_Z) of electric field in an ENZ thin film becomes very strong, and this can lead to very large light absorption in the film. The maximum absorptance of a free-standing thin film is limited to SHAPE * MERGEFORMAT , but it is possible to increase it up to SHAPE * MERGEFORMAT (i.e. PA) in various ways. Here we employ ENZ CPA for ITO thin films.

In a bidirectional inputs system, the left-going wave, I_2 is the time reversal of the right-going wave, I_1. Since the propagation direction of the left-going wave is opposite, the time reversal is equivalent to the negative direction of magnetic field (-H) of the forward wave, assuming the direction of E-field is same. At CPA the destructive interferences should occur in both Outputs. In other words, the right-going wave I_1 only should exist in the incident medium and the left-going wave I_2 only should exist in the substrate, respectively. Therefore the admittance for the backward wave in the substrate becomes negative due to the negative magnetic field (-H) and at CPA the starting admittance of the substrate in the admittance diagram is $-n_{sub.}$

Using the negative admittance matching method, we design 3-layer symmetric CPA thin film at the 1600 nm at 45° oblique incidence of waves as shown Fig. 1(a). Fig. 1(b) shows the irradiances in around 1400 – 1670 nm band are satisfied the perfect absorption as over 99.9 %. Fig. 1(c) shows irradiance of $output_1$ by phase and wavelength. Particularly at 1600 nm, the reference wavelength of this design, the absorption curve by controlling the phase is modulated as 0.216 to 1 repeatedly(Fig. 1(d)).

In this study, we propose broadband CPA designs with ENZ ITO thin films using admittance matching method and scattering matrix method, respectively: bandwith is about 270 nm. These designs can be used as nanophotonic devices such as optical modulator, sensors, switches, detectors, transducers, and notch filters.

P2-Op.012*

Generation of a High Power Laguerre-Gaussian Beam Using a Spiral Phase Plate From a W-band Gyrotron

*유동호, Ashwini Sawant, 최은미
*Dongho. Yu, Ashwini. Sawant, Eunmi. CHOI
울산과학기술대학교.

Keyword : Spiral Phase Plate, Laguerre-Gaussian beam, orbital angular momentum,Gaussian beam, Gyrotron

A Laguerre-Gaussian Beam has characteristics of orbital angular momentums (OAM) and it allows transmitting a lot of independent data streams over the same spatial wireless medium. We investigated a Laguerre-Gaussian beam generated from a W-band high power gyrotron source with a spiral phase plate (SPP). We consider 24 steps of the SPP structure for the effective transmittance. The step height of SPP is decided by a equation,, where is a wavelength, is an azimuthal index, and and are refractive indexes in material and vacuum, respectively. The detail design values of the SPP structure will be presented in the talk. Not only for l=1 OAM mode, but also other higher OAM modes are generated with slightly different step sizes of the SPP. Simulation study shows that the generated LG beam's phase and amplitude is clearly identified as characteristics of orbital angular momentum, which are doughnut shape amplitude and helical phase structure at W-band. Fabrication of the designed SPP is underway.

P2-Op.013*

렌즈를 이용한 은폐와 파장에 따른 은폐 특성 연구

*곽대훈, 김태훈, 류지욱, 김용기
*Dae Hun. Kwak, Tae Hun. Kim, Ji Wook. Ryu, Yong Gi. Kim
공주대학교.

Keyword : "은폐, 배율, 파장, 렌즈 간격"

메타물질의 발견으로 군사기술 등 다양한 응용분야에서 물체를 숨기기 위한 은폐(Cloaking) 기술의 관심이 급증하였고, 일반렌즈와 방해석을 이용해 은폐의 가능성이 증명되었다.[1, 2] 그러나 일반렌즈를 이용한 은폐연구에서 파장 변화에 따른 은폐지점과 배율의 변화에 대한 연구결과는 없었다. 물체의 은폐를 완벽하게 구현하기 위해서는 물체와 상의 비율이 1 되는 배율(Magnification)을 만들어야 한다. 본 연구에서는 4 개의 양볼록렌즈를 이용하여 그림 1 (a)의 오른쪽 아래 삽입된 그림과 같이 은폐장치를 구성하여 렌즈 사이의 간격 거리(d_1, d_2, d_3, d_4) 변화에 따른 물체의 은폐연구를 진행하였다. 그림 1 (a)는 Zemax 를 이용하여 d_1 과 d_3 를 같은 간격으로 변화 시켜 구해진 배율(Magnification) 데이터이며, d_2 는 180 mm, d_4 는 0 mm 로 고정한 경우이다. 이 과정에서 물체의 은폐를 위해 필요한 배율 1 이 되는 d_1, d_3 의 거리는 약 260 mm 이어야 함을 그림 1 (a)에서 알 수 있다. 그림 1 (b)는 Zemax 를 이용하여 d_2 값의 변화에 따른 배율의 관계를 가시광선 영역에서 대표적인 4 개의 파장을 선정하여 계산하였다. 이 때 d_1, d_3 는 260 mm, d_4 는 50 mm 로 고정하였다. 그림 1 (b)에서 알 수 있듯이 d_2 가 증가할수록 파장 632.8 nm, 532 nm 의 배율은 점점 증가하며, 454.5 nm 의 배율은 감소한다. 하지만 렌즈 d_2 의 간격 변화에 관계없이 배율 1 을 가장 잘 유지하는 파장은 503 nm 임을 그림 1 (b)에서 확인할 수 있다. 그리고 d_4 가 50 mm, d_2 가 170 mm 이면 4 개의 파장 모두에서 배율 1 이 되지만, d_4 가 증가할수록 4 개의 파장 모두가 배율 1 을 유지하기 위한 d_2 의 거리 점점 짧아진 사실도 알게 되었다. 본 연구에서는 그림 1 (a), (b)의 데이터를 이용하여 배율 1 을 유지하면서 완벽한 은폐가 가능한 렌즈 사이의 거리 d_1, d_3 는 260 mm 이며 d_2 는 180 mm 라는 사실을 실험적으로 발견하였고 파장 변화에 따른 배율의 변화를 확인하였다.

[1] J.S. Choi and J.C. Howell, “Paraxial ray optics cloaking”, Opt. Express 22(24), 29465-29478 (2014).
[2] J.C. Howell, J.B. Howell and J.S. Choi, "Amplitude-only, passive, broadband, optical spatial cloaking of very large objects", Appl. Opt. 53(9), 1958-1963 (2014).

P2-Op.014*

필드 추적과 광선 추적 기법을 통한 고출력 레이저용 빔 균질 광학계 설계에 관한 연구
A study on the beam homogenizer design for a high-power laser with field tracing method and ray tracing method

*김태신, 유태준
*Tae Shin. Kim, Tae Jun. Yu
한동대학교.

Keyword : Beam homogenizer, High-power laser, Laser peening

레이저 표면개질에 사용할 고출력 레이저 빔 균질 광학계에 대한 시뮬레이션을 수행하였다. 원형의 빔 분포를 사각형의 균질한 분포로 만들기 위한 광학계로서, 높은 출력과 에너지를 고려하여 렌즈들의 초점거리 및 렌즈사이 거리를 초기 설계하였다. 광학계 설계를 위한 광선추적과 함께, 가간섭성이 좋은 광원으로 인해 실제적으로 형성되는 이미지에서의 간섭 및 스펙클 효과를 보기 위해 필드추적을 동시에 수행하였다. 이를 통해 빔 균질기를 통과한 빔의 형태 및 분포를 확인하고 비교하였다.

P2-Op.015*

건조한 노면과 젖은 노면 기상 상태의 광학적 구분

*김태훈, 김성기, 곽대훈, 신용빈, 정동진, 류지욱, 김용기
*taehun. kim, Sung Gi. Kim, DaeHun. Kwag, yong bin. shin, dong jin. jeong, Ji-Wook. RYU, Yong Gi. Kim
공주대학교.

Keyword : "건조 노면, 젖은 노면, 스캐닝, 레이저 다이오드"

최근 자동차들은 기술과 성능의 비약적 발전과 지능형교통시스템(ITS), 차량들 간의 통신 시스템 도입 등으로 점점 고속으로 달릴 수 있게 되었다. 이러한 지능형교통시스템은 운전자들에게 돌발 상황과 교통상황 등 다양한 정보를 제공하고 있지만 도로 노면의 기상 상태는 전혀 전달하지 못하고 있다. 운전자들에게 실시간으로 건조, 젖음, 결빙, 강설 등의 도로 노면 기상상태를 실시간으로 제공 된다면 교통사고 방지를 통해 생명과 재산을 보호 할 수 있다.

최근 국내에서 몇 년간 레이저 다이오드를 이용한 도로 노면 기상 관측 시스템에 대한 연구가 진행되었다. [1] 지금까지 도로 노면 기상 관측 시스템은 고정식으로 고속도로에 여러 지점을 측정하지 못하는 한계가 있다. 본 연구는 스캐닝을 통해 여러 지점에서의 노면 기상 상태를 관측하였다. 스캐닝은 좌·우 관측이 가능하며, AOI(Angle of Incidence)에 따라 수평거리가 변화한다. 장비의 높이는 5 m 로 고정하고, AOI 는 50°, 60°로 하였다. 파장이 905 nm, 1550 nm 인 두 개의 레이저 다이오드의 인가전압을 5 V 로 고정하여 아스팔트 지면으로 쏜 후 후방 산란되는 신호를 디텍터를 통해 수신하였다. 그림 1 의 (c)는 장비의 설치 위치를 기준으로 스캐닝 반경을 90°로 설정하고 45°간격으로 아스팔트 노면의 기상 상태를 건조한 정상적인 노면과 인위적으로 물을 뿌려 젖게 만든 젖은 노면으로 만들어서 실험을 진행하였다. 그림 1 의 (a)(b)는 x-축 0°~45°까지의 신호는 건조한 노면이고 45°이후의 신호는 젖은 노면의 신호이다. 노면이 건조할 때는 일정한 신호가 측정되고 젖은 노면에서는 빛의 흡수로 인하여 신호가 급격히 감소함을 알 수 있다. 이를 통해 아스팔트 도로 노면의 건조와 젖음 기상 상태를 고정된 하나의 지점만이 아니라 스캐닝 기술로 더 많은 지점을 분명하게 구별할 수 있다.

[1] 이서경, 김용기. 새물리, 63(3), 280-287 (2013)

P2-Op.016*

도로노면 기상상태의 비접촉식 측정

*김성기, 정동진, 류지욱, 김용기
*Kim Sung Gi. , dong jin. jeong, RYU Ji-Wook. , Kim Yong Gi.
공주대학교.

Keyword : "노면 기상상태, 스캐닝, 레이저 다이오드, 신호감쇠"

도로 노면의 기상상태에 변화로 인해 고속으로 달리는 도로에서는 큰 사고를 유발한다. 따라서 도로노면 기상 상태를 알 수 있다면 큰 사고를 예방 할 수 있다. 외국에서 개발된 도로노면 기상관측 기술은 고정식 단일지점 관측 기술이다.[1] 그러나 단일지점 관측 기술은 넓은 도로를 파악하기에는 효율적이지 못하다. 본 연구에서는 회전 스캔과 선형 스캔을 통해 넓은 도로노면 기상상태를 파악하는 기술을 연구하였다. 스캐닝은 국내에서도 처음시도 된 기술이며 외국에서도 사례가 없다.
그림 1 의 (a)는 AOI(Angle of Incidence)를 30° 부터 60°까지 좌우로 회전 스캐닝을 하였고, 기상상태의 변화가 없으면 신호의 세기가 일정하게 측정되었다. 신호의 세기가 클수록 노면의 굴곡이나 파임 등 물리적인 변화에 민감하게 반응하는 것을 그림 1 의 (a)의 30°, 35°, 40° 그리고 45° 4 개의 데이터에서 확인하였다. 따라서 노면의 포장상태, 굴곡, 거칠기 등에 덜 민감하게 반응하기 위해서는 빔의 출력 밀도가 낮은 것(50°, 55°, 60°)이 더 균일한 수신신호 획득이 가능함을 알 수 있다. 선형 스캔의 경우 상하로 스캐닝 하였으며, AOI 가 커질수록 레이저 다이오드(LD)에서부터 도로노면까지의 거리가 멀어짐에 따라 그림 1 의 (b)와 같이 지수함수적으로 감소하였고 다음 식을 도출해 내었다.

(1)

식 (1)을 이용하면 LD 에서부터 도로노면까지의 거리만으로 디텍터에 수신되는 신호의 세기가 예측 가능하다. 식 (1)으로 계산된 값과 실험으로 측정된 값을 비교한 결과 그림 1 의 (b)에서 5.0 V 의 경우 0.28 mV(< 1%)의 오차로 도출된 식의 정확성을 확인하였다. 식 (1)에서 표현된 신호감쇠율 값은 아스팔트 노면의 경우 0.45 정도이며, 이 값은 외부변화에 관계없이 일정한 값을 갖는다.

[1] J. Casselgren, M. Sjödahl, and J. P. LeBlanc. "Angular spectral response from covered asphalt". Appl. Opt. 46, 4277-4288 (2007).

P2-Op.017*

테라헤르츠-펌프/테라헤르츠-프로브 분광장치 개발

*김영찬
*Young-Chan. Kim
충북대학교.

Keyword : 테라헤르츠, 펌프/프로브, THz, pump/probe

펌프/프로브 실험방법은 물질의 광특성을 분석하는데 매우 유용한 방법으로 잘 알려져 있다.여기에 테라헤르츠 전자기파를 광원으로 사용하여 테라헤르츠-펌프/테라헤르츠-프로브 분광장치를 만들었다.
테라헤르츠 전자기파는 다양한 물질들에 대해 투과성이 좋으면서 에너지가 낮아 시료에 손상을 주지 않는 특성이 있다. 또한, BiFeO3 를 비롯한 다강체의 magnon 과 잘 공명할 것으로 예상되며, MgB2 등 초전도체의 cooper pair 의 결합 에너지가 테라헤르츠 영역에 있기 때문에 개발된 테라헤르츠-펌프/테라헤르츠-프로브 장치를 사용하여 다강체와 초전도체 등의 광특성을 자세히 연구할 수 있다.
테라헤르츠 전자기파는 비선형 결정인 LiNbO3 와 ZnTe 의 비선형성질을 이용해 생성하였다.
먼저, Pulse Front Tilting 방법과 4-f 시스템을 통해 LiNbO3 결정에서 테라헤르츠 전자기파의 발생이 가능하다.
이러한 방법은 복잡하지만, 펌프용 빔으로 사용하기에 적합한 강한 테라헤르츠 전자기파의 생성이 가능하다.
현재 우리의 펌프용 테라헤르츠 전자기파는 샘플위치에서 2.7mm 크기로 집광되며 50 kV/cm 의 세기를 보이고 있다.
위상정합성이 우수한 ZnTe 결정을 사용하여 보다 쉽게 프로브용 테라헤르츠 전자기파를 생성하였다.
이렇게 생성된 테라헤르츠 전자기파는 0.75 THz 를 기준으로 약 1THz 밴드폭의 스펙트럼을 보이고 있다.
이와 같이 생성된 테라헤르츠-펌프/테라헤르츠-프로브 분광기를 사용하여 다강체:BiFeO3 와 초전도체:MgB2 를 분석할 예정이며, 이 밖에도 다양한 고체물질들에 대해 연구할 계획이다.

P2-Op.018*

The Measurement of Minority Carrier Lifetime Using Millimeter Wave Photoconductivity Decay Technique

*최문석, 이규섭 [1], 유난이 [1], 최은미
*Mun Seok. Choe, Kyu-Sup. Lee[1], Nan Ei. Yu[1], Eunmi. CHOI
울산과학기술대학교. [1] 광주과학기술원.

Keyword : Millimeter wave , minority carrier life time, micro-PCD technique, Quasi-optics

The measurement of minority carrier life time using -PCD (Photoconductivity decay) technique is widely used in research of semiconductor material and examination of wafer defects in industry. Microwave sources (10~20 GHz) for -PCD technique have a limit of wavelength (~ cm) which is too large compared to local region in wafer, therefore we suggest a quasi-optical transmission system using millimeter wave and sub-THz source. In this system, an oversized corrugated horn antenna focuses a beam to a desire target area order of few mm^2. Focused beam through wafer goes to Schottky diode detector which can detect signal in nano-second range. Experimental data is compared with theoretical model to verify this technique as an alternative method instead of -PCD technique.

P2-Op.019*

레이저 빔의 안정화에 따른 전자빔의 특성 분석

*한병헌, 백인형 [1], 조재흥 [2], Nikolay Vinokurov[1], 정영욱 [1]
*Byung Heon. Han, InHyung. Baek[1], JO Jae Heung. [2], Vinokurov. Nikolay[1], JEONG Young Uk. [1]
한국원자력연구원. 한남대학교 물리학과. [1] 한국원자력연구원. [2] 한남대학교.

Keyword : 레이저 안정화, 비선형 현상

현재 한국원자력연구원 양자빔기반방사선연구센터에서는 레이저를 이용하여 전자빔을 발생시켜 가속하는 시스템을 가동 중에 있다. 가속기 시스템에 사용되는 레이저 빔의 경로는 거의 10 m 에 달한다. 레이저 빛이 진행하는 거리가 멀어지게 되면 고려해야 할 사항이 여러 가지가 있는데 그 중에 제일 중요한 것이 전자빔을 발생시키기 위한 레이저 빔의 안정도이다. 빛이 진행하는 경로에 공기의 흐름이 있으면 비선형 현상으로 인하여 빔의 내부에 울렁거리는 현상이 발생하게 된다. 그에 따라 레이저 빔이 불안정하게 흔들리게 되고 레이저 빔이 불안정하게 되면 전자빔을 발생시키는 면에 제대로 입사가 되지 않아서 발생되는 전자빔의 특성에 영향을 주게 된다. 본 논문에서는 레이저 빔의 안정도에 따른 전자빔의 특성을 연구하고자 한다.

P2-Op.023*

공초점 현미경과 PCS 를 사용한 V_20_5 박막의 표면 분석

김현기, 이재란, 강만일, *김석원
Hyunki Kim. , Jaeran Lee. , Manil Kang. , *KIM Sok Won.
울산대학교.

Keyword : 공초점 현미경, correlator, PCS, laser scanning

공초점 현미경은 기존의 광학 현미경에 비해 높은 해상력을 가진 측정용 현미경으로, 요철이 있는 시료면에 대해 시야 전면에 초점이 맞는 고해상도 이미지를 얻을 수 있으며, 비파괴 및 비접촉의 3 차원 형상 계측이 가능하여 바이오 및 여러 산업 분야에서 이미징 장치로 활용되고 있다. 하지만, 이미지만으로 물질의 표면 특성을 정의된 정량적인 값과 동일시하는 것은 어렵기 때문에 이를 보완해줄만한 신호 처리 기술이 필요하다. 본 연구에서는 레이저 주사 공초점 현미경의 시료 표면 주사 기술과 표면에서 반사된 신호의 시간에 따른 상관성을 분석하는 상관함수 분석 기술을 결합하여 시료의 표면 특성을 분석하였다. 레이저 주사 공초점 현미경을 구성하기 위해 아르곤 이온 레이저(MODU-LASER, Stellar-Pro ML/100) 의 488 nm 파장의 빔, 갈바노미러, 대물렌즈(olympus, 60×, NA 1.2), 빔스플리터, PMT(photomultiplier tube) 모듈을 사용하였고, 레이저 주사 공초점 현미경에서 얻어지는 광자신호를 상관함수의 형태로 분석하기 위해서 광자상관분광법(PCS; photon correlation spectroscopy)을 적용하였다. 주사 속도를 1000 Hz 에서 100,000 Hz 까지 변화시키면서 10 μm × 10 μm 면적의 이미지와 PCS 신호를 얻을 수 있었고, 수 마이크로 미터 크기의 표면 요철은 공초점 현미경의 이미지를 통해, 수백 나노미터 이하의 박막의 grain 크기는 PCS 를 통해 분석할 수 있었다. 본 연구 결과는 박막의 표면 거칠기와 같은 특성들을 분석하는 기술로 활용할 수 있을 것으로 보인다.

P2-Op.024*

열 탈분극 효과를 최소화하기 위한 고반복률 페타와트급 티타늄 사파이어 증폭기 설계에 관한 연구
A study of the high-repetition rate petawatt scale Ti:Sapphire amplifier designed to minimize thermal depolarization effects

*조세례요한, 유태준
*Seryeyohan. Cho, Tae-Jun. Yu
한동대학교.

Keyword : Ti:Sapphire amplifier, High-power and High-repetition rate laser, Thermal effect, Optimal design

티타늄 사파이어를 매질로하는 증폭기에서 발생하는 열 탈분극 효과를 최소화 하기 위한 설계 변수를 제안하였다. ASE 의 흡수를 위한 클래딩의 형상 구조와 매질의 냉각 형태를 설계 변수로 하여 열 탈분극 최소화를 위한 설계 조건을 유도하고, 그 효과를 시뮬레이션 하였다. 매질의 클래딩 형상으로 ASE 로부터 얻은 열 에너지를 분배하였고, 매질의 경계부분 냉각 형태를 조절하여 매질의 중심과 경계 간의 온도 차를 최소화 하였다.

P2-Op.028*

변형 Z-scan 법을 이용한 결상렌즈의 초점 상태 확인 기법
Study on the focusing characteristics of converging lenses

*이재현, 남기봉
*JaeHyun. Lee, NAHM Kie Bong.
한림대학교.

Keyword : Z-Scan, 초점거리 측정, 다초점렌즈, IOL, 프레넬렌즈

집광 렌즈의 초점을 실측하는 과정은 주관적 판단에 의존한다. 즉 초점의 크기나 밝기를 목측으로 판단하거나 또는 결상되는 영상의 선명도 등을 측정하거나 하여 이로부터 초점의 위치나 초점거리를 측정 또는 산출한다. 이 과정은 측정자의 주관적 판단에 의존할 수 밖에 없어서 정밀도의 한계가 노출된다. 본 연구에서는 광축을 따라가며 초점 면 주변의 에너지밀도를 측정하는 방법을 통하여 이러한 측정 오차를 제거하는 방법을 연구하였다.
프레넬 렌즈와 같은 다초점 결상렌즈는 이론적으로 다수의 초점이 존재하는 것은 밝혀져 있으나 실제 이를 개별 측정하기에 어려움이 있는 것이, 한 초점에는 다른 다수의 초점에 의한 배경 신호가 존재하여 어느 초점을 명확하게 규명하기가 어렵다. 본 연구에서는 직경 20 마이크로미터의 핀홀을 주사하면서 투과광을 측정함으로써 다수의 초점이 형성되는 상황을 객관적으로 보일 수 있었다.

P2-Op.029*

도플러 편이를 이용한 광섬유 간섭계 내부의 광학 위상 지연자

이승석, 김주하, 엄태중 [1], *최은서
Seung Seok. Lee, Joo Ha. Kim, Tae Joong. Eom[1], *Eun Seo. Choi
조선대학교. [1] *고등광기술연구소.*

Keyword : 도플러 편이, 광섬유 간섭계, 위상천이

물체 표면에서 반사되어 되돌아 오는 빛은 물체의 동적인 움직임에 따라서 원래의 파장 특성이 아닌 다른 특성을 보이게 되는데 이러한 개념이 광계측에서의 도플러 편이의 기본개념이다. 광계측에서 간섭계를 이용하는 경우 샘플의 움직임에 따라서 유도되는 도플러 편이는 간섭무늬에서 변이를 만드는 원인이 된다. 이러한 특징을 이용하여 샘플에서 발생하는 동적 움직임을 분석하여 혈류의 흐름이나 유체의 특성을 분석하는데 활용되기도 한다. 간섭무늬 계측에서 흔히 보이는 평형이동은 위상천이에 의한 것으로 파장 이하의 매우 작은 광경로차의 변화에 의해서 발생한다. 이러한 불안정성을 제어하기 위해서는 미세한 위상천이를 제어할 필요가 있다. 이를 위해서 외부 실험 환경에 가능한 노출되지 않도록 하면서 동시에 신호의 안정성을 확보하기 위한 다양한 기법을 활용해야 한다. 이런 점에서 도플러 편이 정도를 광섬유 내부에서 제어할 수 있게 되어 미세 위상천이를 조절할 수 있다면 있다면 외부 조건에 영향에 둔감하면서도 간섭무늬를 효율적으로 안정적으로 제어할 수 있는 방법으로 활용이 가능할 것이다. 본 논문에서는 광섬유 광학계로 구성된 간섭계의 한쪽 팔에 미세진동을 통해 도플러 편이를 유도하여 이를 이용하여 위상천이가 제어될 수 있음을 실험적인 결과를 통해서 제시하고자 한다. 도플러 편이를 기반으로 유도된 위상천이방법은 광섬유 내부로 전달되는 빛의 도플러 편이를 이용하기 때문에 광손실이 없으면서도 외부 인가신호에 대해서 선형적으로 반응하는 장점을 가지고 있어 매우 정확한 위상천이를 실시간 제어할 수 있는 장점을 가진다. 그러므로 광섬유 간섭계로 구성이 가능한 계측 시스템에 제시한 기법의 적용이 용이할 뿐만 아니라 연속적으로 가능하므로 다양한 기존 위상천이 기법의 대체가 가능하다. 제시한 방법을 이용함으로써 특정 위치에서의 안정적 위상 계측뿐만 아니라 위상정보를 기반으로 하는 의료영상분야에서도 활용도가 높을 것으로 예상되는 바이다.
This work was supported by the Industrial Strategic Technology Development Program, 10047943, ‘Development of Micro-surgical Apparatus based on 3D Tomographic Operating Microscope’ funded by the Ministry of Trade, Industry & Energy(MI, Korea), and Basic Science Research Program through the National Research Foundation of Korea(NRF) funded by the Ministry of Education(grand no. 2014R1A1A2059532).

P2-Op.030

Coherent anti-Stokes Raman scattering 를 이용한 식용유에 섞인 불순물의 정량적 판별

*박창우, 이인구 [1], 고도경 [1]
*Park ChangWoo. , ingu lee. [1], KO Do-Kyeong. [1]
광주과학기술원 물리·광과학과. [1] 광주과학기술원.

Keyword : "coherent anti-Stokes Raman scattering", "올리브유", "불포화지방산", "이중결합"

올리브유는 활성산소를 제거해주는 폴리페놀과 비타민 E 등 항산화 성분이 풍부하고, 포만감을 높여주어 식욕을 억제해 주는 올레산이 다른 식용유에 비해 많이 있어 다이어트에 효과적이다. 참기름은 향이 좋고, 리그난의 일종인 세사민이 들어있어 죽상동맥경화증의 위험 요소인 LDL 콜레스테롤을 감소시키는데 효과가 있다. 이러한 효능 때문에 올리브유와 참기름은 시장에서 다른 식용유에 비해서 3-5 배 비싼 가격에 판매된다. 하지만 제품에 표시되지 않은 성분들을 다량 함유한 올리브유와 식용유의 유통 및 판매에 대한 문제점이 제기되어 왔다. 식용유들은 지방산으로 구성되고, 지방산은 이중결합의 유무에 따라 크게 포화지방산과 불포화지방산으로 나뉜다. 식용유의 종류 마다 불포화지방산이 지닌 일중결합과 이중결합의 비율이 다른 것을 이용한 실험으로 진위를 판별할 수 있다.
본 연구에서는 broad femtosecond pulse 기반의 multiplex coherent anti-Stokes Raman scattering (CARS) 분광 현미경을 이용하여, 시중에 판매되고 있는 올리브유, 들기름, 참기름, 대두유, 옥수수유를 섞어서 불포화지방산의 이중결합이 나타내는 3031 cm^{-1} (=C-H symmetric stretching) 영역을 측정 및 분석하였다. 올리브유에 들기름의 양을 다르게 조성하여 얻은 정규화된 CARS intensity 그래프는 들기름에 이중결합의 비율이 올리브유보다 많기 때문에 들기름의 함량이 높아질수록 CARS intensity 가 증가함을 보인다.

P2-Op.031

Ti:sapphire 오실레이터의 연속 발진 빔 출력

*이신영, 김경남 [1], 김하나 [2], 류우제 [3], 조정상 [1], 이기태 [1], 박성희 [1], 정영욱 [1], Nikolay Vinokurov[1]
*Shin-yeong. Lee, Kyung Nam. Kim[1], Ha-Na. Kim[2], Woo Je. Ryu[3], Jeong Sang. Jo[1], Ki Tae. LEE[1], Seong Hee. PARK[1], Young Uk. JEONG[1], Nikolay. Vinokurov[1]
과학기술연합대학원대학교(UST). [1] 한국원자력연구원. [2] 한국원자력연구원. 충남대학교. [3] 한남대학교.

Keyword : Ti:sapphire, 레이저 오실레이터, 공진기 안정 조건

80 MHz 오실레이터 시스템을 제작하기에 앞서 연속 발진 빔의 발진 특성을 이해하는 것이 중요하다. 펄스레이저를 제작하기에 앞서 접힌 X 자 형태의 연속 발진 오실레이터를 구성하였다. 전체 공진기 길이는 추후 제작할 80 MHz 오실레이터에 맞게 1875 mm 로 설정했다.
공진기의 접힌 각도는 18.8 도로 제작하여 비점수차를 보정하였다. 또한, 양 팔 길이 차의 변화시키며 두 오목거울 사이 거리에 따른 빔 웨이스트를 계산하였고, 같은 조건에서 출력을 측정해 비교하였다. 빔 웨이스트 값이 실수일 때, 레이저 빔이 발진 되며 공진기 안정 영역을 만족함을 알 수 있었다.
양 팔 길이 차가 클수록 발진 되지 않은 영역이 커졌고, 분리된 두 영역 사이에서는 레이저 발진이 되지 않았다.
양 팔 길이를 같게 만들고 3 W 의 여기광(다이오드 펌프 레이저, Verdi-V10)을 주었을 때, 최대 출력은 550 mW 였다. 여기광 대비 출력의 기울기 효율이 ~ 31%였다. 또한, 빔 질을 확인하기 위해 빔 프로파일러로 M^2 값을 측정하였다

P2-Op.032

은 나노선 기반의 가변 테라헤르쯔파 플라즈모닉 소자 제작

홍정택, *안영환
Jung Taek. Hong, *Yeong Hwan. Ahn
아주대학교.

Keyword : 테라헤르쯔파, 은 나노선, 플라즈모닉 소자

투명전극은 고전도도와 높은 투과도 특성을 요구하며, 현재 태양전지, LED, LCD 등의 전자분야에 광범위하게 사용하고 있다. 대부분 ITO 박막 주로 활용되고 있지만 유연성 소자를 제작하기에는 강도가 약하고 고른 박막을 제작하기 어렵기 때문에, 이를 대체하기 위한 여러 가지 물질이 대두되고 있으며, 그 중 하나가 은 나노선(AgNW)이다. AgNW 는 높은 전도성을 가지며, 간단한 공정으로도 좋은 네트워크 구조를 구성할 수 있기 때문에 투명전극으로서의 활용도가 매우 높다. 본 연구에서는 다양한 전도도 및 두께의 AgNW 네트워크 박막을 제작하여 테라헤르츠파 투과 특성을 측정하고, 이를 기반으로 하는 플라즈모닉 소자를 제작하였다. 고전도성 AgNW 박막을 가공하여 슬롯안테나 형태의 플라즈모닉 소자를 제작하고 투과도를 측정한 결과, 매우 우수한 공명 투과 특성을 보였다. 또한, 저항이 높아질수록 공명 투과의 적색편이 현상과 Q-factor 의 감소를 동시에 확인하였다. 즉, 면저항 조절을 통해, 가변적이며 유한한 광학상수를 가지는 플라즈모닉 소자의 개발이 가능할 것이다. AgNW 네트워크 박막은 광학적으로 투명하며 고전도성을 필요로 하는 다양한 광학기기 개발에 활용될 것으로 기대된다.

P2-Op.033

The Color Temperature, Chromaticity Binning control with White LEDs

*박승현, 정상헌 [1], 류상완 [2]
*Seung Hyun. Park, Sang Hern. Jung[1], Sang Wan. RYU[2]
한국광기술원/전남대학교. [1] *케이케이디씨.* [2] *전남대학교.*

Keyword : LED, Color temperature, Chromaticity, Binning, Packaging

백색 LED 에서의 Color Temperature, Chromaticity 의 binning 은 생산수율을 결정하는 가장 중요한 요소이다. Binning 은 LED 를 적용하는 모든 산업분야에 있어서 생산 시간, 수율, 원가등에 가장 중요한 요소로 자리잡고 있으며, 최근 이런 경향이 더욱 강화되고 있다.[1] Color temperature, Chromaticity 에 대한 분류 기준은 ANSI C.78 2008 규격에 제시된 바와 같이 적용되고 있다. Color temperature 에 대하여 균일성이 강조된 백색 LED 를 요구하고 있는데, 백색 LED 의 균일성은 Macadam Ellipse 로 표현되고 있다. 백색 LED binning 은 청색 LED 소자의 특성 분포와 황색,녹색,적색 형광체 소자의 균일한 분포 및 이를 수행할 수 있는 공정이 필수적으로 요구된다.[2] 현재 더 좋은 Beam 품질과 각도별 colordifference 가 달라지는 것을 억제하기 위하여, 해외업체에서는 LED chip 에만 균일하게 coating 하는 Concept 로 Conformal coating 및 remote 방법을 적용하여 백색 LED PKG 를 구현하는 기법이 적용되고 있다.[3] conformal coating 기법은 형광체 sheet 부품을 별도로 제작하고, 이를 백색 LED 에 부착하는 방법으로, Macadam ellipse 를 최소화 할 수 있는 공정법이다.
본 논문에서는 binning 및 Macadam Ellipse 분포 및 개선하기 위한 방법을 이해하기 위하여, Remote phosphor 공정법을 활용한 백색 LED 의 color temperature, Chromaticity 의 분포 상관성을 분석하고, 이를 통해 기존 white LED 생산 방식과 비교하여 향상된 color consistency 를 구현할 수 있음을 제시한다.

[1] S. Chhajed, Y. Xi, Y.L. Li and Th. Gessmann, E. F. Schubert, J.A.P. 97, 054506(2005)
[2] Kewei Chen, Lee, S.W.R, Dept. of Mech. Eng, Hong Kong Univ. 2010 11th international Conference on Electronic packaging technology.
[3] C. Sommer, J. R. Krenn, P. Hartmann, P. Pachler, M. Schweighart, S. Tasch, G. Leising, and F. P. Wenz, Japanese
Journal of Applied Physics, vol. 48, pp.070208, Dec. 2009.

P2-Op.034

전방향으로 발광하는 Bulb 형 LED Lamp 의 광학계 설계 및 분석
(Analysis of Optical System Design for Omni-directional LED Bulb Implementation)

장재현, 원예림, 유영문, 이문재, *김종태
Jae Hyun. Jang, . , . , . , *Jong Tae. Kim
부경대학교.

Keyword : 조명설계, 광학계설계, LED Lamp

현재 전방향으로 발광하는 Bulb 형 LED Lamp 를 구현하기 위해 복잡한 반사판 구조물을 설치하거나 수직방향으로 LED 패키지를 실장 하는 방식으로 제작 되고 있다. 본 논문은 2 차 광학계를 사용하여 Energy Star 규격에 만족하도록 Bulb 형 LED Lamp 를 제작하기 위하여 조명 광학적 시뮬레이션 하였다. 광학계의 주요 구성 요소는 COB LED 패키지, LED Lamp 의 Cap, 반사판, 확산판으로 구성되어 있으며, 조명광학 설계를 위해 시뮬레이션 프로그램은 LightTools software 를 사용하였다. 전방향으로 발광하는 Bulb 형 LED Lamp 의 메커니즘은 광원으로부터 발생된 빛이 Cap 안쪽 면에 부분 코팅된 반사판에 반사되어 후방으로 나아가고 반사된 빛은 확산판을 통과하면서 산란된다. 위의 방식으로 Bulb 형 LED Lamp 는 Energy Star 의 배광 규격과 색도 규격(IES LM-79-08)을 만족 하도록 하였다.

P2-Op.035

LED 광원 확산을 위한 조명용 광학 Lens 설계에 관한 연구
(Illumination Optical Lens Design for LED Source Diffusion)

*김종태, 장재현, 유영문, 박은미
*Jong Tae. Kim, . , . , . .
부경대학교.

Keyword : LED, 조명설계, 광학설계, 확산렌즈

반도체 광원으로 LED 을 이용한 분야가 급속히 증가하면서 LED 광원이 가지고 있는 제한적인 빔 확산성이나 광도분포 특성을 제어하기 위한 방법이 다양한 분야에서 연구와 개발이 이루어지고 있다. 본 연구에서는 LED 광원의 확산각을 확대하기 위한 beam shape 조명 Lens 를 설계 하였으며, 그 응용으로서 LED TV 등과 같은 BLU(Back Light Unit) 광학계에 접목하여 그 성능을 평가하였다. 설계한 광 확산렌즈는 LED 광원과 결합하여 조명용이나 확산용 광원으로 사용할 수 있으며, 다양한 조명분야에 응용이 가능하다.

P2-Op.036

레이저탐색추적기를 겸비한 적외선 공통 광학계 설계

*이혁재
*hyukjae. lee
한화탈레스.

Keyword : "적외선 광학계","레이저탐색추적기","공통광학계"

무장 비행체, 레이더 등의 군용 장치에서 표적을 추적하는 기존의 표적 추적 기술은 영상 추적과 레이저 스폿 추적이라는 두 가지 형태로 추적이 이루어지는데, 각각은 별도의 검출기 및 시스템으로 구성된다. 영상추적기는 주로 적외선을 사용하며, 적외선 광학계는 물체와 배경의 복사량의 차이를 영상화 함으로서, 야간이나 시정이 불량한 대기 상태에서 표적을 탐지할 수 있다.
한편, 레이저는 밝기(Brightness)가 매우 높고, 방향성(Directionality)이 우수하기 때문에 원거리에서 높은 에너지를 방출할 수 있다. 또한 레이저는 단색성(Monochromaticity)의 특성을 가지기 때문에 원하는 파장만 보낼 수도 있다. 이러한 특성으로 레이저 기술은 원격 탐지 및 추적분야에 사용되며, 이는 군사 분야에서 매우 유용할. 레이저 기술은 군사 표적의 손상 및 파괴 분야에도 사용된다.
기존의 광학계 및 추적장치는 레이저 추적 광학계와 적외선 영상 획득 광학계가 따로 분리 되어 있어, 각각의 시스템으로 한가지 기능 밖에 하지 못하는 문제가 있었으며, 레이저 추적 광학계와 적외선 영상 획득 광학계를 한 장비에 장착하더라도, 두 광학계의 센서간 영점정렬을 조절하고 수시로 점검해야 하는 어려움이 있었다.
본 논문에서는 적외선 영역과 레이저 파장을 동시에 검출하며, 레이저 추적 정확도를 향상시킬 수 있는 광학계를 설계하였다.

P2-Op.037

레이저빔 파면보정을 위한 적응광학장치의 측정 정확도 분석

권성옥, 박승규, 김동율, *백성훈
Seong-ok. Kwon, Seung-Kyu. Park, dong-lyul. Kim, *Sung-Hoon. BAIK
한국원자력연구원.

Keyword : 파면측정, 정확도, 적응광학, 파면보정, 샥-하트만센서

대기유동이나 레이저빔의 파면오차 보정을 위한 적응광학장치에서는 파면측정 장치를 사용하여 파면왜곡 상태를 측정하고 파면보정 장치로 이러한 파면왜곡을 보정하게 된다. 따라서 파면측정장치에서의 파면측정 오차는 적응광학장치의 성능저하로 이어지게 된다. 본 연구에서는 CCD 카메라와 배열렌즈를 사용하여 Shack-Hartmann 파면센서를 개발하고, 개발된 파면측정센서의 측정 정확도를 상용의 파면측정 센서와 간섭계와 비교하여 분석하였다.

P2-Op.038

도플러 라이다를 이용한 3 차원 바람장의 측정 및 가시화

권성옥, 박승규, 김동율, *백성훈
Seong Ouk. KWON, Seung-Kyu. Park, donglyul. Kim, *Sung-Hoon. BAIK
한국원자력연구원.

Keyword : Doppler lidar, VAD scan, Wind field, Velocity measurement

도플러 라이다 시스템은 공기분자나 입자에 산란되어 돌아오는 레이저빔 주파수의 변이(shift)를 경계필터를 사용하여 측정함으로써 바람장의 속도나 방향을 측정하는 장치이다. 본 논문에서는 흔히 radar 기술에 사용되는 VAD(Velocity Azimuth Display) scan 방식을 펄스 레이저를 이용한 비간섭 도플러 라이다 장치에 적용하여, 대기중의 바람장의 속도 벡터를 측정하고 이를 3 차원적으로 가시화하였다.

P2-Op.039

고해상도 비냉각 열상 검출기를 이용한 광시계 광학계 설계 및 제작

*이종훈
*JongHoon. Lee
한화탈레스.

Keyword : "고해상도 열상 검출기", "인지", "광시계", "비열화"

본 논문은 차량용 열상 광학계를 제작하기 위해 고해상도 검출기 및 광시계 광학계의 효율을 최적화하는 열상광학시스템을 설계 및 제작하는 과정으로 구성된다. 고해상도의 비냉각 열상 검출기를 적용하여 인지능력을 향상 시켰으며, 광학계는 광시계를 적용하여 운전자의 운용편의성을 증대하였다. 열상광학계에서 중요한 요소인 비열화를 위해 초점구동 방식을 채택하여 온도에 따른 자동 비열화를 구현하였다. MTF 는 Nyquist Frequency 에서 50%이상의 회절한계에 가까운 성능을 만족 하며, 광시계를 가지는 광학계에서 중요한 성능요소인 왜곡은 5% 이내로 광학계를 설계/제작하였다.

P2-Op.040

디지털 홀로그래픽에서의 해상도 향상연구

*나실인, 신상훈 [1], 유영훈
*Na Sil-In. , Shin Sanghoon. [1], YU Young Hun.
제주대학교. [1] 케이피에스.

Keyword : Holography,Digital holography

빛을 이용하여 3 차원 측정하는 방법은 크게 2 가지 방법, 즉 파면을 측정하는 방법과 파면의 기울기를 측정하는 방법이 있다. 파면을 측정하는 방법인 간섭방법은 매우 정밀하게 3 차원 형상을 측정 할 수 있으나 측정하려는 단차가 사용하는 파장보다 큰 경우에는 단차를 정확하게 측정하기 힘들다. 이를 보완하기 위하여 다 파장 간섭법과 액체를 이용하는 방법이 연구 되고 있다. 다 파장 간섭법은 각각의 파장으로 위상 데이터를 구하고 이를 수학적으로 처리하여 원래의 파장보다 큰 가상 파장을 만들어 측정하는 방법으로 매우 성공적으로 사용되고 있다. 또 다른 방법으로 액체를 이용하는 방법은 액체를 이용하여 상대적 경로차를 적게 하여 측정하는 방법으로 단일 파장을 이용하여 실험구성이 간단하고 잡음 증폭 없이 측정할 수 있지만 해상도가 떨어지는 단점이 있다. 본 연구에서는 액체를 이용한 디지털 홀로그래픽에서 해상도를 유지하면서 큰 단차를 측정 할 수 있는 방법에 대하여 연구하였다.

P2-Op.041

Effect of Mn dopant concentration in $Cd_{0.5}Zn_{0.5}S/ZnS$ Core/Shell Quantum Dots on energy-down-shift effect for enhancing Power-conversion-efficiency in Silicon Solar Cells

*이승재, 고윤혁 [1], 모하메드 잘랄라 [1], 심태현 [1], 박재근 [1]
*Seung-Jae. LEE, Yun-Hyuk. Ko[1], Jalalah. Mohammed[1], Tae-Hun. Shim[1], Jeagun. PARK[1]
한양대학교 대학원. [1] 한양대학교.

Keyword : "energy-down-shift ", "quantum dots (QDs)", "silicon solar cells ",

The energy-down-shift having energy-tuning effect of Mn doping concentration in $Cd_{0.5}Zn_{0.5}S$–ZnS core–shell quantum dots on power-conversion efficiency enhancement in silicon solar cells was investigated for the first time. It was found that Mn doped $Cd_{0.5}Zn_{0.5}S$–ZnS core (6.83 nm in diameter)–shell (4.81 nm in thickness) quantum dots (QDs) demonstrated a typical energy-down-shift from 2.76-4.96 eV to 2.05-2.12 eV, which absorbs ultra-violet (UV) light (250–450 nm in wavelength) and emits yellow-orange visible light (583, 602 and 604 nm in wavelength). They showed the quantum yield of ~59 % and their coating on the SiN_X film textured p-type silicon solar-cells enhanced the external-quantum-efficiency (EQE) of ~16 % at 300–450 nm in wavelength, thereby enhancing the short-circuit-current-density (J_{SC}) of ~1.42 mA/cm^2, and the best power-conversion-efficiency (PCE) of ~0.55 % (relatively ~3.19 % increase compared with the reference p-type silicon solar cells without QDs). In particular, it was observed that the PCE of the solar cell was peaked at the 0.064 M Mn doped QD layer. We report effect of Mn dopant concentration in $Cd_{0.5}Zn_{0.5}S/ZnS$ core/shell quantum dots on energy-down-shift effect for enhancing power-conversion-efficiency in silicon solar cells.

P2-Op.042

Passive mode-locking of a mid-IR Cr:ZnS laser with graphene saturable absorber

*김진선, 최선영 [1], 김미혜 [1], 김준완 [1], 이지수, 송동훈, 신동호, 정문연, Fabian Rotermund[1], 조원배
*Jin Sun. Kim, Sun Young. Choi[1], Mi Hye. Kim[1], Jun Wan. Kim[1], JiSu. Lee, Dong Hoon. Song, Dong Ho. Shin, Moon Yeon. Jung, Fabian. Rotermund[1], Won Bae. CHO
한국전자통신연구원. [1] 아주대학교.

Keyword : "Mid-IR". "Cr:ZnS","graphene","saturable absorber","fs laser"

We report on passive mode-locking of a solid-state Cr:ZnS laser by using a transmission-type graphene saturable absorber. To minimize insertion losses in the laser cavity, high-quality monolayer graphene transferred on a CaF2 substrate was placed in Brewster's angle. The mode-locked laser delivers 165 fs pulses at 2.29 μm with a maximum output power of up to 270 mW at 7.3 W incident pump power.

P2-Op.043

주기가변 나선형 교번자장기 특성 분석 및 테스트

*문정호, 정영욱 [1], Nikolay Vinokurov[1], 이기태 [1], 장규하 [1], 박성희 [1], 배상윤 [1], 김현우 [2], 박선정 [3], Sergey Vladimirovich Miginsky[1], 전민용
*Jungho. Mun, Young Uk. JEONG[1], Nikolay. Vinokurov[1], Ki Tae. LEE[1], Kyu Ha. Jang[1], Seong Hee. PARK[1], Sangyoon. Bae[1], Hyun Woo. Kim[2], Pakr Sun jeong. [3], Sergey. Miginsky[1], Min Yong. JEON
충남대학교. [1] 한국원자력연구원. [2] 과학기술연합대학원대학교. [3] 경북대학교.

Keyword : 자유전자레이저, 교번자장기, 테라헤르츠

자유전자레이저의 발진파장은 전자빔의 에너지, 교전자장기의 자기장 세기 및 주기길이에 의해 결정된다. 본 연구는 자기장의 세기를 일정하게 유지하면서 자기장의 주기를 조절하여 파장을 가변 할 수 있는 주기가변 나선형 교번자장기에 관한 것이다. 개발된 교번자장기는 발진되는 빛의 파장이 400 ~ 600 micrometer 사이에서 조절될 수 있도록 주기의 길이를 23.3 ~ 25.6 mm 까지 가변 할 수 있고, 각각의 주기길이에서 교번자장기 갭에서의 최대 자기장은 0.97 T 이다. 주기성(periodicity) 및 자기장 세기의 정밀도는 각각 1%, 0.7% 이하 이고, 주기길이 25.6 일 때 RMS phase error 는 3.7 degree 로 초기 목표치를 만족하였다. 개발된 교번자장기는 보안 검색을 위한 소형 테라헤르츠 자유전자레이저 장치 개발에 적용될 것이다.

P2-Op.044

파장별 대기 투과 특성을 고려한 레이저 원거리 송수신 특성 분석

*윤창준
*Yoon Chang Jun.
한화탈레스.

Keyword : 대기 투과, 레이저 송수신

원거리 레이저 송수신 광학 시스템 설계 및 제작에 있어, 대기 투과 특성 및 대기 왜란 특성 예측이 필요하다.
본 연구는 레이저 송수신에 사용되는 근적외선 레이저 파장이 갖는 대기 특성을 고도별도 분석하고, 분석된 결과를 토대로 대기 투과 특성 모델링을 수립하였다. 이와 함께 대기 왜란 특성도 함께 분석하여 원거리 레이저 송수신 특성을 구체적을 모델링 할수 있게 수립하였다. 본 연구에 사용된 분석 툴은 Modtran 을 사용하여 특성 분석을 수행을 하였다.
그리고, 본 연구를 통해 수립된 대기 투과 특성 모델링을 적용하여, 최대 원거리 레이저 송수신 능력을 추가로 분석하였다.

P2-Op.045

Perpetual rotation of micro-objects by linearly-polarized light in an optical tweezer

*황한석, 김재완
*Hanseok. Hwang, Jae-Wan. KIM
명지대학교.

Keyword : optical tweezer, optical manipulation, optical trapping, orbital angular momentum,

Optical tweezer is technique to manipulate the micro-particle with laser. Study manipulating birefringent micro-particle using laser with optical angular momentum have been reported. We report a perpetual rotation of micro-particle induced by light in our optical tweezer experiment. The light is laser with linearly polarized and TEM00 mode. The particles are composed of non-birefringent material(polystyrene) and have irregular shape. When particles are rotated, the polarization of the light scattered by the particle do not alter almost. The intensity profile of the forward scattered light is significantly modified showing spatial components of zero intensity at the center. We attribute the perpetual rotation of the asymmetric shaped particle to the orbital angular momentum of light transferred to the particle.

P2-Op.046

Flat-type LED 조명에 있어서 산란패턴 방향에 따른 LGP 의 광학적 특성

*신용진, 박소희, 방태환
*SHIN Yong-Jin. , so hee. Park, Bang Tae Hwan.
조선대학교.

Keyword : LED lighting, Light guide panel, Scatterer pattern, Waveguide

Flat-type LED 조명은 측면 광원으로부터 나오는 빛을 반사판 및 도광판을 통해 평면광의 형태로 형성하기 때문에 박형화에 유리하고 비교적 적은 수의 LED 를 사용할 수 있다. 그러나 대면적 조명시스템에 적용되는 고출력 LED 광원은 램버시안(Lambertian) 배광 형태를 지니기 때문에 점 눈부심(point glare) 또는 불쾌 눈부심(discomport glare)을 나타나고 있으며, 전반적으로 휘도 및 균일도의 저하를 가져온다. 따라서 본 연구에서는 도광판의 산란패턴 방향을 조정하여 잔존하는 눈부심을 제거하고, 휘도의 비균일성 및 비효율성의 문제점을 해결하였다. 먼저 전산모사를 통하여 광원의 방향과 수직으로 배열된 산란패턴의 경우 측면으로의 균일성을 향상시키며, 평행하게 배열된 산란패턴은 도파관 역할을 함으로써 낮은 출력의 LED 를 적용하고도 높은 효율성을 높여주는 광학적 특성을 알 수 있었다. 이러한 전산모사의 결과를 초정밀 레이저로 대면적 도광판을 가공하여 Flat-type LED 조명시스템을 구현하였다. 전산모사와 레이저 가공에 의한 도광판의 광학적 특성이 일치하였다. 따라서 대면적 Flat-type LED 조명에 있어서 도광판의 산란패턴의 방향을 조정하는 것이 휘도의 균일도 및 효율성을 높이는데 효과적인 방법이 될 수 있음을 확인하였다.

P2-Op.047

Study on the Light Guide Plate with curved V-Groove Patterns in Edge-Lit Backlight

*박소희, 신용진
*Sohee. PARK, Yongjin. SHIN
조선대학교.

Keyword : back-light unit (BLU), light guide panel (LGP), V-Groove pattern, Luminance

V-Groove pattern for light diffusion was designed as a curve at the bottom of the light guide plate (LGP) to enhance the light incident efficiently optimizing the structure of the LGP that applied to an Edge-Lit Backlight. We performed a comparative analysis of the luminance and uniformity through simulations to predict the optical properties of the proposed scattering pattern by applying appropriate parameters. As a result, the loss of light intensity was able to minimize by arranging the angle-adjusted v-groove pattern as a curve considering the property of the optical to inside of the LGP. Even though the number of the pattern was reduced more than 70% by angle-adjusted v-groove pattern, it was able to fulfill the great improvement of the luminance uniformity.

P2-Op.048

(5,4), (6,4), (7,3) 단일벽 탄소 나노 튜브에서 관측된 이중 방사형 호흡 진동모드들

*신성일, 주태하 [1], 임용식
*Seong-Il. Shin, Tai-Ha. Joo[1], LIM Yongsik.
건국대학교. [1] 포항공과대학교.

Keyword : "SWCNT","RBM","Nanotube","LPSVD"

펨토초 펄스를 사용하여 단일 카이랄 구조를 갖는 단일벽 탄소 나노 튜브에서 여기-탐사방법으로 결맞은 격자 진동을 발생시키고 측정하였다. 모드 잠금된 티타늄 사파이어 레이저를 이용하여 650 nm - 1100 nm 까지 광대역 선폭을 갖는 약 6 fs 극초단 펄스를 발생시켰다. 탐사광 파장 변화는 720 nm - 1040 nm 까지로, 샘플 통과 후 여러 간섭필터 (bandpass filter)를 사용하여 5 nm 간격으로 중심파장을 변화시키는 주파수(파장) 분해 방법을 사용하였다. 이는 주파수(파장) 분해 및 시분해 분광기법을 동시에 적용할 수 있는 측정 기법으로, 기존에 나노 물질 특성 분석을 위해 수행되어 오던 기법들(전자 및 X 선 현미경법, 라만 및 형광 분광측정법 등)에 비해 독특한 여러 장점을 갖는다. 이미 지난 연구에서는 단일 카이랄로 정제된 반도체 특성의 고순도 (6,5) 탄소 나노 튜브로부터 이론적으로 가능한 18 개의 고유 진동 모드들을 계산하였고, 이들 간의 조합모드로 나타난 14 개의 모드들을 검출하고 분석하였다.(1)
본 연구에서는 순간흡수율 변화를 측정하는 여기-탐사기법에서 관측되는 방사형 호흡모드(Radial Breading Mode:RBM, 튜브직경이 호흡하듯 동시에 커졌다가 축소하는)가 하나가 아니라, 두 개(doublet)로 관측됨을 보고하고자 한다. 인접한 주파수를 갖는 진동모드들을 보다 정확하게 분해하고자, 보통 사용되는 고속 푸리에 변환방법과는 다른 푸리에 기법, LPSVD(linear prediction by singular value decomposition)기법을 활용하였다. 관측된 두 개의 방사형 호흡모드들은 각각 기저상태와 제 1 여기( ) 전자 구조와 각각 결합하는 격자진동 준위들로부터 발생될 수 있으며, 관측된 제 1 여기( ) 전자 구조와 결합하는 격자진동 주파수는 튜브 종류에 따라 기저상태와 결합하는 격자진동 주파수보다 더 큰 값을 갖거나, 또는 더 작은 값을 갖는다. 그림 1 과 같은 초기 위상 거동으로부터, (5,4) 튜브(type 1)의 경우에는 기저상태 결합 격자진동 주파수는 373cm-1 이며, 제 1 여기상태 결합 격자진동 주파수는 370cm-1 임을 추론할 수 있었으며, (6,4) 튜브(type 2)의 경우에는 기저상태 결합 격자진동 주파수는 337cm-1 이며, 제 1 여기상태 결합 격자진동 주파수는 333cm-1 임을 추론할 수 있었다. (7,3) 튜브(type 3)의 경우에는 기저상태 결합 격자진동 주파수는 329cm-1 이며, 제 1 여기상태 결합 격자진동 주파수는 326cm-1 임을 추론할 수 있었다. 이는 기저상태 결합 격자진동 주파수만 측정하는 라만 분광법과는 달리, 여기-탐사기법은 기본적으로 기저상태 뿐 만 아니라 여기상태와 결합된 격자진동 준위들을 동시에 측정할 수 있는 제 3 차 비선형 현상으로, 이의 특성을 규명하고자 한다.

P2-Op.050

Yb 첨가 광섬유 레이저의 발진 특성 연구

오민, 김진권, 박준영 [1], 장원종 [1], 이동관 [1], 이한결 [1], 김경융 [1], *이종훈
Min. Oh, Jinkwon. Kim, Jun Young. Park[1], Wonjong. Chang[1], Dong Kwan. Lee[1], Han Gyeol. Lee[1], Kyung Yung. Kim[1], *Jonghoon. Yi
영남대학교. [1] 대구과학고등학교.

Keyword : 광섬유 레이저, 공진기, 출력 특성

Yb 가 첨가된 LMA(Large Mode Area) 광섬유를 다이오드 레이저로 여기하였다. 코어의 직경이 100 um 인 광섬유에서 나오는 여기 다이오드 레이저의 파장은 915, 974 nm 이고 출력은 최대 20 W 이다. Yb 첨가 광섬유의 직경은 6, 10, 25 um 이었다. 여기다이오드의 파장이 각각 915 nm 혹은 974 nm 인 경우에 대하여 출력경의 반사율을 다양하게 변화시키면서 여기 다이오드의 출력에 따른 출력의 변화를 측정하여 최대 출력이 나오는 조건과 문턱 발진 조건, 기울기 효율 등을 조사하였다.

P2-Op.051

Prevention of Whisker Growth in Aluminum Electrodes of Microfabricated Ion-Trap Chips Operating in Ultra High Vacuum

이민재, 홍석준, 천홍진, 안준식 [1], 김태현 [1], *조동일
Minjae. LEE, Seokjun. HONG, Hongjin. Cheon, Jun Sik. Ahn[1], Taehyun. Kim[1], *Dong-il. Cho
서울대학교. [1]SKT.

Keyword : quantum information, ion trap, MEMS, microfabrication, aluminum whisker

Advancements in quantum information processing (QIP) have fostered appreciably increased research interests in large-scale integration of ion trap arrays in recent years. Silicon-based microfabrication is one of the most important candidates for such implementations, owing to the technology's scalability. Au has been commonly used as the electrode material in non-silicon-based microfabrication technologies, but Al is more readily compatible with silicon-based microfabrication [1]. However, a major problem in using Al as the electrode material is the growth of whiskers on electrodes attributed to the intrinsic compressive stress, which is a phenomenon that occurs while baking ion trap chambers to achieve the required ultra-high vacuum (UHV) environment. Since high RF voltages are used to trap ions, the growth of whiskers can lead to the electric arcing between electrodes, which in turn damages the ion trap electrodes. In this paper, a series of experiments with Cu-containing Al to prevent the whisker growth is presented.
[1] Seokjun Hong, Minjae Lee, Hongjin Cheon, Jun Sik Ahn, Min Hyung Kim, Taehyun Kim , and Dong-Il "Dan" Cho "Microfabrication of Trap Chips as a Scalable Platform for Ion Trap Quantum Information Processing", The Korean Physical Society Autumn Annual Conference 2014.
*Corresponding Author: dicho@snu.ac.kr

P2-Op.052

상온에서 동작하는 Yb:YAG 단결정 광섬유를 이용한 고출력 증폭기 시스템 개발

*이성만, 차용호, 김용희, 신재성, 고광훈, 임권, 이림, 박현민, 김택수, 정도영
*Sungman. Lee, CHA Yong-Ho. , Kim Yonghee. , Shin Jae Sung. , KO Kwang Hoon. , Gwon. Lim, anticlimax. , PARK Hyun Min. , KIM Taek-soo. , JEONG Do-Young.
한국원자력연구원.

Keyword : Yb:YAG 단결정 광섬유, 단결정 광섬유 증폭기, ns 펄스 레이저

광섬유 전치 증폭기를 통과한 1030 nm 에서 발진파장을 갖는 레이저 빔의 출력증폭을 위해 상온에서 동작하는 Yb:YAG 단결정 광섬유를 이용하는 출력증폭기 시스템이 설계 제작되었다. 수십 MHz 의 좁은 레이저 선폭을 갖는 DFB 레이저 다이오드에서 발생하는 시드 레이저 빔을 증폭하는 레이저 증폭 계열에서 출력 증폭을 위해 단일모드 광섬유나 PCF (Photonic Crystal Fiber) 광섬유들을 출력 증폭기로 사용할 경우 고품질을 유지하기 위해서 출력 증폭기로 사용되는 상대적으로 긴 길이를 갖는 단일 모드 광섬유에서 발생하는 SBS (Stimulated Brillouin Scattering)을 포함한 강한 비선형 산란효과들이 고품질의 빔질과 고출력을 동시에 갖는 증폭시스템 개발에 제약 조건이 된다. 이러한 고출력 증폭기에서 발생하는 비선형 효과 문제를 완화하고, 고품질과 고출력을 동시에 얻기 위한 Yb:YAG 단결정 광섬유를 기반으로 하는 고출력 증폭기 시스템이 설계 제작되었다. 사용된 Yb:YAG 단결정 광섬유는 1.0 at.%의 Yb-도핑율이 사용되었고, 1 mm 의 직경과 약 40 mm 의 길이를 가지고 있다. 여기용 레이저로 4 개의 100 W 급 레이저 다이오드를 광섬유 빔결합기(4X1)로 결합하여 사용하였으며, 단일 종면 여기 방식에서 레이저 결정 내의 열초점 변화가 계산되었다. 레이저 매질 내의 열초점 변화를 고려한 증폭레이저 시스템의 입사빔의 결합광학계와 여기레이저 빔의 결합광학계가 최적 설계되었으며, 이를 이용한 Yb:YAG 단결정 광섬유 출력증폭기의 상세한 증폭 특성을 보고한다.

P2-Op.053

구면 망막 영상의 외부 추출을 위한 relay lens 기반의 안구 모델 설계
Extracting the image off the human retina: the optical relay system

*최형순, 남기봉
*Hyoung Soon. Choi, NAHM Kie Bong.
한림대학교.

Keyword : "사람의 시력"

사람의 시력에서, 망막은 구면형태를 하고 있어서 눈의 결상광학계가 만드는 영상의 만곡에 대하여 포용범위가 넓다. 그러나 곡면을 따라 형성되는 영상을 평면센서로 감지하는 경우에는 필름의 경우와 동일한 수차의 영향을 받게 된다. 교육용 등의 목적으로 이러한 결상 현상을 직접 확인하기 위해서는 결상소자를 망막, 특히 황반에 해당되는 위치에 두면 되지만, 안구 내부에는 유리체액이 채워져 있어서 CCD 센서를 액체와 접촉하면서 망막에 배치하여 실제 영상을 실시간으로 확인하는 것은 기술적 난제이다.
본 연구에서는 실제 안구에서와 같이 액체로 채워진 안구의 망막에 결상된 영상을 외부로 전달하여 CCD 상에 상면만곡을 최소화하여 결상시킬 수 있는 realy lens 가 부착된 안구모델을 CODE V 로 설계하고 이를 이용하여 실제 안구를 제작하여 이로부터 결상되는 시스템의 특성을 연구하였다. relay 렌즈는 기성 제품 중에서 설계사양에 가장 가까운 것을 사용하여 영상이 얻어짐을 확인하였다.

P2-Op.054

저시력 시뮬레이터용 필름의 광학적 특성 분석

양석준, 육주성, 성훈금, 육소영, 강경환, 김용권, 배석환, *최은정
Seok-Jun. , Ju Sung. Yuk, Hoon Geom. Sung, So Young. Yuk, Kyoung Hwan. Kang, Yong Gwon. Kim, Seok Hwan. Bae, *Eun Jung. Choi
건양대학교.

Keyword : "저시력 시뮬레이터", "투과율", "시력", "백내장"

정상인들이 다양한 안과적 질환을 체험해 볼 수 있도록 고안된 저시력 시뮬레이터(Low vision simulators, Fork in the Road, USA)에 내장된 필름의 광학적 특성을 조사하였다. 필름의 분광투과율을 분광광도계(UV-2450, Shimadzu, Japan)로 가시광선 범위(380 ~ 780 nm)에서 5 nm 간격으로 측정하였다. 분광투과율의 전반적인 경향은 장파장 대역에서는 비교적 일정한 값을 유지하다가 단파장 대역으로 갈수록 서서히 감소하는 추세를 보이고 있었다. 필름은 흰색을 띠고 있는데, 이는 확산 처리된 필름의 표면으로부터 모든 파장의 빛이 산란되기 때문이다. Lamber-Beer 법칙과 최소자승법을 이용하여 도출한 저시력 시뮬레이터용 필름의 평균투과율은 91.92%인 것으로 나타났다. 필름을 겹쳐가면서 시력을 측정한 결과, 시력은 필름의 투과율에 따라 비례하여 감소하는 것으로 나타났는데, 이러한 특징은 백내장으로 인한 수정체 혼탁에서 나타나는 시력 감소와 유사한 특징을 보이는 것이었다. 따라서 연구에 사용된 저시력 시뮬레이터는 백내장 질환을 시늉내는 도구로서 활용될 수 있을 것으로 사료된다.

P2-Op.055

안경 렌즈의 반사 코팅이 투과율에 미치는 영향

양석준, 육주성, 성훈금, 육소영, 조현주 [1], *최은정
Seok Jun. Yang, Ju Sung. Yuk, Hoon Geom. Sung, So young. Yuk, Hyun Ju. Cho[1], *CHOI Eun Jung.
건양대학교. [1] *대덕대학교.*

Keyword : 반사 코팅,안경 렌즈,투과율,반사율

안경 렌즈의 반사 코팅이 안경 렌즈에서 시각적 능력에 주된 영향을 미치는 투과율에 어떠한 영향을 미치는지 연구하였다. Essential 사의 Macleod 를 사용하여 430 ~ 440nm 에서 최대 반사율 5, 10, 15, 20, 25, 30%을 갖는 반사 코팅을 설계한 후 Synopsys 사의 Lighttools 프로그램으로 반사 코팅을 적용시킨 안경 렌즈의 중심부 투과율 변화를 분석하였다. 반사 코팅이 적용된 안경 렌즈의 투과율은 AR 코팅이 적용된 안경 렌즈의 투과율에 비하여 반사 코팅의 반사율이 증가 할수록 중심부의 투과율은 점차 감소하였고 주변부의 투과율은 비슷하였다. 안경 렌즈의 반사 코팅의 반사율 증가는 중심부 투과율에 영향을 미치는 것을 알 수 있었다.

P2-Op.056

안경 렌즈의 반사 코팅으로 인한 미광에 대한 연구

양석준, 육주성, 성훈금, 육소영, 조현주 [1], *최은정
Seok Jun. Yang, Ju Sung. Yuk, Sung Hoon. Geom, So Young. Yuk, Hyun Ju. Cho[1], *CHOI Eun Jung.
건양대학교. [1] *대덕대학교.*

Keyword : 반사 코팅, 안경 렌즈, 고스트 이미지, 미광

안경 렌즈의 반사 코팅에서 고스트 이미지를 발생시키는 미광에 대하여 분석하였다. Essential 사의 Macleod 를 사용하여 안경 렌즈의 반사 코팅 6 가지와 AR(Anti-Reflect)코팅을 설계한 후 Synopsys 사의 Lighttools 프로그램을 사용하여 안경 렌즈의 미광을 분석하였다. AR 코팅을 적용시킨 안경 렌즈와 반사 코팅을 적용시킨 안경 렌즈는 안경 렌즈의 주변부에서 비슷한 값을 나타내었다. 이로써 반사 코팅이 적용된 안경 렌즈의 고스트 이미지를 발생시키는 미광은 AR 코팅이 적용된 안경 렌즈와 비슷함을 알 수 있었다.

P2-Op.057

LED 의 색온도 변화가 색지각 능력에 미치는 영향

양석준, 육소영, 육주성, 성훈금, *최은정
Seok Jun. Yang, So Young. Yuk, Ju Sung. Yuk, Hoon Geom. Sung, *CHOI Eun Jung.
건양대학교.

Keyword : LED, 색온도, 색지각

LED 광원의 색온도의 변화가 색지각 능력에 미치는 영향을 조사하였다. 본 연구에서는 LED 광원이 색온도를 변화에 따라 안질환이 없는 20 대 정상인을 대상으로 색 지각과 색 식별범위의 변화 양상을 파악하는 것을 목적으로 하며, 평가 장비로는 휴테스트(Hue Test, Muncell color, USA)를 이용하여 안질환이 없는 20 대 정상인를 대상으로 색표를 축색하고 육안평가실험을 실시하여 비교, 분석하였다 그 결과 색온도가 증가함에 따라 색인지 능력이 감소하는 경향을 보였다. LED 광원의 색온도 변화에 따라서 색인지 능력이 변하였다. 이로써 광원의 색온도 변화는 색지각 능력에 영향을 미치는 것을 알 수 있었다.

P2-Op.058

안개시 시인성을 고려한 LED 밝기 변화의 허용치

양석준, 육주성, 성훈금, 육소영, *최은정
Seuk Jun. Yang, Ju Sung. Yuk, Hoon Geom. Sung, So Young. Yuk, *CHOI Eun Jung.
건양대학교.

Keyword : 안개, LED, 시인성, 투과율

안개시 시인성을 고려한 LED 광원 밝기의 정도를 연구하였다. 본 연구에서는 시인성을 고려하여 안개시 LED 광원 밝기 변화 허용치가 어느정도 될 것인지를 평가하고자 하였다. 연구 환경을 조성하기 위하여 자체 제작한 가로 높이 1m, 길이 3m 의 경통을 이용하였고, 시력을 측정하며 안개의 투과율을 측정하였다. 그 결과, 안개시 LED 광원의 밝기의 허용치에 대한 지수를 도출할수 있었다. 안개시 LED 광원의 밝기에 따른 전조등 밝기가 낮아짐에 따라 시인성의 정도는 다소 둔화되는 경향을 보였다. 안개의 투과율에 따라서 다양한 시인성을 보였고 이에 따른 LED 의 밝기 허용치가 나타났다, 다양한 변수가 존재하기 때문에 안개의 정도나 실제 환경에 맞게 다양한 변수를 적용 시킬수 있는 가변형 LED 광원이 좋을 것이라고 사료된다.

P2-Pl.001*

Study of Erosion and Redeposition of Plasma Facing Component in KSTAR during 2011 – 2014 campaigns

*이호선, 박준우, 소현섭, 홍석호 [1]
*Hosun. LEE, Jun-Woo. Park, Heon Seob. So, Suk-Ho. HONG[1]
Kyung Hee University. [1]National Fusion Research Institute.

Keyword : PFC, erosion, redeposition, hydrogenated carbon, ellipsometry

We have investigated the optical properties of amorphous hydrogenated carbon (a-C:H) films which were deposited in 2011, 2012, 2013, and 2014 Campaign at KSTAR, and studied the deposition mechanism and the transport characteristics of eroded impurities which follows preferentially magnetic field lines. Eroded carbon atoms and hydrocarbon molecules are deposited on silicon wafers positioned at different toroidal locations of KSTAR vacuum vessel. In order to estimate number of particles incoming towards silicon wafer, a cavity structure has been used. Two types of cavity structures are used to decouple the effect of ions and neutrals: the one is parallel to the magnetic field line, while the other is perpendicular to the field line.
We have analyzed the deposition thickness profile, microstructure, and optical properties of the a-C:H films by using transmission electron microscopy, spectroscopic ellipsometry (SE), and energy dispersive X-ray analysis (EDX). The surface composition of the films was measured by X-ray photoelectron spectroscopy (XPS). The thickness profile and the optical constants (n, k) were measured by SE. Raman spectroscopy was used to measure the microstructure and atomic bonds of the thin films. We have found that stainless steel components such as Fe, Cr, Ni, and Si were incorporated in a-C:H thin films. For the coupons attached near the neutral beam injection (NBI), films contain some percentage of Si came from Si substrate due to the physical sputtering by impact of high energy D ions. The phases of a-Si and Fe3O4 were found and sp2 bonds of a-C:H were ascertained with the overlap of D and G modes, identified by Raman spectroscopy. The width of the thickness profile of a-C:H films of vertical slits (poloidal gap) were narrower than those of horizontal slits (toroidal gap). The optical constants of the films deposited in 2011 and 2014 campaigns could be analyzed by using diamond-like-carbon (DLC) models, whereas effective medium approximation in combination of a-C:H and a-Si was used for the 2012 and 2013 campaigns to accommodate the NBI effect. The optical constants of the a-C:H films in Horizontal slits were different from those of Vertical slits, because the incident particles are both neutral and ion particle in Horizontal slits and are mainly neutral in Vertical slits. The total masses of the carbon erosion during each campaign was estimated and were compared to the total power of KSTAR.

P2-Pl.002

Investigation on the dependence of the local energy balance upon the collisionality in the drift-Alfven model

*안찬용, 김창배, 민병훈
*Chan-Yong. An, Chang-Bae. Kim, Byunghoon. Min
숭실대학교.

Keyword : plasma, turbulence, simulation

Electromagnetic drift wave turbulence of the plasma driven by the pressure gradient in the sheared magnetic field is simulated in the platform called BOUT++. Energy transport basically is balanced between the production due to the pressure gradient, the ExB nonlinear fluxes and dissipative dynamics. In the Fourier space the real part of the nonlinear fluxes redistribute energy
from the linearly unstable scales and the energies are damped out by the dissipations. It is expected that lower collisionality tends to move the peak of the energy spectrum toward larger scale. Characteristics of the nonlinear fluxes will be investigated depending on the size of the collisionality.

P2-Pl.003

Study of the energy-non-transporting nonlinear flux in the ion-temperature gradient plasma turbulence

*민병훈, 김창배, 안찬용
*Byounghoon. Min, Chang Bae. KIM, Chan Yong. An
숭실대학교.

Keyword : ion temperature gradient

Aspects of the nonlinear fluxes that are directly involved in the transport are investigated in the ion-termperature gradient turbulence. This work is motivated by the recent works that reveal the critical role of the anisotropic nonlinear flux in the Hasegawa-Wakatani (HW) model. In the HW model, part of the E×B nonlinear flux in the Fourier space indicates the advection along the diamagnetic drift velocity. Three-dimensional fluid simulations are performed and we analyze various cases of different temperature gradients and the magnetic shears. Cases with or without the zonal flows will be presented.

P2-Pl.004

Bend of Oversized Transmission line for KSTAR LHCD System*

*성태식, 조무현 [1], 남궁원 [1]
*Taesik. Seong, Moo-Hyun. CHO[1], Won. NAMKUNG[1]
포항공과대학교(POSTECH). [1] 포항공과대학교.

Keyword : Ohmic loss, Transmission line, LHCD, KSTAR, Bend

In the KSTAR LHCD system, RF power generated by the klystron is transmitted through waveguide to the Tokamak. As RF pass through waveguide, a current is generated on the surface of the waveguide. Ohmic loss which is generated by the current reduce a transmission efficiency. In the current LHCD system, oversized waveguide is used to reduce ohmic loss. But as the size of the waveguide is increased, a cutoff of the electromagnetic modes is lower. Hence current LHCD system makes the number of possible modes increases. On straight section of transmission line, there is no conversion of electromagnetic mode. On the other hand, the mode conversion occurs in the bending part of transmission line. The Mode conversion that occurs when RF pass through a bent section of transmission line is determined by the structure of bend. We propose a suitable bend for the KSTAR LHCD system that uses oversized transmission line.

P2-Pl.005*

Study of the transport parameter of hydrogen isotopes in CuCrZr for fusion applications

*변우준, 신해원, 서희정, 이석관 [1], 김희수, 노승정
*Woo Jun. Byeon, Hae Won. Shin, Hee Jeong. Seo, Seok Kwan. Lee[1], Hee Soo. KIM, Seung Jeong. NOH
단국대학교. [1] 한양대학교.

Keyword : CuCrZr, hydrogen, deuterium, transport parameters

CuCrZr, which is a precipitation hardened copper alloy, is an attractive heat sink for nuclear fusion because of its high thermal conductivity, good mechanical property, and strong radiation resistance. The permeation of hydrogen and deuterium in CuCrZr was experimentally measured by using the continuous-flow method, and the transport parameters (permeability, diffusivity, and solubility) of both hydrogen and deuterium were determined. We also investigated the isotope effect of the transport in consideration of the quantum mechanical effect based on a harmonic approximation, calculating the transport parameters of tritium by using the hydrogen and deuterium data measured in this study.

---

* "This work was supported by the National Research Foundation of Korea (Project No. 2015M1A7A1A01002234)."

P2-Pl.006

열탈착거동분석장치를 위한 유도결합플라즈마 소스의 빔인출부 최적화 실험
(Optimization of the beam extraction system of ICP Plasma Source for Thermal Desorption Spectroscopic System)

김희수, 이석관 [1], *변우준, 신해원, 서희정, 변재덕, 현준원, 노승정, 김도완 [2], 한준희 [2], 최동민 [2], 이철의 [2]
KIM Hee Soo. , Lee Seok Kwan. [1], *Byeon Woo Jun. , Shin Hae Won. , . , Byun Jae Duk. , HYUN June-Won. , NOH Seung Jeong. , Kim Do wan. [2], Han jun hui. [2], Choi. Dong Min[2], LEE Cheol Eui. [2]
단국대학교. [1] 한양대학교. [2] 고려대학교.

Keyword : 열탈착분석장치(Thermal Desorption Spectroscopic System), 이온빔소스, 수소동위원소

핵융합로에서 플라즈마와 직접 대면하거나 영향을 받는 대면재와 구조재는 수 eV 에서 수백 eV 의 영역을 갖고 있는 이온의 영향을 받는다. 이와 같은 과정에서 이온은 재질내로 침투하거나 표면에서 화학적인 침식, 기체버블을 형성하는 등 재질의 표면변화와 물성의 변화를 야기한다. 특히 핵융합로의 연료로 쓰이는 수소동위원소는 대부분의 재질에 대해서 높은 침투와 체류특성이 있으므로 핵융합로 내부와 외부를 구성하는 핵융합로재질의 역학적 물성의 열화를 이끈다. 재질에 침투한 수소동위원소의 정량적 측정을 위해서 이용되는 대표적인 장치는 열탈착분석장치(Thermal Desorption Spectroscopic System)이다. 보통의 경우 플라즈마 또는 이온조사된 시편을 열탈착분석장치로 옮기는 과정에서 대기에 노출되는 경우가 많으므로 재질내 기체의 정량적 분석에 문제가 있을 수 있다. 본 연구에서는 이온원으로서 유도결합플라즈마를 채용한 이온빔소스를 열탈착분석장치와 결합하여 저에너지 이온조사 후 외기노출없이 in-situ 로 열탈착분석을 수행할 수 있는 시스템을 구축하고 빔 인출조건을 최적화하는 실험을 수행하였다.

---

* "이 연구는 2015 년도 정부(미래창조과학부)의 재원으로 한국연구재단의 지원을 받아 수행되었음(No. 2015M1A7A1A01002234)."

P2-Pl.007

Turbulence spreading as a non-local mechanism of global confinement degradation

*이수민, 권재민, 함택수 [1]
*SuMin. Yi, JaeMin. Kwon, Taik Soo. Hahm[1]
국가핵융합연구소. [1] 서울대학교.

Keyword : tokamak, core ion energy confinement, non-local transport mechanism, turbulence spreading

In tokamak, local transport models tend to underestimate the level of transport and fail to explain important experimental observations. Non-local transport mechanisms can complement the weakness of the local models and provide a better picture to understand the experiments. In this contribution, we report a new non-local mechanism of the global confinement degradation and the profile stiffness. By performing global gyrokinetic simulations, we find that turbulence spreading into a marginally stable zone can increase turbulent transport to a level exceeding the predictions of the local theories. Also, we present the first quantification of the parametric dependence of turbulence spreading and resulting confinement degradation on toroidal rotation shear and magnetic shear: turbulence spreading is significant for high magnetic shears s>0.2, while it is slowed for low magnetic shears. The suppression of turbulence spreading by toroidal rotation shear is only effective for the low magnetic shears, which is in a good agreement with the experimental trends of core confinement improvement. Our findings suggest that the non-local mechanism is indispensable for an accurate transport modeling in tokamak plasmas.

P2-Pl.008*

광학적 방법을 이용한 플라즈마 내부의 티끌입자 진단

*심성용, 오차환, 정규선, 강인제, 박경득
*shim sung yong. , OH Cha Hwan. , CHUNG Kyu-Sun. , Kang In Je. , Park Kyungdeuk.
한양대학교.

Keyword : "plasma dust diagnostics","laser Rayleigh scattering","dusty plasma"

모든 핵융합 플라즈마에서는 티끌입자가 관측되며 토카막 내부에서 형성된 티끌입자는 토카막 운전에 악영향을 줄 수 있다. 본 연구에서는 플라즈마 내부의 티끌입자의 크기와 밀도를 진단함으로써 티끌입자 형성 및 티끌입자가 플라즈마에 미치는 영향을 조사하였다. 플라즈마 내부에서 tungsten 시료에 Nd:YAG pulse laser(wavelength : 532nm, pulse width : ~4ns, pulse energy : 250mJ)를 쏘아서 티끌입자를 생성하였다. 생성된 티끌입자의 밀도는 광학적 방법을 이용해서 진단하였으며, 티끌입자의 크기는 laser Rayleigh scattering 을 이용해서 진단하였다. 진단된 크기는 tungsten 시료의 SEM 사진과 비교하였다.

P2-Pl.009

수소 플라즈마에서 포화 흡수 분광 신호 측정

*박경득, 이원욱 [1], 오차환
*Park Kyungdeuk. , LEE Won Wook. [1], OH Cha Hwan.
한양대학교. [1] 한국원자력연구원.

Keyword : "포화흡수분광","수소플라즈마","Balmer-α 전이선","

본 연구에서는 DC glow discharge 챔버에서 생성된 수소 플라즈마에서 포화흡수분광(Saturated Absorption Spectroscopy) 신호를 측정하였다. 흡수 신호 측정에는 수소의 Balmer-α(n=3→n=2, 656.282nm) 전이선이 사용하였다. Balmer-α 전이선의 fine structure 는 3 개의 lower level 과 5 개의 upper level 로 구성되어 있고, selection rule 에 의해 7 개의 optically allowed transition 을 갖는다. 이에 따라 수소 원자의 흡수 신호는 7 개의 흡수 신호의 중첩으로 나타나고, 포화흡수 신호는 7 개의 주공진선 신호를 갖는다. 그리고 lower 또는 upper level 을 공유하는 두 개의 주공진선 신호들 사이에는 교차공진 신호가 나타나며, 수소의 Balmer-α 전이선의 경우 7 개의 교차 공진 신호가 있다. 해당 전이선의 파장을 갖는 diode laser 를 이용하여 External Cavity Diode Laser (ECDL) system 으로 레이저의 선폭을 $_0e^{\sigma\Delta Nz}$)에 따라 나타내었고, pump 광이 있을 때와 없을 때의 차이를 통해 포화흡수분광 신호를 측정하였다.

P2-Pl.010

Characteristics of Rotation, Temperature and Density Pedestal under non-axisymmetric fields in KSTAR

*고원하, 이형호, 이종하, 이승헌, 서동철, K. Ida[1], 전영무, 인용균, 윤시우, 곽종구, 오영국
*Wonha. KO, H.H.. Lee, J.H.. Lee, S. H.. Lee, D.C.. Seo, K.. Ida[1], Y.M.. Jeon, Y.. In, S.W.. Yoon, J.G.. Kwak, Y.K.. Oh
국가핵융합연구소. [1]NIFS. Japan.

Keyword : plasma rotation, non-axisymmetric fields, KSTAR

The recent tokamak research has been emphasizing that the plasma rotation plays an essential role in determining transport which is related in rotation shear and stability which is affected by increased rotation [1]. The toroidal and poloidal rotation and ion temperature profiles of the carbon impurity line are measured by charge exchange spectroscopy and it enables to understand the behavior of plasma especially for the non-axisymmetric fields in KSTAR [2, 3].
The non-axisymmetric fields make not only ELM suppression but also reduction of rotation in the KSTAR H-mode plasma. The effect of the non-axisymmetric fields appears on rotation, density and temperature profiles for different collisionality in KSTAR. There is being pedestal rotations which is term from intrinsic torque but core rotation disappears during the mode locking by non-axisymmetric fields on KSTAR. The poloidal and toroidal rotation dynamics and its physics is further investigated including the temperature.

References: T Tala, et al., Plasma Phys. Control. Fusion 49, B291 (2007).

Y. M. Jeon et al., Phys. Rev. Lett. 109, 035004 (2012).

W. H. Ko, et al., Nucl. Fusion 55 083013 (2015)

P2-Pl.011*

Effect of Plasma Parameters onf the behaviour of Edge Pedestal

*김상균, 나용수, 권오진 [1]
*SangKyeun. Kim, Yong Su. Na, Oh Jin. KWON[1]
서울대학교. [1] *대구대학교.*

Keyword : Edge pedestal, Pedestal height, EPED, peeling-ballooning

The width of the plasma edge pedestal, formed by the transport barrier, and the pressure at the top of pedestal (pedestal height) strongly affect the confinement of fusion plasma. To achieve the plasma of target performance in future devices (such as ITER, DEMO, etc), effective prediction and optimization of the edge pedestal are required. However, prediction of the pedestal height and width still has many uncertainties and understanding of its physics remains as a challenge. As part of an effort, we investigated the impacts of plasma parameters (such as ,, , , etc) on the edge pedestal. We adopted EPED model [1]; the edge pedestal predictive model which is based on the peeling-ballooning mode [2,3] and the kinetic ballooning mode (KBM) [2,4,5], to predict and understand the behaviour of the edge pedestal in terms of those plasma parameters. Numerical codes HELENA [6] and MISHKA [7] were used to calculate the plasma equilibriums and their stabilities. From this study, we found that triangularity () and largely affect the edge pedestal. To explain the behaviour of the edge pedestal, we propose a simple theoretical model. With this model, it was possible to explain the variation of the edge pedestal with respect to the plasma parameters and to predict its tendencies. Finally, we suggest ways to improve the height of the edge pedestal by modifying plasma parameters.

References: [1] P. B. Snyder et al 2009 Phys. Plasmas 16 056118

[2] J. W. Connor et al 1998 Phys. Plasmas 5 2687

[3] P. B. Snyder et al 2004 Plasma Phys. Controlled Fusion 46, A131

[4] P. B. Snyder et al 2002 Phys. Plasmas 9 2037

[5] F. Jenko et al 2001 Plasma Phys. Controlled Fusion 43 A141

[6] G. T. A Huysmans et al 1996 HELENA Installation and User Guide

[7] A. B. Mikihailovskii et al 1997 Plasma. Phys. Reports 23(10) 844

P2-Pl.013

Design of PAM antenna for 4 MW KSTAR LHCD System

*김지현, 왕선정, JulienHillairet[1], 김해진, 성태식 [2], 황지현 [2], 남궁원 [2], 조무현 [2]
*Jeehyun. Kim, Son Jong. WANG, Julien. Hillairet[1], Hae Jin. Kim, Taesik. Seong[2], Jihyun. Hwang[2], Won. NAMKUNG[2], Moo-Hyun. CHO[2]
국가핵융합연구소. [1]CEA. [2] 포항공과대학교.

Keyword : KSTAR, LHCD, PAM, current drive

Design of 4 MW LHCD system is under study with the aim of operation in 2020. 4MW LHCD system in the design consists of eight 5 GHz 500 kW CW klystron, eight sets of circular transmission lines transmitting TE01 circular mode, and PAM (passive active multijunction) type launcher. The advantage of the PAM are its reliable CW operation due to the cooling and low reflection by the passive active waveguide and multijunction configuraion. KSTAR LHCD PAM launcher was designed to have N// of 2.25 at the frequency of 5 GHz. In this paper, it will be presented the LHCD antenna design with PAM launcher including RF design of multijunction using HFSS and the N// spectrum and reflection coefficient at a various plasma density calculated from ALOHA code.

P2-Pl.014

Z_{eff} measurement study by using prototype new Thomson polychromater in KSTAR

*이종하, 이승헌, 손수현, 고원하, 서동철
*Jong Ha. LEE, Seung Hun. Lee, Soo Hyun. Son, Wonha. KO, Dongcheol. SEO
국가핵융합연구소.

Keyword : Z_{eff}, Thomson scattering, Polychromater, KSTAR

To measure the Z_{eff}, most tokamak machine equipped the filterscope or monochromator system. In KSTAR also the filterscope system have developed for Z_{eff} measurement. Recently, in tokamak machine, there are not enough vacuum windows to measure the plasma parameter because of the many of independent plasma diagnostic system. For this reason, we need to research an integration of plasma diagnostic system. In this research, we developed the integrated diagnostic system which integrated Thomson scattering with filterscope system. In case of Thomson scattering system, to analyze the spectrum, we use the polychromater system. At the inside of polychromater, scattered light separated by 5 bandpass filters that wavelength range is 750 nm ~ 1084 nm. And other wavelengths from the plasma are wasted. We get idea from this measurement mechanism add extra channel to measure 523.8nm wavelength. From this extra channel, we can calculate the Z_{eff} without any independent measurement system. In this paper, we will show the prototype new polychromater that integrated with Zeff measurement system. By using this system, we will show a measuring result of Thomson signal and 523.8nm wavelength to calculate the ne, Te and Z_{eff} in KSTAR experiment.

P2-Pl.015

신개념 RF 전류 구동을 위한 npar 가변형 안테나 연구

*이현우, 김선호 [1], 조종갑 [2], 이현영 [2], 황용석 [2], 이병제
*Lee Hyunwoo. , Kim Sun-Ho. [1], Jo Jong Gab. [2], Lee HyunYeong. [2], HWANG Yong-Seok. [2], Byungje. Lee
광운대학교. [1] 한국원자력연구원. [2] 서울대학교.

Keyword : lower hybrid, fast wave, current drive, comb-line antenna

핵융합 발전의 상용화를 위해서는 정상 상태 운전이 필수적으로 이루어져야 하며, 이에 따른 고성능 운전 모드가 요구된다. 그리고 이러한 고성능 운전 시나리오를 달성하기 위해서는 토카막 플라즈마 중심부 또는 off-axis 의 효율적인 외부 가열 및 전류 구동을 할 수 있는 보조 가열에 대한 연구가 필요한 상황이다. 현재 lower hybrid(LH) 주파수 대역의 slow wave 를 이용한 전류 구동 방법이 가장 높은 효율을 보이고 있지만, 토카막 플라즈마의 중심부까지 RF wave 가 도달하지 못하는 어려움이 있다. 이에 반해, lower hybrid(LH) 주파수 대역의 fa,st wave 는 높은 밀도와 온도에서 플라즈마 중심부까지 RF wave 가 전파되어 중심부 또는 off-axis 의 효율적인 외부 가열 및 전류 구동이 가능하다.
본 연구에서는 높은 밀도와 온도에서 lower hybrid 주파수 대역의 fast wave 를 통한 가열 및 전류 구동에 요구되는 안테나를 제안 및 설계하였다. 안테나는 comb-line 구조로써, 다양한 플라즈마 부하 조건에서도 안정적으로 동작하기 위한 진행파형 안테나 구조를 제안하며, 기존의 가열장치들이 이용하였던 위상 변환기 대신 주파수 가변을 통해 플라즈마에 커플링 및 흡수 특성을 결정하는 npar 을 조정할 수 있는 안테나 구조를 설계하였다. 본 안테나는 효율적인 전류 구동을 위한 npar 가변 범위인 3.5~4.5 를 만족한다. 본 연구는 서울대학교와 한국원자력연구원과 공동 연구로 진행되며, lower hybrid 대역의 fast wave 에 대한 분석적인 연구를 기반으로 안테나 설계를 하였다. 추후 연구를 통해 도출된 안테나와 한국원자력연구원에서 개발 중인 RF system 을 제작하고, 서울대학교의 Versatile Experiment Spherical Torus 에 설치하여 전류 구동 실험을 진행할 예정이다.

이 논문은 2015 년도 미래창조과학부의 재원으로 한국연구재단의 지원을 받아 수행된 국책 연구 사업임 (NRF-2014M1A7A1A03045379)

P2-Pl.016

1kJ 급 Nd:Glass Laser 를 이용한 고에너지밀도 플라즈마의 X-선 관측 기술 연구

*하성용, 한재민, 남성모, 오승용, 임창환
*Ha Sung Yong. , HAN Jae Min. , NAM Sung Mo. , Oh Seong Yong. , LIM Chang Hwan.
한국원자력연구원.

Keyword : nuclear fusion, Nd:Glass Laser, plasma, silicon x-ray

플라즈마 발생에 이용되는 고에너지 레이저 장치는 Nd:Glass 레이저로 1 개의 빔라인 에너지가 250 Joule 이며 총 4 개의 라인으로 구성되어 최대 1KJ 의 에너지로 방출 가능하다. 이 레이저를 이용해서 고에너지밀도플라즈마를 발생시키고 이 때 발생되는 고에너지 전자 및 이온, X-선, 감마선, 중성자등은 플라즈마의 거동을 관측하고 해석하는데 중요한 기초 데이터로 사용된다. 본 연구의 최종 목표는 silicon 재질의 microballoon 의 내부에 중수소 및 삼중수소가스 혹은 DT ice 와 같이 내관 기폭성을 가지는 특별한 핵융합 연료로 채우고 고에너지 레이저를 발진하여 이때 발생된 고에너지밀도플라즈마를 해석하는데 있다. 본 발표에서는 현재까지 개발된 1kJ 급 레이저 시설을 소개하고 그중에서도 진행되고 있는 X-선 관측기술에 대해 설명하려 한다.

P2-Pl.017

레이저플라즈마 발생 충격파 해석을 위한 속도간섭 시스템 개발

*하성용, 한재민, 남성모, 오승용, 이승호 [1], 임창환
*Ha Sung Yong. , HAN Jae Min. , NAM Sung Mo. , Oh Seong Yong. , Lee Seungho. [1], LIM Chang Hwan.
한국원자력연구원. [1] 오사카대학교 레이저에너지연구소.

Keyword : 속도간섭시스템, VISAR, 충격파, Shockwave

속도간섭 시스템의 레이저 간섭방법은 일반적으로 충격이 가해진 시편의 표면 움직임에 대한 속도-시간 프로파일을 얻기 위한 수단으로 사용되는 시스템이다. 본 연구실에서는 충격파를 해석하기위해 VISAR(Velocity Interferometer System for Any Reflector)를 개발 하였다. VISAR 의 출력 신호는 PBS(polarizing beamsplitter)와 두 쌍의 광 검출기에서 획득되는 비편광 신호이다. 이 편광의 위상은 간섭계의 한 방향에 1/8 WP(wave plate)의 사용을 통해 서로에 대해서 위상이 이동한다. 보통의 마이켈슨 간섭 시스템에서와같이 VISAR 시스템은 광 경로상에 에타론(etalon) 혹은 유전체 슬랩(slab)을 설치한다. 에타론을 설치하는 목적은 실제의 미러 위치보다 BS 에 가깍게 가상의 미러 이미지를 생성하기 위해서이다. 따라서 간섭계의 경로는 서로 다른 물리적인 거리차가 생기고 다시 재결합하여 시간이 지연된다. 본 발표에서는 VISAR 시스템을 소개하고 개발된 시스템을 이용해서 Al 타겟에서 발생된 레이저 플라즈마에대한 충격파를 설명하려한다.

P2-Pl.018*

Measurement of local density and magnetic field of a magnetized plasma using Raman scattering from a focused laser pulse

*송형선, 조명훈 [1], 김영국, 강태연, 석희용 [2], 허민섭
*HYUNG SEON. SONG, Myung Hoon. Jo[1], Young kuk. Kim, Te Youn. Kang, Hyyong. Suk[2], Min Sup. Hur
울산과학기술대학교. [1] 광주기초과학기술원. [2] 광주과학기술원.

Keyword : Raman scattering, plasma diagnostics, magnetized plasma, particle-in-cell simulation

We investigated the possibility of pin-pointing the local density and magnetic field of an inhomogeneous, magnetized plasma by Raman scattering of a pump laser pulse focused on a desired position. As the Raman growth rate is proportional to the pump pulse amplitude, the spectral peak shift of the scattered signal is, though it is a spatially integrated one, expected to be determined dominantly by that from the focal position of the pump pulse. From a theoretical estimation, we found a condition of the pulse duration and plasma density for such an expectation to properly work. It was confirmed by two-dimensional particle-in-cell simulations that as long as the pulse duration is long and the length scale of the plasma inhomogeneity is large compared to the Rayleigh length, the spectral bandwidth of the spatially integrated Raman signal can be narrow enough to distinguish the peak position with good enough resolution.

P2-Pl.020

레이저 산란을 이용한 알곤 대기압 플라즈마의 변수 측정

*서병훈, 김대웅 [1], 김정형, 유신재 [2], 유승완 [3], 권지혜 [3]
*BYONG HOON. SEO, Dae Woong. Kim[1], Jung-hyung. Kim, Shin Jae. You[2], Seung-Wan. Yoo[3], Ji Hye. Kwon[3]
한국표준과학연구원. [1] 카이스트. [2] 충남대학교. [3] 서울대학교.

Keyword : 대기압 플라즈마, 톰슨 산란, 라만 산란

최근들어 다양한 영역에서 대기압 플라즈마가 활용되고 있다. 따라서 우리가 원하는 조건의 플라즈마를 발생, 활용 하기 위해서는 플라즈마 변수의 정확한 진단이 요구된다. 본 연구에서는 레이저 톰슨 산란과 라만 산란을 이용하여 플라즈마의 변수인 전자밀도, 전자온도, 중성종 온도를 공간적으로 측정 하였다. 특히, 식품, 의료등에서 대기압 플라즈마를 사용할 경우, 물에 노출된 환경을 쉽게 접할 수 있는데, 이때 플라즈마의 상태가 어떻게 변하는지 확인하기 위해, 플라즈마를 물에 접촉 시켜 변수 분포를 측정 하였다. 그 결과, 물에 접촉 하지 않은 플라즈마의 경우 밀도 봉우리가 하나로 측정 되는 반면, 물에 접촉한 플라즈마는 밀도 봉우리가 두개로 측정 되었다. 이것은 물의 표면이 요동침에 따라 생기는 날카로운 점에 의해 전기장이 분산되어 이러한 분포를 형성하는것으로 이해 된다. 이러한 실험 결과와 물리적 해석을 자세하게 기술 할 예정이다.

P2-Pl.021

The research of TVS triggered condition

*박웅화, 김무상, 손윤규, Philip Dienstbier[1], Andre Michel[2], 이병준
*Wung Hoa. Park, Moo Sang. Kim, Yoon Kyoo. Son, Philip. Dienstbier[1], Andre. Michel[2], Byung Joon. Lee
포항가속기연구소. [1]Erlangen Nürnberg University. [2]Goethe University Frankfurt.

Keyword : vacuum, trigger, pulse, CST, copper, tungsten

The Triggered Vacuum Switch (TVS) is widely used in the high power switch. It discharges high current whithin a micro second after being triggered. The trigger which comes from a external trigger pulse generator supplies a high voltage signal to a trigger pin.The triggered voltage signal depends on the geometry of trigger pin, material, vacuum pressure, and so on. In this paper we have studied for the vacuum pressure and the geometry of trigger pin which is simulated with CST. Our research is accomplished under the condition that material is fixed with the copper electrode and tungsten trigger pin.

P2-Pl.022

대기압 플라즈마 처리시 수용액상에서의 광분해 메커니즘과 활성분자 생성 및 미토콘드리아에 주는 영향

*박주영, 박상후 [1], 김기중, 최원호
*Park Jooyoung. , Park Sanghoo. [1], Kim Ki jung. , CHOE Wonho.
한국과학기술원. [1]KAIST.

Keyword : 미토콘드리아 포텐셜, 제트플라즈마, 광분해, OH 라디컬

대기압 플라즈마는 최근 의학적 치료 도구 및 병리학, 생리학 등의 활용 도구로서 많은 관심하에 다양한 방면으로 연구가 진행되고 있다. 특히, 병리 및 생리학적으로 많은 영향을 끼치는 활성산소종 및 활성질소종의 공급원으로서 대기압 플라즈마에 대한 연구가 진행되고 있다. 본 연구에서는 대기압 플라즈마로부터 공급되는 수용액상의 과산화수소 및 아질산염의 광분해 메커니즘을 이해하고자 하였다. 또한 광분해의 결과로 생성되는 활성분자들에 의해 나타나는 미토콘드리아의 변화를 관측하였다. 아르곤제트 플라즈마(전압 4 kV, 주파수 35 kHz, 유량 6 lpm)에서 방출되는 자외선을 이용하여 과산화수소(H_2O_2) 및 아실잔염(NO_2^-)을 광분해하였으며, 그 과정을 HPLC(High Performance Liquid Chromatography)로 수산기(OH) 라디컬을 측정하여 관측하였고, 또한 광분해 과정 중에 생성되는 과산화물($O_2^{\cdot -}$) 및 산화질소($NO^{\cdot}$) 등의 활성산소 및 질소종들을 EPR(Electron Paramagnetic resonance)를 이용하여 측정하여, 플라즈마에 의한 광분해 과정을 면밀히 파악하였다. 이를 바탕으로 플라즈마 생성되는 과산화물, 산화질소 및 수산기 등이 세포의 미토콘드리아 막에 끼치는 영향을 plate reader 및 FACS(Fluorescence Activated Cell Sporting) 등으로 멤브레인 전압 및 세포 사멸을 확인하였다. 본 연구결과로 수용액상에서 플라즈마 광분해를 통해 활성산소 및 질소종들이 생성되는 과정과 활성분자들이 미토콘드리아에 주는 영향을 이해할 수 있다.

P2-Pl.025*

주입 기체 온도에 따른 농식품 저장 향상을 위한 상압 플라즈마의 오존 농도 제어에 관한 연구

*문아영, 문세연, 유석재 [1]
*Moon A-Young. , Se Youn. Moon, YOO Suk Jae. [1]
전북대학교. [1] 국가핵융합연구소.

Keyword : 대기압 플라즈마, 농식품, 오존 발생, DBD

플라즈마 기술의 적용은 일반 산업체에서뿐만 아니라 미용기기, 소독기, 의료기술 등 실생활에서도 손쉽게 찾아볼 수 있다. 특히 유전체 장벽 방전 플라즈마는 플라즈마 발생시 nitric oxide 와 ozone 등 다양한 활성종들의 생성으로 곰팡이와 같은 균들의 살균과 저장성 증대 효과를 가질 수 있기 때문에 최근 농식품 분야에 적용하는 연구가 활발하다. 하지만 농식품과 오존의 발생, 분해와 농식품을 접목시킨 연구는 미비하다.
따라서 본 실험에서는 유전체 장벽 방전 플라즈마 발생 시 주입한 기체의 온도에 따른 오존 발생량에 대해 연구하였다. 오존 발생량은 오존 감지기를 이용하여 측정하였고 그 결과 주입 기체 온도를 상온에서 120 ºC 까지 증가시킴에 따라 오존농도가 342 에서 168 ppm 으로 감소하였다.
OES 와 전류-전압 측정을 통해 플라즈마의 광학적, 전기적 특성을 분석하였다. 한편 플라즈마 처리 기술이 농식품에 미치는 영향을 알아보기 위해 일반 공기와 플라즈마 처리한 공기에 일정 시간 동안 방울토마토를 보관한 후 Brix 와 손실 중량을 측정하였다. 저장한 시간과 온도에 따라 측정한 결과 큰 값의 차이를 보이지 않았다. 미생물 수는 일반 공기에 보관한 방울토마토의 경우 3 일간 증가하는 경향을 보였지만 플라즈마 처리한 기체에 보관한 경우 12 시간까지 6.18 에서 6.98 Log CFU/g 으로 감소하다가 점차적으로 증가하였다. 주입한 기체의 온도에 따른 미생물 수 변화는 온도가 증가함에 따라 곰팡이의 수가 소폭 증가하는 경향을 보였지만 여전히 일반 공기에 보관한 방울토마토보다 적은 미생물 수를 보였다.

* 이 연구는 2015 년도 정부의 재원으로 국가 핵융합연구소의 지원을 받아 수행되었음.

P2-Pl.028*

대면적 사이즈 고주파 용량성 결합 플라즈마에서의 전자기적 현상 연구

*배효원, Ming-Chieh Lin[1], 조영현, 이해준
*HYOWON. BAE, Ming-Chieh. Lin[1], Younghyun. Jo, LEE Hae June.
부산대학교. [1] *한양대학교.*

Keyword : 플라즈마, 시뮬레이션, CCP, PIC

고주파 용량성 결합 플라즈마(CCP)는 유도성 결합 플라즈마(ICP)와 함께 반도체 및 디스플레이 공정에서 널리 이용되고 있다. 반도체 공정 기술이 고도화 됨에 따라 반도체 생산 수율을 높이는 것이 필요하다. 그 중 한 가지 방법은 선폭을 줄여 반도체의 크기를 줄이는 것이고, 다른 방법으로는 반도체 공정에서의 웨이퍼 사이즈의 크기를 증가시켜서 한 웨이퍼에서 더 많은 반도체를 얻어내는 것이다. 반도체 장비가 커지면서 고밀도 플라즈마를 생성해내기 위해서 용량성 결합 플라즈마 장비에서는 60 MHz 에서 100 MHz 이상의 고주파로 파워를 인가하게 된다. 이로 인해 전자기파의 파장은 짧아지게 되고 특히 장비가 450mm 이상의 대면적 사이즈로 가게 되면서 짧아진 파장의 영향으로 정상파(standing wave)가 발생되어 플라즈마의 균일도가 떨어지게 되고 공정에서 원하는 결과를 얻기가 힘들어지게 된다. 이와 같은 정상파가 플라즈마 공정에 미치는 효과에 대한 연구는 대면적 장비의 활용에 있어 매우 중요하다. 그 연구 방법 중에 한 가지로 컴퓨터 시뮬레이션을 이용하고 있는데, 기존의 반도체 시뮬레이션은 대부분 정전계(electrostatic)로 가정하여 정전기적 현상만 고려하였지만 위에서 언급한대로 대면적 고주파 용량성 플라즈마에서는 전자기적 현상을 모두 고려해야 한다. Maxwell 방정식을 직접 푸는 것은 시간이 오래 걸리기 때문에 본 연구에서는 자기벡터 포텐셜 방법을 도입하여 전자기적 현상을 관찰하는 기법을 개발하였다. 2 차원 입자-셀(Particle-In-Cell) 시뮬레이션을 이용하여 자기벡터 포텐셜을 함께 풀었을 때에는 플라즈마의 정 중앙으로 갈수록 정상파에 의한 전기장이 강해지는 걸 관찰할 수 있었고, 이로 인해 자기백터 포텐셜을 고려하지 않았을 때에 비해 플라즈마가 더 불균일해지는 것을 알 수 있었다. 또한 전자에너지분포함수의 변화를 함께 관찰하고 이를 토대로 대면적 고주파 용량성 결합 플라즈마의 물리적 현상을 파악하였으며 이 영역에서는 반드시 전자기 현상을 고려해야 한다는 것을 확인하였다.

P2-Pl.030

A Study on High Power Quartz Waterload using ANSYS

*선상원, 김해진, 왕선정, 김지현
*Sang won. Seon, Hae Jin. Kim, Son Jong. WANG, Jeehyun. Kim
국가핵융합연구소.

Keyword : waterload, quartz, thermal flow, structure analysis

KSTAR 의 플라즈마 가열을 위한 가열장치 중 하나인 Lower hybrid current drive (LHCD) 시스템은 5 GHz, 500 kW 급의 클라이스트론을 이용한다. 클라이스트론의 RF 출력은 80 m 의 전송선로를 지나 안테나를 통해 방사되고 플라즈마를 가열하게 된다. 이때 플라즈마에 흡수되지 않고 되돌아오는 반사파로부터 클라이스트론 소스를 보호하기 위해 워터로드를 사용한다. 워터로드는 고출력 RF 장치에서 많이 사용되며 전송선로의 종단에 위치하여 microwave 를 흡수하거나 전송선로의 파워 손실을 계산하는데 사용한다.

고출력 quartz 워터로드는 직각 도파관의 수직형태로 위치한 원뿔 형태의 quartz 안에 물을 이용하여 100 kW 의 높은 전력을 흡수하도록 설계하였다. 워터로드에서 흡수된 고출력 전자파에 의하여 발생된 열은 국부적으로 집중되기 때문에, 정상적인 냉각이 이루어지지 못할 경우 고열로 인하여 워터로드의 손상을 발생시킬 수 있다.

본 연구에서는 고출력 quartz 워터로드의 냉각 효율을 높이기 위해 ANSYS CFX 프로그램을 이용하여 열 해석과 냉각수 입/출구의 위치 변화, 유로 보조 장치의 형상 및 냉각수 유량제어를 분석하였다. ANSYS 시뮬레이션 결과를 통해 quart 워터로드 내부 국부 지역의 최고 온도가 낮아짐을 확인하였고 냉각수로 인해 quartz 표면에 발생하는 내부압력을 ANSYS 를 이용하여 구조 해석을 수행하였다.

P2-Pl.031

Regulation of NOx emission using atmospheric air plasma in vehicle exhaust

*김호영, 김진석 [1], 당천우 [1], 이해준 [1]
*Ho Young. Kim, Jin Seok. Kim[1], Tianyu. Tang[1], Hae June. LEE[1]
하이브리드 소재 솔루션 국가 핵심 연구센터. [1] *부산대학교.*

Keyword : Regulation of NOx emission, Atmospheric air plasma, Atmospheric pressure plasma, Plasma simulation

화석 연료의 연소를 이용한 기술이 발달하면서 연소 시 발생되는 NOx 의 처리 중요시되었다. 그 중, 자동차 배기가스에서 나오는 다량의 NOx 성분 때문에 스모그, 산성비, 호흡기 질환 등의 문제가 발생됐다.[1] 이러한 다량의 배기가스를 처리하기 위해 공기의 농도, 환원제 사용(NH_3, $(NH_2)_2CO$), 선택적 촉매환원 기술(Selective Catalytic Reduction (SCR)), 플라즈마 처리 등이 연구 되어 왔다. 그 중 플라즈마와 SCR 기술을 복합적으로 쓴 Hybrid 방법이[2] 있는데 우수한 NOx 감소율을 보였다. 그러나 대기압 공기 플라즈마 안에 있는 활성종과 SCR 에 쓰이는 암모니아와의 NOx 생성 소멸 반응 메커니즘 규명과 다양한 플라즈마 형태에서 나오는 활성종에 의한 NOx 발생량 조절 연구는 아직 미미한 상태다. 플라즈마 시뮬레이션을 통해서 가스 온도, 전극간 간격, 전극 모양에 의한 NOx 밀도 변화를 확인하였다. 가스 온도가 높아질수록 NO 와 NO_2 밀도는 증가 했지만, 일정 온도 이상이 되면 NOx 밀도는 감소되었다. NO 와 NO_2 밀도는 서로 상충관계에 있는데, 반응 메커니즘은 모두 산소원자와 관련이 있다. 플라즈마를 발생시키는 두 전극 사이의 거리에 따른 활성종 변화와 NOx 생성 및 소멸 메커니즘도 알아보았다. 마지막으로 플라즈마 유체 시뮬레이션을 통해 NOx 의 Diffusion 과 전극 모양에 따른 NOx 밀도 변화를 확인하였다.

P2-Pl.032

전극구조에 따른 DBD 방전 특성

*문혜원, 전형원 [1], 엄상흠 [1], 김성봉 [1], 주정훈, 유석재 [1]
*hye won. Mun, . [1], . [1], . [1], . , YOO Suk Jae. [1]
군산대학교. [1] *국가핵융합연구소.*

Keyword : .

최근 생활수준의 향상에 따른 고품질 식품 수요에 의하여 식품 생산 및 공급에 대한 관심이 높아지고 있다. 이에 따라 신선한 식품을 공급하기 위해서는 식품 저장기술과 장기보관을 위한 관련 기술이 요구된다. 식품은 열에 민감하여 저온에서도 변성 될 가능성이 있으므로 변성을 일으키지 않고 살균할 수 있는 비 가열 살균기술의 적용이 필요하다. 대체기술로 인지되고 있는 대기압 저온 플라즈마 기술은 화학적 반응성이 큰 활성 라디칼, 자외선 및 적외선 등이 포함되어 물리화학적 처리가 동시에 가능하고, 생산시간 또한 단축시킬 수 있으며, 인체에 무해한 처리 방법이다. 따라서, 대기압 저온 플라즈마 기술을 식품에 적용하기 위해서는 다양한 식품군에 대한 전극 구조 및 방전특성에 대한 연구가 요구된다. 본 발표에서는 식품과 유사한 floating conductor 를 이용하여 다양한 DBD 전극구조에 따른 I-V, OES, 라디칼 분석을 통해 방전 특성을 평가하였다.

P2-St.001

Exact Partition Function of the Ising Model on Finite Triangular Lattice with Free Boundary Conditions

*김승연
*Seung Yeon. Kim
한국교통대학교.

Keyword : Exact Partition Function, Triangular Lattice, Free Boundary Conditions

The exact partition functions of the triangular-lattice Ising model with free boundary conditions are not known for systems of arbitrary size. To overcome this, Stosic et al. [Phys. Rev. B 41, 11466 (1990)] computed the exact density of states for the Ising model on (equilateral) triangular lattice with free boundary conditions up to L=15 spins on a side (corresponding to 2^120 = 1.329 x 10^36 states) by using an IBM 3090. We evaluate the exact density of states for the Ising model on (equilateral) triangular lattice with free boundary conditions up to L=24 spins on a side by counting all possible spin states with the microcanonical transfer matrix. The total number of states is 2^300 = 2.037 x 10^90 for L=24. Classifying all 2^300 spin states according to their energy values is an enormous work. From the density of states, the exact partition function is immediately given.

P2-St.002

Geometric Analysis of Polymers on a Square Lattice

*이재환, 이주련, 김승연 [1]
*Jae Hwan. Lee, Julian. Lee, Seung-Yeon. Kim[1]
숭실대학교. [1] *한국교통대학교.*

Keyword : Radius of gyration, End-to-end distance

We study conformational transitions of two-dimensional lattice polymers by measuring the radius of gyration and the end-to-end distance, which are known to provide us with information on the collapse transition. Derivatives of the mean square values of both quantities show peaks in the low-temperature region, distinct from the peak corresponding to the collapse transition. Results are compared with those obtained by the specific heat. In addition, the universal ratio of the mean square radius of gyration and the mean square end-to-end distance are calculated for whole temperature region and compared with previous results.

P2-St.003

Surface Growth in Quenched Impurities on a Sierpinski Gasket Substrate

*김수경, 김수진, 박완기, 김진민
*Soo Kyung. Kim, Su Jin. Kim, Wanki. Park, Jin Min. Kim
숭실대학교.

Keyword : Surface growth, Sierpinski gasket, Pinning-depinning transition

We introduce a discrete growth model with quenched impurities on a Sierpinski gasket substrate to understand the pinning-depinning transition. At the critical force F_c, the surface width W shows a scaling behavior $W(t,L) \sim L^\alpha f(t/L^z)$. Near F_c, the steady-state velocity v_s follows $v_s(F) \sim (F-F_c)^\theta$. From the finite-size scaling of the growth velocity, we obtain correlation time exponent ν_t. The nontrivial diffusion behaviors of the underlying substrates are also considered. Because the growing site is considered as the active site of an absorbing state, the interface pinning of the surface model is discussed in connection with the absorbing phase transition.

P2-St.004

Anomalous Behaviors of Generalized Conserved Lattice Gas

*곽우섭, 하미순
*Wooseop. Kwak, Meesoon. Ha
조선대학교.

Keyword : GCLG, temporal scaling behavior, aging effect, absorbing phase transition

We investigate the temporal scaling behaviors of the generalized conserved lattice gas (GCLG), which is a simple variant of the conventional CLG with an effective temperature parameter, . Previous studies on two-dimensional lattices found that the effective temperature yields nontrivial absorbing phase transitions. Resolving the origin of such anomalies, we numerically investigate the aging effects of the GCLG on two-dimensional lattices and random networks.

P2-St.005

Particle in a box with a time-dependent delta-function potential

*백승기, 이수도, 김민재
*Seung Ki. Baek, Su Do. Yi, Min Jae. Kim
부경대학교.

Keyword : Quantum information engine, Time-dependent Schrodinger equation, Time-dependent delta-function potential, Volterra integral equation

In quantum information processing, one often considers inserting a barrier into a box containing a quantum particle. Assuming that the particle initially lies in the ground state without the barrier, we formulate this insertion problem as a one-dimensional Schrodinger equation with a time-dependent delta-function potential. By applying the Laplace transform, we convert the equation into a set of Volterra integral equations, which allows analytic and numerical investigations. We show that even if the strength of the potential diverges within a finite time, the wavefunction converges to the first excited state without any anomalies.

P2-St.006

Experimental test of generalized Jarzynski equality under nonequilibrium feedback Control

*이동윤, Govind Paneru, 박혁규 [1]
*Dong yun. Lee, Govind. Paneru, Hyuk Kyu. PAK[1]
기초과학연구원/UNIST. [1] 울산과학기술대학교.

Keyword : Information thermodynamics, Inforamtion ratchet, Genralized Jarzynski equality, feedback control

Recent studies of the relationship between information and thermodynamics showed that in the presence of feedback control, an information quantity known as the mutual information, should be included in describing non-equilibrium dynamics of fluctuating systems, such as molecular motors, information engine, etc. During the last decade, such relationships have been intensively studied experimentally, but have been limited to a single system. Here, we experimentally test the generalized Jarzynski equality under nonequilibrium feedback control by measurements the mutual information and work of a colloidal particle under the information ratchet suggest by Sagawa and Ueda[1]. We can also transport the Brownian particle in one dimension through feedback control. Our results will be helpful to understand operating engines under feedback control at micro-and nanometer length scale.
[1] Takahiro Sagawa and Masahito Ueda, Phys. Rev. Lett. 104, 090602 (2010).

P2-St.008*

Electrical phenomena at solid-liquid interface during the liquid droplet spreading

*송명원, 이정훈 [1], 문종균 [2], 박혁규
*Myungwon. Song, Jung-Hoon. Lee[1], Jong Kyun. Moon[2], Hyuk Kyu. PAK
울산과학기술대학교. [1]University of Waterloo. [2] 기초과학연구원 (IBS).

Keyword : electric double layer, solid-liquid interface, surface charge distribution

A water droplet spreads rapidly immediately after it makes a contact with a solid surface. And the spreading radius of a droplet on a substrate follows a well-defined power-law dynamics. When the spreading radius of the contact area increases, the area of the electrical double layer increases at the interface between a droplet and a solid simultaneously. Here, we propose a new experimental method of measuring the spreading radius of contact area and the induced electric signals from the modulation of the electrical double layers simultaneously [1, 2]. We used an interferometric technique for nanoscale measurement of spreading dynamics of a droplet interacting with a solid surface. We expect this method for measuring both the mechanical and electrical properties on the solid-liquid interfaces at the same time will be useful in the study of electrical phenomena on solid–liquid interfaces.

[1] Moon, J. K., Jeong, J., Lee, D., & Pak, H. K. (2013). Electrical power generation by mechanically modulating electrical double layers. Nature communications, 4, 1487.
[2] Moon, J. K., Song, M. W., & Pak, H. K. (2015). Investigation of surface charge density on solid–liquid interfaces by modulating the electrical double layer. Journal of Physics: Condensed Matter, 27(19), 194102.

P2-St.009

Greedy adaptive walks on a correlated fitness landscape

*박수찬, Johannes Neidhart[1], Joachim Krug[1]
*Su-Chan. Park, Johannes. Neidhart[1], Joachim. Krug[1]
가톨릭대학교. [1]University of Cologne.

Keyword : Adaptation, Genotype space, Extreme value theory, Asexual population

We study adaptation of a haploid asexual population on a fitness landscape defined over binary genotype sequences of length L. We consider greedy adaptive walks in which the population moves to the fittest among all single mutant neighbors of the current genotype until a local fitness maximum is reached. The landscape is of the rough mount Fuji type, which means that the fitness value assigned to a sequence is the sum of a random and a deterministic component. The random components are independent and identically distributed random variables, and the deterministic component varies linearly with the distance to a reference sequence. The deterministic fitness gradient c is a parameter that interpolates between the limits of an uncorrelated random landscape ($c = 0$) and an effectively additive landscape ($c \to \infty$). When the random fitness component is chosen from the Gumbel distribution, explicit expressions for the distribution of the number of steps taken by the greedy walk are obtained, and it is shown that the walk length varies non-monotonically with the strength of the fitness gradient when the starting point is sufficiently close to the reference sequence. Asymptotic results for general distributions of the random fitness component are obtained using extreme value theory, and it is found that the walk length attains a non-trivial limit for $L \to \infty$, different from its values for $c=0$ and $c = \infty$, if c is scaled with L in an appropriate combination.

P2-St.010

Dependence of the Crossing Time on the Sequence Length in a Diploid Discrete-Time Mutation-Selection Model for a Finite Population

*길원평
*Won Pyong. GILL
부산대학교.

Keyword : diploid model, mutation-selection model, crossing time, finite population, overdominant case

This study examined the crossing time in the diploid discrete-time mutation-selection model in a finite population for a range of dominance parameters and selective advantages by switching on a diploid, asymmetric, bridged landscape, from an initial state, a steady state in a diploid, bridged landscape.
The dependence of the crossing time on the sequence length was examined for a fixed extension parameter, which was defined as the mean Hamming distance from the optimal allele of the initial steady state divided by the sequence length.
The boundary between the deterministic and stochastic regions in the diploid discrete-time mutation-selection model was characterized using the same formula as that in the haploid discrete-time mutation-selection model.
The crossing time in a finite population with various population sizes, dominance parameters and selective advantages began to deviate from the crossing time for an infinite population at the critical sequence length.
The crossing time for a finite population in the stochastic region was found to be an exponentially increasing function of the sequence length, whose rate was unchanged, regardless of changes in the population size, dominance parameter and selective advantage with a fixed extension parameter.
Therefore, the saturation of the crossing time at a long sequence length, which was observed for the overdominant case in an infinite population, could not be realized for a finite population.

P2-St.011

CHARMM force field 의 CMAP 에너지 보정항이 alpha-helix 의 탄성에 미치는 효과

*최승호, 유진우, 설태령, 제갈장환, 박준서
*Seungho. Choe, Jin Woo. Yu, Tae Roung. Seol, Janghwan. , JunSeo.
DGIST.

Keyword : alpha-helix, persistence length, CMAP

단백질의 기능을 이해하기 위해서는 단백질을 구성하고 있는 기본 요소인 alpha-helix 와 beta-sheet 의 물리적 성질을 이해하는 것이 중요하다. 분자동력학 시뮬레이션과 선형 탄성이론을 이용하면 alpha-helix 의 persistence length(또는 영률)를 구할 수 있는데, 본 연구에서는 단백질 backbone 의 구조적인 정확도를 향상시키기 위해 도입된 CHARMM force field 의 CMAP 에너지 보정항 유무에 따라 alpha-helix 의 persistence length 값이 어떻게 달라지는지 살펴본다.

P2-St.012*

Impact of enzymatic gene coexpression of cellular networks on disease comorbidity

*하경균, 이덕선
*Gyeong-Gyun. Ha, Deok-Sun. LEE
인하대학교.

Keyword : "comorbidity", "gene coexpression", "metabolic multiplex network"

The diverse interactions of numerous cellular ingredients in cellular networks have proved to be essential for understanding disease prevalence patterns. For instance, we have previously shown that the metabolites controlled by genetically-correlated enzymes are robust; the prevalence of their associated diseases is low. Yet, it remains elusive how the intricate connectivity pattern of cellular networks affects the relationship - a positive or negative correlation - between distinct diseases. Here we consider the distance between two metabolites at different layers of cellular networks - gene coexpression, protein interaction, and metabolism - and how much they can explain the correlation of distinct disease modules quantified by their comorbidity.

P2-St.013*

Effective Diversity of T Cell Repertoire

*허금, 조정효
*Jin. Xu, Junghyo. Jo
아시아태평양이론물리센터.

Keyword : immune repertoire diversity, thymic selection, optimal coding

To detect countless pathogen invaders in our life, we should equip with diverse immune receptors. Each immune cell expresses copies of one specific receptor. Therefore, we cannot have infinite diversity for receptors with a finite number of cells, but should have an effective repertoire. The immune system shapes the repertoire by filtering immature immune cells that express randomly-generated receptors. The system selects immature cells of which receptors have sufficient, but not too strong, interactions with self peptides in the thymus. The positive and negative selection prevents the maturation of negligible and autoimmune cells. We ask how the repertoire formation, based on only self peptides, can be effective to detect non-self peptides that were never experienced. Here we model T-cell receptors and peptides on major histocompatibility complexes as strings of amino acids, and examine the interactions between strings. Using the model, we test whether the thymic selection minimizes the risk of responding to safe self peptides and ignoring dangerous non-self peptides.

P2-St.014*

Structure and Learning of Neural Network

*송주용, 조정효 [1]
*Juyong. Song, Junghyo. Jo[1]
Postech. [1] *아시아태평양이론물리센터.*

Keyword : Graph Theory, Neural Network Learning, Back-propagation algorithm

Small-world, scale-free and modular structures have been observed in the brain networks, although their functional roles are not yet clear. Therefore, we broadly examine potential benefits of those structural features on machine learning. In particular, we apply the two well-known algorithms of the Boltzmann machine and the recurrent back-propagation for learning certain tasks with various network structures.

P2-St.015

Gating mechanism of nicotinic acetylcholine receptors studied by molecular dynamics simulations

*판티홍탐, 이명기
*Thi Hong Tham. Phan, Myunggi. Yi
Pukyong National University. Busan.

Keyword : Gating mechanism, nicotinic acetylcholine receptor, α4β2 nAChR

Nicotinic acetylcholine receptors (nAChRs) are essential in neurotransmission. Although there are many research on the allosteric mechanism of ligand binding event triggering channel opening in transmembrane domain, the relationship between structure and function in atomic scale is still unclear. In this study, we focused on investigating the gating mechanism of nAChR through either apo form or ligand bound forms. We performed 4 molecular dynamics (MD) simulations of α4β2 nAChR: wild type of apo form (APO), acetylcholine bound wild type (ACH), wild type of BuIA toxin bound form (WT) and toxin bound mutant type (MT) α4β2 nAChRs whose 3 residues of α4 subunit (Tyr185, Asp187 and Arg188) were replaced by 3 corresponding residues of α6 subunit. These three α6 residues are determinants of the toxin α-conotoxin BuIA selectivity of α6 subunit. The pore radius calculations showed that the MT and APO forms had restriction radii of 1.9 and 2.3 Å (Glu261 on alpha subunit, Lys260 on beta subunit), while the same region was broadened in WT and in ACH (radii of 2.6 and 3.4 Å). The result showed that the asymmetric tilting motion of ECD was observed in WT and ACH caused the asymmetric twist angle between ECD and TMD. This motion induced the asymmetrically arranged TMD to become more symmetric. In contrast, an opposite tendency was observed in MT and APO systems. We conclude that the inherent asymmetric arrangement of α4β2 nAChR can be broken by an asymmetric tilting motion of ECD. This motion induces the symmetric arrangement in TMD which makes the channel open.

P2-St.016

Mechanism of proton transfer in Hv1 channel studied by molecular dynamic simulations

*판티뜨엉비, 이명기
*Thi Tuong Vy. Phan, Myunggi. Yi
Pukyong National University. Busan.

Keyword : voltage-gated proton channel, molecular dynamic simulations, water wire

The voltage-gated proton channel (Hv1) has been shown to play important roles in the proton extrusion, pH homeostasis, sperm motility and cancer progression. Hv1 has been shown to be highly expressed in cell lines and in tissue samples from patients with breast cancer. The closed-state structure of Hv1 was recently solved by the X-ray crystallography. No open structure exists. We used this structure to perform MD simulations with electric field and pH conditions to investigate the mechanism of proton transfer in Hv1. The closed-state structure shows that the selectivity filter Asp108 is located in the hydrophobic layer comprising two Phe residues (146 and 179), which might prevent water penetration. We observed a continuous hydrogen-bonded chain of water molecules (a “water wire”) goes through the channel when the channel opens by the moving up of sidechains of 3 Arg on the S4 helix. The increasing of percentage of opening time was consistent with increasing membrane potential. The moving of the selectivity filter Asp108 out of the hydrophobic layer was also observed. In addition, the losing of a hydrophobic layer comprising two Phe residues removes the shield which prevents to form water wire. During simulations, the open channel allows unique water molecules pass through the channel but exclude other ions. This indicated Hv1 channel is highly selective for protons. In the line with previous experimental and simulation observations, our results clearly show that forming of the internal water wire for proton transfer and the opening of channel underlie voltage-and pH-gradient sensing.

P2-St.017

Measurement of the prevalent presence of cations at water-metal interface

*문종균, 조용석 [1], 박혁규
*Jong Kyun. Moon, Yong Seok. Jho[1], Hyuk Kyu. PAK
기초과학연구원 / 울산과학기술대학교. [1] *아시아태평양이론물리센터.*

Keyword : water-metal interface, interfacial charge density, hydronium ions

In spite of tremendous studies and debates over hundred fifty years, it is still controversial why water interface in contact with any materials is charged, and what sign of charge and amount are. Understanding the spontaneous charging of water interface is very important problem in broad fields of science and technology. Here, we developed a new experimental method of measuring the interfacial charge density at water-metal interfaces at the condition of room temperature and atmospheric pressure on the basis of the previous work [1, 2]. We found that the universal preference of the hydronium ions at the metal-water interface regardless of types of metals (Ag, Au, Cu, Pt, ITO, Al). In addition, not only the type of charge, but also the amount of charges at the interface is successfully measured. This information of the interfacial charge density can be considered as a characteristic quantity of the material, and thus be regarded as a complementary property of the material surface which explains an affinity to water/water-ion, like hydrophobicity. We believe that our methods and findings will be important in broad fields of surface sciences in liquid (wet) environment.

[1] Moon, J. K., Jeong, J., Lee, D., & Pak, H. K. (2013). Electrical power generation by mechanically modulating electrical double layers. Nature communications, 4, 1487.
[2] Moon, J. K., Song, M. W., & Pak, H. K. (2015). Investigation of surface charge density on solid–liquid interfaces by modulating the electrical double layer. Journal of Physics: Condensed Matter, 27(19), 194102.

P2-St.018

Restoration of mutual cooperation in the prisoner's dilemma game

*이수도, 백승기, 최정규 [1]
*Su Do. Yi, Seung Ki. Baek, Jung-Kyoo. Choi[1]
부경대학교. [1] *경북대학교.*

Keyword : Prisoner's dilemma, mutual cooperation, Tit-for-tat

One of the most important questions in game theory concerns how mutual cooperation can be achieved and maintained in a social dilemma. In Axelrod's tournaments of the iterated prisoner's dilemma, Tit-for-Tat (TFT) demonstrates the role of reciprocity in the emergence of cooperation. However, the stability of TFT does not hold in the presence of error, and a TFT population is prone to neutral drift to unconditional cooperation, which eventually invites defectors. We argue that a combination of TFT and anti-TFT (ATFT) overcomes these difficulties in a noisy environment. According to this strategy, a player normally plays TFT; turns to ATFT, doing the opposite to what the other player did last time, upon recognizing his or her own error; returns to TFT when mutual cooperation is recovered. The proposed strategy provides simple and deterministic behavioral rules for correcting implementation error in a way that cannot be exploited by the opponent, and suppresses the neutral drift to unconditional cooperation.

P2-St.019

Analyses of optimal investment conditions in the KOSDAQ and KOSPI

*김경식, 임규성 [1], 김수용 [1]
*Kyungsik. Kim, Kyuseong. Lim[1], Soo Yong. Kim[1]
부경대학교. [1] 한국과학기술원.

Keyword : Asset pricing model, Fundamentalist, Chartist, KOSDAQ, KOSPI

The asset pricing models with each different type of the fundamentalist and the chartist are investigated in the Korean financial markets. Two cases are considered as we investigate the statistical properties of the fundamentalist and the chartist. We firstly analyze the overlap values of two prices, as the real closing prices are compared to those simulated from the KOSDAQ and KOSPI. Secondly, the three nonlinear equations for the stock's price are compared and analyzed, and the chaotic behaviors of fundamentalist and the chartist are discussed. Since the fractions of these trader types change over time according to evolutionary process, the fundamentalist and the chartist obtain their forecasting rule upon determinations from optimal investment condition of strategies of future prices.

P2-St.020

Dynamical behaviors in DNA sequences

*김경식, 신기홍, 민승식 [1]
*Kyungsik. Kim, Ki-Hong. Shin, SEUNGSIK. MIN[1]
부경대학교. [1]Korea Naval Academy.

Keyword : Levy walk, Detrended partial cross-correlation analysis, DNA sequences, Genbank

We study the two-dimensional Levy walk and the detrended partial cross-correlation analysis (DPCCA) in several genomic DNA sequences of Genbank. In the generalzed Levy walk, we discuss the prabability distribution, walk behavior, and scaling exponent analysis. In the DPCCA, the partial-correlation technique is applied to quantify the relations of two non-stationary sequences on different time scales. Particularly, we simulate and analyze the DCCA cross-correlation coefficient and compare our result to other findings.

P2-St.021

Modeling diffusion of forest pest under climate conditions

*조우성, 김범준
*WooSeong. Jo, Beom Jun. KIM
성균관대학교.

Keyword : RCP 8.5, pest diffusion, diffusion on network,

Spatial information plays a key role in understanding of disease diffusion in the real world. Especially, climate conditions in space control diffusion pattern of forest pest. We designate climate-dependent diffusive model of forest pest, called Pine Needle Gall Midge. In the model. diffusion is affected by the local temperature and its spatial gradient. From the future climate data in RCP 8.5 which is a scenario with high greenhouse effects, we construct the spatial network in which nodes represent sites by 1km x 1km and link their spatially adjacent neighbors. We simulate the model in the spatial networks and compare with diffusive patterns when the average temperature grows. The result implies that climate conditions are crucial for explaining how pest spreads in the real world.

P2-St.022*

Comparison of Traffic Models for the Korean Bus System

*홍인호, 정우성
*Inho. Hong, Woo-Sung. Jung
포항공과대학교.

Keyword : radiation model, gravity model, Korean bus, human mobility

Traffic models for understanding human mobility induced by populations have been studied for various transportations. The radiation, gravity models and their modifications have deeply been investigated to verify their predictability of traffic flows. In this research, we compared the predictability of radiation and gravity models for two datasets of Korea: nationwide bus passengers and urban bus operations. The radiation model showed better performance for both datasets and for the nationwide and urban scales. The result implies that the radiation and absorption processes in the radiation model explain how people move between populated locations. High deviation issue in both models will be discussed to improve the radiation model.

P2-St.023*

Controllability of systemic risk in economic system

*오갑진, 박아영
*gab jin. oh, AYoung. Park
조선대학교.

Keyword : systemic risk, agent-based model, economic system

Recently systemic risk, characterized by cascading effect among economic objects, is a key concern in a risk management field. Here, we construct a simple agent-based model, including bank, firm, and householder, as an economic system and analyze the system stability by imposing a specific rule. To reduce the systemic risk in the economic system, we propose the bounded information on the interconnection among banks and reduce the systemic risk by controlling the contagion effect. We find that in an agent-based model the systemic risk can be reduced using transparency of information on interconnection between economic objects.

P2-St.024*

Clustering of clans based on marriage pattern in the past

*박혜진, 조우성, 이상훈 [1], 김범준
*hye jin. Park, WooSeong. Jo, Sang Hoon. Lee[1], Beom Jun. KIM
성균관대학교. [1] 고등과학원.

Keyword : clustering, self-oganizing-map

Using Korean family books called ”Jokbo”, we investigate women’s marriage pattern in each clan. We find non-overlapping groups of clans from such patterns. It is observed that clans in some groups are widely spread geographically, while clans in other group are lumped together within a certain limited area. Our result implies the importance of a geographic constraint in the marriage pattern in the past.

P2-St.025

Searching algorithm using true self avoiding walks

*박석종, 육순형, 김엽
*Seok-Jong. Park, Soon-Hyung. Yook, Yup. Kim
경희대학교.

Keyword : complex network, random walk, searching algorithm

다양한 network 위에서의 최적화된 검색 algorithm 을 찾기 위하여 true self avoiding walk (TSAW)에 기반을 둔 algorithm 과 기존의 최적화된 algorithm 으로 알려진 biased random walk (BRW)에 기반을 둔 algorithm 을 비교 분석하였다. BRW algorithm 에서 얻은 mean first passage time 가 최소가 되는 조건은 network 의 degree distribution 과 degree-degree correlation 에 의존하며, 이때 임을 확인하였다. 반면, TSAW algorithm 의 경우 임을 확인하였다. 또한 network 의 구조와 상관없이 TSAW algorithm 의 가 BRW algorithm 의 보다 항상 작음을 보였다. 이를 통하여 TSAW algorithm 이 정보 검색에 있어서 가장 최적화된 algorithm 임을 확인하였다.

P2-St.026

Brownian motion of Ferromagnetic single cube respect to ambient temperature and external magnetic field

*이상혁, 김동현, 이기라 [1], 이유진 [2], 조영훈 [3], 최연석 [3], 박승영 [3]
*Sang-Hyuk. Lee, Dong Hyun. Kim, Gi-Ra. Yi[1], Yuo-Jin. Lee[2], Younghun. Jo[3], Yeon-Suk. Choi[3], Seung young. Park[3]
충북대학교. [1] 성균관대학교. [2] 충남대학교. [3] 한국기초과학지원연구원.

Keyword : Brownian motion, dfiffusivity, magnetic particle, temperature dependence

브라운 운동은 1905 년 아인슈타인의 논문[1]에서 통계적인 특성을 발견한 이후 다양한 연구가 있었다. 이러한 통계적 특성은 비단 입자의 거동을 알아보기 위해서만 연구되는 것이 아니라 많은 다른 현상에도 접목할 수 있는데, 증시변화의 통계적인 연구, 자성체 안에서 스핀의 요동, 에너지수집에 관련된 연구 등을 예로 들 수 있다.
브라운운동의 통계적 특성인 평균 제곱 변위(MSD)는 diffusivity 를 기울기로 하는 시간에 일차함수로 표현되는데, diffusivity 는 입자 주변 유체의 온도와 점성 그리고 입자의 반지름과 관련이 있다.
본 연구에서는 입자 주변 용매의 온도가 변할 때, 브라운 운동의 통계적인 특성이 어떻게 변하는지를 연구하였고. 여기에 더하여 단일 자성 입자에 가하는 외부 자기장을 변화시켜가며 그 특성을 보았다.

[1] A. Einstein, Ann. Phys. 1905, 322, 549

P2-St.027*

The effect of intimacy among members in online communities

*김기범, 김범준
*KIBUM. KIM, Beom Jun. KIM
성균관대학교.

Keyword : intimacy, growing network

In formation of online communities, it is pointed out that effect of intimacy causes decline of the number of total users in communities. We propose a network model to show the effect of intimacy among online community users. In this network, each node represents people in an online community, and each link represents the strength of intimacy. New nodes are added constantly over time. We change the strength of intimacy in the networks and observe the total number of nodes. It takes more time for new nodes to make strong connections to other nodes when the influence of intimacy becomes stronger. This effect makes new nodes into alienated nodes. These alienated nodes exit the network because they have no reason to stay in there. The number of nodes in the community decreases due to this process of elimination. Consequently, the bigger the strength of intimacy is, the more people in the network are eliminated.

P2-St.028*

How to Model Temporal Networks with Activity and Memory

*김혜원, 하미순 [1], 정하웅
*Hyewon. Kim, Meesoon. Ha[1], HAWOONG. JEONG
KAIST. [1] 조선대학교.

Keyword : Time-varying network, activity, memory effect, network modeling

Understanding the structural properties of time-dependent interacting systems, it is necessary to figure out how the network connections are formed along time. While connectivity-driven models, such as Erdös-Rényi random network and growing scale-free networks, are suitable to describe static structural features, they fail to capture temporal properties. To overcome this limitation, the activity-driven model [1] has been proposed and represented temporal structural features of highly dynamical networks. However, the activity-driven model assumes random and Markovian processes, which is not true in most of real-world cases; therefore, we modify the model by including the memory effect [2]. In terms of the modified activity-driven model, we clarify the role of activity and memory in temporal networks, and discuss how it is different from previous suggested models as considering various dynamical processes such as greedy random walk and epidemic process.
[1] N. Perra, B. Gonçalves, R. Pastor-Satorras, and A. Vespignani, Sci. Rep. (2012).
[2] H. Kim, M. Ha, and H. Jeong, arXiv:1508.03545 (2015).

P2-St.029

Long term correlation of the trading interval in the market of London Stock Exchange

*이민영, 오갑진 [1]
*MINYOUNG. LEE, gab jin. oh[1]
POSTECH. [1] 조선대학교.

Keyword : econophysics, time interval analysis, Hurst exponent

This paper investigates the statistical and dynamical properties of ultra high-frequency data for an order-driven market of London Stock Exchange, heterogeneous traders with specific investment strategy dynamically choose the trading times according to execution price and waiting costs. To analyze the nonlinear properties, we first construct the intervals of trade for several investor activities, including the information on the various investment strategies, and analyze the temporal dynamics using the multifractal detrended fluctuation analysis (MF-DFA) method. Our observations assert that for the trading interval regardless of investor type, the Hurst exponent of trading interval is larger than 0.5, which there is long-term correlation.